

SUMMARY OF
SIGNIFICANT
RESULTS IN—

Mineral resources
Water resources
Engineering geology
and hydrology
Regional geology
Principles and
processes
Laboratory and
field methods
Topographic surveys
and mapping
Management of
resources on
public lands
Land information
and analysis
Investigations in
other countries

LIST OF—

Investigations in
progress

GEOLOGICAL SURVEY

RESEARCH 1978



GEOLOGICAL SURVEY PROFESSIONAL PAPER 1100

GEOLOGICAL SURVEY

RESEARCH 1978

GEOLOGICAL SURVEY PROFESSIONAL PAPER 1100

*A summary of recent significant scientific
and economic results accompanied by a
list of geologic and hydrologic investigations
in progress and a report on the status of
topographic mapping*



UNITED STATES GOVERNMENT PRINTING OFFICE, WASHINGTON, D.C.: 1978

UNITED STATES DEPARTMENT OF THE INTERIOR

CECIL D. ANDRUS, *Secretary*

GEOLOGICAL SURVEY

H. William Menard, *Director*

Library of Congress catalog-card No. 68-46150

For sale by the Superintendent of Documents, U.S. Government Printing Office

Washington, D.C. 20402

Stock Number 024-001-03158-2

CONTENTS

	Page		Page
Abbreviations	VII	Regional geologic investigations—Continued	
SI units and inch-pound system equivalents	IX	Rocky Mountains and the Great Plains—Continued	
Mineral-resource and mineral-fuel investigations	1	Environmental geology	56
United States and World mineral-resource		Stratigraphy	58
assessments	1	Igneous rocks	60
Mineral-resources assessment of land areas	2	Precambrian rocks	62
Geologic studies of mineral districts and mineral-		Tectonics	63
bearing areas	4	Basin and Range region	69
Geochemical and geophysical techniques in re-		Mineral-resource studies	69
source assessments	9	Stratigraphic and structural studies	70
Regional geochemical and geophysical studies	9	Igneous rocks	73
Trace elements in minerals	11	Geochronologic studies	74
Geochemical studies of water	11	Pacific Coast region	75
New analytical methods and techniques	12	California	75
Mineral resource information systems and		Oregon	78
analysis	12	Washington	78
Coal	13	Alaska	80
Mineral exploration potential maps	13	General	80
Geotherm file	14	Northern Alaska	81
Coal resources	14	West-central Alaska	82
Reinhardt Thiessen collection now at Reston,		East-central Alaska	83
Virginia	14	Southwestern Alaska	84
Growth of the national coal resources data		Southern Alaska	84
system	14	Southeastern Alaska	85
Coal in New River Gorge area in West		Geologic maps	87
Virginia	14	Water-resource investigations	89
Intertonguing, paleochannels, and faults in		Northeastern region	90
the Wasatch Plateau in Utah	14	Connecticut	91
Montmorillonite in coal partings	15	Illinois	92
Coal rank related to depth of burial and		Indiana	92
buried intrusive rocks	15	Maine	93
Geochemistry of U.S. coal resources	16	Maryland	93
Neutron activation and magnetism of coal	17	Massachusetts	93
Oil and gas resources	17	Michigan	95
Alaska	17	Minnesota	95
Rocky Mountains and Great Plains	18	New Jersey	97
Great Basin and California	20	New York	97
Appalachian Basin and Florida	22	Pennsylvania	98
Offshore areas	23	Rhode Island	99
New exploration and production	23	Vermont	99
Oil-shale resources	25	West Virginia	99
Nuclear-fuel resources	26	Wisconsin	100
Geothermal resources	39	Southeastern region	102
Regional geologic investigations	45	Interstate studies	103
New England	45	Alabama	103
Appalachian Highlands and the Coastal Plains	48	Florida	104
Central region	53	Georgia	106
Kentucky	53	Mississippi	107
Upper Mississippi Embayment	53	North Carolina	107
Lake Superior region	53	South Carolina	107
Missouri	54	Tennessee	108
Rocky Mountains and the Great Plains	55	Central region	108
Economic geology	55	Multistate studies	109

	Page		Page
Water-resources investigations—Continued		Geologic and hydrologic principles, processes, and techniques	167
Interstate studies	110	Experimental geophysics	167
Arkansas	111	Rock magnetism	167
Colorado	111	Geomagnetism	168
Iowa	114	Petrophysics	169
Kansas	114	Applied geophysical techniques	170
Louisiana	115	Geochemistry, mineralogy, and petrology	176
Montana	116	Experimental and theoretical geochemistry	176
Nebraska	118	Mineralogic studies and crystal chemistry	177
New Mexico	118	Volcanic rocks and processes	179
North Dakota	119	Hawaiian volcano studies	179
Oklahoma	119	Columbia River plateau studies	180
South Dakota	120	Chemical evolution of silicic magma chambers	181
Texas	121	Volcanic rocks in Western United States	182
Utah	122	Mineral alteration in volcanic environments	183
Wyoming	123	Submarine volcanism	184
Western region	124	Plutonic rocks and magmatic processes	184
Interstate studies	125	Geochemistry of water and sediments	186
Alaska	125	Diagenetic studies	186
Arizona	126	Experimental studies on chemistry of water	187
California	126	Statistical geochemistry and petrology	188
Hawaii	128	Isotope and nuclear geochemistry	189
Idaho	128	Isotope tracer studies	189
Nevada	129	Stable isotopes	190
Oregon	130	Advances in geochronometry	191
Washington	130	Geothermal Systems	193
Special water-resource program, data coordination, acquisition, and storage	133	Sedimentology	210
Office of Water Data Coordination	133	Variability of sediment-discharge	210
National Water Data Exchange	135	Stream morphology	211
Water-data storage system	136	Modification of Eolian deposits	212
Urban water program	136	Instrumentation	212
Water use	139	Glaciology	212
National water-quality programs	140	Geology and climate	213
National stream-quality accounting network	140	Ground-water hydrology	218
Marine geology and coastal hydrology	144	Aquifer-model studies	218
Coastal and marine geology	144	Artificial recharge	220
Atlantic Continental Margin	144	Miscellaneous studies	221
Gulf of Mexico and Caribbean Sea	148	Surface-water hydrology	225
Pacific Continental Margin	150	Paleontology	227
Alaska Continental Margin	153	Mesozoic and Cenozoic studies	227
Oceanic studies	157	Paleozoic studies	230
Studies of marine and coastal processes	159	Plant ecology	233
Estuarine and coastal hydrology	159	Chemical, physical, and biological characteristic of water	234
Atlantic and Gulf Coast	159	Relation between surface water and ground water	238
Pacific Coast	159	Evaporation and transpiration	239
Management of natural resources on Federal and Indian lands	164	Limnology and potamology	240
Classification and evaluation of mineral lands	164	New hydrologic instruments and techniques	244
Classified land	164	Sea-ice studies	244
Known geologic structures of producing oil and gas fields	165	Analytical methods	245
Known geothermal resource areas	165	Analytical chemistry	245
Known recoverable coal resource areas	165	Emission spectroscopy	246
Coal resource occurrence/development potential maps	165	Neutron activation	246
Known leasing areas for potassium, phosphate, and sodium	165	X-ray fluorescence	247
Waterpower classification—preservation of reservoir sites	165	Analysis of water	247
Supervision of mineral leasing	165	Geology and hydrology applied to hazard assessment and environment	250
OCS lease sales for oil and gas	166	Earthquake studies	250
Cooperation with other Federal agencies	166	Seismicity	250
		Earthquake mechanics and prediction studies	253

	Page		Page
Geology and hydrology applied to hazard assessment and environment—Continued		Land use and environmental impact—Continued	
Earthquake hazard studies	257	Multidisciplinary studies in support of land-use planning and decisionmaking—Continued	
Tectonic framework and fault investigations	257	Puget Sound Project—hazard evaluation on Mount Baker	318
Seismicity investigations	261	Analyses of subsurface data to assist planners in evaluating feasibility of tunneling for rapid-transit systems	318
Ground motion investigations	262	Land use and land cover maps and data and other geographic studies	318
Ground failure investigations	263	Environmental impact studies	322
Engineering geology	264	Methodology of post-EIS monitoring	322
Landslide hazards	265	Modified format for site-specific EIS	323
Reactor hazards	266	Environmental analysis of NPRA	323
Environmental aspects of energy	268	Resource and land investigations programs	323
Geology and hydrology related to national security	273	Technology transfer workshops for State and local officials	323
Geologic aspects of radioactive waste management	275	Integrated surface mine reclamation and land use planning	324
Studies of media	276	Conflict resolution	324
Studies of potential repository sites	277	Impact of western energy development	324
Relation of radioactive waste to hydrologic environment	278	Coastal zone management coordination	324
Hydrologic investigations relative to the disposal of low-level radioactive waste	280	International cooperation in the earth sciences	325
Floods	280	International resources assessment	325
Flood frequency studies	281	Cooperative scientific investigation and exchange	326
Flood mapping	283	Crustal studies	326
Effects of pollutants on water quality	284	Multilateral scientific programs	328
Environmental geochemistry	288	CircumPacific map project	329
Land subsidence	289	International presentation	329
Hazards information and warnings	291	Technical cooperation and participant study	331
Astrogeology	293	International hydrological program and related activities	336
Planetary investigations	293	Review of hydrologic investigations	338
Lunar investigations	295	Summary by countries	338
Lunar sample investigations	298	Argentina, Bolivia, and Paraguay	338
Remote sensing and advanced techniques	301	Brazil	339
Earth resources observation systems program ..	301	Cambodia	339
Data analysis laboratory	301	CENTO countries	339
Monitoring the environment	301	Chile	339
Cooperative projects with the Bureau of Land Management	301	Costa Rica	340
Cooperative projects with States	303	Dominica	341
Cooperative projects with the Bureau of Reclamation	304	Eastern Arabian Peninsula	341
Assessing the impact of surface mining ..	304	Egypt	341
Forest defoliation	305	Guatemala	341
Studying the global environment	305	Indonesia	342
Targeting mineral exploration	306	Israel and Jordan	342
Remote sensing application to geologic studies ..	309	Kenya	342
Applications to hydrologic studies	312	Liberia	342
Applications to cartographic studies	314	Malaysia	343
Landsat-3 investigations	314	Mexico	343
Nighttime images of the Earth from space ..	314	New Zealand	343
Satellite image maps	314	Nicaragua	344
Space oblique Mercator projection	315	Nigeria	344
Parameters for an automated mapping satellite	315	Peru	345
Land use and environmental impact	317	Philippine Islands	345
Multidisciplinary studies in support of land-use planning and decisionmaking	317	Poland	345
Geohydrologic studies to guide exploratory drilling for ground water in Fairfax County, Virginia	317	Saudi Arabia	345
Geologic and hydrologic mapping in the Colorado Front Range Urban Corridor to aid local and regional planners	317	Senegal, Mauritania, and Mali	349
		Sri Lanka	349
		Sudan	349
		Turkey	350
		Yemen	350
		Yugoslavia	350
		Antarctic programs	350

	Page		Page
Topographic surveys and mapping	354	Topographic surveys and mapping—Continued	
Field surveying	354	Cartography and design—Continued	
Aerial profiling of terrain	354	Hardware	357
Minimum safe altitude warning project	354	Software	358
Special leveling projects	354	Digital cartographic data files	358
Photogrammetry	355	DEM files	358
Mapping from high-resolution high-altitude		DLG files	359
photographs	355	File management	359
Resolution measurements with star and bar		Pilot production projects	359
targets	355	Computer technology	361
Microdensitometer study of submerged		Time-sharing system access	361
marine features	355	Batch computing services	361
Comparison of Landsat image products	355	U.S. Geological Survey publications	363
Photoimage mapping	356	Publications program	363
Simulating color in image maps	356	Publications issued	364
Photobase mapping	356	How to obtain publications	365
Satellite image mapping	356	Over the counter	365
Cartography and design	357	By mail	365
Metric quadrangle maps	357	References	367
One-meter contour interval mapping	357	Investigations in progress	383
Space oblique Mercator projection	357	Indexes	419
Digital cartographic applications	357	Subject index	419
		Investigator index	454

ILLUSTRATIONS

	Page
FIGURE 1. —McKelvey diagram for geothermal energy showing derivation of “resource” and “reserve”	41
2.—Index map of the conterminous United States showing areal subdivisions used in the discussion of water resources	89
3.—Counts of fecal coliform bacteria, computed from a reference level of 200 cells per 100 mL, at NASQAN stations during the 1976 water year	141
4.—Counts of fecal coliform bacteria, computed from a reference level of 200 cells per 100 mL, at NASQAN stations during the 1975 water year	142

TABLES

	Page
TABLE 1. —Mineral production, value, and royalty for calendar year 1977	166
2.—Technical assistance to other countries provided by the USGS during FY 1977	331
3.—U.S. Geological Survey remote sensing activities in other countries, 1977	335
4. Technical and administrative documents issued during the period October 1976 through December 1977 as a result of USGS technical and scientific cooperative programs	336

ABBREVIATIONS

A	-----	angstrom	IGCP	-----	International Geological Correlation Program
ABAG	-----	Association of Bay Area Governments	IGU	-----	International Geographical Union
a.c.	-----	alternating current	IHD	-----	International Hydrological Decade
A.D.	-----	anno Domini	IHP	-----	International Hydrological Program
AESOP	-----	Automatic Surface Observation Platforms	IMW	-----	International Map of the World
AGID	-----	Association of Geoscientists for International Development	in	-----	inch
AGWAT	-----	Ministry of Agriculture and Water	IR	-----	infrared
AIDJEX	-----	Arctic Ice Dynamics Joint Experiment	ISAM	-----	Index Sequential Access Method
AMRAP	-----	Alaska Mineral Resource Assessment Program	ISO	-----	International Standardization Organization
AMS	-----	American Management Systems	IUGS	-----	International Union of Geologic Sciences
ANCSA	-----	Alaska Native Claims Settlement Act	J	-----	joule
AOCS	-----	Atlantic Outer Continental Shelf	JECAR	-----	Joint Commission of Economic Cooperation
APD	-----	antiphase domain	JPL	-----	Jet Propulsion Laboratory
ARPA	-----	Advanced Research Projects Agency	JTU	-----	Jackson turbidity unit
ASL	-----	Albuquerque Seismological Laboratory	K	-----	kelvin
ASRO	-----	Advanced Seismological Research Observatories	kbar	-----	kilobar
atm	-----	atmosphere	KCLA	-----	Known Coal Leasing Area
bbl	-----	barrel	KeV	-----	kiloelectronvolt
BLM	-----	Bureau of Land Management	kg	-----	kilogram
BOD	-----	biochemical oxygen demand	KGRA	-----	Known Geothermal Resources Area
B.P	-----	before present	KGS	-----	Known Geologic Structure
Btu	-----	British thermal unit	kHz	-----	kilohertz
°C	-----	degrees Celsius	km	-----	kilometer
CAI	-----	Color alteration index	kb	-----	kilometer
cal	-----	calorie	KREEP	-----	potassium-rare-earth element-phosphorus
CARETS	-----	Central Atlantic Regional Ecological Test Site project	kWh	-----	kilowatt-hour
CCD	-----	Computer Center Division	L	-----	liter
CCOP	-----	U.N. Committee for Coordination of Joint Prospecting for Mineral Resources in Asian Offshore Areas	LARS	-----	Laboratory for Applications of Remote Sensing
CCT	-----	computer-compatible tape	lat	-----	latitude
C/DCP	-----	convertible data-collection platforms	LMF	-----	lithic matrix fragments
CDP	-----	common depth point	long	-----	longitude
CENTO	-----	Central Treaty Organization	m	-----	meter
CEQ	-----	Council on Environmental Quality	M	-----	magnitude (earthquake)
CFRUC	-----	Colorado Front Range Urban Corridor Project	mcal	-----	millicalorie
CGIS	-----	Canada Geographic Information System	MEF	-----	maximum evident flood
cgs	-----	Centimeter-gram-second	mGal	-----	milligal
Ci	-----	curie	mi	-----	mile
cm	-----	centimeter	min	-----	minute
COD	-----	chemical oxygen demand	mg	-----	milligram
COM	-----	computer-oriented microform	ml	-----	milliliter
COST	-----	Continent Offshore Stratigraphic Test Group	mm	-----	millimeter
CPU	-----	central processing unit	MN	-----	meganewtons
CRIB	-----	Computerized Resource Information Bank	mo	-----	month
CV	-----	characteristic value	MPa	-----	megapascal
d	-----	day	MSS	-----	multispectral scanner
d.c	-----	direct current	mV	-----	millivolt
			MW	-----	megawatt
			MWe	-----	megawatts electrical
			m.y.	-----	million years
			μ	-----	micron
			μcal	-----	microcalorie
			μg	-----	microgram
			μGal	-----	microgal
			μm	-----	micrometer
			μmho	-----	micromho
			μstrain/yr	-----	engineering shear
			NASA	-----	National Aeronautics and Space Administration
DCAP	-----	Digital Cartographic Applications Program			
DCS	-----	Data-collection system			
DEROCS	-----	Development of Energy Resources of the Outer Continental Shelf			
DMA	-----	Defense Mapping Agency			
DNPM	-----	Departamento Nacional da Produção Mineral			
DO	-----	dissolved oxygen			
DOMES	-----	Deep Ocean Mining Environmental Study			
DSDP	-----	Deep Sea Drilling Project			
EIA	-----	Environmental Impact Analysis			
EIS	-----	environmental impact statement			
EM	-----	electromagnetic (soundings)			
EMRIA	-----	Energy Mineral Rehabilitation Inventory and Analysis			
emu	-----	electromagnetic units			
EPA	-----	Environmental Protection Agency			
ERDA	-----	Energy Research and Development Administration			
EROS	-----	Earth Resources Observation Systems			
ERTS	-----	Earth Resources Technology Satellite			
ESCAP	-----	Economic and Social Commission for Asia and the Pacific Committee on Natural Resources			
eV	-----	electronvolt			
FAO	-----	Food and Agriculture Organization			
f.l	-----	focal length			
FLD	-----	Fraunhofer line discriminator			
FY	-----	fiscal year			
g	-----	gram			
GIPSY	-----	General Information Processing System			
GIRAS	-----	Geographic Information Research and Analysis System			
GOES	-----	Geostationary Operational Environmental Satellite			
GPa	-----	Giga Pascale			
GRASP	-----	Geologic Retrieval and Synopsis Program			
h	-----	hour			
ha	-----	hectare			
HFU	-----	heat-flow unit			
HIPLEX	-----	High Plains Cooperative Program			
hm	-----	hectometer			
HUD	-----	Department of Housing and Urban Development			
Hz	-----	hertz			
IAH	-----	International Association of Hydrogeologists			
IAHS	-----	International Association of Hydrological Scientists			
ICAT	-----	Inorganic Chemical Analysis Team			
IDB	-----	Inter-American Development Bank			
IDIMS	-----	Interactive Display Image Manipulation System			
IDOE	-----	International Decade of Ocean Exploration			

ABBREVIATIONS

NASQAN ----- National Stream Quality Accounting Network
 NAWDEX ----- National Water Data Exchange
 NCRDS ----- National Coal Resources Data System
 NEIS ----- National Earthquake Information Service
 NEPA ----- National Environmental Policy Act
 ng ----- nanogram
 NLCR ----- nonlinear complex resistivity
 NOAA ----- National Oceanic and Atmospheric Administration
 NOS ----- National Ocean Survey
 NPR ----- Naval Petroleum Reserve
 NRA ----- National Resources Agency
 NRA ----- Nuclear Regulatory Agency
 nT ----- nanotesla
 NTIS ----- National Technical Information Service
 NTS ----- Nevada Test Site
 OAS ----- Organization of American States
 OCS ----- Outer Continental Shelf
 oe ----- Oersted
 ohm-m ----- ohm-meter
 OIA ----- Office of International Activities
 OME ----- Office of Minerals Exploration
 ORNL ----- Oak Ridge National Laboratory
 OWDC ----- Office of Water-Data Coordination
 Ω ----- ohm

PAIGH ----- Pan American Institute of Geography and History
 PCB ----- polychlorinated biphenyls
 pCi ----- picocurie
 ppb ----- part per billion
 ppm ----- part per million
 PSRV ----- pseudo-relative velocity
 R ----- range
 RASS ----- Rock Analysis Storage System
 REE ----- rare-earth element
 RF ----- radio frequency
 RMSE ----- root mean square error
 R/V ----- research vessel
 s ----- second
 SFBR ----- San Francisco Bay Region Environment and Resources Planning Study
 SIP ----- strongly implicit procedure
 SLAR ----- side-looking airborne radar
 SMS ----- Synchronous Meteorological Satellite
 SOM ----- Space Oblique Mercator
 SP ----- self potential
 SRO ----- Seismic Research Observatory
 t ----- tonne
 T ----- township
 TEM ----- transmission electron microscopy
 TIU ----- Thermal-inertia unit
 TL ----- thermoluminescence
 TVA ----- Tennessee Valley Authority

UNDP ----- U.N. Development Programme
 UNESCO ----- United Nations Educational, Scientific and Cultural Organization
 USAID ----- U.S. Agency for International Development
 USBM ----- U.S. Bureau of Mines
 USDA ----- U.S. Department of Agriculture
 USGS ----- U.S. Geological Survey
 USNC/SH ----- United Nations Educational, Scientific and Cultural Organization
 USPHS ----- U.S. Public Health Service
 U.S.S.R. ----- Union of Soviet Socialist Republics
 UTM ----- Universal Transverse Mercator
 V ----- volt
 VDETS ----- Voice Data Entry Terminal System
 VES ----- Vertical electric soundings
 VHRR ----- very high resolution radiometer
 VLF ----- very low frequency
 W ----- watt
 WMO ----- World Meteorological Organization
 WRC ----- Water Resources Council
 WRDD ----- Water Resources Development Department
 WWSSN ----- Worldwide Standardized Seismograph Network
 yr ----- year

SI UNITS AND INCH-POUND SYSTEM EQUIVALENTS

[SI, International System of Units, a modernized metric system of measurement. All values have been rounded to four significant digits except 0.01 bar, which is the exact equivalent of 1 kPa. Use of hectare (ha) as an alternative name for square hectometer (hm²) is restricted to measurement of land or water areas. Use of liter (L) as a special name for cubic decimeter (dm³) is restricted to the measurement of liquids and gases; no prefix other than milli should be used with liter. Metric ton (t) as a name for megagram (Mg) should be restricted to commercial usage, and no prefixes should be used with it. Note that the style of meter² rather than square meter has been used for convenience in finding units in this table. Where the units are spelled out in text, Survey style is to use square meter]

SI unit	Inch-Pound equivalent	
Length		
millimeter (mm)	= 0.039 37	inch (in)
meter (m)	= 3.281	feet (ft)
	= 1.094	yards (yd)
kilometer (km)	= 0.621 4	mile (mi)
	= 0.540 0	mile, nautical (nmi)
Area		
centimeter ² (cm ²)	= 0.155 0	inch ² (in ²)
meter ² (m ²)	= 10.76	feet ² (ft ²)
	= 1.196	yards ² (yd ²)
	= 0.000 247 1	acre
hectometer ² (hm ²)	= 2.471	acres
	= 0.003 861	section (640 acres or 1 mi ²)
kilometer ² (km ²)	= 0.386 1	mile ² (mi ²)
Volume		
centimeter ³ (cm ³)	= 0.061 02	inch ³ (in ³)
decimeter ³ (dm ³)	= 61.02	inches ³ (in ³)
	= 2.113	pints (pt)
	= 1.057	quarts (qt)
	= 0.264 2	gallon (gal)
	= 0.035 31	foot ³ (ft ³)
meter ³ (m ³)	= 35.31	feet ³ (ft ³)
	= 1.308	yards ³ (yd ³)
	= 264.2	gallons (gal)
	= 6.290	barrels (bbl) (petroleum, 1 bbl=42 gal)
	= 0.000 810 7	acre-foot (acre-ft)
hectometer ³ (hm ³)	= 810.7	acre-feet (acre-ft)
kilometer ³ (km ³)	= 0.239 9	mile ³ (mi ³)
Volume per unit time (includes flow)		
decimeter ³ per second (dm ³ /s)	= 0.035 31	foot ³ per second (ft ³ /s)
	= 2.119	feet ³ per minute (ft ³ /min)

SI unit	Inch-Pound equivalent	
Volume per unit time (includes flow)—Continued		
decimeter ³ per second (dm ³ /s)	= 15.85	gallons per minute (gal/min)
	= 543.4	barrels per day (bbl/d) (petroleum, 1 bbl=42 gal)
meter ³ per second (m ³ /s)	= 35.31	feet ³ per second (ft ³ /s)
	= 15 850	gallons per minute (gal/min)
Mass		
gram (g)	= 0.035 27	ounce avoirdupois (oz avdp)
kilogram (kg)	= 2.205	pounds avoirdupois (lb avdp)
megagram (Mg)	= 1.102	tons, short (2 000 lb)
	= 0.984 2	ton, long (2 240 lb)
Mass per unit volume (includes density)		
kilogram per meter ³ (kg/m ³)	= 0.062 43	pound per foot ³ (lb/ft ³)
Pressure		
kilopascal (kPa)	= 0.145 0	pound-force per inch ² (lbf/in ²)
	= 0.009 869	atmosphere, standard (atm)
	= 0.01	bar
	= 0.296 1	inch of mercury at 60°F (in Hg)
Temperature		
temp kelvin (K)	= [temp deg Fahrenheit (°F) + 459.67]/1.8	
temp deg Celsius (°C)	= [temp deg Fahrenheit (°F) - 32]/1.8	

Any use of trade names and trademarks in this publication is for descriptive purposes only and does not constitute endorsement by the U.S. Geological Survey.

MINERAL-RESOURCE AND MINERAL-FUEL INVESTIGATIONS

UNITED STATES AND WORLD MINERAL-RESOURCE ASSESSMENTS

The study of mineral deposits and the geologic factors responsible for their formation is essential if we are to assess national and worldwide supplies and potential for mineral commodities. This continuing effort provided important statements on chromite, fluorite, and alunite resources during 1977. Studies of major U.S. regions produced a deeper understanding of the metalliferous deposits of the West and called attention to the possibility of important undiscovered metallic mineral deposits in a geologic environment that is widespread in eastern and central United States.

Geological analysis of world chromite production

Cumulative world production of chromite from 1797 to 1975 was compiled by B. R. Lipin and T. P. Thayer. World production of chromite totals about 150×10^6 t, of which 130×10^6 t has been produced since 1946. Production since 1946 and world resources are as follows:

Deposit Type	Use*	Production (10 ⁶ tons)		World Resources (10 ⁶ tons)
		1946-70	1971-75	
Podiform				
High-Al ---R		11.3	2.1	15
High-Cr ---M		48.7	16.4	155
Stratiform				
High-Fe ---C+M		22.1	10.5	18,000
High-Cr ---M		12.4	5.7	2,700

* R=Refractory; M=Metallurgical; C=Chemical

Before 1970, 64 percent of all production came from podiform deposits and was mostly high-chromite ore. However, in the period 1971-75, podiform deposits yielded only 53 percent. By 1980, stratiform deposits will be outproducing podiform deposits.

Estimated world demand for chromite from 1976 to 2000 is about 300×10^6 t, which is double the entire production up to 1975. Probable resources of podiform deposits are equivalent to about 170×10^6 t of shipping-grade ore or less than 1 percent of the world total. Present methods of exploration are not adequate to find concealed podiform deposits. South

Africa and Rhodesia will dominate the world chromite market by 1990 by virtue of the immense resources (over 20×10^9 t) in their stratiform deposits.

Fluorine provinces, reserves, and resources of the United States

R. E. Van Alstine's study of fluorine provinces of the United States showed that the fluorine provinces based on fluorspar deposits are concentrated in the Rocky Mountains, the Appalachian Mountains, and the midcontinent region. Fluorine provinces based on fluorapatite in marine phosphate rock are mainly in the Coastal Plain areas of southeastern United States, in Tennessee and Kentucky, in the northern Rocky Mountains, and in California.

The host rocks of productive fluorspar deposits are commonly Precambrian or Paleozoic rocks uplifted along major fault zones; elsewhere the host rocks are of Cretaceous or Tertiary age. Fluorine-bearing phosphate deposits are found in upper Tertiary rocks in the southeastern Coastal Plain and California. They are found in upper Paleozoic rocks in the northern Rocky Mountains and Alaska and in lower Paleozoic rocks in Tennessee and Kentucky. Deposits of fluorapatite phosphate rock were discovered recently in Precambrian rocks of the Upper Peninsula of Michigan (Cannon and Klasner, 1976).

United States reserves of fluorspar total about 16×10^6 t of ore containing about 35 percent CaF_2 or 2.7×10^6 t of fluorine. In addition, 180×10^6 t of fluorspar averaging about 17 percent CaF_2 , which is equivalent to 15×10^6 t of fluorine, are classed as identified resources. About 55 percent of the reserves are in the Illinois-Kentucky fluorspar district. The lower grade resources that are not presently commercial are mainly in Colorado, Illinois, Nevada, New Mexico, Oregon, and Tennessee.

United States reserves of recoverable fluorine in phosphate rock, which contains about 3 percent F, were estimated at 11×10^6 t; an additional 20×10^6 t of fluorine in phosphate rock that is not presently commercial are classed as identified resources (Wood, 1976, p. 386). The chief reserves of phosphate rock being mined are in Florida, Idaho, North Carolina, Tennessee, and Utah. Other reserves and

resources of fluorine in phosphate rock are mainly in Alabama, Alaska, California, Georgia, Montana, South Carolina, and Wyoming.

Alunite resources of the United States

Three main types of alunite deposits are recognized in the United States: (1) veins, (2) replacements, and (3) thin nodular layers of supergene or diagenetic origin localized in argillic sediments. Only the large-tonnage, low-grade metasomatic replacements in hydrothermally and (or) solfatarically altered volcanic terranes in southwest Utah and other western States constitute a significant resource that can in part substitute for imported bauxite and alumina. Alunitic rock must contain at least 30 percent alunite (11 percent Al_2O_3) and very little soluble silica to be considered potentially exploitable. R. B. Hall estimates that there is a total resource of at least 2×10^9 t for the western United States. This is an adequate base for a domestic alumina-from-alunite industry, providing that economic feasibility can be established. Recovery of potassium sulfate fertilizer and sulfuric acid as byproducts is essential.

Potential for massive sulfides in eastern and central United States

Recent studies by Helmuth Wedow, Jr., in connection with research on zinc-lead ore deposits have led to the conclusion that a significant potential exists for undiscovered base-metal resources in massive sulfide ores from the relatively unmetamorphosed Phanerozoic shale sequences of eastern and midcontinent United States. Comparison of the sedimentary environments that contain zinc-lead ore deposits (such as Meggan and Rammelsberg in West Germany, Howard Pass in northern Canada, and Sullivan in British Columbia) with those in the United States suggests that the coincidence of diverse features (such as abrupt sedimentary rises, euxenic off-reef environments, accumulations of catastrophically destroyed pelagic faunas, evidence of deep plutonian, along incipient rift zones, and the occurrence of pyroclastic-derived debris mixed with other sedimentary rocks) can point to a local habitat for the concentration of massive sulfides and related deposits such as iron oxides, barite, and fluorite.

Mesozoic and Cenozoic metallogenesis in the western United States

Geologic phenomena are being fitted increasingly, and apparently successfully, into plate-tectonic mod-

els. P. W. Guild concludes that although the Mesozoic and Cenozoic metallogeny of the western United States seems to have resulted from convergence of the North American and Pacific Ocean plates, subduction alone does not adequately explain the distribution of the ore deposits in Laramide and post-Laramide time when magmatism and mineralization extended irregularly eastward at least 1,500 km from the continental margin. Stable isotopes, lead and initial $^{87}\text{Sr}/^{86}\text{Sr}$, indicate derivation of some rock- and ore-forming elements from continental lithosphere rather than oceanic lithosphere. A gross east-west metals zonation lacks the clearcut divisions evident to the north and south in the Cordillera. Lineaments, difficult or impossible to document unequivocally, probably played some role in localizing mineral belts transverse to plate boundaries.

Guild suggests that mantle convection in a reactivated ensialic backarc, triggered at least in part by subduction on one or more Benioff zones, became increasingly important both with time and with distance eastward from the Mesozoic trench. Small magma pockets were generated episodically by partial fusion of the continental lithosphere, itself probably inhomogeneous, where deep crustal flaws, many ancient but some perhaps newly created, relieved pressure and provided access to the upper crust.

MINERAL-RESOURCES ASSESSMENT OF LAND AREAS

The availability of mineral resources and the assessment of mineral-resource potential is a critical prerequisite to informed land use planning. The USGS continued this work during 1977. Under agreement with the Bureau of Indian Affairs, phase I studies (summary and analysis of existing information) were completed in 13 reservations, and phase II studies (field studies) were underway on 4 reservations. Results of the studies to date include publication of an aeromagnetic map of the Papago Reservation in Arizona and completion of detailed field studies of six 15-minute quadrangles.

The importance of resource appraisal is also recognized in the Wilderness Act of 1964, which directs the USGS and Bureau of Mines to assess the mineral-resource potential of all lands recommended for inclusion in the Wilderness System. That effort began in 1966 and will continue for many years. Significant results of some of the wilderness work in 1977 follows.

Mineral-resource potential of Wambaw Swamp Wilderness Study Area in South Carolina

The mineral-resource potential of Wambaw Swamp was evaluated by C. C. Cameron. An estimated 4×10^5 t of phosphate (P_2O_5) occurs in the northern half of the study area as grains and scattered nodules overlying and in the weathered surface of the Cooper Formation of early Tertiary age; however, the phosphate lies under 12 to 15 m of overburden, and the grade is considerably lower than that presently being mined elsewhere in the United States. Uranium associated with the phosphate is also below the grade currently considered economically feasible to mine; the total amount is only about 250 t of U_3O_8 . Peat is too thin and too high in ash content to be a potential resource. Oil and gas potential is also very slight. Some deeply buried fluvial and beach sands contain 1 to 5 percent potassium feldspar. However, richer deposits occur near the area at the surface. Well-sorted Pleistocene beach sands used for road construction do not extend far into the Swamp; heavy minerals in these sands have little economic value. The only clay body that might be suited for lightweight aggregate or vitreous clay products occurs at depths of 10 to 18 m. The underlying limestone is also too deep to be considered a resource.

Mineral-resource assessment of the Citico Creek Wilderness Study Area in Tennessee

Geologic mapping and reconnaissance geochemical sampling were carried out by J. F. Slack in the 567-ha Citico Creek Wilderness Study Area. Slightly anomalous concentrations of Cu, As, Co, Pb, and Zn were found within one narrow (<150 m thick) stratigraphic unit composed of sulfide-rich graphitic slate and metagraywacke of the Great Smoky Group (Precambrian). No economic potential appears to exist for this horizon. Very minor deposits of sand and gravel and abundant rock suitable for crushing constitute the only known mineral resources in the study area.

Large submarginal iron resources in Mill Creek, Peters Mountain, and Mountain Lake Wilderness study areas in Virginia and West Virginia

Reconnaissance mapping and study of previous drilling data by F. G. Lesure (USGS) and B. B. Williams and M. L. Dunn (U.S. Bureau of Mines) provided data for the calculation of 1.75×10^9 t of submarginal iron resources in the Mill Creek, Peters Mountain, and Mountain Lake Wilderness study

areas in Giles and Crag Counties, Virginia, and Monroe County, West Virginia. The iron is in hematitic sandstone beds of the Rose Hill Formation of Silurian age. The iron-rich sandstone beds range from 1 to 10 m thick and are as much as several kilometers long. They are scattered throughout an interlayered series of red and green shale and sandstone of lower grade that ranges in thickness from 45 to 60 m. The iron content ranges from 10 to 30 percent, and the phosphorous content ranges from 0.05 to 0.8 percent. Mining or quarrying of hematitic sandstone in areas of outcrop would be relatively inexpensive, but beneficiation methods are not yet adequate to permit economic production at existing prices.

New River Gorge in West Virginia

A mineral-resource assessment of 440 km² of the New River Gorge study area in West Virginia was completed by the USGS and U.S. Bureau of Mines on April 1, 1977. Twelve maps were prepared for open-file and printed (Englund and others, 1977a). These include a geologic map of the area at a scale of 1:50,000, a structure contour map, a stratigraphic section, aeromagnetic and gravity maps, maps showing coal resources in the proposed Wild and Scenic River area and in the National Park area, natural-gas-productive intervals and subsurface maps, a geochemical sample localities map, nonmetallic resources map, a landslide map, and extent of mining and reserve base maps. A short text open-file separately summarizes the information on the maps (K. J. Englund and others, 1977b), and a separate open-file lists all analytical data for geochemical samples (D. F. Siems and others, 1977).

Coal resources of 66×10^6 t occur in 12 coalbeds in the area of the proposed Wild and Scenic River, and coal resources of 151×10^6 t are present in 13 coalbeds in the larger area of the proposed national park. The entire New River Gorge area has a potential for natural gas resources, but oil is unlikely to be found within or near the study area. The extensive resources of sandstone and shale are not considered to be economically important in the gorge area. Resources of other nonmetallic materials, including limestone and fire clay, are small or nonexistent. Resources of metallic minerals are not known in the study area.

Mineral resource appraisal of the Washakie Wilderness in Wyoming

A survey by J. C. Antweiler, D. W. Rankin, and F. S. Fisher to evaluate the mineral resource poten-

tial was completed for the Washakie Wilderness in Park County, Wyoming, and contiguous study areas for the North and South Absaroka Wilderness Areas. The survey included preparation of a geologic map, geochemical sampling, and aeromagnetic and ground gravity surveys. Known mineralized areas were studied in detail to determine criteria for recognizing and evaluating precious and base metal mineralization particularly in intrusive centers. Several localities with alteration and mineralization characteristic of copper porphyry deposits occur in the project area. Two of these, Stinkingwater and Eagle Creek, have been known since early in the 20th century; another, Meadow Creek Basin, was staked in 1975; two others were discovered in 1976 as a result of work done on this project.

GEOLOGIC STUDIES OF MINERAL DISTRICTS AND MINERAL-BEARING AREAS

The appraisal of mineral-resource potential demands a thorough understanding of the chemical, physical, and geologic features that lead to the formation of a mineral deposit. This information, obtainable through the study of known deposits or mineral districts, can then be applied in new areas that appear to have similar characteristics.

New studies during 1977 provided further additions to our understanding of mineral deposits, and applications of our knowledge led to further information on their origin and distribution.

Mineralization controls at the Haile gold mine in South Carolina

Planetable mapping by R. W. Luce and Henry Bell at the Sericite Pit of the Haile gold mine in Lancaster County, South Carolina, has revealed that mineralization is concentrated along several northeast-trending fault contacts between foliated argillites and massive pyroclastic units. Sericitic alteration is pervasive throughout a 1.5 km-wide area surrounding the district, but silicification, sulfide mineralization, and gossan formation are most developed at the fault contact of the two units. Pyrite, with which gold is associated, is the dominant sulfide mineral. It was formed in several stages both as a replacement of coarse pyroclastic fragments and as a general dissemination.

Ground checks of aeroradioactivity anomalies in the Atlantic Coastal Plain of South Carolina

Extensive total-count gamma aeroradioactivity coverage in the Atlantic Coastal Plain is now avail-

able as a result of cooperative funding from the Coastal Plains Regional Commission. E. R. Force and Andrew Grosz examined the data for the Charleston, S. C., region and field checked areas with anomalously high levels of radioactivity. Of about 100 anomalies checked, 11 are heavy mineral concentrations in Pleistocene beaches. Five together contain about 2×10^6 t of heavy minerals at roughly economic grades. Radioactivity of the concentrations comes mostly from monazite, rather than zircon. The proportion of hornblende, epidote, and K-spar in the sediments vary widely depending on the extent of weathering since their deposition.

Some anomalies were caused by uraniferous phosphate in silt-size particles in muddy facies of the Cooper Formation. Although the radioactive minerals are more abundant in these silt-size deposits than they are in beach sands, they are too fine grained to permit economic recovery with existing technology.

Radioactivity distribution from aerial surveys were ground checked with gamma logs and chemical analyses. Results show that the area with potential uraniferous phosphate resources extends far beyond the previously known Charleston phosphate district.

Efficient exploration for heavy minerals with aeroradioactivity maps requires extensive use of spectral radioactivity information, geologic and soils maps, and knowledge of detrital minerals likely in the region.

Geologic mapping of Cretaceous and Tertiary kaolin in the Macon-Gordon district of Georgia

A geologic map of the Macon-Gordon district of Georgia, prepared by S. H. Patterson and C. L. Neeley (USGS) in cooperation with B. F. Buie (Florida State University) and J. H. Hetrick (Georgia Geological Survey), shows new information about the kaolin deposits. All of the kaolin was formerly thought to be of Late Cretaceous age; it is now known that some deposits are of this age, but many others occur in Tertiary beds. Much of the Tertiary kaolin is middle Eocene. Lower Eocene and Paleocene kaolin deposits may be present, but as yet they have not been definitely identified. The deposits of Cretaceous age are widely distributed through the central part of the district and occur under overburden too thick for profitable stripping in the southern or downdip part. Deposits of Tertiary age overlap the Cretaceous ones; therefore, the younger deposits under thin overburden are much more widely distributed.

High-calcium marble in the Beaver Creek area of St. Lawrence County in New York

C. E. Brown reports that one of the three belts of marble mapped in the Beaver Creek drainage area in St. Lawrence County, New York, is composed of coarsely crystalline, pure calcitic marble. The belt of marble is exposed in a zone at least 11.2 km in length and 0.8 km wide. All samples analyzed contain more than 92 percent CaCO_3 , and some samples contain as much as 97 percent CaCO_3 with small amounts of MgO and Fe_2O_3 . Some rocks in the other marble belts also are nearly pure calcitic marbles, but the possibility of proving up large tonnages is less.

The extensive deposit in the town of Macomb, west of Beaver Creek, has a chemical composition favorable for specialized chemical, industrial, and metallurgical uses. This coupled with inexpensive water transportation on the St. Lawrence Seaway available at Ogdensburg, N. Y., only 27 km away from Macomb, might make economical exploration of the high-calcium marble possible.

Geology of Port Leyden, New York, heavy mineral deposit

Heavy minerals of the Port Leyden deposit occur in Pleistocene lake delta sands on the east side of the Black River valley in New York (Force and others, 1976). B. D. Stone and E. R. Force found that the deposit is a series of coalescent glacial outwash deltas deposited in glacial Lake Port Leyden (Fairchild, 1912), the water level of which was controlled by a bedrock spillway south of Boonville, N. Y. Melt-water streams that drained the active glacial margin in the Adirondack crystalline upland to the east deposited crystalline-derived sands in delta wedges as much as 80-m thick (Force, Lipin, and Smith, 1976). These wedges overlie slightly older ice-contact fluvial deposits derived from local valley crystalline and sedimentary rocks. The volume of these ice-contact deposits under some delta wedges locally may be large. Heavy minerals are most concentrated in climbing-ripple cross-laminated fine sand in delta bottomset beds. Late glacial eolian dunes, commonly 3-m high, overlie some delta plains and till hills.

Keweenawan igneous complex identified in Michigan

J. S. Klasner and W. F. Cannon have identified by geophysical surveys a swarm of mafic to ultramafic dikes in northern Marquette and Baraga Counties in Michigan. The area is deeply covered by glacial drift, and two outcrops of peridotite form the only surface expression of the dikes. The area was pre-

viously believed to be underlain entirely by middle Precambrian metasedimentary rocks but newly acquired geophysical data indicate a dike swarm about 25-km long in an east-west direction and as much as 2-km wide intrudes the metasedimentary rocks. The dikes can be traced by a complex magnetic anomaly that is in places coincident with gravity and electromagnetic anomalies. Paleomagnetic determinations indicate the dikes were intruded during the early Keweenawan magnetic reversal. The peridotite has anomalously high copper and sulfur content, which is a favorable indicator of copper or nickel sulfide mineralization. Positive electromagnetic anomalies coincident with positive gravity anomalies are attractive targets for further mineral exploration because they may indicate the presence of buried sulfide concentrations in the area.

Previously unreported mineralization found in the Darlington quadrangle of southwestern Wisconsin

W. S. West's field investigation in the Darlington 7½-min quadrangle of Upper Mississippi Valley-zinc-lead district of Lafayette County, Wisconsin, disclosed several previously unreported and unmap-ped areas of mineralization. These areas of mineralization consist of four patches of old lead diggings, some of which are quite extensive. One is in an area about 2.5 km due north of Darlington, one is about 1.5 km south-southeast of Darlington, and two are on the east bank of the Pecatonica River about 4.5 and 5.5 km southeast of Darlington. The discovery of these mineralized localities has enlarged the target area for more detailed prospecting and improves the possibility of finding new zinc-lead orebodies in the eastern part of the mining district.

Peat resources in part of Lake of the Woods County in Minnesota

Field reconnaissance by C. C. Cameron in an area of about 130 km² in northern Lake of the Woods County, Minnesota, reveals vast swamp and marsh peatlands. However, deposits of commercial quality reed-sedge moss and humus peat, thick enough for use as soil conditioner and possible manufacture of natural gas, are largely restricted to areas behind relict barrier beaches formed during the retreat of Glacial Lake Agassiz. Here the peat attains a thickness of at least 1.5 m, and resources are estimated as 4.08×10^6 t of air-dried peat.

The field reconnaissance was undertaken as part of the field exploration of the peat deposits for assessment of peatland use in terms of the environment and the industry.

Faulting in the Duluth Complex in Minnesota

Preliminary results of large-scale (1:24,000) mapping in the Duluth Complex in Minnesota by M. P. Foose and R. W. Cooper for the first time gives evidence for the presence of a large number of faults. Most of the faults appears to have only small (<100 m) normal or strike-slip displacements, but some faults, mostly with northeast-southwest trends, represent major discontinuities of undetermined size. The intense fracturing is similar in style to tensional regimes such as the Basin and Range and suggests a paleorift origin for the Duluth Complex. The recognition of faulting is important in evaluating the continuity of nickle-copper ores in the complex and in estimating the region's nickle-copper resources.

Potential economic significance of gahnite (zinc spinel) in Colorado

During recent field investigations in Colorado, D. M. Sheridan and W. H. Raymond found that gahnite, a zinc spinel, occurs in and near many Precambrian sulfide deposits in the Front Range, Park Range, Wet Mountains, and Salida regions. Although sphalerite, chalcopyrite, and lesser amounts of silver-bearing galena are the principal sulfide ore minerals in these deposits, a newly recognized concept identifies potential economic significance of gahnite (Sheridan and Raymond, 1977). Gahnite may be sufficiently abundant at some of the deposits to constitute an ore mineral. Samples of gahnite-rich rocks from various mines and prospects range in zinc content from 3.5 to 19 percent, and the pure mineral contains up to 27 percent Zn. Moreover, the geologic relations found in some localities suggest that gahnite may be used as a significant guide for prospecting, characterizing favorable lithologic trends, even where cogenetic sulfides are sparse or absent in outcrops.

Production of quartz-muscovite schist from Poncha Pass area in Colorado

A wide extensive zone of Precambrian quartz-muscovite schist is being mined in the Bonanza northeast quadrangle northwest of Poncha Pass, Colo. The schist is excavated from open cuts, transported to nearby Salida for crushing and screening, and then shipped by rail to Denver for use in making bottles; previously it was used in gypsum board, paint, and insulation material. R. E. Van Alstine reports that the steep schist zone locally is more than 150 m thick and extends north from Highway

U.S. 285 for about 1.6 km. It is localized along one of the faults that bound the east side of the north extension of the Rio Grande trough. In 1975 and 1976 schist produced from here was valued at \$100,000 each year (Colo. Div. Mines, 1976, p. 21, 23, 74, and 109; Colo. Div. Mines, 1977, p. 11, 53).

Course of Eocene Wind River locates auriferous sedimentary rocks in the western Wind River Basin in Wyoming

The distribution of roundstone conglomerates in the upper part of the Wind River Formation in the western part of the Wind River Basin was found by D. A. Seeland to coincide exactly with the course of the Eocene Wind River as determined by a study of crossbedding in the sandstones of the Wind River Formation. This is most significant because analysis of panned concentrates from these roundstone conglomerates indicates the presence of a substantial quantity of gold. The volume of conglomerate decreases eastward, but there is no eastward diminution of grade. Thus, if sandstones of this stratigraphic horizon exist to the east and contain similar gold values, then the course of the Eocene Wind River should define the location of a substantial additional volume of auriferous rocks.

Carbonatite dikes in Bear Lodge Mountains, Wyoming

Numerous carbonatite dikes were recognized by M. H. Staatz in cores from deep drilling of alkalic rocks in the southern Bear Lodge Mountains. These intrusive rocks, which dome up the surrounding sedimentary rocks, are principally trachyte and phonolite. At depth they tend to be coarser grained and become fine-grained syenite and nepheline syenite. As many as 22 carbonatite dikes have been encountered in one hole. One carbonatite was subsequently found on the surface during detailed mapping. The dikes range in thickness from about 1 mm to 5 m. Calcite is the principal mineral. Other minerals commonly found in many samples are bastnaesite, ancylite, strontianite, pyrite, pyrrhotite, sphalerite, and galena. In addition at least 14 other minerals have been identified in various samples. These carbonatites, like the massive carbonatite at Kangankunde Hill, Malawi, are both rare-earth and strontium-rich. Samples of the Bear Lodge carbonatites containing 2 to 5 percent rare-earths and 3 to 10 percent strontium are common.

Relationships of copper and gold deposits in the ophiolitic Canyon Mountain Complex in Grant County, Oregon

Until recently, copper and gold veins in the Canyon Mountain Complex in Oregon had been as-

sumed to be related, although they differ in some respects. Recent interpretations of the origins of the two vein groups suggest that they are not related (Thayer, Case, and Stotelmeyer, 1977). The Canyon Mountain Complex is about 160 km² in area; about 50 percent ultramafic and 30 to 35 percent gabbroic rocks form a continuous metamorphosed cumulate sequence. About 20 percent of the complex consists of basaltic dikes and plagiogranite that form a composite sheeted dike unit and cut the gabbro along through-going fractures. The entire complex probably is of Early Permian age.

Chalcopyrite-bearing pyritic quartz veins are localized in the southern part of the gabbro, mostly within 600 m of the contact with the sheeted dike unit. The veins are associated with basaltic dikes, albite granite, and albite-chlorite-epidote alteration along shear zones. Although small epidotic quartz veins and lenses are common with albite granite in the sheeted dike unit, few of them contain sulfides. Sampling by the U.S. Bureau of Mines has indicated about 45,000 tons of material that averages 0.30 to 0.35 percent copper in two deposits. The larger deposit is in a zone about 750 m long that was followed by several basaltic dikes from an offset in the gabbro contact against the sheeted dike unit. The copper veins contain only traces of gold and silver.

Gold occurs in pockety quartz-calcite veins that cut carbonatized gabbro and serpentinite in the northwestern corner of the complex. Goldbearing veins also occur in greenstone and argillite north of the complex, and in Mesozoic rocks 2.5 km west of it. Gold production, mostly from nearby placer deposits, has been about 26,000 kg, with about 400 kg of silver and some platinum. The veins contain no copper. A major difference in ages of the gold and copper veins is indicated by gold veins west of the complex that cut Triassic conglomerate, which contains many clasts of albite granite. The gold veins appear to be related to Upper Jurassic dioritic to granitic plutons in the Blue Mountain region. Petrogenetic relationships between gabbro, basaltic dikes, and plagiogranite are not known (Thayer, Case, and Stotelmeyer, 1977).

The close association of copper veins with basaltic dikes in gabbro suggest that their origin may be similar to the massive cupreous pyritic ores of Cyprus. The Canyon Mountain dikes are interpreted as feeders for pillow lavas that have been eroded away. In Cyprus, deposition of massive sulfides resulted from reaction of seawater with volcanic emanations, and ore-grade mineralization was shallow. It is postulated that the copper veins in the Canyon

Mountain may represent former channels for solutions that formed massive sulfide deposits at higher levels on the Permian seafloor.

Characteristics of a porphyry copper stock in the Globe-Miami district of Arizona

In the Globe-Miami district of Arizona, the porphyry copper deposits are temporally and spatially related to the Schultze Granite, a porphyritic quartz monzonite stock of Laramide age. Recent geologic mapping by S. C. Creasey within the stock has shown that it is composite. The early intrusive phase contains more biotite and is not so conspicuously porphyritic. The intermediate, or main, intrusive phase is lighter in color and contains less biotite and larger and more abundant K-feldspar phenocrysts. The youngest intrusive phases are porphyries. All of the disseminated sulfide mineralization in the district is in, or adjacent to, the porphyries. Although not abundant, breccia pipes are also in, or near, porphyries and mineralized ground. The implication is clear that whatever the nature of the ore-forming process, the formation of porphyries is related to it in some way.

In addition the entire stock is cut by quartz-sericite-magnetite-sulfide veins ranging in width from less than 2 mm to perhaps 3 m, and in length from about a meter to as much as 650 m. These veins occupy fractures and are more abundant near the porphyry copper deposits. Although K-Ar ages on sericite from the veins indicate they are about the same age as the porphyry copper deposits, the small amount of development work on the veins suggests that they were low in base and precious metals. The origin of these veins is not clear, but the possibility of circulating meteoric water comes to mind.

Another model of porphyry copper generation

The orthomagmatic and meteoric water models of porphyry copper genesis find no support and considerable conflict in the data produced during detailed field and petrologic studies of the stocks associated with the Ray, Ariz., porphyry copper deposit, one of the 10 top producers of copper in the country. The studies, which resulted in a new model of ore generation (Banks and Page, 1977) included detailed geologic mapping; thin section and polished thin section petrography; fluid-inclusion work; whole rock major and minor chemistry; electron and ion microprobe analyses of igneous and alteration minerals for Cu, S, Cl, H₂A, F, and major elements; and petrology of the magmatic sulfide minerals. Very little copper and sulfur occur in the

rocks; and the data are best explained if the copper and most of the sulfur, chlorine, and water in the magmas were used by the igneous minerals during crystallization of the magmas. The stocks, and by analogy any parental upper crustal magma, thus were themselves unlikely to produce an ore fluid. Furthermore, not only did the stocks contain little copper and sulfur to supply to an ore fluid of circulating meteoric water, but also copper was more likely added to rather than extracted from the rocks in the outer parts of a circulation cell. Incorporated into the new model is the petrologic confirmation that sulfur is essentially insoluble in siliceous silicate melts, and it is postulated that sulfide minerals accumulate in a zone of partial melting around, but not in, pockets of magma. Some of the magma is mobilized and intruded into the upper crust. The sulfides, however, remain in the zone of partial melting until local or regional cessation of melting allows excess metamorphic and late magmatic water to be present, which remobilizes and transports the sulfides to upper crustal sites. The new model explains the time-space relationship of ore and magma. It also explains the failure of considerable research to discover petrologic and chemical distinctions between "ore" and "non-ore" plutons. The model places renewed emphasis on regional structure in delineating favorable zones and localities for discovery of ore.

Geology of the Cuprite mining district of Esmeralda County in Nevada

Studies by R. P. Ashley show that the Cuprite mining district contains mineralization of two different types and ages. The younger is characterized by intense acid-sulfate alteration that has converted Cambrian siltstones and Tertiary tuffs, flows, and volcanic sedimentary rocks to silicified, opalized, and argillized rocks. Mineral production associated with this alteration includes only minor amounts of sulfur, silica, and clay. Potential for substantial discoveries of commercial sulfur and clay is low, for silica the potential is high, and for gold and mercury it is low to moderate. Alunitic rock exists, but its tonnage is too small and its mineralogy too unfavorable for exploitation by presently contemplated commercial processes.

The older mineralization at Cuprite consists of base-metal veins (mainly copper-lead) with minor precious metal values (mainly silver) in unaltered to locally hornfelsic Cambrian siltstones. This mineralization is probably Mesozoic in age, associated with a buried pluton. These veins have little eco-

nomic potential, but minor potential exists for disseminated copper mineralization at depth.

Molybdenum mineralization in the Battle Mountain mining district of Lander County, Nevada

Numerous base and precious metal deposits in the Battle Mountain mining district are related to Upper Cretaceous and middle Tertiary granodiorites to quartz monzonites emplaced into thick sequences of Paleozoic sedimentary rocks. Molybdenum mineralization occurs sporadically throughout the district, but is especially concentrated in an elongate stockwork system near Copper Basin that is being studied jointly by T. G. Theodore and J. N. Batchelder (USGS) and D. W. Blake and E. L. Kretschmer (Duval Corporation). This system is related to numerous small Tertiary (?) quartz monzonite intrusions. Near Copper Basin the emplacement of most intrusive rocks was controlled by two prominent fracture sets, one striking N. 70° W. and the other north-south. The molybdenite mineralization, including very minor chalcopyrite, is related mostly to the N. 70° W. set. In addition, other mineralized fractures striking approximately N. 45° W. and N. 45° E. acted as important conduits for mineralizing fluids. Many of the molybdenite-stockwork veins and their selvages reflect locally intense potassic alteration, and the veins typically contain potassium feldspar-biotite-calcite-molybdenite, and quartz-molybdenite-calcite ± potassium feldspar ± white mica assemblages. The molybdenite-bearing veins contain abundant liquid plus vapor fluid inclusions. Preliminary fluid-inclusion studies of these veins suggest the bulk of the molybdenite mineralization occurred during circulation of nonboiling to slightly boiling, moderately saline fluids that range mostly between 8 and 12 weight percent NaCl equivalent. Temperatures were approximately 300° to 400°C. The values of $\delta^{18}\text{O}$ of the water calculated to be in equilibrium with hydrothermal quartz from molybdenite-bearing veins are +5.7 to +6.2, an unusually restricted range suggesting significant isotopic exchange with the wallrocks. Last, the molybdenite-stockwork system has been intruded extensively by a series of late north-south-striking, westward-dipping quartz latite porphyry dikes associated with minor lead and zinc mineralization.

West-northwesterly structural zone controlled gold mineralization at Manhattan in Nevada

Geologic mapping by D. R. Shawe in the vicinity of Manhattan shows a major west-northwest-trending zone of faults that was probably a primary con-

trol of late Tertiary gold mineralization. The structural zone also may have localized middle to late(?) Tertiary volcanism, including eruption of volcanic melange or megabreccia.

GEOCHEMICAL AND GEOPHYSICAL TECHNIQUES IN RESOURCE ASSESSMENTS

REGIONAL GEOCHEMICAL AND GEOPHYSICAL STUDIES

Lithochemical studies in Missouri

Regional geochemical studies by R. L. Erickson, E. L. Mosier, and J. G. Viets of "barren" sedimentary rocks of Cambrian age in the Rolla, Mo., 1:250,000-scale quadrangle showed that two distinct suites of trace elements are present in these rocks—an intrinsic suite and an introduced, or epigenetic, suite. This observation should aid in assessment of the mineral resource potential of the quadrangle and may contribute to our understanding of the origin of the southeast Missouri lead belts. This study was based upon spectrographic and chemical analyses of splits of drill hole samples, insoluble residues, and mineral separates obtained from the sample library of the Missouri Geological Survey. Samples from 62 drill holes were selected for study; samples from 31 holes were analyzed (about 4,000 samples). None of the drill hole samples available for study was located in the known ore trends (Old Lead Belt and Viburnum Trends). None intersected economically significant mineralized ground, and some were as much as 40-km distant from known ore trends.

The intrinsic suite of trace elements was found to be unique to the Derby Dolomite, Davis Formation, and Bonneterre Dolomite of Cambrian age, and the distribution and abundance of this suite reflected the lithology of those formations. The suite, in approximate order of abundance, was Fe, Ti, Mn, Ba, Zr, B, Cr, V, Y, Ni, Co, and Be. The mineralogic residences of these elements were clay minerals, micas, glauconite, and detrital heavy minerals such as zircon and iron-oxides. Thus, the shale facies of the Davis Formation, the shaly and silty limestone facies of the Bonneterre Dolomite, and the glauconite-rich zones in any of the three formations contained the highest contents of intrinsic trace elements. Strontium, in amounts ranging from 300 to 1,000 ppm, characterized the limestone facies. Strontium was contained in the calcite lattice, and it was an indicator of high limestone-dolomite ratios. Manganese, in amounts greater than 500 ppm, was

unique to Bonneterre dolomite facies, and it was contained in the dolomite lattice. Cambrian dolomites, overlying any facies of the Bonneterre Dolomite, contained little manganese.

The introduced, or epigenetic, suite of metals that consisted of Pb, Zn, Cu, Ni, Co, Mo, Ag, As, Sb, and Sn were detected in a few samples. The content of individual metals in the original samples commonly was below spectrographic detection limits (apparently barren rock), but their presence was readily detectable and enhanced in insoluble residue samples. The introduced suite and the relative abundance ratios of one metal to another were the same as for the Southeast Missouri Lead Belt ore suite. The most common mineral residence for this suite was pyrite and (or) marcasite. Galena, sphalerite, and chalcopyrite were observed, but they were not common. Stratigraphic zones that contain anomalously high amounts of the epigenetic suite appeared to be solution channelways. The sulfide minerals found in the soluble residues of samples from the channelways recorded the passing of waters (brines?) that carried metal ions. The channelways always occurred in highly porous and permeable carbonate zones that contained only very small amounts of the intrinsic suite of trace metals. Some drill holes showed vertical stacking of several epigenetic metal-rich channelways that were separated by clastic-rich (shale and siltstone) zones characterized by large amounts of the intrinsic trace element suite.

Some metals, such as nickel and cobalt, were common to both suites. However, nickel and cobalt were contained in glauconite and illite when they were intrinsic, and they were contained in sulfide when they were introduced.

Trace elements in silver-lead-gold veins in Idaho

New quantitative analyses obtained by C. M. Tschanz (U.S. Geological Survey Research 1976, p. 2) for samples from veins in Boulder Basin, Idaho, generally confirmed the remarkably high gold, silver, and selenium contents, but the highest gold value found was only 235 ppm. These new analyses show that the productive ore shoots generally contained from 1,000 to 4,300 ppm Ag and 14.5 to 25 ppm Au.

A semiquantitative spectrographic analysis of a sample of steel galena collected by W. E. Hall revealed that the galena contained 15,000 ppm Ag and 200 ppm Au and 200 ppm Hg. The close association of mercury with ore richest in gold and silver suggested that mercury was present in argentiferous tetrahedrite, the most abundant silver mineral and host for most free gold in the samples studied. This

element association suggests that mercury can be used as a pathfinder in the search for the galena-tetrahedrite ores. High concentrations of Hg, Sb, Cu, and high Ag/Au ratios all generally decrease to minimums near or within the zone of optimum gold values in most gold deposits, according to several Soviet geochemists. The extremely high concentrations of these same elements together with the high Ag/Au ratios in the Idaho samples suggest that higher gold concentrations may occur below levels presently explored. Microscopic study of the ore-related minerals revealed blebs and minute veinlets of fine gold up to 75 μm in maximum dimension in tetrahedrite, diaphorite(?), owyheeite(?), and a ruby silver that is usually found in galena. Anomalous radioactivity was not detected by field scintillometer surveys conducted by C. M. Tschanz in any of the veins in Boulder Basin. Subsequent reexamination of the spectrographic film disproved the previous report of 500 ppm U (U.S. Geological Survey Research 1976, p. 4).

Stream-sediment and panned-concentrate investigations, northern Sonora, Mexico

As a result of a regional geochemical exploration study in northern Sonora, Mex., that was conducted in cooperation with the Consejo de Recursos Minerales of Mexico, E. L. Mosier and G. H. Allcott reported that results from emission spectrographic analyses of stream-sediment and panned-concentrate samples delineate a broad belt containing high concentrations of rare-earth elements. Elements included in the rare-earth suite were Th, Y, La, Sc, Nb, and U. The belt was found to be approximately 45 km in width and centered near Cerro del Chile in the northwest corner of the study area. The belt extended 180 km to the southeast, cutting across several north-trending mountain ranges, to a point approximately 20 km northeast of Bacoachi. The host thorium mineral was isolated and identified as thorite.

Reconnaissance geochemical studies in Alaska

Stream sediment samples were collected by P. K. Theobald, Jr., and H. N. Barton in the National Petroleum Reserve Alaska (NPRA) and in the adjoining Brooks Range of Alaska. A heavy-mineral concentrate was separated from part of each stream-sediment sample, and both types of samples were then analyzed. The distributions of regional geochemical anomalies within the NPRA suggested that five types of mineralization may occur there: (1)

Barium anomalies related to concretionary or bedded barium deposits; (2) zinc, silver, and barium anomalies related to zinc-rich massive sulfide deposits; (3) arsenic, lead, and silver anomalies not related to any known source; (4) lead, silver, and zinc anomalies in areas of low barium and not related to any known source; and (5) chromium and associated element anomalies related to ultramafic-associated mineralization south of the NPRA.

T. D. Hessin's studies in the Big Delta quadrangle, east-central Alaska, revealed several areas in the northeastern part where heavy-mineral concentrates from stream sediment contained anomalous concentrations of Sn, W, Mo, Pb, Zn, and Ag. This metal suite was found to be associated with granitic plutons and suggested possible economic tin occurrences. A similar element correlation also exists, to a lesser degree, in the southeastern part of the quadrangle.

Also in Hessin's investigation, samples of heavy-mineral concentrates collected in the Goodnews quadrangle, southwest Alaska, revealed anomalous amounts of copper, lead, zinc, and arsenic in heavy-mineral concentrates collected near Cretaceous and Tertiary granitic stocks in the northeast part of the quadrangle.

Geochemical studies by R. C. Karlson and others (1977) of heavy-mineral concentrates collected in the western part of the Talkeetna Mountains quadrangle in south-central Alaska, revealed several areas containing anomalous amounts of either silver and gold or copper and molybdenum. The results of this survey suggested that as-yet undiscovered metal deposits may occur in these areas.

Geochemical anomalies associated with mercury deposits in Nevada and Oregon

According to J. J. Rytuba, mercury deposits within the McDermitt Caldera, along the Nevada-Oregon border, contained high concentrations of Be, U, As, Sb, Hg, and Mo in association with the deposits. Anomalous concentrations of this same element suite in tuffaceous, sedimentary rocks in other portions of the McDermitt caldera indicated a potential for other mercury deposits.

Soil-gas investigations, Hawaii Volcanoes National Park in Hawaii

Molecular sieve absorbers buried in the ground over a thermal area in Hawaii Volcanoes National Park were used to collect soil gases. These gases were analyzed by mass spectrometry, gas chroma-

tography, and atomic absorption. According to M. E. Hinkle, anomalies of sulfur compounds and helium were found to be present near the Puhimau Thermal Area, and mercury concentrations were very high directly over the thermal area.

In-hole gamma ray studies in Texas

Two sealed sondes, with germanium gamma-ray detectors cooled by melting propane, were field tested by R. M. Moxham, A. B. Tanner, and F. E. Senftle to depths of 79 m in water-filled boreholes at a uranium mine in Bee County, Texas. When used as total-count devices, the sondes were found to be comparable in logging speed and counting rate with conventional scintillation detectors for locating zones of high radioactivity. When used with a multichannel analyzer, the sondes were found to be detectors with such high resolution that individual lines from the complex spectra of the uranium and thorium series could be distinguished. Gamma rays from each group of the uranium series can be measured in ore zones, permitting determination of the state of equilibrium at each measurement point. Series of 10-minute spectra taken at 0.3- to 0.6-m intervals in several holes showed zones where maxima from the uranium group and from the ^{222}Rn group were displaced relative to each other. Apparent excesses of ^{230}Th at some locations suggested that uranium-group concentrations at those locations were severalfold greater some tens of thousands of years ago. At the current state of development a 10-minute count yields a sensitivity of about 80 ppm U_3O_8 . Data reduction could in practice be accomplished in about 5 minutes. The result was practically unaffected by disequilibrium or radon contamination. In comparison with core assay, high-resolution spectrometry (1) allowed a larger volume to be sampled; (2) avoided problems due to incomplete core recovery, loss of friable material to drilling fluids, and errors in depth and marking; and (3) permitted use of less expensive drilling methods. Because gamma-rays from the radionuclides are accumulated simultaneously, the technique also avoided the problems inherent in trying to correlate logs made in separate runs with different equipment.

Geophysical studies in southwestern New Mexico

The Emory Pass Caldera in New Mexico, previously only inferred (Elston, Seager, and Clemons, 1975), was clearly delineated along its southern half by gravity data interpreted by J. C. Wynn. An aero-

magnetic low on the southern margin of the caldera has strong geochemical haloes around it that may be caused by hydrothermally altered rocks beneath the widespread Kneeling Nun Tuff. A gravity ridge was delineated that stretches south from the Copper Flats porphyry copper deposit to an area where anomalous bismuth and tungsten were previously reported. This ridge may come to within a kilometer of the surface at a point about 8 km southeast of Hillsboro, N. Mex.

TRACE ELEMENTS IN MINERALS

Trace elements in galena and sphalerite in the Montezuma district of Colorado

Grains of galena and sphalerite that were hand picked from vein material collected in the Montezuma district of Colorado were analyzed by emission spectrography. According to Theodore Botinelly, the areal distributions of trace elements detected in samples of these two minerals were found to be spatially related to major geologic structures in the district.

GEOCHEMICAL STUDIES OF WATER

Radon analyses of water in Carbon County, Wyoming

W. R. Miller and others (1977) conducted a pilot study in the vicinity of Arrastre Lake in the Medicine Bow Mountains of Carbon County, Wyoming, to determine the most effective exploration methods for uranium in the area. The so-called "Deep Lake Formation," Precambrian X in age, is present in the area and includes slightly radioactive conglomerates. Radioactivity caused by radon was as high as 2,600 pCi/L in waters of the area, much higher than could be accounted for by uranium in exposed rocks. The results indicated that uranium mineralization is present in subsurface rocks.

Stream water sampling in Puerto Rico

In a geochemical investigation of stream water in the Rio Tanama porphyry copper district of Puerto Rico, R. E. Learned and T. T. Chao found that the copper concentrations in water delineated the interfluvial areas of known deposits. The copper concentrations ranged from 1 to 50 ppb. The molybdenum, lead, and zinc contents of stream waters appeared to be much less useful for exploration purposes. The sulfate content of stream water delineated a broad

area of hydrothermal alteration around the deposits and was therefore found to be a useful guide in regional exploration. Low pH measurements were characteristic of small tributaries draining areas of hydrothermal alteration.

Radioactive spring site guides to uranium in southwestern United States

The effects of four major geochemical processes on the chemical composition and properties of radioactive spring and ground waters were identified by R. A. Cadigan and J. K. Felmlee who used multivariate factor analysis of sample information. Similarly, the effects of five major processes involved in the chemical composition of precipitates at spring sites were also identified. Samples used in this study represented 33 localities in Colorado, Utah, New Mexico, and Arizona. Major factors, in order of importance, controlling properties of these radioactive waters (by analysis of variance?) were: (1) total dissolved solids in solution, (2) true alkalinity, (3) temperature, and (4) iron-uranium concentration. Major factors controlling compositional properties of precipitates of spring sites were: (1) amounts of contamination by detritus and migrating salts, (2) manganese precipitation, (3) iron-arsenic-beryllium precipitation, (4) heavy metal precipitation, and (5) barium-radon precipitation. These nine geochemical factors accounted for approximately 70 percent of variation in both sets of data. Differences in water properties and precipitate composition were found to be functions of variation in the intensity at which the nine processes operated in different springs and in different geologic environments. Intensity levels were computed; the result was a set of intensity scores—one for each process, for each water and precipitate sample. Sample localities were also ranked by the use of nonparametric ranking methods in terms of the overall level of intensity at which the controlling geochemical factors were operating. The higher ranked sample sites were considered to be associated with areas having the highest potential for significant uranium mineralization.

Helium and radon in uranium exploration

Helium surveys conducted by G. M. Reimer showed anomalous helium concentrations in soil gas and subsurface water in the vicinity of various types of uranium deposits. The anomalies were difficult to interpret in view of the diverse geologic nature of uranium deposits, but preliminary models were de-

veloped to aid the interpretation (Reimer and Otton, 1976). Several sampling techniques were successfully evaluated in order to enhance helium and radon concentrations before analysis (Reimer, 1977). The results of these continuing investigations indicated that helium data supported by radon analyses can be useful in locating uranium mineralization.

NEW ANALYTICAL METHODS AND TECHNIQUES

New atomic-absorption method for tellurium

A new flame and flameless atomic absorption method for the determination of tellurium in geological materials was developed by T. T. Chao, R. F. Sanzolone, and A. E. Hubert. This method was found to tolerate considerable amounts of iron in a sample and was found to be both sensitive and rapid. A sample is decomposed with a solution of hydrobromic acid and bromine, ferric iron is reduced with ascorbic acid, and tellurium is extracted into methyl isobutyl ketone. An oxidizing air-acetylene flame is used to determine tellurium in the 0.1 to 200 ppm range. For samples containing 4 to 200 ppm Te, analysis is done by the use of a flameless carbon-rod atomizer after washing the organic extract with 0.4 normal hydrobromic acid to remove the residual iron. The flame procedure is useful for rapid preliminary monitoring, and the flameless procedure can determine tellurium at very low concentrations.

MINERAL RESOURCE INFORMATION SYSTEMS AND ANALYSIS

The Mineral Resource Information Systems and Analysis program assists national mineral policy decisionmaking and USGS resource programs by improving methods of assessing and locating mineral resources, as well as methods for the storage, retrieval, manipulation, and display of geologic and commodity information for mineral resource evaluation and prediction.

Highlights of the program for fiscal year 1977 included:

- Development of a model to assess the interrelations between energy and other input prices and depletion on commodity costs with special emphasis on the effect of such costs on substitution and recycling with respect to copper and aluminum.

- Development of a method to quantitatively appraise the resource potential of a mineralized area by using weighted aggregations of geologic attributes including lithology, structure, magnetic intensity, and remotely sensed reflectance. This method will be particularly useful in assessing the resource potential of large regions for purposes of land classification and land use decisions.
- Application of the Arps and Roberts discovery process model, which was initially tested and found to produce very accurate predictions for the Denver Basin, was found to produce nearly as accurate predictions in the much more complex Midland Basin and Gulf Coast OCS regions.
- Investigation of the exploration techniques of firms operating in the Denver Basin, which indicated that operators are making optimal use of information obtained in the discovery history of the petroleum province.
- An analysis of petroleum discovery and production data for the non-Communist world outside the United States and Canada, which indicated that the date of maximum petroleum production for this area will occur during the decade of the 1990's. The peak of total world petroleum production is predicted to occur before then.
- Worldwide computer conferencing on resource data bases and resource-assessment methodologies was implemented and used by 141 geologists representing 10 countries for a total of over 1,100 hours in 15 months, which is the largest amount of data on the use of computer conferencing in an operational environment to date. Applications for the new communications medium include sharing data bases, raising policy issues, and disseminating scientific information.
- International standards and methodologies for resource assessments, primarily in developing countries, were developed and have been accepted by over 40 nations. This provides, for the first time, a means to conduct such studies in a format useful to all nations for assessing mineral resource and reserve endowment.

COAL

To appraise the amount and quality of coal resources, the Coal Resources Investigation program (1) conducts research to determine the physical and chemical characteristics of coal; (2) collects,

analyzes, and evaluates geologic, geochemical, and mining data to provide information for the selection of future mines sites; (4) develops and uses geophysical techniques to aid in assessing the thickness, depth, and composition of coalbeds; (5) determines the geologic processes that partly or wholly control the selection, development, and operation of existing and future mines; (6) studies the organic, metallic, and mineral contaminants in coal as related to depositional environments, diagenesis, and complete geologic history; and (7) continues expansion of the National Coal Resources Data System (NCRDS).

Accomplishments for fiscal year 1977 included:

- Development and implementation of numerical analysis techniques and graphic display capabilities for coal-resource assessment studies. The procedures operate in interactive, time-shared mode on the USGS Multics computers providing the coal-resource analysts with extended analytical techniques and more accurate and rapid methods for conducting assessment studies.
- Conduction of a detailed core drilling and sample analysis study of Bureau of Land Management (BLM) lands in Utah to determine their suitability for leasing activities for evaluating their reclamation potential and for predicting any possible mining and environmental hazards.
- Estimation of the total original coal resources of the Cache coalbed in the Recluse (Wyoming) model area to be 2×10^9 t. Study included geological mapping, core drilling, sample analysis, and environmental analysis to determine that recovery by conventional methods is possible.
- Development of a geophysical technique for correlating coalbeds in areas where little other data are available. Geophysical data from >3,650 m of logging in 50 holes are valuable in defining the geometry and thickness of coalbeds so that potential mining sites may be identified.

MINERAL EXPLORATION POTENTIAL MAPS

An experimental inventory and map showing mineral exploration potential in the Death Valley $1 \times 2^\circ$ quadrangle of California-Nevada has been published, and similar maps and tables for the Needles quadrangle of California-Arizona and Medford quadrangle of Oregon-California are in preparation. The publications clarify and document statements about the exploration potential of these areas.

GEO THERM FILE

The GEO THERM file is a fully operational data base on geothermal resources. It is divided into three subfiles, which are geothermal fields, wells, and chemical analyses. The geothermal fields file contains information of the location, geology, and geothermal characteristics of geothermal fields/areas. There are 290 fields listed from the United States. The well file contains information on well localities, depths, casings, pressures, flows, and temperatures. There are 430 well records from the western United States. The chemical analysis file contains water quality data and temperatures from thermal waters.

COAL RESOURCES

REINHARDT THIESSEN COLLECTION NOW AT RESTON, VIRGINIA

The Reinhardt Thiessen collection of coal thin sections, formerly housed in Columbus, Ohio, (U.S. Geological Survey Research 1974, p. 7) is currently available for reference and study at the USGS National Center in Reston, Va. The collection consists of more than 19 thousand slides from 682 different localities and includes examples of coal from fields in the United States and other parts of the world. Of historic interest are the examples of coal used in early studies on which were based the origin of coal, coal classification, and the first quantitative system of coal petrology. All available sections of coal studied by the U.S. Bureau of Mines and the USGS that used Thiessen's system of petrography are included, as well as some sections of oil shale and peat. The collection is cataloged in USGS Bulletin 1432 (Schopf and Oftedahl, 1976) and is referenced according to coal basins and geographic area. In addition to the slide collection, Thiessen's point count books and photomicrographs are also available for inspection, as are more than 300 hand specimens of coal collected by J. M. Schopf. Arrangements to study all these items may be made by contacting the Branch of Coal Resources, U.S. Geological Survey, Mail Stop 956, Reston, Va. 22092.

GROWTH OF THE NATIONAL COAL RESOURCES DATA SYSTEM

The National Coal Resources Data System (NCRDS) continues to grow in size and use under the direction of M. D. Carter and A. L. Medlin.

A. C. Olson's systems software development is nearing completion

During the year, approximately 60,000 records on coal resources and chemical analyses were added to the system, which raised the total to nearly 86,000 records. Currently, the data base includes 31,000 coal resource tonnage records and 53,000 records of USBM proximate and ultimate analyses, nearly all records reported by coal bed on a State and county basis. In addition, the NCRDS contains 2,300 geotectonically-located records of proximate, ultimate, major-, minor-, and trace-element analyses and associated data from the Branch of Coal Resources geochemical program.

At present the NCRDS has cooperative arrangements with five State geological agencies for collection, correlation, transmission, entry, retrieval, manipulation, and display of drill hole, chemical analyses and other relevant coal resource-related data, and the NCRS hopes for additional joint efforts to promote rapid building of the data base.

COAL IN THE NEW RIVER GORGE AREA IN WEST VIRGINIA

A mineral-resource assessment was made jointly by the USGS and USBM for a proposed National Park or Wild and Scenic River of the New River Gorge area in West Virginia (Englund and others, 1977). In this investigation, a total of 220×10^6 t of original coal resources were mapped and identified. Mining has depleted about 38 percent or 83×10^6 t. Because of the large remaining coal resources, 137×10^6 t, the proposed boundary was reduced substantially to eliminate large blocks of coal from the park area. Core drilling in conjunction with this investigation extended the known distribution of economically important low-sulfur coal in central West Virginia.

INTERTONGUING, PALEOCHANNELS, AND FAULTS IN THE WASATCH PLATEAU IN UTAH

Lithostratigraphic environmental modeling of the Blackhawk Formation and the Star Point Sandstone in the Wasatch Plateau of Utah has resulted in the reinterpretation of the genesis of these rock units by R. M. Flores. Correlations of 125 closely spaced stratigraphic sections in an area of 67 km² show interfingering of the lower part of the Blackhawk Formation with the upper part of the Star Point Sandstone. A 20-m thick zone of this previously un-

known intertonguing was traced for about 10 km in a north-northwest direction in the Muddy Creek area of the Wasatch Plateau coalfield by Flores, P. T. Hayes, J. D. Sanchez, and W. E. Marley. The trend should provide a useful guide to future exploratory drilling in the area. This relationship demonstrates a very limited lateral continuity of the thick, minable coalbeds in the lower part of the Blackhawk Formation. Heretofore, these coalbeds had been identified as having broad lateral extent in the Wasatch Plateau; therefore, modifications in earlier concepts of coal-bed correlation and continuity will be required, and estimates of coal resources in the Wasatch Plateau probably will be lowered. The lateral variations, nature of content, sedimentary structures, petrographic properties, trace- and macro-fossil content, and morphology of the detrital rocks associated with coal suggest a depositional continuum of the Blackhawk Formation and Star Point Sandstone. That is, the lower and middle parts of the Blackhawk Formation represent delta plain deposits that grade seaward into the delta front sediments of the Star Point Sandstone. The Star Point Sandstone was originally interpreted as a barrier bar deposit.

In the central portion of the Wasatch Plateau coalfield, E. G. Ellis has identified paleochannels that cut into coalbeds of the lower part of the Blackhawk Formation. He has also located, within the area of coal-mining interest in the Ferron Canyon 7 $\frac{1}{2}$ -minute quadrangle, some previously unmapped fault zones of the north-trending graben system partially mapped by Spieker (1931).

Mapping by L. F. Blanchard in the Johns Peak 7 $\frac{1}{2}$ -min quadrangle, Sevier County, Utah, has shown a zone of intense normal faulting that trends north-northeast and effectively forms the western boundary of the Emery coalfield. The extreme lenticularity of coalbeds in the Ferron Sandstone Member of the Mancos Shale observed on the outcrop was confirmed by drilling. The investigations also showed that the economically important Last Chance Creek, Upper Last Chance Creek, and Ivie coalbeds in the lower part of the Blackhawk Formation range from 1.2 to 2.7 m in thickness.

MONTMORILLONITE IN COAL PARTINGS

The mineralogy of bentonitic partings in coal is directly related to the environment of the peat swamp during or immediately following peat deposition, according to evidence presented by B. F. Bohor.

Samples of partings in the Fruitland coal in the San Juan Basin, New Mexico, showed that amounts of montmorillonite increased upward in the vertical succession where the coal is overlain by marine beds (Bohor, 1977). These relationships were confirmed at the San Juan mine and at a similar section in the Fruitland coal near Durango, Colo.

COAL RANK RELATED TO DEPTH OF BURIAL AND BURIED INTRUSIVE ROCKS

Twelve channel samples of coal were collected from five different beds by V. A. Trent, J. H. Medlin, and S. L. Coleman at mines in a 38-km² area in McDowell and Tazewell Counties in West Virginia. The coalbeds are distributed through 265 m of strata in the Pocahontas and New River Formations of Early Pennsylvanian age. Standard USBM chemical analyses of the samples show that the rank of the coal spans the medium-volatile range and increases with depth of burial of the bed. There are direct proportional relationships between the depth of burial of the coal and its fixed carbon content and carbon-hydrogen (C/H) atomic ratio, the two most widely accepted indices of rank in carbonaceous materials. Linear regression curves were fitted to the two sets of point data and the calculated correlation coefficients are high for the number of samples.

Research by G. P. Eager indicates that the rank of the Upper Cretaceous coal in the Grand Mesa field in Delta and Mesa Counties in west-central Colorado is related to structural location within the Piceance Creek Basin. Coal rank in the lower part of the Mesaverde Formation changes from high volatile *B* bituminous at an altitude of 1,460 m to subbituminous *B* at an altitude of 2,440 m. Thinning of the Tertiary formations over the structurally higher, lower rank coal implies depth of burial as the primary mechanism for rank variation.

The carbon-oxygen (C/O) ratios (dry basis) in Cretaceous coal in the Somerset coalfield in Gunnison and Delta Counties in Colorado were found to increase from about 5.5 to 30 eastward across the field, which indicates an eastward increase in rank of the coal. J. R. Dyni and D. L. Gaskill attribute this increase in C/O ratios to heating by laccoliths that intrude the coal-bearing strata around the eastern side of the coalfield. Coal having C/O ratios greater than about 7.5 has marginal or better coking qualities; such coal is likely to be found in the east and northeast parts of the coalfield. Carbon-oxygen

ratios may be useful in delineating the boundaries of buried intrusive rocks and in locating areas of methane-enriched coal that may have considerable value for in situ gasification.

GEOCHEMISTRY OF U.S. COAL RESOURCES

Vanadium content in coal

During the past year, 934 coal samples were analyzed by the USGS for 60 to 80 inorganic elements and by the USBM for proximate and ultimate determinations. According to Peter Zubovic, J. H. Medlin, and C. L. Oman, results of analyses on more than 2,700 coal samples from the United States show the following mean values for vanadium content: Pacific Coast coal, 120 ppm; Alaskan coal, 60 ppm; Rocky Mountain lignite, 59 ppm; Rocky Mountain bituminous coal, 14 ppm; Northern Great Plains subbituminous coal, 17 ppm; Northern Great Plains lignite, 7 ppm; and Appalachian bituminous coal, 22 ppm.

Sphalerite-bearing coal in Illinois

As determined by H. J. Gluskoter (Illinois Geological Survey), the sphalerite-bearing Colchester (No. 2), Springfield (No. 5), and Herrin (No. 6) coalbeds in the northwestern part of the Illinois Basin coalfield contain approximate mean values of 629 ppm zinc and 6.0 ppm cadmium. Resources of coal in Fulton, Knox, Peoria, and Stark Counties in Illinois amount to $5,600 \times 10^6$ t. The mineral resources in that amount of coal would be about 63.45×10^6 t zinc and 26×10^3 t cadmium. The abundance of zinc and cadmium in sphalerite-bearing coal must be determined from large samples that are representative of both disturbed and undisturbed parts of the coalbed. Disturbed parts of coalbeds are characterized by fractures, faults, slips, and clay dike intrusions, all of which may contain sphalerite. A sampling program was developed that includes composite auger, composite face channel, composite face grid, channel, and bench samples. Results of zinc and cadmium determinations on certain sample types have a bimodal distribution. The lower mode, which ranges from 100 to 500 ppm zinc, corresponds to samples that were collected in undisturbed parts of the coal beds. Samples of the higher mode, which range from 650 to 1,250 ppm zinc, were collected from disturbed parts of the coalbeds. The origin of sphalerite in coal is thought to be the result of warm, formational brines moving through the coal along structural features such as cleats, fractures,

faults, and clay dikes. It is hypothesized that these brines originated in deeper parts of the basin and migrated updip in response to increasing hydraulic pressures resulting from sedimentary loading in the main part of the basin.

Hydrogenation of coal and sulfide minerals

Lignite from North Dakota and bituminous coal from Illinois have been exposed by I. A. Breger to a methane plasma produced by a radio-frequency discharge in an attempt to obtain detailed information about the chemical structure of coal and thereby determine its best possible use. When in a vacuum at ambient room temperature, the methane and coal appear to react to produce light yellow to dark brown products. The reaction leads to vaporphase products that condense to produce thin, non-crystalline films of the products that have atomic hydrogen-carbon (H/C) ratios as much as 70 percent greater than the ratios in the original coals. The ability to hydrogenate coal under vacuum without a catalyst and at ambient room temperature is of particular interest in the conversion of coal to liquid fuel.

Breger has also exposed several copper and iron-copper sulfide minerals to a hydrogen plasma produced when hydrogen gas is passed through a radio-frequency discharge. A reaction between activated hydrogen and (or) hydrogen-free radicals with the sulfide mineral takes place at ambient room temperature in a vacuum to produce metallic copper. A patent application covering this "invention" will be submitted.

Mass balances of trace elements at powerplants

Peter Zubovic's studies of mass balances of 16 environmentally hazardous elements show that Be, Cr, Cu, Ni, and V are not emitted from powerplants in amounts greater than that associated with the fly ash passing through the entrainment equipment. When this equipment is highly efficient, near zero emission of these metals occurs. Mercury, chlorine, and iodine are almost totally emitted from the powerplants. Other elements have the following emission ranges in percent: As, 0 to 74; Br, 43 to 96; Cd, 0 to 69; F, 0 to 90; Pb, 0 to more than 43; Sb, 0 to 98; Se, 0 to 65; and Zn, 0 to 40. This variability of emissions from six different powerplants is similar to that reported by other investigators.

Environmental pollution of the Everglades in Florida

Pollution of the Everglades from agricultural and automotive sources is revealed by the enrichment of

phosphorus, zinc, and lead analyzed in the uppermost material of peat cores that were taken by Z. S. Altschuler 150 to 200 m from the highway along the Tamiami Trail in Florida. Although the pollution is not extreme, phosphorus and zinc range from 2 to 4 times background, and lead, 10 to 20 times background. These results will aid the National Park Service in evaluating the human impact on the Everglades environment. Also, the anomalies are relevant to understanding trace-element geochemistry in coal for, in the case of phosphorus and zinc, they reveal appreciable and widespread dispersion of soluble allochthonous material from the farming district near Lake Okeechobee; the lead is introduced from automotive traffic.

NEUTRON ACTIVATION AND MAGNETICS OF COAL

The nuclear borehole sonde (U.S. Geological Survey Research 1976, p. 25) was successfully used for in situ elemental analysis by high energy capture gamma-ray spectrometry. A new borehole sonde has been developed by F. E. Senftle, A. B. Tanner, J. L. Mikesell, and R. M. Moxham (USGS) and R. J. Macey (Princeton Gamma Tech., Inc.) to examine the possibility of using low energy capture gamma-ray analyses. Preliminary tests have been made in a coalbed in Harrison County, Ohio, and the data are still under study. Certain elements, such as oxygen, that cannot be seen at high gamma-ray energies can be seen in the low energy end of the spectrum.

Magnetic susceptibility, magnetization, and the Curie constant were measured on about 50 samples of lignite, bituminous coal, and anthracite by F. E. Senftle, A. N. Thorpe, and C. C. Alexander. The magnetic properties varied drastically even in a small hand specimen, and oxidation of the samples took place by merely sitting in air. The Curie constant was related to the carbon concentration and to the heat value. Measurements are being made to determine the source of paramagnetic component of the observed magnetic susceptibility.

OIL AND GAS RESOURCES

ALASKA

Petroleum potential of Lisburne Group in the North Slope

The Lisburne Group, a thick, dominantly carbonate unit of Mississippian and Pennsylvanian age, is an important drilling objective in a large area of

northern Alaska. A comprehensive review of the Lisburne in the subsurface of the eastern Arctic Slope by K. J. Bird indicates possible reservoir rocks in favorable source and migration settings, wherein numerous trapping mechanisms appear to be available. Evaluation of this group is timely because of current exploration programs in the Prudhoe Bay area and in Naval Petroleum Reserve No. 4.

Dolomite and sandstone have been identified as possible reservoir rocks. Oolitic grainstone is a common rock type, but observations indicate little reservoir potential owing to complete void filling by calcite cement. The most important potential reservoir rock, as judged by thickness, areal extent, and predictability, is microsugrosic dolomite of intertidal and supratidal origin. Microsugrosic dolomite is present throughout the Lisburne Group, and it is most abundant near the middle of the sequence. Northward the microsugrosic dolomite decreases in thickness from 300 m to <30 m. Porosity of the dolomite in selected wells averages 10 to 15 percent and has a maximum of slightly more than 25 percent. Net thickness of reservoir rocks (i.e., rocks with greater than 5 percent porosity) in these wells ranges from 40 to 120 m. Oil shows are common, and drill-stem tests have yielded as much as 1,600 bbl/d of oil and 623,000 m³/d of gas in the Lisburne pool of the Prudhoe Bay field and as much as 2,057 bbl/d of saltwater elsewhere. The widespread occurrence of microsugrosic dolomite in the studied area makes its presence in the offshore Beaufort Sea and adjacent Naval Petroleum Reserve No. 4 fairly certain. The presence of a sandstone facies as thick as 40 m in the middle and upper parts of the Lisburne in two coastal wells suggests that larger areas of sandstone may be found to the north in offshore areas. Shows of oil and gas and a saltwater flow of 1,470 bbl/d have been recorded from this sandstone facies.

Shales of Permian and Cretaceous ages unconformably overlie the Lisburne Group, providing adequate sealing beds above potential reservoirs. Impermeable limestone (completely cemented grainstone) and thin beds of shale may serve as seals within the Lisburne, but the possible presence of fractures in these units may negate their sealing capability.

The most favorable source rock for hydrocarbons in the Lisburne Group appears to be shale of Cretaceous age that unconformably overlies the Lisburne east of Prudhoe Bay. This shale is reported to be a rich source rock and is the most likely source for the entire Prudhoe Bay field. A source within the

Lisburne or within the underlying Kayak Shale is postulated for oil shows in the southernmost wells. This postulated source may be in a more basinal facies of the Lisburne and may be similar to dark shale in the upper part of the Lisburne in thrust slices in the Brooks Range. Coal in the underlying Endicott Group is a possible source for dry gas. At present, much of this coal probably is in a gas-generating regime downdip from the Prudhoe Bay field.

Stratigraphic traps involving the Lisburne Group may have resulted from widespread Permian and Cretaceous unconformities. Structural traps related to normal faulting may be present along the trend of the Barrow arch, and faulted anticlines are numerous in the foothills of the Brooks Range. Combination traps are possible along the trend of the Barrow arch.

Petroleum potential of Tertiary formations on Alaska peninsula

Analysis of outcrop samples by I. F. Palmer and J. G. Bolm (USGS) and W. M. Lyle (Alaska Div. of Geological and Geophysical Surveys) suggests that porosity and permeability of sufficient quality to constitute potential petroleum reservoirs exist in younger Tertiary formations on the Alaska peninsula. Kerogen studies indicate a moderately immature to mature regime of hydrocarbon maturation in possible source rocks and a capability for generation of either dry gas or liquid hydrocarbon. Many analyzed samples yield a C_{15}^+ hydrocarbon extract in excess of 300 ppm.

ROCKY MOUNTAINS AND GREAT PLAINS

Hydrocarbon potential of Disturbed Belt in northwestern Montana

The northern part of the Disturbed Belt has a high potential for natural gas accumulations, as determined by D. D. Rice (1977). Petroleum probably was generated in Jurassic and older marine shales and expelled, migrated, and accumulated in stratigraphic traps prior to early Tertiary orogeny. Some of these traps were associated with northeasterly-trending linaments. The oil was thermally cracked, converted to methane-rich gas and condensates, and redistributed into primarily structural traps associated with the thrust faulting and associated structures. The faulted eastern edge of reservoir rocks in the upper plate of a thrust block is probably the primary type of structural trap; associated folding is a secondary type.

The primary reservoir target is carbonate rocks of Mississippian age, which are the primary reservoirs in the Alberta Foothills to the north and in the Sweetgrass arch to the east. Porous zones are developed in areas of secondary dolomitization or organic buildups, such as encrinites. Previously unevaluated reservoirs may be present in underlying Devonian carbonate rocks, such as the Birdbear Member of the Jefferson Formation. Potential reservoirs in clastic rocks, such as the Jurassic Swift and Cretaceous Kootenai Sandstones, are regarded as secondary targets because of clay infilling and diagenetic effects associated with deformation.

Hydrocarbon potential of proposed Great Bear Wilderness in western Montana

The potential for discovery of petroleum and natural gas, but mainly gas, is very high for most of the Great Bear Wilderness in western Montana, according to M. R. Mudge, R. L. Earhart, and G. E. Claypool. Excellent source and reservoir rocks are present in the study area. Surface mapping of structures indicates that subsurface structures favorable for hydrocarbon accumulation may occur at depth. However, they cannot be determined without seismic surveys. Forty-two outcrop samples from the Wilderness and nearby areas were analyzed and evaluated as hydrocarbon source rocks. Organic matter in rocks of Jurassic and Early Cretaceous age has the capacity for generating natural gas, and burial of these rocks beneath thrust plates should have generated significant amounts of gas at a time favorable for trapping. Petroleum probably will not be found in reservoir rocks in most of the study area. However, possible petroleum source rocks of Late Cretaceous age are present near the western part of the study area, and oil occurrences there may have developed when these rocks were deeply buried by thrust plates with thick rock sequences. These data probably explain the production of oil between 1902 and 1906 from a depth of about 150 m in Upper Cretaceous rocks in the east part of Glacier National Park and oil seeps in other parts of the eastern Rocky Mountains in northwestern Montana and adjacent parts of Canada.

New biostratigraphic, paleogeographic, and tectonic data on Cretaceous rocks in Minnesota and eastern South Dakota

Upper Cretaceous strata in mines and quarries of northern and western Minnesota and eastern South Dakota were examined by E. A. Merewether, W. A. Cobban, and G. W. Shurr as part of a regional in-

vestigation of Cretaceous unconformities. Index fossils from outcrops and specimens in collections at the University of Minnesota were identified and related to the ammonite zonation of the Cretaceous Western Interior sequence by Cobban. Many of the Cretaceous beds in Minnesota and eastern South Dakota now can be correlated with strata in the Rocky Mountain area. The ages of the fossils and the altitudes of the fossil localities in Minnesota and eastern South Dakota are interpreted as evidence of slight differential crustal movement in the region during or after early Late Cretaceous time.

The studied Cretaceous beds contain marine fossils of Cenomanian and Turonian Age and disconformably overlie Precambrian igneous and metamorphic rocks. Near Calumet, in northern Minnesota, a basal Cretaceous conglomerate contains the ammonite *Dunveganoceras albertense* (Warren) of later Cenomanian Age, other mollusks, reptilian bones, and fossil wood. The basal strata in the eastern part of the area also contain fossils of brackish-water origin. The marine fossils and conglomeratic beds probably represent a near-shore depositional environment of moderate to high wave energy. Near Bellingham, in western Minnesota, Precambrian granite is overlain by limestone and pebble-bearing shale, which contain *Inoceramus labiatus* (Schlothheim) of early Turonian Age, other mollusks, and abundant fish bones. The basal strata near the town of Milbank, in northeastern South Dakota consist of slightly calcareous pebble-bearing shale, which contains *Collignonicerias woollgari* (Mantell) of early to middle Turonian Age, other mollusks, abundant fish bones, and large fragments of fossil wood. A few of the bedding planes display branching burrows, about 1 cm in diameter, which are probably *Thalassinoides*. The fossils, burrows, and scattered sand and pebbles in the shale and limestone of the Milbank-Bellingham area are interpreted to evidence a near-shore depositional environment of low to moderate wave energy.

Sloan (1964, p. 5) determined that the unconformity at the base of the Cretaceous sequence in Minnesota had a relief of as much as 427 m prior to Cretaceous deposition. The new data support his suggestion (Sloan, 1964, p. 15, figs. 2 and 11) that the Cretaceous sediments accumulated between the islands and peninsulas of a dominantly granitic and metamorphic coastal region during a period of marine transgression.

In northern Minnesota, where the basal conglomerate contains *Dunveganoceras albertense* (Warren)

of late Cenomanian Age, the altitude of the unconformity is 420 to 440 m. At the town of Comfrey, in southern Minnesota, the same ammonite was found in shale at an altitude of about 345 m. The Cenomanian strata in the northern part of Minnesota seem to be about 75 to 95 m higher than beds of the same age in the southern part of the State. In the Milbank-Bellingham area, where the basal strata are of early to middle Turonian Age, the altitude of the unconformity is 290 to 330 m. Thus, the altitude of the unconformity is greater in northern Minnesota than it is in southern Minnesota and adjacent South Dakota. This difference in altitude seems to indicate minor tectonism in the region during or after early Late Cretaceous time, rather than remnant depression of the crust caused by continental glaciers. Depression probably would be directly opposite and greater in northern than in southern Minnesota.

Natural gas resources of shallow, low-permeability (tight) reservoirs of the northern Great Plains

Geological investigations by D. D. Rice and G. W. Shurr and analysis of recent exploration activity in western Canada indicate that major natural gas resources are entrapped in reservoirs of low permeability at depths of less than 1,200 m in the northern Great Plains area of eastern Montana, western North and South Dakota, and northeastern Wyoming. These shallow accumulations of gas, which consist predominantly of methane, are the product of the immature stage of hydrocarbon generation and are referred to as biogenic gas.

Prospective low-permeability (tight) gas reservoirs in the northern Great Plains range in age from late Early Cretaceous to Late Cretaceous and include most of the sequence from the Mowry Shale to the Bearpaw Shale. Individual reservoirs are thin, discontinuous siltstone and sandstone beds enclosed in thick sequence of marine shale. Shale, where naturally fractured, may serve both as a source rock and as a potential reservoir. Laterally continuous marls in the Greenhorn, Carlile, and Niobrara Formations that have high porosity but low permeability, are potential targets for exploration, particularly in the eastern part of the study area. All of these tight reservoirs were formed in sediments deposited in a low-energy, marine-shelf environment along the north-trending Western Interior seaway.

Gas production from tight reservoirs north of the study area is reported from the southern part of 22 m³/km². Using these reserve data as an analog,

the northern Great Plains area should contain resources of natural gas in excess of 3 trillion m³. The volume of recoverable gas will be dependent on the development of recovery technology and on gas prices.

Hydrocarbon accumulation in Cretaceous shallow-marine sandstones of the northern Denver Basin

Surface and subsurface studies by L. W. Kiteley of the Pierre Shale (Upper Cretaceous) in the northern Denver Basin have established a regional lithologic and time-stratigraphic framework for sandstone units within the Pierre Shale. Paleontologic information indicates that the "Shannon" and "Sussex" sandstones of drillers' informal subsurface usage in the Denver Basin are entirely different in age from and depositionally unrelated to the type Shannon and Sussex Sandstone Members of the Steele Shale (Upper Cretaceous) in Wyoming. Stratigraphic correlations indicate that the so-called Shannon and Sussex sandstones are approximately equivalent to the Parkman Sandstone Member and younger beds of the Mesaverde Formation (Upper Cretaceous) in the Powder River basin. Consequently, Hygiene and Terry Sandstone Members of the Pierre Shale should be used in the place of Shannon and Sussex in the Denver Basin.

In the northern Denver Basin the upward increase northwestward from Boulder, Colo., of sandstone interbeds within the Pierre Shale indicates a major eastward regression of the strandline. Analyses of outcrop data suggest that the lower third of the Pierre was deposited in open-marine environments, the middle third in shallow-marine environments, and the upper third in open-marine to very near shore environments. Computed rates of deposition for the Hygiene and Terry Sandstone Members indicate that the source of sand for these members probably was a delta, which lay to the north and northwest in north-central Colorado and south-central Wyoming. Stratigraphic relations and computed rates of deposition of the Hygiene near Boulder, Colo., where it is thickest, indicate rapid accumulation in a locally subsiding basin. The rapid accumulation in this area, where both the Hygiene and the Terry produce oil and gas, is believed to have favored preservation of potential source rocks. Hydrocarbon accumulation in producing sands is in an area of updip facies change from sands to low permeability, lower energy siltstones and shales.

GREAT BASIN AND CALIFORNIA

Permian source rocks, northeastern Great Basin

Initial laboratory analyses of samples of organic-rich shale beds collected by E. K. Maughan from the Permian Phosphoria Formation and Park City Group in Box Elder and Tooele Counties, Utah; Elko County, Nevada; and Cassia County, Idaho; indicate organic-carbon contents as high as 5.4 percent in some beds. Most of the analyses, however, indicate contents of less than 1 percent. The higher organic-carbon values are from the Meade Peak Member of the Phosphoria Formation in the Terrace Mountains in Box Elder County. The Meade Peak Member attains a maximum thickness of 65 m there, but it thins and seems to wedge out westward within Elko County, in northeastern Nevada. A tentative evaluation of the shale beds as a source of petroleum is indicated by their regional extent, volume, and relatively high organic-carbon content. Petroleum may have been generated throughout most of the four-county area, but the better source beds and most likely the center of petroleum generation are in central Box Elder County, near the northern arm of Great Salt Lake in Utah.

Early gas discovery in Cordilleran hingeline area in Utah

A new gasfield has been discovered in an area, the petroleum potential of which had been predicted earlier by C. A. Sandberg and R. C. Gutschick (1977) in U.S. Geol. Survey Open-File Rept. 77-121 released in February 1977. The same prediction was made by these authors and W. J. Sando in Geological Survey Research 1977. The discovery well, American Quasar Petroleum Co. No. 1-20 Hogback Ridge, in sec. 20, T. 13 N., R. 7 E., Rich County, Utah, was first tested in June 1977 and was completed in September and October 1977 producing from two zones: 280,000 m³ of gas per day from the Permian Phosphoria Formation at a depth of 3,070 to 3,120 m and 635,000 m³ of gas per day from the Dinwoody Formation (Triassic) at a depth of 2,887 to 2,936 m. The well is located only 10.5 km northeast of the measured section of the phosphatic shale member of the Little Flat Formation (Mississippian) at Old Laketown Canyon near the south end of Bear Lake in Utah. On the basis of regionally low conodont color alteration index (CAI) values of 1 to 1½ for conodont collections from this and other localities, Sandberg and Gutschick (1977, p. 9-10) successfully predicted in two consecutive years that both the southern Pavant Range and the area around

Bear Lake in northern Utah offer the best prospects for successful petroleum exploration of the Cordilleran hingeline in Utah, that (2) in this area the oil expelled from the phosphatic shale member may have migrated upward into upper Paleozoic or Mesozoic formation, and that (3) the Trap Spring oilfield in Nevada lies within a "cold spot" area where thermal maturation of hydrocarbon has not progressed beyond optimum temperatures.

"Cold spots" were described by Sandberg and Gutschick (1977, p. 8) as the opposite of "hot spots," which are caused by mantle plumes. They theorized that "cold spots" could be caused by convection currents in the mantle and would produce abnormally low geothermal gradients in the overlying continental crust. In such areas, Paleozoic source rocks would have been refrigerated and would have had their thermal maturation retarded so that they are now at or near optimum temperatures for generation and expulsion of petroleum and natural gas.

Rates of sedimentation of petroleum source rocks in Utah, Nevada, and Idaho

C. A. Sandberg and F. G. Poole (1977) proposed a method for determining the rates of sedimentation of petroleum source rocks and non-source rocks by using conodont zonation. They use as a model the depositional basin of the Upper Devonian (Frasnian and lower Famennian) lower member of the Pilot Shale in western Utah and eastern Nevada. It is assumed that the combined length of the Frasnian and Famennian Stages is 13 m.y. based on currently accepted radiometric age dates and divided by the 27 conodont zones in the standard Upper Devonian conodont zonation. Because the zonation is based primarily on the phylogeny of a single conodont genus, *Palmatolepis*, that evolved very rapidly under optimum stable ecological conditions across at least half the diameter of the Earth, the zones are arbitrarily assumed to have a duration of the same order of magnitude. The length of a single Upper Devonian conodont zone can be calculated to represent approximately 0.5 m.y. From this figure and interpretations of the lithologic character of the sediments, it was determined that (1) the better source rocks were deposited at a rate of 32 to 55 m/m.y. and (2) flyschlike sediments that contain fewer source beds and more terrigenous material were deposited at a rate as high as 160 m/m.y. The rate of starved sedimentation, which did not produce source rocks because of aerobic bottom conditions, was only 4.5 to 6 m/m.y. The sedimentation

of aerated shallow-water shelf carbonate rocks surrounding the Pilot Basin took place at a rate of 40 m/m.y. It was also determined by applying the same method to Lower Mississippian rocks that calcareous Antler flysch sediments, which contain interbedded source rocks, were deposited at a rate of 267 to 400 m/m.y. in the Pioneer Mountains of central Idaho.

Many source beds accumulate where a moderate to rapid rate of sedimentation preserves organic matter from seafloor scavengers. However, source beds also can accumulate in starved phosphatic basins where the rate of sedimentation is about 10 m/m.y. Such a slow rate of sedimentation took place in the basin of the Mississippian (Osagean to lower Meramecian) phosphatic member of the Deseret Limestone in Utah. There, dysaerobic (minimal-oxygen) conditions on the seafloor reduced the number of scavengers, so that the organic matter was preserved and source beds were produced.

Mineralogic character of some hydrocarbon reservoirs in Uinta Basin, Utah

Some reservoirs in the Green River Formation (Paleocene and Eocene) at Pariette Bench field are fractured, marginal-lacustrine channel-form sandstone interbedded with calcareous and carbonaceous claystone and some grain-supported carbonate, according to J. K. Pitman and T. D. Fouch. Rocks formed in similar depositional environments produce oil and (or) gas in Utah at Ute Trail, Natural Buttes, and Altamont-Bluebell fields. Petrographic and X-ray diffraction analyses indicate the primary mineral constituent is very fine to fine, subrounded to angular grains of quartz; alkali and plagioclase feldspar, Ca-Mg-Fe carbonate, heavy minerals, and clays are present in minor amounts. Dominant framework grains are monocrystalline quartz exhibiting straight grain contacts. Scanning electron microscope (SEM) analyses indicate that complex detrital and authigenic carbonate, clay, and zeolite assemblages fill intergranular pore space cementing the framework grains. Little evidence for extensive compaction, pressure solution, and quartz overgrowths indicates that much of the cementation may have taken place during early diagenesis. Clay mineral constituents are interstratified mixed-layer illite-smectite and chlorite.

Sedimentation, tectonics, and petroleum potential of California Coast Ranges

Within California, there are principally four Upper Cretaceous depo-tectonic terranes: (1) an arc

terrane (Sierra Nevada-Klamath Mountain crystalline basement), (2) a regional fore-arc basin (Great Valley sequence, sedimentary rocks), (3) a subduction complex (Franciscan assemblage, sedimentary and metamorphic rocks), and (4) a wrench-tectonic(?) borderland (Salinian block; plutonic, metamorphic, and sedimentary rocks). The first three terranes follow the arc-trench gap model of W. R. Dickinson, and reflect underthrusting of the oceanic Farallon plate beneath the continental North American plate. The original distribution of these terranes has been greatly modified because of late Tertiary faulting (San Andreas fault system) between the Pacific and North American plates. Sandwiched within the disrupted pattern of the first three terranes is a relatively young plutonic clastic terrane of the Salinian block. The geologic relations of this allochthonous body suggest a major episode of Late Cretaceous transform faulting. D. G. Howell, J. G. Vedder, and Hugh McLean recognized within the Salinian block, five distinct sedimentary basins, each characterized by abrupt, lateral and vertical lithofacies changes. Locally, the sediments that lie depositionally on plutonic rocks postdate by only 10 m.y. the emplacement age of this crystalline basement. This minor difference in age and the lithofacies patterns suggest active and complex tectonic and depositional relations.

Deposition in restricted basins, such as those in the Salinian block, can provide a favorable setting for petroleum accumulation. Preliminary analyses indicate, however, that the source-rock potential is very low and the quality of reservoir rocks is poor.

APPALACHIAN BASIN AND FLORIDA

Possible stratigraphic controls for Devonian gasfields in the Appalachian Basin

Isopachs of the black shale facies of Middle to Late Devonian age in the Appalachian Basin outline two distinct north-trending belts of thick black shale accumulations separated by a transition zone of thinner black shale, according to L. D. Harris. The thick belts apparently accumulated at different times during separate near-stillstand episodes in the growth of the Catskill delta. The thicker and earlier belt accumulated in the eastern part of the Appalachian Basin during Middle to Late Devonian time; whereas, the second belt accumulated mainly during Late Devonian time in the western part of the basin. Commercial gas production from the black shale facies is confined to the western black shale belt and

part of the adjacent transition zone. The Big Sandy gasfield in Kentucky and West Virginia is centered over two major partly coalesced black shale lobes within the western black shale belt. Limited data suggest that the largest initial and stimulated production occurs from wells drilled along the crestal regions of lobes in the Big Sandy field. Conversely, initial and stimulated production decreases on the slopes of lobes as the thickness of the black shale decreases. Thus, a correlation may exist between thickness of black shale and potential gas production. Other thick lobes, which are relatively untested by modern well completion and stimulation methods, underlie parts of central Ohio.

Hydrocarbon maturation in Kentucky and Virginia

Core samples of black shale of Devonian age from Martin County, Kentucky, and Wise County, Virginia, were cased at the well site. After outgassing in the cans for periods of 3 to 4 months, the amount and chemical composition of the gas, and the stable carbon isotope ratio of the methane in the gas were measured. According to G. E. Claypool and C. N. Threlkeld, differences in the amounts and compositions of the gases are due to the marked difference in temperature history at the two localities. This difference in temperature history is suggested by present depth of burial and published conodont alteration and coal rank studies in the overlying rocks. The difference in thermal maturity is confirmed by geochemical analyses, such as thermal analysis, which indicates that the solid organic matter (kerogen) has evolved to an early post-mature stage at Wise County; whereas, it is in a mature stage at Martin County. The original nature of the organic matter at these localities is believed to have been the same.

Quick evaluation by gamma-ray intensity and density crossplot of Devonian shale in West Virginia

J. W. Schmoker has found that the density crossplot versus gamma-ray intensity from a sequence of shale of Devonian age penetrated by three wells in Lincoln County, West Virginia, is linear. A linear crossplot is predicted from geochemical considerations, assuming that organic content is the only variable producing changes in formation density. Thus, quantitative evidence is obtained that factors such as shale mineralogy, porosity, or pore-fluid type have only a second-order effect upon density changes. The gamma-ray log can be used (1) to distinguish lithologic and stratigraphic units in the

Devonian shale sequence in this area and (2) to estimate their density to $\pm 0.02 \text{ g/cm}^3$ (at a 68 percent confidence level). The crossplot between density and gamma-ray intensity can be used as a preliminary tool to identify intervals that differ from the normal section in that factors other than organic content are contributing to density changes. Such factors could include the presence of siltstone, increased porosity, or gas as a pore fluid, all of which would be favorable for gas production.

Source-rock potential of South Florida Basin

Preliminary studies by J. G. Palacas indicate that in the South Florida Basin, carbonate rocks of Early Cretaceous (Comanchean) age are relatively richer in average organic-carbon content (0.41 percent) than those of earliest Cretaceous (Coahuilan) age (0.28 percent), Late Cretaceous (Gulfian) age (0.18 percent), and Paleocene age (0.20 percent). They are also nearly twice as rich as the average carbonate rock worldwide (0.24 percent).

Possible petroleum source rocks were noted in almost each subdivision of the Coahuilan and Comanchean Series, particularly in the subsurface units of the "Fredericksburg 'B'", upper and lower parts of the Sunniland Limestone, "Trinity 'F'", and Punta Gorda Anhydrite.

Preliminary analyses also indicate that in most of the analyzed carbonate samples, about 80 percent of the solid organic matter is the marine, amorphous, hydrogen-rich, oil-prone type of kerogen. Consistent with this finding is the relatively high apparent conversion of organic matter to hydrocarbons, commonly ranging from 4 to 15 percent, in the majority of these samples, particularly from the Lower Cretaceous.

OFFSHORE AREAS

Oil and gas resources of the Outer Continental Shelf

Geologic assessments of undiscovered resources of oil and natural gas for several areas of the Outer Continental Shelf (OCS) that were proposed for leasing, including the Bristol Basin off Alaska, the Oregon-Washington OCS, the Central and Northern California OCS, and the South Atlantic-Blake Plateau continental margin, have been completed by a USGS team. The assessments (McCulloch and others, 1977; Snavely and others, 1977) suggest that significant quantities of undiscovered recoverable oil and gas may reside in these areas. The Bristol Basin of the Bering Shelf was considered to have

the greatest potential of these four areas with its undiscovered recoverable resources estimated to be 0 to 2.5×10^9 bbl of oil and 0 to 5.4×10^{12} ft³ of gas at the 95 percent and 5 percent probabilities of occurrence of the low and high ranges, respectively. This area was followed closely by the South Atlantic-Blake Plateau continental margin and the Central and Northern California OCS. The Oregon-Washington OCS appears to be least attractive.

Oil and Gas resources of the Gulf of Mexico

A new assessment of the undiscovered oil and gas resources of the western Gulf of Mexico clastic province from east of the Mississippi delta westward and southward to the United States-Mexico border has been completed by a USGS team. The team comprised B. M. Miller, R. S. Pike, E. W. Scott, R. B. Powers, G. D. Lambert, B. T. Vietti, K. H. Carlson, and William Markewich. They were assisted by R. J. Cassidy (USGS) and E. E. Remmenga (Colorado State University). The resource appraisal is a report on (1) assessments of the in-place undiscovered oil and gas resources by major stratigraphic units or depth intervals; (2) assessments of the distributions by size and number of the undiscovered oilfields and gasfields for each of the above units; (3) assessments relating to the distributions by depth of occurrence of the undiscovered resources; and (4) the projected finding-rates for crude oil and natural gas. The results of these assessments are reported in graphic form as probability and frequency distributions for the subprovinces or zones as defined by water depths of 0 to 200 m, 200 to 1,000 m, and 1,000 to 2,500 m within the Gulf of Mexico.

NEW EXPLORATION AND PRODUCTION TECHNIQUES

Detection of marine oil slicks as a petroleum exploration tool

Recent work by R. D. Watson, M. E. Henry, A. F. Theisen, T. J. Donovan, and W. R. Hemphill suggests the suitability of using a Fraunhofer Line Discriminator (FLD), operating in an imaging mode, to detect marine oil slicks. This technique may be used for reconnaissance exploration of submarine oil seeps as well as for pollution monitoring. Airborne measurements of the areal extent of oil from selected seeps in the Santa Barbara Channel in California displayed high sensitivity and real-time display of luminescence gray-level maps that include up to 94 gray levels. No change in luminescence with oil-film thickness occurs for the Santa Barbara

measurements owing to the high specific gravity of the oil. However, laboratory measurement on a suite of oil samples with lower specific gravities, ranging from 0.73 to 0.96, indicates positive correlation between oil-film thickness and luminescence.

Application of stable carbon isotopic ratios to exploration for deep-water source sediments

P. A. Scholle made analyses of the stable carbon isotopic ratios of carbonate carbon from chalks and related deep water limestones of Jurassic to Tertiary age. Closely spaced samples were collected from stratigraphically well-controlled sections in England, Germany, Italy, and Mexico. Preliminary results indicate that maxima carbonate carbon ratios (δC_{13} PDB $\cong +4.0$) occur near the Cenomanian-Turonian and Aptian-Albian boundaries. Minima ratios occur at the Turonian-Coniacian and Maestrichtian-Danian boundaries. These carbon isotopic variations have now been correlated in limestones from five European localities across more than 1,500 km. Apparently, the major positive carbon intervals also correlate with time intervals of accumulation of organic-rich black shales in the North Atlantic Basin as determined from DSDP drilling. Thus, this study may not only provide for isotopic correlation of sediments but also may serve as an indicator of time intervals of unusually high organic carbon preservation in basinal sediments. In turn, it might be predicted that Atlantic basinal sediments of Aptian and Albian, and to a lesser extent of Cenomanian-Turonian Age, may be economically significant source intervals for hydrocarbons.

Studies of eolian deposits aid production problems

Recent findings by T. S. Ahlbrandt that can be applied to petroleum production problems associated with eolianites (Lupe and Ahlbrandt, 1975) include: (1) statistical methods of differentiating eolian bedforms with strike and dip or borehole dipmeter data, (2) detailed analyses of primary and secondary structures in dune and interdune deposits, and (3) recognition within eolian deposits of indigenous hydrocarbon sources and burrows previously thought to be incompatible with eolianites.

Data from an eolian sand trap, developed by S. G. Fryberger and Ahlbrandt, demonstrate that field sand movement rates are less than predicted by wind tunnel studies because of armoring of dune and interdune surfaces. Short- and long-term pulses of wind energy may correlate to individual laminae and

beds, suggesting that the different laminae styles observed in eolian deposits may correspond to wind-energy level.

Application of helium surveys to petroleum exploration

Two new surveys by A. A. Roberts, T. J. Donovan, Mary Dalziel, and R. L. Forgey of the concentration of helium in soil gas over known petroleum reservoirs further demonstrate the utility of such surveys in oil and gas exploration.

A traverse was made across a newly discovered oilfield at Rublesanto, Guatemala, and off-structure southward to a second untested structure. Helium values were found to be high over the known oil reservoir and to drop to background off-structure. High helium values were not found over the second structure; this suggested that drilling there would be unsuccessful. A wildcat well being drilled at the time of the survey was subsequently found to be dry, proving the prediction of the helium survey.

A helium survey was also completed over the Cement oilfield near Chickasha, Oklahoma. A grid of about 150 samples showed an area of high helium values that had the same general shape and size as the oilfield and that lay directly over it. Thus, most of the producing and dry wells would have been correctly predicted had a helium survey been used as an exploration tool.

These two surveys support the hypothesis that near-surface helium anomalies can sometimes be used as indicators of buried petroleum deposits. The helium surveying technique has proved to be a quick, inexpensive, and environmentally non-destructive exploration tool under a wide variety of climatic conditions, from the tropical rain forest in Guatemala to the semi-arid plain in Oklahoma.

New seismic procedure for locating stratigraphic traps

Measurements of the attenuation of seismic waves, made by A. H. Balch, M. W. Lee, and R. T. Ryder, indicate that sand percentage in some rock formations can be estimated by measuring seismic attenuation. An empirical relation between seismic attenuation and sand percentage has been observed in the Minnelusa Formation (Pennsylvanian and Permian) in the Powder River basin in Wyoming. Measurements made in several parts of the Minnelusa in two wells invariably indicated that increased sand percentage was associated with an increase in seismic attenuation.

Vertical seismic profiling was used to make the attenuation measurements. This procedure involves

lowering a special geophone into a well on a conventional logging cable, energizing a seismic source at the surface, and measuring the resultant wave field in the earth. Important acoustic properties of the subsurface reflecting layers are thus measured. Some of these properties may be related to the presence or absence of petroleum. The procedure also permits a better interpretation of surface seismic data because reflected events can be traced from the surface to their source, deep in the ground. If the preliminary results from the Minnelusa Formation can be substantiated by further measurements, a valuable aid to seismic exploration may result.

Accuracy of borehole gravity data

Using the LaCoste and Romberg borehole gravity meter, J. W. Schmoker made repeated subsurface gravity measurements to determine the accuracy of the borehole gravity data and thus the precision of bulk densities calculated from the borehole gravity measurements. Schmoker found that the likelihood of poor interval gravity measurements increases sharply for intervals in the well >45 m, and increases approximately linearly with increasing time between readings. Contrary to expectations, data quality does not improve with the passage of time from the beginning of a survey. In a properly designed borehole gravity survey, the gravity difference between two points in a borehole can be measured to ± 10 μ gals. This translates to a density error of $\pm .02$ g/cm³ or less for vertical intervals >6 m.

Nonconventional natural gas resources

Joint appraisal by government and industry has been made of nonconventional (noneconomic) natural gas resources (gas-in-place), of recoverability of such resources, and of the estimated cost of such recoverability using currently developing production techniques. When experimental techniques such as massive hydraulic fracturing and chemical-explosive fracturing are used, the anticipated increase in natural gas production from tight or low-permeability (0.001–0.050 mD) gas reservoirs is possibly three to five times the production rate of conventionally completed gas wells. However, where a conventionally completed well produces tens of thousands of cubic feet of gas per day, and where a well with improved production techniques might produce a few hundred thousand cubic feet per day, such increased production would be only marginally economic.

OIL-SHALE RESOURCES

Lower Tertiary rocks in the southeastern Uinta Basin of Utah

W. B. Cashion's stratigraphic studies of lower Tertiary rocks in the subsurface of the southeastern Uinta Basin have permitted the delineation of alluvial, marginal lacustrine, and open lacustrine facies in intertonguing beds of the Wasatch (alluvial) and Green River (lacustrine) Formations. Lacustrine deposition became progressively more widespread from Paleocene into middle Eocene time. The sequences of complexly interbedded distal lacustrine and alluvial rocks are likely hydrocarbon traps.

Isolation of zones in oil shale with distinctive chemical characteristics using statistical techniques

Several objective statistical techniques were used by W. E. Dean to isolate six zones of distinctive chemical characteristics within the saline facies of the Green River Formation (Eocene) in the Piceance Creek Basin in Colorado. The data consisted of measured concentrations of Al, Si, Na, K, Ca, Sr, Fe, and S in a 232-m section of the saline facies in the Juhan 4-1 core hole (Dyner, 1974). Statistical techniques used for zonation included analysis of variance (Gill, 1970) and moving correlation coefficients (Dean and Anderson, 1974). Zones chosen by the statistical techniques largely reflect variations in amounts of nahcolite, dawsonite, and pyrite. Oil-yield zones appeared to be poorly correlated with the geochemical zones. However, high positive correlations between oil content and iron during periods of high salinity (as interpreted from zones of high nahcolite content) and low negative correlations between oil content and iron during periods of lower salinity suggested that the affect of organic content on iron diagenesis, probably through controls on pH and Eh, was maximized by whatever geochemical conditions were unique to the Green River lake during deposition of nahcolite.

Intertonguing of the Green River and Uinta Formations in Rio Blanco County, Colorado

Investigation by J. R. Donnell showed significant intertonguing between the Green River and Uinta Formations along the Cathedral Bluffs in the southwestern part of the Sagebrush Hill quadrangle of northwestern Piceance Creek Basin in Rio Blanco County, Colo. The upper part of the Green River Formation between the "Mahogany" bed and "Big 3" oil-shale zone (Pitman and Donnell, 1973) was

found to be approximately 122 m thick and consisted almost entirely of oil shale. In the northeastern part of the quadrangle the interval between the same stratigraphic markers was almost doubled and consisted of roughly equal amounts of oil shale (Green River Formation) and tongues of tuffaceous siltstone (Uinta Formation), three of which are well developed. In the Sagebrush Hill quadrangle the lowermost tongue of the Uinta Formation was found near the stratigraphic position of the wavy bedded tuff (Pitman and Donnell, 1973); it wedged out along a west-trending line approximately 3 km north of the southern boundary of the quadrangle. Earlier mapping in the quadrangle to the north showed that the Uinta tongue occupied intervals stratigraphically as low as the "Mahogany" marker (Pitman and Donnell, 1973).

Contact between the Parachute Creek Member of the Green River Formation and the Uinta Formation of south-central Piceance Creek Basin in Colorado

Recent mapping by W. J. Hail in the Mount Blaine quadrangle of Garfield County, Colorado, shows a southward stratigraphic rise in the contact between the Parachute Creek Member of the Green River Formation and the Uinta Formation; this rise was effected by intertonguing. Thus, most of the Uinta Formation as mapped to the north was found to be laterally equivalent to the upper part of the Parachute Creek Member as mapped in this part of the southern Piceance Creek Basin.

Geology of the Bates Knolls quadrangle of east-central Uinta Basin in Utah

G. N. Pipiringos completed geologic mapping of the Bates Knolls quadrangle of Uintah County, Utah. The base of the Uinta Formation as mapped by Keighin (1977) in the adjoining Cooper Canyon quadrangle to the east, was traced across the Bates Knolls quadrangle. However, many of the sandstone beds in the lower 158 m of the Uinta Formation were found to thin westward and were replaced by barren marl and low grade oil shale.

The "Mahogany" oil-shale bed, the richest oil-shale unit in the Parachute Creek Member of the Green River Formation averages about 2 m in thickness. It was traced completely across the southern part of the quadrangle, and underlies approximately 90 percent of the mapped area.

The Douglas Creek Member of the Green River Formation, which underlies the Parachute Creek Member, crops out in the southwest and south-east corners of the mapped area. In all areas ex-

amined, at least the upper 10 m were found to consist of sandstone whose matrix contained dried hydrocarbon.

Geology and oil-shale resources of the South Elko Basin in Nevada

Geologic mapping of portions of the Elko West and Elko East quadrangles of Elko County, Nevada, was completed by B. J. Solomon and C. A. Brook. Mapping revealed a maximum thickness of 375 m for the Elko Formation (Oligocene or Eocene) in the South Elko Basin.

The Elko Formation has been subdivided into five informal units: (1) chert-pebble conglomerate with interbedded lean oil shale and mudstone; (2) rich oil shale of approximately 25 m with interbedded siltstone and minor lignite; (3) lean oil shale, mudstone, and minor thin beds of calcareous siltstone and limestone; (4) basal tuffaceous siltstone overlain by lean oil shale, mudstone, siltstone, and minor tuff and lignite; and (5) basal air-fall tuff overlain by shale, siltstone, tuff, and ash beds. At the Laramie Energy Research Center, Department of Energy, analyses of oil shale from member 2 showed that the richest beds yield up to 357 L/t of oil.

Strata of the Elko Formation and associated Eocene and lower Oligocene rocks dip eastward and are transected by several north-trending normal faults. These rocks are unconformably overlain by subhorizontal beds of air-fall tuff and andesite. Biotite from the tuff, dated by E. H. McKee, gave a K-Ar age of 37.1 ± 1.0 m.y. A whole rock K-Ar date from the andesite gave an age of 31.0 ± 1.0 m.y. These early and middle Oligocene dates differ significantly from the late Miocene age that has been assigned to these volcanic rocks on previously published reconnaissance maps of the region. Such data, in conjunction with the faulted and tilted nature of the underlying lower Oligocene and older rocks, suggested that the South Elko Basin was subjected to tensional stress in the early Oligocene. Post-middle Oligocene Basin-and-Range crustal extension uplifted the South Elko Basin as a discreet block bounded by range front faults, with little concurrent deformation within the basin.

NUCLEAR-FUEL RESOURCES

Sedimentological guide to uranium deposits in southern Utah

Recent studies by Fred Peterson (U.S. Geol. Survey Circular 753) in the Henry Mountains mineral belt of south-central Utah showed that uranium de-

posits in the Salt Wash Sandstone Member of the Morrison Formation occur in sandstone beds that are closely associated with dark grey mudstone beds that were deposited in offshore lacustrine environments. Thus, locating the grey mudstone beds is an important guide to undiscovered uranium deposits, but because they are thin (<1 m thick), covered by talus or soil, or underground, methods other than direct identification are needed to locate the areas most likely underlain by the grey mudstones. An indirect method of determining the approximate location and areal extent of the grey mudstones is based on their lateral gradation shoreward into marginal lacustrine sandstone beds that are more conspicuous and easier to recognize. The marginal lacustrine sandstones generally contain 80 percent or more horizontally laminated bedding, are moderately to well sorted, do not vary appreciably in thickness, and locally are well burrowed. The lacustrine sandstones are readily distinguished from the numerous fluvial sandstone beds in the region in that the fluvial sandstone beds contain about 10–30 percent horizontal laminations, are poorly to moderately sorted, vary in thickness because of scours and channels at the base, and generally lack burrows. The area with the highest probability of containing the grey mudstones and associated uranium deposits lies in an offshore direction from the marginal lacustrine sandstones. This relationship can be a helpful exploration guide to undiscovered uranium deposits, and it can be used in subsurface studies where cores, cuttings, and geophysical logs are available.

Uranium in the Date Creek Basin area of west-central Arizona

Uranium occurs in Eocene(?) and Miocene(?) tuffaceous, carbonaceous lacustrine rock in the Date Creek Basin of west-central Arizona. The total resources of the basin are estimated by J. K. Otton to be [50 to 100] 4.57×10^3 t of U_3O_8 in low-grade ores (0.03 to 0.1 percent). The Chapin Wash Formation (Miocene?) is the most important host unit, with occurrences at the Anderson mine, Black Butte, and the Lincoln Ranch Basin. At these localities, uranium is associated with tuffaceous siltstones and mudstones, rich in organic debris, which have been partly silicified. The Anderson mine is presently undergoing development by Union Minerals and Uranengesellschaft. Uranium also occurs in the basal part of the Artillery Formation (Eocene?) near Artillery Peak and in the Ester Basin.

Genesis of tabular uranium bodies in Triassic and Jurassic basins in Eastern United States

Field studies conducted by C. E. Turner-Peterson in the Newgate mine area of the Hartford Basin in Connecticut provide new evidence that uranium mineralization in the Triassic and Jurassic basins of the eastern United States is facies controlled. The model proposed to explain mineralization in the Newark Basin of Pennsylvania and New Jersey (Turner-Peterson, 1977) requires the intercalation of nearshore lacustrine flat-laminated to massive sandstones with offshore lacustrine black mudstones in the mineralized areas. In this model, pore-water chemistry and hydrology would have favored mineralization of the sandstones during early burial, with humic acids being supplied by the compacting mudstones and uranium being supplied by ground water. If the model has validity, a similar facies relationship is to be expected in association with other uranium occurrences in similar basins. The presence of flat-laminated to massive lacustrine sandstones and offshore lacustrine black mudstones in association with uranium in the Newgate mine and vicinity therefore lends support to the model.

Examination of facies in the Gettysburg Basin of Pennsylvania and the Danville-Dan River basins of Virginia and North Carolina indicates that lacustrine facies similar to those in the Newark Basin occur in other Triassic and Jurassic basins of the East. The nearshore lacustrine sandstone facies of these basins may therefore be good exploration targets. The model proposed for the Newark Basin and extrapolated to other Triassic and Jurassic basins of the East also has bearing on the genesis of tabular ore bodies in general, in particular those of known lacustrine associations such as in the Basin and Range province.

Uranium mineralization at the Upper Cretaceous Fox Hills Sandstone—Lance Formation interface

Studies by H. W. Dodge, Jr., of the northeastern Powder River basin in Wyoming and southeastern Montana indicate that uranium mineralization at the Upper Cretaceous Fox Hills—Lance (Hell Creek) interface is patchy and quite variable in quality. Where seen, mineralization is generally confined to organic-rich, thin-bedded siltstone and sandstone interbedded with claystone. These sediments were deposited in ancient estuaries and tidal flats. Organic plant detritus was concentrated at the freshwater-saltwater interface during and following a period of fluvial erosion, which cut into offshore-marine and transitional-marine shale and fine-

grained sandstone, and into shoreface and beach sandstones.

Uranium in Triassic rocks in southeast Utah

In southern Utah, R. D. Lupe found that the Chinle Formation (Upper Triassic) was deposited as a series of fluvial-lacustrine sediments. Regionally, uranium mineralization is related to these environments. Significant uranium deposits exist in areas dominated by the transition between proximal and distal braided stream deposits in the lowest part of the Chinle. Locally, rocks that host uranium were deposited low in the alluvial plain, in low energy, distal environments, such as abandoned channel fill, point bar deposits, and Gilbert-type delta deposits. Features common to rocks of these distal environments, which may have influenced uranium mineralization, include lenticular geometry, a complex distribution of porosity and permeability, and the presence of clays and preserved plant material. These host-rock bodies are spottily distributed because of their depositional habit and erosion by the overlying, extensive proximal braided stream deposits. The sandstones of these braided stream deposits probably served as the conduits for mineralizing solutions. This geologic model for the relationship between depositional environments and uranium in the Chinle was used to assess resources for a 15,000 km² area in the San Rafael Swell-Moab region. The formation contains between 30,000,000 to 70,000,000 kg U₃O₈ in grades similar to that produced to January 1977.

Facies change related to ore deposition

Sites of uranium ore deposition in the Powder River basin of Wyoming are, in part, spatially related to facies changes in the Wasatch Formation. By plotting sandstone-mudstone ratios calculated from subsurface data, E. S. Santos found that a high-energy facies with ratios greater than 1.0 makes up the formation near the southern and western margins of the basin. Eastwardly, across the southern part of the basin, there is a progressive change to where the ratios are less than 0.5 near the eastern extent of the formation in the basin. All of the uranium ore deposits in the Turnercrest and Pumpkin Buttes areas occur where sandstone-mudstone ratios are less than 1.0. Those deposits near the southern margin of the basin occur where the ratios are greater than 1.0 but extend to areas where the ratios are less than 0.5. The data indicate that the sediments in the southern part of the basin

were introduced from the south and west. Ore deposition tends to occur in sandstone units that extend out from the high-energy facies into areas where the Wasatch Formation is mostly shale and siltstone.

Uranium deposits at Copper Mountain in Wyoming

As a result of mapping by R. E. Thaden, uranium deposits of possible economic significance appear to be confined largely to rocks within a complex east-west-trending, 3- to 8-km-wide, graben along the south face of Copper Mountain in central Wyoming. The fault at the south margin of the graben separates the Wind River Formation of early Eocene age on the south from the graben-filling Wagon Bed Formation of middle and late Eocene age. Precambrian and Paleozoic rocks, as well as rocks of the Wind River Formation, crop out in subsidiary horsts within the main graben. The north fault is an extensive zone of faulting in the Precambrian granite.

The known deposits of uranium are confined largely to a basal conglomerate in the Wagon Bed Formation and to broken zones in the granite near the north side of the graben. Ponding, or redirection of the movement of ground water north (updip) of the south fault resulted in extensive decomposition of the granite and extensive zeolitization of the Wagon Bed, possibly releasing and transporting uranium from both units. The north fault zone was the avenue of access of petroliferous fluids, now inspissated, from Cretaceous rocks at depth, which may have acted as the principal reductants for the precipitation of the uranium. Humic matter incorporated in surface waters that flowed southward across the granite north of the graben may also have been an important component of the reducing agents.

Neither the geology nor the structure, as presently understood, precludes the existence of concentrations of uranium within the zone of ponding in the graben for perhaps 10 km, both east and west, of those uranium concentrations now known.

Uranium potential of the Lower Cretaceous, Piceance Basin of Colorado

Studies by L. C. Craig have identified two relatively thick lobes of sandstone in the Burro Canyon Formation (Lower Cretaceous) that extend beneath the southwest margin of the Piceance Basin, one lobe near Whitewater and one lobe near Delta, Colo. These lobes might have served as "pipelines" for the transport of uranium-bearing solutions. If a reductant was present in the sandstone in the sub-

surface of the basin, uranium might have been deposited at an oxidation-reduction interface. The size of such deposits is difficult to predict, but analogy with known uranium deposits in sandstone of this stratigraphic position suggests that they might range from scattered deposits containing only a few tons of ore to one or more multimillion-ton deposits.

Stratigraphic relations in the Whitsett Formation in south Texas

The Calliham and Tordilla Sandstone Members of the Whitsett Formation (Upper Eocene) in south Texas have been considered by Eargle (1972) to be stratigraphic equivalents. He used the term Tordilla for a fine-grained beach sandstone unit in western Karnes County and the term Calliham for medium to coarse-grained sandstone deposited in distributary channels in Atascosa and McMullen Counties to the southwest. Studies by K. A. Dickinson of new exposures provided by the uranium mining in Karnes County show that the Calliham channels were scoured into the Tordilla beach sand, and though they are deposited physically at about the same horizon, the Calliham deposits are younger. The Calliham is equivalent in age to the Fashing Clay Member, which overlies the Tordilla in Karnes County.

Character of the conglomerate of the Shinarump Member of the Chinle Formation at Window Rock in Arizona

According to R. E. Thaden, the Shinarump Member of the Chinle Formation (Triassic) cropping out on the flanks of the Defiance Upwarp near Window Rock, Ariz., bears many of the characteristics that accompany uranium orebodies elsewhere on the Colorado Plateau and are thought to be requisite for the deposition of ore. Near Window Rock it is 20 to 22-m thick except where it has incised paleochannels into the upper part of the De Chelly Sandstone (Permian). The channels underlie 2 to 10 percent of the formation and are incised as much as 11 m. The largest known channel is 180 m wide and 5,560 m long. Scour pockets in the base of the channels were detected on surface outcrops and can be seen in channel cross sections exposed in the walls of canyons cut on the flanks of the Defiance Upwarp. The channels, trending northwest to north-northwest and showing northerly sediment transport, branching, and anastomosing, contain abundant clay and abundant fossil vegetation including retained carbonaceous trash. The channels also have bed access to organic fluids both from the Shinarump and from the overlying part of the Chinle Formation

(Triassic). The Shinarump is confined under relatively impermeable clayey zones of the basal part of the Chinle in many places.

Uranium possibilities of Marfa Basin in Texas

The Marfa Basin in southwestern Texas offers good potential for uranium deposits. C. C. Reeves, Jr. (1974), in discussing exploration possibilities for Tertiary and Quaternary fill of the basin, has pointed out that “* * * uranium shows, uraniferous source rocks, and the existence of alluvial and lacustrine host rocks suggest the possibility of classic uranium roll fronts within the basin fill.”

Field reconnaissance and consultation of geologic reports by C. T. Pierson and M. W. Green indicate the presence at the basin margins of (1) possible source rocks consisting of Tertiary alkalic igneous rocks containing as much as 50 ppm U_3O_8 ; (2) a number of ore-grade uranium occurrences as disseminations in Tertiary carbonaceous sandstone and freshwater limestone, as well as vein-type occurrences in Tertiary igneous rock; (3) permeable sandstones and conglomerates that could act as conduits for uranium-bearing solutions, or as host rocks for deposits; (4) interstratified siltstone and mudstone aquicludes; and (5) uranium-precipitating carbonaceous material in the form of lignite interbedded with freshwater limestone, and as plant debris in the clastic rocks.

Examination of the basal part of the Tertiary clastic-volcaniclastic sequence exposed along the eastern margin of the basin showed that a general decrease in the energy levels of the depositional environment of the rocks takes place from a high level in the Chisos Mountains-Lajitas area along the Rio Grande River to a low level in the Anderson Ranch area 90 km to the north. At the Anderson Ranch, uranium occurs in lignite interbedded with lacustrine limestone of the “Pruett Formation” of Eocene(?) or late Eocene age. At the 02 Ranch, 25 km south of the Anderson Ranch, uranium is found in carbonaceous fluvial sandstone and conglomerate of the so-called Pruett.

Efficient search for uranium deposits in the Marfa Basin, which according to Shurbet and Reeves (1977, p. 612) contains a 6,000-ft thickness (1,829 m) of Tertiary and Quaternary basin fill, will require detailed outcrop studies of facies trends as well as availability of sufficient subsurface information to trace these trends into the basin as a guide to drilling.

Uranium mineralization in the Morrison Formation at the Dennison-Bunn Prospect in New Mexico

Uranium investigations by J. L. Ridgley in outcrops on the eastern margin of the San Juan Basin have shown that uranium mineralization at the Dennison-Bunn claim (Chenoweth, 1974) south of Cuba, N. Mex., occurs in stacked fluvial channel sandstones of the Westwater Canyon Member of the Morrison Formation. Based on the configuration of the channel sandstones and on the pattern of uranium mineralization at the outcrop, the channel sandstone beds and uranium deposits appear to be elongate east to west. The uranium deposits, ranging from 0.001 to 0.067 percent U_3O_8 , are irregular in cross section. Generally, iron-mineral concentrations separate oxidized from unoxidized rock. Such a configuration suggests the deposits may be related to the formation of small roll-fronts within the channel sandstones of the Westwater Canyon Member.

Geology and mineral resources in north-central Arizona

General geologic studies and mineral-resource assessment of the Paria Plateau-House Rock Valley area in north-central Arizona determined the area to be only moderately favorable for the discovery of additional small deposits of uranium in sandstone formations of Triassic age. The potential for economic quantities of other minerals in the area is considered low to non-existent. The studies and assessments were made by M. W. Green and C. T. Pierson (Green and others, 1977) for incorporation into the Navajo Land Selection Environmental Impact Statement now being prepared by the U.S. Bureau of Indian Affairs.

The area, which is located on the southwestern edge of the Colorado Plateau physiographic province in an area underlain by about 5,000 m of fossiliferous marine and continental sedimentary rock ranging in age from Precambrian through Quaternary, is bounded on the west by the East Kaibab monocline and on the east by the Echo monocline. The Paria Plateau, bounded on the south by the scenic Vermillion Cliffs, is composed of continental red beds of Triassic and Jurassic age.

With the exception of a relatively small quantity of uranium mined from sedimentary rocks of Late Triassic age (Shinarump Member of the Chinle Formation) near Lee's Ferry on the east side of the Paria Plateau, mineral resources have not been found in the area, even though oil, gas, helium, and coal have been produced from similar strata in

adjacent areas to the north in the Kaiparowits Basin and to the east in the Black Mesa Basin.

Intermontane basin uranium occurrences in Arizona

Field reconnaissance by C. S. Bromfield in three widely separated intermontane basins in Arizona showed uranium to occur in several ages and types of basin host rocks. Occurrences along the south flank of the Muggins Mountains in the Gila Valley near Yuma are in Miocene lacustrine mudstones and limestone. At the north foot of the White Hills on the east side of Detrital Valley in Mohave County, anomalous concentrations of uranium occur in the Pliocene part of the Muddy Creek Formation through a 50-m-thick section of limestone, mudstone, sandstone, and minor gypsum. Here the highest concentrations of uranium, judged by radiometric readings, are in the limestones. Occurrences in the Gila Valley, about 25 km southeast of Safford at the northwest end of the Whitlock mountains, are in Pliocene and Pleistocene paludal-lacustrine marl, mudstone, diatomite, and silty sandstone. The best concentrations of uranium appear to be in a several-meter thick diatomaceous zone. Also in the Gila Valley, an anomaly was found during this study in Pliocene and Pleistocene lacustrine limestone located 60 km northwest of Safford.

In all three of these widely scattered Arizona basin-fill localities, regardless of host rock, lithology or age, the highest concentration of uranium is in association with silicification that produced irregular cherty or opaline layers and nodules, and in lacustrine beds lying unconformably on or near older Tertiary volcanic rocks.

Uranium, thorium, and gold in Precambrian conglomerate in Black Hills, South Dakota

The Estes Conglomerate (Precambrian X), near the village of Nemo in Lawrence County, S. Dak., is primarily a poorly sorted, polymictic conglomerate. However, F. A. Hills has found that part of the Estes consists of beds of well sorted quartz-pebble and quartzite-pebble conglomerate, which have several of the characteristics of gold-uranium conglomerates in the Witwatersrand district of South Africa and in the Elliot Lake district of Ontario. The well sorted beds contain anomalous concentrations of uranium, thorium, and gold; and pyrite is abundant in the matrix of these beds.

The Estes Conglomerate lies unconformably on the Benchmark Iron-formation, a banded specularite-magnetite-quartz rock, and although some of the

poorly sorted nonradioactive beds of the Estes contain abundant pebbles and grains of iron-oxide minerals derived from the Benchmark, detrital grains of magnetite and hematite are scarce in the well sorted, pyrite-bearing, radioactive beds. In the radioactive beds, detrital iron-oxide minerals are partially replaced by pyrite, and banded pebbles derived from the Benchmark Iron-formation show replacement rimming of the iron-oxide minerals by pyrite near the surfaces of pebbles, but iron-oxide minerals remain in pebble interiors. Evidently sulfidization of iron oxides occurred during diagenesis or during metamorphism.

Although economic concentrations of uranium, thorium, and gold are not yet known in the Estes Conglomerate, the well sorted beds of the Estes constitute good exploration targets for all three. Up to 100 ppm of uranium, 800 ppm of thorium, and 1.4 ppm of gold were found in samples of Estes Conglomerate that was collected from outcrop. An average Th-U ratio of approximately 7 was determined. However, lead isotope analyses indicate (1) that during weathering uranium has been severely leached relative to thorium and (2) that the average Th-U ratio of radioactive conglomerate below the zone of leaching is probably between 2 and 3.

Uranium-bearing, quartz-pebble conglomerate found in Sierra Madre, Wyoming

Uranium bearing, quartz-pebble conglomerate has been discovered by P. J. Graff and R. S. Houston in the Sierra Madre in Wyoming. This pyritic quartz-pebble conglomerate is similar to that reported earlier in the Medicine Bow Mountains of southeastern Wyoming. This uraniferous conglomerate is in metasedimentary rocks that equate to the "Deep Lake Formation" of middle Precambrian age in the Medicine Bow Mountains. It has been mapped in five localities of the northwestern Sierra Madre. The quartz-pebble conglomerate has been traced for 4.8 km in one outcrop, and this conglomerate exceeds 100 m in thickness, locally. Oxidized surface samples contain up to 131 ppm uranium. Inasmuch as uranium is probably largely removed from surface outcrops by weathering, these conglomerates may contain commercial quantities of uranium at depth.

Emplacement of uranium into Midnite mine deposits

Several hypotheses of uranium emplacement into uranium deposits of the Midnite mine in Stevens County, Wash., have been developed by J. T. Nash

(1977) including (a) penesynthetic accumulation during sedimentation or diagenesis of the Togo Formation, (b) hydrothermal emplacement during or following intrusion of a radioactive quartz monzonite, and (c) supergene introduction after the pluton was exhumed in the Eocene. The hydrothermal hypothesis is favored because of the apparent restriction of uranium mineralization to zones of pre-intrusion faulting and unusual amounts of fluid release (evidenced by abundant aplite and pegmatite). According to the hydrothermal hypothesis the magma became saturated in volatiles in a volatile-rich, oxidizing zone at the top of the pluton, and upon pressure release, a uranium-rich fluid evolved and uranium was transported upward and outward. The uranium was reduced and fixed in metapelite wallrocks by reaction with iron sulfides or graphite. The metamorphic aureole probably contained relatively low concentration of uranium that was later leached and redeposited in permeable zones to create ore.

Structural and lithologic controls for uranium at the Pitch mine in Colorado

Preliminary studies of complexly faulted sedimentary rocks in the Pitch mine in Saguache County, Colo., by J. T. Nash in collaboration with geologists of Homestake Mining Co. clarify the structural and lithologic controls on ore distribution. Oxidized and reduced uranium minerals occur in highly fractured and internally faulted rocks of the Leadville Limestone (Mississippian) and Belden Formation (Pennsylvanian) in a reverse fault zone adjacent to Precambrian granite and schist. Coarse to very fine sandstone, shale, and coal of the Belden Formation occur in thin fault slices along with dark gray and rusty dolomite of the Leadville Limestone. Dark dolomite, containing dispersed fine-grained pyrite, is a favored host for uranium where the dolomite is thoroughly brecciated. Oxidation of pyrite creates rusty dolomite to depths of more than 125 m; this rock now contains little or no uranium. Sandy and coaly rocks of the Belden are less favored hosts, and mineralization in them generally produced low uranium concentrations.

High radioactivity in basement rocks of Michigan

Reconnaissance studies of the lower Precambrian (>3,000 m.y. old) granites and granitic gneisses that constitute most of the exposed basement complex in the region between the Marquette iron district in northern Michigan and the Iron Mountain

area of Michigan reveal that many have significantly high radioactivity. M. R. Brock reports that levels of radioactivity are approximately three to five times those obtained on granites and granitic gneisses in the younger (2,750–2,700 m.y. old) complex located to the north of the Marquette iron district.

The southern complex with its higher content of uranium and thorium, and adjacent sedimentary basins, offer good potential for resources of these two metals in the form of large, low-grade deposits as well as lode deposits within crosscutting shear zones. Anomalous concentrations of uranium ranging between 0.01 and 0.9 percent U_3O_8 (Kallio-kowski, 1976) occur in these environments within the region but, as yet, no exploitable deposits have been detected. Targets showing the best potential include: biotite-rich variants within the granitic rocks, such as schlieren, greissen, and pegmatoid bodies; shear zones located in the more radioactive rocks and black slates; supergene-enriched fracture zones beneath erosional unconformities which are, or have been, overlain by coarse clastic sedimentary rock; and quartz-pebble conglomerates and phosphatic zones in sedimentary rocks of lower middle Precambrian sequence.

Stratigraphy of volcanic rocks as a guide to uranium in the Thomas Range, Utah

The stratigraphy in volcanic rocks in the Thomas Range and Drum Mountains of Utah is being revised on the basis of new geologic mapping and dating. According to D. A. Lindsey, the following four groups of volcanic rocks are now recognized: (1) flows, agglomerates, and tuffs of intermediate composition (41 m.y.); (2) rhyolitic ash-flow tuffs (30–38 m.y.); (3) tuffaceous sediment, water-laid tuff, and topaz rhyolite (21 m.y.); and (4) water-laid tuff and topaz rhyolite (6–7 m.y.). Each group overlies an angular unconformity. Unconformities beneath the third and fourth groups are overlain by porous volcanoclastic rocks that should be excellent hosts for uranium. This conclusion is confirmed by the occurrence of every known deposit of uranium and beryllium (which uranium commonly accompanies) in tuff and sandstone of the third group near Spor Mountain, in the Thomas Range.

Uranium and Tertiary volcanic rocks in the Marshall Pass district of Colorado

In the Marshall Pass district of Colorado, geologic mapping by J. C. Olson has shown that siliceous ash-flow tuff and waterlaid tuff, as well as andesitic flows, probably covered most of the district before

being partially removed by erosion. Patches of welded tuff atop Lime Ridge, 1.4 km north of the Pitch mine, together with larger areas of the same rocks to the south near Marshall Creek, suggest that the base of the tuffs may have been very near parts of the uranium deposits. At the time of deposition of the tuffs, the Precambrian crystalline rocks on the east side of the Chester fault probably stood above the Paleozoic sedimentary rocks to the west as a faultline scarp, against which the Tertiary volcanic rocks accumulated. The siliceous tuffs are of interest as a possible source for the uranium in the uranium deposits of the district. The only Tertiary intrusive rocks that have been found in the district are two small rhyolite plugs, 150×225 m and 275×450 m in size. The larger plug is exposed on both sides of Duncan Creek just above its confluence with Marshall Creek, and the smaller plug is about 200 m southwest of the larger plug. The rhyolite plugs cut and are therefore younger than the dark andesite flows of Tertiary age that are common in the southern part of the district.

Uranium studies in western Alaska

Field mapping of the Eagle Creek alkaline dike swarm in the southeastern Seward Peninsula of Alaska was completed by T. P. Miller and B. R. Johnson. These alkaline dikes occur as part of a Cretaceous dike swarm covering over 250 km² in the southeastern Seward Peninsula and contain anomalous amounts of uranium, generally in the range of 35 to 80 ppm. The dikes typically consist of bluish-gray, fine-grained to slightly porphyritic dense pulaskite; other varieties are more coarse-grained, brownish-gray, and contain abundant pseudoleucite phenocrysts as much as 3 cm across. The dikes are 3 to 15 m thick, obtain lengths of 2.5 km or more, and are steeply dipping with a consistent northeast strike. Most of the dike swarm occurs inside the large composite Kachauik pluton composed of monzonite, syenite, and granodiorite; a smaller number of dikes occur in the Precambrian schistose marble country rock.

The alkaline dikes have sharp contacts and are crosscutting. Some alkali metasomatism has occurred in granodiorite immediately adjacent to the dikes, resulting in a decrease in the amount of quartz and the formation of aegerine and riebeckite. Metasomatism in syenite wallrock adjacent to the alkaline dikes has resulted in the formation of nepheline and allanite.

Allanite-rich replacement bodies occur in syenite in the north central part of the dike swarm. These

bodies occur on either side of a pulaskite dike at distances as close as 3 m and as far away as 300 m. These allanite-rich syenite bodies contain as much as 1,500 ppm uranium and 9,500 ppm thorium. It is suggested that the uranium and thorium in these dikes is related to a late uranium-rich magmatic episode in the emplacement of the Kachauik pluton. This magmatic pulse resulted in the formation of replacement uranium-thorium deposits consisting of allanite-rich pegmatitic zones in monzonite-syenite country rock.

An occurrence of parsonite, a secondary uranium mineral, in west-central Alaska

Parsonite, a hydrous phosphate of lead and uranium, was identified as occurring in alaskite of the Wheeler Creek pluton in the Purcell Mountains of west-central Alaska by T. P. Miller. The parsonite occurs as soft earthy yellow to brown mineral coating fracture surfaces in a narrow (<16 m wide), strongly radioactive fracture zone in the alaskite. The identification was confirmed by X-ray diffraction.

This is the first reported occurrence of secondary uranium minerals in west-central Alaska and suggests the possibility of primary uraninite in the uraniumiferous alaskite and (or) secondary enrichment of uranium.

Stable isotope studies of thorium-bearing veins in the Wet Mountains of Colorado

Thorium-bearing quartz-barite veins are genetically and spatially related to three Cambrian alkalic complexes that intrude Precambrian Y metamorphic rocks in the Wet Mountains area of Colorado. According to T. J. Armbrustmacher, these veins are found throughout a 100 km² area and are typically vertical, about 1 m thick, and occur chiefly along structures in the Precambrian rocks, some of which can be traced for over 10 km. In addition to varying but usually abundant amounts of smoky quartz and barite, the veins commonly contain specular and earthy hematite, goethite and microcline, irregular amounts of calcite, thorite, and galena, and sparse amounts of pyrite, chalcopyrite, dolomite, chlorite, siderite, cerussite, xenotime, brockite, sphalerite, rutile, and other minerals. Small euhedral vugs in the veins suggest the hydrothermal dissolution of earlier phases. Studies of light stable isotope minerals in the veins by R. O. Rye show that physical-chemical conditions for thorite deposition were remarkably uniform throughout the area. The $\delta^{18}\text{O}$

values of quartz range from 9.3 to 12.1 permil and indicate that the hydrothermal fluids had a uniform thermal history throughout the area. The $\delta^{34}\text{S}$ values for coexisting barite and galena range from 5.1 to 8.1 permil and -14.1 to -24.3 permil, respectively, and suggest that the hydrothermal solutions derived their sulfur from igneous sources and that vein deposition occurred under a rather limited range of pH and fO_2 conditions.

Multiple-intruded carbonatite dike in the Wet Mountains of Colorado

Two distinct types of carbonatite occur side-by-side to form a multiple-intruded dike at McClure Gulch in the Wet Mountains area of Colorado, according to T. J. Armbrustmacher, I. K. Brownfield, and L. M. Osmonson. One type, sulfide-bearing carbonatite, consists mainly of white calcite surrounding dark brown knots of iron-oxide-stained dolomite and pyrite; small amounts of synchisite, bastnaesite, ancylite, strontianite, barite, and iron oxide minerals are also present. The other type, coarse-grained carbonatite, consists of coarse-grained calcite with minor amounts of barite, biotite, apatite, and rare-earth minerals. The multiple nature of this dike and certain details of the mineralogy and geochemistry are thus far unique when compared with other carbonatite dikes that occur in the vicinity of the intrusions of the Wet Mountains alkalic province.

Iron sulfide minerals and sulfur isotopes associated with roll-type uranium deposits

R. L. Reynolds and M. B. Goldhaber found significant similarities and differences in the mineralogy and texture of iron-sulfide minerals associated with five roll-type uranium deposits in Wyoming and Texas. At least two temporally distinct episodes of sulfide formation are present in each deposit. The earlier episode of sulfidization, constituting a necessary form of host-rock preparation, preceded uranium mineralization. In deposits that contain carbonaceous matter, pre-ore iron sulfides are primarily framboids and related textures of probable bacterial origin. In deposits that lack indigenous organic debris, pre-ore iron sulfides, dominantly pyrite, occur as replacements of detrital iron-titanium oxide minerals, as interstitial cement, and as large euhedral crystals. Framboids are absent in these deposits. In each deposit, marcasite, formed as a result of a mineralization process, occurs as rims around pre-ore pyrite adjacent to the redox boundary. In a deposit containing carbonaceous matter, ore-stage marcasite

is confined to zones within about a meter of the redox boundary, whereas in organic-free deposits ore-stage marcasite may extend several meters above and below the redox boundary. The distribution of marcasite may reflect zonation of pH conditions related to hydrogen-iron production and consumption as influenced by the absence or presence of carbonaceous matter. Post-mineralization introduction of fault-derived H_2S into the host rock of two deposits in south Texas led to a third generation of iron-sulfide minerals. In zones beyond the former oxidized tongue in both re-reduced deposits, pyrite related to the last stage of sulfidation rims both pre-ore pyrite and ore-stage marcasite.

In one of the re-reduced deposits, petrographic study has, to date, not produced criteria for independently recognizing the former oxidized tongue. However, stable isotopic analysis of sulfide minerals by Goldhaber, Reynolds, and R. O. Rye does provide such criteria. Sulfide minerals outside the inferred position of the formerly oxidized tongue are isotopically light (enriched in ^{32}S compared to ^{34}S). The ^{34}S values range from -26 to -46 permil in these sands. Sulfur isotopes from the formerly oxidized tongue are comparatively heavier ($+26$ to -13 permil) and are systematically distributed, with the isotopically heavy sulfides grading to lighter sulfides with distance updip. The lightest sulfide in this sequence, -13 permil, occurs 1 km updip from the nose of the roll. If it is assumed that the source of sulfide is located downdip from the present roll, then it follows that the mechanism of isotopic fractionation between fault-derived H_2S and solid-phase sulfides is via partial equilibration of the two sulfur reservoirs. Sulfur isotopic equilibrium of this type has not previously been recognized in low temperature ($<100^\circ C$) systems. The striking isotopic contrast between sulfides in ore and those related to the re-reduction episode suggests that stable isotope measurements may be effectively used in exploration programs in south Texas.

Pyrite oxidation and the origin of roll-front uranium deposits

Research by M. B. Goldhaber in collaboration with R. L. Reynolds has been directed toward understanding the role of pyrite oxidation in forming sedimentary roll-front uranium deposits. Two previously proposed genetic models for these deposits suggest either bacterially produced sulfide, or abiologically generated metastable sulfur species such as thiosulfate ($S_2O_3^{2-}$) as the sulfur source for ore-stage pyrite. Pyrite oxidation by ground water

is considered to be the source of sulfate for bacterial reduction, or alternatively, the mechanism for generation of metastable sulfur species. Under acidic conditions the oxidation of pyrite is known to proceed by a rapid reaction with ferric ion to produce ferrous iron and sulfate ion. Because this mechanism requires ferric iron in solution, it is unlikely to apply to roll-front formation. Iron oxides and oxyhydroxides have been observed in both Texas and Wyoming deposits whose textures are pseudomorphic after pyrite. Such textures imply incomplete dissolution of the iron component during sulfide oxidation. The experiments were conducted at constant pH, controlled temperature and constant oxygen concentration. Rate of addition of base necessary to maintain a constant pH was monitored. Samples were withdrawn periodically and analyzed for total sulfur in solution, thiosulfate, tetrathionate ($S_4O_6^{2-}$) and sulfide (SO_3^{2-}). At pH 6 and an oxygen concentration of 0.33 millimolar, half the aqueous sulfur occurs as tetrathionate and the remainder is sulfate. As pH increases at a constant oxygen concentration, tetrathionate and sulfate both decrease at the expense of thiosulfate and sulfite. The rates of hydrogen-ion generation and iron-oxide formation were found to increase markedly with increasing pH. Oxidation at pH greater than neutrality was shown to produce pseudomorphic textures similar to those observed in the deposits. These results are consistent with, but do not prove, an abiological origin for some uranium rolls.

Geochronology of uranium ores

A study by K. R. Ludwig of the U-Pb isotope apparent ages of uranium ores and ore-minerals from the Gas Hills and Crooks Gap districts in Wyoming shows that mineralization in both districts occurred sometime in the interval of 55 to ~ 26 m.y. ago. This conclusion was reached from analyses of U-Pb isotopes in 15 ore samples and 14 uraninite-coffinite or pyrite mineral separates, and it firmly establishes an Oligocene or pre-Oligocene time of last major uranium mineralization.

An investigation by Ludwig into the magnitude of the effects of initial radioactive-daughter disequilibrium on the U-Pb isotope and apparent ages of very young uranium ores has shown that a surprisingly large effect exists even at ages of several million years. Typical low-temperature uranium ores form with very low $^{230}Th/^{238}U$ and $^{231}Pa/^{235}U$ activity ratios and so are markedly out of radioactive equilibrium for several half-lives of ^{230}Th and ^{231}Pa .

The effect on the stable Pb daughters, however, persists to much longer times than necessary to attain secular equilibrium, so that the error in assuming secular equilibrium is over 10 percent at 1 m.y. and still analytically significant at 30 m.y. Thus, rigorous evaluation of the U-Pb isotope apparent ages of young, closed-system U-ores, must take into account this effect.

Analyses by Ludwig of cogenetic zircon, apatite, and uraninite mineral suites from granitic rocks of the Granite Mountains in Wyoming have given the most accurate and precise age dates yet from these rocks and have distinguished two intrusive events of similar ages in the area. An earlier granite was emplaced at $2,640 \pm 20$ m.y. ago, followed by a much larger body of granite at $2,595 \pm 40$ m.y. ago. Both granites suffered isotopic disturbance during Laramide uplift. Analyses of epidote, zircon, and apatite from silicified/epidotized zones in the 2,595 m.y. old granite further revealed that these altered zones were probably formed deuterically from the host granite, and that an early middle Proterozoic disturbance affected the region.

Electron microprobe analyses of uraninite and coffinite

Electron microprobe analyses of uraninite and coffinite by R. I. Grauch indicate that both uranium phases contain essential calcium and silicon. Samples of coexisting uraninite and coffinite pairs from three different uranium deposits (Gas Hills and Crooks Gap, Wyo., and Woodrow Pipe, N. Mex.) have been analyzed. Although the absolute values of the measured elemental quantities may not be accurate because of uncertainties in the standards and correction procedures, the values are at least internally consistent and indicate that both phases have variable amounts of uranium, calcium, and silicon. Uranium has been assigned a valence value of +4 because both uraninite and coffinite are historically considered to be "reduced" phases, and in the case of uraninite the measured values of uranium are consistent with a unit formula calculation using UO_2 , not U_3O_8 . Uraninite compositions are in the range: UO_2 , 93 to 95 weight percent; CaO, 1.4 to 3.2 weight percent; and SiO_2 , 2.9 to 6.1 weight percent, with sums of oxide weight percent from 100.7 to 101.4. Coffinite compositions are in the range: UO_2 , 76.9 to 82.3 weight percent; CaO, 1.0 to 2.4 weight percent; and SiO_2 , 13.4 to 15.6 weight percent, with sums of oxide weight percent from 93.8 to 98.0. The consistently low oxide sums for coffinite suggest a systematic error in the correction pro-

cedures, the presence of U^{+6} , and (or) the presence of structural OH^- . The analytical data suggest that the compositions of coexisting phases vary sympathetically (high calcium and high silica uraninites seem to coexist with high calcium and high silica coffinites respectively). This suggests the possibility that one phase formed by replacement of the other or that both phases grew in similar or the same local chemical environment. If the partitioning of calcium and silicon between uraninite and coffinite is systematic, a program to examine the kinetics and phase equilibria in the system $\text{UO}_2\text{-CaO-SiO}_2$ should yield information that would permit the definition of the physicochemical conditions of ore formation.

Characterization of granitic uranium source rocks

Previous studies (Rosholt and others, 1973; Stuckless and Nkomo, 1978) have demonstrated that the granitic rocks in the Granite Mountains in Wyoming have lost large amounts of uranium and that the timing of the uranium loss is compatible with the age of ore deposition in the three nearby uranium districts (Stuckless and Nkomo, 1978; Ludwig, 1977). These facts and the proximity of the granite to the Gas Hills, Crooks Gap, and Shirley Basin uranium districts suggest that the granite was the major source rock for the sedimentary uranium deposits. Characteristics of the granite that may be common to other granitic uranium source rocks may include: (1) a mineralogy dominated by quartz and two feldspars with biotite, primary epidote and locally abundant magnetite, (2) a fairly homogeneous bulk chemical composition that approximates the granite minimum in the system quartz-albite-orthoclase, (3) an anomalously high concentration of lithophile trace elements such as the rare earths, (4) proportionalities among radioelement concentrations that differ markedly from normally accepted values for similar rock types, (5) high initial isotopic ratios such as $^{87}\text{Sr}/^{86}\text{Sr}$ or $^{207}\text{Pb}/^{204}\text{Pb}$ relative to rocks of similar age, and (6) isotopic disequilibrium within the ^{238}U -decay chain.

Uranium mobility during interaction of rhyolitic glass with alkaline solutions

Based upon preliminary results of experimental leaching of rhyolite glass shards, R. A. Zielinski has identified some criteria for recognizing likely volcanic source rocks of uranium. Well-flushed columns of rhyolitic shards may release significant

uranium through a mechanism of glass dissolution. Silica and uranium are released in the same weight fraction as present in the glass (congruent dissolution) while lithium and potassium removal is enhanced by additional ion exchange. Residual glass is apparently unaltered but shows signs of dissolution as devitrified rims and small (<10 microns) etch pits. Additional field guides for recognizing partially dissolved rhyolitic glass include abnormally low lithium content, underlying accumulations of secondary silica precipitates (sometimes uraniferous) and (or) lithium-rich clays.

Uranium in secondary silica as a guide for describing uranium mobility

Continuing research by R. A. Zielinski in the Shirley Basin in Wyoming indicates that the uranium content of secondary silica may provide a fossilized record of the relative uranium concentration of ancient ground water. Uranium concentration of cryptocrystalline silica veinlets collected at the base of a thick sequence of Oligocene rhyolitic ash increases basinward. One dated veinlet is at least 20 million years old. Silica was precipitated from uraniferous, silica-saturated ground water percolating downward through overlying rhyolitic ash. Uranium concentration ranges from 10 to 250 ppm and is homogeneously distributed (in silica separates). Uranium content and age estimates of silica precipitates can be used to evaluate possible source rocks and identify areas of prior uranium concentrations that may relate to nearby sedimentary uranium deposits.

Conceptual-mathematical models of uranium ore formation in sandstone-type deposits

J. S. Leventhal and H. C. Granger (1977) have estimated the time required to produce a roll-type ore deposit of a given size in sandstone, using reasonable assumptions for the removal of uranium from igneous source rocks by ground water, for uranium content of the ground water, ground-water flow rate, uranium entrapment efficiency, and host-rock porosity and density.

Mass-balance calculations indicated that removal of half of the uranium from a relatively small volume of source rock having a specific gravity of 2.6 and originally containing 10 ppm uranium would yield 10 t of uranium. This amount is equivalent to that obtained from weathering and leaching a 300 m² area of granite to a depth of 8.5 m, or a 3 km² area of volcanic ash about 8.5 cm thick. The time required to remove that amount of uranium from

such source rocks depends in part on their porosity and permeability that, in turn, are related to the extent of fracturing in the granite or the grain size of the ash and the solubility of the uranium. The amount of weathering and access of meteoric water into the ground-water system are additional essential factors. Ten million cubic meters of water containing 10 ppb uranium are needed to form a 10-t uranium deposit. If the rainfall is 25 cm/yr, this amount of water would fall on the granite area noted in about 44,000 years and the ash in 440 years. These are minimum estimates because the uranium may not be removed in this time, and it is unlikely that all of the rainwater would enter the ground-water system. If only 10 percent of the rainwater infiltrated the rock, the above time periods would be increased by a factor of 10.

A reasonable calculation has been made of the time required to form a roll-type deposit having a 5-m average width and containing 10 t of uranium. If the deposit averages 0.25 percent uranium, it contains about 4,000 t of ore. If this ore has a specific gravity of 2, it has a volume of 2,000 m³. The 10⁹ m³ of uranium-bearing solution needed to supply the 10 t of uranium, assuming 10 ppb and 100 percent precipitation, is about 500,000 times the volume of the ore deposit. The calculation flow rate using a hydraulic gradient of 9.4 m/km in a medium grained sandstone is 5.3 m/yr. This means that each year a volume of water about equal to that of the resulting orebody flows through the roll; therefore, it takes about 500,000 years to form the orebody. If the solution contained 50 ppb uranium, it would take only 100,000 years to form the same orebody.

Organic materials and conditions of uranium fixation

Experiments performed by J. K. Jennings and J. S. Leventhal (1976) to test the degree of uranium fixation by humic acids as well as by synthetic ion-exchange and chelating resins over a broad pH range showed in most cases that the form of soluble uranium changes with pH. At pH below 4, the uranyl cation UO^{+2} predominates, but at pH above 5 the uranyl dicarbonate complex $UO_2(CO_3)_2(2H_2O)^{-2}$ is the dominant soluble form, which at higher pH gives way to greater proportions of the uranyl tricarbonate complex $UO_2(CO_3)_3^{-4}$. The reactive sites of humic acids also change with increasing pH due to deprotonation and (or) hydration. Because of these changes in soluble uranium species and reactive sites of humic acids, the degree of interaction between acids is strongly pH-dependent. The conditional stability constants for reaction

products were determined by measuring the reactivity between uranyl carbonate solutions and several ion-exchange and chelating resins both in the presence and absence of humic acids under controlled pH conditions. Preliminary results indicate that fixation is strongly pH-dependent and involves both ionic and chelate interaction. Humic acids will complex the greatest quantity of uranium in the near neutral pH region.

Computer modeling of roll-type uranium deposits

C. G. Warren (1977) simulated roll-type uranium deposits in a computer model that emphasized the interrelationships of geochemistry and hydrology. In the model, ground water carrying dissolved oxygen flows through a confined aquifer containing pyrite-bearing sandstone. The oxygen destroys the pyrite on contact and creates a distinctive crescent-shaped alteration zone that is similar to the shape of the alteration zone observed in nature. In the model, the velocity profile of the ground water partly determines the shape of the altered zone but transverse dispersion of oxygen further modifies the shapes. Impermeable mudstones above and below the sandstone aquifer were found to exert profound control over the entire system. Ground water is inferred to move very slowly along the boundaries with the result that oxygen is essentially delivered to the boundary areas by only one process—transverse dispersion. In the model, any impermeable surface, such as clay layers suspended in the aquifer, exerts this kind of control.

Thermoluminescence of sand grains near a uranium deposit

Previous workers' attempts to use thermoluminescence (TL) as an indicator of uranium mineralization were thwarted by the inability to separate the effect of radiation on TL from the natural variation in the susceptibilities of the samples to TL. C. S. Spirakis, M. B. Goldhaber, and R. L. Reynolds (1977) found that variation in the susceptibility can be normalized, however, by ratioing TL measurements from two different temperature ranges. With this normalizing technique, radiation-induced TL related to the mineralizing process, was detected around a south-Texas uranium rollfront deposit. This anomalous TL may form the basis of a new uranium-prospecting tool.

Mobile helium-detection equipment used in uranium exploration

Helium surveys conducted by G. M. Reimer have shown anomalous helium concentrations in soil gas

and subsurface water in the vicinity of various types of uranium deposits. The anomalies are difficult to interpret in view of the diverse geologic nature of the uranium deposits, but preliminary models are being developed to aid the interpretation (Reimer and Otton, 1976). Several sampling techniques have been successfully evaluated in order to enhance the helium and radon concentrations before analysis (Reimer, 1977). The results of these continuing investigations indicate that helium detection, supported by radon analyses, can be useful in the search for uranium.

Uranium anomaly in Cañada de la Cueva, New Mexico

Studies by K. J. Wenrich-Verbeek of uranium concentration in the surface waters north of Ojo Caliente, N. Mex., have shown that the sources of anomalously high uranium concentrations are springs (both cold and hot) that are (1) flowing out of the Sante Fe Formation in Cañada de la Cueva and (2) located near the mouth of Cañada de la Cueva in the valley of the Rio Ojo Caliente. Uranium concentrations here are between 40 and 150 $\mu\text{g/L}$ (ppb), whereas in the well-known hot springs of Ojo Caliente the uranium concentrations are $<7 \mu\text{g/L}$. Other springs and streams throughout the area are $<5 \mu\text{g/L}$. Thus, the area of anomalous uranium appears to be restricted to the area of Cañada de la Cueva and does not indicate generally high uranium values for all hot or cold springs in the Ojo Caliente region.

Water sampling for uranium exploration

A detailed geochemical study was conducted by K. J. Wenrich-Verbeek of water and stream sediments in an area containing anomalous uranium concentrations in water. The high uranium concentrations in the surface water were not reflected in the corresponding stream sediments. The low uranium content of the stream sediments from these high uranium waters can be explained by (1) the presence of a ground water source for the uranium, and (2) insufficient time for the uranium in the water to be adsorbed onto the sediments. Although a stream sediment anomaly in these streams cannot be established with a size fraction $<150 \mu\text{m}$ (<100 mesh), enough uranium has been adsorbed by the fine fraction that a small local anomaly can be outlined using the fraction size $<90 \mu\text{m}$ (<170 mesh). This anomaly is so small though, that it probably would not have been recognized in a regional reconnaissance study. Thus, in a case where ground water

is the contributing source for uranium, stream-sediment sampling alone, even using the fine fraction, is not an effective technique for detecting uranium anomalies. This emphasizes the necessity of water sampling in conjunction with stream-sediment sampling.

Spring-deposited radioactive barite in the Great Salt Lake area of Utah

Barite and calcite are being chemically precipitated at Stinking Hot Springs northeast of the Great Salt Lake in Utah. One hard porous radioactive sample shown by X-ray diffraction to be monocrystalline barite contains radium equivalent to 17,000 ppm uranium. This concentration of radium by natural processes of coprecipitation is the highest found by J. K. Felmlee and R. A. Cadigan in their reconnaissance of mineral springs in eight Western States. The occurrence at this site may result from the mixing of barium-rich sulfide-bearing water associated with a local fault aquifer and radium-rich water from a more widespread aquifer that may be fed by fault systems close to the Wasatch Range. Geologic evidence indicates that the radium and barium have their sources in the Precambrian and Paleozoic rocks in the area rather than the Tertiary and Quaternary sediments.

Uranium in two-mica granite in northern New England

A significant occurrence of uranyl-phosphate minerals has been reported in two-mica granite near Lake Sunapee, N.H. (Boudette, 1977). Two-mica granite is recognized for its anatectic genesis and anomalous content of ore-forming elements including uranium, tin, tungsten, beryllium, lithium, and fluorine, (de la Roche and others, 1976). Field studies by E. L. Boudette determined that the two-mica granite at Lake Sunapee is part of the westernmost of three belts of two-mica granite in New Hampshire (see Boudette, 1977) that compose the Concord Granite. Recent isotope dating of the two-mica granite has shown it to be younger than previously interpreted, probably of Mississippian age (Lyons and Livingston, 1977) indicative of widespread Hercynian (Variscan) plutonism in New England. Rocks of the Lake Sunapee two-mica granite belt are peraluminous with a silica content ranging from 72.6 to 75.1 percent, alumina content ranging from 14.9 to 15.3 percent, and total alkali content ranging from 7.7 to 8.7 percent. These rocks are moderately enriched in potash and have a $^{87}\text{Sr}/^{86}\text{Sr}$ initial ratio of 0.7142 (Lyons and Livingston,

1977). The thorium content of the Lake Sunapee rocks ranges from 2 to 14 ppm and average 8 ppm. The uranium content ranges from 8 to 32 ppm and averages 15 ppm. The thorium-uranium ratio ranges from 0.1 to 1.6 and averages 0.72. The combination of strontium initial ratio value and thorium-uranium ratio indicate a crustal origin for the two-mica granite. The easternmost belt of two-mica granite (Milford belt) in New Hampshire can be observed to be sheet-form and routed in embrechite. The embrechite is part of a lithostratigraphic unit that has been previously called "Massabesic Gneiss" of local usage, but is more accurately termed the Massabesic Migmatite which is exposed in southeastern New Hampshire. The crustal origin indicated by geochemistry and spatial association of the two-mica granite with migmatite, in turn, indicates that the two-mica granite was generated by anatexis of protoliths of the Massabesic.

Intragranitic syngenetic uranium deposits in France (Poty, 1977) are located in Hercynian-age two-mica granite sheets or related rocks. The close comparison of the age for two-mica granite in the Central and Armorican Massifs of France with the Concord Granite in New England has an important metallogenic significance because it is possible that these rocks comprise a coextensive province prior to continental breakup and formation of the present Atlantic Ocean. Thus, the two-mica granite in New England, as well as elsewhere in the Appalachian orogen, emerges as an important exploration terrain for uranium as well as other resources.

Two-mica granite is assigned to peraluminous irruptive suite. Whether or not this suite is transitional into the calc-alkalic suite is problematic, but both relate in time and space to orogenic stages. It is unlikely that the peraluminous suite is transitional into the alkalic suite that is normally related to epeirogenic or anorogenic environments. Rocks of the late Mesozoic age White Mountain batholith of New Hampshire present tectonic-geometric contrasts to the two-mica granite, and show a different uranium-thorium distribution pattern. The thorium content ranges from 4 to 391 ppm and averages 59 ppm. The uranium content ranges from 2 to 32 ppm and averages 13 ppm. The thorium-uranium ratio ranges from 1.3 to 23.3 and averages 4.4. The later value is essentially a normal value for rocks with mantle geochemical affiliations.

Uranium fractionation followed by syngenetic and dispersed uranium deposition is possible for granitic rocks emplaced in (1) calc-alkalic, (2) peralumi-

nous, or (3) alkalic irruptive suites. Each suite, however, presents a unique genetic model, which has important consequences in exploration.

Uranium, thorium, carbon, and sulfur in Devonian black shale from West Virginia, Kentucky, and New York

Samples of Devonian black shale from drill core obtained by J. S. Leventhal and M. B. Goldhaber in three eastern States were analyzed for uranium, thorium, carbon, and sulfur. The uranium shows variations from 1.5 to 38 ppm. These variations reflect regional extremes, but even in a given core uranium variations range from 1.5 to 15.8 ppm (West Valley, Cattaraugus County, New York), 3.2 to 38 ppm (Perry County, Kentucky), 3.4 to 36.6 ppm (Lincoln County, West Virginia), 3.4 to 21 ppm (Jackson County, West Virginia).

The thorium shows the most constant value, 15 ppm, near the mean values of 12.0 ppm reported for shales. Thorium-uranium values >3 are indicative of lithologic changes that may be useful for stratigraphic correlation. Uranium and carbon are generally higher than the average values quoted for shales of 3.7 ppm for uranium and 2.1 percent for carbon. Uranium shows a covariance with both organic carbon and sulfur (iron sulfides). The plots of the carbon, sulfur, and uranium with depth for Perry County, Kentucky, and Jackson County, West Virginia, show a good covariance for uranium and carbon. In this core, the uranium and sulfur relationship is not good at the top but is as good as carbon and uranium in the lower portion.

Earlier work (Kehn, 1955; Bates and Strahl, 1957) on the Gassaway Member of the Chattanooga Shale of Devonian age from DeKalb County, Tennessee, showed much higher amounts of uranium (averages of 50–60 ppm) and carbon (11 percent). At that locality there was a smooth trend of more carbon corresponding to more uranium. These earlier results are different from ours obtained from the Kentucky, New York, and West Virginia localities. In general, our units are thicker, and because of probable dilution of the carbon and uranium with inorganic material, we see values that are generally only 50 percent as high for the uranium and carbon values. This may be due to a shallow-barred or land-locked sea in the area of DeKalb County, Tennessee, (Conant and Swanson, 1961; Breger and Brown, 1963), whereas our samples from the region to the north represent deltaic to open-ocean environments where the organic material and uranium could be diluted by clay minerals.

Electromagnetic methods aid in detection of mineralization associated with uranium

B. D. Smith, J. W. Cody, D. L. Campbell, J. J. Daniels, V. J. Flanigan, and L. J. O'Connor, using nonradiometric geophysical methods in hardrock and sedimentary-rock terranes, have demonstrated that the geophysical data can successfully be used to map and detect geological features that indicate favorable areas for uranium mineralization (Smith and others, 1976). A sufficient number of surveys have been conducted in hardrock terrane to draw a few tentative conclusions about the general design of geophysical surveys in relation to types of uranium deposits.

A number of geophysical surveys have also been conducted in sedimentary terranes to demonstrate that electrical and magnetic methods can detect suitable variations in physical properties of sediments associated with uranium deposits. These subtle variations in geological and geochemical properties of sediments may constitute much larger targets than the uranium mineralization itself. Consequently, surface geophysical surveys may be capable of detecting much deeper uranium mineralization than previously suspected. Laboratory petrophysical measurements indicate that uranium mineral deposits may have a much larger geological halo than previously suspected.

GEOTHERMAL RESOURCES

Snake River Plain, Idaho, geothermal well studies

Geothermal waters may be a potential source of energy for a central heating system for Sugar City, an eastern Idaho town that was largely destroyed in the Teton Dam disaster of June 5, 1976. E. G. Crosthwaite reports that water temperatures in nine selected wells in the region of the potential energy resources ranged from 23° to 49° C. Aquifer temperatures, estimated by geochemical thermometers, ranged from 45° to 145° C when Si concentrations were used and from less than 10° C to 205° C when Na-K-Ca concentrations were used. Preliminary results of oxygen-isotope data show that the cold and warm waters have essentially the same ^{18}O contents.

Several water samples were collected by H. W. Young and R. E. Lewis from wells near Twin Falls in southern Idaho. In one local area, more than 15 wells were drilled in the past 2 years for space heating, catfish farming, and swimming pools. These wells are generally 300 m deep and have reported

water temperatures ranging from 35° to 60° C. In one well, flowing about 95 L/s, Si and Na-K-Ca geothermometers indicated temperatures of 106° C and 88° C, respectively. Mixing models showed a temperature of about 185° C, with an 84-percent cold-water fraction.

A 220-m deep well, drilled in the bottom of the Snake River Canyon, reportedly penetrated Idavada Volcanics(?) of Miocene age. It had a reported shut-in pressure of 15 kg/cm², a flow of about 170 L/s, and a water temperature at the surface of 42° C. Silica and Na-K-Ca geothermometers indicated temperatures of about 120° C and 90° C, respectively, with a mixing-model temperature of 215° C.

Geothermal water studies in the Verde Valley of Arizona

Preliminary water-quality inventories of wells and springs in the Verde Valley indicate some anomalously high geothermal temperatures. According to P. P. Ross and C. D. Farrar, the Verde Hot Springs are the focal point of the investigation and have surface temperatures of 40° C and indicated geothermal temperatures of 118° C when the SiO₂ method is used and 146° C when the Na-K-Ca method is used. Indicated water temperatures in wells sampled as far as 32 km north of the Verde Hot Springs have been calculated as high as 135° C when the SiO₂ method is used and 125° C when the Na-K-Ca method is used. The well- and spring-sampling program is continuing to define the extent of the geothermal reservoir. If the reservoir proves to be continuous from Verde Hot Springs to the wells north of Camp Verde, the reservoir may be of adequate size to designate it as a known geothermal resource.

Geothermal water studies in the Coso Hot Springs of California

Temperature measurements made by W. R. Moyle, Jr., (1977) in the Coso Hot Springs area of California ranged from 4° C in a mountain spring to 42° C at the bottom of the deepest well. The temperature gradients below land surface range from 1.1° C per 33.3 m in nonthermal areas to 24.4° C per 33.3 m in thermal areas. Only six areas were found to have water or ground temperatures greatly above the local average air temperature: Coso Hot Springs, Devils Kitchen, Nicol area, Wheeler Prospect, and areas on the west and northeast sides of Sugarloaf Mountain.

The water quality is considered good throughout the study area except where water is evaporated for

discharging playa surfaces or steaming ground. All temperatures measured in springs surrounding Coso Hot Springs and Devils Kitchen indicate that the springs are non-thermal and are strongly influenced by the ambient air temperature. One spring measured twice showed a variation of 21° C between summer and winter.

Geothermal potential northeast of Clear Lake in California

The northward progression of ages of eruptions in the Clear Lake Volcanics implies that a heat source at depth has moved relatively northward, according to J. M. Donnelly, B. C. Hearn, Jr., and F. E. Goff (Donnelly and others, 1977). The area of youngest volcanic activity (<0.2 m.y.) lies along the northeast side of Clear Lake and further northeast of the lake, a distance of 3 to 13 km northeast of a high-level magma chamber inferred from geophysical data. That magma chamber may have been left behind to cool and crystallize, while the deep heat source may now be warming up the area northeast of Clear Lake. This young focus of igneous activity may have considerable geothermal potential, as shown by the wider halo of thermal springs, but existing geophysical and geological data are insufficient to assess the potential.

Seismic refraction at Raft River in Idaho

The Raft River geothermal system in southeastern Idaho is a convective hot water system presently being developed to demonstrate the production of electricity from low-temperature (~150° C) water. Interpretation by H. D. Ackermann of seismic-refraction recordings made in the Raft River geothermal area yielded compressional velocities from near the surface to the crystalline basement at a maximum depth of approximately 1,600 m. The results show a complex sequence of sediments and volcanic flows overlying basement. Velocities in the sedimentary section vary laterally. Correlation with well data suggests that zones of higher velocities correspond to zones where sediments are hydrothermally altered. Flowing hot wells occur near the boundary between inferred shallow altered and unaltered rocks. The basement surface does not appear to be displaced by any large faults, although there is ample surface evidence of faulting. The deep circulation of hot water necessary for a convective system may be through many small faults and fractures. Fracturing is suggested on the basis of lateral velocity variations within the basement complex.

Crustal melting at the San Francisco volcanic field in Arizona

E. W. Wolfe, R. B. Moore, G. E. Ulrich, R. F. Holm, and C. G. Newhall report that basalt vents are conspicuously rare within the major centers of intermediate to silicic eruption in the San Francisco volcanic field in Arizona. However, the close proximity of these centers to large numbers of basaltic vents of broadly similar age indicates that the basalts and non-basalts are related in origin. Perhaps large volumes of basalt magma invading the crust caused local melting that produced silicic liquids. Such liquids may be represented by felsic xenoliths that were partially melted and now contain silica-rich glass. The silicic melts may have mixed with basaltic liquid to produce andesite that erupted at many places in the central part of the volcanic field, including San Francisco Mountain. The andesite tends to differentiate readily. Four andesite vents south and west of San Francisco Mountain enclose more silicic central plugs (two are rhyolitic), and an andesite flow contains large segregations of dacite with hornblende gabbro xenoliths. Additional evidence that melts from crustal rock are important components in the intermediate and silicic rocks comes from O'Leary Peak, a differentiated vent just east of San Francisco Mountain where M. A. Lamphere determined unusually high Sr-isotope ratios in both andesite and rhyodacite.

Terminology for geothermal resource assessment

During late 1976 and 1977, the USGS cooperated with the National Electric Agency of Italy in evaluating methodology for regional geothermal resource assessment, under the sponsorship of the U.S. Energy Research and Development Administration, recently absorbed into the new Department of Energy. Analysis of methodology and recommendations for uniform terminology were presented at the Larderello Workshop on Geothermal Resource Assessment and Reservoir Engineering, along with a test application to central and southern Tuscany in Italy (Muffler and Cataldi, in press; Cataldi and others, in press).

Given the need for a consistent, agreed-upon term for geothermal resource assessment, Muffler and Cataldi proposed a logical, sequential subdivision of the geothermal resource base, accepting its definition as being all the thermal energy in the Earth's crust under a given area, relative to mean annual surface temperature. That part of the resource base that is shallow enough to be tapped by production drilling is termed the accessible resource base, and it in turn is divided into useful and residual components.

The useful component (i.e., the thermal energy that could reasonably be extracted at costs competitive with other forms of energy at some specified future time) is termed the geothermal resource. This in turn is divided into economic and sub-economic components, based on conditions existing at the time of assessment.

In the format of a McKelvey diagram (fig. 1), this logic defines the vertical axis (degree of economic feasibility). The horizontal axis (degree of geologic assurance) contains identified and undiscovered components. Reserve is then designated as the identified, economic resource. All categories should be expressed in units of thermal energy, with resource and reserve figures calculated at wellhead, prior to the inevitable large losses inherent in any practical thermal use or in conversion to electricity.

The proposed terminology is internally logical and is consonant with pre-existing terminology used to describe mineral and petroleum resources.

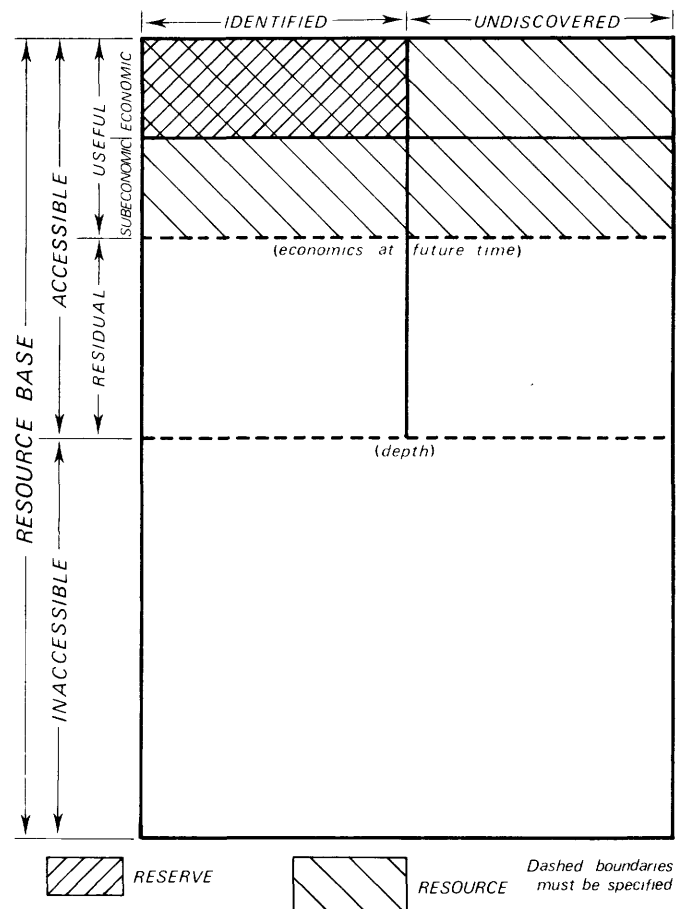


FIGURE 1.—McKelvey diagram for geothermal energy showing derivation of "resource" and "reserve" (Muffler and Cataldi, 1978, fig. 1). Scales are arbitrary; relative sizes of rectangles have no relation to relative magnitudes of categories.

Lithium-rich rocks in Nevada

E. F. Brenner-Tourtelot reported that lithium concentrations in the Miocene part of the Horse Spring Formation at Lava Butte near Henderson, Nev., are related to: (1) the degree of aridity reached in this ancient playa as indicated by the presence of evaporite minerals such as halite; (2) influx of volcanic ash as indicated by vitroclastic textures and the presence of zeolite and feldspar minerals; and (3) the presence of hot springs. One 40-m section at Lava Butte contains an average of 0.1 percent Li. The lithium was leached probably from the volcanic ash by circulating hot water of the springs and was concentrated evaporatively in the brines of the playa. Final deposition of the lithium was by the interaction of tuffaceous playa sediments with the lithium-rich playa brine to form a hectorite-like clay mineral on bedding planes and joint surfaces of the dolomite and dolomitic tuff of the playa mud.

Tuffaceous sediments of a similar ancient playa near Socorro, N. Mex., in the Popotosa Formation were found to contain as much as 0.15 percent Li. Samples from this area confirmed G. O. Bachman's discovery of a lithium anomaly in 1976. The maximum lithium values are lower than those found at Lava Butte, Nev.; the mineralogy of the sediments of the Popotosa indicates a less concentrated brine but a drier environment than for the Horse Spring. Very little gypsum and no halite have been found in the Popotosa Formation.

Geophysical characterization of brine deposits

Field geophysical surveys by Bruce D. Smith shows that the northeast end of Fish Lake Valley in Nevada is dominated by a NW to SE gravity gradient that obscures any subtle expression of low density sediments in the gravity data. Direct current resistivity and electromagnetic sounding surveys have defined a very limited area of conductive sediments that might contain brine-bearing zones. In contrast, Columbus Salt Marsh, north of Fish Lake Valley, has a pronounced gravity low that indicates the presence of a thick sequence of low density sediments. Electrical geophysical surveys indicate that these sediments contain zones of low resistivity. Thus, Columbus Salt Marsh appears to be favorable for the occurrence of brines that may contain lithium.

Limited laboratory measurements of the electrical properties of playa sediments indicate that high precision electrical geophysical methods can be used

to distinguish between brine-bearing sediments and other electrically conductive sediments. Although more work needs to be done on this topic, the results of this work suggest that high precision electrical surveys could play an important role in the future exploration for lithium-bearing brines.

Origin of lithium in sedimentary rocks and brines

J. D. Vine lists two requirements for the accumulation of lithium in sedimentary rocks and brines: (1) a source for lithium in solution that provides an unusually large proportion of lithium in comparison to the major cations, Na, Ca, Mg, and K, and (2) a mechanism for evaporative concentration of these waters to precipitate some of the major constituents as limestone, dolomite, gypsum, and halite or similar chemical evaporite deposits, thereby concentrating the lithium in the residual brines. Once concentrated, the lithium may enter into such clay minerals as hectorite, or remain in the final brines. Favorable conditions for a lithium-rich source are found in hot springs associated with volcanic activity where the ratio Li:Cl may be as high as 1:100. Conditions for evaporative concentration occur in a number of undrained basins in the western Cordillera of both North America and South America and possibly on other continents.

New occurrences of the lithium-rich smectite, hectorite

R. K. Glanzman found significant amounts of lithium-rich clay very similar to the type hectorite at Hector, Calif., in the McDermitt caldera in northern Nevada and southern Oregon, and the Date Creek Basin in central Arizona near Wickenburg. The clay in the McDermitt caldera is interbedded with the zeolites, clinoptilolite, erionite, and analcime, in a sequence of altered tuffaceous sediments of Miocene age. Clay associated with clinoptilolite and erionite contains as much as 3,600 ppm Li. Clay associated with analcime contains as much as 6,500 ppm in individual whole-rock analyses. The highest amount of lithium reported for type hectorite is 5,100 ppm. Lithium is also associated with mercury and uranium deposits in the caldera. Lithium enrichment is caused by a combination of diagenetic and hydrothermal alteration.

Uranium-bearing lacustrine sediments of Tertiary age in the Date Creek Basin contain several clay zones that have up to 2,300 ppm Li. This occurrence is a southerly extension of the lithium-rich trend from the Horse Spring Formation in the Lake Mead area (southern Nevada) through the Big Sandy Formation near Wikieup, Ariz., and the "Lyles"

lithium deposit near Kirkland, Ariz. The trend suggests that the Colorado Plateau-Basin and Range physiographic transition zone may be a zone of lithium enrichment.

California phosphorite

A. E. Roberts reported that phosphorite deposits in Santa Barbara and Ventura Counties are a potential resource for phosphate. The deposits are in sedimentary sequences ranging in age from Saucian through Mohnian Stages of the California Miocene Series. The phosphatic facies consists generally of brown to gray, laminated to medium beds of massive to graded pelletal and nodular phosphate, phosphatic mudstone, mudstone, siltstone, and some fine-grained sandstone. The pellets range from very fine to medium sand-size, and the nodules range from coarse sand to medium pebble-size. They are generally structureless aggregates of submicrocrystalline carbonate-fluorapatite containing terrigenous clay, silt, and sand particles, and diatoms or shell fragments. Faunal assemblages and sedimentary structures in the phosphatic facies suggest formation as an offshore mud-shelf deposit. Phosphate was precipitated in the shelf mud during prolonged calm-water conditions interspersed with occasional high-energy conditions that winnowed away the finer grained material and rounded the pellets and nodules.

Gold and silver in ash of incinerated sewage sludge

R. A. Gulbrandsen discovered that the phosphate (16.6 percent P_2O_5) contained in the ash of incinerated sewage sludge at Palo Alto, Calif., is a significant resource that can be used in the manufacture of fertilizer. The ash also contains high contents of gold (30 ppm) and silver (660 ppm). Copper (0.8 percent), tin (0.3 percent), palladium (4 ppm), and zinc (0.38 percent) in the ash are also of economic interest. Most commercial interest is focused on the recovery of gold, the most valuable component of the ash. In addition to a yearly production of about 2,000 t of ash, Palo Alto has an accumulation of 10,000 t of ash in the city dump. The latter comprises a gold deposit with an apparent value of about 1.5 million dollars.

Phosphate resources in the southeastern United States

Recent drill data indicate the presence of extensive deposits of phosphate in DeSoto County, Florida, as well as in the Osceola National Forest in northern Florida and in southern South Carolina.

According to J. B. Cathcart, these deposits will be more costly to mine and process than the nearly depleted deposits currently being exploited in Florida and North Carolina. In addition, there are environmental restrictions for some areas. Nonetheless, it is probable that these deposits will become economically viable.

Physical and chemical properties of bentonite

By comparing the cation-exchange properties of 347 bentonites of Cretaceous age from Wyoming and Montana with their physical properties, C. W. Frahme found that samples with desirably high viscosity values, such as might be used in the drilling-mud industry, exhibited low filtrate loss, $pH > 8$, and 30–180 milliequivalents water-soluble cations. Detrimentally large filtrate losses occur in samples with a $pH < 9$, low to moderate amounts of exchangeable sodium, and low exchangeable $Na/Ca+Mg$.

Lithium in flint clays

H. A. Tourtelot reported that maximum concentrations of lithium found in samples of flint clay and associated rocks of Pennsylvanian age in different States are: Missouri—5,100 ppm; Pennsylvania-Maryland—2,100 ppm; Kentucky—890 ppm; Ohio—660 ppm; Alabama—750 ppm; and Illinois—160 ppm. Maximum concentrations in kaolin deposits in the Coastal Plain province extending from New Jersey to Texas and in a deposit in Idaho, range from 64 to 180 ppm. The maximum concentration found in the Arkansas bauxite region is 460 ppm, and the maximum concentration in flint clay in Colorado is 370 ppm. Samples from areas other than Pennsylvania, Maryland, Kentucky, and Missouri are relatively few in number, represent mostly commercially valuable clays, and represent only a part of the refractory clay deposits in the United States. Data are not available on associated clays that could be unuseable because they contain too much lithium, as well as other deleterious elements. In both Pennsylvania and Missouri, lithium contents vary regionally between districts and vary locally between deposits. In samples containing more than 2,000 ppm Li, the lithium occurs in a dioctahedral chlorite mineral very similar to cookeite, which previously has not been recognized in sedimentary clays. The clays associated with the cookeite-like mineral consist chiefly of well-crystallized kaolinite. The dioctahedral chlorite, however, seems to be most abundant where diaspore and boehmite occur along with the

kaolinite. Barium, chromium, copper, phosphorus, and strontium are present in some samples in amounts of several hundred parts per million or more, and may contribute to the failure of some clays to perform satisfactorily in firing tests.

Carbonate rocks for sulfur dioxide gas recovery

Limestones, chalks, and marls, as well as secondary carbonate from industrial processes, are among the carbonate rocks most suitable for scrubbing SO_2 emissions from coal-fired generators. C. M. Shifflett found that calcite sludge from the Kraft paper process shows higher reactivity with SO_2 than natural carbonates under laboratory conditions. Waste lime derived from the production of acetylene gas was found to have higher reactivity and fewer problems with plugging and scaling than virgin lime or limestone. This may be caused by a different oxidation rate in the scrubber.

Phosphate resources of the Hawley Creek area in Idaho

Phosphate resources in the Retort Phosphatic Shale Member of the Phosphoria Formation (Permian) in east-central Idaho ($113^{\circ}05'$ to $113^{\circ}15'$ W. Long. and $44^{\circ}35'$ to $45^{\circ}45'$ N. Lat.) were examined by Peter Oberlindacher and R. D. Hovland. The Retort crops out for about 18 km in the area. The member is poorly exposed but generally forms a distinct swale between more resistant dolomite beds in the upper part of the Park City Formation and the overlying Tosi Chert Member of the Phosphoria Formation. The Retort is intensely folded and faulted in much of the mapped area caused by regional thrusting (Lucchitta, 1966; Ruppel, 1978).

Two bulldozer trenches and several measured sections indicate an average thickness of 22 m for the Retort. One of the trenches contained 0.7 m of high-grade (31+ percent P_2O_5) phosphate rock; 4.3 m medium-grade (24+ percent P_2O_5); and 11.2 m low-grade (16+ percent P_2O_5).

REGIONAL GEOLOGIC INVESTIGATIONS

NEW ENGLAND

Vassalboro-pre-Vassalboro stratigraphic relations

Studies by P. H. Osberg in the Bangor, Maine, 2° sheet have shown that the Vassalboro Formation is in the flanks of a complexly faulted antiform, the trace of which extends from Gardiner, Maine, to Bangor (index map, loc. 1). The basal part of the Vassalboro Formation consists of thinly laminated, slightly calcareous wacke containing a distinctive, highly aluminous pelite. This sequence lies on different lithologic units of the pre-Vassalboro sections, which suggests that the Vassalboro Formation is disconformable to older rocks.

The pre-Vassalboro rocks belong to two sections that have uncertain relations. A western section consists of light colored quartzo-feldspathic gneisses

and dark colored biotite-rich amphibolites, light gray quartzo-feldspathic gneiss, and intercalated marble and lime-silicate granulite; an eastern section consists of thinly bedded quartzite and pelite. Both pre-Vassalboro sections are intruded by well foliated granite, granodiorite, and migmatite. Wones (1974) reports a minimum zircon age of 430 million years for one of these migmatite complexes.

Possible Lake George faulting

Isachsen (1975) found from studies of geodetic leveling data in the Adirondack Mountains of New England that contemporary uplift is taking place at the rate of 3.7 mm/yr. R. J. Wold recently conducted a geophysical survey in Lake George, (loc. 2) in the southeast corner of the Adirondack dome, in search of evidence of faulting as a result of this uplift.



High resolution seismic data over an old boundary fault that forms one edge of the graben occupied by Lake George indicates some disturbance in the unconsolidated sediments. This disturbance may be evidence of reactivation of this fault, presumably as a result of the contemporary doming. If recent faulting can be established, it has far reaching implications for the neotectonics of the northeast.

Deglaciation in the Leominster-Fitchburg area, Massachusetts

Surficial mapping by B. D. Stone in northeast-central Massachusetts (loc. 3) from Leominster to the New Hampshire State line shows that ice-contact deltaic sediments were deposited in three successively lower ice-dammed lakes in headwater tributaries of the Nashua River west of Fitchburg: (1) Wyman Pond basin (285 m elevation spillway), (2) Rice Meadow Pond (265 m), (3) Flag Brook basin (255 m). Ice-marginal deltas graded to the Flag Brook waterplane extend 6 km up Whitman River valley to Baldwin Hill, indicating a north-west-trending ice front barrier from Notown Reservoir to South Ashburnham. Younger fluvial deposits in Whitman River valley and Phillips Brook Valley are graded to local ice-dammed lakes in the Fitchburg area; thus, no sediment from these headwater tributaries entered the early high-stage levels of glacial Lake Nashua to the east. The northwest-trending ice margin positions form a regional pattern along the eastern front of the plateau, indicating development of a re-entrant in the receding glacier front over the plateau while a retreating active ice lobe occupied the Nashua River valley to the east.

Zone of detachment in the Hoosac Mountain area

N. M. Ratcliffe mapping in the Tolland Center, Williamstown, Pittsfield West, North Adams, and Cheshire quadrangles (loc. 4) as well as integrating and organizing the mapping efforts of D. B. Potter, E-an Zen and D. S. Harwood, obtained a regional comprehensive picture of the bedrock geology of western Massachusetts. Working closely with R. S. Stanley in the Hoosac Mountain area they jointly concluded that a major pre-metamorphic detachment zone exists along the contact of two lower Paleozoic formations, the Hoosac Formation and the Rowe Schist. This detachment zone may well be part of the zone of derivation of much of the allochthonous rocks in the Taconic Range.

Glacial Lake Housatonic was complex

In the area around Lee and Stockbridge in Massachusetts (loc. 5), C. R. Warren has found deltas and other evidence that record glacial lakes at about 10 different levels. Spillways that probably controlled most of these lake levels have been identified. The more accurate vertical data that are now available show that the Konkapot col of Taylor (1903) is too low to have controlled glacial Lake Housatonic at the time Taylor's "Lenox Dale moraine" was deposited and, allowing for post-glacial tilt, probably too high to have controlled the lake into which the Glendale delta was deposited. Thus, Taylor's correlation of the Lenox Dale delta with the Glendale delta is no longer acceptable, and the alignments of the ice front that Taylor inferred require revision.

Fitchburg pluton in Massachusetts

R. D. Tucker and Peter Robinson, University of Massachusetts, report that in the Wachusett Mountain area of Massachusetts (loc. 3), the west side of the Fitchburg pluton is a complex series of laterally continuous east-dipping sill-like sheets of varied composition intruding metamorphosed sedimentary rocks of probable Silurian and Early Devonian age. The stratified rocks, consisting of Silurian (?) biotite-quartz-plagioclase granulite with minor quartzite and sulfidic schist and gray-weathering pelitic schist contain evidence of four stages of folding post-dating the emplacement of the plutonic rocks. The earliest folds (F_1) are isoclinal and recumbent with axial surfaces parallel to the regional east-dipping foliation. Later isoclinal and recumbent folds (F_2) plunge gently ENE and their axial surfaces dip E. North-northeast-trending (F_3) folds deform F_1 and F_2 axial surfaces and show a weakly developed north-west-dipping axial plane schistosity and west-side up asymmetry. Late open (F_4) folds, with steeply north-south-trending axial surfaces deform older structural features.

Age of rocks in Lake Char fault zone in south-central Massachusetts

H. R. Dixon reports that the trace of the mylonite zone marking the Lake Char fault makes an abrupt bend from north-northeast in the northern part of the Oxford quadrangle and continues east to north-east across the Oxford, Worcester South, and Grafton quadrangles of Massachusetts (loc. 6). The mylonite is poorly exposed across much of this distance, although its presence can be inferred in places by mylonitic boulders. Exposures are more abundant

in the northern part of the Grafton quadrangle and in the northeast extension of the belt in the Shrewsbury and Marlboro quadrangles. The belt is continuous with the Burlington mylonite belt of Castle and others (1976).

The type Milford Granite shows intrusive relationships with the metasedimentary rocks and amphibolites of the Westboro Quartzite, and probably with the Sterling Plutonic Group equivalent in Massachusetts (observed in boulders, but not seen in outcrop). Good exposure of an intrusive contact is on the west side of Nipmuck Lake in the Blackstone quadrangle of Massachusetts. The Milford of the Milford quarries has been dated by Zartman (personal commun.) as about 610 million years. Thus, the rocks intruded by the Milford must have been formed and metamorphosed prior to 610 million years and this date puts an older age limit on the Lake Char faulting.

Hoppin Hill unconformity, new fossils

E-an Zen, Richard Goldsmith, and P. C. Lyons visited a well-known outcrop near Hoppin Hill in Attleboro, Mass. (loc. 7), where Cambrian fossils have previously been found. It was discovered that the Cambrian quartzite immediately adjacent to the granitic rocks shows cross-stratification at three places, all unequivocally indicating the quartzite rests on the granite nonconformably. A good Cambrian stratigraphic sequence leading up to the fossiliferous red limestone was pieced together. A virtually identical sequence, also resting on granite ("Joe's Rock Granite" of the older literature), was reported by A. F. Foreste (1899) around the turn of the century, but it has been overlooked since then. Goldsmith revisited and verified the locality early in the season. Later, Goldsmith, Lyons, and Zen found a quantity of Cambrian fossils.

Granite gneiss terrane in southeastern Massachusetts

Richard Goldsmith reports that a terrane of gneissic granitic rocks with screens of medium- to high-grade metavolcanic-metasedimentary rocks extends from the Westport area south of Fall River in Massachusetts through New Bedford northeast to Wareham in Massachusetts (loc. 8), where the granitic terrane becomes completely covered by glacial drift. North of this terrane, non-gneissic to locally gneissic granitic rocks form part of the Dedham Granodiorite terrane of eastern Massachusetts. The zone of gneissic granites strikes about N. 60° E., but the zone may curve in a more northerly direction

in its poorly exposed eastern part. Gneiss in a core from the Pilgrim Nuclear Reactor site near Plymouth may be from this terrane. The granitic rocks range from fairly massive alaskitic and biotite granite gneiss to layered biotite and hornblende gneiss. The compositions of the gneissic rocks are similar to compositions of granite gneisses in southeastern Connecticut and Rhode Island, west of Narragansett Bay, and are probably the same age as the granites in the Dedham terrane to the north. The screens of metavolcanic rocks are in the amphibolite facies, although grade seems to decrease westward and northward. At Acushnet, Mass., a metamorphosed diorite was intruded by granite gneiss. Nonmetamorphosed diorite masses are present along the shore of Buzzards Bay in the Westport-South Dartmouth area. The zone of gneisses and diorite corresponds approximately with a zone along the north shore of Buzzards Bay that has a magnetic signature slightly higher than that to the north shown on the map of Harwood and Zietz (1976). The boundary between the gneissic and non-gneissic rocks is not sharp in detail but is fairly continuous and linear at a scale of 1:250,000. It is interpreted as a boundary between rocks metamorphosed at different crustal levels and may be analogous to the boundary between the Dedham and Milford terranes southwest of Boston, Mass.

Correlation of Scotland Schist and Hebron Formation in eastern Connecticut with Oakdale Formation in Massachusetts

Rocks assigned to the Oakdale Formation in Massachusetts have been traced by M. H. Pease, Jr., southwestward into the northeast corner of Connecticut (loc. 9), where they are probably correlative with the Scotland Schist and part of the Hebron Formation. The Oakdale is composed mostly of well layered, thinly layered quartz-biotite-feldspar metasilstone and very fine grained metasandstone. Lenses of highly aluminous schist and metamorphosed claystone occur at several horizons particularly near the top. The aluminous schist is increasingly common to the southwest, and in Connecticut it has been mapped as the Scotland Schist resting on the Hebron. Aluminous silicates in the schist coarsen greatly with increasing metamorphic grade toward the southwest; the metasilstone maintains a remarkably uniform fine grain size even at sillimanite grade of metamorphism. The metasilstone in eastern Connecticut that has been correlated with the Oakdale of Massachusetts probably should no longer be included in the Hebron Formation. Inconclusive contact relations suggest that the Hebron

that lies west of the Oakdale correlatives stratigraphically overlies the Oakdale. This Hebron is consistently coarser grained; it is in fault contact with rocks of the Southbridge Formation on the west.

Syntectonic faults in eastern Connecticut

Tectonic dislocation under high temperature and stress has formed a complex of steep to essentially horizontal fault zones in eastern Connecticut along which apparent displacements are extremely varied. These fault zones, according to M. H. Pease, Jr., characterize the structural style of the crystalline rocks of eastern Connecticut east of the Triassic and Jurassic basin. Layering and foliation are commonly subparallel across these fault zones, and orthogneiss and pegmatite commonly are intruded along them. Thus, their surface traces, which may extend over a relatively broad zone, may be quite obscure. Metamorphic rocks from apparently unrelated stratigraphic sequences are juxtaposed along many of these fault zones. Along others, tectonic dislocation subparallel to layering and foliation may be considerable although apparent stratigraphic displacement is negligible. Direction and amount of dislocation is difficult to measure and may vary widely along a single fault zone.

These fault zones are believed to have initiated as syntectonic compressional features at depth. Their physical expression in outcrop is evidenced by such features as rotated tectonic blocks (Wintsch, 1976), stacked asymmetric folds, sheared fold noses, strong penetrative lineation that may obliterate layering and foliation, and alinement of metamorphic minerals. Such features tend to increase in abundance toward a syntectonic fault zone and tend to be oriented in the general direction of transport. Cataclasis, including mylonite, blastomylonite, and ultramylonite, is also a conspicuous feature along many of these fault zones. Cataclasis appears to be a late event and locally affects the syntectonically emplaced intrusive gneisses associated with these zones.

Nature of Cambrian trilobite-bearing rocks from Beavertail Point

Skehan and other (1977) reported on the major discovery by A. T. Smith and a coworker of a Middle Cambrian trilobite fauna at Beavertail Point on Conanicut Island in Rhode Island (loc. 10) in rocks previously thought to be Carboniferous in age. Skehan and others (1976) gave detailed local relations. E-an Zen examined the rock, which is the matrix of one of the trilobite specimens, at the re-

quest of Skehan's co-author A. R. Palmer. The rock is a glossy, grey, low-grade schist in hand-specimen, showing tiny ($1/2$ mm) dark specks of porphyroblasts. X-ray study shows muscovite, chlorite, dolomite-ankerite, quartz, plagioclase, and a suggestion of paragonite. In thin section, the specks prove to be ankerite pseudomorphs after some mineral having monoclinic outline, which is suggestive of amphibole. Around these porphyroblasts are whiskers of other minerals now also replaced by carbonate. There is a strong bimodal distribution of size between porphyroblasts and matrix ($<50\mu$). The rock clearly never attained the regional metamorphic grade of the nearby Pennsylvanian rocks (staurolite-garnet-kyanite schist, suggesting a temperature not less than 600° C and a pressure exceeding 4 kbars) even prior to the retrograde reactions, which are not evident in the Pennsylvanian rocks. The present juxtaposition, thus, must be post-metamorphic and post-Carboniferous-Permian, possibly along a major fault that now bounds the southeast edge of the Narragansett Basin. The southeast extremity of Massachusetts and southern margin of Rhode Island may belong to a geologic terrane different from adjacent parts of the two States.

Coal and stratigraphy in the Narragansett Basin of Massachusetts

In the course of detailed observations throughout the Narragansett Basin of eastern Massachusetts, P. C. Lyons has found about a dozen new Pennsylvanian plant fossil localities (Lyons, 1977). A significant find is the location of the uppermost coalbed in the Narragansett Basin just below the Dighton Conglomerate. Lyons concluded that the volcanic rocks of Plympton, shown as carboniferous on all existing maps, are in reality pre-Carboniferous metamorphic rocks. On the other hand, Lyon established that the supposed Carboniferous volcanic rocks around Attleboro, Mass., are indeed within the Carboniferous stratigraphic section. These rocks are of different chemical compositions and are, in contrast to the Plympton rocks, not metamorphosed or severely deformed.

APPALACHIAN HIGHLANDS AND THE COASTAL PLAINS

Upper Triassic stratigraphy in the Culpeper Basin of Virginia and Maryland

After the completion of fieldwork, the Upper Triassic stratigraphy in the Culpeper Basin (index map, loc. 2) is being redefined by K. Y. Lee into the

APPALACHIAN HIGHLANDS
AND COASTAL PLAINS STATES

Manassas Formation, 149 to 1,060 m thick, the Balls Bluff Siltstone, 76 to 1,690 m thick, and the Bull Run Formation, 249 to 5,152 m thick. The Manassas Formation consists of, in ascending order, the Reston Member, Rapidan Greenstone Conglomerate Member (proposed new name), Tuscarora Creek Limestone Conglomerate Member (proposed new name), and Yorkshire Sandstone Member (proposed new name). The Bull Run Formation is divided into the Leesburg Limestone Conglomerate Member, basaltic flow-bearing clastics member, and Culpeper Greenstone Conglomerate Member (proposed new name). The basaltic flow-bearing clastics member of the Bull Run contains the proposed Mount Zion Church basalt flow, 3 to 142 m thick, the proposed Hickory Grove basalt flow, 79 to 212 m thick, and the proposed Sander basalt flow, 136 to 545 m thick.

The clastic sediments were derived from adjacent Proterozoic (Precambrian Z) and lower Paleozoic uplands and deposited in the basin by streams. The lacustrine deposits of the Balls Bluff Siltstone grade into and intertongue with the fluvial deposits of the Manassas and Bull Run Formations (Lee, 1977).

Devonian black shale stratigraphy

Recent stratigraphic studies of the Devonian black shale sequence in the Appalachian Basin by J. B. Roen, Wallace de Witt, Jr., R. C. Kepferle, L. G. Wallace, and M. N. West have confirmed suggested

correlations of previous workers and have indicated new significant correlations of regional extent. Data used for this study were primarily gamma-ray logs of oil and gas wells augmented where possible by lithologic logs of well cuttings and detailed surface sections. These logs were used to prepare a series of six stratigraphic sections across the basin. Some data included in the regional stratigraphic synthesis were supplied by A. M. Van Tyne and L. V. Rickard of the New York Geological Survey, R. G. Piotrowski and S. A. Krajewski of the Pennsylvania Geological Survey, A. Janssens of the Ohio Geological Survey, D. G. Patchen and J. F. Schweitering of the West Virginia Geological Survey, E. N. Wilson and J. S. Zafar of the Kentucky Geological Survey, and F. R. Etensohn of the University of Kentucky, as a part of the Eastern Gas Shales Project's stratigraphic framework study.

The physical stratigraphy demonstrated in this series of sections indicates that the Cleveland Member of the Ohio Shale is equivalent to the upper unit of the Gassaway Member of the Chattanooga Shale of Tennessee. The Three Lick Bed of Provo, according to Kepferle and Potter (1977) is equivalent to the middle unit of the Gassaway and is here thought to be equivalent to the thin distal portion of the Chagrin Shale of Ohio that separates the Cleveland Member from the underlying Huron Member of the Ohio Shale. The stratigraphy indicated here confirms the opinion of Hass (1956, p. 20) that "The conodont fauna of the youngest beds of the Gassaway is like that in the upper part of the Ohio Shale (Cleveland Shale Member) of Ohio and Kentucky . . ."

The Huron Member of the Ohio Shale can be traced from central Ohio into eastern Ohio, where it intertongues with the Chagrin Shale. In addition to separating the Cleveland from the Huron, the Chagrin also divides the Huron into an upper and lower part. The upper part of the Huron thins eastward but can be traced across northwest Pennsylvania into western and central New York, where it becomes the Dunkirk Shale Member of the Perrysburg Formation. This correlation supports that of Schweitering (1970, unpublished Ph.D. dissertation, Ohio State Univ., p. 33).

The middle part of the Huron, which is equivalent to a tongue of the Chagrin Shale, thins from north-eastern Ohio southward. The upper and lower parts of the Huron merge and thin toward eastern Kentucky and northern Tennessee. The position of the Huron relative to the overlying Three Lick Bed of

Provo, Kepferle, and Potter (1977) suggests that the Huron is mainly correlative with the lower unit of the Gassaway Member of the Chattanooga Shale of Tennessee.

The Rhinestreet Shale Member of the West Falls Formation is a recognizable unit in New York. Gamma-ray logs and lithologic sections were used to extend this black shale unit to western Pennsylvania and to the eastern half of Ohio, where it thins to extinction against an unconformity. By means of gamma-ray signatures the Rhinestreet equivalent was recognized as far south as southwestern Virginia and eastern Tennessee. In Tennessee this unit is the Dowelltown Member, the lower member, of the Chattanooga Shale. In Tidewater-Wolf's Head Well in Scott County, Virginia, the Rhinestreet is correlative to a sequence of black to very dark gray shale approximately 10 m above a cherty argillaceous limestone. According to recent sample descriptions by Zafar of the Kentucky Geological Survey, our Rhinestreet equivalent unit of the Tidewater-Wolf's Head Well contains a bentonite zone near the base. This 960-km correlation of the Rhinestreet was confirmed by a Late Devonian age determination made from a conodont study by Anita Harris (USGS). The conodont collections were keyed to Dennison and Boucot's (1974) measured section at Little War Gap, Hawkins County, Tennessee, and included samples from within their "Tioga Bentonite" zone. Harris identified *Palmitolepis punctata*, a Late Devonian form found in the Rhinestreet Shale Member of the West Falls Formation of New York. The paleontologic data confirm the extension of the Rhinestreet equivalent to southwest Virginia and corroborate the correlation of the Rhinestreet of New York and the Dowelltown Member of the Chattanooga Shale of Late Devonian age. In addition, the presence of an Upper Devonian bentonite zone in the beds identified as the Rhinestreet equivalent in the Tidewater-Wolf's Head Well and the Little War Gap section further confirms that these beds are equivalent to the Upper Devonian Dowelltown, which includes the Center Hill Bentonite Bed in Tennessee. It then seems reasonable to assume the bentonite zones of Scott County, Virginia, and Hawkins County, Tennessee, may be equivalent to the Center Hill Bentonite Bed of the Dowelltown Member in DeKalb County, Tennessee.

This work was performed in cooperation with the Eastern Gas Shales Program (EGSP) of the Department of Energy (interagency agreement number EX-76-C-01-2287) and through the cooperation of EGSP contractors.

Inner Piedmont Deformation

The South Carolina Inner Piedmont rocks were affected by at least three folding events and by two post-Proterozoic (Precambrian Z) thermal events according to A. E. Nelson (loc. 10). The first recorded folding is represented by rootless intrafolial folds; these folds are probably Precambrian in age. The second folding episode is represented by the northeast-trending regional fold structures. These folds appear to have developed during deformation associated with the first thermal or middle Paleozoic regional metamorphic event. The third folding episode is represented by small symmetrical and asymmetrical folds superposed on the earlier folds. A crenulation cleavage has developed along the flanks of these third generation folds. Locally, gentle warping may represent a still later episode of folding. Prominent shear zones were deformed during several phases over a long time interval. Deformation ranges from mylonitization, to minor cross folding of sheared rocks and incipient cleavage development, to final brittle fracturing. Mylonitization probably occurred at high temperatures during the first thermal event or period of regional metamorphism. The cross folding and cleavage development may have occurred during the third period of folding, but this is uncertain. The fracturing may have occurred at lower temperatures accompanied by retrogressive metamorphism, which represents the second thermal event.

Ordovician clastic rocks of eastern Pennsylvania

Detailed geologic mapping in upper Lehigh and Berks Counties, Pennsylvania, (loc. 1) by A. A. Drake, Jr., P. T. Lyttle, and G. G. Lash (Lehigh University) has confirmed earlier observations that there are at least three Ordovician clastic sequences in this part of eastern Pennsylvania: the Martinsburg Formation, the "Shochary" sequence, and Hamburg klippe sequence. The Martinsburg Formation is well known (Drake and Epstein, 1967) and rocks of the Hamburg klippe are reasonably well known from the work of Alterman (1972).

The "Shochary" sequence consists of the so-called Shochary Sandstone that contains an abundant Middle Ordovician ("Sherman Fall") shelly fauna and an unnamed interbedded pelite and thin graywacke unit that contains abundant Middle Ordovician pelecypods and graptolites, probably the lower part of zone 13. These rocks have turbidite features but lack the other characteristics of flysch. A prodelta environment for these rocks seems likely

since burrowing is common and the graptolites present apparently are shallow water, near surface dwellers. As such, these rocks contrast greatly with the flysch of the Martinsburg on the north. This fault, the Eckville fault, is a fairly steep thrust (50°). On the south and east, the "Shochary" rocks are in fault contact with rocks of the Hamburg klippe.

In this part of eastern Pennsylvania, the east and south margins of the Hamburg klippe are marked by a polymictic wildflysch that has overridden its own debris on a hard thrust. This low angle thrust zone contains a strong smear lineation showing transport from the east-southeast. The thrust has been folded subsequent to emplacement.

Georgia subsurface studies

Isopach maps have been prepared for all major lithologic units of the Georgia coastal plain by Howard R. Cramer (Emory University) and Peter Popenoe (USGS). These maps show that lower Cretaceous rocks onlap onto the Coastal Plain from the southwest, and are in a trough-shaped configuration. Upper Cretaceous rocks are overlain by Midwayan Paleocene rocks in western Georgia and by Upper Paleocene (lower Wilcox) rocks everywhere else, suggesting a regional unconformity following middle-Paleocene uplift. Lower Eocene to Holocene rocks overlie these with local unconformities relating to strand-line fluctuations. Jurassic rocks were identified in the extreme southwestern corner of Georgia, which appear to be equivalents of an updip extension of the Cotton Valley Group of Alabama. Structures created during the Paleocene and post-Oligocene uplifts have been identified. These are largely normal faults, some of which persist across the State of Georgia in northeast- and northwest-trending zones.

Tectonic model for northeast Virginia Piedmont

Mapping completed by Louis Pavlides in the Salem Church (loc. 3) and nearby quadrangles of Virginia has resulted in the formulation of a tectonic model to explain the manner of formation of the refolded synform (Ramsey type II interference fold) that occurs in the Salem Church and southern quadrangles of the northeast Virginia Piedmont. The stratigraphic framework of this model consists of a crystalline basement, the "Fredericksburg complex," on whose west side the Chopawamsic Formation (metavolcanic rocks) lies unconformably. The Quantico Slate (mostly metapelite) with a discon-

tinuous quartzitic (metasandstone and metawacke) layer at its base, was deposited unconformably on the Chopawamsic to the west and the "Fredericksburg complex" to the east. This stratigraphic package was differentially deformed in several stages. Initially, to the west, the Quantico and Chopawamsic occupied an upright syncline. To the east the anticline complementary to this syncline developed into a westward verging recumbent anticline placing biotite-hornblende-plagioclase gneiss of the "Fredericksburg complex" structurally above the younger Quantico Slate on its overturned limb. This superposed gneiss occupied a northwest-trending synformal flap of the overturned part of the westward verging recumbent or reclined fold. Later, folding of this northwest-trending synform about a northeast trending antiformal axis resulted in the interference fold pattern of this region.

This pattern of refolded folds is believed to extend as an anticlinorium at least from the Whispering Creek anticline of the central Virginia Piedmont northeastward through the Salem Church area up into the Occoquan region of northeast Virginia. It may belong to a tectonic front of nappes that recently have been recognized in the eastern Piedmont of Maryland.

New information on tectonic framework of the Culpeper Triassic and Jurassic basin

Recent investigations by R. P. Volckmann and W. L. Newell demonstrate that the eastern margin of the Culpeper Triassic and Jurassic basin (loc. 4) consists of a series of high angle faults that displace horizontally to steeply dipping sediments ranging from silty shales to boulder conglomerates against cataclastically deformed piedmont metamorphic rocks. Fault movement probably occurred during and after Triassic and Jurassic sedimentation.

Major faulting has occurred along two principal orientations; one ranges from N. 10° E. to N. 30° E., the other from N. 70° E. to N. 85° E. The more northerly trending faults appear to be truncated by the more easterly trending faults that can be traced into the Piedmont rocks. The major border faults are offset by a series of minor fractures which trend generally north-south to N. 20° W. Offset along these smaller faults is, in most cases, left-lateral, which suggests that the resolution of movement along the major border faults is left-lateral as well as vertical. Parallelism of the Triassic and Jurassic border faults, particularly those which are

north-northeast-trending, with those in the Stafford fault zone suggests that they may be related to the same tectonic framework.

Age of basal Cretaceous in North Carolina

Earlier reports have dated the basal outcropping formation in the North Carolina Coastal Plain (loc. 5), the Cape Fear Formation, as either Early Cretaceous (Aptian and Albian) or earliest Late Cretaceous (Cenomanian). Field studies and paleontologic investigations by J. P. Owens, R. A. Christopher and B. W. Blackwelder now indicate that it is Late Cretaceous (Turonian or Santonian). Correlating the Cape Fear either with units north along the Fall Line in Virginia and Maryland (Potomac Group, Lower Cretaceous part) or with units to the south mapped as Tuscaloosa Formation (Cenomanian) no longer seems warranted.

Triassic and Jurassic rocks in the South Carolina Coastal Plain

Three deep test holes, Clubhouse Crossroads No. 1, No. 2, and No. 3, drilled in Dorchester County, South Carolina, (loc. 6), have penetrated up to 377 m of pre-Upper Cretaceous volcanic and sedimentary rocks. According to G. S. Gohn and B. B. Higgins, a minimum of 120 m of unfossiliferous, feldspathic red beds underlie about 257 m of sub-aerial basalt flows. Potassium-argon ages (M. Lanphere) for basalt from CC No. 2 (204 ± 4.1 m.y., 162 ± 3.2 m.y., 186 ± 3.7 m.y.) are significantly older than previously reported ages for geochemically altered basalt from CC No. 1. The new dates confirm Late Triassic and Early Jurassic age for the basalt, and by inference a similar age for the underlying red beds, as previously suggested from other data by Peter Popenoe, Isidore Zietz, and David Gottfried. Major, minor, and trace element analyses of basalt from all three holes by Gottfried indicate that these rocks are predominantly quartz-normative tholeiitic basalts that are petrochemically similar to other Eastern North American lower Mesozoic basalts.

Geomorphology of the Augusta, Georgia, area

W. L. Newell and M. J. Pavich report that the deeply dissected inner coastal plain terrain of the Augusta, Ga., area (loc. 7), exhibits a complex history of weathering, erosion, and generation of surficial deposits. High permeability of marine sand units has resulted in extensive weathered horizons underlying broad uplands. These horizons are characterized by thick (1 to 12 m), white sandy leached

zones containing pale-brown lamellae, grading down through a mottled undulatory contact into an equally thick or thicker red oxidized zone.

The uplands are commonly bordered by back-wasting scarps that locally expose the weathered horizons. Colluvium and alluvium from these scarps and from the upland surfaces contain hematitic-limonitic pebbles derived from the semi-indurated oxidized zone of the upland residual mantle. Thus, the surficial deposits can be distinguished lithologically from all underlying Cretaceous and Tertiary sediments even where texture, bedforms, and morphostratigraphic position are uncertain.

The terraces, fans, and imbricated sheets of colluvium document a complex history of floods and mass movement influenced by fire and land use. Some deposits originated within historic times; others, as indicated by deep weathering and dissection, are much older. Locally, within one surficial deposit, unconformities between similar sediment units can represent deposition during vastly different time periods.

Nearshore sedimentation in Upper Cretaceous deposits in Western Georgia

Subenvironments within a barrier island complex can be recognized for each of the nearshore marine Upper Cretaceous units along the eastern margin of the Gulf Coastal Plain (loc. 8). The distribution and extensiveness of these barriers determined the degree of hydrologic restriction within back barrier environments. The barriers themselves are composed largely of coarse sand containing heavy mineral concentrations which may be locally economic deposits. Sedimentary structures, including trough crossbeds up to 3 m thick and abundant *Ophiomorpha* burrows, indicate that most of the sand was deposited as inlet filling sequences or as subaqueous off-shore bars. The seaward subtidal shelf deposits are typically bioturbated glauconitic sand to marl. Most of this Upper Cretaceous terrigenous sediment grades to chalk composed of nannofossils in central Alabama.

Synorogenic mudflow deposit

Spicular chert clasts in pebbly mudstone (non-marine mudflow) deposits in the basal part of the Rockwell Formation (Lower Mississippian) of western Maryland (loc. 9) are associated with clasts of Middle and Upper Devonian rock types and may define the inception of early Alleghenian folding and

thrusting in the central Appalachians according to W. J. Perry, Jr. The chert clasts are no younger than Middle Devonian and may be as old as Silurian.

CENTRAL REGION

KENTUCKY

New evidence supports Nebraskan age for origin of Ohio River drainage system

Detailed mapping in north-central Kentucky by W. C. Swadley and A. B. Gibbons has revealed several deposits of glacial drift that support a Nebraskan age for the origin of the Ohio River drainage system. These deposits, which include both deeply weathered till and outwash occur at low topographic levels in Trimble and Carroll Counties, Kentucky, in the area of the pre-Pleistocene Madison divide. The degree of weathering indicates these deposits are older than Illinoian Drift exposed in a comparable topographic position 17 km up the Ohio Valley near Carrollton, Kentucky, but the low topographic position, well below the preglacial drainage levels, requires an age younger than the high-level drift that ponded the Pliocene drainage and initiated the development of the Ohio River in this region. Therefore, the presence of two pre-Illinoian tills in the area would indicate the high-level till that occupies preglacial valleys is Nebraskan in age and the lower till was deposited in Kansan time following a long period of erosion during which the Madison divide area was deeply dissected and much of the present Ohio River system was developed.

Tentative dating of pre-Pleistocene deposits along the Kentucky River of central Kentucky

Several levels of fluvial deposits have been mapped along the Kentucky River in an area of central Kentucky west of Lexington. These deposits are preserved as terrace remnants in abandoned valley segments and meander cutoffs. Similar deposits mapped along an abandoned valley of the preglacial Kentucky River that extends northeastward from Carrollton, Ky., to Lawrenceburg, Ind., are overlain by glacial drift that has been identified as Nebraskan (Swadley, 1971; Ray, 1974). Tracing of terrace remnants along the Kentucky between these two areas by W. C. Swadley and upstream projection of the gradient established for the valley northeast of Carrollton indicate that deposits in central Kentucky at an elevation of about 220 m are of latest Pliocene age and were deposited just prior to the onset of

glaciation in the region. Glacial ponding of the Kentucky River caused the northern part to be abandoned and, with the breaching of a major drainage divide at Madison, Ind., initiated the development of the Ohio River drainage system. Rapid downcutting to the newly established base level during the Pleistocene produced the deeply incised valley of the present Kentucky River.

UPPER MISSISSIPPI EMBAYMENT

Late Cenozoic history of the upper Mississippi embayment

Studies by W. W. Olive indicate that continental deposits of the so-called Lafayette Formation of the northern Mississippi embayment were deposited during Miocene(?) and Pliocene time as coalescing alluvial fans. Deposition of the sediments was the result of a climatic cooling trend that gave rise to greater than present snow accumulation, greater spring runoff and increased stream discharge. With the advent of the Pleistocene, precipitation and runoff in headwater areas of streams heading in unglaciated areas decreased, and the ability of the streams to transport coarse sediments also decreased. As a result, growth of alluvial fans ceased. Eventually, as base level was lowered because of eustatic changes in sea level, streams with steepened gradients began to incise their valleys into the fan deposits.

During successive changes in base level in response to eustatic fluctuations in sea level during the Pleistocene, the streams alternately eroded and alluviated their channels. During early glacial stages the valleys were deepened. During maximum and waning glacial stages, they were alluviated, but to levels below those of previous stages. Thus, former floodplains that correspond to the four glacial stages are now represented by alluvial terraces that correspond to the Williana, Bentley, Montgomery, and Prairie terraces of Fisk (1938, p. 149-172; 1940, p. 63-113) and Waterways Experiment Station (1949, pl. 5).

LAKE SUPERIOR REGION

Structural evolution of the Vermilion district of Minnesota

Two generations of folds have been recognized (Hooper and Ojakangas, 1971; Sims, 1976) in the metavolcanic-metasedimentary succession in the western part of the Vermilion district in northeastern Minnesota, an early episode of isoclinal fold-

ing with subhorizontal hinge lines (F_1 or Embarrass-Lake Vermilion generation) and a younger episode of open to near-isoclinal folding with steeply plunging hinge lines (F_2 or Tower generation). From detailed studies of finite strain and metamorphic fabrics in bedded metasedimentary and pyroclastic rocks in the extreme western part of the district, Hudleston (1976) concluded that the F_1 folds probably were of soft sediment origin, for he recognized no internal strain in the rocks prior to the F_2 folding. He postulated that F_1 resulted from slow downslope slump movements induced by tilting within the volcano-sedimentary basin.

Geologic mapping by P. K. Sims and D. W. Southwick in the Soudan and Eagles Nest $7\frac{1}{2}$ -min quadrangles, just east of the study area of Hudleston, provides new data that bear on the origin of the two generations of folds, as well as on the regional structure. The mapping shows that F_1 folding involved metavolcanic rocks, mainly pillow basalt, as well as the better bedded sedimentary rocks, and that this episode of folding mainly controls the distribution of major geologic units in the western part of the district. In this part of the area, F_2 folding is rarely discernible and, where observed, the folds are small scale features.

If the correlation of fold episodes between the area mapped by Sims and Southwick and that studied by Hudleston is correct, an origin by soft sediment deformation for F_1 is questionable. It is unlikely that systematic folds in both well-bedded rocks and poorly bedded submarine volcanic rocks over an area of a few hundred square kilometers could have resulted from soft sediment deformation.

Geologic interpretation of aeromagnetic map of part of northern Wisconsin

A generalized bedrock geologic map (scale 1:250,000) of about 50,000 km² in northern Wisconsin has been completed by P. K. Sims and W. F. Cannon (USGS), and M. G. Mudrey, Jr., (Geological and Natural History Survey, University of Wisconsin-Extension). The geology is based largely on interpretation of a recently published aeromagnetic map (Zietz, Karl, and Ostrom, 1977). The map delineates for the first time the broad geologic relationships of the Precambrian rocks in the poorly exposed area between the Gogebic iron range and central Wisconsin.

The geology of northern Wisconsin is similar to that of northern Michigan. Except for the Gogebic range, the basement is Archean (formerly Precam-

brian W) gneiss and amphibolite. Z. E. Peterman's preliminary rubidium-strontium data on gneisses from localities near Mellen, Wis., indicate a model age of about 3,200 million years. The gneiss occurs at the surface throughout about one-third of the region as exhumed, uplifted fault blocks. Supracrustal metasedimentary and metavolcanic rocks, roughly equivalent to the Marquette Range Supergroup (Proterozoic, Precambrian X), overlie the gneiss in the north-central part of the region and in the vicinity of Wausau, in central Wisconsin. In this sequence, metavolcanic rocks increase southward relative to metasedimentary rocks, in the same way as in Michigan, and the metavolcanic rocks are spatially associated with large masses of Precambrian X granitic rocks about 1,800 million years old.

The fault pattern is complex and as yet poorly understood. An older fault system consisting mainly of northwest- and north-northeast-trending faults appears to be present throughout the region. The faults are steep, commonly have wide zones of mylonite, and were reactivated repeatedly through Precambrian time. A younger fault set consisting of steep, straight fractures that trend N. 50° to 55° E. appears to be confined to the northwest part of the region; these are interpreted as late Keweenawan (Proterozoic, Precambrian Y) faults related to late stages in the development of the mid-continent rift system. The pronounced northwest-dipping homocline of the Gogebic range probably resulted from tilting of fault blocks during this episode of extension.

The economically important volcanogenic massive sulfide deposits known in northern Wisconsin occur in the southern part of a large, east-trending, differentiated volcanic pile that traverses the state at about 45°30' N. lat. The volcanic mass is more than 250 km long, suggesting that the potential for the discovery of additional deposits in this belt is excellent.

MISSOURI

Distinct volcanic assemblages identified in Missouri Precambrian

W. P. Pratt's review of the exposed Precambrian of Missouri, based on recent detailed and reconnaissance mapping, shows that widespread volcanic rocks, previously characterized as rhyolites and felsites, comprise three megascopically distinct petrographic assemblages with an apparently simple gross stratigraphy. The oldest assemblage consists of quartz latites and soda-rhyolites (using the

chemical classification of Rittmann, 1952) and is distinguished by plagioclase phenocrysts; it predominates in the southern and central St. Francois Mountains. It is overlain by a rhyolite assemblage in which plagioclase and alkali feldspar phenocrysts are subequal. The youngest assemblage comprises alkali-rhyolites (distinguished by alkali feldspar phenocrysts) and makes up most of the St. Francois Mountains north of about $37^{\circ} 27' N.$ Lat; alkali-rhyolites also form the Eminence Mountains, where they are unusually rich in potassium. All three assemblages include abundant ash-flow tuffs; one ash-flow tuff unit may be as much as 2 km thick and is exposed locally over an area 40 km wide north-south and 60 km long east-west. Some evidence exists for several calderas, but they have not been positively identified.

ROCKY MOUNTAINS AND THE GREAT PLAINS

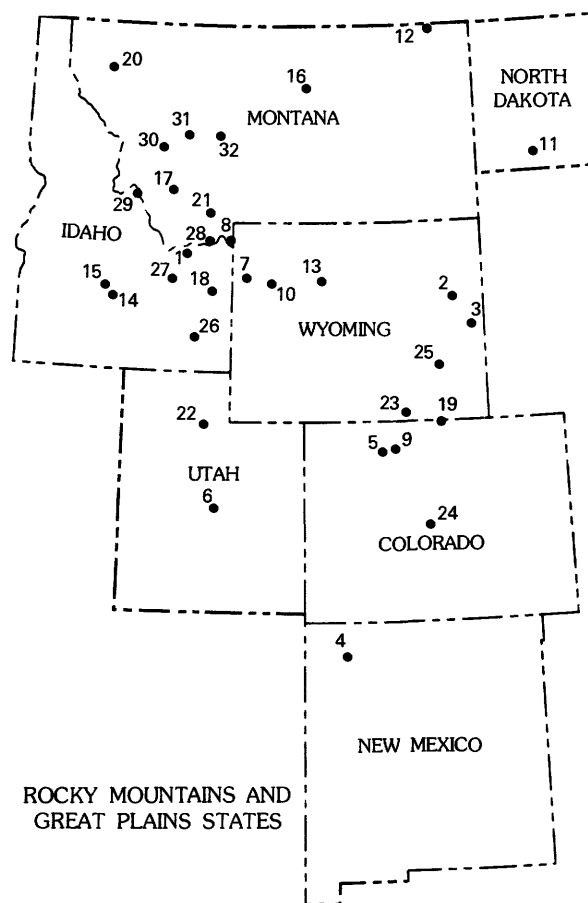
ECONOMIC GEOLOGY

Hydrocarbon potential north of Snake River Plain of Idaho and Montana

According to B. A. Skipp and M. H. Hait, Jr., stacked allochthons north of the eastern Snake River Plain, in an area near the Idaho-Montana border (index map, loc. 1) approximately bounded by lat $44^{\circ}00'$ and $44^{\circ}45' N.$ and long 112° and $113^{\circ} W.$ have structural and stratigraphic settings favorable for hydrocarbon accumulation. The Lima stack (Skipp and Hait, 1977) contains Paleozoic and Mesozoic cratonic sequences—Cretaceous marine shale, Triassic and Jurassic limestone and sandstone, and upper Paleozoic carbonate rock and sandstone—known to include both source and reservoir rocks in the similar structural setting of the Idaho-Wyoming thrust belt (Powers, 1977). The Lima stack is overridden on the west by the Lemhi stack, which is characterized by thick middle Proterozoic (Precambrian Y) rocks overlain by thick Paleozoic miogeoclinal carbonate sequences. The Paleozoic carbonate sequences associated with possible source beds of the McGowan Creek, Big Snowy, and Phosphoria Formations also would provide possible reservoirs if repeated at depth by thrusting, as suggested by Skipp and Hait, (1977, fig. 1).

Coal in Powder River basin in Wyoming

Early Tertiary deformation appears to have influenced deposition and subsequent erosion of coal



beds in the upper part of the Fort Union and lower part of the Wasatch Formations of eastern Powder River basin in Wyoming (loc. 2). In the Reno Junction-Antelope Creek area, at least two important faults coincide with zones where the Wyodak coalbed (Fort Union) splits into the Anderson and Canyon coalbeds, which are separated by as much as 90 m of intercoal sediments. Comparison of structure-contour and coal-thickness maps prepared by N. M. Denson, J. H. Dover, and L. M. Osmonson (1978a, b) showed the Wyodak and Anderson coalbeds to be relatively thick in synclines and anomalously thin or absent over anticlines. Some structures in the Fort Union Formation do not affect the overlying Wasatch, and those that do are more subdued than they are in the Fort Union, indicating that deformation culminated prior to deposition of the Wasatch. Field work by Denson combined with subsurface data indicated that the Wasatch-Fort Union contact in this part of the basin is an unconformity having a few hundred meters of relief. Variations in thickness of the Wyodak and Anderson coalbeds are a result of structurally controlled depositional patterns and (or) accelerated pre-Wasatch erosion

related to this unconformity. Recognition and delineation of the variations in thickness of these coalbeds is critical to their efficient development and reclamation throughout eastern Powder River basin.

Proterozoic rocks and iron deposits, Hartville Uplift, Wyoming

G. L. Snyder mapped a sequence of Proterozoic metasedimentary and metavolcanic (?) rocks, including muscovite, biotite, and chlorite schists, amphibolite, and dolomite in the Hartville uplift, Wyoming (loc. 3). These rocks are probably equivalent to part of the "Libby Creek Group" in the Medicine Bow Mountains in Wyoming. They have been intruded by quartz monzonite-granodiorite-diorite stocks, possibly remobilized older basement. All the above rocks are cut by dikes of pegmatite and two ages of amphibolite. Metamorphism ranges from chlorite to sillimanite grade. The area has been block-faulted in post-Pennsylvanian time, possibly along zones of weakness inherited from Precambrian structures.

Deposits of arsenic, beryllium, copper, and gold occur in the Uplift, but the main economic deposits are of hematite and supply iron ore for the mills in Pueblo, Colo. At least three ages of hematite deposits are present:

- Early Pennsylvanian, related to karstic solution of Mississippian and older carbonate rocks;
- Early Mississippian, related to karstic solution of Precambrian carbonate rocks;
- Pre-Mississippian, possibly Precambrian, hematite schists.

ENVIRONMENTAL GEOLOGY

Surficial deposits in San Juan Basin of New Mexico

G. R. Scott reported that the surficial deposits overlying the strippable coal of the Fruitland Formation (Cretaceous) in the San Juan Basin of New Mexico (loc. 4) consist of alluvium, fan alluvium, colluvium, and eolian sand. Along the San Juan River, the alluvium is bouldery glacial outwash in terraces ranging from early to late Pleistocene in age. Along the Chaco River and its tributaries, the alluvium is pebbly non-glacial material in terraces and on pedimentlike bedrock surfaces and is middle to late Pleistocene in age. The two youngest terraces are composed of sandy to silty alluvium; they lie along the bottoms of most valleys and are late Holocene in age. Fan alluvium covers some outwash terraces along the San Juan River. Silty to clayey colluvium lies on slopes below bedrock prominences.

The eolian sand, which Scott concluded is the most useful and widespread material for rehabilitating mined areas, is medium-grained and, although generally thin, locally exceeds 6 m in thickness. Well developed soils are formed on the eolian sand and on all but the youngest alluvium.

Landslides in northwestern Colorado

Cross-cutting relations between landslides and stream terraces are common in the area of the Craig 1:250,000-scale topographic map (loc. 5). At several places, the stream terraces can be assigned reliable relative ages chiefly because of their position with respect to volcanic ash or glacial deposits, the chronologic sequence of which has been established. Study of these cross-cutting relations led R. F. Madole to the following conclusions: (1) morphologic expression of landslides can persist in the landscape for hundreds of thousands of years, (2) only a minority of the landslides in the area mapped are as young as Holocene, and (3) the destruction of landslide forms with time parallels the repeatedly described weathering and erosion of glacial deposits.

Active faults in central Utah

Two generations of active faults were recognized by I. J. Witkind in central Utah (loc. 6). One set of faults (including the Wasatch fault) trends north and clearly belongs to the group of range-front, high-angle, normal faults that characterize the Basin and Range province. These faults appear to have been active since late Tertiary time, and fresh scarps in alluvium and alluvial fans indicate that they have been active in the Holocene. The second set of faults trends northeast and appears to be confined to the crest and flanks of the Wasatch Plateau. These faults, too, are high-angle normal faults and commonly bound grabens. Several of them cut and displace large amphitheater-like basins that are probably cirques. If these beheaded basins are indeed cirques, then it is clear that these faults were active during the late Pleistocene and possibly even during the Holocene. It would appear that this second fault set was established long after movement began along the Basin and Range type faults.

Hot springs in Jackson Hole in northwestern Wyoming

The hottest springs in Jackson Hole, Wyo., (maximum temperature 72° C) emerge along the trace of the Teton normal fault, which here has a displacement of 4,600 to 7,600 m, on the west side of Jackson Lake (loc. 7). The springs were not shown on the Grand Teton topographic map of 1899 or on

later topographic maps and were not described prior to construction of the Jackson Lake dam (1906-7; failed in 1910; rebuilt 1911-16). The dam raised the lake level 12 m. The 1977 drawdown of Jackson Lake almost to its original pre-dam level, because of drought and increased irrigation requirements in Idaho, briefly exposed the hot springs during September and October, allowing a brief reconnaissance study by J. D. Love and R. E. Lewis, Jr.

The total areal extent and flow of the springs are not known, but an estimated half of them were visible at the time of the study. This estimate is based on the abundance of nonflammable gas that accompanied the visible hot springs plus the area in which gas emerged through the lake water for more than 100 m offshore. About 2.5 km southeast of the hot springs, another elliptical area of gas seeps more than 100 m in diameter was noted in the middle of Jackson Lake where the September-October 1977 lake depth was 3 m, but the volume of water that accompanied the gas and its temperature are not known.

The visible springs extended along the west shoreline of Jackson Lake for approximately 520 m. Their combined flow was at least .021 m³/s. Water temperature generally ranged from 60° C to 72° C. The springs emerged from limestone rubble at the base of a cliff of Madison Limestone (Mississippian) on the upthrown side of the Teton fault. Rocks on the downthrown side below the Quaternary lake sediments may be Cretaceous. No Cenozoic igneous rocks are exposed in the area, but the source of the heat could be a hitherto unrecognized igneous body intruded along the Teton fault.

The pH of the water ranged from about 6.68 to 6.78. A moderate amount of sulfur in white strings emerged with the water. A scintillator detected no radioactivity, either in the water or in precipitates from it. Several springs produced a white astringent salt precipitate, one spring had a film of oil, and several had iridescent films or iron compounds. Samples of water and precipitates were taken for additional analysis.

Soil development and age of Bull Lake Glaciation in the Rocky Mountains

Particle size analyses of soils from five deposits in the Rocky Mountains assigned to the Bull Lake Glaciation showed increased clay content similar to that in soils from dated deposits near West Yellowstone, Mont. (loc. 8). The end moraines near West Yellowstone were dated by combined obsidian hy-

dration and potassium-argon methods as about 140,000 years old (isotope stage 6 of the marine record) and therefore older than the last interglaciation (K. L. Pierce and others, 1976). In order to make this comparison, Pierce used a crude but simple method of quantifying the total clay increase. Estimating the percent clay increase in the B-horizon(s) (present clay content minus a range of estimated original clay contents) and multiplying this by the appropriate horizon thickness gives the clay increase expressed as an equivalent thickness of clay.

Based on analyses of two soil profiles by R. C. Burke (written commun., 1975) the clay increase in the soils of the dated West Yellowstone moraines is estimated to be between 1.1 and 3.3 cm. Based on averages of analyses by Shroba (1976), the clay increase in soils from four moraines in the central and southern Rocky Mountains assigned to the Bull Lake Glaciation is estimated to be between 1.6 and 2.4 cm. Based on analyses by Machette and others (1976), soils from alluvium near Denver correlated with the Bull Lake have an estimated clay increase between 1.5 and 2.7 cm. Thus, on the basis of clay increase in B horizons, these deposits assigned to the Bull Lake Glaciation would seem to be similar in age to the deposits near West Yellowstone dated as 140,000 years old.

Time of Pinedale deglaciation in the Park Range of Colorado

Bog and lake sediments potentially useful in paleoclimatic studies are common along the summit of the Park Range south of Mount Ethel in north-central Colorado (loc. 9). Meyer Rubin determined radiocarbon ages of peat from two such sites sampled by R. F. Madole near the Continental Divide at Buffalo Pass. From the two radiocarbon ages (9,240 ± 200 years before present (B.P.), W-3804, and 7,730 ± 250 years B. P., W-3806) and related stratigraphic data, Madole concluded that the Pinedale ice cap probably had disappeared from the southern part of the Park Range by 10,000 years ago, a date much earlier in this area than has hitherto been generally accepted. Although evidence of subsequent glacial expansion has not been observed in this part of the range, Holocene cirque glaciation is recorded in the higher, more rugged part of the range north of Mount Ethel.

Glaciation near Togwotee Pass in the Wind River Mountains of Wyoming

W. L. Rohrer identified the sources of glacial erratics that now lie several miles southeast of Tog-

wotee Pass near the head of Wind River in Wyoming (loc. 10). Some scattered erratics are composed of the distinctive intrusive rock that forms the prominent Pilot Knob, a short distance south of Togwotee Pass, which has been K-Ar-dated at 3.4 million years. Other erratics composed of a non-intrusive rock, formerly attributed to a source north of Brooks Lake (Rohrer, 1966), also came from the vicinity of Togwotee Pass. More abundant erratics of a third kind were derived from the basalt of Lava Mountain, south of the Pass, which is about 480,000 years old, based on dates supplied by J. D. Obradovich. The erratics represent the earliest glaciation recognized in the area. They lie upon surfaces above 2,743 m in elevation (600 m and more above Wind River) and indicate a large ice mass west of the Pass, possibly dating back to approximately 480,000 years, since which time the land surface has been reduced to present levels by subsequent glaciations and post-glacial erosion.

Pingo scars in southwestern North Dakota

Large circular geomorphic features, 1,500 to 2,600 m in diameter, consisting of an outer ridge, a central dome, and an intervening moat and formed in the Fort Union Formation (Paleocene) southwest of Mott in Hettinger County in North Dakota (loc. 11), were identified as pingo scars by D. E. Trimble. These features, whose topographic expression is shown on the Mott Southwest and Mott South 1:24,000-scale topographic quadrangle maps, have as much as 17 m relief. They lie about 56 km west of the maximum position of the continental ice sheet in North Dakota, indicating periglacial permafrost far beyond the Pleistocene ice front. Similar, but smaller, features near De Kalb, Ill., have been described by Flemal, Hinkley, and Hester (1973).

Middle Wisconsinan glacial lake near Scobey, Montana

R. B. Colton discovered photogeologic evidence of a large glacial lake near Scobey in northeastern Montana (loc. 12), which was confirmed by Colton and R. D. Feltis during field examination of the lake deposits. The lake formed when a lobe of ice advanced north up the Poplar River and blocked the drainage. Bars, spits, hooks, and beaches were identified and indicate that crustal rebound in that area has been as much as 0.8 m/km. The area covered by the lake included at least 400 km² in northeastern Montana and at least that much more in Canada. The minimum age of the beach deposits is inferred to be 34,000 years.

STRATIGRAPHY

Correlation and structure of Eocene rocks in southwestern Bighorn Basin of Wyoming

The Aycross Formation, earlier recognized only in the northwestern Wind River Basin and adjacent southern Absaroka Mountains, is, according to T. M. Bown, well developed in the Grass Creek-Owl Creek area of the southwestern Bighorn Basin in Wyoming (loc. 13). It comprises at least 250 m of mudstone, sandstone, tuffaceous sandstone, conglomerate, tuff, and flow breccia. These rocks, referred to the Pitchfork Formation by Hay (1956) and most subsequent authors, are lithologically indistinguishable from the Aycross Formation of Love (1939) and contain an abundant and a varied vertebrate fauna. Fifty vertebrate-fossil localities are now known in Aycross rocks of the Bighorn Basin, and three of these are important microvertebrate quarries. Bown determined that the mammalian fauna of at least forty species contains diagnostic forms suggestive of an early middle Eocene age. The recovery of several new taxa and the unusual faunal associations of some of the mammals support Black's (1967) contention that the hitherto unknown middle Eocene faunas of upland areas peripheral to the major Tertiary basins of Wyoming might record different paleo-environmental settings.

In the southwestern Bighorn Basin, the Aycross Formation is overlain by at least 350 m of the Tepee Trail Formation. Bown found that portions of the Tepee Trail have become detached from in situ masses and have been transported across an erosion surface developed on the Aycross Formation. The detached segments are of two kinds: (1) highly deformed heterogeneous rock masses of considerable areal extent, and (2) highly deformed homogeneous rock masses less than 1.0 km² in area. Both before and during the episode of detachment faulting, the Aycross acted as a plastic unit. It is intensely deformed subjacent to the detached masses and is thrust and drag-folded over much of its outcrop area. The age of the detachment faulting is probably late Tertiary or Quaternary.

Revised thickness of Hailey Conglomerate Member, Wood River Formation of central Idaho

The Hailey Conglomerate Member (Middle Pennsylvanian), basal member of the Wood River Formation, was reported to be 300.5 m thick at its type locality (loc. 14) on the west side of the Big Wood River opposite Hailey, Idaho (Thomasson, 1959). In the course of extensive mapping, W. E. Hall and J. N.

Batchelder found that the Hailey is discontinuous in outcrop and thins to the east and north of the Hailey-Bellevue area, where its maximum thickness, except for the type locality, is about 122 m. The variation in thickness and discontinuity were attributed to steep normal faulting (Ross, 1934) and to nondeposition and facies change (Thomasson, 1959). However, the Hailey everywhere is intensely sheared, and its discontinuous masses are readily explained as boudins in a thick thrust-fault zone between the Milligen (Devonian) and Wood River Formations. Thus, the westward thickening of the Hailey is a result of deformation rather than original deposition.

At the type locality, the Hailey strikes approximately north and dips steeply west. It is underlain on the west by the Milligen Formation of Devonian age. Hall and Batchelder had considered the possibility that the type section is repeated in a steep isoclinal syncline, but they had not been able to examine the eastern contact to prove this hypothesis because access is difficult where the river flows against the west valley wall. Because of the drought in 1977, the Big Wood River was very low and this area was accessible. They found that the Milligen Formation does crop out on the east side of the Hailey about a half mile north of Hailey. The whole section is intensely sheared, the conglomerate is indeed in a steep isoclinal syncline, and the true thickness of the conglomerate is approximately 122 m. The conglomerate was folded by being squeezed between two north-striking faults on the west side of the valley and dropped possibly as much as 1220 m. This fault zone forms the remarkably straight west wall of the Wood River Valley. The new thickness eliminates evidence of westward thickening of the Hailey Conglomerate Member and opens the possibility that the Hailey might have been derived from an eastern emergent terrane on the Copper Basin Formation (Mississippian) as was documented by Skipp and Hall (1975) in the case of other Wood River conglomerates in the Fish Creek Reservoir area.

Paleozoic strata and Eocene(?) granites along eastern margin of Idaho batholith

Preliminary geologic mapping by C. M. Tschanz in the Smoky Mountains of central Idaho (loc. 15) revealed large outcrops of Paleozoic sedimentary rocks, pink Eocene(?) granites, and older Eocene(?) subvolcanic porphyries of intermediate composition in an area covering several hundred square kilometers, all of which are shown on published recon-

naissance geologic maps as either Idaho batholith (Cretaceous) or Challis Volcanics (Tertiary). Two slightly metamorphosed sedimentary units of pre-Pennsylvanian age, previously included in the Wood River Formation (Pennsylvanian part) (Ross, 1930), were recognized in the Little Smoky and Willow Creek mining districts. Together these discoveries greatly modify the geologic picture as previously mapped.

The pre-Pennsylvanian units are exposed in a north-trending belt along the eastern contact of the Idaho batholith for a distance of 16 km along the crest of the Smoky Mountains south of Carriatown and also for several kilometers east of the West Fork of Big Smoky Creek, about 20 km farther north. The Wood River Formation is extensively, although intermittently, exposed east of this belt, but its contact with the older units is not exposed north of Warm Springs Creek. According to W. E. Hall and J. N. Batchelder, in the Little Smoky district the two pre-Pennsylvanian units are separated by thrust faults, and the younger one is thrust on the Wood River. It appears that the two units are allochthonous and were thrust on younger rocks before the emplacement of the Idaho batholith late in Cretaceous time. The two units have been affected by low-grade regional metamorphism that also affected the Milligen Formation (Devonian) in the Wood River region but did not affect equivalent rocks farther east or the Wood River Formation. Although fossils have not yet been found, both units probably correlate with some part of the Silurian to Upper Devonian transitional sequence exposed on the northeast flank of the Boulder Mountains northwest of Trail Creek Summit.

The lower, more deformed unit consists chiefly of rusty weathering, pyritic, banded, light-gray siltite containing innumerable thin seams of dark argillite. It resembles most of the allochthonous type Trail Creek Formation of Silurian age. The thicker upper unit consists predominantly of dark gray, carbonaceous, silty limestone and calcareous siltstone. It is the host of the argentiferous lead-zinc veins in the Little Smoky district and in the northern outcrop area. It apparently includes locally some subphyllitic argillite with crinkle cleavage that is indistinguishable from rocks in the Milligen Formation of Devonian age, but it could be partly older or younger. Both units are several hundred meters thick.

These previously unmapped outcrops of Paleozoic rocks are scattered over several hundred square kilometers in the Galena, Baker Peak, Frenchman Creek, and Boyle Mountain quadrangles of Idaho. They are

intruded by many dikes and irregular bodies of Eocene(?) subvolcanic porphyry that are contemporaneous with and similar to the overlying Challis Volcanics. In four cirques surrounding Norton Peak, they are also intruded by pink granite (or quartz monzonite) that is correlated with the Boulder Mountain stock and the Sawtooth batholith, which are 44 million years old.

IGNEOUS ROCKS

Ages of alkalic igneous activity in north-central Montana

B. C. Hearn, Jr., R. F. Marvin, R. E. Zartman, and C. W. Naeser have dated about 60 rocks from alkalic igneous centers in north-central Montana (loc. 16) by K-Ar analysis of mica, feldspar, hornblende, and pseudoleucite, and by fission-track analysis of apatite, sphene, and zircon (Hearn and others, 1977). Ages suggest that peak igneous activity occurred between 53 and 48 million years ago, in early and middle Eocene time. However, major intrusions in the Little Rocky Mountains and part of the Judith Mountains are significantly older—Late Cretaceous or Paleocene. Significantly younger ages were obtained from some intrusions in the Little Belt and Judith Mountains, from the Missouri River Breaks diatremes and dikes, and from Smoky Butte near Jordan. Age ranges are, from oldest to youngest in millions of years:

Judith Mountains	80(?)–46
Little Rocky Mountains	66–58
Little Belt Mountains	58–41
(Marvin and others, 1973)	
Bearpaw Mountains	55–49
Sweetgrass Hills	52–49
Highwood Mountains	52–48
Missouri River Breaks	51–46
Eagle Buttes	50–48
Smoky Butte	27

Thus the total span of igneous activity may be as much as 50 million years. Dates suggest a 3- to 4-million-year life of individual centers, similar to time spans of major basic-silicic magma systems in Western United States. Ore deposits are typically late at each center and range in age from Late Cretaceous and Paleocene to Eocene. Major uplifts of the Judith and Little Rocky Mountains in Late Cretaceous and Paleocene time probably influenced the early migration of oil and gas in the western part of the Williston Basin.

Chemical trends of Tertiary volcanic rocks in the Pioneer Mountains of Montana

E-an Zen obtained chemical analyses of 10 Eocene volcanic rocks and a Miocene volcanic rock from the Vipond Park area in southwestern Montana (loc. 17), all dated by K-Ar whole-rock methods in cooperation with R. F. Marvin. The chemical data show that the rocks range from basaltic andesite and andesite, through dacite, trachyandesite, and rhyodacite, to rhyolite (all names according to Rittmann's system), the intermediate members being predominant and evidence of bimodal distribution lacking. The one Miocene rock is not chemically or mineralogically different from the Eocene rocks. Harker variation diagrams of the data show moderate to excellent rectilinear correlation. Plots of K_2O against SiO_2 show these rocks to be chemically different from the broadly contemporaneous Challis Volcanics of central Idaho, in spite of some petrographic similarity. At SiO_2 values of 55 or 60 percent, the corresponding weight percent K_2O gave values that, applying the plots of Dickinson and Hatherton (1967; Hatherton and Dickinson, 1969) as was done for the Tertiary volcanic rocks of the Western United States by Lipman, Prostka, and Christiansen (1972), would yield nominal "depth of derivation" of about 160 km, which fits very well with the western or trailing edge of Lipman and others' eastern downgoing slab, and the geographic location of the Pioneer Mountains fits their map well.

The hypothesis of Lipman, Prostka, and Christiansen has recently been revived (Dickinson and Snyder, 1977), and the chemical data from the Pioneer Mountains suggest that, whatever the true explanation of the relations, the hypothesis does provide a correlational tool of predictive value. On the other hand, a similar plot of the Pioneer batholith rocks, Late Cretaceous in age, yields a similar fictive depth of magma derivation, even though the initial strontium values refute an upper mantle origin (unless crustal contamination of isotopic ratios is allowed). The Elkhorn Mountain Volcanics and the main series (Tilling, 1973) of the Boulder batholith, both Late Cretaceous in age, yield fictive depths of about 260 km, which could fit the hypothesis of Lipman, Prostka, and Christiansen because the area is at the junction of their two downgoing slabs. All of which seems to indicate that the hypothesis has hit upon a real correlation but not a real explanation yet.

Tectonic implications of granite ages, southwestern Montana

The Pioneer batholith in the Pioneer Mountains of Beaverhead County in Montana (loc. 17), mapped by E-an Zen, has yielded isotopic K-Ar ages of biotite and hornblende ranging from 80 to 62 million years. Most of the rocks contain biotite and hornblende and have minimum ages of about 68 million years, whereas, the only 62 million-year-old pluton is the only two-mica granite found so far, both micas being products of liquids crystallization on the basis of textural relations. Similar relations also occur elsewhere in southwest Montana. J. M. Hammarstrom's microprobe data showed no halogen in the mica; therefore, unless (improbably) lithium is abundant in the micas, the two-mica granites must have crystallized at pressures of 3 kbar (10-km load) or more (Chatterjee and Johannes, 1974). On the other hand, the biotite-hornblende plutons show field evidence (miarolitic cavities, etc.) of having formed at shallow depths of only a few hundred bars (1- to 2-km load). Thus between 68 and 62 million years ago, the Pioneer Mountains and other parts of southwestern Montana must have received about 8 km of extra tectonic load. Zen interprets this as being caused by the emplacement of the Sapphire tectonic block at about this time; the dates are not in conflict with known age relations now being considered for the Sapphire block (Chase and Hyndman, 1977) and in fact could provide ages for the distal parts of the block. Study of the western Pioneer Mountains should shed critical light on this problem.

Strontium-isotope data from Pioneer batholith in southwestern Montana

E-an Zen's study of the Pioneer batholith in southwestern Montana (loc. 17) was provided major new insight by two initial strontium values of two plutons determined by J. G. Arth. One, a tonalite about 70 million years old, has a value of .7116, and a nearby granite of the same age has a value of .7130 (both $\pm .0002$). These numbers show that the two rocks are not just phases of the same crystallizing magma, a point strongly suggested by field data but difficult to prove. The values are very high compared to the values of the Boulder batholith, which range from .7055 to .7092 $\pm .0006$; the two sets do not overlap at the level of twice the standard deviation. Consanguinity of the rocks of the "sodic series" of the Boulder batholith, with rocks of the Pioneer batholith, was previously conjectured (Zen, Marvin, and Mehnert, 1975; Tilling, 1973) because they

have comparable K_2O/SiO_2 relations, are similar in age, and in the Boulder batholith the rocks of the sodic series tend to occur toward the Pioneer batholith. The isotope data seem to disabuse us of that hypothesis.

Arth also obtained an excellent 4-point isochron from four rocks of the pre-Belt crystalline-basement gneisses from the same area, and an isochron age of $1,639 \pm 36$ million years. On the basis of U-Th-Pb ages of a zircon from one of the rocks, this is probably a metamorphic isochron. The strontium isotopic values of these four pre-Belt rocks 70 million years ago nicely bracket the values of the two plutons mentioned in the paragraph above. Thus, on the basis of the strontium value, a supposition can be made that the magma was derived by melting the upper-crustal basement material. The Boulder batholith is north of the Willow Creek fault zone, but the Pioneer batholith is south of it. The isotopic difference between the two batholiths could mean that their magmas were generated from different blocks of the crust. The high initial strontium values of the intrusive rocks of the Pioneer Mountains suggest that the source of the magma was not in oceanic crust.

The Heise caldera in southeastern Idaho

From their mapping and detailed study of the volcanic stratigraphy of the Heise-Kelly Mountain-Willow Creek area of southeastern Idaho (loc. 18), H. J. Prostka and D. J. Doherty concluded that this area lies just within a huge resurgent caldera of Pliocene age. A rhyolitic, crystal-rich, eutaxitic, lithophysal, welded ash-flow tuff, informally designated Heise A, was erupted along a ring fracture zone, part of which is exposed in the canyons of Willow Creek and Meadow Creek. This tuff overlies Mesozoic clastic sedimentary rocks throughout most of the map area. At the base of the Heise Cliffs, however, it lies upon a massive banded flow of devitrified porphyritic rhyolite, which is exposed along most of the Heise Cliffs and Kelly Mountain. The caldera collapsed during the late stages of this ash-flow eruption. Caldera collapse was followed by several stages of rhyolitic volcanism, the products of which are well exposed at Kelly Mountain and along Willow Creek.

Prostka and Doherty recognized two post-collapse ash-flow tuffs separated by up to 300 m of devitrified rhyolite flows and followed by a densely welded ash-flow tuff probably from a distant source in the Snake River Plain.

All these eruptive rocks were then uplifted in several small domes just inside the ring-fracture zone. Next, late-stage resurgent volcanism produced thick pumiceous ash-flow and air-fall tuffs, which are thickest in Little Kelly Canyon but are absent from the top of Kelly Mountain. The sequence closed with the eruption of additional welded ash-flow tuffs. With the exception of the one densely welded ash flow mentioned, all the tuffs and flows were erupted from sources close to the Heise-Kelly Mountain dome. Base-surge features characterize some of the tuffs (Doherty, 1976). The stages of activity match very closely stages 2 to 6 of the development of resurgent calderas described by Smith and Bailey (1968). The same general sequence occurred during formation of the Island Park and Yellowstone calderas to the northeast (Hamilton, 1965; Keefer, 1971; Christiansen and Blank, 1972).

Carbonate-rich kimberlite in southeastern Wyoming

Carbonate-rich, massive to porphyritic or brecciated kimberlite has been recognized by M. E. McCallum, C. B. Smith, and H. G. Coppersmith (Colorado State University) in diatremes of the Colorado-Wyoming State Line and Iron Mountain, Wyo., districts (loc. 19). Carbonate-rich phases are texturally similar to the more serpentine, rich kimberlite varieties (Smith and others, 1977), but contain appreciably greater amounts of calcite and dolomite. Phenocrysts (olivine), xenocrysts (primarily olivine, enstatite, Cr-diopside, pyrope, Mg-ilmenite, and phlogopite), and xenoliths of crustal and upper mantle origins are commonly suspended in a matrix composed chiefly of carbonate with minor amounts of chaotically distributed serpentine, phlogopite, apatite, and secondary hematite and leucoxene after magnetite and perovskite. In some phases, phenocrysts, fragmental inclusions, and serpentinous matrix material may be completely carbonatized, and the rock may contain as much as 90 percent carbonate.

Preliminary chemical analyses indicate that the carbonate-rich kimberlite contains the largest amounts of La, Ce, Nd, Cs, Ba, Be, Pb, Sr, and Zn, in addition to CaO and CO₂ of all the kimberlite phases in the area. However bulk chemical composition is remarkably similar to that of average serpentine-rich phases. This similarity apparently results from the tendency of carbonate-rich kimberlite to contain dolomite and greater amounts of "foreign" SiO₂ in the form of granitic fragments and silicified groundmass constituents. Petrographic

and field evidence indicates that some of the carbonate-rich kimberlite crystallized from a magma containing immiscible silicate and carbonate fluid phases. Diatreme formation by fluidization and explosive boring apparently was initiated in portions of kimberlite dike systems where the carbonate-rich fluid phase was most concentrated, and where fluid pressures exceeded load pressures.

PRECAMBRIAN ROCKS

Copper in Belt rocks of Montana

J. E. Harrison extended mapping of the several formations of the Ravalli Group of the Belt Supergroup northward in Montana into the area of the Kalispell 1:250,000-scale map (loc. 20), where they had not previously been differentiated. Because stratabound copper occurs in rocks of the Ravalli Group, subdivision of the group to improve understanding of its depositional history is of more than academic interest. Harrison's preliminary studies suggested that the upper unit of the Ravalli, the Spokane Formation, which was derived from the northeast, contains tongues of the middle unit of the Ravalli, the Revett Formation, which was derived from the south. The tongues of Revett are about 30 m thick, are composed of quartzite, and are in envelopes of green laminated argillite and siltite about 10 m thick that contain anomalously large amounts of copper sulfide. Further mapping is needed to determine the extent and persistence of the copper occurrences.

Archean age of major sedimentary sequences in southwestern Montana

Rubidium-strontium analyses by C. E. Hedge of samples collected by Hedge and H. L. James during the past several years from various localities in the Ruby, Tobacco Root, Madison, and Gallatin Ranges of southwestern Montana (loc. 21) showed that the major pre-Belt metasedimentary sequences have a minimum age of $2,726 \pm 13$ million years. These sequences, now generally metamorphosed to the level of amphibolite facies, include thick units of dolomite and quartzite as well as widely distributed thin beds of iron-formation.

W. M. Cady reported that the Archean rocks of the Ruby Mountains include paragneiss, metabasalt, and ultramafic intrusive rocks, in addition to quartzite, marble, and iron-formation. This mixture of rocks is characteristic of both eugeosynclinal and

miogeosynclinal assemblages of Proterozoic and Phanerozoic time.

Farmington Canyon Complex, Wasatch Mountains, Utah

Proterozoic (Precambrian) rocks of the Farmington Canyon Complex in the region between Ogden Canyon and Mill Creek southeast of Bountiful, Utah (loc. 22), were found by B. H. Bryant to consist of complexly deformed high-grade metasedimentary rocks, migmatite, granitic gneiss, pegmatite, and lenses of amphibolite. No infolds or slices of younger, less metamorphosed Precambrian rocks occur in this part of the Wasatch Mountains.

In the northern part of the complex the predominant rock is fine- to medium-grained quartz monzonite gneiss containing amphibolite and calc-silicate lenses, which range from a few meters to a kilometer in length. This gneiss grades into migmatitic gneisses containing various amounts of biotite, hornblende, and garnet, and enclosing numerous pegmatitic lenses and stringers, the contacts of which are generally indistinct. To the south, near Farmington Canyon, the effects of migmatization decrease, biotite-feldspar-quartz layers increase, and many pegmatites several meters thick with sharp contacts are present. South of Bountiful Peak, the complex locally includes interbeds of coarse-grained white quartzite as much as several meters thick. Individual beds of quartzite can be traced less than a kilometer. Farther south at Mill Creek, layers of calc-silicate gneiss are abundant.

Throughout the complex, sillimanite is preserved in layers of biotite schist not greatly affected by later retrogressive metamorphism. Field observation suggested to Bryant that sillimanite formed during the metamorphism that produced both mineral lineation and west-trending minor folds.

Zones of shearing and retrogressive metamorphism under greenschist-facies conditions are widespread, especially in the central part of the complex between Weber and Farmington Canyons. Many of the shear zones have low to moderate dips that truncate more steeply dipping older foliation and layering, but other shear zones parallel the older structures. The rocks along these shear zones are more thoroughly sheared through a much greater thickness than along the Ogden thrust, which passes beneath the Farmington Canyon Complex at its north end and is marked by a thin zone of retrograde rocks and many fractures. The shear zones must have formed in a deeper environment somewhat before the Ogden thrust or even much earlier, perhaps in Proterozoic (Precambrian Y or Z) time.

Mafic complex at Mullen Creek in the Medicine Bow Mountains of Wyoming

Continued study by M. E. McCallum of the mafic complex at Mullen Creek in southeastern Wyoming (loc. 23) revealed a number of significant structural, petrographic, and geochemical trends. The complex consists of a variably layered sequence of Precambrian meta-igneous mafic rocks that reflect wide ranges of metamorphism and hybridization, the latter associated with intrusion of felsic magma. Relict cumulate textures and zones of rhythmic layering are common, and crossbedding and minor scour channels of igneous origin have been observed (Donnelly and McCallum, 1977). Structural and compositional data indicate that the complex has been folded anticlinally about a slightly overturned axis plunging steeply to the northwest, and subsequent refolding is represented by a shallow westerly plunging synantoclinal fold.

Metagabbro, metadiabase, and metaleucogabbro predominate, but metapyroxenite and variably metamorphosed anorthosite, troctolite, olivine gabbro, and norite are abundant locally. Basaltic to diabasic dikes record several intrusive episodes, and later felsic intrusive rocks are abundant in the central part of the complex. Preliminary geochemical and petrographic data indicate compositional variations that are consistent with those of other layered mafic intrusions. Concentration of leucocratic phases, ratios of Fe to Mg, and content of Na, Ti, V, Zr, and P increase, and Ni decreases toward the inferred top of the complex.

TECTONICS

Paleocene deposition and Eocene deformation in South Park, Colorado

In central Colorado, the South Park Formation (Sawatzky 1967; Wyant and Barker, 1976) filled a structural basin (loc. 24) between the Laramide Sawatch anticline and the Front Range early in Tertiary time. The formation rests unconformably on Upper Cretaceous rocks and was folded, faulted, and overridden by the western margin of the Front Range uplift along the Elkhorn fault. R. F. Marvin, H. H. Mehnert, and V. M. Merritt determined K-Ar ages of biotite from crystal-lithic tuffs from the base, the upper middle (Link Spring Tuff Member), and the top of the South Park Formation. The ages are 65.5 ± 1.6 , 59.7 ± 2.0 , and 56.3 ± 1.3 million years, respectively, showing that the filling of the South Park basin took place throughout Paleocene time.

Fission-track ages of zircon from the same samples, determined by C. W. Naeser, are compatible with the biotite ages.

B. H. Bryant concluded that folding and faulting of the South Park Formation closely followed its deposition, for boulder beds near the top of the formation include abundant fragments derived from the margin of the Front Range uplift east of the Elkhorn fault. This deformation must have occurred near the beginning of Eocene time.

Tectonic significance and post-Laramide giant boulders in southeastern Wyoming

Conspicuous deposits of giant boulders of Precambrian rocks have long been known on both flanks of the Laramie Range in southeastern Wyoming (loc. 25). The deposits are nonfossiliferous, and previous workers have called them Paleocene, lower Eocene, Oligocene, Miocene, Pliocene, or Pleistocene. They are not related to faults, and their tectonic significance has not previously been recognized.

J. D. Love identified three major episodes of boulder deposition: (1) middle Eocene, (2) Oligocene and Miocene, and (3) Pliocene and Pleistocene. The middle Eocene boulder deposits are confined to the west flank, and in places extend to the crest of the Precambrian rock core of the Laramie Range. The younger boulder deposits are on the east flank and extend eastward onto the High Plains. No lower or middle Eocene rocks are known on the east side of the range south of the Powder River basin. Love postulated the following tectonic, erosional, and depositional events to explain the distribution of giant boulders through Cenozoic time and their present positions with respect to the Laramie Range, the High Plains to the east, and the basin to the west:

- Early in Eocene time, drainage from the Laramie Range and the Granite Mountains in central Wyoming was to the north through the Powder River basin (Love, McGrew, and Thomas, 1963, p. 203 and fig. 7; Seeland, 1976, p. 36). The area east of the Laramie Range was high and has yielded no record of early Eocene deposition.
- At the beginning of deposition of middle Eocene rocks, the Laramie Range and probably the basin area to the east (northern part of the Denver-Julesburg structural basin) were uplifted high enough and tilted westward steeply enough to block eastward drainage and to permit catastrophic floods, aided by a wet humid climate and abundant airfall plastic ash debris,

to spread 30 m or more of giant Precambrian boulders, many 3 to 7 m in diameter, 8 to 16 km westward from the Laramie Range out onto Cretaceous rocks. The apron of boulders covered an area of at least 400 km².

- The same region tilted eastward during Oligocene time and eastward-flowing drainage was established across the Laramie Range. The range never again was a significant barrier to streams flowing from the basin on the west into the basin to the east.
- During later Oligocene to Miocene time, the east flank of the Laramie Range and the High Plains to the east sagged 500 m or more and became the site of deposition of several hundred meters of conglomeratic strata including zones of large boulders of Precambrian rocks. These boulders are not as big or as abundant as the boulders deposited, 300 m or more topographically higher on the opposite side of the range in middle Eocene time.
- In Pliocene to Pleistocene time, another catastrophic event, possibly triggered by a combination of sudden lowering of base level east of the Laramie Range, rise of the range itself, and tremendous floods, resulted in the eastward spread of giant granite boulders, many 3 to 5 m in diameter, for 30 km or more onto a nearly flat terrain of Miocene rocks. No unquestioned glaciation of the east flank of the range has yet been recognized, but meltwater from some ancient stage could have been involved. No comparable boulder deposits of this age are present on the west side of the range.
- After deposition of the boulders in event 5, the general land surface 16 km or more east of the Laramie Range was eroded down about 150 m, leaving remnants of these giant boulders on interstream divides.

Middle Proterozoic tectonics in the Wyoming Age Province

A search through the USGS Radiometric-Age Data Bank for available geochronologic data on Archean rocks of the Wyoming Age Province revealed systematic patterns in Rb-Sr and K-Ar biotite ages that are interpreted to be the result of major vertical tectonic events in middle Proterozoic time. A general decrease in mineral ages from the center to the periphery of the Wyoming Age Province has been known for many years. The compilation of all existing data by Z. E. Peterman emphasized and extended this pattern. Biotite ages in

central and northern Wyoming were stabilized by uplifting and cooling in the latest Archean or earliest Proterozoic time. Biotite ages in southern Wyoming and in southwestern Montana are lower by as much as one billion years. The regional conformity of these lower ages and narrow transition zones with regions of greater ages suggest vertical uplift and cooling as the major tectonic cause of the age patterns. The transition zones that are marked by steep gradients or discontinuities in biotite ages are zones of major crustal dislocation along which several kilometers of vertical movement must have occurred in middle Proterozoic time.

Geology of the northern Portneuf Range in southeastern Idaho

M. K. Corbett (Idaho State University) briefly indicated some of the results of geologic mapping in the northern part of the Portneuf Range in southeastern Idaho (loc. 26). The range is composed of several upper Proterozoic (Precambrian Z) to lower Paleozoic east-dipping units of general north-south trend; elevated western portions of the range consist primarily of Proterozoic (Precambrian) quartzite and argillite, which are successively overlain by Cambrian to Silurian carbonate rocks in an eastward direction.

The major structures, which offset, repeat, omit, and otherwise interrupt the homoclinally dipping sequence, are associated with two main tectonic events: (1) thrusts related to development of the Idaho-Wyoming thrust-fold belt during the Sevier orogeny of Cretaceous time, and (2) younger block faults produced by regional extension. The larger of two thrust faults resulted in the eastward displacement of Proterozoic (Precambrian) quartzites and argillites for several kilometers over a lower plate consisting primarily of Paleozoic carbonate rocks. Several sets of high-angle faults cut all map units and have displacements of a few hundred meters. The eastwest and northsouth sets appear to have developed concurrently, as no definite pattern of relative age could be determined with any consistency. The boundary fault on the west side of the northern Portneuf Range, the Bonneville fault, consists of a zone of one or more slip surfaces, all with similar sense of movement. The zone has stratigraphic throw of nearly 1,200 m and, based on the disturbance of Tertiary gravels, appears to be the most recent fault mapped. It offsets, but never is offset by other high angle faults of the area. Folding is essentially absent from the Portneuf Range.

Late Paleozoic depositional patterns suggest separate crustal responses north and south of eastern Snake River Plain

B. A. Skipp noted that the Mississippian, Pennsylvanian, and Permian Systems in southern Idaho and adjacent areas are very different on the north and south sides of the Snake River Plain west of longitude 113°. North of the plain in central and eastern Idaho, (1) Lower Mississippian rocks consist of more than 3,500 m of coarse-grained deep-water foreland-basin flysch that grades eastward into extensive shale and siltstone (Skipp and Hait, 1977; Nilsen, 1977; Sandberg, 1975); (2) Upper Mississippian rocks consist of 1,250 m of limestone that grades westward into coarse-grained partly shallow-marine strata deposited on the site of the earlier Mississippian flysch basin (Skipp and Hait, 1977; Nilsen, 1977); and (3) Pennsylvanian and Permian rocks were deposited in two marine basins separated by the Copper Basin highland (Skipp and Hall, 1975; Skipp and Hait, 1977). The western Wood River basin contains Middle Pennsylvanian to Permian sandstone, limestone, argillite, and minor conglomerate and chert, more than 4,760 m thick (Hall, Rye, and Doe, in press; Skipp and Hait, 1977). The eastern Snake Canyon Basin contains a Lower Pennsylvanian to Permian sequence 1,425 m thick including limestone, dolomite, sandstone, and a thin Phosphoria Formation (Skipp and Hait, 1977).

South of the plain, (1) Lower Mississippian rocks are mostly fine-grained orogenic and nonorogenic deposits, not known to be more than 1,400 m thick (Poole and Sandberg, 1977); (2) Upper Mississippian rocks are more than 2,100 m thick, consist of fine- to coarse-grained synorogenic sediments deposited as a series of coalescing deltas in a narrow trough (Brew, 1971), and thin eastward across northern Nevada into northwestern Utah (Poole and Sandberg, 1977; Skipp, in press); and (3) Pennsylvanian and Permian sandstones and limestones appear to thicken from east to west across southeastern Idaho west of Pocatello but nowhere are thinner than 2,000 m (R. L. Armstrong, oral commun., 1977; Leland Cress, written commun., 1977; J. Fred Smith, written commun., 1977); no evidence of two separate basins is known.

Skipp concluded that these different depositional patterns and histories indicate different paleotectonic settings during late Paleozoic time on opposite sides of a zone that parallels the trend of the late Cenozoic eastern Snake River Plain.

Structure and volcanism in eastern Snake River Plain of Idaho

Detailed reconnaissance mapping at a scale of 1:24,000 of the eastern Snake River Plain (loc. 27), an area of about 19,000 km² east of longitude 114° 15' W. and north of latitude 43° N. was completed by M. A. Kuntz. These studies show that this continental basalt province is characterized by distinctive structural and volcanic features.

The major structural features of the area studied in the eastern Snake River Plain are volcanic rift zones, which are defined by rectilinear distribution of structural and volcanic features such as grabens, extensional faults, cinder cones, eruptive fissures, shield volcanoes whose vents are elongated over inferred rifts, and non-eruptive open fissures. These features are typically arranged along the rift zones in the order listed above from the north margin of the Plain to the Plain axis. Similar relationships are not clearly recognized near the south margin of the eastern Plain, probably owing to erosion and deposition of sediments by the Snake River. The largest number of rift zones trend northwest or north, normal to the long axis of the Plain. These include the Great Rift, Arco, Spencer-High Point, Menan, Hells Half Acre-Lava Ridge, and Rock Corral Butte rift zones. A few rift zones with northeast or east trends are present in the study area, but they are short and relatively discontinuous. Some rift zones are narrow and have had volcanism centered on them for only short periods of time (Menan rift); others are narrow zones in which volcanism has been sporadic over long periods of time (Hells Half Acre-Lava Ridge); and others are broad zones with indistinct boundaries where volcanism has also been sporadic (Great Rift and Arco). Rhyolite domes (Big Southern Butte, East Butte, and Middle Butte?) and a ferro-latitude volcano (Cedar Butte) all are at the intersections of NW-SE rift zones with rift zones of different trends.

Nearly all of the Pleistocene and Holocene volcanoes in the study area represent rift-controlled eruptions; their distribution is not random as has been stated by some workers. Although various volcanic landforms occur, shield volcanoes located near the center of the Plain, covering areas between 200 and 500 km² and having volumes on the order of 50 km³, make up most of the volcanic pile along the axis of the eastern Snake River Plain. In contrast, the marginal parts of the eastern Plain are made up of volcanic products chiefly of cinder cones, spatter ramparts along eruptive fissures, and smaller shield volcanoes, and interlayered sediments.

Volcanic rift zones that intersect the Plain margins (those having northwest and north trends) are aligned with range-front faults and older structures in mountain ranges adjacent to the Plain. The fault zones beyond the Plain margins and their rift-zone extensions onto the Plain define continuous, nearly rectilinear structural systems, all parts of which are related to the regional northeast-southwest extension that characterized the late Tertiary and Quaternary stress field of the northeastern Great Basin. Dominant dip-slip or strike-slip fault movement has been documented in the mountains north and south of the Plain, whereas extensional fissures are the only obvious expression of strain at the surface near the axis of the eastern Plain. The continuation of these structural systems across the margins of the eastern Plain, the absence of identifiable faults at the boundaries of the eastern Plain, and the lack of clear geophysical evidence of such faults suggested to Kuntz that the eastern Plain is not a graben decoupled from the surrounding mountains but is rather a downwarp similar to that originally proposed by Kirkham (1931, p. 473-479).

A major left-lateral strike-slip fault in the Wood River area of Idaho

W. E. Hall and J. N. Batchelder mapped a major strike-slip fault that strikes N. 70° E. for a distance of 40 km from Wolfstone Creek on the west to the head of the East Fork of the Big Wood River on the east (loc. 14). The shatter zone along the fault is tens of meters to 300 m thick. Regional mapping of the Milligen and Wood River allochthons indicates that the fault has an overall left lateral displacement of approximately 5 km. The most recent movement, however, has been right lateral. This is indicated by a 1.6 km offset of the Wood River graben, which is bounded by strong fault zones that abruptly end against the strike-slip fault. The strike-slip fault probably merges at its northeast end with a thrust fault between the Milligen Formation (Devonian) and older rocks of the Pioneer Mountains gneiss dome and hence is deflected around the south end of the dome. There is no evidence that the fault cuts the gneiss dome. Hall and Batchelder recognized this fault on ERTS and low altitude photographs as extending both northeast and southwest of the area mapped for a total distance of 105 km.

The fold and thrust belt in southwestern Montana

The eastern edge of the Cordilleran fold and thrust belt in southwestern Montana appears to be

a continuation of the corresponding edge of the Wyoming thrust belt, projected beneath the Snake River Plain across the region of the Targhee uplift in east-central Idaho. The thrust trace is mostly concealed, but E. T. Ruppel interpreted stratigraphic and structural relations as suggesting that the thrust crosses the Montana line near the middle of the Centennial Mountains (loc. 28), trends westward beneath the Red Rock Valley and thence northward to Fleecer Mountain near Butte. From there it apparently extends westward into northern Idaho. No structural tie with the Montana disturbed belt is evident.

Ruppel identified several major component plates in the thrust belt, each containing a distinctive sequence of rocks different in composition and structural style from the cratonic sequence. The plates are characterized by pervasive overturned folds and imbricate thrust faults, structural styles unusual in cratonic rocks. The lower plates, which form most of the eastern edge of the thrust belt, seem to have been moved about 20 to 40 km. Their rocks are somewhat similar to those of the craton but differ abruptly in details of thickness, composition, age, or stratigraphic sequence from the cratonic succession across the edge of the thrust belt. The overlying plate is much larger and consists mainly of miogeoclinal rocks originally deposited perhaps 150 to 175 km farther west. These rocks differ in most respects from those in the lower plates, and they differ even more from those on the craton. The lower plates probably are slightly younger than the upper plate, and radiometric evidence from the Pioneer Mountains in Montana (Zen, 1977) suggests that the thrust belt was in its present position by about 76 million years ago.

The cratonic rocks were folded before thrusting, and the resulting broad anticlines and synclines are overridden by the eastern edge of the thrust belt.

New light on the Beaverhead Mountains in Idaho

Mapping and preliminary reconnaissance by David Lopez in the vicinity of North Fork in Lemhi County, Idaho (loc. 29), indicated that the backbone of the Beaverhead Mountains is made up predominantly of a medium to coarse-grained facies of the Big Creek Formation of the Lemhi Group (middle Proterozoic, Precambrian Y). Rocks of the Gunsight Formation, the uppermost unit of the Lemhi Group, and the pre-Lemhi Yellowjacket Formation occur along the western flank of the range. Rocks of both the Big Creek and the Gunsight Formations

have been thrust eastward over Yellowjacket rocks. A system of northwest trending range-front normal faults has broken the thrust sheets. Isolated blocks of Challis Volcanics (Tertiary) are preserved where dropped down between faults of the range-front system.

Three structural styles in the Sapphire thrust belt in western Montana

C. A. Wallace and M. R. Klepper identified three styles of tectonic deformation in the Sapphire thrust belt in the John Long Mountains and northern Flint Creek Range of western Montana (loc. 30). Each style of deformation can be related to the physical characteristics and age of the strata displaced by the overthrust system.

In Precambrian strata, thrust-fault zones are characterized by incoherent and coherent breccia, and wall-rocks are in general greatly shattered. Folds are rare in thrust plates of Precambrian rocks and, where present, are broad open structures. Precambrian rocks reacted in a brittle manner to deformation, probably because the thickness of quartz-cemented sandstone and siltstone in Precambrian strata is greater than in younger rocks.

Thrust-fault zones in lower Paleozoic carbonate rocks are characterized by coherent breccias and silicified breccias, whereas thrust faults in shaly rocks are represented by sheared zones and incoherent breccia or gouge. Shattered rocks are much less common in lower Paleozoic strata than in Precambrian rocks. Chaotic folds are common within thick limestone and dolomite units, but adjacent shaly rocks are only locally folded with carbonate rocks because thrust faults generally form the boundaries of the carbonate units. Shale and shaly carbonate units formed closed folds only in the immediate area of thrust zones. The lower Paleozoic carbonate rocks apparently behaved as coherent units that deformed internally in a plastic manner, whereas numerous, discrete shear-planes formed in shaly strata between carbonate units, which prevented development of large-scale fold systems in shaly rocks.

In upper Paleozoic and Mesozoic rocks, thrust faults only locally formed discrete breccia zones. The most striking characteristic of these rocks is the presence of abundant, large-scale, isoclinal, vertical, and overturned folds in thrust plates. Relatively thin, poorly indurated beds of sandstone apparently maintained little strength during compression, so that the entire thickness (more than 4,000 m) of strata deformed plastically.

Despite the different structural styles of the three major subdivisions of strata, decollement zones between tectonic units of different physical properties have not been identified. Therefore, it seems probable that the lateral stratigraphic separation of brittle older rocks has been translated into tight isoclinal folds and numerous bedding-plane-slip surfaces in more plastic younger rocks. If a decollement zone is present in the Sapphire thrust belt, it probably underlies the brittle Proterozoic (Precambrian Y) Belt sequence.

Major deep-seated faults near Helena, Montana

It has long been recognized that a zone of fundamental crustal discordance extends from the vicinity of Helena, Mont. (loc. 31), northwestward across western Montana and northern Idaho to eastern Washington. This zone, known as the Lewis and Clark line, separates crustal blocks of profoundly contrasting structural style and gross lithology that have been juxtaposed by a combination of large-scale horizontal and vertical fault movements. Two major deep-seated faults, discovered in recent years in the vicinity of Helena, are believed to mark the eastern segment of the Lewis and Clark line. One, named the Helena Valley fault, forms the northern boundary of the line; the other, named the Bald Butte fault, forms the southern boundary of the line. Geologic mapping in 1977 by R. G. Schmidt in the Canyon Creek, Granite Butte, and Elliston quadrangles and earlier mapping by J. W. Whipple in the Stemple Pass quadrangle provided new data on the location and structural characteristics of these faults in the area northwest of Helena, which is here summarized by Schmidt.

The Helena Valley fault has been traced 35 km northwestward from Helena Valley to the Continental divide near Stemple Pass. Beyond that point the fault is covered by volcanic rocks of Tertiary age, and its location is uncertain, but Landsat imagery suggests that it extends northwestward along the eastern and northern margins of Lincoln Valley and joins the St. Mary's fault, which defines the northern limit of the Lewis and Clark line across much of northwestern Montana. The Bald Butte fault lies 10 to 15 km south of the Helena Valley fault. It has been traced 40 km northwestward from Helena to the south base of Bald Butte in the Elliston quadrangle and thence to the Continental Divide near Nevada Mountain, beyond which its location has not been accurately established. Reconnaissance studies suggest, how-

ever, that it extends far to the northwest and is possibly a splay from the St. Mary's fault.

The rocks immediately north of the Helena Valley fault are mainly the Greyson Shale and Spokane Formation of the Ravalli Group of the Belt Supergroup. Broad northwest-trending folds and a major thrust fault in these rocks terminate abruptly at the Helena Valley fault and have not been recognized south of the fracture. The rocks immediately south of the Bald Butte fault are the Helena Dolomite of the Belt Supergroup and Snowslip Formation, Shepard Formation, Mount Shields Formation, Bonner Quartzite, and McNamara Formation of the Missoula Group of the Belt Supergroup. These rocks form the eastern flank of the northwest-trending Black Mountain syncline, which terminates sharply against the Bald Butte fracture. Between the two faults is a linear strip of rocks of the Greyson Shale, Spokane Formation, Empire Formation, Helena Dolomite, Snowslip Formation, Shepard Formation, and Mount Shields Formation, which are deformed into broad irregular folds and broken by large normal faults of predominantly northwest trend. Small plutons of Late Cretaceous and early Tertiary age are scattered along the length of the intervening strip. Significantly, much of the seismic activity in the Helena region is concentrated along the Bald Butte and Helena Valley faults and along several normal faults within the deformed strip of rocks between the major fractures.

The traces of the Helena Valley and Bald Butte faults are exceptionally straight, and the faults are interpreted as vertical or near-vertical fractures that extend deep into the Earth's crust. The abrupt termination of structures against the faults and the profound change in regional structure and lithology across them are believed to have resulted mainly from large strike-slip movement along the breaks. This horizontal translation, which perhaps occurred mainly during Laramide tectonism in Late Cretaceous and Paleocene time, may have amounted to several kilometers, but the absolute displacement cannot be determined from existing geological data. Later movement, which perhaps took place largely in Eocene time, appears to have been normal dip slip, for stratigraphic offset along the faults indicates upthrow to the northeast. Maximum stratigraphic separation on the Helena Valley fault is about 1,500 m and on the Bald Butte, about 3,000 m.

Thrust faults near the Lewis and Clark line in Montana

Structural trends in the northern Montana disturbed belt change in orientation from north-north-

west to east-southeast where the disturbed belt intersects the major tectonic boundary known as the Lewis and Clark line. Displacements on thrust faults north of the line decrease toward it; in the area of the strike change, successively lower thrust faults first break from anticlines, then increase in amount of displacement eastward. Successively lower thrust faults along the line involve older rocks of middle Proterozoic (Precambrian Y) age than do faults north of the line. M. W. Reynolds determined that horizontal displacement on the lowest principal thrust fault at the north end of the Big Belt Mountains (loc. 32) is at least 15 km and probably exceeds 25 km. The total shortening across the thrust faults may exceed 60 km. Changes in the style of folding associated with the thrust faults and in the structural trends noted may have resulted from lateral shear along the Lewis and Clark line partly contemporaneous with thrusting.

BASIN AND RANGE REGION

MINERAL-RESOURCE STUDIES

Mineralized volcanic arc in westernmost Idaho and adjacent Oregon

F. G. Poole reported that volcanogenic bedded- and porphyry-type base-metal sulfide deposits occur in allochthonous Permian and Triassic mafic to felsic volcanoclastic rocks, lavas, and plutonic rocks of the predominantly volcanic Seven Devils Group and re-

lated rocks in westernmost Idaho and eastern Oregon (index map. loc. 1). Massive sulfide deposits in the volcanic rocks are believed to be contemporary with some porphyry deposits in granitoid plutons; the two associations may be cogenetic in the island-arc environment. Temporal and spatial relations of the sulfide mineral deposits to the ancient arc are analogous to those in comparable settings in other parts of the world, such as the Miocene Kuroko deposits of Japan. Accordingly, the Seven Devils and related volcanic rocks have the potential for large base-metal sulfide deposits in addition to the relatively small deposits already known.

Age of volcanism and mineralization in Tonopah mining district, southwestern Nevada

M. L. Silberman, R. P. Ashley, H. F. Bonham, Jr., and L. J. Garside (Nevada Bureau of Mines and Geology) have completed a detailed geochronological study of Tertiary volcanic rocks and hydrothermal ore deposits in the Tonopah mining district and vicinity, Nye and Esmeralda Counties in Nevada (loc. 2). More than 60 potassium-argon and fission-track ages were determined on whole rocks and mineral separates from volcanic units, hydrothermal veins, and hydrothermally altered wall rocks.

Four episodes of Tertiary volcanism between 35 and 10 million years ago produced a large variety of intrusive and extrusive rocks ranging in composition from basalt to rhyolite and in mode of emplacement from ignimbrites and tuffs to lavas, flow-dome complexes, dikes and sills. Two of the four major episodes of volcanism were accompanied by hydrothermal activity that produced epithermal precious-metal vein deposits worth about \$150 million.

The earliest volcanic episode (35 to 25 million years ago) included eruption of now largely altered rhyolitic ash-flow and air-fall tuffs, and flow-dome complexes. About 24 to 18 million years ago a large granitic batholith is thought to have been emplaced in the subsurface, and major volcanic centers, including the Tonopah and Divide centers, developed over cupolas of the batholith. Early in this episode, lavas of intermediate composition, including trachyandesites and dacites of the Mizpah Trachyte (host rocks for ore deposits at Tonopah), erupted from stratovolcanoes. Cooling and differentiation of the batholith probably concentrated silicic magmas in the cupolas, which resulted in the eruption of several major rhyolitic ash flows and the intrusion of rhyolite dikes, sills, domes, and flow-dome complexes. During this time, hydrothermal activity produced the epithermal silver-gold veins at Tonopah.



About 17 to 15 million years ago, resurgence of granitic magma caused eruption of trachyandesite to rhyodacite lavas north of Tonopah and rhyolitic to quartz latitic pyroclastic rocks, flows, and domes south of Tonopah near Divide. Hydrothermal activity accompanied volcanism at Divide and deposited silver- and gold-bearing epithermal veins 16 to 15 million years ago.

Crustal extension began about 16 million years ago and resulted in eruption of rhyolite pyroclastic debris, trachybasalt and basaltic andesite flows, and rhyolitic lavas from numerous vents. Much of the pyroclastic debris was reworked and deposited in basins that were formed during crustal extension. Volcanism ceased about 10 million years ago.

STRATIGRAPHIC AND STRUCTURAL STUDIES

Quaternary faulting in Clayton Valley in southwestern Nevada

Geomorphic investigations by J. R. Davis in Clayton Valley in Esmeralda County, Nevada (loc. 3), have revealed evidence of Quaternary faulting. Studies of alluvial slopes and fault scarps along the eastern margin of Clayton playa suggest that faulting was episodic and caused segmentation and entrenchment of alluvial fans. The scarps display two distinct trends which intersect at an acute angle; one trend strikes about N. 30° E. and the other N. 65° E. The most recent episode of faulting is represented by a set of small, steep scarps. If the rates of scarp-profile degradation in Clayton Valley are comparable to those in north-central Nevada (Wallace, 1977), the last episode of faulting may have occurred 12,000 years ago or less.

Triassic rocks in southern Toiyabe Range in central Nevada

The Candelaria Formation (Lower Triassic) has been recognized by F. G. Poole about 12 km southwest of Manhattan in the southern Toiyabe Range in northern Nye County, Nevada (loc. 4). Correlation with the type Candelaria, located 80 km to the southwest, is based on similar lithology, sedimentary features, and fauna. Sparse limestone beds in the dominantly platy argillite and siltite flysch sequence have yielded age-diagnostic fossils. Ammonites and bivalves identified by N. J. Silberling (USGS) and conodonts identified by B. R. Wardlaw (USGS) and J. W. Collinson (Ohio State University) are Early Triassic (late Griesbachian to early Dienerian) in age and are comparable to those found in the type locality. Lithology and fauna of the marine Candelaria indicate that it was deposited mainly by tur-

bidity flows in an elongate basin in moderately deep water. The Candelaria flysch is believed to have formed during the Sonoma orogeny of Silberling and Roberts (1962).

Digital aeromagnetic data set for Nevada

A composite aeromagnetic map of the State of Nevada was created from approximately 125 different data sets that were adjusted to a barometric elevation of 12,500 ft. The data sets were made by digitizing contour maps compiled from surveys having different line spacings and elevations and flown over several years. The aeromagnetic map has been a useful aid in geologic mapping, in exploration for new mineral deposits, and in delineating areas of geothermal potential.

Mississippian flysch in Toiyabe Range in central Nevada

Autochthonous sandstone and conglomerate of probable Mississippian age has been recognized by F. G. Poole in the Toiyabe Range in northwestern Nye County, Nevada (loc. 5). The sandstone and conglomerate unit rests with angular unconformity on the strongly deformed Ordovician Vinini Formation and is overlain disconformably by a 60 m-thick fossiliferous marine limestone unit of Late Mississippian age. The sandstone and conglomerate unit, which is as much as 275 m thick, was deposited in a depression on the denuded and subsided Antler orogenic belt.

Allochthonous Devonian chert in northern Shoshone Range in north-central Nevada

Microfossils obtained by C. T. Wrucke, Jr., and D. L. Jones from chert layers in the Roberts Mountains allochthon in the northern Shoshone Range, Lander County, Nevada (loc. 6), have provided additional information on ages of Paleozoic rocks that comprise the allochthon. Most previous dates on these eugeosynclinal rocks were based on fossils from sparse limestone beds and abundant, but poorly exposed, shale and argillite units. Unfortunately, the fossils obtained were from too few localities to permit adequate age assignments of many thrust sheets that also lacked lithologic characteristics diagnostic of a particular formation. Recently, age-diagnostic radiolarians, conodonts, and other microfossils have been found in chert layers at numerous localities in north-central Nevada, and owing to the abundance of chert in most thrust sheets of the allochthon, these fossils will help decipher the stratigraphic and structural complexities of these strongly

deformed rocks. The fossils were freed from the rock using the HF leaching method developed by Pessagno and Newport (1972). Samples collected from outcrops in the Mount Lewis and Crescent Valley 15-minute quadrangles indicate that the Devonian Slaven Chert is more widespread than previously thought, has intercalated greenstone units, and is as young as Late Devonian (Famennian). This date is in accord with the Famennian conodont fauna reported by Poole and others (1977) from the upper part of the Slaven Chert in the northern Shoshone Range.

Devonian Woodruff Formation in central Nevada

Allochthonous Devonian Woodruff Formation has been recognized by F. G. Poole and G. A. Desborough (USGS) about 37 km south-southwest of Eureka in the Fish Creek Range in southern Eureka County, Nevada (loc. 7). Physical and geochemical correlation with the type Woodruff, located 155 km due north in the Piñon Range in southwestern Elko County, has been corroborated by Brian Holdsworth (University of Keele, England) who identified radiolarians of early Late Devonian (Famennian) age collected by R. K. Hose (USGS) from a chert layer within the strongly deformed eugeosynclinal mudstone, siltstone, and chert sequence. Lithology of the Woodruff indicates that it was deposited in a continental-rise setting in moderately deep water.

Proterozoic (Precambrian Z) stratigraphy clarified in Deep Creek Mountains of westernmost Utah

Stratigraphic studies by H. T. Morris in the east-central Deep Creek Mountains in Juab and Tooele Counties, Utah (loc. 8), have shown that the Goshute Canyon Formation of Bick (1959) consists of the Mutual Formation and the upper part of the "Sheeprock Group" (local usage). Earlier failure to identify the Mutual Formation apparently resulted because it is intensely bleached in the Deep Creek Mountains where the Mutual does not exhibit its characteristic red-purple to lavender colors. Recognition of the Proterozoic (Precambrian Z) Mutual Formation and "Sheeprock Group" in the Deep Creek Mountains will simplify correlation with equivalent strata in the "McCoy Creek Group" of eastern Nevada (local usage) and the more widespread Proterozoic (Precambrian Z) strata of central and western Utah.

Thrusts in City Creek Canyon near Salt Lake City, Utah

Recent mapping on the south slopes of City Creek Canyon, northeast of Salt Lake City, Utah (loc. 9),

by M. D. Crittenden, Jr., and R. H. Van Horn has delineated complex structures that may be a north-westward extension of folded thrusts exposed in the Wasatch Mountains farther southeast. Throughout most of City Creek Canyon, rocks of early Paleozoic age strike N. 50–70° E. and dip vertically. On the ridge south of Rotary Park, these vertical beds are truncated by a gently dipping thrust, above which rocks of the Mississippian Deseret, Humbug, and Doughnut Formations dip gently southward, parallel to the fault. To the south and upward within the plate, folding on northeast-trending axes becomes more pronounced, finally becoming nearly isoclinal with axial planes overturned to the south. At its south edge the gently dipping plate is bounded by a steeply dipping folded (?) thrust parallel to bedding in dark shales of the Doughnut Formation. Although the possible northeastward extent of this fault is uncertain, it occupies the same stratigraphic position as the western part of the Mount Raymond thrust on the opposite limb of the Parleys Canyon syncline southeast of Salt Lake City. Interest in the possible continuity of these folded thrusts is heightened because the Mount Raymond thrust appears to be the southwestward extension of the Absaroka thrust of Wyoming (Crittenden, 1977). Field data may be insufficient to establish the extent of the City Creek Canyon structures because they disappear to the northeast beneath a cover of Tertiary conglomerate. Connections northward to thrusts in the Morgan and Ogden Canyon areas are possible.

Strike-slip faults in Lake Mead area of southern Nevada

Geologic mapping by R. G. Bohannon in the vicinity of Lake Mead northeast of Las Vegas in Clark County, Nevada (loc. 10), has revealed a large, northeast-trending system of left-slip faults that extends from the Colorado Plateau-Basin and Range physiographic border near the Virgin River Canyon in Arizona to the southern part of Las Vegas Valley in Nevada. At least 65 km of left-slip motion occurred along the fault system as shown by offset beds beneath an unconformity and matching unique clast-types to a known source area. Some of the faults associated with the strike-slip zone have some unusual characteristics. The trend of these faults changes by as much as 140° and the sense of displacement also changes. Most of these faults also have large-magnitude left-slip movement, but some pass into right-slip faults as their trend changes. The right-slip parts of these faults are truncated by other faults that have left-slip movement. Although the origin of these unusual faults is not well under-

stood, the left-slip zone probably absorbed differences in extensional spreading rates of the crust between the southern Basin and Range province in Arizona and the northern Basin and Range province in Nevada and Utah, but it also may manifest south-west-directed mantle flow from the Basin and Range margin into that province.

Reinterpretation of Grand Canyon geomorphology

C. G. Bowles reported that the Colorado River eroded the Grand Canyon in Mohave and Coconino Counties of Arizona (loc. 11) during two major erosional cycles beginning in late(?) Oligocene or early Miocene time. Throughout much of the first cycle, the Colorado River flowed westward within the Grand Canyon between Nankoweap and Spencer Canyon before turning southward through Spencer, Hindu, Lost Man, and the ancestral Peach Springs Canyons. By middle Miocene time, uplift along the Hurricane fault in the western part of the canyon blocked this stream course and halted incision of the Grand Canyon. Erosion of the canyon walls continued and the outer canyon and Esplanade surface were formed. The Esplanade surface was tilted by uplift of the Kaibab Plateau while concurrent displacement along the Butte fault at the east side of the Kaibab Plateau dammed the flow of the Colorado River at Nankoweap Canyon and ended the first erosional cycle in late Miocene time.

The second erosional cycle of the Grand Canyon began with headward erosion of the lower segment of Marble Canyon. It is postulated that a lake, which formed behind the dam at Nankoweap Canyon, backed up into Marble Canyon and recharged the aquifer of the Mississippian Redwall Limestone. Ground-water flow along fractures parallel to the Butte fault developed solution piping in the limestone and fed springs that discharged into the gorge of the Little Colorado River opposite Cape Solitude. As the pipes enlarged, a spring-fed stream eroded headward to carve the lower segment of Marble Canyon. This new canyon eventually drained the lake and re-established flow of the Colorado River in the Grand Canyon. Similarly, lateral piping of ground water to Grand Wash (Hunt, 1969) caused headward erosion of the west end of the Grand Canyon across the Hualapai-Sanup Plateau. By late Pliocene time, the Colorado River was re-established throughout the Grand Canyon and commenced erosion of the inner canyon.

Cenozoic volcanism and tectonism in west-central Arizona

The area mapped by Ivo Lucchitta and N. H. Suneson near the Bill Williams River in southern Mohave County, Arizona (loc. 12), includes a major Cenozoic volcanic field of strong bimodal characteristics. There are four main sequences of volcanic rocks of this field interlayered with a variety of basin deposits of different ages. The oldest volcanic rocks include a thick sequence of trachybasalt to trachyandesite that is steeply dipping and vertical, highly shattered, brecciated, and mineralized with hematite and copper minerals. At one locality these rocks are directly overlain by the widespread Peach Springs Tuff of Young (1966; Miocene, 18 m.y.), which provides a regional time marker. The second sequence consists of widespread high-silica and high-potassium (8–10 wt. percent K_2O) rhyolite domes, dikes, flows, tuffs and associated quartz-bearing "basalt" flows. The third volcanic sequence was emplaced at or near the end of basin filling, about 10 million years ago, and consists of basalt and basaltic-andesite flows that now cap high mesas. The youngest sequence of volcanic rocks includes alkali-olivine basalt flows that post-date development of the through-flowing drainage. The youngest of these flows occurs at present stream level and retains vent and flow features, indicating that it may be as young as Quaternary. Rhyolite intrusions, flows, and tuffs are intimately associated with these young basalts, and hence also are possibly Quaternary in age.

The earliest volcanic rocks in the area (trachybasalt and trachyandesite) appear to predate onset of high-angle normal faulting, whereas the latest alkali-olivine basalts are in part synchronous with the basin-range faulting and are virtually unfaulted. The young rhyolite and basalt was intruded along faults and at intersections of faults. These fault-controlled intrusions may be a local manifestation of the strongly linear west-northwest trend of silicic volcanic centers in the region. The trend probably follows a regional zone of structural weakness, such as a zone of transcurrent faults.

Reserve graben of west-central New Mexico

According to J. C. Ratté, the Reserve graben is the deepest part of a northeasterly trending zone of parallel horsts and grabens about 50 km wide near Reserve in Catron County, New Mexico (loc. 13). The Reserve graben is about 20 km wide and is *en echelon* with the San Augustin plains, a much larger extensional structure northeast of Reserve. Oligo-

cene ash-flow tuffs, lava flows, and fanglomerates are downthrown as much as 1,000 m within the Reserve graben, and Quaternary basalt flows also may be offset within the graben.

Subvolcanic intrusive rocks are probably alined along faults of both the Reserve and San Augustin grabens. The intrusive rocks range in composition from intermediate to silicic and are Oligocene to middle Miocene (10–15 million years) or younger in age. The intrusions may be the roots of volcanoes that were alined along the graben faults. Some hydrothermal alteration (weak argillization and oxidation) occurred locally near the alined intrusive rocks, but there are no strong indications of mineralization related to them.

Mississippian rocks of Pedregosa basin in southwesternmost New Mexico and adjacent Arizona

New faunal information obtained by A. K. Armstrong (USGS) and B. L. Mamet (University of Montréal, Canada), enables more precise correlation of the Escabrosa Group and overlying Paradise Formation in southwesternmost New Mexico and adjacent Arizona (loc. 14). Basal beds of the Keating Formation of the Escabrosa Group contain foraminifers of Zone pre-7 of Mamet and Skipp (1970a,b) and megafossils of late Kinderhookian age. Member B of the Keating contains Zone 7 microfossils at its top and an early Osagean megafauna. The top of the overlying Hachita Formation of the Escabrosa Group represents Zones 14 and 15 of late Meramecian age. Zones 8 through 13 are missing, which indicates that a major hiatus separates the Keating and Hachita Formations.

Goniatites from the base of the overlying Paradise Formation were assigned to the *Goniatites americanus* Zone by Mackenzie Gordon, Jr. Microfossils from the same level represent Zones 14 and 15. The Paradise Formation contains microfossils representing Zones 15 through 19 (uppermost Chesterian). The overlying basal Pennsylvanian strata yield foraminifers of Zone 20 of Mamet and Skipp (1970a), indicating no significant hiatus at the Mississippian-Pennsylvanian boundary.

Multiple deformation of gneiss dome near Rincon Mountains in southeastern Arizona

Recent mapping by H. D. Drewes and C. H. Thorman north of the gneiss dome near the Rincon Mountains in Pima and Cochise Counties in Arizona (loc. 15) has revealed new evidence supporting multiphase development of the crystalline core rocks and tectonically mixed crystalline and sedimentary

carapace rocks of the dome. There are at least two phases of movement on low-angle or bedding-plane faults. Pre- and post-Oligocene deformation is indicated by the presence of unfaulted Oligocene "turkey-track" porphyry as intrusive pods along earlier thrust faults and as part of a sequence within a gravity slide plate. In addition, some remobilized granitoid rocks are cut by the earlier thrust faults, and some thrust faults, excluding glide faults, are cut by remobilized granitoid rocks. This evidence supplements that evidence based on (1) variations in styles of deformation, (2) a thrust plate of Precambrian nonmetamorphosed granitoid rock that is interleaved in the carapace rocks and has no root in the dome, (3) conglomerate clasts derived from a terrane now represented only within a gravity slide plate, and (4) the local unconformable overlap of thrust-faulted Cretaceous and older rocks by Oligocene deposits commonly found in gravity slide plates on all sides of the gneiss dome.

IGNEOUS ROCKS

Jurassic plutonism and volcanism in south-central Arizona

According to J. A. Briskey, Jr., and G. B. Haxel, Jurassic igneous rocks that crop out in the Comobabi Mountains and Ko Vaya Hills in Pima County, Arizona (loc. 16), represent the subvolcanic environment near the interface between a large near-surface plutonic complex and its overlying volcanic pile. The igneous complex includes plutons of porphyritic to equigranular quartz monzonite, granite, granodiorite, diorite, and quartz syenite, and hypabyssal porphyritic intrusions and flows, flow breccias, and welded tuffs of andesite, trachyandesite, rhyodacite, trachyte, rhyolite, and dacite. Lenses of immature, mainly volcanoclastic, continental sedimentary rocks are locally intercalated with the extrusive rocks. Near contemporaneity of the extrusive and intrusive rocks is suggested by the close spatial association of the volcanic and plutonic rocks and by ambiguous intrusive relations. Volcanic flows are intruded by quartz monzonite porphyry, which in turn is intruded by sparse, small vesicular dikes apparently identical to the flows. In addition, breccia within some of the plutons contains fragments of the plutonic rock in a matrix closely resembling rocks of the volcanic suite. Features indicative of shallow-level emplacement of the plutonic and hypabyssal rocks include: (1) ubiquitous pronounced porphyritic textures, (2) abundant brecciation along contacts and within individual intrusive masses, (3)

presence of copious comminuted rock as breccia matrix, (4) angular vugs within breccia masses, (5) miarolitic cavities, (6) abrupt and seemingly random changes in rock composition and texture over short distances, (7) finely-crystalline margins adjacent to sharp intrusive contacts, (8) vesicular hypabyssal intrusions, (9) lack of strong contact metamorphism, (10) widespread micrographic (granophyric) textures, and (11) the common occurrence of completely altered oxidized ferromagnesian minerals.

Calc-alkalic intrusive rocks at Mineral Mountain, south-central Arizona

Geologic mapping by T. G. Theodore and W. J. Keith has clarified geologic relations surrounding a complex of four distinctive calc-alkalic intrusive bodies near the southwestern corner of the Mineral Mountain 7½-minute quadrangle in Pinal County, Arizona (loc. 17). A porphyritic quartz monzonite belonging to the widespread Ruin Granite (Proterozoic, Precambrian Y) has been intruded by a small leucocratic two-mica granite initially emplaced presumably also during Proterozoic (Precambrian Y) time. Both of these plutonic rocks are cut by Proterozoic (Precambrian Y) diabase. The two-mica granite has also been intruded by a biotite-hornblende quartz monzonite which crops out in a 3-km² area; it was affected by sparse copper mineralization. Primary phenocrystic biotite from the biotite-hornblende quartz monzonite has been dated as 71 million years in age by S. C. Creasey using the K-Ar method. Secondary biotite is widespread throughout the two-mica granite and has been dated as 66 million years in age. A small body of granodiorite crops out just north of the biotite-hornblende quartz monzonite, and both intrusions were faulted intensely by conspicuous north- to northeast-striking faults related to prominent range-front faults.

Tertiary volcanic rocks in southwestern New Mexico

D. C. Hedlund reported that Tertiary calc-alkalic volcanic rocks along the Knight Peak Range and Little Burro Mountains in Grant County, New Mexico (loc. 18), are as much as 2,000 m thick and represent a well-defined sequence of extrusive andesite, tuff, rhyolite, and latite flows. The Knight Peak Range is a down-faulted, east-northeast-tilted fault block of Tertiary volcanic rocks surrounded by Proterozoic (Precambrian Y) rocks (1,270–1,550 million years old) of the Big Burro Mountains. The volcanic rocks in the Little Burro Mountains rest on Precambrian rocks and Cretaceous Beartooth Quartz-

ite and Colorado Shale. All of these rocks in the Little Burro Mountains occur in a tilted fault block that dips 15° to 30° ENE.

The volcanic rocks vary along the 40-km length of the Knight Peak Range. To the south in the vicinity of JPB Mountain, volcanoclastic rocks are abundant and rhyolite domes, plugs, and flows are common; the total thickness of volcanic rocks is at least 2,000 m. To the north, the volcanic section is much thinner (~600 m), and volcanoclastic rocks and rhyolite are less common. The JPB Mountain section from top to bottom is as follows: (1) latite of Malpais Ridge (0–200 m); (2) Kneeling Nun Tuff (0–170 m) with K-Ar age of 33.7±0.8 million years; (3) volcanoclastic rocks, tuff breccias, and thin basalt flows (0–450 m); (4) rhyolite dome-flow complex of Burro Cienega Canyon and rhyolite plugs (500 m+); (5) volcanoclastic rocks (90 m); (6) latite and andesite of JPB Mountain (400 m+); (7) conglomerate of JPB Mountain (20–25 m); and (8) andesite lava (120 m).

The Knight Peak section from top to bottom is as follows: (1) latite of Malpais Ridge—200 m, (2) Kneeling Nun Tuff—50 m, (3) ash-flow tuffs of C-Bar Canyon—330 m, and (4) andesite lava—0–20 m.

In the Little Burro Mountains the volcanic rocks are very similar to those in the Knight Peak Range but the section is generally thinner, about 600 m or less. The generalized sequence from top to bottom is as follows: (1) latite of Malpais Ridge (~90 m); (2) welded ash-flow tuff (0–200 m) lithologically similar to the Kneeling Nun Tuff but is much thicker than in the Knight Peak section and lacks the accessory mineral sphene that is characteristic of the Kneeling Nun Tuff; (3) air-fall tuff (0–180 m); (4) tuff breccias and volcanoclastic rocks (0–45 m); and (5) altered andesite and andesitic breccias (0–90 m) which are of probable Paleocene and (or) Late Cretaceous age.

In the Schoolhouse Mountain area at the northern end of the Big Burro Mountains in New Mexico, the volcanic rocks are different from those described above and may have a different source (Wargo, 1959).

GEOCHRONOLOGIC STUDIES

Age of quartz diorite at Bishop Spring in northwestern Oregon

A radiometric age has been obtained on a sample of quartz diorite collected by F. G. Poole and G. A. Desborough at Bishop Spring in the Powder River Canyon in Baker County, Oregon (loc. 19). The

biotite K-Ar age of 213 ± 5 million years, determined by R. F. Marvin, H. H. Mehnert, and L. B. Schlocker, probably records Middle Triassic oceanic plutonism in a mid-ocean ridge or volcanic arc setting. In either case, the ophiolitic quartz diorite and associated gabbro and plagiogranite plutons probably were transported eastward a great distance during formation of the pre-Upper Triassic serpentinite mélangé in northeastern Oregon and adjacent Idaho.

PACIFIC COAST REGION

CALIFORNIA

Garnet clues for lost Sierra Nevada tail

Reconnaissance geologic mapping and sampling studies in the basement rocks of the San Emigdio and Tehachapi Mountains, by D. C. Ross have uncovered a widespread, but until now, little publicized terrane of dark gneissic rocks of diorite and quartz diorite composition that is abruptly terminated along the San Andreas fault. Probably the most dramatic feature of this terrane is the presence of red garnet crystals, in part euhedral and as large as 10 cm. These garnet plums with white haloes in a dark diorite pudding have now been found at more than 30 localities and should serve as an effective "index fossil" in identifying ripped-off chunks of the southern Sierra Nevada basement, wherever they may be.

Upper Cenozoic basaltic and phonolitic lavas in central Sierra Nevada

Basaltic lavas erupted from numerous vents in the last 11 million years in central Sierra Nevada and its eastern bounding fault zone have been studied by F. C. Dodge and J. G. Moore. In the 20,000 km² area between 36° and 38° N. latitude, these rocks are provisionally divided into three petrographically, chemically, and geographically distinct groups: (1) alkali olivine basalt (AOB), restricted to the eastern fault zone and the Kern Canyon fault, covering a total area of ~100 km²; (2) potassic olivine basalt (POB), of the Sierran block, ~100 km²; and (3) ultrapotassic phonolite (UPP), closely associated with POB, ~0.5 km².

All the rocks contain phenocrysts of olivine and clinopyroxene, but AOB bears plagioclase and UPP biotite phenocrysts. Groundmass plagioclase and clinopyroxene are common to the three groups, bio-

tite is present in POB, and biotite, sanidine, leucite, and abundant apatite are other major groundmass minerals in UPP. The ratio $K_2O:K_2O+Na_2O$ of 117 analyses typically ranges from 0.2 to 0.4 for AOB, from 0.4 to 0.6 for POB, and >0.6 for UPP. AOB and POB range from 42 to 53 percent SiO₂ with <1 percent P₂O₅, whereas UPP ranges from 48 to 56 percent SiO₂ and 1.4 to 1.7 percent P₂O₅. MgO ranges from 4 to 11 percent in AOB, from 8 to 16 percent in POB, and from 5 to 12 percent in UPP. Analyses generally yield normative *ol*, but AOB and POB have either *hy* or *ne* (or *ac*).

Basaltic rocks west of the Sierran crest are limited to three broad zones, apparently genetically related to AOB-rhyolite volcanic centers to the east. POB and UPP occur in two distinct zones, one west of the Big Pine volcanic field. The Kern Canyon AOB-rhyolite suite occurs west of the Coso volcanic field.

Melones fault zone in the northern Sierra Nevada

Work by A. M. Hietanen on the large ultramafic body that is exposed on the west side of the Melones fault in the Bucks Lake quadrangle (Hietanen, 1973) shows that it continues to the Onion Valley quadrangle in the southeast. This body, bordered by the Rich Bar fault in the west, is about 6 km wide in the central part of the Onion Valley quadrangle, but wedges out in its southernmost part, and the Rich Bar fault ends. The southern tip of the ultramafic body, bordered by faults, penetrates the northern part of the circular mass of amphibolite that is exposed on the west side of the Melones fault in the southeastern part of the Onion Valley and northeastern part of the La Porte quadrangles. Schist and blastoclastic quartzite, similar to rocks of the Shoo Fly Formation on the east side of the Melones fault, are exposed in the center of the amphibolite mass and between its northeastern part and the Melones fault. These metasedimentary rocks continue farther to the north forming a wedge between the large ultramafic body on the west and the Melones fault on the east. South of the circular mass of amphibolite the Melones fault branches: (1) the eastern branch, labeled as Melones fault on geologic maps, passes to the south through Downieville, and (2) the western branch is along Goodyears Creek. Only the Goodyears Creek fault is accompanied by ultramafic rocks. Schist and metachert, which are rocks similar to the Calaveras Formation, occupy the area between these two faults.

Water chemistry predicts occurrences of Great Valley sequence

In the Geysers-Clear Lake area, F. E. Goff, J. M. Donnelly, J. M. Thompson, and B. C. Hearn, Jr., have found that thermal waters which have passed through undisputed Franciscan assemblage rocks contain less than 300 mg/L chloride, whereas thermal waters which have passed through "Great Valley"-sequence rocks contain more than 300 mg/L chloride. Thus, the occurrence of chloride-rich waters can be used to infer the concealed extent of "Great Valley" rocks beneath the Clear Lake Volcanics, and to predict the presence of exposed or concealed Great Valley rocks northeast of the Clear Lake Volcanics. High chloride waters suggest the presence of previously unrecognized areas or under-thrust slabs of "Great Valley" sequence along the east side of the Bartlett Springs fault zone, underlying the "Cache Formation," and beneath the ophiolite sheet north of Wilbur Springs (Goff and others, 1977; Goff and Donnelly, 1977).

Plate tectonics and The Geysers geothermal anomaly

Evaluation of regional tectonics in The Geysers-Clear Lake geothermal area has led R. J. McLaughlin (1977) to suggest that late Tertiary to Quaternary crustal extension enabled movement of magma into the upper crust and accompanied or closely followed northward propagation of the San Andreas fault system in northern California. Using the right-lateral slip rate of 5.5 cm/year postulated by Atwater and Molnar (1973) for motion between the Pacific and North American plates, the Mendocino triple junction and, by inference, the propagating edge of the San Andreas shear system would have been opposite the Clear Lake region about 3 million years ago. Presumably, subduction of the Farallon plate beneath the Clear Lake region was terminated at this time. Donnelly, Hearn, and Goff (1977) pointed out that consideration of timing of the northward migration of Tertiary and Quaternary volcanism in this area and of the timing of oldest Sonoma volcanism and youngest Clear Lake volcanism indicates about a 0.5- to 1.0-million-year time lapse in volcanism between 2.9 and about 2.0 million years ago. This time lapse may be related to development of extensional fractures within the newly propagated segment of the San Andreas shear system, enabling magma generated in the upper mantle and lower crust to move to high levels in the crust. This tectonic model suggests that any significant undiscovered geothermal resources are most likely to be found north and northeast of the Clear Lake re-

gion, within the confines of the San Andreas shear system, or northeast and considerably inland of Cape Mendocino, where subduction has recently been, or is presently active. The San Andreas shear system by this modeling appears to be a broad zone of discontinuous right lateral shear with some thrust components that in part bends westward into the Mendocino fracture zone, and extends nearly to the west edge of the Sacramento Valley over a large area of northern California.

Tectonics and sedimentology of upper Tertiary fluvial deposits along Maacama fault studied

Detailed geologic mapping and sedimentologic studies by T. H. Nilsen and R. J. McLaughlin in deformed fluvial and lacustrine deposits along the Maacama fault zone southwest of The Geysers steam field in California may provide important information on sedimentation processes that accompany the propagation of major transform fault systems. The Maacama fault zone is a major active branch of the San Andreas fault system. The unnamed fluvial and lacustrine deposits occupy a steep sided, narrow structural depression aligned with the fault zone. Preliminary data indicate that these sediments were supplied to a northwest flowing fluvial system by alluvial fans and debris flows that periodically blocked the narrow drainage, producing deep lakes. The structural basin appears to have been created by complex extension, thrusting, and strike slip within the Maacama fault zone, that preceded and accompanied deposition. Detritus was entirely locally derived, suggesting the absence of any major through-going drainage, and basal strata locally consist of extremely coarse breccias with clasts up to several tens of meters in diameter, apparently shed from active, growing fault scarps. Intense local deformation slump folding, and sedimentary structures that may have been earthquake induced attest to a long record of active tectonics in this region.

Serpentine emplacement, Northern California Coast Ranges

Many ultramafic and serpentine bodies in the Coast Ranges are associated with pillow lava and other mafic igneous rocks. This association has been described as an ophiolite complex and the ultramafic and volcanic rocks have been interpreted as ancient oceanic crust (Bailey, Blake, and Jones 1970) at the base of the Great Valley sequence. Although pillow lava of Late Jurassic age does underlie and inter-finger with mudstone and sandstone at the base of the Great Valley sequence (R. D. Brown, 1964), some

of the serpentine was clearly emplaced much later. Field relations mapped by Brown in the Snow Mountain Wilderness Study area show that one linear serpentine body, 13 km long, invades a north-west-trending high-angle fault. This fault cuts folded pillow lava of Late Jurassic age in a klippe, and it offsets a major low-angle thrust fault that truncates bedding and structure at the base of the klippe. The serpentine along the high-angle fault produces a linear magnetic anomaly about 100 gammas greater than the total field intensity nearby. Both the serpentine and the magnetic anomaly can be traced southeastward into the Stony Creek fault zone, which separates the Coast Ranges physiographic province from the Great Valley to the east. Although the serpentine in this area may be derived from oceanic crust of Jurassic age, most of it must have been emplaced in its present structural setting after a long and complex episode of crustal deformation.

Maximum temperature of formation of Franciscan mélangé

Although Franciscan mélanges commonly contain exotic blocks of eclogite and blueschist facies, the metamorphic grade of the mélangé as a whole is generally quite low. Quantitative data on the temperature of formation, however, are difficult to obtain. In the Franciscan rocks of the Nacimiento block of the central California coast, V. M. Seiders found that a common type of exotic block is a chert-pebble conglomerate, lithologically quite similar to conglomerate in the lower part of Great Valley sequence. The chert pebbles contain rich radiolarian faunas that are still being studied. Two localities yielded pebbles with conodont faunas that were examined by A. G. Harris. The conodonts, of Silurian and Late Triassic age, have a color alteration index (Epstein, Epstein and Harris, 1977) of only 1 to 1½, indicating that the host rocks were never hotter than about 60° C. This agrees well with the unmetamorphosed aspect of many of the Franciscan rocks of the area and points out that at least the final step of the process of mélangé formation can take place at very low geologic temperatures.

Deep-water sedimentation influenced by an actively-shifting source terrane

Stratigraphic studies of the Santa Margarita Formation by R. T. Ryder (USGS) and A. F. Thomson (Shell Oil Co.) in the southern Temblor Range in California indicate that the conglomerate and sandstone units were deposited as submarine canyon and submarine fan-channel complexes in outer neritic

to upper bathyal water depths. Moreover, it appears from the detailed mapping of these units that the Salinian block shifted northwestward along the San Andreas fault while shedding coarse debris to progressively younger submarine fans in the adjacent basin to the east. Specific evidence for this proposed relation includes: (1) sandstone units in the McLure Shale Member of Monterey Shale and the Reef Ridge Shale, (2) conglomerate units containing distinctive white flow-banded felsite clasts in the Santa Margarita Formation on the east side of the range, and (3) metamorphic-clast assemblages in the Santa Margarita Formation on the west side of the range which all occupy progressively higher stratigraphic levels in a northwest direction subparallel to the trace of the San Andreas fault.

Deformational regime assessed

Focal-plane solutions determined by R. F. Yerkes for 100 out of 630 earthquakes recorded during 1970–1975 by the USGS Western Transverse Ranges network (area covered: N. Lat 33°45' to 34°45' × W. long 118°30' to 120°30') yield east-trending reverse fault mechanisms with well-defined subhorizontal P axes oriented within 35° of normal to the "Big Bend" of the San Andreas fault. This north-south maximum compressive stress has been assumed to explain the orientation and habit of the Transverse Ranges structures. The extreme compressive deformation of the Western Transverse Ranges is well reflected in the anomalously high elevations and estimated rates of uplift (greater than 7.7 m per thousand years over the last 40,000 years) of marine terraces along the east-trending Point Conception–Santa Monica shoreline, as compared to equivalent dated terraces to the northwest and southeast.

Cucamonga fault scarps

Since the 1971 San Fernando earthquake in California, considerable attention has been given to the fault system on which this earthquake occurred. This thrust fault system bounds the south front of the San Gabriel Mountains, and in the easternmost 25 km is called the Cucamonga fault zone. The most youthful appearing and best preserved scarps are developed along the eastern half of the Cucamonga fault zone. There are five well-preserved scarps here on a well developed alluvial fan that heads at Day Canyon. Results from detail mapping and profiling of the youngest-appearing scarp by D. M. Morton and F. K. Miller yield several tentative conclusions.

Measured scarp heights range between 2 and 40 m; most scarps appear to be the result of surface displacements by multiple earthquakes. Irregularities at 2- to 3-m intervals on an individual scarp cutting alluvium of different ages appear to have been produced by different seismic events, and are in keeping with an average scarp height of 2- to 3-m produced during surface displacement earthquakes. Comparison with 2- to 3-m high thrust fault scarps produced during historic earthquakes suggests individual earthquakes are $\geq M$ 7 to 7.7. The number of such earthquakes producing these scarps is estimated at 20 to 30. Based upon degradation of scarp profiles the last surface displacement earthquake is estimated to have occurred 700 to 900 years B.P.

OREGON

Radiolarians from Mesozoic rocks in western Oregon

Chert samples collected by W. N. Blair from Mesozoic rocks in the western part of the Medford 2° quadrangle sheet yielded several suites of radiolarians and other micro-fossils. Scanning electron microscope studies have revealed excellent preservations of many radiolarian specimens so that identifications and definite age determinations are possible. As the rocks are complexly faulted and folded and have otherwise yielded scant evidence of their age, these studies offer the first hope of sorting out the age and stratigraphic relations of subtly different terrains. In fact radiolarians collected from the widespread Dothan Formation are the first fossils which can be positively assigned to the Dothan Formation in the Medford quadrangle.

WASHINGTON

Age of the last major scabland flood of eastern Washington

Beds of volcanic ash in deposits associated with the last major flood that crossed the channeled scabland of eastern Washington indicate that the flood occurred about 13,000 years ago according to D. R. Mullineaux. Until recently, the flood had been thought to be about 20,000 years old. Fe-Mg mineral suites and chemical compositions indicate that the ash beds are downwind components of pumice layers of tephra set S from Mount St. Helens volcano. Tephra set S, in turn, can be dated at and near the volcano as about 13,000 radiocarbon years old. That date is supported by another radiocarbon date of

about 13,000 years for peat that directly overlies downvalley deposits of the flood near Portland, Oregon.

Potential petroleum reservoirs within Tertiary *mélange*, coastal Olympic Peninsula and adjacent OCS

Large infolded "loaves" of sandstone and conglomerate 5 to 10 km long and 2 to 5 km wide "float" in middle Eocene as well as in lower to middle Miocene *mélange* in the coastal part of the Olympic Peninsula and on the adjacent continental shelf. The intensely sheared siltstone in these two *mélanges* are mature with respect to the temperature history required for hydrocarbon generation and are potential source beds for petroleum. This geologic setting has led P. D. Snively, Jr., and J. E. Pearl to speculate that these loaves of coarse clastic sedimentary rock may form a unique reservoir for petroleum where they are deeply buried as in middle Miocene underthrust zones. Hydrocarbon generated from either the middle Eocene or the lower to middle Miocene siltstones in regions of higher temperatures in underthrust zones would most likely migrate into the floating loaves of coarse clastic sediments. The siltstone units would, therefore, act as both a source bed for petroleum as well as a "cap" rock surrounding the loaves.

Faults south of Wenatchee, Washington

A previously unrecognized zone of north- to north-west-trending faults and monoclines was discovered south of Wenatchee, Wash., by D. A. Swanson and G. R. Byerly. The zone lies more or less along the southward extension of the Entiat fault, which forms the east edge of the Chiwaukum graben. The faults and monoclines displace the Grande Ronde Basalt, indicating post 15-million year tectonism. Basalt flows are sheared and tilted to 65 degrees in a narrow zone in which the Columbia River flows past Rock Island Dam. The faults in this area appear to define a complex horst with perhaps 100-200 m of displacement. The zone of deformation can be traced at least 30 km south of the Rock Island Dam area. Displacement decreases southward, and the faults become monoclines north of Quilomene Creek.

Revision of Naches Formation

Recent mapping by R. W. Tabor, V. A. Frizzell, Jr., W. C. Gaum, and K. L. Marcus in central Washington has shown that the Naches Formation, first named by Smith and Calkins (1906) and redefined by Stout (1964) is complexly folded and faulted up-

per Eocene and Oligocene(?) volcanic rocks and sediments that can be subdivided into several lithologic units. The formation unconformably overlies pre-Tertiary metamorphic rocks and is unconformably overlain by less intensely deformed upper Oligocene and Miocene pyroclastic rocks that are probably correlative with the Ohanapecosh or Stevens Ridge Formation (Fiske, Hopson and Waters, 1963). Generalized lithology and ages from youngest to oldest units are:

- Interbedded basalt, and basaltic tuffs and breccias and arkosic sandstone with minor rhyolite tuffs and flows as well as andesite flows(?)—The lower part of this heterogeneous unit contains thick rhyolite flows and ash flow tuffs (Kachess Rhyolite of Smith and Calkins, 1906, p. 5) with zircon fission track ages of about 34 to 39 million years (Joseph Vance and Charles Naeser, written commun., 1977). On the southeast this unit is predominantly arkosic sandstone with abundant intercalations of rhyolite and minor basalt.
- Commonly columnar jointed, black, dense olivine basalt flows and basalt breccias that appear to overlie the next lower unit unconformably—Thick rhyolite flows underlain by a widespread ash flow tuff. On the east the unit contains considerable andesite flow rock and breccia (Taneum Andesite of Smith, 1904). A fission track age on rhyolite tuff near the base is 45 ± 5 million years.
- Arkosic sandstone with minor shale, and conglomerate and some coal beds—This is the Manastash Formation of Smith (1904) with flora unlike the Eocene part of the Swauk Formation or Roslyn Formation (upper Eocene; Stout, 1964, p. 327) but correlative with the Clarno Formation (Eocene and Oligocene). Palynomorphs in the Manastash are like the type Swauk (Newman, 1977).

The gross structure of the Naches Formation appears to be a north-northwest-trending complex syncline, with older rocks exposed to the south (northwest plunge). On the east it is partially faulted against older rocks by the southern continuation of the Straight Creek fault and on the west overlain by rocks correlative with the Ohanapecosh and (or) the Stevens Ridge Formation.

Potential submarine landslides in Puget Sound

Detailed bathymetry on the Nisqually delta foreslope and bottom slope of the southern Puget Low-

land shows submarine morphology, which suggests that the delta foreslope has been subject to instability and submarine sliding. Elongate ridges, closed depressions, and irregular hummocky terrain with local relief of about 10 m characterize the bottom morphology at the base of the delta foreslope. It is postulated by M. J. Chrzastowski and Fred Pessl, Jr., that this irregular morphology may be caused by submarine landslide deposits that moved down glide planes subparallel to the delta foreslope and were deposited at the base of the foreslope and seaward into Nisqually Reach. Such submarine sliding may cause ground instability at the delta front and may induce tsunami-like waves threatening some nearshore development in the southern Lowland.

Possible Quaternary faulting in the Puget Sound region

Detailed geologic mapping and stratigraphic studies east of Discovery Bay on the northeast corner of the Olympic Peninsula by H. D. Gower have shown that conglomerates previously mapped as part of the Lyre Formation (upper Eocene) belong to at least two different stratigraphic units separated by a pronounced angular unconformity. Several north-trending faults were identified between Discovery Bay and Puget Sound. Steeply dipping Quaternary sediments exposed along one fault, about 4 km west of Port Ludlow, suggest possible Quaternary fault movement.

Possible continental transform fault in northwest Washington

The Devils Mountain fault, a major east-west-trending left-lateral fault, links thrust-bound terranes in the San Juan Islands with the western Cascade Range, according to recent mapping by J. T. Whetten. The "Trafton" sequence, a Mesozoic mélange on the mainland, is offset about 60 km and reappears on San Juan Island (a correlation first noted by W. R. Danner, University of British Columbia, in 1957). The youngest rocks cut by the fault are Eocene or Oligocene; younger Tertiary rocks are not present, and Quaternary glacial deposits do not appear to be offset. The fault is not older than Cenomanian or Turonian, the age of the youngest marine rocks known on southern Lopez Island. The fault appears to bend to the northwest and southeast at its western and eastern extremities, respectively, and becomes tangent to thrusts separating complexly deformed Mesozoic terranes. The time of thrusting may be approximately the same as the time of movement on the Devils Mountain fault, which suggests that thrusting and strike-slip

faulting may have occurred as the block south of the Devils Mountain fault moved east relative to the block on the north.

Mesozoic thrust-bound terranes in the San Juan Islands, Washington

Recent studies by J. T. Whetten, D. L. Jones, and R. E. Zartman (USGS), D. S. Cowan (University of Washington), and Emile Pessagno, Jr., (University of Texas, Dallas) indicates that the southern San Juan Islands are underlain by a succession of highly deformed thrust-bound terranes that include a Jurassic ophiolite, a Triassic volcanic arc-derived assemblage, and a mélangé composed of crystalline and sedimentary rocks ranging in age from Cambrian to Jurassic. Mesozoic elements have been identified in all terranes, including those that previously were thought to be only Paleozoic. Thrusting may have occurred in two episodes, the Late Cretaceous and the early(?) Tertiary. The former event probably corresponds to the Late Cretaceous thrusting postulated by Peter Misch (University of Washington) in the Northern Cascade Range; the latter appears to have thrust the highly deformed rocks of the southern San Juan Islands over relatively undeformed Triassic to Upper Cretaceous rocks of the northern San Juan Islands.

Geologic mapping and Pb-U dating of zircons strongly suggest that there are two distinct sub-parallel southeast-trending ophiolite belts in the western Cascades-San Juan Islands area of Washington. The inner belt extends from Blakely Island to Silverton and is about 170 million years old. The outer, about 155 to 160 million years old, begins near Arlington and may be discontinuously exposed at least as far as Rimrock Lake, where rocks of similar lithology and age were described by C. A. Hopson (USGS) and J. M. Mattinson (University of California, Santa Barbara). The latter belt crosses the Olympic-Wallowa lineament and constrains the amount of strike-slip motion that could have occurred along faults associated with the lineament since the time of ophiolite emplacement.

ALASKA

Significant new scientific and economic geologic information has resulted from many regional and topical investigations conducted in Alaska during the past year. Discussions of the recent findings of these studies are grouped under six major geographic regions and a general statewide category.

GENERAL

Mineral appraisals of Alaska on schedule—levels of studies

Mineral appraisals of Alaska are carried on by the USGS at four levels. Level I studies comprise statewide (152 million ha) compilation of geologic-terrane and mineral-deposit data at 1:2,500,000 scale. These studies were completed and administrative and open-file reports made available for governmental use in June 1977. Level II studies, informally known as RAMRAP, the acronym for Regional Alaskan Mineral Resource Assessment Program, include compilations and syntheses of basic geological, geophysical, geochemical, and earth-satellite data for regional (1:1,000,000 scale) resource assessment. These studies are completed for all of Alaska except for the southeastern panhandle and part of the North Slope where there are no known metallic mineral resources; the reports and maps will be published in January 1978. At Level III, the ongoing AMRAP (Alaska Mineral Resource Appraisal Program) studies comprise field studies leading to multidisciplinary resource assessment of 1:250,000-scale quadrangles. To date, studies in 15 quadrangles have been completed. Four more studies are underway. Folios of mineral-resource assessment for 14 quadrangles, an aggregate of approximately 19.2 million ha, have been published or are in press or advanced preparation. Level IV comprises studies of ore genesis and other mineral-deposit research problems. Such studies are underway or completed in five mining districts notable for copper or gold deposits. These assessment programs, largely coordinated by H. C. Berg, are being carried out mainly by geologists and subprofessionals of the Branch of Alaskan Geology with the collaboration of specialists from other branches and subactivities in the Geologic Division. In addition, geoscientists from the State of Alaska Division of Geological and Geophysical Surveys and the University of Alaska are collaborators.

Microplate tectonics of the southern part of Alaska

D. L. Jones recognized that the southern part of Alaska constitutes a mosaic of microplates, of widely differing ages and lithologies, that assembled during late Mesozoic time. Some fragments, such as Wrangellia, originated in equatorial regions and were rafted northward with respect to North America a minimum of 3,000 to 6,000 km.

Two major microplates (Wrangellia and Alexander terrane) have been recognized, plus a large

number (20 or more) of smaller fragments distributed throughout southern, southeastern, and southwestern Alaska. The northern limit of these allochthonous terranes appears to be the Tintina Trench in east-central Alaska.

NORTHERN ALASKA

Early or Middle Pleistocene glaciation in the National Petroleum Reserve in Alaska

Studies by W. E. Yeend showed a piedmont-type glacier covering a substantial portion of the northern slope of the western Brooks Range within NPRA, and extending into the northern foothills portion of the Range in early or middle Pleistocene time. This glaciation had been previously recognized in the extreme eastern portion of NPRA where it reached almost to the Colville River (Chapman, Determan, and Mangus, 1964). As the Range becomes progressively lower to the west the ice was correspondingly more restricted in areal extent and did not extend west of the Utukok River drainage basin because no source area was available at a sufficiently high elevation to nourish annual ice development. Much of the till deposited by this ice sheet has been eroded leaving resistant erratics scattered on bedrock. Ice sculpture produced rounded, low, subdued hills and ridges and broad valleys up to and within the high portions of the Range. Remnants of gravel outwash terraces are generally 40 to 60 m above the major north-flowing tributaries of the Colville River and the Colville River itself. These deposits could be an important source of aggregate for local use. Although not draining glaciated terrain, the Kokolik River drainage west of the Utukok River also exhibits gravel terraces 40 to 60 m above present river levels. These alluvial terraces can be traced into a suspected beach gravel at the inland margin of the coastal plain at an elevation of 120 to 150 m. If the correlation is as suggested then the high sea level marked by the beach gravel would most likely correlate with the interglacial period immediately following the extensive glaciation discussed above.

Paleotransport directions in Nanushuk Group

During the 1977 summer field season, 22 sections (14,425 m of section) were measured in rocks of the Nanushuk Group primarily in the western part of the North Slope of Alaska. Field investigators include T. S. Ahlbrandt, project chief, J. E. Fox, A. C. Huffman, F. E. May, C. G. Mull, Ira Pasternack,

R. A. Scott, and Susan Winkler. The paleotransport direction for the Nanushuk Group is to the north-east in the western part of the North Slope as determined from symmetrically filled fluvial troughs. The northeasterly transport direction for this region is consistent with the orientation of shorelines for these rocks determined by Chapman and Sable (1960); but differs from the north-south orientation suggested by Smiley (1969). Exploration trends related to depositional environments are significantly affected by this transport interpretation.

A western and eastern depocenter can be differentiated in rocks of the Nanushuk Group. The two depocenters differ in detrital composition, stratigraphic sequence, and reservoir potential. The western depocenter, based upon preliminary data, has less reservoir potential (fewer and thinner reservoir sandstones) than the eastern sequence. Coals in the western area occur stratigraphically higher in the section relative to the stratigraphic position of coals in the eastern section. Depositional environment, which can be differentiated in Nanushuk rocks by sedimentary structures and trace fossils, is a major factor controlling reservoir quality. Higher energy environments, particularly foreshore (beach) sandstones have the best reservoir potential because they have (1) an adjacent hydrocarbon source (marine shales), (2) lateral continuity along the paleoshoreline, and (3) a more diagenetically stable composition due to the removal of unstable grains under high energy conditions.

A biostratigraphic zonation study of the Nanushuk Group with dinoflagellates, spores and pollen, and foraminifera is in progress. Spores and pollen have been recovered from rocks previously thought to be barren of them. A dinoflagellate zonation has been completed for the Fish Creek test well, and the zonation is being applied to other sections by F. E. May.

Offshore permafrost in the Prudhoe Bay region

D. M. Hopkins reports that, using the shorefast ice as a platform, four boreholes 30 to 70 m deep completed during spring 1977 were added to the three boreholes completed during spring 1976. In the Prudhoe Bay area, the subbottom sediments are at temperatures below 0°C throughout the continental shelf at least as far offshore as the 15-m isobath, which lies more than 17 km offshore. Negative thermal gradients indicate that ice-bound sediment is present at depths of several tens of meters, but only one of the boreholes actually penetrated ice-bound material (at a depth of 30 m). Sediments as deep as

68 m below sea level and as cold as -2.3°C in another borehole were not ice-bonded, though they may have been ice-bearing; evidently interstitial brine is saltier than normal seawater.

Comparison between borehole data and seismic reflection and refraction studies indicates that the top of permafrost in the Prudhoe Bay area is an irregular and, commonly, gradational boundary. The irregularity is probably the result of the tendency for large, warm, thermokarst lakes to develop on land near the rapidly encroaching shoreline. Permafrost thaws more rapidly and deeply beneath these fresh-water lakes than beneath the cold seawater. Areas on the continental shelf that once were thermokarst lakes thus are more deeply thawed than areas that had been tundra prior to encroachment by the sea.

Gravel resources and erosional problems on the coast of Beaufort Sea

A study of beaches and barrier islands in the Beaufort Sea by D. M. Hopkins, R. W. Hartz, R. E. Nelson, and P. A. Smith indicated that the coast of the Beaufort Sea is carved in unconsolidated, ice-rich sediments that in many places contain little gravel. The naturally gravel-poor beaches fail to protect the coast, in many places resulting in extremely rapid coastal erosion. Gravel could be removed by quarrying from "sediment sinks" such as recurved spits, but gravel mining in other areas would aggravate the rapid coastal erosion.

Many of the barrier islands of Beaufort Sea are relict features now separated from their original sources of sand and gravel. If the islands were quarried for gravel for causeways or artificial islands, they would not be reconstructed by natural processes.

Strata-bound lead-zinc mineralization, Philip Smith Mountains quadrangle

Upper Devonian rocks in the Philip Smith Mountains quadrangle contain anomalous occurrences of lead, zinc, and several other metallic elements, according to J. T. Dutro, Jr. Samples from a measured section of Frasnian strata were analyzed spectroscopically for Mn, Cr, Co, Ni, Zn, Cu, Pb and V. Atomic absorption values were also secured for zinc (D. E. Detra, written commun., 1977). At eight levels, all in deeper water portions of minor depositional cycles, five or more elements attain peak values. These high values suggest that the Hunt Fork Shale, particularly, could have been the source of subsequent concentration of metals in

promising structural settings. Anomalous concentrations of Cu, Pb, Zn and Ag were found at one place above the pre-Frasnian unconformity on a structural high (Detra, 1977). Original high metallic values in the dark shales could have been concentrated during or after burial and the highly metalliferous fluids might have migrated later into favorable stratigraphic or structural traps at the unconformity, above structural highs, or both.

WEST-CENTRAL ALASKA

Basal Cretaceous rocks discovered at south margin of Yukon-Koyukuk province

A basal Cretaceous rock unit of probable Neocomian Age, previously unknown along the south margin of the Yukon-Koyukuk province, was mapped by R. M. Chapman and W. W. Patton, Jr., in 1977. The unit, at least 300 m in thickness, consists of andesitic volcanic, volcanoclastic, and fine-grained tuffaceous and shaly sedimentary rocks, and is exposed only on the Melozitna River at the first bluff above the mouth (Ruby quadrangle). Lithologically this unit is very similar to the basal Cretaceous (Neocomian) unit of andesitic volcanic rocks (Kv) mapped farther north in the Melozitna quadrangle (Patton and others, 1977).

A few fossil ferns, collected in 1977 from the Melozitna River section, are not well-enough preserved to demonstrate details of venation or other specific characters, but the size and shape of the pinnules conform quite nicely with those of the genus *Cladophlebis*, which is common in the Mesozoic. Also, no ferns in the North American Permian resemble these specimens (S. H. Mamay, written commun., 1977). Ferns of this genus are present in Albian(?) or Upper Cretaceous rocks about 32 km west along the Yukon River (Hollick, 1930).

The rock types plus the fossil evidence strongly favor a Neocomian Age for the rock sequence at the Melozitna River site. A correlation with the Rampart Group, which immediately underlies Cretaceous clastic rocks east of the Melozitna River, seems unlikely because the volcanic rocks of this group are predominantly basaltic, rather than andesitic, and only Permian fossils have been found in the sedimentary rocks of the Rampart Group elsewhere.

A narrow belt of the andesitic rock unit might be concealed in the covered areas east and west of the Melozitna River, but the mapping east of the river strongly suggests that post-Neocomian Cretaceous conglomeratic rocks overlap and conceal the ande-

sitic rock unit along this part of the south margin of the Yukon-Koyukuk Basin. A few kilometers south and west of the Melozitna River site the Cretaceous rocks are right-laterally offset by the Kaltag fault (Patton, 1973). Only post-Neocomian rocks are exposed to the west on the north side of the fault and the Yukon River. If the andesitic rock unit is present at or near the surface to the southwest, it is concealed by the broad, featureless Yukon River valley.

Probable pre-Ordovician age of metamorphic complex in northern Kuskokwim Mountains

New evidence was discovered in the Medfra quadrangle that establishes the age of the metamorphic complex in the northern Kuskokwim Mountains as definitely pre-Permian and probably pre-Ordovician. On a tributary of Meadow Creek in the north-central part of the quadrangle, pelitic schists and greenstones of the metamorphic complex were found to be overlain by a massive basal conglomerate of Permian age. The conglomerate contains large angular blocks of the metamorphic rocks that are set in a sandy quartz-carbonate matrix that carries an abundant brachiopod fauna. The presence of these large clasts of metamorphic rocks in the Permian strata demonstrates clearly that the age of metamorphism is pre-Permian and rules out the possibility that large-scale horizontal dislocations has occurred between the Permian beds and the metamorphic complex. A pre-Ordovician age for the metamorphic complex is strongly suggested by the fact that 25 km east of Meadow Creek Permian strata overlie unmetamorphosed carbonate rocks of earliest Ordovician to Middle Devonian age with no angular discordance.

Landslides near Melozitna River Canyon

Eight large landslides and several small slides and earthflows within a 100-km² area 10 km northwest of the Melozitna River Canyon in the Ruby quadrangle were identified by R. M. Chapman and W. W. Patton, Jr., in 1977. These prominent features, which had been noted and photographed from the air in 1974, superficially resemble cirques, and apparently Eakin (1916) interpreted them as evidence for small glaciers that left only insignificant deposits.

The large landslides, six of which are southerly facing, descend from altitudes of 610 to 700 m at the heads of small stream valleys, and range from 0.8 to 1.4 km in width at the head and from 0.8 to 1.6 km in length from crown to toe. They ap-

parently formed as rotational slumps, consisting of slump blocks and debris from the Upper(?) Cretaceous conglomerate, sandstone, siltstone, and shale bedrock. A few tiny lakes occupy shallow depressions in some of the slides. The slides are in, or close to, east-northeast-trending axial zones of an anticline and a syncline where the beds dip 10° or less. The rupture planes are not along bedding planes and no control by faults, joints, or axial deformation could be detected.

The large slides apparently have long been essentially stable and are thinly to moderately covered by brush and small trees except on the steep main and flank scarps. They are probably at least a few thousand years old, and perhaps as old as late Pleistocene. Some of the small slides may be considerably younger.

EAST-CENTRAL ALASKA

Radiolaria date chert in Big Delta quadrangle as late Paleozoic

Red, green, and gray chert interlayered with greenstone and associated with ultramafic rocks in the northeastern part of the Big Delta quadrangle is yielding radiolaria and conodonts. Preliminary identifications by D. L. Jones indicate a Late Pennsylvanian or Early Permian age for the chert. These are the first pre-Pleistocene fossils found in the Big Delta quadrangle and give the first confirmation of a Paleozoic age for at least some of the metamorphic rocks of the quadrangle.

The ultramafic rocks, greenstone, and chert compose a distinct terrane of oceanic origin that appears to have been thrust over adjacent greenschist facies rocks that include marble, quartzite, meta-volcanic rocks, and metamorphosed coarse arenite deposits of continental affinities.

Aluminosilicate minerals in the Big Delta quadrangle

Metamorphosed pelitic rocks had been considered comparatively scarce in the Yukon-Tanana Upland, until H. L. Foster and her coworkers recently mapped an area of sillimanite gneiss, bordered on the north and east by kyanite-bearing schist. The map covers an estimated area of more than 1,200 km² in the west-central part of the Big Delta quadrangle.

The central part of the sillimanite gneiss may be a gneiss dome (Foster, Weber, and Dusel-Bacon, 1977, p. B33) and consists of medium-grained quartz-biotite-muscovite sillimanite gneiss. The north side of the gneiss dome is bordered by gar-

netiferous schists, some of which have kyanite (Foster, Dusel-Bacon, and Weber, 1977). One thin section of schist has the rare occurrence of all three polymorphs, kyanite, sillimanite, and andalusite. Kyanite crystals occur in abundance on the north-east side of the gneiss and some are more than 3 cm long. The three aluminosilicates occur with biotite, muscovite, quartz, garnet, and staurolite. A complex metamorphic history may be indicated.

SOUTHWESTERN ALASKA

Lawsonite in Hagemeister Island quadrangle

J. M. Hoare and W. L. Coonrad identified lawsonite in thin section and by X-ray diffraction in specimens from two localities in the Hagemeister Island quadrangle. The lawsonite occurs in altered volcanic rock (basalt flow?) on the east side of Cape Pierce and in plagiogranite on Tokomarik Mountain at the base of Cape Newenham peninsula. Both localities are structurally aligned with previously reported blue amphibole localities (Hoare and Coonrad, 1977). The only other reported lawsonite occurrence in Alaska, also associated with blue amphiboles, is on the northwest coast of Kodiak Island (Carden and Forbes, 1976). The Kodiak locality is a short distance northwest of the Border Ranges fault, which is interpreted (MacKevett and Plafker, 1974) as a Mesozoic plate boundary. The Aleutian Trench southeast of Kodiak Island is generally recognized as an active parallel plate boundary; it is reasonable to think that the occurrences of lawsonite in southwestern Alaska may be related to an old plate boundary.

Post-caldera airfall pumice at Aniakchak caldera

T. P. Miller reports that an extensive post-caldera airfall pumice was identified and partially mapped both inside and outside Aniakchak caldera in the Alaska Peninsula. A new carbon-14 age locality was sampled northeast of the caldera; the age determined from this locality may help resolve the problem of one versus two major catastrophic eruptions. Preliminary field studies of Aniakchak caldera were essentially completed with only a few additional days work needed to complete the geologic map of the area.

SOUTHERN ALASKA

Sedimentary facies in Tertiary rocks in the Tyonek quadrangle

Studies of the Kenai Group in northwestern Cook Inlet area of southcentral Alaska by K. A. Dickin-

son and J. A. Campbell reveal three fluvial depositional facies that they term *proximal-braided*, *distal-braided*, and *distal*. The *proximal-braided* facies consists mainly of medium- to thick-bedded clayey or sandy conglomerate beds that display lenticularity, low angle forests and channels and were deposited largely by mudflows and near-source braided stream systems. The *distal-braided* facies consists of sandstone, coal, and conglomerate. The sandstone units are as much as 25 m thick and consist of fine- to medium-grained generally well-sorted sandstone containing tabular crossbeds. The coalbeds are as much as 15 m thick and consist of dark-brown and black lignite with wood fragments. The *distal-braided* facies includes some sequences that fine upward from conglomerate to mudstone and coal near the toe of Capps Glacier. This facies mainly represents deposition on a broad plain by a braided fluvial system, but may include some deposition by meandering rivers. The *distal* facies is predominantly mudstone and sandstone with smaller amounts of conglomerate and coal. The rocks of the *distal* facies are similar to those of the *distal-braided* facies, except that they contain more mudstone and that sandstone units are thinner and less well sorted. The *distal* facies probably represents reworking of earlier *proximal-braided* and *distal-braided* units by braided streams on a broad plain.

Tectonic significance of newly discovered lower Paleozoic strata in the Healy A-6 quadrangle

Geologic mapping in the Healy A-6 quadrangle by Béla Csejtey, Jr., and W. H. Nelson disclosed two massive limestone beds of Silurian and Devonian age. The beds, each about 20 m thick, vertical, and striking northeasterly, are exposed about 200 m apart in the canyon walls of the lower reach of Long Creek. Both are massive to thickly bedded, are medium gray in color, contain considerable shelly fragments, have undergone only moderate recrystallization, and are enveloped by poorly exposed, dark gray shales, graywackes, and argillites of uncertain age. The contacts between the limestones and the enveloping rocks are not well enough exposed to determine whether they are depositional or tectonic contacts.

Fossils from both limestone beds have been identified by W. A. Oliver, Jr. One bed yielded massive stromatoporoids and *Dendrostella* sp. of probable Middle Devonian age and the other *Labechia* sp. and *Favosites* sp. of Silurian or Devonian age. Whether the two limestone beds are of the same age, Devonian, or one is Devonian and the other is Silurian,

cannot be determined on the basis of presently available information.

The occurrence of these newly discovered lower Paleozoic strata of probable continental-margin origin in the upper Chulitna Valley is of great tectonic significance because they are located only about 5 km southeast of ophiolitic rocks determined to be of Devonian age by D. L. Jones. The present close spatial relationship of these probably continental-margin-type limestones to the ocean-floor ophiolites, all of the same or similar age, is additional evidence for large-scale alpine-type tectonic displacements, due to subduction and suturing, in south-central Alaska.

SOUTHEASTERN ALASKA

New data on Ketchikan and Prince Rupert quadrangles

H. C. Berg, R. L. Elliott, J. G. Smith, and R. O. Koch (in press) report that the Ketchikan and Prince Rupert quadrangles contain three main geologic terranes. The eastern half of the area is underlain mainly by the Coast Range batholithic complex, a heterogeneous group of plutonic rocks and amphibolite-facies metamorphosed bedded rocks. The plutons range in emplacement age from Eocene to Miocene, in structure from gneiss to massive, and in composition from gabbro to granite, with granodiorite predominant. Metamorphic age of both plutonic and bedded rocks is Eocene. Structural trends, isograds, and lithologic units strike north to north-northwest. The northeasternmost part of the terrane is underlain by relatively less metamorphosed Triassic and Jurassic volcanoclastic and plutonic rocks. Mineral occurrences consist of porphyry molybdenum deposits in Miocene granite plutons, and of sulfide vein and disseminated deposits of gold, silver, copper, lead, and zinc in the metamorphic rocks.

The central third of the map area is underlain by greenschist-to-amphibolite facies metamorphosed sedimentary and volcanic rocks and by variously metamorphosed plutonic rocks ranging in composition from gabbro to quartz monzonite and in emplacement age from Cretaceous to Miocene. Regional metamorphic grade increases northeastward. K-Ar studies show Cretaceous metamorphic ages. Pre-metamorphic ages of the bedded rocks probably are late Paleozoic to late Mesozoic, with tectonic inliers of rocks possibly as old as Precambrian. Structural trends, isograds, and lithologic units strike north-

west to west. Mineral occurrences include traces of molybdenite in some plutons, and sulfide vein and disseminated deposits of antimony, gold, silver, lead and zinc in the metamorphic and plutonic rocks.

The remaining sixth of the area lies southwest of the central terrane and contains the most varied lithology, the most complete suite of stratified rocks, and the least-metamorphosed pre-Tertiary rocks in the Ketchikan and Prince Rupert quadrangles. The bedded rocks range in age from Silurian or older to Late Jurassic, and the plutonic rocks from Silurian or older to Cretaceous. Especially distinctive units include a Silurian or older stock of leucocratic trondhjemite, a middle(?) Paleozoic rhyolite, and a Jurassic or Cretaceous zoned ultramafic complex that contains spectacular zones of rhythmically layered dunite and peridotite. Mineral occurrences include copper-bearing barite veins in the Paleozoic rhyolite, veins carrying gold, silver, and other metals in Upper Jurassic andesitic metatuff, and stratiform titaniferous magnetite deposits in the zoned ultramafic rocks.

Selected highlights of the Ketchikan-Prince Rupert map area include:

- The boundary between the central and eastern terranes is an abrupt structural discordance that may be the metamorphosed trace of a major late Mesozoic tectonic suture.
- The central terrane contains a swarm of Cretaceous garnet-bearing feldspar (plagioclase) porphyry stocks and smaller plutons that intrude variously metamorphosed pelitic and andesitic rocks. The swarm of plutons, which has been traced for at least 80 km northwest of the map area (Berg and others, 1976), terminates abruptly at the boundary of the eastern terrane.
- The central terrane contains northeast-dipping to nearly flat thrust faults and fault zones that probably were regionally metamorphosed in Cretaceous time. The thrusts are roughly parallel to axial surfaces of semi-recumbent folds overturned to the southwest.
- A potentially economic porphyry molybdenum deposit occurs in a Miocene granite porphyry stock in the eastern terrane. Molybdenite also occurs in the eastern terrane in Miocene quartz porphyry dikes, in the Triassic and Jurassic rocks at the northeastern corner of the map area, and in at least one of the Cretaceous feldspar porphyry stocks in the central terrane.

Paleomagnetic results from the Alexander terrane and from eastern North America agree on Paleozoic paleolatitudes

Paleomagnetic research on the enigmatic Paleozoic rocks of the Alexander terrane was initiated by Sherman Grommé (USGS) to determine their original position relative to North America. Last year about 120 samples of Devonian and Carboniferous graywacke, volcanic rock, limestone, and red beds from Prince of Wales Island were analyzed by Meridee Jones and Rob Van der Voo (University of Michigan). Jones and others' (1977) study of demagnetization shows large amounts of present-day field magnetic overprinting. Characteristic magnetization directions were obtained with east-southeast declinations and inclinations between 0° and -50°. Paleolatitudes that have been calculated from the inclinations approximately match those to be expected for southeastern Alaska by extrapolation from eastern North America paleomagnetic data. The large confidence limits of the Alaskan and eastern North American results do not allow more than the tentative conclusion that relative (northward) motion of the Alexander terrane has been small or absent.

Platinum-group metals in the Douglas Island Volcanics, Juneau quadrangle

Platinum, palladium, and rhodium in 28 samples of Cretaceous greenstone (upper part of Douglas Island Volcanics) were analyzed by Joseph Haffty and A. W. Haubert as part of a study by A. B. Ford and D. A. Brew of the geochemical and petrologic nature of this extensive metavolcanic unit. The rocks are compositionally olivine tholeiites (Ford and Brew, 1977a). Palladium content is above its determinability limit in 97 percent, platinum above its limit in 17 percent and rhodium above its limit in none of the samples. Palladium content averages 12 ppb, platinum content averages 6 ppb, and the ratios Pt/Pd and Pt/(Pt+Pd) respectively average 0.51 and 0.34. Because of the many platinum results below the limit of determinability, Ford and Brew calculated the above averages by assuming qualified values at half of that limit for those samples. The metavolcanic terrane lies in the subgreenschist outer fringe of a Barrovian metamorphic belt (Ford and Brew, 1977b). The degree of element redistribution during metamorphism is presently unknown but is not believed great in view of low variability in major-element abundances and lack of other evidence of metasomatic change.

Content of nonplatinum-group minor metals in the Douglas Island Volcanics, Juneau quadrangle

Quantitative spectrographic analyses of selected minor metals in 28 samples of Cretaceous greenstone (upper part of Douglas Island Volcanics) by R. E. Mays indicate that the terrane has nearly normal amounts of copper, cobalt, chromium, nickel, scandium, and vanadium compared to average basalt. Major-element chemistry and study of field relations by A. B. Ford and D. A. Brew show that the parent rocks were mostly submarine basalt flows, tuffs, and agglomerates having the composition of olivine tholeiite (Ford and Brew, 1977a). The spectrographic analyses show the rocks to contain an average of 62 parts per million (ppm) cobalt (range 25 to 95 ppm), 207 ppm chromium (46 to 340), 92 ppm copper (36 to 200), 62 ppm nickel (22 to 220), 44 ppm scandium (21 to 74), and 222 ppm vanadium (140 to 280). The tectonic setting of volcanism is uncertain because the present data are nondiscriminatory as to whether the rocks are ocean-basin or island-arc tholeiites. An island-arc tholeiitic composition may be suggested by the low nickel and chromium averages.

Contacts of the gabbro at Mount La Perous, Mount Fairweather quadrangle

R. A. Loney, G. R. Himmelberg, and G. K. Czamanske continued their detailed field and laboratory study of the layered gabbro intrusion at Mount La Perous, concentrating their efforts on the contact zone. The western contact, probably including at least part of the north and south contact, is a vertical zone of high temperature shearing, ranging from a few meters to more than 200 m in thickness. The zone is composed mostly of interlayered garnet-bearing gneiss and garnet-bearing biotite-hornblende gneiss, through which are scattered blocks and lenses of gabbro and amphibolite at Mount La Perous, which is identical to the major amphibolite terrane that borders the zone on the west. Many of these gabbro and amphibolite blocks contain garnets, suggesting that they were subjected to some of the same metamorphism as the gneiss but somehow escaped penetrative deformation. In addition to garnet, the gneisses of the contact zone contain metamorphic sillimanite, cordierite, and staurolite. This assemblage is indicative of the amphibolite facies, except that the occurrence of cordierite and the purple color of some of the garnets suggest a transition with the granulite facies.

In contrast, the eastern contact with the major biotite schist terrane shows no shearing but appears

to be a somewhat irregular intrusive contact with fine- to medium-grained garnet-biotite schist at the contact. The schist within 20 m from contact contains a metamorphic mineral assemblage indicative of the amphibolite facies, similar to that of the western contact zone. Therefore, it is probable that the gabbro initially intruded the biotite schist terrane, and later while solid but still hot, it was faulted along with at least adjacent parts of the schist terrane against the amphibolite terrane to the west along a deep-seated fault that may extend north and south into the country rock.

Distribution of intrusive rocks in the Fairweather Range, Glacier Bay National Monument, Alaska

Completion of reconnaissance geologic mapping in the high part of the Fairweather Range in Alaska by D. A. Brew, B. R. Johnson, A. B. Ford, and R. P. Morrell shows that about 30 percent of the Fairweather geologic province (MacKevett and others, 1971) is underlain by intrusive rocks of diverse types and ages. The oldest groups are the layered gabbros of inferred Precambrian or early Paleozoic age (Brew and others, 1977a) which form a crude belt intruding mainly a regionally extensive hornblende schist and gneiss unit. Locally foliated biotite-hornblende quartz diorite, diorite, and granodiorite of inferred Tertiary or Cretaceous age occur both within and northeast of the belt of layered gabbros and in a regionally extensive biotite schist unit. Bodies of unfoliated leucocratic biotite granodiorite and tonalite, garnet- and muscovite-biotite granite and granodiorite, and hornblende-biotite tonalite, granodiorite, granite, and quartz diorite of inferred middle Tertiary age occur throughout the province, but the greatest volume is near its northeastern boundary where the biotite schist unit grades locally into phyllite and graywacke semischist.

Previous studies (Brew and others, 1977b) indicated the existence of many of these bodies, but the most recent work has shown the presence of three more relatively inaccessible major bodies of the inferred Cretaceous or Tertiary quartz diorite, diorite, and granodiorite and has clarified the relations of all the bodies to the country rocks.

Tarr Inlet suture zone, Glacier Bay National Monument, Alaska

Recent reconnaissance geologic mapping by D. A. Brew, R. P. Morrell, and B. R. Johnson west of Tarr Inlet in Glacier Bay National Monument and compilation by Morrell of those data together with pre-

vious mapping to the south as far as Taylor Bay on Icy Strait suggest that a 5- to 12-km wide and 100-km long zone of complex geology between the predominantly metamorphic rocks of the Fairweather Range province (MacKevett and others, 1971) to the west and predominantly intrusive rocks of the Geikie province to the east represents a relatively old suture between significantly different terranes.

The suture zone extends to the north into British Columbia underneath the Grand Pacific Glacier; no geologic mapping is available for about 100 km in that direction. To the south the zone projects towards the Inian Peninsula on Chichagof Island, a controversial area which Loney and others (1975) show as dominantly Mesozoic country rocks to the west separated by intrusive rocks from probable middle Paleozoic country rocks to the east and which Plafker and others (1976) in contrast place entirely to the east of the Border Ranges fault, which they infer to be "a late Mesozoic plate boundary that juxtaposes regionally metamorphosed upper Paleozoic rocks on the north[east] against predominantly upper Mesozoic deep marine rocks" on the southwest.

Brew and Morrell interpret the available evidence as suggesting that the Tarr Inlet suture zone resulted from the collision, sometime between Permian and middle Cretaceous, of a large block of probably Precambrian or lower Paleozoic rocks to the west with the very large block of middle Paleozoic rocks that is an essential element (Brew, Loney, and Muffler, 1966) of what is now called the Alexander terrane (Berg, Jones, and Richter, 1972).

GEOLOGIC MAPS

Useful applications of map data file

A map data retrieval service, still under development, is supplying diverse types of information frequently requested. All published 7½-min quadrangles are examined for about 150 bits of information. In July 1977 a preliminary list was retrieved giving latitudes and longitudes of 7½-min quadrangles where landslide deposits or scars have been mapped. In November 1977, lists giving map references to known soapstone, talc, serpentine, and "asbestos" mines (mines which may contain chrysotile asbestos) were furnished to the EPA through the U.S. Bureau of Mines.

In addition, computer-generated topical maps, displaying selected items in the data file, can be produced. A preliminary map displaying quad-

rangles where landslide deposits and scars have been mapped was produced in July 1977 to accompany the printed list.

Chronometric-geologic charts for Precambrian, United States and Mexico

Preliminary chronometric-geologic charts for the Precambrian of the United States and Mexico have been compiled by the 35 members of the IUGS Working Group, J. E. Harrison, Chairman. Detailed charts cover five "provinces" of the United States, Alaska, and Mexico. In addition, a generalized chart for the entire area has been compiled for the Working Group by Harrison. The charts are of great aid in correlating Precambrian rock bodies and events between the scattered exposures characteristic of the regions, but they also reveal the vast uncertainties of age and geologic history for many areas. The lack of obvious breaks in the continent-wide record suggests that subdivisions of the Precambrian are not marked in North America by single and sweeping geologic events.

Quadrangle compilation manuscript available for 1976 geologic map of Arkansas

Geologic information for the new Geologic Map of Arkansas (1976) was placed on topographic quadrangle maps (scale 1:24,000 or 1:62,500) prior to reduction to the scale (1:500,000) of the new map. The geologic quadrangle maps are available for inspection at the office of the Arkansas Geological Commission, 3815 West Roosevelt Road, Little Rock, Arkansas 72204, and reduced copies (scales of 1:48,000 or 1:62,500) may be ordered.

Geologic-Tectonic map of the Caribbean

Compilation of a new geologic-tectonic map of the Caribbean region at scale of 1:2,500,000 has been completed. This compilation, which will be published in multicolor, portrays the onland and offshore geology and tectonics of the entire Caribbean region between 5° and 24° N. lat and 54° and 98° W. long. More than 100 earth scientists from more than 23 nations were active contributors to the project during the 5-year compilation, led by J. E. Case (USGS) and T. L. Holcombe, U.S. Naval Ocean Research and Development Activity. Data on structure and thickness of sedimentary sequences were compiled from seismic data along many thousands of kilometers of ship traverse, provided by numerous oceanographic institutions. New geologic data from recently pub-

lished or unpublished geologic maps of many nations provided an up-to-date summary not available on previous summary maps of the region. New national maps were available for Mexico (1976), El Salvador (1974), Honduras (1974), Nicaragua (1973), Panama (1976), Colombia (1977), and Venezuela (in press).

Rio Grande rift system in Colorado

A 1:1,000,000-scale tectonic map of the Rio Grande rift system in Colorado, prepared by O. L. Tweto, identifies faults that have had late Tertiary (Neogene) and younger movements. Neogene sedimentary rocks are concentrated in grabens of the fault system whose elements define a broad belt that trends northerly through the central mountain region of Colorado from the New Mexico border to the vicinity of the Wyoming border. A major part of the rift system is caused by reactivation of a north-northwest-trending system of Precambrian faults that extends more than 300 km through the mountains of Colorado and probably farther beneath the adjoining sedimentary basins. Movements occurred repeatedly on these faults in Precambrian, Paleozoic, early Mesozoic, Laramide, and Neogene time, and several record Pleistocene and Holocene movements. Whether of ancient or Neogene origin, faults of the rift system are of special concern because (1) mineral deposits, notably of fluor spar, are associated with them; (2) the most promising geothermal areas in the State are associated with them; and (3) because of the recency of movements on some of them, they constitute the most likely sites of seismic activity in the State and are potential geologic hazards that must be considered in construction and urbanization.

Quaternary map of the conterminous United States

Completed Quaternary maps at scale 1:1,000,000 of nine north-central and northeastern glaciated States have been submitted to G. M. Richmond, editor for review. Compilation has begun in an additional 30 States. This nationwide effort has been undertaken in cooperation with various state geological survey and university personnel. In addition to surficial deposits, the maps will show Quaternary volcanic rocks, Quaternary structures, and submarine deposits. The integrated map, with individual authors, will be printed in color on 50 sheets of the World Map series; an ultimate product is a single sheet map in color at a scale of 1:2,500,000.

WATER-RESOURCE INVESTIGATIONS

The mission of the USGS's Water Resources Division (fig. 2) is to provide, interpret, and apply the hydrologic information needed for the optimum utilization and management of the Nation's water resources. This is accomplished, in large part, through cooperative programs with other Federal and non-Federal agencies.

The USGS also cooperates with the Department of State in providing scientific and technical assistance to international agencies.

The USGS conducts systematic investigations, surveys, and research on the occurrence, quality, quantity, distribution, use, movement, and value of the Nation's water resources. This work includes (1)

investigations of floods and droughts and their magnitudes, frequencies, and relations to climate and physiographic factors; (2) evaluations of available waters in river basins and groundwater provinces, including assessments of water requirements for industrial, domestic, and agricultural purposes; (3) determinations of the chemical, physical, and biological characteristics of surface and ground water and the relation of water quality and suspended-sediment load to various parts of the hydrologic cycle; and (4) studies of the interrelation of water supply with climate, topography, vegetation, soils, and urbanization.

One of the USGS's most important activities is



FIGURE 2.—Index map of the conterminous United States showing areal subdivisions used in the discussion of water resources.

disseminating water data and the results of investigations and research by means of reports, maps, computerized information services, and other forms of public releases.

The USGS coordinates the activities of Federal agencies in the acquisition of water data for streams, lakes, reservoirs, estuaries, and ground waters, maintains a national network, conducts special water-data-acquisition activities, and maintains a central catalog of water information for use by Federal agencies and other interested parties.

Supportive basic and problem-oriented research is conducted in hydraulics, hydrology, and related fields of science to improve the scientific bases for investigations and measurement techniques, and to provide sufficient information about hydrologic systems so that quantitative predictions of their responses to stress can be made.

During FY 1978, data on streamflow were collected at 7,696 continuous-record discharge stations and at 9,741 lake- and reservoir-level sites and partial-record streamflow stations. About 12,200 maps of flood-prone areas in all States and Puerto Rico have been completed to date, and about 825 pamphlets covering areas susceptible to flooding have been published in the past 5 years. Studies of the quality of surface water were expanded; there were 6,818 water-quality stations in the United States and in outlying areas where surface water was analyzed by the USGS. Parameters measured include selected major cations and anions, specific conductance or dissolved solids, and pH. Other parameters, measured as needed, include trace elements, phosphorous and nitrogen compounds, detergents, pesticides, radioactivity, phenols, BOD, and coliform bacteria. Streamflow and water-temperature records were collected at 4,055 of the water-quality stations. Sediment data were obtained at almost 1,380 locations.

Annually, about 500 USGS scientists report participation in areal water-resource studies and research on hydrologic principles, processes, and techniques. There is a total of 1,498 active water-resource projects; 446 of the studies in progress are classed as research projects. Of the current water-resource studies, 147 are related to urban-hydrology problems, 172 are energy-related projects, and 39 are related to water-use.

In FY 1978, 764 areal appraisal studies were carried out. Maximum and mean areas of the studies were about 1.5×10^6 km² and 0.062×10^6 km², respectively. Total areal appraisal funding was \$35 to \$50 million. Ground-water studies have been made

or are currently in progress at some degree of intensity for all of the Nation. Long-term continuing measurements of ground-water levels were made in about 28,000 wells, and periodic measurements in connection with investigations of ground-water were made in many thousands of other wells. Studies of saline-water aquifers, particularly as a medium for disposal of waste products, are becoming increasingly important, as are hydrologic principles and analytic and predictive methodologies for determining the flow of pollutants in ground-water systems. Land subsidence caused by ground-water depletion, the possibilities for induced ground-water recharge, and the practicality of subsurface disposal of wastes are under investigation. Ground-water supplies for energy development and the effects of coal-mining activities on both ground- and surface-water resources are being intensively studied.

The use of computers—in research studies of hydrologic systems, in expanding data-storage systems, and in quantifying many aspects of water-resource studies—continued to increase during FY 1978. Records of about 320,000 station-years of streamflow acquired at about 17,600 regular streamflow stations are stored on magnetic tape, and data on about 570,000 wells and springs have been entered in a new automated system for storage and retrieval of ground-water data. Digital-computer techniques are used to some extent in almost all of the research projects, and new techniques and programs are being developed continually.

NORTHEASTERN REGION

Johnstown in Pennsylvania, was again the site of an extreme flood caused by local downpours of from 254 to 305 mm on July 19–20, 1977. Flood peaks in the Johnstown area generally exceeded those of 1936. Frequencies were estimated to be in excess of those expected every 100 years. Runoff was as great as $341.6 \text{ m}^3 \text{ s}^{-1} \text{ km}^{-2}$ computed for a 15.18-km² drainage area in the Little Conemaugh River basin. The Conemaugh River at Seward, Pa., draining 1,873 km², had a peak discharge of $14.7 \text{ m}^3 \text{ s}^{-1} \text{ km}^{-2}$. Seven earthen dams in and near Johnstown are known to have failed as a result of the extremely high runoff rates. The flood left 73 dead and 2,696 injured. Damage was estimated to be more than \$200 million.

Though most publicity concerning the drought of 1976–77 was focused on the West, many other areas

were severely affected. For example, in some of the Great Lakes States, especially Minnesota, Wisconsin, and Michigan, thousands of private and small municipal wells, most of which were marginally productive in the past, went dry. Many were small diameter (50 mm) shallow wells (6–12 m deep), sited for convenience rather than for hydrologic favorability. In some parts of the Upper Peninsula of Michigan and locally elsewhere, aquifers are thin and areally small, but even in these places, closer attention to well location and construction would have eased the drought situation.

Intensive studies were begun throughout the coal-producing States of the northeastern region to assess the impact of mining on water resources, particularly on water quality. Comprehensive data are being gathered to evaluate surface- and ground-water quality in both bituminous and anthracite coalfields to assess restoration and reclamation efforts in mined areas and to aid in evaluating management alternatives.

Reclamation of spent coal mines may also affect aquifers. In Illinois, a study of a strip-mined area, reclaimed by disposing wet sewage sludge on the area, indicated that onsite ground-water quality was highly degraded compared with offsite ground-water quality.

Ground-water models were built for two watersheds in Ohio, where strip mining is practiced. The models enabled simulation of premining steady-state flow, and will be used in an environmental impact study.

Leachate from landfills, sewage lagoons, and burial sites for low-level radioactive wastes can degrade ground-water quality. Studies in Indiana and Illinois suggested that leachate does move downward into aquifers, and that degree and areal extent of aquifer contamination depend on the duration of leaching.

A modified computer program for a two-dimensional digital model for use in wetland hydrology studies was prepared. The program can simulate interactions among swamps, aquifers, and streams.

In February 1977, 136 m³ of organic cyanide (acrylonitrile) was spilled on snow-covered ground near Guilford, Ind. An aquifer near the site was contaminated. Advice of USGS investigators prompted the removal of cyanide, except for trace amounts, from the aquifer by pumping.

CONNECTICUT

Evaluation of the stratified-drift aquifer in the Pootatuck River valley

F. P. Haeni completed an analysis of ground-water availability in part of the Pootatuck River valley. A digital model of the stream-aquifers system incorporated data on aquifer characteristics and recharge that was collected for this study and for previous investigations (Grossman and Wilson, 1970; Wilson, Burke, and Thomas, 1974). Model simulation indicated that 0.17 m³/s can be withdrawn from the aquifer under average conditions. Induced recharge from the Pootatuck River would supply 0.11 m³/s, or 65 percent of the total pumpage. At one of the hypothetical pumping centers, the 90-percent duration flow of the adjacent stream would be reduced from 0.13 m³/s to 0.04 m³/s.

An assessment of water quality indicated that the water of the Pootatuck River meets the Connecticut standards for drinking water, with the exception of coliform bacteria. Although ground water generally meets the State standards, samples from two test wells had excessive cadmium concentrations.

Appraisal of ground-water availability and quality in Farmington

D. L. Mazzaferro used an analytical model to evaluate three areas in Farmington, Conn., that are supplied by wells tapping a stratified-drift aquifer. Estimated long-term yields ranged from 0.05 to 0.11 m³/s.

Chemical analyses of water from 11 wells tapping the aquifer indicated generally good chemical quality. The only exception is in the vicinity of the town's landfill, where concentrations of several constituents exceed the maximums specified by the State.

PCB concentrations in bottom sediments of the Housatonic River

F. P. Haeni made a preliminary evaluation of bottom sediments in Lake Zoar and Lake Lillinonah on the Housatonic River. Seismic reflection surveys showed that 0.9 to 1.2 m of sediment covered the bottom of these impoundments. Gravity coring indicated that the bottom sediments are composed predominantly of organic-rich silt.

Samples of the sediment were analyzed for PCB because of an upstream facility that had manufactured this compound. PCB concentrations ranged from 660 to 1,500 µg/kg within a single core and

from 570 to 2,100 $\mu\text{g}/\text{kg}$ in the samples analyzed. Concentrations did not increase or decrease uniformly with depth below the sediment-water interface.

ILLINOIS

Sludge-irrigation hydrology

The ground-water quality in a strip-mined area in Fulton County, Ill., being reclaimed by applying sludge from sewage-treatment plants, is different from that in the surrounding area, according to R. F. Fuentes and G. L. Patterson. Specific-conductance data from about 70 wells indicated that differences are most marked in concentrations of sulfate, sodium, calcium, manganese, and dissolved solids. Maximum onsite concentrations of sulfate were about 2,500 mg/L compared with offsite concentrations of less than 200 mg/L; onsite specific conductances were as great as 3,800 μmho compared with offsite specific conductances of 1,000 μmho . The limited data indicated that the differences were caused by mine-spoil material and that 5 years of sludge application had not significantly affected ground-water quality.

INDIANA

Saline ground water near Vincennes

R. J. Shedlock reported that a plume of saline water in the bottom of the Wabash River alluvial aquifer was at steady state with pumping of the Vincennes, Ind., municipal well field. Saline water is entering the well field, but, during 1977, the well-field effluent remained within the concentration range of from 25 to 30 mg/L chloride. In addition, the boundaries of the plume shifted only slightly because of seasonal changes in pumping.

Observation wells within the plume showed an upward movement of water from the bedrock to the alluvium and also showed that there was little, if any, leakage of saline water from abandoned oil wells in the plume into the alluvium. An inference made from lineaments mapped on aerial photographs of the plume region was that saline water was coming up through fractures in the bedrock.

The effect of increased pumping on the upwelling rate of the saline water is uncertain. Nevertheless, transport-model simulations for two and four times the present upwelling rate were run for double the 1977 pumpage. The model showed effluent chloride concentration of 100 mg/L for two times the upwell-

ing rate and 150 mg/L for four times the upwelling rate.

Geology and hydrology of the Indiana Dunes National Lakeshore Area

A study by William Meyer and Patrick Tucci showed that the 55 m of unconsolidated deposits in the Indiana Dunes National Lakeshore area may be grouped into four major units. These units consist of 12 to 37 m of a basal clay till that is overlain by 0 to 24 m of fine to medium sand; this sand is overlain by 0 to 9 m of clay and silt, and there is 1.5 to 15 m of fine to medium sand at the surface. The sands had hydraulic conductivities averaging 5.67×10^{-2} cm/s.

Monitoring of ground-water levels showed that the fly-ash settling ponds of a neighboring power-plant caused mounding in the unconfined ground-water system. Because of this mounding, water is present on adjacent wetland areas throughout the year.

Availability of ground water in the Upper White River basin

An unconfined alluvial sand-and-gravel aquifer and four relatively thin, discontinuous confined sand-and-gravel aquifers are being mapped within the drift of the upper West Fork of the White River basin by L. D. Arihood, W. W. Lapham, and J. P. Reussow. Deeper sand-and-gravel units also exist in bedrock valleys cut before glaciation. Exploratory drilling is defining the thickness and areal extent of these aquifers and the head distribution in them. Preliminary drilling indicated that the drift ranges in thickness from 0 to 152 m.

The unconfined aquifer, which ranges from 0 to 46 m in thickness and from 0 to 4.8 km in width, has the greatest potential for producing large amounts of water. Compared with the alluvial system, the confined aquifers will probably yield only small amounts.

A map of the head distribution in the limestone beneath the drift indicated that water in the limestone is discharged into streams in the basin.

Unconsolidated aquifers near Logansport

The thickness and areal extent of the unconsolidated sand and gravel aquifers in the Logansport, Ind., area were determined by D. C. Gillies and Angel Martin, Jr. An extensive test-drilling program provided stratigraphic information to supplement that contained in drillers' logs for wells scattered throughout the 500-km² study area. The

aquifer of primary interest is the sand and gravel deposit at or near the bottom of preglacial Teays Buried Valley, which crosses Cass County from east to west 5 to 6 km north of the Wabash River. This aquifer is buried beneath 30 to 60 m of drift, and it is bounded beneath and on the sides by limestone bedrock. Over the axis of the buried valley, the deposit has a maximum thickness of 30 m. The aquifer ranges from 2 to 3 km in width. Although the general location, depth, and configuration of Teays Buried Valley aquifer in Cass County had been known previously, this study produced detailed information regarding the nature of the material filling the valley, thus allowing delineation of the permeable sand and gravel deposits.

Leachate movement in opposite directions in outwash aquifer separated into two units by clay

Sewage lagoons and a landfill overlie the glacial outwash aquifer in Marion County, Ind. The aquifer, directly below the landfill and lagoons, is separated into an upper and lower sand-and-gravel unit by a clay layer. Leachate from the 30-year-old sewage lagoons has affected ground-water quality in both the upper and lower units, whereas leachate from the 8-year-old landfill has affected ground-water quality only in the upper unit, according to R. A. Pettijohn.

Directly below the landfill and sewage lagoons, ground-water and leachate movement in the upper unit is southeastward toward the White River, and that in the lower unit is northwestward toward the industrial pumping.

Analyses of water from wells between the sewage lagoons and the industrial wells showed that leachate is being highly attenuated as it moves through the aquifer toward the center of industrial pumping.

MAINE

Ground-water resources in the Portland area

A study of surficial geology and ground-water resources of the Portland area of Maine by G. C. Prescott, Jr., (1976) indicated a lack of productive aquifers from which well yields of 3.15 L/s or more can be obtained. Marine deposits, which consist of silt, clay, and fine sand are widespread and reach a maximum thickness of more than 60 m in the valley of the Fore River. Outwash sand overlies the marine deposits in places and yields enough water for domestic use. Ice-contact deposits contain only about a meter of water-saturated sand and gravel and are not a source of water. Wells in bedrock generally

yield enough water for domestic supplies but not enough for public or industrial supplies. The average yield of wells drilled in rock is 0.7 L/s, and the median yield is 0.3 L/s. Much of the area is served by a public water supply, the Portland Water District, which obtains most of its water from Sebago Lake

Geohydrology of the Androscoggin Valley Regional Planning area

A study of the geohydrology of part of the Androscoggin River valley by G. C. Prescott, Jr., (USGS) (1968) and J. W. Attig, Jr., (Androscoggin Valley Regional Planning Commission) indicated that substantial supplies of ground water are available in ice-contact and outwash deposits, especially where these deposits are adjacent to and in hydraulic continuity with the Little Androscoggin River, which serves as a source of induced recharge. The maximum reported yield is 126 L/s from an individual public-supply well. The water is of calcium bicarbonate type, and it is of good to excellent chemical quality; it is low in dissolved-solids concentrations (18–186 mg/L), and it is soft to moderately hard (2–110 mg/L). Iron and manganese cause problems locally where large amounts of recharge are being induced from the Little Androscoggin River.

MARYLAND

Two-dimensional model of the Piney Point aquifer

A two-dimensional model of the Piney Point (Eocene) aquifer in Maryland was calibrated by J. F. Williams. The Piney Point is an unconsolidated, confined Coastal Plain aquifer and is a major water source for cities, communities, industries, and domestic users in southern and eastern Maryland.

For the past several years, water levels have been rising in the large cone of depression centered at Cambridge, Md. This is due to reduced withdrawals from the Piney Point in that area. Simulated model predictions indicated that if projected future pump-ages are correct, water levels in Cambridge will be 4.5 m higher by 1990 than they were in 1976. Additional simulation predictions indicated that water levels will decline (generally <6 m) in southern Maryland between 1976–90.

MASSACHUSETTS

Results of water-level survey at Martha's Vineyard

D. F. Delaney's studies, which included test drilling and water-table mapping, of the water resources

of Martha's Vineyard in Massachusetts show that the principal aquifer is glacial outwash underlying the southeastern two-thirds of the island east of the Gay Head-Martha's Vineyard terminal moraine, which contains imbricated thrust beds of fine-grained Tertiary sediments. The water table in the outwash is highest (>5 m above mean sea level) near the moraine and slopes southeastward across the center of the island; it slopes toward the coastline near the northern, eastern, and southern shores. Owing to seasonal changes in evaporation and transpiration, annual fluctuations of the water table are less than 1 m. Test drilling in the aquifer to a clay layer 40 m deep at one site near the shore indicated that freshwater flow toward the sea was nearly horizontal and sufficient to displace the saltwater-freshwater interface offshore.

Trace metals in ground water on Cape Cod

A reconnaissance of ground-water supplies on Cape Cod, Mass., by M. H. Frimpter and F. B. Gay indicated that the trace metals As, Cd, Co, Cn, Pb, Hg, Se, and Zn were found in concentrations no greater than one-tenth of the maximums recommended for drinking water, and chromium concentrations were not greater than one-fifth of the recommended maximums. Only concentrations of iron and manganese (0.3 and 0.05 mg/L, respectively) were greater than the recommended maximums. Iron and manganese in ground-water supplies are troublesome at scattered locations, but particularly in Provincetown, an area consisting largely of post-Pleistocene sand dunes. Where concentrations of these metals are above recommended levels, the water is both acidic and reducing.

Iron and manganese oxide or hydrous oxide coatings on the sediment particles are the sources of these metals in ground water. In most of the study area, ground water is oxidizing (median DO, 7.75 mg/L) and acidic (median pH, 6.1), and it does not readily dissolve iron or manganese. In places, however, ground water is reducing (devoid of oxygen), owing to the effects of decaying organic matter in landfills, septic systems, and marsh deposits buried by eolian sand. In this reducing environment, ground water dissolves both iron and manganese from the coatings on sediment particles.

Freshwater-saltwater relations on Cape Cod

J. H. Guswa and D. R. LeBlanc reported that specific conductance and water levels were measured periodically, and water samples were collected for

determination of chloride concentrations at 30 test-well sites on Cape Cod, Mass., to locate and describe the boundary between fresh and saline water. There is an average of four wells, each screened at different depths, at each site.

Generally, the transition zone between fresh and saline water along the outer Cape and on the southern and western shores of the inner Cape is 5 to 16 m thick, and its position is in close agreement with that predicted by a hydrodynamic model. No seasonal movement of this freshwater-saltwater boundary was observed. At two locations on the southern shore of the inner Cape, inland saline surface water (chloride concentration exceeding 6,500 mg/L) enters the upper parts of the aquifer and is diluted (chloride concentration, 1,000 mg/L at a depth of 30 m) by the fresher ground water as it moves downward.

Along the northern shore of the inner Cape, freshwater (chloride concentration less than 250 mg/L) was penetrated to a depth of at least 30 m at several locations and to bedrock at a depth of 90 m. Glaciolacustrine clay and silt layers, common along the northern side of the Sandwich moraine, have created local confining conditions, which have resulted in a displacement of the freshwater-saltwater transition zone downward and seaward of the position that would have been predicted by using water-table heads in a hydrostatic model.

Ground-water assessment in the lower Merrimack River basin

The most productive aquifers in the lower Merrimack River basin of Massachusetts are glacial deposits of sand and gravel, which are scattered throughout the basin, according to F. B. Gay and D. F. Delaney. These aquifers, which range from 0.2 to 1.1 km in width and from 0.6 to 3.2 km in length, are capable of supplying 6 to 19 L/s to individual wells. Within these aquifers are zones of sufficient volume and transmissivity (370 m²/d) to sustain yields in excess of 19 L/s to individual wells. The bedrock aquifer is capable of supplying only about 0.5 L/s to wells.

Ground-water quality is generally good throughout the basin, and the water is suitable for most uses. Water ranges from soft to moderately hard (0-120 mg/L), except that from wells near the Merrimack Estuary, tidal marshes, or the ocean, where water ranges from hard to relatively very hard (121 to >180 mg/L). At many places in the basin, iron and manganese concentrations commonly exceed the maximums recommended for drinking water (0.3 and 0.05 mg/L, respectively).

Analyses of base-flow measurements showed that streamflow at the annual minimum 7-day mean flow at the 10-year recurrence interval ranges from no flow for many streams draining less than 26 km² to 26.5 m³/s for the Merrimack River just below its confluence with the Concord River at Lowell, where the river drains 12,005 km².

Ground-water development on Cape Cod

From 4 to 5 percent of the estimated annual recharge to ground-water reservoirs on Cape Cod, Mass., is withdrawn from public-supply wells, according to D. R. LeBlanc and J. H. Guswa. An inventory of the total pumpage by public water-supply systems on Cape Cod showed that 23.5 hm³ of water was pumped for public supply in 1976. Estimates of the total annual recharge to the aquifer system determined by the Thornthwaite empirical method ranged from 447 to 579 hm³/yr. Most of the water pumped for public supplies, as well as most of the water pumped from private wells, is returned to the aquifers as septic-tank and sewage-treatment-plant effluent.

A water budget for Nantucket Island

A water budget for Nantucket was prepared by E. H. Walker. Input of freshwater was from precipitation, which averages 1,110 mm/yr. The major item of discharge was evapotranspiration, which is estimated to return an average of 625 mm of water yearly to the atmosphere. Runoff was estimated at 25.4 mm/yr because the only streams on the sandy island are a few small brooks that drain swamps and cease to flow during the growing season. The remainder of the water from precipitation, 460 mm/yr, recharges the ground-water reservoir and then discharges to the ocean along the coast. This amounts to 47.7 million m³/yr over the 104 km² of the island that is not composed of salt marsh and sandbars. Ground water pumped for public supplies and drained to sewage-treatment lagoons close to the southern shore of Nantucket amounts to 833,000 m³/yr. Thus, pumping for public supplies captures less than 2 percent of the natural outflow of ground water.

MICHIGAN

Reevaluation of water resources of the Marquette Iron Range

Iron-ore mining and beneficiation processes in the Marquette Iron Range are placing extensive de-

mands on the water resources of Marquette County, Michigan, according to Norman Grannemann. These demands compete with the need to supply adequate water for domestic and recreational uses. In recent years, reservoir with capacities of 6.53 and 28.7 hm³ were built to more fully use the water supply. Expanding mining operations increased the number and size of tailings basins, and interbasin diversions added to the complexity of the water-resource system. Substantial amounts of ground-water, surface-water, and quality-of-water data were obtained in the area. These data are being used to reevaluate the water resources in the Marquette Iron Range.

Agricultural land use related to chemical and physical erosion

A study by T. R. Cummings to determine the relationship of agricultural land use to erosion in the Upper St. Joseph River basin of Michigan established base-line conditions against which future changes can be judged. In cooperation with the Michigan Department of Agriculture, 42 sites in the basin were sampled. Correlations were strong among runoff, the loads of various forms of nitrogen and phosphorus transported, and suspended sediment loads. Relationships of stream quality, type of land use, and seasonal variations are being determined.

MINNESOTA

Hydrology and ground-water quality in a potential mining area in northeastern Minnesota

D. I. Siegel and D. W. Ericson reported that ground-water discharge to streams in much of the proposed copper- and nickel-mining area of northeastern Minnesota is restricted because of a general lack of surficial aquifers. During the recent drought, streamflow receded from well above normal levels in the spring of 1976 to record- or near-record minimum flows 10 months later. Rivers having many in-channel lakes maintained large flows longer than other rivers.

Potential development of ground-water is essentially restricted to the glaciofluvial sediments underlying the Embarrass and Dunka Rivers and filling buried valleys near Aurora. Wells tapping these surficial aquifers may yield from 10 to 20 L/s.

Ground-water quality varies according to aquifer lithology. Water from surficial aquifers is generally a mixed calcium and magnesium bicarbonate type. Water from mafic rocks in the Duluth Complex is more variable, ranging from sodium bicarbonate to

sodium chloride types. Cu, Ni, Pb, Co, and Cr were present in surficial aquifers in concentrations generally ranging from less than 0.1 to 50 mg/L. Higher concentrations of most constituents were found in ground-water samples collected adjacent to a mineralized outcrop. Concentrations of copper and nickel were as much as 3.8 and 0.4 mg/L, respectively, in shallow ground water adjacent to the site. Selenium was not detected. Where mercury and silver were found, they generally occurred in concentrations of less than 50 ng/L.

Interflow in uncased multiaquifer wells

Hydraulic head differences between the upper carbonate aquifers and the underlying St. Peter Sandstone aquifer are as much as 85 m in the karst area of southeastern Minnesota, according to M. F. Hult. The intervening Decorah Shale and Glenwood Shale constitute confining beds between the two aquifers.

Because of the large difference in head, abandoned multiaquifer wells were assumed to be the path for contaminants reaching deep aquifers. However, study results indicated that the multiaquifer wells are physically unstable and tend to bridge-over or collapse. Well inventories showed that nearly all abandoned wells are shallow, single-aquifer wells that do not penetrate the St. Peter Sandstone.

Appraisal of a sand-plain aquifer in central Minnesota

J. O. Helgesen (1977) reported that well yields of 30 L/s can be obtained in much of a 2,000-km² shallow outwash-sand aquifer, and yields may exceed 125 L/s in some parts of the aquifer. A numerical-model analysis showed that present withdrawal of 44 L/s has no significant effect on ground water storage in the system. Simulations of hypothetical withdrawals of 1,700 to 3,400 L/s resulted in computed maximum water-table declines of 3.7 m in heavily pumped areas.

Availability of ground water in southwestern Minnesota

D. G. Adolphson reported that test augering and well data indicated that sustained yields of 65 L/s may be available from wells in shallow sand and gravel aquifers locally in an eight-county, water-poor area of southwestern Minnesota. The sand and gravel deposits occur as outwash and crevasse-filling deposits associated with a series of parallel terminal and recessional moraines and in a network of six melt-water channels. The melt-water channels are

long, narrow features underlying the present drainage.

Planning study in the Pelican River sand plain

H. W. Anderson, Jr., reported that augering is a feasible method of determining the areal extent and thickness of ice-contact deposits in the Pelican River sand plain, an area of about 500 km² in west-central Minnesota. Augering of test holes was unsuccessful at only 1 of 21 sites; at that one site, material too coarse to penetrate was encountered. The ice-contact deposits ranged in thickness from 7 to 37 m and ranged in saturated thickness from 0.3 to 21 m. Depth to water ranged from 1.5 to 21 m.

Augering near Pearl and Floyd Lakes indicated that the Pelican River sands aquifer extends westward beneath till. Additional test drilling is needed to define the boundaries of the buried part of the aquifer.

Appraisal of the Buffalo aquifer

By means of extensive test augering, R. J. Wolf found that the Buffalo aquifer in western Minnesota is 64 km long and ranges from 1.5 to 6.5 km in width. Unconsolidated sand and gravel beds that compose the aquifer are roughly triangular in section and are surrounded by fine-grained glacial-lake deposits and clayey till. The maximum depth that could be augered indicated that the aquifer exceeds 46 m in thickness at several locations and that the sand and gravel deposits are not directly connected hydraulically to the South Branch Buffalo River, which parallels the aquifer. However, a series of low-flow measurements in the river showed several losing reaches that indicated possible recharge to the aquifer.

Ground-water appraisal in sand plains of Benton, Sherburne, Stearns, and Wright Counties

According to G. F. Lindholm, test augering indicated that surficial outwash is as thick as 30 m in parts of the Sherburne National Wildlife Refuge in Sherburne County. Outwash is thickest where it fills buried valleys in underlying till.

About 300 irrigation wells are concentrated in a 5-km-wide band adjacent to the Mississippi River in Sherburne County. About 50 percent of the wells are completed in confined or semiconfined drift aquifers, 25 percent are completed in unconfined drift aquifers, and 25 percent are completed in the Paleozoic sandstone aquifers which underlie the eastern third of the county.

In eastern Stearns County, where coarse sand and gravel locally exceeds 30 m in thickness, a rapid development of water supplies for irrigation is taking place.

In the spring of 1977, following the severe drought of 1976 and early 1977, water levels in the unconfined aquifer reached the lowest level in the 9-year period of record.

NEW JERSEY

Water-resources potential of the Wharton Tract

A study by R. S. Poggioli and O. S. Zapecza of about 100 geophysical logs throughout the New Jersey coastal plain confirmed previous indications that the upper Tertiary Cohansey and Kirkwood Formations are hydraulically connected in much of the coastal plain. A segment along the southeastern coast of the State is the only exception. From central Ocean County to Cape May Point, the Cohansey aquifer is separated from the Kirkwood aquifer by a dense clay confining unit with an average thickness of 100 m. This confining layer extends updip from the coast to approximately 30 km inland, where it grades laterally into a more permeable silty sand, producing a composite Cohansey-Kirkwood aquifer system.

Water level measurements throughout the Mullica River basin in late August 1977 indicated that the unusually dry year had caused groundwater levels to decline approximately 3 m in interfluvial areas.

NEW YORK

Effects of wastewater-management schemes on ground-water reservoir evaluated

An evaluation of the effects of wastewater-management schemes on the ground-water reservoir of Long Island in New York involved the use of a regional three-dimensional analog model. A. W. Harbough, G. E. Kimmel, and T. E. Reilly (Harbough and Reilly, 1976, 1977; Kimmel and Harbough, 1976) evaluated the effects of sewerage, and various techniques intended to minimize detrimental effects of sewerage, such as a lowered water table and reduced streamflow.

The simulations improved estimates of future water-table declines; for example, the water table may decline as much as 5 m in Nassau County and as much as 1.8 m in Suffolk County by the 21st century. These declines could be remedied in several

ways, including artificial recharge and water conservation.

Position of freshwater-saltwater interface on South Fork, Long Island

Studies by Bronius Nemickas and E. J. Koszalka (Nemickas, Koszalka, and D. E. Vaupel, 1977) indicated that the freshwater-saltwater diffusion zone ranges from 6 to 18 m in thickness on South Fork, Long Island. The lenticular configuration of the freshwater reservoir follows the Ghyben-Herzberg principle in the southern part of South Fork, but in the northern part, the interface is much closer to the land surface than the water-table altitude would indicate. This is a result of a high degree of aquifer anisotropy in the northern part.

Heavy ground-water withdrawals at a single location may sufficiently lower the head in the freshwater aquifer to cause vertical leakage of saline water from a shallow or deeper aquifer. Saltwater may encroach on South Fork from the shoreline, but it is more likely to encroach by vertical leakage.

Diversion of the Hudson River in Pleistocene time

The Jameco Gravel of pre-Sangamon Pleistocene age occurs in a deep buried valley in central Queens County, Long Island. Julian Soren (1978a) reported that numerous large fragments of diabase in the Jameco deposits indicated stream transport by an ancestral Hudson River that was diverted through Queens from the Palisades, which form the western side of the present Hudson channel between New York and New Jersey. The fact that the buried channel of the Hudson in the Continental Shelf is in better alignment with the buried valley in Queens than it is with the present lower Hudson channel between New York and New Jersey supports this conclusion.

Extraction of chromium and cadmium from aquifer material

Core samples of aquifer material in a plume of industrial discharge were analyzed by oxalate and dithionite-citrate-bicarbonate extraction methods for the presence of chromium and cadmium. Results, reported by H. F. H. Ku, B. G. Katz, D. J. Sulam, and R. K. Krulikas (1978), indicated that median concentrations of chromium and cadmium in the aquifer material were 9.7 and 1.65 mg/kg of soil, respectively, and that maximum concentrations were 19.2 and 2.3 mg/kg of soil, respectively.

Glacial deposits may be thin at artificial-recharge site

According to T. M. Robison, D. A. Aronson, G. A. Brown, and R. K. Krulikas, information obtained from drilling numerous observation and injection wells at the Meadowbrook artificial-recharge site in central Nassau County, Long Island, suggested that the upper glacial aquifer is thinner in this area than was previously thought. The upper surface of the underlying Magothy Formation of Cretaceous age is apparently uneven and may come to within 15 m of the land surface in places.

Dye used to study mixing of waters of the Hudson River estuary

G. C. Gravlee, Jr., and Bernard Dunn supervised a major dye-dispersion study on September 21, 1977. Fluorescent dye (Rhodamine-WT) was continuously injected into the Hudson River near Cornwall, N.Y., during a 7-hour period. The resulting dye cloud was monitored by fixed and mobile sampling equipment over a 30-hour period. The close tracking of the dye cloud provided the Federal Power Commission with the data they needed for designing the proposed Cornwall pumped-storage plant on the Hudson River.

Beds of clay impose limits on available fresh ground water on Shelter Island

Ground-water investigations by Julian Soren (1978b) on Shelter Island, Suffolk County, showed that glacial sand and gravel beds containing fresh water lie between the water table at 0 to 1.5 m above sea level and the surface of underlying marine clay beds at 20 to 30 m below sea level. The saline water in the clay is probably connate. Because saline water also occurs beneath the clay beds, the sole source of fresh ground water on Shelter Island is precipitation, which recharges the glacial sand and gravel beds.

A water-table altitude of more than 1.5 m above sea level in parts of the island indicated that fresh-water should occur to depths of more than 61 m below sea level, according to the Ghyben-Herzberg principle. The clay beds, however, limit the fresh-water zone to about half this depth.

Water-table recovery causes flooding problems

In 1947, New York City ceased pumping all ground water for Brooklyn's public water supply because of saline-water infiltration to the aquifer. The subsequent water-table rise flooded basements and subway tunnels in central Brooklyn. In 1974, when the city ceased pumping in the Woodhaven section

of adjacent Queens County for the same reason, the rate of water-table rise increased in the nearby East New York section of Brooklyn.

Studies by Julian Soren (1976) showed that the water table in the central East New York section of Brooklyn was about 1.5 m below sea level in 1947. It had recovered to 1.5 m above sea level by 1973 and to 2.4 m above sea level by 1976. Ultimately, the water table in the central East New York section of Brooklyn could rise as high as 4.6 m above sea level. If this happens, pumping out flooded structures will be difficult, and satisfactory disposition of the pumped-out water may be equally as difficult.

Areas of contamination delineated in ground water in Suffolk County

Julian Soren (1977) reported that analyses of water samples collected from 1972-75 from observation wells screened at shallow depths below the water table at 171 sites in Suffolk County indicated no significant contamination from pesticides or radioactivity. Areas contaminated by nitrate and synthetic detergents were delineated. The main source of such contamination in western Suffolk County was cesspool effluent. The main source of nitrate contamination in eastern Suffolk was fertilizer leachate from farming areas.

Although pesticides have been used for decades in the heavily farmed parts of eastern Suffolk County, their concentration in ground water was insignificant, which suggested that the pesticide compounds are either held in the upper soil zone or break down into simpler and less hazardous substances in the lower soil zone.

Radioactive fallout from the atmosphere, which would be the main source of radioactive contamination to ground water in Suffolk County, was not apparent from 1972-75.

PENNSYLVANIA**Nutrient and sediment discharges for agricultural land**

A nonpoint source discharge study by D. A. Eckhardt and J. R. Ward indicated that nutrient and suspended-sediment yields from the Pequea Creek basin in the Appalachian piedmont in south-central Pennsylvania are among the highest annual yields in the State. The 383-km² study area, a rural agricultural watershed in Lancaster County, is chiefly underlain by Cambrian and Ordovician carbonate rock and supports productive dairy farms and cropland. The suspended-sediment yield from the area

for the 1977 water year was 165,000 kg/km²; this was calculated from continuous streamflow records and water-quality samples collected near the confluence of Pequea Creek and the Susquehanna River since February 24, 1977. The yield of total nitrite plus nitrate as N was 1,120 kg/km². The yield of total kjeldahl nitrogen as N was 508 kg/km², and the yield of total phosphorus as P was 158 kg/km². The sediment, phosphorus, and organic part of kjeldahl nitrogen were transported primarily in suspension during intense storms, although significant quantities were also transported in solution. Nitrate, however, was transported almost completely in solution, especially during wet spring months and was discharged into the stream chiefly as baseflow.

RHODE ISLAND

Measurement of aquifer characteristics in the Pawcatuck River basin

Drilling and aquifer testing resulted in the delineation of a highly permeable body of stratified drift in the lower Wood River area of the Pawcatuck River basin. H. E. Johnston and D. C. Dickerman found from analyses of lithologic logs of more than 85 test wells that the drift, which fills and conceals the preglacial channel of the Wood River, consists of an upper coarse-grained unit of high permeability, and a lower fine-grained unit of low permeability. Maximum thickness of the sediments is about 90 m. The coarse unit, which is chiefly sand and gravel, is lens shaped, has a maximum thickness of about 45 m, and occupies an area 7 km long and 0.9 to 1.2 km wide. Twenty-centimeter-diameter test wells constructed at 11 sites in the coarse unit were pumped for 48 hours at rates ranging from 21 to 40 L/s during controlled aquifer tests. Yields of larger diameter wells at these sites should be in the range of 35 to 100 L/s. Preliminary analyses of the aquifer-test data indicated that hydraulic conductivity of strata adjacent to screens in the pumped wells ranges from 46 to 358 m/d and averages about 160 m/d.

VERMONT

Ground-water resources in the Rutland area

Results of a water-resource investigation of the Rutland area in the southwestern part of central Vermont by R. E. Willey (USGS), David Butterfield and J. W. Ashley (Vermont Department of Water

Resources) indicated that a sufficient quantity of water is available from bedrock and glacial aquifers to supply domestic needs nearly everywhere in the area.

Bedrock-aquifer yields depend on the secondary porosity and permeability of the formations. Well yields ranged from less than 0.01 to 9.4 L/s, with a median yield of 0.38 L/s.

Ice-contact deposits along the western side of the Green Mountains and along small tributary valleys yield water in sufficient quantities for domestic, light industrial, and commercial purposes—the deposits yield as much as 7.9 L/s in some places. Areas favorable for developing large-capacity wells, yielding in excess of 16 L/s, are located in coarse stratified-drift deposits in larger stream valleys.

Dissolved-solids concentrations in water from bedrock and glacial aquifers are low—less than 500 mg/L. Iron and manganese are problem constituents in the ground water. The median concentration of iron and manganese, 0.26 and 0.04 mg/L, respectively, is higher than that in water from wells finished in bedrock. Owing to road-salt application or storage, the quality of ground water is poor; sodium and chloride concentrations reached 240 and 700 mg/L, respectively.

WEST VIRGINIA

Effects of deep mining on base flow

Two basins in West Virginia were selected by W. A. Hobba, Jr., and S. M. Ward to study the effects of deep mining and deep-mine collapse on hydrology. Buffalo Creek and Indian Creek basins both contain active and abandoned deep mines in the Pittsburgh coal, which lies 60 to 120 m below major stream drainage. Seventy measurements of base flow and mine pumpage in the fall of 1977 generally showed that lowest yields were from basins underlain by active deep mines, the highest yields were from basins underlain by abandoned deep mines, and intermediate yields were from basins having no deep mining activity. These findings are comparable to those for Roaring Creek and Grassy Run basins, which are underlain by abandoned deep mines in the Kittanning coal, which lies above major stream drainage. Available flow data for these basins showed that the yield of the mined area is greater than the yield of the unmined area at low base flow in the fall. In the winter, base flow of the mined area is nearly twice as great as that of the unmined area.

Hydrology of the Guyandotte River basin

Fractures and bedding-plane partings on valley walls and bottom are probably the major sources of ground water in the Guyandotte River basin and possibly in the Appalachian Plateaus Province. The cause of the fractures and partings is probably elastic rebound caused by erosion of the valley. The results of three pumping tests by J. S. Bader, J. W. Borchers, and G. G. Wyrick indicated that fractures in the valley walls are nearly parallel to the valley, and their depth is restricted. The depth to which the bedding-plane partings reach below the valley floors is not known, but it may be great. Alluvium covering the sides and floor of the valley serves as a seal, so nearly all heavy precipitation runs off. The fracture system is recharged high on the valley walls, where the alluvial cover is thin.

Wells near the center of the valley would probably yield the most water because there the unloading effect would be greatest, and bedding planes would be opened widest. Wells too close to the valley walls might penetrate unfractured rock.

WISCONSIN

Low-flow characteristics of small streams in 32 basins

S. J. Field determined the low-flow characteristics for 278 streams in 32 basins being considered for work under provisions of Public Law 566. These characteristics were the annual minimum 7-day mean flow at 2-year ($Q_{7,2}$) and 10-year ($Q_{7,10}$) recurrence intervals; $Q_{7,2}$ estimates ranged from 0 to 3.85 m³/s, and $Q_{7,10}$ estimates ranged from 0 to 2.66 m³/s.

Effects of a powerplant on streamflow and lake levels

The possible effects of using water from Lake Koshkonong for powerplant cooling were investigated by W. R. Krug. A continuous streamflow- and reservoir-routing model was used to simulate daily streamflow of the Rock River and daily stage of Lake Koshkonong for consumptive use ranging from 0 to 1.13 m³/s. With a consumptive use of 1.13 m³/s, the simulated stage of Lake Koshkonong was as much as 0.13 m lower than the simulated stage with no consumptive use. Duration of simulated lake stage below the regulatory minimum stage of 3.60 m, which would be exceeded once in 10 years, increased from 83 to 132 days as simulated consumptive use increased from 0 to 1.13 m³/s.

Low-flow characteristics at gaging stations on the Wisconsin, Fox, and Wolf Rivers

Low-flow characteristics were determined at 11 gaging stations on the main stem of the Wisconsin, Fox, and Wolf Rivers in Wisconsin by W. A. Gebert and B. K. Holmstrom. The low-flow characteristics determined were the annual minimum 7-day mean flow at 2-year ($Q_{7,2}$) and 10-year ($Q_{7,10}$) recurrence intervals.

To provide accurate and consistent low-flow characteristics for uniform evaluation, the 1915–75 period of streamflow record was used for the analysis; data included long-term streamflow conditions and various degrees of regulation by storage reservoirs.

The $Q_{7,10}$ discharge on the Wisconsin River ranged from 3.96 m³/s at Rainbow Lake near the town of Lake Tomahawk to 79.0 m³/s at the Muscoda gaging station. On the Fox-Wolf Rivers, the $Q_{7,10}$ ranged from 10.2 m³/s at Fox River at Berlin to 26.9 m³/s at Fox River at Rapide Croche Dam near Wrightstown. The low-flow characteristics were found to vary \pm 30 percent at some gaging stations, depending on whether or not the period of record used in the analysis included the severe drought of the 1930's.

Low-flow characteristics of streams in the lower Wisconsin River basin

Low-flow characteristics were determined for streams in the lower Wisconsin River basin by W. A. Gebert. Included were estimates of low-flow frequency and flow duration at 11 gaging stations, low-flow frequency characteristics at 26 low-flow partial-record stations, and 70 miscellaneous measurement sites. For 26 low-flow partial-record stations and 2 gaging stations with drainage areas of less than 388 km², the average low flow for 7 consecutive days with a recurrence interval of 2 years ($Q_{7,2}$) and 10 years ($Q_{7,10}$) was 0.0031 and 0.0024 m³ s⁻¹ km⁻², respectively. These basin averages are significantly higher than the State average of 0.0022 m³ s⁻¹ km⁻² for $Q_{7,2}$ and 0.0015 m³ s⁻¹ km⁻² for $Q_{7,10}$.

Multiple-regression equations were developed for determining low-flow characteristics at ungaged sites. Two sets of equations were determined, one for sites without additional streamflow data and the other for sites with base-flow measurements. The standard error of estimate of $Q_{7,10}$ was 54 percent for the first equation and 32 percent for the second equation. The most significant characteristics in explaining the variation in low flow were drainage

area, forest cover, soil-infiltration rate, and base-flow index.

Low-flow characteristics estimated for the lower Wisconsin River basin had a high degree of reliability when compared to those for other basins in Wisconsin. Reliable estimates were related to the relative uniformity of the factors that control low flow—mainly precipitation, geology, and evapotranspiration.

Preimpoundment conditions in a small drainage basin

P. A. Kammerer, S. M. Hindall, M. G. Sherrill, and R. S. McLeod studied hydrologic and water-quality characteristics of the Nederlo Creek basin before construction of a flood-retention structure and a multipurpose reservoir. The basin is typical of farmland in the "driftless area" of southwestern Wisconsin. Streamflow consists primarily of groundwater runoff about 90 percent of the time, but sudden rises in stage caused by snowmelt or heavy precipitation may lead to flash flooding. Rugged topography, easily erodible soils, and land use are factors contributing to relatively large quantities of suspended sediment, total phosphorus, and total nitrogen transported during the short time that runoff is a significant contributor to streamflow. From 70 to 80 percent of total phosphorus, 35 to 55 percent of total nitrogen, and 74 to 86 percent of suspended sediment are transported when runoff is contributing to streamflow. Mean annual suspended-sediment loads measured during 1968–74 ranged from 4.6 to 21 t/km²; total phosphorus and total nitrogen loads during the same period were 0.007 to 0.024 and 0.14 to 0.28 t/km², respectively.

Water in the Nederlo Creek basin is a calcium magnesium bicarbonate type that is similar in chemical quality to surface water and ground water in the surrounding area. The DO content of stream water during the summer is generally between 7 and 13 mg/L. The daily ranges and extremes of water temperature are influenced by the proximity of springs. Temperatures exceeding 26°C are rare, and maximum temperatures near springs are lower.

Concentrations of toxic heavy metals in water from wells in Wisconsin

C. A. Harr, in cooperation with the Wisconsin Geological and Natural History Survey, made a reconnaissance of the natural concentrations of minor elements in ground water. Samples were collected from a statewide network of observation wells tapping principal aquifers. Median and average con-

centrations, respectively, were: As, 0 and 2.5 µg/L (217 wells); Cd, 0 and 0.5 µg/L (213 wells); Co, 0 and 0.8 µg/L (196 wells); Cu, 0 and 13 µg/L (227 wells); Pb, 2.0 and 3.9 µg/L (269 wells); Ni, 1.0 and 2.6 µg/L (82 wells); Se, 0 and 0.3 µg/L (180 wells); and Zn, 60 and 273 µg/L (268 wells). Concentration of mercury was less than 0.5 µg/L, and that of chromium was less than 10 µg/L in water from all wells sampled.

Arsenic concentration in water from one well known to be contaminated was 250 µg/L; however, the water is not used. Zinc concentration in water from one well in the lead-zinc district in southwestern Wisconsin was 6,600 µg/L.

Low-flow characteristics of streams in the Rock-Fox River basin

Low-flow characteristics were determined for 13 gaging stations, 32 low-flow partial-record stations, and 78 miscellaneous sites in the Rock-Fox River basin by B. K. Holmstrom. The low-flow characteristics determined were the annual minimum 7-day low flow at 2-year ($Q_{7,2}$) and 10-year ($Q_{7,10}$) recurrence intervals.

For the 32 low-flow partial-record stations and 4 gaging stations with drainage areas of less than 388 km², average $Q_{7,2}$ is 1.1×10^{-3} (m³/s)/km², and average $Q_{7,10}$ is 6.6×10^{-4} (m³/s)/km². These basin averages are significantly lower than the State averages of 2.2×10^{-3} (m³/s)/km² for $Q_{7,2}$ and 1.5×10^{-3} (m³/s)/km² for $Q_{7,10}$.

Multiple-regression equations were developed to determine $Q_{7,2}$ and $Q_{7,10}$ of ungaged sites and at sites having one base-flow discharge measurement. The equation for $Q_{7,10}$ had a standard error of estimate of 62 percent for sites having one base-flow measurement. Drainage area and base-flow index were the most significant parameters for this analysis.

Low-flow characteristics of streams in the Trempealeau-Black River basin

Low-flow characteristics were determined for 9 gaging stations, 20 low-flow partial-record stations, and 41 miscellaneous sites in the Trempealeau-Black River basin by B. K. Holmstrom. The low-flow characteristics determined were the annual minimum 7-day low flow at 2-year ($Q_{7,2}$) and 10-year ($Q_{7,10}$) recurrence intervals.

The average $Q_{7,2}$ is 3.5×10^{-3} (m³/s)/km² and $Q_{7,10}$ is 2.6×10^{-3} (m³/s)/km² for gaging stations and low-flow partial-record stations in the "driftless area" with drainage areas of less than 388 km². For stations in drift areas, average $Q_{7,2}$ is 3.3×10^{-3} (m³/s)/km², and $Q_{7,10}$ is 2.2×10^{-4} (m³/s)/km².

These compare with State averages of 2.2×10^{-3} (m^3/s)/ km^2 for $Q_{7,2}$ and 1.5×10^{-3} (m^3/s)/ km^2 for $Q_{7,10}$.

Multiple-regression equations were developed to determine low-flow characteristics for ungaged sites having one base-flow discharge measurement in the "driftless area" and drift areas in the Trempealeau-Black River basin. The equation for $Q_{7,10}$ for sites in the "driftless area" having one base-flow measurement had a standard error of estimate of 20 percent. Drainage area, precipitation and snowfall, and base-flow index were significant parameters for this analysis. The equation $Q_{7,10}$ for sites in drift areas having one base-flow measurement had a standard error of 85 percent. Drainage area and base-flow index were the significant parameters for this analysis.

SOUTHEASTERN REGION

Hydrologic studies of environment, energy, and the increasing demand for water by agriculture, industry, and municipalities continued to be emphasized in the southeastern region. To meet the requirements of current and projected needs, long-established programs for the collection of data were modified and strengthened.

Water-resource investigations associated with coal mining were started or continued in Alabama, Georgia, Kentucky, and Tennessee; studies were made of stream discharge, water quality, and sediment from basins in which surface mining is planned or underway. The USGS and the Kentucky Geological Survey are conducting a joint study on the feasibility of using abandoned water-filled underground coal mines in eastern Kentucky for public water supplies.

Studies of the hydrology and hydraulics of low-level nuclear-waste disposal sites in Kentucky, Tennessee, and South Carolina are continuing. In Kentucky, burial of low-level wastes was halted when there were indications of leakage of radioactive material from trenches. D. A. Webster (1977) completed a report on the history of radioactive-waste disposal at Oak Ridge National Laboratory in Tennessee. C. A. Spiers began a study of the hydrogeology of salt domes in the central Gulf Coast area as part of a larger investigation to determine the feasibility of using salt domes for storage of high-level nuclear wastes.

In Florida, several studies were focused on the effects of phosphate mining on water resources. A report on the hydrologic impact of potential mining in the Osceola National Forest (J. A. Miller, G. H. Hughes, R. W. Hull, John Vecchioli, and P. R. Seaber, 1978) was recently released. In central Florida, studies are underway to determine how water resources will be affected by decreased mining activity in Polk County and increased mining activity in Manatee County.

Ever greater demands for water for agriculture, industry, and municipal supplies are putting increased stress on the carbonate-rock aquifer (known as the Floridan aquifer in Florida) that underlies much of the Southeast and is the principal artesian aquifer in surrounding states. In Florida, studies to better define the hydrogeology of the aquifer are continuing; models are being designed for northeastern and west-central Florida, and studies of the quality of water in the system are underway. Outside of Florida, the principal demands on the aquifer were for industrial pumpage in the Brunswick and Savannah, Ga., areas. Increased pumping from the aquifer at Hilton Head, S.C., on the northern edge of the Savannah cone-of-depression, probably will affect the potentiometric head and the quality of water in the aquifer. Within the past 2 years, extensive development of the aquifer for irrigation has taken place on the Dougherty Plain in southwestern Georgia and southeastern Alabama.

Because of increasing demands for water in areas where the Floridan aquifer contains poor-quality or unusable water, or where the aquifer is in danger of saltwater encroachment, interest in overlying surficial aquifers has increased. The Biscayne aquifer, a surficial aquifer in the Miami-Dade County area, is being considered for designation as a "sole-source" aquifer. In central Florida, surficial aquifers are not only being studied as sources of water for various uses but also as important sources of recharge to the underlying Floridan aquifer. In northeastern Florida, surficial aquifers are being studied primarily as alternate or supplementary sources of water.

Flood-frequency studies were completed in Alabama, Georgia, and Tennessee, and were nearing completion in Florida, Puerto Rico, and South Carolina. In North Carolina and Alabama, regional studies of low-flow characteristics indicated that reliable methods can be developed for estimating low flow of ungaged streams.

INTERSTATE STUDIES

Results of long-term monitoring for saltwater in the Savannah area of Georgia and South Carolina

Saltwater encroachment in the principal artesian aquifer in the Savannah area of Georgia and South Carolina has shown only limited increases in the past 14 years, according to H. B. Counts. This conclusion was reached after examination of water-level and chloride data acquired over a 20-year period from seven monitoring wells. Between 1964 and 1977, water samples from two of the wells showed increases of about 40 mg/L in chloride concentration in the main water-bearing zone. Both of these wells are located about 40 km northeast of Savannah on Hilton Head Island, S.C., where resort and residential development has taken place. The increase in chloride in these two wells is probably due to local pumpage rather than to that from the major pumping center at Savannah.

ALABAMA

Statistical analyses of water quality

Regression and correlation analyses, with specific conductance and instantaneous discharge as the independent variables, were used to quantify relationship between 11 water-quality constituents at 31 surface-water sites throughout the State. Using data collected between 1970 and 1976, T. N. Russo found good correlation between specific conductance and dissolved solids, bicarbonate, hardness, calcium, and magnesium. These parameters can be estimated within 35 percent of the mean of the dependent variables.

The mean value of specific conductance for approximately 3,000 samples was 147 $\mu\text{mho}/\text{cm}$, and ranged between 10 and 1,200 $\mu\text{mho}/\text{cm}$. The lowest values occurred in the southwestern part of the State and the highest values occurred in industrial areas near Birmingham. In general, the distribution and areal variation of related physical and chemical parameters were the same as specific conductance. Greater variation in a given constituent was common at stations affected by waste-water discharge.

The relationships between discharge and specific conductance and sulfate were good at those stations where contamination of water resources is known to occur. Poor correlation of these parameters at the other stations is due primarily to the small range in concentration of the dependent variables.

Effects of surface coal mining on the hydrology of Warrior coal field

Celso Puente and J. G. Newton studied the effects of surface coal mining in the Warrior coal field on the hydrology of Crooked Creek and Turkey Creek basins of Jefferson County. Results indicated significant water-quality degradation, increased sediment yields, and increased low flow in most tributaries draining mined areas in the study basins. The augmenting of low flows in the mined tributaries during periods of little or no precipitation results from springs emanating from storage in spoil areas and water impoundments in mined areas.

The maximum values of specific conductance, sulfate, hardness, and dissolved-solids concentrations in samples collected during low-flow conditions from several mined tributaries were 2,430 μmho , 1,300 mg/L, 1,400 mg/L, and 1,060 mg/L, respectively; nearly neutral pH probably resulted from neutralization of acid waters by carbonate rocks.

Samples collected during low-flow conditions in tributaries draining unmined areas of the study basins had low specific conductance ($<100 \mu\text{mho}$), and very low dissolved solids concentrations ($<60 \text{ mg/L}$).

The estimated maximum mean annual suspended-sediment yield for a tributary draining a mined area was 5,110 t/km², whereas the estimated minimum mean annual suspended-sediment yield for a stream draining an unmined area was only 180 t/km².

The impact on water quality of inflow from tributaries draining mined areas to the main stem of Turkey Creek was insignificant because of large dilution ratios (1:30–1:300) while the impact of inflow on water quality from tributaries draining mined areas to the main stem of Crooked Creek was significant because of the lack of dilution.

Streamflow and water-quality data from the tributaries of less than 50 km² draining mined areas within and outside the study area were used to develop simple linear-regression equations for estimating on a regional basis specific conductance, sulfate, and dissolved solids, which served as excellent indicators of mine drainage. The standard error of estimate of the regression equations ranged from 11 percent to 14 percent.

Relation of geology to low flow in Alabama streams

By relating geology to low flow, R. H. Bingham developed a preliminary regression equation to estimate the 7-day 10-year low flow of Alabama's streams. The relation of geology to low flow is defined by the recession slope of the streamflow hydro-

graph. Using geology, contributing drainage area, and mean annual precipitation as independent variables, Bingham determined that the standard error of estimate of the regression equation is 38 percent. One equation applies statewide to all natural-flow streams; the equation does not apply to streams where flow is significantly altered by activities of man.

FLORIDA

Pumpage shutdown in industrial area yields significant information on recovery of water levels

A labor strike at paper pulp mills at Fernandina Beach, Fla., in September and October 1977 afforded a unique opportunity to observe the response of water levels in a deep and extensive cone of depression in the Floridan aquifer during a prolonged period when 10 of 13 large industrial wells were shut down. C. B. Bentley reported that artesian water levels rose about 1 m at a distance of 15 km from the center of pumpage, 9 to 10 m at a distance of 2½ km from the center of pumpage, and 38 m (from 42 m below sea level to 4 m below sea level) at the center. It was estimated that recovery at the center of pumpage would have been an additional 10 to 15 m if the remaining industrial and all municipal wells had not been in operation. Preliminary calculations of hydraulic characteristics of the upper part (Eocene Ocala Limestone) of the aquifer from water-level recovery curves indicated a transmissivity of between 2,500 and 6,000 m²/d and a storage coefficient of about 0.0006.

Top of Floridan aquifer mapped

A map prepared by G. W. Leve (1978) shows the altitude and configuration of the top of the Floridan aquifer in Jacksonville, Fla. The map shows two inferred concealed faults generally trending north-south through the area; the maximum vertical displacement of the top of the aquifer at these faults is about 50 m. Some saltwater intrusion into freshwater zones of the aquifer occurring in the vicinity of one of these faults may be caused by vertical movement of saline water through the fault from deeper zones in the Floridan aquifer.

Availability of water from a shallow limestone aquifer in the Jacksonville area

Test wells drilled at 13 sites in the Jacksonville area tapped a semiconfined to confined limestone aquifer at depths of 12 to 30 m below land surface.

L. V. Causey and G. G. Phelps reported that preliminary analyses of aquifer tests indicated that transmissivities of the limestone aquifer are about 50 to 70 m²/d. The limestone yielded between 163 and 545 m³/d to wells during pumping tests. The quality of water generally is acceptable for most domestic, commercial, and industrial uses, but locally the iron concentration exceeds 0.3 mg/L and the water is very hard.

Water from shallow aquifers in St. Johns County

A study to provide information on the availability of potable water from the shallow-aquifer system in St. Johns County, Fla., is being conducted by the USGS in cooperation with St. Johns County. According to E. C. Hayes, preliminary data from test wells drilled at three locations indicated that the aquifers and confining beds are discontinuous. Aquifers in test wells drilled to the top of the Miocene Hawthorn Formation (approximately 30 m) were located at depths ranging from 7 to 20 m, and yielded from 24.5 to 229 m³/d.

Availability of water in the Santa Fe River subbasin

Adequate supplies of water are available for most municipal and industrial uses in the Santa Fe River basin of northern Florida at the present time and for the foreseeable future, according to J. D. Hunn. The Floridan aquifer, the principal source of ground water, yields 0.06 to 0.3 m³/s to individual wells in the western part of the basin. Two additional sources of ground water, shallow aquifers that overlie the Floridan aquifer, supply many domestic supplies in the eastern part of the basin. Ninety percent of the time, the Santa Fe River discharges about 25.5 m³/s near Fort White and about 5.7 m³/s near High Springs.

Water quality and well yield of the Ochlockonee River basin

According to C. A. Pascale, water samples collected at selected depths from wells tapping the Floridan aquifer in the Ochlockonee River basin of northwestern Florida showed that dissolved-solids content did not increase measurably with sampling depth. The sampled wells ranged from 40 to 80 m in depth in the southern (coastal) part of the basin to more than 200 m in depth in the northern part of the basin.

Dissolved-solids content of the water generally was less than 500 mg/L in the southern part of the basin, and ranged from 150 to 200 mg/L in the central and northern parts of the basin. In the south-

ern part of the basin, one well, cased to 52 m and drilled open hole in limestone to 80 m, yielded water with dissolved-solids concentrations ranging from 900 mg/L at 56 m to 918 mg/L at 80 m; concentrations of the major constituents, calcium and sulfate, were 120 mg/L and 320 mg/L at 56 m and 80 m, respectively. A well in the northern part of the basin, cased to 132 m and drilled open hole in limestone to 208 m, yielded 27 L/s for 24 hours. Dissolved-solids content increased from 150 mg/L to 180 mg/L during the pumping period.

Specific capacities of the sampled wells were as great as $14 \text{ L s}^{-1} \text{ m}^{-1}$ near the gulf coast, but they declined inland in the central and northern parts of the basin. The largest specific capacity of the inland wells was $4 \text{ L s}^{-1} \text{ m}^{-1}$ in the northern part of the basin.

Leaky confined-aquifer conditions indicated in a sand-and-gravel aquifer at Pensacola

Henry Trapp, Jr., reported that the response of water levels in a pair of observation wells 18- and 54-m deep, indicated that the main producing zone of the sand-and-gravel aquifer acts as a leaky confined aquifer under prolonged stress. However, the possibility that the aquifer is vertically anisotropic and unconfined cannot be ruled out.

Hydrographs based on monthly measurements showed that from 1971 to 1977 levels in the 18-m-deep well in the upper part of the aquifer were generally 0.3 to 1 m higher than those in the 54-m-deep well open to the main producing zone. Beginning February 1, 1977, a new public-supply well 76 m from the paired observation wells was put into nearly continuous service, pumping about $8.8 \times 10^{-2} \text{ m}^3/\text{s}$. By April 11, the water level in the deeper observation well had fallen about 4.8 m, while the level in the shallow well had fallen only 0.4 m. By using a transmissivity of $7.7 \times 10^{-3} \text{ m}^2/\text{s}$ estimated from the specific capacity of the production well, it was determined that the theoretical drawdown in the deeper observation well would have been 9.9 m with no leakage and a storage coefficient of 5.5×10^{-4} (average of values derived by Jacob and Cooper, 1940), or 4.2 m under unconfined conditions and an assumed storage coefficient of 2.5×10^{-1} .

Effects of phosphate mining on the Floridan aquifer

W. E. Wilson III (1977) is investigating the effects that decreased phosphate mining in Polk County and increased phosphate mining in Manatee County would have on the Floridan aquifer. Preliminary results of the study indicated that by the year

2000, the maximum rise in water levels in Polk County would be about 9 m and the maximum decline in water levels in Manatee County would be about 4.4 m. Wilson's analyses are based on the application of a digital model of two-dimensional ground-water flow in west-central Florida.

Identification of a limestone aquifer in southern Hendry County

According to T. H. O'Donnell, a thick limestone in southern Hendry County represents a northern extension of a limestone locally known as the Ochopee Limestone (lower Pliocene and upper Miocene) which occurs throughout much of southwestern Florida. Water wells that penetrate this unit yield as much as $95 \text{ m}^3/\text{d}$. In southern Hendry County, water from this unit is used primarily for irrigation of sugar, citrus, and vegetable crops.

Water-bearing zone in the Hawthorn Formation identified in Lee County

T. H. O'Donnell reported that a test drilling program led to the identification of the principal water-bearing zone in the lower part of the Miocene Hawthorn Formation in Lee County. This zone forms the uppermost part of the Floridan aquifer in southwestern Florida. The chloride concentration in water from this zone ranged from 440 to 1,600 mg/L. The artesian pressure ranged from 15 m above mean sea level in the northeastern part of Lee County to 6 m above mean sea level in the southeastern part of Lee County.

Saltwater intrusion causes abandonment of municipal-supply wells

Salinity data gathered over a 4-year period by W. B. Scott and G. W. Hill showed that saltwater intrusion in a shallow aquifer was an immediate threat to wells that usually supply the Village of Tequesta in northern Palm Beach County. The well fields have been abandoned, at least for the present, and water is being imported by pipeline from another area.

Potential sources of pollution to the Biscayne aquifer

Results of a study of the Biscayne aquifer of southeastern Florida by Howard Klein and J. E. Hull suggested that potential sources of pollution to the nonartesian Biscayne aquifer are (1) urban runoff into the aquifer and into canals that are cut into the aquifer, (2) thousands of septic tanks scattered throughout southeastern Florida, (3) many

solid-waste disposal areas, (4) discharge of treated sewage effluent from scores of treatment plants into canals and soakage pits, and (5) runoff into canals and infiltration of runoff from interior agricultural areas.

Induced infiltration to new well fields

Supply wells for the proposed Three Squaremile well field west of Hialeah in Dade County, Fla., probably will be located along the west property boundary, 2 miles from Snapper Creek Canal, the nearest source of canal-water infiltration. According to Howard Klein and J. E. Hull, estimates based on predicted drawdowns indicated that if one well on the western boundary were pumping constantly at a rate of $1.89 \times 10^5 \text{ m}^3/\text{d}$, diversion of water from the Snapper Creek Canal toward the pumping well would begin about 10 days after pumping started.

Saltwater intrusion in well fields

According to W. A. J. Pitt, Jr., a chloride-monitoring network of wells in the shallow aquifer in Hollywood, Fla., has shown a continuing advance of saltwater each year during the dry season. A primary area of intrusion is developing in the northeastern part of the city's well field, where a finger canal used to remove floodwater is not controlled with a salinity barrier, and seawater moves inland from the coast and enters the aquifer through the canal.

Chloride levels in monitor wells in Hallandale, Fla., continue to increase each year during the dry season as a result of lowering water levels partially caused by increased pumpage. Salt-front movement is primarily in the northeastern part of the city's well field, but another threat is developing in the southeast.

Contamination of a shallow aquifer by irrigation

According to W. L. Miller, extensive use of highly mineralized irrigation water from the Floridan aquifer in agricultural areas of St. Lucie and Martin Counties is affecting water quality in the shallow aquifer. During periods of low rainfall and reduced infiltration to the aquifer, chloride concentrations rapidly increase in the upper part of the shallow aquifer in the vicinity of irrigated lands; increases of as much as 700 mg/L were observed in water from some wells. Many municipal and private wells draw water from the upper part of the aquifer. Geologic data were collected at 55 sites as part of an investigation to determine the thickness and extent of producing zones in the shallow aquifer.

GEORGIA

Variations in low-flow characteristics

Analyses of low-flow characteristics of streams in Georgia by R. F. Carter and S. A. Putnam have demonstrated that although there are variations in flow per unit of drainage area, the flows do not relate to the physiographic provinces throughout the State. Low flows for 7 consecutive days with a 10-year recurrence interval vary from 0 to more than $10.9 \text{ L s}^{-1} \text{ km}^{-2}$. In the Blue Ridge province in the northern part of the State, unit low flows range from 3 to $9 \text{ L s}^{-1} \text{ km}^{-2}$.

There is a contrast in unit rates of low flow between the upper part of the Coastal Plain where most low flows are large, and the lower part where most low flows are small. Flows in the upper Coastal Plain are in the range of 1 to $11 \text{ L s}^{-1} \text{ km}^{-2}$, but in the lower Coastal Plain they range from 0 to $0.3 \text{ L s}^{-1} \text{ km}^{-2}$; only the largest streams, those that head in the Piedmont, have appreciable flow during low-flow periods.

In a companion study, R. F. Carter's preliminary analysis indicated that storage requirements for streams in Georgia can be expressed as a family of regional curves showing storage required to maintain various rates of flow if low-flow index values for individual streams are known.

The regional analyses indicated that the State must be divided into subregions, approximately conforming to physiographic boundaries, in order to achieve a good definition of the storage-requirement values.

Determination of depth to saltwater in the Albany area

Results of a study of the ground-water resources of the Albany, Ga., area by R. E. Krause (USGS) and R. S. Lynch (Georgia Department of Natural Resources) indicated the presence of poor-quality water directly underlying aquifers of middle Eocene to latest Cretaceous age used for the area's water supply. A test well completed in Upper Cretaceous (lower Maestrichtian) sedimentary rocks yielded a sodium bicarbonate type water with dissolved solids and chloride concentrations of 1,610 and 410 mg/L, respectively.

Water from this aquifer could pose a threat to the ground-water resources of the area as the head is about 45 m higher than that in aquifers used for a water supply. At present, there is no indication of contamination of the overlying aquifers. Confining beds between the aquifers are high in clay content and appear to be essentially impermeable.

Dewatering operation indicates yield potential of crystalline rocks

Dewatering operations at the site of a "people mover" tunnel being constructed at Atlanta's Hartsfield International Airport is providing information about the relationship between topography, geology, and well yields in the Piedmont, according to C. W. Cressler. The tunnel site, which extends in an east-west direction for nearly 1.6 km, is being dewatered along the north and south sides by 103 wells drilled at intervals of 30 m. The wells are 34 m deep, gravel packed to bedrock, and have slotted casing to total depth. Observation wells 18 m or more deep are spaced every 61 m along both sides of the tunnel to permit monitoring of water levels.

As expected, the largest yields (1 to 5 L/s) were obtained from wells in or a few meters down-dip from the channels of intermittent streams and from wells penetrating the contact zones between rocks of contrasting character, such as hornblende gneiss, mica schist, and granite. Wells in interstream areas underlain by homogeneous rocks generally supplied only 0.06 to 0.6 L/s.

Information obtained thus far confirms earlier studies that showed that (1) topography is the best single indicator of the yield potential of well sites in the Piedmont and (2) by using topography in conjunction with the attitude, lithology, and physical properties of the underlying rocks, it usually is possible to select high-yields well sites in crystalline rocks.

MISSISSIPPI

"Tuscaloosa aquifer system" in Mississippi

E. H. Boswell reported that in a study of the major aquifers in Mississippi, he has applied the term, "Tuscaloosa aquifer system," to the water-bearing sand and gravel beds in the Upper Cretaceous Tuscaloosa Group and to those underlying hydraulically connected beds of Early Cretaceous age that contain freshwater. The thickness of the aquifer system ranges from a few meters to more than 600 m in northern Mississippi. The base of the aquifer system is at the top of the Paleozoic rocks in the north and within beds of the Lower Cretaceous in the south part of the area of occurrence.

In the northern part of the area, the Tuscaloosa forms one principal aquifer, but in the southern part the system comprises two major aquifers: (1) the lower sand-and-gravel unit of the Gordo Formation (the Gordo aquifer), and (2) the basal sand of the

Coker Formation and hydraulically connected sand beds of the underlying Lower Cretaceous Series (the Coker aquifer). Minor aquifers occur in irregular sand beds in the upper parts of both the Gordo and the Coker Formations.

NORTH CAROLINA

Water sources and geology along the Blue Ridge Parkway

"Good" and "fair" areas for wells and inferred fracture zones, based upon an assessment of topography and saprolite thickness, were depicted on topographic maps of the Blue Ridge Parkway in North Carolina. The purpose of the investigation was to describe sources of ground water for existing and future recreation facilities along the parkway so that the National Park Service can plan for its best use. According to M. D. Winner, Jr. (1978), the best areas to develop ground water are in broad draws and in stream valleys where draws open to the valleys. Saprolite thickness in some places exceeds 15 m and provides adequate ground-water storage, and yields from some wells along the parkway exceed 1.6 L/s.

SOUTH CAROLINA

Saltwater encroachment in the principal artesian aquifer for Beaufort, Colleton, Hampton, and Jasper Counties

According to L. R. Hayes, the principal artesian limestone aquifer that is the main source of ground water for Beaufort, Colleton, Hampton, and Jasper Counties in South Carolina becomes increasingly salty with depth so that only the top 30 to 50 m, the upper permeability zone, is used for industrial, municipal, and domestic needs for the area. Saltwater encroachment of the upper permeability zone of the aquifer has already occurred on many of the sea islands and parts of the mainland, thus making the water unusable. In order to establish the freshwater-saltwater boundary and to monitor the saltwater movement, wells were tested and sampled. Application of both the Ghyben-Herzberg principle and its modified version were used on data obtained from two wells 3 m apart, with a difference of 53 m of open-hole section.

From test results, L. R. Hayes concluded that: (1) the depth to a freshwater-saltwater boundary depends on the heads and densities of both the freshwater and saltwater; (2) large errors can result from calculations based on freshwater data

alone; (3) depth to a freshwater-saltwater boundary calculated from the equation is only an approximation, mainly because conditions at the boundary fail to fully satisfy all of the assumptions of the equation; and (4) the only way to accurately determine the depth of a freshwater-saltwater boundary is through a series of samples for geochemical analysis taken at different depths at the same test site.

Geochemical analysis revealed saltwater contamination even when the chloride concentration had increased by only a few milligrams per liter. It also was used to compare water from different zones within the same aquifer, to show progressive changes in chemical quality of water as it moved away from recharge areas, and to analyze water from different aquifers.

TENNESSEE

Ground-water exploration in carbonate rocks

Forty-four test wells were drilled at 24 sites in the crystalline carbonate rocks of central Tennessee in order to test concepts of ground-water occurrence and movement near the southern edge of the central basin. The wells were drilled in two groups; among the first group of 16 wells, one-third of the wells produced between 0.9 and 10 L/s, and the rest were dry. Only one-fourth of the sites were productive. The site-selection criteria used for the most productive wells were then used to locate the second group of 28 wells at 5 sites. Among the second group, two-thirds of the wells produced between 0.9 and 10 L/s and the rest were dry. More than one well was drilled at each site, and all 5 sites were productive.

Drilling revealed that the potential aquifers, or those rocks that are more soluble and therefore have a greater potential than most for being permeable, comprise only one-fifth of the section and each is less than 15 m thick. Water quality indicated that as little as 5 m of nonaquifer material overlying a potential aquifer drastically reduces circulation.

E. F. Hollyday and P. A. Zurawski concluded that 96 percent of the zones yielding more than 1.2 L/s are at depths of less than 27 m and 50 percent are at depths of less than 12 m because of the combination of stratigraphic features and the fact that the rocks are relatively flat-lying. Zones yielding less than 1.2 L/s were encountered at depths as great as 84 m. Solutioning appeared to be enhanced where the rocks dip more steeply than normal (1° - 3°).

The most significant well-location criteria included: (1) a potential aquifer at or near the land

surface, (2) dry reaches of stream upflow from large streambank springs, and (3) folds, faults, or fractures that enhance underground flow and storage.

CENTRAL REGION

In 1977, hydrologic activities in the central region again strongly emphasized studies related to the environment and to energy development. Long-established programs for the collection and publication of diverse water-resource data continued. Intensive hydrologic investigations related to coal development continued in North Dakota, Montana, Wyoming, Utah, Colorado, and New Mexico, and were begun in coal areas of east-central Oklahoma; also, studies related to oil shale in Colorado, Utah, and Wyoming continued. Hydrologic studies of small basins that are representative of potential surface coal-mining areas were again emphasized. Results of these studies are expected to be applied to leasing decisions, environmental-impact statements, mining procedures, and specifications for reclamation of mining areas.

Numerous water-quality studies are underway throughout the central region. USGS scientists, in cooperation with personnel of other agencies and with Canadian scientists, are studying the water quality of the Poplar River of Montana and Saskatchewan, Canada, in relation to a coal-fired power-plant near Coronach, Saskatchewan. Intensive baseline water-quality studies are being made in coal areas, especially in Colorado, Montana, New Mexico, North Dakota, Utah, and Wyoming. The energy-related water-quality investigations include studies of sediment, bed material, water chemistry, and aquatic biota in selected streams. Lake and reservoir studies concerned with algal production and identification and with salt leaching are underway in several reservoirs on the North Platte River of Wyoming and in several North Dakota prairie lakes.

Widely varied surface-water activities again were an important part of the regional program. Because of increased activities in energy-related projects, gaging-station networks continued to expand in Colorado, Montana, New Mexico, North Dakota, Utah, and Wyoming. Monitoring efforts were dominant in most areas, but some systems modeling was begun. Digital-model analyses will be used for coal and oil-shale areas where surface-water supplies are inadequate, to evaluate availability and indicate maximum utility of future water resources of the mining areas.

The mapping of flood-prone areas continued in a few districts, but at a generally reduced level of activity. Several districts continued to make HUD type-15 insurance studies, but this effort also is decreasing. Flood-frequency studies continued in Colorado, Louisiana, and Missouri, and studies were completed in Texas. Reports on hydraulic conditions at bridge sites were prepared in Arkansas, Kansas, Louisiana, and Montana.

Studies of regional aquifer systems were initiated in the northern Great Plains of Montana, Wyoming, North Dakota, and South Dakota and in the High Plains of Texas, New Mexico, Colorado, Oklahoma, Kansas, Wyoming, Nebraska, and South Dakota. The intensive studies include: (1) the assessment of the aquifer-system boundaries and characteristics and (2) the determination of the storage capacity and natural discharge and withdrawals, sources and amounts of recharge, anticipated yields, and effects of pumping on supplies. The studies also will be used to determine the extent of past ground-water mining and the estimated economic life of an aquifer under various assumptions as to rates of withdrawal and susceptibility of the aquifer to operation and management on a "sustained-yield" basis.

Studies of artificial recharge to aquifers by spreading ponds continued near Lubbock, Tex., and in El Paso County, Colorado. An investigation of the feasibility of artificial recharge to an alluvial aquifer by means of naturally filtered river water in an injection well continued in south-central Nebraska.

Hydrologic research in the central region included many activities related to energy development, such as investigations of the hydrochemistry of surface and ground water in oil-shale and coal-bearing terrane, the development of modeling techniques for the prediction of solute transport in ground water, and modified runoff and sediment transport from areas undergoing surface mining in several hydrologic regimes. The development of techniques for estimating numerical values for parameters and boundary-condition values for ground-water systems continued. Also included was research in sediment transport, channel-geometry changes, and fluvial processes in coal areas.

An investigation of special significance to coal development is an evaluation of the water-yielding potential of the Mississippian Madison Limestone—an important, deeply buried aquifer underlying large areas in the Powder River basin in Wyoming, Montana, North Dakota, and South Dakota. A preliminary numerical model of the aquifer system con-

tinued to be used for planning further studies and for designing a data-collection program. The location of the third deep exploratory well to be drilled through the Madison Limestone was selected; drilling and hydraulic testing of the first two test wells was completed.

Field investigations of the hydrology of geothermal systems are continuing in Colorado and Montana. Also, development and testing of instruments, tools, and interpretative techniques for use in the extreme heat of geothermal systems is continuing.

In Nevada, water-resource investigations continued at the Nevada Test Site, where intensive investigations of the feasibility of high-level radioactive-waste disposal were initiated. Also, studies of the Paradox Basin in Utah and Colorado were begun to determine the hydrologic conditions that might affect the use of deeply buried evaporites for waste disposal.

MULTISTATE STUDIES

Solute-transport model for ground water

The versatility of a two-dimensional solute-transport model, based on the method of characteristics, was previously demonstrated by its applications to field problems that represent a variety of hydrogeologic settings. Recent modifications by L. F. Konikow to the computer code have improved its accuracy, precision, efficiency, and applicability. The revised program uses a particle-tracking procedure to represent convective transport and a two-step explicit procedure to solve a finite-difference equation that describes the effects of hydrodynamic dispersion, fluid sources and sinks, and divergence of velocity. This explicit procedure has several stability criteria, but consequent time-step limitations, which usually are not severe, are automatically determined by the program. An analysis of several test problems indicated that the error in the mass balance will be generally less than 10 percent. Accuracy and precision of the numerical solution is sensitive to the initial number of particles placed in each cell and to the size of the time increment. Mass-balance errors are commonly the greatest during the first several time increments, but those errors tend to decrease and stabilize with time. In the case of one-dimensional flow, agreement with analytical solutions is nearly exact, but in that of plane radial flow, a small amount of numerical dispersion occurs.

INTERSTATE STUDIES

Hydrogeologic considerations for an interstate ground-water compact on Madison aquifer, northern Great Plains

The development of an interstate ground-water compact for the Madison aquifer in the northern Great Plains may provide a framework to allocate equitably this large ground-water resource while avoiding possible future interstate legal conflicts. However, L. F. Konikow (1978) noted that some technical problems will have to be resolved to allow the development of an interstate ground-water compact that is hydrologically sound, logical, and equitable. A compact designed to regulate or to allocate the available ground water will have to be written in very precise, legally acceptable definitions. The required definitions may infer a degree of accuracy of measurement that cannot be technically or economically provided. A compromise may be required between those who wish to preserve natural conditions and those who prefer that beneficial use of the ground-water resource be allowed.

Shallow ground-water flow systems in the northern Powder River basin

Field data from more than 2,000 wells in the northern Powder River basin supported the initial concept of two distinct ground-water flow systems described by geochemical models of previous years for small areas—an upper system comprising water with the primary chemical constituents Na^+ and SO_4^- and a lower system with the primary constituents Na^+ and HCO_3^- . Expansion by R. W. Lee of the mapping to larger areas indicated that the concept is applicable to the entire northern Powder River basin.

Potentiometric data further substantiate the concept. Potentiometric maps prepared by S. E. Slagle depict localized movement of ground water, which generally reflects the topography in the shallow system and regional flow in the deeper systems that discharge to the major drainages.

Analyses of water samples collected during base-flow investigations on the major streams showed the major chemical constituents to be Na^+ and SO_4^- , and indicated that the major portion of the ground-water contribution to the streams is from the shallow system.

B. D. Lewis and W. R. Hotchkiss reported that analyses of data obtained from selected geophysical logs used to define the geologic framework for the occurrence of ground water above the Cretaceous

Pierre Shale in the Powder River basin in Montana and Wyoming have produced the following statistics for Tertiary and Cretaceous units currently being used for the development of a five-layer digital model:

	Max	Min	Mean
Tongue River Member Fort Union Formation and Wasatch Formation			
Thickness (meters) -----	1208	35	435
Sandstone thickness (meters) -----	686	26	230
Sandstone percentage -----	91.3	16	53.6
Lebo Member Fort Union Formation			
Thickness (meters) -----	924	37	212
Sandstone thickness (meters) -----	235	3	64
Sandstone percentage -----	93.2	6.3	32.2
Tullock Member Fort Union Formation			
Thickness (meters) -----	593	55	231
Sandstone thickness (meters) -----	375	18	113
Sandstone percentage -----	96.6	21.1	52.6
Hell Creek confining unit (Approx. upper 2/3 of Hell Creek Formation)			
Thickness (meters) -----	369	30	150
Sandstone thickness (meters) -----	128	12	49
Sandstone percentage -----	87.6	9.4	34.7
Fox Hills-Hell Creek aquifer (Fox Hills Sandstone and approx. lower 1/3 of Hell Creek Formation)			
Thickness (meters) -----	637	87	227
Sandstone thickness (meters) -----	335	34	114
Sandstone percentage -----	93.8	24.7	50.9

Only the data from geophysical logs are included, and these data, do not account for thinning of the units in outcrop areas.

Tests of the above units indicated hydraulic conductivities ranging from about 3×10^{-5} to about 6 m/d for coal and from about 0.5 to 3 m/d for sandstone.

Rehabilitation potential of coal lands in the central region evaluated

The potential for rehabilitation of surface-mined coal lands was determined for areas in North Dakota, Montana, Wyoming, and New Mexico by L. M. Shown, F. A. Branson, R. F. Miller, I. S. McQueen, and R. F. Hadley. Data were collected on soil moisture, vegetation, soil erodibility, and sediment yield in six study areas that are representative of western coal fields where surface mining is proposed and where other land-use and land-management problems may exist.

Rehabilitation potential is dependent on several factors including climate, soils, and topography. In the six study areas, the rehabilitation potential covers a wide range. In Dunn County, North Dakota, the usually favorable spring precipitation, deep and fertile soils, and low topographic relief combine to produce highly favorable rehabilitation conditions. At the other extreme, in south-central San Juan County, New Mexico, a climate characterized by low annual precipitation, intense thunderstorms and prolonged winds, and fine-textured, relatively impermeable soils presents an unfavorable combination of factors for rehabilitation. Other areas in Montana

and Wyoming have characteristics that lie between these extremes.

Quality of water in abandoned zinc mines in northeastern Oklahoma and southeastern Kansas

Correlation analyses of water in abandoned, interconnected zinc mines in northeastern Oklahoma and southeastern Kansas showed that several chemical constituents, including dissolved solids, total hardness, and dissolved sulfate, calcium, magnesium, and lithium, are linearly related to specific conductance. None of the constituents of mine-shaft water tested are significantly linearly related to pH. However, values of dissolved aluminum, zinc, and nickel transformed to natural or Napierian logarithms, are linearly related to pH.

S. J. Playton and R. E. Davis reported that from September 1975 to June 1977, the water level in the interconnected mine workings rose at an average rate of 0.37 m/mo. Generally, the water-level rise was greater than average following periods of relatively high rainfall, and it was less than average during periods of relatively low rainfall.

Digital-computer model simulates ground-water flow in the lower Mesilla Valley of Texas and New Mexico

J. S. Gates, E. R. Leggat, and D. E. White constructed a three-dimensional, digital ground-water model of the lower Mesilla Valley area of Texas and New Mexico, just northwest of the city of El Paso, Tex. The model indicated that increasing the 1968-75 average withdrawals of ground water from the intermediate and deep zones in El Paso's Canutillo well field in the Mesilla Valley from 16.6 million to 37 million m³/yr would almost double the depth to water in observation wells. The model predicted an increase from 5.6 to 11.0 m in depth to water in an observation well in the intermediate zone and increases from 9.33 to 20.6 m and from 16.7 to 34.6 m in depth to water in two observation wells in the deep zone. Most of the simulated declines would occur within a few months. At the end of a simulated 5-year period of pumping at the increased rate, the water levels would be essentially stable because of leakage from a shallow zone.

ARKANSAS

Water-resource literature for Arkansas annotated

R. T. Sniegocki (1976) compiled and annotated a bibliography of more than 300 USGS reports on Arkansas water resources and related subjects. The

reports, prepared between the late 1800's and 1975, were in many forms, including memorandums, hydrologic atlases, water-supply papers, professional papers, annual reports, bulletins, brochures, geologic atlases, open-file reports, and basic-data tabulations.

COLORADO

Benthic invertebrates in Piceance Creek, northwestern Colorado

Preliminary results of studies made from October 1976 to September 1977 by K. J. Covay and T. R. Ford indicated that benthic invertebrates are well established in Piceance Creek in Colorado and that colonization is enhanced by the stable substrate in the stream channel. The upstream reach of Piceance Creek supports communities composed of a large number of species. The downstream reach supports only a few species probably because of the increased concentrations of dissolved solids and alkalinity in the downstream reach of the creek.

Two tributaries to Piceance Creek are quite different in that one has a channel with a fairly unstable substrate and the other has a channel where silt and mud accumulate. The benthic communities in these tributaries have a smaller number of species than are found in the upper reaches of Piceance Creek.

Availability and quality of ground water in the Gunnison-Crested Butte area

Hydrologic data are being collected to identify the availability and chemical quality of ground water in the Gunnison-Crested Butte area of Colorado. Because of an increase in winter-sports activities in recent years, parts of the area have undergone rapid population growth that has resulted in an increased demand for additional domestic, industrial, and municipal water supplies. T. F. Giles reported that ground-water supplies of as much as 6 L/s are available from wells in the alluvial aquifers and as much as 4 L/s are available from wells in the Cretaceous Dakota Sandstone and the Jurassic Entrada Formation. Ground-water supplies from other aquifers are generally less than 1.6 L/s. Calcium magnesium bicarbonate water is the predominant water type in the study area. Water quality is generally suitable for all uses; dissolved-solids concentrations range from 30 to 829 mg/L and average 203 mg/L throughout the study area, and values for water hardness range from 20 to 400 mg/L.

Water quality in Boulder County

D. C. Hall, E. L. Boyd, and D. L. Cain studied the water resources of Boulder County to determine the quality of surface and ground water. Precambrian crystalline rocks occur in the mountains in the western half of the county, and Paleozoic through Holocene sedimentary rocks underlie the plains in the eastern half of the county. Quality of the surface water is best in the mountains and declines rapidly after the rivers leave the canyon mouths. The fecal-coliform bacterial concentration in Boulder Creek is less than 1 colony/100 mL of water at a site in the mountains, and 37,700 colonies/100 mL of water at a site on the plains. The specific conductance of St. Vrain Creek is 21 $\mu\text{mho/cm}$ at a site high in the mountains and 1,780 $\mu\text{mho/cm}$ at a site on the plains. The specific conductance is higher in the winter when the streamflow is minimal. At 33 streamflow sites sampled, the State's recommended maximum concentrations of pollutants in surface water were exceeded for aquatic life at 18 sites, for raw municipal drinking water at 13 sites, and for agricultural use at 7 sites.

Maps were made to show concentrations of specific conductance, chloride, and nitrite plus nitrate in ground water. Ground-water quality in the alluvial aquifers was closely associated with the quality of the surface water. This was indicated by parallel increases in specific conductances with distance from west to east across the county. Specific conductance in ground water from the unconsolidated aquifers increased with lateral distance away from the streams. Specific conductance in water from bedrock aquifers increased from west to east across the county; it reached the highest values in the northeastern corner of the county. In contrast to specific conductance in ground water, chloride and nitrite plus nitrate are distributed in localized areas of high concentrations surrounded by areas of low concentrations. This may indicate degradation of ground water by man's activities.

Countywide, coliform bacteria occurred in water from 168 of 643 wells (26 percent). Coliform bacteria occurred in water from 99 of 292 wells (33 percent) completed in the unconsolidated aquifer, in water from 15 of 41 wells (16 percent) completed in the Laramie-Fox Hills aquifer, and in 33 of 171 wells (19 percent) completed in the crystalline-rock aquifer. Countywide, fecal-coliform bacteria occurred in water from 51 of 643 wells (8 percent). Fecal-coliform bacteria occurred in water from 33 of 292 wells (11 percent) completed in the uncon-

solidated aquifers, in water from 1 of 91 wells (1 percent) completed in the Laramie-Fox Hills aquifer, and in water from 9 of 171 wells (5 percent) completed in the crystalline-rock aquifer. Counts of coliform and fecal-coliform bacteria in water from the Pierre Shale aquifer were about the averages of those in other counties.

Water-table aquifers in the Boulder-Fort Collins-Greeley area of the Front Range Urban Corridor

The principal water-table aquifers occur in the alluvium and terrace deposits in and adjacent to the valleys of the South Platte River and its major tributaries. D. E. Hillier found that depth to the water table in the sedimentary deposits underlying the eastern three-fourths of the study area ranged from 0 to about 15 m during 1976-77. Depth to water in the river valleys generally was less than 3 m. Long-term records of water level showed that there are no areas of major water-level decline; the maximum decline since the late 1950's has been about 1½ m. Water of suitable quality for drinking is found in terrace deposits near Fort Collins and Loveland, in the alluvium of Boulder, Left Hand, and St. Vrain Creeks just east of the mountain front, and in the mountainous western part of the area. Elsewhere, the dissolved-solids concentrations exceed 500 mg/L and generally exceed 1,000 mg/L. Arsenic, chloride, fluoride, iron, magnesium, manganese, nitrite plus nitrate as nitrogen, selenium, and sulfate locally occur in water in concentrations that exceed maximums recommended by the State for drinking water.

Water-management plans for the South Platte River valley

The USGS developed a digital-computer model for the South Platte River valley, in northeastern Colorado, that simulates the interrelationships between the various components of the hydrologic system to provide planners and managers with a means of testing alternative management plans. The model was calibrated by using monthly data collected from January 1967 to December 1971. Two examples of alternative water management, one a predominantly surface-water plan and the other a predominantly ground-water plan, were prepared to show how the model might be used. According to R. T. Hurr and A. W. Burns, these examples represent the extremes in operational management of the present diversion and withdrawal system.

Total diversions, the sum of surface-water diversions for direct application, surface-water diversions for storage, and ground-water withdrawals are

about the same for both plans. Application, however, is about 20 to 25 percent less for the predominantly surface-water plan because of the large volume of canal flow sluiced back to the river as indicated by the model calibration. Surface-water outflow—the streamflow at Julesburg, Colo.—is about the same for both plans. The change in ground-water storage under the predominantly surface-water plan was an increase of approximately $9.25 \times 10^8 \text{ m}^3$ from 1951 to 1974, whereas the change under the predominantly ground-water plan was a decrease of approximately $1.85 \times 10^9 \text{ m}^3$. These changes were based on an original volume in storage of approximately $10.6 \times 10^9 \text{ m}^3$.

On an annual basis, the predominantly ground-water plan more efficiently reduces potential crop evapotranspiration than the predominantly surface-water plan. This is due principally to the larger total volume of application, but it is partly due to better timing of application by the ground-water plan.

Effects of proposed "Narrows" reservoir on South Platte River

Preliminary data from gain-loss studies conducted by D. R. Minges indicated that a 42-km reach of the South Platte River, encompassing the site of the proposed "Narrows" reservoir near Fort Morgan, Colo., gains an average of $3.0 \text{ m}^3/\text{s}$. Gains for six of seven subreaches examined were found to be closely related to saturated thickness of the valley-fill aquifer. Averages for seven gain-loss studies indicated a gain of $0.14 \text{ m}^3 \text{ s}^{-1} \text{ km}^{-1}$ for the upstream 6.6-km subreach, where the saturated thickness of the aquifer is generally 36 m or more, and no gain for the downstream 7.2-km subreach where the aquifer generally has a saturated thickness of 3 m or less. Gains in all but one of the remaining subreaches showed a similar relationship to saturated thickness. The exception is the subreach encompassing the "Narrows," a pronounced constriction of the river valley. Data from prior studies indicated that a steepening of the water-table gradient toward the river through this subreach, resulted in a higher gain than might be predicted from saturated thickness alone.

The gain-loss studies are being conducted as part of a program to determine existing streamflow, water-quality, and sediment-load characteristics of the river so that the effects of the reservoir can be determined both during and following construction. Downstream irrigators, in particular, are interested in reservoir effects on return flow, which comprises a large part of their irrigation supply. In addition,

gain-loss data will be used in conjunction with reservoir-modeling studies.

Piceance Basin model

S. G. Robson and G. J. Saulnier, Jr., reported that a three-dimensional ground-water flow and dissolved-solids solute transport model of Piceance Basin was constructed and successfully calibrated against the steady-state ground-water flow conditions that presently exist in the basin. The model was used to simulate the long-term effects of ground-water pumpage from two hypothetical mines located at Federal-lease tracts C-a and C-b in Piceance Basin.

Reconditioning of geohydrologic test holes in an oil-shale formation

The observation-well network in the Piceance Basin contains a number of wells that provide only a composite water level of the upper and lower aquifers because the wells were left open to both aquifers, according to F. A. Welder. To prevent the exchange of water between the aquifers and to provide better water-level information, eight wells were reconditioned. Inflatable packers were set in six wells, and cement plugs were placed above the packers to isolate the lower aquifer from the upper aquifer. Two bridged wells were cleaned out. The wells are now being monitored to determine the effectiveness of reconditioning. The reconditioned wells will serve as additional observation sites to monitor the effects of proposed oilshale development on the aquifer system.

Water quality of springs and productivity of wells in the Piceance Basin

Springs in the Piceance Basin were sampled for major and trace constituents during the spring and the fall. According to G. J. Saulnier, Jr., results of the analyses of water from these springs indicated that the quality of water from each spring is consistent throughout the year. On an areal basis, discharge from the springs has a net increase in dissolved solids from recharge to discharge areas. The water type changes from a mixed-cation bicarbonate water in the recharge area to a sodium bicarbonate water in the discharge area. The dominance of sodium over the other major cations is due to (1) inputs of sodium bicarbonate water from deeper aquifers in the basin, (2) ion-exchange reactions that exchange calcium for sodium, and (3) precipitation of calcium carbonate.

Strontium concentrations increase an order of magnitude within 16 km of the recharge area, thereby indicating a source of soluble strontium in the aquifer. The milliequivalent and weight ratios Mg^{2+}/Ca^{2+} increase from recharge to discharge areas caused by calcite deposition and dissolution of dolomite from marlstones.

The magnitudes of spring discharge and well yields appear to be related to the basin's fracture system. The probability of completing a well that produces large quantities of water is increased by locating the well near a spring that produces from a fracture zone.

Water-level fluctuations and residential waste-treatment systems

D. C. Hall reported that annual fluctuations of water levels in 11 observation wells in the fractured crystalline-rock aquifer in Jefferson County, Colorado, ranged from less than 1 to 4.5 m. The lowest water levels generally occurred in February and the highest occurred sometime during the warmer months. There was no apparent relationship between amount or seasonal distribution of precipitation and fluctuations in water levels.

Aeration and septic residential waste-treatment-system efficiencies were studied. Samples from the treatment tanks and from the soil-absorption systems were analyzed and compared. If concentration of a particular constituent in one system was more than 50 percent greater than in the other, the concentration was considered to be significantly higher. The aeration system was significantly higher in oxidized products of treatment such as nitrite, nitrate, sulfate, and phosphate. The septic system was significantly higher for bacteria, dissolved solids, detergents, and BOD. For example, the average concentrations for nitrate-nitrogen were: aeration-treatment tank, 3.39 mg/L; septic-treatment tank, 0.04 mg/L; aeration-system soil-absorption field, 90.2 mg/L; and septic-system soil-absorption field, 7.9 mg/L. Average concentrations of BOD (5-day, 20° C) were: aeration-treatment tank, 344 mg/L; septic-treatment tank, 609 mg/L; aeration-system soil-absorption field, 19.5 mg/L; and septic-system soil-absorption field, 32.0 mg/L.

Two-dimensional finite-difference model developed for the closed-basin area of San Luis Valley

C. J. Londquist converted an existing digital-computer model of the closed-basin area of the San Luis Valley to a finite-difference model for simulation of two-dimensional ground-water flow. Several preliminary model simulations made to test a proposed

water-salvage plan indicated that about 100 hm³ of water can be pumped annually from the unconfined aquifer and that, after 50 years of pumping, the projected drawdown will be less than 0.6 m at the project boundaries.

Results of an aquifer test conducted in the area indicated that the transmissivity is 325 m²/d, and the storage coefficient is about 0.0002 in a zone about 15 to 50 m below land surface.

IOWA

Iowa sediment-data compiled

All fluvial-sediment data for Iowa, which had been published by the USGS and other Federal agencies, were compiled into one volume by J. R. Schuetz and W. J. Matthes, Jr. (1977). Their report includes data through September 30, 1973, on daily extremes and monthly summaries of sediment concentrations and loads, particle-size analyses of suspended sediment and of bed materials, and summaries of reservoir-sedimentation studies on streams.

Drought effect and recovery noted in Iowa carbonate aquifers

In eastern Iowa, water levels generally fluctuate on a seasonal basis with declines occurring from June through February and with recovery occurring in March, April, and May. Normal seasonal water-level fluctuations in the Silurian aquifers are about 1.5 m; however during a 3-year period of below-normal precipitation (July 1974–July 1977), seasonal recoveries were drastically reduced, and declines continued or even accelerated. As a result, a general decline of 4 to 5 m occurred throughout the aquifer.

From late July through October 1977, greater-than-normal rainfall occurred, and even though water levels would normally have been in a seasonal decline, recovery began in updip areas immediately, and by November it amounted to about 4.5 m. In downdip areas, water-level recovery was delayed in time and by November amounted to about 1.5 m. If a normal seasonal water-level recovery of 1.5 m occurs in the spring of 1978, the aquifers will have recovered from a 3-year drought in less than 1 year.

KANSAS

Ground-water mining in west-central Kansas

M. E. Pabst and E. D. Gutentag reported that from 1950 to 1977 ground-water withdrawals for irrigation in west-central Kansas increased from

about 49 to 690 hm³/yr, and the number of large-capacity wells increased from 250 to 2,850 during the same period. Measurements in about 290 observation wells in the Ogallala Formation showed that, during the same period, the water level in wells declined as much as 21 m in areas of greatest development and the saturated thickness of the aquifer in those areas declined as much as 79 percent. The mean water-level decline was 8 m, and the mean percentage decline in saturated thickness was 30 percent.

Geohydrology of saline water occurrence in the Wellington Formation in central Kansas

The potentiometric surface of saline water in a linear, northerly trending solution-collapse zone along the eastern margin of the Hutchinson Salt Member of the Permian Wellington Formation was determined from water-level measurements. According to A. J. Gogel, the measurements indicated that hydraulic continuity exists along the entire 210-km trend, which was formed by dissolution of the salt by circulating fresh ground-water and the subsequent collapse and subsidence of overlying shale.

A potentiometric high exists in an area between Hutchinson and Buhler, Kan. The potentiometric surface slopes downward from the high towards two discharge areas. One discharge is near Salina in Kansas, and the other is near the Geuda Springs-Adamsville area of Kansas.

Modeling of river valleys in north-central Kansas

L. E. Stullken and D. G. Jorgensen reported that modeling of the first of five principal stream-aquifer systems in north-central Kansas, and collection of data for the first and second models were completed.

Results of the model study indicated that appreciably more water is stored in the aquifer beneath irrigated areas than before irrigation began because surface-water irrigation provided increased recharge that raised the water level in the aquifer.

Seepage-salinity measurements in streams indicated that nearly 20 years of irrigation has not appreciably altered the quality of the water at base flow.

Streamflow losses in the Arkansas River, western Kansas

In the Arkansas River Valley in Kearny and Hamilton Counties of Kansas, strong relationships exist among recent water-level declines, decreasing streamflow, and less-than-average precipitation. R. A. Barker and K. R. Watts reported that analyses of historic variations in gains and losses

along a 30-km reach of the Arkansas River between the Colorado-Kansas State line (near Coolidge, Kans.) and Syracuse, Kans., indicated that there was no net annual loss prior to 1965; the average stream gain from 1951 to 1964 was approximately 14 hm³/yr, or nearly 10 percent of the gaged flow at Coolidge. Data for years after 1964, however, indicated an almost consistent year-to-year loss; the average annual loss was 3 percent of the flow at Coolidge. During the 1976 drought period, the Arkansas River apparently lost 46 percent of its flow between Coolidge and Syracuse.

The time of distribution of these river losses was consistent with the trend of declining water levels in the area. The change in the river gain-loss relationship between Coolidge and Syracuse apparently occurred in response to water-level declines that resulted most directly from (1) increasing ground-water withdrawals, (2) decreasing river flow across the Colorado-Kansas State line, and (3) less-than-normal precipitation in a recent succession of years.

Chloride concentration of ground-water discharge to Smoky Hill River in Kansas

The immediate source of the natural pollution of the Smoky Hill River in Kansas is the brine in cavities in gypsum beds of the lower part of the Wellington Formation. The contact of the lower part of the Wellington Formation and the overlying valley alluvium is characterized by many sand- and (or) gravel filled cavities. J. B. Gillespie reported that the brine, which has a chloride concentration of 60,000 mg/L, mixes with the ground-water in the valley alluvium. Consequently, ground-water discharging to the Smoky Hill River has a chloride concentration of 5,000 mg/L and increases the chloride concentration of the water in the river to about 500 mg/L.

LOUISIANA

Time of travel of solutes in Louisiana streams

A. J. Calandro compiled data to summarize the traveltime and dispersion of solutes in 18 streams in Louisiana that were surveyed by injecting a fluorescent tracer in the water. Nine of the streams were surveyed at varying discharges, and graphs showing the relation of unit concentration, traveltime, and discharge were prepared.

Standard multiple-linear-regression techniques, relating traveltime and dispersion characteristics to basin parameters, were used to develop equations for estimating traveltime, dispersion of solutes, and peak concentrations for unsurveyed streams in

Louisiana. The equations can be used for all streams and stream reaches below dams in Louisiana that have drainage areas of less than 5,000 km². The standard errors of estimate for the leading edge, peak, trailing edge, and peak unit concentration are 27, 25, 27, and 39 percent, respectively.

Ground-water resources of Washington Parish

According to H. L. Case III, test drilling in Washington Parish in Louisiana, 3 km north of Bogalusa, showed that water in the "1,300-foot" sand of the Bogalusa area has a low-iron concentration and a pH of about 8.8. This discovery extends the known northern limit of the low-iron area of the aquifer. The "1,300-foot" and "1,500-foot" sands are the only sources of low-iron ground water in the Bogalusa area in southeastern Louisiana. Another test hole showed that the "1,500-foot" sand (the major source of supply for the city of Bogalusa) extends at least 5.5 km northwest of the city limits. Another significant finding of the project was that the "100-foot" sand, a major source of industrial water, is hydraulically connected to the Pearl River.

Fresh ground water mapped in St. James Parish in Louisiana

Test drilling in St. James Parish revealed a potential source of good-quality water in an area of the Norco aquifer that was previously thought to contain only water of much poorer quality. D. C. Dial has found that the aquifer contains a narrow lobe of fresh, soft water that extends southward from Sorrento to Welcome, a distance of about 14.5 km. The width of the lobe is more than 5 km at Sorrento and narrows to about 1.6 km at Welcome, on the southwestern side of the Mississippi River. Northeast of the river on both sides of the lobe, the aquifer contains salty water.

The discovery that the freshwater lobe extends across the river near Welcome is especially significant because only hard water having a high concentration of iron was previously known to be available in that area of St. James Parish.

Fresh and brackish water in the Norco aquifer is used for domestic and industrial supplies on the northeastern side of the river. The aquifer is composed of fine to coarse sand with some gravel, and ranges in thickness from 24 to 30 m; the depth to the top ranges from 60 to 125 m in the areas of test drilling.

Freshwater anomalies over three Louisiana salt domes

Within the Arcadia-Minden area of northern Louisiana, the Arcadia, Gibsland, and Minden salt

domes have caused pronounced local anomalies in the base of freshwater. The two major aquifers in this area are in the lower Tertiary Sparta Sand and the Wilcox Group and are separated by 60 to 90 m of clay. The Sparta Aquifer contains freshwater, but the Wilcox aquifer which is deeper, contains saltwater in much of the area. However, according to G. N. Ryals, the Wilcox contains freshwater on the flanks of the domes, usually in areas of 2.5 km² or less. The freshwater bodies in the Wilcox are either crescent shaped or completely encircle the dome, and are probably the result of recharge along fault zones over the dome.

Ground-water in lignite areas of De Soto Parish

USGS investigators drilled test holes and installed observation wells to obtain data on the Wilcox aquifer in southeastern De Soto Parish in Louisiana. The data will provide a base from which the effects of future surface mining lignite can be assessed, according to J. L. Snider. During the drilling, a sand overlying the lignite in the Wilcox Group was found to be thicker, coarser, and more extensive than was indicated by previous studies. This sand is a potential source of water for public supplies in southeastern De Soto Parish. Surface mining of lignite planned for the area would disrupt the sand and diminish its usefulness as an aquifer. Because the sand is extensive, dewatering for mining will affect water levels in adjacent areas.

Changes in ground-water quality caused by realignment of the Red River in northern Avoyelles Parish

M. S. Whitfield, Jr., observed that water-quality changes are occurring in the Red River alluvial aquifer in an area where the Corps of Engineers, U.S. Army, realigned the Red River. In northern Avoyelles Parish, the chloride concentration in one USGS observation well near a cutoff increased from about 70 to 110 mg/L. Other observation wells in this same area showed smaller changes. Data indicated abrupt changes in water quality both laterally and vertically within the aquifer. Changes in the direction of ground-water flow and in the hydraulic gradient, caused by realignment of the Red River, probably account for the changes in water quality.

MONTANA

Ground-water resources of the Poplar River basin, northeastern Montana

A study of the ground-water resources in the Poplar River basin in northeastern Montana indi-

cated that the river serves as a drain for the shallow aquifers. R. D. Feltis reported that water-level contours based on measurements in shallow wells showed that ground-water movement is toward the river from both the eastern and western sides of the stream valley. Water samples from wells indicated that the Paleocene Fort Union Formation generally contains sodium bicarbonate type waters, except near an area where gravel of the upper Tertiary Flaxville Formation overlies the Fort Union—there the water is a magnesium or calcium bicarbonate type. Dissolved-solids concentrations in ground water ranged from 523 to 1,470 mg/L, and boron concentrations ranged from 300 to 2,800 $\mu\text{g/L}$.

Thermal ground water

Most of the hot (38°) springs in southwestern Montana issue from fractured crystalline rock or from valley fill. Results of recent drilling near typical springs of each type indicated that adequate supplies of hot ground water are available for space heating, greenhouses, and domestic use.

Maximum water temperatures of 68°C and 89°C were measured in wells drilled to a depth of 61 m in fractured intrusive rock near Helena (Broadwater hot springs) and in wells drilled to a depth of 103 m in valley fill near Ennis (Thexton hot springs). R. B. Leonard reported that the maximum temperatures of the well waters exceeded the temperatures of the associated springs, but the well water temperatures were lower than reservoir temperatures predicted from chemical geothermometers.

An aquifer test at a flowing thermal well near Helena indicated that the transmissivity of the fractured crystalline rock is about $560\text{ m}^2/\text{d}$, and the potential yield of wells is more than 130 L/s.

Site-specific coal-land reclamation study near East Trail Creek, southern Montana

W. R. Hotchkiss and J. D. Stoner studied the reclamation potential for strippable coal deposits at East Trail Creek, a small part (20 km^2) of the Hanging Woman Creek coalfield, about 31 km east of Decker, Mont. Ephemeral runoff was monitored in 1977 at a gaging station 1.5 km upstream from the mouth of the East Trail Creek Basin (approximately 81 km^2). The most significant runoff occurred after a June 1977 rainstorm that had a measured intensity of 61.0 mm in 6 hours. Following the event, flow at the station peaked rapidly at about $0.84\text{ m}^3/\text{s}$ and receded to no flow in less than 7 days. Major constituents in the water from sampled runoff events were sodium, magnesium,

and sulfate. Dissolved-solids concentrations ranged from 2,390 to 4,510 mg/L.

Sixteen test holes drilled in the area indicated that the 8.9-m-thick Anderson and the 3.0-m-thick Dietz coalbeds were the most significant shallow-aquifer units of the Tongue River Member of the Fort Union Formation. Wells in the coalbeds produced from 0.02 to 0.76 L/s of water. Aquifer testing of the coalbeds yielded transmissivities from 0.06 to $1.5\text{ m}^2/\text{d}$ with storage coefficients of about 2.5×10^{-4} .

Data from test drilling across the alluvial valley of East Trail Creek during the fall of 1977 suggested a losing-stream configuration of the fall water table. Aquifer tests indicated that the transmissivity of the alluvium was about $147\text{ m}^2/\text{d}$ with a storage coefficient of 0.005.

Major constituents in water from the coalbeds were sodium and bicarbonate. Major constituents in water from the alluvium were sodium, magnesium, and sulfate. Dissolved solids in water from all wells ranged from about 2,200 to 6,300 mg/L.

Water quality of selected streams in the Fort Union coal area, southeastern Montana

According to J. R. Knapton and P. W. McKinley, water-quality characteristics of streams draining the Fort Union coal region of southeastern Montana are largely influenced by whether the water was contributed to the stream as runoff or as baseflow. The baseflow component had high dissolved-solids concentrations that were dominated by sodium and sulfate. Many of the downstream concentration changes in major ions, rather than being gradual, were abrupt and appeared to correlate with changes in lithology.

Surface runoff was generally characterized by lower concentrations of dissolved ions made up principally of the calcium and magnesium cations and the bicarbonate anion. The surface-runoff component also often carried a significant amount of suspended sediment that was contributed from overland flow, channel scour, and bank erosion. Because of the affinity that certain trace metals and nutrients have to clay particles, suspended sediment acted as a transporting mechanism for some constituents.

Localized saline seep development in Hailstone Basin in Montana

Saline seeps are areas that have become progressively less productive because of seepage of saline ground water. B. D. Lewis studied the factors contributing to saline seeps at a site in the

Hailstone Basin of Montana. The formation of a saline seep is related to several hydrogeologic factors, including the presence of a local, shallow perched ground-water flow system, and precipitation percolating below the root zone. Hydrogeologic factors also determine where the saline seep occurs; these factors include shallow depth to an impermeable unit, local surface and subsurface topography, stratigraphy, hydrology, and lithology.

The ground-water flow system at the study site is local, perched, and shallow. The mean specific conductance of the ground water, which is a sodium sulfate type, is 8,400 $\mu\text{mho/cm}$. The nature of the weathering at the study site qualitatively suggested that weathering is the source of the ions. There was as much as 855 mg/L of nitrate in the ground water; the nitrate may be related to conversion of organic nitrogen to nitrate in response to cultivation, rather than in response to application of fertilizer.

Second test well completed in the Madison aquifer

As a part of the regional evaluation of the geology, hydrology, and geochemistry of the Madison aquifer, Madison Limestone test well 2 was bottomed 28.7 m below the top of Precambrian rocks at 2,860 m below land surface on March 23, 1977. The well is in T. 1 N., R. 54 E., sec. 18, Custer County, Montana (D. L. Brown, and others, 1977).

According to E. M. Cushing, 19 cores were taken from selected depth intervals, ranging in age from Late Cretaceous to Precambrian. Core recovery was 220 m out of 230 m attempted. Seventeen drill-stem and packer-swabbing tests were attempted in formations ranging in age from Cretaceous to Cambrian. Geophysical logs available included electric, induction electric, gamma, guard, neutron, acoustic, density, three-dimensional velocity, temperature, and caliper. The well was cased into the top of the Madison aquifer at about 1,978 m below land surface. The open-hole part of the well begins about 6 m below the top of the Madison Limestone (Mississippian) and ends about 37 m above the base of the Red River Formation (Ordovician) at a depth of about 2,569 m. Two cement plugs were placed in the bottom of the well—one from about 2,860 to 2,770 m and the other from about 2,710 to 2,570 m below land surface—to block upward leakage of the highly saline water in the lower geologic units. Water from the open-hole part of the well had a dissolved-solids concentration of about 4,400 mg/L. It had a pressure of 2,296 kPa and flowed at a rate of 2.8 L/s with a pressure loss of 2,275 kPa. The temperature

of the water, measured at land surface, was about 49°C.

NEBRASKA

Shrinking channels of the North Platte and Platte Rivers

A reconnaissance investigation was made by G. P. Williams to determine whether the channels of the North Platte and Platte Rivers in western and central Nebraska have been changing in character since the latter part of the 19th century and, if so, the general nature and extent of such changes. The 480-km study reach extended from Minatare in Nebraska on the North Platte River to Grand Island on the Platte River.

The channels have indeed changed considerably. Most of the former river channel is now overgrown with vegetation. Changes in the 365-km reach between Minatare and Overton differ in magnitude and sometimes in character from the 115-km downstream stretch between Overton and Grand Island. By 1969, the channel between Minatare and Overton was only about one- to two-tenths as wide as it was in 1865; in 1969 the channel was less braided and slightly more sinuous than it was in 1938. (No data are available for braiding and sinuosity prior to 1938.) In 1969, the channel between Overton and Grand Island was about six- to seven-tenths as wide as it was in 1865, and various changes in braiding and sinuosity took place between 1938–69.

The decreases in channel width are related to decreases in water discharge. Such flow reductions resulted primarily from the regulating effects of major upstream dams and man's greater use of river water.

NEW MEXICO

Ground water near Capulin

According to D. L. Hart, Jr., and C. S. Smith, preliminary results of a ground-water investigation of a closed basin west of Capulin in New Mexico indicated two potential sources of water. Alluvial deposits and volcanic cinders within this basin have sufficient transmissivity to yield large quantities of water to wells. Wells tapping the alluvial deposits yield from 0.06 to 60 L/s and wells tapping the volcanic cinders yield as much as 125 L/s. The area of saturated alluvium is about 80 km², and the area of known saturated cinders is about 5 km². The two aquifers are highly productive only in an 18-km² area.

The alluvial deposits are as much as 56 m thick, but average less than 15 m thick. The depth to water

in the alluvial deposits ranges from 0 to 21 m below the land surface. The volcanic cinders are less than 21 m thick, and depth to water generally ranges from 5 to 15 m below the land surface.

The water from these aquifers is a calcium-bicarbonate type with a specific conductance that ranges from 350 to 750 $\mu\text{mho}/\text{cm}$.

NORTH DAKOTA

Ground-water flow model of Harmon lignite at Gascoyne mine, North Dakota

A digital ground-water flow model of the Gascoyne lignite mine in Bowman County of North Dakota indicated that the Harmon lignite bed of the Tongue River Member of the Paleocene Fort Union Formation has high lateral transmissivities beneath several of the major stream valleys in the mine area, according to M. G. Croft. The valley's parallel major regional lineaments are probably fracture zones that conduct large quantities of water. The model indicated that values for lateral hydraulic conductivity may be as high as 7.6 m/d. The model also suggested that the lignite is fractured to a much lesser degree beneath the interstream areas, where the value for lateral hydraulic conductivity is less than 0.3 m/d. Soils are poorly permeable and vertical recharge is less than 1.5 mm/yr.

Hydrologic evaluation of mining and reclamation in the Beulah Trench area of North Dakota

M. E. Crawley reported that results of test drilling in the Beulah Trench area indicated that ground-water movement is generally eastward from the glacial-till-covered highlands west of the trench. Water levels in observation wells indicated a possible hydraulic connection between water in the Sentinel Butte aquifer and the glacial Antelope Creek (Beulah Trench) aquifer. Ground-water samples from the Antelope Creek aquifer were basically a calcium-sodium bicarbonate type, whereas ground-water samples from the Beulah-Zap lignite aquifer were a calcium-magnesium sulfate type. Samples from the underlying Tongue River aquifer were strongly sodium bicarbonate in type and had pH values of 8.7 to 8.8. Trace-metal concentrations in all ground- and surface-water samples were very low except for isolated occurrences of iron and manganese.

Buried glaciofluvial aquifer system in southeastern McIntosh County in North Dakota

R. L. Klausing reported that test drilling revealed a buried glaciofluvial aquifer system in the south-

eastern part of McIntosh County in North Dakota. The sand and gravel aquifer system underlies an area of about 150 km². Mean aggregate thickness of the aquifer system is about 12 m. The ground water is predominantly a sodium bicarbonate type; it has a mean sodium-adsorption ratio value of about 4, and a high-salinity, low sodium hazard (C_3-S_1). The aquifer appears to have good irrigation potential if the water is to be applied to well-drained soils.

OKLAHOMA

Geohydrology of the Arbuckle aquifer, south-central Oklahoma

The Arbuckle aquifer, in the Arbuckle Mountains of south-central Oklahoma, consists of limestone and dolomite of the Arbuckle Group (Cambrian and Ordovician) and sandstone and limestone of the Simpson Group (Ordovician). These rocks were intensely folded and faulted in Pennsylvanian time. Data collected by Roy Fairchild and R. E. Davis indicated that springs and seeps issuing from the aquifer within the area of outcrop of the two groups are the sources of baseflow to perennial streams of the area. Many of the springs and seeps are associated with faults. Winter (1976-77) baseflow in the eastern two-thirds of the area amounted to about .007 (L/s)/km² for a total of nearly 6 m³/s.

Wells tapping the Arbuckle aquifer range from a few meters to as much as 915 m in depth, but most are 30 to 60 m deep. Well yields generally range from 1.25 to 300 L/s, but one well yields more than 1,500 L/s (nearly 24,000 gpm).

Recharge to the aquifer is derived directly from precipitation. Water levels generally respond quickly to precipitation events, which indicates that fractures and solution openings provide a means of rapid entry and movement of water. Fluctuations of water levels in wells ranged from 1.5 to 16 m during 1977.

In the outcrop area, water in the aquifer is generally of good quality and usually has a dissolved-solids concentration of less than 500 mg/L. In the west-central part of the area, water in the Simpson Group contains various amounts of organic matter (oil), which is troublesome in domestic supplies. About 3 km from the outcrop area, the aquifer dips below younger rocks, and water in the aquifer becomes highly mineralized.

Quality of ground-water varies in prospective coal-lease areas of east-central Oklahoma

A study of three prospective coal-lease areas near Blocker, Spiro, and Rock Island in east-central Okla-

homa showed that ground-water quality is extremely variable. J. S. Havens reported that specific conductance ranged from 100 to 6,000 $\mu\text{mho}/\text{cm}$, and pH ranged from 4.9 to 8.8 in water samples from about 150 wells. Specific conductance of surface-water samples collected from seven sites in the area ranged from 60 to 850 $\mu\text{mho}/\text{cm}$; the higher conductances reflected low-flow conditions during the summer. The specific conductance of about 20 samples collected from streams within the areas ranged from 66 to 420 $\mu\text{mho}/\text{cm}$. The pH of these samples ranged from 5.6 to 8.2, but most samples were within the 6.5 to 7.0 pH range.

Water levels in observation wells in each of the three areas generally showed rises caused by local recharge in response to precipitation. All three wells responded quickly to daily and regional barometric fluctuations.

Stream-water quality in eastern Oklahoma coalfield

During the summer of 1977, 89 streams throughout the coalfields of eastern Oklahoma were inventoried for discharge, specific conductance, pH, DO, and iron, chloride, and sulfate content. The maximum discharge was 0.71 m^3/s , and median discharge was 0.008 m^3/s . Approximately 70 percent of the streams were either dry or pooled but not flowing. Generally, flowing streams occurred in areas of active mining.

Preliminary analyses of the data by Joanne Kurklin indicated that, for the most part, the quality of water in the streams was good. Eighty percent of the specific-conductance values were less than 1,000 $\mu\text{mho}/\text{cm}$ at 25°C; few pH values were less than 6.5 (the lowest was 5.5); all iron values were less than 1 mg/L; and sulfate values exceeded 100 mg/L in only 25 percent of the samples.

Specific-conductance values greater than 1,000 $\mu\text{mho}/\text{cm}$ at 25°C and sulfate values greater than 100 mg/L generally occurred in streams draining active mining areas.

Quality of water in Oklahoma's abandoned coal pits

During the summer of 1977, 28 water-filled strip-mine pits in the southern part of the eastern Oklahoma coalfields were inventoried by S. J. Playton and R. E. Davis for selected morphometric, physical, and chemical properties. The maximum depths of most of the strip-mine pits were between 4.5 and 9 m; however, some were as shallow as 1.5 m, and others were as deep as 18 m. In general, water in strip-mine pits with depths greater than 4 m was

stratified, with pH, water temperature, DO, and dissolved sulfate decreasing and specific conductance increasing with depth.

The hypolimnetic waters in some strip-mine pits were anaerobic. Reducing conditions prevailed in these strata, and dissolved manganese and iron concentrations were greater than in the oxygenated epilimnetic zone.

Generally, the quality of water in the strip-mine pits was good. Few acidic water conditions were observed; most specific conductances were less than 1,000 $\mu\text{mho}/\text{cm}$ at 25°C; and large, oxygenated epilimnia were present. Also, flourishing communities of aquatic flora and fauna were found in most strip-mine pits.

SOUTH DAKOTA

Major outwash aquifers located in southeastern South Dakota

Major glacial aquifers of outwash sand and gravel were found by drilling 100 test holes and inventorying approximately 600 municipal, irrigation, domestic, and stock wells in Aurora and Jerauld Counties, a 3,200- km^2 area of till plains and hills in southeastern South Dakota. L. J. Hamilton (USGS) and L. S. Hedges (South Dakota Geological Survey) reported that the glacial aquifers were found in nine different areas at depths ranging from 3 to 130 m. During 1977, 14 irrigation wells yielding 10 to 50 L/s were completed at depths of from 8 to 30 m in these aquifers.

Madison Group only a part of a major aquifer system in South Dakota

Analyses of available data by L. W. Howells indicated that major water-bearing units in Paleozoic rocks below the Mississippian Madison Group probably are interconnected over a wide area and, together with the major water-bearing zones in the Madison Group and Pennsylvanian and Permian Minnelusa Formation, form a complex aquifer system. Recharge to this aquifer system is at the outcrop of Madison rocks in the Black Hills. The major natural discharge of the system in South Dakota is to aquifers in overlying Mesozoic strata in the central and eastern parts of the State.

Big Sioux aquifer in parts of eastern South Dakota extends beyond stream valleys

A digital-model study of a major shallow aquifer in Brookings and Hamlin Counties in eastern South Dakota by N. C. Koch indicated that in some areas, the aquifer extends beyond the valleys of the Big

Sioux River and its tributaries. Water in the aquifer is under water-table conditions where it occurs in the stream valleys but is under artesian conditions where it underlies the till beyond the stream valleys. The aquifer covers about 780 km² in the study area, averages 8 m in thickness, and contains about 1.2 billion m³ of water in storage. There are about 150 irrigation wells and a number of municipal wells in the study area. Wells in the Big Sioux aquifer yield as much as 126 L/s.

A thick glacial-drift deposit contains several outwash aquifers in Miner County

Extensive preliminary test-hole drilling in Miner County in southeastern South Dakota revealed a glacial-drift deposit up to 100 m thick. Jack Kume found several outwash bodies that are aquifers within this drift deposit. These aquifers are located in many parts of the country, but they are of significant size only in the western and southeastern parts.

The aquifer with the greatest, areal extent, the Floyd aquifer, occurs in the western one-fifth of the county. It consists of buried outwash sand and gravel up to 11 m thick. Other unnamed aquifers that occur in the southeastern part of the county consist of buried outwash sand and gravel up to 10 m thick.

Extensive aquifers occur in alluvium and outwash deposits in Walworth County

Well-site inventories and test-hole drilling completed in Walworth County in north-central South Dakota revealed several extensive aquifers in alluvium and outwash deposits. Jack Kume mapped four major and several minor glacial outwash and alluvium aquifers.

Major aquifers that occur in surface or near-surface outwash deposits include the Bowdle aquifer in eastern Walworth County and the Selby aquifer in north-central Walworth County.

Major aquifers in buried deposits of outwash are the Grand aquifer in the northwestern and west-central part of Walworth County and the Java aquifer in the east-central and southeastern part of the county. Minor aquifers occur in outwash and alluvium in the drainage channels of Swan Creek and an unnamed tributary to Blue Blanket Creek.

Large ground-water yields in northeastern South Dakota

L. J. Hamilton (1978) reported that maximum well yields ranged from 12 to 126 L/s from six major glacial aquifers at depths ranging from 2 to 180 m in Clark County, an area of 2,528 km² of roll-

ing to hilly glacial-till plains in northeastern South Dakota. Storage of water in the aquifers totals about 6,600 million m³ and annual recharge averages about 12 million m³. Pumpage during 1976 totaled 4.4 million m³; pumpage was much greater than normal because of large withdrawals through 24 irrigation wells during a period of severe drought. At four sites, responses of aquifers to pumping indicated that the transmissivities vary from about 30 to more than 3,000 m²/d. Hydraulic conductivities ranged from 3 m/d in clayey, silty sand and gravel in the deepest aquifer to as much as 150 m/d in medium to coarse sand and gravel.

TEXAS

Jasper aquifer mapped in the Coastal Plain of Texas

The Jasper aquifer, one of several highly productive aquifers in the Texas Coastal Plain, was mapped from the Sabine River to the Rio Grande by E. T. Baker, Jr. A series of 12 strike-and-dip sections illustrates the aquifer's stratigraphic and hydrogeologic framework. The Jasper ranges from about 60 to 975 m in thickness; the maximum thickness occurs within the region of highly saline water in the aquifer. The average range in thickness within the zone of fresh to slightly saline water is from about 180 to 300 m.

The Jasper contains more sand in the eastern part of the Coastal Plain of Texas than in the southern part. In some places near the Sabine River, where it is composed almost entirely of sand, the Jasper attains a thickness of more than 700 m, and fresh to slightly saline water saturates the aquifer to a depth of about 900 m below sea level.

Geohydrology of the northeastern Texas salt-dome basin

J. E. Carr and H. B. Peters are evaluating the regional geohydrology of the northeastern Texas salt-dome basin. Preliminary maps of the potentiometric surfaces of the Eocene Carrizo Sand and the underlying Eocene and Paleocene Wilcox Group show a general south-southeast ground-water flow system. The occurrence of natural ground-water discharge from these units was indicated in the upstream areas along the Trinity and Sabine Rivers and in the respective outcrop areas.

A preliminary map of the potentiometric surface of the overlying Eocene Queen City Sand shows a regional pattern of ground-water flow from the topographically higher divides to the major river

valleys. The hydraulic head in the Queen City Sand is greater than the heads in the Carrizo Sand and Wilcox Group over most of the salt-dome area. A structural-contour map of the top of the underlying Paleocene Midway Group, which is a major basal confining layer for the freshwater aquifers within the basin, shows that the regional dips of the western side of the basin range from 9.5 to 14 m/km, and increase in the southern part of the basin. Definite uplift of the Midway Group is shown at the Mount Sylvan and Palestine salt domes.

UTAH

Evaluation of aquifers in southern Utah

R. M. Cordova collected data on unconsolidated aquifers in the mainly consolidated-rock terrain of southern Utah. These aquifers occur in alluvium of Tertiary or Quaternary age deposited by streams on broad rock terraces east of Kanab and southeast of Hurricane. The aquifers are as much as 75 m thick and yield 10 to 40 L/s of water to wells. The deposits containing the aquifers are covered by young fine-grained material. The deposits were identified from lithologic logs of wells.

Traveltime and dispersion characteristics of the White River in the Uinta Basin oil-shale area

By using fluorescent dye, D. W. Finn and K. L. Lindskov studied time-of-travel and dispersion characteristics of the White River in the oil-shale area of the southeastern Uinta Basin of Utah, to determine the effects of movement of contaminants in the major stream in the basin. During 1975-76, data were collected on two different flow conditions for a 90-km reach of the White River between the gaging station near Bonanza and the mouth of the river near Ouray, Utah. Relations were developed from the data to predict when wastes will reach downstream locations, how long it will take wastes to pass, and probable maximum concentrations. Standard equations were used to predict traveltimes of the leading edge, peak, centroid, and trailing edge of soluble material entering the river. Total traveltimes for the entire reach varied from about 35 hours at average flow to 75 hours at 15 percent of average flow. Passage time ranged from 10 to 25 hours for the respective flows. In addition, the unit-concentration technique was used to estimate the maximum probable concentrations of soluble substances at any location downstream from a slug injection.

Navajo Sandstone source of ground water for future energy-related development in southeastern Utah

The lower Mesozoic Navajo Sandstone, a major aquifer in southeastern Utah, is a probable future source of water for energy-related development in that arid area. The sandstone is an important water source in the area between the Henry Mountains and the San Rafael Swell because it underlies much of the area and is thick—from about 150 m thick northeast of Hanksville to slightly more than 300 m thick in the vicinity of Capitol Reef National Park. Deep-well cores showed that the undisturbed sandstone is nearly isotropic and that its hydraulic conductivity averages about 0.15 m/d, within the range of that for unconsolidated clay. The primary permeability, however, is enhanced by secondary permeability where the sandstone has been folded and fractured. Large-diameter, partially penetrating test wells near Caineville were pumped at 180 to 200 L/s. Aquifer tests on these wells showed a transmissivity of about 140 m²/d for the 270-m section of sandstone, thus indicating hydraulic conductivity of 0.52 m/d, which is triple that of the undisturbed formation.

Recharge to the Navajo Sandstone probably is small. Radioisotope analyses of water from wells 5 to 24 km from formation outcrops gave uncorrected ages of about 7,000 to 30,000 years for water in the sandstone, thereby indicating slow movement of a small amount of water under natural gradients of 1.9 to 3.8 m/km. Data also indicated local leakage to the sandstone from both above and below. A test hole northwest of Caineville yielded a brine from the sandstone; the brine probably originated in the overlying Jurassic Carmel Formation. The water level in the Carmel is above that in the Navajo, and the Carmel contains some halite. Elsewhere, limited data indicated upward leakage from underlying formation that are under high artesian pressure.

Reasons for deterioration of the Bonneville Salt Flats

Findings of a 2-year study of the Bonneville Salt Flats recently completed by G. C. Lines indicated that most of the damage to the world-famous Bonneville Racetrack and surrounding salt crust can be attributed to (1) a wet-weather cycle that extended through the 1960's and early 1970's, (2) the collection of brine from a shallow aquifer for the production of potash, and (3) the construction of Interstate Highway 80 across the salt.

On the bases of transmissivity data and the configuration of the density-corrected potentiometric

surface of the shallow-brine aquifer, 10^6 t of salt were estimated to have been removed for the production of potash from the area of the racetrack by subsurface flow during 1976. Re-resolution of the salt crust and recharge to the shallow-brine aquifer were accelerated because of the wet-weather cycle. Re-resolution of the salt crust and accumulation of sediment on the surface also were accelerated in man-made ponding areas created on the windward side of surface-drainage barriers, such as the roadfill for the interstate highway.

Several previously suggested remedial measures, such as the construction of subsurface-drainage barriers, were evaluated. Study findings indicated that none of the remedial measures will eliminate completely the conflict between uses or will transform the Salt Flats to its original state.

Declining ground-water levels in the Beryl-Enterprise area of southwestern Utah

Ground-water levels are declining in the Beryl-Enterprise area of the Escalante Valley in southwestern Utah, mainly as a result of pumping for irrigation, and of the drought in that part of the State, according to R. W. Mower and G. W. Sandberg. The declines were large enough to create a closed depression that encompasses at least 155 km^2 in the water table. The depression will continue to deepen and expand laterally after precipitation returns to normal or above normal because current annual pumpage, which is about 96 million m^3 , is much greater than recharge resulting from precipitation. The rate of water-level decline in the pumped area will diminish slowly, however, as more of the water in the outer reaches of the depression moves into the heavily pumped parts. Because thickness of the aquifer exceeds 200 m over an extensive area and the average decline in 1977 was less than 0.5 m in the heavily pumped parts of the aquifer, no serious depletion problems are expected.

Navajo Sandstone evaluated as an alternative source of water for energy development in the Kaiparowits Plateau area in south-central Utah

In the Kaiparowits Plateau of south-central Utah, the Navajo Sandstone of Triassic(?) and Jurassic age lies from 300 to 600 m below the coal-bearing Straight Cliffs Formation of Cretaceous Age. Data compiled by Donald Price indicated that in this area, the Navajo Sandstone can yield more than 60 L/s of fresh to slightly saline water to individual wells. Aquifers in the Navajo would be essentially unaffected by mining of the Straight Cliffs coal or by

subsidence in mined-out areas and, therefore, could be a dependable source of water for coal-mining activities or related energy development, such as electric-power generation, in the area.

Principal constraints to development of water in the Navajo in the Kaiparowits Plateau area are the depths to the aquifers and the relationship of water in those aquifers to Lake Powell. Because the aquifers lie 600 to 1,200 m beneath the plateau surface, drilling and pumping costs would be high. Also, because the aquifers receive recharge from Lake Powell during rising lake stages (Don Price and Ted Arnow, 1974, p. C11), applications to divert large quantities of water from the aquifers could lead to complex legal problems.

Spring discharge and water-quality data on coal areas of east-central Utah

Hydrologic data collected by C. T. Sumsion in the Book Cliffs-Wasatch Plateau coalfield area of east-central Utah includes data on selected springs, mostly in the Upper Cretaceous and lower Tertiary Mesa Verde Group, North Horn Formation, and Flagstaff Limestone. Spring discharges range from 0.006 to 5.7 L/s, and specific conductance of spring water ranges from 100 $\mu\text{mho}/\text{cm}$ at 25°C in the Price River Formation to 2,950 $\mu\text{mho}/\text{cm}$ in the Star Point Sandstone. Most springs are perennial in the Wasatch Plateau, but are seasonally intermittent in the Book Cliffs.

WYOMING

Preliminary digital model of the Sweetwater River basin

A preliminary digital flow-system model of the Arikaree aquifer was developed by W. B. Borchert, who used limited, poorly distributed available data, an estimated distribution of recharge, and a conceptual model of the aquifer flow system. Calibration of the model was based on the reproduction of the potentiometric surface and the base flow of the Sweetwater River in November 1975. Calculated steady-state heads were within 15 m of the observed heads in about 98 percent of the nodes. The calculated leakage from the Arikaree aquifer to the Sweetwater River in the western area was within 12 percent of the leakage of 0.48 m^3/s determined by gain-and-loss studies.

Analysis of runoff from small drainage basins in Wyoming

G. S. Craig, Jr., and J. G. Rankl (1977) defined the magnitude and frequency of flood volumes and

flood peaks to be expected from drainage basins smaller than 28.5 km² in the plains and valley areas of Wyoming. Rainfall and runoff data, collected for the months of April through September for 9 years, were used to calibrate a rainfall-runoff model on each of 22 small basins. Long-term records of runoff volume and peak discharge were synthesized for these basins and flood volumes and flood peaks of specific recurrence intervals (2, 5, 10, 25, 50, and 100 years) were then related to basin characteristics. Flood volumes were related to drainage area, maximum relief, and basin slope. Flood peaks were related to drainage area, maximum relief, basin slope, and channel slope.

Digital model predicts water-level declines and streamflow depletions near Wheatland

D. T. Hoxie developed a digital ground-water flow model for the Arikaree aquifer in a 1,000-km² area near Wheatland in north-central Platte County. The model was used to assess the effects of projected ground-water withdrawals for irrigation and proposed ground-water withdrawals for industry. At expected average pumping rates for both irrigation and industry, it was found that streamflow in the Laramie and North Laramie Rivers would be reduced by 0.16 and 0.10 m³/s, respectively, and that water-level declines of more than 2 m would occur over a 300-km² area.

Stream-temperature model for the Green River basin in Wyoming

Temperatures of streams in the Green River basin of Wyoming can be estimated by using a regional model developed by H. W. Lowham. The model was developed by describing annual temperature patterns at 43 measured sites in the basin and by applying the harmonic function $T = M + A [\sin(0.072 t + C)]$, where T is mean daily temperature, M , A , and C are harmonic coefficients calculated from data for each stream-temperature station, and t is the day of the water year. Application of the equation for estimating temperatures at unmeasured sites required regionalized estimates of M , A , and C ; these estimates were developed with the aid of multiple-regression techniques, whereby the calculated harmonic coefficients were regressed against physical and climatic characteristics of the stream-temperature stations. Stream elevation was found to be a significant factor affecting water temperature.

Analyses of areal and temporal variations in temperature showed that springs, irrigation return

flows, and reservoir storage were affecting reaches of several major streams.

WESTERN REGION

Drought ravaged most of the western region in 1977 for the second consecutive year. Discharge of the Columbia River was the lowest since records began in 1878. In California, North Fork American River had the least discharge in 36 years of record, and Smith River had the least discharge in 46 years of record. The annual discharge of the Snake River near Heise, Idaho, was the lowest in 67 years of record, and that of the Spokane River at Spokane, Wash., was the lowest in 86 years of record.

When the water year ended on September 30, 1977, contents of major reservoirs in California averaged only 34 percent of normal. Water stored in Shasta Lake, on the Sacramento River, amounted to about 24 percent of normal, the Bridgeport Reservoir in the Sierra Nevada was dry, and water stored in the Rye Patch Reservoir on the Humboldt River of Nevada amounted to 38 percent of normal.

Southern California water agencies that were able to meet minimum needs by drawing upon the Colorado River voluntarily waived their allotments of water from northern California supplied through the California Water Project. Other necessary inter-agency adjustments were made throughout the region, but generally surface water was in short supply.

As a result of the drought, hydroelectric-power supplies diminished; consequently, the use of more costly fossil fuel in generating plants increased. Irrigation-water supplies were curtailed and agriculturists reactivated wells or drilled new wells by the thousands. In the heavily cultivated San Joaquin Valley of California, the renewed heavy draft on ground-water resources resulted in declining pressure heads, and renewed aquifer compaction was recorded on USGS instruments used in land-subsidence research.

In many areas, water rationing was imposed on domestic-supply users dependent on surface-water sources, and voluntary cutbacks of 25 to 50 percent of normal usage were achieved. However, in some places especially in the San Francisco Bay region, rationing of domestic supplies was imposed and buttressed with penalties for excessive household use with ludicrous results in at least one instance. In Palo Alto, Calif., the fire department extinguished a small roof fire by using household water to avoid damage that would have been caused by using

high pressure hoses; the homeowner was charged a penalty for overuse of water. Overall, rationing was accepted with good grace and considerable effectiveness.

Westerners became familiar with a new word "graywater" as householders, who were denied use of tapwater for flower and tree irrigation, turned to rinsewater from dishwashing and laundering for their supply. Operators of ski resorts closed down operations for lack of snow, or resorted to costly machine-made flaky ice for their slopes. Owners of freshwater marinas watched retreating shorelines remove their means of livelihood as reservoir levels dropped. Massive forest fires destroyed brush and timber over hundreds of thousands of hectares, leaving behind the promise of mudslides when the next rains came.

The effects of the 1976-77 drought forced Federal, State, and local water-management agencies to make some decisions that depended on information—lake and reservoir stage, surface-water discharge, water quality, and ground-water levels—obtained from the USGS. The USGS increased the frequency of measurements and expanded the scope of its data-gathering activities. The Congress assisted that effort by appropriating supplemental funds for drought-related investigations. In several affected States, the USGS, with the concurrence of its cooperating agencies, reoriented parts of its project studies, and postponed various investigations in order to concentrate on obtaining information almost daily on changing water conditions, or locating supplemental sources of water. USGS personnel sat on or advised drought-emergency panels appointed by governors of several western States.

Alaska had unusually heavy precipitation and runoff in most areas as a persistent high-pressure system off the California coast displaced Pacific storm tracks far to the north. Hawaii, Guam, and the Trust Territory Islands experienced intermittent, seasonal shortages of water; however, shortages were generally comparable to those of normal years, and prolonged periods of water shortage did not occur on the islands.

In 1977, the USGS assisted EPA in two studies relating to "sole-source" aquifers. Under the Safe Drinking Water Act (PL 93-523), EPA is required to determine, upon petition or its own initiative, whether aquifers declared to be the sole or principal sources of drinking water are or may be subject to pollution. EPA requested the USGS to evaluate existing information on the aquifers underlying the Fresno area of California (K. S. Muir, 1977)

and the areas of Rathdrum Prairie area of Idaho and the Spokane Valley area of Washington (B. W. Drost and H. R. Seitz, 1977).

USGS scientists, in cooperation with the National Park Service, continued to study geomorphology, erosion, and sediment-transport in the Redwood National Park of California (R. J. Janda, 1978). The purpose of the study is to provide information to Congressional subcommittees, representatives of the lumber industry, and members of conservation groups so that they can reach a decision on expansion of the park area.

INTERSTATE STUDIES

"Sole-source" study

The Spokane Valley-Rathdrum Prairie aquifer extends from northern Idaho southward to about the latitude of Spokane, Wash., then swings westward into the Spokane Valley. B. R. Drost and H. R. Seitz made a study of the aquifer for EPA. EPA's tentative designation of the Spokane Valley-Rathdrum Prairie aquifer as a "sole-source" aquifer is based on the information contained in the investigators' final report (Drost and Seitz, 1977). The aquifer apparently has a balance between recharge and discharge at an average rate of 37.4 m³/s. The average rate of withdrawal from the aquifer in 1976 was 7.05 m³/s. The water is generally of good quality; less than one-half of 1 percent of the 3,300 analyses available had constituent-concentration levels that exceeded those specified in the National Interim Primary Drinking Water Regulations. Alternative water sources for the area supplied by the aquifer are less desirable owing to poor-quality water, remoteness to the areas, or insufficient supply.

Using a digital model to define the hydrologic-flow system, Seitz found that recharge to the Rathdrum Prairie aquifer is mostly leakage from surrounding lakes, runoff from adjacent highlands, and precipitation on the aquifer. Operation of a dam at the outlet of Pend Oreille Lake has significantly affected the ground-water levels since 1952. In the southern part of the aquifer, water levels are affected by Hayden and Coeur d'Alene Lakes and leakage from the Spokane River.

ALASKA

Large springs north of Delta Junction

According to D. E. Wilcox and G. L. Nelson, large quantities of water are discharged from the

perennial springs that feed Clearwater, Sawmill, and Granite Creeks, Clearwater Lake, and the Tanana River, north of Delta Junction, Alaska. In September 1977, discharge at the Clearwater Creek gaging station and the outlet of Clearwater Lake totaled 34.4 m³/s. Waller, Feulner, and Tisdell (1962) suggested that the aquifer is recharged by seepage losses from the Delta River and Jarvis Creek in the vicinity of Fort Greely, and that the ground water flows northeastward to feed the springs. The springs may also be fed by groundwater recharge from the Tanana River east of the springs, the Gerstle River, and several small streams draining the north face of the Alaska Range.

ARIZONA

Water use may double in Apache County

In 1975, the last year of record, about 37 hm³ of water was used in the 10,600-km² area of southern Apache County. About 70 percent was from surface water and about 30 percent was from ground water. Water use is expected to increase almost 100 percent by 1980, owing to the growing demand for domestic, irrigation, and industrial supplies. Because most of the reliable surface-water supplies are allocated, ground water will be used to meet the future demand.

According to L. J. Mann, nearly all geologic units that underlie the area locally yield water to wells and springs. The Coconino aquifer—which consists of the Permian Coconino Sandstone, the uppermost part of the underlying Supai Formation, and the overlying Kaibab Limestone—probably underlies the entire area. In 1975, the aquifer furnished about 9.5 hm³ of water to wells, and water levels generally have not declined appreciably.

The water in the Coconino aquifer contains less than 500 mg/L of dissolved solids in the southwestern and west-central parts of the area but contains 1,000 to 3,000 mg/L in the southeastern part and most of the east-central parts. In the northern part of the area, the water contains from 3,000 to more than 60,000 mg/L of dissolved solids, which precludes its use for human or livestock consumption, irrigation supplies, and most industrial needs.

CALIFORNIA

Studies show pollution of streams

J. G. Setmire reported that a "one-time-only" intensive sampling was made of the New River at

Calexico in Imperial County, California; field tests were made every 45 minutes for 90 hours.

Pollutant discharges were generally identifiable by an increase in turbidity. Closely paralleling the rise in turbidity was a concurrent increase in pH, with values going from a pre-discharge level of 7.6 to a maximum of 8.8 and back to 7.7 when the discharge had passed. Samples measured for total and dissolved organic carbon had background values ranging from 10 to 20 mg/L, whereas during discharge, highs ranging from 34 to 42 mg/L of dissolved organic carbon and 80 to 161 mg/L of total organic carbon were observed. COD reached 510 mg/L during a waste discharge. No trace elements indicative of industrial pollution were detected.

The river-profile study showed a sharp decrease in DO concentrations between river mile 16 (measured from the International Boundary) and river mile 11—DO concentrations dropped from 3.8 to 0.3 mg/L. The DO minimum was in evidence from river mile 11 to river mile 3.5, and the zone of active deoxygenation extended from river mile 3.5 to river mile 0. The length of the zone of oxygen minimum was variable.

Setmire also reported that results of an urban-runoff study in the basin of Tecolote Creek near San Diego showed the impact of high total-residue loads on Mission Bay; the maximum instantaneous level was 2,730 t/d. The geometric mean concentration of total residue for the study was 1,540 mg/L.

COD of the Tecolote Creek runoff had a geometric mean of 176 mg/L during the study period. The maximum observed concentration of COD was 630 mg/L; however, the load was only 0.44 t/d as compared with 196 t/d during one of the peak discharges when the concentration was 250 mg/L.

High concentrations of lead were observed in the Tecolote Creek runoff. The maximum observed concentration for the study was 3,900 µg/L, whereas the geometric mean was 398 µg/L. The highest lead concentration occurred during low discharge, and exhibited a commonly observed first-flush effect.

Geometric means of phosphorus and total nitrogen were 0.26 and 4.0 mg/L, respectively. The pesticides, chlordane, malathion, and diazinon, occurred in amounts that exceeded the maximums set by EPA.

Geothermal gradient is 800°C at Coso Hot Springs

W. R. Moyle, Jr. (1977), reported that temperature measurements made in the Coso Hot Springs area of Inyo County in California ranged from near freezing (4°C) in a mountain spring to above boil-

ing (142°C) at the bottom of the deepest well. Temperature gradients below land surface ranged from 35°C/km in nonthermal areas to nearly 800°C/km in thermal areas. Six areas have water or ground temperatures that greatly exceed the local average air temperature; these are Coso Hot Springs, Devils Kitchen, the Nicol area, Wheeler Prospect, and areas on the western and north-eastern sides of Sugarloaf Mountain. All temperatures measured in springs surrounding Coso Hot Springs and Devils Kitchen indicated that the springs are nonthermal and are strongly influenced by the ambient air temperature. One spring measured twice showed a variation of 21°C between summer and winter temperatures.

Nitrogen studied in the Santa Ana River basin

A major effort to control and maintain the quality of water in an alluvial aquifer, which is being recharged with imported surface water, is currently underway in the Upper Santa Ana River basin of California. To help meet this objective, the USGS is making a study of nitrate in the unsaturated zone.

Water-level rises in 1968 and 1969 following above-average precipitation were accompanied by measurable increases in the dissolved nitrate-nitrogen concentration in the water. Earlier studies showed that plans to increase the water-table elevation by artificial recharge might cause additional nitrate from the unsaturated zone to dissolve in the water. To evaluate this possibility, J. M. Klein and W. L. Bradford examined core samples taken from the unsaturated zone at depths to 55 m at various land-use locations in order to determine the relative areal and vertical nitrate-nitrogen concentrations.

In general, nitrate in the interstitial water of the unsaturated zone decreased significantly with depth except for occasional zones of higher nitrate which seldom exceeded values observed at the land surface. The observed nitrate-nitrogen concentrations at the land surface ranged from 0.8 to 193 milligrams of nitrate per kilogram of soil, whereas calculated total nitrogen in the test holes ranged from 87 to 1,035 milligrams of nitrate-nitrogen. In general, land that required fertilization and irrigation was underlain by the largest nitrate-nitrogen concentrations.

In order to better understand the sources of nitrogen and to study isotopic fractionation of nitrogen as water percolates through the unsaturated zone, nitrogen-isotope ratios of soil-water extracts were determined. The mechanisms acting in the nitrogen cycle control the isotopic fractionation in the soils

of the unsaturated zone and thus account for the observed range of isotopic (δN^{15}) values. According to Klein and Bradford, nitrogen is preferentially fractionated in favor of N^{14} , the lighter isotope; however, the enrichments are generally small. Fractionation of the nitrogen isotopes is thought to be associated with most reactions in the nitrogen cycle.

Observed soil-nitrogen isotopes ranged from $\delta N^{15} = -6.7$ to $\delta N^{15} = 15.4$. Significant areal and vertical variations in the nitrogen isotopes were noted in the 14 holes drilled. These variations are attributed to varying soil types, land uses, soil moisture, and the degree of completeness of the nitrogen-mineralization nitrification or denitrification reactions.

Ground-water studies in desert basins

Water supplies in Death Valley National Monument in California and its vicinity are limited to ground-water sources, almost without exception. Ground water underlies the entire area, but its availability and suitability for use are greatly restricted by its chemical quality and, to a lesser extent, by the permeability of water-bearing materials. G. A. Miller (1977) reported that promising areas for additional ground-water supplies on the valley floor are (1) the Eagle Borax Spring-Bennetts Well area, (2) near Midway well and Triangle Spring, and (3) northern Mesquite Flat. Data indicated that ground water in those areas contains 500 to 1,500 mg/L of dissolved solids and locally is under sufficient artesian pressure to flow from wells. Because of the paucity of subsurface hydrologic data, test drilling is necessary to appraise the ground-water resources of these areas.

Johnson Valley, an alluvial ground-water basin in the Mojave Desert, is a relatively undeveloped area that is being considered for conjunctive use of water imported from northern California. According to J. J. French (1978), the basin contains about 310 hm^3 of water in storage, of which about one-half can be considered recoverable. This water could conceivably be used as a supplemental water supply for the water-short areas of the desert before imported water becomes available.

About 310 hm^3 of void space in the unsaturated alluvium is available for storage of imported water from the California Aqueduct by way of the proposed Desert Pipeline, but not all of the recharged water could be recovered. The ground water is satisfactory for public supplies, although water from some areas is high in fluoride concentration and

should be mixed with water of low-fluoride concentration.

The water level in two areas of Lucerne Valley declined a maximum of 18 m from 1954 to 1976. D. H. Schaefer inferred that the declines are the result of heavy pumping for the irrigation of alfalfa. The lowering of water levels has caused many shallow domestic wells to go dry. Well yields in the valley generally range from about 1 to nearly 65 L/s. About 300 hm³ of ground water was extracted from 1950 to 1976, and about 2,100 hm³ remains in storage.

An area of poor-quality water (dissolved-solids concentration of more than 2,000 mg/L) exists in the valley around Lucerne Lake and borders the two pumping depressions. The poor-quality water did not show any definite sign of movement toward the pumping depressions from 1954 to 1976, but the possibility exists for future movement.

Lucerne Valley may be hydrologically suitable for artificial-recharge operations of some type. Preliminary data suggested an area for artificial recharge that would benefit most of the areas affected by the water-level declines; however, a detailed investigation is needed before recharge operations are begun.

Water supply at Beale Air Force Base unchanged

Recharge to the well field at Beale Air Force Base near Yuba City in California is principally by ground-water inflow from the north. R. W. Page estimated that ground-water inflow in 1975 was 5 hm³/yr. Discharge from the well field is by pumping and by ground-water outflow generally southward. In 1975, discharge from the well field by pumping was about 3.8 hm³, and about 1.0 hm³ by ground-water outflow. The difference between ground-water inflow and ground-water outflow nearly equaled pumpage at the base, and water levels at the base were about the same for spring 1975 and spring 1976.

HAWAII

Wailuku River basin characterized

The first of two synoptic surveys was made to determine the baseline characteristics of the Wailuku River, which heads at an altitude of about 3,350 m on the eastern slope of Mauna Kea on the Island of Hawaii. From its head, the river flows over a 37-km course to the ocean at Hilo Bay where the average discharge is 7.7 m³/s. The stream is

characterized by numerous waterfalls and pools interspersed with short, almost level reaches. The streambed is volcanic bedrock overlain by boulders and coarse gravel derived from the bedrock. Land use within the basin is 1 percent urban, 3 percent cultivated crops, 46-percent forest, 20 percent pasture, and 30 percent conservation.

J. J. S. Yee and C. J. Ewart II found that above an altitude of 1,000 m, the stream fauna is sparse and consists mostly of aquatic insects. At lower altitudes, the fauna increase and includes atyid shrimp, chironomid larvae, damselfly nymphae, and hihiwai (*Neritina granosa*, a snail). Guppies, gobies, and crayfish are common in lower reaches of the stream. At the 325-m level, the dissolved-solids concentration of the water is about 50 mg/L and the hardness is seldom greater than 20 mg/L.

Ground-water yields small in Truk Islands

In observations made during an intensive drilling program on the island of Moen in the Truk lagoon, Eastern Caroline Islands, D. A. Davis confirmed earlier estimates that indicated that the volcanic rocks of the Truk Islands are generally poor water-bearing materials. The greatest yields at the test holes and wells came from sections of basaltic and andesitic saprolite that still retains the relict textures of the original rock. Among the holes tapping water in the saprolite, specific capacities during pumping ranged from 1 to 6 L s⁻¹ m⁻¹. Among those drilled in unweathered rock and in weathered rock reduced by decomposition to nearly homogeneous clay, the specific capacities ranged from about 0.004 to 0.1 L s⁻¹ m⁻¹. The productive saprolite, which occurs without predictable patterns in irregular, discontinuous zones of variable size, makes up only a small part of the rocks penetrated by the test holes and wells.

IDAHO

Ground-water stress in southeastern Idaho

H. R. Seitz reported that increased urbanization near Pocatello, increased phosphate mining near Soda Springs, and increased irrigation throughout the Bannock, Bear Lake, and Caribou Counties may stress groundwater resources in the three-county area.

Dissolved-solids concentrations in water from 103 wells ranged from 170 to 1,800 mg/L. Hardness of water in the study area ranged from 80 to 1,800 mg/L. The high hardness values are associated with water from travertine deposits.

Values of nitrate plus nitrite as nitrogen (N) ranged from 0 to 29 mg/L. The high values are in water from sediment in Marsh Creek Valley. Other high values of 15 to 19 mg/L were noted in Gem Valley north of Soda Springs.

Coliform-bacteria determinations indicated an absence of pathogenic bacteria in ground water of the study area.

Water resources in Camas Prairie

Ground-water withdrawals in Camas Prairie in south-central Idaho increased from 1.7 hm³ in 1957 to 12.3 hm³ in 1977. A study by H. W. Young indicated that declines in the potentiometric surface for the same period exceeded 9 m. An inventory of more than 200 wells indicated that ground water occurs under watertable and artesian conditions in both sand and gravel of valley-fill deposits and in basalt of the Bruneau Formation. Recharge, estimated to be 33.3 hm³ annually, is from percolation losses from adjacent streams and from precipitation on the valley floor.

NEVADA

Waste brines are rich in metals

Waters having a wide range of dissolved-solids concentrations and pH (measured ranges from 1,100 to 100,000 mg/L and 1.8 to 11.3 pH units, respectively) are associated with ore processing at a copper mine in Lyon County. A. S. Van Denburgh reported that the acid, sulfate-rich brines contain large concentrations of several constituents normally present only in trace amounts. Measured values, in milligrams per liter are: Al, 6,400; As, 42; B, 11; Cr, 9; Co, 28; Cu, 330; F, 470; Fe, 30,000; Mn, 420; Ni, 21; P, 990; Pb, 3; U, 6.2; and Zn, 56. These brines are the result of waste disposal in evaporation ponds, whereas the much more dilute fluids are recycled. The measured specific conductance of shallow ground water less than about 0.5 km downgradient from the disposal and recycling areas characteristically ranges from 1,000 to 25,000 $\mu\text{mho/cm}$, with higher values near the ponds. Measured conductances for shallow waters more than 0.5 km away range from 400 to about 1,000 $\mu\text{mho/cm}$.

Water supply stable in Fort McDermitt Indian Reservation

Water quality and availability in the Fort McDermitt Indian Reservation in north-central Nevada are satisfactory for current needs, according to F. E. Arteaga. The valley-fill reservoir is more than 370 m

thick in at least one place near McDermitt, and at least 107 m thick at a site near Hog John Ranch (the reservation is comprised of two separate areas, one near McDermitt and the other at the ranch). Water levels have remained virtually unchanged in the McDermitt area for the last 12 years. They have remained unchanged also in the Hog John Ranch area for nearly 30 years. Measured transmissivities at seven wells in the McDermitt area ranged from 59 to 1,020 m²/d. Two short pumping tests made near the ranch indicated transmissivities of 59 and 153 m²/d. Water quality in the ranch area apparently tends to improve with depth, at least in the upper 76 m for which data are available.

Hydrology and geology of the Carson City area

In a cooperative program, the USGS and the Nevada Bureau of Mines and Geology evaluated hydrologic and geologic conditions and hazards in the rapidly urbanizing Carson City area. T. L. Katzer and C. V. Schroer (USGS) and Dennis Trexler (Nevada Bureau of Mines and Geology) mapped geology, ground-water levels, and aquifer yields, and delineated potential hazard areas of floods, sediment movement, and geology; the hazard areas are on the urbanizing alluvial fans west and north of downtown Carson City. Water levels near Carson City's main public-supply wells declined about 1.5 m/yr from 1973 to 1977.

A gravity survey by F. E. Arteaga determined that the alluvial thickness is as much as 670 m in Eagle Valley. This is part of the information being acquired for use in a two-layered, finite-element ground-water model for the valley, which includes Carson City. Ground-water pumpage in the valley increased from about 1.2 hm³ in 1965 to 5.7 hm³ in 1975. A moratorium is in effect prohibiting new subdivisions until additional sources of water are assured. The model will provide a more quantitative approach to estimating ground-water availability in the area, and it will be used to evaluate the intermediate and long-term impacts of development alternatives.

Overdraft in Pahrump Valley

Pahrump Valley is an arid basin about 110 km west of Las Vegas, Nev. The valley has been a prominent agricultural area for many years, and is currently undergoing residential development. J. R. Harrill reported that ground-water pumpage increased from about 0.6 hm³/yr in 1913 to nearly 50 hm³/yr in 1975. The ground-water budget is esti-

mated to have had about 27 hm³/yr of inflow and outflow under natural conditions. However, the perennial yield was estimated to be only about 15 hm³/yr because a substantial quantity of ground water leaves the valley by subsurface outflow through carbonate-rock aquifers. Ground-water pumpage has exceeded the perennial yield since the 1940's. However, because some pumpage has been recycled back to the ground-water body as return flow, a substantial overdraft did not develop until the early 1950's when annual pumpage first exceeded 25 hm³. Water levels have declined appreciably in response to the heavy pumping. Net declines since pumping began range from 1 m in areas remote from pumping to slightly more than 30 m near areas of heavy pumping. By 1975, the declines had dried up two large springs, resulting in the capture by pumping of about 12 hm³/yr of former spring discharge.

Aquifers underlie Carson Desert

The Fallon area is in Carson Desert, the terminal valley of the Carson River basin in northwestern Nevada. The alluvial ground-water basin is saturated nearly to land surface, but most of the water is saline and not potable. According to P. A. Glancy, a basalt aquifer of limited area and volume, imbedded within the much larger alluvial system, is the major known source of potable ground water in the Carson Desert. An electrical-resistivity study generally outlined the basalt aquifer (Zohdy, Bisdorf, and Glancy, 1977). The aquifer commonly yields about 4,000 L/min, with a drawdown of about 1 m during prolonged (several-day) pumping periods.

An alluvial aquifer, about 5 to 10 m below land surface, that is more areally extensive than the basalt furnishes domestic water to many residents within the Newlands Irrigation Project. The shallow aquifer seems generally related to and dependent on infiltration of irrigation water from the project lands. A similar shallow alluvial aquifer peripheral to the irrigated lands is generally saline. Two years of biweekly water-level measurements at about 30 sites in the shallow-aquifer systems disclosed that water levels beneath irrigated areas characteristically fluctuated 0.5 to 1.5 m annually; those beneath nonirrigated areas generally fluctuated less than 0.5 m during the year.

OREGON

Ground water in southern Douglas County

Wells in the Myrtle Creek-Glendale area in southwestern Oregon produce water of variable quantity and quality. According to F. J. Frank, the wells in the area have an average depth of about 33.5 m and produce from less than 0.63 to about 4.7 L/s from Jurassic, Cretaceous, Tertiary, and Quaternary rocks. Dissolved-solids concentrations generally range from 150 to 500 mg/L. However, water with as much as several thousand milligrams per liter of dissolved solids is found in places.

Streets contribute much lead to urban runoff

A comparison was made between concentrations of lead in street-sweepings and the ratio of lead to suspended sediment during storm runoff from two urban basins near Portland, Oreg., by T. L. Miller and S. W. McKenzie. In one basin, they measured 820 mg of lead per 1 kg of street sweepings and 630 mg of lead per 1 kg of suspended sediment in the stream. The second basin yielded street-sweepings with 750 mg of lead per 1 kg and suspended sediment in the stream containing 260 mg of lead per 1 kg. These comparisons suggested a possible relationship between the concentration of lead in street-sweepings and the ratio of lead to suspended sediment in urban runoff. A comparison made for zinc, however, showed the ratio of zinc to suspended sediment to be as much as 13 times higher than the zinc in street-sweepings.

WASHINGTON

Studies on Indian Reservations

Colville (No Name Creek Basin).—No Name Creek Valley is a narrow trough cut in granitic bedrocks and has a low alluvial divide in the northern one-third of the valley separating it into the No Name Creek Basin on the south and the Omak Creek Basin on the north. Omak Creek is the larger stream and enters the valley through a narrow gorge in the eastern granite wall. The valley is partly filled with unconsolidated gravel, sand, and silt to depths as great as 50 m, and contains a ground-water reservoir that supplies four irrigation wells and several domestic-supply wells. The ground-water reservoir also feeds springs that give rise to No Name Creek and it contributes some water to the Omak Creek Basin to the north.

Before 1976, the ground-water divide was naturally about 0.9 km north of perched Omak Creek where it enters the valley. About 0.72 hm³ of leakage from Omak Creek recharges the No Name Creek ground-water reservoir. By 1977, ground-water withdrawal of 1.23 hm³/yr in No Name Creek Basin had caused the ground-water divide to shift to a position about 1.2 km north of the topographic divide. This increased the drainage area contributing to the No Name Creek ground-water reservoir for about 3 months so that during a year of normal flow, a total of about 0.74 hm³ of leakage from Omak Creek could be captured. In 1977, however, drought caused Omak Creek to go dry for a short period, and recharge was about 0.06 hm³ less. According to D. R. Cline (1978), as much as 1.36 hm³/yr can be pumped from the central part of the ground-water reservoir. This pumpage would cause the ground-water divide to shift farther northward, resulting in the capture of additional recharge from Omak Creek; the total leakage would be about 0.86 hm³.

Lower Elwha.—A large quantity of water of good chemical quality and uniform temperature is needed on the Lower Elwha Indian Reservation, Clallam County, for use in a salmon hatchery and several large rearing ponds. According to K. L. Walters, wells capable of yielding at least 125 L/s can be developed from alluvial deposits that underlie most of the reservation. The Elwha River flows through the reservation and contains sufficient water of excellent chemical quality, but the temperature fluctuates between 2° C and 13° C. The chemical quality of ground water on the reservation is nearly identical to that of the Elwha River, but the temperature range is better in that it fluctuates only between 7° C and 9° C.

Makah.—According to K. L. Walters, test drilling on the Makah Indian Reservation in Clallam County indicated that ground-water supplies sufficient only for individual domestic use can be developed. Streams are the only sources of water large enough to supply an expanded community water system and proposed tribal fish-rearing facilities, but these streams carry considerable amounts of suspended sediment during winter high-flow periods. The chemical quality of surface water on the reservation is generally good, but without storage the quantity may be barely adequate in late summer and early fall for the proposed new uses.

Port Gamble.—Ground water occurs generally in two aquifer systems beneath the Port Gamble Indian Reservation in Kitsap County, according to W. E. Lum II. Wells tapping a shallow aquifer yield

only enough water to supply individual households. A deeper artesian-aquifer system yields as much as 4 L/s to wells. The estimated natural discharge of ground water from the deeper aquifer is about 14 L/s; about 6 L/s of this amount could be withdrawn without greatly increasing the danger of seawater intrusion.

Port Madison.—W. E. Lum II reported that about 200,000 m³/yr of ground water is available on a long-term basis on the Port Madison Indian Reservation. This represents enough water to meet the domestic needs of more than four times the present population. Of nine streams on or near the reservation, average later-summer low flows for a 7-day period every 2 years were 8.5 L/s or less. No evidence of major pollution of ground or surface water now exists, but seawater intrusion into the ground-water system could accompany increased ground-water development.

Swinomish.—Average inflow to the hydrologic system of the Swinomish Indian Reservation in Skagit County is about 680 L/s, virtually all of which is natural precipitation. Outflow equals inflow and consists of evapotranspiration (400 L/s), subsurface outflow (190 L/s), and surface-water outflow (90 L/s). Recharge to the ground-water system is about 230 L/s. B. W. Drost reported that three major, hydrologically distinct, unconsolidated units were identified by seismic refraction, test drilling, driller's logs, and surficial mapping. Human interaction with the hydrologic system is negligible; the average rate of water use is about 2.5 L/s. Tidal efficiencies of up to 42 percent were observed in shoreline wells. The freshwater-saltwater zone of diffusion is at least 45 m thick. Ground-water development in the area can probably be increased to a net rate of withdrawal of 45 L/s or more without adversely affecting the hydrologic system.

Tulalip.—Total recharge (precipitation minus actual evapotranspiration) during the 1977 water year in the Tulalip Indian Reservation was about 168 mm, well below the mean of 460 mm, and the lowest in 43 years of record. B. W. Drost reported that this drought condition resulted in the lowest ground-water levels on record and mean streamflows 52 to 58 percent below those of the previous year. Increased precipitation since the beginning of the 1978 water year (October 1, 1977) has restored ground-water levels and mean streamflows to near-normal conditions.

Yakima.—A four-layer ground-water model of the aquifer system in the Toppenish Creek Basin was calibrated by J. A. Skrivan. A steady-state analysis

of 1954 conditions indicated that annual recharge to the 1,600-km² basin was 36 hm³ from precipitation and about 5 hm³ from underflow from adjacent basins. The transient analysis used historical records for the period 1954–72, during which time there were measured water-level declines of as much as 29 m in the basalt aquifers. A projection of conditions to 1982 showed that basalt-aquifer water levels could drop as much as 11 m/yr between 1978–82 if pumpage during that period were to increase 80 percent.

Coal-hydrology studies

Maximum and minimum recoverable water reserves within the Roslyn mines for emergency use during drought were estimated at about 34 and 15 hm³, respectively. These reserves occur in 10 separate reservoirs in mined-out parts of three coal seams in Kittitas County. Water quality was judged to be good, except for sulfide content which can be managed by aeration. F. A. Packard suggested six well locations for draining the maximum possible volume of water from the mines. Major potential problems are surficial subsidence and prior ground-water rights.

Surface-water quantity and quality in the Wilkeson Carbonado mining district in Pierce County is adequate for hydraulic mining of coal; however, according to Packard and W. L. Haushild, during low-flow periods, some storage may be necessary for mining on small streams such as Wilkeson Creek. Water-quality samples taken during an experimental borehole hydraulic-mining test indicated that suspended sediment would be a major problem associated with disposal of waste water from hydraulic mining in the district. Where presently abandoned mines are to be reentered, dissolved sulfide will present a waste-disposal problem.

F. A. Packard, L. A. Fusté, and M. O. Fretwell reported that analyses of water samples from 50 abandoned coal mines indicated that environmental problems from coal-mine drainage should be of only moderate concern. Results from the detailed study of a typical drainage site showed that there are some significant mixing-zone effects on stream quality and biology. However, when complete mixing is achieved, no significant change in the aquatic biology can be found and the chemical-quality changes are small. On the basis of mine-drainage analyses, detailed mine-drainage-study data, and baseline data gathered over a 1-year period, a biologic- and water-quality monitoring system was proposed for two

stream basins where underground coal mining will occur in the near future.

Test well drilling in Washington State

H. E. Pearson and W. E. Lum II reported that a test well in the Yakima River canyon between Ellensburg and Yakima penetrated basalt of the Miocene Columbia River Basalt Group to a depth of about 183 m. The well had a strong artesian flow of about 100 L/s at a depth of about 90 m. The temperature of the water was 23°C and the shut-in pressure of the well was about 1.1 kg/cm². Little additional water was encountered in the depth interval between 90 and 183 m. A second test well, which was drilled in the Badger Pocket area about 16 km southeast of Ellensburg, established that the basalt of the Columbia River Basalt Group is overlain in that area by more than 220 m of unconsolidated materials.

Irrigation increased in Horse Heaven Hills

According to Dee Molenaar, surface and ground water are being used increasingly for irrigation in the semiarid to arid Horse Heaven Hills region formerly characterized by dryland wheat farming. In 1977, about 26,000 ha were irrigated—about 24,400 ha by surface-water diversions from the Columbia River and about 1,500 ha from ground water (W. G. Gerlitz, written commun., 1977). Much of the ground-water irrigation is in an area where well development has disclosed the existence of an extensive artesian aquifer in the Miocene Yakima Basalt; several wells have flows of 100 L/s or more.

Lake studies

Primer on limnology.—A primer on lakes in Washington was written to acquaint the lay reader with the basic physical, chemical, and biological processes operating in Washington lakes. According to N. P. Dion, the report includes discussions of lake origins, lake-water chemistry, typical aquatic organisms, and the aging of lakes. In addition, the report contains a glossary of commonly used limnological terms and numerous references pertaining to lakes in general and the lakes of Washington in particular. The report, to be published by the Washington Department of Ecology, will also give readers a better understanding of the results reported in previous technical papers that describe present conditions in more than 700 lakes in the State.

Nutrient loading and budget of Wilderness Lake.—The results of a water-budget study of Wil-

derness Lake (in King County), a candidate for lake-quality restoration, indicate that 68 percent (449,000 m³) of the inflow to the lake is by ground-water seepage and that 73 percent (484,000 m³) of the outflow is on the surface. Based on the results of the water budget, the theoretical water-renewal time of the lake is 2.6 years. According to N. P. Dion, the rates of the external nutrient loading of Wilderness Lake from precipitation and ground water alone are 0.96 and 0.33 g of nitrogen and phosphorus, respectively, per square meter of lake surface per year. Nutrient contributions from other sources, such as the numerous bathers who use the lake, were not assessed but could be significant.

Salmon propagation in Ozette Lake.—A study of the Ozette Lake drainage basin in Clallam County indicated that the lake, its tributaries, and the lake-outlet stream have many of the characteristics that are generally supportive of good sockeye-salmon production, even though the run of sockeye to the lake has decreased appreciably over the past 25 years. Among the characteristics studied were (1) suitability of spawning gravels in the tributaries and along the lake shoreline, (2) water temperatures in the lake and tributaries, and (3) DO concentrations at all depths of the lake. According to G. C. Bortleson and N. P. Dion, Ozette Lake compares favorably with eight other Washington and Alaska sockeye-producing lakes in respect to concentrations of zooplankton, the chief food source for sockeye salmon.

Nisqually, an undeveloped lake.—Because of the unique location near U.S. Army artillery ranges, the existing water resources of the Nisqually Lake study area are almost undeveloped. According to H. E. Pearson and N. P. Dion, the only surface waters significant in the study area are Muck Creek, Nisqually Lake, and the outflow channel of a spring. The absence of wells in the area precludes any firm conclusions on the availability of ground water, although it probably does occur in unconsolidated and poorly consolidated glacial materials. Nisqually Lake has no natural surface-water inflows or outflows; however, water is diverted into the lake from Muck Creek during the winter and spring months. The lake is too shallow to stratify thermally; the warm surface-water temperatures observed in late spring and summer extended to the bottom of the lake. Because of the lack of a cooler layer of water at depth, the lake would probably be better suited to warm-water fish species than to cold-water species.

Cyclic variations in drain-water quality

An assessment of water quality in the irrigation drains of the Sulphur Creek Basin of Yakima County during the 1976 irrigation season and the following nonirrigation season showed that sediment and nutrient concentrations and discharges varied in an annual cycle that can be described by harmonic (sine-wave) mathematical approximations. P. R. Boucher and M. O. Fretwell reported that the rankings of the subbasins of Sulphur Creek according to sediment yield correspond directly with their rankings according to average land slope of the irrigated parts. Although nitrate concentrations are generally higher during the nonirrigation season than during the irrigation season, nitrate discharges are generally larger in the irrigation season because of greater streamflow.

Model predicts snowmelt runoff

W. V. Tangborn employed a hydrometeorological model that uses existing observations of runoff and precipitation to predict seasonal snowmelt runoff on the Skokomish, Nisqually, and Cowlitz Rivers in Washington. Runoff from those drainages is used for hydroelectric-power generation by the Tacoma City Light public utility. Accuracy was within the given error limits, even though a record drought occurred during the 1977 season (Tangborn, 1977). Evaluation of the model's applicability was made for the Lewis, Cedar, Tolt, and Baker Rivers in Washington in preparation for experimental predictions for those basins during the 1977-78 season. The model was also tested on the South Fork Flathead River of Montana and the Salt and Verde Rivers of Arizona. Results of retrospective predictions for the previous 10 to 20 years indicated that this model reduces the mean prediction error by 20 to 50 percent on those drainage basins. Accuracy and versatility were increased by revising the computer program to use daily rather than monthly increments of runoff and precipitation data. Predictions can now be made on any day each month, and the prediction season can be of any number of days in length.

SPECIAL WATER-RESOURCE PROGRAMS, DATA COORDINATION, ACQUISITION, AND STORAGE

OFFICE OF WATER DATA COORDINATION

The Office of Water Data Coordination (OWDC) continued to implement Office of Management and

Budget Circular A-67, which sets forth guidelines for coordinating certain water-data-acquisition activities by Federal agencies. During FY 1978, progress was made in several major areas of OWDC's coordination program. These areas included compiling new editions of the "Catalog of Information on Water Data," and releasing the introduction and chapter 5 of the "National Handbook of Recommended Methods for Water-Data Acquisition."

The "Federal Plan for the Acquisition of Water Data, Fiscal Years 1978 and 1979" (U.S. Geological Survey, 1978a) summarizes the 1978 regional plans (U.S. Geological Survey, 1978b) from each of the 21 major water-resources regions, presenting information from all Federal agencies on active, planned, and needed activities related to streamflow and stage, surface-water quality, and ground-water quality. The Federal plan also documents several other activities related to the coordination effort, including the National Water Data Exchange (NAWDEX), the stream-quality and stream-quantity components of the Level I accounting element of the National Water Data Network, the National Water Quality Surveillance System of EPA, and the water-data-acquisition activities of several divisions of the USGS.

The computer file of the "Catalog of Information on Water Data" (U.S. Geological Survey, 1978c) was updated through 1977, and 21 volumes (one for each of the 21 Water Resources Council's regions) were prepared. Each volume contains information on streamflow and stage, surface-water quality, and ground-water quality activities. Short-term data activities (station activities with less than 3 years of continuous record) of all participating agencies are now included in the catalog. In addition, a separate catalog prepared during this period summarizes areal investigations and miscellaneous activities for all 21 WRC regions (U.S. Geological Survey, 1978d).

A special edition of the catalog was printed—a four-volume "Index to Stations in Coastal Areas," containing one volume each for the Atlantic, Gulf, Pacific, and Great Lakes Coasts (U.S. Geological Survey, 1978e). Because of the great interest shown in the coastal zone, a new edition is tentatively planned for next year.

Another special edition of the catalog (U.S. Geological Survey, 1978f) was developed to meet the burgeoning need for knowledge about water-data activities in coal-resource regions of the U.S. This edition lists water-data-acquisition activities in counties with coal resources and includes informa-

tion on streamflow and stage, surface-water-quality stations, and ground-water-quality stations.

As a result of recommendations made by working groups of the Advisory Committee on Water Data for Public Use, a National Water-Use Data System has been designed and is managed by the USGS's Water Resources Division. The system, described in more detail in another section of this report, will ascertain the degree of use and the status of development of the Nation's water resources. In this cooperative program, State and local agencies will handle most of the collecting, storing, and retrieving of data, and the USGS will help finance the program by matching State and local monies.

The "National Handbook of Recommended Methods for Water-Data Acquisition" is nearing completion. The handbook presents water-data-acquisition methods recommended by over 180 scientists representing 30 Federal agencies and more than 100 specialists representing non-Federal organizations. When complete, the new handbook will consist of 10 chapters on surface water, ground water, sediment, biological and bacteriological quality of water, chemical and physical quality of water, soil moisture, drainage-basin characteristics, evaporation and transpiration, snow and ice, and hydro-meteorological observations. In addition, an appendix in the handbook will contain recommendations on metric units, conversion factors, precision of metric measurements, and metric conversion of equipment for all measurements related to hydrologic data. To develop greater non-Federal participation, discussions were held with many standards-developing societies.

Each of the handbook chapters will be published and distributed as it becomes available. The introduction and chapter 5 ("Chemical and Physical Quality of Water and Sediment") were released (U.S. Geological Survey, 1977), and over 6,000 copies were distributed to requesters in the United States. The handbook is being published in looseleaf form so it can be continuously updated to incorporate the latest technology. The working group for chapter 5 has already developed an update of new and revised methods for release in early 1978.

Each of the USGS Water-Resources Division district offices, all State agencies concerned with water-resources planning and management, and all local "208" planning groups, were given complete sets of the 13 reports of the Willamette River assessment so that they could be advised of the intensive river-quality assessment program. The USGS is studying

a proposed 5-year program to speed up the intensive water-quality assessments on estuaries, lakes, and reservoirs, as well as on large river systems. The river-quality assessments of the Chattahoochee River basin of Georgia, and the Yampa River basin, in Colorado and Wyoming, progressed during the year.

The series of uniform, nationally consistent 1:500,000-scale hydrologic unit maps (U.S. Geological Survey, 1974), prepared by the USGS in cooperation with the U.S. Water Resources Council, are being used extensively. The series (consisting of 47 separate maps covering the 50 States and Puerto Rico) accurately delineates U.S. drainage basins averaging about 1,800 km² in area. The four-color maps show a distinct numeric computer code assigned to each river basin and provide information on drainage, culture, hydrography, and hydrologic boundaries for each of the 21 regions and 222 subregions designated by the Water Resources Council. They also depict the boundaries and codes of 349 accounting units within the National Water Data Network and the approximately 2,100 cataloging units of the USGS's "Catalog of Information on Water Data." The hydrologic units nest hierarchically within each other, and range from the smallest (cataloging units) to the largest (regions). Also included on the maps are State and county codes that conform with the numerical codes of the Federal Information Processing Standards (FIPS).

OWDC prepared a nontechnical pamphlet describing State hydrologic unit maps and their varied uses. Released as a USGS pamphlet, the publication depicts a portion of one of the four-color maps with its legend and with information on price and addresses where these maps can be obtained. Digitization of all hydrologic-unit boundaries at a scale of 1:500,000 was completed, thus permitting (1) computation of all drainage-basin areas, (2) computer plotting of boundaries at various scales, and (3) computer conversion of locations by latitude and longitude coordinates into locations by hydrologic-unit code.

Small-scale National hydrologic unit maps also were prepared. The maps show all regions, subregions, and accounting units in the 50 States and Puerto Rico at scales of 1:3,168,000 and 1:7,500,000.

The [Federal] Interagency Advisory Committee on Water Data met in Gettysburg, Pa., September 15-16, 1977. At the meeting, progress reports from the Working Group on Precipitation Quality, the Working Group on Water Quality Data Needs for Small Watersheds, and the Coordinating Council for

Water Data Acquisition Methods were presented. The Committee recommended that the draft report of the Working Group on Precipitation Quality be reviewed by the non-Federal Advisory Committee, which had expressed interest in precipitation quality at the 11th (joint) meeting.

The Committee also discussed current problems and future trends in publishing water data, the "Catalog of Information on Water Data," developments in the ground-water component of the National Water Data Network, and agency program plans and needs for water-data in fiscal year 1978 and 1979. Representatives of 24 agencies and 15 observers attended the 2-day meeting. A summary of the meeting was printed and distributed (Interagency Advisory Committee on Water Data, 1978).

The Advisory Committee on Water Data for Public Use (non-Federal) met in Houston, Tex., November 29-December 1, 1977. The Committee discussed the program made over the past year and the implementation of Office of Management and Budget Circular A-67, the progress made on the Federal interagency project to develop the "National Handbook of Recommended Methods for Water Data Acquisition," a report of the Committee's Working Group on River-Quality Assessment, and current developments in the ground-water component of the National Water Data Network. Ad hoc working groups were impaneled at the meeting for one day to consider (1) current practices and future trends in publishing water data, (2) the National Water-Use Data System, and (3) a national ground-water information base. Recommendations of the three working groups were presented the last day of the 3-day meeting and were published in a printed summary of the meeting (Advisory Committee on Water Data for Public Use, 1977).

NATIONAL WATER DATA EXCHANGE

The National Water Data Exchange (NAWDEX) provides assistance to users of water data in the identification, location, and acquisition of needed data. NAWDEX consists of a membership of over 100 organizations throughout all levels of Federal, State, and local governments, as well as interstate organizations, universities, and private organizations that work together to make their water data readily and conveniently available. Membership is voluntary and open to any water-oriented organization that wishes to take an active role in NAW-

DEX activities. There are no dues or fees for membership.

NAWDEX services are available through a program office located at the USGS National Center in Reston, Va., and a nationwide network of Local Assistance Centers (LAC's). A total of 53 LAC's are operating in 45 States and Puerto Rico. Most centers are equipped with computer terminals, thereby providing an extensive telecommunication network for access to the computerized directory and indexes maintained by the NAWDEX Program Office. These centers have direct access to the computerized files of the National Water Data Storage and Retrieval System (WATSTORE) of the USGS, and they provide referral services to data systems maintained by NAWDEX members.

Systems available through members include several State-level data systems, the Water Resources Scientific Information Center of the U.S. Department of the Interior, the Environmental Data Service of NOAA, and the Water Resources Document Reference Centre of the Inland Waters Directorate of the Canadian Department of Fisheries and the Environment. Access to data from the Storage and Retrieval system of EPA is also provided by the NAWDEX Program Office in Reston, Va., and the LAC facilities provided by the Texas Natural Resources Information System in Austin, Tex.

NAWDEX maintains a computerized Water Data Sources Directory which identifies organizations that have water data available, locations within these organizations from which data may be obtained, the types of data available, the geographic areas in which the data are collected, the media in which the data are available, and alternate sources for acquiring an organization's data. Over 400 organizations have been registered in the Directory. A computerized Master Water Data Index is also maintained that identifies individual sites for which water data are available, the locations of these sites, the organizations collecting the data, the hydrologic disciplines represented by the data, the periods of record for which data are available, the major parameters for which data are available and the frequency of measurement of these parameters, and the media in which the data are available. Over 180,000 sites operated by 318 organizations have been indexed.

Through its Water Data Sources Directory, Master Water Data Index, and services provided by its membership, NAWDEX serves as a central source of information on water data available from a large number of data collectors.

WATER-DATA STORAGE SYSTEM

The National Water-Data Storage and Retrieval System (WATSTORE) is a large-scale computerized system developed to process and disseminate water-resource data collected by the USGS. Representative WATSTORE products are: computer-printed tables and graphs, statistical analyses, digital plots, and data in machine-readable form. The computer system consists of a central computer located in Reston, Va., and remote terminal facilities in nearly every State.

During 1977, several major WATSTORE files grew significantly. The Daily Values File, which contains data on daily discharge, was expanded to include about 10,600 regular streamflow stations. Data in this file are compatible with a variety of statistical programs for analysis on the basis of calendar years, water years, climatic years, or any other period desired.

By March 1978, the Ground-Water Site-Inventory File contained hydrologic, geologic, and well-inventory data on more than 580,000 ground-water sites. To facilitate file management, the data base was divided into four files, each of which corresponds to one of the four water-resource areas.

The Peak-Flow File, which contains nearly 400,000 measurements of annual maximum-streamflow and gage-height values at surface-water sites, is being revised so that it will be more compatible with other files in the system. The new version of the Peak-Flow File will enable partial peak data to be sorted, eliminate duplication of station header data, improve input and output formats, and increase retrieval capabilities.

Newly acquired access to the Taxonomic Biological Data File of the Central Laboratory System provides users with additional methods for obtaining statistical analyses and publication tables.

Minicomputers are being used in some States to maintain local files, to reproduce maps, plots, and other graphics, to do local surface-water modeling, and to process or preedit some data before it is included in WATSTORE.

URBAN WATER PROGRAM

The objective of the USGS urban-hydrology program is to provide generalized relationships for estimating hydrologic changes due to urbanization, and hydrologic conditions under urbanization. To implement this program, runoff data are being collected

on 244 fully or partially urbanized catchments, about half of which are less than $2\frac{1}{2}$ km² in area (H. H. Barnes, Jr., and M. E. Jennings, 1977). Storm-water quality data collected on only a few of these catchments are being analyzed as they become available.

Data management and instrumentation

M. E. Jennings, R. A. Miller, H. C. Mattraw, Jr., L. D. Wilson, and W. H. Doyle, Jr., developed a data-management and analysis system for urban watershed flow and water-quality research on four small land-use catchments in Broward County, Florida. The system was used to reproduce data reports and to perform statistical analyses and deterministic modeling computations.

Mattraw reported that four improvements in the USGS urban-hydrology monitor were tested on a stormwater installation near Miami, Fla. These are a sampler for rainfall, a status check by telephone, a recording conductivity bridge for better selection of water samples for chemical analysis, and improved means for processing records.

Source of urban runoff in southern Florida

Rainfall and storm-water-runoff data were collected for 100 storms at a 23.5-ha catchment in southern Florida. Rainfall totals of up to 76 mm were recorded. According to R. A. Miller, runoff is about 18 percent for rainfalls of less than 35 mm and about 23 percent for larger rainfalls. Because the hydraulically connected impervious area of the catchment is about 18 percent of the total, Miller concluded that in southern Florida, runoff from rainfalls of less than 35 mm comes solely from the impervious area.

Flood-frequency studies

Fred Liscum and B. C. Massey developed equations that included the application of earlier methods (S. L. Johnson and D. M. Sayre, 1973) for estimating flood-peak frequency characteristics of streams in the Houston, Tex., metropolitan area. The parameters used were drainage area, bankfull channel conveyance, and percentage of developed drainage area.

Preliminary analyses by H. E. Allen, Jr., of records for 80 crest-stage gages and 28 continuous-record gaging stations in urbanized northeastern Illinois indicated that the percentage of impervious area, basin and channel storage, drainage area, slope, and rainfall intensity are significantly related

to flood magnitude. The impervious area in 15 watersheds was determined from aerial photographs. Regression analyses provided a reliable relationship for estimating the amount of impervious area from population density; this relationship was used for the remaining 93 watersheds.

O. G. Lara (1978) evaluated the impact of urban development on the magnitude and frequency of flooding in the lower reach of the Walnut Creek basin, a 200-km² area on the west side of Des Moines, Iowa. A mathematical model, HEC-1, was calibrated by using concurrent rainfall and runoff data collected at three gaging stations in the basin. Model parameters were regionalized to provide future users with the capability of estimating flood characteristics of ungaged streams within the basin. Long-term rainfall data for two nearby stations were used to synthesize annual peak discharges corresponding to selected degrees of urbanization as measured by the percentage of impermeable area. Five synthetic flood series which corresponded to 5-, 20-, 30-, 50-, and 100-percent impermeability were generated. The results indicated that for 50 percent impermeability, impact of the 100-year flood was 39 percent greater, and the impact of the 2-year flood was 81 percent greater than for zero impermeability.

Comparison of USGS urban-basin model and rational-method estimate of peak discharge

According to M. A. Lopez and R. F. Giovannelli, rainfall and streamflow data for Allen Creek near Largo, Fla., were used to determine a preliminary calibration for the USGS urban-basin model. Allen Creek watershed is a 4.87-km² urbanized area in which 70 percent of development is residential and 30 percent is commercial. About 36 percent of the watershed has impervious cover.

Long-term (1905-52) rainfall data for Tampa, Fla., were used with the model to simulate a 47-year record of annual flood peaks for Allen Creek. A flood-frequency distribution was determined for simulated peaks. Flood-peak discharges from the frequency distribution were compared with peak discharges estimated by using the rational method (a commonly used procedure for estimating urban-area peak discharges). Rational-method peak discharges were an average of 30 percent lower than frequency-distribution discharges for the 5-, 10-, and 25-year recurrence intervals, and were approximately equal for the 50- and 100-year recurrence intervals.

Artificial recharge

R. C. Prill and E. J. Oaksford reported that a 102-day ponding test of highly treated municipal sewage effluent in a basin of outwash sand and gravel deposits in Suffolk County, New York, showed that high infiltration rates can be maintained for extended periods of time. Data collected during the test also showed that the unsaturated zone can be effective in removing organics and viruses and in converting ammonium to nitrate. Because of surface clogging by suspended solids in the effluent, the infiltration rate dropped rapidly during the first few days of the test; however, subsequent degradation of the clogging material by biological activity arrested further clogging, and the infiltration rate stabilized at approximately 2.5 m/d. Measurements of the nitrogen suite when ammonium was present in the effluent showed that ammonium was converted to nitrate by the time the effluent reached the water table at a depth of 7.5 m. Ammonium conversion was generally most pronounced in the lower part of the unsaturated zone. Most of the polio viruses added to the effluent were removed by the time water had percolated to a depth of 3 m. Ammonium conversion and virus removal were probably affected by organic material present as a coating over individual grains throughout the unsaturated zone and as deposits in the interstices between grains. The soil materials provide a medium for sorption of solid particles as well as a nutrient source for microbiological growth.

M. S. Garber applied filtered secondary- and tertiary-treated municipal sewage to sand-packed columns so that the effects of infiltration could be observed. The secondary-treated effluent, although filtered, caused clogging within 1 hour in the top segments of columns containing (1) a field sample, medium to coarse sand, (2) Ottawa sand, and (3) glass beads the size of fine sand. Tertiary-treated effluent was applied to two columns for about 60 days. Flow rate gradually decreased as pore spaces clogged. Both columns reached unsaturated flow state after about 40 days. Unsaturated state extended from the base of the columns to a point near the upper surface, thereby indicating that the clogging in this test was a surface phenomenon. Clogging was probably caused by suspended solids and a gelatinous mixture of iron compounds and alum in the wastewater used; both could have been the result of poor quality control in the tertiary-treatment process.

Water-quality studies

Results of a study by T. L. Miller and S. W. McKenzie indicated that substantial reductions in constituent concentrations in urban storm water may be achieved by settling for 1 hour. Average percent reductions for five constituents were: 5-day BOD, 32-percent reduction for 15 samples; COD, 50-percent reduction for five samples; ammonia, 0-percent reduction for five samples; total organic nitrogen, 36-percent reduction for five samples; and total phosphorus, 51 percent reduction for five samples.

A new urban storm-water data-management system designed by R. A. Miller facilitated computation of storm-water runoff at a residential site and a transportation site in Broward County, Fla. Loads were computed for 23 different water-quality constituents by H. C. Matraw, Jr. Due to the nature of the hydrological interconnection of impervious areas, runoff at the transportation site was approximately three times higher than at the residential site. Nitrogen and phosphorus concentrations were higher at the residential site, but total loads were lower than at the transportation site, owing to differences in runoff. COD and lead were higher in runoff from the transportation site.

Many aquifers favorable for large-scale water supplies in Connecticut are overlain by urban and industrial areas and are, therefore, susceptible to contamination. Data collected by E. H. Handman, I. G. Grossman, J. W. Bingham, and J. L. Rolston on more than 1,400 possible sources of contamination in the State indicated that about 10 percent of all oilspills and leaks, uncovered road-salt stockpiles, solid-waste disposal areas, and industrial-sludge disposal sites have altered ground-water quality. Wells as far as 2,700 m downgradient from a disposal site have been affected. The numerous incidents of contamination identified in the course of this study are believed to represent only a small part of the total.

According to B. J. Prugh, Jr., a recently completed water-quality study at Bloomington and Normal, Ill., showed three basic variations in water-quality parameters in response to climatic and hydrologic stresses: (1) Stream temperatures and concentrations of DO, ammonia nitrogen, total phosphorus, BOD, and fecal bacterial varied seasonally; (2) conductivity, pH, chloride, and suspended-solids concentrations were closely related to stream discharges; (3) total organic carbon, total nitrogen, total phosphorus, BOD, fecal-coliform and fecal-streptococcal bacteria concentrations exhibited

looped parameter-discharge variations indicative of initial flushing action in response to storm runoff.

The atmospheric contribution to the various constituent loads in storm-water was investigated by R. A. Miller. Data were obtained from two storms on one residential, one highway, and one commercial catchment. The atmospheric contribution (bulk precipitation) included both rainfall and fall of particulate matter between storms. Suspended solids contributed from the atmosphere ranged from about 10 to nearly 100 percent of those in the runoff. Although none of the inorganic-carbon load came from the atmosphere, from 0 to 45 percent of the total carbon load did. The atmospheric contribution of COD ranged from 45 to 55 percent. Approximately 100 percent of the total nitrogen on the residential and highway sites and 50 to 89 percent on the other two sites came from the atmosphere. Likewise, the atmosphere contributed 100-percent of the total phosphorus on the highway site but contributed from 10 to 60 percent on the other two sites. The lead contribution from the atmosphere was 95 percent on the commercial site.

Model studies

M. E. Jennings and T. N. Keefer (1977) compared results from kinematic-wave routing and storage routing of flows in storm drains to results from the MLSR (multiple-linearization storm-drain-routing) method. The MLSR method gave very good results without incurring the numerical solutions or damping problems of other methods.

Jennings, K. M. Waddall, B. C. Massey, and L. D. Wilson developed a modified STORM computer program for application to the Houston Metroplex urban water-quality study. Ten water-quality constituents from seven watersheds contributing to the Houston Ship Channel were simulated on a daily mean-load basis by the use of rainfall data for the 1948-75 calendar years. Special programs for data management, treatment of reservoirs, and statistical analyses were appended to the basic STORM program.

W. M. Alley and W. H. Doyle, Jr., developed and tested an urban storm-water planning model for use in USGS urban flood-frequency studies.

WATER USE

Estimated use of water in the United States in 1975

According to C. R. Murray, the preliminary water-use data for 1975, reported in Professional

Paper 1050 (C. R. Murray and E. B. Reeves, 1977a), were updated as required and published in USGS Circular 765 (Murray and Reeves, 1977b). Quantities were given in U.S. gallons rather than metric units to facilitate comparisons with data reported in the five previous quinquennial water-use circulars. Because of a major expansion in the USGS water-use data collection program, a considerable improvement is expected in the accuracy of future data.

Irrigation increasing in southwestern Georgia

According to R. G. Grantham, the use of ground water for irrigation in Georgia has increased rapidly since 1975. There were more than 2,900 self-propelled irrigation systems in southwestern Georgia in 1977, about twice the number reported in 1975, and the area under irrigation in 1977 was more than 24,000 ha, almost double the area reported in 1975.

Because of severe drought conditions during the late spring and summer of 1977, many of the irrigation systems were in continuous operation for more than 2 months. In Seminole, Decatur, Miller, Mitchell, and Baker Counties, the total quantity of water used averaged 500,000 m³/d, assuming uniform withdrawal for 365 days. In late December of 1977, the ground-water system was beginning to recover in response to winter rains, but the full impact of the drought on the ground-water system will not be known until the spring of 1978.

Water use in Hawaii in 1975

R. H. Nakahara reported that the largest use of water in Hawaii in 1975 was for production of thermoelectric power; of this use, which amounted to about 40 percent of the total, nearly 90 percent of the water was pumped from the ocean or from near-shore seawater wells. The greatest use of freshwater was in agriculture; irrigation of sugarcane fields accounted for about half of the fresh water used. Surface-water sources supplied about 65 percent of the total water (both freshwater and seawater) used and about 45 percent of the freshwater used. Recycled water (mostly effluent from wastewater-treatment plants and water reclaimed from sugarcane-processing facilities) amounted to about 2 percent of the total used; recycled water was used for irrigation and for some industrial purposes.

Water use in Washington for 1975

Results of a canvass of water users in 39 counties and 62 drainage basins of Washington indicated that

9.4×10^9 m³ of water was used in 1975 for municipal, industrial, and irrigation purposes. According to N. P. Dion and W. E. Lum II, that amount represents a 10-percent increase over water use in 1965, but it represents a slight decrease from that of 1970.

According to A. J. Hansen, Jr., water use in 1975 on the Kitsap Peninsula averaged about 56,000 m³/d. About 26,000 m³/d was diverted from a stream in the Gold Mountain upland, and about 30,000 m³/d was ground water withdrawn from two aquifers. Total water use by 1995 is projected to be about 86,000 m³/d. Most of the projected increase—30,000 m³/d—most be obtained from local aquifers. Ground-water development potential seems adequate to meet the expected demand as an additional 18,000 m³/d probably can be obtained from each of the two aquifers. However, at several localities, this increased rate of withdrawal may cause saltwater intrusion in the lower aquifer.

NATIONAL WATER-QUALITY PROGRAMS

Estimating regional water use and residuals output from energy development

One goal of the USGS's river-quality assessment program is to devise methods for identifying potential river-quality problems and for evaluating planning alternatives in terms of their impacts upon the quality of the river. According to J. E. Schefter, one such assessment is currently being conducted in the Yampa River basin of northwestern Colorado.

The Yampa River basin contains large deposits of coal which may be strip mined at a rapid rate in the near future. The impact of this coal development on the rate of consumption of water and the water quality of the Yampa River will depend not only on the rate at which the coal is mined, but also on how and where the coal is used.

Estimates of water consumption and residuals output resulting from coal mining and coal use can be derived by using plant-level models descriptive of the type of coal mining and coal-use processes to be employed within the basin. These plant-process models generally use the engineers' materials-balance approach to predicting water consumption and residuals output.

However, such a procedure provides estimates of only the water consumed and the residuals generated directly by the coal-mining and utilization processes. It does not provide estimates of water consumption and residuals generation by economic activity indirectly associated with the coal-energy develop-

ment, and induced by such development. Water consumed and residuals generated by, for example, increased activity in the retail-trade and services sectors of the economy would be overlooked by the plant process-materials balance approach to impact assessment.

Economic input-output (I/O) analyses were used to predict water consumption and residuals output under various energy-development conditions in the Yampa River basin. Results of the analyses indicated that plant-process models provide estimates of water consumption and process-related residuals output that are lower (although generally within 10 percent) than those obtained by using I/O analyses. However, estimates of the output of population-related residuals (e.g., BOD, COD, N, and P) derived by using only plant-process models are generally less than 10 percent as large as those obtained by using I/O analysis. This is because the plant-process models, unlike any I/O model, provide estimates of only the direct effects, and neglect the indirect effects.

NATIONAL STREAM-QUALITY ACCOUNTING NETWORK

The National Stream-Quality Accounting Network (NASQAN) was established by the USGS to provide a nationally uniform basis for continuously assessing the quality of United States rivers. According to J. F. Ficke, the stations generally are located to represent flow from the 349 water-quality accounting units (subregional drainage basins) which collectively encompass the entire land surface of the Nation. At the end of 1977, there were 445 NASQAN stations; there are plans to expand the network to 525 stations by 1979.

More than 4 years of data are now available from NASQAN. The data show geographic patterns of water quality that reflect climate, geology, soil types, agricultural practices, human and animal populations, water pollution, and pollution-control practices. Generally, the quality of rivers in the United States can be determined on the basis of analyses of several dozen sets of national water-quality maps developed from NASQAN data for the 1974-77 water years.

Water-quality conditions

Chemical and biological characteristics of streams as described by NASQAN data indicated that water quality is best (especially in regard to inorganic

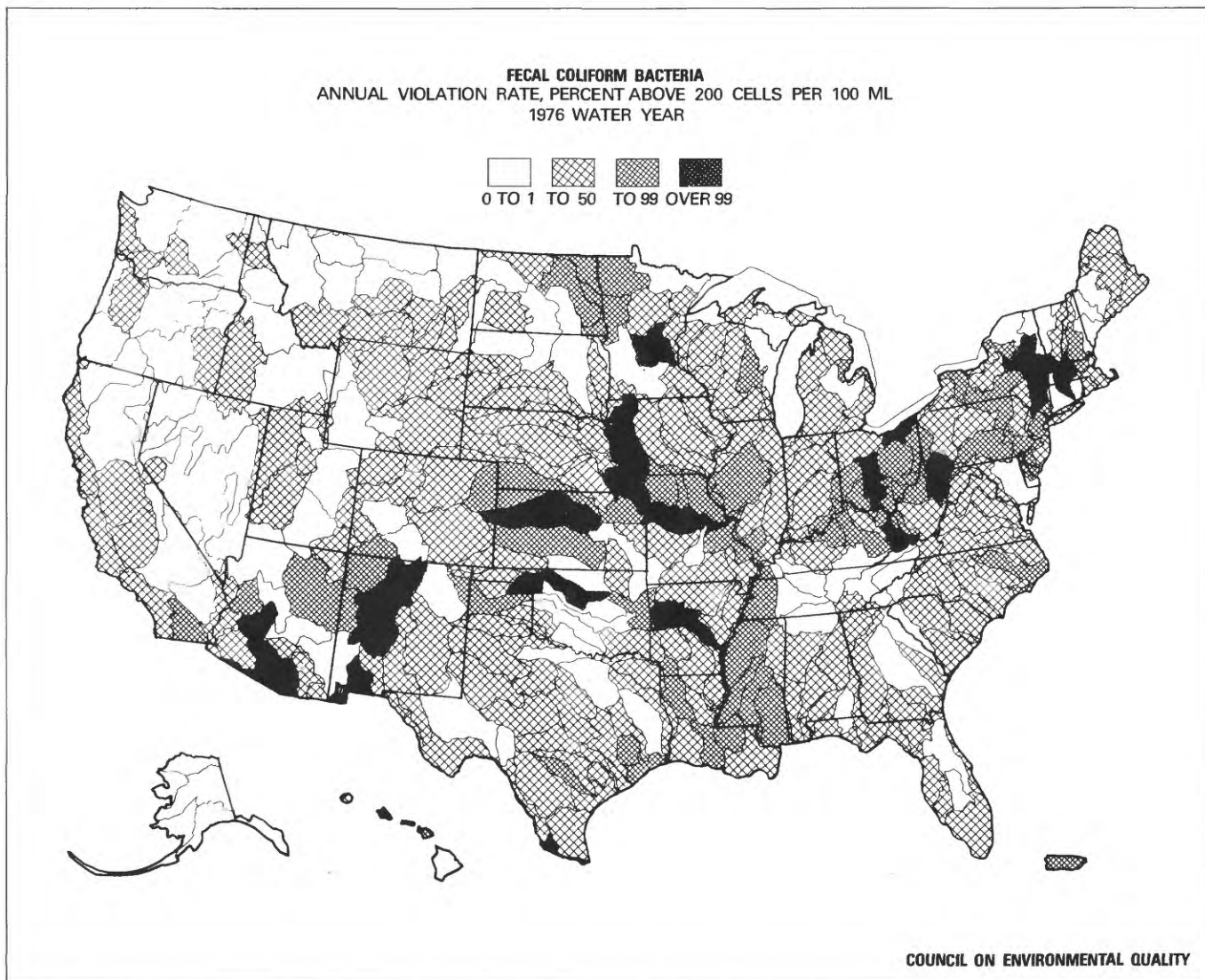


FIGURE 3.—Counts of fecal coliform bacteria, computed from a reference level of 200 cells per 100 mL, at NASQAN stations during the 1976 water year. Map is shaded to show station data representing flow from the accounting unit.

substances) in the Northeast, Southeast, and Northwest. Water in those regions is generally low in dissolved solids and the major and minor chemical constituents, soft (except in Florida), and carries relatively small amounts of sediment. However, many streams in these areas carry moderate to high levels of major nutrients and have correspondingly high populations of plankton and attached microflora. High counts of indicator bacteria also indicated local pollution, particularly in regions of the country where there are large human or animal populations. In the Northeast, there are some concen-

trations of heavy metals at moderate levels, but these do not exceed the maximums specified by water-quality criteria.

Rivers in most of the Midwest and Southwest are characterized by moderate to high levels of dissolved major and minor constituents—sediment, nutrients, floating and attached aquatic plants, and indicator bacteria. In addition, the highest incidences of pesticides in stream and bottom sediments were in these regions.

Concentrations of dissolved solids, major nutrients, phytoplankton, and zinc in the Mississippi

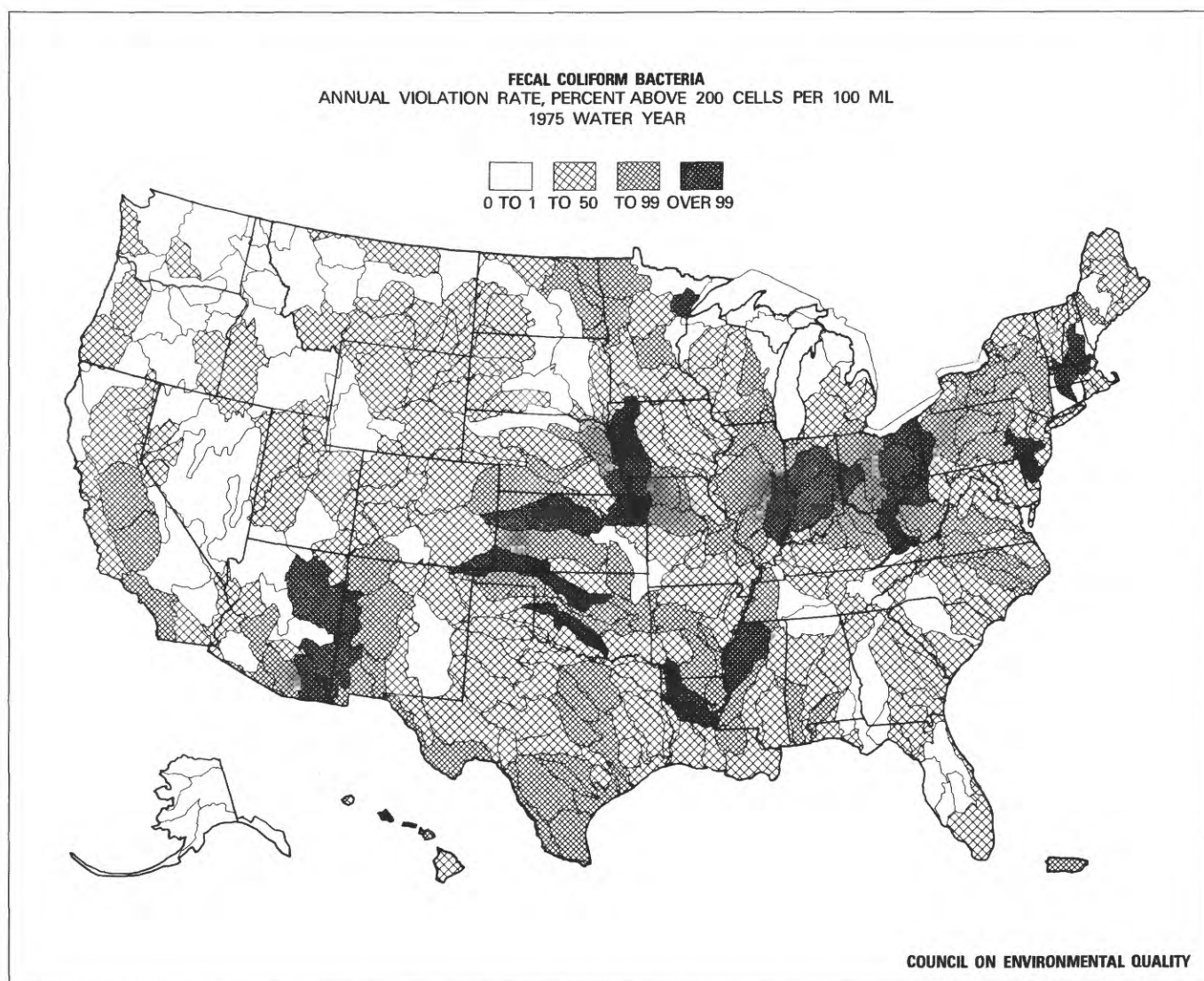


FIGURE 4.—Counts of fecal coliform bacteria, computed from a reference level of 200 cells per 100 mL, at NASQAN stations during the 1975 water year. Map is shaded to show station data representing flow from the accounting unit.

River above Memphis, Tenn., were intensively studied. Flow volume greatly influences concentrations of these substances. Stations with low concentrations of major nutrients generally had low phytoplankton populations.

Water-quality changes

Because of the short period (1975–77 water years) for which nationwide coverage is available from NASQAN, only tentative statements can be made about changes in water quality. It is not pos-

sible to rigorously define trends in hydrologic systems only from data available for a 2-year period because of the variations between relatively wet and dry years. There were, however, what appeared to be significant regional differences in water quality between the 1975–77 water years, differences that may be indicators of trends or changes. For example, the national patterns of counts of fecal coliform bacteria (figs. 3 and 4) as measured at NASQAN stations showed decreases in many accounting units. The decreases were most evident in the Northeast and in several units in the Mississippi

River basin; on the other hand, a few accounting units showed increases.

Although the data were limited, some reasons for changes in water quality were indicated. Large regional improvements in water quality were primarily attributed to pollution-control measures and

hydrologic variations. The drought in 1976-77 probably aggravated pollution. On the other hand, many new sewage-treatment plants began operating during that period, and it is possible that the new facilities effected an improvement in water quality.

MARINE GEOLOGY AND COASTAL HYDROLOGY

COASTAL AND MARINE GEOLOGY

ATLANTIC CONTINENTAL MARGIN

Stratigraphy and structure of the Atlantic Continental Margin and adjacent deep-sea floor

The continued collecting and processing of geophysical data is providing an increasingly accurate and detailed basis for the analysis and interpretation of geologic relationships, associated mineral resource potentials, and the environment of our Nation's continental shelves. For example, with 1,650 km of multichannel seismic-reflection data now available for analysis of the Georges Bank basin off New England, J. S. Schlee is able to distinguish four major acoustic units (depositional sequences) that are bounded by prominent regional unconformities. On the basis of their acoustic properties and extrapolation of Scotian Shelf well data, the inferred units are: (1) Triassic(?) and Lower Jurassic nonmarine clastic and evaporite rocks (0-8 km thick), (2) Middle and Upper Jurassic nonmarine sedimentary rocks and marine carbonate rocks (0-4 km thick), (3) Cretaceous marine and nonmarine sandstone and shale (0-2 km thick), and (4) Cenozoic marine and glacial deposits (0.2-0.5 km thick). Like other eastern North American basins, the Georges Bank basin appears to have undergone a rifting phase with deposition of nonmarine strata and evaporite deposits followed by a broad subsidence phase of prevailing marine conditions.

Similarly, J. A. Grow (USGS) and C. O. Bowin (Woods Hole Oceanographic Institution) have now integrated approximately 39,000 km of marine gravity data collected during 1975 and 1976 with data obtained by the U.S. Navy and others to construct a more detailed free-air gravity anomaly map for the U.S. Atlantic Continental Margin between Florida and Maine. A band of maximum gravity values (-10 to +70 mGal) is present along the edge of the continental shelf (or outer margin of the Blake Plateau), and another of minimum values (-20 to -130 mGal) exists along the base of the continental

slope. Although these high and low values are largely dependent on continental slope topography and the sharp change in crustal thickness across the margin, the maximum and minimum longitudinal trends nevertheless terminate abruptly at discrete transition zones along the margin. The transition zones appear to mark major fractures that separate the subsided continental margin and adjacent oceanic crust into a series of segmented basins and platforms. Differential subsidence of bounding crustal blocks during early stages (Jurassic?) of rifting from Africa presumably caused most gravity transitions along the margin. The major transition zones presently identified lie southeast of Cape Fear, east of Cape Hatteras, near Norfolk Canyon, off Delaware Bay, just south of Hudson Canyon, and south of Cape Cod.

The regional gravity field averages -20 to -30 mGal over the continental rise and near zero over the continental shelf. This abrupt change in the longer wavelength components implies either a difference between upper mantle densities beneath the continental crust and the adjacent oceanic crust or an abrupt change in regional dynamic stresses across the continental margin.

In a continuing analysis of aeromagnetic survey data, K. D. Klitgord and J. C. Behrendt note substantial correlations with multichannel seismic data in areas of distinct seismic reflections. The magnetic data support the seismic interpretation of 14 to 15 km of nonmagnetic sediments above acoustic basement in the deepest sections of the Baltimore Canyon trough. The east coast magnetic anomaly has also been interpreted as the boundary between oceanic and continental crust. Werner deconvolution magnetic depths computed from steep gradients along this east coast anomaly, however, suggest causative sources at 6 to 9 km. These source depths are substantially shallower than those of the seismic and magnetic basements of the Baltimore Canyon Trough to the west and the continental rise to the east. The shallow depths occur in an area where seismic reflections are indistinct. These considerations lead to geologic interpretations of either an

uplifted basement ridge (at much greater depths than that proposed by early investigators on the basis of seismic refraction data) or intrusion of dikes and sills within deeper parts of the sedimentary section.

A close agreement of comparisons between magnetic estimates and multichannel seismic reflection profiles for depth-to-basement allows use of the magnetic information to interpolate basement structures in regions between the profiles. Therefore, using a new aeromagnetic anomaly map (Klitgord and Behrendt, 1977) with depth-to-magnetic basement estimates in its margins, Klitgord has outlined the pattern of deep sediment-filled basins and intervening shallow platforms along the East Coast continental margin. Basins include the deep Baltimore Canyon Trough, the Georges Bank Basin, and a number of smaller troughs on the Long Island platform. The Connecticut Valley Triassic and Jurassic Basin can be traced beneath Long Island; another large Triassic and Jurassic basin is suggested for the region east of the Newark Basin; and a small Triassic (?) and Jurassic (?) basin can be identified between the islands of Nantucket and Martha's Vineyard.

Petroleum potential of the Mid-Atlantic continental margin

Continuing study of samples and logs from the stratigraphic test well that was drilled by industry to a depth exceeding 4,800 m, 1,546 km east of Atlantic City, New Jersey (COST No. B-2 well), and integration of the study results with those obtained through processing and interpretation of multichannel seismic reflection profiles is providing an increasingly clear picture of the petroleum potential of the continental shelf off the central East Coast of the United States. R. E. Mattick reports that the abundance of terrestrial rather than marine organic matter in well samples favors the presence of natural gas instead of oil in rocks of the Baltimore Canyon Trough. Thick, potential reservoir sands, possible source beds (organic carbon contents of as much as 12 percent), potential cap rocks (shales), and large structures and pinchouts provide favorable conditions. A "bright spot" analyses suggests the possibility of at least one substantial gas accumulation.

R. E. Mattick, O. W. Girard, Jr., P. A. Scholle, J. A. Grow, and J. S. Schlee attach particular significance to a continuation in seismic records of the buried Lower Cretaceous continental shelf to distances of as much as 20 to 30 km seaward of the present shelf edge. Seismic velocities in the Lower

Cretaceous increase markedly between the COST B-2 well and the Lower Cretaceous shelf edge, and together with indications of faulting, arching and other structures, lead to interpretation of carbonate reef deposits along the buried margin. This interpretation implies zones of high porosity which could serve as oil and gas reservoirs within the reef deposits. Shale beds, which overlie the buried shelf margin, would provide the relatively impermeable seal needed to trap the migrating fluids; middle Cretaceous black shales of the continental rise could serve as source beds for oil and gas which migrated up-dip into the Lower Cretaceous shelf-edge structures. K. D. Klitgord and J. C. Behrendt note approximate coincidence of the buried reef edge and the East Coast magnetic anomaly, which they attribute to an underlying basement ridge or the presence of deep intrusive bodies.

Using multichannel seismic reflection data, W. P. Dillon reports that the surface of an unconformity at the top of presumed Triassic rocks deepens abruptly to the southwest of a hinge zone that crosses the Blake Plateau in a southeasterly direction off Charleston, S.C. The hinge zone coincides with large magnetic and gravity anomalies and with the landward extension from the ocean basin of the Blake spur fracture zone. The inflection appears to be a major structural lineament crossing the continental margin and probably represents the boundary between thinned continental crust to the northeast and transitional oceanic crust to the southwest. It may also relate to the Charleston seismicity trend that includes the epicenter of the earthquake that destroyed much of Charleston in 1886.

In a preliminary study of seismic velocities within sediments composing the Blake Ridge off Cape Fear, N.C., Dillon found very high velocities (apparently more than 3 km/s) within the upper .5 km of sediment. Beneath this high velocity layer, the velocities seem to drop well below those of sound in water (1.5 km/s). These preliminary results suggest the likelihood of a several-hundred-meter-thick layer of free gas that has been trapped beneath sediment and "lithified" by frozen gas hydrates.

Geologic environment of the Atlantic Continental Shelf

In addition to its resource studies off the Atlantic Coast, the USGS is also gathering and interpreting data on baseline conditions and geologic hazards that pertain to oil and gas development on the Outer Continental Shelf. Along the eastern Atlantic Coast, effort is concentrated within three large areas

having greatest potential for significant petroleum discoveries: the Georges Bank Basin off New England (North Atlantic), the Baltimore Canyon Trough off New Jersey (Middle Atlantic), and the Georgia Embayment (South Atlantic).

Currents and bottom sediment movement on Georges Bank

At Georges Bank, high current speeds associated with the large tidal range, common storms, and shallow water provide a widely recognized and significant hazard to offshore development. Bradford Butman and M. A. Noble used instruments mounted on a tripod frame to obtain time-lapse bottom photographs and simultaneous measurements of currents, light transmission, pressure, and temperature off the southern side of Georges Bank (85 m water depth) from November 1976 to March 1977. The photographs and measurements show frequent resuspension and movement of the surficial sediments and suggest that sediment motion in winter results primarily from tidal currents (typically 20 cm/s near bottom at this location) and wave-induced bottom currents. Similar measurements made in the Great South Channel (January 1977), on the northern flank of the bank (July–August 1977), and near the southwest crest (May 1976) indicate frequent surficial bottom-sediment movement. Long-term moored current observations on the southern flank of Georges Bank from 1975 to present indicate a persistent southwestward flow, parallel to the shelf edge (4 cm/sec at 75 m; 8.5 cm/sec at 45 m). Observations of currents at several other locations on Georges Bank during 1976 and 1977 suggest an anticyclonic (clockwise) circulation around the bank; the near-surface flow on the northern side was to the northeast, and near-bottom flow in Great South Channel was northward into the Gulf of Maine. The anticyclonic current circulation may impede flushing and prolong the residence time of suspended particulates, nutrients, and biological populations in the region. The frequent resuspension and movement of near-bottom sediment, coupled with measured imperfections in the clockwise circulation, suggest that from the southern flank of the bank some sediment moves northward into the Gulf of Maine and some moves westward along the shelf.

Vertical distribution of trace metals in sediments of Georges Bank

M. H. Bothner and R. J. Fabro have determined trace metal contents of acid-leached sediment from 20 sediment cores collected on Georges Bank. The

abundances for zinc ranged from 0.2 to 10.7 ppm; for copper, from 0.3 to 4.2 ppm; and for chromium, from 0.9 to 5.5 ppm. The distribution of these metals with depth is uniform, without higher concentrations at the surface where modern industrial pollutants might be expected. The concentrations are low compared to average abundances in crustal materials, but generally characteristic of coarse-grained sediments that have not been contaminated with abnormal amounts of trace metals. The study offered no evidence of anthropogenic trace metal additions to the sediments.

Pb-210 profiles in continental shelf sediments—an index to rates of sediment reworking

Pb-210 is a naturally occurring radioisotope of lead that has a half-life of about 22 years and has proven useful for estimating rates of recent sediment accumulation. M. H. Bothner and S. D. Locker have shown that Pb-210 profiles can also be used to determine the rates and depths of sediment mixing on Georges Bank and in the vicinity of the Baltimore Canyon Trough where sediments are not accumulating at present. At these places they observed a typically fast mixing rate that can homogenize the upper 5 to 10 cm of sediment in less than 5 years and a slower mixing rate within the underlying 10 to at least 20 cm of sediment. The data have particular relevance to the prediction of residence times for new pollutants that are introduced into continental shelf sediments.

Glacial deposits of the continental shelf

D. W. Folger notes that although high current velocities and sediment movement constitute the most significant hazards, attention must also be paid to potentially unstable foundations and to the prospect of upper continental slope slumping when planning offshore structures in the vicinity of Georges Bank. Continuing study of samples and data collected in the course of the 1976 Atlantic Margin Coring project (Hathaway and others, 1976) has included tests of engineering properties that will help define foundation conditions for rigs and platforms. Glacial deposits that underlie the surface of Georges Bank are at least 80 m thick and will serve as the main strata to support platform legs.

Postglacial sea levels on the Inner Continental Shelf of southern New England

R. N. Oldale and C. J. O'Hara report 22 new radiocarbon dates for samples collected from the

seabed off southeastern Massachusetts. The data allow evaluation of published eustatic sea-level curves (Curry, 1965; Milliman and Emery, 1968; Dillon and Oldale, 1978) that have been used to establish postglacial sea levels on the Inner Continental Shelf off southern New England. The oldest significant date, 13,200 yr B.P., is on freshwater peat sampled from the base of a deposit 56 m below sea level. This date plots on Curry's curve, with the implication of a local sea level below the curve at that time. Six dates for shells are in the range 10,000 to 8,000 yr B.P. and appear to fit Curry's curve. The shells, however, have probably been transported shoreward thereby exaggerating the amount of submergence. For the period, 8,500 to 5,000 yr B.P., dates on freshwater peats provide more reliable indicators of maximum possible submergence. These also fall on Curry's curve and again indicate that it is too shallow. Finally, a freshwater peat date of 5,510 yr B.P. plots below all three curves. Oldale and O'Hara, therefore, conclude that a sea-level curve for the Inner Continental Shelf south of New England should be generally lower than the Curry curve. Between 13,000 and 8,500 yr B.P., it may be fairly represented by the Dillon and Oldale curve that is shallower than the Milliman and Emery curve for that time interval. The local curve for the past 6,500 years may plot below all three evaluated curves, and correspond most closely to the curve offered earlier by Redfield and Rubin (1962).

Evidence from Massachusetts onshore and offshore areas for thrust coastal end moraines and a fluctuating ice margin of Woodfordian age

Ridges, which are morphologically similar to ice-thrust ridges found elsewhere in North America and Europe, occur at many places within Woodfordian end moraines on Martha's Vineyard, Nantucket, the Elizabeth Islands and Cape Cod. The ridges on Martha's Vineyard consist of thrust and folded sediments of pre-Pleistocene age. Elsewhere the ridges are composed of drift in which evidence for ice thrusting is less easily recognized. Features which are interpreted as evidence of overthrust drift include folding and faulting within the drift, the presence of glaciolacustrine clays and delta beds high up on the front of moraine ridges, and northward dips of bedded deposits that terminate at morainal fronts. These may be contrasted with features that are considered products of overriding ice as, for example, till overlying stratified drift and angular unconformities atop stratified drift.

R. N. Oldale and C. J. O'Hara interpret some reflectors of offshore seismic profiles across submerged portions of the Nantucket and Buzzards Bay moraines as evidence for thrusting of preglacial and glacial sediments. Beneath Cape Cod Bay, they infer northward dipping imbricated reflectors to be subglacial tills that were deposited as ice advanced over sublacustrine drift. Thrusting is thought to have occurred when ice advanced against the north-facing escarpment of the pre-Pleistocene coastal plain cuesta, in the case of the Nantucket moraine, and against ice-contact slopes of earlier outwash plains, in the case of the Buzzards Bay and Sandwich moraines. The disappearance of Woodfordian ice from southeastern Massachusetts appears to have involved alternating periods of ice front advance and stagnation zone retreat, perhaps similar to that described for northern Illinois (Frye and Williams, 1973). If so, the alternating advances and stagnation imply short-lived and possibly severe variations in Woodfordian glacial climates.

Environmental studies of the Mid-Atlantic Outer Continental Shelf

D. W. Folger and H. J. Knebel report the addition of appreciable amounts of detail to knowledge concerning the distribution of surface sediments on the Mid-Atlantic Continental Shelf, using vibracore techniques to collect information to depths of several meters. Mapping reveals significant areas in which the characteristic surficial sands are absent and the underlying widely distributed muddy unit is exposed. With thicknesses attaining as much as 75 m, this muddy unit clearly constitutes a factor that must be considered in planning the construction of platforms and emplacement of pipelines. Shallow subbottom seismic-reflection profiles show large actively moving sand waves around the head of Wilmington Canyon. Most movement of the sand waves probably takes place during storms and hurricanes.

Knebel concludes that (1) seasonal variability of suspended sediment within the water column may be attributed chiefly to the numbers of diatoms and silico-flagellates and that (2) in general, terrigenous matter is a quantitatively important component of only the suspended particles that are nearshore and near the bottom. Seasonal deployment of tripods comparable to those used for the studies on Georges Bank shows that most sediment movement takes place during winter storms when waves are large and bottom currents are strong (>30 cm/s). Folger notes that sediment may be transported as much as 20 to 30 km during a single storm and that

surface sediment and associated pollutants may therefore be spread across most of the shelf in the course of a year or two.

Environmental organic geochemistry of Mid-Atlantic shelf sediments

R. E. Miller and D. M. Schultz continued studies of hydrocarbon variability within sediments from the Mid-Atlantic Continental Shelf in conjunction with the Environmental Assessment Program of the Bureau of Land Management. These second year results show natural variability of the aliphatic hydrocarbons ranging from 1.0 to 5.0 $\mu\text{g/g}$ sediment. The aromatic hydrocarbon fractions occur in concentrations of generally less than 0.01 $\mu\text{g/g}$ sediment, with those identified having gas chromatograph/mass spectrometer fragmentation patterns characteristic of fused ring aromatics in the classes of anthracene, phenanthrene, fluoranthene, pyrene, and chrysene. The source of these aromatic hydrocarbons is not known. The very low concentrations and relatively even distribution, however, indicate the probability of a very well mixed source, such as that which could be expected of airborne particulates transported from land to the ocean basins.

Environmental assessment of the South Atlantic Continental Shelf

Serving as principal investigator on a contract, Orrin Pilkey (Duke University) reports that more than 1,500 samples from the South Atlantic Continental Shelf have been analyzed in order to prepare maps showing the distributions of grain size, color, composition, and lithofacies of surface sediments. The maps indicate that nearshore sediments tend to be fine sand, those covering the Outer Continental Shelf are medium and coarse sand, and those on the Upper Continental Slope are mud and muddy sand. In general, the post-Pliocene sediments are thin (<5 m) and consist of a relict non-carbonate sand fraction and a younger carbonate fraction that have been thoroughly mixed by both biological and physical processes. The areal patchiness of sediment colors, however, shows that regional mixing and long distance transport are not important processes. Other than skeletal debris from organisms and grains eroded from underlying sediment, present day shelf sedimentation apparently involves little addition of material.

Analyses of sidescan sonar and high resolution seismic records for the Carolina to Florida Continental Shelf

Peter Popenoe examined sidescan sonar and high resolution seismic records and concluded that sand-

size sediments compose most of the continental shelf surface east of Charleston, S.C., and Brunswick, Ga., and that hard bottoms form a few small areas. East of Charleston, sediments are coarser, hard bottoms are more extensive, and beyond the shelf break the profiles display structures indicative of downslope sediment creep. A reef appears to be generally continuous along the outer edge of the Georgian and South Carolinian Shelf. Present limited seismic coverage suggests confinement of most hard bottoms to three poorly defined, irregularly shaped and discontinuous zones that lie subparallel to the coast at distances of 55, 100, and 140 km from the shore.

Organic geochemistry of heavy hydrocarbons in Florida-Hatteras Outer Continental Shelf sediments

D. M. Schultz and R. E. Miller have determined the distribution, concentration and composition of the C_{15}^+ heavy hydrocarbons and fatty acid methyl esters within samples from Hole 6,004 that was drilled and penetrated sediments of Late Cretaceous age during the Atlantic Margin Coring project (Hathaway and others, 1976). Low total organic carbon contents (generally less than 0.5%) and low concentrations of fatty acids indicate that organic productivity in the water column may have been correspondingly low during Late Cretaceous and Tertiary time. Samples of lower Miocene sediments that contain total organic carbon exceeding 1.0% provide an exception.

The aliphatic and aromatic hydrocarbons identified in the samples from Hole 6,004 do not appear to be the product of thermal maturation processes associated with the formation of liquid petroleum hydrocarbons. Instead, they probably reflect the nature of the precursor source organic matter and are attributed chiefly to marine organisms and, to a lesser degree, high plant waxes.

GULF OF MEXICO AND CARIBBEAN SEA

Multichannel seismic data raise questions concerning the Mesozoic age of the crust beneath the Gulf of Mexico

Using recently acquired multichannel seismic data recorded aboard a research vessel of the University of Texas Marine Science Institute at Galveston, Tex., R. G. Martin has identified a prominent seismic reflection unit beneath the Challenger Salt of the Sigsbee Plain in the central Gulf of Mexico. The unit extends downward from the base-of-salt reflector to average subsalt depths of about 0.5 seconds (two-way travel time), and apparently, at some places, to

as much as 1.0 second or more. Layer-velocity determinations yield an average velocity of about 5.0 km/s, providing a thickness range of from 1.0 to more than 2.5 km for this reflection unit. The subsalt reflection unit and its equivalents are extensive beneath the Sigsbee Plain and can be traced to the margins of the deep Gulf basin where they appear to extend unbroken into the deep foundations of the Florida and Campeche carbonate platforms to the east and south. Remarkably, throughout distribution of the unit, reflections reveal no evidence of major, or even moderately significant, tectonic events. The widespread distribution of this relatively thick, undeformed, pre-salt seismic unit suggests: (1) that the minimum age of the oceanic crust beneath the central Gulf of Mexico must be at least earliest Mesozoic, and possibly older, and (2) that Triassic pull-apart theories for origin of the Gulf need further study, if not total revision.

Sediment deposition and movement, Gulf of Mexico Continental Shelf

C. W. Holmes and E. A. Martin have determined rates of sediment deposition for the past 150 years at 22 sites on the Continental Shelf and on the Upper Continental Slope of the northwestern Gulf of Mexico using a radiometric lead (Pb-210) dating method. In an area of rapidly accumulating sediments (>7 mm/yr) on the central Texas shelf south of Matagorda Bay, trace metal profiles indicate significant increases in the amounts of barium and lead during the past 25 years. The data also indicate that the metal-contaminated sediment is migrating southward over the Texas shelf at a rate of 2 km/yr. With offshore petroleum exploration and development on the shelf of the northern Gulf having begun in earnest during 1952, one can reasonably attribute the increase in barium content and its dispersal during the past 25 years to drilling activity. Results demonstrate the applicability of the combined barium content—lead dating method for determining rates of sediment deposition and transport in any area having offshore drilling activity.

Submarine landslides on the Mississippi Delta

L. E. Garrison and his associates identify submarine landsliding as one of the principal ways to move deltaic sediments from river mouths across continental shelves. The processes involved in the movement are not well understood because methods for observing mechanisms and identifying the resulting features have not been available until recently. Now, however, detailed seafloor maps made

from side-scan sonar mosaics permit identification of submarine landslide morphologies, and development of techniques for making in situ measurements of physical changes during times of marine sediment failure supply data that was not previously available.

In many cases, submarine landsliding can be shown to begin at circular depressions a few tens of meters across on shallower parts of a delta front. The depressions are abundant on the Mississippi Delta, and although their formation has not yet been observed, they probably are initiated by a combination of factors including slope angles and sediment strengths. Failure on slopes of less than 0.5° is common, and greatly reduced sediment strength results from the inclusion of methane gas in amounts that cannot be measured precisely. The studies of Garrison and his associates have also shown that weak sediment masses respond to fluctuating surface wave pressure with measurable movements that shift sediment characteristics toward their failure points.

Whatever the complex initiating causes of failure, once begun it is likely to continue in a sequence that transfers sediments great distances from their original sites of deposition. Through successive failures, the small depressions elongate upslope and laterally as the disrupted material flows downslope to be deposited on lower parts of the delta front. This process, whether essentially continuous or episodic, goes on until the axial slope profile of the developing feature approaches the angle of stability for existing conditions. It produces an upslope area of deflation that is connected to a downslope area of overlapping mudflows by a long sinuous chute that channels the sediment.

Early bathymetric maps reveal the chutes as "gullied" areas adjacent to the Mississippi River passes. Prior to initiation of USGS studies, however, the role of the chutes in sediment transport was not apparent. With the new perspectives provided by the continuing studies, it is now clear that they are of critical importance to the engineering of offshore structures.

Sediments of Corpus Christi Bay

Corpus Christi Bay and its estuary, Nueces Bay, form about 450 km² of the south Texas coast. Corpus Christi Bay is a saucer-shaped depression with a remarkably uniform depth of 3 m. Nueces Bay is even shallower (<1 m) and has numerous oyster reefs. The bay system has had a recent increase in drilling activity. Drillers working in the central por-

tion of the system have experienced difficulties caused by failure of jackup legs to encounter sediments that are firm enough to raise and set rigs for drilling.

Using results of a high resolution subbottom survey of the bay system, C. W. Holmes has identified the bed and meandering valley of an ancient Nueces River that is 20 to 30 meters below present sea level and is nearly filled with modern sediments. In the upper reaches of Corpus Christi Bay, profiles of the subbottom survey also reveal extensive oyster reefs a few meters above the ancient valley floor. The absence of comparable reefs in the overlying sediments suggests a rapid rise of sealevel and presence of a sediment trap during the later stages of bay development. Such conditions would favor rapid deposition of sediments with relatively weak bearing capacities. Thus, where sediments are thickest in central portions of the bay, difficulty in positioning structures can be expected.

Suspended sediments of Corpus Christi Bay, Texas

G. L. Shideler and Frances Firek have determined the spatial and temporal variability of suspended sediments within Corpus Christi Bay by means of quasi-synoptic water sampling and vertical transmissivity-temperature profiling at seven monitoring stations; to access seasonal factors, they acquired field data and samples on six dates spanning the 16-month interval, October 1975 to February 1977. The water-column transmissivity measurements indicate generally turbid conditions ($<40T/0.25$ m) throughout most of the bay, and increasing turbidity with depth—conditions that apparently reflect the bay's shallowness and frequent resuspension of bottom sediment by wave surge. A series of *t*-statistic tests for predicting conditions between separate sampling dates generally indicate no significant seasonal differences in overall mean sediment concentrations in terms of total mass.

Shideler and Firek also found that compositionally the bay sediment consists of a nonorganic silt-clay fraction and a generally subordinate organic fraction dominated by diatoms. The organic to nonorganic ratio varies with time and was highest during the months of January and February. Significant variations in sediment texture (mean size, sorting) that were found on several sampling dates can probably be attributed to variations in the proportion of organic constituents.

Dispersal paths of river sediments on the north shelf of Puerto Rico

Sediment is brought to the narrow northern shelf of Puerto Rico by a number of major rivers, almost exclusively in times of floods. Because the mineralogy and dark color of the river sediment differ markedly from that of the light-colored skeletal carbonate grains of the insular shelf sands, O. H. Pilkey (Duke University) and J. V. A. Trumbull (USGS) were able to trace dispersal patterns of the river sediment on the shelf with ease. They found that river sand is transported across the shelf to a depth of about 20 m and then moves laterally to both the east and west. Mud continues seaward to a depth of about 40 m, and then it moves to both the east and west. Thus, the inner shelf is bypassed by the river sediment and is formed predominantly of skeletal carbonate fragments. The offshore zone of lateral rivers and transport merits investigation as a possible source of commercial amounts of sand that is uncoupled from the sand regime of the shoreline and its beaches.

PACIFIC CONTINENTAL MARGIN

California to Washington

The Pacific Continental Margin, like the Gulf and Atlantic Margins, is a region of continuing marine geological and geophysical studies, many directed toward solving problems of petroleum resources and their development. The southern California borderland, like the Gulf, is a region of proven offshore reserves that are now being exploited; the region to the north is like the Atlantic with potentials that remain unknown and untested. Unlike margins to the east, the Pacific Margin lies within a zone of active and intense deformation of the earth's crust; many USGS activities focus on implications of the difference.

Faulting in coastal south-central California

The role of faulting along the southern part of the west coast is illustrated in part by the pattern of tified on land and offshore and are shown on a map of the south-central coast of California (Buchanan-Banks and others, 1978). The pattern is a northward extension of one shown on a map of the southern California borderland issued in 1974. To derive it for the nearshore shelf, D. S. McCulloch, A. T. Long, and P. A. Utter interpreted many relatively close-spaced single channel intermediate and high

resolution seismic reflection records and much aeromagnetic data. Movement and seismic events associated with the faults shown on the maps can be expected to affect coastal and offshore installations.

Geology of the Monterey Bay region

H. G. Greene examined geophysical data and samples from the seafloor of Monterey Bay and adjacent portions of the central California Continental Shelf and Slope. He concluded that the region has had a complex late Cenozoic tectonic history of vertical and strike-slip fault movements. This late Cenozoic history begins with development of an extensive erosional surface on upper Mesozoic granitic basement rocks and subsequent incision of an ancestral Monterey Canyon into this surface. Marine sedimentary rocks of Miocene and Pliocene age overlie the surface and may have filled the canyon. In fact, the canyon may have been filled and exhumed at least twice since its inception.

Using seismic reflection results, Greene identifies the presence of two prominent, intersecting, northwest-trending fault zones in the Monterey Bay area. The Palo Colorado-San Gregorio fault zone forms a major structural boundary. It is at least 200 km long, about 3 km wide and appears to connect with faults mapped on land near Ano Nuevo Point and Point Sur. The Monterey Bay fault zone, between Santa Cruz and Monterey, is a diffuse zone that is approximately 10 to 15 km wide and consists of en echelon faults. Faults within this zone may connect with faults on land near Monterey. The zone is probably truncated by the Palo Colorado-San Gregorio fault zone west of Santa Cruz.

Plotted epicenters of more than 110 earthquakes (1968-76) form two clusters, one at the intersection of the Monterey Bay and Palo Colorado-San Gregorio fault zones, and the other in a northwest-trending linear belt along the Palo Colorado-San Gregorio fault zone. Trends and right-lateral strike-slip displacements of individual faults within the Monterey Bay fault zone correspond to those of the San Andreas, whereas properties of faults within the Palo Colorado-San Gregorio fault zone are similar to those of the Hayward fault. Interrelationships of movement between the onshore and the offshore faults may help explain problems associated with each. Intermittent late Cenozoic movements along the offshore faults can also explain the present configuration of unusual seafloor features, such as the headless Pioneer and Ascension Canyons that ap-

pear to be displaced and recently exhumed lower segments of ancestral stages of Monterey Canyon.

Sedimentological features and growth of the Monterey deep-sea fan off central California

Using geophysical survey records, W. R. Normark and G. R. Hess have determined that the southern sector of the Monterey fan is the chief area of present fan growth. The western portion of the fan appears to receive only occasional dilute turbidity flows and in places has a mantle of pelagic sediment. Discrete basins and basement troughs, as well as isolated seamounts and volcanic ridges that form basement highs, have controlled directions of fan growth.

On the basis of a detailed survey, Normark and Hess showed that the irregular hummocky topography of the upper Monterey fan forms a series of sinuous crests and troughs. These features have amplitudes of 10 to 20 meters, wavelengths of 1 to 2 km, and overall lengths of 1 to more than 4 km and apparently are associated with the deposition of channel levees. The present active sediment distribution system on the fan is a complex mixture of main channels with branching distributaries that may rejoin in some cases. Irregular topography and weak, diffuse seismic signals that differ from those for turbidite deposits were used to identify a recent large debris flow at the base of the continental slope to the south and east of the upper Monterey fan valley and downslope of an area of active faulting and seismicity. This flow covers 688 km² of seafloor, has a maximum observable thickness of 89 m and calculated volume of 23.3 km³.

Beach-sand retention landward of a nearshore submarine canyon

Providing foci for high energy wave conditions, the heads of several submarine canyons lie close to the shore of Monterey County, California. J. R. Dinger has found that, despite exposure of a nearby beach to the high energy conditions, sand is retained on the beach. Here, sand retention appears to be related to a combination of sand supply, offshore trapping by large bedforms, and biologic stabilization.

Recent faulting of seafloor off Humboldt Bay in California

Based on their interpretations of two multichannel seismic profiles and a high resolution seismic record, D. S. McCulloch, A. T. Long, and P. A. Utter suggest the presence of relatively young thrust

faulting associated with, and roughly parallel to, the axis of a clearly defined anticline that has an east-west trend and lies seaward of Humboldt Bay in northern California. One interpretation of the high resolution record would provide a seafloor offset of as much as 20 meters with upward displacement of the north side. The fault may be an offshore expression of the North Spit fault on the adjacent mainland.

Petroleum resources potential and geologic hazards of the Oregon-Washington Outer Continental Shelf

On the basis of an interim synthesis of existing information, P. D. Snavely, Jr., J. E. Pearl, and D. L. Lander concluded that no one can now assess the petroleum potential of the continental shelf off Oregon and Washington with any degree of confidence because of the paucity of geophysical and subsurface geological data. More than 6,000 m of Tertiary marine sedimentary rocks, the presence of many untested structural and stratigraphic traps, and indications of petroleum in Neogene strata of coastal Washington provide ample reason for additional exploration and drilling of the region.

Without question, the most critical factor controlling the accumulation of petroleum on the Oregon-Washington OCS is the availability of reservoir rocks. Based on interpretation of onshore geologic mapping and stratigraphic studies, Snavely, Pearl, and Lander concluded that a sand source existed near an ancient shelf edge and that sand from this source may have moved through channels into deep marginal basins off Coos Bay, Newport, Astoria, and Grays Harbor. The most favorable prospective areas, therefore, may lie seaward of onland source areas where upper Eocene to middle Miocene deltaic deposits accumulated near a former shelf edge.

Many large anticlinal structures that have been drilled onland and at several places offshore have "bald" cores of lower and middle Eocene basalt flows and breccias, intensely deformed lower and middle Eocene sedimentary rocks, or sheared siltstone and *mélange* of diapiric structures. The best target horizons for petroleum exploration may lie along the flanks of these large structures where stratigraphic traps may result from onlap of upper Eocene to middle Miocene units onto the pre-middle to late Eocene structures.

At most places, the structurally complex siltstones and mudstones of early to middle Miocene age are mature with respect to the generation of hydrocarbons. The overlying upper Miocene and Pliocene

sequence contains sandstone beds that are potential reservoir rocks. However, whether or not the Pliocene sediments above the larger anticlines and diapiric structures have cap rocks of sufficient thickness for capture of petroleum is debatable. In fact, many diapirs penetrate the entire upper Miocene and Pliocene sequence and reach the seafloor.

Potential geoenvironmental hazards are known to exist on the Oregon-Washington OCS, but cannot be fully evaluated because of the lack of enough high-resolution seismic data and sufficient seafloor samples. Geologic and seismic evidence indicates continuing tectonic activity through the Tertiary and Quaternary to the present. Warping and offset of the seafloor and areas of submarine sliding are identifiable on the few available high-resolution seismic profiles. Geologic mapping of coastal areas indicates the presence of many faults that deform or offset Pleistocene deposits and several that displace recent soil profiles. Vertical tectonic activity has apparently been relatively intense along the Olympic Coast and on the inner Washington OCS, as demonstrated by the record of rapid uplift of the Olympic Mountains during the past 5 million years.

Separate and superimposed equilibrium bedforms—a synthesis of flume and San Francisco Bay observations

D. M. Rubin has compared results of flume experiments on the relationships of bottom sediment bedforms and water shear velocities with records of side-scan sonar surveys of bedforms in central San Francisco Bay and determinations of associated hydrodynamic conditions. He concludes that the kind of bedform present at a given place, either in a flume or in the Bay, is related directly to the shear velocity of the flow. The shear velocity is greatest above large sand waves and least above flat beds with no sediment transport, and has intermediate values over beds with ripples, small sand waves, and flat beds with sediment transport.

Where small bedforms are superimposed on large bedforms, the shear velocity near the bed is in equilibrium with the large bedforms. For example, where ripples are superimposed on sand waves, the flow within a distance of several ripple heights from the bed has a shear velocity within the ripple range; the overlying flow (within several sand-wave heights of the bed) has a shear velocity within the sand-wave range. These observations allow the prediction of velocity profiles above the bed of San Francisco Bay on the basis of bedform distribution. They may also be used to construct profiles when a change in bedform has been recorded by a bottom-mounted

rotating side-scan sonar that is currently being used in studies of bay currents (Rubin, McCulloch, and Hill, 1977).

Heavy-mineral assemblages of Willapa Bay in Washington

Gretchen Luepke identified two basic heavy-mineral assemblages within the modern sediments of Willapa Bay. One assemblage within sands delivered by rivers draining into the bay from the south and east is rich in clinopyroxene, commonly in amounts that exceed 70 percent of the total assemblage. The other assemblage within sands of the bay's beaches, tidal flats, and rivers draining from the north is rich in hypersthene and hornblende (with the river sands generally richer in hornblende). Sands of terraces bordering the eastern shore of Willapa Bay contain the same assemblages, apparently reflecting comparable controls of sand distribution in the past.

Interactions of oil and burrowing fauna experiment at Willapa Bay

Major unresolved questions concerning petroleum spillage include the degree to which oil modifies the behavior of burrowing fauna and, conversely, the extent to which the fauna incorporates oil into the sediment. H. E. Clifton conducted experiments at Willapa Bay to help answer these questions. The experiments involved emplacing small quantities of North Slope crude oil in plots of 1 m² on sandy tidal flats riddled by burrows of the decapod crustacean, *Callinassa*. One experiment tested the effect of oil applied topically to burrow openings at the sediment surface; a second determined the effect of a thin layer of oil buried several centimeters beneath the surface. Adjacent control plots provided a measure of the influence of oil on the fauna.

The oil applied topically during a low tide had no significant effect on the number of burrow openings. Small slicks, however, emanated from the burrows for several days following application, indicative of some oil having been incorporated into the sediment column. In contrast, the buried oil drastically reduced the number of burrow openings, apparently because the oil-saturated sand formed a barrier through which the *Callinassa* could not burrow. Even after two months, only a few burrows near the margin of the plot penetrated the oil layer. Accordingly, it appears that for some time burrowing activity has not redistributed the buried oil significantly.

ALASKA CONTINENTAL MARGIN

Environmental geologic studies, northeastern Gulf of Alaska

B. F. Molnia has recognized four morpho-geographical segments, each with a unique sedimentologic regime and geologic character, along the 250-km coastal area between Cape Suckling and Yakutat Bay on the northeastern margin of the Gulf of Alaska. The segments are (1) Bering Glacier foreland, (2) Yakataga to Umbrella Reef, (3) Icy Bay mouth, and (4) Malaspina Glacier foreland. All are subject to aperiodic tectonic uplift and variable isostatic adjustment.

The Bering Glacier foreland, characterized by outwash plains and broad, thick (>100 m) sand beaches, has large wash-over fans that are offsetting stream mouths and burying forests. Rivermouth spits accrete westward (max. rate: 6 km/30 yr) as the coastline actively recedes (max. rate: 20 m/yr). The shore from Yakataga to Umbrella Reef has thin beaches separated by eroding bedrock outcrops. A receding scarp as much as 6 m high bounds the inland side of the beaches. The Icy Bay mouth segment is the most dynamic and complicated with recent rapid deglaciation, and shoreline erosion of as much as 4.5 km since 1922. Parts of the area are underlain by melting ice. Deposition of sediment at Point Riou Spit averages about 5×10⁶m³/yr. The Malaspina Glacier foreland consists of eastern and western outwash plains and a large recessional moraine at Sitkagi Bluffs. Sediment from the stagnating glacier and erosional resistance of the moraine cause an essentially stable shoreline. Blizhni Point is the only major depositional site.

Despite active, continuing erosion, the Cape Suckling to Yakutat Bay coast must still be classed as an accretionary zone. A periodic uplift of the seafloor produces new land that, although attacked immediately by erosion, is subsequently raised above reach of the shoreline processes.

Since Icy Bay deglaciation began in 1904, intense erosion has caused adjacent Gulf of Alaska shoreline retreat of several kilometers. For the shore east of the bay mouth, retreat amounts to more than 1.3 km since 1941 and as much as 4.5 km since 1922. The western shore has receded at least 4.8 km since 1922, removing a land area of more than 8.2 km² between 1922 and 1976. Development of Point Riou Spit began as soon as longshore transport could supply sediment to the area that ice occupied in 1904. By 1922, the spit had a length of 3.18 km and by 1957 had grown to 6.86 km. A major storm between 1957 and 1971 breached and shortened the spit and

formed Severed Bar. In 1976, Point Riou Spit was 6.60 km long. If it continues to grow at its 1971 to 1976 average annual rate, it will seal off the mouth of Riou Bay within 20 years and within another 15 years will fill Moraine Harbor, the proposed site for a Chugach Natives, Inc., development. Between 1922 and 1971, sedimentation added more than $3.5 \times 10^7 \text{ m}^3$ of material to Point Riou Spit, including growth of the spit into an area of open water with a previous depth exceeding 75 m. This may be compared to filling of Vancouver's Icy Bay that, on the basis of available geographic and bathymetric data, probably took place between 1807 and 1837 and required a sediment volume of about $5 \times 10^8 \text{ m}^3$.

K. A. Kvenvolden and G. D. Redden measured hydrocarbon gas contents in nearshore, near-surface sediment samples from 12 sites along the north and northeast margins of the Gulf of Alaska. Methane (C_1) concentrations ranged from 0.32 to 23.0 nl/g of wet sediment. Hydrocarbon gases of high molecular weights (ethane (C_2), propane (C_3), isobutane (i-C_4), n-butane (n-C_4), ethylene and propylene) were also detected in most samples, but at concentrations at least an order of magnitude less than those of C_1 . A sample of clayey silt from near the mouth of the Copper River contained the highest amounts of C_1 , as well as of C_2 , C_3 , and n-C_4 . Relatively high gas concentrations were also found in clayey silt samples from southeast of Kayak Island. For all samples concentrations and proportions of the various hydrocarbons are consistent with a low-temperature biochemical origin involving decay of organic material incorporated in the sediments.

For the same areas, seismic records have discontinuous reflectors that suggest the presence of gas-charged sediments. If this deeper gas had a thermogenic origin associated with the formation of petroleum, any leakage would produce anomalous ratios in the surface-sediment concentrations of hydrocarbons. Lacking anomalies, gas of the deeper sediments is thought to be the product of biologic activity like that of the analyzed samples.

Further offshore, the northeast Gulf of Alaska Continental Shelf is cut by at least eight major valleys. According to P. R. Carlson, T. R. Bruns, B. F. Molnia, and J. C. Hampson, Jr., evidence of glacial processes as a cause of their present morphologies includes: (1) U-shaped cross sections, both surficial and on the top of buried Pleistocene surfaces; (2) concave longitudinal sections that commonly shoal at their seaward ends; (3) till-like sediment samples from the valley walls and adjacent shelf; and (4) local partial fill of sediment with

seismic properties typical of glacial deposits. Buried Pleistocene erosion surfaces along thalwegs of the valleys have depressions with tens of meters of relief. These depressions have been partially smoothed by the seaward-thinning wedge of post-glacial flour (clayey silt) that is filling these valleys and blanketing the inner shelf at rates of as much as 15 mm/yr (as determined by Pb-210 measurements).

Although glaciation had the dominant role, the modern morphologies of the submarine valleys may also be partly attributed to structural controls. For example, seismic records indicate that the center of deposition of a shelf basin underlies the landward end of the Yakutat Sea Valley, and various structurally controlled topographic highs of the shelf (i.e. Tarr Bank, Kayak Island, and Pamplona Ridge) apparently influenced movement of the glacial lobes.

Seaward of the Malaspina Glacier, the northeastern Gulf of Alaska Continental Shelf has bottom features that P. R. Carlson interprets to be products of mass movement. The slump structures lie in water depths of 70 to 150 m on slopes of less than 0.5° , are about 0.5 km from front to back, have irregular surface relief of 2 to 5 m, show disrupted bedding in acoustic profiles, and consist of low-strength, poorly sorted, clayey silt. Slump "blocks" reflect progressive failure that may be attributed to lateral extension or stretching of an underlying sedimentary unit at a depth of 35 to 50 m in the Holocene deposits. Slump features of similar size and shape off the mouth of the Copper River are thought to be products of intense ground shaking that accompanied the 1964 Alaska earthquake. Those southwest of the Malaspina Glacier cannot be related to a specific earthquake event; however, a fault on the south side of Icy Bay, numerous earthquakes near the mouth of Icy Bay, and three magnitude-6 shocks at nearby Pamplona Ridge during 1970 indicate that the shelf is subject to frequent ground shaking of sufficient intensity to cause mass movements.

South of Kayak Island in the northern Gulf of Alaska, the outer edge of the continental shelf is the site of small surficial step faults underlain by deeper listric faults, according to T. R. Bruns, P. R. Carlson, and W. C. Schwab. The surficial step faults are clustered in two areas of 100 km² and 125 km² at water depths of 150 to 225 m. Individual scarps have relief ranging from 2 to 5 m. Fault planes are traceable on high resolution seismic records to depths of about 150 m and offset strata of Pleistocene age. Some fault blocks provide evidence of backward rotation; however, the seismic records fail to show seaward curvature of the slip planes.

The deeper listric faults, which are interpreted from multichannel seismic records, are present discontinuously over a distance of 50 km, and affect strata of Pleistocene and possible Pliocene age to a depth of 1 km. The fault planes appear to be curvilinear, concave-upward, slip surfaces. Fault-block rotations have caused wedges of material to be displaced seaward. The faults are considered a consequence of continued growth of an underlying anticlinal structure that has caused uplift and gravity sliding of the overlying material. The surface faults, in turn, may be due to settling within the seaward-moving wedges. Masses of slumped sediment on the continental slope adjacent to the faulted areas represent an ultimate effect.

Continental Shelf structure, northwestern Gulf of Alaska

Based on analyses of multichannel seismic and other geophysical records, R. E. von Huene and M. E. Fisher report that the Continental Shelf adjacent to Kodiak Island has three basins with areas exceeding 3,500 km² and several smaller basins. Gently deformed sediments of probable Oligocene or Miocene and younger age fill the basins and overlie intensely deformed strata of Oligocene and older age. Anticlines that form the edge of the Continental Shelf also appear to form dams at the seaward margins of all large basins. The stratigraphy of the shelf area is complex because erosion and deposition by glaciers, turbidity currents, and other processes create features that lie at right angles to the direction of folding, faulting, and other effects of regional tectonic forces.

Bedform movement in lower Cook Inlet

A. H. Bouma and M. A. Hampton have extended their studies of bedforms within the lower Cook Inlet region to a ramp that exists off the south point of the Kenai Peninsula and has depths of 70 to 140 m exceeding by 10 to 80 m those within the inlet itself. Here, as elsewhere, each bedform type covers a small elongate field a few hundreds of meters in breadth and several kilometers in length. In general, the ramp is considered to be a constructive progradational wedge, building slowly to the south.

Navarin Basin complex, Bering Sea Outer Continental Shelf

Summer 1977 marine operations included the collection of more than 4,000 km of geophysical data including 24-channel seismic reflection profiles in the Bering Sea. The data revealed that Navarin Basin, between Siberia, USSR, and St. Lawrence

Island, Alaska, actually is a complex of three distinct basins. M. S. Marlow, A. K. Cooper, D. W. Scholl, Hugh McLean and J. R. Hein reported that the three subshelf basins lie beneath shallow water (less than 200 m) and that each contains more than 9,000 m of sediments. The thick sections of sedimentary fill are separated by a series of northwest-trending basement ridges. In one basin, the fill has been deformed compressionally and then truncated. Seismic records of the sedimentary layers contain numerous acoustic anomalies that are suggestive of hydrocarbon deposits and warrant further investigation.

Heat flow data for the Bering Sea Basin

A. K. Cooper, B. V. Marshall, and J. R. Childs acquired instruments formerly used on the *T3* ice island to measure heat flow in deepwater sedimentary basins and adapted them for use aboard USGS research vessels. During June 1977, measurements were obtained at 6 of 10 heat flow test sites within the Bering Sea Basin. Preliminary interpretation of the results indicates an average heat flow value of about 1.5 $\mu\text{cal}/\text{cm}^2/\text{s}$, which is slightly higher than the world average for ocean basins. The successful measurements span an area that is known to have a buried igneous basement with relief of 3 km; the lack of heat flow anomalies indicate that these basement features do not have active heat sources. The projection of surface temperature gradients downward into the known thicker (3 to 9 km) sedimentary rock sequences, however, provides sufficiently high heat values for the generation of heavier hydrocarbons of oil and natural gas. Thus, Cooper, Marshall, and Childs conclude that the thermal regime of the Bering Sea Basin favors the presence of petroleum deposits.

Thermogenic gas seep on the sea floor of Norton Sound

C. H. Nelson and K. A. Kvenvolden undertook an intensive study of a portion of Norton Sound about 40 km south of Nome, Alaska, in response to the 1976 discovery of a plume of hydrocarbon gases that was reported by Cline and Holmes (1977). Gases of the reported plume were assumed to have a thermogenic origin based on chemical composition and to reach the water column through a fault zone in the seafloor. The follow-up studies included running closely spaced 2- to 5-km transects throughout the 200-km² plume area. Data obtained with high resolution seismic profiling equipment (Uniboom, bubble detector, 3.5 kHz, and 12 kHz), side-scan sonar,

underwater TV, and gas chromatogram analysis of core samples failed to produce evidence for thermogenic gas in sediments of the reported plume area. They did, however, lead to discovery of a new area 9 km south of the plume center and associated fault zone where both geophysical and geochemical evidence suggest the presence of thermogenic hydrocarbons in the sediments.

In an area of about 2 km² at the newly discovered location, the seismic records contain acoustic anomalies that terminate all subbottom reflectors, suggesting the presence of gas-charged sediments. Within this same area, the records also provide evidence for a fault that parallels the trend of the fault zone in the plume area to the north. Analyses of hydrocarbon gases in samples from a 1.6 m core collected at the location gave anomalously high concentrations for hydrocarbon gases that are heavier than methane. The ratio of methane to ethane and propane had minimum values of 7 at the bottom of the core, and the maximum concentrations of ethane, propane, *n*-butane, and isobutane were as much as 7, 3, 6, and 52 times greater, respectively, than concentrations of these gases in three cores within and to the north of the plume area. The low ratio and high concentrations of heavier hydrocarbons are considered indicative of a dominantly thermogenic origin for the gases and of the possibility of subsurface petroleum deposits within the region.

Effects of a major storm on the northern Bering Sea coastline

During November 1974, a major storm caused extensive damage to coastal communities on the northern Bering Sea coast of Alaska. Along much of the coast, reported wave heights of as much as 3 to 4 m were superimposed on storm surge elevations of about 4 m above sea level. The wind, waves, and surge lifted and broke bottomfast ice that had begun to form along beaches and in shallow lakes and lagoons before the storm and drove the resulting ice cakes as far as 100 m inland.

A. H. Sallenger and R. E. Hunter compared vertical aerial photographs taken before and after the storm and found that tundra bluffs in the vicinity of Nome had been eroded as much as 45 m. Giant pre-storm cusps spaced at intervals of about 350 m were destroyed and replaced by still longer cusps spaced at roughly 1,000 m. The new giant cusps controlled the location and extent of overwash on barrier spits east of Nome—the overwash extending further landward within embayments of the rhyth-

mic shoreline topography. The new spacing also resulted in a complex pattern of post-storm shoreline erosion and accretion. Sallenger and Hunter also noted that melting the following summer caused deposition of sediment and vegetation that was frozen to the bottom of shore-driven ice cakes. They conclude that lifting and movement of sediment attached to ice cakes may be a major factor in maintaining or deepening the lakes in low coastal areas of northern Alaska.

Bottom boundary layers and sediment transport on the floor of Norton Sound in Alaska

D. A. Cacchione and D. E. Drake successfully deployed and recovered three GEOPROBE tripods in Norton Sound, Alaska, during the periods September–October 1976 and July–October 1977. Data from two consecutive GEOPROBE records taken at a site about 50 km south of Nome showed that currents during spring tidal sequences are sufficiently strong to generate a turbid, sediment-laden bottom layer whose thickness and intensity waxes and wanes in the course of the tidal cycle. Net transport of material is accomplished by a weak to moderate mean flow toward the Bering Strait. The 1977 data also showed that a chance storm produced relatively large amounts of suspended sediment about 2 m above the seafloor. Such storm-generated sediment activity, combined with the tidal stress effects, may explain the relatively low sediment accumulation rates in western Norton Sound.

Bottom velocity shear measured with four vertically arranged electromagnetic current meters on the GEOPROBE reflected development of intense stresses at the seafloor during the storm and peak spring tidal currents. These high shear measurements correlate with low transmission and high scattering data for light.

Shipboard measurements during the 1976 and 1977 cruises provided evidence for one and possibly two remnant water masses above the seafloor of eastern Norton Sound. This mass probably represents water formed during freezing and associated convection the previous winter. Relatively high suspended sediment levels of this bottom water probably result from tidal processes.

The 1977 shipboard and moored current-meter data indicate a general cyclonic circulation in western Norton Sound, providing a major transport pathway for Yukon River materials toward the Bering Strait. The eastern portion of the sound exhibits no well-defined mean water circulation pat-

tern, and therefore diffusion apparently is the major exchange process.

Rates of arctic marine geologic processes

Following several years of study, P. W. Barnes, Erk Reimnitz, D. E. Drake, and L. J. Toimil have arrived at general estimates of the rates of arctic marine geologic processes about which little was known in the past. Rates of seafloor ice gouging and barrier island movement provide examples.

Repetitive side-scan sonar and precision bathymetric surveys over a 5-year period, 1973 to 1977, in the Beaufort Sea enable the identification of changes in microrelief resulting from ice gouging. Superimposition of gouges and the crispness of gouge flanks serve to distinguish new gouges. With measurements on fathograms of cross-sectional gouge relief, a conservative estimate of 0.36 km of gouging within a 10-km segment of trackline took place between 1973 and 1975 (19 m/km/yr). Measurements on 1976 records indicate a similar rate of ice gouging (12 m/km/yr). Assuming that no area is gouged more than once, the rates would lead to reworking of the bottom of the entire survey area within 50 to 80 years. The estimated gouging rates are conservative because (1) they exclude very small gouges on the gouge flanks and (2) the actual area of the bottom disturbed by a blunt ice keel is probably much greater than the measured width of a gouge. With average gouge depths of 0.3 m and an inner shelf sedimentation rate of less than 1 m/1,000 yr., surface sediments will be reworked several times before being buried deep enough to escape ice action. Seaward of the study area in the stamukhi zone, where ice activity is greatest, rates and intensities of ice gouging are probably much greater.

Three sand and gravel islands off the north coast of Alaska near Prudhoe Bay have remarkably similar rates of erosion and apparent migration at 6 to 7 m/yr on their seaward sides. The islands of Cross, Spy, and Thetis are becoming narrower through erosion and longer through spit accretion at their ends. Although the dominant northeasterly winds and resulting westerly longshore transport control the general shapes of the islands, ice push from the northeast onto the beaches also has an apparent role, bringing material from several meters depth offshore onto the beaches and thereby accelerating rates of morphologic change. Because the islands lack an apparent outside source of sand and gravel from rivers, longshore transport, or offshore, it can

be concluded that the Islands are self sustaining or gradually disintegrating.

Sediment transport on the inner shelf of the Beaufort Sea

Side-scan sonar records obtained by L. J. Toimil and Erk Reimnitz in the 2-m water depths of Leffingwell Lagoon on the north coast of Alaska reveal a herringbone pattern of linear reflectors with branching diagonals. The major longitudinal reflectors are spaced 10 to 30 m apart and have no detectable relief of 20 cm or more. Toimil and Reimnitz believe the patterns represent the traces of current-aligned, helical cell boundaries recorded in unresolvable microrelief or in textural differences of the silty fine sand on the lagoon floor. Three-dimensional flow of the Taylor-Görtler type, consisting of an array of pairs of counter-rotating helical vortices with axes lying parallel to the primary direction of flow provides a likely mechanism to explain the observed sonar patterns. Reasons for the flow are unclear but may be related to the development of centrifugal instability of ebb flow along the concave surface of the tidal inlet, or to constriction and intensification of tidal flow in the shallow lagoon under a growing winter ice canopy.

D. E. Drake used water samples and a beam transmissometer to determine the concentrations, composition, and distribution of suspended particulate matter in the inner shelf of the Beaufort Sea during both ice-covered and open-water seasons. Sluggish water movement and extremely low concentrations of suspended particles during the ice-covered season suggest that winter sediment transport is only a small fraction of summer transport. Drake also found that the great bulk of suspended matter transport takes place within 5 to 15 km of the shore, that discharge of the Coleville River overshadows that of smaller rivers, that wind-driven water motion apparently controls the fate of suspended particles, and that as a result of dominant northeasterly wind, net sediment transport is westward along the coast.

OCEANIC STUDIES

Sediment-nodule geochemistry of deep sea manganese nodules

Using results of chemical and petrographic analysis of manganese nodules and associated sediments from three of NOAA's Deep Ocean Mining Environmental Study (DOMES) sites, J. L. Bischoff and D. Z. Piper have compared the geochemical characteristics of three widely separated areas within

the Equatorial North Pacific Manganese Nodule Province. Sediments at these sites consist of varying proportions of terrigenous clay, biogenic debris, volcanogenic grains, and hydrogenous material. The sediments of DOMES sites A and B have higher concentrations of biogenic phases (apatite, organic carbon, and opaline silica) than those of site C. The sediments at site C, in turn, have a significant metalliferous component that is high in iron and manganese and low in Al_2O_3 and that is essentially absent at sites A and B. The terrigenous components of samples from the three sites have uniform chemical compositions that are nearly identical to average Pacific pelagic clay. The hydrogenous component, as characterized by the amounts of nickel and manganese, is significantly higher at site C than at sites A and B. In each area, Cu, P, Mo, and Ba correlate closely with Mn and Ni of the sediments, as in manganese nodules.

In general, the averaged chemical compositions of manganese nodules from the areas are surprisingly similar in light of the rather striking differences in bulk compositions of the associated sediments. Variations of compositions among nodules within each area, however, are rather large and, together with nodule abundance, appear to have a close relationship to seafloor relief.

Coral caps on seamounts of the Emperor Seamount Chain

Seismic reflection records collected during a cruise to the Emperor Seamount Chain northwest of Hawaii in September-October 1976 contain evidence of northward displacement of the Emperor Seamount chain as predicted by the hot-spot hypothesis. Analyses of the seismic records by H. G. Greene and G. B. Dalrymple (USGS), and D. A. Clague (Middlebury College) show that ancient coral reefs as much as 400 m thick cap the principal seamounts of the Emperor chain as far north as lat $45^{\circ}30'$ N. Even the southernmost of these reefs, at lat 35° N. is presently well north of the northern limit of active reef growth. In addition, existing oxygen isotope data indicate ocean surface temperatures during the Cenozoic were never warm enough to permit reef growth north of about lat 33° - 34° N. From the data and other information, Greene, Dalrymple, and Clague (1978) concluded that the Suiko Seamount, which is now at lat $44^{\circ}30'$ N. and is the northernmost examined, was formed about 58 million years ago and has been displaced a minimum of 10° northward relative to the geographic equator. They also concluded that the youngest fossil reef organisms on seamounts in the submerged chain have a late

Eocene or older age. These conclusions have subsequently been substantiated, at least in part, by drilling on Ojin, Nintoku, and Suiko Seamounts conducted during July to September 1977 in the course of Leg 55 of the International Program of Ocean Drilling.

Deep-tow studies of the East Pacific Rise, Pacific Ocean Basin

W. R. Normark and G. R. Hess successfully matched deep-tow data collected during a second cruise to the crest of the East Pacific Rise with data from an earlier (1974) cruise. Side-scan and photo data were used to correlate the two data sets and construct a detailed bathymetric map. Analyses of about 4,000 stereo-paired photographs allowed preparation of a large-scale geologic map to aid in delineating the distribution of hydrothermal events within the spreading center axial zone and to help determine the relations of these events to processes of deep-sea mineralization.

In a cooperative deep-tow experiment with Cal Tech's Jet Propulsion Laboratory, Normark and Hess successfully deployed and tested a "chirp" reflection profiling system. Preliminary results indicate the system will provide quantitative information on internal structures and geo-engineering properties of marine sediments.

In the course of the deep-tow experiments, four dredge hauls from a 3.3 km-wide zone at the axis of the East Pacific Rise recovered fresh tholeiitic basalt. Petrologic studies, including major element chemical analyses, indicate a range of moderately fractionated basalt varieties with one sample enriched in iron and titania. The samples show no symmetrical compositional zonation across the ridge axis; however, the youngest and least fractionated were from the east side of the axis.

Nannofossil ages for East Pacific Rise fast spreading sites

Cores for use in studying the nature of young crustal rocks in areas of rapid seafloor spreading were obtained at two clusters of deep-sea drilling sites in the eastern Pacific Ocean near the Siqueros Fracture Zone on the East Pacific Rise (approx. lat 9° N., long 106° W.) and near the Galapagos spreading center (approx. lat 1° N., long 86° W.) during leg 54 of the International Program of Ocean Drilling. J. D. Bukry reported that preliminary study of nannofossil assemblages from the 11 sites indicate Quaternary ages for the oldest sediment of most cores and Pliocene ages for 4. Two of the latter come from sites that are more

than 200 km from the axis of active spreading. One of these contains an assemblage identified as the upper Pliocene early *Discoaster surculus* Subzone, with an age of about 2.5 m.y. The indicated spreading rate of 8.2 cm/yr is similar to other fast rates that have been reported for the East Pacific Rise south of the Clipperton Fracture Zone (Van Andel and Bukry, 1973).

Hypersaline epoch in the Black Sea

In another contribution of studies supporting the deep ocean drilling effort, F. T. Manheim has found that interstitial waters of cores from the Black Sea contain evidence of both a fresh-water lake stage and a hitherto unidentified hypersaline stage about 400,000 years B.P., in late Pleistocene time. Measured interstitial salinities of nearly 100 ‰ (compared with current values of 23 ‰ for Black Sea bottom waters) characterize deeper formation fluids and are considered indicative of former evaporite minerals that have been removed by diffusion.

STUDIES OF MARINE AND COASTAL PROCESSES

Mercury release from contaminated estuarine sediments

In experiments in Puget Sound, M. H. Bothner demonstrated continuing release of dissolved mercury from mercury-contaminated anoxic sediments. The results are contrary to the previously predicted immobilization of mercury by sulfides in the pore fluids of anoxic sediments, and they lead to the conclusion that contaminated sediments can be a lingering source of mercury discharge after removal of a primary industrial source.

Reef destruction by boring organisms

The presence of stress bands of known age within corals killed by weather in 1969 allows realistic estimates of the rate at which boring organisms degrade dead corals (i.e., reef limestone). To make such estimates, E. A. Shinn, J. H. Hudson, and B. H. Lidz took several cores from the same coral head over a 3-year period. By measuring downward from the surface formed by the boring organisms to an identifiable stress band, the amount of material, and rate of coral skeleton removal was determined. Shinn, Hudson, and Lidz concluded that a 1-m high coral head can be completely converted to sediment in 100 years.

Daily cycles in coastal dune deposits

Cross-strata of some ancient eolian sandstones display cyclic tendencies that are not well understood. In a search for modern analogues, R. E. Hunter found cyclic structures in sediments of active dunes along the Oregon coast. The modern cycles are produced by daily variations in wind velocity associated with the sea-breeze regime. Like most sedimentary cycles, the daily cycles in the dune deposits lack absolute regularity; on some days wind speeds are too low to form layers, and on others disturbing events introduce complexities. The thicknesses of the cyclic layers relate to dune height and to wind speed, as well as to the daily regime. A comparison with time intervals represented by the cycles of ancient eolian sandstones remains questionable because, for example, the cyclic layers in the Navajo Sandstone of Utah are so thick and the required wind velocities of a comparison are so high that an interpretation invoking daily layering is difficult to accept.

ESTUARINE AND COASTAL HYDROLOGY

ATLANTIC AND GULF COAST

Estuarine sediment sources of the Potomac estuary

As a part of a program to determine sediment sources, transport and deposition patterns, and transport rates, J. L. Glenn began a reconnaissance study of bottom and suspended sediments in the Potomac estuary from Washington, D.C., to Chesapeake Bay. Bottom sediments are chiefly silt and clay size with sand common only in shoal areas in the upper estuary. Suspended-sediment concentrations at four 24-hour sampling stations along the estuary varied with tidal and river current velocities; concentrations were generally higher at higher velocities at all stations and were highest at a station near the upstream limit of marine saltwater.

Distribution of biologically reactive substances in the Potomac estuary

Initial findings from a late summer (August–September, 1977) hydrographic survey of the Potomac River and estuary by T. J. Conomos and D. H. Peterson show the presence of a massive waste-related phytoplankton bloom in the upper fresh-water portion of the system. As a result, the major river to estuary variations in dissolved gases (O_2 , CO_2), suspended particulate carbon and nitrogen,

dissolved ΣCO_2 , NH_3 , NO_2 , NO_3 , pH, and alkalinity correlate with phytoplankton biomass and activity. An unusual down-river variation in alkalinity may be explained by a phytoplankton growth-mineralization process that causes variations in the dissolved NH_3 (associated with alkalinity increases) and NO_3 (alkalinity decreases) concentrations. A simple model for transport of substances is, however, inadequate when describing oxygen, carbon, and nitrogen distributions in the upper estuary (0–10 ‰ salinity). Presumably, an additional source from the Chesapeake Bay is required for a mass balance.

Circulation modeling and turbidity monitoring in Tampa Bay, Florida

A model analysis of Tampa Bay, Fla., indicated that circulation is enhanced by nonuniform distribution of inertia in tidal flows. According to C. R. Goodwin, inertial characteristics of water masses in an estuary depend, to a large degree, on water depth. Inertial differentials produce differences in times of tide reversals that cause adjacent water masses to move in opposite directions for considerable lengths of time. As a result, Tampa Bay flood-tides predominate in many of the deep parts of the bay and ebb-tides generally prevail in the shallow near-shore areas.

Turbidity plumes are being monitored in Tampa Bay near dredge construction areas by using 35-mm aerial photographs and water-quality sampling by boat. Sample positions are chosen by an observer in the aircraft that is in radio communication with the boat. Samples for turbidity and other parameters are collected while photographic overflights are made. Results indicated that turbidity plumes are highly variable in appearance, depending on type and color of dredge material, water depth and clarity, speed and turbulence of the current, type and size of the dredge, and effectiveness of floating, plume-containment screens.

In areas where long gray-white plumes overlie clear, deep water, turbidity differences of 1 to 2 JTU are easily detectable from the air. In slow-moving water that contains dark sediments, turbidity differences of 20 JTU or more are difficult to detect.

Potential saltwater encroachment in southwestern Louisiana

The principal aquifer for southwestern Louisiana is the Chicot aquifer, which in the coastal area is more than 300 m thick, including intercalated clays. The top of the sand in the coastal area is about 60

m below the surface. Studies by D. W. Nyman, S. T. Mumme, and J. R. McKay showed that the water-level gradient was coastward before ground-water development in the Chicot, but because of heavy agricultural and industrial pumping, the gradient was reversed and is now gently landward. Studies in the coastal zone indicated that some areas are susceptible to saltwater encroachment, whereas others are afforded some natural protection. The latter areas are those where the underlying upper sands in the Chicot aquifer are less permeable and contain intercalated clays that act as barriers to saltwater movement. In these areas of lower permeability, the freshwater-saltwater interface is relatively steep; northward, the base of freshwater is deeper than in the adjacent areas that are more susceptible to encroachment.

The susceptible areas are underlain by thick, continuous, permeable sands that extend gulfward and contain saline water. In these areas the northward sloping freshwater-saltwater interface is relatively gentle.

According to Nyman, routine observations of salinity indicated no significant encroachment since monitoring began in 1963. However, if large quantities of ground water were developed near the susceptible areas, the steepened landward water-level gradient could induce northward movement of the interface.

Saltwater intrusion into the Old Bridge Sand Member of the Magothy Formation of New Jersey

F. L. Schaefer and R. L. Walker, Jr., used field observations of water levels and chloride concentrations to determine the source and extent of saline water in wells tapping the Old Bridge Sand Member of the Magothy Formation in Keyport and Union Beach Boroughs of Monmouth County, New Jersey. Analyses of the changes in hydraulic and chloride concentrations indicated that saline water has moved into the Old Bridge aquifer from the submerged outcrop beneath Raritan Bay and has reached some of the near coastal-area wells at Keyport and Union Beach. Ground-water pumpage in this area had lowered the hydraulic head in the center of the cone of depression to 15 m below mean sea level by January 1977.

Data for 1950–68 indicated that background chloride concentration in this area was generally less than 5 mg/L. However, by March 1977, chloride concentrations had increased to a maximum of 660 mg/L at one well in Union Beach and 98 mg/L at one well near Keyport. Estimates of ground-

water flow rates for November 1973 and January 1977 are 47 and 89 m/d, respectively. Any increases in withdrawal rates in this area that tend to decrease the freshwater hydraulic head will accelerate the saltwater intrusion.

Water budget of Pamlico Sound, North Carolina

According to G. L. Giese, freshwater losses through evaporation from 5,335-km² of Pamlico Sound in North Carolina may sometimes exceed freshwater gains from inflow and precipitation, thus resulting in a net inflow of ocean water through Oregon, Hatteras, and Ocracoke inlets, which makes up the difference. The 30-consecutive day, 10-year minimum freshwater inflow to Pamlico Sound from all land areas and Albemarle Sound is only about 85 m³/s. If this inflow were to occur in June, when average evaporation from the sound is about 433 m³/s, and if precipitation during that particular month were negligible, then the net rate of loss of freshwater from Pamlico Sound would be about 347 m³/s, amounting to 900 million m³ for the month. Any such water losses would be made up by ocean water entering through the inlets. On an annual basis, Pamlico Sound receives an average of 233 m³/s (1,380 mm) of freshwater from precipitation, 805 m³/s of runoff from land areas draining directly into Pamlico Sound or indirectly through Albemarle Sound and loses about 153 m³/s (906 mm) of water from evaporation, for a net freshwater inflow of about 885 m³/s.

PACIFIC COAST

Current-measurement studies in San Francisco Bay

To augment the understanding of transport processes and to implement modeling studies of estuarine hydrodynamics in San Francisco Bay, R. T. Cheng initiated a hydrometeorological data-collection program. His initial efforts were directed toward developing techniques for measuring currents in a shallow estuary under the strong influence of wind-generated waves. An instrument tower that supported instruments free from the conventional mooring motion was designed and placed in South Bay during spring, 1977. During a 2-month period, four types of recording current meters (Savonius rotor, tethered shroud-impeller, drag-inclinometer, and electromagnetic) were tested and compared. These evaluations were conducted in conjunction with continuous wind and tide-height measurements. The results indicated that all types of current

meters are, to some degree, susceptible to mooring line motions. Among the instruments tested, the shroud-impeller current meter showed the least influence owing to strong wave motions. In contrast, most instruments gave relatively clean records when they were supported free from mooring lines. Results of tests suggested that carefully designed instrument must be used for any current meter in future shallow-wave-zone current measurements.

Migration of sand waves in central San Francisco Bay

D. M. Rubin and D. S. McCulloch are conducting a continuous, long-term experiment with a rotating side-scan system in central San Francisco Bay. The sand waves, which are 1 to 2 m high and 15 m apart at the study site, migrated several meters in the first 6 weeks of the experiment. Migration rates measured in the bay are being compared with predicted rates and with migration rates measured in other tidal and unidirectional flows.

Hydrographic framework of San Francisco Bay

A conceptual framework describing the physical processes controlling the distributions of properties of San Francisco Bay is being further quantified by T. J. Conomos. The northern reach receives 90 percent of the mean annual river inflow and 24 percent of the waste-water inflow to the bay. It changes from a partially mixed estuary, with a vertical salinity gradient of 10 ‰ during high river inflow, to a well-mixed estuary with a vertical salinity gradient of 3 ‰ during low summer inflow. The southern reach also has seasonably varying water properties. The variations are determined by water exchange from the northern reach and the ocean and from direct waste inflow (70 percent of total bay waste inputs). Salinity stratification is present during winter, whereas during summer the water is nearly isohaline because of wind and tidal mixing.

The northern reach of the bay has a permanent estuarine circulation cell largely maintained by the salinity-controlled density differences between river and ocean waters. Although wind and barometric-pressure variations alter this circulation, it is largely modulated by the timing and magnitude of the highly seasonal river inflow. This nontidal circulation is nearly equivalent to tidal diffusion in controlling the water replacement rates that vary from weeks (winter) to months (summer). The southern reach, in contrast, has seasonally reversing but sluggish near-bottom and surface nontidal currents

that are generated by prevailing summer and episodic winter-storm winds and by winter flows of low-salinity water from the northern reach. Although the diffusion of substances by the strong tidal currents are notable, the relative importance of diffusion by strong tidal currents and the episodic advective processes in controlling water replacement mechanisms and rates has not been fully determined.

Distribution of biologically reactive substances in northern San Francisco Bay

D. H. Peterson related the distributions of dissolved biologically reactive substances (O, C, N, and Si) in northern San Francisco Bay to spatial and temporal variations with dynamics of the estuary. The influence on the estuary of moderate or higher (>500 m³/s) river flow is impressive; at such rates of inflow, estuarine-water replacement time is probably less than 1 month and relative effects of additional sources and sinks of the dissolved constituents (waste inputs, phytoplankton production-mineralization, atmospheric-benthic exchange processes) appear to be small. Dissolved O, C, N, and Si are, therefore, often near-conservative, and their replacement (turnover) times are on the order of weeks or longer.

Marked departures from near-conservative O, C, N, and Si distributions occur during low river flow (<200 m³/s) when the local sources and sinks may exceed river and ocean outputs. In general, however, the rates of many processes are of the same magnitude and no one factor is dominant; dissolved oxygen is typically 5 to 10 percent below saturation concentrations, dissolved CO₂ is 150 to 200 percent above saturation concentrations and in balance with oxygen consumption, phytoplankton production is apace with waste inputs of N, and dissolved silicon is maintained above concentrations that limit phytoplankton growth rates.

Many differences between the inner estuary and the outer estuary can be explained by differences in water circulation and diffusion. For example, dilution rates are probably at least an order of magnitude greater in the outer estuary than in the inner estuary, which is a fortunate circumstance as most waste input is located near the mouth rather than the head of the estuary. If the reverse were true, oxygen depletion in northern San Francisco Bay could be a critical problem.

Estimates of phytoplankton productivity in San Francisco Bay

In situ measurements of nutrient use and oxygen and carbon production by D. H. Peterson showed

that phytoplankton productivity is light limited. Carbon assimilation per unit area is less than might be expected (<1 g C/m²/d) because the euphotic depth is shallow (0.5–6 m). Evening (dusk to dawn) losses of daylight oxygen production and carbon assimilation varies widely, but averages 25 and 20 percent, respectively. Particulate nitrogen assimilation, however, continues at night at an average rate proportional to previous light exposure; a light compensation value where 24 hour net nitrogen assimilation equals zero is estimated at 0.7 ± 0.3 (Einsteins/m²)/d. Twenty-four-hour average light-limited rates of dissolved oxygen production and particulate carbon and nitrogen assimilation appear internally consistent. For example, if NH₃ concentrations are maintained above 2 μg at/L, NO₃ uptake is suppressed (NH₃ is preferred); in this instance oxygen production is approximately 13 times NH₃ assimilation. When NH₃ concentrations are lower, oxygen production increases (13 times NH₃+17 times NO₃ assimilation). Effects of light inhibition, which appeared in all experiments, are probably an artifact of the experimental design.

In vivo fluorescence studies in the San Francisco Bay

Gregory McMurray analyzed the variability of in vivo fluorescence in San Francisco Bay waters between September and December, 1977. Extracted chlorophyll, assayed spectrophotometrically ranged from 0.5 to 46.1 μg chlorophyll *a*/L. Fluorescence ratios (fluorescence: extracted chlorophyll *a*) ranged sevenfold and were inversely and curvilinearly related to turbidity. Fluorescence blank values from 0.45-μm filtered samples increased landwards and accounted for up to 38.5 percent of the total fluorescence. DCMU ratios (fluorescence:fluorescence after addition of DCMU [3-(3,4-dichlorophenyl)-1, 1-dimethylurea]) for a single cruise ranged from 1.61 to 2.40 and could be related to photosynthetic capacity of the phytoplankton. Multiple linear regression of fluorescence results indicated the existence of spatial and temporal species differences affecting in vivo fluorescence in San Francisco Bay.

Seasonal phytoplankton distributions in San Francisco Bay

Using results of field studies and literature reviews, J. E. Cloern is defining seasonal phytoplankton distributions in San Francisco Bay.

Seasonal changes in phytoplankton species composition are apparently related to seasonal succession at the system's two important boundaries, the

delta and the ocean, but causes of temporal variation in standing stock are not so obvious. The southern and central parts of the bay generally have maximum phytoplankton densities in early spring to midsummer (apparently coincident with the timing of coastal upwelling), while the northern part of the bay attains maximum standing stocks from midsummer to fall (coincident with the timing of low freshwater inflow and maximum densities in the Sacramento River). Population dynamics and productivity of phytoplankton in the southern and central parts of the bay are apparently most strongly coupled with marine coastal waters, while behavior in the northern part of the bay is governed most strongly by events in the delta.

Species composition and density of phytoplankton exhibit distinct patterns of spatial and temporal variation. The dominant spatial feature is a pronounced summer maximum of standing stock in the null zone of the northern part of the bay where water residence time is lengthened during low river inflow. The exact location of this maximum varies diurnally with the tides and annually with the seasonal pattern of delta outflow. Marine stenohaline species (particularly centric diatoms) dominate in the saline central and southern parts of the bay; euryhaline forms (neritic, centric, and freshwater diatoms) persist over the wide salinity range of northern part of the bay; freshwater stenohaline species are restricted to the less saline eastern portion of the northern part. Because the southern part of the bay has little freshwater inflow and strong vertical mixing, its longitudinal salinity gradient is small and phytoplankton composition is more homogeneous.

Benthic-community structure in San Francisco Bay

Data collected in the San Francisco Bay estuary over the last 65 years showed that numbers of macrofaunal species are greatest in the marine environment of the central region near San Francisco, decreasing toward the north and south. This distribution has traditionally been attributed to absolute values of salinity and to sediment texture. Re-

cent studies by F. H. Nichols of both the benthos and the physicochemical environment near the bottom of the bay suggested that species distributions are related more to temporal variations in salinity and in sediment texture and stability, as well as to man's introductions of exotic species.

Maximum values of total benthic biomass, in contrast to numbers of species, are found in the southern part of the bay, probably reflecting the reduced variability of salinity and sediment-stability there and the large quantities of potential food (high sewage waste loadings, high concentrations of suspended particulate matter, and moderate to high standing stock of primary producers) as a result of shallow depth and lack of strong water circulation. High biomass can also be attributed to the successful establishment of several large and abundant introduced species which thrive in the southern reach.

The effects of waste disposal on the benthos are now often masked by natural perturbations resulting from biotic and abiotic disturbances of surface sediments and by heterogeneous distributions of animals. Anthropogenic influences on benthic community structure, other than those resulting from the introduction of exotic species, will become increasingly difficult to quantify and, therefore, to predict. Probably there will be additional changes in the biota if reductions in fresh water flow into the estuary continue.

Estuarine sediment sources in the Tillamook estuary in Oregon

Compositional analyses of bottom and subbottom sediment samples from the Tillamook estuary were completed by J. L. Glenn. Three sources of sediments filling the estuary were identified from differences in mineralogy. The riverine source dominates in the eastern and southeastern parts of the estuary, and in the southern part of the central estuary. Sediments from a "marine" source are abundant along the western estuary margin and in the northern part of the central estuary. Shoreline erosion and small streams draining recently logged uplands provide most of the nearsurface sediments along the southwestern part of the estuary.

MANAGEMENT OF NATURAL RESOURCES ON FEDERAL AND INDIAN LANDS

The Conservation Division is responsible for carrying out the USGS's role in managing the mineral and potential water-resource development sites on Federal and Indian lands, including the Outer Continental Shelf; that includes, in particular, the conservation and evaluation of the leasable mineral resources and waterpower or reservoir site potential of these areas and the development of the leasable mineral resources. Primary functions are (1) mapping and evaluation of mineral lands; (2) delineation and preservation of potential public-land reservoir and water power sites; (3) promotion of orderly development, conservation, and proper use of mineral resources on Federal lands under lease; (4) supervision of mineral operations in a manner that will assure protection of the environment and the realization of a fair value from the sale of leases and that will obtain satisfactory royalties on mineral production; and (5) cooperation with other agencies in the management of Federal mineral and water resources.

CLASSIFICATION AND EVALUATION OF MINERAL LANDS

The organic act creating the USGS gave the Director the responsibility of classifying and evaluating the mineral resources of public-domain lands. There are about 101 million ha of land for which estimates of the magnitude of leaseable mineral occurrences have been only partially made. Such appraisals are needed so that the rights to valuable minerals can be retained in the event that the land

surface is disposed of and so that the extent of U.S. mineral resources can be determined. Estimates are based on data acquired through field mapping and the study of available geologic reports, in addition to spot checks and investigations made in response to the needs of other Government agencies. As an aid in this assessment of certain minerals, guidelines have been prepared setting forth limits of thickness, quality, depth, and extent of a mineral occurrence that are necessary before land is considered mineral land.

CLASSIFIED LAND

Mineral-land classification complements the leasing provisions of the mineral-leasing laws by reserving to the Government, in disposals of public land, the title to energy resources such as coal, oil, gas, oil shale, asphalt, and bituminous rock and fertilizer, and industrial minerals such as phosphate, potassium, sodium minerals, and sulfur.

These reserved minerals on public lands are subject to development by private industry under the provisions of the Mineral Leasing Act of 1920. All minerals in acquired lands and on the Outer Continental Shelf are subject to development under comparable acts.

As a result of USGS investigations, large areas of Federal land have been formally classified as mineral land. At the end of calendar year 1977, more than 17 million ha of land had been formally classified, and an additional 951 million ha had been designated prospectively valuable for a leasable mineral:

Commodity	Formally classified lands, ha		Prospectively valuable lands, ha	
	During calendar year 1977	Total at end of calendar year 1977	During calendar year 1977	Total at end of calendar year 1977
Asphaltic materials -----	0	0	0	7,262,766
Coal -----	183,428	16,999,187	0	142,040,070
Geothermal resources -----	0	0	177,605	41,761,632
Oil and gas -----	0	1,714	-2,015,654	595,321,498
Oil shale -----	0	0	0	5,815,256
Phosphate -----	20,464	186,924	27,118	12,410,689
Potassium -----	0	0	2,932,124	35,683,548
Sodium -----	1,586	254,536	0	108,303,594

KNOWN GEOLOGIC STRUCTURES OF PRODUCING OIL AND GAS FIELDS

Under the provisions of the Mineral Leasing Act of 1920, the Secretary of the Interior is authorized to grant to any applicant qualified under the act a noncompetitive lease to prospect for oil and gas on any part of the mineral estate of the United States that is not within any Known Geologic Structure (KGS) of a producing oil or gas field. Lands within such known structures are competitively leased to the highest bidder. During calendar year 1977, 129,610 ha of onshore Federal land was determined to be in KGS's—the total at the end of the year was more than 7 million ha.

KNOWN GEOTHERMAL RESOURCE AREAS

The Geothermal Steam Act of 1970 provides for development by private industry of federally owned geothermal resources through competitive and non-competitive leasing. During calendar year 1977, 94,602 ha was included in known Geothermal Resources Areas (KGRA) and brought the total to 1,347,738 ha.

KNOWN RECOVERABLE COAL RESOURCE AREAS

The Federal Coal Leasing Amendments Act of 1975 provides for the development of federally owned coal lands by private industry through competitive lease and authorizes the Secretary of the Interior to designate Known Recoverable Coal Resource Areas (KRCRA). During calendar year 1977, 469,813 ha of coal land was included in KRCRA's and brought the total to 5,657,536 ha. Contract drilling in support of coal land classification during 1977 totaled 168,696 m for 1,323 holes completed, at an average depth drilled of 127 m/hole.

COAL RESOURCE OCCURRENCE/DEVELOPMENT POTENTIAL MAPS

Conservation Division personnel completed a total of 89 7½-min quadrangles in the western States of Colorado, Montana, New Mexico, North Dakota, Utah, and Wyoming as part of the Geological Survey's ongoing Coal Resources Occurrence/Coal Development Potential (CRO/CDP) mapping program. An additional 506 CRO/CDP maps have been contracted outside the Geological Survey. These quadrangles are scheduled for completion by the middle of calendar year 1979.

KNOWN LEASING AREAS FOR POTASSIUM, PHOSPHATE, AND SODIUM

During calendar year 1977, Known Phosphate Leasing Areas were increased by 6,093 ha for a total of 33,105 ha. The total of 116,515 ha in Known Sodium Leasing Areas and 174,545 ha in Known Potassium Leasing Areas remained unchanged during 1977.

WATERPOWER CLASSIFICATION— PRESERVATION OF RESERVOIR SITES

Suitable sites for water-resource development are valuable natural resources that should be protected to assure that they will be available when they are needed. The waterpower classification program is conducted to identify, evaluate, and protect from disposal and injurious uses those Federal lands located in sites having significant potential for future development. USGS engineers review maps, aerial photographs, and streamflow records to determine potential dam and reservoir sites. Topographic, engineering, and geologic studies are made of the identified sites to determine whether the potential value warrants formal classification of affected Federal lands. These resource studies provide the land-administering agencies with information that is basic to management decisions on land disposal and multiple use. Previous classifications are reviewed as additional data become available and as funds permit. If the sites are no longer considered suitable for development, the classification of the affected Federal lands is revoked. If the lands are not reserved for other purposes, they are returned to the unencumbered public domain for possible disposition or other use. During calendar year 1977, about 3,400 ha of previously classified lands in five Western States was released, and reviews of classifications were conducted in six river basins in California, Oregon, and Wyoming.

To assure consideration of potential reservoir and waterpower sites in the preparation of land use plans, information concerning such sites was furnished to the Bureau of Land Management and the U.S. Forest Service for several planning units in Western States and Alaska.

SUPERVISION OF MINERAL LEASING

Supervision of competitive and noncompetitive leasing activities for the development and recovery

TABLE 1.—*Mineral production, value, and royalty for Calendar Year 1977*

Lands	Oil (tonnes)	Gas (1,000 m ³)	Gas Liquids (liters)	Other (2) (tonnes)	Value (dollars)	Royalty (dollars)
Outer Continental Shelf -----	41,636,048	105,852,992,831	7,776,551,156	-----	5,764,595,348	918,153,431
Federal Onshore -----	22,529,794	29,550,689,383	1,003,644,926	56,806,393	3,084,498,863	300,234,964
Indian -----	3,429,125	3,483,996,719	133,073,526	28,182,026	557,940,483	69,995,851
TOTAL -----	67,594,967	138,887,678,933	8,913,269,608	84,988,419	9,407,034,694	1,288,384,246

of leasable minerals in deposits on Federal and Indian lands is a function of the USGS, delegated by the Secretary of the Interior. It includes (1) geologic and engineering examination of applied-for lands to determine whether a lease or a permit is appropriately applicable, (2) approval of operating plans, (3) inspection of operations to insure compliance with regulations and approved methods, and (4) verification of production and the collection of royalties (see table 1).

Before recommending a lease or a permit, USGS engineers and geologists consider its possible effects on the environment. Of major concern are the esthetic value of scenic and historic sites, the preservation of fish and wildlife and their breeding areas, and the prevention of land erosion, flooding, air pollution, and the release of toxic chemicals and dangerous materials. Consideration is also given to the amount and kind of mining-land reclamation that will be required.

OCS LEASE SALES FOR OIL AND GAS

Two sales of Federal Outer Continental Shelf (OCS) leases for oil and gas were held in calendar year 1977. One lease sale was held in June for leases in the Gulf of Mexico OCS and the other was held in October for leases in the lower Cook Inlet. In the Gulf of Mexico sale, Sale No. 47, 223 tracts

totaling 434,859 ha were offered for lease. High bids totaling \$1,170,093,432.03 were accepted on 124 tracts totaling 245,016 ha. In the Lower Cook Inlet sale, Sale CI, 135 tracts totaling 311,040 ha were offered for lease. Of these 135 tracts, 89 were offered on a royalty bid basis with a fixed cash bonus. High bids totaling \$398,471,313.00 were accepted for 87 tracts totaling 200,448 ha. Thirty of the 46 tracts offered for royalty bidding were leased for royalties ranging from 20.11 percent to 63.44 percent. Prior to each sale, USGS geologists, geophysicists, and engineers evaluate each tract to be offered to insure that the Government receives a fair market value for each tract.

COOPERATION WITH OTHER FEDERAL AGENCIES

The USGS acts as consultant to other Federal agencies in their land disposal and multiple use cases. In response to their requests, the USGS determines the mineral character and water-resource-development potential of specific tracts of Federal lands under their supervision that are proposed for sale, exchange, or other disposal. The USGS also determines the possible effect and advisability of permitting other uses during the interim between withdrawal and development of lands withdrawn as potential waterpower or reservoir sites. About 2,000 such reports were made during the calendar year 1977.

GEOLOGIC AND HYDROLOGIC PRINCIPLES, PROCESSES, AND TECHNIQUES

EXPERIMENTAL GEOPHYSICS

ROCK MAGNETISM

Paleomagnetic poles from the Valdez(?) and Orca Groups, Alaska

Sheeted dikes and tholeiitic pillow basalt, associated with flysch deposits, occur in two linear belts in the southern Kenai and Chugach Mountains. The presumably older mafic belt, a part of the Valdez (?) Group of Late Cretaceous age, is exposed along the length of Resurrection Peninsula (Tysdal and others, 1977). The younger belt, a part of the Orca Group of early Tertiary age, occurs in Prince William Sound and is best exposed on Knight Island. Paleomagnetic results obtained by J. W. Hillhouse and C. S. Grommé from dikes and pillow basalt of Resurrection Peninsula give a pole at 31.9° N., 170.4° E. ($\alpha_{95} = 13.0^\circ$). This anomalous pole position indicates that the Resurrection Peninsula may have originated 15° to 30° south of its present position relative to North America. In addition, the Resurrection Peninsula has been rotated counterclockwise 90° about a pivot point located in Prince William Sound. In contrast the igneous rocks of Knight Island give a pole at 55.8° N., 235.7° E. ($\alpha_{95} = 20.9^\circ$), as determined from seven normally polarized sites and two reversed sites. Although the pole from Knight Island is not well-defined, there is no compelling evidence for long-distance transport of the Orca igneous rocks.

Geomagnetic polarity event from Cobb Mountain in California

Paleomagnetic measurements by E. A. Mankinen and C. S. Grommé and potassium-argon age determinations by J. M. Donnelly on silicic volcanic rocks from Cobb Mountain in the Clear Lake volcanic field in California have been completed. Potassium-argon ages of these rocks range from 1.06 to 1.12 m.y., a time within the Matuyama reversed polarity epoch that is significantly older than the Jaramillo normal polarity event. The oldest unit has an intermediate direction of magnetization that is from 80° to 100° different from a reversed axial dipole

field direction. This unit is overlain by a flow that is reversely magnetized. The youngest unit exposed is also reversely magnetized but with a somewhat shallow direction. The intermediate direction of the oldest unit is interpreted to represent the beginning of a brief normal polarity event, and the shallow direction of the youngest unit to be recording a subsequent excursion. These results provide the first confirmation from subaerial lavas that a brief polarity event occurred at about this time as has been suggested by studies of some mid-oceanic magnetic anomalies and marine sedimentary cores. This new event probably had a duration of about 0.01 m.y. or less, and the best estimate of its age is 1.12 ± 0.02 m.y.

Revised late Cenozoic geomagnetic polarity time-scale

New data on the atomic abundance and decay activities of ^{40}K have led to the adoption of new values for the constants used in potassium-argon dating. The adoption of new constants is always troublesome, but it is especially critical in time-scale applications and when comparing new data with old. Because of the importance of the late Cenozoic potassium-argon geomagnetic polarity time-scale as a correlation and dating tool on both the continents and the sea floor, E. A. Mankinen and G. B. Dalrymple have updated the compilation of data used to define this time-scale. The new compilation includes all age and polarity data in the interval from 0.01 to 5 m.y. published through September, 1977, that meet the minimum criteria for acceptability, and all ages have been recalculated using the refined K-Ar constants. In addition, since the last compilation 5 years ago, the number of data in this interval have nearly doubled, enabling the major polarity epoch boundaries to be more accurately determined. Recalculation of these boundaries has yielded ages of 0.73 m.y. for the Brunhes-Matuyama, 2.48 m.y. for the Matuyama-Gauss, and 3.40 m.y. for the Gauss-Gilbert boundaries.

Paleomagnetic dating of glacial sediments underlying Taylor Dry Valley in Antarctica

As part of an investigation of the glacial history of Antarctica, the National Science Foundation has drilled several core holes into glacially-derived sediments (diamictites and laminated sediments) that underlie the dry valleys near McMurdo Sound. Microfossils are not abundant in these sediments and the species that occur are not particularly useful in determining the age of the rocks. To aid in dating these materials, D. P. Elston and H. R. Spall have measured the paleomagnetic record of geomagnetic reversals in the longest of the cores (324 m) from Taylor Dry Valley. The polarity zonation in the core matches the known timing of geomagnetic reversals during the interval from 10 to 2.4 million years ago. This chronology means that glacial erosion had cut the original Taylor Dry Valley more than 10 million years ago and that sedimentation from the base of an ice sheet into the fiord continued until approximately 2 million years ago, after which time the area was elevated above sea level.

Origin of natural remanent magnetization in red sedimentary rocks of the Moenkopi Formation in Arizona

In order to use the paleomagnetic record of geomagnetic reversals to construct stratigraphic correlation in sedimentary rocks such as sparsely fossiliferous continental red beds, it is necessary to show that the natural magnetization was acquired by the sediment during or shortly after its deposition in the geomagnetic field. D. P. Elston and M. E. Purucker have conducted a detailed investigation of the natural magnetization and magnetic mineralogy of the magnetization of these red beds was acquired Mountain in Arizona. They have found that most of the magnetization of these red beds was acquired prior to small-scale intraformational deformation and that this magnetization is stable at high temperatures and resides in detrital specular hematite. The part of the magnetization that resides in very fine-grained hematite pigment is erased after heating to moderate temperatures. The Moenkopi Formation has recorded many reversals of the Earth's magnetic field. The results of this study indicate that the observed paleomagnetic reversals are accurately recorded time horizons within the formation, so that they may be used to construct regional stratigraphic correlations.

Underground fires in coal mines located by geophysical surveys

Ground-level magnetic and electrical surveys have been made over two burning coal mines in Wyoming

and Colorado by D. E. Watson and D. B. Hoover, who have found that these techniques can be used to locate the fires in the underground coal seams. During a period of five months, Watson observed an increase of 400 nT in a magnetic anomaly over a burning mine near Acme, Wyo. The anomaly is due to an increase by a factor of 100 to 1000 in the remanent magnetization of the rock overburden as it is progressively baked by the coal fire. Similar magnetic anomalies were observed in a preliminary survey over an abandoned mine near Marshall, Colo. At the same localities, self-potential and apparent-resistivity surveys were performed by Hoover, who found self potential anomalies of 50 to 100 mV near the hot zones in both mines. Self-potential measurements appear to be more effective in delineating the hot zones than do resistivity measurements, while total-field magnetic surveys can be used to determine the total area extent of the burn. A combined self-potential and magnetic survey is capable of estimating both direction and rate of advance of the fire fronts.

GEOMAGNETISM

Geomagnetic observatories

Standard geomagnetic observatory operations were continued at Barrow, Sitka, and College, Alaska; Guam, Mariana Islands; Newport, Wash.; Boulder, Colo.; Fredericksburg, Va.; San Juan, P.R.; and Tucson, Ariz.

In 1975 the instrument piers at the Barrow Observatory were redesigned and rebuilt and an automated fluxgate-proton magnetometer was installed in place of a standard photographic recording magnetograph. Since that time the observatory has been operated without a resident observer; personnel from the College Observatory visit Barrow every 6 weeks to make absolute observations, change records, and service the equipment. In a recent analysis of data from the Barrow Observatory, J. B. Townshend (1978) found that as a result of the new pier construction and instrumentation the ranges in the base-line data were reduced by a factor of 15 for horizontal intensity, 9 for declination, and 5 for vertical intensity.

In a comparison of data recorded simultaneously by digital fluxgate and standard magnetograph systems, L. R. Wilson (1977) found that the precision and accuracy of the digital data was as good or better than standard magnetograph. However, equipment malfunctions led to a loss of about 5 per-

cent of the data with the electronic systems but less than 1 percent with the conventional system; this points to the need for greater redundancy in the digital systems.

Magnetic stations for the International Magnetospheric Study

Under sponsorship from the National Science Foundation, final assembly testing and calibration was completed for most of the magnetometer systems that are being supplied to various investigators by the USGS. According to R. W. Kuberry, several of those systems are already in operation in the Arctic. At most sites, data are telemetered to Wallops Island by satellite and then telemetered to Boulder by land line so that data is available to investigators in almost "real time". Data recovery has been better than 90 percent during initial operations.

U.S. and World Magnetic Charts

E. B. Fabiano has found that the current international model of the Earth's magnetic field, IGRF 75, now shows errors (due primarily to secular variation estimates) of the order of 700 nT in the southeastern section of the United States. This is of most concern to exploration geophysicists attempting to match up survey results obtained at different times in the same or adjacent regions. For the U.S. charts the recent acceleration in the rates of secular change has contributed to degrading the accuracy of results extrapolated from the current (1975) series of maps. However, the current secular estimates, though linear, are more accurate than estimates derived from world models that depended almost exclusively on observatory annual means. Use of repeat station data evidently has contributed to producing regional estimates that are more reliable.

Geomagnetic secular change

N. W. Peddie (1977) has derived unique new mathematical models of the geomagnetic field that are based on optimum sets of one through four unconstrained magnetic dipoles and one through four circular current loops. The new models, representing refinements of some earlier work, are the results of multiple computer runs using random initial parameter values and stricter convergence criteria. The representation achieved by the new models is generally better than that achieved by the traditional spherical harmonic analysis of the same data using a comparable number of parameters. The

radii of the current loops range from 800 km to 2,980 km and are often close to, but never outside, the core-mantle boundary. The possibility is being examined that such models may provide superior representations of secular variation that, when extrapolated in time, may provide predictions of the field.

In a study of selected observatory annual measurements, J. C. Cain (USGS) and Takeshi Yukutake (Earthquake Research Institute, University of Tokyo) found that there is a double solar cycle period in the external field variation that is related to the frequency of magnetic storms. Also, there is an induced component from the solar cycle variation as well as an internal variation unrelated to the external variation with a period of a little over 6 years.

Geomagnetic diurnal variation

The ionospheric diurnal variation as determined by analysis of surface magnetic observations was previously thought to be a consistent and predictable phenomenon. However, J. C. Cain has found that the results of the POGO magnetic survey showed a high variability with longitude and with time even over periods of a few hours. Since many of the new data are taken over areas devoid of surface magnetic observations, it will not be easy to explain this result.

Deep mantle conductivity estimated from geomagnetic variations

Using observed surface observations of magnetic variations, L. R. Alldredge has made new estimates of the conductivity of the deep mantle. An earlier study had shown that sources in the Earth's core produced surface variations with periods of 25 years and amplitudes as large as 60 nT; approximately six times the amplitudes of variations with periods of 15 years. Assuming equal amplitudes for all periods at the core-mantle interface and a power law decrease of conductivity with radial distance, an estimate of 10^5 mho/m was derived for the conductivity at the core-mantle interface. This is three orders of magnitude higher than earlier estimates and nearly eliminates any large discontinuity in the conductivity at the core-mantle interface.

PETROPHYSICS

Electrical properties in a geothermal environment

G. R. Olhoeft has completed construction of the Petrophysics Laboratory facilities for studying electrical properties of rocks under simulated geo-

thermal conditions. The laboratory now has the capability to study electrical properties at temperatures from 4.2°K to 1,473°K and pressures from vacuum to 1 GPa. The first measurements of basalt saturated with an aqueous salt solution (0.1 m NaCl) have been performed from ambient conditions up to a temperature of 593°K and a hydrostatic pressure of 20 MPa. The resistivity of the basalt varied essentially independently of pressure and frequency; however, it displayed the same temperature dependence as the pore solution up to 353°K, but above that temperature the resistivity of the basalt decreased faster with increasing temperature than did that of the pore (NaCl) solution. This suggests that the pore walls have a surface conductance that becomes more important than the pore solution volume conduction above 353°K. Thus, the familiar Archie's Law relationship between the rock resistivity in terms of the rock porosity and the resistivity of the pore solution is not valid above 353°K in basalt. Preliminary results were reported in G. R. Olhoeft (1977).

Nonlinear complex resistivity applied to ground-water and mineral chemistry

G. R. Olhoeft continued the development of an electrical technique for measuring nonlinear complex resistivity. The technique was demonstrated to be a viable research tool with many promising applications for remotely measuring ground-water and mineral chemistry. Laboratory studies showed distinctly different nonlinear signatures for sulfide and clay minerals. A computer program series was developed to analyze, parameterize, and statistically test the data. The nonlinear response of a mineral varies according to its chemical state and its chemical environment. Nonlinear complex resistivity measurements show great promise as a borehole logging technique to determine the relative ranges of ground-water pH and Eh, as well as the oxidation state of the minerals and relative concentrations of sulfide versus clay minerals. Further development of this capability should produce a technique to assist in characterizing mineral (especially sedimentary uranium) deposits before beginning a solution mining process.

Infrared spectral behavior of fine particulate solids

G. R. Hunt measured the transmission and emission spectra of clouds and layers of fine particulate samples of quartz, magnesium oxide, and aluminum oxide in the 6.5 to 35 μ m wavelength range. The results demonstrate (1) that the behavior of layers

of particles constitutes a good analog for a cloud of particles; (2) that individual micrometer-sized particles emit most where they absorb most; (3) that as the size of the particle is increased, the emission features reverse polarity and the spectrum approaches that of one obtained from a polished plate; and (4) that as the particle layer-thickness increases, radiative interaction becomes increasingly important so that the emission maximum shifts from the stronger to weaker features, or produces a maximum at the Christiansen wavelength.

APPLIED GEOPHYSICAL TECHNIQUES

Magnetic and gravity expressions of the Lewis and Clark Line

The Lewis and Clark Line is a tectonic feature expressed as a linear zone 15–50 km wide that extends at least 500 km west-northwest across western Montana and northern Idaho. Studies by M. D. Kleinkopf and M. W. Reynolds reveal that the feature is expressed as a nearly continuous 15 mGal gravity gradient zone with anomaly values lower on the south. The zone separates prominent northwesterly trending gravity anomalies on the north from predominately northeasterly trends to the south. Wavelengths of anomalies on the north exceed those on the south by nearly twofold. The magnetic data show both strongly aligned contours along the zone and small closed anomalies that define locations of plutons concentrated within the zone along much of its length. Both the gravity and magnetic fields show regionally higher values north of the line. The Lewis and Clark Line appears to be a major and long-lived intraplate tectonic boundary. It forms the northeast limit of late Cenozoic basin and range faulting, geothermal activity, a magnetically quiet basement, and a region of low gravity, all associated with the Cordilleran thermotectonic anomaly defined by Eaton and others (1976).

Circum-Caribbean mafic-ultramafic belts

J. E. Case reports that most circum-Caribbean mafic-ultramafic belts and their associated mineral deposits coincide with active or inactive plate boundaries. The emplacement ages of most of the belts are late Mesozoic and early Cenozoic. Most of the belts are ophiolites, in the modern context of plate tectonics, but some ultramafic bodies in Venezuela are of Alaskan type rather than Alpine. Most of the belts are associated with Mesozoic metamorphic rocks that include blueschists in Guatemala, Cuba, Jamaica, Hispaniola, and Venezuela.

The belts in Guatemala occur in a suture-zone between blocks of continental crust with local slices of oceanic crust. Those in the Greater Antilles appear to rest on oceanic crust. Those in Venezuela may occur on continental crust at present, but they have been displaced southward from a province of oceanic crust. Some of those in Colombia occur along a late Mesozoic suture between oceanic and continental crust; others to the west occur mainly on oceanic crust. Ophiolites of Panama and Costa Rica are mainly sites of oceanic crust. Gravitational expression of the belts is variable. Displaced ophiolite belts have little expression. Ophiolites in place are normally expressed by strong, positive anomalies. Magnetic expression is exceedingly variable, and no diagnostic patterns have yet been interpreted.

Geophysical anomalies in the Mississippi Embayment

A study of the Bouguer gravity and aeromagnetic anomalies by J. D. Hendricks and T. G. Hildenbrand in the Mississippi Embayment suggest the Embayment is a graben-like depression oriented in a northeast direction and is approximately 80 km wide. The Precambrian basement deepens from about 2-3 km on the northwest edge to as much as 7 km in the center. The deepest (to Precambrian) part of the Embayment is some 30 km west of, and parallel to, the present course of the Mississippi River. The northwest edge of the Embayment is characterized by a line of intense positive gravity and magnetic anomalies that extend from Little Rock, Ark., northeastward to Broomfield, Mo. These anomalies are typical of those associated with basic igneous intrusions. Although the ages of the intrusions are unknown (except at Little Rock, where Upper Cretaceous nepheline syenite crops out), the igneous rock may have been injected along a crustal zone of weakness active since Precambrian time.

Upper-crustal structures near Charleston, South Carolina

H. D. Ackerman, D. L. Campbell, and J. D. Phillips have constructed a model of upper-crustal structures in the Charleston, S. C., earthquake area using magnetic, gravity, refraction-seismic, and geoelectric data. Basement rocks of the Charleston block are deeper, more magnetic, and produce less-lineated aeromagnetic-map patterns than typical Piedmont rocks. Several mafic or ultramafic intrusions are present in the Charleston block. One such intrusion near Summerville seems to be differentiated, having a crown and shoulders that are less magnetic than its flanks. Its top is at a depth of about 1,400 m and is characterized by high electrical resistivity and a

P-velocity of 6.1-6.4 km/s. This body partly intrudes a layered sequence, which can be divided geophysically into four units. The uppermost is a sedimentary unit extending from the surface to a depth of from 600 m in the north to 900 m in the south; it has a seismic velocity of about 2.2 km/s, a resistivity of about 20 ohm-m, and is nonmagnetic. The top of the second unit, which consists of volcanic flows, has a P-velocity in the range from 4.5 to 5.8 km/s but no clear electric or magnetic definition. The third unit is distinguished mainly by its moderate magnetic character. Its top is at a depth of about 1,400 m, suggesting that it may represent an unconformity surface that corresponds to the top of the Summerville intrusion. This unit may represent moderately magnetic, crystalline basement rocks of variable resistivity, or it may be a deep sedimentary unit containing some dikes or flows. It has no clear seismic contrast with the overlying unit. The fourth unit lies at a depth of about 3,000 m and has resistivity greater than 100 ohm-m; it represents the crystalline basement or a unit within the crystalline basement.

Caldera on Snake River Plain

Gravity and aeromagnetic surveys on the eastern Snake River Plain have defined regional anomalies associated with a caldera that had previously been identified on the basis of geologic studies. D. R. Mabey reports that the geophysical data appear to define the boundary where it underlies young basalt. The caldera is about 45 km in diameter and centered near Rexburg. A residual gravity low of about 15 mGal is associated with the caldera with prominent gravity gradients along about 70 percent of the caldera boundary. Magnetic expression of the caldera is not as pronounced, but some local magnetic anomalies appear to be controlled by the boundary of the caldera. Three areas of known hot water occur along the inner side of the caldera edge. One of these thermal areas, comprising Heise Hot Springs and nearby Elkhorn and Hawley Warm Springs, is in the area of a local 10 mGal gravity high and on the crest of more extensive 500 gamma magnetic high (at 750 m above the ground surface). The nature of the dense mass producing the gravity high has not been determined, but the magnetic anomaly appears to reflect a large intrusive body underlying the Snake River Plain where the Swan-Grand Valley structure intersects the plain. Similar magnetic highs occur at three of the four locations where major Basin and Range valleys intersect the south side of the Snake River Plain.

Audio-magnetotelluric measurements on the Papago Indian Reservation in Arizona

An audio-magnetotelluric (AMT) survey was made by C. L. Long in the Santa Rosa Mountains area of the Papago Indian Reservation in Arizona to assess its utility as an effective reconnaissance tool for mapping the substructure. Sixty-six soundings were made at a station density of one per eight km², using the natural fields between 7.5 Hz to 6.7 Hz and VLF radio source-fields at 10.2 kHz and 18.6 kHz. Scalar resistivity contour maps derived from these measurements at various frequencies (corresponding to differing depths of investigation) provided complementary information for interpreting regional gravity and aeromagnetic data, particularly along the flanks of the outcropped rocks. Compatible interpretations of the geoelectric section made from galvanic and telluric current studies in a few areas demonstrated the cost-effectiveness of the AMT survey.

Gravity data reveal buried ophiolite belt in California

H. W. Oliver's compilation of 2,128 gravity stations in the Fresno 1° by 2° quadrangle in California reveals a 100-km long line of gravity highs over Quaternary alluvium along the eastern edge of the San Joaquin Valley between Fresno and Porterville. The gravity highs have amplitudes of 10 to 30 mGal and extend into the Sierra Nevada south of Porterville where they are associated with the Kings-Kaweah ophiolite belt and related mafic intrusions (Oliver and Robbins, in press). The Kings-Kaweah belt contained deposits of commercial chromite which have been largely mined out. Thus, the regional gravity data reveal the location of the shallow-buried ophiolite belt and indicate areas where detailed geophysical exploration for chromite might be successful.

Self-potential anomalies on volcanos

In analyzing the results of a self-potential (S.P.) survey of Kilauea's lower east rift zone (Puna district, Hawaii), C. J. Zablocki (1978) concluded that (1) four distinct, large amplitude anomalies delineated in the area are related to magma or hot intrusion at depth; (2) the probable source mechanism for these potentials is an electrokinetic phenomenon resulting from thermally-induced, differential ion-displacement in the waters that overlie deeper-seated hot zones; and (3) whereas three of the anomalies are elongate parallel to the rift zone, one is transverse to the trend of the rift zone. It

also is coincident with the epicentral area of recurrent, shallow (4 km) earthquake swarms in past years. These factors, together with some hydrologic and geologic inferences, collectively suggested that the transverse S.P. feature reflects permeable, vertical fractures that contain water in the liquid and vapor phase that is heated by a broad heat source at depth. The results and conclusions derived from this study were instrumental in siting a test hole drilled to a depth of 1,962 m, which encountered temperatures of about 350°C. A self-potential anomaly of 4 V has been measured by D. B. Hoover on the south flank of Mount Hood, Oreg. This anomaly, the largest on record, occurs where near surface resistivities are very high, and the high resistivities may in part be responsible for the large amplitude. A large, 100 mv, diurnal potential was also noted that is not caused by induction from the diurnally varying magnetic field. The source of these large potentials is not known.

Schlumberger soundings near Moorhead, Minnesota

A survey consisting of 192 Schlumberger resistivity soundings was made by A. A. R. Zohdy and R. J. Bisdorf near Moorhead, Minn., to delineate the course of a large buried stream channel. The channel, which ranges in width from about 0.5 km to about 2 km and has a length of about 50 km, is an important aquifer. Using the sounding data obtained over 12 profiles, it was possible to (1) map the course of the buried stream channel, (2) evaluate this thickness of the buried stream channel sand and gravel, (3) evaluate the depth to basement, and (4) clearly delineate areas where the sedimentary rocks are composed of clays. The interpretation results also revealed (1) the presence of older buried channels that have carved their course into the basement rocks, (2) the presence of sand deposits beneath clay layers, and (3) the depth to basement increases from north to south, and the depth to basement (275 m) in the southern part is much larger than previously anticipated.

Analysis of stress-concentration mechanism for intraplate earthquakes

D. L. Campbell has performed an analytical follow-up of the stress concentration mechanism proposed by M. F. Kane (1977) for intraplate earthquakes. The analysis is of a circular or elliptical mafic or ultramafic intrusion into a felsic continental plate. A differential stress concentration factor, defined as the amount by which the radius

of Mohr's circle increases in the vicinity of the intrusion when the plate is subjected to various systems of horizontal stresses, is calculated. For a certain class of intrusive rock, including those serpentized, the intrusive rock may be stronger than the plate at depths of 0 to 5 km, but weaker at depths of 10 to 15 km. The analysis predicts: (1) possible seismicity at the shallow depths anywhere within the intrusive rock and within one radius of the boundary in the surrounding plate, with maximum activity of about 30° horizontally from the direction of maximum regional stress P_1 ; (2) possible seismicity at the intermediate depths within one radius of the boundary in the surrounding plate only, with maximum activity 90 degrees horizontally from the direction of P_1 ; (3) a zone of no seismicity in between the above depths (the hypocenters will die out at 35° and then reappear deeper down at 90°); (4) distinctive focal mechanisms for earthquakes in the two depth ranges; and (5) prospective upper bounds on expected earthquake magnitudes that depend on the chemical make-up of the intrusive rock, its size, its shape with respect to the regional stress field, the mechanical characteristics of plate and intrusive rock, and the magnitude and type of the regional stress field.

Geophysical studies of the Silver Cliff area in Colorado

M. D. Kleinkopf reports that gravity, aeromagnetic, and seismic refraction data provide new information about the thickness distribution of volcanic rocks and geometry of volcanic structures in the Silver Cliff and Rosita Hills volcanic areas. Geophysical surveys consisted of gravity measurements at 318 stations, low level aeromagnetic coverage flown at 0.8-km spacings, and two seismic refraction profiles across the Silver Cliff volcanic area. Negative gravity anomalies at the Silver Cliff and adjacent Johnson Gulch areas are interpreted to be caused by up to 1,200 m of low density breccias, tuff, and glasses preserved in volcanic subsidence features in Precambrian crystalline terrane. Anomalies in the Rosita Hills are smaller indicating more restricted volcanic subsidence. The magnetic data reflect both lithologic variations of Precambrian crystalline gneisses and distribution of the Tertiary volcanic rocks. Two north-south seismic refraction profiles across the Silver Cliff volcanic area provided more specific quantitative data that complemented the gravity and magnetic studies in defining the configuration of the volcanic subsidence areas in delineating possible associated local vents.

Crustal magnetic anomalies from satellite data

The magnetic anomaly maps at a height of 630 km from the ground reflect spatial changes in the average magnetization of large crustal blocks and regional changes in the thickness of the magnetic crust. Analysis of these data by B. K. Bhattacharyya reveals that along the continental margins the magnetization contrasts caused by gross compositional differences between oceanic crust and continental crust produce apparent gradients in the maps. Patterns in the magnetic field over the conterminous United States indicate variations in remanent magnetization and variations in the thickness of the magnetic crust related primarily to regional temperature gradients.

Magnetic depth estimates

Estimations of the depth to magnetic sources using the spectral properties of magnetic anomalies generally require long arrays that reduce resolution. R. J. Blakely developed a method that uses the maximum entropy power spectrum to calculate depth to source. The predictive nature of the maximum entropy technique permits the use of shorter windows of data. The method operates by dividing a profile into overlapping windows, calculating a maximum entropy power spectrum for each window, linearizing the spectra, and calculating with least-squares the various estimates of depth. The assumptions of the method are that the source is two-dimensional and that the intensity of magnetization includes a random component; knowledge of the direction of magnetization is not required. Application of the method to theoretical data and observed marine anomalies over the Peru-Chile trench yields encouraging results. Specifically, for the eastern margin of the Nazca plate, analyses indicate a continuous magnetic basement extending into the subduction zone. The basement is shallow seaward of the trench axis and deepens as the plate approaches the convergent margin. This apparent deepening is postulated to be caused by the thickening of the oceanic crust and the deterioration of its magnetization, possibly caused by the compressional disruption of the basaltic layer. Landward of the trench axis, the depth estimates indicate possible uplift of the oceanic material into the lower slope of the continental margin.

Radar-transparent oil shales

D. L. Campbell and F. R. Olhoeft (1977) report that laboratory measurements of dielectric properties of oil shales and alkali salts from Piceance Creek

basin in Colorado indicate that these materials should be fairly transparent to radar waves. Water-bearing gouge and fault zones, on the other hand, are reflectors. Radar, therefore, may be a useful way to search out bad ground ahead of an advancing mine opening in oil shale operations.

New magnetotelluric field processing system

A new microcomputer based magnetotelluric (MT) data acquisition and real-time processing system has been developed. The system is based on readily available commercial circuit cards and software developed by W. D. Stanley. Software for the system is designed around unique new MT analysis algorithms that allow error reduction caused by statistical power spectral estimation uncertainties. MT data acquisition and high quality processing is possible over a frequency range of 10^{-4} to 5×10^2 Hz. The system was designed for rapid and inexpensive duplication by private industry.

Geomagnetic array data processing

Programs for spectral analysis have been added to the geomagnetic array data processing system. D. V. Fitterman reports that programs for computing Fourier transforms auto and cross power spectra, auto and cross correlation, spectral smoothing, and scalar impedance estimation have been developed. In addition, programs that plot the results of the spectral analysis are available. A new high speed plotting routine has been added to the system that allows plotting of daily magnetograms with higher resolution, and much less computer time.

Electrokinetic potential and magnetic anomalies

D. V. Fitterman has also completed an analysis of the electric potential and magnetic anomalies produced by a pressure source in a layered half-space. The analysis has shown that for a pressure source with radial symmetry there is no magnetic field produced at the Earth's surface. This result is true for any number of layers. Furthermore, since any pressure distribution can be synthesized by a collection of point sources (delta functions), no surface magnetic field can be produced for any pressure source in a layered half-space. The results have application in the areas of earthquake prediction and geothermal exploration.

EM modeling and inversion programs

W. L. Anderson (1977) has inverted extra-low frequency (ELF) data obtained in the southern Raft

River valley in Idaho and the results showed good agreement with previously published Schlumberger sounding data (Zohdy, Jackson, and Bisdorf, 1975). The ELF equipment was operated in the 1 to 2,000 Hz frequency range with station receiver-transmitter spacings from 1,480 to 3,057 meters. For these spacings and frequency range, resolution of both shallow and very deep layers were poor, compared to the intermediate layer solution. A hot water zone was located about 400–600 m from the surface by the method. New improvements in computing Hankel transform integrals and finite integrals about a wire source developed by Anderson and J. P. Kauahikaua greatly enhanced the inversion of controlled source data in both accuracy and speed of the computations—thus making the entire inversion process now practical.

Noise problem in audiomagnetotelluric survey

A significant source of noise in audiomagnetotelluric and other material natural source electromagnetic surveys in the audio range has been identified by D. B. Hoover as transient voltages on the Earth return of power distribution systems. Little information is available on the magnitude of current returned through the earth, but typical estimates are in the range of tens of amperes. Transients on the power system, and these occur continuously, are a source of broad band noise source of indeterminate location. These signals are difficult to distinguish from natural signals, may be much stronger than natural signals, and generally tend to give erroneously high AMT apparent resistivities.

A plastic detector for aerial gamma-ray surveys

A 113-liter plastic detector weighing 218 kg has been used by J. S. Duval in experimental aerial gamma-ray spectroscopy surveys. Using the count rate in the T-208 energy window, the plastic detector was determined to be approximately equivalent to 41 L of sodium iodide costing several times as much. In addition to lower cost, the plastic detector offers the advantages that it is not hygroscopic and, therefore, does not require periodic cleaning and repackaging to maintain detector energy resolution, and it is less susceptible to thermal or physical shock. The plastic detector does not, however, have as good an energy resolution as sodium iodide that causes the final result obtained with the plastic detector to have a wider noise envelope than similar measurements obtained with sodium iodide. To provide a direct comparison with data obtained using sodium iodide, part

of an earlier aerial survey was repeated using the plastic detector. Contour maps of the two data sets show that the distribution of high and low values are essentially the same for the two types of detectors.

Optimum size source for borehole gamma-ray analysis

A study by F. E. Senftle has been made in an artificial borehole to see if smaller ^{252}Cf neutron sources can be used in mineral exploration sondes at shorter source-to-detector distances and still retain the capture gamma-ray sensitivity of larger neutron sources at relatively large source-to-detector distances without additional hazard to the detector (Intrinsic Ge or Ge(Li)). The fast and thermal neutron flux from a $3.7\ \mu\text{g-}^{252}\text{Cf}$ neutron source was first determined as a function of the source-to-detector distance in air, water, an iron ore-concrete mixture, and dry sand. Integral gamma-ray counts across the spectrum and gamma-ray intensity measurements of specific spectral lines at low and high energies were then made in the iron ore-concrete mix for the same source-to-detector distances. Using a graphical method, the intensity of selected gamma-ray lines were determined from the data as a function size of the neutron source. Two limits were used in the calculation: (1) the fast neutron flux at the detector and (2) the count rate above which resolution is lost because of poor circuit response. It is shown that the latter imposes the most serious limits on the method, and if this limitation is removed by using fast electronic circuits, a substantial gain in sensitivity can be realized even with relatively small neutron sources.

Digital terrain corrections for gravity data

Donald Plouff reported that digital elevation data on terrain tapes of the National Chart and Information Center have been tested for use in a gravity terrain correction program (Plouff, 1977). The ground spacing of the digital data is 63.5 m derived from maps at a scale of 1:250,000. Average elevations for 5,600 half-by-half minute compartments that were previously estimated by hand methods for areas in Oregon and Colorado were compared with average values from digital terrain tapes and revealed an average elevation difference of only 10 m—after correction for hand errors that exceeded 100 m. An average difference of 15 m was obtained for an area in the Sierran Foothills from a comparison tape digitization with 680 quarter-by-quarter minute compartments, which were derived from 3-by-3 sec-

ond compartment estimates done by hand methods. These results indicate that data from the terrain tapes in these areas are quite satisfactory for use in computing gravity terrain corrections. Testing in specific areas, however, may be needed to determine if individual variances from the average differences where there are steep topographic gradients introduce unacceptable errors into the gravity terrain correction.

Detection of shallow faults

The use of geophysical surveys to detect shallow faults has been tested by V. J. Flanigan. Where the contrast in physical properties between the fault zone and surrounding medium is high and where overburden was not masking the underlying anomalies, the geophysical surveys proved effective. In a Virginia test area the Dumfries fault produced a clearly recognizable resistivity anomaly. Near Houston, Tex., faults occurring in sedimentary rocks could not be detected because of a lack of contrasting physical properties and very conductive near surface materials. Faults in crystalline rocks in Colorado produced gravity and magnetic anomalies as well as resistivity anomalies. The selection of geophysical method and survey field procedure should be determined by the geologic environment of the faults being studied.

Physical properties changes associated with uranium deposits can be detected by borehole geophysical measurements

Comprehensive borehole geophysical investigations by J. H. Scott and J. J. Daniels in Texas, Utah, and Wyoming show that physical properties changes associated with uranium deposits can be detected with borehole geophysical tools. These physical properties changes are related to the geological and geochemical environment of the uranium deposit as described by Daniels and others (1977). Changes in the oxidation state across the uranium bearing zone cause variations in pyrite, clay, calcite cement, and magnetite content. Variations in pyrite content and clay type (montmorillonite vs. kaolinite) can be determined with induced polarization. Total clay and calcite cement content can be estimated by resistivity measurements. Variations in magnetite content can be determined with magnetic susceptibility measurements.

Hole-to-hole electrical measurements can be used to determine resistivity and induced polarization anomalies that exist between boreholes. An interpretation scheme using a layered earth computer

model facilitates the interpretation of hole-to-hole electrical data.

The economic significance of this research accrues from the finding that physical-property anomalies are detectable from geophysical measurements made in drill holes that span the zone of mineralization associated with a uranium orebody. Therefore, these anomalies can be used as pathfinders that indicate the possible presence of ore deposits between widespread drill holes during the reconnaissance stage of exploration.

GEOCHEMISTRY, MINERALOGY, AND PETROLOGY

EXPERIMENTAL AND THEORETICAL GEOCHEMISTRY

Experimental studies in the MgO-CaO-SiO₂-H₂O-HCl system

Equilibrium constants for the reactions: (1) talc + 6H⁺ → quartz + 3Mg²⁺ + 4H₂O, (2) tremolite + Mg²⁺ + 2H⁺ → 2 talc + Ca²⁺, and (3) 4 diopside + Mg²⁺ + 2H⁺ → tremolite + 2Ca²⁺ have been determined at 500°C and 600°C and 2 kbar pressure by R. W. Luce and J. J. Hemley using the hydrochloric-acid buffering technique. The equilibrium constant for the reaction: wollastonite + Mg²⁺ → diopside + Ca²⁺ was determined from 500°C to 700°C and 2 kbar pressure in unbuffered runs at 4M, 2M, and 1M total chloride concentration. A lowering of the equilibrium constant for this reaction with lower chloride concentrations indicates that there is an increase in magnesium chloride complexing above 600°C. Results of this study outline the stability fields of these important skarn minerals and provide basic data to compute more complex equilibria.

Modern day formation of a uranium orebody in Bee County, Texas

It has been concluded by R. W. Potter, M. A. Clynne, and R. C. Erd, after studying the mineralogy of the cores and the chemistry of the waters, that the Pawnee orebody, Bee County, Texas, is being formed. The mineralogical studies show that pyrite, clinoptilite, uraninite, and amorphous UO₂ are contemporaneous, which is in agreement with the stabilities predicted by the chemical analyses of water samples taken from the formation waters. The most conclusive evidence comes from analyses of the Eh and uranium contents of the formation waters. The Eh drops 60 mv from the oxidized side to the reduced side of the orebody, and correspond-

ingly, the uranium concentration decreases from 6 ppb to 0.06 ppb. In other places the uranium content in the formation waters reaches 110 ppb on the oxidized side and drops to 0.06 ppb on the reduced side. Uranium isotope distribution also strongly suggests that the ore deposit is currently forming. Thus, there is the opportunity to collect data from an actively forming ore deposit and to gain a deeper insight into the processes responsible for forming uranium deposits.

High temperature magnetic separation tests of titaniferous magnetites

Harry Klemic and P. J. Loferski's high temperature magnetic separation tests made on titaniferous magnetite concentrates from the Little Pond deposit, Essex County, New York, show that at furnace temperatures between 500°C and 540°C some of the magnetite was above its curie temperature and could be recovered as a nonmagnetic fraction. This was expected because electron microprobe studies of the ore had shown variations in composition within grains and between grains, particularly in their titanium and aluminum contents; thus the different particles of such magnetites should have different Curie temperatures. However, the high temperature magnetic and nonmagnetic fractions showed very little difference in bulk composition as determined by spectrographic analyses. Apparently finer grinding and more refined magnetic separation methods are required to achieve satisfactory compositional separations.

Heat capacities of feldspars and kaolinite

The heat capacities (C_p^o) for the alkali feldspars low albite, analbite, microcline, and high sanidine, and for kaolinite have been measured by R. A. Robie and B. S. Hemingway between 350°K and 1000°K by differential scanning calorimetry (DSC). Their data were combined with the cryogenic adiabatic calorimetry data on feldspars obtained by Openshaw and others (1976) and the low temperature data on kaolinite of King and Weller (1961) to give C_p^o for the four feldspars between 298°K and 1400°K and for kaolinite between 298°K and 800°K.

Compact, low-power telemetry controller and transmitter unit for volcanic gas monitoring

K. A. McGee has designed, built, and tested an economical, compact electronic unit that can automatically control the operation of a solar panel, gas pump, data multiplexer, radio transmitter, data input multiplexer, voltage to frequency converter, reference voltage source, and ambient temperature sen-

sor. The unit consists of only five integrated circuits and an assortment of transistors, diodes, and other small parts, and requires only 10-20 mA at about 12V. The central frequency of the transmitted signal can be set at the standard frequencies of seismic telemetry system. Although the unit is designed primarily for volcanic gas monitoring application, it may turn out to be just as useful for many similar remote sensing and telemetry applications.

Thermodynamic behavior of titanomagnetite

Motoaki Sato (USGS) and Mariano Valenza (guest investigator from University of Palermo) have determined, using the Sato double cell method, the equilibrium fO_2 values between 800°C and 1200°C of assemblages of the magnetite-ulvöspinel solid solution with wüstite, silica plus fayalite, or metallic iron. The fO_2 data were used to obtain alpha plots, activities, and activity coefficients for both magnetite and ulvöspinel at 1000°C, 1100°C, and 1200°C. The alpha plots show that the solid solution is not ideal and changes the solution behavior in the mid-composition range. The Henry's law constant for magnetite is as small as 0.2.

The above findings indicate that the estimated fO_2 of basaltic rocks, based on the assumption of ideal solution behavior of titanomagnetite, could be higher than real fO_2 by as much as two orders of magnitude and strongly point to the necessity of direct measurement.

A new ultramicrochemical analytical technique for fluid inclusions

E. W. Roedder has developed a new analytical procedure for the chemical analysis of individual minute fluid inclusions, making use of the tremendous sensitivity of the electron microprobe. There have been several studies published recently by others that used the electron microscope to analyze qualitatively individual solid phases in fluid inclusions. Special methods of sample preparation were also used that were not applicable to analyzing the liquid phase. The new method involves taking a very tiny mineral fragment containing an inclusion of interest, cracking it open under clean conditions, adding (under the microscope) a micro drop ($\sim 10^{-7}$ g) of pure water to the crushed debris, transferring this liquid by micropipette to a hydrophobic-coated planchet of beryllium or copper, adding an appropriate amount of a water-soluble organic glassformer, evaporating to form a tiny disk of organic glass containing the $\sim 10^{-8}$ g of water-soluble ions from the inclusion fluid, uniformly dis-

tributed, and then probing the whole disk with an electron beam for Na, K, Ca, Mg, S, and Cl. Since the most effective glass-former found to date is corn syrup (a mixture of sugars that effectively interfere with each other's crystallization forming an organic glass), the resulting tiny sample disk is essentially a sugar glass. As such, it is, in effect, a miniature lollipop, hence the procedure has been dubbed the "minimillimicrolollipop method". A number of other organic glass formers are still to be tried, but the requirements of the method are surprisingly restrictive in this selection. The most important function of the glass former is to prevent the crystallization of the inclusion salts on drying, thus yielding a sample with a maximum concentration of salts homogeneously distributed throughout a minimum volume of uniform glass. The volume minimum is set by the depth of penetration of the electron beam into the glass. Preliminary studies indicate that valid ratios of Na:K:Ca:Mg:S:Cl can be obtained with the method, but considerably more developmental and calibration work will be required.

MINERALOGIC STUDIES AND CRYSTAL CHEMISTRY

Crystal structure of hydrochlorborite

The crystal structure of the rare playa mineral, hydrochlorborite, from the Salar Carcote in Antofagasta, Chile, has been determined by J. R. Clark (USGS) and G. E. Brown (Stanford University); its chemical formula is $Ca_2[B_3O_3(OH)_4 \cdot OB(OH)_3](Cl \cdot 7H_2O)$. The mineral is monoclinic, space group $I2/a$, $Z=8$, $a=22.783$, $b=8.745$, $c=17.066\text{Å}$, $\beta=96.70^\circ$ (Hurlbut, Aristarain, and Erd, 1977). The structure contains isolated, modified borate poly-anions, each formed by corner-sharing among two tetrahedra and one triangle, plus an extra tetrahedron, $3:(\Delta+2T)+T$. Each calcium cation is coordinated by two oxygen anions, three hydroxyl ions, and three water molecules, average $Ca-O=2.474\text{Å}$. These polyhedra share corners to form isolated groups of four polyhedra linked by Ca-O and Ca-OH bonds to the borate polyanions. The chlorine anions do not coordinate calcium, which is an unusual feature. Instead, each Cl receives eight hydrogen bonds, which is a record number for Cl in an inorganic structure (average $Cl \dots O=3.296\text{Å}$). Of the seven water molecules, six coordinate to calcium cations, and one is hydrogen-bonded only. A network of hydrogen bonds completes the structural linkage. The mineral is found only in dry seasons, and the nature of the structure suggests that crys-

tallization occurs only when the concentration of chlorine ion in the brines becomes high.

Fine structure of orthopyroxene

G. L. Nord, Jr., showed that lunar and terrestrial orthopyroxenes in the enstatite-hypersthene composition range contain one to five unit-cell-wide zones of calcium-rich orthopyroxene. These zones are similar to "Guinier-Preston" zones in alloys. The zones are constrained coherently along (100) plane of the host, with the *a* cell edge increased by 1.7 percent over that of the host.

The Guinier-Preston zones have been determined by X-ray energy spectroscopy in a scanning transmission electron microscope with a 100-Å beam size to be richer in calcium than the host orthopyroxene. The slightly increased *a* cell edge and volume abundance of 6 percent is consistent with the zones having ~25 mol percent wollastonite content. The presence of *a*-glide violations from only the Guinier-Preston zones reduces the space group to *Pbc2*₁; this requires ordering of calcium into one of two M2 sites. This model results in one-half of the unit cell having a composition of diopside and the other having the composition of orthopyroxene.

The zones dissolved into the host at 950°C for one unit-cell-wide zone and at 1,050°C for five unit-cell-wide zones; annealings were for 1 week. The presence of Guinier-Preston zones instead of the equilibrium phase is due to the necessity of orthopyroxene to expel calcium; the zones take up this calcium when supersaturation is low (slow cooling or low wollastonite content) or nucleation sites are absent (augite requires nucleation, Guinier-Preston zones may require none).

New alkali metal sulfides from California

Three potassium-iron sulfides and a sodium-iron sulfide have been found by G. K. Czamanske in the mafic alkalic diatreme at Coyote Peak, Humboldt County, California, establishing this as a unique locality. Two of the minerals, $K_3Fe_{10}S_{14}$ and $NaFeS_2$, are new minerals; in fact, no sodium sulfide phase had ever been found before in nature.

Coyote Peak is only the second locality where a third mineral, rasvumite, has been found. Careful microprobe analyses of type rasvumite and the material at Coyote Peak have established their identity and show that the original Russian description presents an improper formula based on incorrect analysis for potassium. The proper formula is KFe_2S_3 , establishing rasvumite as a potassic

analog of cubanite. A fourth mineral appears to be a cuprian and nickeloan djerfisherite, $K_3Cu(Fe,Ni)_{12}S_{14}$, but because of its fine-grained nature this has not yet been confirmed by X-ray. Both $K_3Fe_{10}S_{14}$ and KFe_2S_3 have been dated by the $^{40}Ar/^{39}Ar$ technique. $K_3Fe_{10}S_{14}$, a massive phase, gives an age of 29.4 m.y. in agreement with the age obtained on two samples of coexisting phlogopite. KFe_2S_3 , a bladed, fibrous phase that broke up during sampling, apparently lost Ar at some point and gives an age of 26.5 m.y.

Health aspects of the asbestos minerals as they relate to the mining industry

Malcolm Ross has completed a review study of the asbestos and health problem as it relates to the mining and quarrying industries. Presently only four types of commercial asbestos are used in the United States; approximate per annum consumption in metric tons is: chrysotile (766,000), crocidolite (33,800), amosite (8,500), and anthophyllite (998). Chrysotile, composing about 95 percent of the asbestos used in the United States, is mostly imported from the Thetford Mines region of Quebec. All crocidolite and amosite are imported from South Africa.

Although all four forms of commercial asbestos can cause scarring of lung tissue (asbestosis), this disease can be controlled by maintaining reasonably low dust levels. By monitoring the worker's chest X-rays lung damage can be detected and the employee can be placed in jobs with little or no exposure to dust. More serious is the risk of lung cancer and pleural and peritoneal cancer (mesothelioma) to those who are exposed to certain kinds of asbestos dust. Epidemiological studies of many different types of workers (asbestos shipfitters, asbestos textile workers, insulators, crocidolite miners, amosite miners, chrysotile miners and millers) indicate that there is a very serious hazard associated with the use of crocidolite, a sodium and iron-rich clin amphibole. It also appears that the abnormal frequency of the disease mesothelioma is associated mostly with this mineral. Health risks associated with chrysotile asbestos are particularly important, for this is the most common form of asbestos. Health studies in Quebec, Canada, since 1966 show that there is only a slight excess of lung cancer in a group of 11,000 chrysotile miners and millers. Only seven cases of mesothelioma have been reported since 1936 among the asbestos workers of Quebec. This rather positive health history is particularly impressive in view of the fact that the dust levels in the

Thetford Mines region has been extremely high for more than 70 years; only in the last 10 or 15 years have the dust levels been at their present low level because of application of modern dust control technology. The Quebec miners and millers presently developing lung disease were exposed to these historically high dust concentrations of the period up to about 1960–65. Those coming into the labor force since then can expect to show a much lower incidence of lung disease. Also, mining companies are requiring their asbestos workers to refrain from smoking; non-smoking asbestos workers have an incidence of lung cancer about the same as that of the non-smoking general population.

There is then every reason to believe that if the quarrying and mining industries of North America maintain dust levels between 400,000 and 4,000,000 particles per cubic foot (14 to 140 particles/cm³), values presently obtained by the Quebec chrysotile mining industry, little increase in the incidence of asbestos lung diseases will occur in the labor force over a 50 year working lifetime. On the other hand, the use of crocidolite should be carefully controlled. Most is used in asbestos-cement pipe; perhaps a substitute could be found.

VOLCANIC ROCKS AND PROCESSES

HAWAIIAN VOLCANO STUDIES

Activity at Kilauea Volcano in 1977

After a 21-month period of quiescence, Kilauea Volcano began to erupt on September 13, 1977. Three minor seismic swarms occurred in the months preceding, and a major seismic event heralded the eruption. Rapid deflation of the summit began 22 hours prior to the outbreak of surface activity on the central east rift. Microearthquakes and harmonic tremor during the episode traced the underground movement of magma, the lava fountaining, and the relief of stresses generated in the adjacent south flank of the volcano.

The first spatter cones formed along a discontinuous, en echelon, 7-km-long fissure system trending N. 70° E. between two prehistoric vents, Kalalua and Puu Kauka. During the first week, eruptive activity was concentrated at two spatter cones, one near the center and one at the west end of the new fissure.

The third and most voluminous phase of the eruption began late on September 25, 1977. An irregular spatter rampart formed along a 500-m segment near the center of the new fissure. Within 24 hours,

the activity became concentrated at the east end of this segment. One flow from the new, breached, 40-m-high cone at this site moved rapidly southeast, reaching a point 700 m from the nearest house in the evacuated village of Kalapana on October 1, 1977. The staff of the Hawaiian Volcano Observatory, working closely with the State of Hawaii's Office of Civil Defense throughout the eruption, recommended the evacuation on September 29, 1977.

The total volume of material produced during this 19-day eruption is estimated to have been 25–50 × 10⁶ m³. Samples from active flows indicate that a differentiated tholeiitic basalt was erupted. Plagioclase was the only significant phenocryst, and augite and minor olivine accompanied it as microphenocrysts. This mineralogy, although uncommon in Kilauea lavas, is similar to that of the 1955 basalt. Systematic variation in bulk composition occurred throughout the eruption, and the last basalt produced appears to have been differentiated. The lava chemistry suggests that the magma that had erupted had been previously stored in the rift and that the magma that entered the rift during summit deflation has not yet erupted.

Rate of inflation slows at Mauna Loa Volcano

Geodimeter, dry tilt, and level surveys at the summit of Mauna Loa Volcano have shown that the rate of magmatic inflation has slowed during the past year. Microseismic activity remained at essentially low levels, with most epicenters of micro-earthquakes located beneath the summit caldera and along the Northeast Rift Zone. Fumarolic activity has increased dramatically at the July 1975 vents, however, and native sulphur is now being deposited, in contrast to the earlier absence of sulphur phases in the hot fumarolic gases.

A major effort to establish the recurrence interval of prehistoric Mauna Loa eruptive activity has resulted in the discovery of over 60 charcoal sample sites beneath prehistoric lavas. Carbon-14 dates on these samples range from less than 200 to more than 12,000 years and have established the fact that the maximum age of Mokuaweoweo caldera is 520 ± 200 years.

Structural evolution of Mauna Loa Volcano

Mauna Loa, the world's largest basalt shield volcano, is structurally complex in comparison with terrestrial and extraterrestrial shields, probably in large part owing to the buttressing effect of adjacent volcanoes on Hawaii Island (Lipman and Lock-

wood, 1977). The 50-km-long Southwest Rift Zone, historically active along most of its length, extends from the summit to the sea, and has a conspicuous 40° change in strike in its middle part. In contrast, the historically active sector of the Northeast Rift Zone is only 15-hm long, does not extend to sea level as a clearly defined feature, and is nearly straight. Radial vents are common between the rift zones on the northwest flank of the volcano, but are entirely absent on the southeast side. Some of these structures may have developed early in Mauna Loa's history and are probably related to gravitational "edifice effects" of the adjacent older Mauna Kea and Hualalai Volcanoes. Other structural complexities of Mauna Loa appear to reflect interaction with the concurrently growing Kilauea Volcano. In particular, as Kilauea developed into a sizable volcano, it began to form a southern barrier to Mauna Loa swelling. As a result, the lower part of the Northeast Rift Zone of Mauna Loa became buttressed, resulting in reduced rates of volcanism along this part of the rift, and the Southwest Rift Zone began to migrate westward, producing the conspicuous bend in its middle sector.

Paths of magma ascent in the earth

The tensile strength of partly molten rock and the criteria of tensile failure are of key significance to the condition of accumulation of magma at the source of melting and the subsequent path of ascent to volcanic conduits. The melting rate, conditions of accumulation, and rates of transport are all governed by mechanical factors determined by tectonic work rates. This conclusion was tested by H. R. Shaw by comparing the magma transport volumes of Kilauea Volcano with the hypocentral distribution and energy spectrum of earthquakes there. Direct correlations were found between volumetric work rates related to extensional failure criteria of magma transport and seismic energy release rates. Eruption records therefore provide a quantitative clue to recurrence intervals for earthquakes of given magnitudes, and conversely earthquake records provide information on details of magma conduit paths in the lithosphere.

COLUMBIA RIVER PLATEAU STUDIES

Olympic-Wallowa lineament influenced Cascade-Columbia River volcanism

An abrupt facies change in the Ellensburg Formation, a sequence of sedimentary deposits interbedded

with and overlying the Grande Ronde Basalt, was found by D. A. Swanson and G. R. Byerly to take place across the north edge of the Kittitas Valley in central Washington. All Ellensburg deposits north of the valley, including those in the Wenatchee Mountains and along the Columbia River, are arkosic; no trace of freshly erupted andesitic and dacitic material was found. In and south of Kittitas Valley, however, floods of such volcanoclastic debris, including large pumiceous clasts and laharic deposits, comprise the bulk of the Ellensburg, although arkosic components are also present. This previously unrecognized facies change is intriguing because it occurs across the Olympic-Wallowa lineament, suggesting that about 15 million years ago active volcanism in the Cascades was confined south of the lineament or that perhaps the lineament had topographic expression and was guiding the course of rivers heading in the Cascades. In any case, the facies change provides still more circumstantial evidence that the lineament exerted some control, tectonic and (or) magmatic, on development of the Columbia Plateau and adjacent Cascade Range.

Gently dipping feeder dikes for Columbia River Basalt Group

At least 10 gently dipping (20°) dikes were discovered by D. A. Swanson and T. L. Wright south and east of Milton-Freewater, Oreg. These are the first dikes of the Columbia River Basalt Group known to depart from nearly vertical attitudes. The dikes can be traced across more than 750 m of section with no tendency to steepen upward. They apparently fed flows of the Frenchman Springs Member of the Wanapum Basalt that caps the ridgecrests. The dikes are from 1 m to 70 m thick, generally coarser-grained than flows, and have glassy margins. The gently dipping dikes, which strike north-south, a little more easterly than vertical, are apparently coeval, "normal" dikes in the area. The gently dipping dikes occur in two north-south zones; those in the western zone dip eastward, and those in the eastern zone dip westward. The dikes may be analogous in origin to ring dikes, except they are linear rather than arcuate. The dikes cross but are not offset by the Olympic-Wallowa lineament.

Picture Gorge Basalt coeval with middle part of Grande Ronde Basalt

The age relation of the Picture Gorge Basalt and Grande Ronde Basalt was clarified by D. A. Swanson (USGS) and R. D. Bentley (Central Washington University) in north-central Oregon. Magnetic polarity determinations and geologic mapping in

the Butte Creek-Thirtymile Creek area combine to show that the Picture Gorge Basalt is interbedded with the middle part of the Grande Ronde Basalt, specifically with magnetozones N_1 and R_2 . This indicates that the known Picture Gorge is decidedly younger than the Imnaha Basalt to the northeast, previously considered as correlatives. The Imnaha underlies the lowermost known Grande Ronde Basalt (magnetozone R_1).

Petrogenesis of Columbia River Basalt Group

The petrogenesis of Columbia River Basalt Group has been inferred from study of whole-rock major and minor element chemistry and of major element chemistry of glass associated with flows or dikes of known chemistry. T. L. Wright has shown that glass rock chemical trends are systematic and differ from chemical trends relating different whole-rock compositions. From this he infers that crustal (low pressure) fractionation is not an important process in producing the lava compositions. Incompatible element ratios are generally incoherent between chemical types, which implies an origin by melting in a mantle that is mineralogically and chemically heterogeneous. Lava compositions are inferred to be close to parental melt compositions and their relatively low MgO and high CaO and Al_2O_3 contents suggest that melting took place in a relatively MgO-poor mantle where mineralogy is dominated by pyroxene rather than olivine.

CHEMICAL EVOLUTION OF SILICIC MAGMA CHAMBERS

Emplacement sequence and chemical evolution of Pleistocene rhyolites in Coso Range, California

Attempts to decipher the detailed sequence of dome emplacement in the Coso volcanic field with K-Ar ages, obsidian hydration rind ages, and overlapping field relations have been frustrated by incomplete and imprecise data. On the assumption that chemical similarity reflects temporal similarity, W. A. Duffield and C. R. Bacon have now assigned the domes to seven age groups indicated by recently acquired trace element analyses of fresh glass from each dome. The age of at least one dome in each of the seven groups is known from one or more of the above mentioned dating techniques, and such ages define unique periods of time for each group.

The oldest age-chemical grouping consists of a single dome emplaced about 1 million years ago, and the youngest grouping consists of 14 domes that are 0.08 million years old or younger. Most of

the domes were emplaced within the last 0.25 million years. A plot of the aggregate volume of domes in each grouping shows an almost exponential increase from older to younger, a relation that invites speculation about future eruptive activity.

The general sequence of dome extrusion indicated by the age-chemical grouping defines no simple geographic progression. In some groupings, domes were emplaced across the entire length of the developing field; in other groupings, emplacement was limited to the central part of the field; and in one grouping, single domes were emplaced at the north and south limits of the field.

For all of the age-chemical groupings, the relative abundances of the analyzed elements are very similar to those of the Bishop Tuff (Hildreth, 1977) and silicic rocks of the Valles volcanic system, including the Bandelier Tuff (R. L. Smith, oral commun., 1977). Such similarity suggests that the same fractionation process or processes affected all three silicic systems. The Bishop Tuff represents the product of a nearly instantaneous sample of a large silicic magma body possessing internal chemical gradients, while the silicic rocks of the Valles volcanic system record chemical evolution before, during, and after emplacement of the Bandelier Tuff, a much longer period of time. By analogy with these well-studied silicic systems, Bacon and Duffield infer that the Coso domes, at least those emplaced during the last 0.25 million years, were tapped from the top of a single, fractionating magma chamber. Microprobe analyses of coexisting plagioclase and sanidine phenocrysts in Coso domes show that the degree of magma fractionation and the apparent equilibrium growth temperature of the feldspar vary inversely, consistent with Hildreth's (1977) data on the Bishop Tuff and with a general model for the origin of chemical zonation in silicic magma bodies, proposed by Shaw, Smith, and Hildreth (1976).

Trace element abundances fluctuate between age-chemical groupings of Coso domes from relatively "primitive" to relatively "evolved", and trace element abundances show an overall depletion of "evolved" constituents throughout the life of the dome field. These temporal fluctuations probably reflect a delicate balance between the rate of eruption and the rate of chemical fractionation. Magma apparently was bled off the magma chamber faster than fractionation could reestablish original chemical gradients over the life of the field; whereas, fractionation outstripped eruption between some of the age-chemical groupings.

Rocks similar to the highly faulted and shattered granitic basement at the surface probably also form the roof of the magma chamber, and may control the degree of chemical fractionation that is possible at Coso. Such mechanically weak rocks with the superimposed effect of east-west tectonic extension probably favor intermittent emplacement of domes and (or) flows over prolonged, undisturbed fractionation that might eventually result in voluminous pyroclastic eruptions.

Petrology of post-caldera rhyolites in Long Valley, California

The post-caldera rhyolites of Long Valley caldera consist of two generally coeruptive petrographic and chemical types: (1) aphyric to sparsely porphyritic pyroxene-bearing rhyolites and (2) coarsely porphyritic hornblende-biotite rhyolites. The two types form sub-parallel trends on oxide variation diagrams, with the porphyritic being slightly higher in FeO, MgO, CaO, TiO₂, and P₂O₅ and lower in Al₂O₃ and K₂O. Electron microprobe and major- and trace-element studies by R. A. Bailey demonstrate that the two types and their chemical trends are related by crystal fractionation, mainly separation of plagioclase, hornblende, and pyroxene. The aphyric to sparsely porphyritic lavas apparently represent high-temperature magma (800–850°C) circulating in the main part of the Long Valley magma chamber, while the prophyritic lavas represent water-enriched lower temperature magma (700 to 750°C) crystallizing along the roof and walls of the chamber. Crystallization separation of mainly biotite, hornblende, and plagioclase along the margins of the chamber and possibly convective accumulation of these minerals deeper in the chamber, produces a core magma that becomes progressively richer in silica and depleted in most other major oxides with time. The process results in concentric zonation similar to that observed in silicic plutons with silicic centers and more mafic margins; it contrasts with the vertical zonation, inferred from ash-flow studies, which probably is not often preserved in the plutonic stage owing to its removal by eruption of the ash-flow themselves. Vertical chemical zonation apparently develops during an early magmatic stage when magmatic temperatures are relatively high and thermal gradients are maintained relatively constant, whereas concentric zonation develops during a later stage when magmatic temperatures are declining, and the chamber is crystallizing. Thus, the Long Valley post-caldera rhyolites provide both (1) an explanation for the contrasting zonation inferred from petrologic studies of ash-

flow deposits and plutons and (2) a link between the volcanic and plutonic environments in cauldron complexes.

Potential volcanic activity near Clear Lake in California

The span of eruptive activity from about 2 million years to 10,000 years ago and the presence of a magma chamber inferred from gravity, aeromagnetic, and teleseismic data show that the Clear Lake volcanic system is potentially active, according to B. C. Hearn, Jr., J. M. Donnelly, and F. E. Goff (Donnelly, Hearn, and Goff, 1977). The age span and the absence of ash-flow tuffs suggest that the system could be in an early evolutionary stage that is preliminary to major ash-flow eruption and caldera collapse of the type shown by other silicic magma systems, such as Long Valley, Calif., Valles, N. M. and Yellowstone, Wyo., and would be a major volcanic hazard. However, because it lies in a different tectonic setting within the right-lateral stress system of branches of the San Andreas fault, the Clear Lake system may not follow the same evolutionary course. Instead, the walls and roof of the magma chamber may be cracking often enough so that frequent leakage of magma prevents the build-up of volatiles necessary for the voluminous ash-flow eruption. In addition, the northward movement of the heat source, inferred from the northward decrease in ages of eruptions, may preclude a duration of heating sufficient to generate the volume of volatile-rich silicic melt necessary for large-volume ash-flow eruption. Future eruptions would probably be mafic, similar to the youngest cinder cones and flows, although the presence of the 90,000-year rhyolite of Borax Lake indicates that silicic eruptions are a possibility. Locations of eruptions are likely to be close beneath, or northeast of Clear Lake, in the area of the youngest past eruptions and above the apparent current focus of heating. Eruptions are likely to be of phreatomagmatic type near the lake, and to produce cinder cones and small flows away from the lake. Phreatomagmatic eruptions would pose hazards to the lakeshore area and within a few kilometers of the vent. Eruptions away from the lake would be hazardous to smaller areas, as a result of ash falls and cover by flows.

VOLCANIC ROCKS IN WESTERN UNITED STATES

Tertiary volcanic sequence at Mineral Mountain in Arizona

Additional geologic mapping in the Mineral Mountain 7½-min quadrangle by W. J. Keith and

T. G. Theodore has clarified relations within an extensive suite of Tertiary sedimentary and volcanic rocks cropping out there. The oldest rocks in the sequence are some pebbly grits derived principally from the underlying Pinal Schist (Precambrian X), but also containing angular fragments of rhyolite. The rocks are overlain by an extensive suite of water-laid tuff that forms prominent and picturesque buff-colored cliffs. Locally, the water-laid tuff is cut by intrusive rhyolite and quartz latite that are essentially coeval in that they each display intrusive relations with the other. Rhyolite and quartz latite flows, however, are also interbedded with water-laid tuff. Nonetheless, the quartz latite appears to have been the last to erupt in the volcanic pile, and it locally overlies water-laid tuff and rhyolite as a topographic high in the northeastern part of the quadrangle. A K-Ar age of 15 m.y. has been obtained from quartz latite by S. C. Creasey, about the same age as those obtained previously from the volcanic sequence in the adjacent Teapot Mountain 7½ min quadrangle.

Folds in Huckleberry Ridge Tuff (Pleistocene) in eastern Idaho

G. F. Embree (Ricks College) and H. J. Prostka (USGS) have mapped a zone of 60- to 90-m-high folds in the Pleistocene volcanic sequence in the Teton Canyon, eastern Idaho. The folds range in form from chevron to strongly overturned to the southwest and involve about 35 m of basalt and unconsolidated gravel and the overlying 70- to 100-m-thick Huckleberry Ridge Tuff (1.9 m.y.). The tight folds pass into horizontal beds upcanyon and into subdued slippage features downcanyon. Internal zoning in the tuff indicates that it had been emplaced and was beginning to develop compaction foliation, flattened pumice fragments, and a basal vitrophyre, and that while still hot and viscous, it began to flow internally forming a basal zone of recumbent small-scale folds, a middle shear zone of small thrusts, and an upper zone of viscous pull-aparts. Perhaps closely following this, the deformation involved the underlying gravel and basalt down to a detachment between the basalt and a diatomite unit below.

Some of the deformation was clearly contemporaneous with emplacement and cooling of the Huckleberry Ridge Tuff. Deformation of the gravel and basalt along with the tuff perhaps suggests some kind of subregional uplift, such as resurgent doming of the caldera after ponding of the tuff.

Age of volcanism at Togwotee Pass area in Wyoming

Two geographic features give clues to the age of volcanism in the Togwotee Pass area of northwestern Wyoming. Pilot Knob is a biotite-augite intrusive rock located about midway (4.5 km) between Togwotee Pass on the Continental Divide in Teton County and a volcanic vent on Lava Mountain in western Fremont County. During the late Pliocene(?), Pleistocene, and very early Holocene, about 26 basalt flows erupted from the vent on Lava Mountain.

A sample collected by W. L. Rohrer from Pilot Knob and dated by J. D. Obradovich yielded a K-Ar age of 3.40 ± 0.06 m.y. (Pliocene). Whole rock samples of the 19th basalt flow (above the base) on Lava Mountain gave a K-Ar age of 0.48 ± 0.06 m.y. A cinder cone remnant caps Lava Mountain and obscures the vent. Based on geomorphology, Rohrer infers that the cinder cone eruptive phase occurred during the late Pleistocene or very early Holocene.

Two theoretical curves were generated by plotting the age data on a semi-log chart. One curve shows that the intrusive on Pilot Knob and the extrusive flows on Lava Mountain are time related and consequently, generically related and that the volcanic phase is complete. The other indicates that the two features are either unrelated or very complexly related and that the volcanic phase is incomplete. The data points are inadequate to establish which curve is most realistic, but in the latter case it appears that the Lava Mountain volcanism began 1.5 to 2 million years B.P.

MINERAL ALTERATION IN VOLCANIC ENVIRONMENTS

Solubilities in the system Al_2O_3 - SiO_2 - H_2O

The metasomatic or silica-dependent reactions relating the minerals kaolinite, pyrophyllite, andalusite, diaspore, boehmite, and corundum have been investigated by J. J. Hemley, and the stability relations of these minerals have been established. This information elucidates the physical-chemical conditions of formation of a variety of alteration mineral assemblages and their associated ores, notably precious metal deposits in volcanic environments and the upper levels of some porphyry copper deposits. Sericite-kaolinite and sericite-pyrophyllite (\pm andalusite) are the more characteristic of these associations, but diaspore or corundum-bearing assemblages are also occasionally observed.

SUBMARINE VOLCANISM

Carbon dioxide-filled vesicles in deep-sea basalt

J. G. Moore, C. G. Cunningham, and J. N. Batchelder have found that volatile-filled vesicles are present in minor amounts in all samples of mid-ocean basalt collected down to depths of 4.8 km. When such vesicles are pierced in liquid under standard conditions, the volume expansion of the gas is 0.2 ± 0.05 times the eruption pressure in bars or 20 ± 5 times the eruption depth in km. Such expansion relations could be used as a measure of eruption depth.

A variety of techniques that indicate that CO_2 comprises more than 95 percent of the vesicle gas volume in several submarine basalt samples from the Atlantic and the Pacific are: (1) vacuum crushing and gas chromatographic, freezing separation, and mass spectrographic analyses, (2) measurements of phase changes on a freezing microscope stage, (3) microscopic chemical and solubility observations, and (4) volume change measurements. The amount of CO_2 in the vesicles is about equal to or greater than that presumed to be dissolved in the glass (melt) and amounts to 400 to 900 ppm of the rock. The rigid temperature of the glass is 800°C to $1,000^\circ\text{C}$ and increases for shallower samples. Sulfur gas also was originally present in subordinate amounts in the vesicles but has largely reacted with iron in the vesicle walls to produce sulfide spherules.

These facts indicate that CO_2 -rich gas must enter sea water in large amounts above oceanic spreading ridges as volatiles stream up from subjacent magma chambers, as lavas are erupted on the ocean floor, and as the submarine lavas and underlying gabbros are weathered.

Red Sea opening

According to M. M. Donato and R. G. Coleman, in early Miocene time (~ 22 m.y. ago) dike swarms, layered gabbros, granophyres, and basalts of the Tihama Asir ophiolite in southwest Saudi Arabia were emplaced during the initial stages of Red Sea rifting and separation of the African and Arabian plates. As rifting began, dikes invaded Paleozoic and Mesozoic sedimentary and Precambrian metamorphic rocks of the Arabian plate along a northwesterly trend paralleling the axial trough of the Red Sea. With increased separation along the rift edge, new crust was accreted to the continental margin. This crust consisted of a 4-km-wide zone of subparallel dikes having chilled margins against one another and lacking screens of older continental

rock. This dike complex is analogous to the sheeted dike swarms described from the Cyprus, Oman, and Newfoundland ophiolites. Layered gabbros and granophyric intrusions within the dike swarm are products of magmatic differentiation developed during the initial stages of rifting. The differentiation trends indicate that the parent magma was tholeiitic and evolved by crystal fractionation in much the same manner as lavas at Thingmuli Volcano in Iceland. Late Miocene tilting of the sedimentary rocks and dike swarm toward the Red Sea axis and later erosion have exposed the continental-oceanic crust boundary along a narrow zone. The continental Baid Formation (18 m.y.) rests unconformably on the Tihama Asir ophiolite.

PLUTONIC ROCKS AND MAGMATIC PROCESSES

The Baltimore Complex, a disrupted ophiolite

The Baltimore Complex extends 150 km southeast from southeastern Pennsylvania across Maryland to northern Virginia and constitutes one of the largest assemblages of mafic and ultramafic rocks in the Appalachian system within the United States. Recent work on the complex by B. A. Morgan has shown that these rocks are part of an ophiolite sequence that was disrupted during emplacement and subsequently severely deformed and metamorphosed. In terms of an ophiolite stratigraphy, the complex includes the following units: (1) Serpentinized peridotite including dunite with podiform chromitite and pyroxenite; (2) Gabbro, commonly norite, containing ultramafic cumulus layers of "herzolite" and "websterite" and at many places metamorphosed to an epidote-amphibolite containing serpentinite layers; (3) Quartz gabbro and diorite containing hornblende and relict pyroxene; (4) volcanic rocks that include an association of pillow basalt, keratophyre, and minor intrusions of plagiogranite dikelets into the underlying gabbro. Units 1, 2, and 3 can all be considered as parts of a cumulus sequence characterized by the disappearance of olivine before the crystallization of cumulus plagioclase and clinopyroxene and by the appearance of postcumulus hornblende in the more differentiated rocks. The Baltimore Complex was thrust westward into broken diamictite and boulder gneiss of the Wissahickon Formation. The geologic evidence suggests that the minimum age for emplacement was Ordovician, but conflicting data from U-Pb zircon ages suggest that the time of emplacement may have been as old as Early Cambrian or latest Precambrian.

Jurassic zoned tonalite-trondhjemite pluton in Trinity Alps of Klamath Mountains in California

The Upper Jurassic Canyon Creek pluton (Lipman, 1964), one of eleven compositionally zoned intrusive bodies of the Trinity Alps in the central Klamath Mountains in California shows concentric zoning from marginal mafic tonalite to central trondhjemite. A geochemical study of this pluton by Fred Barker and H. T. Millard, Jr., shows that SiO_2 increases from 61 percent at the margin to 73 percent in the center, whereas Al_2O_3 , iron oxides, MgO , CaO , TiO_2 , Sr, Sc, and Co decrease uniformly from margin to center. Light rare earth elements (REE's) increase slightly from border to center (from 40 to 60 times chondrites) but heavy REE's decrease (from 8 to 4 times chondrites). There are no Eu anomalies. The general heavy-REE-depleted character of the pluton suggests generation by partial melting of amphibolite or quartz eclogite. The changes in REE patterns from the relatively mafic margin to the central trondhjemite are interpreted to be the result of fractionation of tonalitic magma by separation of hornblende and minor plagioclase during ascent of the pluton.

New data on modification of K-Ar ages by Tertiary thrust faulting in eastern Nevada

Tertiary K-Ar age dates in Late Precambrian and Lower Cambrian metasedimentary and Jurassic igneous terranes are incompatible with the idea of cooling with uplift based on studies of 60 new K-Ar ages by D. E. Lee, R. F. Marvin, and H. H. Mehnert from igneous, metamorphic, and detrital minerals mostly from eastern White Pine County, Nevada. They instead relate the anomalously young ages to Tertiary movement along regional thrust faults. Ages of mica from the metasedimentary rocks may indicate time of metamorphism, but more likely reflect degassing of the mica in response to stresses resulting from late movements along thrust surfaces.

These new data also suggest a working hypothesis for the history of the plutons exposed in and near the area of study as follows:

- Intrusion of plutonic rocks penecontemporaneous with and spatially related to thrust faulting during middle Mesozoic time. This would imply a genetic relation between the thrust faulting and the magmatic activity.
- Cooling and crystallization of the igneous rocks.
- Renewed activity along the thrust surfaces (as recent as 17-18 m.y. ago in the southern Snake Range) leading to stress, shearing, or even cata-

clasis in the associated plutons, partial to total degassing of the constituent micas, and consequent post-crystallization K-Ar ages for those micas. Thus, near thrust faults, Tertiary K-Ar (mica) ages for these plutons should be regarded with caution unless confirmed by other data.

Magmatic diversification and crust-mantle structure in Colorado

Compilation of 225 new rock analyses by George Phair, supplemented by 486 previously determined rock analyses compiled by Young (1972) make possible the tracing of geographic changes in magma type of Cretaceous and Tertiary intrusive rocks in Colorado in a detail not previously possible. A plot of Peacock Index (P.I.) for 29 intrusive suites on a map of Colorado by Phair shows that three belts of magmatism having distinctive chemical properties radiate from the central Front Range: (1) a southward trending alkalic to alkali-calcic belt characterized generally by Na_2O in excess of K_2O ; (2) a north-westward-trending alkalic to alkali-calcic belt characterized by generally high K_2O relative to Na_2O ; and (3) a southwestward trending "porphyry belt" that is alkalic to alkali-calcic in character in the Front Range and that becomes calc-alkalic as it widens throughout a broad region to the west.

The alkalic and calc-alkalic suites tend to cluster in separate regions; whereas, the alkali-calcic types tend to characterize the intervening areas, and the emplacement of a specific magma type within a particular region was recurrent throughout the Late Cretaceous through Miocene time interval, all of which suggests the plutonic activity was subject to deep seated crust-mantle control.

Such a petrogenetic interpretation is supported by:

- The variation in P.I., which shows that alkalic suites in Colorado tend to concentrate in old highland areas and calc-alkalic suites in old basins of deposition and that alkali-calcic rocks extend into intervening areas.
- The variation in density of the upper mantle (Jackson and Pakiser, 1965; Pakiser, written commun., 1976) within the "porphyry belt" shows that alkalic suites tend to be associated with an upper mantle having a high average density close to 3.43 g/cm^3 , alkali-calcic suites tend to be associated with an upper mantle of intermediate density ($3.43\text{--}3.36 \text{ g/cm}^3$), and calc-alkalic rocks tend to be associated with an upper mantle of still lower density ($3.3\text{--}3.36 \text{ g/cm}^3$).

- A plot of P.I. for 29 intrusive centers against the mean regional gravity anomalies developed in the surrounding country rocks shows a strong correlation, with alkalinity increasing as gravity increases. Brinkworth and Kleinkopf (1972) have shown that a high component of the variation in measured Bouguer gravity in Colorado reflects changes in density of the underlying upper mantle.

Petrochemistry trends, distribution coefficients, and quality of minor element data

Geochemical studies by N. G. Banks near Ray, Ariz., have shown that distribution coefficients and petrochemical trends for minor elements may be of doubtful value if they are based on comparisons of data from petrochemically unrelated samples. Measurable amounts of Cl, F, H₂O, S, and, particularly, Cu occur in relatively few igneous minerals in the rocks near Ray, Ariz. Essentially all of the magmatic Cl, F, H₂O, and most of the magmatic S occurs in biotite, apatite, and hornblende. Most, if not all, of the magmatic copper occurs in magmatic sulfide minerals. On the other hand, incipient alteration of biotite in the samples results in an extreme but erratic enrichment of copper in biotite alteration products and as much as a threefold increase in H₂O, a total loss of sulfur and chlorine, and moderate loss of fluorine. Thus, depending on the relative amounts of biotite, apatite, and hornblende in the rock, significantly aberrant results and erroneous petrogenic conclusions concerning these ore fluid components can be generated. Care must be used in analyzing unevaluated whole rock and mineral-separate data for a relatively fresh rock with glassy feldspars where only 10 percent of the biotite is altered. Also apparent in the Ray data is the occurrence of very different abundances of minor elements in minerals from petrographically and chemically similar but genetically unrelated rocks.

Calc-alkaline intrusive relations at Mineral Mountains in Arizona

Geologic mapping by T. G. Theodore and W. J. Keith has clarified the geologic age relations of four distinct calc-alkaline intrusive bodies near the southwest corner of the Mineral Mountain 7½-min quadrangle of Arizona. A porphyritic quartz monzonite belonging to the regionally extensive Ruin Granite of Precambrian Y age has been intruded by a small leucocratic two-mica granite initially emplaced also during Precambrian Y time although a 66 m.y. age has been determined by the K-Ar method on second-

ary biotite from this body. Both of these plutonic rocks are cut by Precambrian Y diabase. The two-mica granite has also been intruded by a biotite-hornblende quartz monzonite, cropping out in an approximately 3 km² area and containing widely scattered indications of sparse copper mineralization. Primary phenocrystic biotite from this quartz monzonite has been dated at 71 m.y. by S. C. Creasey, using the K-Ar method. A very small body of granodiorite crops out just north of the biotite-hornblende quartz monzonite that probably has the same emplacement age as the quartz monzonite. The biotite-hornblende quartz monzonite and the granodiorite have been faulted intensely by conspicuous north to northeast striking faults related to prominent range-front faults just west of the quadrangle.

Semiquantitative spectrographic data from granitoid rocks of the Basin-Range province

Preliminary study by D. E. Lee of new semiquantitative spectrographic analyses of granitoid rocks from 34 samples from 17 Precambrian plutons and 196 samples from 98 Phanerozoic plutons from the Basin-Range province show that Precambrian plutons are richer in zirconium and rare earths than the Phanerozoic plutons. Moreover a plot of barium against calcium for all 230 samples shows a strong tendency for the two to increase together. If decreasing calcium values are regarded as a measure of differentiation, this relation of barium to calcium is contrary to the generally accepted view that barium tends to increase in late differentiates.

GEOCHEMISTRY OF WATER AND SEDIMENTS

DIAGENETIC STUDIES

Thermal history in siliceous shales

The temperature-sensitive silica mineralogy of Upper Cretaceous-Paleocene, Eocene-Oligocene, and Miocene siliceous shales was determined over a large part of southern Diablo Range of California by K. J. Murata. The shales are cristobalitic in most places, thus indicating a depth of burial of 1 to 2 km. In a small area at Panoche Hills, Upper Cretaceous-Paleocene Moreno Shale which still retains opaline diatoms attests to an extraordinarily shallow depth of burial (<1 km). Several thermal anomalies in the form of restricted areas of quartzose shale in a generally cristobalitic province correlate with piercements of serpentine or with hidden underlying bodies of serpentine previously delineated magneti-

cally. The presence of shales with highly disordered cristobalite adjacent to the San Andreas fault suggests that heat sufficient to raise the ambient temperature of the shale by 20°C to 30°C has not been generated along the fault during the past several million years.

Laumontite alteration

Petrographic observations by M. L. Holmes, R. J. Lantz, T. H. McCulloh, and B. D. Ruppel of feldspathic sandstones from well cores in the Santa Fe Springs oilfield, in Los Angeles County, California, indicated that threshold subsurface conditions for formation of the zeolite mineral laumontite from intermediate plagioclase in marine sandstones without volcanic detritus are $120.5 \pm 0.5^\circ\text{C}$ at ~ 300 bars (30,000 kPa). A further requirement appears to be abundantly available hyposaline water (17,000–20,000 ppm) dominated by Na^+ and Cl^- and at a pH near 7 in sandstones initially of reservoir quality (average porosity of 20 percent and average permeability of $0.025 \mu\text{m}^2$).

Probably because of their superior permeabilities, petroleum reservoir feldspathic sandstones appear to be selective targets for laumontite formation when other threshold conditions are satisfied. Destruction or serious degradation of reservoir quality and petroleum producibility are direct results of practical consequence.

EXPERIMENTAL STUDIES ON CHEMISTRY OF WATER

Coprecipitation of metals with manganese oxide

By using chemical thermodynamics, J. D. Hem evaluated cyclic process of manganese oxidation and disproportionation. Such a cycle can be maintained in natural aqueous systems by circulating aerated water. It leads to a manganese oxide solid near the composition MnO_2 and a manganese solubility in the range commonly found in river water. Coupling of the cycle to other metals, especially lead and cobalt, can scavenge them from solution to maintain very low steady-state concentrations. The concentrations to be expected can be calculated by using thermodynamic principles. Agreement between observed and calculated concentrations of cobalt was found in a number of Colorado stream waters affected by drainage from metal mines.

Adsorption of lead at variable-charge mineral surface

Investigation by D. W. Brown involved the integration of two theoretical models for quantifying

the pH-dependent adsorption of cations of lead and other heavy metals in aqueous media on suspended particulate oxide or silicate surfaces. Brown developed a computer program that takes into account the actual non-Nernstian rise in surface potential with pH and the effect of adsorbed metal cations on the surface potential and avoids the faulty assumption that the dielectric constant of water near the surface is independent of solution parameters and distance from the surface.

Lead hydroxide formation constants

C. J. Lind determined formation constants of lead hydroxide complexes by means of polarography in 0.01 M sodium perchlorate at 25°C. Log values for β'_1 , β'_2 , and β'_3 were calculated to be 6.59, 10.80, and 13.63, respectively. Log values of these constants corrected to zero ionic strength are 6.77, 11.07, and 13.89, respectively. Previously reported values of all three constants were measured primarily in high ionic strength media, and those values of β'_1 varied by two orders of magnitude. Accurate evaluation of these constants at low ionic strength is basic to the consideration of lead species distribution in most freshwaters.

$\text{NO}_3\text{-N}$ uptake by algae in a streamlike environment

V. C. Kennedy and M. J. Sebetich reported that most rapid changes in $\text{NO}_3\text{-N}$ uptake by algae in a flume occurred within a 3-hour period just after daybreak and just after sunset. Hence, sampling to determine $\text{NO}_3\text{-N}$ uptake by stream biota should be done in mid-afternoon or just before daybreak, when rate of change in $\text{NO}_3\text{-N}$ appears to be least. That considerable metabolism occurred at night was indicated by the nighttime removal of 50 to 60 percent of the added $\text{NO}_3\text{-N}$.

Kinetic controls on ground-water chemistry in a volcanic aquifer

A. F. White compared compositions of ground waters found within Rainier Mesa in southern Nevada with compositions of waters produced by experimental dissolution of vitric and crystalline tuffs that comprise the principal aquifers. The two tuff phases of the same bulk chemistry produce aqueous solutions of different chemistry. Rapid parabolic release rates for sodium and silica and the retention of potassium within the vitric phase supported previous predictions concerning ground-water compositions associated with vitric tuffs. Parabolic dissolution of the crystalline tuff results in solutions high in bivalent cations.

The parabolic release of cations from the vitric phase can be described empirically as:

$$Q = Q_0 + kt^{1/2}$$

where Q is the total mass transfer of a species into solution up to time, t , Q_0 is the intercept at $T=0$ and equal to the surface exchange reaction, and k is the parabolic rate constant. Extrapolation of the equation to long time periods successfully reproduces, at comparable pH, the cation composition of Rainier Mesa ground water.

Aqueous geochemical kinetics studies

A digital kinetic model describing the diffusion-controlled dissolution of a rhyolitic glass was developed by H. C. Claassen and A. F. White. This model takes into account variations in surface-to-volume ratio, pH, and temperature. The effect of solute concentration variations on reaction rate is described by use of a Freundlich sorption isotherm.

Initial reaction consists of a rapid ion exchange on the solid surface and establishment of a metastable equilibrium. Mass transfer is subsequently controlled by the various hydrogen ion-cation codiffusion rates. Diffusion of zerovalent species is pH-independent; however, charged species have diffusion rates that are dependent on hydrogen-ion concentration—and bivalent ions are more dependent than monovalent ions. This results in a solution composition that is determined by the pH of reaction and explains the composition of ground waters associated with vitric tuffs in parts of southern Nevada.

Obtaining a sorption isotherm for natural material from kinetic data allows meaningful comparisons to be made between different materials and predictions to be made of sorption behavior of species not subjected to laboratory scrutiny.

STATISTICAL GEOCHEMISTRY AND PETROLOGY

Anomalous geochemical variability in Washington County, Missouri

R. J. Ebens and J. J. Connor (1977), in a study of geochemical patterns in the carbonate residuum of southern Missouri, found that copper, lead, zinc, and barium in the residuum of Washington County have not only high mean concentrations but high variabilities as well even though the variabilities were measured on logarithmic scales to correct for the commonly-observed relationship between the mean and variance. The frequency distributions of

these elements in the residuum of Washington County and of the other counties taken as a group are approximately lognormal. The residuum is a clay-rich product of highly-weathered, carbonate bedrock. Most of the barite mining district of southeastern Missouri is in Washington County. The relatively high concentrations of copper, lead, zinc, and barium, and the high variabilities may be related to the occurrence of these metals in known barite deposits although no detailed relation between high geochemical values and known deposits was observed.

Frequency distributions of elements

A. T. Miesch reports that frequency distributions of both major and minor chemical constituents in some common rock types follow three-parameter lognormal and gamma functions significantly better than they follow the commonly assumed normal and two-parameter lognormal distributions or the two-parameter gamma distribution. If this property of geochemical data is found to be widespread, it will have an important bearing on any statistical procedure used in geochemistry that involves probability theory, but it will be especially important in some of the procedures being used to identify geochemical anomalies in exploration and to establish baseline concentrations in environmental geochemistry. It may also be important in statistical predictions of reserves that are based on the nature of the frequency distributions of elements in the earth's crust. It appears now that the three-parameter lognormal density function may be generally applicable in geochemistry, even where the observed frequency distribution is apparently symmetrical or even negatively skewed. A series of three FORTRAN programs has been completed to use in further studies: (1) Program RDIST is used to generate simulated data from any of nine different kinds of frequency distributions; (2) Program GDIST, adapted from a USBM program (Alldredge and Bolstad, 1977), is used to test any of the nine distributions for goodness-of-fit to observed data; and (3) Program FDIST is used to compute the ordinate values or the percentiles for any of the nine distribution types.

A number of changes were made in the GDIST program, the more significant of which are options added to fit (1) three-parameter lognormal distributions with either positive or negative skewnesses and (2) three-parameter gamma distributions. The third parameters for the distributions are location parameters and are estimated by a numerical method.

J. O. Kork modified the section of GDIST that estimates the parameters of the gamma distribution. Although the maximum likelihood method is used, the maximum likelihood equations cannot be solved explicitly and are highly unstable under certain conditions. Therefore, an iterative technique has to be used to find the approximate solutions.

Geochemical anomalies

Areas within a geochemical map are commonly recognized as anomalous not by the presence of extraordinarily high geochemical values but by the clustering of values that are only moderately high. A number of methods for identifying statistically significant clustering have been developed by geographers and plant ecologists, but most of them require considerable computation in their application. A. T. Miesch has explored the problem by computer simulation and developed criteria that can be used wherever the map values correspond approximately to a grid pattern and tend to be normally distributed. A cluster is defined as two or more map values higher than a given number of standard deviations above the mean that occur within map cells that are contiguous on a side or corner. If the geochemical map has 9 values, clusters of 2 or more values higher than one standard deviation above the mean are significant—that is, they occur only 5 times out of 100 by chance alone. If there are 49 values, clusters of 6 or more are significant. Similarly, for 100 values, clusters of 9 or more, and for 225 values, clusters of 11 or more are significant. If the geochemical values are more than 2 standard deviations above the mean, clusters of 2 or more are significant if the map contains fewer than 225 values. Each of these estimates is based on 1,000 computer trials and on simulated map areas that were square. However, a few experiments indicated that the estimates are approximately correct even if the dimension of the map in one direction is twice that in the other. The presence of a significant cluster indicates only that the clustering is unlikely to be fortuitous; it might be the result of many geologic factors other than the presence of a mineral deposit.

ISOTOPE AND NUCLEAR GEOCHEMISTRY

ISOTOPE TRACER STUDIES

Strontium isotopic variation in a compositionally zoned granitic pluton

The Tuolumne Intrusive Series is a compositionally zoned pluton in the central Sierra Nevada being

studied by R. W. Kistler, P. C. Bateman, D. L. Peck (USGS) and Bruce Chappell (Australian National University). Rock types range from tonalite in the outer margin to granite in the core of the pluton. Several slightly different models that all rely on fractional crystallization of an originally homogeneous magma were developed in earlier studies to explain the compositional zonation observed in the pluton.

Strontium isotopic compositions were determined for 18 specimens from a traverse across the pluton. Initial $^{87}\text{Sr}/^{86}\text{Sr}$ values increase from the margins to the center of the pluton. When $^{87}\text{Sr}/^{86}\text{Sr}$ is plotted against $^{87}\text{Rb}/^{86}\text{Sr}$ on a strontium evolution diagram for all the samples, two parallel lines can be drawn through the points. Regression of these lines yields two different initial $^{87}\text{Sr}/^{86}\text{Sr}$ values of 0.7059 and 0.7064 for the rocks. A single sample is well off the two lines and has an initial $^{87}\text{Sr}/^{86}\text{Sr}$ value of 0.7057.

The strontium isotopic data indicate at least two isotopically discrete source materials are involved in the rock series and the compositional zonation in the pluton is not due to fractional crystallization of a single magmatic source material.

Source of lead in ores of the San Juan Mountains in Colorado

In the San Juan volcanic area of southwestern Colorado, B. R. Doe, T. A. Steven, M. H. Delevaux, J. S. Stacey, P. W. Lipman, and F. S. Fisher found the isotopic composition of lead in ores and ore prospects of Cenozoic age to range widely: 17.72 to 21.13 for $^{206}\text{Pb}/^{204}\text{Pb}$; 15.50 to 15.81 for $^{207}\text{Pb}/^{204}\text{Pb}$; and 37.21 to 38 for $^{208}\text{Pb}/^{204}\text{Pb}$. Examination of the lead isotope data indicates that once deposition of lead minerals begins, further exchange of lead between fluid and wall rock is insignificant. This conclusion is supported by the relatively constant isotopic composition of the lead in individual ore deposits, which is not affected by the grade of ore mineralization or type of wall rock. The values of $^{206}\text{Pb}/^{204}\text{Pb}$ in some vein-type deposits exceed the maximum value known for all Mesozoic and Cenozoic igneous rocks of the Rocky Mountain region. These isotopic relations show that if ore-forming solutions contain meteoric water, as indicated in studies of light stable isotopes, they must have penetrated deep enough to acquire lead from Precambrian rocks or sediments derived from them. The fact that some of these vein ores are now in Cenozoic igneous rocks indicates the ore fluid had an upward vertical component to its movement. The lead isotope data therefore support a circulating cell hypothesis for these kinds of ores,

as suggested by many recent studies of light stable isotopes as related to mineralization.

Some other deposits (Summitville, Jasper, Red Mountain district) have values of $^{206}\text{Pb}/^{204}\text{Pb}$ similar to those of the large volumes of altered rock that enclose them ($^{206}\text{Pb}/^{204}\text{Pb}$ of 18.5), suggesting that in places the lead may have been locally derived by leaching of the adjacent rocks or by derivation from magmatogenic fluids.

When the lead isotope data are treated in detail, the rocks and galenas of the Platoro caldera complex, the central San Juan caldera complex, and the Baughman Creek center appear to contain significant components derived from source materials that are 1.4 to 1.5 billion years old and 1.7 to 1.8 billion years old. These also are the ages of the two main groups of rocks that comprise the Precambrian basement under the San Juan volcanic area. Although the data from the western San Juan caldera complex scatter considerably, the only obvious source for the lead seems to be the rocks that are 1.7 to 1.8 billion years old or detritus of such age in Phanerozoic sediments. Where the involvement of sources that are 1.4 to 1.5 billion years old is greatest, the Th-U ratio is small (calculated to be about 0.7), whereas the Th-U ratio of the 1.7- to 1.8-b.y. source material appears to be 2.3 to 3.3. The largest Th-U values are from the western San Juan caldera complex.

STABLE ISOTOPES

Hydrothermal system of the East Tintic district in Utah

J. N. Batchelder and J. R. O'Neil are doing a fluid-inclusion and light-stable-isotope study on selected samples of quartz, barite, sphalerite, and galena from the fissure and replacement orebodies at the East Tintic district in Utah. Preliminary results indicate that filling temperatures of fluid inclusions in quartz and barite range from 150°C to 300°C, and salinities range from <0.1 to 3.1 equivalent weight percent NaCl. Present-day spring waters in the East Tintic district have a δD of approximately -120 permil and a $\delta^{18}\text{O}$ of -15 permil. Water liberated from fluid inclusions in quartz yields δD values ranging from -121 to -118 permil. Calculated $\delta^{18}\text{O}$ values for water in equilibrium with quartz range from -5.1 to 0.0 permil. Water liberated from fluid inclusions in sulfide samples has δD values generally ranging between -114 to -101 permil and, in the coarsest galena sample, a value of -84 permil. These preliminary data from quartz

suggest a hydrothermal system that was dominated by meteoric waters that underwent partial exchange with the host rocks. In contrast, the data from the sulfides indicate that substantial amounts of magmatic water may have been present during ore deposition.

Sulfur isotope distributions at Balmat in New York

Underground mapping of the Balmat Zn-Pb deposit has distinguished 16 stratigraphic units that consist of alternating siliceous- and carbonate-rich layers with minor anhydrite lenses. The section is part of the Grenville Series (Precambrian). Anhydrite occurs in at least seven of the marble units but is best developed as 15 to 25-m and 45 to 60-m-thick lenses in two of the marble units that are 215 m apart stratigraphically. Numerous zinc-pyrite deposits occur in the top nine units of the section, some of which are physically associated with anhydrite.

On the basis of their large volume, lithologic associations, $\delta^{34}\text{S}$ distributions and $\delta^{13}\text{C}$ and $\delta^{18}\text{O}$ of associated marbles, J. F. Whelan and R. O. Rye have concluded that the anhydrite lenses are marine evaporitic in origin. The lower and upper anhydrite lenses have $\delta^{34}\text{S}$ values ranging from 7.6 to 10.2 permil and 24.1 to 30.2 permil respectively, with values in both lenses increasing from bottom to top of the unit. The within lens variations of $\delta^{34}\text{S}$ values can be attributed to simultaneous bacterial reduction of sea-water sulfate and evaporite formation. The between lens variations indicate extremely rapid variations in the $\delta^{34}\text{S}$ of sea water sulfate in the Grenville ocean. These variations were apparently much more rapid than occurred in the Phanerozoic.

The $\delta^{34}\text{S}$ values of averaged bulk samples from 23 ore occurrences range from 13.2 to 16.2 permil, indicating that sea-water sulfate was the source of sulfur in the deposits. The $\delta^{34}\text{S}$ values of the deposits, however, are distinctly different from the $\delta^{34}\text{S}$ values for sea water during the deposition of the sedimentary section as indicated by the anhydrite data. Thus, the deposit must have formed after the entire host section was deposited, probably by some kind of lateral secretion process.

^{18}O and δD values of Hawaiian basalts and xenoliths

In a study by J. R. O'Neil the $\delta^{18}\text{O}$ values of submarine basalts dredged from the East Rift Zone of Kilauea range from +4.7 to +6.3 and are correlated positively with degree of differentiation. The chemical and isotopic relations of these basalts are con-

trolled by olivine. Subaerial Hawaiian tholeiites $\delta^{18}\text{O}$ values range from +5.2 to +5.8. Unaltered alkali olivine basalts and xenoliths, on the other hand, are generally more ^{18}O -rich with values of $\delta^{18}\text{O}$ between +5.8 and +7.7. These oxygen-isotope data indicate isotopically distinct sources for alkali olivine basalts and tholeiites and imply a possible genetic relation between alkali olivine basalt and xenoliths in Hawaii. Oxygen isotope reversals are observed in mineral separates from several xenoliths.

Values of δD are positively correlated with H_2O contents and eruption depths of Kilauean submarine basalts and indicate contamination of the molten basalts with seawater. Hawaiian tholeiites contain a maximum of 0.26 to 0.31 weight percent magmatic water that has a δD value between -69 and -80. The calculated quantities of seawater are too low to affect the chemical and oxygen isotope compositions of the basalts or to mask the detection of any rare gas anomalies.

ADVANCES IN GEOCHRONOMETRY

K-Ar dating of the Albian

Continued geochronologic work by J. D. Obradovich and W. A. Cobban on Albian bentonites indicate that this stage may have been quite lengthy. Two biotite-bearing bentonites were collected along the northwest flank of the Black Hills uplift in Wyoming. The upper bentonite (99.6 m.y.), from the base of the Newcastle Sandstone, lies in a barren interval between the *Miliammina manitobensis* and *Haplophragmoides gigas* foraminiferal zones. The lower bentonite (104.4 m.y.), from the bottom of the Skull Creek Shale, lies near the base of the *H. gigas* Zone. The lower part of the *M. manitobensis* Zone is older than the *Neogastropilites* Zone, and *H. gigas* Zone is younger than the *Gastropilites* Zone. The *Gastropilites* fauna is of basal late Albian Age based on the occurrence of *G. cantianus* in the *Diploceras cristatum* Subzone. Therefore, the middle-late Albian boundary is older than 104 m.y. With the Albian-Cenomanian boundary placed at 96 million years B.P. (based on revised decay constants for ^{40}K), the late Albian spans at least 8 million years. A third bentonite, collected from the upper part of the Hulcross Member, Commotion Formation, Fort St. John Group, near Hudson Hope, British Columbia, Canada, lies below occurrences of *G. cantianus*. The underlying Gates Member of the Commotion con-

tains *Beudanticeras affine* of early Albian Age. A preliminary K-Ar age of 108 m.y. on plagioclase from this middle Albian horizon indicates that the latter half of the Albian may have lasted 12 m.y. Previously published U-Pb ages of 114 m.y. on zircon and monazite from plutons that intrude the Allisitos Formation and correlatives (late Aptian and possibly early Albian in age), Baja, Calif., help place constraints on the age limits of the early Albian. These results place only a minimum age on this time interval but do suggest that the Albian Stage may have lasted 18 m.y. or more.

Fission-track dating of the type Ordovician and Silurian

An investigation by C. W. Naeser, R. J. Ross, and G. A. Izett has produced the first isotope ages ever determined on the type sections for the Ordovician and Silurian Systems in the United Kingdom. Zircons have been separated from bentonite beds that are biostratigraphically controlled. These zircons were then dated with the fission-track method. The ages are as follows:

System	Stage	Age
Silurian	Ludlovian	397 ± 9, 398 ± 12
	Wenlockian	404 ± 9, 410 ± 10
Ordovician	Caradocian	450 ± 20, 454 ± 17
	Llanvirnian	464 ± 10, 462 ± 10
	Arenigian	478 ± 11

Discordancy of zircons in the Saudi Arabian Shield

J. S. Stacy (USGS) and J. A. Cooper (University of Adelaide) have found that 650-800 m.y. old zircons in the southern Arabian Shield do not appear to have been disturbed by the Pan African uplift and orogeny about 600 m.y. ago, even though many K-Ar systems were reset at that time (Fleck and others, 1976). On the other hand the zircons do seem to have suffered lead loss in a more recent event that was presumably the uplift and rifting that formed the Red Sea. This more recent event did not affect the K-Ar systems although it did affect some Rb-Sr systematics.

It is hypothesized that the U-Pb systems in the zircons were not disturbed (damaged by radiation) by the Pan African event because they were not sufficiently metamict. In Tertiary time, however, lead loss occurred from the then metamict zircons because of their uplift into the level of low temperature ground-water activity.

Uranium-trend dating of alluvium deposits

A new concept in uranium-series dating called uranium-trend dating has been tested extensively over the past year by J. N. Rosholt to determine the reliability of this technique in estimating the time of deposition of alluvium deposits over the time range of 10,000 years to about 900,000 years ago. The dating technique consists of determining an isochron from analyses of several samples covering the various soil horizons in a given alluvium unit; approximately four to nine samples of each alluvium unit are analyzed. In each sample an accurate determination of the abundances of U-238, U-234, Th-230, and Th-232 is required. The results of these analyses are plotted where $(^{234}\text{U}-^{238}\text{U})/^{238}\text{U}$ versus $(^{238}\text{U}-^{230}\text{Th})/^{238}\text{U}$ ideally yield a linear relationship where the resulting slope, $\Delta(^{234}\text{U}-^{238}\text{U})/\Delta(^{238}\text{U}-^{230}\text{Th})$, increases with increasing age of the alluvium deposition for a given half-period of the flux controlling the migration of uranium in the alluvium environment. A mathematical model using the first derivations of Bateman's equations describing the growth and decay of ^{234}U and ^{230}Th requires a variable factor called the half-period of this flux. The value of this factor, $F(0)$, is determined as a function of the intercept of the isochron on the x-axis ($y\text{-axis}=0$ in fig. 1) and a $^{230}\text{Th}/^{238}\text{U}$ apparent isochron calculated in the same manner as that for ionium dating of volcanic rocks (Allegre and Condomines, 1976). A significant number of soil profiles on different alluvium units have now been analyzed (15 units comprising about 94 samples), and the results appear very encouraging.

Samarium-Neodymium systematics in gabbro from Fairweather Range in Alaska

In a cooperative work with G. K. Czamanske, Mitsunobu Tatsumoto has studied the Sm-Nd and Rb-Sr systematics of the LaPerouse layered gabbro from the Fairweather Range of Glacier Bay National Monument in Alaska.

The emplacement age of the ultramafic pluton has been debated among ages from no older than Precambrian to late Paleozoic. Because of the low susceptibility of Sm-Nd systematics to metamorphic events and existence of measurable amounts of samarium and neodymium in ultramafic rocks, the Sm-Nd method seems to be a good method to date such ultramafic rocks. The $^{87}\text{Sr}/^{86}\text{Sr}$ ratios are rather primitive and range from 0.7041 to 0.7047 among plagioclase, olivine, and pyroxene fractions. The ratios are similar to that of continental basalt but are slightly higher than those of oceanic ridge

tholeiites. The $^{143}\text{Nd}/^{144}\text{Nd}$ ratios ranged from 0.51293 to 0.51299 although $^{147}\text{Sm}/^{144}\text{Nd}$ ratios ranged from 0.128 to 0.293 for whole rock, plagioclase and pyroxene fractions. The virtual identity of the Nd-isotopic compositions among the mineral separates clearly implies that the rock age is not older than 100 m.y., assuming that the Sm-Nd systematics were not disturbed by later metamorphic events.

Minor element geochemistry and strontium isotopes of Tertiary stocks in Colorado mineral belt

Rocks of the northeast portion of the Colorado mineral belt form two petrographically and chemically distinct rock suites: (1) a silica saturated, high alkali, monzonite suite and (2) a silica oversaturated, lower alkali, granodiorite suite. E. C. Simmons and C. E. Hedge have found that these rock suites are also distinct on the basis of their trace element and Sr-isotope compositions. Rocks of the monzonite suite generally have strontium contents greater than 1,000 ppm, highly variable rare-earth elements (REE) patterns and $^{87}\text{Sr}/^{86}\text{Sr}$ initial ratios less than 0.706. Rocks of the granodiorite suite generally have strontium contents less than 1,000 ppm, subparallel REE patterns, and initial $^{87}\text{Sr}/^{86}\text{Sr}$ ratios greater than 0.707.

Despite forming simple, smooth trends on major element variation diagrams, trace element data for rocks of the granodiorite suite indicate that they were not derived from a single magma. These rocks are derived from magmas having similar REE patterns, but variable rubidium and strontium contents, and Rb/Sr ratios. The preferred explanation for these rocks is that they are derived by partial melting of a mixed pyroxene granulite-pyroxenite source.

Rocks of the monzonite suite are chemically and petrographically more complex than the granodiorite suite. They are subdivided here into alkalic and mafic monzonites and quartz syenites. The geochemistry of these three rock types require derivation from separate and chemically distinct magma types. The preferred explanation for rocks of the monzonite suite is derivation from a heterogeneous source having the composition of alkali basalt and the mineralogy of eclogite.

The Sr-isotope systematics of the majority of these rocks are interpreted to be largely primary and not the result of crustal contamination. The positive correlation of Rb-Sr and $^{87}\text{Sr}/^{86}\text{Sr}$ ratios for the least fractionated samples indicate that the sources from which parent magmas of both the

granodiorite and monzonite suites were derived are Precambrian in age.

GEOHERMAL SYSTEMS

Two and three dimensional modeling of geothermal systems

Geothermal modeling by J. W. Mercer concentrated on (1) implementing a concept of vertical equilibrium in geothermal modeling, (2) improving the matrix equation solution technique for both two-and three-dimensional models, and (3) applying a vertical equilibrium, areal model to the Wairakei, New Zealand geothermal field. The model currently being used for field problems incorporates the concept of vertical equilibrium. It solves for only two space dimensions (areal), includes gravity terms, and the finite-difference equations are solved using Newton-Raphson iteration on source and accumulation terms. The resulting matrix equations are solved sequentially using D4 ordering and Gauss-Doolittle decomposition.

Chemical modeling of geothermal waters

Chemical modeling of natural waters involves the mathematical distribution of the cations among all complex forming ligands to the strength that the complexes form. For example, magnesium is distributed among the following species: Mg^{2+} , $MgOH^+$, $MgSO_4^0$, $MgHCO_3^+$, $MgCO_3^0$, $MgH_2PO_4^+$, $MgHPO_4^0$, and $MgPO_4^-$. Chemical modeling of geothermal waters from hot springs and shallow wells provides information of the natural solubility controls of the dissolved constituents. This information may be used to predict dissolved concentrations from wells drilled down to hotter waters. It is also useful in understanding the natural controls on dissolved toxic trace elements in geothermal effluents. This information may be used to promote removal of the toxic trace elements through natural processes. This is likely to be the least expensive method for reducing to acceptable levels the concentration of toxic trace elements in effluent geothermal waters.

A. S. Van Denburgh, E. A. Jenne, J. W. Ball, and J. M. Burchard studied a suite of well-water samples from the Soda Lakes geothermal area near Fallon, Nev. It appears that most of the waters are in equilibrium with sepiolite ($MgSiO_4$) within the combined error of the sampling, analyses, and thermodynamic data. About one-third of the waters are in apparent equilibrium with amorphous silica (SiO_2).

Sulfate appears to limit the concentrations of barium, as the mineral barite ($BaSO_4$) in half of the

waters and calcium, as the mineral gypsum ($CaSO_4$) in three samples.

The fluoride levels in the well waters appear to be too low to be solubility controlled.

Oxides of arsenic and calcium arsenate are greatly undersaturated. Arsenic levels in these hot waters are probably controlled by sulfide levels.

Transient pressure analysis in vapor-dominated geothermal reservoirs

In a continuing effort to understand the processes occurring in vapor dominated geothermal systems, A. F. Moench designed a computer model for the horizontal, radial flow of steam in the presence of an immobile vaporizing or condensing liquid phase. This model was adapted from the model of Moench (1976) and is described in the summary report by Moench and Atkinson (1977). Dimensionless plots of pressure drawdown and buildup have been obtained for a well discharging steam at a constant rate for a specified time. Drawdown computations show that the existence of a vaporizing liquid-water phase is manifested only by a shift in the horizontal direction from that expected for a noncondensable gas and can be explained as an apparent increase in steam compressibility. Pressure buildup computations, on the other hand, show characteristics markedly different from that expected for noncondensable gas. Initially, pressure rises rapidly because the steam is superheated in the vicinity of the well bore. When pressure in the reservoir becomes equal to the saturated-vapor pressure, condensation occurs and pressure remains nearly constant for a period of time. Continued rise in pressure occurs slowly and is due to reservoir heating through release of latent heat. If phase change plays a significant role in pressure transient well testing of vapor-dominated geothermal reservoirs it should be manifested in pressure buildup tests.

Chemical character of ground water associated with the Soda Lakes geothermal area near Fallon, Nevada

Data from 15 shallow to moderately deep test wells (perforations 9–150 m below water table) indicate that water quality within and adjacent to the Soda Lakes geothermal area near Fallon, Nev., differs considerably from place to place. According to A. S. Van Denburgh, the hottest sampled fluids ($144^\circ C$) contain about 5,000 mg/L of dissolved solids, dominated by sodium and chloride. The much cooler waters of two wells hydraulically upgradient from the hottest area are considerably fresher (600 and 1,300 mg/L) and are chemically different from

each other and from the hottest waters. Down-gradient from the hottest area, the dissolved-solids concentration of sampled ground waters is wide in range. The deeper waters (more than 15 m below water table) are relatively fresh (900 to 4,100 mg/L). They presumably reflect mixing and dilution of the hot water as it moves down the hydraulic gradient. The three shallowest well waters, in contrast, contain 4,800–8,800 mg/L of dissolved solids, suggesting that the dilution process is counteracted at shallow depths by the concentrating effects of evapotranspiration.

Thermal conductivities of rocks

In the disposal of radioactive waste in the earth, the heating effects on the containing rock salt, shale, limestone, or igneous rock must be accounted for, and the thermal conductivity of the rock is perhaps the most important property used in estimation and design for possible sites. Tabulations of conductivity are inherently unwieldy and uncertain, and actual measurements on rock samples require much effort, and on friable rocks are often impossible. E. C. Robertson has developed easily usable charts from which conductivities of rocks can be obtained from the textural and mineral data of the rocks. Thermal conductivities of all the common rocks have been found to vary with the square of solidity (one minus porosity), linearly with content of quartz in granite, and linearly with pressure (about 3 percent/kbar) in all nonporous rocks. The variation with water content can be taken as linear in nonporous rocks, and the variation with temperature is strongly negative for felsic rocks and salt and is positive and small for mafic rocks. Anisotropy can be important, the values normal and parallel to bedding or foliation differing by 20 percent in some rocks, but is usually less than 5 percent. The conductivity charts clearly are usable for geothermal resource purposes and in heat flow calculations and thermal gradient estimates in regions of known lithology but without rock samples for conductivity measurement.

Newberry Volcano in Oregon

The flanks of Newberry Volcano in central Oregon, formerly mapped as consisting of basalt flows and cinder cones, are as complex as the caldera at Newberry's summit. Geologic mapping by N. S. MacLeod has resulted in the identification of numerous ash-flow-tuff units on the east and west flanks interbedded within sequences of basaltic-

andesite to dacite flows, other tephra deposits, and sediments. Fifteen ash-flow-tuff units, some consisting of as many as 10 individual ash flows, have been mapped. They range in composition from andesite to rhyolite, are mostly pumiceous and lithic-rich, and are up to 50 m thick. Many are widespread, others occur only in a few scattered localities and appear to have been confined to paleo-channels. Units on the west and east flanks do not apparently correlate, suggesting that ash flows were derived during segmental collapse of the complex summit caldera. Nineteen rhyolitic bodies (domes, flows, explosion craters, etc.) have been mapped on the flanks; some occur in zones radial to the caldera. Basalt flows form most of the north and south flanks but are younger than the ash flows of the east and west flanks and probably veneer them. The geothermal potential is probably highest in the caldera that has been withdrawn from geothermal development, but the abundant rhyolitic rocks, some younger than 6,700 years, on the upper northeast and southeast flanks may also be associated with areas of high geothermal potential.

Earthquake swarms in Imperial Valley, California

Three earthquake swarms occurred in northern Imperial Valley in November and December 1976. G. S. Fuis found that together they roughly outline the trend of the Brawley fault (NNW) that has been inferred from past seismicity, but two of them appear related to structures with different trends. The first and largest swarm occurred during the period November 4–10, 1976. It generated 213 locatable events, including nine events of $M_L \geq 4$ during the first 12 hours. It began with a cluster of events about 8 km west of Calipatria. The largest event in the swarm, $M_L = 4.9$, occurred in this cluster and was followed within an hour by events defining a steeply-dipping, planar zone extending 5 km west-southwest of the cluster. These observations are consistent with slip on a fault conjugate to the inferred trend of the Brawley fault, triggered by the $M_L = 4.9$ earthquake. The second swarm occurred during the period November 11–17, 1976. It generated 62 locatable events; the largest, $M_L = 3.4$. It began with a tight cluster of events under Obsidian Butte, about 7 km northwest of the first cluster in the first swarm; $2\frac{1}{2}$ days later seismicity shifted and clustered 1 km north-northeast of Obsidian Butte. The axis of these clusters is at a high angle to the inferred trend of the Brawley fault. Events in this swarm cluster tightly in depth. The third swarm occurred during the period December 17–20,

1976. It generated 12 locatable events; the largest, $M_L = 3.5$. It began with a tight cluster of events 7 km north-northwest of Obsidian Butte followed 2 days later by a cluster 3 km farther north-northwest. The axis of these two clusters does have the trend of the Brawley fault. The temporal earthquake clusters during this 2-month period is suggestive of a north-northwestward migrating displacement on the Brawley fault that triggers displacements on related structures. Similar spacial-temporal patterns of seismicity have been noted farther along the Brawley fault (Hill, Mowinckel, and Lahr, 1975; Johnson and Hadley, 1976).

New seismic instrumentation for geothermal surveys

A sophisticated seismic data acquisition and analysis system has been developed to aid in geophysical investigations of geothermal areas. P. A. Reasenbergs reports (Reasenbergs, Cessaro, and Wilson, 1977) the data acquisition system consists of a portable 96-station seismic array, radio telemetry equipment and an analog tape recorder. The data analysis system includes a minicomputer capable of performing both interactive graphic data presentations and advanced numerical analysis programs. Results of system tests indicate that the system produces high quality seismic data. Data collected at the Coso volcanic field in California are currently in use in two studies of crustal structure in that region.

Strike-slip faulting and crustal spreading in the Coso Range, California

Studies of current seismicity at the Coso geothermal area by C. S. Weaver and A. W. Walter have defined a conjugate strike-slip fault system, trending northeast and northwest across the volcanic rocks of the Coso Range. These faults define a zone of crustal spreading, where surface geothermal features are present and earthquake swarms are observed.

Seismicity of The Geysers-Clear Lake geothermal area in California

Microearthquake activity in The Geysers-Clear Lake region of northern California has been monitored continuously since 1975. The seismogenic zone across the geothermal area and gravity low is relatively shallow; earthquake focal depths are less than 5 km. The absence of deeper earthquakes is consistent with the hypothesis of elevated temperatures associated with a magma body at depth. C. G. Bufe and S. M. Marks found that the present tectonic stress orientation, deduced from *P*-wave first

motions, indicates maximum compression at N. 30° E., minimum compression at N. 60° W. over most of the region. This stress orientation is rotated 30° clockwise from that producing maximum right lateral shear on faults subparallel to the San Andreas, possibly accounting for the diffuse pattern of epicenters in the region. Most fault-plane solutions suggest right lateral strike-slip motion on short, possibly en echelon faults trending more northerly than the geologically well-defined Macama, Mercuryville, or Collayomi systems. Most of the earthquakes between magnitude (M_L) 1.0 and 4.0 in the region occur in The Geysers geothermal development area and are characterized by a very large increase in number of microearthquakes with decreasing magnitude.

Refraction study of the southeast coast of Kilauea

In November 1976, a series of 26 shots were detonated in the water along a 100-km line that is roughly perpendicular to the Kau Puna coast on the southeast flank of the big island of Hawaii. The shots were recorded on the USGS permanent Hawaii net stations and at five other locations using portable 5-day recorders. Record sections from the shots show well-defined *P_n* branches having little scatter from a straight line. D. P. Hill and J. J. Zucca report that the apparent velocities of these branches cluster around 8.0 km/s. The rays that have traveled solely through the crust show more complicated first-arrival patterns. Later arrivals are difficult to correlate from trace to trace in the record section and are correspondingly difficult to interpret. Because of the nature of the shot-receiver geometry, little data in closer than 20 km were obtained. *P_n*-intercept times (uncorrected for water depth and elevations) are slightly greater than 6 seconds over the volcano flanks and along the coastal areas. Intercept times are somewhat lower, between 5.7 and 5.9 seconds over the rift zones of the volcanoes and in the summit areas of both Kilauea and Mauna Loa. These data provide additional evidence on the nature of the high-velocity core beneath the summit and rift zones of the Hawaiian volcanoes.

Seismicity and tectonics at Yellowstone National Park

A series of earthquakes up to magnitude 6, beginning in March 1974 and continuing through 1976, define a northwest-trending zone of seismicity, 5 km wide and 25 km long, which cuts across the north-central boundary of the Yellowstone caldera. The northwest end of the seismic zone coincides with

several north to northwest-trending normal faults in 600,000 year old rocks. First order level line changes indicate 20 to 30 mm of displacement may have occurred on a 5-km-long segment of one of these faults between 1960 and 1975. No surface faulting has been observed in the 70,000- to 150,000-year-old rocks at the southeast end of the seismic zone within the caldera.

According to A. M. Pitt, the current seismic activity suggests that the long-term Yellowstone regional tectonic pattern of north to northeast extension is propagating across the young volcanic rocks within the caldera and that the caldera is not tectonically isolated from the surrounding region.

Hydrothermal alteration in Carnegie I Drill Hole, Upper Geyser Basin, Yellowstone Park

C. N. Fenner of the Geophysical Laboratory, Carnegie Institution of Washington, directed the drilling in 1929 of the world's first research core hole in a geothermal area. This hole, now distinguished as Carnegie (C-I), is near the center of the Myriad Group of hot springs in the Upper Geyser Basin. Fenner (1936) made a detailed study of the hydrothermal mineralogy that was superb for its time and methods of study then available. T. E. C. Keith and D. E. White have studied the small pieces of preserved core to compare the primary lithology and hydrothermal mineralogy with core obtained from USGS research drill holes Y-1 (Honda and Muffler, 1970), Y-7, and Y-8 (Keith, White, and Beeson, in press), located in other parts of Upper Geyser Basin. Improved methods and understanding of mineral relationships permit several revisions in Fenner's conclusions. His "orthoclase" consists of three types, each with a different origin: (a) primary phenocrysts of sanidine, (b) sanidine from devitrification of rhyolite during cooling, and (c) hydrothermal "sanidine" (or adularia). Fenner identified a hydrothermal mineral as heulandite, but this mineral is actually clinoptilolite (Mumpton, 1960).

Carnegie I drill hole penetrates the same rocks as those of other Upper Basin drill holes. A thin layer of sinter overlies streambedded obsidian sand and gravel, now hydrothermally altered. The lowest unit is Biscuit Basin rhyolite flow, consisting of two parts, an upper vitrophyric flow breccia and a lower pumiceous tuff. Fenner identified the flow rock as dacite, but R. L. Christiansen (oral commun., 1977) includes it with rhyolites from its silica content and normative feldspar compositions.

Hydrothermal mineral relationships of C-I are similar to those of Y-8. The assemblaged-cristoba-

lite-clinoptilolite is interlayered with analcime-quartz in the upper part, but potassium-feldspar-quartz is the dominant assemblage in most of the section. Chalcedony often occurs as open space deposits, followed by quartz. Veinlets in the rhyolite are lined with varying proportions of quartz and potassium-feldspar. Electron microprobe analysis by M. H. Beeson on veinlet potassium-feldspar shows 98.5 Or. The potassium-feldspar and quartz found throughout C-I reflects higher potassium content and higher temperatures of upflowing waters, relative to Y-1, Y-7, and Y-8.

Unusual and scarce hydrothermal minerals in C-I are truscottite, gyrolite and wairakite, found co-existing with calcite in open spaces above -28 m and with marcasite in a cavity at -45 m. An unidentified white acicular mineral from a veinlet at -80.5 m is being studied.

Ages and continuities of most New Zealand geothermal systems not well-defined

The geothermal systems of New Zealand have been drilled and studied extensively over the past 25 years but relatively little is known of the timespan and continuity of activity of individual systems. A major problem is that young lava flows and tephra are abundant and generally conceal all evidence of surface activity prior to ~25,000 years ago. However, three major systems (Wairakei, Broadlands, and Kawerau) have revealed evidence for considerable age, perhaps as much as 500,000 years. P. R. L. Browne (New Zealand Geological Survey) recently reported (written commun., 1977) that drill core from Kawerau contains a hydrothermal explosion breccia with incompatible fresh and hydrothermal mineral assemblages in adjacent fragments. The breccia is older than a welded tuff of ~260,000 years and is younger than another welded tuff with a probable age of about 390,000 years. The evidence from Wairakei also consists of a hydrothermal explosion breccia that is not precisely dated but has an estimated age of 300,000 to 500,000 years. Both areas also contain young explosion breccias, but evidence that bears directly on continuity of activity between the old explosion breccias and young sinter breccias is lacking.

The Orakeikorako area contains two sequences of siliceous sinter that were formerly interpreted as different parts of a once continuous sinter sheet from a single spring vent area. The western 15-m sequence has no presently associated thermal activity and is mantled by 10 to 15 m of tephra that range up to 20,000 years in age. The silica mineral

of the upper sinters of this sequence is β -cristobalite, ($d_{101} = \sim 4.10 \text{ \AA}$) the middle part gradually changes downward to α -cristobalite ($d_{101} = \sim 4.07 \text{ \AA}$), and the basal part consists of chalcedonic sinter with local α -cristobalite ($d_{101} = \sim 4.05 \text{ \AA}$). This is the most systematic diagenetic conversion of silica minerals yet found in hot-spring sinters, and is strikingly similar to the diagenesis of Miocene siliceous shales described by Murata and Larson (1975). Conversion of amorphous opal to β -cristobalite at the top of the western Orakeikorako sequence required at least 20,000 years at temperatures initially near 100°C but were thereafter much lower. The comparable diagenetic step in siliceous shales required roughly 9 million years near 50°C , and the conversion of α -cristobalite to chalcedony required approximately 11 million years near 110°C . Comparable times and temperatures for chalcedonization of hot spring sinter is not known, but many tens of thousands of years at temperatures near 120°C are probably required.

Temperatures and heat flow in wells near the Raft River geothermal area of Cassia County in Idaho

The Raft River area of Idaho contains a geothermal system of intermediate temperatures ($\sim 150^\circ\text{C}$) at depths of about 1.5 km. Outside of the geothermal area, temperature measurements made by Manuel Nathenson, T. C. Urban, and W. H. Diment in three intermediate depth wells (200–400 m) and one deep well (1,500 m) indicate that the heat flow is about $2.5 \mu\text{cal}/\text{cm}^2/\text{s}$ or slightly higher, and that temperature gradients range from 50°C to $60^\circ\text{C}/\text{km}$ in the sediments, tuffs, and volcanic debris that fill the valley. Within and close to the geothermal system, temperature gradients in intermediate depth wells (100–350 m) range from 120 to more than $600^\circ\text{C}/\text{km}$. The latter value was found close to the site of a former hot spring. Temperatures measured in three deep wells (1–2 km) within the geothermal area indicate that two wells are in or near an active upflow zone while one well shows a temperature reversal. Vertical seepage velocities in the formation are estimated from temperature data in the two wells to be $0.05 \text{ m}/\text{yr}$ in RRGE-1 and $0.01 \text{ m}/\text{yr}$ in RRGE-2 and the combined convective and conductive heat flows are estimated to be $20 \mu\text{cal}/\text{cm}^2/\text{s}$ in RRGE-1 and $8 \mu\text{cal}/\text{cm}^2/\text{s}$ in RRGE-2. From shut-in pressure data and the estimated velocities, the average vertical permeabilities are 0.6 and 0.2 mdarcy, respectively. The total heat flow from the system is estimated to

be at least $1.3 \times 10^6 \text{ cal}/\text{s}$, a value at the low end of values obtained for systems in northern and central Nevada.

Geology and thermal history of Mammoth Hot Springs

K. E. Bargar reports that the Mammoth Hot Spring thermal area, located about 8 km inside the northern entrance to Yellowstone National Park, consists of nearly 100 hot springs scattered over a score of steplike travertine terraces. The travertine deposits range in age from late Pleistocene to present-day deposition (Bargar and Muffler, 1975). Sporadic records of hot spring activity suggest that most of the current major springs have been intermittently active since at least 1871.

Water moving along the Norris-Mammoth fault zone is heated by partly molten magma and enriched in calcium and bicarbonate. Upon reaching Mammoth this thermal water (temperature about 73°C) moves up through the old terrace deposits along preexisting vertical linear planes of weakness. As the water reaches the surface, pressure is released, carbon dioxide escapes as a gas, and bicarbonate in the water is partitioned into more carbon dioxide and carbonate; the latter then combines with calcium to precipitate calcium carbonate, forming travertine. The travertine usually precipitates rapidly from solution and is lightweight and porous; however, dense travertine, such as is found in core from the 113-m research drill hole Y-10 located on one side of the upper terraces, forms beneath the surface by deposition in the pore spaces of older deposits.

The Mammoth terraces abound with hot spring deposits such as terracettes, cones, and fissure ridges. Semicircular ledges (ranging in width from about 0.3 m to as much as 2.5 m), called terracettes, are formed by deposition of travertine around slowly rising pools. Complex steplike arrangements of terracettes have developed along runoff channels of some hot springs. A few hot springs have deposited cone-shaped mounds, most of which reach heights of 1–2 m before becoming dormant. However, one long-inactive cone attained a height of about 14 m. Fissure ridges are linear mounds of travertine deposited from numerous hot spring vents along a medial fracture zone. The ridges range in height from about 1 to 6 m and in length from a few meters up to nearly 300 m; width at the base of a ridge is equal to or greater than its height. In some places, water from new hot spring activity becomes ponded behind fissure ridge bar-

riers or dams, so that travertine deposits and eventually large flat terraces develop.

Aquifer pressure lowering at Cerro Prieto, Mexico, causing boiling and temperature decrease

A. H. Truesdell (USGS) and Alfredo Manon (Comision Federal de Electricidad, Mexico) report production drillholes at Cerro Prieto, Mexico, were found to tap two-phase fluids at depth with an average of 3 percent excess steam in 1974 increasing to an average of 7.5 percent excess steam in 1977. Some wells show 20 percent decreases in chlorine contents. Evidently decreased reservoir pressures have caused boiling in the reservoir and mixture with more dilute, lower temperature fluids. The result of both these processes is a decrease of reservoir temperature (indicated by silica) which is an average of 12°C lower in 1977 than in 1974. Temperature decreases since the start of production (1970) may exceed 30°C. This hitherto unrecognized field behavior may make reinjection of separated water imperative.

Relation of mercury mineralization to The Geysers hydrothermal system

Studies of the age and paragenesis of mercury deposits on the southeastern and southwestern periphery of The Geysers steam field in northern California by D. H. Sorg and J. M. Donnelly, in conjunction with regional mapping by R. J. McLaughlin, reveal similar evolutionary histories for the ore deposits and have significant bearing on the age of The Geysers hydrothermal system. The silica carbonate host rock of these mercury deposits is formed from hydrothermal alteration of elongate serpentinite sheets that are shown from the mapping to be aligned along steeply northeast dipping thrust separating imbricate slabs of upper Mesozoic rocks of the Franciscan assemblage. Regional tectonics and local field relations indicate that many of the thrust faults bounding these serpentinite bodies have sustained recurrent movement, in part as strike-slip faults, during the past 2 to 3 million years. Frequent fault movement is thought to have established and maintained deep-rooted, permeable fracture zones in the bedrock that enabled thermal meteoric waters heated by magma to move into shallow crustal levels beneath The Geysers-Clear Lake area. These thermal waters reacted with serpentinite to produce the silica carbonate bodies and deposit mercury.

The relatively simple mineral assemblage of silica-carbonate rock, produced from replacement of serpentine minerals, consists of cryptocrystalline to macrocrystalline quartz, ankerite, and (or) dolomite, and magnesite. Ore stage minerals consist of pyrite and (or) marcasite, cinnabar, solid and liquid hydrocarbons, quartz, dolomite, minor clay minerals, and native mercury.

Sorg found that during formation of the silica-carbonate rock, up to six distinct periods of fracturing and brecciation occurred, each followed by partial to complete healing of the newly formed fractures by various forms of quartz. The early quartz is largely chalcedonic, with a trend toward macrocrystalline, vuggy, euhedral quartz in each successively younger period of fracturing. Iron sulfides almost always predate cinnabar deposition, although a slight overlap in deposition was recognized at the Helen mine, southeast of The Geysers. Deposition of cinnabar in these mercury deposits was confined to a single post-fracturing episode occurring very late in the paragenetic sequence. Liquid hydrocarbons and native mercury were in part contemporary with, and also post-dated cinnabar deposition. Euhedral vug-forming quartz and dolomite encrust all other minerals and were the last minerals to be introduced.

Sorg has found that some of the post-cinnabar quartz contains scarce fluid inclusions that yield filling temperatures <100°C. The occurrence of high gravity, liquid hydrocarbons contemporaneous with cinnabar from the Helen mine further indicate that temperatures during cinnabar deposition probably could not have exceeded 100°C–120°C since liquid petroleum rapidly converts to low density compounds at temperatures $\geq 120^\circ\text{C}$ (K. K. Landis, 1967).

The time framework for mercury deposition is inexactly known at present, but it appears to have accompanied or closely followed introduction of magma sources for the 2.0 ± 0.03 million year Clear Lake Volcanics. This conclusion is supported by the presence of a basaltic andesite intrusion at the southeast edge of The Geysers steam field, which is locally the host rock for mercury mineralization. The whole-rock K–Ar age of this andesite was determined by Donnelly to be 2.05 ± 0.3 m.y., indicating that mercury deposition accompanied or post-dated earliest Clear Lake volcanism. Another significant constraint to the timing of mercury mineralization is found at the southwest edge of The Geysers steam field in the older terraces of Little Sulphur Creek, whose tributaries drain the Culver

Baer mercury mine. The highest terrace remnants were found to contain cobbles of cinnabar-bearing silica carbonate rock derived from the Culver Baer area. Based on their physiographic maturity and soil profile development, these terraces are thought by E. J. Helley to be about one-half million years old, suggesting that mercury deposition had occurred in this area and that the deposit was being actively eroded by about one-half million years ago. The data thus suggest that hydrothermal activity related to mercury deposition in the southwest to southeast periphery of The Geysers steam field began during or following early Clear Lake volcanism and is probably closely related to The Geysers hydrothermal system. Regional tectonics suggest however that older mercury deposits may be present further to the southeast, and that even younger deposits exist to the northeast, in the younger part of the Clear Lake volcanic field.

P-wave delay studies in geothermal areas

Preliminary results from a teleseismic *P*-wave delay study of The Geysers-Clear Lake geothermal area, California, indicate the presence of very large *P*-wave delays, strong attenuation, and signal shape changes in the geothermal area. The study by Mahadeva Iyer, D. H. Oppenheimer, and Tim Hitchcock used data collected by permanent and portable seismic networks. Two seismic stations, one in the vicinity of the steam production zone at The Geysers and one near the center of the gravity low around Mount Hannah, show delays of about 1.5 seconds relative to the surrounding area. Delays of 0.5–1 second are also found at the other stations located over the gravity low. If the delays are caused by a magma body, the spatial patterns of the delays and other geophysical data do not permit it to have a diameter greater than about 15 km. To produce the observed large delays in such a finite body, drastic change in material properties inside the body are required. Hence, careful evaluation of other contributions to the delays is required to assess the effect caused by the presence of magma under The Geysers.

Pressurized fractures in hot rock

The three-dimensional form of several large sheet intrusions near Shiprock, New Mexico, and on the San Rafael Swell, Utah, was investigated by D. D. Pollard. Of particular interest are the fingered nature of the intrusion periphery and the many offset, en echelon segments of each intrusion. These geometric features of sheet intrusions may be used to deduce

propagation direction and some of the physical conditions during emplacement, such as stress, pressure, rock properties. The detailed maps and data on intrusion form produced during this fieldwork are being compared to theoretical mechanical models.

At four localities on the San Rafael Swell (Willow Wash, Moroni Slopes, Cathedral Junction, and South Desert) the relationship between sheet intrusions and volcanic necks was investigated. Detailed maps of host rock deformation, breccias, and igneous forms were prepared and are currently being analyzed. These volcanic necks appear to grow by a process of selective brecciation of the wall rock of a sheet intrusion. The field data will be used to help formulate a theory of brecciation.

Ground surface deformation over igneous dikes was studied on Kilauea Volcano, Hawaii. After visiting several areas, the December 1974 fissure eruption on the southwest rift near the summit was selected for future detailed mapping. Excellent examples of surface cracks and faults are preserved off the ends of the fissures. This deformation will be compared to a theoretical model of the interaction of large fluid-filled cracks with the earth's surface.

The en echelon form of fracture segments is attributed to the propagation of a fracture into a region with either a planar anisotropy at a new orientation or a new orientation of the least principal stress. The second alternative was investigated and a theory derived that relates the length of en echelon segments to the rate of change of stress orientation.

The mechanical interaction between a fluid pressurized fracture and the earth's surface was investigated by solving the elastic problem for a crack of arbitrary inclination buried beneath a free surface and subjected to an arbitrary pressure distribution. The fracture behaves essentially as if it were in an infinite region if the depth-to-center is greater than three times the half-length. Shallow fractures should propagate preferentially toward the surface requiring less pressure as they grow in length. Deformation of the Earth's surface increases markedly as the fracture approaches and is most pronounced for small inclinations. The theory explains some of the features of volcanic rift zones, such as crack distribution and graben formation in a qualitative way.

Thermal regime of Leach Hot Springs area of Grass Valley in Nevada

A total of 82 holes ranging in depth from 18 to 400 m were drilled for thermal and hydrologic

studies in a 200-km² area of Grass Valley, Nev., near Leach Hot Springs. A. H. Lachenbruch (1977) R. J. Munroe, J. H. Sass and J. P. Ziagos, (USGS) H. A. Wollenberg and D. E. di Somma (Lawrence Berkeley Laboratory) report that outside of the immediate area of Leach Hot Springs, heat flow ranges from 1 to 6.5 HFU with a mean of 2.4 HFU (1 HFU = 10^{-6} cal/cm²/s = 41.8 mWm⁻²). Within 2 km of the springs, conductive heat flow ranges between 1.6 and >70 HFU averaging 13.6 HFU. Besides the conspicuous thermal anomaly associated with the hot springs, two additional anomalies have been identified. One is associated with faults bounding the western margin of the Tobin Range near Panther Canyon, and the other is near the middle of Grass Valley about 5 km south-southwest of Leach Hot Springs. The mid-valley anomaly appears to be caused by hydrothermal circulation in a bedrock horst beneath about 375 m of impermeable valley sediments. If the convective and conductive heat discharge within 2 km of the Leach Hot Springs is averaged over the entire hydrologic system (including areas of recharge), the combined heat flux from this part of Grass Valley is about 3 HFU, consistent with the average regional conductive heat flow in the Battle Mountain High. The hydrothermal system can be interpreted as being in a stationary stable phase sustained by high regional heat flow, and no localized crustal heat sources (other than hydrothermal convection to depths of a few kilometers) need be invoked to explain the existence of Leach Hot Springs.

Models of an extending lithosphere and heat flow in the Basin and Range province

Reduced heat flow in the Basin and Range province is characteristically greater by 50–100 percent than that in stable regions; in the hotter subprovinces such as the Battle Mountain High, it is greater than 300 percent. A. H. Lachenbruch and J. H. Sass (in press) report evidence for distributed tectonic extension and magnetism throughout the province suggests that much of the anomalous heat is transferred from the asthenosphere by convection in the lithosphere in the solid state by stretching and in the magmatic state by intrusion. Simple steady-state thermo-mechanical models of these processes yield relations among reduced heat flow, asthenosphere flux, lithosphere thickness, extension rate, and basalt production by the asthenosphere. Thermal effects in an extending lithosphere lead to decreased estimates of temperature and increased

estimates of lithosphere thickness in the Basin and Range province. Moderate extension rates can account for high heat flow in the province without calling on anomalous conductive flux from the asthenosphere. The heat and mass budgets of bimodal volcanic centers suggest that they occur at points where the lithosphere is pulling apart rapidly, drawing up basalt to fill the void. For a range of plausible models of distributed extension, the anomalous heat flows increases roughly 1 HFU (10^{-6} cal/cm²/s) for every 1 to 2 percent/m.y. increase in extension rate; the relation suggests extension rates in the Great Basin consistent with estimates from structural evidence. It also suggests much more rapid local extension in the hotter subprovinces, an inference supported by limited evidence from other sources.

Heat flow in the United States and the thermal regime of the crust

A contour map of heat flow based on 625 observations now available in the conterminous United States shows new detail. According to A. H. Lachenbruch and J. H. Sass (1977) subprovinces of exceptionally high heat flow [>2.5 HFU (1 HFU = 10^{-6} cal/cm²/s = 41.8 mW/m²)] in the Western States are beginning to emerge as regional features. The Battle Mountain High, previously described in north-central Nevada, probably extends northeastward to Utah and Idaho and westward almost to California. With the eastern Snake River Plain, a region that probably has large convective loss, it could form a zone of exceptionally high heat loss that extends almost continuously for 1,000 km from the vicinity of Steamboat Springs near Reno, Nev., to Yellowstone Park in Wyoming and possibly northward into the Idaho batholith. A sinuous high heat flow subprovince of comparable length is emerging in the Rio Grand Trough in New Mexico and southern Colorado. The linear relation between surface heat flow and radioactive heat production, so successful in the Sierra Nevada and eastern United States provinces, does not apply in the Basin and Range province. There the variations in heat flow caused by hydrothermal and magmatic convection are probably greater, by a factor of 3 or 4, than those caused by crustal radioactivity, and heat flux into the lower crust is not uniform; it is probably controlled by the mass flux of intruding magma. Modal values of reduced heat flow can be used to construct generalized crustal temperature profiles for comparison with profiles for more stable areas and with melting

relations for crustal rocks. Theoretical profiles are consistent with the widespread magmatic manifestations observed in the Basin and Range province. Laterally extensive silicic partial melts are possible at midcrustal levels in "hot" subprovinces like the Battle Mountain High. Effects of hydrologic convection, whether driven by thermal density differences or regional piezometric conditions, are important to an understanding of regional heat flow, especially in tectonically active areas. The "Eureka Low," a conspicuous subprovince ($\sim 3 \times 10^4$ km²) with anomalously low heat flow in southern Nevada, is probably caused by interbasin flow in deep aquifers fed by downward percolation of a small fraction of the annual precipitation. Heat flow observations in such areas provide useful information on regional hydrologic patterns.

Helium-3 in Yellowstone, Lassen, and The Geysers' fluids indicates mantle connection

Hot spring waters and gases of The Geysers in California, Lassen National Park in California, and Yellowstone National Park in Wyoming were found to be highly enriched in helium-3 (similar to mantle helium) in an investigation by A. H. Truesdell (USGS) with William Jenkins and Tom Torgensen (Woods Hole Oceanographic Institution). The ³He/⁴He ratio of these fluids was 5.8×10^6 at The Geysers and ranged from 2.4 to 12.0×10^6 at Yellowstone and 3.9 to 9.9×10^6 at Lassen compared to 1.2×10^6 for the atmosphere and about 0.1×10^6 for the crust. This geochemical technique may be very important in indicating present and past zones of weakness in the crust and in prospecting for geothermal resources.

Geothermal gradients in the Northern Great Plains

Temperature data taken in Paleozoic formations in the Northern Great Plains from over 2,300 oil, gas, and waterwells plus seven temperature profiles were collected in a study by K. T. Kilty. The data were corrected for the influence of the borehole environment and metal casing. Gradients were then established based on a non-linear function of temperature versus depth. Maps of the area showing the geothermal gradient present in the Paleozoic rocks were compiled. Maps for the temperature-of-formation for the Minnelusa Formation and the Madison Group (or Limestone) were also made for the same area. The results of this study are being used to help delineate areas of ground-water recharge, discharge, and subsurface flow.

Organic gases in geothermal fluids

N. L. Nehring and A. H. Truesdell found that three end member patterns can be distinguished for organic gases in geothermal and volcanic steam samples:

- A volcanic pattern with relatively little total hydrocarbons, little methane, more unsaturated than saturated C₂ and C₃ hydrocarbons, a large amount of an unidentified C₄ and C₅ gas and no benzene. This pattern was found in Kilauea, Hawaii, St. Augustine, Alaska, and Mount Hood, Oreg., fumarole gases.
- A volcanic-geothermal pattern where a geothermal system is developed in volcanic or crystalline rocks. In this pattern more total hydrocarbons, about 10 times more methane than in the volcanic pattern, and variable amounts of benzene are found with saturated C₂ and C₃ hydrocarbons predominant over unsaturated hydrocarbons. This pattern was found at Lassen Park, Calif., the eastern part of Yellowstone National Park, Wyo., Steamboat Springs, Nev., and Roosevelt Hot Springs, Utah.
- A sedimentary-geothermal pattern characterized by a relatively large amount of total hydrocarbons, near absence of unsaturated hydrocarbons other than benzene, and the appearance of numerous branched hydrocarbons in large amounts. Patterns of this type, found at The Geysers, Calif., Lardarello, Italy, and Cero Prieto, Mexico, are nearly identical despite large differences in sedimentary rock type and geothermal character. Some gases from western Yellowstone also approach this type.

Geoelectrical investigations in the Coso Hot Springs area in California

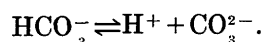
D. B. Jackson reports that completion of the telluric *J* value map in the Coso Range shows a trend of resistivity highs that coincide with the zone of arcuate faults mapped by W. A. Duffield and C. R. Bacon (1977) to the northwest, north, and northeast of Coso Hot Springs. Healing of the faults and fractures by magmatic intrusion could account for the higher resistivities observed in this zone. Two dimensional modeling of telluric *J* values along or east-west profile across the Coso Range supports the interpreted presence of a conductive zone of less than 1 ohm-m (originally interpreted from a magnetotelluric sounding) at about 3-km depth beneath

the rhyolite dome field of the eastern Coso Range. This conductive zone is within a region of earthquake swarms that extend to at least 6-km depth, (A. Walters and C. Weaver, personal commun.); therefore, it appears highly unlikely that the conductive zone represents a magma chamber.

Improved estimates of carbonate alkalinity in geothermal waters

Carbonate alkalinity is one of the important characteristics of geothermal waters. It has generally been thought that carrying out the alkalinity titrations in the field results in the most accurate estimates of alkalinity. However, recent studies of Yellowstone National Park geothermal waters by D. V. Vivit, J. W. Ball, and E. A. Jenne indicated that the field analyses were less precise and less accurate than subsequent laboratory determinations. There are several reasons for this situation. These waters are supersaturated with carbon dioxide (CO_2) and contain highly variable amounts of dissolved sulfide ions (H_2S , HS^- , and S^{2-}). The CO_2 undergoes exsolution for a period of time. If alkalinity titrations are made on the hot water, the pH may actually increase following acid addition and stirring, making it very difficult to distinguish between CO_3^{2-} and HCO_3^- . The variable exsolution of H_2S and oxidation of dissolved sulfide also causes inaccuracy in the titration alkalinity. Additionally, time dependent changes in the polymerization of silicic acid in conjunction with the protonation of the dissolved $\text{H}_2\text{SiO}_4^{2-}$ and H_3SiO_4^- species that occur in the alkaline waters also causes inaccuracies in the titration alkalinity.

It was found that more accurate estimates of carbonate alkalinity could be obtained by (1) determining the titration alkalinity after all supersaturated CO_2 has exsolved, remaining sulfides have oxidized, and silica polymerization has largely ceased; (2) determining the noncarbonate alkalinity by back titration with base to the pH of the sample at the time the titration alkalinity was determined; and (3) subtracting out the noncarbonate alkalinity and calculating relative amounts of carbonate and bicarbonate as a function of pH, temperature, and the equilibrium constant for the reaction:



This results in a significant decrease in the degree of supersaturation of these waters with calcite.

Distribution of radioactivity with depth in the Front Range Uranium and Thorium provinces

George Phair obtained uranium, thorium, and potassium heat production data on 73 samples used by Birch (1950) for measurements of thermal conductivity in his study of heat flow in the Adams Tunnel in the north-central Front Range, and on 124 samples used by Decker (1969) in his study of heat flow in the Roberts Tunnel in the central Front Range. Twenty-three of the Roberts Tunnel samples came from the Montezuma stock of Tertiary age; the remainder came from the segment of the tunnel lying to the southeast that cuts a mixed assemblage of Precambrian metamorphic and igneous rocks. In addition, heat production data of a similar type was obtained on 17 rocks from the metamorphic section exposed along Clear Creek near Golden, the site of a borehole used by Decker (1969) for heat flow studies.

A plot of the heat flow data of others at the four localities against the Survey's heat production values yielded a good straight line defined by the equation:

$$Q = 1.1 + 9.5A.$$

According to the model of Roy and others this equation indicates that all heat flow in the Front Range, above a threshold of 1.1 heat flow units (HFU) attributable to the underlying crust and mantle, originates within a radiogenic outer crust that is 9.5 km thick. The measured total heat flows in this uranium and thorium province (Phair and Gottfried, 1964) range from a low of 1.5 HFU to a high of 2.24 HFU in the Precambrian section cut in the Roberts Tunnel. The pattern of distribution of heat sources in the Front Range throws light on the manner in which the radioactive province originated and subsequently developed.

Noble and active gases in the Larderello Geothermal Field in Italy

A suite of gas and steam condensate samples was collected by Emanuel Mazor (Weizmann Institute in Israel) along a south to north (Castelnuovo to Gabbro) section across the Larderello geothermal field. The section was from shallow, older wells in the south, near possible recharge areas, to deep, newer wells in the north. Analyses of the samples indicated that there is a good correlation between reactive gases, atmospheric noble gases (argon, krypton, xenon) and radiogenic noble gases (^4He , ^{40}Ar), and a possible excess of primordial xenon in

the steam. The observed patterns are interpreted as showing deep circulation of fluids with thorough mixing of atmospheric, crustal, and possibly mantle components.

Isotope and active gas analyses made on the same suite of Larderello steam samples showed (1) a south to north increase in ^{18}O from -5.0 permil to 0.4 permil with little change in deuterium (-42 ± 3 permil); (2) a south to north increase in total gas/steam from $.003$ to $.05$ mole fraction; (3) generally constant CO_2 (95 ± 2 percent, nearly constant H_2 (2 ± 1 percent), H_2S ($1.5 \pm .5$ percent), CH_4 ($1.5 \pm .7$ percent), N_2 (0.8 ± 3 percent), and no O_2 in the dry gas; (4) C_2 to C_6 hydrocarbons independent of CH_4 and highest in the Gabbro wells; and (5) hydrocarbon abundances generally as follows: $\text{C}_1 \gg \text{C}_2 > \text{C}_6 > \text{C}_3 > \text{C}_4 \cong \text{C}_5$, with C_4 to C_6 variably branched.

These observations are interpreted as showing that (1) either more oxygen-shifted deep water mixed with less oxygen-shifted recharge water or an oxygen-isotope shift in the deep northern waters followed by distillation of steam from the north towards the south (three plates at $\sim 220^\circ\text{C}$); (2) total evaporation of water containing decreasing gas with depth so that the older southern wells contain little gas; (3) synthesis of CH_4 from H_2 and CO_2 buffered by rock reactions so that these components have relatively constant amounts in the gas fraction; and (4) extraction of higher hydrocarbons (and H_2S) from rock organic matter with variations caused by variations in the source rock. No evidence of magmatic contributions was found in the isotope and active gas compositions.

Geochemistry of geopressed geothermal waters

Detailed chemical and isotopic analyses of 90 formation water samples from 18 oil and gas fields in coastal Texas and Louisiana by Y. K. Kharaka showed that the salinity of water in the geopressed zone may be higher than previously believed, ranging from about 15,000 to 270,000 mg/L dissolved solids. Samples from many gas wells yielded low salinities that are not representative of the true salinity of formation water because of dilution by condensed water vapor produced with natural gas. Kharaka and others (1977) showed that chemical geothermometers and fluid production data can be used to estimate the true salinity of the diluted samples. Salinities lower than about 30,000 mg/L are observed in "effluent waters" squeezed from shales and siltstones; salinities higher than about 80,000

mg/L result from interaction with salt beds; intermediate salinities may result from membrane filtration and interaction with sediments.

The analyses also showed that the concentration of problem components H_2S , SiO_2 , Hg, and As are low and the concentration of toxic components (boron, ammonia, and others) are moderately high. Subsurface injection will probably be the only acceptable method of disposal of spent geothermal waters because of the high salinities and relatively high concentration of toxic contaminants.

A study of organic acid anions in 95 samples from oil and gas fields in Texas and California (Carothers and Kharaka, in press) indicates that decarboxylation of these acid anions may be the main source of the natural gas; these acid anions contribute up to 100 percent of the measured alkalinity.

Conductive component of total heat flow in research drill holes of Yellowstone Park and relation of heat flow to vegetation patterns

In high-temperature convection systems, the modes of heat flow become increasingly complex as a single liquid phase at depth rises and boils. In the near-surface environment, heat is transferred in liquid and vapor in springs, geysers, fumaroles, and hot ground, and significant transfer also occurs by conduction in locally very high thermal gradients. Because of these near-surface complexities that differ greatly in mode and magnitude over short distances, the physical measurement of total heat flow from a system is both difficult and imprecise; where conditions are appropriate, a chemical method (Fournier, White, and Truesdell, 1976) is much faster and more reliable.

D. E. White determined the conductive component of total heat flow in 13 research core holes drilled by the USGS in 1967-68, with depths that range from 73 to 332 m. Temperatures, depths, methods of measurement, and other data were published by White, L. J. P. Muffler, R. O. Fournier, and A. H. Truesdell (1975). New data on thermal conductivities of the core permit calculation of conductive heat flows for the different depth intervals selected in each hole. Interval boundaries were determined from changes in gradient with depth, generally with no common basis between holes. The uppermost interval distinguished in the 13 drill holes range from 45 to 660 heat-flow units (HFU); the world conductive average is about 1.5 HFU, which emphasizes the magnitude of the Yellowstone anomalies. The deepest intervals range from -3 (temperature decreasing with depth) to 36 HFU. Heat flow through

the uppermost interval of individual holes is generally at least 10 times higher than that of the lowermost interval.

The distribution of lodgepole pines correlates with near-surface heat flow. Pines with normal characteristics grow near drill holes with near-surface conductive heat flows of 200 HFU or less (6 holes). Heat flows from 230 up to 330 HFU are characterized by stunted, sparsely-spaced trees (5 holes), and the two holes with near-surface conductive heat flow near 600 HFU evidently are too hot at root-zone depths for pines to grow. These relationships permit crude but rapid extrapolation of local variations in heat flow over large areas that lack subsurface data.

Characteristics of a Hawaiian geothermal system

Measurements by Hawaiian Volcano Observatory staff in the Puhimau geothermal area on the upper east rift of Kilauea Volcano in Hawaii have revealed patterns of variations in physical and chemical parameters that may prove useful in geothermal exploration elsewhere. Systematic sampling of soil gases revealed high values of soil moisture across the entire area, but a peaking in the emission of CO_2 and sulfur compounds only at and near its margins. In contrast, both soil mercury and aerometric mercury are highest in the center of the area, and fall off toward the margins. Resistivity soundings showed high apparent resistivities between depths of 75 and 400 m and lower values at depths below 400 m. Electrical self-potentials are highest in the interior of the geothermal area and magnetic values, lowest. The flora of the area revealed an irregular, concentric zonation of plant species. At least one species observed does not occur elsewhere on the volcano at comparable elevations. The leaves of myrtle trees downwind from the area show the effects of atmospheric transport of mercury and an exponential decay of mercury with distance.

Precipitation of quartz in convecting hydrothermal systems

Hydrologic models of hydrothermal systems that are dominated by meteoric water and that have high-temperature heat sources located at relatively shallow depths (2 to 10 km) must consider variations in the solubility of quartz at high temperatures and high pressures. R. O. Fournier found that the precipitation of quartz presents no problem for maintaining deep circulation cells where the maximum temperature attained by the solution is less than 300°C . However, where higher solution temperatures are attained, the precipitation of quartz

is a major obstacle to maintaining convective circulation. Solubility maxima are attained from 330°C to about 480°C at pressures of 128 to about 715 bars. These pressures would be attained at depths of about 1.25 to 7.5 km where hydrostatic pressure is fixed by cold, dilute meteoric water flowing into the system. Under these conditions dilute water heated at a depth of 2 km ($\cong 200$ bars) will dissolve quartz until about 800 mg silica per kg of solution is attained at about 340°C . Further heating at that depth will cause quartz to precipitate. At a given depth, then, decreased permeability owing to quartz precipitation should limit the temperature attained by dilute water circulating into the system. At 4 km, 370°C can be attained before permeability is decreased, and at 6 km, about 400°C can be attained.

Isotopic and chemical studies of geothermal gases

Seven deep geothermal production wells and seven hot springs and mudpots at Cerro Prieto, Mexico, were sampled for gas by Harmon Craig (University of California, San Diego). Analyses were obtained for total condensable gas ($\text{CO}_2 + \text{H}_2\text{S}$) and for non-condensable gas (H_2 , Ar, O_2 , N_2 , CH_4 , CO) including helium, He^3/He^4 and He/Ne. Several geothermal gas samples from the Imperial Valley have also been analyzed. This work has demonstrated a remarkable uniformity in the He^3/He^4 ratio of all these gases (approximately five to seven times the atmospheric ratio) and a similarity in non-condensable gas chemistry (most notably the presence of small amounts of CO, 0.05–1.8 percent, and in deep well samples from Cerro Prieto a fairly uniform H_2/CH_4 ratio of ~ 1). Preliminary calculations suggest the $\text{H}_2 - \text{CH}_4 - \text{CO}_2 - \text{CO}$ assemblage is at equilibrium at down-hole temperatures at Cerro Prieto.

Steam samples taken from a steam well in the main caldera at Hakone Volcano, Japan, have been analyzed for helium-isotope ratio and non-condensable gas chemistry. The He^3/He^4 ratio at Hakone (6.2) is similar to that observed in Marianas Island hot springs (5.3 to 7.0), indicating that convergent plate boundaries are also sites for mantle helium loss.

Uranium-isotope ratio characterization of geothermal waters

Wide isotopic variations of dissolved uranium ($\text{U}-234$ and $\text{U}-235$ and their ratio $\text{U}-234/\text{U}-235$) in ground waters can be used to characterize water sources. For example, the amount of mixing of geothermal water with cooler near surface ground water can be deduced. J. K. Osmond and J. B.

Cowart (Florida State University) used this approach to characterize geothermal waters from Long Valley, Calif., and other geothermal areas. Data from the high temperature systems at Yellowstone Park and at Mount Lassen demonstrated that geothermal waters usually have U-234/U-238 ratios closer to equilibrium and lower uranium concentrations than other deep ground waters. This is because high temperature processes lead to isotopic equilibration and geothermal systems are highly reducing so uranium is immobilized as insoluble U⁺⁴ compounds. On the other hand, thorium appears to occur in higher than normal concentrations in geothermal systems, and Th-228/Th-232 ratios are unusually high.

Noble gases and dissolved ions in geothermal exploration

A wide range of natural tracers, including the noble gases, were collected at Lassen Volcanic National Park. A study of these data by Emanuel Mazor (Weizmann Institute in Israel) plotted with results from previous work, revealed the following patterns:

- The water phase of hot springs contains dissolved He, Ne, Ar, Kr, and Xe in relative abundances close to those of air dissolved in water at 5°C to 15°C. Thus, these gases originated with the recharging water.
- The concentrations of Ne, Ar, Kr, and Xe in the water phase are low compared to air-saturated water at 5°C. The water phase has, thus, lost 90–95 percent of its argon and corresponding amounts of Ne, Kr, and Xe.
- The relative abundances of Ne, Ar, Kr, and Xe in the gas and water phase per total gas vary over two orders of magnitude. It seems, thus, that the gas phase was separated from the original fluids under conditions that caused little or no fractionation. One mechanism may be boiling at high temperatures (above about 150°C) at which the solubility factors are almost the same for all the noble gases.

Delineation of buried thermal bodies by precision releveling and gravity reobservations

Finite element solutions for crustal uplift that can result from buoyant forces or excess pressure acting on the walls of a magma chamber was determined by R. B. Smith (University of Utah). In addition, a theory relating gravity change to the displacement field resulting from the deformation was developed. Although the theory provides an analytic

formulation of the problem for any crustal rheology and any continuous displacement field, it has been simplified and adapted for use with numerical solutions in linear elasticity. Thus both surface displacement and gravity change information is obtained from the same finite element deformation model. To accompany the theoretical modeling, a microgravimetry base network was established at Yellowstone National Park in Wyoming. One hundred forty, first-order leveling benchmarks were reoccupied by means of La Coste and Romberg gravimeters D26 and G461 during August and September 1977.

Evaluation of geothermal systems using teleseisms

The lateral variation of seismic attenuation observed from teleseisms was mapped by R. W. Ward (University of Texas, Dallas) to infer location and extent of potential geothermal systems. Preliminary attenuation data previously obtained from Coso Hot Springs was interpreted to indicate a zone of elevated attenuation deep beneath the springs area. A maximum differential attenuation (δt^*), variation of 0.1 second, is observed that shifts location for events from different azimuths. A two-dimensional ray-tracing scheme is being developed to better define the location and depth of the attenuation anomaly in a zone lying between Coso Hot Springs, Sugar Loaf Mountain, and Volcano Peak.

The *P*-waves from 22 teleseismic events recorded by a 14-element portable seismograph array deployed by the USGS in The Geysers-Clear Lake region were analyzed to map the lateral variation of differential attenuation. A maximum differential attenuation of 0.3 seconds is observed and indicates a shallow attenuation anomaly within the upper 8 km beneath Mount Hannah associated with a magma chamber. A shallow attenuation anomaly is also observed above the vapor-dominated hydrothermal reservoir near the Collayami fault.

Geothermal potential of the eastern margin of the Basin and Range province in Utah

Studies of the petrology and geochronology of Tertiary and Quaternary volcanic rocks in the eastern margin of the Basin and Range province in Utah, by F. H. Brown and W. P. Nash (University of Utah) showed that rhyolite and basalt have been erupted episodically over the past 6 million years in west-central Utah. Rhyolites have been dated at 0.39 m.y. (White Mountain), 3.4 m.y. (Smelter Knolls), 4.7 m.y. (Honeycomb Hills), and 6.2 m.y.

(Thomas Range and Fumarole Butte). Tholeiitic basalt and basaltic andesite were erupted at 6.0 and 0.88 m.y., respectively, at Fumarole Butte, and 6.1 and 0.31 m.y., respectively, at Smelter Knolls. Younger mafic volcanism has been extensive in the region surrounding White Mountain, which also contains Holocene hot spring deposits.

High angle normal faults extend south 12 km from Fumarole Butte to Smelter Knolls. This fault system has been active recently, and has apparently affected the locus of volcanism over the past 6 million years. Thermal springs (94°C) are present at Fumarole Butte. The waters yield a Na-K-Ca temperature of 155°C. The heat source may be either the young igneous activity or the deep circulation along major faults in this area of high regional heat flow.

Geophysical mapping of the Central Cascades

Aeromagnetic mapping by R. W. Couch (Oregon State University) of the Central Cascades between lat. 43° and 44° N. and long. 121° and 122° W. at 1.6-m spacing revealed many high-amplitude anomalies coincident with mapped volcanic centers. Several anomalies over volcanic centers are negative and suggest the major portion of the volcanic rock was erupted prior to the last reversal of the Earth's magnetic field. Removal of a regional field from completely terrain-corrected gravity measurements obtained earlier shows a striking gravity low immediately west of the "High Cascades" volcanic rocks. The north-trending gravity low coincides with a zone of hot springs and thermal wells. Gravity gradients that strike northeast and northwest in the area from the High Cascades to the edge of the survey area at long. 121° W. suggest major structural changes in the upper crust possibly associated with the location of post-Pliocene eruptive centers.

Aeromagnetic mapping in the Vale-Owyhee area of Oregon

The Vale-Owyhee region of Oregon exhibits surface manifestations of geothermal activity within and marginal to the Vale depositional basin. R. W. Couch (Oregon State University) found, from aeromagnetic mapping between lat. 43°15' and 44°15' N. and long. 117°00' W. at 1.6-m spacing, many high-amplitude elongate anomalies associated with outcrops of great sections of basalt flows and volcanoclastic sediments. The anomalies generally strike north-south in the southern part of the approximately 8,500-km² area and northwest-southeast of the northern part of the area. Magnetic anomalies in the northeast sector are longer in wavelength and

lower in amplitude than in the rest of the area similar to previously mapped gravity anomalies. Steep gravity gradients in the area suggest block faulting. The coincidence of steep gradients and hot springs and wells suggests that the surface manifestations of thermal activity are structurally controlled.

Crustal thinning over area of high heat flow

Analysis of unpublished seismic refraction data by K. F. Priestly (University of Nevada) from two profiles through the central and western Battle Mountain High (BMH) in central Nevada and published refraction results for eastern Nevada indicate a crustal thinning in the heat flow area, the BMH, and crustal thickening in the area of the Eureka Low (EL). The minimum crustal thickness occurs in the area of the Lahontan depression in northwest Nevada. These conclusions were confirmed by a second, more densely sampled profile through northwest Nevada by means of single-component, narrow-band instruments and three component, broad-band digital instruments. These broad-band data provide important information on attenuation across the heat flow high in addition to shear-wave velocities.

Analysis of intermediate surface waves from several events for paths across the heat flow high indicates phase velocities 0.1–0.2 km/s lower within the BMH than in the area of more normal Basin and Range heat flow to the east. In light of the thinner crust inferred from the refraction analysis, these lower-phase velocities indicate low shear-wave velocities in the lower crust and upper mantle of the BMH.

Geothermal hydrology and geochemistry of the Klamath Falls area in Oregon

Approximately 400 geothermal wells exist in the Klamath Falls urban area in Oregon with temperatures ranging from 40°C to 115°C. A study conducted by J. W. Lund (Oregon Institute of Technology) showed that over 100 of these wells have had measurements and data gathered on temperature profiles, water level, and chemistry. Twelve key wells have been monitored over a 4-year period to determine changes in temperature, surface water level, and chemistry. A pump test was performed over a 28-hour period on a major well (County Museum) in the downtown area, with 10 adjacent wells monitored to determine drawdown and temperature changes. From this an estimation of the transmissivities was made for the reservoir. Permeabilities appear to be higher in the northwest-

southeast direction along major fault structures in the area. An inventory and documentation of all artesian and pumped wells in the area was made to estimate the influence on adjacent wells. In addition, four continuous water-level monitors were placed in key wells to measure daily fluctuations in the surface water levels. A 2-m temperature probe is being carried out in the urban area to locate hot springs and to relate these to geology and water flow in the fractured rock.

Geochronology of the San Francisco volcanic field in Arizona

The chronology of geologic events within the San Francisco volcanic field was refined and the paleomagnetic time scale improved by P. E. Damon (University of Arizona). The cumulative number of dated samples from the volcanic field is 75. The Pliocene and Pleistocene extrusion of basaltic and silicic lavas was found to be broadly contemporaneous. Basaltic volcanism was quasi-continuous without a significant time gap between 1.25 million years and 931 years B.P.

Relation of mercury to geothermal areas in Yellowstone National Park in Wyoming

All thermal areas in Yellowstone National Park in Wyoming investigated by P. R. Buseck (University of Arizona) were found to contain anomalous amounts of mercury (up to 300:1 peak to background ratios). These anomalies extend outward for only a few hundred meters from the surface expression of the geothermal system and are narrow and well-defined, independent of whether the surface expression is a single vent or a major geyser basin.

Norris Geyser Basin, Mammoth Hot Springs, and the Mud Volcano area show significant differences in the distribution and concentration of mercury. The lack of broad anomalies suggests, at least in Yellowstone, that the 1.6-km sampling interval may be too large for a regional exploration program.

Viscosity of water and ionic substances

Measurements of the viscosity of water in the temperature range of 20°C–150°C and the pressure range of 0–30 MPa were completed by Joseph Kestin (Brown University), and the data was evaluated and prepared for publication. Also completed were measurements of the viscosity of sodium chloride solutions in the temperature range of 20°C–150°C, the pressure range of 0 to 30 MPa, and the full composition range to saturation. The results were

processed and correlated by an equation that reproduces them over the whole range with the same uncertainty (± 0.5 percent) as that of the experiment. The density of potassium chloride solutions was correlated in preparation for the measurements of viscosity of this system. A preliminary design drawing of a new viscometer was completed.

The principal investigator participated in the international standardization effort of the properties of water substance that resulted in new agreements on the viscosity, thermal conductivity, and surface tension.

Magnetotelluric survey of the Southwest

J. F. Hermance (Brown University) completed collection of magnetotelluric data from four major sites in the southwest and solved the problems of transferring the digitally recorded data to IBM-compatible nine-track tape. Preliminary analysis of a portion of the data indicates that a highly conducting structure is present 5 to 10 km beneath the Southern Rio Grande Rift and probably represents a major magnetic intrusion.

A d.c. SQUID magnetometer for geothermal exploration

A low frequency magnetotelluric system for geothermal exploration was tested in the laboratory by J. Clarke and H. F. Morrison (University of California, Berkeley) and has operated with minor modifications satisfactorily during preliminary field tests. The instrument used is a three-component d.c. SQUID magnetometer that operates at frequencies as low as 10^{-4} hertz, which permits resolving of deep conductivity structures. A large planar thin-film gradiometer was fabricated that will permit more sensitive monitoring of magnetic field gradient fluctuations. Results may be significant to both geothermal exploration and earthquake monitoring.

Water-rock reaction in the Salton Sea geothermal field in California

Petrological studies of several geothermal systems in the upper Cenozoic deltaic sediments of the Salton Trough were completed by W. A. Elders (University of California, Riverside). Dramatic changes in the density, porosity, and permeability of reservoir rocks, caused by water-rock reaction at elevated temperatures, were documented in systems with a range of solute concentrations of from 3 to <250 g/kg and measured maximum temperatures ranging from 100°C to 365°C. Lack of equilibrium between geothermal brine and hydrothermal minerals in the

East Mesa system was used to demonstrate that this system has experienced a significant change in its hydrology. The reservoir rocks are giving up their heat to cooler, more dilute, water that has recently entered the system. A similar cooling has apparently occurred in the Heber system where stages in the progressive hydrothermal alteration of a diabase intrusion were studied.

Such minor intrusions may be significant sources of heat in these systems. For example, rhyolite and basalt dikes are encountered in the Salton Sea geothermal field. In this system, progressive alteration of detrital sediments to quartz, albite, epidote, biotite, garnet hornfels occurs. Differences between the distribution of hydrothermal minerals and of the observed temperatures occur partly because of original variations in permeability. However, mineral isograds and fluid-inclusion data also record a series of successive thermal pulses that have affected the system.

Variations in superconducting gravimeters

Comparison of records from two superconducting gravimeters ran in the same vault at the same time were continued by J. M. Goodkind (University of California, San Diego) at the Pinon Flat Observatory. The uncorrelated part of the secular gravity variations is of order $1 \mu\text{Gal}$ over periods of days or months. It comes partly from differing effects of the barometric pressure and (or) temperature changes at different locations in the vault and partly from differing secular tilts of the gravimeter mounts. The pressure effect probably appears also as a result of tilting of the vault and piers by atmospheric loading or thermal expansion. The tilts involved ($\sim 10^{-5}$ radians) are larger than those usually observed with tiltmeters, and show that the tilt of the instrument must be monitored and corrected for measurements at the μGal level.

Calibration of new instruments, relative to one instrument at Pinon Flat, can be accomplished with a 1-day record to the accuracy of 0.1 percent. The small non-linear part of the response of the instrument can be determined also in 1 day of experimenting when simultaneous records from two instruments are used.

Potential geothermal reservoirs in southern Colorado

Analysis by J. C. Romero (Colorado Division of Water Resources) of geophysical surveys made by the Colorado School of Mines in the northern San Luis and upper Arkansas Valleys in Colorado deter-

mined several resistivity lows that are considered to be manifestations of geothermal reservoirs. It was concluded that the potential reservoirs are intermediate to high temperature hydrothermal convection systems with water being the predominant fluid. The heat source is believed to be the combined effects of rifting and deep igneous rock.

Analyses of water from the thermal springs in the area indicate that water withdrawn during geothermal development might be of relatively high quality. The effect geothermal development might have upon the region's water regimes is possibly problematical, as water in many areas peripheral to, or downstream from, the thermal areas is of marginal quality.

Mercury anomalies in the Long Valley California geothermal area

R. W. Klusman found that mercury anomalies occur within the A₁-horizon soil samples of the Long Valley, Calif., caldera geothermal area with high values especially noted on the resurgent dome in the west-central part of the caldera. High mercury levels also were noted along fault lines. A cumulative frequency plot indicated the presence of a background mercury population and an anomalous mercury population. There is a sizable transition zone because of the influence of secondary parameters upon background mercury levels. Of these secondary parameters, the organic carbon concentration of the soil is the most significant. However, the mercury anomalies caused by geothermal leakage are of such high magnitude that the influence of secondary parameters is relatively small.

Analysis of variance results suggests that a regional variation in mercury levels occurs in Long Valley caldera with a smaller scale variation superimposed on it.

Numerical analysis of convection and thermoelastic effects in fault effecting geothermal systems

The onset of convection in a box of water-saturated porous material was examined by R. P. Lowell (Georgia Institute of Technology). Particular attention was paid to the special box geometry that corresponds to a deep, vertical fault or fracture zone within the Earth's crust. Such fault-fracture zones may control the sites of some continental and submarine geothermal systems. Results were obtained for cases in which the vertical boundaries are (1) insulated and the permeability is anisotropic and (2) isothermal and the permeability is isotropic.

The principal results for the insulated vertical boundaries case are that at the critical number, the convection takes the form of rolls, the axes of which are parallel to the shortest box dimension. The critical Rayleigh number may be significantly greater or less than the critical number for an isotropic medium depending on whether the vertical permeability is greater or less than the horizontal permeability. Depending on the fault-fracture zone length relative to the depth and the permeability ratio, the aspect ratio of the rolls may be lengthened or shortened significantly relative to the isotropic case. These results, applied to the Double Hot Springs in the Basin and Range province of northern Nevada, suggest that the permeability of the fault zone may be anisotropic, and vertical permeability is greater than the horizontal permeability.

The principal result for the isothermal vertical boundaries is that the effect of isothermal vertical walls is to substantially increase the critical Rayleigh number for the onset of convection. The results obtained to date are only approximate, and presently a more accurate method is being implemented. If the approximate results prove to be valid, it may be that convection in fault-fracture zones can only take place in highly fractured rock and that even in such systems, convection may take place near the critical number.

Worldwide three-dimensional seismic crustal studies

Detailed studies of three-dimensional seismic structure in the crust and upper mantle under large seismic arrays around the world, including NOR-SAR (Norway), LSDS (Montana), Yellowstone, Alaska, Hawaii, central California, and several areas in Japan and Italy were made by Keiiti Aki (Massachusetts Institute of Technology). These revealed that the crustal velocity anomaly always shows a strong correlation with geology and other geophysical data in young areas, but in old stable areas the correlation becomes poor. Strong small-scale heterogeneities in the upper mantle were found in all areas.

The method using teleseismic *P*-wave data, originally developed by Aki, Christofferssen, and Huseby, was extended to include the *P*-wave times from local earthquakes. It has also been refined by incorporating three-dimensional ray tracing in the iterative inversion process.

Geothermal reconnaissance of southwestern Montana

Preliminary assessment by R. A. Chadwick (Montana State University) of southwestern Montana hot springs for geothermal potential, using geologic mapping and geophysical surveys, indicates many of the hot springs are located within or along the margins of fault-block valleys. Deep faults or fractures evidently permit circulation of water to depth. Regional heat flow from the mantle furnishes sufficient heat to provide the base temperatures indicated. Shallow d.c. resistivity surveys were conducted at Silver Star, Ennis, White Sulphur, Bozeman, Hunters, Norris, Jackson, and Wolf Creek hot springs. In addition, hammer-seismic surveys were run at Silver Star, Ennis, Norris, and White Sulphur. Geological and geophysical data suggest that Silver Star and Ennis waters may ascend from depth beneath the Jefferson and Madison Valleys, respectively, and reach the surface along valley-margin faults. At both Hunters and Norris, thermal waters probably rise along the intersection of a fault zone and anticlinal axis.

Geothermal potential of Western United States related to silica geothermometry of nonthermal ground waters and regional heat flow

Substantial additional information about subsurface temperatures may be obtained by application of the silica geothermometer to non-thermal waters. From the 40,000 non-thermal ground-water records studied from Western United States by C. A. Swanberg (New Mexico State University) a close correlation between silica geotemperatures and regional heat flow provinces was found for the following areas: Battle Mountain High, $q=125 \text{ mWm}^{-2}$, $\text{TSiO}_2=105^\circ\text{C}-130^\circ\text{C}$; Basin and Range, $q=90 \text{ mWm}^{-2}$, $\text{TSiO}_2=75^\circ\text{C}-95^\circ\text{C}$; Colorado Plateau, $q=55 \text{ mWm}^{-2}$, $\text{TSiO}_2=40^\circ\text{C}-60^\circ\text{C}$; Sierra Nevada, $q=30 \text{ mWm}^{-2}$, $\text{TSiO}_2=40^\circ\text{C}$. This correlation is thought to reflect the depths to which ground-waters may circulate and the temperatures at those depths. The boundaries between these provinces are generally less than 50 to 75 km. Numerous geothermal areas have been located using the silica and Na-K-Ca geothermometers within a province. Numerous new potential areas have been delineated, while other previously known areas verify the utility of applying geothermometers to non-thermal waters. The geothermal areas generally correlate with recent volcanic rocks, deep sedimentary basins, or basement linears reflecting the origins of the thermal waters.

Low heat flow values in the Southeastern United States

D. L. Smith (University of Florida) completed reconnaissance of heat-flow values and radioactive heat generation values in the southeastern United States. Over 30 new heat flow values and over 300 values of radioactive heat generation (from uranium, thorium, and potassium abundances) were determined for Virginia, North Carolina, South Carolina, Georgia, Alabama, Tennessee, and Florida. The data indicated no obvious geothermal resources but does suggest an area of thermal properties distinct from those characterizing the east-central U. S. thermal province. A separate thermal province with reduced heat flow of 0.3 HFU is proposed for much of the southern Appalachian Basin. Anomalously low heat flow (<1 HFU) is seen in the Charlotte Belt, southern Valley and Ridge province, and southern Appalachian Plateau province. Higher temperature gradients and relatively high-heat flow (1.6 HFU) are observed in the Atlantic Coastal Plain. Heat flow in Florida and much of the southern Coastal Plain is modified by ground-water flow. The linear relationship between heat flow and radioactive heat generation appears to exist within the southeastern United States.

SEDIMENTOLOGY

Sedimentology, the study of sediment and sedimentary rock, encompasses investigations of principles and processes of sedimentation and includes development of new techniques and methods of study. The USGS sedimentological studies are directed toward (1) the solution of water-resource problems and (2) the determination of the genesis of sediment and the application of this knowledge to sedimentary rocks to gain a more precise interpretation of their depositional environments. Many USGS studies involving sedimentology have applications to other topics, such as water-resource investigations, marine, economic, and engineering geology, and to regional stratigraphic and structural studies; these studies are presented elsewhere in this volume under their appropriate headings.

Studies of fluvial sediment are directed toward the solution of water-resource problems involving water-sediment mixtures. Sediment is being considered more and more as a pollutant. Inorganic and organic sediment, transported by streams to sites where deposition takes place, carries major quantities of sorbed toxic metals, pesticides, herbicides,

and other organic constituents that accelerate the eutrophication of lakes and reservoirs. A knowledge of erosion processes, the movement of sediment in rivers and streams, and the deposition of sediment in stream channels and reservoirs is of great economic importance to the Nation.

VARIABILITY OF SEDIMENT DISCHARGE

Analyses of long-term sediment records

H. P. Guy and D. E. Walling developed criteria by which daily base flow can be separated by computer from daily flow to yield daily storm runoff on long-term records of perennial streams. The exclusion of base-flow data makes it easier to isolate and evaluate parameters that cause variability of sediment discharge. The immediate objective of this work is to determine the length of sediment record needed to yield sediment-discharge information of specific quality.

Irrigation return flows in the lower Yakima River basin of Washington

According to L. M. Nelson, the annual 1975 and 1976 suspended-sediment discharges from irrigation return flows in the lower Yakima River basin ranged from 59,000 t in the Sulphur Creek Wasteway to less than 90 t in Wamba Drain. In the Yakima Indian Reservation, suspended-sediment discharges ranged from 10,000 t in Marion and Satus Drains to about 340 t in Coulee Drain. Data also indicated that there is a poor correlation between suspended-sediment concentrations and concurrent water discharges, turbidity, and specific conductance. Effect of drainage-area size on sediment yield.

P. R. Jordan found that the average annual sediment discharge per unit of drainage area in the plains region of the Missouri River basin varies with the -0.12 power of the size of the drainage area and is identical to that in the Upper Mississippi Basin.

Bedload-transport rates

W. W. Emmett and L. B. Leopold compared measured bedloads-transport rates with those computed by using existing formulas. The results often showed discrepancy between the two rates, and indicated that existing bedload equations are inadequate to predict transport rates for many rivers.

STREAM MORPHOLOGY

Relationship between channel gradient and mean discharge

According to W. R. Osterkamp, a study of alluvial streams of Kansas indicated that the relationship between channel gradient and mean discharge can be described by a family of power-function equations. All of the equations have the same exponent, -0.25 , but the coefficients vary with size characteristics of bed material. For mean discharge, channel gradients tend to increase with median particle size of bed material. The study also showed that gradients of braided channels are generally greater than gradients of meandering or straight streams of similar discharge.

Storm-event aggradation of ephemeral streams

Two high-intensity summer thunderstorms in 1977 caused significant aggradation in the main channel of a small drainage basin area (2.6 km^2) in northwestern Colorado. In a study of sediment transport from hillslope source areas through the drainage network, D. G. Frickel surveyed 10 channel cross sections after each storm. In a 1,097-m-long reach of the main channel, immediately upstream from the mouth of the basin, the average area of the channel cross sections was reduced 22 percent as a result of the two thunderstorms. Cross sections surveyed after several low-magnitude storms showed little change in area. These data tended to substantiate the hypothesis that, in a semiarid environment with ephemeral streams, sediment is seldom transported through the drainage network in a single storm event, even in small headwater basins.

Effects of the Teton Dam failure

Failure of the Teton Dam of Idaho on June 5, 1976, drastically altered the geomorphic character of the North Fork Teton River system for several kilometers below the damsite. According to R. P. Williams, vast gravel deposits in the channel appeared to have considerable stabilizing effect on downstream sediment-transport processes. Data collected during the 1977 flow season were indicative of the relative stability of the channel. Measured hydraulic variables included measurements of slope, depth, width, velocity, and particle-size distribution of bed material, and, indirectly, channel roughness.

The study also showed that suspended-sediment loads at five sites along a 43-km reach of the river downstream of the dam ranged from 1,500 t to 1,800 t (mostly fine sand and silt) for a 6-month

runoff period. Daily flows ranged from 0.003 to $18.2 \text{ m}^3/\text{s}$, and suspended-sediment concentrations ranged from 2 to 400 mg/L at these sites. Mean particle sizes of the bed material and of the suspended load were approximately 15 and 0.5 mm, respectively. Bedload rates were estimated to be about 10 percent of the total load.

Effects of clearcutting redwoods in the Redwood National Park of California

R. J. Janda and K. M. Nolan reported that a study of sediment discharges of streams within the Redwood National Park of California showed that streams draining areas recently clearcut and tractor-yarded yielded more than 17 times as much suspended sediment during the 1975 and 1976 storm seasons as comparable nearby uncut basins. Streams with drainage basins that were harvested in this manner more than 10 years ago still yielded more than two times as much suspended sediment as uncut basins. Bedload discharges appeared to be affected at least as severely as suspended-sediment discharges. These increases in sediment loads changed stream-channel geometry, which, in turn, appeared to have damaged the aquatic and riparian resources of the park. Numerous streamside trees were killed or in a state of declining vigor because of bank erosion, burial by coarse-grained streambed material, or drowning by locally elevated water tables. Furthermore, the aquatic habitat appeared to have declined in its capability to support the normal level of population and diversity because of toppling of shade-providing streamside vegetation, filling of summer rearing pools, burial of stable substrates, such as bedrock blocks and large logs, and more frequent shifting of streambed materials.

Sediment accumulation rates in stream valleys of Wisconsin

In a continuing study of sediment deposits in the Coon Creek basin of Wisconsin, S. W. Trimble (1977) and S. C. Happ established maximum rates of sediment accumulation by the two techniques of budgeting the total accumulation in the main valley and of measuring accumulation in small reservoirs built in the 1930's and 1940's. Peak annual rates, determined at six locations in the main valley by dating levels of sediment accumulation, ranged from 2,100 to $2,900 \text{ m}^3/\text{km}^2$; the accumulation occurred between 1930 and 1945. Five small reservoirs on small subbasins built and filled with sediment from 1936 to 1945 indicated an areally weighted average annual accumulation rate of $3,300 \text{ m}^3/\text{km}^2$. The two

rates are comparable, considering the relative sizes of the drainage areas.

MODIFICATION OF EOLIAN DEPOSITS

Bioturbation traces

T. S. Ahlbrandt and Sarah Andrews suggested that a cold climate modifies eolian deposits in at least four ways: It reduces the rate of dune migration. It deforms stratification by melting snow or ice layers. It develops dissipation structures, a type of contorted bedding, by infiltration of meltwater. It produces and preserves minor structures that normally would be destroyed.

Although bioturbation traces in rocks of unknown depositional environment are commonly cited as evidence against an eolian origin, bioturbation is also a common, if not ubiquitous feature of eolian deposits. Flora and fauna, adapted to the eolian environment since Carboniferous time, usually make root moulds and burrows in many forms, orientations, and sizes. The different kinds of disruptions are generally distinguishable in eolianites.

INSTRUMENTATION

Helley-Smith bedload sampler

D. W. Hubbel and H. H. Stevens, Jr., found that, under the conditions of a flat bed, high transport rate, and bed material finer than 0.4 mm in diameter, the standard Helley-Smith bedload sampler tended to clog and sample with a very low efficiency in the Rio Grande Conveyance Channel at San Acacia, N.M. Because this finding correlates with previous laboratory studies, it is apparent that the sampler should not be used in sandbed streams where the median diameter of bed material is less than about 0.5 mm.

Sampler for large streams

During 1976 and 1977, C. F. Nordin, Jr., and J. V. Skinner (1977) found that a special point-integrating sampler, designed to sample isokinetically for large streams, performed satisfactorily in a field study of the geochemistry and sediment load of the Amazon River of Brazil.

Design requirements for pumping samplers

J. V. Skinner and J. P. Beverage established hydraulic design requirements for pumping devices used to automatically sample the concentration of

suspended sediment. An optimum balance between sampling efficiency and power requirements was usually attained when flow in the intake tubes had a Reynolds number between 3,000 and 4,000.

Suspended-sediment analysis by laser-light methods

M. C. Goldberg and E. R. Weiner showed that the intensity of Mie, Rayleigh dipole, and Fraunhofer diffraction scattering from a laser-excited sample cell is the product of the function between the excitation wavelength and the particle mean size. By ratioing the forward angles, it is possible to separate the total scattering function into its components and thus to identify each particle size in a mixed sample. At back angles usually greater than 150°, the scattering is due to multiple reflections that tend to depolarize the light. This effect, when viewed at back angles, is indicative of the amount of sample present. It was found that a curvilinear relationship exists between the sample concentration and the depolarization ratio of incident to scattered light.

GLACIOLOGY

Snowfall on Alaskan glaciers in 1976-77

During the 1976-77 winter, while most of the continent received unusually low amounts of snowfall and rainfall, the coastal glaciers of Alaska received unusually large amounts of snowfall, according to L. R. Mayo and D. C. Trabant. The Wolverine and Gulkana Glaciers received the heaviest snowpacks in 10 years of record. Wolverine Glacier near the south-central coast (Kenai Peninsula) received snowfall equivalent to 4.6 m of water, compared to an average of 2.3 m. Gulkana Glacier, which is inland (Eastern Alaska Range), received snowfall equivalent to 1.7 m of water.

Southern Cascade Range borehole drilling program

The continuing program to use boreholes to investigate the basal water system of a glacier in the southern Cascade Range of Washington resulted in several new findings, according to S. M. Hodge. Borehole water levels are probably representative of an area of at least 100 m in extent rather than the 10 m indicated earlier. The surface motion of the glacier correlates well with the water level in a borehole, thus lending strong support to the hypothesis that the sliding of a temperate glacier is dominated by the basal water pressure. The basal water system is probably not as widespread as in-

licated by the original drilling experiments, and the water may be concentrated more in discrete channels. It is more difficult to connect to the basal water system with a borehole than was suggested by the original drilling, and allowance for this must be made in future investigations.

Increased ablation in the Western United States in 1977

Approximately 2,400 km² (0.39 percent of the total area) of the Columbia River drainage basin in the Western United States and Canada is covered by permanent snow and ice. W. V. Tangborn's studies indicated that greater than normal ablation occurred during summer 1977 because the record low snowfall of the previous winter allowed exposure of ice and firn having low albedo (reflectivity) early in the season, thereby causing increased absorption of incoming shortwave radiation. The estimated decrease in average glacier albedo of at least 12 percent corresponded to an increase in ablation of 150 mm of water. Thus, an unexpected 300 GWh (10¹⁵ J) of electrical energy was produced by the increased runoff from these glaciers. The increased hydroelectric power produced by this runoff would have been worth an additional \$9 million to the power-generating utilities of the Columbia River system had it been anticipated and planned for early in the season.

R. M. Krimmel reported that in 1977, the South Cascade Glacier in Washington received only 1.6 m of water, the snowfall equivalent of about one-half the normal precipitation, and runoff from the basin averaged 4.3 m, slightly above normal runoff. High runoff had been expected because of increased melting of firn and ice from the glacier.

Subglacier dye-injection test

R. M. Krimmel reported that Rhodamine-WT dye was injected directly into the subglacial water system at the bed of South Cascade Glacier to determine the transit time of water from the bed to the terminus as compared to the transit time from the surface to the terminus. The transit time of the dye from the bed to the terminus was 2 days until the first indication and 2.5 days until the peak. The transit time of the dye from the surface, 210 m above the bed, to the terminus was about 1/2 day until the first indication and 2 days until the maximum was observed. The concentration peak from the surface injection was broader and of lower amplitude than that from the basal injection. These results suggested that the dye from the surface injection became diffused, perhaps by following many

different paths to the terminus, whereas the basal injection acted more as a concentrated slug.

Hot-water drill for use in temperate glaciers

P. L. Taylor and S. M. Hodge reported that a successful hot-water drill was developed for use in temperate glaciers. Drill rates of 70 to 160 m/h were obtained; these rates are approximately 20 times faster than those of conventional thermal-electric drills. The problem of maintaining a vertical hole was overcome by using a stiff, lightweight hose, and by using an electric motor to lower the drill. The drill easily penetrates dirty ice and is not susceptible to burnouts.

Volcanic effects on snow and ice on Mount Baker, Washington

D. G. Frank and R. M. Krimmel observed that a massive section of the glacier on the northern rim of Sherman Crater on Mount Baker, Washington, was undercut by thermal activity, and in July 1977, collapsed into the crater. About 350,000 m³ of snow and ice and some rock spread across half of the crater floor and completely covered the crater lake and the fumarole clusters near the eastern breach of the crater rim. Much of the debris gradually melted so that the covered thermal area was again exposed by September. Another debris avalanche occurred in late summer in an area of hydrothermally altered material on Sherman Peak; about 35,000 m³ of mostly snow and ice and some mud traveled about 3 km down Boulder Glacier. This avalanche was a repetition of similar debris avalanches that have occurred every 2 to 4 years since at least 1958; the preceding Boulder Glacier avalanche of this type occurred in 1973. Mapping of thermal ground, as interpreted from snow and ice features, indicated that newly developing outlets for fumarolic activity are shifting from the eastern to the western parts of Sherman Crater. After the sudden development of greater and hotter fumarolic emission throughout the crater in 1975, at least three clusters of fumaroles in the western half of the crater either enlarged in area or increased in temperature during 1976 and 1977. Through the end of 1977, these local changes did not seem to indicate an increase in the overall level of thermal activity.

GEOLOGY AND CLIMATE

Climate is considered by many to be an atmospheric phenomenon, but those who realize the interplay of the atmosphere with other surface features

of our globe—the oceans, ice sheets, and the land—know that the impact of climate is plainly imprinted on the geologic record. For nearly a century, earth scientists of the USGS have been among those studying the record of past climatic change and the geological consequences of our present climate.

The broad goals of climatic research are to improve our understanding of how the climate system works, what it may do in the future, and what may be the effects. Earth science has three major roles to play toward the achievement of these goals:

- (1) Defining the long-term record of climatic variability,
- (2) Determining geologic, geochemical, and geophysical factors that contribute to climatic change, and
- (3) Estimating the physical and biological consequences of possible future climates.

The responsibilities of the USGS lead to a heavy concentration of its efforts on research in the continental environment. Climate leaves its mark on and around the continents in an extraordinarily large number of ways that are preserved in the geologic record. Although most investigations of this record by the USGS are concerned primarily with other objectives, nearly all yield information pertinent to understanding our present climate, past climates, and the effect of climate on land and water resources. The results described below are representative of the range of this research.

Impact of climate on the Erie Canal

The importance of predicting the effect of climate on water projects was emphasized by W. B. Langbein (1976) in an historical account of the Erie Canal. Efforts to cope with water shortages in the canal were never fully successful. The primary cause of the persistent shortages was the method used to estimate the available flow of streams during extended dry spells. Ad hoc, spot measurements of streamflow consistently led to overestimation of the dependable supply.

Land-use climatology

A research team in the Geography Program analyzed the effects of urban land use on the climate of Baltimore, Maryland, and Washington, D.C., by evaluating the exchange of energy between the Earth and its atmosphere. The analysis depended on mapping aspects of land use and on numerical modeling of the effects of land use on local climate.

At Baltimore, using measurements of obstacles in 324 representative parcels of land, a close association was found between aerodynamic roughness and the simulated energy balance. More generally, it was demonstrated that surface roughness, and the resulting effects on surface climate, can be estimated from a knowledge of urban land use. At Washington, urban temperatures over periods of time ranging from a day to a month were predicted, using an energy budget model. The results gave good predictions of minimum temperatures, as well as some predictions of maximum temperatures, although the predicted variation in temperature for single days tended to be less than the range actually observed. The land use information was also examined for its applicability to air quality planning. Such information, when incorporated in models of atmospheric diffusion, was found to have potential use in implementing various air pollution control strategies, for selecting sites for air-sampling stations, and for predicting the effects of proposed changes in land use on the distribution of pollutants and the level of air quality.

Climatic assessment of rehabilitation potential

Meteorological data were used to assess the spatial and temporal variation of climatic characteristics affecting the magnitude of water deficiency and, hence, the facility of revegetation on surface-mined lands in the Powder River basin of Wyoming and Montana and the Delores and San Juan River basins in Colorado, New Mexico, Arizona, and Utah. The findings by T. J. Toy (University of Denver) indicate that growing-season length, irrigation water requirement, and mean monthly precipitation are potentially the most useful parameters for evaluating rehabilitation potential. A series of isoline maps with explanatory text were prepared for use in rehabilitation planning.

Tree rings and alluvial history on Black Mesa, Arizona

The chronology provided by tree-ring records has enhanced the understanding of climatic changes on Black Mesa in Arizona and has led to a more accurate correlation of these changes with the alluvial history (T. N. V. Karlstrom, 1976). Former episodes of drought were found to be expressed geologically by gaps in deposition of alluvium, as demonstrated by remains of juniper forests that took root in soils on former valley floors, and subsequent episodes of wetter climate were identified as accounting for burial of these trees by later buildup of alluvium.

The ages of such buried forests, as identified by Jeffrey Dean (University of Arizona), coincide with times of drought established from other tree-ring records; namely, the years 1325–1500, and about 1525, 1600, 1700, 1800, and 1900. A gap dated at about 1950 in alluvium deposited since 1900, as marked by scattered pieces of glass, metal, and plastic, was found to coincide with a drought expressed in tree rings, as well as by modern weather records. Gully erosion of this alluvium began in places between 1969 and 1975, apparently because of the onset of a drier climate at that time.

Pleistocene and Holocene climate in central Mexico

The late Pleistocene and Holocene climate of central Mexico was investigated by interpreting the habitats of fossil diatoms and pollen. Diatoms collected and identified by J. P. Bradbury in the Cuenca de México (19° N. lat., 99° W. long.) indicated that the late Pleistocene climate 15,000–10,000 years ago was cooler and drier than at present. In the part known as the Chalco Basin, a cool and fresh, but very shallow marsh existed, probably nourished by meltwater from glaciers that then reached 1,000 m below their present altitude on the adjacent volcanoes, Popocatepetl and Iztaccíhuatl. The amount of meltwater from glaciers that then reached 1,000 m, however, was sparse, and water that drained northward from Chalco to ancient Lake Texcoco was sufficient only to form shallow, saline pools.

With the close of the Pleistocene about 10,000 years ago, the fossil diatoms show that the climate became warmer and probably wetter than before. Runoff began to fill basins in the Cuenca de México, and brackish water from Lake Texcoco rose and inundated the Chalco Basin, thereby providing a habitat for brackish-water diatom communities. Then, beginning about 4,000 years ago, lake levels again fell, probably because of a return to a drier and cooler climate. The fossil diatom floras of Lake Chalco reflect this climatic change by indicating fewer inundations of saline water from Lake Texcoco, although the lacustrine environment of Chalco did not regain its Pleistocene character.

Pollen analyzed by Lauro Gonzalez Quintero (Instituto Nacional de Antropología e Historia) supported this interpretation of the early Holocene climate. Saline lakes at a high level in the Chalco Basin were indicated by large increases in pollen from sedges and other aquatic plants that characterize such an environment. Further, the pollen samples contained species representative of a cloud

forest, a circumstance that is considered to indicate generally moist conditions and a lack of a dry season. These findings suggested that the early Holocene lakes of central Mexico were the product of a distinctive climatic regime of warmth and moisture and not simply a local hydrologic phenomenon.

Climate and glaciers

In the northern Cascades of Washington, one of the constraints in deducing changes in climate by mapping and dating the position of alpine glaciers is that moraines of early Neoglacial (Holocene) glaciers on the western side of the range were mostly overridden and obliterated by later glacial advances. This circumstance does not apply to the Alpine Lakes Wilderness Area, on the comparatively dry eastern side of the Cascades, where R. B. Waitt and J. C. Yount found distinctive sets of older and younger Neoglacial moraines. The older, informally named the Brisingamen moraine, was found to be as much as half a kilometer beyond the outer edge of the younger, which was informally named the Brynhild moraine. Between them is a striated bedrock surface. By measuring a range of features indicative of age, Waitt and Yount identified a significant hiatus between the Brisingamen and Brynhild Neoglacial advances. The features measured were the amount of lichen growth, depth of circular weathering pits in bedrock and boulders, depth of weathering along joints, the height of resistant minerals above surfaces etched by weathering, the thickness of rinds on glacial cobbles on moraines, and the depth of oxidation of soil on the moraines. The results suggested that the Brisingamen moraine correlates with glacial deposits on Mount Rainier dated at 2,500–3,000 years B.P. The Brynhild moraine was estimated to have accumulated during the last several centuries, a time generally referred to as the "Little Ice Age."

Size of glacial streams in Yellowstone National Park

By considering the characteristics of the glacial climate in Yellowstone National Park, K. L. Pierce estimated that the annual streamflow was then at least twice the present discharge. In one calculation, discharge from the drainage basin occupied by the northern Yellowstone glacier, which covered 3,400 km² at an average thickness of 700 m, was estimated to have been 3.8 km³/yr, as compared to the present annual discharge of 1.6 km³. The calculation was based on decreases in evaporation and evapotranspiration and on the increased height of the glacial

surface. Precipitation was assumed to have been the same as at present. Another calculation, based on consideration of water derived by glacial melting, resulted in an even larger estimate of annual discharge of 4 km³. This calculation depended on information about the volume of snow that accumulates yearly in analogous environments.

Water temperature of corals shown by isotopic analysis

Analyses of ¹⁸O and ¹³C in cores of living corals have confirmed that certain characteristics of their annual growth bands are related to water temperature. The analyses were done by Cesare Emiliani (University of Miami) on cores provided by a USGS research team at Miami Beach, Fla. Previous work had shown that growth of some dense bands, called stress bands, correlate with unusually cold winters in the Florida Keys. By taking 144 samples from 11000 bands of a living coral that grew during the past 30 years, each year being represented by about 4 samples, Emiliani demonstrated a relation between the isotope ratios and temperature.

Three-million-year isotopic record of paleoclimate at Death Valley in California

A measure of the Pliocene and Pleistocene paleoclimate of the southern Great Basin has been gained by documenting fluctuations in the abundance of ¹⁸O and ¹³C in calcitic veins and by dating laminae in these veins by the ²³⁴U/²³⁸U radioactive clock. Such veins at Furnace Creek in Death Valley were deposited by low-temperature ground water and were probably conduits for ancient springs. The veins rise steeply through fan conglomerate of Pliocene and Pleistocene(?) age (Funeral Formation), and the youngest laminae of one of them were dated from 1.0 to more than 2.2 million years old. A projection of average growth for this vein (1 mm/50,000 yr) suggested that the oldest laminae are at least 3 million years old. The laminae show small, but clearly defined, oscillations in ¹⁸O/¹⁶O and ¹³C/¹²C ratios (<1 and <3 permil, respectively) that are thought to reflect variations related to the former climate. A younger, crosscutting vein has been dated at 120,000 ± 65,000 years. These findings follow a detailed study of the hydrodynamics of the existing ground-water system. A knowledge of these isotopes in the calcite, as well as the ratio of ¹⁸O/¹⁶O, ²H/¹H, and the content of ¹⁴C, in the modern ground water provides information on the geologic age of this flow system and the paleoclimate. The study is a joint effort by I. J. Winograd, B. J. Szabo, and Tyler

Coplen (USGS), and by James Cowart (Florida State University).

Three million years of climate history at Searles Lake

Initial results of a joint study of a 930-m core, taken near the middle of Searles (dry) Lake in southeastern California indicated that the core provides a continuous sedimentary record—and a record of the paleoclimate—for all the Pleistocene and some of the Pliocene. The core is the property of the Kerr-McGee Corporation, which gave permission to the USGS to publish a description of the core and to coordinate additional scientific studies (the Corporation itself had previously logged the core and had analyzed several hundred samples taken from it). The current studies are being evaluated by G. I. Smith (USGS) and V. J. Barczak and G. F. Moulton (Kerr-McGee Corp.). Special studies of certain samples have been made by Smith, J. C. Liddicoat (Lamont-Doherty Geological Observatory of Columbia University; paleomagnetic properties), and R. L. Hay (University of California, Berkeley; silicate minerals), and portions of these samples have been given to D. G. Frey (Indiana University; microorganisms), E. B. Leopold (University of Washington; pollen), and A. M. Sarna-Wojcicki (USGS; volcanic ash).

The upper 693 m of the core consists of alternating lacustrine muds and evaporite deposits, which are thought to represent a paleoclimatic record. Between 693 and 915 m the sediments are alluvial arkosic sand and gravel, perhaps reflecting some tectonic influence. The bottom 15 m of the core is quartz monzonite.

Layers of salt-free, lacustrine mud were found in the upper part of the core at depths of 21 to 25 m, 38 to 67 m, 214 to 291 m, 403 to 425 m, and 542 to 690 m. The lack of salt indicated that these layers represent long periods of deep water under a wet climate. The upper three layers were correlated with the Tioga, Tahoe, and Sherwin Tills in the Sierra Nevada, to which the Searles Valley was formerly connected by surface drainage, and the lower two layers were considered to be correlative with the McGee and Deadman Pass Tills. Ages for these lacustrine intervals were suggested by preliminary paleomagnetic measurements by Liddicoat, who found a sequence of changes in direction of magnetism that could be reasonably correlated with the Brunhes, Matuyama, and Gauss epochs and the Olduvai, Reunion, Kaena, and Mammoth events. The Brunhes-Matuyama boundary (0.7 m.y.) was

found at a depth of 185 m, or 29 m above the layer of lacustrine mud that was correlated with Sherwin Till. Interestingly, the Sherwin Till in its type area is overlain by a volcanic deposit also dated at 0.7 m.y., the Bishop Tuff. The Kaena and Mammoth events, which are approximately dated at 3 m.y., were found at depths between 620 and 685 m. This interval is in the middle of lacustrine sediments thought to correlate with the Deadman Till, which lies between volcanic deposits dated at 2.8 and 3.1 m.y. Two conspicuous layers of volcanic ash at depths of 684 and 691 m, approximately at the level that seems to represent the beginning of the Mammoth event, were provisionally correlated with units of tuff in the nearby Coso Formation, which have been dated by G. B. Dalrymple (Duffield and Bacon, 1977) at about 3 m.y., using the potassium-argon method.

Geologic response of southern California to contemporary climate

According to H. G. Wilshire and J. K. Nakata (USGS) and Bernard Hallet (Stanford University), a windstorm in the southern San Joaquin Valley on December 20–21, 1977, caused severe stripping of soil and weathered rock. The newly exposed bare ground, and the unstable deposits of windborne material that accumulated on leeward slopes, made the region notably vulnerable to fluvial erosion by heavy rain that fell a few days later. The rain resulted in damaging floods and mudflows. The effects of wind erosion were seen in a belt of grazing land 5 km wide around the 145 km perimeter of the Tehachapi and San Emigdio Mountains, as well as in 1,500 km² of farmland in the San Joaquin Valley. The susceptibility of the foothill belt to wind erosion apparently was increased by stresses brought on by 2 years of drought and grazing, and deflation of the dry soil of farmlands seemingly was aggravated by a lack of windbreaks. Removal of protecting plants in newly developed urban areas, extensive denudation of oilfields north of Bakersfield, and destruction of soil by recreational off-road vehicles also contributed to the ruinous response to wind and rain. Although the normal rate of erosion in this area is already comparatively high, the erosion rate during the windstorm was estimated to have increased more than 2,000 times.

Duststorm of 1977 in the High Plains

J. F. McCauley, C. S. Breed, and M. J. Grolier (1978) reported that the greatest duststorm yet recorded by a weather satellite began in the High

Plains of eastern New Mexico and Colorado on February 23, 1977, after 2 years of drought. Two enormous dust plumes spread over most of the southeastern States and out into the mid-Atlantic during a 2-day period, as tracked by the GOES-1 satellite. The source of one plume, that in the Clovis-Portales region of New Mexico, showed local amounts of wind scour as deep as 1 m. This erosion was accomplished in less than 12 hours when northwesterly winds blew at velocities of as much as 100 km/hr. Lobate layers of fine sand up to a meter thick and several kilometers long were deposited downwind from the places of wind scour. McCauley, Breed, and Grolier attributed this erosion to a combination of factors: (1) the prolonged western drought, which had dried the soils; (2) the dry air carried by these unusually strong winds, this being the first storm that had broken through a long-lasting Pacific atmospheric high (the Pacific high had prolonged the drought by diverting storms northward during the winter of 1976–1977); (3) the presence of the Llano Estacado escarpment, an obstacle 200 m high that fostered erosion of the upland plains immediately downwind by creating additional turbulence; (4) the susceptibility of unconsolidated geologic deposits in the area to wind erosion, especially river sediments, old dunes, and blankets of wind-laid sand; and (5) the practice of clearing protective grass and shrubs from sandy land for farming.

Climatic changes on Mars

Climatic changes deduced for Mars are of interest in studies of terrestrial climate in that they provide an independent means of assessing the relative effects of variations in solar radiation and of periodicities in orbital geometry. Working with high resolution imagery of the Martian surface, M. H. Carr found evidence of both long term progressive cooling and of shorter term cyclic variations.

The evidence for progressive cooling came largely from relict fluvial features. Much of the old terrain on Mars is heavily dissected by what are apparently stream channels, whereas younger surfaces are progressively less dissected, and the youngest surfaces have no channels whatever. Such channels are incompatible with the existing temperature and atmospheric pressure of Mars, an environment in which water cannot exist in liquid form. The declining development of stream channels therefore implies progressive planet-wide cooling to the present waterless condition.

The evidence for cyclic variations came largely from alternating deposition and erosion of a thick sequence of stratified deposits at the poles. These eroded deposits are so young that they have no impact craters. The deposits are interpreted to be largely eolian, and their stratification is thought to have been caused by cyclical variations in wind patterns. Cyclical wind activity also appears to account for the repeated episodes of covering and stripping. Such changes in wind patterns were attributed by Carr to climatic changes that were induced by oscillations in the obliquity of Mars to its orbital plane or by variations in solar radiation.

GROUND-WATER HYDROLOGY

USGS research on ground-water hydrology has the common objectives of better understanding ground-water systems and developing and applying new techniques of study to improve management of ground water as an important national resource.

During FY 1978, model simulation was applied to many aspects of ground-water hydrology. The process of heat storage in a ground-water reservoir was simulated by a numerical finite-difference model. Land-surface subsidence as well as water-level decline was simulated by a three-dimensional model. A model was developed to simulate the effects of waste-water irrigation on a local ground-water system. Also developed, was a model that simulates the effects on ground-water recharge resulting from paving.

Investigations of artificial recharge as a means of supplementing the natural ground-water supply were carried out. Research was conducted on the chemical interaction between rock and water and the effects of mixing injected and native water on water quality. Several methods of analysis were applied to determine the suitability of storm-water basins to recharge reclaimed waste water. Other experiments included the use of natural filtration through the ground to remove suspended sediment from river water used for artificial recharge, and the use of sewage effluent irrigation water for recharge.

Other studies include work on subsurface waste disposal and saltwater intrusion. Bromide and gold were used as ground-water tracers. A method of predicting barometric-induced water-level fluctuations was developed. A significant discovery was the finding of two 150 m-thick freshwater lenses, extending more than 100 km off the New Jersey coast, which have kept saltwater from intruding along the coast.

AQUIFER-MODEL STUDIES

Simulation of heat-energy storage in a ground-water reservoir

According to S. P. Larson, in an experiment conducted by Auburn University, the physical processes of storing heat energy in ground-water reservoirs was successfully simulated by a numerical finite-difference model. Although difficulties encountered during the experiment (Molz, Warman, and Jones, 1976) diminished the reliability of some of the data, predicted temperatures of recovered water compared very favorably with measured values.

The ratio of horizontal to vertical permeability in the aquifer and the heat capacity of the rock matrix were the most important parameters for this simulation. These parameters had the most significant impact on the radial extent of injected fluid. Parameters such as porosity and hydrodynamic dispersivity had a moderate effect on the steepness of the temperature front but had negligible impact on the spatial position of the front.

Model of the Chicot and Evangeline aquifers in Houston, Texas

The model of the greater Houston area of Texas has been enlarged to encompass about 69,930 km² on a 63×67×5 node variable grid. According to W. R. Meyer, J. E. Carr, C. J. Loskot, and W. M. Sandeen, simulated water-level declines computed by the model were compared with field data for the Chicot and Evangeline aquifers for the periods 1890–1953, 1890–1960, 1890–1970, 1890–1973, and 1890–1975. In most areas, the comparisons were good.

During the simulation period (1890–1973), 31.7 percent of the water pumped was derived from aquifer storage; 22.9 percent was derived from clay storage (54 percent from clays in the Chicot aquifer and 46 percent from clays in the Evangeline aquifer); and 45.4 percent of the water pumped was supplied by recharge from precipitation, return flow from irrigation, and seepage from streams.

The model simulation of land-surface subsidence for 1890–1973 was 2.5573 m, while the measured amount of subsidence for the period was 2.5908 m. The maximum error was about 0.4572 m.

Effects of waste-water irrigation on ground-water conditions

M. G. McDonald and W. B. Fleck reported that the Muskegon County, Mich., waste-water management system disposes of 112,000 m³/d of waste water by spray irrigating 2,200 ha of corn. Irrigation and leakage from 688 ha of lagoons causes ground-water mounding at the site. Drainage

ditches, buried drainage tiles, and pumping wells have been installed to reduce the effect of mounding.

A digital model was developed to study the effects of irrigation, lagoon leakage, and tile drainage on the local ground-water system. A ground-water sink has been caused by drainage ditches and drainage tiles installed below preconstruction ground-water levels. The digital model indicated that a ground-water sink will exist under normal operating conditions throughout most of the waste-water site. Even if irrigation rates were doubled or the effectiveness of the drainage tiles were reduced by 75 percent, a ground-water sink would remain, although about 30 percent of the irrigated land would be waterlogged. In the northwestern corner of the waste-water site, where the few drainage tiles are generally above the water table, heavy irrigation has caused water levels to rise as much as 8 m; immediately outside the site the rise has been about 1 m.

Hydrogeologic system simulation

According to R. L. Cooley, techniques of nonlinear regression were applied to estimate the hydrogeologic parameters (transmissivity or hydraulic conductivity), recharge, discharge, and boundary fluxes for steady-state, ground-water-flow models of two field areas—a cross section in the Hula Basin, Israel, and Truckee Meadows, Nevada. Statistical techniques were used to estimate the degree of nonlinearity of the models, the fit of the models to field data, and the reliability of predictions made by the models. Analysis of model fit included estimated reliability and significance of computed parameters and reliability of computed head distribution. It was found that (1) both cases analyzed behaved at least approximately linearly (based on Beale's measure of nonlinearity); (2) variable reliability of observed head data had to be incorporated into the analysis for Truckee Meadows; (3) residuals transformed to eliminate heteroskedasticity and intercorrelation could be assumed to be independently normally distributed in the case of Truckee Meadows (testing was not carried out for Hula Basin because of possible lack of model fit); and (4) standard errors of parameters for both cases were large, thus indicating nonuniqueness of the solution, even though model fit was good for Truckee Meadows and was fair for Hula Basin. Reliability of the predicted drawdown distribution and pumping rate was estimated for a gravel-pit operation in Truckee Meadows. In spite of the nonuniqueness problem, predictions of these quantities at a level of significance

of 0.05 were not significantly different from the observed values.

Measured values of the hydrogeologic parameters and fluxes together with estimates of their variances were incorporated into the nonlinear regression model. A field application of these procedures to a cross section in west-central Canada indicated that unique estimates of principal components of hydraulic conductivities for several rock layers may be difficult to obtain unless reliable estimates of some of the parameters are available.

Paving does not necessarily reduce ground-water recharge

According to C. H. Tibbals, the percentage of paving that can occur in Floridan aquifer recharge areas in east-central Florida and not reduce the net recharge to the Floridan aquifer is a function of many variables that include rainfall, depth to water table, depth to potentiometric surface of the Floridan, evaporation from paved areas, evapotranspiration from unpaved areas, runoff, pattern of paving, and leakance coefficient of the confining beds. Equations that incorporate these variables, except pattern of paving, were developed and coupled to produce a conceptual model that estimates relative amounts of water available for recharge and percentage of unpaved area below which Floridan aquifer recharge rates must increase. An assumption inherent in the use of the conceptual model is that the excess water that runs off the paved areas is placed in the nonartesian aquifer in the unpaved area so that the water table builds up and thus increases the hydraulic head difference between the nonartesian and Floridan aquifers. Thus, water is driven across the confining beds and into the Floridan aquifer at a rate that is sufficiently increased to make up for the area, reduced by paving, under which recharge actually occurs.

The purpose of this simplified model is to show approximate mathematical interrelations of rainfall, runoff, evapotranspiration, percentage of paving, and Floridan aquifer recharge, and to make quantitative estimates of amounts of water available for Floridan aquifer recharge before and after paving. The allowable percentage of paving calculated in four examples ranges from 86.8 percent to 3.6 percent.

Steady state flow conditions simulated for potential strip-mining areas in Ohio

J. O. Helgesen and E. J. Weiss reported that in several 20-ha watersheds underlain by stratified shale, sandstone, limestone, and coal, the aquifers

are separated by slightly permeable clays that underlie the top two coal units (the top unit is to be mined). Initial aquifer test data indicated aquifer hydraulic conductivities of 0.01 to 0.001 m/d. The top aquifer discharges as springflow and evapotranspiration along the outcrop of the top coal unit. The second aquifer system is connected to the local stream network, and in some watersheds underflow occurs across the surface drainage divides. Application of a quasi-three-dimensional flow model to two of the watersheds enabled simulation of steady-state flow conditions.

Simulation of pumping in Dane County, Wisconsin

R. S. McLeod used a digital model to evaluate the effects of ground-water pumping on the hydrologic system in Dane County, Wis. Model results indicated that the aquifer system underlying the county should be able to meet the water needs of the area well beyond the year 2000. By the year 2000, water levels in the sandstone aquifer are expected to decline 3–9 m, and water levels in the overlying upper aquifer are expected to decline 4.5–15 m; annual streamflow from the upper Yahara basin, the area where most development is occurring, is expected to decline concurrently an additional 7 percent. The model will be used to evaluate the impact of alternate development plans.

ARTIFICIAL RECHARGE

Effects of mixing injected and native waters

A preliminary tracer test made by injection of ground water into a well tapping the Ogallala Formation near Stanton, Tex., indicated that dispersion along discrete beds may be small. According to W. W. Wood, D. C. Signor, and E. P. Weeks, the characteristic dispersive length computed from the breakthrough curve of iodide tracer in piezometers near the injection well is on the order of a few centimeters in length. However, dispersivity values determined by model calibration during water-quality modeling studies commonly are several meters in length. These values appear large probably because they generally are based on analyses of water samples collected from fully penetrating observation wells, rather than from piezometers. Hence, the calculated dispersivity includes the effects of mixing of water moving at different velocities in the different beds comprising the aquifer, as well as the hydrodynamic dispersion induced by pore tortuosity and interconnection.

A small-diameter gas-driven sample pump was developed by D. C. Signor in support of tracer tests for artificial-recharge studies. The pump fits in a 51-mm-diameter well and pumps continuously and automatically by positive displacement of a double-acting piston. The pump produces about 250 mL/m and has been continuously operated for as much as 48 hours on a 8.5 m³ tank of nitrogen. Because the gas has no contact with the water, alkalinity and pH values are little affected by the sampling procedure.

Storm-water basins for aquifer recharge with reclaimed water

D. A. Aronson (1976a, 1976b, 1978) reported that a study of 205 storm-water basins in Nassau County, New York, showed that 14 of the 50 largest basins are suitable for infiltration of reclaimed wastewater. Mathematical, numerical, and analog-model analyses of basin performance during infiltration, and the effects of such recharge on the local and regional water table, indicated that (1) all 14 selected basins can conditionally accommodate both reclaimed water and runoff from large-magnitude storms without overflowing; (2) the most efficient method of supplemental recharge requires partitioning of each basin so that runoff and reclaimed water can be applied alternately to each basin half; (3) the partition height of the basin governs duration of the application-rest cycle for infiltration of reclaimed water; (4) the duration of storm-runoff containment and the height of the water-table mound that develops beneath a basin are the principal limiting factors in supplemental recharge; (5) the quantity of reclaimed water that can infiltrate to the aquifer through the 14 basins, from postulated-design rates of recharge, is 146,000 m³/d; (6) the regional water-table rise resulting from supplemental recharge by the 14 basins will partly offset the water-table decline caused by sewer installation in parts of Nassau and Suffolk Counties; and (7) the 14 basins cannot compensate for the estimated 350,000 m³/d long-term water deficiency anticipated in Nassau County.

Natural filtration used in artificial recharge investigation

W. F. Lichtler (USGS) and D. I. Stannard and Edwin Kouma (Nebraska Water Resources Center) reported that natural filtration through the ground is being used in east-central Nebraska to purify Platte River water before it is artificially recharged into a sand and gravel aquifer that is in hydrologic connection with the river, thereby eliminating treatment costs.

A well about 1 km from the Platte River withdraws essentially purified river water in an area where seepage from the river prevents appreciable water-level decline despite heavy withdrawals and delivers the water via pipeline buried below the frostline to a recharge well 4.8 km distant in an area where the water level is progressively declining. The system is designed to minimize plugging of the well and the aquifer by suspended sediment, air entrainment, and bacterial contamination. Suspended sediment in the recharge water is less than 0.1 mg/L. Recharge rates in excess of 4,000 m³/d have been maintained for more than 60 days with only 5 m of water-level buildup in the recharge well, and considerably higher recharge rates are possible. Elimination of the need for water treatment facilities or frequent well redevelopment greatly increases the possibility that large-scale artificial recharge of ground water through wells will be economically feasible in many areas.

Artificial recharge with wastewater

J. R. Díaz reported that, after 11 months of application, sewage-effluent irrigation water reached the aquifer at the Fort Allen, Puerto Rico, recharge project. Continuous 15–20 cm/wk effluent applications in a sugarcane plot area induced water to percolate through the unsaturated zone, a distance of 7.5 m. Different schemes of time and quantity of effluent applications were tested during 1976 and 1977, but only rates from 15 to 20 cm/wk, in a 3-dry-, 4-wet-days application, proved to be effective to recharge the aquifer.

Water samples were recovered from porous cups at depths of 1 m, 1.2 m, 1.5 m, and 2 m in the unsaturated zone. Soil tests in the area adjacent to the porous-cup nests indicated a 3–15 percent increase in moisture content.

A progressive increase in specific conductance and chloride-ion concentration was recorded in the observation well located in the immediate plot area. The water level rose about 15 cm higher in the observation well in the plot area as compared with levels in outside observation wells. The rise in water level and specific conductance in this well indicated for the first time that recharge water had reached the water table. The time of effluent travel to the aquifer was estimated to be 34 days.

The sugarcane lot was harvested during the first week of July 1977. Total production was estimated to be 7.2 t of cane plus 3.6 t of seeds and trash. Sugar-mill analysis of the cane indicated a relative high yield (10.35 percent) for this variety as com-

pared with other cultivated areas in the south coast of Puerto Rico.

Monthly field tests and bacterial analyses were made of water from observation wells and Fort Allen's public-supply wells. Correlation of specific-conductance measurements with previous water-quality data for these wells, indicated that the chemical character of the ground water in the Fort Allen area remained unchanged during the 11-month period of this investigation.

MISCELLANEOUS STUDIES

Subsurface waste disposal

A 1,888-m-deep test well was drilled to determine the feasibility of subsurface waste storage in the Orlando area of Florida. C. H. Tibbals reported that the well penetrated sedimentary rocks composed chiefly of limestone and dolostone before entering metamorphic basement rock at a depth of 1,866 m. A zone of high transmissivity suitable for injection of large volumes of waste was not encountered below the base of freshwater in the Floridan aquifer, which is estimated to be at a depth of about 722 m. Transmissivity of the brine-containing strata lying between the 738-m and 1,888-m depths was estimated at 14.9–44.6 m²/d; the most transmissive part was the interval from 1,646 m to 1,798 m.

Results of a recent backflow experiment conducted at a subsurface waste-injection facility near Milton in northwestern Florida showed that the injected waste is being altered within the receiving limestone aquifer. According to C. A. Pascale (C. A. Pascale and J. B. Martin, 1977; 1978) and John Vecchioli, injection of a treated industrial waste that is moderately acidic and high in concentrations of nitrate, organic nitrogen, and organic carbon began in June 1975; at the end of 1977, about 2.5×10^6 m³ of waste had been injected into a confined saline-water limestone aquifer. During the experiment, the backflowed waste was discharged from the injection well into a holding pond for about 72 hours at a rate of 13 L/s. Analyses of the recovered waste indicated that nitrate and organic nitrogen concentrations decreased from 210 mg/L to 104 mg/L and from 190 mg/L to 86 mg/L, respectively, during the backflow period. Conversely, nitrite and ammonia increased from 1.3 mg/L to 9.2 mg/L and 38 mg/L, to 108 mg/L, respectively. Dissolved nitrogen and nitrous oxide gases also increased in concentration from 24 mg/L to 43 mg/L and from 42 mg/L to 92 mg/L, based on samples collected after 24 hours and 66 hours of backflow. These changes, as well as

other chemical changes, apparently resulted from bacterial activity in the receiving aquifer.

C. A. Pascale investigated two underground waste-injection systems in western Florida, one near Pensacola and the other near Milton, in which liquid industrial wastes are being injected into a confined saline-water limestone aquifer of low transmissivity. The injection sites are about 13.7 km apart. Since 1963, more than 53×10^6 m³ of acidic industrial waste has been injected at the site near Pensacola. By 1978, injection rates averaged about 145 L/s, and wellhead pressures at the two injection wells averaged 1,180 kPa. The pressure at two deep monitor wells (3.1 km north and 2.4 km south of the injection site) in the injection zone averaged 830 kPa and 870 kPa, respectively. At the injection site, pressure in a shallow monitor well in the artesian aquifer immediately above the 67-m-thick confining bed averaged about 62 kPa and continued to decline slightly. Bicarbonate and dissolved organic carbon concentrations at the south monitor well have continued to increase since the arrival of the dilute waste at the well in mid-1973. Alkalinity (reported as bicarbonate) has increased from a background level of 270 mg/L to 650 mg/L; the concentration increased about 30 mg/L in 1977. Methane-gas concentration decreased from 70 mg/L in August 1970 to 40 mg/L in October 1977, while carbon dioxide gas concentration remained essentially unchanged at 50 mg/L. No changes in water chemistry were detected in the north monitor well or in the shallow monitor well.

Injection began at the site near Milton in June 1975, and, since then, more than 2.5×10^6 m³ of treated industrial waste have been injected. This deep-well waste-injection system uses the same injection zone as the similar system near Pensacola. By 1978, the injection rate averaged 32 L/s and wellhead pressure at the injection well averaged 610 kPa above the preinjection zone 2.5 km northeast, 0.31 km southwest, and 0.48 km south of the injection well averaged 160 kPa, 320 kPa, and 370 kPa, respectively. At the injection site, the water level in a shallow monitor well in the artesian aquifer immediately above the 65-m thick confining layer declined slightly and averaged 21.0 m below land surface. Bicarbonate and dissolved organic-carbon concentrations at the southwest monitor well have continued to increase since arrival of the dilute waste in February 1976. Bicarbonate increased from a background level of 390 mg/L to 1,860 mg/L in December 1977. Since August 1976, bicarbonate and dissolved organic-carbon concentrations at the south

monitor well have ranged from 370 mg/L in September 1976 to 700 mg/L in December 1977; dissolved organic-carbon concentrations ranged from 4.0 mg/L to 25 mg/L. Concentrations of total nitrogen and sulfate also have increased slowly in water from the southwest and south monitor wells. No changes in water chemistry were detected at the northeast monitor well or the shallow monitor well.

The Cambrian and Ordovician Arbuckle Group is a freshwater aquifer in southeastern Kansas and adjacent parts of Missouri, and in equivalent rocks in Oklahoma, and Arkansas. It also serves as an important hydrocarbon reservoir in central and south-central Kansas and is used for disposal of large quantities of brine and industrial wastes throughout the State. A. J. Gogel reported that values of vertical compressibility for the Arbuckle were calculated from several hundred sonic logs. Storage coefficient values were then calculated by a method formulated by C. E. Jacob (1950, p. 334). Computed values of the storage coefficient for the Arbuckle ranged from 1.04×10^{-6} to 1.76×10^{-4} ; indications are that the higher values are associated with thicker intervals (>130 m) of Arbuckle rocks, while lower values are represented by thinner intervals (<20 m) of Arbuckle.

Saltwater intrusion in Florida

The fern-growing industry on the northern extreme of the De Land Ridge and on the Crescent City Ridge in northwestern Volusia County, Florida, requires a large amount of good-quality water for irrigation and an even larger quantity for freeze protection by spray irrigation; the source of most of this water is the Floridan aquifer that contains brackish water in the surrounding flatwood areas. The potentiometric surface of the aquifer is mounded in the ridges and slopes to the flatwood areas. A. T. Rutledge reported that ground-water pumping by the fern-growing industry for freeze protection causes the head in the Floridan aquifer in Pierson to decline approximately 8 m after two nights of pumping. The drawdown about 1 km from the fern-growing area is about 2–3 m. It takes about 2 days of recovery for the head in the Pierson area to return to within 1 m of the prepumping head. Large drawdowns caused by pumping may be causing salty water in the aquifer to migrate laterally and vertically, which could render many wells useless.

D. E. Barr (Northwest Florida Water Management District) and L. R. Hayes (USGS) reported that ground-water levels in the upper limestone of

the Floridan aquifer at Fort Walton Beach, northwestern Florida, have declined as much as 52 m since 1940 because of heavy pumping. Henry Trapp, Jr., C. A. Pascale, and J. B. Foster (1977) concluded, on the basis of specific capacity tests, that the transmissivity of the upper limestone decreases sharply toward the Gulf of Mexico. Recent aquifer tests supported this conclusion.

The water from some wells near the gulf and bays contains more than 250 mg/L of chloride, primarily from saline ground water in the surficial aquifer entering the wells through leaky casings. The overlying Miocene Pensacola Clay and underlying Oligocene Bucatunna Clay Member of the Byram Formation are confining beds that protect the upper limestone of the Floridan aquifer from the vertical movement of saline water. As the potentiometric surface in the aquifer declines, however, the potential for encroachment of saline water is increased.

Iodide- and bromide-tracer studies in carbonate rocks

D. I. Leap and R. J. Sun compared radioactive sulfur-35 and tritium with nonradioactive bromide and iodide salts in a variety of different combinations during tracer tests in southern Nevada. The tests comprised single-well pulse, multiple-well point source, and two-well recirculating configurations. Analyses of tritium and sulfur-35 were accomplished by liquid scintillation, and analyses of bromide and iodide were accomplished by post-sampling neutron activation. Results showed that bromide is a conservative tracer in highly permeable dolomitic rocks and can be used in place of tritium. Iodide can be detected at lower concentrations than bromide but is more sorbable than bromide. These results are significant in that nonradioactive bromide can be used in places where radioactive materials are undesirable or prohibited by law.

Anion complex of gold as ground-water tracer

A new tracer with apparent potential for use in ground-water investigations was developed by L. L. Thatcher. The tracer, a cyanide complex of gold, was not affected by geochemical reactions with a wide variety of aquifer materials. In laboratory tests with columns of quartz sand, field sand, montmorillonite, kaolinite, calcium carbonate, and reducing mud, the tracer was shown to be conservative. The gold-cyanide complex gave the same breakthrough curve as bromide, a known conservative tracer, in every case. The gold tracer is detected with extreme sensitivity by neutron activation analysis. One gram

of gold, which can be detected in 2×10^8 L (166 acre ft) of water provides the sensitivity required for tracing in sites of moderate size, such as nuclear waste-disposal areas.

Barometric effects on water levels in unconfined aquifers

Water levels in wells screened only below the water table in unconfined aquifers respond to barometric effects. According to E. P. Weeks, these effects result from the fact that air movement (through the unsaturated zone) caused by a barometric change is slowed by the resistance of unsaturated materials to air flow and by their capacity to store or release air during a change in pressure. Because, on the other hand, a barometric change is transmitted instantaneously down a well bore, a temporary pressure imbalance between water in the well and in the aquifer occurs, thereby resulting in a water-level fluctuation that dissipates with time. Unlike barometric-induced fluctuations in confined aquifers, these water-level fluctuations generally are advanced in phase from barometric fluctuations, and their amplitudes may exceed those of barometric fluctuations under certain conditions.

Barometric-induced water-level fluctuations often can be accurately predicted by use of step-function response and numerical approximation of the convolution integral if the pneumatic diffusivity, a quantity analogous to hydraulic diffusivity, is first determined by trial-and-error analyses of simultaneous barometric and water-level records.

Surface resistivity used in locating major aquifer

J. N. Fischer reported that the use of resistivity soundings and profiles to locate changes in water quality and lithology within the shallow aquifer of eastern Palm Beach County, Fla., confirmed the existence of a highly permeable zone in the aquifer. A successful test-drilling program, based on the resistivity data, was economical in terms of both time and money.

Effects of carbonate facies and faulting on hydrogeology of the Edwards aquifer

Permeability and secondary porosity within the Edwards aquifer in the San Antonio area of southern Texas increase from Uvalde County in the west toward Bexar and Comal Counties in the east. The general eastward increase in permeability and porosity is attributed to the changes in the carbonate facies forming the Edwards aquifer and to the increased intensity of faulting towards the San Mar-

cos arch, which extends through the eastern part of the San Antonio area (Maclay and Small, 1976).

The changes in carbonate facies are related to three depositional environments—the Maverick Basin, the Devils River trend, and the San Marcos arch. The Maverick Basin, in the western part of the San Antonio area, contains deep-water marine carbonates that were deposited under relatively uniform conditions through most of their depositional history. These carbonates typically are relatively homogeneous, dense, nonporous, and poorly permeable mudstones that contain few sedimentary structures to enhance porosity development. The Devils River trend bounds the Maverick Basin and underlies much of the central part of the San Antonio area. This trend consists of an aggregate of shallow-water marine carbonates, including rudistid reefs, mounds, and tidal flats. The typical facies include skeletal grainstones, rudistid boundstones, and miliolid grainstones, wackestones, and mudstones that commonly are separated by local unconformities. They were deposited under moderate-to high-energy marine environments, and most lithofacies contain textural fabrics and sedimentary structures that contribute to high porosity and intrinsic permeability.

The San Marcos arch is underlain by shallow-water lagoonal, tidal, and salt-flat carbonates that have been subjected during times of emergence, especially during the Cretaceous Period, to extensive diagenetic alteration. These carbonates contain collapse breccias; selectively leached, burrowed, and honeycombed rocks; and porous dolomites. Secondary porosity development resulted in highly permeable zones that are laterally extensive throughout the eastern part of the San Antonio area.

The Edwards aquifer lies partly within the Balcones fault zone, and displacement along faults has contributed both to the formation of highly permeable zones near the fault planes and to abrupt changes in permeability resulting from the placement of permeable rocks opposite less permeable rocks. Periodic vertical movement near the San Marcos arch has produced rotated, normal-fault blocks that are generally uplifted toward the arch. At some places, rotated fault blocks are depressed toward the arch, thus producing scissor faults between the oppositely rotated blocks. The hinge zones between adjacent rotated blocks probably create geologic and hydrologic continuity between the blocks.

Tectonic movement along fault blocks occurred during Cretaceous and Tertiary time, but some movement may have occurred during Quaternary time. These displacements have disrupted previously

established ground-water flow patterns within the aquifer framework, but the effect of faulting on aquifer development is only partially understood. Transverse faulting, lateral and vertical displacement along normal faults, and rotation were recognized, but their hydrogeologic significance has not been determined.

Freshwater in offshore aquifers

According to F. A. Kohout, one of the most significant discoveries made during the AMCOR (Atlantic Continental Margin Coring) Project was that relatively fresh ground water (chloride, 5,000 ppm) forms a flat-lying lens about 150 m thick extending more than 100 km off the New Jersey coast. In general, very low-chlorinity ground water (<1,000 ppm) occurs at distances within 16 km of the Delaware-Maryland-New Jersey coast, but as far as 120 km off the Florida coast. The anomaly probably represents infiltration of freshwater into Shelf sediments during the Pleistocene glacial maximum when land extended far seaward of the present coastline. This conclusion is an agreement with the inferred origin of anomalously deep freshwaters found by pore fluid extraction in drill cores from Nantucket Island, about 60 km off the Massachusetts coast (Kohout and others, 1977). The freshwater now remains trapped beneath clay confining beds that have protected it from vertical intrusion of the overlying sea water since the Shelf was flooded about 8,000 years ago. An implication of the present work is that saltwater would have intruded into coastal well fields long before now, had it not been for the existence of the offshore, fresh ground-water lens.

The position of the freshwater-saltwater transition zone is a fundamentally important initial condition for mathematical models of saltwater encroachment and helps to explain why predictions of 40 years ago, made by using the Ghyben-Herzberg principle, have not been fulfilled. The present data, which are based on very few test holes, can easily be refined by the use of small barge-mounted drill rigs.

Pumpage shutdown yields water-level recovery information

According to C. B. Bentley, a labor strike at paper-pulp mills in Fernandina Beach, Fla., in September and October 1977, afforded a unique opportunity to observe the response of water levels in a deep and extensive cone of depression in the Floridan aquifer when 10 of 13 large industrial wells were not in operation. Artesian water levels rose

about 1 m at a distance of 15 km from the center of pumpage, 9–10 m at a distance of $2\frac{1}{2}$ km from the center of pumpage, and 38 m (from 42 m below sea level to 4 m below sea level) at the center of pumpage. It is estimated that recovery at the center of pumpage would have been an additional 10–15 m if the remaining industrial and all municipal wells had not been in operation. Preliminary calculations of hydraulic characteristics of the upper (Ocala Limestone) part of the aquifer from water-level recovery curves indicated a transmissivity of between 2,500 m^2/d and 6,000 m^2/d and a storage coefficient of about 0.0006.

Long-term storage of freshwater in saline aquifer

F. W. Meyer reported that tests support the use of saline artesian aquifers underlying southeastern Florida as a management option for the storage, conservation, and ultimate recovery of freshwater. During third injection-storage-recovery cycle, 787,000 m^3 of water was injected and stored for at least 6 months, and 318,000 m^3 of water was recovered before the chloride concentration exceeded 250 mg/L.

Base of freshwater above salt domes

Selected salt domes in Mississippi are being considered as repositories of radioactive wastes. C. A. Spiers observed that the base of freshwater above some of the domes is considerably higher than the regional base of freshwater. The study is concentrated on 5 of 49 relatively shallow piercement-type salt domes in southern Mississippi. The shallowest and largest of these is Richton dome; depth to the salt stock is 220 m and its cross-sectional area, at the 900-m depth, is about 16 km^2 . The base of freshwater over the top of the domes is 190 m higher than the regional base of freshwater.

SURFACE-WATER HYDROLOGY

The objectives of research in surface-water hydrology are to provide techniques for estimating the magnitude and variability of streamflow in time and space, under natural and man-modified conditions, to understand the flow process in stream channels and estuaries, and to define rates of movement and dissipation of pollutants in streams.

Estimating flow characteristics at ungaged sites

When R. H. Simmons and D. H. Carpenter first related several flood-peak characteristics of Delaware streams to four basin characteristics, the

standard errors ranged from 57 to 70 percent. The addition of two soil parameters, which were based on a soil classification system developed by the Maryland Department of State Planning, reduced the standard errors to about 40 percent.

R. W. Lichty and Fred Liscum developed an improved method of estimating flood-frequency at gaged sites on small streams. Their method uses a mapped climatic factor developed from synthetic annual floods generated by applying long-term rainfall records to a parametric rainfall-runoff model. Map estimates of the climatic factor and calibrated values of the model parameters were used to compute flood characteristics for 98 small gaged streams in a six-State study area. The improved estimate is a weighted average of computed and observed characteristics.

Using flow data for natural streams in Connecticut, M. P. Thomas showed that the 7-day, 10-year low flow within a major drainage basin is directly related to geology. For drainage areas underlain by stratified drift, this flow characteristic ranged from 0.0016 to 0.0055 $\text{m}^3/\text{s}/\text{km}^2$; in areas underlain by till and bedrock, it was approximately 0.00030 $\text{m}^3/\text{s}/\text{km}^2$. This information and streamflow data were combined to show the 7-day, 10-year low flow of streams in central Connecticut in map format.

B. L. Neely, Jr., used data from 91 gaging stations to develop equations for estimating discharges at 25- and 50-percent duration on ungaged streams in Louisiana draining less than 8,000 km^2 . Variables used were drainage area and mean annual precipitation; standard errors were 46 percent and 78 percent, respectively. The stage corresponding to the 25-percent duration discharge can be computed from discharge, channel cross section, channel slope, and channel-roughness coefficient.

Applications of modeling

In order to evaluate the effects of surface mining on runoffs, the infiltration component of a calibrated rainfall-runoff model was changed by 1-percent increments to reflect changes in the basin infiltration. J. G. Rankl found that a 1-percent change in infiltration resulted in a 10-percent change in runoff for a 4.45- km^2 semiarid watershed near Recluse, Wyo.

J. T. Armbruster used a multisite streamflow model to generate annual flow sequences at three sites in the Juniata River basin of Pennsylvania. The model preserves the mean, variance, and cross correlations of the observed data; it is also capable of preserving the Hurst coefficient. The generated

annual flows were disaggregated into monthly sequences by using a modification of the Valencia-Schaake model. The base-flow frequency and flow-duration characteristics of the generated monthly flows, with length equal to the historical data, compare favorably with the historical data, but 1-, 3-, and 6-month low-flow characteristics based on 100-year generated sequences were generally lower than those computed from historical flows for recurrence intervals greater than 20 years.

C. O. Peek and P. R. Jordan evaluated various methods of estimating peak discharge-frequency relations for use in drainage design by using rainfall and runoff data collected from urbanized drainage basins in and around Wichita, Kans. The method found most suitable for these basins is the SCS (Soil Conservation Service) synthetic hydrograph method with a modified method for calculating basin lag time. The method is sufficiently accurate for design flood calculations in the Wichita area if accurate information on soil conditions and land use is available.

Chintu Lai (1977a) applied an improved computer model of two-dimensional unsteady shallow-water flows by the method of characteristics to both hypothetical and actual embayments. The improvements include techniques of two-dimensional interpolation (Lai 1977b). The model performs better for tidal embayments than for flood plains. Simulation of two-dimensional unsteady flows requires much more computer storage and time and more manpower than one-dimensional simulation.

E. R. Holley and Nobuhiro Yotsukura (1978) completed the derivation of mathematical thermal boundary conditions for the free surface and the bed of an unsteady open-channel flow. Both boundaries are assumed to be in motion and the water is assumed to be carrying suspended sediment. Conditions considered include a variety of radioactive, advective, and diffusive fluxes of heat, and the possibility of some solar radiation reaching the bed.

Nobuhiro Yotsukura (USGS) and W. W. Sayre (University of Iowa) derived a two-dimensional transport equation for nonconservative solute in a steady river flow. The work is an extension of their previous derivation of a steady-state solute transport equation that employed a two-dimensional natural coordinate system following the meandering streamflow direction and a stream-tube concept using cumulative discharge rather than distance as the transverse independent variable (Yotsukura and Sayre, 1977).

L. F. Land prepared a generalized computer model for routing streamflow in an alluvial channel hydraulically connected to an aquifer. The model has the ability to predict the flow between a stream and an aquifer caused by bank storage and well pumpage and the outflow from the reach.

M. E. Jennings prepared a computer model for generalized uncontrolled reservoir routing including upstream routing. The program can be used with arbitrary but unique storage-outflow relationships.

Jennings and Land (1977) studied flow and sediment transport in the Atchafalaya River basin of Louisiana by using a calibrated model supplied by the U.S. Army Corps of Engineers. Three 50-year simulators for alternative channel conditions were examined. The analyses indicated a general trend of aggradation in the lower part of the floodway with a consequent trend toward increasing inundated area, especially at higher floodflows.

Land documented an unsteady-flow routing model based on a linear implicit finite-difference scheme. The model was applied to a reach of the Chattahoochee River of Georgia.

Jennings and Nobuhiro Yotsukura examined and summarized all surface-water and related modeling activities in the USGS Water Resources Division.

J. O. Shearman further developed a package of river-basin modeling programs and assisted in several applications in the Yampa River of Colorado and the Coreen River of Kentucky. Shearman (1977) also completed documentation of a user's manual for step-backwater and floodway studies.

H. E. Jobson and T. N. Keefer (1977) developed coupled flow, temperature, and transport models and verified them by using two extensive sets of data collected under highly unsteady flow conditions on a 27.9-km reach of the Chattahoochee River between Buford and Norcross, Ga. Existing solution techniques, with minor improvements, were applied to verify flow- and transport-modeling concepts. A linear-implicit finite-difference flow model was calibrated by using a depth profile obtained during steady low flow and by using unsteady-flow data obtained during March 1976. The flow model was verified by using dynamic stage and discharge data obtained in October 1975. The verification results were considered to be very good, particularly for flows of less than 100 m³/s.

Dye was added to the upstream end of the river reach at a constant rate while the river flow was highly unsteady. The transport model closely simulated observed dye concentrations in the river.

Even without calibration, the temperature model was capable of predicting temperature changes as large as 5.8°C through the reach with a root-mean-square error of 0.32°C (based on data for October 1975) and 0.20°C (based on data for March 1976).

Hydropulsation has significant effects on the water temperature below Buford Dam. These effects are very complicated because they are quite dependent on the timing of the release with respect to both the time of day and past releases.

Channel width as an indicator of discharge characteristics in Idaho

C. A. Thomas developed relations between channel widths at measuring sections and flow characteristics at gaging stations in Idaho. Data were available for nearly 120 sites for which the 10-year flood, Q_{10} , was measured by using standard methods in natural channels. The relation between Q_{10} and the channel width at the measuring section at that discharge, W_{10} , is expressed by the equation, $Q_{10} = 0.5 W_{10}^{1.9}$. The standard error of estimate is about 23 percent. Likewise, the relation between mean discharge for the period of record, Q_A , and width at the measuring section at the corresponding discharge, W_A , can be expressed by $Q_A = 0.09 W_A^{1.9}$. The standard error of estimate is about 18 percent.

The two equations indicate that for streams with Q_{10}/Q_A less than 6 (perennial streams with high base flows), channels tend to be rectangular or, in other words, $W_{10} = W_A$. For ephemeral streams, those with large ratios of Q_{10}/Q_A , ratios of W_{10}/W_A are greater than 1, and channels tend to be trapezoidal.

Standard errors of estimate for the described relations between widths and discharges are lower than any other relations between basin characteristics and streamflow characteristics investigated in studies by Thomas. On the basis of available data, the relations apply statewide. Evidently at least two "dominant" discharges determine channel widths. With appropriate interpretations and methodology, channel widths at typical measuring sites may have considerable potential for estimating streamflow characteristics at ungaged sites.

H. C. Riggs (1978) described the need for and the physical basis of equations for estimating streamflow characteristics from channel size, compared published estimating relations, examined reliability of flow estimates, and made some proposals for improving estimates.

PALEONTOLOGY

Research by USGS paleontologists involves biostratigraphic, paleoecologic, taxonomic, and phylogenetic studies on a wide variety of plant and animal groups. The results of this research are applied to solving specific geologic problems related to the USGS geologic mapping and resource investigation programs and to providing a biostratigraphic framework for synthesizing the geologic history of North America and the surrounding oceans. Some of the significant results of paleontological research conducted during the past year are summarized in this section by major geologic age and area. Many additional paleontologic studies carried out by USGS paleontologists in cooperation with their colleagues are reported in other sections of this publication.

MESOZOIC AND CENOZOIC STUDIES

Paleocene vertebrates from southern Hijaz Province, Kingdom of Saudi Arabia

Fossil vertebrates collected by D. L. Schmidt, C. T. Madden, and I. M. Naqvi from 17 localities at Jabal Umm Himar, near Turabah, southern Hijaz province, Saudi Arabia, represent the first Paleocene vertebrate fauna known from the Arabian Peninsula. These vertebrates, identified by F. C. Whitmore, designated the Jabal Umm Himar local fauna, include goblin sharks (cf. *Scapanorhynchus*), sand sharks (*Odontaspis macrota*), nurse sharks (*Ginglymostoma blackenhorni* and *G. maghrebianum*), angle sharks (*Squatina*), eagle rays (*Myliobatidae*), catfish, a large lungfish (*Ceratodus humei*); very large side-necked turtles (*Pleomedusidae*), and primitive crocodiles (cf. *Dyrosaurus*). The Paleocene age determination for the fauna is based upon first and last appearance data; the first appearance of *Odontaspis macrota*, *Ginglymostoma blackenhorni* and *G. maghrebianum*, and of catfish, are in the Paleocene; the last appearances of *Ceratodus* and African *Scapanorhynchus* are in the same epoch. The association of *Ginglymostoma blackenhorni* and *Ceratodus humei* suggests a late early or early late Paleocene age, one correlating with the late Danian or early Thanetian of Europe.

The paleoenvironment of Jabal Umm Himar was estuarine. The presence of such a coastal environment at the locality indicates that at least a shallow seaway must have existed in the At Ta'if region during the earliest Tertiary.

Pliocene and Pleistocene holarctic correlation of microtid rodents

In the past fifteen years concentrated study by paleontologists in nearly all countries of Europe has established a rather precise biostratigraphy of the upper Miocene, Pliocene, and Pleistocene continental deposits of that subcontinent. This biostratigraphy has been based largely upon the rodent family Microtidae, the meadow mice and their relatives. Four Pliocene (one at least partly equivalent to the late Miocene Messinian Stage) and two Pleistocene mammalian ages have been recognized on the basis of the faunal composition of these rapidly evolving rodents.

As the pattern of faunal succession became evident, it became obvious that the distinctive changes were derived not only through evolution of the population but also through repeated invasion by new forms from an extra-European source. At least five waves of immigration are recognized during the last 5 million years of European history. Because of the temperate to arctic preferences of the microtid rodents and of the occurrence of similar forms in North America, it is inferred that the source of the immigrants was Asia, although studies of the fossil microtid rodents of this great land mass are few. It was further concluded, through correlation with glacial events, that the invasions marked periods of climatic optimum for the spread of grasslands, and their contained meadow mice, from Asia westward into Europe.

The record of fossil microtid rodents in North America has never shown evidence of repeated waves of immigrants from Asia, as has been found in Europe, and their biostratigraphy has not been as useful. It seems possible that the climatic events presumably responsible for the dispersal of microtid rodents from Asia into Europe were holarctic in extent and that, if these rodents were able to disperse westward into Europe, they might also have been able to spread eastward into North America. On this assumption C. A. Repenning (USGS), in collaboration with Oldrich Fejfar (Czechoslovakian Geological Survey), decided to take a closer look at the fossil microtids of North America. Although major revision of the classification and identification of North American fossil microtids is required, preliminary work has established the fact that each of the five invasions of Europe is also recognizable in the Pliocene and Pleistocene of North America. These define sharply the beginnings of the North American mammalian ages, or their subdivisions: early Blancan (5 m.y.), middle Blancan (3.5 m.y.),

late Blancan (2.5 m.y.), Irvingtonian (1.7 m.y.), and Rancholabrean (0.7 m.y.).

Through holarctic cross correlation, radiometric dates and identifiable magnetic events of each continent may now be applied to the microtid chronology of the other, strengthening both. And identification of microtid lineages in both continents has enabled the recognition of evolutionary trends and stages, which permits further subdivision, by provincial evolution, of the biohistoric units defined by holarctic dispersal waves. Never before have the late Neogene mammalian faunas of North America been so precisely datable.

Dinoflagellates and acritarchs prove useful in the biostratigraphic and paleoecologic analysis of Santonian-Age formations in southwestern Arkansas

Because of the sparcity of calcareous mega- and microfossils, the age and paleoecology of the Tokio Formation (Upper Cretaceous) of southwestern Arkansas have been difficult to determine. Abundant and well-preserved dinoflagellates and acritarchs (both groups are acid-resistant, organic-walled marine palynomorphs) were recovered from the middle part of the Tokio Formation of Sevier County, Arkansas, by F. E. May. This microflora indicates a Santonian Age.

Inland limit of the Croatan sea; Pliocene and Pleistocene beds at Fountain, North Carolina

Mollusks from deposits at 22.9 m elevation near Fountain in Pitt County, North Carolina, correlate with the molluscan assemblages of the Croatan Formation from farther east in North Carolina. At the Martin Marietta Fountain Quarry these fossiliferous beds overlie a large pinnacle-shaped body of metagranite, and most macrofossils are in a unit 3 m above the contact. This body of metagranite is unique in being located so far east (35 km from the Fall Line) and in its position within 9 m of the 30 m elevation land surface. The molluscan fauna, studied by B. W. Blackwelder and L. W. Ward, contains the bivalves *Crassostrea virginica* and *Mulinia lateralis* in abundance and suggests a shallow water near shore environment of deposition. Just to the east of the quarry shallow augering yielded a more open marine assemblage, which suggests an early Croatan age representing approximately the same horizon as the lowermost bed exposed at Colerian, on the Chowan River, North Carolina. The fauna from the Fountain Quarry exposure suggests very close proximity to the inland extent of the Croatan sea.

New age data, Early Cretaceous, Colorado Plateau

Samples collected by R. H. Tschudy, B. D. Tschudy, and L. C. Craig yielded palynomorphs that permit definite age assignments to the upper parts of the Cedar Mountain and Burro Canyon Formations. The Cedar Mountain samples yielded assemblages of palynomorphs dominated by primitive tricolpate and monosulcate pollen species including *Striatopollis paraneus*, *Retitricolpites vulgaris*, *Asteropollis asteroides*, and *Clavatipollenites* cf. *C. hughesii*. These taxa are present in the Albian, and in the Western Interior of North America they are limited to middle Albian and younger rocks. *Striatopollis paraneus* appears to be limited to the middle and upper Albian. The absence of tricolporate or triporate pollen in an otherwise good assemblage indicates a pre-upper Albian Age. The upper part of the Cedar Mountain Formation is therefore of Albian, probably middle Albian Age.

The Burro Canyon samples yielded Early Cretaceous taxa such as *Coronatispora valdensis* and well-preserved specimens of *Clavatipollenites hughesii*. Not even a single specimen of primitive tricolpate pollen was present in the assemblage. *C. hughesii* has not been reported from pre-Albian rocks from the Western Interior, but is known from the Barremian of England and from the Aptian and lower Albian of eastern United States. Based on the absence of tricolpate pollen, the upper part of the Burro Canyon Formation thus appears to be somewhat older than the upper part of the Cedar Mountain Formation. Palynomorphs indicate an age for the upper part of the Burro Canyon no older than Aptian and no younger than early Albian.

North Atlantic Cenozoic mollusks in northern Alaska

Preliminary interpretation by L. N. Marincovich of Cenozoic mollusks from near Ocean Point, on the lower part of the Colville River of the Alaskan North Slope, indicates that the fauna is of entirely Atlantic affinities. Discovery of this Atlantic fauna was unexpected and was made during investigations of overlying strata bearing an anticipated Pacific mollusk fauna. Precise age with the Cenozoic of this Atlantic fauna is not yet known, but it must predate the Miocene and Pliocene opening of Bering Strait. Because only one other Cenozoic fauna of Atlantic affinities is known from Alaska (and that has a species composition entirely different from the Ocean Point fauna), this latest find provides new insight into the character of the Atlantic-Arctic

mollusk fauna previous to the opening of Bering Strait. After Bering Strait opened, Pacific species flooded north and largely displaced the established Arctic fauna. The Ocean Point mollusks allow correlation with Cenozoic faunas across the present North Atlantic margin and better relate the opening of Bering Strait to synchronous events in the Atlantic Arctic.

Miocene diatoms from the Montesano Formation of Weaver (1912), Washington

The Montesano Formation of Weaver (1912) near Aberdeen, Washington, contains early late Miocene diatoms in the upper two thirds of its type section. Benthonic foraminiferal assignments of this section to the Mohnian and Delmontian Stages are thereby refined. Diatom studies by J. A. Barron reveal correlation with the upper Mohnian Stage in California and with the Empire Formation near Cape Blanco, Oreg. The type Empire Formation at Coos Bay, Oreg., on the other hand, contains younger diatoms of late late Miocene age. This represents the first application of refined diatom biostratigraphy to Oregon and Washington.

Cretaceous time scale for North America

M. A. Lanphere and D. L. Jones reviewed the Cretaceous time scale from North America in a symposium on the geochronologic time scale at the 25th International Geological Congress (Lanphere and Jones, *in press*). The Upper Cretaceous strata of the Western Interior of North America contain a rich molluscan fauna and abundant intercalated bentonites. This combination has permitted the development of detailed time scale for the Late Cretaceous. Volcanic rocks are rare in the Lower Cretaceous of North America. Several isolated time-scale points have been reported for Lower Cretaceous rocks, but the Early Cretaceous time scale is not well defined. Nearly all of the available isotopic ages are K-Ar mineral ages. Data have been recalculated using decay constants for ^{40}K based on the refined activity for ^{40}K based on the refined activity for ^{40}K proposed by Beckinsale and Gale (1969) and the isotopic abundance of ^{40}K measured by Garner (Garner and others, 1976). The best current estimates for system and series boundaries are: Cretaceous-Tertiary boundary—65–66 m.y.; Lower Cretaceous-Upper Cretaceous boundary—96 m.y.; Jurassic-Cretaceous boundary—138 ± 3 m.y.

A new Upper Cretaceous ostracode zone

A study of the ostracodes of the Severn Formation of Maryland by Elisabeth Brouwers has resulted in the establishment of a multitaxon-concurrent-range-zone (Oppel-zone) in the upper part of the Navarroan Provincial Stage of the Atlantic and Gulf coastal province. The fauna characteristic of this Upper Cretaceous biostratigraphic unit, named the *Ascetoleberis hazardi* Oppel-zone, has been traced from New Jersey to Arkansas. The ostracode zone is approximately equivalent to the *Globotruncana gansseri* planktic foraminifer subzone of middle Maestrichtian Age.

Cretaceous biostratigraphy in Arkansas

The Brownstown Marl, Ozan Formation, Annona Chalk and Marlbrook Marl of southwestern Arkansas contain abundant ostracodes. Data gathered by Elisabeth Brouwers and J. E. Hazel suggest that deposits of these Austinian and Tayloran units can be placed in six ostracode zones. The study has resulted in a more precise correlation of the rocks of the various outcrop areas of southwestern Arkansas and southeastern Oklahoma, and with other coastal province localities. Some of the conclusions are that the so-called "beerjoint chalk" of southeastern Oklahoma is of early Tayloran Age and not Austinian as has been commonly supposed; the Marlbrook Marl in the Columbus Quadrangle is the biostratigraphic equivalent of the Annona Chalk and the overlying Marlboro of the quadrangle farther to the west; the Marlbrook of the north-eastern outcrop area (Antoine and Hollywood quadrangles) is equivalent only of the upper part of the Marlbrook to the southwest, and rocks mapped as Ozan Formation are biostratigraphic equivalents of the middle part of the Marlbrook and the middle part of the Ozan to the southwest; no Annona or late Ozan-age rocks seem to be present in the north-eastern outcrop area.

PALEOZOIC STUDIES

Radiolarian age-dating of Paleozoic cherts

It has been known for 5 years or more that Mesozoic radiolarian cherts can be dated accurately by means of radiolarians freed by hydrofluoric acid leaching. Little work had been done on Paleozoic cherty rocks, however, and they remained essentially undatable. During the past year, a reconnaissance survey was conducted by D. L. Jones, B. R. Wardlaw, A. G. Harris, and J. E. Repetski

(USGS) and Brian Holdsworth (University of Keele, England). Many Paleozoic cherts were found to yield well-preserved radiolarians and conodonts. The joint occurrence of these two fossil groups in the same sample has allowed rapid and accurate calibration of radiolarian faunas, so that now there is a crude outline of basic morphological types ranging in age from Ordovician to Permian.

Many Paleozoic cherts in Alaska, British Columbia, Washington, Oregon, and Nevada now have been dated. In many cases, the ages obtained are widely at variance with previously suspected ages based on presumed relations to other fossiliferous rocks. These changes in age have had profound effects on the interpretation of the geologic history of many rock units.

New floral zone in Mississippian of Virginia and West Virginia

Paleobotanical studies in connection with Pennsylvanian System stratotype study have identified a new floral zone in Upper Mississippian strata underlying the Pennsylvanian System stratotype section. The occurrence of this zone, predicted by Read and Mamay (1964, p. K6), was confirmed by W. H. Gillespie (West Virginia Department of Agriculture and University of West Virginia) and H. W. Pfefferkorn (University of Pennsylvania) who found *Stigmaria stellata*, *Sphenopteris elegans*, *Sphenophyllum tenerimmum* and *Lepidodendron veltheimii* in the flora between zones 3 and 4 of Read and Mamay (1964).

New information about the evolution of mollusks during the Cambrian and Ordovician

John Pojeta, Jr. (USGS), in cooperation with Bruce Runnegar (University of New England, Armidale, Australia), is continuing his studies of the early evolution of the Phylum Mollusca. Some 50,000 specimens of Ordovician pelecypods have been examined. This material is largely from the tri-State area of Kentucky, Ohio, and Indiana, but the collection has been supplemented significantly by the borrowing of specimens from most of the museums in North America and Australia and from a few museums in Europe.

It can now be demonstrated that pelecypods probably evolved from the pseudobivalved rostroconchs, which in turn are descended from the univalved helcionellacean monoplacophorans. There is a series of morphologically intermediate forms, from the Early and Middle Cambrian, between these three classes that make these conclusions likely. During the Ordovician, pelecypods diversified into 125 known

genera that can be placed in seven subclasses; the subclasses are based upon the first major adaptive radiation of the Pelecypoda in the Ordovician. By the end of Ordovician time, pelecypods are ecologically highly diverse and include: (1) infaunal burrowing deposit feeders, (2) infaunal burrowing suspension feeders, (3) siphonate infaunal suspension feeders, (4) endobysate (semi-infaunal) suspension feeders, (5) facultative boring suspension feeders, (6) nestling suspension feeders, and (7) epibysate (epifaunal) suspension feeders.

The pseudobivalved rostroconchs are important elements of Early Ordovician faunas around the world, but they gradually diminished in diversity throughout the Ordovician and only two genera survived into the Silurian. This decrease in the diversity of rostroconchs is probably because of competition with the pelecypods, the latter class being much more efficient at burrowing.

New information about Ordovician scaphopods from central Kentucky and Late Cambrian rostroconchs from Australia suggests that scaphopods evolved from elongate rostroconchs and that the class Scaphopoda evolved in Ordovician time rather than in Devonian time as was previously thought.

The discovery of Early Ordovician polyplacophorans in Australia and the reexamination of various previously-described Cambrian and Early Ordovician polyplacophorans indicate that *Matthevia*, previously thought to be the sole known member of a separate class of mollusks, is the oldest known polyplacophoran. Polyplacophorans probably evolved from the shell-less Aplacophora in Late Cambrian time.

Lower-Middle Ordovician boundary in south-central Appalachian Basin-conformity and unconformity—the Beekmantown Group "updated"

Analysis of conodont fauna in thick carbonate sections that contain the Lower-Middle Ordovician boundary in the Great Valley of Maryland and in the northern part of the Shenandoah Valley of Virginia (a belt at least 240 km long) studied by A. G. Harris and L. D. Harris shows that:

- No unconformity separates rocks of Early and Middle Ordovician age in the Great Valley of western Maryland, as similarly suggested by Sando (1957). His conclusion was based on the absence of physical evidence of an unconformity, but could not be supported, at that time, by faunal evidence. Conodonts, virtually the only fossils of biostratigraphic value within the chiefly dolomite sequence, now show a com-

plete faunal succession from upper Canadian (Lower Ordovician) through middle White-rockian (Middle Ordovician) in the upper 200 m of the Rockdale Run Formation of the Beekmantown Group; succeeding Whiterockian and Chazyan faunas occur in the overlying Pinesburg Station Dolomite of the Beekmantown Group (Boger and Bergström, 1976). Thus, in western Maryland, the passage from Lower to Middle Ordovician is continuous and lies within the upper part of the Beekmantown Group.

- The same late Canadian to Whiterockian conodont faunal succession also occurs in the upper part of the Beekmantown Group in the northern part of the Shenandoah Valley as far south as Rockingham County, Virginia. Physical and faunal evidence for an Early Middle Ordovician unconformity occurs first in the vicinity of Lexington, Va.

These data are significant to the exploration for strataform zinc deposits in the Appalachian Basin, as much of the zinc production in the basin comes from porosity zones in Lower Ordovician dolomites associated with the Lower-Middle Ordovician unconformity.

Conodont-based Lower Ordovician correlations in eastern Pennsylvania

The Rickenbach Formation (Lower Ordovician) of eastern Pennsylvania has yielded identifiable fossils. As part of a larger study of Early Ordovician conodonts of the central Appalachians, J. E. Repetski systematically sampled the dolomites of the Rickenbach Formation at the type locality in central Berks County. A sparse fauna from a sample 1.5 m above the base of the exposed section includes *Acontiodus iowensis* s.f., *Clavohamulus densus*, *Loxodus bransoni*, and *Paltodus bassleri*. These taxa are characteristic of North American midcontinent Early Ordovician conodont Fauna C of Ethington and Clark (1971), and the latter three taxa are limited to that fauna. No fossils have been reported previously from the Rickenbach Formation except for a few non-identified dolomitized mollusks. The presence of Fauna C conodonts in the lower member of the formation shows that this part of the Rickenbach is correlative, at least in part, with the upper part of the Stonehenge Formation in sections to the west and southwest.

A dolomite farther to the east, near Buckingham in Bucks County in Pennsylvania collected by Repet-

ski and A. A. Drake, Jr., yielded *Acontiodus iowensis* s.f. and *Acodus oneotensis* (another Fauna C indicator). This sample shows that faunally, as well as lithically, the Rickenbach Formation may be recognized as far east as Bucks County.

Coral zones and problems of Mississippian stratigraphy in the Williston Basin

Study of Mississippian corals from the Madison Group in seven well cores from the Williston Basin of Montana and North Dakota by W. J. Sando resulted in a reassessment of the value of corals for resolving problems of subsurface stratigraphy. Coral zones are useful for correlation of subsurface sections with outcrop sections and are more useful for correlation within the Williston Basin subsurface than previously thought. The distribution of corals in the Charles Formation and Mission Canyon Limestone indicates that the Charles is a time-transgressive unit of late Osagean and early Meramecian age and is partly equivalent to the Mission Canyon Limestone of outcrop. The base of the Charles transgresses the Osagean-Meramecian boundary, climbing basinward in the well cores studied. The occurrence of corals also indicates that the Charles is separated from the overlying Kibbey Formation (Chesterian) by a disconformity that represents an erosion interval ranging from middle Meramecian into early Chesterian.

Paleoecology and biofacies of Osagean conodonts

C. A. Sandberg (USGS) and R. C. Gutschick (University of Notre Dame) (1977a, b) postulated a sedimentological model to explain the paleoecology and biofacies of Early Mississippian (Osagean) conodonts. The model is based on conodont faunas recovered from transported and in situ sediments in the deep-water (± 300 m) phosphatic shale member of the Deseret Limestone and its shallower equivalents on the slope and carbonate shelf to the east. The model assumes that conodonts are hard parts of a group of unknown soft-bodied organisms that had both nektic and nektobenthic habits, and that these hard parts fell to the seafloor, where they either remained or were transported seaward by turbidity currents and debris flows. The model also assumes that nektic conodonts had depth-stratified habitats—either close to the surface in an upper, photic zone or at intermediate depths of the aerobic zone—and that nektobenthic conodonts lived within the aerobic zone on the slope and carbonate shelf. Nektobenthic conodonts probably did not inhabit the dysaerobic (minimal-oxygen) zone in the deep

basin, and all conodonts found there are interpreted to have originated in the overlying aerobic zone or to have been transported seaward from the slope. These assumptions are strongly supported by interpretations of the character of the sediments and of the contained planktic radiolarian and foraminiferan and benthic agglutinate foraminiferan faunas. On the basis of this model, interpretations of the paleoecology of the conodont faunas were made that the ubiquitous *Polygnathus communis communis*, *Anchignathodus penescitulus*, and a species close to *Bispathodus stabilis* were nektic and lived in the upper, photic zone. However, *A. penescitulus* ranged much farther seaward. *Doliognathus latus* and *Scaliognathus anchoralis* were nektic and lived at intermediate depths above the basin, slope, and shelf. Species of *Bactrognathus* also were nektic and lived at intermediate depths, but they did not venture as far seaward. Species of *Gnathodus* and *Pseudopolygnathus* were nektobenthic and lived both on the carbonate shelf and its westward slope. *Eotaphrus burlingtonensis* inhabited shallow, aerated water of the upper slope and shelf, whereas *Polygnathus communis carina* lived only in very shallow water of the carbonate shelf.

Permian-Triassic boundary in western Wyoming and parts of Idaho and Montana

William Schock (University of Wyoming), working with B. R. Wardlaw and E. K. Maughan (both USGS), has defined a new unit within the Park City Formation and has clarified the Permian-Triassic boundary in a study of Upper Permian and Lower Triassic strata in western Wyoming and adjacent parts of Montana and Idaho. The new unit is lithologically and spatially intermediate between the Ervay Member of the Park City Formation and the Shedhorn Sandstone and comprises chiefly paleorange to light-grayish-brown-weathering calcareous and siliceous mudstone. Lithologically, the rocks of this new unit closely resemble rocks of the overlying Dinwoody Formation (Triassic), but the former are characterized paleontologically by *Echinauris*, a spiny productoid brachiopod that probably is Wordian (early Guadalupian) in age. The unconformably overlying Dinwoody is characterized paleontologically by sparse *Claraia* and *Lingula* and comprises lateral and vertical sequences of transgressive-regressive facies deposited upon a nearly planar, horizontal shelf. Scattered chert and phosphorite grains derived from the Phosphoria Formation are found as high as 30 m above the base in most sections of the Dinwoody. The superficial resemblance

between rocks of the newly defined unit of the Park City and those of the overlying Dinwoody has led to the conclusion that Permian fossils have been retrieved from the Triassic Dinwoody (Gere, Schell, and Moore, 1966; Waterhouse, 1973). This erroneous conclusion has been used in arguments by Waterhouse (1976) and Waterhouse and Bonham-Carter (1976) for placing the Griesbachian Stage in the Permian rather than at the base of the Triassic.

PLANT ECOLOGY

Wetland vegetation reflects hydrology

A study in Wisconsin by R. P. Novitzki showed that the hydrology of a wetland site influences the plant community and soil-formation processes that occur in the wetland. Grassy wetlands are typically too wet during some periods to allow trees or shrubs to grow. Brushy areas are drier, and flood-plain forests are dry most of the time. Forested bogs, cedar swamps, and hardwood swamps may be wet, but peat or muck accumulations are so thick that the surface is dry enough to allow shrub and tree growth. Peat and muck accumulate in areas that are almost continuously wet and where water movement is minimal; accumulation continues during wet periods until it is balanced by decomposition or burning during dry periods.

Water-quality differences also are reflected in a wetland plant community. Cedar swamps occur where ground-water inflow provides a source of nutrients, whereas bogs exist on the limited nutrients supplied by direct precipitation on the wetland.

Distribution of forest plants reflects differences in environment

R. A. Sigafos found that the distribution of plants in the forest surrounding the USGS National Center at Reston, Va., reflects differences in underlying bedrock, surface water, and past land use. Northern red oak grows only in areas underlain by diabase and hornfels of Triassic age. Chestnut oak is most abundant in, and nearly limited to areas underlain by pelitic schist, and, before the American chestnut was killed by chestnut blight in the 1920's, it also grew only in these areas. Black tupelo and red maple are predominate in poorly drained areas that are wet most of the year. The largest unit in the forest consists of several species of oaks, but red oak, chestnut oak, black tupelo, and red maple are absent as canopy trees. Dense stands of 50- to 60-year-old Virginia pine grow where cultivation was

abandoned after World War I. Tulip trees have reproduced in moist to wet areas that were lumbered almost 35 years ago.

Tree-growth rates reflect changes resulting from drainage construction

R. L. Phipps and D. L. Ierley reported that loblolly pines (*Pinus taeda*) growing in the Great Dismal Swamp of North Carolina and Virginia contain tree rings that were sensitive to hydrologic change resulting from drainage construction. Regression analysis of data, representing a time period prior to ditching, and climatic and prior growth factors explained nearly 85 percent of the tree-ring width variance, but data representing the time since ditch construction explained only 70 percent of the variance. Prior to ditching, growth was most limited by dry summers that followed dry summers. Tree-ring growth after ditching was less limited by precipitation and more limited by temperature. It appeared that, following ditching, the root systems of the trees increased in size, and that size increase resulted in increased ring growth. Apparently, this "root release" following lowered water levels is analogous to crown release following lumbering.

National wetland-classification system

The USGS and the U.S. Fish and Wildlife Service developed a new national wetland-classification system for the Fish and Wildlife Service's current national wetlands inventory. According to V. P. Carter, wetlands classes, subclasses, and dominance types are based upon vegetation, soils, and hydrology. The system allows a nationwide comparison of inventory data by ecological system, by physiographic region, by wetland class and subclass, and by drainage basin or hydrologic unit.

Perennial streams and wetlands of Arizona

D. E. Brown (Arizona Game and Fish Department), N. B. Carmony (USGS), and R. M. Turner (USGS) (1977a) compiled a 1:1,000,000-scale map that shows perennial streams and important wetlands in Arizona. Three categories of perennial streams are shown—unregulated streams, regulated streams, and streams containing only effluent or wastewater. Important wetlands, the other major category shown, are separated into two size categories and classified by regulatory criteria similar to those for perennial streams. Regulation of flow by dams causes changes in the streamflow pattern and the water-temperature regime. The effects of these

changes on the aquatic and riparian biota usually result in new assemblages of mainly introduced plant and animal species (Brown, Carmony, and Turner, 1977b). Because saltcedar (*Tamarix chinensis*), for example, is poorly represented on unregulated perennial streams but is usually found along regulated streams and streams of effluent, inferences concerning its distribution can be drawn from the map.

CHEMICAL, PHYSICAL, AND BIOLOGICAL CHARACTERISTICS OF WATER

Effects of land use on water quality of rivers

A recent study by D. J. Lystrom and F. A. Rinella III (1978) showed that land use has a measurable effect on water-quality characteristics of subbasins of the Susquehanna River basin in Pennsylvania and New York. Lystrom and Rinella studied 11 water-quality characteristics, including mean concentrations and calculated yields of suspended sediment, dissolved solids, and various chemical species of nitrogen and phosphorous. Water-quality characteristics were related to land use, climatic, and physiographic characteristics of subbasins by using multiple-regression analysis. Usable regression models were defined for 10 of the 11 water-quality characteristics. These models explain from 58 to 89 percent of the variation of the water-quality characteristics, with standard errors of estimate ranging from 17 to 75 percent. The 10 models can be used to estimate water quality at specific stream sites or to simulate the generalized effect of a specific basin characteristic, such as land use, on water quality. In the Susquehanna River basin, land use was associated with higher concentrations and yields of the water-quality constituents. The greatest effect noted was on nitrate, for which the range of observed yields was 20 times higher than the simulated range under background conditions; this difference was attributed primarily to agricultural fertilization, animal waste, and urbanization.

Green River basin water-quality investigations

Dissolved-solids concentrations and loads can be estimated from streamflow records by using a regression model derived by L. L. DeLong from chemical analyses of monthly samples. The regional salinity model takes seasonal effects into account by the inclusion of simple-harmonic time functions. Monthly mean dissolved-solids loads simulated for a 6-year period at USGS water-quality stations

in the Green River basin in Wyoming agree closely with corresponding loads estimated from daily specific-conductance records. In a demonstration of uses of the model, an average gain of 114,000 t/yr of dissolved solids was estimated for a 6-year period in a 110-km reach of the Green River from Fontenelle Reservoir to the town of Green River, including the lower 48-km reach of the Big Sandy River.

M. J. Engelke, Jr., determined aquatic populations and biological communities including population distribution patterns, community edge effects, the energy budget, the food pyramid, and nutrition levels between various kinds and types of plants and animals in Salt Wells Creek, a low-nutrient plains stream in the Green River basin of Wyoming. The algae and stream invertebrates were studied to determine base-line data and biological indicators of water quality. Phytoplankton, periphyton, and benthic invertebrates were collected to determine the chemical ranges and food chains of aquatic indicators of water quality.

Chemical quality of streams in North Carolina

The water quality of large rivers in North Carolina is being studied in order to relate the present water quality to past water quality and to "natural" water quality of pollution-free streams in the same geologic region. Fifteen sampling sites, representing nine major watersheds in the State, were chosen for this study. To date, studies of the French Broad and Neuse River basins have progressed to the point where preliminary results can be reported. M. S. Weiner and D. A. Harned found that water in the French Broad River basin contains a predominance of bicarbonate, sulfate, sodium, and silica. Pollution, as indicated by increased concentrations of sulfate, sodium, and chloride in the stream system, increased from 1958-67, and decreased from 1974-76. Similar analyses show a decrease in pollution during 1974-76 for the Neuse River basin.

Chemical-quality data collected from 47 small streams in North Carolina were used to estimate average concentrations for naturally occurring constituents during periods of high and low streamflow. The streams have drainage areas ranging from 0.8 to 44 km², have no known point sources of pollution, and generally represent natural conditions. Water samples collected during base flow represent the quality of ground water, and flood-flow samples represent overland runoff quality. C. E. Simmons reported that concentrations of most of

the major constituents correlated well with the geology of the region whereas concentrations of nitrogen and phosphorus correlated with land-use characteristics. No correlation was found between trace metal values and rock type, land use, or physiographic region.

New Jersey water-quality investigations

J. C. Schornick, Jr., and D. K. Fishel investigated the impact of storm runoff on a small stream draining a planned residential community in southern New Jersey. Stream samples collected during periods of storm runoff from a 23.7-km² study area were analyzed for up to 86 parameters (including total and dissolved phases of many parameters). Fifty-nine parameters were found in detectable amounts at some time during the study. Most of the parameters not detected were toxic metals, insecticides, or herbicides. Calculation of mean loads for 38 of the 59 detected parameters showed that the 9.92-km² residential area is contributing significantly less of the total load than is the 13.8-km² nonresidential area. Notable exceptions to this are 2, 4-D, silvex, lead, and suspended iron. Measured maximum concentrations of As, Fe, Pb, Mn, 2, 4-D, silvex and total coliform bacteria exceeded acceptable maximum concentrations. For mean concentrations, however, only suspended and dissolved iron, dissolved manganese, silvex, and total coliform bacteria exceeded the recommended maximums. Coliform values were high under all flow conditions.

The USGS, in cooperation with the New Jersey Department of Environmental Protection, is studying the effects of trial releases from Round Valley Reservoir to a nearby stream. The study area includes the South Branch Rockaway Creek, Rockaway Creek, and the Lamington River. The various aspects incorporated into the study include streamflow, channel geometry, time of travel, sediment transport, water quality, and aquatic biology.

M. C. Yurewicz reported that computations for erosion sites indicated no overall trend, although there was significant erosion of the bank opposite the release point. Concentrations of nutrients and common inorganics decreased due to the dilution effect during releases. Sediment concentrations increased significantly during the initial release period but dropped off rapidly. Data collected during a 3-day release period indicated a gradual decrease in turbidity. During each release, the suspended-sediment peak concentration decreased in the downstream direction.

Assessment of water quality in an Ohio watershed

Eight times over a period of 13 months, physical, chemical, and biological data were collected at eight sites in the Rattlesnake Creek watershed in Ohio. Land use in this basin is approximately 85 percent agricultural. K. F. Evans investigated effects of, and recovery from, sewage effluent entering the stream system in the upper portion of the watershed. Ammonia (as N) concentrations were as high as 23 mg/L, but they decreased with concomitant increases in other forms of nitrogen (NO₃, organic nitrogen) downstream. Nitrate concentrations generally were about 1.5 mg/L at all sites during the low-flow periods of summer and fall, but during the winter and spring runoff period, nitrate concentrations were between 5 and 10 mg/L. Concentrations of heavy metals in bottom materials were low (less than 40 μg/g). Pesticide residues in bottom materials were also low (0–3.0 μg/kg) except for chlordane which, at two of three sites, was 10 μg/kg. Benthic samples indicated moderate to heavy pollution stress (diversity indices, less than 2.0), in the upper portion of the watershed. Coliform counts at times were high (up to 72,000 colonies/100 mL for total coliform bacteria) and usually indicated animal or mixed animal-human sources (fecal coliform-fecal streptococcus ratios generally less than 2.0). The lower portion of the watershed generally showed significant improvements in water quality, thus indicating strong recovery from conditions upstream.

Chemical reactivity of sediment in aqueous systems

Sediment surfaces in natural water systems acquire coatings of solid organic and inorganic materials and layers of adsorbed ions by a wide variety of sorption and chemical reactions with dissolved chemical species. The distribution of a given constituent between dissolved and solid forms depends on system parameters such as pH, ionic strength, temperature, and nature of the sediment surfaces. Sediments can act as sources or sinks of particular chemical species, depending on how these factors may change in the natural aquatic environment. Experimental methods for investigating surface reactions with respect to their applications to natural water-sediment systems can be evaluated by many different techniques. However, according to M. C. Goldberg and E. R. Weiner, it appears that only photon spectroscopy is useful for in situ measurements of reactions at the solid-water interface. Direct measurements of surface species surface re-

action mechanisms, and adsorbent-adsorbate bonding properties have been made mainly on pure adsorbents and adsorbates with homogeneous and regular structure. It is suggested that there now is enough reference data on these model systems to allow the useful application of photon spectroscopy to a systematic study of natural water-sediment systems.

Analyses of Willamette River bottom material and elutriates

Bottom material from the Willamette River of Oregon was mixed separately with waters of the Columbia River and the Willamette River, and their respective elutriates were analyzed as part of an evaluation of potential environmental effects of a planned dredging operation that would include dredging the Willamette bottom material from the Portland Harbor, loading it onto a hopper barge with water-sediment overflow, and transporting and dumping the nutrient-enriched material into the Columbia River. According to J. F. Rinella and S. W. McKenzie (1977), the bottom-material analyses revealed chemicals that could possibly be toxic to aquatic life, and indicated that the elutriates also should be analyzed for these chemicals. The elutriate analyses indicated that ammonia, manganese, copper, and zinc must be diluted by receiving water to achieve the EPA's recommended maximum levels. The pesticides present in the bottom material were not detected in the elutriates.

Chemical quality of ground water in Kansas

Approximately 300 wells were sampled as part of network investigations in Kansas. According to C. D. Albert, the very limited chemical analyses showed that ground-water quality in Kansas is highly variable and reflects the State's wide range of geologic formations. In many wells in south-central Kansas, concentrations of chloride and sulfate exceed maximums recommended for drinking water. Other isolated samples gave analyses results showing excessive nitrate and selenium. Chemical analyses for organic substances on a limited number of samples indicated that they were not present in measurable quantities.

High nitrate concentrations found under a Nebraska prairie

Unexpectedly high nitrate-nitrogen concentrations were found by W. F. Lichtler (USGS), D. I. Stannard, and Edwin Kouma (Nebraska Water Resources Center) in water from a well tapping a Pleistocene sand and gravel aquifer beneath a 1-hm² plot of virgin prairie in east-central Nebraska. The source of

the nitrate (N) concentrations, which were as high as 330 mg/L, is unknown. The aquifer is overlain by approximately 30 m of unsaturated fine sand, silt, and loess. Other wells developed in the same aquifer and located about 200 m from the well that yielded the high concentrations of nitrate, yield water with a nitrate-nitrogen concentration of less than 10 mg/L. One possible source of the high nitrate-nitrogen was discovered by analyses of core samples from above the aquifer. The analyses show zones of nitrate concentration as high as 32 mg/kg associated with two fossil soils that are 9 and 20 m below land surface, respectively. Other investigations by University of Nebraska personnel also uncovered high nitrate-nitrogen concentrations beneath prairie soils.

Analyses of cores from beneath a nearby slough did not show high nitrate concentrations associated with the soil zones; however, natural recharge is high beneath the slough and it is possible that much of the nitrate already has been flushed from the soil in that area. Another possible source of the nitrate was a small abandoned dairy located about 300 m from the site. However, an analysis of nitrogen isotopes by Roy Spalding (Conservation and Survey Division of the University of Nebraska) indicated that animal or human wastes probably were not the source of the nitrate. Fertilizer applied to the extensive cornfields surrounding the prairie plot is another possible source of nitrate. However, water from wells in and near the cornfields generally contains nitrate-nitrogen concentrations of less than 10 mg/L.

Chemistry of geothermal waters

Chemical modeling of natural waters involves the mathematical distribution of cations among all complex-forming ligands according to the strengths of the complexes formed. For example, magnesium is distributed among the following species: Mg^{2+} , $MgOH^+$, $MgSO_4^0$, $MgHCO_3^+$, $MgCO_3^0$, $MgH_2PO_4^+$, $MgHPO_4^0$, and $MgPO_4^-$. Chemical modeling of geothermal waters from hot springs and shallow wells provides information on the natural solubility controls on the dissolved constituents. This information may be used to predict dissolved concentrations when power development wells are drilled down to hotter waters. It is also useful in understanding the natural controls on dissolved toxic trace elements in geothermal effluents. This information may be used to promote natural processes of removal of the toxic trace elements, it is likely to be much cheaper

than imposing some other treatment approach upon the effluent waters to reduce their toxic trace-elements concentrations to acceptable levels. Studies by A. S. Van Denburg, F. H. Olmsted, E. A. Jenne, J. W. Ball, and J. M. Burchard on a suite of samples from the Carson Desert of Nevada indicated that most of the samples were in equilibrium with sepiolite (MgSiO_4) within the combined error of the sampling, analyses, and thermodynamic data. About one-third of the samples were in apparent equilibrium with amorphous silica (SiO_2).

Sulfate appeared to limit the concentrations of barium—as the mineral barite (BaSO_4)—in half of the samples and appeared to limit the concentrations of calcium—as the mineral gypsum (hydrous CaSO_4)—in three samples; carbonate appeared to limit the concentration of magnesium—as the mineral magnesite (MgCO_3)—in about half of the samples. The fluoride levels in the hot springs and shallow wells appeared to be too low to be solubility controlled. Oxides of arsenic and calcium arsenate were greatly undersaturated. Arsenic levels in these hot waters are probably controlled by sulfide levels.

Carbonate alkalinity is one of the important characterizations of geothermal waters. It has generally been thought that carrying out alkalinity titrations in the field results in the most accurate estimates of alkalinity. However, recent studies of Yellowstone National Park geothermal waters by D. V. Vivit, J. W. Ball, and E. A. Jenne indicated that field analyses were less precise and less accurate than subsequent laboratory determinations. The waters are supersaturated with carbon dioxide (CO_2) and contain highly variable amounts of dissolved sulfide ions (H_2S , HS^- , and S^{2-}). The CO_2 undergoes exsolution for a period of time. If alkalinity titrations are made on the hot water, the pH may actually increase following acid addition and stirring, thereby making it very difficult to distinguish between CO_3^{2-} and HCO_3^- . The variable exsolution of H_2S and oxidation of dissolved sulfide also causes inaccuracy in the titration alkalinity. Additionally, time-dependent changes in the polymerization of silicic acid in conjunction with the protonation of the dissolved $\text{H}_2\text{SiO}_4^{2-}$ and H_3SiO_4^- species that occur in the alkaline waters also causes inaccuracies in the titration alkalinity.

The investigators found that accurate estimates of carbonate alkalinity are obtained by (1) determining the titration alkalinity after all supersaturated CO_2 has exsolved, remaining sulfides have oxidized, and silica polymerization has largely

ceased; (2) determining the noncarbonate alkalinity by back titration with base to the pH of the sample at time the titration alkalinity was determined; and (3) subtracting out the noncarbonate alkalinity and calculating relative amounts of carbonate and bicarbonate as a function of pH, temperature, and the equilibrium constant for the reaction: $\text{HCO}_3^- \rightleftharpoons \text{H}^+ + \text{CO}_3^{2-}$. This results in a significant decrease in the degree of supersaturation of these waters with calcite.

Radium-228 found in water from a geopressured-geothermal well

V. J. Janzer reported that relatively high levels of ^{228}Ra were found in water from a geopressured-geothermal test well drilled approximately 40 km south of Lafayette, La. Preliminary results indicated that ^{228}Ra is present at concentrations of 300 pCi/L or more in brine samples obtained from the well. This is equal to or greater than the levels of ^{226}Ra found in the same samples. Radium-228 is a beta-emitting decay product of naturally occurring thorium-232 that is probably present in the mineral assemblages that constitute the aquifer.

Organic compounds in the Lower Mississippi River

F. C. Wells investigated volatile and semivolatile organic compounds in the Mississippi River in Louisiana. Water samples were collected at five locations in December 1976 and in June and October 1977. Volatile samples were analyzed by using the "Bellar sparging technique." Semivolatile organics were extracted with dichloromethane at three pH levels—at the prevailing pH of the sample (neutral extraction), pH of 1 (acid extraction), and pH of 11 (base extraction). Approximately 20 organic compounds were identified in the samples collected in December and June. Benzene, toluene, and chloroform were the most frequently detected volatile organics; however, concentrations of these compounds did not exceed $5 \mu\text{g/L}$ except for benzene, which was detected at $10.6 \mu\text{g/L}$ at Luling, La., on June 14, 1977. The most frequently detected semivolatile organics were phthalate compounds. These included dibutylphthalate, dioctylphthalate, butyl benzyl phthalate, and bis(2-ethylhexyl)phthalate. Concentrations of these compounds did not exceed $5 \mu\text{g/L}$ except for dibutylphthalate, which was detected at $6.4 \mu\text{g/L}$ at Luling, La., on December 1, 1976. In more than 50 percent of the samples, atrazine, a popular herbicide, was present in concentrations ranging from 0.32 to $2.6 \mu\text{g/L}$.

Investigations of volatile organic compounds and gases in streams

R. E. Rathbun determined the rate coefficients for the volatilization of acetone and the absorption of oxygen for a range of mixing conditions in a stirred water bath. Comparison of the coefficients showed that the oxygen-absorption coefficient varied about nineteenfold and the acetone volatilization coefficient varied about fourfold over the range of conditions considered. Results are consistent with the two-film theory of mass transfer for slightly soluble and very soluble substances.

Using acetone as a substrate, D. J. Shultz studied the growth characteristics of a mixed natural bacterial population in a series of laboratory respirometer experiments. An inverse relation between the acetone concentration and the adenosine triphosphate concentration was found. A series of experiments were performed to determine the Monod kinetics parameters k_m and K_s for the system. The experimental data were consistent with Monod kinetics during log-phase growth but were inconsistent with these kinetics during the initial period of growth.

D. W. Stephens determined in laboratory experiments that virtually no acetone was absorbed by unialgal cultures of *Anabaena flos-aqua* or *Chlorella vulgaris* over time periods of about 450 hours. One experiment with a penicillin-treated blue-green alga (*Oscillatoria*) from a natural-water source showed no losses initially but large losses at later times. These losses were believed to be the result of decline in the bacteriostatic action of the penicillin followed by degradation of the acetone by endogenous bacteria.

D. J. Shultz developed a model which simulates the variation with time of the concentration and δO^{18} of DO in a natural system. The model considered sorption of atmospheric oxygen, photosynthetic production of oxygen, and biologic respiration. The calibrated model qualitatively simulated a set of experimental data but did not reproduce it exactly. The worst fit was for the daylight hours, which was an indication that there is a problem with the assumption of a constant rate of photosynthetic production of oxygen.

D. W. Stephens compared the floating dome method with the distributed equilibrium method and a modified tracer method of measuring reaeration rates in standing water. The lack of agreement between the dome method and the other methods was attributed to limitations in the polarographic instruments commonly used to measure oxygen in

the dome method. In techniques where polarographic probes are used to monitor changes in dissolved or gaseous (dome) oxygen, the ratio of the dome volume to volume of the water column under the dome must be kept below 0.02 to minimize instrument error to less than 10 percent of the predicted oxygen transport.

Red colonies on fecal-coliform-bacteria plates identified

During a water-quality study by the USGS in the Bear Creek basin of Jackson County, Oregon, stream samples were taken for bacteria determination. According to L. A. Wittenberg, red- to pink-colored colonies were found growing on an agar that was supposedly selective for fecal-coliform organisms. One of these pink colonies was isolated and identified as an organism known as *Klebsiella*, a bacteria associated with log ponds. Because of the large number of log ponds in the Pacific Northwest, this organism occasionally occurs on fecal-coliform plates. Careful counting of only the blue colonies should prevent false determinations of fecal coliforms present.

RELATION BETWEEN SURFACE WATER AND GROUND WATER

Modeling lake drawdown caused by well pumpage

A three-dimensional finite-difference model (P. C. Trescott, 1975) was used to simulate water-level decline in Horsehead Lake, Oneida County, Wisconsin, by a proposed ring of dewatering wells around the lake. The Office of Inland Lake Renewal, Wisconsin Department of Natural Resources, had requested a report on the feasibility of using this method to drain the 3-m-deep lake and dewater most of the 3 to 10 m of organic lake-bottom sediment (95 percent water). If the lake were drained, air drying and resultant compaction of the sediment would help to alleviate the lake's eutrophic condition.

In working with the model, H. L. Young used an upper water-table layer containing lakes and a lower leaky-artesian layer in which the proposed wells were to be finished; lakes were interconnected with aquifers, both vertically and horizontally, by assuming a leakance coefficient for the lake sediment. Lakes were modeled as a highly transmissive layer with a storage coefficient of unity.

Two simulations used data on 32 wells, pumping at 2,450 m³/d each and then at 4,900 m³/d each. After 152 days of simulated pumping at the lower

rate, the lake level declined about 3.5 m. Only 25 percent of the water pumped was from the lake and, coincidentally, only 25 percent of the sediment was dewatered. Adjacent to the lake, drawdown in the artesian aquifer was as much as 10.5 m, and, at a distance of 0.6 km, a lake was lowered 1.3 m. In the second simulation, drawdown in the artesian aquifer far exceeded that necessary to cause maximum infiltration from the lake. After simulation of 45 days of pumping, lake drawdown was almost identical to that of lake drawdown after 76 days of pumping in the first simulation; however, aquifer drawdown near the lake was almost doubled. At least 220 days would be required to lower the lake level by 10 m. An optimum initial pumping rate would be between 2,450 and 4,900 m³/d, but the allowable reduction in pumpage to maintain maximum leakage was not determined.

The Office of Inland Lake Renewal used this information to determine that the costs of the rehabilitation technique were too great.

Soil temperatures indicate gaining and losing streams

In the Lebanon, Mo., area thermocouples were installed at a depth of 0.76 m at three locations in gaining and losing reaches of Bear, Dry Auglaize, Conns, and Deberry Creeks. According to John Skelton and E. J. Harvey, the interpretation of soil-temperature measurements made by thermocouples supported the conclusions of a thermal-imagery study made in Missouri in 1974. During winter and early spring, soil temperatures in the gaining reaches of the streams averaged 1.3°C higher than those in dry reaches; in late spring and summer, soil temperatures in the gaining reaches averaged 0.4°C lower than those in losing reaches. In the summer, changes in vegetative cover seemed to have a measurable effect on ground temperatures, thereby complicating data interpretation. As a hydrologic tool for identifying gaining and losing streams, the analysis of soil temperatures is not as practical as direct measurements of surface flow and ground-water levels.

Water-table configuration related to lake seepage

In modeling ground-water flow near lakes, T. C. Winter found that outseepage through lakebeds is eliminated if (1) the water-table mound between the lake and a regional ground-water discharge area is sufficiently high (Winter, 1976) and (2) the water-table gradient on the side of the mound facing the discharge area is sufficiently small. Two ground-

water systems of different overall dimensions were examined by digital simulation—the ground-water system thickness-to-length ratio of the first was 0.0037 and the ratio of the second was 0.0045. In the first system there was no outseepage from the lake if the water-table gradient from the mound to the regional discharge area was less than 0.0090. For the second setting, the critical gradient was 0.0110. For settings of the given dimensions that have water-table gradients greater than the two critical values, outseepage took place through part of the lakebed.

EVAPORATION AND TRANSPIRATION

Evaporation from water surfaces and the combined evaporation and transpiration (evapotranspiration) from vegetated land surfaces play a major role in hydrology. The processes return an average of about 70 percent of the incident precipitation in the conterminous United States to the atmosphere. Moreover, changes in vegetative cover or land use may change the amount of water lost to evapotranspiration, thus affecting the availability of water for other uses. Consequently, knowledge of evapotranspiration rates under various land-use and climatic conditions is needed to assess the environmental impact of land development and to evaluate possible water-management schemes, such as phreatophyte eradication.

Most of the significant results of evaporation and transpiration studies during 1977 year were obtained from water- and energy-budget data on flood-plain vegetation and from natural desert vegetation.

Evapotranspiration from saltcedar in the Gila River flood plain in Arizona

T. E. A. van Hylekama studied the weather in and above a stand of saltcedar on the flood plain of the Gila River near Buckeye, Ariz., in order to determine evapotranspiration by micrometeorological methods. There was evidence that evapotranspiration from saltcedar plants is limited during periods of high evapotranspiration demand by stomatal closure. That transport constants for momentum, heat, and vapor were equal for more than 80 percent of the record, was indicated by the fact that plots of wind speed versus temperature at different heights and wind speed versus humidity at those heights fell on straight lines. However, during hot afternoons when temperatures exceeded 40°C, vapor

fluxes and photosynthesis (as indicated by carbon dioxide flux) diminished. These data suggested that stomatal resistance increases under those conditions.

Additional evidence of stomatal closure during periods of peak evapotranspiration potential was obtained by comparison of evapotranspiration values computed by using the combination mass-transfer and energy-budget method with simultaneous evapotranspirometer (water budget) data. The combination-method results were higher than the water-budget data during daylight hours. However, when stomatal and aerodynamic resistances were taken into account, the calculated values agreed well with the measured ones. This agreement suggested that saltcedar reacts to extremely high wind speeds and temperatures by stomatal closure restricting evapotranspiration even though water is readily available (as it is in evapotranspirometers with favorable water and soil conditions).

That riparian vegetation always uses water at a potential rate cannot be taken for granted, and quantitative estimates of salvageable water based upon that assumption may at times be greatly overestimated.

Hydrologic effects of saltcedar control on the Pecos River flood plain in New Mexico

Phreatophytes, predominantly saltcedar, were cleared from approximately 77 km² of the flood plain of the Pecos River between Acme and Artesia, N.M., beginning in March 1967. It had originally been estimated (Mower and others, 1964, p. 91) that as much as 3.5×10^7 m³ of water could be salvaged annually by these control measures. However, base-flow analyses detected little or no water salvage in the form of increased base flow of the river, according to G. E. Welder. Possible reasons that the anticipated amount of salvaged water has not been found are: (1) Transpiration before clearing may have been less than early studies suggested, and evaporation after clearing could be larger than had been expected and (2) the phreatophytes were cleared by mowing from 1967 until late 1972, when the practice of root plowing was instituted. Regrowth was vigorous following mowing and may not have been effectively curtailed until about 1976; consequently, salvaged water may have just begun to appear in the river in 1977.

Soil moisture along a bajada in southern Arizona

Water use by three different vegetation types—Sonoran desert, grassland, and oak woodland—was

monitored by gathering soil moisture and climatological data at 11 stations along the bajada on the western side of the Santa Rita Mountains near Tucson, Ariz., during the period 1963–66. The stations range in altitude from 850 to 1,400 m above mean sea level. Climatic data were obtained by the Institute of Atmospheric Physics, and soil moisture measurements were obtained by the USGS.

Preliminary multiple-regression analysis by T. E. A. van Hyleckama showed that quantities of moisture, y , in the top 0.6 m of the soil can be predicted quite accurately (correlation coefficients 0.88 and higher) by the equation, $y = a + bx_1 + cx_2 + dx_3$, in which x_1 is potential evapotranspiration (H. L. Penman, 1956), x_2 is rainfall during the week, and x_3 is antecedent soil moisture as computed from the previous week (but not for the first week, when it was measured). The values a , b , c , and d are constants that vary with the altitude and other characteristics of the station.

Analyses of air temperatures and rainfall showed that, as expected, there is a trend toward cooler temperatures and more rainfall as the altitude increases. Because minimum temperatures tend to increase with altitude, relatively, stations at low altitudes are exposed to much higher ranges of temperature than stations at high altitudes. The effects of temperature ranges are apparent in the composition of vegetative cover.

LIMNOLOGY AND POTAMOLOGY

Although the term "limnology" originally applied only to the study of lakes, in its current usage it also refers to the study of streams and rivers. The term "potamology" is more restrictive, applying only to river investigations. Limnology is the study of sources and nature of fresh water, its motion and changing condition and, perhaps most significantly, the life it supports.

Limnology of Maine lakes

D. J. Cowing and Matthew Scott (Maine Department of Environmental Protection) evaluated sampling methods and parameters to be used in a trophic classification of Maine lakes. The current method of classification, using Secchi disk transparency, was not applicable to lakes with colors greater than 30 platinum-cobalt units. Regression analyses among chlorophyll a , total phosphorus, and Secchi disk transparency yielded data for calculating equivalent

trophic state for highly colored lakes. Vertical lake profiles of dissolved oxygen, temperature, specific conductance, and pH during late winter ice cover and later summer thermal stratification yielded valuable supplemental information on trophic condition of the 43 lakes.

Three methods for calculating hydraulic retention time of lakes were tested. (The Maine Department of Environmental Protection used these values to estimate vulnerability of a lake to cultural eutrophication.) The best method of estimating hydraulic retention time was found to be the "Empirical Formula Method." This method used an empirical formula based on basin characteristics to calculate mean annual flow at ungaged sites. These flow figures are then used to estimate annual mean hydraulic retention times.

Marsh plants depend on nitrogen and phosphorus from sediments

According to J. T. Turk, sediments taken from a marsh in Lake Champlain showed that nitrogen and phosphorus played an important role in plant production. Concentration of nitrogen and phosphorus in the pore water in the sediments decreased continually during the growing season and were replenished in winter and early spring. A mass-balance analysis of (1) the nutrient decrease in the pore water during the growing season, (2) the nutrient supply from other major sources, and (3) uptake by plants showed that the pore water supplied 42 percent of the nitrogen and 9 percent of the phosphorus used by the plants. The nitrogen and phosphorus were available even when supplies from tributary streams were minimal. Proposed regulation of the level of Lake Champlain during the spring high-water period could dewater some of the sediments and transport nitrogen and phosphorus from the marsh to Lake Champlain.

Large concentrations of ferromanganese nodules found in Oneida Lake, New York

According to W. E. Dean, Oneida Lake, N.Y., contains the most concentrated deposit of freshwater ferromanganese nodules (in terms of amount per unit area) yet reported. The mineralogy and bulk chemistry of these saucer-shaped nodules are similar to those of deep-sea ferromanganese nodules, but the nodules in Oneida Lake contain considerably lower concentrations of trace metals, especially cobalt, nickel, and copper. Budgets for iron and manganese in waters from Oneida Lake and its

tributaries indicated that approximately 122 t of iron and 23 t of manganese are lost each year from the lake waters, presumably by incorporation into sediments and ferromanganese nodules. Estimates based on nodule abundance and age of the lake suggested that iron and manganese are being incorporated into ferromanganese nodules at rates of 13 and 22 t/yr, respectively. Most iron lost from the lake waters is apparently incorporated into sediments, which contain an average of 10 times more iron than manganese. Most manganese lost from the lake waters is apparently incorporated into ferromanganese nodules, which contain an average of 1.7 times more manganese than iron. Very high rates of phytoplankton productivity combined with almost continuous wind mixing to the lake bottom provide high-pH and high-O₂ conditions in most of the lake. Algae also provide an effective means of concentrating and transporting iron and manganese and thereby aid in the extensive development of ferromanganese-nodule deposits.

Water quality of active and inactive log ponds

Active log ponds, sampled during the summer of 1977, in Douglas County, Oregon, generally were found to have higher color and lower pH and dissolved oxygen concentrations than comparable inactive log ponds. J. F. Rinella found that active ponds had colors ranging from 200 to 1,200 platinum-cobalt units compared to less than 100 units in inactive ponds. Active ponds had dissolved oxygen concentrations of less than 30 percent saturation and pH values ranged from 5.8 to 6.8 near the water surface; in contrast, inactive ponds had dissolved oxygen concentrations between 50 and 95 percent saturation and pH values ranged from 6.8 to 8.4. In active ponds, total dissolved solids were generally higher and transparency lower than in inactive ponds. Concentrations of hardness, conductivity, and alkalinity were similar in the two types of ponds.

Copper cycles and copper sulfate algicidal capacity in two California lakes

J. F. Elder (USGS) and A. J. Horne (University of California) investigated copper toxicity to algae in a new reservoir in southern California and a large eutrophic lake in northern California. Results of bioassay experiments showed significant copper depression of chlorophyll *a*, photosynthesis and nitrogen fixation at concentrations of 5–10 µgCu/L. Bluegreen algae are especially susceptible to copper. Following an algicide treatment, field measure-

ments of the reservoir confirmed the expected stability of dissolved copper and elevated concentrations persisted for several weeks. The investigations concluded that algicidal effectiveness of copper is quite variable but likely to be greatest in lakes where nitrogen-fixing bluegreen algae are abundant.

Flow and salinity modeling of proposed reservoirs in the Yampa River basin

The Yampa River basin is an unregulated stream system covering 21,000 km² in northwestern Colorado and south-central Wyoming. As a consequence of energy resource and associated economic development, demands for available surface water supplies in the basin are increasing. The construction of as many as 30 reservoirs has been proposed that would impound 41 percent more water than the equivalent long-term streamflow yield of 1.9 billion m³ annually. Present reservoir feasibility studies have considered only individual projects.

Four of the proposed reservoirs were modeled by T. D. Steele, R. H. Dale, D. B. Adams, and D. P. Bauer in order to evaluate multireservoir effects on downstream flows and dissolved solids. These four reservoirs represent 57 percent of the maximum proposed reservoir capacity for the basin. The modeling analysis permitted comparison of hydrologic conditions before and after reservoir construction. Reservoir-operating rules that would redistribute existing seasonal patterns of flow and salinity in the Yampa River downstream from each reservoir were assumed for the model simulations. The analyses indicated that the amount of surface water yield from the basin could decrease as much as 6 percent owing to evaporative losses from all the proposed reservoirs. The study showed that salinity loads in the Yampa River would not be affected by implementation of the reservoirs. However, impounded snowmelt runoff of lower salinity water released during the remainder of the year would reduce the annual time-weighted dissolved solids concentrations downstream by an estimated 34 percent.

Algal growth potential of North Platte reservoirs

Trends in algal growth potential and phytoplankton community composition were assessed in the four major reservoirs of the North Platte River, Wyo. For 3 years, S. J. Rucker IV sampled dissolved nutrients, temperature, dissolved oxygen, specific conductance and phytoplankton composition regularly. Algal growth in the reservoirs began each

year in June and continued until late October. Diatoms were the dominant phytoplankton during the early part of the growing season. In late June, *Anabaena* dominated, but a wide diversity of species remained. *Aphanizomenon* appeared at the end of July, and by the middle of August it clearly became the dominant genus. At that time large mats of *Aphanizomenon* form on the lake surface. In 1975 and 1976 blooms in Glendo Reservoir apparently stressed fishes enough that they left the reservoir through the outlet in great numbers. Solute nutrient concentrations were greatly reduced during blooms.

Lake Koocanusa water quality program

J. R. Knapton (USGS), in cooperation with the U.S. Army Corps of Engineers, has monitored various limnological parameters in Lake Koocanusa (northwestern Montana). Vertical profiles were made for temperature, dissolved oxygen, specific conductance, pH, and transmissibility. Samples collected at various depths were analyzed for plant nutrients, chlorophyll *a*, organic carbon, major ions and minor elements. Primary productivity measurements were made in the euphotic zone. The Lake Koocanusa program was supplemented by present river quality records and several years of streamflow and water quality data for the Kootenai River prior to the construction of Libby Dam in 1972. Data are being used to study the effects of river quality of the impoundment.

Water quality of selected reservoirs in Texas

Periodically since October 1961, the USGS, in cooperation with State, Federal, and local agencies, conducted comprehensive water quality surveys of selected reservoirs in Texas, according to H. B. Mendieta. During the 1977 water year, 47 comprehensive water quality surveys were made for 16 reservoirs. Quality constituents determined were major ions, minor elements, nutrients, pesticides, total coliforms, fecal coliforms, fecal streptococci, total organic carbon, biological oxygen demand, Secchi disk transparencies, turbidities, and color. Specific conductance ranged from 145 to 6,750 μ mho in the 16 reservoirs. Seasonal depletion of oxygen and accompanying changes in ionic and organic composition of the lake hypolimnion were delineated.

Reconnaissance of lakes in the National Petroleum Reserve in Alaska

As part of a hydrologic study of the National Petroleum Reserve in Alaska directed by C. E.

Sloan, a reconnaissance of 120 lakes was conducted in July-August 1977. The Reserve is located on the northwest Arctic slope and extends from the summit of the Brooks Range across the Arctic foothills and Arctic coastal plain to the Beaufort Sea. Data collected for these lakes included major ions, organic carbon, algal growth potential, lake depth, turbidity, Secchi disk transparency, and sediment type. Numerous lakes exist on the Coastal Plain and most are shallow (<2 m). Lakes in the sand dune region south of Teshekpuk Lake were generally deeper with some nearly 20 m. Dissolved solids were low in most lakes during summer, but a few near the coast were clearly influenced by marine conditions. Dissolved solids concentrations increase under ice during winter and became highly concentrated in shallow lakes that have frozen to near the bottom. Because of persistent wave action, turbidity caused by suspended sediment was common in the shallow lakes. Primary productivity rates were low in all the lakes.

Benthic invertebrates in a north-flowing stream and a south-flowing stream in Brooks Range, Alaska

K. V. Slack, J. W. Nauman, and L. J. Tilley compared benthic invertebrate fauna in two fifth-order streams, the Atigun River flowing northward and the Dietrich River flowing southward from the Continental Divide in the Brooks Range in Alaska. Aquatic insects comprised 88 percent of the taxa and 97 percent of the individuals from the Dietrich River and 73 percent of the taxa and 97 percent of the individuals from the Atigun River. Taxa with the greatest numbers of individuals were the same in both streams. Cluster analysis showed a high degree of resemblance between the fauna of the rivers. Both within and between streams faunal resemblance decreased with increasing distance between stations. The evidence for faunal resemblance is stronger than for faunal differences, although some taxa may occur in only one of the streams. Other studies have shown that differences in total radiation associated with differences in valley direction (aspect) affect local climate, hydrology, and distribution of terrestrial plants and animals. However, during a 4-day, late summer study, the benthic fauna of the Atigun and Dietrich Rivers were remarkably similar. Factors that operate independently of aspect (possibly freezing solid in winter) may control the occurrence of species in these streams.

Biology of the upper Chattahoochee River in Georgia

The upper Chattahoochee River in Georgia was intensively sampled to evaluate water quality conditions in selected river reaches and two impoundments in the drainage. Potential for algal growth and environmental factors adversely affecting biological communities were determined according to B. W. Lium and R. N. Cherry.

In general, diversity of benthic invertebrates was low throughout the study area. Lowest diversities were found between Buford Dam (hydroelectric power generation) and Atlanta. Diversities were highest in mountain areas and middle reaches of West Point Lake. Cell counts of phytoplankton were generally higher downstream than upstream of Atlanta. Phytoplankton genera in the mountain reaches differed from those in lakes and in downstream reaches of the river. Rates of nitrification in the upper Chattahoochee River were comparatively low, but nitrification was shown to be an important source of oxygen consumption 45 miles downstream of Atlanta area wastewater treatment plants. Algal growth potentials in West Point Lake decreased and phytoplankton concentrations increased from the upstream to the downstream end of the impoundment. Algal growth potential decrease and phytoplankton increase downstream were related to temperature variations. Empirical equations were derived relating change in algal growth potential and phytoplankton cell density to water temperature.

Water-quality effects of underground coal mining

Water quality measurements made near an abandoned coal mine in western Washington were used by F. A. Packard, L. A. Fuste, and M. O. Fretwell to design a monitoring program for underground coal mines. Over a 10-month period chemical, physical, and benthic invertebrate data were collected monthly at stations upstream from the mine, in the effluent mixing zone and in the completely mixed zone. Data on approximately 50 benthic taxa were used in a Spearman's rank correlation matrix, together with associated chemical measurements, to determine indicator community assemblages. Statistical evaluation of the biological data showed significant ($\alpha=.10$) differences between the least and the most severely affected stations.

Benthic invertebrates of the lower Mississippi River

Four sites on the Mississippi River were examined for 1 year to determine differences between

upstream and downstream benthic communities in Baton Rouge and New Orleans, La. Sediment samples were collected and analyzed for benthic invertebrate composition, particle-size distribution, and loss on ignition. Each site was sampled at five locations in the cross section. Results of this study by F. C. Wells and C. R. Demas, in cooperation with the Louisiana Department of Transportation and Development, indicated that the most common organisms in the lower Mississippi River are the *Molluscan Corbicula* and tubificid worms. Substrate type and stability, channel geometry, river velocity, vegetation, and salinity apparently influence benthic community structure. Wastes discharged into the river may have less effect on the benthic community structure than the above natural factors.

NEW HYDROLOGIC INSTRUMENTS AND TECHNIQUES

D. I. Leap reported that commercially available field-data acquisition and processing systems were interfaced to provide data in a form readily compatible with the USGS's new Honeywell MULTICS computer system. Analog signals from field transducers, thermocouples, barometers, and flow meters were interfaced with a multichannel analog-digital converter, recorded digitally in ASCII code on a magnetic-tape cassette and concurrently printed with channel and time identifiers. The tape cassette can be retrieved from the field and read directly into the MULTICS system for processing and plotting. This system was tested in the Amargosa Desert of southern Nevada and the Osceola National Forest of Florida. Its use demonstrated a new and potentially useful approach to the collection and processing of field data.

A minicomputer-based pulse height analyzer with 8,192 channels was used in the laboratory with a variable borehole model designed by D. E. Eggers to emulate a uniform distribution of gamma-emitting isotopes outside the borehole. Spectral data were obtained by using known concentrations of Co^{60} , Cs^{134} , Cs^{137} , Mn^{54} , and Na^{22} in tubes within the model to calibrate and determine detection limits. The pulse height analyzer has software for use in extensive analyses of gamma spectra.

F. C. Koopman reported the development of several new hydrologic instruments. These include a new solid-state electronic timer that is compatible with USGS water-stage recorders; one-hundred units were built and are undergoing field testing. A

digitizer also was developed for use in monitoring the output from a Price current meter to compute water velocity. An interface between a commercially available electromagnetic flow meter and USGS recorders was developed, and 15 prototype units are being evaluated under field conditions. A prototype battery-operated water-quality monitor was developed to operate unattended in an automatic mode. This monitor uses circuitry that was developed and thoroughly tested in line-powered models that were operated by the USGS for several years. Initial tests of the prototype monitor were run as a prelude to production of 25 units for field use.

C. D. Kauffman, Jr., reported that the Geostationary Operational Environmental Satellite (GOES) Data Collection Platforms (DCP) and the GOES data-collection system were tested at nine gaging stations in the Juniata River Basin of Pennsylvania. The first data (river stage) was successfully transmitted from the basin via the GOES system on April 5, 1976. Much of the early data was either lost or of poor quality, but subsequent improvements increased its reliability and usefulness. The most reliable DCP was at gaging station 01560000, on Dunning Creek at Belden, Pa., where it has been operating almost perfectly since its installation and initiation on March 9, 1977. During the first 3 months, the data was continuous except for 11 days of partial gage-height record and 2 days of missing record, none of which was attributed to faulty DCP operation. The remaining 6 $\frac{2}{3}$ months of record were continuous and complete. Similar success was experienced with two other DCP's in the basin. Since about January 1, 1977, the DCP's at the remaining six sites operated an average of about 130 days (range, 3–236 days) before stoppage or faulty timing occurred. Initial tests of a telemetry system by using a commercial satellite also were successfully begun in late 1977, but performance statistics have not yet been developed. As part of a joint USGS-COMSAT General demonstration, the USGS's Pennsylvania and Oregon Districts are each instrumenting five stream-gaging stations with DCP's designed to communicate with a commercial satellite.

SEA-ICE STUDIES

Results of AIDJEX main experiment

W. J. Campbell reported that final analyses of the surface, aircraft, and satellite data obtained in the AIDJEX main-experiment study area in 1975–76 were completed. Aircraft passive-microwave data

were used to distinguish first-year and multiyear ice types and concentrations, and the data revealed new information on ways to observe ice mixtures and thin-ice types. The data showed that large areas of the Arctic summer pack ice have concentrations as low as 50 percent—previously, the lowest summer ice concentration was considered to be 90 percent. This information can be used for determination of ocean-air interaction, weather forecasting, and climate studies.

The combined SLAR and scatterometer data of the sea ice in the AIDJEX area was “first-of-its-kind” data; its interpretation is of great importance to the Seasat-A satellite program because Seasat will be the first satellite to carry radar and a scatterometer. The combined active- and passive-microwave sensor data results presented proof that this combination of sensors gives the best information on sea ice.

Radar imagery study of Beaufort Sea ice

Analysis was completed of April–May 1974 radar imagery of near-shore Beaufort Sea ice obtained by a USGS aircraft. According to W. J. Campbell, the data yielded information on the mesoscale dynamics of the region with a far greater accuracy than was obtained by using other remote-sensing techniques. Results of the study will be applied to interpretation of the forthcoming Seasat-A synthetic-aperture radar imagery of sea ice.

Mapping of the Greenland ice sheet

W. J. Campbell reported that USGS and NASA scientists analyzed GOES-III satellite altimetry data for the southern Greenland ice sheet. These data provided a capability for mapping the area to an accuracy of ~ 1 m. Previously undetected features, such as large-scale undulations, were observed, and small-scale undulations, domes, and ice divides were easily detected and monitored. This type of mapping will be repeated by the forthcoming Seasat-A satellite radar altimeter. It can provide very accurate maps of the Greenland ice sheet, and information on ice-sheet growth and retreat.

Sea-ice model

L. A. Rasmussen, W. J. Campbell, and C. H. Ling developed a time-dependent, quasi-steady-state numerical model of the dynamics of sea ice. It computes the extent and concentration of sea ice, data necessary for global circulation models. The model was derived from 1974 “twice-daily” synoptic pres-

sure data, which were used to generate surface wind-stress fields; electronically scanning microwave radiometer imagery for the same time segment in the Antarctic region was used in conjunction with the pressure data. The model is being applied to the Antarctic ice pack.

ANALYTICAL METHODS

ANALYTICAL CHEMISTRY

Sample preparation effects elements extractions of soils

Differences in DTPA extractable element concentrations in soil related to two methods of sample preparation were investigated by R. C. Severson and J. M. McNeal. Samples of A- and C-horizon soils from the Northern Great Plains were prepared by disaggregating and grinding. Preparation methods had a significant effect on extract concentrations of Fe, K, Mg, Mn, and Na in A-horizon soils but no effect for concentrations of Cd, Co, Cu, Ni, Pb, and Zn. Significant effects of extract concentration of Cd, Fe, K, Mg, Mn, and Zn were noted for sample preparations of C-horizon soils, and those elements showing no effect were Cu, Na, Ni, and Pb.

Analytical methodology and its usefulness in geochemical exploration

F. N. Ward has evaluated several analytical methods and their application to geochemical exploration (Ward and Bondar, 1978). Atomic absorption and emission spectrography are the methods of analysis most widely used in geochemical exploration. Development of nonflame atomizers, particularly electrothermal devices and reduction cells for atom and metal-hydride generation, has expanded the application of atomic absorption spectrometry by pushing detection limits of many elements well into the parts per billion range and by reducing detection limits for others, such as As, Se, Te, and Sn, to levels useful in lithochemical surveys. The recent promotion of inductively coupled plasma sources for excitation, as well as other variations such as use of echelle gratings, has increased the number of available spectrographic methods for multi-element surveys and has simplified the application of partial extraction techniques in emission spectrography.

Other methods that require mass spectrometers and gas chromatographs are being used to measure volatile indicator elements and compounds such as helium and sulfur gases. Analytical techniques in-

cluding those based on voltammetry, ion-selective electrodes, and the use of partial or selective extractions are finding increased application as analytical tools and as aids in determining metal speciation so as to better understand geochemical processes of dispersion and concentration.

Evaluation of analytical methods for the geochemical exploration of uranium

Existing methods of uranium analysis were evaluated by F. N. Ward. Current interest in uranium exploration has sparked a major effort to develop new or improve existing analytical methods for the determination of uranium and related radionuclides. Exploration geologists may now choose conventional fluorimetry, delayed neutron activation, X-ray fluorescence, laser-induced fluorescence, and nuclear-fission track techniques for the determination of uranium. The choice will depend on sensitivity required, sample media being analyzed, chemical species of the uranium to be determined, turnaround time required, and cost considerations. Two of the methods described, conventional fluorimetry and laser-induced fluorescence, can be adapted for use in the field.

While recent developments of exotic techniques and apparatus have greatly expanded the number of useful analytical techniques in exploration geochemistry, each one has its own problems and limitations as well as its applications. A panacea for analytical problems does not yet exist—except perhaps in the skilled analyst, whose ingenuity in developing and applying new methods augments diligent application of tried and true procedures.

Determination of beryllium in geologic materials

A method has been developed by E. Y. Campbell and F. O. Simon for the atomic-absorption determination of beryllium in geologic materials using electrothermal atomization after separation by solvent extraction. Samples were decomposed with HF and HNO₃ in teflon-lined pressure decomposition vessels. Beryllium was isolated by its extraction into xylene as beryllium acetylacetonate at pH 8 and by its subsequent back-extraction in 3M HCl. The method was successfully applied to the determination of beryllium in 14 USGS standard rocks. Four subsamples from four bottles of each standard sample were analyzed in random order. The mean beryllium contents determined were (in ppm Be): AGV-1, 1.98; PCC-1, 0.024; MAG-1, 2.84; BHVO-1, 0.90; DTS-1, 0.026; SCo-1, 1.74; SDC-1, 2.52; BCR-1, 1.44; GSP-1, 1.22; SGR-1, 0.86; QLO-1,

1.83; RGM-1, 2.21; STM-1, 8.75; G-2, 2.29. The analysis of variance showed that all samples may be considered homogeneous at $F_{0.95}$ except AGV-1 and DTS-1, which may be considered homogeneous at $F_{0.99}$.

Thallium contents of 16 USGS standard rocks

F. O. Simon, E. Y. Campbell, and P. J. Aruscavage determined thallium in 16 USGS standard rocks by atomic absorption spectroscopy in which a heated graphite atomizer was used after extraction as thallium iodide into amyl acetate. Four subsamples from four bottles of each standard sample, except G-1 and W-1, were analyzed in random order, and the average thallium contents in parts per million (as Tl) were AGV-1, 0.41; GSP-1, 1.63; G-2, 1.08; BCR-1, 0.35; SDC-1, 0.80; MAG-1, 0.79; BHVO-1, 0.049; SCo-1, 0.79; SGR-1, 0.34; QLO-1, 0.23; RGM-1, 1.07; STM-1 0.30; DTS-1, <0.005; and PCC-1, <0.005. The analysis of variance showed that all samples may be considered homogeneous at $F_{0.975}$ and only GSP-1 may be considered heterogeneous at $F_{0.95}$. The Tl contents of G-1 and W-1 are 1.0 and 0.12 ppm, respectively.

EMISSION SPECTROSCOPY

Argon inductively coupled plasma in the analysis of geological materials by atomic emission spectrometry

An argon inductively coupled plasma (ICP) is being used in the spectrometric analysis of geochemical materials. This emission source is characterized by its bright atomic spectra, stability, chemical inertness, and high temperature, which are conducive to sensitive elemental analyses that are both precise and accurate. The ICP was applied by D. W. Gollightly in trace-element analysis and in basic studies of geochemically coherent elements, such as zirconium and hafnium. J. L. Seeley and P. J. Lamothe have applied the ICP to As, Sb, Al, and Si determinations at the low ppb levels on rock-water interactions and on uranium ore leach solutions at the 100 ppb level.

NEUTRON ACTIVATION

Instrumental neutron activation of geological materials

Instrumental neutron activation has been applied to the determination of 24 to 30 elements in rocks, minerals, and coals by J. J. Rowe and P. A. Baedecker. An automated system was used to analyze more than 2,000 samples per year. Each sample was counted four times over a 2-month period using

both low energy planar intrinsic germanium and large Ge(Li) detectors. Eight detectors, each with an automatic sample changer, were interfaced to a multichannel analyzer with magnetic tape output for processing by computer.

Data processing was carried out on a Honeywell computer with the Multics operating system. Spectral data were smoothed using the Savitzky and Golay (1964) technique and analyzed by the SPECTRA 3 program of Baedecker (1976) which used the first derivative for peak location and either the TPA or Wasson method for photopeak integration (Baedecker, 1971). Partially resolved multiplets were analyzed by simple non-iterative procedure of Baedecker (1977). After SPECTRA 3, SUMMARY 1 was executed, which called data from disk and averaged results of multiple lines to generate an "Initial Summary Report." After all countings were completed, SUMMARY 2 averaged all results with weighting according to estimated counting errors to provide the "Final Analytical Report". Fission product corrections were applied to the results for Zr, La, Ce, Nd, and Sm. The final report included a computer plot of chondrite normalized rare earth distribution patterns.

X-RAY FLUORESCENCE

Scanning electron microscopy study of the accessory minerals in coal

Scanning electron microscopy (SEM) provides an ideal method to evaluate trace elements in coal minerals. Results from the detailed study by R. B. Finkelman of the accessory minerals in the Waynesburg coal. Taking into account solid solution in titatively occur in discrete mineral phases.

Clearly, the Cr, REE, Y, Zr, Zn and Ni were almost completely inorganically bound in the Waynesburg coal. Talking into account solid solution in pyrite, copper and lead were probably totally bound in mineral phases. It appeared that Th, W, Sn, and Mo were predominantly in discrete mineral phases while only one-third of the titanium can be accounted for as titanium oxide. Some titanium was bound in clays as well as other accessory minerals (sphene, pyroxene), but as much as 50 weight percent may be organically bound. A similar situation appeared to exist for barium and strontium. The SEM and the "Lexan" technique indicated that no more than one weight percent of the uranium was inorganically bound. The bulk of the uranium was associated with the RE phosphates, the remainder in zircons. It is this type of information that can

help us predict the behavior of these elements during combustion, liquefaction, gasification, weathering, and leaching of a coal.

XRF glass disc fusion method for silicate rock analysis

A glass disc fusion method for silicate rock analysis has been refined by H. N. Elsheimer and B. P. Fabbi for trace element analysis of silicate rocks. The technique provides a significant improvement in speed, accuracy, and precision over pressed-pellet techniques and was applicable for many elements at the ppm level including Ba, Sr, Zr, Cr, and Ni (10, 20, 20, 30, and 6 ppm, respectively). The method, originally designed for major element silicate analysis, is now appropriate for 15 of the common rock forming elements.

ANALYSIS OF WATER

Specific conductance and pH

D. E. Erdmann and H. E. Taylor developed a procedure to simultaneously determine both specific conductance and pH of natural water samples. These determinations are carried out under thermostatically controlled conditions in a continuous-flow system. The measurement of pH is by direct electrometry in the range of 4 to 9. The conductance measuring system is designed to automatically switch ranges in order to accommodate conductances ranging from 0 to 15,000 $\mu\text{mho/cm}$. The sampling rate for this procedure is 30/h. Results of a study comparing this method with a manual procedure, showed that the average difference was 1.3 percent for specific conductance and 0.07 pH unit for pH.

Boron in natural water

R. R. Spencer and D. E. Erdmann developed an AutoAnalyzer procedure for determining boron in natural water. An intensely colored complex is formed between boric acid and azomethine H, the condensation product of 8-amino-1-naphthol-3, 6-disulfonic acid and salicylaldehyde. This procedure is relatively free of interference. The analytical range is 0 to 400 $\mu\text{g/L}$, and the sampling rate is 30/h.

Plasma emission spectrometry

Methods were developed by J. R. Garbarino and H. E. Taylor (1977) for the simultaneous quantitative determinations of Ca, Mg, Na, Sr, Ba, B, Be, Cd, Cr, Co, Cu, Fe, Mn, Mo, V, and Zn by an induc-

tion coupled argon plasma emission spectrometer. The methods are suitable for the direct determination of these elements occurring as dissolved constituents in water samples having specific conductances of less than 2,500 $\mu\text{mho}/\text{cm}$ at 25°C. A rotating refractor-plate background-correction system was used to eliminate or greatly minimize interelement interference effects. Sensitivities and detection limits approaching those of conventional atomic-absorption spectrometric techniques were easily obtained.

Arsenic and selenium

An automated method to determine both inorganic and organic forms of arsenic in water, water-suspended sediment mixtures, and streambed material was developed by M. J. Fishman and R. R. Spencer (1977). Organic arsenic-containing compounds are decomposed either by ultraviolet radiation or by sulfuric acid-potassium persulfate digestion. The arsenic so liberated, together with all inorganic arsenic originally present, is reduced to arsine with sodium borohydride. The arsine is stripped from the solution with nitrogen and is then decomposed in a heated (800°C) tube furnace placed in the optical path of an atomic absorption spectrometer. Thirty samples per hour can be analyzed at arsenic concentration levels of 1 $\mu\text{g}/\text{L}$ or more.

A somewhat similar automated method to determine both inorganic and organic forms of selenium in water was evaluated by G. S. Pyen and M. J. Fishman. Organic compounds containing selenium are first manually decomposed by hydrochloric acid-potassium persulfate digestion. The Se(VI) so liberated, together with all inorganic Se(VI) originally present, is reduced to Se(IV) with stannous chloride and potassium iodide and then to hydrogen selenide with sodium borohydride. The hydrogen selenide is stripped from the solution with nitrogen and is then decomposed in a heated (800°C) tube furnace placed in the optical path of an atomic-absorption spectrometer. Thirty samples per hour can be analyzed at selenium concentration levels of 1 $\mu\text{g}/\text{L}$ or more.

Anodic stripping voltammetry

J. E. Bonelli and H. E. Taylor found that trace amounts of Cu, Zn, Cd, and Pb in natural water samples can be determined simultaneously at a hanging mercury drop electrode by differential pulse anodic stripping voltammetry. Techniques were developed for minimizing the copper-zinc amalgam intermetallic compound-formation interference effect and the interelement interference caused by excessive

iron in the sample. A buffered citrate-supporting electrolyte was used along with an automated microprocessor-controlled polarograph. By increasing deposition time, sensitivities approaching those obtainable by graphite-furnace atomic-absorption spectrometry can be achieved.

Determination of acetone

D. Y. Tai developed a direct aqueous injection gas chromatographic technique for the determination of acetone in water samples. Concentrations of from 10 to 300 mg/L were determined with a precision of about 2 percent. Concentrations in the microgram-per-liter range can be determined by using a head space sweeping and trapping procedure with a precision of about 10 percent.

Organic solutes

Several uncharged macroreticulate XAD resins were tested by R. L. Malcolm, E. M. Thurman, and G. R. Aiken as a means of concentrating organic solutes from natural waters. The resins tested included XAD-1, -2, and -4 (styrene-divinylbenzene copolymers), and XAD-7 and -8 (acrylic ester copolymers). The uncharged polyacrylic XAD-8 resin was found to be the most efficient in solute sorption and desorption. The XAD-1, -2, and -4 resins were undesirable because (1) the small pores of these resins become clogged with large natural polyelectrolytes (humic and fulvic acids), and (2) irreversible sorption of polyaromatic solutes occurs as a result of the formation of charge transfer complexes with the aromatic matrix. The XAD-7 resin was undesirable because it cannot be cleaned of various impurities. The large pores of the XAD-8 resin enables efficient utilization of its extensive surface area and also makes possible the quantitative sorption and desorption of both large and small organic solutes. Irreversible sorption caused by charge transfer complex formation is not possible with XAD-8 resin inasmuch as it has no aromatic character.

Hydrophobic organic acids

The hydrophobic acid fraction isolated from surface and ground waters using XAD-8 resin is a mixture of both simple and complex organic acids. E. M. Thurman and R. L. Malcolm separated these acids into high- and low-molecular-weight fractions by exclusion column chromatography using a new porous polyacryloylmorpholine gel called Enzacryl.

They found that the high-molecular-weight fraction consists almost entirely of humic and fulvic acids, whereas the low-molecular-weight fraction is predominately a mixture of C_4 to approximately C_{18} organic acids. This fractionation permits gas and liquid chromatographic identification of the low-molecular-weight acids without interference from humic substances. It also facilitates the characterization of humic and fulvic acids, which are then free of interferences of the low-molecular-weight acids.

Pesticides

A method for the determination of residues of 10 triazines in natural water samples was developed by T. R. Steinheimer. It is applicable to raw surface water, ground water, and many industrial effluents. The procedure utilizes methylene chloride extraction followed by adsorption chromatography on aluminum oxide and subsequent gas chromatographic separation and quantitative measurement. Identification is made by selective gas chromatographic analysis with the use of two or more dissimilar column packing materials. Nominal sensitivity is $1 \mu\text{g/L}$. The method can measure residues of ametryne, atratone, atrazine, cyprazine, prometone, prometryne, propazine, simazine, simetone, and simetryne.

Humic acids

Humic acids, the most abundant organic compounds in soils and natural waters, have been studied extensively, but very little progress has been made in the elucidation of their chemical structure because humic acids form molecular aggregates that are held together by hydrogen bonding and other weak bonding mechanisms. In the past, workers have been forced to use drastic degradation procedures in order to fragment the molecules and obtain structural information. The fragments isolated, however, have generally been too small to provide more than the most rudimentary structural data.

A better approach to the problem of the determination of the chemical structure of humic acids is that of disrupting the hydrogen bonding, separating out the various chemical species of the aggregates, and then applying specific degradation techniques to each of the fractions. In order to accomplish this, R. L. Wershaw and D. J. Pinckney (1978) developed a permethylation procedure that allows

greater methylation of carboxylic acid, and also of phenolic and alcoholic groups, than was previously possible. When these groups are derivatized they can no longer participate in hydrogen bonding, and disaggregation takes place.

Biological Methods

A high-pressure liquid chromatographic (HPLC) method was developed by W. T. Shoaf III for the determination of chlorophyll *a* and *b*. The method was automated with the use of an autoinjector and a computing integrator, thereby reducing analysis time as compared to analysis times required for thin-layer chromatographic methods.

Shoaf also developed a procedure for the identification and enumeration of periphytic diatoms.

Lithium isotopes

H. E. Taylor and L. J. Schroder II (1978) developed a dual-beam atomic-absorption spectrometric technique for measuring the ratio of trace levels of lithium-6 to lithium-7 in water samples. The method involves simultaneous measurement of the absorbances of lithium-6 and lithium-7 isotopes in a single sample portion. The absorbances are then electronically ratioed by a microprocessor to yield an output that is directly proportional to the isotope ratio. Ratios can be measured on samples with total lithium concentrations as low as $100 \mu\text{g/L}$.

Stable isotope ratios

The accurate, fast determination of the stable-isotope ratios of H, C, N, O, S, and Si is of fundamental importance in chemistry, geology, biology, and geochemistry. Recently, the null technique, used on double-collecting mass spectrometers since 1950, was improved by using a voltage-frequency conversion and totalizer system (VF system). T. B. Coplen II made a further improvement in isotope-ratio analysis by employing a passive filter on the major ion beam electrometer, which was adjusted so that the response speeds of both ion beam electrometers are identical. The outputs are measured several times a second with a programmable calculator-digital voltmeter system, and software is used to reject spikes. This is a significant improvement over the VF system in that it provides for spike rejection and is less expensive to implement.

GEOLOGY AND HYDROLOGY APPLIED TO HAZARD ASSESSMENT AND ENVIRONMENT

EARTHQUAKE STUDIES

SEISMICITY

National Earthquake Information Service

The USGS National Earthquake Information Service (NEIS) serves as a focus for seismological information from an international and national group of cooperating seismic observatories. Three principal services are provided to a wide variety of users in the scientific, governmental, private, and public sectors. These services are: (1) determining earthquake parameters, primarily hypocenters and magnitudes, which provides a data base for a substantial part of all research in seismology; (2) performing a clearinghouse function for timely general information about earthquake phenomena; and (3) providing early information on location, magnitude, and relevance of all large and damaging earthquakes and filling a need for notification to disaster relief agencies, scientists, and the public.

The USGS provides public information services on recent earthquakes in response to increasing demands from the general public. In order to do this on a timely basis, NEIS operates a continental aperture seismic array, centrally recorded in Golden, Colo., and an Early Earthquake Alert that is staffed on a 24-hour, 7-day week basis. Depending on the shock size and location, information was usually provided within hours to concerned agencies and media in the United States and overseas. In addition to the fast release of data and results, NEIS continued to publish the Preliminary Determination of Epicenters (PDE), Monthly Listing of Epicenters and the Earthquake Data Report (EDR). The first two publications provide summary data on location, magnitude, and human and property losses, whereas the EDR provides both the summary data and station data reported as of the publication date. This permits other researchers to add data and carry out their own investigations.

According to NEIS records, W. J. Person found that there were 3,000 deaths caused by earthquakes

in 1977, 1,500 were from the magnitude 7.2 Rumanian shock of March 4, 1977. For the year, there were 14 earthquakes of magnitude 7 or larger, but casualties and damages were relatively light because most of the major shocks occurred in oceanic or otherwise sparsely populated areas. For the larger shocks in or about the Pacific Basin, seismic data arriving at NEIS Golden Headquarters was rapidly processed and forwarded to the Tsunami Warning System in Honolulu, Hawaii, which is operated by the National Weather Service of NOAA.

C. W. Stover reports that 71 earthquakes in 19 States were canvassed for felt and damage data by use of a newly revised questionnaire more acceptable for computer evaluation. The questionnaires plus additional data, from the media or USGS official collaborators, were evaluated for intensity, and the results are in preparation for publication.

The largest earthquake (magnitude $M_L=4.8$) in the United States occurred near Willets, Calif. (39.45°N. , 123.26°W.), with a Modified Mercalli intensity VIII. An unusual shock, of smaller magnitude, occurred in northeast Utah with little or no damage in the epicentral area; however, Grand Junction, Colo., inhabitants, about 140 miles away, were alarmed by the shock.

According to M. A. Carlson, the U.S. Seismic Network became truly national in scope during fiscal year 1977 with the addition of several stations in the Northeast. This expansion, as before, takes advantage of existing stations and regional recording centers in order to increase NEIS recording capability at minimal add-on expense. Though recording capability is compromised due to the lack of stations in the far Southeast, and upper and lower Midwest, there will be no further expansion until a feasibility study for an upgraded National Seismic Network, currently underway, is finished.

At the present time the network is used to establish the occurrence of an earthquake and to determine the data requirements for an adequate location and magnitude. The enlarged aperture of the U.S. Seismic Network, particularly with Honolulu, Hawaii, Palmer, Alaska, and other fast reporting

facilities, greatly improves the NEIS capability to locate large and destructive shocks. There are now 60 short-period vertical (SPZ) elements and 5 long-period vertical (LPZ) channels. Another area where the network has made quite an impact is rapid determination of magnitudes. At the present time, 16 data channels are calibrated and the response curves stored in a magnitude program called "mag" for rapid determination of m_b , m_s , M_L and other magnitudes, interactively, as required, by NEIS personnel. This is particularly useful for the Earthquake Early Alert staff of NEIS in the early stages after the occurrence of an important earthquake.

In addition to the 60 SPZ recorded at Golden, Colo., 10 of the SPZ are recorded at the Newport Observatory in Washington where staff are available to report data to the NOAA/Tsunami Warning System whenever the alarms are triggered. A mini-computer has been purchased and efforts are underway to automatically detect events and establish a usable data file at NEIS Golden. This represents a continuing effort to upgrade the services of this center.

Observatory and seismic data systems

According to H. M. Butler, 13 advanced seismograph systems, called Seismic Research Observatories (SRO) are being installed as part of a program to upgrade the worldwide seismic data network. The SRO system was created by combining a recently developed broadband borehole seismometer and a software-controlled recording system. Digital recording of gain-ranged data provides an amplitude of nearly 120 B (20 orders of magnitude). The network of SRO stations will be an important new data resource for seismological investigations, especially for those studies that require computer processing of the data. Butler also notes that the High-Gain Long Period Systems (HGLP/ASRO) continue to provide high-gain long period digital and analog data to USGS researchers and others that require high quality data to study source mechanisms, structure, attenuation, and other earthquake parameters.

The USGS continues to operate the Worldwide Standardized Seismograph Network (WWSSN) in 29 different states and territories of 50 foreign countries. Albuquerque Seismological Laboratory (ASL) provides support to these stations that provide a significant amount of the high quality data to NEIS for global seismicity studies. R. P. McCarthy notes that the timing accuracy of less than 50 milli-

seconds error per 24-hour period was evidenced at about 60 percent of the stations and, of the remainder, most were under 100 milliseconds.

L. H. Jaksha and colleagues have expanded seismic studies in the New Mexico rift zone. The seismic network of the rift zone has been enlarged to 13 stations over a monitoring area that includes the Albuquerque, Estancia, and parts of the Socorro and Santo Domingo Basins. Routine analysis of ongoing seismicity indicates three primary zones of earthquake activity: The South Albuquerque-Socorro Basins, the Estancia Basin, and the area northeast of Grants, N. Mex. Normal faulting is indicated as the preferred source mechanism of the earthquake activity.

The Systems Engineering Group supports engineering activities at the Albuquerque Seismological Laboratory in conjunction with various worldwide seismic and observatory activities. Under this program, new microprocessor-based seismic instrumentation systems and circuits are being designed, developed, and tested to improve seismic systems performance and lower the cost of new systems. H. E. Clark, Jr., reports that the use of microprocessor systems reduces all system costs by 40 percent to 60 percent of present system costs.

Tsunami seismic and tide systems

H. E. Clark, Jr., also points out that for the USGS-NOAA/NWS Tsunami Systems Development Project the most important result obtained was the large cost reduction in Tsunami data systems. The use of microprocessor-based data systems reduced the cost of conventional Tsunami Tide Systems from \$4,000 per system to \$300 per system. The microprocessor-based Tsunami Seismic System reduced the cost of conventional Tsunami Seismic Systems from \$6,000 per system to \$500 per system. In addition, the microprocessor-based Tsunami systems has greatly increased capacity and expanded capabilities.

Seismicity and seismic parameters research

Aftershock hypocenters of the October 1974 Peruvian earthquake, determined from regional network data, lie southward of the main shock ($M_s=7.8$) and define a 25 km-thick, 'T'-shaped zone that is composed of two linear trends, according to C. J. Langer and W. J. Spence. These trends, which seem to mimic the location and shape of the main shock, are 80 to 100 km offshore and are parallel to the coast for a length of about 220 km. The other trend is perpendicular to the first at its approxi-

mate midpoint and dips 20° E., extending for about 150 km to beneath the coastal town of Chilca, Peru, about 50 km south of Lima, Peru. A composite focal mechanism solution for the latter trend is well-defined and suggests underthrust motion, very similar to that inferred for the main shock. Each of the aftershock trends has a b -value of about 0.65, and the total data set is complete above magnitude 3.6. The measured after shock area is about $10,000 \text{ km}^2$ (10^{14} cm^2), implying an equivalent mainshock magnitude of $M_s = 7.7$ (Utsu relationship: $\log_{10} A = M_s + 6.3$).

In a related study, Spence and Langer found a well-defined space-time distribution for the 1974 Peru aftershocks in a study combining regional and teleseismic data. Space-time seismicity studies of the teleseismically- and regionally-located aftershocks to the M_s 7.8, October 3, 1974, Peru earthquake indicate six distinctive groupings of epicenters. The entire aftershock sequence occurred to the south of the main shock. The first grouping of aftershocks consisted of four teleseismically-located aftershocks that occurred near the extremities of the subsequently developed aftershock zone. The next four groupings show that earthquakes alternate, almost exclusively, between a parallel-to-coast trend of aftershocks and a second trend perpendicular to the first, each grouping lasting from 2 to 3 days. The last three of these groupings include regionally-located aftershocks, down to the magnitude 3.6 level, and confirm both the gross space-time characteristics and the internal sequencing of earthquakes within each group. In particular, the two groups occurring in the offshore limb show a geometrically-regular oscillation of activity between its northern and southern ends, skipping the mid-portion of this zone. The sixth grouping lasted about 3 weeks and showed a more random-space-time distribution of epicenters. It is remarkable that the primary aftershock series was terminated by the two largest aftershocks of the series (November 9, 1974, ($M_s = 7.1$); November 14, 1974, ($m_b = 5.4$)). Since November 14, teleseismically-located earthquakes of this region are occurring at the periphery of the primary aftershock zone. The observed space-time seismicity pattern may reflect a continuing tectonic instability of this region. These observations are being refined by relocating these aftershocks by a joint hypocenter method.

J. W. Dewey and D. W. Gordon engaged in a study to improve historical earthquake locations. It has been noted by a number of researchers that the U.S. earthquake catalog has inconsistencies that can

compromise seismic risk, tectonic, and other types of studies requiring good locations. Over 100 instrumentally-recorded shocks that occurred in the United States east of 85° W. longitude in the years from 1918 to 1976 have been relocated by the method of joint epicenter determination (JED) and 90 percent-confidence ellipses assigned to their epicenters. Dewey and Gordon show that the vast majority of the above-mentioned 100 instrumentally-recorded shocks cannot be located to within 20 km (at a 90 percent level of confidence) using the data reported in the standard seismological bulletins, even when the effect of source-station bias is minimized by use of the joint epicenter method. Therefore, it is pointless to use routinely determined epicenters to try to resolve tectonic structures in the east with dimensions smaller than several tens of kilometers. The resolution of small-scale (dimensions less than several tens of kilometers) tectonic structures in the east requires dense networks of regional seismographic stations, such as those in New York, New England, and South Carolina. The method of JED in which calibration events are used is not optimum for large sections of the eastern United States in which seismic events are widely spaced. For these regions, we have written a form of JED in which travel-time tables are calibrated using calibration stations assumed to have zero bias. An apparent east-west trend of epicenters through Charleston, S.C., is probably spurious. The earthquakes had occurred prior to the installation of the South Carolina network. Recomputed epicenters are not significantly different from the Middle Gardens source region recently defined by the South Carolina network and believed to mark the source of the destructive 1886 earthquake.

B. R. Julian reports that considerable progress has been made during this period in developing programs with which to study earth structure as well as the earthquake mechanism. It is now generally recognized that the use of ray theoretical techniques (such as the use of $T-\Delta$ or $\frac{dT}{d\Delta}$) are

inadequate and in some cases misleading for the purpose of inverting for an earth model. The main effort, therefore, has been to develop programs to produce synthetic waveforms that properly account for non-ray theoretical effects, as well as attenuation, that are incurred by body waves propagating through the earth. Available on the Multics are programs to generate synthetics in the time or frequency domains and Fourier components of certain

body waves by using a frequency-dependent full-wave theory.

Research is being conducted to extend the capability of the full wave theory. G. L. Choy (USGS), in cooperation with Vernon Cormier (Cooperative Institute for Research in Environmental Science) developed a technique that enables the full wave theory to treat body waves whose propagation paths interact with a series of first order discontinuities in a spherically symmetric but radially varying earth model. This development is now being applied to synthesize *SH* body waves. These synthetic *SH* waveforms are being used both to study upper mantle structure and to examine the consequences of assuming the validity of ray theory.

EARTHQUAKE MECHANICS AND PREDICTION STUDIES

The National Earthquake Information Service has been receiving earthquake predictions for many years. Almost all of them come from sincere people who claim to have new geophysical theories, physical sensations, or psychic powers. R. N. Hunter and J. S. Derr report that for the last 2 years, these predictions have been logged and scored by a computer program that rates the failure or degree of success of the prediction, as well as its value based on the seismicity of the predicted area. Any such method of scoring must necessarily be subjective. However, even a fairly liberal definition of "success" results in the vast majority of predictions being failures. Statistical manipulations of the data are currently underway. There is a possibility that some predictions will be statistically significant, depending on the scoring criteria used. Hunter and Derr cited an analysis of over 2,300 predictions from over 230 filed sources that shows that none of the predictions has achieved a high enough score to merit consideration.

A significant part of the U. S. earthquake prediction program has been concerned with the near field stress regime. During the preparation phases of great earthquakes, major changes in the associated regional stress field apparently occur. These stress changes result in a set of physical precursors to impending great earthquakes; some of these precursors are observable in the far field. Thus seismologists have the opportunity to use remote seismograph networks to monitor earthquake zones for possible seismic precursors. W. J. Spence and L. C. Pakiser held a special conference in Denver, Colo., to ex-

plore present and future research in global seismology, emphasizing prediction of large earthquakes. Thirty-two participants from 11 institutions discussed and speculated on the questions at hand. The major conclusions, which are consistent with the inclusion theory of earthquake occurrence, of the group were:

- Temporal patterns of seismicity (and aseismicity) exist on a global scale, on a regional scale, and on a local scale. Certain of these seismicity patterns precede the occurrence of large earthquakes. The systematic location of worldwide earthquakes by the USGS National Earthquake Information Service provides a data base for monitoring zones of possible great earthquakes for precursory seismicity patterns.
- Waveforms that originate from small to moderate earthquakes occurring in the region of a forthcoming great earthquake may change their character in relation to the evolving regional stress conditions. The new digital recording broadband seismograph systems now being installed by the USGS may permit monitoring of suspect seismic zones and detection of prognostic waveform changes as a large stress regime approaches failure.
- A definite reduction of low to intermediate magnitude earthquake activity occurs in the aftershock zone of a large earthquake. At the same time there is often a small burst of activity near the hypocenter of the forthcoming large earthquake, which is then followed by relative quiescence. These observations are consistent with the inclusion theory of earthquake occurrence.

Land deformation

J. C. Savage and W. H. Prescott conclude from annual remeasurement of Geodolite lines along the San Andreas fault between Cajon and Tejon passes in Calif. that compression normal to the fault and right-lateral shear strain across the fault are accumulating at about the same rate (0.2 microstrain/yr) along the entire section in the period 1973-77. There is no significant accumulation of strain parallel to the fault. The uniformity of this strain accumulation is confirmed by comparing several individual networks along the section. The amount of compression relative to the amount of shear is about four times larger than might be expected from simple models of the Big Bend of the San Andreas.

Further analysis of the historic geodetic record by R. O. Castle shows that the southern California uplift is but a single event in an apparently continuing deformational process. Thus, the identification of an earlier episode of uplift that grossly mimicked the modern uplift probably began sometime after 1902. It shows that large parts of southern California, lying generally astride the San Andreas system, have sustained major, more-or-less cyclic, aseismic crustal deformation characterized by one-half century periods.

R. C. Jachens established a network of high-precision gravity stations in the tectonically active regions of southern California during the first 3 months of fiscal year 1977. The purpose of the work was to establish a gravity datum against which future gravity measurements can be compared in order to detect, monitor, and study changes in gravity associated with crustal deformation. Relative gravity was remeasured at 32 stations scattered throughout the network during May 1977. Computed standard errors for apparent changes in gravity referred to a primary reference station in Riverside, Calif., averaged $9 \mu\text{Gal}$. Apparent changes in gravity that exceeded two standard errors were found at five isolated stations. The largest apparent change in gravity (-37 ± 9 (s.e.) μGal) was found at a station located 40 km northeast of Lucerne Valley, Calif. Apparent changes in gravity at stations located within 10 to 15 km of the point of maximum change were $< 10 \mu\text{Gal}$.

D. F. Barnes reported that a preliminary reoccupation of gravity base stations southwest of Anchorage, Alaska, has revealed a surprisingly small gravity change along a traverse on which precise releveling has indicated more than half a meter of relative uplift since the 1964 earthquake (Brown and others, 1977). Both NOAA and the USGS established gravity bases on this line in 1965, and both sets of bases were reoccupied in 1977. All the accurately reoccupied stations showed changes of less than $40 \mu\text{Gal}$, and a running average of changes at station pairs is usually less than $10 \mu\text{Gal}$ suggesting that the measured gravity change is both less than the probable uncertainty of the data and much less than the $150 \mu\text{Gal}$ change that might be expected from the free-air difference caused by the elevation change. Furthermore, the change measured during the 1964 earthquake was also anomalously small in this area and was not clearly established until several years after the earthquake. Thus both stress release and probable stress accumula-

tion seem to be accompanied by gravity changes much smaller than a free-air gradient would indicate for the elevation changes. A probable explanation is a process that involves large mass changes such as elastic deformation with a low Poisson's ratio or dilatancy in a crystal-magma melt.

R. O. Burford compared creepmeter records from several sites along the Calaveras fault in Hollister Valley with results from a high-precision multi-wavelength distance-measuring (MWDM) system operated from a hilltop in Hollister since September 1975 and concludes that (1) aseismic fault slip extends to considerable depth (about 10 km) on the Calaveras fault north of Hollister; (2) deep slip episodes are characterized by long periods of accelerated slip (several weeks in duration), as seen on long MWDM lines, in contrast to the typical near-surface fault response seen on creepmeter records (event durations of hours to days); (3) the deep slip activity can precede the near-surface response by several weeks; (4) clusters of seemingly isolated creep events at the surface may be related to a single episode of deep-seated aseismic movement; and (5) the observed behavior suggests a rigid block model overlain by a thick layer (3 to 5 km) of unconsolidated sediments. The thick surface layer is loaded to failure (resulting in a detectable surface creep event cluster) by the deeper episodic slip detected by the MWDM system.

Arrays of relatively inexpensive tilt, strain, and magnetic instruments, installed by M. J. Johnston, C. E. Mortensen, A. C. Jones, and B. E. Smith, along active faults in Western United States, are being used to provide details of both seismic and aseismic (creep) fault failure. Of particular interest is the detailed fault mechanics sequence that results in earthquakes. Preliminary results indicate that (1) precursive slip seen most clearly for earthquakes larger than magnitude 4 occurs before and dominates the earthquake process (an earthquake prediction scheme has therefore been designed around automatic detection of these strains and tilts); (2) surface expression of aseismic slip (creep) does not appear to be associated with large-scale strain field changes; and (3) change in crustal stress fields, as inferred from magnetic measurements, can apparently have a scale exceeding several tens of kilometers. Magnetic field changes since 1973 have been observed near Palmdale in southern California, and these appear to be related in detail to changes in level in the region.

Analyses of seismic data

A compilation of seismicity in southern California since the installation of the USGS Mojave and San Bernardino networks (July 1974–September 1976) (G. S. Fuis and others, 1977) has revealed a number of intriguing features. Seismicity in the central Mojave Desert is characterized by earthquake swarms and earthquake-aftershock sequences that are not conspicuously interrelated spatially or temporally. Seismicity in the Little San Bernardino-Eagle Mountains area is characterized by earthquake swarms that interconnect spatially and temporally to define the Blue Cut seismic lineament and the Porcupine Wash and Smoketree Wash seismic lineaments. The Desert Hot Springs seismicity belt is parallel to but northeast of the Banning-Mission Creek fault. A seismicity cross section through this belt indicates seismically active crust to the northeast and seismically inactive crust to the southwest; the interface between these regions appears fairly sharp and dips 35° to 40° to the northeast. The Brawley fault is outlined strikingly by seismicity. Between this lineament and the Desert Hot Springs belt is a seismicity gap on the Banning-Mission Creek fault. It is interesting to note that the steepest gradient (and possibly the greatest strain) on the newly-developed eastern lobe of the Southern California Uplift (Thatcher and others, 1976) occurs in the area of this gap. It must be pointed out, however, that this gap has existed for at least 45 years (Hileman and others, 1973). A seismicity boundary between seismically active and inactive parts of the Mojave Desert is parallel to the dominant structural grain of the Mojave Desert between latitudes of about 34° to 35° and conjugate to the dominant structural grain south of 34° lat.

F. W. Klein studied the seismic trends associated with the 1975 Kalapana earthquake, which occurred adjacent to an otherwise seismically active and deforming volcanic zone. The poorly understood interaction between large earthquake and volcanic rift produced a complex aftershock sequence that is long in duration and spread laterally outward in all directions as it progressed.

Detailed analysis has been made by W. H. Bakun, R. M. Stewart, and C. G. Bufo of the magnitude-4.1 January 15, 1973, earthquake and associated aftershocks that occurred on the San Andreas fault 25 km south of Hollister, Calif. This event was preceded by a sequence of foreshocks that began in December 1972. Of particular interest are two foreshocks on December 12, 1972, at 0351 and 0355 GMT with magnitudes 2.9 and 2.8, respectively,

that have nearly identical hypocenter locations and fault-plane solutions. Observed seismograms for these two events at 25 stations within about 50 km of and surrounding the epicenters are systematically different in a pattern that is consistent with different directions of rupture for the two events. In contrast to the more bilateral rupture propagation of nearby aftershocks, the 0351 GMT foreshock rupture propagated unilaterally from near the northwest edge of the aftershock volume toward the southwest into the aftershock volume, and the 0355 GMT foreshock rupture propagated unilaterally toward the northwest away from the aftershock volume.

W. H. K. Lee has continued making refinements in methods of inverting *P*-arrival times recorded by microearthquake networks and in tracing seismic rays through a heterogeneous medium. He has successfully adapted the method of singular value decomposition to the generalized inversion scheme and applied the adaptive finite difference techniques to two-point seismic ray tracing.

Equipment development

R. V. Allen has demonstrated that very powerful recognition and timing algorithms are now practical in automatic earthquake processing because of the availability and applicability of low-priced microprocessor systems. An algorithm developed originally on large general-purpose computers has now been operated successfully in a microprocessor of a kind that can form the basis of future field and office-based systems.

J. R. Vanschaack completed design, development, and construction on 100 portable seismic recorders with cassette tape storage for observing up to 10 seismic refraction shots at predetermined set times. The system will automatically turn on, calibrate itself, and record for a period of up to 16 minutes at each preselected recording time.

Hydrofracturing

Stress measurements were made to depths of 344 m in Atlantic Coastal Plain sediments near Charleston, S.C. The magnitude of the least principal compressive stress was found to be sufficiently below lithostatic to result in normal-type fault motion on favorably oriented faults. Because stratigraphic evidence suggests the existence of normal faults in the area, M. D. Zoback interprets these results to suggest that normal faults in Coastal Plain sediments near Charleston are currently active. It is not clear, however, if this process is re-

lated to either the 1886 Charleston earthquake or the current seismicity. Zoback also conducted seismic refraction and borehole studies at three sites in the region of the New Madrid earthquakes. Analysis of the refraction profiles, which cross lineaments bounding Reelfoot Lake in northwest Tennessee, show that each is apparently a normal fault. Thus the lake, which reportedly formed at the time of the major earthquake, appears to occupy a graben bounded on each side by a normal fault dipping beneath it. Investigations of Crowley's Ridge, a prominent northeast-trending scarp near the town of Dexter, Mo., showed that the feature was not a fault. Laboratory experiments were designed by Zoback to determine fracture toughness, or critical stress intensity factor of a variety of rock types. This parameter is extremely important for development of theoretical models of hydraulic fracture propagation in situ. Three types of crystalline rock were investigated: Westerly Granite (82 bar-cm^{1/2}), "Sierra" granite (78 bar-cm^{1/2}), and "Academy" gabbro (102 bar-cm^{1/2}). Berea Sandstone (30 bar-cm^{1/2}) and "Leudere" limestone (58 bar-cm^{1/2}) were also investigated.

M. D. Wood found that by carefully recording small ground tilts during massive hydraulic fractures, he could infer the fracture geometry reasonably well.

Laboratory studies

Preliminary preseismic fault slip experiments have been conducted by J. H. Dieterich, D. W. Barber, and Gerald Conrad using a large-scale biaxial deformation apparatus. The sample consists of a 150 cm×150 cm×40 cm granitic block with a resurfaced sawcut oriented 45° to the loading axes. Variable amounts of preseismic slip were observed for all seismic slip events. Duration of slip is proportional to the magnitude of stress irregularities along the slip surface and inversely proportional to loading rate. The results also confirmed a previous prediction that the amount of preseismic slip displacement increases with fault dimensions. This suggests that preseismic slip may be a significant precursor at the dimensions for earthquake faulting. J. D. Byerlee found that creep on faults at high pressure takes place at first by a decaying primary creep followed by a constant secondary creep and finally by an accelerating Tertiary creep that ends in sudden strike-slip. His experimental results suggest that earthquakes in areas of constant rate fault creep should be preceded by a period of accelerating creep rate. S. H. Kirby completed a comprehensive

study of the creep properties of synthetic alpha quartz crystals with the objective of elucidating the hydrolytic weakening mechanism. The creep rates follow a thermally activated power law with the activation energy for creep $E_c^* = 40 \pm 5$ Kcal/mole and stress exponent $n = 3.3$. The rate controlling mechanism is the diffusion of impurity water. A change in activation energy to 10 to 20 Kcal/mole occurs when the temperature is in the -quartz stability field.

Compressional wave velocities in Franciscan rocks could be predicted, with an error of 2 percent, by R. M. Stewart using a linear function of temperature, pressure, porosity and density, over the range 0°C to 300°C, 2 to 8 kb, 0.5 to 6.5 percent, 2.55 to 2.95 g/cm³. Extrapolated to 10 kb and 0 percent porosity, the linear function agrees well with Birch's law. The results, combined with seismological and geological data, imply that a major lithologic change occurs beneath the Franciscan terrain of northern and central California, at a depth of 12 to 15 km, from Franciscan metasediments to a more mafic rock, possibly oceanic crust. Stewart also studied compressional and shear velocities in metavolcanic and amphibolite rocks from the region of Oroville, Calif. Results for saturated rocks under low uniaxial stress (250 bars) show that observed seismic velocity in the Oroville area is compatible with a several-kilometer-thick layer of metavolcanic and amphibolite rocks and that pore pressures cannot be a substantial fraction of the lithostatic pressure in any large seismically monitored volume of the crust of the Oroville area.

Compressional and shear velocities were measured in Westerly Granite samples as functions of independently variable high temperature and pressure. The technique adopted was designed to insure that no cracking occurred in the samples during the experiment. The results are in general agreement with previous measurements of velocity in intact granitic rocks, but disagree with results obtained for Westerly Granite subjected to extensive thermal cracking. In particular, the Poisson's ratio of the intact sample is insensitive to pressure and temperature, and incomprehensibility decreased smoothly with temperature. Both these results contrast sharply with the results for the thermally cracked granite. Louis Peselnick measured compressional velocity to 8 kbar and 275°C on three orthogonal cores of a harzburgite rock from the Antalya ophiolite complex in Turkey. On the basis of its mineralogy and texture, such rocks are considered to represent the upper mantle underlying an oceanic

crust. The mode (percent by volume) for the sample is 74 olivine, 22 orthopyroxene, 1.5 clinopyroxene, 1.5 spinel, and 1.0 serpentine. The apparent porosity is 0.5 percent and the bulk density is 3.32 g/cc. For pressures greater than 2 kbar, the velocity is adequately described by a linear dependence on pressure and temperature. A strong anisotropy in the velocity was observed of 8.57 ± 0.07 km/s along crystal axis (100), 7.98 ± 0.06 along axis (010), and 7.87 ± 0.06 along axis (001). Thus, seismic anisotropy would be expected for the oceanic upper mantle. The average pressure and temperature derivatives of the velocity for the three directions are 14 m/s kbar and -0.6 m/s °C. He considers these values to be representative of Antalya oceanic uppermost mantle. The critical thermal gradient calculated from these values is $7.5^\circ\text{C}/\text{km}$. Estimates of geothermal gradients in the upper mantle are about $7-10^\circ\text{C}/\text{km}$. Thus, the high thermal gradients could in part be responsible for the low velocity zone.

EARTHQUAKE HAZARD STUDIES

TECTONIC FRAMEWORK AND FAULT INVESTIGATIONS

Seismogenic zones of Alaska and adjacent continental shelf

J. I. Ziony and W. H. Diment in collaboration with D. M. Perkins and S. T. Algermissen completed a preliminary analysis of the seismotectonic framework of Alaska and adjacent continental shelves. Twenty-five source zones that encompass regions with distinctive geologic conditions and earthquake potential were delineated. Many of the zones are large because seismicity for much of Alaska could not be closely associated either with specific geologic features exposed at the surface or geophysical trends indicative of deep structures.

Earthquake source areas likely to produce relatively frequent large to great events in southern Alaska are associated with (1) segments of a seismically well-defined subduction zone, which is broad and shallow near the Gulf of Alaska and steepens abruptly down-dip toward the northwest, and with (2) nearby tectonic units suitably oriented to respond to subduction-related regional stress. An interlacing system of narrow source zones represented by Holocene strands of the Denali, Totschunda, Fairweather, Chatham Strait, and Queen Charlotte Island strike-slip faults generally bounds the subduction region on the northeast. Zones of markedly lower seismicity, and presumed lower earthquake potential, locally are interposed westward of the strike-slip fault; these zones include

the Wrangell Mountains, underlain by Quaternary and upper Tertiary volcanic rocks, and the relatively underformed shelf area between Cross Sound and Icy Bay. A broad seismogenic zone with potential for large shallow earthquakes was identified with a series of faults subparallel to the Denali between the Alaska Range and Yukon River. The largest historic event north of the subduction zone—the poorly located magnitude 7.7 earthquake of 1904—may be associated with this zone.

The inner Bering Sea and southwestern Alaska north of the Aleutian arc comprise a broad zone with relatively low potential for earthquakes. Several major fault systems such as the Denali, which to the east is seismogenic, extend into this region, but none are considered active within the zone. In contrast, the outer shelf of the Bering Sea appears to have potential for infrequent moderate to large earthquakes. An elongate west-trending seismogenic province likely to produce infrequent but potentially destructive earthquakes has been outlined across interior Alaska, the Seward Peninsula, and parts of Norton Sound, Hope Basin, and the Chukchi Sea. The zone is inferred to represent a regime of extensional tectonics that has recently been established across diverse older central Alaska tectonic elements.

Source zones in northern Alaska generally coincide with the Brooks Range and adjacent Arctic Foothills-Coastal Plain physiographic provinces. Seismicity is low, diffuse, and cannot be associated with known geologic features. An exception is an arcuate source zone in the Beaufort Sea between Camden Bay and Mackenzie Bay; this zone encompasses moderate seismicity apparently associated with late Cenozoic faulted folds that flank the Romanzof Mountains. Significantly, this zone eastward may merge with the Richardson-Mackenzie Mountains seismic belt of northwestern Canada that has been the site of several magnitude 6 and larger earthquakes.

The 1899 Yakutat Bay earthquakes

Early seismograph records and vertical uplift data constrain the fault slippage that occurred during 1899 in three magnitude 8+ earthquakes located in the eastern Gulf of Alaska. According to W. R. Thatcher the seismic moments of these earthquakes cannot be accounted for by deformation only within Yakutat Bay, and significant seismic slippage in adjacent regions is required. The most consistent explanation of all available seismic, coastal uplift, and tsunami wave data is that underthrust-

ing along ~200 km of the Chugach-Saint Elias thrust zone produced ~5 m of plate convergence during these 1899 earthquakes.

Tectonic framework of the San Francisco Bay Region

D. G. Herd reported the discovery of a major normal fault zone along the west side of the San Joaquin Valley in San Joaquin, Stanislaus, and Merced Counties, California. The newly found structural feature, which was named the San Joaquin Valley fault zone, occurs at the foot of the monocline that bounds the east side of Diablo Range. Differential offset in Quaternary deposits displaced by the fault zone has indicated that the San Joaquin Valley was repeatedly downthrown during the Pleistocene along the east side of the fault zone. Uplift of the Diablo Range locally along the fault zone has been in excess of 90 m since early Pleistocene time. Preliminary analysis of seismic records indicated that the San Joaquin Valley fault zone is seismically active, and that it may be part of a much longer, although yet unmapped, fault zone along the west side of the entire San Joaquin Valley.

Studies by E. E. Brabb demonstrated that the onshore trace of the San Gregorio fault has juxtaposed two major tectonic blocks with markedly different stratigraphic sequences. In the Pigeon Point block southwest of the San Gregorio fault, porphyritic silicic rocks are overlain by at least 2,600 m of Upper Cretaceous clastic strata. Cretaceous strata are not present in the La Honda and Ben Lomond blocks northeast of the fault where more than 10,000 m of Paleocene to Pliocene rocks rest on a pre-Tertiary granitic basement. Paleocene and Eocene rocks are not present in the Pigeon Point block. Oligocene and middle Miocene strata occur in the La Honda and Ben Lomond block is missing fauna, and bathymetry on opposite sides. A thick upper Miocene to lower Pliocene mudstone section in the La Honda and Ben Lomond block is missing west of the fault. The differences in stratigraphic sequences across the San Gregorio fault in the Santa Cruz Mountains and comparison with sequences near Bodega Head suggest right slip movement of at least 125 km since the late Miocene, or at least 1.25 cm/yr.

Southern California tectonics

In an investigation in Fremont Valley, Calif., M. M. Clark, J. M. Buchanan-Banks and T. L. Holzer found that creep is presently occurring along normal faults associated with the Garlock

fault zone. Although the faults are tectonic and record several meters of displacement in Holocene time withdrawal of ground water from Fremont Valley may be causing the modern creep. Pumping of the unconsolidated sediments within the valley during the past 20 years depressed ground-water levels more than 74 m in a cone that is partly concentric with the creeping faults. Benchmarks in the valley show subsidence relative to surrounding terrain. Most of the creep is dip slip, but some displacement consists of opening perpendicular to the faults that has led to the formation of large earth fissures. Maximum modern dip slip has increased from 300 mm in 1971 to 600 mm in 1977. Although modern fault creep is in the same sense as past tectonic movement, a tectonic origin of the creep seems unlikely. No creep is recognized on the Garlock fault beyond the boundaries of Fremont Valley. Geodetic surveys reveal no present movement of crustal blocks across the valley, and most modern creep postdates the beginning of major water-level declines.

The late movement history of the Imperial fault in California was documented by R. V. Sharp from data gathered in a trench excavated across the fault between the All-American Canal and the Mexican border. The trench was dug in fluvial and lacustrine sediments and intercepted two fault strands that moved during the 1940 Imperial Valley earthquake. Vertical separations of strata at each of the faults, with one exception, were less than 12 cm. One stratum that was offset 12 cm was both underlain and overlain by layers displaced by smaller amounts, indicating that at least part of the vertical separation could have been caused by the effect of horizontal slip on beds whose thicknesses change along the strike of the fault. The narrow width of the rupture zones, as well as additional evidence based on a projected intersection of a distinctive channel boundary with the main fault trace, suggested that strata in the trench probably suffered only one episode of large-scale slip—that of 1940. A lack of shelly material or charcoal prohibited an accurate assessment of the age of the trench sediments. However, an analysis of the sedimentation rate in Imperial Valley at a location 37 km northwest of the trench site suggested by extrapolation that the last pre-1940 seismic event associated with major slip on the Imperial fault might have occurred more than 900-1,000 years ago.

Two creepmeters 6.95 km apart on the Imperial fault in southern California recorded a total of 14 mm and 23 mm of right lateral slip over a 2-week

period during April 1977 (Gilman and others, 1977). These separate events of slip were thought to be related and to represent a single patch of slip. From a careful air-photo reconstruction of the 1940 surface rupture of the Imperial fault and a spatial and temporal analysis of surficial breakage of manmade features between and beyond the offset features, R. V. Sharp concluded that the recent creep events occurred on two separate surficial strands of the fault. No data gathered since 1940 confirms the presence of a throughgoing single fault at the surface in this area although the approximate coincidence of movement in time implies that there may be continuity at depth. Thus, the two surface observations of creep in April 1977 could reflect a discontinuity of surface slip similar to that developed in the 1940 earthquake rupture—one that tends to mask deepseated continuity of slip.

Sharp prepared a new map showing traces of fault strands along part of the Brawley fault in south-central Imperial Valley. Two kinds of features are displayed on the map—fractures in the ground surface that were observed at the time of the earthquake swarm of January to February 1975 (Sharp, 1976) and fault scarps and linears visible on aerial photographs of this region taken in 1937 by the U.S. Department of Agriculture. Superposition of these two sets of data revealed:

- Within the limits of error (approximately ± 5 m), the 1975 surface fractures coincide nearly exactly with the positions of the fault traces as mapped from the 1937 photographs. This relation implies that the next movements of the Brawley fault in this area are most likely to reoccur along the fault traces shown on the map. Furthermore, the general spatial coincidence of the surface ruptures with the lines of prehistoric movement together with earthquake foci in basement rocks, and the en echelon character of the fractures provide compelling evidence that the surface fractures and associated vertical offsets of 1975 reflect tectonic displacement at depth.
- Two small apparent divergences of the 1975 surface fractures from the earlier trace occur, but these fall within an expected "normal width of disturbances along a fault trace.
- The surface faulting of 1975 probably developed along four and possibly five separate preexisting strands within the zone of the Brawley fault.

California coastal tectonics

K. R. Lajoie reported that amino acid analysis of molluscan fossils from four marine terrace localities ranging in elevation from 6 m to 240 m along a 50-km section of the Santa Barbara and Ventura County, California, coastlines indicates all localities are roughly 40,000 years old. The cool-water aspect of the molluscan faunas supported the interpretation that the presently discontinuous marine terrace on which these fossils lie was cut during the middle Wisconsinan highstand of sea level when ocean temperatures were significantly cooler than they are today. Molluscan fossils from a marine terrace at about 20 m yielded age estimates of 6,000 to 7,000 years. The maximum tectonic uplift rate derived from the highest part of the 40,000 year old terrace and the Holocene terrace is ≥ 7.7 mm/yr, which agrees with uplift rates of ≥ 10 mm/yr derived by others from geodetic data. These values are the highest known uplift rate outside the isostatically rebounding Puget Sound area (~ 8.5 mm/yr) on the west coast of the conterminous United States. The rapid vertical crustal movements are an expression of the north-south compressional tectonic pattern presently affecting this region.

Seismotectonics of Utah and Nevada

Earthquake epicenters in southwestern Utah are distributed in diffuse zones that trend northerly and east-northeasterly. From field studies and interpretations of published geologic maps of the area, R. E. Anderson concluded that the zones coincide with major structural features. One zone that extends southward from the intermountain seismic belt into Arizona coincides with the faulted western part of the Colorado Plateau province, commonly referred to as the transition zone between the Colorado Plateau and the Basin and Range provinces. Another zone extends east-northeasterly from southern Nevada into southwest Utah where it follows a major structural corridor to its intersection with the Colorado Plateau. The apparent coincidence of the seismic zones with major structures suggests a distinction between the intermountain seismic belt and the southern Nevada seismic belt.

Studies of late Quaternary faults in western Utah by R. C. Bucknam and R. E. Anderson showed that there are large areas in western Utah, mainly along the seismic belts, where there is a fairly close association of late Quaternary fault scarps and earthquake epicenters. Elsewhere in Utah, there are areas of several thousand km² in extent where neither

late Quaternary scarps nor earthquakes are located. The picture is not simple, however, for there is a west-northwest-trending corridor 75 km wide and 150 km long in central west Utah where fault scarps are common and earthquake epicenters are not. The generally good correlation between late Quaternary fault scarps and epicenters was not apparent when only the Holocene record of western Utah was considered. Though data that permit a rigorous discrimination between Pleistocene and Holocene fault scarps are scant, there appear to be large portions of the seismic belts in Utah that lack evidence of Holocene faulting and others that contain such evidence. Studies of the geomorphic characteristics of fault scarps together with C^{14} age dating and studies of trenches excavated across faults succeeded in documenting Holocene faulting in only one small area (Braffits Creek, 10 km northeast of Cedar City) in the Richfield and Cedar City 2° quadrangles, yet the major zone of seismicity in southwestern Utah passes through these quadrangles.

The analysis of displacements and lengths of young faults in north-central Nevada by R. E. Wallace indicated that over a few tens of thousands of years the largest earthquakes to have occurred had a seismic moment corresponding to a local magnitude of no more than 7.5. The earthquake of 1915 in Pleasant Valley was of this general size.

Seismotectonics of the Mississippi embayment

Offsets, possibly representing the first evidence for Holocene surface faulting in the upper Mississippi embayment, were identified by D. P. Russ in a trench dug across the Reelfoot Lake scarp in Lake County, Tennessee. A zone with >3 m normal displacement occurs near the base of the scarp. This zone may be contiguous with a subsurface fault interpreted from seismic-refraction data, or it may represent draping of surficial sediments over a buried fault. Truncation of sandblow conduits and offsets mapped in the trench together with the geomorphic history of the vicinity strongly suggest that ground motion strong enough to liquify sediments occurred at least twice before 1811 in the Reelfoot Lake area.

T. G. Hildenbrand and M. F. Kane reported that the Bouguer gravity map and aeromagnetic map of the Mississippi embayment reveal several prominent anomalies that appear to reflect the presence of major geological structures. Of particular interest is a broad zone of subdued magnetic and gravity expression that divides a region typified by higher intensities and gradients. The graben-like expres-

sion is approximately 75 km wide and trends northeast for about 300 km. Hildenbrand and Kane proposed that the subdued zone is the expression of a rift that has been active through much of geologic time since the Precambrian. Recent earthquakes have been concentrated within the rift zone and are sparse along the rift's boundaries. The epicentral line corresponding to the New Madrid earthquake series of 1811 and 1812 also lies within the margin of the rift. A linear trend of epicenters striking southwest along the axis of the proposed rift suggests that the rift is presently active or that the axis represents a zone of crustal weakness along which strain produced by present-day tectonic forces is being relieved.

Surficial geology and tectonics in the Snake River Plain

Studies by W. E. Scott of alluvial and glacial deposits and calcic soils in basins north of the Snake River Plain and directly north of the Idaho National Engineering Laboratory provided preliminary conclusions regarding the age, magnitude, and location of Quaternary deformation. Along the fault-bounded east sides of Big Lost River, Little Lost River, and Birch Creek basins about 40 km to 70 km north of the Snake River Plain, stratigraphy and the degree of soil development indicate that faults displace surfaces 15,000 to 30,000 years old by as much as several meters. In the southern parts of the basins, faulted surfaces have soils that are older than those mentioned above whereas surfaces with less well-developed soils are not faulted. Preliminary dating by several methods and comparison of these soils with better dated soils elsewhere suggest that these surfaces are on the order of 100,000 to 200,000 years old. Small remnants of surfaces with older soils may be on the order of 500,000 years old. The distribution of surfaces of these ages and their height above present drainage suggest that there is a zone of uplift trending transverse to the basins and subparallel to the northern margin of the plain. The zone is about 15 km to 20 km wide and crosses the basins about half way between the plain and the Salmon River divide. The zone is characterized by vertical separation of these alluvial surfaces of several ten's of meters to 100 m compared with a few meters to 10 m to 20 m south and north of the zone. The pattern of deformation is also indicated by bedrock relations in the adjoining ranges.

Geomorphology of fault scarps

R. E. Wallace (1977) included the height of a fault scarp in a list of several variables that can

influence the rate at which scarps are modified. The concept that scarps decrease in steepness with age in a generally regular manner was used by R. C. Bucknam and R. E. Anderson to group into general age categories late Quaternary fault scarps that they mapped in western Utah. Recent work done in support of that mapping focused on defining the relationship between scarp height and slope angle. The most complete set of data was based on 40 detailed profiles of a swarm of fault scarps on the east side of the Drum Mountains in Millard County, Utah. The scarps there, which are estimated to be about 10,000 years old, are developed on a bajada sloping about 1° to 4° . The measured scarps range in height from 0.5 m to 6.7 m and corresponding slope angles range from 6° to 25° . The well-defined curve described by the data suggests that for a given age, the slope angle of the scarp is proportional to the log of the scarp height. The standard deviation of slope angle on log scarp height is 2° . The wide range in slope angle on a scarp of a single age and generally similar materials shows that scarp height can be an extremely important variable if slope angle is used to estimate absolute or relative ages of fault scarps.

Trench investigation of faults

In cooperation with R. V. Sharp, M. G. Bonilla supervised the excavation of a trench across the 1940 traces of the Imperial fault just north of the United States-Mexico border. This site was useful for evaluating trenching as a technique for identifying faulting because a large strike-slip displacement had occurred in 1940 without noticeable vertical component and the bedding in the sediments was nearly horizontal. Theoretically under these conditions evidence of the faulting could be very difficult to see; however, although the dip of the beds was only about 1° , variation in bed thickness locally resulted in more than 0.1 vertical separation of the beds. Along a narrow zone the bedding was obscured by shearing and other processes.

A trench excavated across the 1915 Pleasant Valley normal fault in Nevada was mapped by H. A. Villalobos and T. A. Kaplan-Henry. Exposures in the trench show that the 1915 displacement at the site was about 0.5 m and that a displacement of about 0.3 m occurred prior to 1915. Based on a probable age of less than 5,000 years for some rodent bones found in the trench wall and interpretation of structural relations, it is tentatively concluded that the pre-1915 displacement occurred less than 5,000

years ago and that a cumulative displacement of more than 3 m occurred in the same time span.

Relationship of carbon dioxide to seismogenic zones

Natural CO_2 discharges are virtually restricted to zones of historical seismicity according to Ivan Barnes and W. P. Irwin. Similar to the pattern of global seismicity, most of the CO_2 discharges are concentrated along the boundaries of major crustal plates. There are two major concentrations—one along a narrow circum-Pacific belt, and the other along the great Alpine orogenic belt of Europe and Asia Minor. Both phenomena are absent or sparse in regions of old cratonic rocks. The CO_2 originates variously from metamorphism of marine carbonate-bearing rocks and organic material and from the mantle. The generation of CO_2 in active orogenic zones is a long-term event, compared to the historical record of seismicity, and thus may be a useful parameter in regional seismic zoning.

SEISMICITY INVESTIGATIONS

Charleston, South Carolina

In eastern South Carolina the recorded earthquake activity was in two distinct source regions, according to C. J. Langer. Near Middleton Place the epicenters have defined a zone that is 3 km wide and 25 km long. This zone is in the region of highest intensity of the 1886 Charleston, S.C., earthquake. Near Bowman, about 100 km northwest of Charleston, there has been a low level of seismic activity; most of the earthquakes occurred as a swarm between September and December 1976.

Kermit, Texas

About 135 earthquakes were located near Kermit, Tex., by A. M. Rogers, but these earthquakes cannot be correlated with known faults. Most of the events had focal depths within the sediments above the basement, which is at a depth of 3.7 km. The trend of epicenters is subparallel to the Central Basin Platform. The largest events were near to the Keystone and the Dollarhide oilfields. Focal mechanisms indicate normal faulting on a plane striking north-northwest.

Southern Alaska

A detailed study by J. C. Lahr and C. D. Stephens of the seismicity at Icy Bay, Alaska, which is within the source area of the great Yakutat Bay earthquakes of 1889 and 1900, showed that the epicenters

define a linear northeast trend about 30 km long, possibly along a single fault structure. The epicenters may be related to the northeast-trending thrust fault inferred along the southern margin of Chaix Hills or to a northeast-trending thrust fault found offshore 25 km to the southwest or to both.

J. C. Lahr and J. W. Reeder (Stanford University) used data from seismograph stations around Cook Inlet to study various aspects of the Mount Augustine volcanic eruptions that began on January 23, 1976. A 15-hour swarm of earthquakes of magnitude 3 or less preceded the first series of eruptions that consisted of 15 distinct events occurring over a 35-hour interval. Ground vibration, believed to be caused by the transport of high-pressure gases and material through the volcano, was recorded to distances of 220 km. Following seven of the last eight eruptions, distinctive signals with a velocity of about 0.3 km/s were recorded to a distance of 318 km in a northeasterly direction. These are interpreted as atmospheric pressure waves generated by northeasterly-directed explosions that disintegrated the northeast part of the crater wall. Increased seismic activity did not precede a smaller series of eruptions in February; no pressure waves were detected.

Guatemala

Local monitoring of the aftershocks of the February 4, 1976, earthquake in Guatemala revealed secondary southwest-trending alignments of epicenters splaying from the western end of the main rupture on the east-west trending dextral strike-slip Motagua fault. According to C. J. Langer, these alignments are characterized by normal faulting and correlate spatially with mapped surface lineaments and, to some degree, with patterns of ground breakage accompanying the earthquake. The observed features of the secondary splays of aftershocks are compatible with the theoretical pattern of fracturing at the end of a strike-slip fault.

GROUND MOTION INVESTIGATIONS

Source of earthquake energy

D. J. Andrews proposed a physical model to explain the source of earthquake energy. In an earth subject to internally generated stresses, faulting decreases the total energy in the elastic field. Over a period of time following the faulting, distant viscoelastic regions can be expected to respond in such a way as to return stress in the seismogenic region

to a value appropriate to steady flow. In the course of this response, work will be performed on the brittle seismogenic region to increase elastic field energy smoothly throughout the region. This work of tectonic loading contributes to the stored elastic energy of the seismogenic region only at long wavelengths, and therefore supplies energy only to the largest earthquake. The stored elastic energy released in small earthquakes can arise from larger earthquakes loading shorter wavelengths. An earthquake, while smoothing the stress and slip distributions on the fault at length scales on the order of the rupture dimension, must leave the fault in a rougher state at smaller length scales.

Seismic intensities of the 1906 California earthquake

A detailed investigation by R. D. Nason of the seismic damages caused by ground shaking in the 1906 California earthquake showed that the damages were more widespread than previously thought. On alluvial ground, the collapse of chimneys and parts of unreinforced walls were observed to distances of 80 km from the earthquake fault.

Ground response in the Los Angeles region

A. M. Rogers recorded ground motion at many sites in the Los Angeles, Calif., metropolitan area from underground nuclear explosions at the Nevada Test Site to study the geographical variability in ground response to seismic shaking. The amplification of long-period (0.6–3.0 s) motion recorded on unconsolidated sediments relative to rock displays a strong dependence on the depth to crystalline basement, increasing by a factor of four as the depth to basement increases from 1 to 5 km. The amplification of short-period (0.2–0.6 s) motion also tends to increase as depth to crystalline basement increases but exhibits a stronger decrease as depth of alluvium increases. Other factors that seem to influence short-period amplification are age of alluvium, lithology (for example, clay-silt or sand), and void ratios near the surface.

Ground response in the San Francisco Bay region

R. D. Borcherdt, J. F. Gibbs, and T. E. Fumal continued a pilot study to detail the shallow shear-wave velocity structure in the San Francisco Bay region. Downhole shear and compressional velocities, geologic logs and standard penetration have been measured in the upper 30 m of eight geologic units at a total of 59 locations. Preliminary results indicate that shear-wave velocity can be correlated with

average spectral amplification of horizontal ground motion recorded from distant events, with variations in intensity observed during historic earthquakes and with several physical parameters that can be easily measured in the field including texture, penetration resistance, color, and depth in unconsolidated sediment, and fracture spacing and hardness in rock.

Ground response in the Salt Lake City region

Data on the amplification of ground motion of different types of rocks and soils have been recorded at more than 50 sites in the Salt Lake City, Utah, region using nuclear explosions, quarry blasts, and earthquakes. According to W. W. Hays, there are significant differences in the level of ground response throughout the region with the ground motions recorded on water-saturated alluvium as much as 8 to 10 times greater than those on rock.

Estimation of design ground motions

From a statistical analysis of strong ground motion recordings, R. K. McGuire concluded that spectral response amplitudes around 1-second period cannot be reliably estimated from a single peak ground motion parameter, such as peak acceleration or velocity. For example, a widely used scheme based on peak ground motion parameters underestimates the spectral amplitudes significant for high-rise buildings by as much as a factor of two at large distances from the earthquake source. More reliable estimates of spectral amplitudes, especially for large magnitudes and at large distances, can be obtained from regression analyses that include earthquake magnitude, distance from the source, and local site geology as variables.

Processing of strong motion records

W. B. Joyner developed a simple and economical new method for baseline correction and integration of strong motion records using a recursive high-pass filter. The filter is a two-pole Butterworth filter, and the record is passed through the filter twice, once forward and once backwards to attain zero phase distortion. A key element of the method is the order in which the processing steps are carried out. First the acceleration is integrated to give the velocity. The velocity is then high-pass filtered and a least-squares straight line is removed. The result is differentiated to give corrected acceleration and integrated to give displacement.

Dynamic response of soils to shear

In laboratory tests D. G. Anderson and K. H. Stokoe (University of Texas, Austin) found an increase of shear moduli with time of confinement in sustained pressure resonant-column tests on soils. The increase was characterized by two phases: primary consolidation and the long-term effect. The duration of primary consolidation and the magnitude of the long-term time effect varied with factors such as soil type and stress conditions. The long-term time effect was exhibited by all soils and was shown to occur at shearing strains greater than 10^{-3} . The conclusions from these investigations are that shear moduli must be defined at the completion of primary consolidation and that the long-term time effect must be considered when using laboratory moduli to interpret in-situ soil response.

GROUND FAILURE INVESTIGATIONS

Landslides

Careful study of landslides in local and foreign earthquakes by E. L. Harp and G. F. Wieczorek showed that rock falls and shallow debris slides are numerically the most common types of earthquake-induced landslides. The studies showed that such slides usually involve weakly consolidated and cemented rocks and soils and extensively jointed rocks. The distribution of slides suggests that topography plays a fundamental role in amplifying the ground motion that triggers them. Earthquake-induced rockfalls are generally restricted to slopes steeper than 50° . Debris slides occur mainly on slopes steeper than 30° and most extensively within thin residual soils containing little clay. Failure apparently occurs as a decoupling at the soil-bed-rock interface.

Land stability in Salt Lake City in Utah

The relative stability of the land surface during earthquakes for southeastern Salt Lake City in Utah and adjacent mountains is shown on a new map prepared by Richard Van Horn and J. N. Van Driel (1977) as an aid in land-use planning. The map is a computer-generated interpretive map derived from source maps of the 7.5-m Sugar House quadrangle superimposed on the standard 1:24,000-scale topographic map of the quadrangle. The four source maps show relative slope stability, thickness of loosely packed materials, texture of grain size, and depth to top of the principal aquifer. The interpretive map delineates four types of areas ac-

ording to their relative ability to withstand landslides, soil liquefaction and subsidence that can accompany earthquakes. The most stable areas are in the mountainous region to the east, including part of the Wasatch National Forest, where bedrock is exposed on much of the surface. The least stable areas are to the west in lower, more developed parts of Salt Lake City and its suburbs where surficial deposits are thickest, mostly fine grained, and water saturated near the surface.

Deformational structures in soft sediments

J. D. Sims found additional deformational structures in Quaternary lacustrine sediments in California that are suggestive of earthquake shaking. Outcrops of Holocene sediments of ancient Lake Cahuilla in the Coachella Valley contain deformational structures similar to those interpreted as earthquake induced in the nearby Imperial Valley. Structures found in cores collected by SCUBA techniques from Upper Van Norman Reservoir, San Fernando Valley are similar to and probably correlative with deformational structures in Lower Van Norman Reservoir about 2 km to the southeast. Other similar structures were found in the Bouse Formation (Pliocene) near Vidal.

SEISMIC ENGINEERING STUDIES

From measurements of the resonant periods of tall structures in Guatemala City, Guatemala, Raul Husid found that fundamental periods of vibration for typical buildings undamaged by the Guatemalan earthquake are longer than for similar size structures in California. Most Guatemalan structures were designed using the code written by the Structural Engineers Association of California (SEAOC) including the formula for calculating fundamental period of vibration. Because the design load calculated from the SEAOC code diminishes as the period of vibration increases, the lateral design loads usually used in Guatemala exceed those for analogous structures in California.

Strong-motion recording program

Sixty-seven strong-motion records were obtained in the year beginning July 1976, according to R. B. Matthiesen. The amplitude of peak ground motion ranged from insignificant to 0.14 of gravitational acceleration (Porcella, 1976, 1977a, b). A basic plan for a national strong-motion instrumentation plan was completed, and a preliminary plan for Central and South America was prepared.

ENGINEERING GEOLOGY

Research in rock mechanics

The influence of rock properties on the construction of an underground oil-storage facility near Mount Waldo, Maine, is being studied by F. T. Lee and T. C. Nichols, Jr. Long-term deformation and high in-situ stress can influence rock stability. Stress relief measurements at three sites in the granite show that near-surface horizontal stresses are compressive and unequal with initial magnitudes as high as 14.5 (MN/m²). Creep stabilized in about 20 days after coring with additional strains of up to three times the initial strain relief. Quarries in the granite exhibit deformed and offset drill holes. Recent near-surface subhorizontal shear failures in quarries were accompanied by the formation of fault gouge. Dale (1907) described a violent rock burst that occurred near our measurement locations and produced a northwest-trending vertical fault extending the length of the quarry, further attesting to the rock-breaking magnitudes of the in-situ stresses.

Initial studies show that excavations in the upper several meters can be subject to damage from abrupt brittle failures in addition to long-term deformation. In order to determine the integrity of large excavations at greater depths, the ratio of horizontal to vertical stresses must be known as well as stresses associated with sheeting, and the location of vertical faults and joints.

Research in soils engineering

A procedure has been developed by T. L. Youd and D. M. Perkins (1977) for using geologic and seismologic information in making preliminary maps showing liquefaction-induced ground failure potential. The procedure requires the superposition of two constituent maps, a ground-failure-opportunity map and a ground-failure-susceptibility map. Ground-failure opportunity occurs when the intensity of seismic shaking reaches a level strong enough to cause liquefaction in susceptible materials and consequent permanent ground displacements. Thus, ground-failure opportunity is a function of the seismicity and the ground-motion attenuation characteristics of an area. Techniques applying probability concepts and empirical correlations were developed for mapping ground-failure opportunity on a regional basis.

Ground-failure susceptibility refers to the relative ease with which the materials under a particular site can be liquefied and permanent ground

displacements can occur. Qualitative criteria were developed for assessing or mapping on a regional basis the likelihood that susceptible materials are present in various geologic settings. These criteria will undoubtedly be adjusted and expanded as information is gained from future earthquakes.

The maps are combined to form a single map showing the potential for liquefaction-induced ground failure, which can be used for preliminary planning and decisionmaking.

Research in geologic hazards

In August of 1977, a reconnaissance investigation by T. L. Youd, R. F. Yerkes, and M. M. Clark, was made to evaluate the influence surface faulting during the 1971 San Fernando, Calif., earthquake has had on subsequent land use in that fault zone. Fault displacements of up to 2.4 m during the 1971 event severely damaged nearly every structure astride a major surface fault rupture. The rupture zone is 15 km long, 9 km of which is in urban areas, and up to 100 m wide. The 1977 reconnaissance revealed that, with the exception of the zone change at one site from hospital (now forbidden by law) to commercial-industrial, the 1971 faulting has had no apparent influence on land use in the fault zone. Buildings have been repaired, new buildings have been built, land is actively being traded, and a major freeway interchange has been constructed across the trace of the 1971 fault rupture. None of these uses are in violation of any state or local building codes.

Geophysical surveys near Picacho, Arizona

In conjunction with work by T. L. Holzer, seismic refraction and gravity surveys were conducted near the town of Picacho, Ariz., across a zone of earth fissures and surface faults associated with land subsidence related to ground-water withdrawal. The zone includes the Picacho fault, a modern surface fault on which vertical offset has been mapped along more than 15 km of its length. Two seismic spreads, each 2.7 km long, were run westward from the Picacho Mountains, and three shorter spreads, each 345 m long, were run across the center of the zone of fissures. Gravity was measured at 90-m spacing along a 4-km survey line west from the Picacho Mountains and at closer spacing along two profiles straddling the zone of fissures.

The preliminary interpretation of the longer seismic spreads indicates a six-layer structure. The upper two layers are nearly horizontal, but the

lower four show progressively steeper dip westward, away from the mountain front. The upper surface of the deepest layer (velocity=5.6 km/s) is approximately 650 m deep beneath the fissures and has a dip exceeding 20°. The shorter spreads recorded only the upper four layers. In the immediate vicinity of the fissures, a lithologic structure or change is suggested by a basinward decrease of velocity in layer four from 3.7 km/s to 3.1 km/s.

The gravity results show a smooth decrease in Bouguer anomaly values away from the mountain front with a slight steepening of the horizontal gradient in the vicinity of the Picacho fault. The smooth basinward decrease in Bouguer anomaly values reflects the basinward increase in thickness of sedimentary rocks. The steepening of the horizontal gradient in the vicinity of the fault could result from a basinward decrease in water table height or small offsets or changes in density in the sedimentary layers directly beneath the fault. No local anomalies exceeding about 0.04 mGal were found associated with the zone of fissures. This indicates that the bulk density of material near the surface in the vicinity of the fault is within a few percent of the density of the surrounding material.

LANDSLIDE HAZARDS

Landslide data available for Pacific Palisades area in Los Angeles, California

The report of a special Congressionally authorized landslide study of the Pacific Palisades area of Los Angeles in California prepared by the Corps of Engineers in cooperation with the USGS (1976), was released to city and other officials and the public. The technical appendix, prepared by J. T. McGill (USGS), consists of a detailed map showing landslides in Pacific Palisades (McGill, 1973) and a table giving summary data on each of the 130 individual landslide areas delineated on the map. The table provides information on the time and type of movement and the kinds of materials involved as well as pertinent available data on the location, dimensions, configuration, and volume of the landslide; the topographic and geologic setting; and seepages, heavy rains, grading operations, and landslide damages. The staff geologist of the Los Angeles Department of Building and Safety described the technical appendix as the single most useful geologic report available to that office.

Landslides related to fracture systems in Fairfax County, Virginia

S. F. Obermeier conducted a field investigation of landsliding in Fairfax County, Virginia. The materials are typical Coastal Plain sediments of the Potomac Group that extends from Baltimore, Md., to Richmond, Va. Laboratory tests of intact samples of Potomac sediments indicated that the materials were much too strong to fail by landsliding; yet landslides are a significant problem in the region. The object of the investigation was to determine if Potomac sediments have joints, fractures, and shears that are commonplace, predictable in orientation, and possibly related to the initiation of landslides. It was shown that (1) fracture systems are common in massive clay and plastic silt deposits, (2) there is a preferred regional orientation of the fracture systems, predictable from Landsat imagery, and (3) these systems contribute significantly to landsliding.

The effect of scale on seismic-induced landslides

Large earthquakes trigger a diverse range of sizes and styles of landslides. Field studies by R. C. Wilson of landslides triggered by the 1976 Guatemala earthquake indicated that this range was characterized by two "end members": (1) closely spaced, small ($<10^4$ m³), shallow (<5 m), soil slips and rockfalls that occurred on slopes steeper than 70 percent in soil or in weathered or weakly cemented rock and (2) large ($>10^6$ m³) slumps and block-glides that occurred on gentler slopes and perhaps involved more competent (but usually fractured) rock. This observation suggests that the scale (absolute size) of the landslide body may be related to the mechanism of seismic-induced landsliding.

Ancient landslide dated in The Geysers steam field, California

In cooperation with geologic investigations for the USGS geothermal program, Union Oil Co., principal operators of The Geysers steam field, furnished a sample of carbonized wood from a landslide on the northwest flank of Cobb Mountain. The sample site was from the 12- to 18-m depth in a rotational depression in the block-type slide previously mapped by R. J. McLaughlin. This wood sample from near the bottom of the sediment deposits in the depression was dated by S. W. Robinson in the Menlo Park Radiocarbon Laboratory and found to be $13,200 \pm 160$ years old. This age probably postdates earliest landslide movement, suggesting that many of the large dissected block-type landslides in The

Geysers region and elsewhere in the Coast Ranges formed in pre-Holocene time.

Stability of highwalls in surface coal mines, western Powder River basin

Field and theoretical investigations by W. Z. Savage and W. K. Smith of highwall slopes at an abandoned open-pit mine in Sheridan County, Wyoming, indicated that highwalls may become unstable as much as 20–25 years after abandonment. A large landslide which occurred in 1975 and several smaller failures developed in an abandoned highwall. The large slide continued to move through 1977. Samples have been collected at the mine for determination of material properties. Preliminary calculations of long-term highwall stability have been performed by finite element and limit-equilibrium methods. The purpose of the analyses is to develop methods for predicting time to failures.

Streamside landsliding near Redwood National Park

As part of an ongoing investigation of landsliding and stream sedimentation in the vicinity of Redwood National Park, D. R. Harden, R. J. Janda, and K. M. Nolan analyzed rainfall records and historical accounts that indicate individual storms comprising a late 19th century series of flood-producing storms in northwestern California were similar in magnitude and spacing to six particularly damaging storms that occurred between 1953 and 1975 in this same area. However, the limited number of active and revegetated streamside landslide scars discernible along Redwood Creek on aerial photographs taken in 1936 and 1947 suggest that the recent storms initiated more streamside landslides along Redwood Creek than the comparable older storms that occurred prior to extensive road construction and timber harvesting. Construction and logging activities on some marginally stable streamside hillslopes directly contributed to recently increased landslide activity. Recent land-use changes and severe storms increased stream-sediment discharges and caused a shift to a wider, shallower channel configuration. Streambank cutting attendant to the increased channel width also contributed to increased streamside landsliding along Redwood Creek.

REACTOR HAZARDS

Topical and areal research

A great variety of research on faults, earthquakes, volcanic hazards, aseismic faulting, landslides, and

solution cavities is underway in the USGS, the results of which are reported under other appropriate topical and areal headings in this volume. Results not included elsewhere are described here.

Fort Yuma Earthquake of 1852

During the course of USGS review for the Nuclear Regulatory Commission of the operating license application for Sundesert, Calif., it was determined that the 1852 Fort Yuma, Ariz., earthquake probably occurred within the San Andreas fault zone in Imperial Valley, Calif., rather than northeast of Yuma, Ariz.

Youngest movement on Melones fault zone in California

Four small dacite and rhyodacite intrusive bodies near Mokelumne Hill in Calaveras County, Calif., are intruded into and locally overlain by the Mehrten Formation, an upper Tertiary volcanoclastic unit. Dating the intrusions thus establishes an age for the upper part of the Mehrten in this area. This age has special significance because recent work in the Sierra Nevada foothills metamorphic belt by Woodward-Clyde Consultants for Pacific Gas and Electric Company has revealed that the Mehrten Formation is displaced by the Mother Lode fault, one of several faults making up the Melones fault zone, in the vicinity of the intrusive bodies. The base of the Mehrten is offset by as much as 30 m (down to the northeast), and a trench excavated across the fault adjacent to one of the rhyodacite intrusions shows that the highest exposed Mehrten on the ridge crest is juxtaposed with younger colluvium containing clasts of rhyodacite apparently identical to the nearby intrusion. The minimum offset on the colluvium-Mehrten contact is about 5 m.

Two of the intrusions yielded K-Ar ages of 4.03 ± 0.26 and 4.12 ± 0.11 m.y., which are analytically indistinguishable. The latest movements on the Mother Lode fault, therefore, are more recent than the youngest part of the Mehrten Formation, and because colluvium containing blocks of rhyodacite from one dated intrusion is involved in the faulting, the latest movements must be more recent than 4 m.y.

Southern Elsinore fault zone in California

Three northwest-striking groups of normal faults have been identified in the southern part of the Elsinore fault zone that cut sedimentary deposits as young as Holocene—one fault zone lies at the foot of the Laguna Mountains escarpment and crosses

into the Peninsular Ranges block to the south. The zone, en echelon with, and east of the Elsinore fault zone, is one which crosses the foot of the Tierra Blanca Mountains. The third zone lies at the foot of the Vallecito Mountains on the east side of Carrizo-Vallecito-Mason Valleys. The valleys form a complex, northwest-trending graben whose narrow northern end merges into the Elsinore fault in Banner Canyon. The Peninsular Ranges block to the west is an upfaulted block, the bounding faults of which extend into the block. In this part of the Elsinore fault zone, no strike-slip movement has taken place since middle Cretaceous time—batholithic structure and Quaternary sedimentary deposits cross the zone without lateral offset. Prior to normal faulting, crystalline rocks were thrust over Pleistocene sediments locally.

Santa Maria River fault, California

Geologic mapping and analysis of subsurface data in the vicinity of Santa Maria, Calif., by C. A. Hall, Jr., has proved the position and extent of a significant subsurface fault named the Santa Maria River fault. To the southeast this fault joins the Foxen Canyon fault, which in turn joins the Little Pine fault; to the northwest this fault appears to go to sea near Oceano and then probably parallels the coast, approximately 1 km offshore, between Port San Luis and Port Buchon. The Santa Maria River fault juxtaposes different middle Tertiary stratigraphic sections and, therefore, appears to have played a major part in the formation of the Santa Maria basin. The youngest fault activity along this zone may have occurred as recently as late Quaternary, somewhat later than the previously known movements on the Little Pine fault.

In-situ stress on Barre Granite in Vermont

From measurements made on a $10 \times 10 \times 5.7$ -m block of Barre Granite, before, during, and after quarrying, it was determined that an initial stress drop of about 10 MPa occurred upon quarrying. Time-dependent strains occurred on the surfaces of the block and cores retrieved from the block after quarrying. These strains were in most cases approximately the same magnitude as the initial strains. Moreover, additional stresses remain in the block after quarrying (Nichols, Savage, and Brethauer, 1976). In addition, it was determined that the stresses measured before and after quarrying are too large to be explained by calculated gravity stresses. From these data, it is concluded

that the measurement of initial rapid-strain response does not give an adequate estimate of deformations caused by quarrying.

Expected ground motion at proposed nuclear power plant sites

In accordance with longstanding arrangements, seismic conditions to be encountered for planned nuclear power plants were reviewed for the Nuclear Regulatory Commission of the Department of Energy. The purpose of the review is to consider all seismological aspects in or near a proposed plant and to evaluate, confirm, or deny the recommended maximum expected ground motion within the design life of the structure. For the reporting interval final reviews were made by J. W. Dewey for Pilgrim Unit II in Massachusetts and by W. J. Spence for Pebble Springs in Oregon, wherein 0.20 g and 0.25 g, respectively, accelerations were deemed to be appropriate for the Category I structures.

ENVIRONMENTAL ASPECTS OF ENERGY

Geology contributes to archaeology and climate studies in northeast Arizona

Richard Hereford has mapped a multiple sequence of upland gravel deposits northwest of Black Mesa in Arizona. The gravels have young eolian mantles and range in age from Tertiary through Pleistocene. One fossil locality (Blancan provisional mammal age) and pending fission-track dating of a tuff found associated with an intermediate-age gravel unit will facilitate correlation of this detailed alluvial record with that of the upland gravel sequence of "Shonto" (Blancan) and "Dilkon" (Blancan and Irvingtonian) age, in the southern part of the area, with the K-Ar-dated erosional record of the Little Colorado drainage, and with the history of the San Francisco volcanic field, all of which may be related to the geomorphic development of the region.

Field checking of photo-delineated vegetation zones has been completed by J. P. Schafer, along with some mapping of the distribution of upland eolian units and of bedrock that has been baked and fused by burning of coal beds in the Wepo Formation. Work continues on the stratigraphic analyses of the Carbon-14-dated alluvial and colluvial record of the Dakota Bench area. The alluvial section provides an unusually continuous depositional record from about 10,000 years B.P. to present. Charcoal from this section records a significant vegetational

shift on the Mesa from forests with ponderosa pine to present day juniper-and-pinyon-pine-forest type sometime prior to 7,500 years B.P. (the classic "altithermal" period).

Surficial geologic mapping by B. C. Philpott has delineated a multiple sequence of upland gravel units and associated eolian deposits along the southeastern border of Black Mesa. These gravels are inset into, and thus are younger than, the upper alluvial Pliocene member ("Roberts Mesa" of Shoemaker and others, 1957, 1962) of the Bidahochi Formation.

H. E. Holt mapped upland gravel deposits across several unconnected upland areas of Black Mesa. There, valley-fill deposits in the headward areas of intervening valleys are of Holocene age, and pre-Holocene deposits are restricted to the valley fills of lower valley reaches bordering the Little Colorado River drainage. Unstratified fine-grained cave deposits about 1-1.2 m thick in Stanton's cave, about 43 m above the present level of the Colorado River in Grand Canyon, were sampled and paleomagnetically measured. The results suggests that only the upper few centimeters of these deposits are of Holocene age, and that the lower part, which shows a marked magnetic excursion, is pre-Wisconsinan in age.

T. N. V. Karlstrom (USGS) with E. Karlstrom (University of Wyoming) assisted in the location and sampling of different types of buried and surface soils for detailed pedologic analysis. Well-developed soils, stratigraphically positioned between upper Pleistocene and upper Holocene deposits, and including Hack's (1942) "altithermal" soil of Jeddito valley, are identified as Typic Haplargid soils with profiles as much as 200 cm thick and probably representing intense weathering intervals on the order of one or more thousands of years duration. In contrast, weak soils separating the dated upper Holocene "T" through "Z" depositional units are identified as Fluventic Camborthid type soils with simple profiles (mainly oxidized B Horizons), generally less than 20 cm thick. Based on tree-ring and carbon-14 dating of overlying and underlying deposits, these buried soils appear to represent less intense weathering intervals of the order of 100 to 200 years duration. The regional distribution of these soil types in the absence of other criteria provides a functional field method for separating surface deposits of Pleistocene age and older (deep soils) from those of Holocene age (shallow soils).

Environmental geology of coal development, Powder River basin in Wyoming

The surficial geology was mapped in all or part of eight 7½-min quadrangles in the area underlain by surface-mineable coal that extends the length of Campbell County. Fieldwork, thus, is completed for surficial geologic maps of 44 7½-min quadrangles and half of each of 2 15-minute quadrangles. Publication of this series of maps has begun with the maps listed below.

Using a format evolved for the Powder River basin Surficial Mapping Project by V. S. Williams, geologic and topographic constraints to development have been delineated in the Gillette East 1:24,000-scale quadrangle. A single black-and-white map was constructed by superimposing generalized maps for each constraining factor, then giving each area on the composite map an identifier consisting of a series of single-digit numbers, each of which indicated one of the constraints existing in the designated area. Maps with such a format now are being prepared for about eight critical 7½-min quadrangles along the surface-mineable coal belt of the western Powder River basin. The constraints shown are: (1) land underlain at shallow depth by thick coal that can be economically surface mined, (2) land underlain by a source of aggregate, (3) hard rock near the surface, (4) potentially unstable hill slopes, (5) land subject to flooding or shallow ground water, and (6) rough land requiring road building for four-wheel drive access. Information on these constraints was derived from surficial geologic maps prepared by the project in combination with bedrock geologic maps, topographic maps, well logs, and color aerial photographs. Advantages of this format are threefold. First, all delineated geologic constraints for a given site can be identified by referring to a single map. Secondly, special-use derivative maps can be prepared by the user by employing his own coloring patterns. Williams thus could emphasize certain combinations of factors, or lump factors. For example, areas of high ground-water table, hard rock near the surface, and potentially unstable slopes may be colored out to make a single map emphasizing areas unfavorable for septic waste-disposal systems. The third advantage of the format is that such maps are economical and quick to produce so that coverage of a wide area is possible at a useful scale and at a reasonable expense. Development along the coal outcrop is expected to be widely dispersed, rather than in a concentrated urban form, and extensive map coverage will be required. Potential disadvantages

of this format, however, are also threefold. First, these maps are more difficult to use than published colored maps. Second, the time required to color the maps may discourage some users. And third, information must be less detailed and boundaries more generalized than for separate maps of each factor.

Stratigraphic investigations in the Caballo Creek drainage basin and part of the Belle Fourche River valley in eastern Powder River basin in Wyoming by D. S. Fullerton resulted in identification of four stratigraphic units of Pleistocene age and several units of Holocene age. The oldest recognized Pleistocene unit is resistant coarse gravel, 6 to >6m above the present valley floors; it records deepening and widening of major valleys by shifting perennial streams. Two younger alluvial units next were deposited on valley floors, also in response to higher base levels than at present. Both are intensely weathered and locally have well-developed (buried) soil profiles. The younger of the two units is the Arvada Formation. The fourth Pleistocene unit, the Ucross Formation, locally may be a channel facies of the Arvada Formation. All Pleistocene units are thin, discontinuous, and poorly preserved. A major interval of soil formation and very extensive erosion occurred after deposition of the Ucross gravel and before deposition of the oldest Holocene alluvium. Early Holocene time was characterized by formation of extensive alluvial fans, followed by cutting of arroyos in the fans, and subsequent filling of the arroyos. Middle Holocene time was characterized by a long interval of weathering and extensive erosion, followed by partial filling of arroyos and aggradation on valley floors, by ephemeral streams, and subsequent development of an altithermal soil. The lower Holocene alluvial units were intensely dissected and the present bedrock floors of major valleys were scoured during the middle Holocene erosion interval; channels of major streams were incised 3-6 m below the beds of present channels. A return to aggradation resulted in partial filling of the incised channels; a truncated altithermal soil is exposed locally on the fill surface. The early part of late Holocene time was characterized by slope wash deposition on hillslopes and extensive filling of valleys by fine-grained alluvium of ephemeral streams. Nearly all older Holocene sediments were buried by slope wash and valley fill alluvium, the Kaycee Formation. At least two pulses of Kaycee deposition, separated by at least one short interval of erosion, are recorded. The Kaycee surfaces have textured soil B-horizons and are the loci of surface archeologic sites of the "McKean" technocomplex,

indicating that the surfaces have been stable for at least 3,000 years. Kaycee deposition was followed by incision of meandering (perennial?) streams into the valley fills, with consequential formation of a Kaycee terrace and one or more lower ("Moorcroft") cut terraces. The streams were incised more than 3 m below the present streambeds in most places. A return to aggradation results in deposition of more than 3 m of fill, the Lightning Formation. At least two pulses of Lightning deposition, separated by erosion, or locally, by soil formation, have been identified. The present flood plains and stream channels are inset into the Lightning fill.

Fission track dates were ascertained by C. W. Naeser on zircons from a suite of five samples collected by D. A. Coates at a locality where natural burning of a thick coal bed has baked overlying rocks. Close clustering of the ages around 7×10^5 years B.P. demonstrates that the burning of coal in place can anneal zircons and that at least some burning in the region has occurred long enough in the past so that fission track dating is possible. This apparently is a new application of fission track dating.

Seismic surveys by C. H. Miller indicate that a low-seismic-velocity layer overlies a high-velocity layer throughout much of the Powder River basin. The shear modulus of the low-velocity layer is about one-tenth that of the high-velocity layer, suggesting significant differences in strength properties. The difference in strength properties between the two layers is supported by drill hole information and physical-property test data of core samples from a site 12 km south of Sheridan, Wyo. Therefore, it is concluded that the low-velocity layer may be a major factor in slope stability in many areas of the basin.

In situ seismic measurements of clinker (rocks altered by burning of coal beds) indicate that clinker has low strength properties relative to those of small intact samples tested in the laboratory. These measurements point up the necessity for field-site, in situ tests of materials prior to their use as sites for heavy construction. Electromagnetic, magnetic, gravity, and seismic refraction surveys intended to locate the bounds of abandoned underground coal workings were only marginally successful.

A. F. Chleborad and W. F. Ebaugh, mapping landslide deposits in an area extending from Sheridan, Wyo., to the northern end of the Wolf Mountains in Montana, have found extensive landslides in the Tertiary Fort Union and Wasatch Forma-

tions of Tertiary age. Earthflows, debris slides, and slumps are numerous throughout the area, especially along the western escarpment of the Wolf Mountains. Landslides in the Wolf Mountains typically occur in colluvium or poorly consolidated, clay-rich mudstone or shale beds underlying steep hilltops of baked and fused rocks (clinker) or resistant ledge-forming sandstones. The abundance of landslides indicates the possibility of serious slope stability problems for future construction, mining, or logging activities.

Borehole inclinometer data from an instrumented landslide in the Wasatch Formation near Sheridan, Wyo., indicate movement associated with the melting of heavy spring snows. The five inclinometer boreholes monitored show differential movement above 5.3 m depth. A stability analysis (Morgenstern and Price method) led to the conclusion that the slide occurred after development of 2.4 m of artesian ground-water head within the slope. An effective cohesion of 11.0 kPa and an effective angle of internal friction of 26.8° were also determined. Landslide factor mapping, considering geology, slope, and extent of irrigation, was used to produce a relative slope stability map of the Big Horn quadrangle in Sheridan County, Wyo.

E. N. Hinrichs, in the course of engineering geologic mapping in the Sheridan and Hultz Draw quadrangles, found partings of airfall tuff in the Smith, Roland, Burgess, and Bar N coal beds. These partings probably will prove useful in correlation of coal beds and for fission-track age dating. Excavations in the Sheridan area for water and sewer lines and for house foundations have exposed a paleosol, the Kaycee Formation, over a calcareous and gravelly unit, the Ucross Formation, which is underlain by a weathered sandy gravel, the Arvada Formation.

S. P. Kanizay, from mapping and compilation on the southeast part of the Crow Indian Reservation in Montana affirms earlier mapping by W. T. Thom, who noted three distinct physiographic units in the area. The main stream drainage, the Little Big Horn, is incised moderately into the Parkman Sandstone (Upper Cretaceous) and separates Upper Cretaceous shale on the west from Upper Cretaceous and lower Tertiary sandstone on the east. The Wolf Mountains on the eastern edge of the reservation owe their relief to resistant red clinker from coal burns in the Tongue River Member of the Fort Union Formation. Large deposits of coal exist in the Wolf Mountains.

Investigation was begun of highwall failures in

an abandoned surface mine. These failures, which first occurred 20 years after abandonment of the mine, are now being monitored for continuing movement. Movements greater than 6 cm occurred on one slide between June and September 1977. W. Z. Savage and W. K. Smith noted in investigations of highwall slopes of strip mines that such walls may become unstable as much as 20–25 years after excavation. In the continuing study of highwall stability in the western Powder River basin emphasis is now being placed on investigation of long-term stability of final highwalls and of slopes on reclaimed land. Such considerations are important in light of the Surface Mining Control and Reclamation Act of 1977 (P. L. 95–87).

An investigation was conducted by C. R. Dunrud and F. W. Osterwald regarding the feasibility of constructing a strip-mine firebreak to contain a fire beneath an area of prime grazing land that is located about 20 km north of Sheridan, Wyo. The fire is burning an estimated 1,200 acres of abandoned mine workings and is spreading at an alarming rate into thick unmined coal beds. It not only is wasting energy resources but also is polluting the atmosphere with smoke, steam, and toxic gases. Although the lands affected by the fire are owned by individuals or corporations with very diverse interests and priorities, such as cattle ranchers and coal companies, all parties contacted so far feel that the fire must be contained before its effects reach disastrous proportions.

R. J. Marrs (University of Wyoming) has conducted a grant-funded study to delineate and produce maps of natural landforms, natural vegetation, and present-day land use in Sheridan, Johnson, and Natrona Counties in Wyoming. Each county set of maps was published by the Wyoming Geological Survey as part of their County Map Series. Marrs' maps are designed to be of use in decisions regarding post-coal-mining landscape restoration and re-vegetation of disturbed lands.

Fairway crested wheatgrass (*Agropyron cristatum* (L.) Gaertn.) was analyzed to determine the possible effects of coal spoils on the chemical composition of this widely-used reclamation species. J. A. Erdman and R. J. Ebens report that concentrations of 8 of the 26 elements tested by analysis of variance showed significant differences between the samples growing in 10–15 cm of topsoil covering the spoils and samples from normal soils nearby. Generally, samples from the mined areas showed about 50 percent higher concentrations. Concentrations of manganese and uranium, however, were about 150 percent and 200 percent higher,

respectively. Concentrations of the trace elements cobalt, manganese, and zinc—essential in animal nutrition—ranged from deficient levels in the “control” samples to adequate or marginal levels in samples from the reclaimed spoils. The phosphorus content, on the other hand, was less by one-third in samples that grew on spoil material, to the point where this grass may be nutritionally deficient in phosphorus as a forage for cattle.

The two greatest geochemical impacts on the western landscape resulting from large-scale coal development are likely to be geochemical alteration at stripmine sites by overturn and geochemical alteration adjacent to electric-generating sites through coal combustion. The first tends to be a rather localized effect but the second may have regional impact. The environmental interest in the chemical composition of the natural landscape arises from fears that disturbed (or restored) landscapes may exhibit visibly changed compositions. For all practical purposes, this interest focuses on the chemical potential of disturbed or restored materials in supporting a desirable vegetative cover, which in turn can support animal life of interest (including animals used directly by humans). Based on a literature survey (J. J. Connor, 1977) the following impacts appear probable. Stack emissions contain a large variety of elements or their components, the most worrisome of which appear to be sulfur dioxide, hydrofluoric acid, and elemental selenium and mercury. Chemical leaching of combustion wastes seems likely if percolating solutions are distinctly acidic, although molybdenum mobilization may be important under wider pH ranges and trace-element leaching of overburden may be greatly enhanced in the presence of oxidizing pyrite. All of these effects may well impact the local vegetative cover rather rapidly and in important ways. Examples of such impact observed to date in coal-bearing areas of the Western United States, include fluorine-induced damage to pines, sulfur-induced damage to shrubs, altered Cu-Mb ratios in sweet-clover growing on spoil banks, slightly increased concentrations of cadmium, cobalt, fluorine, uranium, and zinc in crested wheatgrass growing on reclaimed spoils, slightly increased concentrations of zinc in wheat growing on reclaimed spoils, and elevated concentrations of sulfur, selenium, copper, lead, zinc, and strontium in native vegetation growing within 5 to 10 km of at least one, large coal-fired electric-generating plant. Lowered copper-molybdenum ratios might induce molydenosis in ruminants, and cadmium, fluorine, selenium, and lead are known poisons.

Environmental geology of oil shale and coal lands in northwest Colorado

Pinyon and juniper roots exposed on steep, south-facing slopes in the Piceance Creek area of Colorado were sampled by P. E. Carrara. Twenty root sections were collected from each of five sites in the Barcus Creek Southeast quadrangle. In the majority of samples, the amount of time that roots have been exposed to weathering processes can be inferred from annual growth ring patterns and (or) other features. These data, combined with the height of each root section above the present ground surface, leads to an estimation of erosion rates on south-facing slopes in a semiarid environment in the pinyon-juniper ecosystem. Times of root exposure range from 25 to 600 years. Preliminary analyses indicate that the erosion rate for the last 100 years has been far higher than any previous 100-year period during the last 400 years. Results are: 0–100 years ago, 1.72 mm/yr; 100–200 years ago, 0.48 mm/yr; 200–300 years ago, 0.25 mm/yr; and 300–400 years ago, 0.27 mm/yr. Data prior to 400 years are sparse and may be unreliable. The sharp increase in erosion rates about 100 years ago roughly corresponds with the beginning of arroyo entrenchment in this region.

Approaches to the development of oil shale in the region are shifting from surface retorting of material produced by surface and underground mining methods to retorting of material in place at depth, according to J. W. Whitney. Potential impacts of in situ development differ considerably as they relate to geologic factors. Less disruption of the surface, less waste material stored or disposed of at the surface, and fewer surface facilities reduce potentially adverse impacts, but high temperatures and changes in volume of materials underground present possibilities for as yet unknown surface impacts. Principal relations between oil shale development and geology include effects on water quality, oil shale as a resource, geochemistry of soils and rocks, and erosion processes and rates. Man-caused disturbances in the past, such as heavy grazing, have caused erosion processes and rates to change, and, once changed, the process continues inexorably in search of equilibrium. Average annual precipitation amounts are generally low so that increases at higher altitudes do not add significantly to erosion rates, but, rather, increase in amounts of vegetation tends to stabilize slopes. Furthermore, vegetation at higher altitudes recovers more quickly after disruption, and therefore the terrain at higher altitudes is less fragile. Where average precipitation

is low and vegetation is sparse, the terrain is fragile and particularly subject to process and rate changes. Adding to the problem is the unusual pattern of summer rains. Storms tend to be extremely heavy but unusually local in extent. Thus, although average precipitation is low, the storms are major influences on erosion processes, leading to episodic fluctuations of rate and unpredictable geographic distribution of influences on processes.

Coal production from surface and underground mines in the project area is increasing, but impacts on geology or caused by geologic factors are relatively few. R. B. Raup, Jr., reports that the geographic distribution of mineable coal, its structural setting, and the nature of the host rocks minimize adverse impacts on surface water patterns, aquifers, sediment yield, and agricultural lands. The principal geologic hazard in the region is unstable slopes, but the potentially hazardous rock types are rare at mine sites and are subject to control by construction practices common to major civil engineering works. Unstable slopes are more problematic where population increases are causing rapid community development. These accumulations of minor engineering projects are less able to cope with stability problems and the problems also tend to be adequately identifiable only after site-specific study.

Surficial geology and geologic hazards in the Williston Basin in North Dakota

Photo interpretation of about 100,000 km² of the Williston Basin in North Dakota by D. E. Trimble determined that major landslides were present in four areas: (1) the flanks of the high buttes in southwestern North Dakota, (2) the Heart River valley between Dickinson and Mandan, (3) the valley of the Little Missouri River along its eastward course, and (4) the valley of the Des Lacs River between Kenmare and Donnybrook. A number of subsidence areas over old areas of underground mining were also noted.

The landslide areas and subsidence areas were field checked, and an additional type of ground instability that was not recognized on the high-altitude aerial photographs was found to be widespread south of the Missouri River. Earthflow scars are almost ubiquitous on slopes of 15° or more where they are underlain by Fort Union Formation. This type of ground instability is limited both in areal extent of individual earthflows and in depth, but is so widespread as to constitute a geologic hazard of significance.

Trimble also interpreted the circular geomorphic features to be pingo scars. These features lie almost 100 km west of the maximum position of the continental ice sheet in southwestern North Dakota and denote periglacial permafrost far beyond the ice margin.

Delicate environment of Alaska's coal lands

Field investigations were initiated by H. R. Schmoll and L. A. Yehle in the Beluga-Tyonek region where strip mining of coal is most anticipated. A variable thickness of Quaternary glacial, lacustrine, alluvial, colluvial, and probably marine deposits overlies coal-bearing Tertiary sedimentary rocks in most of the region. Landslides ranging in size from minuscule to those covering many square kilometers appear to have occurred shortly after deglaciation for the most part; some sliding activity continues to the present, and occurrence of major sliding cannot be ruled out, especially where disturbance from large-scale open-trench mining might occur. Termini of two large glaciers occur in the region. Preliminary observations indicate that the front of Triumvirate Glacier may have been fairly stable during the last 25 years, but Capps Glacier appears to have retreated at least several hundred meters.

Geologic aspects of off-road vehicle use

H. G. Wilshire made measurements of the modification of soil physical properties by the establishment of roadways in the Bisti and Star Lake quadrangles in New Mexico and of soil losses resulting from construction, off-road vehicle use, and maintenance of unpaved roads. Preliminary examination of the scope of accelerated erosion problems was made in urban areas that have undergone rapid population increase as a result of coal strip-mining. Wilshire studied quantitative studies of vehicle impacts and erosional consequences of those impacts at a number of sites in arid, semiarid, and Mediterranean climatic zones of California and adjacent states. The common types of modifications are: (1) rapid disruption of natural soil stabilizers, (2) increased bulk density and decreased soil moisture at depths critical to seed germination, root growth, and normal animal activity, (3) increased surface strengths to levels inhibitory to seedling emergence, increased diurnal temperature range, and reduced organic carbon contents.

Accelerated erosion, including direct mechanical erosion by the vehicles, has caused soil losses in directly impacted areas from 7 kg/m² to 1,180

kg/m². Erosion rates at two off-road vehicle sites are estimated to be 11,000 and 6,000 t/km²/yr, the difference being related to the extent of land modification. Reclamation costs at one site used by motorcycles for about 20 years are as much as \$2,000/acre with, as yet, a low chance of success.

GEOLOGY AND HYDROLOGY RELATED TO NATIONAL SECURITY

The USGS, through interagency agreements with the U.S. Department of Energy and the Department of Defense, investigates the geologic and hydrologic environment of each site within the Nevada Test Site (NTS) where underground nuclear explosions are conducted. In addition, the USGS compiles geologic and hydrologic information pertaining to underground nuclear explosions conducted within the Soviet Union. Geologic and hydrologic data are needed to assess the safety, engineering feasibility, and environmental effects of nuclear explosions. The USGS does research on specialized techniques needed to acquire geophysical and hydrologic data at nuclear explosion sites; some of the results of this research are summarized in the paragraphs that follow.

Geologic and geophysical investigations at the NTS in support of the Los Alamos Scientific Laboratory, the Lawrence Livermore Laboratory, the Sandia Laboratories, and the Defense Nuclear Agency (DNA) have continued to develop a clearer understanding of Quaternary alluvium, Tertiary volcanic rocks, and Paleozoic carbonate and clastic rocks and their structural setup in the Great Basin.

Interdisciplinary communication within the USGS has worked well to provide this clearer understanding: isopach maps of the alluvium and total Cenozoic fill under Yucca Flat in eastern NTS have been updated by A. T. Fernald and D. L. Healey on the basis of new drillhole information; D. C. Muller's geophysical logging interpretations have provided points for magnetic and gravity resolutions; G. D. Bath's interpretation of magnetic anomalies in Yucca Flat has delineated near surface structures, and D. L. Healey's gravity work describes the configuration of the Paleozoic surface; P. P. Orkild and E. C. Jenkins have updated cross sections and completed an appraisal of future nuclear test site potential of Pahute Mesa (in northwestern NTS); and postnuclear test surface effects, described and mapped by F. M. Byers, Jr., and

J.P. Ohl, show near-surface structures and stress-strain relationships at or near test sites.

As part of the geologic investigations for two nuclear events sited in a tunnel under Rainier Mesa (northern NTS), a complete fault documentation program was initiated by J. R. Ege and continued by G. S. Corchary. Approximately 25 faults were instrumented to determine explosion-induced fault movement. Each exact fault location, attitude, and apparent displacement were recorded on a map. Four steel pins were embedded in each rib of the tunnel to form corners of a rough parallelogram surrounding the fault trace. A "tattletale" patch of sulfaset was installed across each fault trace. Measurements were taken from pin to pin and across the tunnel several times preshot and postshot. Each location was photographed preshot and postshot and marked for easy postshot recovery and excavation. Gross explosion-induced movement and gross direction of movement were detected by this method. Greatest movement occurred on faults located closest to ground zero.

Other work performed in the Rainier Mesa tunnels gave geomechanical support to DNA. W. L. Ellis, J. E. Magner, and J. D. Kibler performed the following three investigations:

- Rock-stress investigations provided data concerning residual-stress effects of underground nuclear explosions (events). Comparisons of pre-event stress conditions with postevent field measurements near the source of explosions indicate that significant alterations in the in situ stress field were induced by the explosions. These induced stress changes are believed to be significant with regard to effective containment of underground nuclear explosions. While results of the field measurements are not entirely conclusive, they do indicate the presence of an enhanced compressive stress field near the explosion-produced cavity. These findings are qualitatively consistent with predictions based on mathematical model calculations. Data derived from this program have been beneficial in gaining better insight into nuclear containment phenomenology.
- In situ stress investigations provided a unique opportunity for a substantial compilation of stress data within a relatively small and geologically well understood area. While a generally consistent pattern of stress magnitude and orientation exists within this area, significant

perturbations in this pattern sometimes occur in geologically complex areas. It has also been noted that even relatively insignificant geologic faults are often accompanied by variations in stress magnitudes near the fault plane or zone. While a consistent correlation between in situ stress variations and geologic structure has not been apparent, there is evidence of a cause-effect relationship. Past stress determinations made near a fault that exhibited shock-induced displacement suggested that significant stress changes accompanied the displacement. This has prompted a future investigation of stresses near a fault that is expected to undergo shock-induced displacement. It is hoped that through this program a more comprehensive understanding of the interrelationship of stress, geologic structure, and fault-motion mechanics may emerge.

- Overcore and hydrofracture in situ stress evaluation techniques have been compared and experience has indicated that shut-in pressures obtained from hydrofracturing are normally within 20 percent of the minimum stress magnitude determined by the overcoring method. However, it has been found that the hydrofracturing results often exhibit considerable scatter, and that is necessary to conduct several tests at a location for proper evaluation of the results. There seems to be no correlation between hydrofracture results and drill-hole orientation. Although hydrofracturing has been accepted as a reliable method for estimating stress conditions in deep vertical drill holes, experience in this project indicates hydrofracturing is also a viable method in horizontal drill holes that extend from underground workings. Definition of the complete state of stress may not be attainable by the hydrofracture technique, but it can be used to indicate changes in minimum stress conditions at drill-hole depths beyond the capability of other methods. Hydrofracturing can also be used to estimate stress conditions in areas where core discing or other difficulties prevent successful overcore measurements.

G. E. Brethauer and colleagues established a physical-properties data base and retrieval programs, collectively called USGS/DNA Storage and Retrieval System, for the computer. This system provides a central computer source of geologic and physical properties pertinent to DNA-sponsored

underground nuclear events that can be rapidly scanned and retrieved. Data can be sorted and retrieved using 11 different parameters, and optional statistical calculations can be made. Example parameters for retrieval include specific drill holes, drill holes associated with a certain nuclear event, certain lithologies, or a given radius around the working point of a nuclear event. This retrieval activity exists on a request basis; tabularized output is available. The system is excellent for quick comparative studies of and access to all physical properties associated with a nuclear event or a particular parameter.

A major drainage area at the NTS was selected for study to determine if radionuclides are being moved across the test site boundaries by means of sediment transport. D. D. Gonzalez reports that an analysis of high-resolution gamma-ray spectrometry of two suites of sediment samples taken along the main channel and several tributaries of Fortymile Canyon shows that there are no detectable traces of radioactivity in the channel sediments.

At the Almedro nuclear explosion site, temperatures in the cavity region have finally dropped sufficiently so that perforation of the lower regions may soon be feasible, according to D. D. Gonzalez. Geophysical logs and analyses of water samples indicate that the casing has been sheared several hundred meters below predetonation water levels as a result of nearby testing.

The hydrologic investigations are being made in relation to underground nuclear explosions: Drill holes UE2ce and UE7nS were completed in Paleozoic rocks in Yucca Flat for the purpose of monitoring water levels and water quality near underground nuclear explosion sites. Both holes were equipped with submersible pumps and pumped for water samples. As reported by G. C. Doty, the sustained yield of well UE7nS was too low (0.6 L/s) for aquifer characteristics to be obtained. Hole UE2ce was pumped several times at a rate of about 1.9 L/s. The transmissivity of the carbonate aquifer for periods of pumping less than 36 hours is about 6 m²/d; for longer periods of pumping, discharging boundary conditions become apparent. A pronounced increase in tritium content of the pumped water has been noted in hole UE2ce, which is less than 200 m from the Bourbon explosion site.

In addition, G. C. Doty has continually monitored a long, narrow tension crack in Yucca playa. In 1969 the crack opened and drained within a few hours the accumulated runoff from recent precipitation. The crack is about 1.6 km long and has since

opened because of erosion to a width of 6 to 7 m in the widest places. A system of berms and 10 Parshall flumes was installed in 1974 to obtain estimates of the quantity of water draining into the crack. The monitoring system was discontinued in August 1977 after a violent thunderstorm washed out structures. Data for some runoff events have not yet been evaluated, but Doty has calculated as much as 23,000 m³ of inflow for a single flow event.

Although no nuclear testing has been done in northern Nye County in central Nevada for years, hydrologic investigations relating to the Faultless event are still in progress. The depth and the radiochemistry of water in the Faultless rubble chimney have been continually monitored in a reentry hole since the underground nuclear test was conducted on January 19, 1968. G. A. Dinwiddie and D. D. Gonzalez report that the water levels had remained stable at 518 m below the local water level for nearly 7 years after the explosion before beginning to rise. In October 1974 water levels in the reentry hole began to rise, initially at a rate of 0.3 m/d for 3 months, then the rate of rise decreased to about 0.12 m/d as of November 1977. Water levels are now 370 m below predetonation levels. Radiochemical analyses show that during the stable period, tritium concentrations remained fairly constant, and during the initial period of abrupt water-level rise, concentrations decreased, presumably because of dilution. Current radiochemical analyses show tritium concentrations vary from the greatest near the bottom to the least near the top of the water column; the maximum concentrations are in excess of 10³ pCi/L.

GEOLOGIC ASPECTS OF RADIOACTIVE WASTE MANAGEMENT

Efforts to find suitable repositories in geologic formations for radioactive waste from the nuclear fuel cycle continued in 1977. In cooperation with the Energy Research and Development Administration (ERDA), which became part of the U.S. Department of Energy (DOE) during the year, USGS studied the properties of salt, anhydrite, shale, and crystalline rocks as potential storage media, and the regional geology of the Salina salt basin of New York and Ohio, the Paradox Basin of southeast Utah, and the Pierre Shale of South Dakota. Detailed studies of potential repository sites were carried out at the Nevada Test Site. An area east of

Carlsbad, N.M., was investigated as a possible repository for radioactive waste from military activities.

USGS scientists made a survey of some of the geologic aspects of radioactive waste disposal (Bredhoeft and others, 1978) and concluded that research is needed on (1) techniques for exploring possible repository sites without extensive drilling; (2) the effects of the excavation and the waste on the surrounding rock; (3) the chemistry and mechanical behavior of salt-brine mixtures; (4) the properties and reactions to waste of geologic formations other than salt; and (5) the details of ground-water flow systems, especially flow through fractures and sorption-desorption phenomena. They also felt that uncertainties of geologic prediction for the long times during which wastes will remain hazardous require a multiple-barrier or "defense-in-depth" philosophy for radionuclide containment. Such a philosophy employs a succession of independent barriers to nuclide migration. The waste form, the host rock, and the ground-water flow path to the biosphere all provide potential barriers. Continuing research is needed to measure the efficacy of these barriers and to obtain a better understanding of the processes involved.

STUDIES OF MEDIA

Salt and anhydrite

The physical chemistry of salt-brine systems is important in evaluating potential repositories in both domed and bedded salt. In particular, it is necessary to know the properties of any fluids which may become concentrated in the vicinity of the waste. The densities, vapor pressures and enthalpies of these fluids may have a significant effect on waste containment even though there may be relatively small amounts of fluids present.

Portions of the systems $\text{NaCl-CaSO}_4\text{-H}_2\text{O}$ and $\text{NaCl-CaSO}_4\text{-KCl-MgCl}_2\text{-H}_2\text{O}$ are being explored by R. W. Potter, M. A. Clynne, and colleagues. The latter system includes components of many of the brine inclusions in domed and bedded salt. These inclusions have been found to be highly concentrated bitterns, not simple NaCl solutions. In the experiments, soluble starting materials are allowed to equilibrate under pressure at a series of controlled temperatures; temperature-pressure relations and the solubilities of the salt in the concentrated brines are then determined.

Addition of components to the simple $\text{NaCl-H}_2\text{O}$ system restricts the two-phase field in which gas

(steam) and solid are in equilibrium. Depending on the extent of this effect, brine, not gas, will be the fluid in equilibrium with salt at repository conditions. The proportion of brine to solid greatly affects the strength of rock salt. The greater the number of components, the greater the proportion of brine to solid at any given temperature and pressure.

The solubility relationships of anhydrite were determined in brines saturated with both NaCl and CaSO_4 to temperatures of 435°C and pressures of 220 bars. The solubility relationships of CaSO_4 in NaCl-saturated brines are complex, being retrograde (less CaSO_4 can be dissolved as the temperature is increased) up to approximately 230°C and prograde at higher temperatures. Despite the increased solubility in most brines, CaSO_4 remains relatively insoluble even up to the highest temperatures studied.

The retrograde solubility of CaSO_4 means that brine inclusions will not migrate to a heat source ($<230^\circ\text{C}$) within anhydrite. This property, the low solubility in brine, and the fact that freshwater infiltrating anhydrite can be fixed by the formation of hydrated minerals, suggest that anhydrite, where present in sufficient thickness, may be a suitable waste containment medium.

Results for the more complex system containing MgCl_2 being studied show that ion-pairing processes are significant at 200°C , causing MgCl_2 -rich solutions to become acid (to pH 2). The temperature dependence of the formation of HCl in the gas phase is being accurately determined as preliminary results suggest limiting values may be attained. It is probable that the increased acidity caused by ion-pairing phenomena would increase the corrosion of metal canisters.

Crystalline rocks

The USGS has initiated reconnaissance studies of holocrystalline intrusive igneous rocks, gneisses, schists, amphibolites, and Precambrian metavolcanic rocks to assess their suitability for radioactive waste disposal. The great tectonic stability of the Lake Superior region, where many of these rock types occur, has been documented through isotopic studies by Z. E. Peterman. Tectonic stabilization occurred in the earliest Proterozoic, and the area has remained stable since. In the Wyoming age province of the Precambrian, biotite ages of central and northern Wyoming reflect stabilization, uplift, and cooling in the latest Archean or earliest Proterozoic. Biotite ages in southern Wyoming and in southwestern Montana have been lowered by up to a

billion years. The regional consistency of these lowered ages and narrow transition zones with regions of higher ages suggest vertical uplift and cooling as the major tectonic cause of the age patterns. The transition zones that are marked by steep gradients or discontinuities in biotite ages are zones of major crustal dislocation along which several kilometers of vertical movement must have occurred in middle Proterozoic time.

U-Th-Pb and U-disequilibrium studies provide insight into the migration of elements in crystalline rocks, and can help determine the magnitude and rates of radionuclide migration during the last 250,000 years. Available data on Precambrian and younger crystalline rocks have been reviewed; they suggest that intermediate daughter products move readily in exposed crystalline rocks and in samples obtained from shallow drill holes. In contrast, the few data available from deep drill holes indicate little if any movement of radionuclides.

U-Th-Pb studies, coupled with independent geochronologic methods, also provide key data in assessing fluid migration in crystalline rocks. Recent studies of an Archean (2,600-million years-old) granite in Wyoming demonstrate widespread migration of uranium to depths of at least 500 m. In this area, fluid migration and uranium mobility were undoubtedly facilitated by fracturing of the granite during the Laramide uplift.

Thermal properties

In the disposal of radioactive waste in the earth, the heating effects on the containing rock must be accounted for, and the thermal conductivity of the rock is perhaps the most important property used in estimating these effects and designing repositories. Tabulations of thermal conductivity are inherently lengthy and difficult to assess; actual measurements on rock samples require much effort and on friable rocks are often impossible. E. C. Robertson has developed easily usable charts from which conductivities of rocks can be obtained from the textural and mineral composition of the rocks. Thermal conductivity (K) in all the common rocks has been found to vary with the square of solidity (one minus porosity). In granites, sandstones, and shales, K varies linearly with quartz content. In basalts, K varies linearly with olivine content. In all rocks with low porosity, K varies linearly with pressure (about 3 percent/kbar) and water content. The variation with temperature is strongly negative for felsic rocks and salt and is positive and small for mafic rocks. Anisotropy can be important; the

values of K normal and parallel to bedding or foliation differ by 20 percent in some rocks. The conductivity charts are also useful in estimates of geothermal resource and in estimation of heat flow and thermal gradients in regions of known lithology.

Regional studies in Paradox Basin in Utah

Part of the Salt Valley anticline, northwest of Arches National Park in Grand County, Utah, is under study as a potential site for underground storage of nuclear waste in salt. Field studies have located an area along the collapsed axis of the anticline, where the salt core lies about 245 m below the ground surface, that is attractive for intensive subsurface study as an area that appears to be typical of salt diapirs in the Paradox Basin (Gard, 1976).

Reprocessing of existing petroleum seismic data indicates that the lower frequencies and coarse spacing of shots and receivers used in the petroleum industry are not appropriate for mapping the thin, complexly folded intersalt layers. A raypath model computer study indicates that the high salt velocity and complex structure cause a divergent lens effect and relatively few rays penetrate the salt. Seismic sources and receivers must be placed in the salt to minimize this effect.

Examination of existing subsurface data indicates that the salt mass averages about 84 percent halite. The maximum penetration of pure halite rock in this area is 400 m and numerous boreholes intersect 155 m or more of uninterrupted halite. All boreholes in this area show the salt mass to be complexly folded and faulted.

STUDIES OF POTENTIAL REPOSITORY SITES

Nevada Test Site

Investigations related to radioactive waste disposal were greatly expanded at the Nevada Test Site (NTS) in Nye County, Nevada, during 1977. Potential disposal media were identified in the Timber Mountain caldera on the western edge of NTS (Byers and others, 1976), in the Climax stock near the northeast corner, and in the Eleana Formation in the northcentral part of the site. At the same time as geological and geophysical studies of these media were underway, the U.S. Department of Energy (DOE) carried out investigations on the compatibility of a waste disposal site at NTS with nuclear weapons testing, which is the primary function of NTS. The scope of future exploration of NTS

for a waste repository will depend on this compatibility study.

Data from three drill holes totaling 2,267.6 m, gravity data interpreted by D. L. Healey (USGS), and previous work by D. L. Hoover (USGS) and J. N. Hodson (Fenix and Scisson, Inc.) indicate that argillite in the upper unit (J) of the Eleana Formation of Mississippian age is 600–700 m thick. The unit underlies about 30 km² at depths of 300 m to at least 1,000 m in the Syncline Ridge area of Nevada Test Site. During the Jurassic Period, argillite was completely deformed by thrust faulting, folding, lateral faulting, and intense shearing. Preliminary examination of Quaternary alluvial deposits and landforms and of known faults, suggests that the Syncline Ridge area, although surrounded by Tertiary and younger faults, has been structurally stable since pre-Tertiary time.

The Climax stock is a composite intrusive composed of quartz monzonite and granodiorite of Cretaceous age. The properties of the stock were summarized by Florian Maldonado (1977) in support of a DOE experiment to determine the response of these rocks to heat that would be generated by emplaced radioactive waste. The heater experiment site is located underground in the quartz monzonite phase of the Climax stock where 18 holes had previously been drilled. The cored quartz monzonite is light gray to medium light gray, porphyritic, medium grained and contains feldspars, quartz, and biotite phenocrysts. Potassium-feldspars as much as 10 cm long are common. The quartz monzonite has a fracture density of 3 to 15 fractures/m. All of the fractures at depth are filled with quartz, potassium-feldspar, pyrite, calcite, sericite, chloride, clay and limonite.

Southeast New Mexico

E. W. Roedder and H. E. Belkin have examined samples of cores of salt beds from the Energy Research and Development Administration (ERDA) no. 9 borehole near Carlsbad, N.Mex., the site of a proposed underground nuclear waste repository in the Permian salt beds of the Salado Formation. Their aim was to help understand the origin and geological history of the basin and the diagenetic mineral assemblages in the Salado Formation and to anticipate what problems fluid inclusions might cause during long-term waste storage. The available data from fluid inclusions indicate that 99 percent of the salt has been recrystallized at some time since its original deposition 225 million years ago.

The recrystallization occurred in the presence of extremely saline bitterns that may actually be the original bitterns from which the salt crystallized. The total amount of inclusion fluid in the samples as prepared is generally less than 1 percent by volume; an additional amount is present in intergranular pores.

RELATION OF RADIOACTIVE WASTE TO THE HYDROLOGIC ENVIRONMENT

One of the few unresolved problems facing the nuclear-power industry in the United States is the management of radioactive-waste material generated in the nuclear-fuel cycle. Most of the waste is in liquid or solid form; consequently, liquids or leachates derived from the solids could become part of the hydrologic environment during disposal or storage.

Geohydrology of the proposed Waste Isolation Pilot Plant, southeastern New Mexico

In cooperation with the U.S. Department of Energy, the USGS is studying the geohydrologic regime associated with the proposed Nuclear Waste Isolation Pilot Plant near Carlsbad, N.Mex. J. W. Mercer and B. R. Orr evaluated the geology and made hydrologic tests in 11 exploratory test holes drilled to study the geohydrologic systems both above and below Permian bedded salt deposits. Shallow fluid-bearing zones are located in the Culebra Dolomite Member and Magenta Member of the Rustler Formation and at the contact of the Rustler Formation and the underlying salt-bearing Salado Formation. Preliminary values of transmissivities of the fractured dolomite units ranged from 10^{-5} to $13 \text{ m}^2/\text{d}$, whereas preliminary values for the transmissivities of the Rustler-Salado contact ranged from 10^{-2} to $10^{-5} \text{ m}^2/\text{d}$. Potentiometric surface maps of the dolomites indicated that fluid movement across the site is to the southwest in the Magenta and to the southeast in the Culebra. Concentrations of total dissolved solids in fluids in the Culebra Dolomite Member ranged from 23,700 to 118,300 mg/L; in the Magenta, dissolved-solids concentrations ranged from 10,400 to 20,700 mg/L. Fluids moving along the Rustler-Salado contact were nearly saturated with respect to chloride (260,000–300,000 mg/L), and ranged from 311,000 to 325,800 mg/L in total dissolved solids.

Drilling and testing indicated that the sands of the Bell Canyon Formation of the Delaware Mountain Group contained fluid that was moving slowly eastward across the site. Dominant chemical constituents in the fluid were sodium, calcium, magnesium, and chloride, with a concentration of total dissolved solids of 189,000 mg/L.

Simulation of the effects of containment of nuclear wastes in layered salt deposits

The computer program, DYNAMO, was used to develop a geologic simulation analysis of the hypothetical repository in a halite member of an evaporite sequence separated from a sandstone aquifer by shale interbeds at a depth of about 600 m. The computer code simulated inputs and feedback, coupling, considering interaction of the following factors: radioactive heat sources, rock deformation, cracking of shale layers, and access of ground water to salt and its consequent effects on solution rates of salt. H. R. Shaw computed amounts of salt removal for different sets of boundary conditions in order to provide sets of reference data to evaluate the significance of hydrologic factors to the stability of layered salt. Salt-transport calculations were carried out on time scales from 1,000 to 1,000,000 years. Significant salt transport is theoretically possible for the shorter timescale, assuming access of water from aquifers of high transmissivity for a range of realistic ground-water conditions.

Hydrologic investigation of the Eleana Formation, Nevada Test Site

G. A. Dinwiddie reported that a comprehensive evaluation of the potential of the Nevada Test Site for nuclear-waste disposal was started in April 1977. As part of this program, two holes were drilled into the Mississippian and Devonian Eleana Formation in the Syncline Ridge area, and tests were made primarily to define the hydraulic characteristics necessary for an engineering assessment of the feasibility of constructing a waste repository in the argillite of the Eleana Formation. One 914-m-deep hole (UE16d) penetrated successively alluvium, the Permian(?) and Pennsylvanian Tippihah Limestone, and the Eleana Formation. An aquifer in the Tippihah that was pumped at a rate of 3,100 m³/d had an indicated transmissivity of more than 200 m²/d. The water table in this hole is about 230 m below land surface, but below a depth of about 465 m, the heads increase significantly. The other hole (UE16f), drilled to a depth of 451 m, penetrated alluvium and the Eleana For-

mation; as in hole UE16d, heads increased with depth. In general, the most permeable rocks in the Syncline Ridge area were limestone and quartzite, and, as far as could be determined, the massive argillite was of low permeability.

Hydrology of subsurface waste disposal, Idaho National Engineering Laboratory in Idaho

Aqueous, low-level radioactive waste has been discharged to the basaltic Snake River Plain aquifer at the Idaho National Engineering Laboratory in southeastern Idaho for 25 years. The waste is from a nuclear-fuel reprocessing facility, and disposal is through a 183-m well. The waste contains tritium, strontium-90, cesium-137, iodine-129, and salts. The dispersion and movement of the plumes of various waste components in the aquifer were monitored and mapped.

Because iodine-129 was not reported as a waste product until recently, is discharged in low concentrations, and requires a large sample for detection by neutron activation, it was only recently discovered and mapped by J. T. Barraclough. Because of its long half-life (1.6×10^7 yr), it is significant in long-range studies of the effects of radioactive wastes on the hydrologic environment. Iodine-129 was dispersed over about 8 km² of the aquifer and had migrated about 4 km downgradient from the discharge well. Tritium was dispersed over about 72 km² of the aquifer and had migrated about 12 km downgradient. The strontium-90 plume was about 4 km² in area and extended about 2.4 km from the discharge site. Cesium-137 was not detected in the aquifer. Studies of these low-level wastes documented some of the characteristics of solute migration in a fractured basaltic aquifer.

Gamma spectral borehole logging, West Valley, New York

W. S. Keys and R. E. Hodges logged holes drilled through covered radioactive-waste disposal trenches at the West Valley, N. Y. waste-disposal site. The gamma spectral logs were recorded by using an 8,000-channel minicomputer-based pulse-height analyzer. A. E. Hess and L. J. Bishop adapted the analyzer to field use. Ordinarily, field conditions, such as extremes in temperature and humidity, rough roads, and dust, are hostile environments for a minicomputer, but no problems have been encountered.

Detection of gamma-emitting radioisotopes in boreholes

W. S. Keys, D. E. Eggers, and F. E. Senftle compared the responses of sodium iodide and high-purity germanium detectors in boreholes at the

radioactive-waste disposal site at Oak Ridge National Laboratory of Tennessee. Each of these detector systems has unique advantages for the identification of gamma-emitting radioisotopes that may migrate from such sites in ground water. Germanium detectors have much higher resolution and good efficiency at low gamma energies. In contrast, sodium iodide detectors have much greater efficiency at high gamma energies.

HYDROLOGIC INVESTIGATIONS RELATIVE TO THE DISPOSAL OF LOW-LEVEL RADIOACTIVE WASTE

Existing commercial low-level radioactive-waste burial sites are rapidly being filled or are closed because of potential release of radioactive material. If the nuclear-power industry, industrial processors, laboratories, and hospitals are to continue to produce and use radioactive materials, additional burial grounds will be needed for their waste products. Because ground water is one of the most probable mechanisms by which radionuclides will be transported from a properly managed burial site, investigations by the USGS are directed toward defining and quantifying the parameters controlling solute transport by this mechanism. The USGS is investigating hydrology and transport at existing disposal sites to evaluate parameters as they occur under field conditions; numerous sites that reflect widely different hydrologic settings are being measured. The data and analyses obtained from these investigations will provide a basis for developing hydrogeologic site-selection criteria that can be used by other Federal and State agencies.

Hydrologic evaluation of radioactive waste buried near Beatty, Nevada

Investigations have recently begun near Beatty, Nev., in an arid area containing thick zones of unsaturated alluvial-fan material. W. D. Nichols reported that the studies were designed to evaluate recharge to the ground-water system, including direct measurements of infiltration, by using neutron meters in specially constructed access holes. Also, a 1.5-m-diameter shaft was drilled 11 m below the surface to allow the installation of tensiometers and thermocouple psychrometers. Micrometeorological data are being collected to compute evaporation from the area.

Hydrologic evaluation of a radioactive-waste burial site near Sheffield, Illinois

The geologic environment of a radioactive-waste burial site near Sheffield, Ill., consists of glacial deposits of silt, loess, clay, and sand overlying a Paleozoic shale. J. B. Foster reported that 36 test wells were drilled in the 8-ha burial site to evaluate the hydrology, geology, and movement of radionuclides. In five of these wells, tritium in concentrations significantly above background levels was detected. The tritium moved at least 23 m from the nearest burial trench in less than 3 years. Apparently, there were no other radionuclides moving in the ground water at this site.

Hydrologic evaluation of radioactive waste buried in Barnwell County, South Carolina

In a radioactive-waste burial site in Barnwell County, S.C., Coastal Plain sediments overlying crystalline rocks were drilled and tested for hydrologic, geologic, and radiochemical data. Samples collected from test holes drilled near a trench used to bury solid low-level radioactive waste indicated the presence of tritium concentrations significantly above background levels. J. M. Cahill reported that the tritium was found in the unsaturated zone above the trench floor, and may be moving upward because of the high evaporation potential of the area during periods when there is no rainfall.

FLOODS

Three major categories of flood studies by the USGS are (1) measurement of stage and discharge, (2) definition of the relation between the magnitude of floods and their frequency of occurrence, and (3) delineation of the extent of inundation of flood plains by specific floods, or by floods having specific recurrence intervals.

Floods of June 1976 in Culbertson, Montana

Rainfall of 44 mm on June 4, and 124 mm on June 12, 1976, caused flooding at Culbertson, Mont. M. V. Johnson determined the magnitude of peak flows in areas where damage was greatest. Indirect discharge measurements indicated that Diamond Creek had a peak discharge of 37.4 m³/s on June 4. Maximum discharge of an unnamed tributary (tributary no. 5) of the Missouri River was 37.7 m³/s on June 12.

Appalachian flood of April 1977 in Kentucky, Tennessee, Virginia, and West Virginia

Heavy rains that fell over the Appalachian region of Kentucky, Tennessee, Virginia, and West Virginia from April 2–5, 1977, caused record flooding. Rainfall amounts of 100 to 400 mm were observed. G. S. Runner (1977) reported that flood discharges along the upper Guyandotte River; Tug Fork, and Levisa Fork in the Big Sandy River basin; the Cumberland River; and Clinch and Powell Rivers in the Tennessee River basin exceeded those previously known. Severe flooding also occurred along the Holston River and the North Fork Kentucky River. Recurrence intervals of flood discharges were greater than 100 years at 29 streamflow-measurement sites. The highest rates of discharge ranged from 404 m³/s from a drainage area of 51 km² (Prater Creek at Vansant, Va.) to 140 m³/s from a 1,980-km² drainage area (Emery River at Oakdale, Tenn.).

Daily suspended-sediment discharges on Guyandotte River near Baileysville, W.Va., and Tug Fork at Glenhayes, W.Va., were 49,700 and 263,000 mg/d, respectively, on April 5, 1977.

Twenty-two lives were lost and total property damages reportedly exceeded \$400 million in flooded parts of the four-State area.

Floods of July 1977 in the Johnstown area of western Pennsylvania

S. A. Brua reported that extensive flooding throughout an eight-county area in western Pennsylvania resulted from intense rainfall during the night of July 19, 1977. Locally, 250 to 300 mm of rain fell in a 7-hour period on a 500 km²-area northeast of Johnstown, Pa. Flooding was severe along the Conemaugh River, Crooked Creek, Mahoning Creek, Red Bank Creek, West Branch Susquehanna River, and the Juniata River. Seven earth-fill dams in the Conemaugh River basin were breached.

Peak discharges were the highest of record on many streams, and recurrence intervals exceeded 100 years at some sites. Flood stages and discharges were determined at 57 sites. Runoff rates were as high as 34.6 m³s⁻¹km⁻² from a 15-km² drainage area in the Little Conemaugh River basin. Maximum rate of runoff of Conemaugh River at Seward (drainage area, 1,852 km²) was 1.49 (m³/s)km².

At least 77 lives were lost and property damage reportedly exceeded \$200 million.

Floods in Missouri and Kansas in 1977

Outstanding floods occurred September 12–13, 1977, in the Blue River, Little Blue River, and Sni-A-Bar Creek basins in the metropolitan area of Kansas City, Missouri, and Kansas City, Kansas, as a result of rainfall that exceeded the 100-year 24-hour frequency. A total of about 400 mm of rain fell in two 6-hour bursts.

L. D. Hauth and W. J. Carswell, Jr., reported that peak discharges were determined at 31 sites. Recurrence intervals of peak discharges exceeded 100-years at 18 sites. The highest rates of runoff, 24.6 m³s⁻¹km⁻² from a 15.2-km² drainage area (Round Grove Creek at Raytown Road near Raytown, Mo.) and 14.8 m³s⁻¹km⁻² from a 15.1-km² drainage area (Brush Creek at 63rd Street, Mission, Kans.) were comparable to the highest runoff rates in southeastern Kansas during the great flood of July 1951.

Profiles of the maximum water surface were obtained along Big Blue River, Little Blue River, Brush Creek, and Rock Creek (Kansas).

Twenty-five persons lost their lives and property damages reportedly were more than \$50 million.

Scour at a bridge in Mississippi

Scour of sand-bottomed channels at bridge piers during floods changes rapidly with time, according to K. V. Wilson, who surveyed a channel 26 hours after a bridge collapsed and found little or no indication of a scour hole believed to have been more than 6 m deep a day earlier. Peak flow November 21, 1977, at the State Highway 8 bridge over Batawpan Bogue Creek at Grenada, Miss., was about 850 m³/s, stage 55.291 m (National Geodetic Vertical Datum of 1929). There had been at least three higher floods since 1947, but a large drift accumulation on a pier caused the scour that destroyed the bridge during a flood with a recurrence interval of less than 10 years. The concrete pier with spread footing, supported by 6-m timber piling, collapsed "straight down," according to an observer. Several weeks after the piers collapse, a Corps of Engineers probing survey determined that some parts of the 18-m span were 6-m below the streambed. The 24-m span was not located.

FLOOD FREQUENCY STUDIES

Magnitude and frequency of floods in metropolitan Atlanta, Georgia

H. G. Golden and E. J. Inman developed a method of estimating the magnitude and frequency of floods on urban streams in metropolitan Atlanta. The method is based on adjustments to the natural

stream flood-frequency and rainfall-frequency characteristics of the local area as defined by urban flood studies in other areas.

The effects of urbanization on flood-peak runoff were estimated from the percentage of drainage basin that is impervious and the percentage of drainage area served by storm sewers. Equations were developed for estimating the 2-, 5-, 10-, 25-, 50-, and 100-year flood peak discharges for basin sizes between 1.5 and 260 km² in the Atlanta area. The general form of the equation is:

$$Q_x(u) = C_1 A^{.60} (R_L^{-1}) + C_2 A^e (7 - R_L),$$

where $Q_x(u)$ is the urban peak discharge for recurrence interval, x ; C_1 and C_2 are constants depending on recurrence interval, x ; A is the drainage area in square miles; R_L is an adjustment factor to account for the effect of urban development; and e is an exponent that varies with recurrence interval, x .

Data from 12 urban streams in the Atlanta area were used to obtain a qualitative verification of the 2- and 100-year estimating equations.

Flood-depth frequency relations on natural streams in Georgia

Multiple-regression analyses were used by McGlone Price to define relations between flood-depth frequency and 10 physical and climatological basin characteristics in Georgia. Drainage area of the basin was the most significant variable. Regional relations were defined for estimating the depth of water for floods having recurrence intervals of 10-, 50-, and 100-years on streams with natural flow. Five separate regions having distinct flood-depth frequency characteristics were delineated. The developed relations apply to virtually any site in Georgia where the drainage area is between 2.6 and 2,600 km² and the flow is natural.

Flood-frequency model for small streams in Massachusetts

The USGS rainfall-runoff model (D. R. Dawdy and others, 1972) with subsequent modifications was used by S. W. Wandle, Jr., (1977) to improve the flood-estimating relations for rural streams draining less than 26 km². Multiple-regression techniques were used to develop the relationship between available flood-peak data and a set of basin characteristics.

The model is being calibrated at each of 10 gaging stations with drainage areas of 1.27 to 19.50 km² and with maximum peak discharges of 0.33 to 2.79 m³s⁻¹km⁻². Basin lag time, calculated from the ratio of main-channel length to main-channel slope, ranges from 1.1 to 4.2 hours.

Flood elevations of canalized stream in Mississippi

Extensive canalization of the Yalobusha River watershed in north central Mississippi has reduced elevations of small floods but has had relatively little effect on the elevation of the 25-year flood, according to J. D. Shell. The new channel at Calhoun City contains the 2-year flood within its banks whereas prior to canalization the 2-year flood overtopped the banks by 1.1 m. Although canalization of the stream has reduced the elevation of the 25-year flood, it has increased the discharge of the 25-year flood so that the net reduction in water surface elevation is less than 0.5 m.

Magnitude and frequency of floods in St. Louis County, Missouri

Results of modeling 30 basins in St. Louis County, Mo., using the USGS rainfall-runoff model indicated a general correlation of the model parameters to the variation in surface geology and manmade changes in the basins.

D. W. Spencer and T. W. Alexander derived equations by multiple linear-regression methods for estimating the magnitude and frequency of floods at ungaged sites. Of the three independent variables, drainage area, mean channel slope, and percent imperviousness, only drainage area and percent imperviousness were statistically significant at the 5-percent level. Where the mean channel slope was retained in the equation, there was no significant improvement in the results.

Magnitude and frequency of Ohio floods

E. E. Webber and W. P. Bartlett, Jr., used regression techniques to estimate the magnitude and frequency of floods on Ohio streams. Flood records from 249 streamflow gaging stations with 10 or more years of record were analyzed in accordance with techniques presented in U.S. Water Resources Council Bulletin 17, "Guidelines for Determining Flood Flow Frequency" (1976). Five regions of similar flood hydrology in the State were established, and regression analyses were used to develop peak discharge flood equations for recurrence intervals between 2- and 100-years in each region. Records from 215 stations with drainage areas between 0.03 and 19,200 km² with natural (unregulated), nonurban flow were used in the analyses. The five significant parameters were drainage area, main-channel slope, storage, average basin elevation, and average annual precipitation. The resulting standard error of estimate for the 30 developed equations ranged from 26 to 41 percent with an

average of 32 percent. A summary of flood and watershed data for gaging stations with 10 or more years of record and a plot of drainage area versus peak discharge for all documented Ohio floods were developed.

Flood-frequency estimates based on censored samples

The form of flood-frequency distributions usually is not known and can only be approximated in most cases by comparing distributions of empirical flood data with known distributions. Moment estimates of flood frequencies may suffer from considerable error if the assumed fitting distribution is different from the true distribution of the data. I. C. James II, T. S. Wyant, and J. A. Smith reported that one potential method for reducing this error is to censor the sample so that the shape characteristics of the distribution in the lower tail has little effect on these estimates. The parameters of the joint distribution of the order statistics of the censored samples are estimated.

Results from Monte Carlo studies with samples of size 50 indicate that substantial reductions in root mean square error of T -year estimates ($T=100, 50, 20, 10, 5, 2$) can be achieved by censoring for cases where the fitting distribution is dissimilar in shape to the generating distribution. Optimal censoring can be defined where both distributions are known. Continuing research will develop optimal censoring strategies to minimize expected error conditioned on the level of uncertainty as to the true generating distribution.

FLOOD MAPPING

Flood-insurance study for Belt, Montana

M. V. Johnson and R. J. Omang used stepbackwater and photogrammetric techniques to prepare flood boundary maps along Belt Creek, which flows northward across Belt, Mont. The 100- and 500-year flood discharges were 320 and 439 m³/s, respectively. Although the reach of Belt Creek within the city is contained by a levee, floods overtop parts of the levee at times.

Flood-hazard mapping in Kansas

D. B. Richards, K. D. Medina, C. O. Peek, and S. V. Bond reported that hydraulic analyses based on stepbackwater and photogrammetric techniques were used to define and update flood-prone areas and floodways along streams in Wichita, Lindsborg, Lawrence, and other communities and counties in

Kansas. Areas inundated by the 100- and 500-year flood discharges were delineated on topographic maps. Flood-frequency relations on regulated streams, obtained from other Federal agencies, were incorporated into the hydrologic analyses where appropriate.

Flood hazards in Carson City, Nevada

The existence and severity of flood hazards in the rapidly urbanizing Carson City area of Nevada were evaluated in a recent investigation. According to C. V. Schroer, the most severe flooding in the city historically has been caused by Kings and Ash Canyon Creeks during winter storms. Flooding conditions in recent years generally have been aggravated by inadequate storm-drain capacity and blockage of drain entrances. Nevertheless, the study showed substantially less flooding than was expected, and many areas previously designated as subject to sheet flow were judged not to pose special flood hazards to structures.

Maps of flood-prone areas

Areas inundated by the 100-year flood are outlined on topographic maps as part of the National Program for Managing Flood Losses. The objective of this program is to rapidly inform cities and towns of the general extent of their potential flood problems. According to G. W. Edelen, Jr., nearly 13,000 such maps have been completed for all the States, the District of Columbia, and Puerto Rico.

The maps identify the flood-prone areas of most of the developed and developing parts of the Nation. Flood-hazard maps are used extensively to meet local planning needs and to meet the objectives of the National Flood Insurance Act of 1968 and the National Disaster Protection Act of 1973.

Basin and climatic characteristics to define flood discharges of selected recurrence intervals at ungaged sites on unregulated streams were determined in all States.

A pilot study to evaluate regional techniques for defining flood hazards is in progress. The study compares 10 different procedures of defining the 2-, 10-, and 100 year flood peak discharges at ungaged sites.

Inundation maps of urban areas

Maps showing areas inundated by major floods, flood profiles, discharge-frequency relationships, and stage-frequency relationships were published during the current year as Hydrologic Investigation Atlases

for the Naguabo area, eastern Puerto Rico (Haire, 1978), and Matewan to Williamson, West Virginia-Kentucky (Runner, 1978).

EFFECTS OF POLLUTANTS ON WATER QUALITY

PCB and suspended-sediment transport in the Hudson River

J. T. Turk reported that during the 1977 water year, daily suspended-sediment stations were operated on New York State's Hudson River at the following locations (in downstream order): Glens Falls, Schuylerville, Stillwater, and Waterford, to monitor the transport of PCB. The Glens Falls station is upstream from the suspected source of PCB. The Waterford station was operated for the entire year, whereas the other three stations began operation in late March 1977. Although PCB was not detected in water samples from the Glens Falls station (detection limit $0.1 \mu\text{g/L}$), it was commonly detected at the other three sites. Preliminary data indicate that at river discharges of less than $5 \times 10^5 \text{ L/s}$ ($17,700 \text{ ft}^3/\text{s}$), a relatively constant load of PCB is being transported. The apparent constant loading rates of PCB at the three stations were Schuylerville, 4.0 kg/d ; Stillwater, 5.2 kg/d ; and Waterford, 3.8 kg/d .

At discharges of greater than $5 \times 10^5 \text{ L/s}$, PCB concentrations at Schuylerville and Stillwater can be approximated by PCB versus suspended-sediment regressions and, at Waterford, by a PCB versus log discharge regression. During the high discharge of April 24–May 2, 1977, transport rates at the three sites were Schuylerville, 370 kg ; Stillwater, 360 kg ; and Waterford, 390 kg . The transport of PCB at Waterford during the entire year was approximately $2,600 \text{ kg}$, half of which occurred during low-flow periods, the remainder during high flows.

Fate of wood preservatives in ground water

J. B. Robertson and D. F. Goerlitz studied a field site where ground water was contaminated by wood preservatives, pentachlorophenol (PCP) and creosote, that leaked from a commercial wooden-utility-pole treatment facility.

Methods for the collection and analyses of aquifer material contaminated by creosote and PCP were developed. Gas chromatography was used for the determination of both creosote and PCP. A very rapid, direct, and simple technique for analyzing water and earth material for PCP used high-performance liquid chromatography (HPLC). In an-

other study of ground water contaminated by explosives, HPLC was used to determine TNT, RDX and picric acid. The HPLC equipment proved to be sufficiently rugged to withstand transportation to both field sites thus permitting on-site analyses.

Analyses of samples from more than 25 observation wells indicated that the PCP dispersion plume extended downgradient at least 600 m and spread laterally more than 200 m . Some components of creosote dispersed in a similar pattern, although many creosote components are less soluble and less mobile than PCP in ground water. PCP appeared to behave relatively conservatively in the saturated zone with no significant amount of adsorption. Studies by G. G. Ehrlich indicated that PCP can be aerobically decomposed by microorganisms present in the soil and ground water. However, the contaminated saturated zone is probably anaerobic, or nearly so, in which case biodegradation appears to be considerably slower or nonexistent. Data from two specially constructed monitor wells indicated that neither PCP nor creosote have migrated more than about 120 m laterally in a deeper ($25\text{--}65 \text{ m}$) zone of the aquifer.

Transport of organic solutes by in situ oil shale retorting

J. A. Leenheer and H. A. Stuber reported that processed oil shale was found to be a basic sorbent that sorbed organic acids in retort water preferentially to organic bases. Total organic solute concentrations in retort waters studied ranged from $1,000$ to $5,000 \text{ mg/L}$ dissolved organic carbon with organic acid concentrations greater than neutral organic compound concentrations greater than or equal to organic base concentrations. Significant concentrations of thiosulfate and thiocyanate were found in retort waters. Thiosulfate was unstable in ground waters associated with an in situ retort, but thiocyanate persisted. A diverse range of processed shale materials was found in a sampling trench dug into a burned in situ retort. Retort water was found to dissolve the calcium carbonate and organic-matter coatings from soil colloids.

Organic contamination of the Arkansas River in Pueblo County, Colorado

K. E. Goddard reported that there were greater than normal concentrations of CBOD (carbonaceous biochemical oxygen demand) and ammonia in the Arkansas River in Pueblo County, Colorado, as a result of effluent discharged by the Pueblo sewage-treatment plant and the CF&I Steel Corporation plant. Upstream from these effluent outfalls, CBOD

concentrations ranged from 1 to 2 mg/L, and the ammonia concentration was generally less than 0.05 mg/L. Just downstream from these outfalls, which are located within 100 m of one another, the CBOD concentration was about 16 mg/L and the ammonia concentration was about 3.8 mg/L. The removal of CBOD and ammonia proceed at abnormally rapid rates downstream from these discharges. The rate of CBOD removal, 1.0/d, is ascribed to biological extraction. Large populations of *Nitrosomonas* bacteria are thought to be present in the effluent from the CF&I plant and result in rates of ammonia oxidation as great as 8.0/d.

Characterizing levels of chronic toxicity

The use of embryo-larval, early-juvenile bioassays with rainbow trout, *Salmo gairdneri*, to determine concentrations of heavy metals, singly and in combination, that affect growth and reproduction, the most critical components of population survival, was examined by H. V. Leland. Assays were conducted on Cu, Zn, Pb, and (Cu+Zn) at sublethal concentrations. Ultrastructural analysis of liver tissue from Cu- and Zn-exposed fish showed structural features indicative of storage and (or) toxic abnormalities. Ultrastructural abnormalities of liver cells of Pb-exposed juveniles were less well defined.

Bioavailability of sediment-bound lead and zinc to estuarine clams

Field surveys conducted in a wide variety of estuaries showed little correlation exists between trace-metal concentrations in sediments and concentrations in animals ingesting sediments as food (deposit feeders). S. N. Luoma developed methodology for estimating the biologically available fraction of sediment-bound zinc and lead in estuaries, and used this methodology to predict zinc and lead concentrations in deposit-feeding clams based upon sedimentary characteristics. The lead concentrations in clams from 17 estuaries in southwestern England were controlled by lead concentrations in sediment as modified by the inhibitory effects of sediment-bound iron. Lead concentrations in clams from estuaries polluted by industrial, domestic, or mining wastes were accurately predicted from the Pb-Fe ratio extracted from sediments. Zinc concentrations in clams from San Francisco Bay were predicted from a more complex model, which estimated the form of zinc in sediments from the relative abundance of sedimentary substrates that might absorb the metal (organics, oxides of iron and manganese). Seasonal changes in iron, manganese, and organics

in the sediments explained most of the seasonal variation in the zinc content of clam tissues.

Investigation of nitrogen in ground water on Long Island, New York

Nonpoint sources have been shown to be the major contributor of nitrogen to the water-table aquifer of Nassau County, New York. In the sewered area of the county, elevated nitrate concentrations in ground water are attributed mainly to recent and current inputs of nitrogen from fertilizers. In the unsewered area, fertilizers and domestic wastes from cesspools and septic systems are the major contributors. These findings are based on analyses of 25 years of regional, temporal, and individual-well data on nitrogen species. B. G. Katz, S. E. Ragone, G. E. Kimmel, and J. B. Lindner concluded that although sewers can effectively prevent ammonium and nitrate in domestic wastes from entering ground water, they cannot prevent large amounts of ammonium from landfills and nitrate from nonpoint sources, such as fertilizers and storm runoff, from entering the aquifer, as evidenced by the ubiquity of total dissolved nitrogen among sewered and unsewered areas of the water-table aquifer.

Nitrate in ground water

Nitrogen-isotope ratios were used to indicate sources of ground-water nitrate in Queens, Nassau, and Suffolk Counties, Long Island, New York. According to S. E. Ragone and B. G. Katz (USGS) and C. W. Kreitler (University of Texas at Austin), the nitrogen-isotope values (δN^{15}) in 40 ground-water samples from the water-table aquifer and deeper Magothy aquifer seemed to reflect land use at the time of aquifer recharge. High δN^{15} values were found in samples from the water-table aquifer in a heavily populated area (Queens County), where the probable source of nitrate is animal wastes, and low δN^{15} values were found in an agricultural area where inorganic fertilizers had been applied. Intermediate values of δN^{15} , which reflect a mixture of animal wastes and inorganic fertilizer, were found in both the water-table aquifer in Nassau County and the deeper Magothy aquifer in both Nassau and Suffolk Counties.

Studies by H. F. H. Ku and D. J. Sulam of an unsewered area in southeast Nassau County, New York showed that where thickness of the unsaturated zone exceeds 9 m, almost all nitrogen species in shallow ground water are in the form of nitrate. Ammonium concentration was found to be higher where the unsaturated zone is relatively thin, which

suggests that the relative concentrations of nitrate and ammonium in the water-table aquifer may be controlled by the thickness of the unsaturated zone.

In comparing ground-water quality of adjacent sewered and unsewered areas, the study showed that where the water table was near the surface, the average ammonium concentration was 0.1 mg/L in the sewered area, and 1.8 mg/L in the unsewered area. Average DO concentrations were 4.3 mg/L in the sewered area, and 2.4 mg/L in the unsewered area. Interception of sewage by sewers was assumed to be the principal factor responsible for lower ammonium and higher DO concentrations in shallow ground water in the sewered area.

Movement of bacteria in the Cretaceous Magothy Formation

E. M. Godsy and G. G. Ehrlich found small numbers of bacteria, such as are commonly found in anaerobic sludge digestors, at a point 6.1 m from where tertiary-treated sewage had been injected through a well into the Magothy Formation on Long Island, N.Y. Samples from the injection well and at a distance of from 30 m and 60 m contained microbial populations typical of the undisturbed aquifer. It was concluded that nutrients in the injectant had penetrated at least 6.1 m but not as far as 30 m into the formation; nutrients near the injection well were removed by extensive pumping at the conclusion of the recharge study. Water from all points sampled had elevated COD levels higher than those of native water. No unusual tastes or odors were discernible, however.

Monitoring ground-water quality in Nevada

J. O. Nowlin developed a program for monitoring ground-water quality in Nevada. The program consists of five major elements: (1) An inventory of sources of contamination, (2) background-quality monitoring, (3) surveillance monitoring, (4) intensive site surveys, and (5) a comprehensive data file on ground-water quality. Nevada has been divided for planning purposes into 255 separate hydrographic areas. Two indices were developed to assign monitoring priorities to each area: (1) A Hydrographic Area Priority Index (HPI) that sets priorities for surveillance monitoring, and (2) a Development Potential Index (DPI) that ranks the areas by priority for background monitoring. These indices were used to select candidate basins for the design of detailed monitoring networks.

Pollution of the Snake Plain aquifer

R. E. Lewis reported that a monitoring network of wells and springs was established along the northern rim of the Snake River between Twin Falls and Bliss, Idaho, to monitor the probable effects of nonsewered housing development on ground-water quality. Ten wells and 13 springs were sampled for chemical and bacterial analyses in December 1977. Combined discharge from multiple vents at several spring sites ranged from about 340 to 34,000 L/s. Results of chemical analyses are incomplete. Preliminary interpretation of bacterial analyses indicated the presence of fecal streptococcal bacteria in varying concentrations in nine of the spring samples; however, densities were all below 25 colonies/100 mL.

Ground-water contamination from percolation ponds

W. A. J. Pitt, Jr., reported that analyses of water samples from multiple depth wells drilled adjacent to five percolation ponds in Broward County, Fla., receiving secondary treated domestic sewage indicated some movement of leachates into the underlying aquifer. Sodium, chloride, lead, and nutrient concentrations were found to be as much as two orders of magnitude higher in ground water adjacent to the percolation ponds than in ground water from similar sites away from the percolation ponds.

Effects of mining on water quality

J. H. Barks reported that in the Joplin area of Missouri dissolved zinc concentrations averaged 9,400 $\mu\text{g/L}$ in flooded-mine water and 16,000 $\mu\text{g/L}$ in runoff from tailings areas. During a summer storm, dissolved zinc, lead, and cadmium concentrations in runoff from a 0.028-km² tailings area varied inversely with discharge, and had maximum concentrations of 200,000; 400; and 1,400 $\mu\text{g/L}$. Mine water discharges caused dissolved zinc concentrations in receiving streams to increase from a background of about 40 to about 500 $\mu\text{g/L}$ during periods of low flow. The higher concentrations were sustained during high flow by runoff from the tailings areas.

The hydrologic effects of strip mining in the 989-km² New River basin in Tennessee is being investigated by R. S. Parker. Approximately 65 percent of Tennessee's total annual production of coal comes from this basin. Added importance has been given to the water resources of the New River basin since the enactment by Congress of PL-93-251, which proposes a Big South Fork National Recreation Area

just downstream from this basin. The New River basin is located in the Northern Cumberland Plateau and consists of relatively flat-lying conglomerate, sandstone, siltstone, and shale. Coal seams are found predominately in the upper layers. Because of the relief in the basin, coal extraction is done primarily by contour stripping and subsequent augering.

The neighboring watershed of Clear Fork with a drainage area of 704 km² merges with the New River to form the Big South Fork of the Cumberland River. The Clear Fork basin has relatively little coal-mining activity. A comparison of conductance and major chemical constituents sampled near the outlets of both basins showed a nearly tenfold increase in dissolved solids in the New River basin. The pH remained near neutral and DO remained fairly high for a variety of hydrologic regimes in the New River. Trace metals were found in suspension rather than in solution. Metals in suspension appeared to be carried by the fine-grained suspended sediment. By far the biggest impact on stream environment from mining is sediment. At the basin outlet approximately 95 percent of the suspended sediment was composed of silts and clays (<62 μ m). Suspended-sediment concentrations were high in upstream actively mined subbasins. One basin with a drainage area of approximately 1.3 km² yielded sediment concentrations as high as 115,000 mg/L at a discharge of 0.57 m³/s during a summer storm event in 1977.

According to L. G. Toler data from 16 sampling sites on streams in strip-mined areas in southern Illinois were used to relate sulfate loads from mine drainage to the area of mined land in the stream basin. The estimated annual sulfate loads per square mile of drainage area (2.6 km²) ranged from 28,300 to 200,000 kg/km².

The differences in sulfate load were related to the percentage of the drainage area disturbed by strip mining. A linear regression showed good correlation between the annual loads per km² of drainage area versus the percent of strip-mined land in the basin. From this relationship, annual sulfate loads of 840,000 kg/km² were obtained in strip-mined land, as compared to annual sulfate loads of 19,300 kg/km² for unmined land.

A. M. Diaz and C. D. Albert reported that chemical analyses of samples from streams draining coal-mined areas in southeastern Kansas indicated that the principal chemical constituents and chemical properties affecting the quality of water of the streams are sulfate, iron, manganese, dissolved solids, total hardness, and pH. Concentrations of

dissolved constituents exceeded recommended maximums for drinking water at all stages of streamflow except during periods of flood flows when concentrations of dissolved constituents varied inversely with streamflow. However, total iron, total manganese, and acidity as H₂SO₄ increased proportionately with water discharge. At Cow Creek near Weir, Kans., (drainage area approximately 400 km²) acidity ranged from 16,300 kg/d at base flow to 127,000 kg/d at a discharge of 180 m³/s.

Impact of phosphate mining on the hydrology of Osceola National Forest, Florida

The impact of potential mining on the hydrologic system of the Osceola National Forest was evaluated preparatory to consideration by the U.S. Department of Interior of issuance of phosphate-mining leases on the federally owned lands. According to P. R. Seaber, a detailed study of the forest and a nearby active phosphate mining area led to the following conclusions based on a hypothetical mining plan developed by the U.S. Bureau of Mines:

- Overall effects on streamflow would be small, except in the effluent-receiving stream, and after mining ceases streamflow characteristics would virtually return to premining conditions.
- The effluent-receiving stream would have near-average concentrations of dissolved solids. (Sulfate, phosphorus, nitrogen, and fluoride might be higher than under natural conditions but would not, except perhaps for fluoride, exceed maximum levels recommended for drinking water.) Radium-226 concentrations probably would not be increased above natural levels. Changes in the quality of water in the Floridan aquifer would not be detectable and changes in the quality of the water in the surficial aquifer would be localized in the area of the mining operations.
- Lowering of the Floridan aquifer potentiometric surface because of pumping for mining would be less than 2 m at the nearest population centers. The average flow of the Suwannee River below White Springs would essentially be unaffected.

Radium-228 found in Montana hot springs

Preliminary tests by V. J. Janzer indicated the presence of approximately 20 pCi/L of radium-228 in water from an Alhambra, Mont., hot spring. The levels found were about one-third the concentration

of radium-226 reported by Leonard and Janzer (1977) for the same water. The combined radium-226 and radium-228 levels were about 90 to 100 pCi/L, almost 20 times the maximum contaminant level for radium in community drinking water as recommended in the Federal Register (U.S. National Archives, 1976). If used for drinking, this water should be treated with an ion-exchange water-softening system or some other method to remove the radium.

ENVIRONMENTAL GEOCHEMISTRY

Geochemical survey of the western energy regions

Base lines for as many as 45 chemical elements have been established for 30 regional landscape units spread throughout the coal-bearing regions of the Northern Great Plains and the Powder River, Bighorn, Wind River, and San Juan Basins, and the oil shale regions of Colorado, Wyoming, and Utah (U.S. Geological Survey, 1977b). These units include bedrock formations, stream sediments, ground waters, soils, and plants.

In addition to the regional work, a variety of topical studies has been undertaken, most of its focusing on problems of geochemical change in vegetation because of powerplant operation or strip-mine reclamation. B. M. Anderson, J. J. Connor, and J. R. Keith demonstrated that of 29 elements suspected as contaminants on three species of native vegetation downwind of the Dave Johnston powerplant in Wyoming all but six (S, Se, Cu, Pb, Zn, and Sr) reflect windborne soil, or flyash derived from an exposed pile at the powerplant. J. A. Erdman and L. P. Gough have shown that levels of Ca, Cu, Fe, Mo, S, Zn, and B were abnormally high in winter wheat collected from top-soiled spoils at the Big Sky mine in Montana when compared to 17 samples of winter wheat taken from farm storage bins throughout the Northern Great Plains. T. K. Hinkley and H. E. Taylor compared pond-water and stream-sediment chemistry in two watersheds of Hidden Water Creek in Wyoming, one of which includes a large abandoned strip mine, and found that the general chemical character of the water may be strongly influenced by the presence of the mine. However, stream-sediment chemistry is only weakly influenced.

Soil geochemistry in the Uinta and Piceance Basins

R. R. Tidball and R. C. Severson found no difference in the chemical composition of alluvial soils

regardless of where the soils are located *within* a given small watershed in the Uinta or Piceance Creek Basins of Utah and Colorado. However, significant chemical differences were found *between* basins for the elements Co, Cr, Fe, Ga, Na, Rb, Ti, and Zn, with the high concentrations generally occurring in the Piceance Basin.

W. E. Dean, Jr., (USGS), C. D. Ringrose, and R. W. Klusman (Colorado School of Mines) have related map patterns of major, minor, and trace element in soils of the Piceance Creek Basin in Colorado to the regional geology and hydrology of the basin using *R*- and *Q*-mode factor analyses. Most soils in the northern and central parts of the basin are developed on sandstone of the Uinta Formation overlying the Green River Formation, and generally contain lower trace element concentrations than soils in the southern part of the basin. The latter soils are developed on the Green River Formation, which contains higher concentrations of trace elements than overlying and underlying sandstone units. Soils in both the northern and southern parts of the basin are characterized by relatively high concentrations of calcium carbonate. In the southern part of the basin the carbonate is derived directly from marlstone of the Green River Formation. However, in the northern part of the basin, low-carbonate sandstone-derived soils are secondarily enriched in calcium carbonate by precipitation from saline-rich ground waters. Precipitation of carbonate in soils in the northern part of the basin may also be aided by the fact that this part of the basin receives less rain and snow than most of the rest of the basin, and presumably has a higher rate of evaporation.

Availability of soil elements to native plants

R. C. Severson, L. P. Gough, and J. M. McNeal assessed the availability of several elements in soils to selected native plants of the Northern Great Plains coal regions using samples from 21 sites having diverse soil chemistry. Availability of Ca, Cd, Co, Cu, Fe, K, Mg, Mn, Na, Ni, Pb, and Zn was measured by extraction with DTPA (diethylenetriaminepentaacetic acid) EDTA (ethylenediaminetetraacetic acid), and ammonium oxalate. At each site samples were taken of A and C horizons of uncultivated soils, western wheatgrass (*Agropyron smithii*), silver sagebrush (*Artemisia cana*), and an above-ground biomass composite. Although a few significant ($p < 0.05$) simple correlations (r) exist between the concentrations of specific elements in the plants (dry weight base) and in the soil extracts, no consistent patterns were noted between plants or

between elements and none of the coefficients of determination (r^2) exceeded 0.50. Multivariate relations between elements in plants (dependent variables) and independent variables, such as extracted elements and additional soil physical and chemical properties (pH, cation exchange capacity, mineralogy, and others), were evaluated by multiple regression analysis. In general, more than two-thirds of the significant ($p > 0.05$) multivariate relations explained less than 50 percent of the variation between variables. Of those relations explaining more than 50 percent, independent variables such as mineralogy (percent calcite, dolomite, plagioclase, siderite, and quartz) and soil pH occurred most commonly.

Mercury outgassing in Hawaii

Reports of elevated mercury in the atmosphere and in hair of workers at the Hawaiian Volcano Observatory prompted a field test of the use of native vegetation to monitor the local atmosphere for this element. Accordingly, leaves of the Ohia tree were collected by J. J. Connor and C. W. Connor at approximately geometric intervals downwind of the Puhimau Thermal area near the observatory. T. F. Harms and C. S. E. Papp analyzed them for mercury in the Plant Analysis Laboratory in Denver. An exponential decrease of mercury in Ohia leaves within 3 km of the thermal area demonstrates that it constitutes a local source for atmospheric mercury.

LAND SUBSIDENCE

Subsidence rate decreasing in the Houston-Galveston area of Texas

After many years of increased pumping, the rate of ground-water pumping in the Houston-Galveston, Tex., area fluctuated in a narrow range from 1967-76. During this period, the rate ranged from 21.4 to 23.3 m^3/s . As a result, the rate of water-level decline decreased in much of the area, beginning as early as 1969 in some wells. Borehole extensometer records indicated a decrease in the rate of compaction of the aquifer system beginning about August 1976. At locations where interpretive data were available, the time lag between the alteration of water-level trends and subsidence was 4 to 5 years.

R. K. Gabrysch estimated that, by 1978, importation of water from Lake Livingston, a new source of surface water to the Houston-Galveston area, resulted in a decrease of 3.1 m^3/s in the rate of ground-water pumping in the area of greatest subsidence; most of the decrease occurred in 1977.

In the southern part of Harris County in Texas the potentiometric surface of the ground-water reservoir had risen at least 6 m by January 1978, and rises of as much as 20 m were measured at some production wells where pumping had been curtailed. Additional decreases in subsidence rates are likely to occur as water levels continue to recover because of further decreases in ground-water pumping.

Subsidence investigation in central Arizona

R. L. Laney reported that water levels declined more than 61 m, and locally as much as 137 m, because of ground-water withdrawals from 1923-77. More than 311 km^2 of land subsided at least 2.1 m, and maximum subsidence was 3.8 m from 1952-77. Earth fissures continued to form on the periphery of the basins adjacent to areas of large water-level declines.

Along a 100-km section of the proposed Central Arizona Project aqueduct in Maricopa and Pinal Counties in Texas, the land surface subsided as much as 0.06 m/yr from 1971-77, and, in places, earth fissures were actively forming and enlarging. A joint study by the USGS and the Bureau of Reclamation is estimating the amount of future subsidence and determining areas most likely to develop earth fissures along the proposed aqueduct. An extensive data-collection program includes drilling, selective coring, and borehole geophysical logging of 30 test wells; surface geophysical surveys; precise surveying of bench marks to detect vertical and horizontal ground movement; installing extensometers to monitor long-term compaction; laboratory consolidation tests on selected cores; and large-scale aquifer tests to locally induce stress on the aquifer and measure resultant strain on nearby extensometers.

Drought verified changed storage parameters in California

Heavy ground-water pumping during the 1976-77 drought years caused unusually rapid water-level declines and renewed subsidence in the San Joaquin Valley of California, according to B. F. Lofgren. After 3 decades of pumping overdraft and widespread subsidence, water levels in the western and southern part of the San Joaquin Valley rose rapidly due to importation of canal water. Renewed overdraft during drought years verified earlier conclusions that permanent changes in storage characteristics of compressible aquifer systems occur during a first cycle of ground-water depletion. Water squeezed from the pore spaces during the first cycle

of stressing (water of compaction) is a one-time source of water to wells. It was an important part of the total pumpage during the first cycle of water-level decline, but water of compaction is not available during a second or successive cycle of loading through the same stress range.

At Cantua Creek, Calif., more than 6.1 m of subsidence occurred from 1926 to 1970; by 1975, water levels had risen to their 1946 levels and subsidence had stopped. During 1976, hydrographs and extensometer records showed little change in pumping rates. Heavy pumping began early in 1977, however, and had an abrupt effect on water levels and compaction rates. By early February, when water levels were only 4.9 m below the seasonal high, compaction of the aquifer system began. By March 30, water levels had fallen 15.2 m (to about their 1948 levels) and a maximum rate of seasonal compaction was occurring. By August 20, 1977, water levels had declined 51.2 m—as much decline during one season of second-cycle decline as had occurred during 14 years of first-cycle overdraft. This suggested that even though the more permeable beds of the aquifer system in early 1977 were preconsolidated to hydraulic stresses of the low 1967 water levels, a significant number of the less-permeable, slow-draining interbeds were preconsolidated only to stresses of the mid-1940's.

Although the above rates apply specifically to one site in the San Joaquin Valley, the concepts and principles apply to compressible aquifer systems generally.

Application of subsidence model

D. C. Helm applied a one-dimensional mathematical model that calculates idealized aquifer-system compaction and expansion to observed water-level fluctuations at six sites in the Santa Clara Valley of California. The simulation of observed compaction and expansion of the confined-aquifer system at these sites was good to excellent. By using independently prescribed values at each site for (1) total cumulative thickness of fine-grained interbeds within the confined-aquifer system, (2) weighted-average thickness of these interbeds, (3) initial distribution of preconsolidation pressure, and (4) average recoverable vertical compressibility of the skeletal matrix, it was possible to estimate model values for vertical components of hydraulic conductivity, K' , and nonrecoverable compressibility, S'_{skv} , by trial-and-error fit of calculated to observed compaction history. Estimated values of K' ranged from 1.7×10^{-7} to 3.8×10^{-6} m/d; those for S'_{skv}

ranged from 4.6×10^{-4} to 2.0×10^{-3} m. Although simulation improves greatly when model-parameter values are allowed to vary as functions of calculated preconsolidation pressure (Helm, 1976a), it was found that constant values could be used for at least five decades (Helm, 1976b) for two sites in the Santa Clara Valley.

By using carefully corroborated model-parameter values, future compaction (subsidence) can be predicted for prescribed stress history (projected water-level fluctuations). Subsidence of as much as 4 m occurred in the Santa Clara Valley from 1916 to 1970. Water levels started rising during the mid-1960's, and by 1970, subsidence rates had diminished to near zero. According to the subsidence model, if water levels at the sites studied were returned to and held at their mid-1960 historical lows, additional residual compaction (subsidence) of as much as 3 m could be expected. The degree of confidence of prediction depends on the appropriateness (queness) of estimated model-parameter values (Helm, 1976b).

Effects of continuing land subsidence in Las Vegas Valley, Nevada

Several effects of land subsidence were observed by G. C. Doty during an evaluation of damage claims against the U.S. Department of Energy in the Las Vegas, Nev., area. These included damage to street paving, cracking of concrete slabs around well casings, rupture of well casings at depth, protrusion of well casings, and earth fissuring. In 1977, a casing protrusion of 5 cm was measured at a well on the eastern side of the North Las Vegas Air Terminal. This land subsidence is believed to be caused by pumping of ground water.

Solution mine subsidence hazards

The collapse of the ground surface into underground cavities, created by solution mining of salt or other evaporite deposits, can be a hazard to life and property according to C. R. Dunrud. Large, sudden subsidences at Grand Saline, Tex., in 1976, Hutchinson, Kans., in 1974 (Walters, 1976), and Grosse Ile, Mich., in 1971 (Landis and Piper, 1972), are recent examples of hazards that may result from underground cavities caused by solution mining.

Unstable conditions around underground cavities are more common in areas where salt was produced without consideration of future subsidence problems than in areas where subsidence control was considered during mining. Solution mining prior to

the mid-1900's often created cavities with large spans of roof rock that either are unsupported or poorly supported. Some of these early brinefields are now abandoned. Subsequently, the land surface has been developed for industrial, residential, or recreational use. Local areas in Texas, Kansas, Michigan, and Ohio are examples where development has taken place near or within abandoned solution mine fields.

At present it is not possible to predict whether unstable cavities are present near the subsidence areas mentioned above or in other States with extensive past or present solution mining activities such as New York, West Virginia, Alabama, Louisiana, and Utah. The solution cavities may be stable, or they may be unstable and are migrating upward by successive, intermittent roof collapse—a process that might take many years or decades before collapse occurs at the surface in areas where the overburden is thick. Overburden above solution mined salt beds in the United States commonly ranges in thickness between about 100 and 1,200 m.

In order to identify and evaluate any potential subsidence hazards that may exist, underground cavities must be located and then delineated as to size, shape, and depth below the surface by drilling and subsequent sonar measurements or by other geophysical methods. Based on these factors and on the geologic conditions, their stability may then be evaluated and, if warranted, a notification of potential hazard, a hazard watch, or a hazard warning can be issued depending on the completeness of the evidence and the estimated time frame of subsidence (Federal Register, Tuesday, April 12, 1977, p. 19292–19295).

Studies of solution mine subsidences indicate that collapse commonly is preceded by precursory events that could help alert authorities of a possible failure, and thus might reduce the hazard to life and property if proper actions were taken. These events include local lowering of the ground surface a few months or years before collapse and earth tremors a few minutes to a few days prior to collapse. Surface depressions can be identified and delineated by periodic leveling surveys, by anomalous ponding of water, and by cracks and bulges in the ground, pavements, and floors or walls of buildings. Earth tremors can be detected by seismic instruments or they may be felt by local residents. The subsidence above solution salt mine cavities at Windsor, Ontario, in 1954 (Terzaghi, 1969) dramatically revealed that accelerated lowering of the ground surface that is accompanied by earth tremors, can

mean that a collapse is imminent, which, in turn, can constitute a serious hazard to any people and structures in the area.

Surface faulting in Arizona induced by ground-water withdrawal coincident with a geologic fault

Exploratory drilling, directed by T. L. Holzer, of the Picacho fault indicates that modern surface faulting is attributed to ground-water withdrawal (Holzer and others, 1977) and is spatially coincident, and consistent in nature of offset, with a preexisting, normal fault. The fault cuts the eastern margin of the Eloy-Picacho subsidence bowl in south-central Arizona and offsets the ground surface about 0.5 m. Bedrock beneath the modern fault is approximately 300 m deep and is offset by 30 m across the preexisting fault.

Elastic expansion of the lithosphere caused by ground-water depletion

Analysis by T. L. Holzer (1977) of geodetic data indicated crustal uplift from 1948–49 to 1967 in the lower Santa Cruz basin in south-central Arizona. The crustal uplift was detected from measurements of benchmarks on bedrock in a region where adjacent land areas underlain by alluvium are subsiding in response to ground-water level declines. Uplift was attributed at least in part to elastic expansion of the lithosphere introduced by the removal, and subsequent loss by evapotranspiration, of approximately 4×10^{13} kg of ground water from alluvium. The uplift, relative to an apparently stable area west of the unloaded area, was observed in two areas and amounted to 6.3 and 7.5 cm. The interpretation by Holzer leads to a more general conclusion that mass loss associated with ground-water removal and regional land subsidence can induce crustal uplift that may, over centuries of time, compensate for part of the subsidence.

HAZARDS INFORMATION AND WARNINGS

Potential fault hazard in Ventura, California

A potential earthquake fault hazard is represented by a young fault scarp that extends eastward for 10 km through the north margin of the City of Ventura, California (Sarna-Wojcicki, William, and Gerkes, 1976). The fault features form a band as much as 300 meters wide and the scarp is as much as 12 m high. The fault, when combined with its 40-km long offshore extension (Pitas Point fault), is

inferred to be capable of an earthquake of as much as magnitude 7.

Potential surface faulting related to ground-water withdrawal in Las Vegas Valley, Nevada

T. L. Holzer has recognized that previously published maps of land subsidence in Las Vegas Valley (Harrill, 1976) are compatible with the interpretation that ongoing differential subsidence across faults may be precursory to surface faulting related to ground-water withdrawal. The zone of potential faulting intersects a region of dense urban development. Recognition of a potential for surface faulting in Las Vegas Valley is based on the results of an investigation of the Picacho fault in south-central Arizona. Research there led to the conclusion that differential subsidence induced by ground-water withdrawal across a preexisting fault preceded formation of the modern fault scarp.

Solution mine subsidence hazards

The collapse of the ground surface into underground cavities, created by solution mining of salt

or other evaporite deposits, often constitutes a hazard to life and property. The subsidences in Grand Saline, Tex. (1976), Hutchinson, Kans. (1974), and Grosse Ile, Mich. (1971), are recent examples of hazards that may result from underground cavities.

At present it is not possible to predict whether there are unstable cavities in other areas near the subsidence areas mentioned or in other States with extensive solution mining areas.

Potential rockfall at Billings, Montana

A large wedge-shape mass of rock about 30 m long, 14 m high and more than 4 m wide at the top is located above several homes in Billings, Mont. This free standing mass of rock is in a precipitous position and poses a potential danger to the homes below. A notice of potential hazard was sent to the Mayor indicating the hazard, and recommendations were offered for mitigating the problem.

ASTROGEOLOGY

PLANETARY INVESTIGATIONS

The Viking Mars Mission

The four Viking spacecraft, two landers and two orbiters, continued intensive scientific exploration of Mars during 1977. A number of USGS scientists have continued their involvement both in the analysis and interpretation of the new Viking data, as well as in supporting mission operations to acquire additional data. The mission is expected to continue through 1978.

M. H. Carr, Harold Masursky and L. A. Soderblom maintained continual involvement in Viking Orbiter mission operations, data reduction, and analysis. Over ten thousand additional orbital images were acquired during 1977. Between approximately April and September 1977 global dust storms cloaked the planet obscuring the surface. A substantial amount of new information was compiled on the detailed nature and evolutionary patterns of such storms. During the dust storms the orbital periapsis altitudes of the two Viking Orbiters were lowered by more than a factor of five to 300 km allowing much higher resolution examination of the surface than ever before possible. The new resolution limits is about 15 m/line-pair.

Analyses of the Viking Orbiter pictures of Mars have yielded important conclusions regarding the geologic history of Mars (Carr, Crumpler, and others, 1977; Carr, Greely, and others, 1977; Masursky and others, 1977). The Tharsis volcanic region has apparently been active for billions of years. The eruptions have been at extremely large rates by terrestrial standards and extremely intermittent; the lava properties are consistent with very mafic lavas. Fluvial activity has occurred throughout much of the planet's history, although most floods and the intense dissection of old cratered terrain was restricted to very early periods. Accumulation of sediments at the martian poles to form the layered terrain was apparently a relatively recent event in the history of Mars. Additionally, erosion of the old cratered terrain by

processes of mass wasting has occurred extensively to form fretted and knobby terrain; extensive areas of the northern plains have undergone numerous episodes of mantling and stripping. Mars has had an extremely complex history, most of which remains to be unravelled. Over much of the surface the effects of volcanism and tectonism are complexly interwoven with the products of mass-wasting and aeolian, fluvial and glacial processes.

The Viking Orbiter cameras are equipped with a series of color filters making it possible to acquire black and white images in different parts of the visible spectrum. In this way color images can be reconstructed from frames obtained in violet, green, and orange-red of a single scene. Additionally spectral reflectance information, related to the mineralogy and physical state of surface materials, can be derived for small areas. In this way L. A. Soderblom, K. L. Edwards, and E. M. Eliason constructed the first global colorimetric map of Mars from Viking Orbiter images. The map is in Mercator format covering latitudes from 30° N to 60° S. for 360° of longitude. The map reveals subdivision in color and albedo of a variety of ancient and modern martian lithologies and aeolian deposits often not distinguishable in simple black and white images.

The landing site selection and certification effort for the Viking mission was supported by USGS science and engineering staff under the direction of Harold Masursky. The effort involved preliminary selection based on earth-based radar and Mariner 9 data, final selection based on Viking orbital data after arrival in Mars orbit, and the post-landing evaluation during late 1976 and 1977. Orbital television and infrared data and earth-based radar observations of candidate landing sites were used to evaluate hazards. These observations effectively minimized hazards but could not identify specific hazards, principally large blocks of the scale of the spacecraft; a factor of 100 increase in resolution would have been necessary. Additional instruments have been identified that will allow automatic hazard avoidance for future lander missions to Mars.

E. C. Morris has continued analysis of the images as a member of the Viking Lander Imaging Team. Viking 1 landed on volcanic terrain in the plains of Chryse. Stereo pictures acquired and analyzed in late 1976 and 1977 reveal an undulating topography (Binder and others, 1977). Bedrock is exposed along several ridge crests. Blocks are more numerous than can be attributed to impact ejecta. The apparent presence of a variety of rock types suggests in situ weathering of extrusive and near-surface basaltic igneous rocks along a linear volcanic vent. Fine-grained sediment is present in drift complexes and isolated drifts. During the course of the Viking mission a small patch of fine-grained sediment slumped down one of the drift faces. Otherwise, no morphological changes unrelated to spacecraft activity have been observed. Viking 2 landed on a flat plain of fine-grained sediment overlain by dispersed, evenly distributed boulders (Mutch and others, 1977). The fine-grained material is probably part of a high-latitude mantle comprising material swept south from the polar regions. The boulders, which have distinctive deep pits, or vesicles, may be the residue of an ejecta deposit from the crater Mie. Alternatively, they may be the remnants of lava flows that formerly covered the region. Polygonal sediment-filled cracks seen in Viking Orbiter images of the second landing site may have been formed by ice wedging, similar to the process that occurs in terrestrial permafrost regions. Alternatively, they may be desiccation polygons. H. J. Moore, a member of the Viking Lander Physical Properties Team, has continued analysis of the martian surface properties using mechanical sensors aboard the two Viking Landers that have operated successfully since landing on July 26, 1976, and September 3, 1976. Continued operation of the surface samplers have provided improved estimates of angles of internal friction and cohesion of the surface materials of Mars.

Priestley Toulmin III, H. J. Rose, and R. P. Christian (USGS), in conjunction with B. C. Clark (Martin Marietta Aerospace), A. K. Baird (Pomona College), Klaus Keil (University of New Mexico) and other members of the Viking Inorganic Chemical Analysis Team (ICAT), report the acquisition and analysis of eleven additional samples of martian surface materials by the Viking landers and the on-board X-ray fluorescence spectrometers. The results confirm the previously reported overall compositional homogeneity of the surface materials, but some differentiation, apparently related to surface processes, is apparent. At the Utopia site

(Viking 2), material sampled underneath small boulders has a lower iron content than surface fines. At the Chryse Planitia site (Viking 1), material from a "dune" is homogeneous to the sampled depth of 23 cm; some surface patches are high in iron. Sulfur is variably enriched in material that occurs as cemented aggregates of fines, supporting the early inference of a caliche-like crust made in part of sulfate minerals. Despite repeated attempts, no pebble-size rock fragments have been collected at either Viking site; all such particles (2 to 12 mm diameter) have proved to be cemented aggregates of the very fine-grained surface "dust." In view of the visual evidence for abundant rock cobbles and boulders in the sampling area, the intriguing question as to why are there no rock fragments in the pebble-size range thus remains unanswered. Sample acquisition and analysis is continuing through 1977 on both Viking landers. Details of the results obtained during the Primary Mission (up to March 31, 1977) have been published (Toulmin and others, 1977, two references; Clark and others, 1977; Baird and others, 1977).

Additional data bearing on the mineralogical character of the martian surface fines are derived from the Gas Chromatograph-Mass Spectrometer (GCMS) experiments, which indicate that a significant amount of H₂O, remaining in the material even after prolonged heating at 350°C, can be driven off by subsequent heating briefly to 500°C. Such behavior is consistent with the presence of smectite clays, as hypothesized earlier (Toulmin and others, 1977b). GCMS data on the evolution of CO₂ and volatile sulfur-containing species are consistent with the presence of stable carbonate and sulfate minerals (Biemann and others, 1977).

Planetary geologic processes and histories

B. K. Lucchitta reports results of a comparative study of terrestrial and martian mass-wasting processes. Analysis of a large martian landslide on the south wall of Gangis Chasma indicated that at least 100 km³ of material was involved, some of which moved as far as 60 km across the valley floor. The landslide mass consists of slump blocks at the head, hummocky deposits farther out, and a vast apron of longitudinal ridges and grooved material at the toe. Craters are superposed on adjacent slides of equal freshness suggesting that the slide is not recent. The martian landslide was compared to many large catastrophic terrestrial slides. Common features of landslides on both planets include

(1) the relative order of slump blocks, hummocky deposits, and aprons with respect to the source area, (2) fan-like shape, (3) decreasing thickness with distance from the source, and (4) the presence of lateral and distal rim ridges. The martian slide differs from most terrestrial slides in that it lacks transverse ridges. It is similar, however, to landslides in Alaska that have longitudinal ridges and grooves, have moved over glacial ice, and have relatively low coefficients of friction for their respective weights.

The Sherman landslide (Alaska) particularly resembles the martian slide. This Alaskan slide was described in detail by Shreve (1966) who attributed its high efficiency to gliding on a cushion of air and to the inclusion of snow. There is some evidence that the Sherman slide was wet when emplaced. This evidence includes its resemblance to wet-snow avalanches and the lack of marginal dust deposit. The water may have been derived by rapid melting of snow and ice as heat was generated during the slide. Assuming that the martian landslide had a similar mechanism of emplacement, it is suggested that it may also have contained water. The water could have been generated from ice stored in the source rock of the landslide. The martian slide may have originated by a massive collapse of the canyon wall following melting of supporting ground ice in the wall. The material from the lower wall then flowed and slid out over the trough floor in a thin, fan-like sheet; layers of material from the upper wall fell as rotational slump blocks.

C. S. Breed and J. F. McCauley (USGS) in collaboration with W. A. Ward (University of Washington) report results of comparisons of terrestrial and martian windforms. Earth-like relationships of spacing, width, length, and height have been found among both dunes and yardangs on Mars. The close similarities to terrestrial wind-formed features suggest that the martian dunes and yardangs may be relics of a period of aeolian activity when the atmosphere of Mars may have been more like that of the Earth. Some of the close terrestrial analogs to martian dunes are the megabarchanoid ridges common to the sand seas of the Inner Gobi Desert, the Sahara, the eastern Rub al Khali, and the Karakum Desert of eastern U.S.S.R. These forms, which occur mainly in extremely arid, inland basins, are morphologically very similar to the most abundant type of dunes observed on Viking Orbiter pictures of the martian circumpolar sand seas and crater dune fields. A detailed inventory of large-scale martian wind features, based on approximately 1,500

Mariner 9 and Viking Orbiter pictures was made to evaluate the dominant wind patterns and their interaction with materials on the dry, debris-mantled surface of Mars. Features that were considered indicative of past or present wind directions include dunes, yardangs, and streaks. In parallel, an inventory of large-scale aeolian features on Earth has been completed using Landsat, Skylab, Apollo-Soyuz satellite pictures, and aerial photographs. A global classification of these features was made on the basis of field observations of numerous aeolian landforms in Arizona and adjacent states. Type areas of linear, star, dome, climbing and falling crescentic dunes, and yardangs eroded in two types of bedrock (sandstone and siltstone, with a variety of structural influences) were studied in both the field and with aerial and orbital photography. Because many of the martian yardangs seem to be structurally controlled, structural influence must be carefully evaluated if yardang orientations are used to interpret wind directions on Mars. The relationship of both depositional features (dunes of various types and compositions) and erosional features (deflation hollows and wind-fluted cliffs as well as yardangs) to wind regimes and local topography is currently under study.

D. H. Scott reports that the systematic geologic mapping program of Mars using Mariner 9 photographs is nearing completion. Mapping was started in 1972 and involved 30 quadrangles covering the planet at a scale of 1:5,000,000. In addition, a geologic map of the planet at 1:25,000,000 scale representing a compilation with revisions of the larger scale efforts was completed and is in press.

Among the more interesting results of the recent mapping investigations were the concepts of canyon capture (higher order by lower order) and the existence of large, enduring lakes along the Valles Marineria system developed by J. F. McCauley (1978) to explain rhythmically stratified deposits in the canyon floors. Ring structures in Sabaeus Sinus in the form of faults concentric to the Hellas impact basin some 3000 km distant were recognized by H. J. Moore. Multiple episodes of volcanism in the Phoenicis Lacus quadrangle separated by periods of erosion were recognized around the shields of Arsia and Pavonis Mons (Masursky, Strobell, and Dial, 1978).

LUNAR INVESTIGATIONS

Basin and crater studies

J. F. McCauley, D. E. Wilhelms, and C. A. Hodges studied the general characteristics and stratigraphic

relationships of impact facies around large lunar basins. Approximately 50 such lunar basins have been identified. A variety of ejecta types are distributed about these basins, including continuous ejecta, lineated inner basin ejecta, smooth inner basin ejecta, and secondary craters. These results are presented in the form of generalized model of basin formation and evolution on a terrestrial planet.

E. C. T. Chao, J. A. Minkin, and C. L. Thompson conducted laboratory research, description, and interpretation of materials acquired from the Ries meteorite crater in Germany. Additional field evidence from principal exposures has more firmly established the constraints that must be considered in developing a model that delineates the cratering phenomenon for the Ries multiring structure (Chao, 1977; Chao and Minkin, 1977). Of particular importance is the evidence of downward confining pressure on the crater wall and crater rim in excess of the compressive strength of the constituent limestones. Such pressures are considerably greater than could be attributed solely to the weight of the ejecta moving over the crater wall and rim. Pressures of this magnitude could be exerted by ejecta transported nonballistically in a roll-glide, cascading motion. These investigations were carried out in cooperation with H. Schmidt-Kaler (Bavarian Geological Survey) and R. Hüttner (Geological Survey of Baden-Württemberg).

D. J. Roddy developed a parallel set of analogs for natural impact and explosion craters (Roddy, 1977a). Both types include bowl-shaped, flat-floored with central uplift, and flat-floored with multirings. Roddy also completed a study of the pre-impact geologic setting for the Flynn Creek impact crater (Roddy, 1977b). The impact may have occurred in a shallow Devonian sea. A detailed study of the underground motions in an explosion cratering experiment was also completed using a three dimensional matrix of markers and acceleration gages (Roddy and others, 1977). A study was completed on experimentally produced shatter cones in tonalite under pressures of 20 to 60 kbar (Roddy and Davis, 1977).

Volcanism and tectonism studies

In a continuing program of dating of lunar volcanic plains based on crater density and crater morphology, J. M. Boyce, D. A. Johnson, J. A. Watkins and J. M. Diaz, have determined that emplace-

ment of flow units in the eastern maria spanned at least 1.25 b.y. from about 3.75 to 2.5 billion years ago. Working in collaboration with the Lunar Geoscience Consortium, they have found that the lunar surface remanent magnetic field decreases with age of mare units in a manner suggesting that the magnetizing field was generally decreasing from about 4 to 2.5 billion years ago (Soderblom and others, 1977). In addition, mare units of Apollo 12 and Apollo 15 ages have been identified in Mare Humorum that coincide with units detected by spectral reflectance maps.

D. H. Scott investigated the regional deformation of mare surfaces (Scott, Diaz, and Watkins, 1977). Lunar lava flows forming the maria had very low viscosities and were erupted in large volumes, enabling them to spread thinly over vast areas. Apparently their original depositional surfaces were relatively flat, and large topographic variations were caused by subsequent tectonic modifications. In this study, the amount of deformation of selected maria was measured, and the degree to which isostatic adjustment has been attained was estimated. In order to accomplish this goal, the orientation of rilles on the maria was studied for correlations between their orientations, which followed downslope directions when formed, and their present attitudes. Relationships were obtained between the frequency distribution of rilles and their directions of slope, gradients, and relative age, as well as other parameters, such as rille widths and meander wavelengths along their sinuous channels. Results indicate that correlations between rille ages, rille orientation ratios of rille width, and wavelength suggest fluid velocities in the realm of turbulent flow.

B. K. Lucchitta analyzed mare ridges and scarps along the Apollo 15 and 17 ground tracks in Mare Imbrium and Oceanus Procellarum. The morphology of the scarps was studied using Apollo metric photographs (Lucchitta, 1977). The azimuthal trends of the scarps were compared with those of global structures forming the lunar grid, basin related structures, and buried topography. Results show that the gross topography in southern Mare Imbrium and northern Oceanus Procellarum correlates well with the buried structure and deposits of the Imbrium basin and its rim. Many of the regional slopes in the maria are depositional and reflect the preexisting major features of the basin. Postdepositional, local distortion of the mare surface, however, is present and in many places

associated with mare ridges. Many mare ridges are concentric to the Imbrium Basin suggesting that they are influenced by basin structures. Morphologic diversity of mare ridges suggests that not all have the same origin; volcanic activity apparently took place along some of them. Most mare ridges are associated with faults. The faults could be reverse and associated with a shrinking of the Moon; however, some ridges parallel slopes and could be interpreted as decollement thrust faults along gliding horizons or as vertical faults caused by differential gravitational settling along lines that separate areas that are thinly flooded on topographic highs from areas that are thickly flooded in adjacent lows.

G. G. Schaber, H. J. Moore, and D. W. G. Arthur investigated lava flows in the Tharsis region of Mars as viewed from the Viking Orbiters. To date a total of 1.5×10^6 km² have been mapped on six 1:1,250,000-scale subquadrangles. Twenty lava flow heights have been determined using a new photometric technique developed by Arthur. Results show that a total of six individual eruptive sequences emanated from the Arsia Mons shield volcano and covered up to 2 billion years of shield construction. The height of flows ranges from 11 m to 60 m. The crater densities measured on individual lava flows suggest concentrations of craters with diameters larger than 1 km/10⁶ km² ranging from 4,000 (same as the average lunar mare) to 100 (2.5 percent of the average lunar mare). The youngest eruptive sequence of lavas in the Tharsis region completely surrounds and truncates the lava flows from the Olympus Mons shield and has a crater density of 100 craters that are ≥ 1 km/10⁶ km². These youngest and perhaps most extensive eruptive deposits appear to have emanated from fractures radial to the Tharsis uplift. Depending on the actual crater flux in the vicinity of Mars, these young eruptive materials may be between 40 and 85 million years in age.

H. J. Moore investigated the rheology of lunar, martian, and terrestrial flows. Analyses of flows of lavas and impact melts based on pictures of the Moon and Mars taken from orbit provide broad estimates of their compositions and rheological properties. These data were compared with Moore's measurements of terrestrial flows, which generally show that yield strengths of the flows increase as silica content increases. In the analyses, the flows are treated as Bingham Plastics. Other variables such as volatile content and entrained solids may cause variations in yield strength. Yield strengths of

flows of impact melt, in and around lunar impact craters, are variable and may result from variations in the volume fraction of solids entrained in the melts. Yield strengths of martian flows on Olympus Mons, as well as on and near Arsia Mons, indicate the lavas have low silica contents. Indicated silica contents for the Arsia Mons flows are probably near 45 percent silica, and those of Olympus Mons are higher and probably near 55 percent silica.

Geochemical, geophysical, and geological consortium studies

L. A. Soderblom has found that within the maria, a correlation exists between natural radioactivity, remanent magnetic fields, and absolute age (Soderblom and others, 1977; Eliason and Soderblom, 1977). The oldest provinces are strongly magnetized and weakly radioactive. This suggests that the magnetic field was declining early in mare history and the more radioactive regions had prolonged volcanic history, and are therefore younger and record a weaker field.

Lunar radar studies

G. G. Schaber reports that radar backscatter studies, aimed at improving geologic applicability of radar remote sensing, were concentrated during 1977 on analysis of 1964 Strategic Air Command 3-cm radar images of the Cottonball Basin in Death Valley, Calif. The study focused on comparison of small scale roughness determined from field observations and its correlation with radar images. The final product was a color-coded, computer generated, hypsometric map of the Cottonball Basin, showing the distribution of roughness (roughness scale 0 to 75 cm). Photogrammetrically derived high resolution terrain roughness statistics for the basin were also obtained during 1977. These data were reduced by sophisticated terrain analysis developed by the USGS for Apollo trackability studies. Additionally, an aluminum template capable of obtaining profiles of fine scale roughness directly in the field, was developed as an alternate cheaper method. The specular power data collected in April 1976 overflight were found to coordinate well with roughness statistics. These new roughness data were used to derive preliminary models for radar backscatter. For the first time, millimeter roughness scale statistics are available for a natural terrain covered by abundant SLAR images and numerous other remote sensing data.

LUNAR SAMPLE INVESTIGATIONS

Consortium studies of Apollo 17 breccias

Following the Apollo 17 mission, a consortium of USGS and non-USGS investigators from a variety of fields was established to study two especially significant lunar breccias (samples 73215 and 73255). O. B. James both coordinated the consortium research and carried out petrologic investigations of the samples. These Apollo 17 samples were chosen for such a concentrated study because they apparently formed as aggregates of melt and clasts produced during formation of the Serenitatis impact basin and were never significantly reheated; hence, their crystallization ages might yield the date of the Serenitatis event, and their chemistry might yield information on the nature of the lunar crust prior to formation of the major basins. During the past year, studies were made by James of three clasts of anorthositic gabbro and one of felsite taken from these samples. The anorthositic gabbros appear to have been the dominant rock type in the source terrane. Petrologic studies of the anorthositic gabbros (James, 1977; James and Hammarstrom, 1977) have shown that they did in fact form as heated, partly melted, and (or) recrystallized polymict breccias. Studies of Rb-Sr and ^{40}Ar - ^{39}Ar by other consortium members yielded ages 4.25 b.y. for these clasts. The petrologic data suggest that the best interpretation of these ages is the date of melting/recrystallization of the parent polymict breccias. This implies that there may have been a period of intense and widespread heating of the lunar crust at about 4.25 b.y. Petrologic studies of the felsite clast (James, 1977; James and Hammarstrom, 1977) indicate that the parent rock crystallized from a highly differentiated melt. Prior to the breccia-forming event the parent rock was fractured and injected with melt derived from identical felsite. At the time the clast was incorporated in the breccia, the injected melt was still mobile and the temperature of the bulk clast was $\geq 990^\circ\text{C}$. Transmission electron microscopy (TEM) studies of the clast (Nord and James, 1977) demonstrate that a unique K- and Ca-rich plagioclase precipitated during the original igneous crystallization of the parent rock. Single-phase plagioclase of this composition is unknown from natural terrestrial occurrences or from laboratory crystallization experiments. Because the mineral grains show little or no evidence of having been deformed, the injection of felsic melt

into the fractured parent rock was not accompanied by significant shock. After brecciation the clast was probably never significantly reheated. Radioisotope age estimates by other consortium members yield an age of about 3.90 b.y. for the clast. The petrologic and TEM data from this study indicate that this age is the date of the breccia-forming event, the South Serenitatis impact.

Samples of the matrix of Apollo 17 breccia (73215) were studied by O. B. James (USGS) in collaboration with H. W. Müller and O. A. Schaeffer (State University of New York at Stony Brook) using laser-probe techniques that permit determination of ages of very small volumes of material located with a petrographic microscope. The age of a felsic glass clast determined by this method is about 3.9 b.y., the age interpreted as the date of the breccia-forming event. The age of melt-derived groundmass (~ 4.0 b.y.) probably has no chronological significance; as it appears that the small clasts, or the melt, were not completely outgassed. Clasts of plagioclase show ages ranging from 4.10 to 4.17 b.y.; these ages are lower limits on the times of the last significant heatings of these materials prior to the breccia-forming event. These results are of profound significance for interpretation of all ^{40}Ar - ^{39}Ar stepwise heating data on lunar breccias. Although gas release from bulk chips of matrix showed good plateaus, the ages varied widely from sample to sample, and the laser data demonstrate that the ages do not have chronological significance.

Petrology of Apollo 16 samples

E. C. T. Chao, J. A. Minkin, and C. L. Thompson report investigations of Apollo 16 lunar samples 67455 and 67475, which were collected from a large white boulder thought to be an ejected block representing a major lithologic component of the stratigraphic section penetrated by the North Ray cratering event (Hodges, Muehlberger, and Ulrich, 1973). Sample 67455, a polymict white feldspathic impact ejecta breccia (Chao, Minkin, and Thompson, 1977; Minkin, 1977), appears to be representative of the clast assemblage of the boulder, and 67475 is an impact melt believed on the basis of present evidence (Minkin, Thompson, and Chao, 1977) to have been produced by the same event that produced sample 67455.

Distinguishing characteristics of sample 67455 and some others found near the rim of North Ray

Crater include: (1) more iron-rich olivines and pyroxenes than those of other Apollo 16 anorthositic rocks (Minkin, Thompson, and Chao, 1977; McCallum, Okamura, and Ghose, 1975); (2) higher plagioclase contents than most other Apollo 16 breccias (Chao, Minkin, and Thompson, 1977; Lindstrom and others, 1977; McCallum, Okamura, and Ghose, 1975; Minkin, Thompson, and Chao, 1977); and (3) a unique meteoritic component not found in other Apollo 16 samples (Hertogen and others, 1977a and b). These distinctive compositional features suggest that these North Ray Crater anorthositic breccias came from a different source area than did other Apollo 16 light matrix breccias. It is hypothesized that the event that produced 67455 and 67475 transported this assemblage to the site in the foothills of the Smoky Mountains where the white boulder was subsequently excavated by the North Ray cratering event. Final interpretation of whether the white boulder represents ejecta from the Nectaris event must await age determinations on selected glass clasts from samples 67455 and 67475 (Minkin, Thompson, and Chao, 1977).

Samarium-neodymium chronology of lunar samples

Mitsunobu Tatsumoto (USGS) and visiting scientist Dr. Noboru Nakamura (Colorado School of Mines and Kobe University, Japan) studied the Sm-Nd systematics of the basalt 15065 from station 1 of the Apollo 15 mission in attempts to determine lunar basalt evolution history. Although the Sm-Nd fractionation-ratios vary widely, ranging from 0.17 to 0.24, the light-colored pyroxene core sample and the Sm-Nd data for the basalt sample define an isochron that corresponds to $3.34 \pm 0.09 \times 10^9$ yr and an initial $^{143}\text{Nd}/^{144}\text{Nd}$ ratio of 0.50844 ± 0.00011 . This Sm-Nd internal isochron age confirms the Rb-Sr internal isochron age of 3.28×10^9 yr reported for the rock by Papanastassiou and Wasserburg (1973) as being the crystallation age, and confirms that Rb-Sr and Sm-Nd internal isochron ages do agree when there has been no severe postcrystallizational disturbance. We are now more confident that the 4.37×10^9 yr Sm-Nd and 4.36×10^9 yr Rb-Sr ages for norite 77215 (Nakamura and others, 1976) represent the crystallization age rather than the brecciation age. We also conclude that the 4.37×10^9 yr age represents the oldest reliable crystallization age yet obtained for lunar samples.

Using the Moore County eucrite initial ratio (Nakamura and others, 1977) the $^{147}\text{Sm}/^{144}\text{Nd}$ ratio for the source of basalt 15065 is calculated to be 0.1998 for a two-stage model. The ratio is large compared to the Juvinas value of 0.194 (Lugmair, Scheinin, and Marti, 1975), indicating that heavy rare earth elements (REE) are enriched in the source and the REE distribution pattern (compared to chondritic distribution) is convex upward. Similar distribution patterns are often observed for terrestrial pyroxenites and mid-ocean ridge tholeiites, and it is quite possible that the source material is a pyroxene cumulate in the lunar mantle. This means the single-stage Nd evolution hypothesis (Lugmair, Scheinin, and Marti, 1975) cannot properly explain the lunar mantle evolution if the primary lunar differentiation occurred over a period of a few hundred million years.

Studies of lunar pyroclastic eruption mechanisms

Apollo 17 orange glass (sample 74220) is generally believed to be the product of lunar lava fountaining. Opposing views were expressed by some investigators on the ground that water vapor pressure, which is the driving force for terrestrial pyroclastic eruption, was absent and no alternative gas pressure source was found. Motoaki Sato investigated the oxygen fugacity behavior of the orange glass and observed that the glass underwent self-reduction above 1130°C under 1 atm, which is characteristic of carbon reduction (Sato, 1977). From these results it was deduced that the magma that produced the orange glass must have been under a few hundred bars of CO gas pressure immediately before the eruption, and that the CO gas was generated by a slow, heterogeneous reaction of minute suspended flakes of graphite with ferric iron in the magma during pooling in a magma chamber.

Late-stage differentiates in mare lavas

Edwin Roedder (USGS) and P. W. Weiblen (University of Minnesota) report that on the basis of about 1,000 analyses, there are three compositional types of late-stage melts in the mare lavas (Roedder, Edwin, and Weiblen, 1977): immiscible "high-iron" and "high-potassium" melts, and a possibly contemporaneous but enigmatic "low-potassium melt. The explanation of these three melts is clouded by the fragmental nature of the record and by crystallization of the trapped melt. The composi-

tional data differ from sample to sample, thus permitting a grouping and recognition of some rock types; they verify but do not explain the previously reported strongly bimodal distribution of K_2O values for inclusions in ilmenite; and they delineate some differentiation trends such as increasing SiO_2 , K_2O , and $FeO/FeO+MgO$, but some unanswered questions remain. Thus, silicate liquid immiscibility seems to occur at about 2 percent K_2O , but the stage cannot be specified exactly. The origin of the low-potassium, high-silicon melt inclusions in ilmenite reported earlier remains obscure.

REMOTE SENSING AND ADVANCED TECHNIQUES

EARTH RESOURCES OBSERVATION SYSTEMS PROGRAM

The Earth Resources Observation Systems (EROS) program supports and coordinates research in remote-sensing applications and conducts demonstrations of these applications within Bureaus and Offices of the Department of the Interior. The EROS Data Center in Sioux Falls, S. Dak., has become a focal point within the Department for advances in remote-sensing technology, improving the quality of imagery by digital image enhancement, and improving methods of image interpretation by interactive computer systems. Remote-sensing training courses offered to international, Federal, and State agencies now include a 2-week session in the Data Center's Data Analysis Laboratory where the most advanced techniques of digital image analysis are demonstrated to users.

The EROS Data Center is the principal distributor of remotely sensed data from satellites and aircraft. An expanded transaction processing system was installed to provide interactive access to a data base of approximately seven million frames of imagery and to aid in the daily workload of order processing, accounting, and production. The EROS Program Applications Assistance facilities in Mississippi and Alaska and regional offices of the USGS National Cartographic Information Center have access via computer terminal to the computer system in Sioux Falls to assist the public in searching for and ordering data.

DATA ANALYSIS LABORATORY

The Data Analysis Laboratory led the planning for the EROS Digital Image Processing System (EDIPS) to be installed shortly after the launch of Landsat-C. George Harris reported that the system is now being integrated with software.

D. D. Green (Technicolor Graphic Services, Inc.) reported that techniques of composite mapping and diverse data aggregation were developed that improve the accuracy of classifying land-cover

types. By means of Defense Mapping Agency's digital terrain data, topographic elevation grid cells were resampled to achieve registration to a classification of land-cover type on a Landsat image. Topographic slope and aspect are also derived from the elevation data so that three new observations (elevation, slope, aspect) can be used to refine the classification of cover types. For example, vegetation communities that tend to exist in elevational strata may be differentiated even if spectral characteristics are similar. Errors in classification owing to differences in solar illumination, such as shading, can be corrected by means of slope and aspect information.

S. K. Jenson and C. A. Nelson (Technicolor Graphic Services, Inc.) installed a series of multivariate analysis programs for laboratory experimentation. A Landsat scene of the Black Hills of South Dakota was chosen for evaluating and testing the programs. Principal components analysis and canonical analysis programs were processed on a three-date, twelve-band image. Evaluations of the enhancements for applicability to various disciplines were made by applications scientists.

Principal-components analysis has a long history of theoretical evaluation and application in statistics and biometrics. The emphasis has been on phenomenological interpretations based on relationships among the variables. The same analysis, known as the Karhunen-Loeve Expansion in the engineering and pattern-recognition disciplines, has been used predominantly as a dimensionality reduction transformation. The two approaches to the same analysis have come together in the field of remote sensing where interpretation and dimensionality reduction are simultaneously important.

MONITORING THE ENVIRONMENT

COOPERATIVE PROJECTS WITH THE BUREAU OF LAND MANAGEMENT

The EROS Data Center conducted a series of remote-sensing training courses and demonstration projects to provide Bureau of Land Management

(BLM) personnel training and experience in digital image analysis for resource classification and to provide assistance in developing specifications and plans for image analysis equipment. The Federal Land Policy and Management Act of 1976 requires BLM to maintain an inventory of the resources of public lands. Remote-sensing technology offers a feasible and economical way to fulfill this responsibility. The demonstration projects were conducted with emphasis on vegetation classification, geology, and geohydrologic analysis.

Vegetation classification

W. G. Rohde, W. A. Miller, and C. A. Nelson (Technicolor Graphic Services, Inc.) reported that Landsat digital data, taken on August 1, 1976, of approximately 118,000 ha, were analyzed by the use of an interactive image analysis system to classify wildlife vegetation and other land cover types near Denali, Alaska. A clustering technique was used to derive statistics representative of land cover types in the area. These statistics were input to a maximum likelihood algorithm to classify the picture elements (pixels) into nine land cover types. Evaluation of initial results indicated that areas of barren land on steep north-facing slopes were misclassified as water. Geological Survey 1:62,500-scale maps were used to outline mountainous, barren areas where lakes were not present. Pixels within the barren areas, originally classified as water, were reclassified into the barren land class. This stratification procedure resulted in a 13 percent change in classification within the water and barren classes.

After classification, a series of control points was selected to develop a transformation that registered the classification results to Geological Survey 1:62,500-scale maps. A clustered-stratified random sampling procedure was used to estimate the accuracy of the land cover types displayed on the map overlays. Based on the area classified, it was estimated that to achieve the classification accuracy of each cover type with a confidence interval of ± 5 percent at the 0.05 probability level, it would be necessary to sample 2,050 plots of 0.45 ha each. Proportional allocation was used to determine the number of plots to be sampled within each cover type. Five-pixel by five-pixel clusters were randomly selected until the calculated sample size for each cover type was achieved. Each cluster was plotted onto color-infrared aerial photographs, and each pixel within each cluster was interpreted and identified as one of the land cover types.

By use of sampling for proportion statistics, the overall classification accuracy was estimated to be 84.5 percent ± 4.2 percent at the 0.05 probability level. Accuracy statements were calculated for each of the nine land cover types as follows: (1) water, 100 percent; (2) sediment-laden water, 99.1 percent ± 0.6 percent; (3) barren, 99.4 percent ± 0.3 percent; (4) tall shrub, 100 percent; (5) low shrub, 84.3 percent ± 4.4 percent; (6) tundra, 89.8 percent ± 3.9 percent; (7) open conifer/low shrub, 85.2 percent ± 2.7 percent; (8) open conifer/tall shrub, 58.8 percent ± 5.1 percent; and (9) dense conifer, 52.3 percent ± 6.2 percent.

The cost of Landsat data, aerial photographs, computer time, and man-hours required to analyze the data and verify results for mapping wildland resources over 118,000 ha was estimated to be \$0.039/ha.

D. O. Ohlen and W. G. Rohde (Technicolor Graphic Services, Inc.) reported on a project to map and inventory the Bear Butte Creek watershed (580.45 km²) in western South Dakota, an area of rangeland converted to cropland. The procedure used was interpretation of color-infrared aerial photographs taken in September 1975 and September 1976 at a scale of 1:124,500 and 1:112,600, respectively. Overlays were made with a dot grid showing cropland for each date. It was estimated that 455 ha of rangeland had been converted to cropland in 1 year. The cost of this procedure for mapping and inventorying the area of rangeland converted to cropland was estimated to be \$0.012/ha.

W. C. Draeger (Technicolor Graphic Services, Inc.) reported that Landsat imagery was used to monitor an area of approximately 400,000 ha in central South Dakota, primarily devoted to grazing of mid-grass prairie species, to determine the net area converted from grassland to small grain (mostly wheat) production during 1973-76. Landsat color-composite images at a scale of 1:250,000, acquired in May 1973 and August 1976, were interpreted. The area of crops was delineated manually, and the areas of land-use change were measured using a simple dot-grid mensuration procedure. Aerial photographs were used to evaluate accuracy. Based on the average area estimates, there was a net increase in cropland area of 18,369 ha in the study area from 1973 to 1976. This represents an increase of 26 percent, equivalent to approximately 5 percent of the total study area, in 3 years.

To verify the satellite image interpretation proce-

ture, approximately 15 percent of the study area was interpreted on high-altitude 1:120,000-scale photographs. Cropland area determined from the aerial photographs was compared with cropland area determined from a Landsat image of the same date (May 1975). A discrepancy of only 2 percent was found. The cost of deriving this information was \$200 for imagery, and 5 man-days for interpretation.

Geology

C. A. Sheehan (Technicolor Graphic Services, Inc.) reported that several techniques of computer enhancement of Landsat digital data were performed to determine the optimum image for mapping geomorphic features and surficial materials in lowland areas near Denali, Alaska.

On standard Landsat color-composite images, geomorphic features are partially obscured by vegetation cover. Four linear contrast enhancements were made to minimize the masking effect of vegetation in the lowland areas. Contrast in bands 4 and 5 was increased to reveal the maximum amount of detail in areas of primary interest. On band 7, contrast was reduced within vegetation types in the lowland areas and was increased for the vegetation type associated with the lowland-mountain boundary. The resulting image had clearer detail in the mottled lowland area and sharper land-water boundaries, features which aid in the location of terrace deposits, moraines, and outwash deposits.

An image that was contrast and edge enhanced with the EROS digital enhancement system emphasized structurally related drainage in the highland area, but it was not advantageous for studying lowland features. Ratio and hybrid images were also produced, but they provided no additional information.

Geohydrologic analysis

J. K. Richard (Technicolor Graphic Services, Inc.) conducted a demonstration with BLM personnel using digitally enhanced Landsat data and low-altitude color infrared photography to assess potential ground-water development sites in the Denali area of Alaska. Four interpretive overlays, delineating drainage, drainage basins, and landforms at two scales, were made on the basis of initial analysis of the data. The accuracy of the interpretations was verified in the field. These surface features provided information about subsurface conditions from which preliminary ground-water interpretations were made. A preliminary hydrologic model was devel-

oped to serve as a foundation for the final model, which will integrate Landsat, photographic, and field data.

COOPERATIVE PROJECTS WITH STATES

Pacific Northwest Demonstration Project

The Pacific Northwest Regional Commission (PNRC), National Aeronautics and Space Administration (NASA), and USGS are cooperating on a five-phase project designed to determine the usefulness of Landsat data for regional resource inventory, planning, and management in the States of Oregon, Washington, and Idaho. During Phase III, regional personnel participated in analysis of the Landsat and supporting aircraft data and provided ground data for verification of the statistical accuracy and precision of the classifications.

D. R. Hood reported that Phases IV and V of the project, currently nearing completion, were designed to investigate, document, evaluate, and recommend a resource information system that best serves the needs of each State's resource planning and management agencies. In order to provide input to the final recommendation, several studies were undertaken: An economic evaluation of the project, a survey of the information needs of State agencies, an assessment of the currently available remote-sensing data analysis systems, a survey of current State-owned computer hardware and related equipment, and documentation of Phases II and III.

South Dakota

Dennis Hood reported on the status of a cooperative project of the South Dakota State Planning Bureau and the EROS Data Center to incorporate statewide land-use inventory data into the State's geographic information system. Digital analysis and verification of data are now complete for 90 percent of the State.

System Improvements.—Software was modified to significantly upgrade the strength and reliability of the discriminant function classification.

Data were added to the information system to broaden the base available for multidimensional analysis.

Verification and accuracy analyses were performed on land use/land cover data sets, and several geographic areas were reclassified to improve overall accuracy.

Agreements were negotiated with Department of Agriculture's Soils Conservation Service to provide

annual ground data verification on a long-term basis.

Applications.—Multidimensional analyses were performed in Sully County to determine the extent and rate of conversion of rangeland to cropland.

Land-use/land cover data for Fall River County were prepared for TVA for use in assessing the environmental impact of uranium development.

Land use/land cover statistics were provided to the multicounty planning districts in the State for their use in HUD 701 Comprehensive Planning.

In addition, preliminary negotiations were completed for a series of studies using imagery from satellites and aircraft of irrigation suitability/capability and an analysis of land use change in the Black Hills.

Maine

W. D. Carter, detailed as an Intergovernmental Affairs Fellow in Maine, with personnel from the Maine Geological Survey and the subdistrict office of the USGS Water Resources Division, explored current and proposed applications of Landsat data. W. B. Caswell, a Maine Geological Survey hydrologist, was given a grant to attend an EROS Data Center workshop on hydrologic applications of Landsat data. Carter conducted a lineament analysis of 10 Landsat color-composite images at a scale of 1:250,000. The lineament map made from the analysis was reduced to a 1:500,000 scale to fit the geologic map of Maine and is currently being evaluated. Two enhanced images were also provided to be studied by Maine resource inventory agencies for other potential applications.

COOPERATIVE PROJECTS WITH THE BUREAU OF RECLAMATION

The EROS Program is supporting a project at the Engineering and Research Center of the Bureau of Reclamation to measure the amount of irrigated land, to detect land use change, and to map wildlife habitat along the Colorado River. R. L. Hansen and H. D. Newkirk (Bureau of Reclamation) reported that an inventory of irrigated crops in the Grand Valley project in western Colorado is being conducted on Landsat data using a system of interactive digital analysis supplied by the University of California. The minimum distance classifier was used on training areas within four stratified zones of the project area from one Landsat image. A statistical model was generated for input to the maximum likelihood classifier.

The minimum distance and maximum likelihood classifiers were also used to map water surfaces and land use on Landsat digital imagery of a test area in the west Texas high plains, as an initial step of a Total Water Management Study of the playa lakes in the 210,000-km² area.

R. L. Hansen and G. A. Teter (Bureau of Reclamation) reported that the clustering program (ISOCAS) and maximum likelihood analysis programs (CALSCAN) were modified to accommodate the thermal band of Landsat-C into the multi-parameter image processing system used at the Engineering and Research Center. Users' manuals and additional support documentation were prepared for each of the programs used for reformatting Landsat computer compatible tapes on the Bureau of Reclamation's minicomputer system.

ASSESSING THE IMPACT OF SURFACE MINING

D. M. Carnegie and J. A. Sturdevant demonstrated that changes from August 1975 to August 1976 in a phosphate surface mine in southeastern Idaho could be measured on small-scale (1:120,000) NASA aircraft color infrared photographs. Two techniques for detecting changes, by manual comparison and by mirror stereoscope, on color infrared enlargements (to a scale of 1:24,000) of photographs of the mine were used to: (a) locate and measure vegetation types destroyed or altered by new road construction, new waste dumps, new pits and expansion of mine facilities; (b) detect waste piles upon which reclamation activity had been started; (c) monitor seasonal grazing use; and (d) assess effects of weather upon plant development and water availability. The change-detection analysis performed demonstrates that small-scale aerial photographs are a valuable tool for acquiring information needed to comply with the Surface Mining Control and Reclamation Act of 1977.

W. G. Rohde, D. O. Ohlen, and C. A. Nelson (Technicolor Graphics, Inc.) reported on the application of Landsat data for mapping surface mined areas in a deciduous forest near Fork Mountain in Tennessee. Landsat digital data taken in April 1973 were analyzed using image-enhancement and image-classification procedures. Landsat data of approximately 118,000 ha were digitally enlarged, contrast enhanced, geometrically corrected, and recorded onto film. The enhanced image was enlarged to a scale of approximately 1:63,560 and interpreted to show the area of disturbed lands. A standard Landsat color composite was photographically en-

larged and interpreted in the same way as the digitally enhanced image.

An interactive image-classification system was also used to classify the area of disturbed lands. A clustering technique was used to derive training statistics for use with a maximum likelihood classification algorithm. After classification, a series of control points were selected to develop a transformation that registered the classification results to a Geological Survey 1:24,000-scale map.

A stratified random sampling scheme was used to estimate the classification accuracy of each map overlay. Based on the area classified as disturbed lands, it was determined that sampling of 61 plots of 0.4 ha each was necessary to achieve an accuracy estimate with a confidence interval of 10 percent at the 0.05 probability level.

J. V. Taranik (USGS), J. R. Lucas (Technicolor Graphic Services, Inc.), and F. C. Billingsley (NASA) reported that an 11-county rural area in south central Iowa was selected to test the effectiveness of various digital and photographic image enhancement techniques for classification of strip-mined land. Five classes of land use were delineated on 1:125,000-scale Jet Propulsion Laboratory (JPL) computer-enhanced products. Photographic enhancement techniques for standard Landsat products developed and documented at EDC proved as useful as the JPL computer-enhanced products. However, EROS Data Center Digital Image Enhancement System (EDIES) products proved inferior because the truncation limits were established for the entire scene, rather than for a specific area. A subscene of the Ottumwa, Iowa, area was analyzed with a computer multispectral analysis system, and limits for contrast enhancement were interactively established. Images were produced on a drum-type film recorder in raw and contrast-enhanced form. Photo-optically enhanced raw data compared favorably with digitally enhanced data. This investigation determined that digital-enhancement techniques should be used for cosmetic enhancement, geometric correction, and efficient recording of Landsat data over a photographically useful density range on film. Photo-optical enhancement techniques can be used at little expense in a photographic laboratory to enhance selected landscape features without repeated use of an expensive computer system. Photo-optical enhancement proved to be a more efficient method than the application of additional computer processing for selectively enhancing land classification categories related to surface mining.

FOREST DEFOLIATION

G. R. Johnson (Technicolor Graphic Services, Inc.) reported that digital multispectral scanner data taken over an eastern hardwood forest were used to map the extent and severity of forest canopy defoliation by the gypsy moth (*Porthethria dispar*). Training statistics were developed on the interactive image analysis system describing the spectral characteristics of both forest and non-forest land cover classes. These statistics were used to train a maximum likelihood algorithm to classify Landsat digital data into several land cover classes, including non-defoliated hardwood forests and three levels of canopy defoliation: light, moderate, and heavy. Classification results were geometrically corrected and color coded to display the extent of defoliation levels on overlays registered to Geological Survey 1:24,000-scale maps.

A stratified random sample of individual pixels was used to estimate the accuracy of the Landsat classification results by comparison with sampled pixels on corresponding aerial photography.

STUDYING THE GLOBAL ENVIRONMENT

Cloud top temperature monitoring

Olin H. Foehner (Bureau of Reclamation) reported on a project, supported by the EROS program, to develop better methods to enhance precipitation from winter orographic cloud systems. Digital data from the Geostationary Operational Environmental Satellite (GOES) were analyzed to determine the mesoscale features and major precipitation-producing characteristics of the orographic cloud systems affecting the Sierra Nevada. Synoptic systems that moved into the area in March 1977 were embedded with distinct convective bands of clouds 20- to 50-km wide and 75- to 200-km long. The data were recorded on film loops by the Colorado State University's automatic digital video analysis system (ADVISAR), a method of portraying the mesoscale features, their rate of motion, and duration. By videotaping the moving film loops, permanent records are produced for future analysis and archival. Satellite analysis of mesoscale features represents a breakthrough in stratifying natural phenomena that may be major sources of precipitation.

South America

Because of growing interest in the use of satellite-relayed data collection systems in South America,

the EROS Program conducted workshops, led by R. W. Paulson, in Argentina and Peru and loaned several data collection platforms (DCP) to Bolivia and Chile to collect hydrologic and meteorological data. Landsat and Landsat/GOES convertible platforms were loaned to the Servicio Geologico de Bolivia to test the capabilities of the systems in Bolivia. Landsat-relayed data are received by the NASA/Colinas tracking station near Santiago, Chile, and relayed via Lima to La Paz on a commercial aviation radio network. The Landsat/GOES System functioning in the GOES mode is received by NOAA/NESS at Suitland, Md., and relayed via commercial telegraph to La Paz. Three Landsat/GOES platforms loaned to the University of Chile Electronics Laboratories are operating in the Landsat mode and received by the NASA/Colinas tracking station. As a result of these initiatives, Argentina purchased a test platform, and Brazil and Peru expressed interest in joining the system. W. D. Carter and R. W. Paulson prepared an information manual describing DCP technology to be published by the UNESCO Committee on Space Research. It is now conceivable that a network of satellite-relayed data will be developed that covers the entire Western Hemisphere. Such a network would vastly increase our understanding of dynamic environmental phenomena.

Atlas of glaciers

Richard S. Williams, Jr., and Jane Ferrigno initiated a project to prepare a satellite image atlas of glaciers. Computer searches were made by the EROS Data Center for the best available Landsat images of the 13 major geographic areas of the world with extant glaciers. Personnel from the Glaciology Project of USGS Water Resources Division and from the National Environmental Satellite Service of the National Oceanic and Atmospheric Administration agreed to contribute either to Part I, Geographic Distribution of Glaciers, or to Part II, Topics of Glaciology and Related Environmental Phenomena.

It was determined that glacier movements or changes as small as 0.1–0.2 km can be measured on Landsat images where there is a fixed reference point. Imagery of Greenland and Svalbard was obtained and compared with available literature and published maps.

Trust territories

At the request of the Department of the Interior, the National Aeronautics and Space Administration

(NASA) acquired Landsat images of the U.S. Trust Territories of the Pacific; Yap, Ngulu Atoll in the western Caroline Islands; Anguar, Babelthaup, and the Velasco Reef area in the Palau Islands; the islands of Savaii, Upolu, Tutuila, Manua, Swains, and Rose, in Samoa; the Fonualei Volcano and the Vavau Group of the Tonga Islands. The data, in the form of 70-mm positive transparencies, were initially screened to select land areas. Selected images were enlarged to 1:1,000,000-scale negatives and printed as black-and-white paper prints. The negatives were used in constructing color-composite transparencies by the diazo process, using blue for band 4, yellow for band 5, and red for band 7. The resulting color composite showed the exposed island areas as red, shallow water reefs as green, and deep water reefs as blue. Comparison with hydrologic charts of the area indicated that the deepest parts of the Velasco reefs are at least 6.3 fathoms (36 ft or 12 m) below the ocean surface. Computer compatible tapes of some of the best images were selected to be used in experiments with interactive computer analysis systems.

Integrated terrain mapping

C. F. Hutchinson applied digital Landsat data to integrated terrain mapping in the Mojave Desert of California with the objective of classifying the land into units suitable for management, primarily cattle grazing. Land classes based on multispectral radiance statistics can be sampled on the ground and described according to their geomorphic, vegetative, and soil characteristics.

TARGETING MINERAL EXPLORATION

William T. Pecora Memorial Symposium

The third William T. Pecora Memorial Symposium, on applications of satellite data to petroleum and mineral exploration, was held in Sioux Falls, S. Dak., in October 1977. The Symposium was sponsored by the American Society of Petroleum Geologists, in cooperation with the USGS and NASA, and was attended by more than 600 participants from 30 nations. Proceedings of the first symposium, sponsored by the American Mining Congress, were published by the USGS (Professional Paper 1015).

Effects of atmosphere on Landsat data

J. V. Taranik (USGS) and C. M. Trautwein (Technicolor Graphic Services, Inc.) conducted an

investigation on the effects of the atmosphere on data collected by the Landsat multispectral scanner. Atmospheric scattering increased the brightness of data collected in band 4 (0.5–0.6 μm), band 5 (0.6–0.7 μm), and band 6 (0.7–0.8 μm), while atmospheric absorption decreased brightness of band 7 (0.8–1.1 μm). Radiometric corrections for atmospheric effects were investigated. Corrections for molecular (Rayleigh) and particulate (Mie) scattering, and for oxygen, ozone, and water vapor were theoretically derived and applied to Landsat data of the Goldfield area, Nevada (Scene ID 1072–18001), acquired on October 3, 1972. Regional weather maps supplied by the National Weather Service were used to determine atmospheric water vapor content on that date for the Goldfield area. Calculated brightness values for maximum scene reflectance were exceeded by values observed on Landsat computer compatible tapes. Ground-based spectral measurements could not be precisely correlated with Landsat MSS spectral measurements when atmospheric corrections were applied because of the lack of accurate data on the relationships between detector output voltage and multiplexer digital number and on the radiometric adjustments applied in the production of CCT's. However, the atmospheric corrections on a color composite display of data improved the display of radiometric patterns related to rock and soil cover.

Nickel laterites

J. V. Taranik and W. D. Carter reported that many small islands between Borneo and New Guinea are being investigated for the occurrence of nickel laterites (Reynolds and others, 1973). Ground-based exploration in this area is costly and difficult because of the remote location, dense vegetation, and the ubiquitous lateritic soils that develop over diverse types of iron-rich rocks. Ground-based investigations of islands west of Waigeo Island have documented landscape cover conditions related to nickel laterite occurrence (Reynolds and others, 1973, p. 317). Areas having laterites at or near the surface are often marked by stressed or sparse vegetation or by the presence of particular species.

Landsat computer compatible tapes (CCT) for two islands near Pulau Waigeo were analyzed. An interactive multispectral analysis system was used to classify areas of known laterite occurrence on Pulau Gag. Contrast enhancement techniques increased the contrast between areas with exposed red lateritic soil and areas with dense, healthy vegetation. A parallelepiped classification algorithm

was employed in a supervised mode to determine the integrated spectral response from vegetation and lateritic soil over the laterite areas. The enhancement and classification techniques applied to known areas on Pulau Gag were used for unknown areas on Pulau Kawe, and similar integrated signatures for the sparse and stressed vegetation and exposed red bare soil combination were identified there.

Other techniques, including principal component analysis, were tested in identifying potential areas for targeting nickel laterite exploration, but these techniques were less successful.

Correlation of Landsat data with geophysical data

S. K. Sahai (University of Akron in Ohio) conducted a study of the correlation of geophysical data with Landsat data in an interactive digital image analysis system. Magnetic data collected by aircraft, more readily available at less expense than other forms of geophysical data, were directly correlated with data from Landsat for targeting sites for mineral exploration. Magnetic data were easily displayed as a gray level or color-coded image on a cathode ray tube showing features not apparent on a contour map of the data. The digital analysis system software was used to enhance local gravity and magnetic anomalies. Computer algorithms tested included second derivative calculations, Fourier filtering, continuation of field, and trend surface algorithms. The interactive multispectral analysis system proved extremely useful for the rapid display and analysis of geophysical data and comparison of these data with data from Landsat.

Stereoscopic projection system to interpret Landsat data

J. V. Taranik (USGS) and W. B. Hall (University of Idaho) reported the development of a stereoscopic projection system for training geologists to interpret Landsat imagery. Color oblique stereo aerial (COSA) 35-mm photographs were acquired of various types of landforms, drainage patterns, and land cover. These photographs were used with 35-mm slides in stereo pairs of black and white photographs from low and high altitudes, color photographs from ultra high altitudes (U-2 and RB-57 aircraft), and photographs from manned spacecraft. Two Kodak carousel projectors were mounted on a platform so that one projector could be remotely adjusted in three orthogonal directions for image registration. The projectors were equipped with polarizing filters, and the students

wore polarizing spectacles. The projected stereo image was viewed on a lenticular screen while the monoscopic Landsat image was simultaneously projected on an adjacent screen.

Multidisciplinary study in New Mexico

W. A. Fischer reported that several large playas, anomalous to their surroundings, are present in the north-central part of the 33,000-km² study area near the city of Vaughn, N. Mex. Geochemical analysis of solids and brines from these playas showed minimal concentrations of strontium; waters in the playas and vegetation surrounding them are toxic to cattle. The lack of correlation between the persistence and the amount of water in these lakes and the size of surrounding internal drainage areas suggests the possibility of sub-surface interconnections among the lakes. Large magnetic anomalies, including relatively high magnetic fields beneath the playas, are present within the area. Some other magnetic highs are related to the topographic form (largely buried) of Precambrian basement, as observed in the field or deduced from geologic mapping (Kelley, 1972). Some of the strongest anomalies do not seem to be related to the playas or basement configuration and remain under investigation.

Playa surface mapping

Playa surface mapping experiments by W. S. Kowalik in western Nevada are being used as a local extension of Landsat investigations of Andean evaporite basins conducted earlier by W. D. Carter and Kowalik. Initial results at Fourmile and Garfield Flats and Artesia Lake during Landsat-2 overpass periods indicated a high degree of correspondence between Landsat radiance values, determined by an unsupervised clustering algorithm, and measurements of soil moisture, salt and clay content, and surface macroroughness of field units. Estimation of the distribution of surface types in unknown or less accessible playas should be successful when based on ranges or normalized Landsat digital values found over known surfaces. This methodology will aid playas mineral exploration by showing the distribution of salt and mud at playa surfaces and by showing the seasonal changes in playa surface characteristics. In addition, it will provide information on the hydrologic setting of a playa and aid the planning of transportation development.

Circular feature in Pennsylvania

Study of a previously unrecognized circular drainage pattern 24 km in diameter east of Scranton, Pa.,

that W. S. Kowalik found on Landsat imagery has yielded several clues as to its origin. W. D. Carter reported that reconnaissance of the Devonian Catskill Formation at the surface shows no obvious structural anomalies. Aeromagnetic data show a 70-gamma high over the southeastern quadrant of the drainage pattern. A detailed gravity survey (368 stations) of the area shows a 0.8 mGal gravity high over the aeromagnetic high. Thin sections of surface conglomeratic sandstones did not contain oriented planar features or extensive fracturing in quartz crystals, features which might be expected in strata at or below the surface of an astrobleme. The aeromagnetic and gravity data suggest a body at depth, but the exact origin of the circular drainage feature remains unknown.

Luminescence studies

R. D. Watson reported that the Fraunhofer Line Discriminator (FLD) is now operated routinely from a fixed-wing aircraft. Only pertinent data such as established by a selected luminescence threshold or within a selected range of luminescence values are recorded. A line-scanner imaging system has also been designed, built, and mounted on the Geological Survey's Cessna 337 aircraft, permitting the FLD to operate also in an imaging mode. Performance tests of the imaging system showed that an aircraft speed of 45 m/s and an altitude of 2,382 m above terrain is required to cover 80 percent of the area by the circular field of view (without overlap) at a ground resolution of 45 m. A television system, bore-sighted with the FLD scanner, permits identification of surface features and correlation of these features with measured luminescence. The imaging system was used to map the areal extent of oil slicks from selected seeps in Santa Barbara Channel, Calif., and to map uranium-bearing sandstone outcrops of the Galisteo Formation, Sandia Mountains, N. Mex.

Quantitative study of Landsat data

Stuart Marsh reported that a project was initiated to study the quantitative relationships of surface geology and near surface spectra to satellite radiometric data. Mapping and spectral sampling of a variety of terrain types was done in the Yerington, Nev., area at a time corresponding with two satellite passes and nearly zero cloud cover and relatively consistent meteorological conditions. Measurements were taken on a square grid systems of each site, ranging in size from two to six pixels,

with either 9 or 16 samples per pixel. Calculations to determine the minimum number of samples based upon a "t" distribution and a 95-percent capability of approximating the data mean indicated that nine samples per pixel were sufficient to be within 2.0 to 1.5 percent of the mean reflectance.

REMOTE SENSING APPLICATION TO GEOLOGIC STUDIES

Mapping altered rocks using multispectral aircraft images

Evaluation of Landsat images for distinguishing altered and unaltered rocks has identified two important limitations imposed by mineralogical composition and the multispectral scanner (MSS) bandpasses: (1) limonitic unaltered rocks, such as ferruginous sandstones and hematitic tuffs and flows, cannot be distinguished from limonitic altered rocks, and (2) bleached, limonitic-poor rocks are not discriminable because of the common occurrence of unaltered rocks with intrinsically high albedos (Rowan and others, 1974).

Rowan and R. P. Ashley (USGS), and A. F. H. Goetz (Jet Propulsion Laboratory, Pasadena, Calif.) have noted that in situ reflectance spectra for altered rocks in parts of Nevada and Utah have a prominent absorption band near 2.2 μm because of the presence of hydroxyl-bearing clay minerals, alunite, or pyrophyllite. This absorption band is absent in all unaltered volcanic and intrusive rock spectra examined, which suggests a basis for alleviating the above stated problems in arid and semi-arid areas. Sedimentary rocks containing hydroxyl-bearing minerals commonly have a 2.2- μm band, however.

To test the effectiveness of this spectral band for mapping altered rocks, NASA 24-channel multispectral aircraft images have been evaluated for three areas in the Great Basin. In the Cuprite, Nev., mining district, located 17 km south of Goldfield, bleached opalized and silicified rocks were discriminated from unaltered volcanic rocks through analysis of a color-ratio composite image (Rowan and others, 1974) that included the 2.2- μm spectral band (Abrams and others, 1977). Ashley made petrographic analyses of field samples and visible and near-infrared (VNIR) reflectance spectra acquired at the sample sites with a portable reflectance spectrometer to correlate mineral composition with characteristics of the aircraft data. The results demonstrate that the ratio 1.6 μm /2.2 μm is proportional to the total amount of clays and alunite pres-

ent. A density slice of this ratio image provides a map showing relative variations in total alunite and clay content. The ratio of the band at 1.6 μm to the band centered at 0.48 μm , or any of several ratios of bands centered between the 0.66 μm and 1.0 μm to each other or to the 0.48- μm band, can be used to map relative variations in limonite content. Image processing and field spectrometry were done in cooperation with the Jet Propulsion Laboratory in Pasadena, Calif.

In the Silver Peak Range to the west, tan, pink, and red unaltered hematitic tuffs are widespread and are indistinguishable from limonitic altered rocks in Landsat color-ratio composite images (Rowan and others, 1977). These tuffs were correctly mapped as unaltered rocks in a color-ratio composite aircraft image using the 2.2- μm band (Abrams and others, 1977).

The third area, located in the central part of the East Tintic Mountains in Utah, has a wider range of host and altered rocks and more vegetation than the Nevada areas. Although these conditions required the use of a different color composite of aircraft ratio images, problematical rocks, such as limonitic flow rocks and non-limonitic silicified rocks, were accurately mapped by incorporating the 2.2- μm band.

Because of these results and the availability of a large volume of supporting field spectra, the 2.2 μm band has been recommended to NASA for inclusion on the Thematic Mapper of Landsat D.

Remote sensing for uranium exploration

A study of Landsat images of the southern Powder River basin in Wyoming by G. L. Raines and T. W. Offield has provided the basis for a regional facies analysis for uranium deposition in the Wasatch Formation. This analysis is based on two observations: (1) vegetation cover density is often a sensitive indicator of bedrock lithology, and (2) the ratio of Landsat bands 5 and 6 is directly related to vegetation cover density. Thus, it is possible to map very subtle changes in lithology by mapping vegetation density on ratioed Landsat images. Application of this technique to the Wasatch Formation in the southern Powder River basin provided data for a facies map that is supported by regional well log studies. Raines and Offield conclude that the uranium deposits are consistently associated with a particular, very restricted, facies of the Wasatch Formation. This previously unappreciated facies control of uranium deposition suggests that

certain areas heretofore overlooked may be good exploration targets.

Spectral signatures of minerals in the visible and near-infrared regions of the spectrum

The utility of multispectral remote sensing techniques for discriminating among materials is based on the differences that exist among the spectral properties of the materials. The properties of critical importance are those caused only by the composition of the material and result in spectral features that appear in the visible and near-infrared (0.325 to 2.5 μm) bidirectional reflection spectra of minerals. These features are caused by a variety of electronic and vibrational processes, such as crystal field effects, charge-transfer, color centers, transitions to the conduction band, and overtone and combination tone vibrational transitions. Spectral variations that occur as a consequence of target condition and environmental factors are distinct from those described above and are not considered here.

A "spectral signature" diagram that summarizes the optimum intrinsic information available from the spectra of particulate minerals was constructed by G. R. Hunt, based on data from a large selection of minerals. The diagram provides a ready reference to the interpretation of visible and near-infrared features that typically appear in remotely sensed data because the rock and soil surfaces observed display the characteristic spectral information of their constituent minerals. In the visible near-infrared region, the most commonly observed features in naturally occurring materials are due to the presence of iron in some form or other, or to the presence of water or hydroxyl (OH) groups.

Origin of bands in mineral and rock spectra in the three-micrometer range

G. R. Hunt studied the potential of the three micrometer spectral regions for providing diagnostic information about naturally occurring minerals and rocks, and found that most features in this range are due to the presence of the hydroxyl (OH) group in some form. A broad band centered near 2.9 μm indicates the presence of molecular water, which may be physisorbed, included, or internal, whether essential to the crystal structure or not. To effectively characterize a specific OH group, it is usually necessary to interpret spectral changes that occur as a result of evacuation, heating, and isotopic substitution, as well as to acquire data from other spectral regions. Very sharp bands

at shorter wavelengths (2.74 μm) indicate the presence of constitutional OH groups in the bulk of the material, and typically they occur in layer silicates for which the intensity and form of the bands provide particularly diagnostic information. At still shorter wavelength (2.7 μm), features are produced by free surface silanol groups. When OH groups enter into hydrogen bonding, the features that are produced occur over a range from 2.63 μm to 4.37 μm , depending on the strength of the bond formed.

Evaluation of algorithms for geological thermal-inertia mapping

The errors incurred in producing a thermal-inertia map are of three general types: measurement, analysis, and model simplification. To emphasize the geophysical relevance of these errors, Kenneth Watson and S. H. Miller have developed a technique to express them in terms of uncertainty in thermal inertia and to compare these uncertainties with the thermal-inertia values of geologic materials. The errors calculated in this study were determined assuming site and seasonal parameters corresponding to data acquired at the Raft River, Idaho, and the results serve to illustrate the magnitude of the errors. However, the error analysis used can be directly applied to other sites and conditions by using appropriate parameters.

Measurement errors introduced by multispectral scanning systems commonly range from a noise-equivalent-temperature difference ($NE\Delta T$) of 0.1 K for aircraft systems to 1 K for satellite systems. The resulting uncertainties in thermal inertia range from 15 TIU to 150 TIU, where TIU (thermal-inertia unit) = $1 \text{ watt} \times \text{s}^{1/2}/\text{m}^2/\text{K}$.

Three surface temperature algorithms—linear Fourier series, finite difference, and Laplace transform—were evaluated to estimate the analysis errors. In terms of resulting errors in thermal inertia, the Laplace-transform method is the most accurate (260 TIU), the forward finite-difference method is intermediate (300 TIU), and the linear Fourier series method is the least accurate (460 TIU). However, the two more exact methods require more computer time, and both lack the ability of the Fourier-series algorithm to illustrate the physical significance of individual terms. By comparing the errors with the range of thermal inertias of geologic materials, it is possible to select the most cost-effective algorithm for a particular application.

Model simplification errors result from three sources: transient effects, topography, and surface coating effects. For example, flux of 35 watts/ m^2

(equivalent to a water evaporation rate of 1.2 mm/d) would produce a thermal-inertia error of about 200 TIU. If no topographic corrections are made, a 10° southwestern slope causes an error in thermal inertia of about 350 TIU. A hematite surface coating 1-cm thick on a rock will produce an error of approximately 200 TIU, whereas a 1-mm layer thickness will have a negligible effect (25 TIU).

The total system errors in thermal inertia are placed in geologic context by noting the separation in thermal-inertia values for various geologic materials. For example, the thermal-inertia separation between limestones and dolomites is typically 1,200 TIU. The error analysis technique indicates that thermal-inertia discrimination should be possible between black shale and gabbro (separation of approximately 450 TIU); discrimination between these two materials is not possible using Landsat spectral-reflectance data.

Errors in thermal inertia can be translated into errors in bulk density and moisture content. Thermal-inertia mapping from aircraft ($NE\Delta T = 0.1$ K) has an accuracy of about 1 percent in bulk density or the equivalence thereof and a sensitivity of 0.3 percent in water content. Thermal-inertia mapping from satellite ($NE\Delta T = 1$ K) has an accuracy of 9 percent in bulk density and a sensitivity of 3 percent in water content.

A practical evaluation of the error analysis was demonstrated by using the results of a field study by R. J. Kline at the Raft River in Idaho. He demonstrated that alluvium and some tuffaceous sedimentary rocks can be discriminated from lava flows on a thermal-inertia image. Other tuff units are indistinguishable from the surficial deposits. The Watson and Miller study indicates that the thermal-inertia values of the tuffaceous material overlap both the values of alluvium and the values of the lavas. The overlap of the tuff and the separation of alluvium from lava are consistent with the topographic errors in thermal inertia that are derived from the error analysis technique and are associated with the average slopes on which these materials are inclined.

Landsat filters for rock type discrimination

Ratio values of the reflected energy available through different Landsat bandpass filters were determined by G. R. Hunt based on laboratory spectra of 284 particulate rock and soil specimens. The potential for using these data to discriminate among rocks types was examined. On the basis of only spectral information related to the composition of

the materials as detected in the multispectral scanner bands, thereby excluding texture, slope, relief, and vegetation as effects, Hunt concluded that the ratios can be generally used to discriminate lithologic types. However, only mafic and ultramafic rocks and alteration involving ferric oxide typically display sufficiently characteristic spectral properties to allow specific identification. Certain unique spectral features, such as those produced by the presence of chromium in some chloritic quartzites, can be used for discrimination of certain rare rock types.

Presentation and interpretation of aerial radiometric data

Gamma-ray spectrometric data from an aerial survey in the southern part of the Powder River basin in Wyoming were prepared by J. S. Duval in the format of a color-composite image. The color image highlights the presence of Eolian sand extending from the sand hills west of the survey area and the sandy channel of the Dry Fork of the Cheyenne River. Neither of these features shows up very well in the normally used contour maps. The color image also emphasizes the geologic contact between the Fort Union and Wasatch Formations.

By means of the criterion that an anomaly is any area of relatively small extent that has color characteristics different from the general surroundings, a number of radiometric anomalies were identified. Those anomalies that were checked in the field were found to be associated with evidence of alteration and (or) known uranium mineralization.

Landsat investigations of the northern Paradox Basin, Utah and Colorado

Image processing by computer, followed by lineament analysis of selected Landsat frames of the Paradox Basin in Utah and Colorado, by J. D. Friedman and S. L. Simpson, has yielded new information on the structural geology of the salt anticline region in the northwest quadrant of the 2° Moab quadrangle. A northeast-trending lineament set extends through the incised meander pattern of the Green River to the area of Yellowcat Dome, in a region of northeast-trending basement wrench faults, as interpreted by Hite (1975). The set includes, southwest of Crescent Junction, the heretofore unmapped Tenmile Canyon lineament that marks the eastern termination of Tenmile graben underlain by a salt diapir (Joesting and Case, 1962, p. 1881), and which cuts Courthouse

syncline, Moab anticline, and Salt Valley graben. Previous structural mapping (Williams, 1964) indicates a major change in trend or possible dislocation of Salt Valley anticline and the Moab fault system. This suggests that the Tenmile graben diapir was once continuous with the Moab diapir and has subsequently been dislocated or severed from the Moab structure along the proposed Tenmile Canyon lineament.

Lineament patterns interpreted from radar images of the Mississippi embayment

A lineament map of the Mississippi embayment, compiled by D. W. O'Leary and S. L. Simpson from SLAR images, suggests that the Ozark uplift is intricately and closely faulted, and that the fault pattern extends as far south as the Ouachita Front. A pronounced system of lineaments strikes N. 60° W.; a more fragmented, less consistently oriented set strikes N. 40° E. Within the embayment the N. 40° E. set is evident, but the N. 60° W. set is negligible. The lineament pattern near the northern end of the Nashville dome is quite different; northwest-trending lineaments are weakly developed and northeast-trending lineaments bend into a strong N. 60° to N. 70° E. direction. These patterns suggest that (1) the embayment is a zone of structural discontinuity separating the evolution of adjacent Paleozoic upland structures, (2) the alluvial part of the embayment has strong structural affinities with the Ozark dome, and (3) the alluvial part of the embayment is a narrow trough trending N. 40° E. that received its morphological identity since the dissection of inliers bounded by N. 40° E.-trending lineaments. Since the latest prealluvial deposits in the area are possible early Pleistocene in age, that would mean the embayment achieved its present configuration within the last 2-3 million years.

Orland lineament and structural control in eastern Maine

The Orland lineament is a major terrane feature in eastern Maine; it extends from the town of Orland to East Holden, a distance of 64 km, along a N. 25° E. trend. From East Holden it extends in a more easterly direction, and with less distinction, to the New Brunswick border. It essentially marks the boundary between the "Bays of Maine" plutonic complex and the folded eugeosynclinal rocks to the south.

The lineament is almost entirely within the calcareous Siluro-Ordovician Bucksport Formation that has a well-defined foliation striking about N. 25° E., dipping steeply east. Landforms in the lineament

are strongly controlled by close, regular cross-jointing and clean-foliation cleavage. The eastern edge of the lineament is bordered by a zone of evenly layered hornfels contacted by the Lucerne Granite of local usage. The western border is marked by older, higher grade units, mylonitized Bucksport Formation, or (especially in the northern area) less closely jointed, less deformed Bucksport rocks. Southwest of Orland the lineament is not clearly expressed on Landsat images; here bedrock consists of rusty schist and quartzite of the Penobscot Formation, which does not provide structural control for aligned landforms.

Field investigations by D. W. O'Leary and B. S. Rhea revealed that mylonite and brecciated mylonite are exposed in the Long Pond-Dressers Mount area within the lineament. Microdisplacements in some of the mylonite indicate right-lateral movement. Nevertheless, clear evidence of faulting is not present in the area. The projection of the lineament to the east bank of the Penobscot River intersects bedrock exposed almost continuously for a distance of nearly a kilometer. At least three zones of intense shearing and brecciation are present with open shear fractures, as well as solid mylonite layers. The exposures are also notable for abundant aplite, with inclusions of Penobscot Formation, and local gabbro bodies. Slices of Penobscot Formation and gabbro are included within a broad zone of shearing.

In the Great Pond quadrangle, intense mylonitization and brecciation over a zone almost a kilometer across mark the trace of the lineament. It is not known how this structure relates to the Norumbega fault, which passes through this zone. Mapped fault segments farther northeast along the lineament, combined with the observations mentioned here, indicate that the Orland lineament is the trace of a zone of major shearing and faulting that was certainly active in late Devonian time. The presence of open shear fractures and brecciation suggests that this zone is one of present-day weakness. It seems clear that the Orland lineament marks an important regional shear zone with major implications to the structure of surrounding terrane, especially where it can be projected along the northern edge of Penobscot Bay.

APPLICATIONS TO HYDROLOGIC STUDIES

Research on the hydrologic applications of remote sensing continued during FY 1978. Aerial photographs and Landsat data were tested or used on

an operational basis to locate sites for test wells and to delineate and monitor wetlands. In addition, there were some preliminary and experimental results from surface-water and quality-of-water applications.

Using infrared aerial photographs for ground-water exploration

Black-and-white infrared aerial photographs were used by E. F. Hollyday to locate test-well sites in central Tennessee. Test drilling in the dense, fractured limestones at these sites resulted in the discovery of solution cavities that produce as much as 12.6 L/s of water. Site selection was based on the hypothesis that large amounts of ground water may occur near dry streams; runoff in small drainage basins may be mostly in surface streams or mostly underground. Information from other wells in the Lincoln County study area tends to support this site selection principle.

The Tennessee Valley Authority acquired black-and-white infrared aerial photographs (1:24,000 scale) taken of northern Lincoln County during a dry period in February 1977. U.S. Geological Survey investigators analyzed the photographs and delineated a number of dry reaches where streamflow normally would have been expected. Water appears black on these photographs, whereas bare soil and rock in dry streambeds appear in very light tones.

Eleven test wells were drilled along two of the dry reaches. Five of the test wells produced less than 0.2 L/s; the other six test wells produced from 0.5 to 12.6 L/s and had an average yield of about 5.5 L/s. Other wells in northern Lincoln County have an average yield of less than 0.3 L/s.

Wetland vegetation studies

Vegetation maps of the Great Dismal Swamp of Virginia and North Carolina were produced from digital Landsat data by P. T. Gammon and Virginia Carter (USGS) and L. J. Shima (NASA) (1977). A variety of computer analyses and classification procedures were tested by using both single-date and temporally registered Landsat data. The accuracy of categories on the resulting maps is being checked on the ground and by interpretation of aerial photographs to determine the feasibility of using Landsat data to monitor the vegetation succession resulting from various land-management practices.

Carter and J. H. Burbank (Tennessee Valley Authority) (1978) developed a wetlands-classifica-

tion system for the Tennessee Valley region. This system was used to prepare thematic maps (1:24,000 scale) of classes of wetlands and adjacent land use for 15 quadrangles in western Tennessee. The classes were interpreted and delineated on high-altitude color-infrared photographs, transferred to maps, and checked on the ground.

The USGS, in cooperation with the Jet Propulsion Laboratory and the U.S. Fish and Wildlife Service, is testing the potential of Landsat data to prepare updates of the National Wetlands Inventory. According to Carter, these data may have immediate use for wetlands monitoring in remote areas, such as parts of Alaska.

Landsat surveillance of water turbidity and color

Satellite surveillance is considered a costly way of obtaining information on water turbidity and color, but the application of this technique may have considerable benefits in several areas of study. These include the use of turbidity as an indicator of streamflow velocity and of the productivity of lakes, estuaries, and oceanic fishing grounds.

Recently completed research by G. K. Moore showed that the turbidity and color of water can be measured optically by using imagery provided by remote sensors; reflectivity of light increases with increased turbidity, whereas color is caused by the differential absorption of light in water.

Surface-water applications of Landsat data

Preliminary research by G. K. Moore showed that (1) the area of saturated soil in a drainage basin may be related to rate of streamflow and (2) the digital values of a group of Landsat picture elements may be related to flow velocity vectors.

Saturated soils appear gray to nearly black on positive Landsat band-7 (0.8–1.1 μm wavelength) images. A series of 13 images of an area near Tupelo, Miss., made from October 1975–April 1976, show a wide variation in areas covered by dark soil tones adjacent to the streams. The changes in soil tone apparently are related to increases and decreases in streamflows.

Patterns of Landsat digital picture-element values can be related to water depth and to other factors that determine flow-velocity vectors. Arrays of digital values in Landsat band 5 (0.6–0.7 μm wavelength) and band 7 were examined for reaches of the Tennessee and Ohio Rivers. Band-7 digital values were used to define river boundaries in the

arrays; band-5 values were then used to outline anomalously high and low numbers. The patterns formed by the high and low values were consistent with theoretical flow patterns in the rivers and in a reservoir.

R. A. Baltzer and Virginia Carter are making a similar study of Port Royal Sound, S.C., to determine the relationship between Landsat digital values and water depths in the sound and surrounding wetlands. If Landsat data prove to be a reliable index of water depth and show the presence or absence of water in wetlands, they can be used as input to a digital model of circulation in the sound.

APPLICATIONS TO CARTOGRAPHIC STUDIES

Investigations into further aspects of cartographic applications of space data were continued during fiscal year 1978.

LANDSAT-3 INVESTIGATIONS

Landsat-3, launched on March 5, 1978, carries longer focal length Return Beam Vidicon (RBV) cameras that provide substantially improved resolution and geometric fidelity as compared with the RBV's of earlier Landsats. Preliminary evaluation of the RBV images determined that while the normally produced images were lacking in image quality, specially processed images were excellent. When the NASA digital Image Processing Facility (IPF) and the EROS Digital Image Processing System (EDIPS) become operational in the fall of 1978, normal image quality is expected to be much better.

- The geometric quality of the RBV image tested approaches 1:50,000-scale mapping requirements in horizontal accuracy.
- Based on a study of resolution compared with the multispectral scanner (MSS), the RBV has an advantage approaching 3 to 1.
- The geometric quality of a sample MSS image was also improved as compared with MSS imagery before the launch of Landsat-3.
- A project was started to determine if an improved color composite or lithographic prints can be produced by combining the RBV image and the MSS images. The combination should benefit from the high resolution of the RBV and the multispectral quality of the MSS bands.

- Early generation reproductions of Landsat-3 images have been transmitted to scientists at the University of Arizona, University of Georgia, and Ohio State University. Evaluations by these investigators are expected to complement our own investigations.

NIGHTTIME IMAGES OF THE EARTH FROM SPACE

Investigation of the new improved Defense Meteorological Satellite Program (DMSP) to record information related to Earth resources is being continued. A 1-year contract has been arranged with Stanford Research International to pursue the investigation, with Dr. Thomas Croft serving as principal investigator. Dr. Croft conducted a study of the earlier DMSP data in 1977.

SATELLITE IMAGE MAPS

Temporal mapping with Landsat data

A 1:500,000-scale color image map of Chesapeake Bay and Vicinity, Winter 1976-77 was printed using three Landsat-1 scenes. The map portrays the area under the most severe winter conditions on record and is a true temporal map as well as a historical portrayal of thematic data. The entire Chesapeake Bay was imaged in a 50-second period on February 7, 1977. On the following day the western part of the bay and the Potomac River were imaged, and the changes that occurred in the ice within 24 hours are recorded.

Enhancement of the imagery at the EROS Data Center introduced digital one-dimensional (scan-line) clipping and stretching to accentuate the various ice conditions. Edge enhancement was also used to increase contrast. This one-dimensional enhancement has been referred to as the EROS Digital Image Enhancement System (EDIES). This system will be superseded by the more sophisticated EDIPS.

Upper Chesapeake Bay

A third edition of the Upper Chesapeake Bay color image map was printed at 1:250,000 scale using a precision-processed edge-enhanced image digitally processed by IBM Corporation. The larger scale map shows more color contrast and information and improved geometric accuracy as compared with the two previous editions. The first edition was produced by conventional photographic processing and the second used an image that had been precision processed by digital methods. Since all three editions contain the same basic data (the Landsat-1

image recorded October 11, 1972, valid comparison of results is possible, and the advancement in image processing techniques is evident. An estimated 100 percent increase in both information content and geometric accuracy has been achieved through improved processing. An accuracy test of the map as printed is significant because the root-mean-square error is only 61 m. This indicates that Landsat data, when properly processed, and referenced to ground control, can be printed in multicolor image form and meet U.S. National Map Accuracy Standards for 1:250,000 scale.

Montana/Wyoming image maps

Single scenes of coal-rich areas in Montana were enhanced by EDIES processing and reproduced in color at 1:500,000 scale to demonstrate the quality of image maps that can be produced from Landsat images of that geographic area. The three image maps covering nominal 100 by 100 nautical miles (nmi) are identified as (1) Pumpkin Creek, Mont., (2) Dry Fork Cheyenne River, Wyo., and (3) Medicine Bow River, Wyo.

Wenatchee, Washington

An experiment was completed testing the use of Landsat images for theme extraction of open water, vegetation, and natural shaded relief on the 1:250,000-scale Wenatchee, Wash., quadrangle. The vegetation and natural shaded relief data and the image map background were combined with the line map data. However, it was found that the time of year and Sun angle of the image need to be carefully selected for a complete water plate. This map was selected by the member States of the Commission on Cartography of the Pan American Institute of Geography and History (PAIGH) as the standard model for preparation of the PAIGH 1:250,000-scale unified Hemispheric Mapping Series for areas where no topographic coverage is available.

SPACE OBLIQUE MERCATOR PROJECTION

In 1974, Alden P. Colvocoresses proposed a new map projection that would permit continuous mapping of satellite imagery, especially Landsat—the Space Oblique Mercator (SOM) projection. Until then no map projection had been devised to show the satellite ground track continually true to scale for an orbiting satellite combined with a rotating Earth. In 1977, a contract with Dr. John Junkins of the University of Virginia resulted in development

of a complex set of universal equations that can be applied to noncircular orbits and other general cases. At the same time, an independent investigator, John Snyder, developed simpler equations defined specifically for Landsat. Since then, Snyder has refined and improved the equations, and they can be applied to other polar-orbiting satellites. Snyder's equations have been programmed on the USGS IBM-370 computer. Copies of the program and documentation are available and have been initially distributed to other government agencies and some commercial interests. When fully adopted, Landsat processing based on the SOM will contribute to the automated production of image maps in a few days after the imagery is obtained.

PARAMETERS FOR AN AUTOMATED MAPPING SATELLITE (MAPSAT)

Although the Landsat program is experimental, it has demonstrated the operational utility of Earth sensing from space. This consideration and the revolutionary effects of automated digital processing on the mapping process led to the development of a proposed design for an operational satellite as a key element in an automated mapping system. The proposed design includes stereographic as well as orthographic viewing of the Earth. Specific parameters of the design are as follows:

- ORBIT—919 km, 9:30 a.m. imaging time (same as Landsat-1, -2, and -3).
- SENSORS—Linear arrays plus three optic: two optics, tilted fore and aft about 24 degrees, panchromatic (0.47 to 0.70 μm), high resolution 10 to 30 m pixel; one optic, vertical with 3 (or 4) multispectral linear arrays (MLA).
 - Band 1—0.47 to 0.57 μm , 30 to 90 m pixel
 - Band 2—0.57 to 0.70 μm , 10 to 30 m pixel
 - Band 3—0.76 to 1.05 μm , 30 to 90 m pixel
 A possible alternative for band 3 is two bands at 0.70 to 0.80 μm and 0.80 to 1.05 μm .
- STABILITY—Rational rates within 10^{-6} deg/s. deg/s.
- POINTING ACCURACY—Within 0.1 degree of vertical.
- POINTING DETERMINATION—Within 5 to 10 arc seconds.
- ACQUISITION MODES—Variable as to resolution, base-height ratio, and division (portion) of swath width.
- TRANSMISSION MODES — Fixed antenna, direct to ground and relay to United States and (or) onboard recording.

- DATA TRANSMISSION RATE—15 Mb/s (same as Landsat-1, -2, and -3).
- DATA PROCESSING—Automated, based on one-dimensional data correlation, ephemeris data, and (or) limited ground control.
- PRODUCTS—Multispectral stereoscopic digital data compatible with 1:50,000-scale topographic, planimetric, and thematic mapping. Positional accuracy of 7 to 25 m relative and 50 to 100 m independent of control.

LAND USE AND ENVIRONMENTAL IMPACT

MULTIDISCIPLINARY STUDIES IN SUPPORT OF LAND-USE PLANNING AND DECISIONMAKING

Many of the scientific and economic results reported elsewhere in this volume have application to natural-resource planning and management. The Earth Sciences Applications Program of the Land Information and Analysis Office sponsors a series of projects designed not only to support and encourage the application of those results but also to stimulate the development and application of earth-sciences information for resource-use decisionmaking on a broader scale nationwide.

GEOHYDROLOGIC STUDIES TO GUIDE EXPLORATORY DRILLING FOR GROUND WATER IN FAIRFAX COUNTY, VIRGINIA

The Coastal Plain and Triassic and Jurassic Lowland were selected as the most favorable areas to explore for supplemental public water supplies in Fairfax County, Virginia, based on preliminary results of the Fairfax County environmental geology study (Johnston and Froelich, 1977; Johnston and Larson, 1977). The Fairfax County Board of Supervisors, acting on these preliminary results, recommended—and the Fairfax County Water Authority agreed to fund—an exploratory drilling and aquifer test program.

In the Coastal Plain, high transmissivity aquifers in the Cretaceous Potomac Group are relatively narrow, sinuous sand deposits that fill paleochannels (Johnston and Froelich, 1977). As these sand bodies are for the most part poorly defined at depth (averaging 120 m), the chief problem is to locate thick sand sections and to determine their areal extent and hydraulic characteristics.

In the Triassic and Jurassic Lowland, the principal aquifers are fractured sandstone and siltstone with zones of highest permeability apparently related to bedding plane partings and interconnected fracture systems. Ongoing studies of joints, faults, and lineaments identified on aerial photos and Land-

sat images are being used to select favorable target areas for exploration. As the highest yields are from deep wells (180 to 300 m) in which the ground water is relatively high in dissolved solids, the natural quality of water is another important consideration. Thus the chief problems are: (1) To determine if chemical water quality is a function of depth or if it is related to a specific geologic formation and (2) to try to locate fractured zones of above average permeability by applying the results of lineament studies.

GEOLOGIC AND HYDROLOGIC MAPPING IN THE COLORADO FRONT RANGE URBAN CORRIDOR TO AID LOCAL AND REGIONAL PLANNERS

County geologic and planning personnel are using maps of mountain soils along the eastern Front Range to fill several pertinent voids in their information needs for existing and future land-use studies, including the generation of computer-based land-use maps. Field use of the maps by county personnel has substantiated a high reliability factor. Along with the land-use information these maps contain, users have found the definitions of the five map units and their presentation in a tabular text tailored to their needs. Demands for these soils maps prepared as a part of the Survey's Front Range Urban Corridor study have exceeded expectations.

The principal water table aquifers in the Boulder-Fort Collins-Greeley area of the Front Range Urban Corridor occur in the alluvium and terrace deposits in and adjacent to the valleys of the South Platte River and its major tributaries. Depth to the water table in the sedimentary deposits underlying the eastern three-fourths of the study area ranged from 0 to 15 m during 1976-77. Generally, the depth to water in the river valleys was less than 3 m. Based on long-term records of water levels, there are no areas of major water-level decline; the maximum decline since the late 1950's has been about 1.5 m. Water of suitable quality for drinking is found in terrace deposits near Fort Collins and Loveland, in

the alluvium of Boulder, Left Hand, and St. Vrain Creeks just east of the mountain front, and in the mountainous western part of the area. Elsewhere, the dissolved-solids concentrations exceed 500 mg/L and generally exceed 1,000 mg/L. Arsenic, chloride, fluoride, iron, magnesium, manganese, nitrite plus nitrate as nitrogen, selenium, and sulfate locally occur in water in concentrations exceeding State standards for drinking water.

PUGET SOUND PROJECT—HAZARD EVALUATION ON MOUNT BAKER

On July 13, 1977, a major snow and ice avalanche occurred in Sherman Crater on Mount Baker, partly filling the East Breach, where acidic water drains from the crater. Data from a previous study of the effects of recent volcanic activity on water quality of Baker Lake (Bortleson and others, 1977) were used by Puget Sound project personnel to assess the hazard potential of a possible damming of the crater water by the avalanche and later suddenly releasing the accumulated acid water. The evaluation was released to the public by the Mount Baker Information Committee, a group formed by Federal, State, local, and power company officials concerned over possible effects of the increased activity of Mount Baker. Fortunately, the drainage was only partially blocked, and the potential hazard did not materialize.

ANALYSES OF SUBSURFACE DATA TO ASSIST PLANNERS IN EVALUATING FEASIBILITY OF TUNNELING FOR RAPID-TRANSIT SYSTEMS

Tunneling-feasibility studies for rapid-transit systems, funded by the Department of Transportation, were completed in 1977 for the central business districts of Minneapolis-St. Paul in Minnesota and Los Angeles in California. These projects were designed to assess the need for, and the availability of, hydrologic and geologic data relevant to the construction, maintenance, and operation of underground transit systems.

Analyses of nearly 900 wells and shallow borings, as well as existing maps and reports for the downtown Los Angeles area showed that the ground is generally firm and dry to depths of 30 m, allowing relatively easy tunneling for subways. Some areas, however, may contain troublesome pockets of oil and gas, and ground water and active faults are present locally. Near and beneath the Los Angeles

River, the material is soft and contains boulders that can cause difficulties for tunneling. The soft ground below the water table may shift or flow during the excavation, so that detailed knowledge of the location of, and depth to, ground water is required in advance of excavation. Data on wells, shallow borings, and recently excavated tunnels, and estimated rates of tunneling for boring machines are given in the summary report of the study.

The Minneapolis-St. Paul tunneling feasibility study, conducted jointly by USGS and Minnesota Geological Survey personnel, found that there are a number of ideal routes for cross-town traffic tunneling that could be selected for consideration by planners. Tunneling by shield mole and continuous-lining system is probably a feasible operation in areas underlain by thick Quaternary deposits. Ground water is likely to occur locally. Therefore, dewatering may be required in places, but generally should be feasible. Existing sewer and highway drains might present problems when tunneling in the St. Peter Sandstone.

LAND USE AND LAND COVER MAPS AND DATA AND OTHER GEOGRAPHIC STUDIES

Land use and land cover mapping and data compilation and related research being carried out by the Geography Program of the Land Information and Analysis Office can be divided into the following major activities:

- Release of land use and land cover maps and related overlays at scales of 1:250,000 or 1:100,000, depending on the availability of the new 1:100,000 maps at time of publication.
- Experimentation with and demonstration of land use and land cover mapping at scales larger than 1:100,000 for specific applications.
- Experimentation with Landsat data for consistent mapping results and measurement of spatial and temporal changes in land use and land cover.
- Research on and development of a Geographic Information Retrieval and Analysis System (GIRAS) for handling land use and land cover data in conjunction with environmental, socioeconomic, demographic, and other data.
- Analytical and interpretative studies on land use patterns, problems, and trends.

Land use and land cover mapping

The land use and land cover mapping and data compilation being conducted by the Geography Program began in 1974 to provide a systematic and comprehensive mapping and analysis of land use and land cover on a nationwide basis. The Geography Program provides program development, specifications, quality control, accuracy checks, and consultation, while the basic compilation of land use and land cover maps is done in the Topographic Division's Mapping Centers.

Land use and land cover maps are being compiled at a scale of approximately 1:125,000. Overlays showing Federal land ownership, hydrologic units, counties, and census county subdivisions are also being compiled for each land use and land cover map produced. State land ownership is shown when such information is made available by the appropriate State agency. The land use and land cover maps and accompanying overlays are keyed to the standard topographic map series at 1:250,000 scale and, for specific areas, to the new base maps being prepared at 1:100,000 scale by the Topographic Division. By September 1977, land use and land cover data had been compiled for 134 quadrangles, and 99 quadrangles were in production.

These compiled maps include 70 percent of the Atlantic coastal area, 80 percent of the coastal area of the Gulf of Mexico, 40 percent of the coasts of California, Oregon, and Washington, and other areas such as the Western coal areas (covered by the Ekalaka, Gillette, Newcastle, Miles City 1:250,000-scale sheets) in Montana and Wyoming.

Land use and land cover data are categorized according to the classification system presented in Professional Paper 964 (Anderson and others, 1976). Specifications for compilation of these maps entitled "Specifications for Land Use and Land Cover and Associated Maps" (Loelkes, 1977) were issued as USGS open-file report 77-555. The minimum mapping unit for Urban or Built-up Uses, Water Areas, Confined Feeding Operations, Other Agricultural Land, and Strip Mines, Quarries, and Gravel Pits is 4 ha. All other categories are delineated with a minimum unit of 16 ha. Federal land holdings are shown for tracts of 16 ha or larger.

Land use and land cover maps and accompanying overlays are being digitized in a polygon format. Polygons can be converted to grid cells of varying sizes when desired for statistical data development.

Land use maps and associated overlays, initially available as black-and-white products at 1:250,000

scale, are placed in open file at the USGS Mapping Centers. Enlargements to scales such as 1:125,000 can be requested from the Mapping Centers. When an enlargement is made, however, the positional accuracy of the base map on which the land use and land cover data have been plotted still remains that of the 1:250,000-scale map. The maps can be used for many purposes in the scale range 1:100,000 to 1:250,000.

After the land use and land cover data and other map overlays are digitized, computerized graphic displays and statistical data on current land use and land cover become available for use in conjunction with other data. Statistical data are compiled for counties for areas of Federal ownership, by river basins and subbasins, and by statistical units such as census tracts or other census county subdivisions.

Cooperative land use mapping and data projects

Cooperative agreements between the USGS and State agencies have provided land use and land cover and associated maps for the following States: Alabama, Arkansas, Florida, Georgia, Kansas, Louisiana, Missouri, Pennsylvania, and West Virginia.

Land use and land cover maps for the States of North Carolina and Hawaii are presently being compiled under a cooperative agreement. Digital data on magnetic tape have been delivered for the States of Arkansas, Florida, Kansas, and Louisiana.

Geographic information systems software development

The Geography Program continued research and development work on a Geographic Information Retrieval and Analysis System (GIRAS) to extend and improve its capability for computer-aided storage, editing, manipulation, and retrieval of a geographic data base for the land use and land cover mapping and data compilation effort and other USGS land use and land cover research projects. The system includes (1) contract and in-house digitization of land use and land cover maps and other environmental data; (2) editing and correction of the geographic data base; and (3) manipulation and retrieval of those data in order to perform area measurements, map compositing analysis, and statistical and other computer-aided operations.

Twenty land use and land cover sets were digitized under commercial contract, and 49 additional overlays of related environmental data were digitized in-house. The Geography Program's graphic

input procedures were used to edit and correct the digital data for 32 sets of land use and land cover and associated environmental data. Statistics derived from compositing land use and land cover maps with their associated environmental overlays (census county subdivisions, political units, hydrologic units, and Federal land ownership) have been produced for eight quadrangles.

The publication of USGS Professional Paper 1059 (Mitchell and others, 1977) provides a general system description of the facilities and procedures of GIRAS I, the batch-oriented geographic information retrieval and analysis system now operational in the Program. In addition to a detailed description of the data structure being used in GIRAS I, Professional Paper 1059 describes the procedures for data capture and editing, data retrieval, data manipulation, and data output and establishes the design features for an interactive GIRAS II, which has been under development since 1975.

Technical assistance was provided to the States of Florida, Kansas, Pennsylvania, Alabama, Maine, and Missouri, and to the Atlanta Regional Commission and the U.S. Forest Service. Digital data were provided to the States of Florida, Kansas, Missouri, Alabama, and Maine, the Atlanta Regional Commission, U.S. Forest Service, Pennsylvania Power and Light Company, the Delaware River Basin Commission, and the Army Corps of Engineers. Training was conducted for Missouri and Kansas and the U.S. Forest Service.

Land use and land cover research and analysis

D. W. Davis and J. L. Place have completed research on land use changes resulting from the development of the oil and gas industry along the Louisiana coast over the past 40 years. Among the lessons learned from the study of Louisiana's coastal petroleum industry is that social and land use patterns are significantly modified by such developments. Since maritime transportation is the principal link to wells drilled in water-covered sites, the industry's support businesses are developed lining the available waterfronts. There is a pronounced shift of population from scattered rural homesites to the urbanized strips where higher paying jobs are available. In addition, there is an influx of skilled labor from other regions. The businesses needed to support oil and gas extraction include: (1) Boat and helicopter transportation to and from the oil or gas wells; (2) manufacture of support boats; (3) manufacture or supply of well platforms, equip-

ment, and pipe; (4) catering of food and other services; and (5) special repair, rescue, and training facilities. A major activity that employs workers and has impacts on the natural environment is the moving of oil or gas by pipeline inland to refineries or other processing plants. Where these pipelines, which form a dense network in Louisiana, cross the marshy or swampy coastal plain, it is easier to excavate or dredge canals in which to lay and maintain pipe than to bear the high cost of road building in the wetlands. This canal network inevitably affects the hydrologic, vegetative, and wildlife environment. During the extraction and moving of large quantities of oil, some leakage occasionally occurs, and this pollution persists with unknown long-term consequences. Heavy traffic by boat and ocean-going ships in the coastal and inland waters results in chemical pollution of the water and erosion of the channel banks and bottoms, the channels tending to broaden and replace more and more land. This is especially significant where oil or gas wells are drilled in wetland or very shallow water and are served by a network of canals. Without question, the economy of the Louisiana coast has been stimulated at least temporarily by these developments, and much of the Nation's need for oil and gas has been assuaged, but major changes in land surface configuration and in land use have resulted, with indirect effects on the water, flora, fauna, and social structure of the coastal areas.

Growing out of work done on the Central Atlantic Regional Ecological Test Site (CARETS), R. W. Pease, C. B. Jenner, J. E. Lewis, and F. W. Nicholas in the Geography Program reported on research dealing with the interface relationships between land use and atmospheric systems. In one study, Washington, D.C., served as a test site for the development of a method for predicting the urban temperature field over time spans ranging from 1 day to 1 month. This involved: (1) The modification of a clear-sky surface energy budget model to make the prediction of screen height temperature possible for a variety of synoptic conditions; (2) the extension of the model to treat a matrix of subareas within a metropolitan region; and (3) the use of land as a surrogate for surface characteristic parameters and anthropogenic heat release estimate. Results indicate relatively good model performance in predicting the pattern of minimum, and some degree of success in the prediction of maximum temperatures, although predicted temperature ranges for single days tended to be conservative under all conditions.

In related work, aerodynamic roughness, an important surface parameter in urban climate simulation modeling, was estimated from obstacle element descriptions acquired from 324 land use samples in Baltimore, Md. Urbanization changes the radiative, thermal, hydrologic, and aerodynamic properties of the Earth's surface. Knowledge of these surface characteristics, therefore, is essential to urban climate analysis. An evaluation of the physical association, as well as the statistical association, between land use and surface roughness was examined. Results indicate that a close association exists between particular land use regions and simulated energy balance changes. Further results demonstrated how the surface roughness parameter can be estimated from a knowledge of urban land use together with the aerodynamic implications to the surface climate.

These two studies contributed to a broader analysis of the impact of land use on climate and focused on two analytical techniques for investigating Earth-atmosphere energy interactions—remote sensing and numerical computer simulation. Integration of these two analytical approaches was applied to the Baltimore-Washington area. Results indicated that the understanding of the relationship between climate and land use can be significantly enhanced through the combination of simulation and remote-sensing techniques.

In cooperation with the Bureau of Outdoor Recreation, measurement was completed of various land cover uses of barrier island areas on the Atlantic and Gulf coasts. This project, under the direction of H. F. Lins, Jr., is aiding in the formulation of an effective plan by BOR for protecting, through State and local ordinances, all remaining unspoiled coastal barrier islands from uncontrolled use or development. An initial step in this research used existing USGS land use and land cover data to ascertain the number and area of developed islands, undeveloped but protected islands, and undeveloped and unprotected islands.

In conjunction with its mission to complete a land use and land cover inventory nationwide, and to analyze and update this data base, the Geography Program in the Land Information and Analysis Office is developing automated techniques using multispectral and multitemporal data from Landsat. Work proceeds on three fronts: (1) applications demonstration and staff training in general; (2) specific application to the USGS program for nationwide inventory, analysis, and update; and (3) advancements in applicable states-of-the-arts.

During 1976-77, demonstrations were underway at test sites in several States, testing different applications or techniques, and in concert with different user groups or collaborating State or Federal agencies. For the Washington urban area in Washington-D.C., Maryland, and Virginia, for example, the experimental land cover map compiled earlier by computer processing of 1973 Landsat data was prepared for publication by making color separation plates for printing directly from the land cover classification in magnetic tape form. Area measurements of land cover, also made by computer, accompany the printed map (Gaydos and Wray, 1977). For those who want to process the same data into other cartographic or statistical forms, the Washington land cover data are also available in computer tape form (Gaydos, Wray, and Guptill, 1977).

In Louisiana, an Applications System Verification Test (ASVT) conducted jointly with NASA's Earth Resource Laboratories, at Slidell, is examining ways to update the existing polygon-format land use and land cover map of Louisiana prepared by photo-interpretation with digital-format land cover map prepared by computer processing of multispectral data from Landsat. The multitemporal coverage from Landsat is also being examined for ways to establish priorities for updating land use and land cover maps no matter how the update inventory itself is compiled. A research project began in 1977 to determine the need for updating existing land use, land cover, and associated maps and to select the most appropriate time frame for this work. Valerie A. Milazzo is evaluating alternative remotely sensed data sources for change detection and map update and is investigating the use of complementary conventional remote-sensing sources and those of new or advanced technology to assess levels of accuracy and cost-effectiveness. Alternative approaches and techniques of change detection and map update are being considered to establish the best procedures for implementing an operational nationwide map update program.

In cooperation with NASA and the Pacific Northwest Regional Commission, demonstrations in Washington, Idaho, and Oregon tested uses of Landsat digital analysis techniques in specific urban and agricultural applications identified by State and local agencies. In Idaho, USGS analysts helped to inventory land cover in Ada County, Metropolitan Boise. They also helped to map irrigated and non-irrigated agricultural lands along the Snake River, including areas flooded by the failure of the Teton Dam. In the Puget Sound region, USGS technical

support helped to produce regional land cover maps from 1974 and 1975 Landsat digital data. Separate maps were also produced for individual counties. A land cover map of the Portland, Oreg., urban area demonstrated a "signature extension" technique, whereby statistical land cover classes developed for the Seattle urban area were applied to data for the Portland urban area acquired by satellite only 20 seconds in time down orbit, thereby saving the cost of developing and verifying the classes. For the National Petroleum Reserve on Alaska's North Slope, an environmental assessment was begun preparatory to oil production and impact assessment. One part of the environmental assessment is a vegetation or land cover map of 38,000 mi² prepared by machine classification of 1976 Landsat digital data plus field data acquired during the summer of 1977. The results in cartographic and statistical form will be adapted to provide interim coverage in the nationwide land use and land cover program. Similar activities in North Dakota and Nevada seek ways to combine source materials and interpretation techniques.

Meanwhile, a series of three metropolitan region land use and land cover maps for Atlanta, Ga., Kansas City, Mo., and Pittsburgh, Pa.—all derived by photointerpretation—are demonstrating various cost-saving ways to produce lithoprinted map products in color. So far, most land use and land cover maps produced are available only as open-file reproducible lacking shading or coloring to aid visual interpretation of spatial patterns.

Finally, a project to test the accuracy of land use and land cover maps and land use boundaries showed that all sheets tested to date have been found to meet or exceed an expected accuracy of 85 percent. Sampling, using a systematic stratified unaligned sample and binomial probability theory, has been found to provide the most reliable data for assessing the accuracy of land use and land cover maps in our nationwide program.

ENVIRONMENTAL IMPACT STUDIES

The Environmental Impact Analysis (EIA) Program provides an integrated USGS response to the National Environmental Policy Act (NEPA) requirements for the preparation and review of environmental impact statements (EIS's). It supplies direction, coordination, and expertise in the preparation of EIS's for which the USGS has lead or joint-lead responsibility; furnishes technical information and expertise to support the preparation of EIS's to which the USGS is a contributor; provides tech-

nical analysis, review, and comment on EIS's prepared by the USGS and other agencies; and stimulates, promotes, and conducts environmental research related to EIS's and the anticipated needs of the program.

At the beginning of FY 1978, EIA was administering the USGS lead or joint-lead responsibility with States in 12 EIS's; 11 of these were energy related (8 coal, 2 oil and gas, and 1 oil shale) and 1 concerned mining law reform. Five others were initiated during the fiscal year. Those scheduled for completion during the year involve the Coal Creek coal mine, the Caballo coal mine, the Pronghorn coal mine, the East Gillette coal mine, and the Rochelle coal mine, all in Wyoming.

The USGS participated in the preparation of 18 additional EIS's under the lead of other Federal agencies—namely, the Bureaus of Indian Affairs and Land Management, Bonneville Power Administration, Tennessee Valley Authority, and the U.S. Forest Service. Fourteen were energy-related, and one dealt with a land dispute. The USGS also provided technical information to the U.S. Forest Service for four EIS's on geothermal energy resources and to the Bureau of Land Management for six EIS's on oil and gas leasing on the Outer Continental Shelf.

EIA Program staff members reviewed and commented on 1,800 to 2,200 statements and related documents to support in-house environmental studies and to assist other agencies in areas of USGS jurisdiction and expertise. Improvements in the quality of environmental statements continue to be made. Topically, most of the deficiencies are related to ground-water resources with fewer inadequacies in regard to surface water and geology.

METHODOLOGY FOR POST-EIS MONITORING

L. G. Marcus has developed a methodology for monitoring the impacts predicted in EIS's using the EIS on phosphate development in southeastern Idaho as a case study. A monitoring system based on this methodology would: (1) coordinate comprehensive, interdisciplinary, intergovernmental monitoring efforts; (2) document the major impacts that result, thereby improving the accuracy of impact predictions in future EIS's; (3) help agencies control impacts by warning them when critical impact levels occur and by providing feedback on the success of mitigating measures; and (4) limit monitoring data to the essential information that agencies need to carry out their regulatory and environmental protection responsibilities.

MODIFIED FORMAT FOR SITE-SPECIFIC EIS

F. J. Anderson led the preparation of a site-specific EIS on the Mobil-Consolidation Pronghorn mine in Wyoming using a modified EIS format designed to make the EIS more readable and to eliminate repetitious coverage. The Department of the Interior's mandated format of eight chapters was set aside for this effort and replaced by a format consisting of four sections: (1) synthesis of the EIS, (2) description of the proposed Federal action (including the applicant's proposal), (3) analysis of anticipated impacts of the proposal, and (4) analysis of alternatives to the proposal. All the substantive information contained in the EIS is synthesized in narrative form in section 1, so that decisionmakers and the public can ascertain the significant features of the Federal proposal and the findings and conclusions of the EIS from this section. Section 2 is the applicant's proposal as mitigated by requirements of the law, which consists of statutes, executive orders, operating procedures, and directives from the local managers. Section 3 is the environmental analysis that was performed by the task force, and it contains the adverse and beneficial environmental effects of the Federal proposal as well as an analysis of the effects of possible failure of the mitigations and an estimate of the probability of failure. Section 4 contains both administrative and technical alternatives to the Federal action, including those mitigations proposed by the task force that are not currently required by law or committed to by the local managers. These alternative mitigations can be adopted by the Secretary of the Interior if he so chooses.

ENVIRONMENTAL ANALYSIS OF NPRA

An environmental analysis of alternative procedures for the development, production, transportation, and distribution of oil and gas from the National Petroleum Reserve in Alaska (NPRA) is being prepared by a multibureau task force under the leadership of W. J. Schneider. Under contract, a socioeconomic data base was prepared, and analyses of the socioeconomic impacts related to oil and gas development on the North Slope residents were made. A second contract provided discussion of feasible transportation routes and distribution points for oil and gas from NPRA and impacts of their use. A wetlands classification study, hydrologic and geologic data collection, seismic net analysis to

determine potential earthquake hazards, and the preparation of vegetation maps were completed. This information is being used to complete the environmental analysis of the various alternative procedures based on assumed locations and sizes of potential oil and gas fields in NPRA and on development scenarios prepared by the Office of Mineral Policy and Research Analysis.

RESOURCE AND LAND INVESTIGATION PROGRAMS

TECHNOLOGY TRANSFER WORKSHOPS FOR STATE AND LOCAL OFFICIALS

The nature of Outer Continental Shelf oil and gas exploration and development and the associated onshore impacts were the subjects of six workshops for State and local officials. Lectures, exercises, discussion, and "games" were used to provide participants with information and techniques to use in assessing and planning for onshore activities and facilities. Of the 427 attendees at the workshops, 126 were State representatives; 154, local; 99, regional and other; and 48, Federal. The workshops were held in the north, middle, and south Atlantic coast regions; the Gulf coast region; and the Pacific coast and the Alaska regions. A seventh workshop was held in Reston, Va., for Federal officials. Attendees were provide with "take-home" materials including the "Factbook" and "Estimates" developed through a joint project of the New England River Basins Commission (1976a, b) and the Resource and Land Investigations Program of the USGS, a Source Book (American Society of Planning Officials, 1977), an annotated bibliography (Pattison, 1977), and a two-volume manual tailored to the individual workshop sessions. The workshops were funded jointly by the Environmental Protection Agency and USGS and were carried out through a contract with the American Society of Planning Officials. Faculty came from the USGS, Environmental Protection Agency, American Society of Planning Officials, and New England River Basins Commission and included two consultants. Resource people were supplied by the Office of Coastal Zone Management, the Bureau of Land Management, the Geological Survey's Conservation Division, the Fish and Wildlife Service, and the American Petroleum Institute. State and local officials were involved in developing the workshop curriculum through a user information needs survey and through contact with indiv-

idual officials. A comprehensive evaluation by attendees after the final session was used to make adjustments in subsequent workshops and provided input in developing a curriculum for a second series planned for 1978.

INTEGRATED SURFACE MINE RECLAMATION AND LAND USE PLANNING

Joseph T. O'Connor, Edgar A. Imhoff, and others conducted and reported (1978) the results of a planning officials' workshop held in Fulton County, Ill., on October 6-7, 1977, to focus on science information and analytical methods needed in order to select rationally from the alternative future actions: (a) to mine and reclaim, (b) to refrain from mining, or (c) to keep options open through such devices as minerals preservation zoning. Observations of workshop exercises that involved all participants in simulated decisionmaking suggest that properly interpreted science information can change public plans.

In a presentation to the American Association for the Advancement of Science, Edgar A. Imhoff and J. Ronald Jones summarized the results of USGS research in 1977 to enhance the capabilities of local governments in mineral resources planning.

CONFLICT RESOLUTION

The American Arbitration Association began a project to investigate methods for resolving environmental-development conflicts short of litigation. This project is sponsored by the USGS and the Council on Environmental Quality. A series of individual cases within the Department of the Interior have been examined for potential investigation. Criteria were applied to help identify about five cases for detailed study. The criteria include: (1) The potential for use of some mediation approach, (2) the representation of a range of cases spanning the interests of the Department, and (3) the relevance of cases to the National Environmental Policy Act. In addition, work was begun on a handbook on the state-of-the-art of environmental mediation.

IMPACT OF WESTERN ENERGY DEVELOPMENT

As part of a project for the USGS and other Federal agencies, the Denver Research Institute developed a methodology for analyzing socioeconomic and secondary environmental impacts of energy development. The methodology uses employment forecasts from industry development plans and includes an economic base technique to evaluate the total employment of communities. Population and worker characteristics and the housing requirements are forecast. Housing-supply and public-sector revenues and expenditures are derived. Policies for impact mitigation are also included.

COASTAL ZONE MANAGEMENT COORDINATION

Completion of the first year of a new coordination effort for the USGS was marked by the publication of a paper (Schoen, 1978) emphasizing the importance of earth-science information to successful coastal management. The paper called for States to anticipate their need for an atlas that inventories the physical and biological framework of their coasts, for site specific detailed studies, and for a mechanism to provide long-term monitoring and surveillance of those coastal environments, such as estuaries, that are especially fragile. This paper was one of 16 presented by USGS authors at Coastal Zone 78, a major symposium in San Francisco attended by scientists, lawyers, planners, and politicians involved in coastal zone management.

To respond to the quickening pace of review and approval of State coastal zone management plans, a system was set up to assure a substantive review that includes the concerns of the USGS.

Workshops were held for Water Resources Division district chiefs of the USGS and other interested Survey personnel in the southeast and western regions to familiarize them with the responsibilities and opportunities for the USGS resulting from the Coastal Zone Management Act. To increase participation in all relevant aspects of State coastal zone management, a statement of USGS interests and concerns with the program, approved by the USGS Director, was sent to all State Coastal Zone Managers.

INTERNATIONAL COOPERATION IN THE EARTH SCIENCES

For more than 35 years, international cooperation in the earth sciences has been a significant activity of the USGS, mostly on behalf of the Department of State and under the authority of the Foreign Assistance Act. Technical cooperation and participant study to strengthen national earth-science institutions in developing countries were the principal components of the program during the earlier years, but emphasis has gradually changed to greater USGS involvement in cooperative scientific investigations and exchange, reflecting a growing technical sophistication around the world. At present, USGS international activities, covering a wide range of disciplines and technologies, can be separated into four categories, as follows: (1) International resources assessment; (2) cooperative scientific investigation and exchange; (3) international representation; and (4) technical cooperation and participant study. During the past year there has been new emphasis on the study of world energy and energy-related resources on behalf of other U.S. agencies and in cooperation with other governments. Substantial progress has been made on a number of major cooperative scientific and exchange programs in which the Survey is involved. Highlights of progress in all four categories of USGS international activity are summarized in the following paragraphs.

INTERNATIONAL RESOURCES ASSESSMENT

Energy resources studies on behalf of other agencies

At the request of the Department of State and other agencies, the USGS has been involved with resource assessments of selected areas of concern to the United States, such as areas along international boundaries that may be in dispute. Such studies may involve continental margins and shelves. Compilations of known and potential resources of selected countries provided the Departments of State and Energy with a basis for formulating a cooperative international program of non-nuclear energy

alternatives. Also, for the Department of State, the Survey investigates the known and potential resources of oceanic areas for reference in relation to the international negotiations on the Law of the Sea. Study of the known resources and resources potential of Antarctica, at the request of the National Science Foundation, provides a basis for formulating U.S. policy regarding exploration and development in that continent.

A program headed by the Department of Energy to assist developing countries in assessing their energy options was started in 1977. The Geological Survey was asked to take the lead in studying the resources of fossil fuel geothermal energy, nuclear raw materials, energy-related minerals, and hydro-power, with cooperation from the Bureau of Mines and Bureau of Reclamation. The first phase of the program will involve preliminary compilation and evaluation of available data on energy resources and energy-development options for selected countries. A second phase will involve more comprehensive studies and evaluations by U.S. specialists and their counterparts in the selected countries. The plans for the Phase II studies will be established early in 1978.

Cooperative studies such as these provide information that can help the developing nations, most of which are only partially explored, assess and develop their own natural resource potential. Such studies may also contribute to the overall world supply of raw materials.

Resources Attache and Reporting Program

A major responsibility of the Department of the Interior is to appraise the present and future supplies of mineral and energy raw materials in relation to the Nation's requirements. In 1975, a major part of these requirements was imported. In the field of energy, imports of petroleum represented 36 percent of consumption in 1975, 41 percent in 1976, and an estimated 43 percent in 1977. We are dependent on foreign sources for more than half our supply of 24 important minerals, including such as manganese,

chromium, asbestos, tin, and nickel. In addition we import more than 25 percent of 10 other minerals, including iron, gold, and silver. It is expected that the United States will be increasingly dependent on foreign sources in the years ahead.

The two bureaus primarily involved in developing information about energy and mineral raw materials are the Bureau of Mines for present supplies and known reserves, and the Geological Survey for undiscovered resources and future supplies. To help meet the need for data on reserves and resources in foreign countries, the Bureau and the Survey are cooperating with the Department of State in a Resources Attache and Reporting Program. The program is expanding and will ultimately include at least 20 regional Resources Attaches; 12 resources attache positions have been established, of which 11, in Australia, Belgium, Bolivia, Brazil, India, Indonesia, Japan, Mexico, South Africa, Thailand, and Venezuela, are staffed. Information is also received from officers reporting on a part-time basis in many countries. Comprehensive reports on mineral resources matters are received regularly from the attaches, supplementing numerous published and unpublished geological and resources reports transmitted to the Survey and the Bureau of Mines through established bilateral channels. In 1977 a total of 145 reports was received from the attaches.

A briefing for Resources Attaches assigned to Asian posts (Tokyo, Bangkok, Canberra) and officers from Jakarta and Manila was scheduled in Manila concurrent with the annual meeting of the Committee for Coordination of Joint Prospecting for Mineral Resources in Asian Offshore Areas (CCOP). J. A. Reinemund reviewed the scope and status of CCOP and the objectives of the joint CCOP-IOC-IDOE in Southeast Asia. M. J. Terman, F. H. Wang, and W. A. Fischer also took part in the briefing.

COOPERATIVE SCIENTIFIC INVESTIGATION AND EXCHANGE

CRUSTAL STUDIES

The Worldwide Standardized Seismograph Network (WWSSN) was established in the 1960's to provide data needed for fundamental research in seismology and global tectonics. This network consists of about 113 continuously recording stations distributed over much of the land area of the world.

The USGS is responsible for siting, installing, and maintaining the global seismograph station network. Since the WWSSN was installed, there also have been important advances in instrument technology—long-period signal detection thresholds have been lowered through refinement of seismic sensors, and recording techniques have been much improved through the application of digital electronics. These new technologies have been used and applied to a program to upgrade selected stations for the WWSSN.

The USGS, in cooperation with the Defense Department's Advanced Research Projects Agency, and participating research centers, is currently installing new seismic digital data systems at a number of strategic locations overseas. The various systems are known as the Seismic Research Observatories (SRO), High-Gain Long Period (HGLP), Modified HGLP (ASRO), and Worldwide Standard Seismograph Network-Digital Recording (WWSSN-DR). The digital data acquisition systems differ slightly in sensor, sensor emplacement, channels recorded, and dynamic range.

So far SRO systems have been installed at Albuquerque, New Mexico; Bogota, Colombia; Chiang Mai, Thailand; Guam; Mashad, Iran; Narrogin, Australia; Taipei, Taiwan; and Wellington, New Zealand. Stations will be installed in 1978 at Ankara, Turkey; Shillong, India; Quetta, Pakistan; Bangui, Central African Empire; and Graefenberg, Germany. Station personnel from Quetta were trained on the operation and maintenance of the SRO system at the Albuquerque Seismological Laboratory (ASL). Station personnel from Ankara were provided six months scientific training at Menlo Park, Calif., and Golden, Colo.

ASRO stations were installed at Kabul, Afghanistan, and Matsushiro, Japan. Station personnel from these two stations were provided with extensive training on the operation and maintenance of the ASRO seismic system at ASL. Additional ASRO stations have been installed at Charters Towers, Australia, and La Paz, Bolivia.

The USGS Program to monitor global seismicity requires a well integrated system of international cooperation. This program involves the interpretation of seismograms, data transmission, and processing of seismic data to determine the origin time, location, and magnitude of earthquakes whenever and wherever they are experienced. To do this, arrival time and amplitude data recorded at observa-

tories throughout the world are sent to the USGS National Earthquake Information Service (NEIS) at Golden, Colo. as expeditiously as possible, where the data are processed by computer and the results are released to agencies and the user public. Nearly all countries that operate seismic facilities, including the U.S.S.R. and People's Republic of China, now contribute to this voluntary program that annually determines source parameters of about 6,000 seismic events. Approximately 1,000 of these events could be sensed or cause damage if they take place near population centers.

For disaster response and expeditious field study efforts, NEIS operates a 24-hour standby system that computes earthquake locations and magnitude as soon as possible after major shocks and provides these data to agencies concerned with public safety and disaster relief, the news media, and others who have previously specified their reporting criteria or who request up-to-date data shortly after a particular event. Summary data may be obtained, on an after hours basis, by dialing (303) 234-3994. Depending upon the location of the shock and, of course, data availability, the early results are usually released in bulletin form in one to several hours.

Resultant data from large shocks located outside of the United States are provided to the Department of State-AID Disaster Relief Center and to the World Meteorological Organization (WMO) that rapidly disseminates the information to appropriate offices throughout the world. WMO also provides communications facilities whereby a number of observatories report data routinely to NEIS in this manner. Forty bulletins were released in 1977. Frequently, in the case of destructive earthquakes, communications into and out of the epicentral region are impaired. In this event NEIS may call on the special relationships engendered with recently established regional centers in Strasbourg, France; Manila, the Philippine Islands, and Lima, Peru. These centers routinely facilitate two-way data exchanges, and in 1977 they effectively aided NEIS in receiving station data and releasing results for:

- Romanian shock of March 4, 1977: killed 1,500 and injured 10,500, extensive damage. The Centre Seismologique Europeo-Mediterraneen, established by the Intergovernmental European Seismological Commission with members in Europe, Western and Central Asia, and North Africa, rapidly forwarded data via telex to NEIS and disseminated NEIS bulletins to Romania and others concerned with disaster re-

sponse and field studies of the earthquakes. A very accurate hypocenter was available much faster than before, owing to the cooperative effort and previously established means of communication.

- Philippines shock of March 18, 1977: 1 killed and 9 injured, damage in northern Luzon. Extensive data exchange with John Hodgson, Director of the Regional Seismological Centre for Southeast Asia, located at Manila, sponsored by UNESCO-U.N. Development Programme.
- San Juan Province, Argentina shock of November 23, 1977: killed 70 and injured 200; extensive damage. Communications were nil and NEIS received station data and transmitted bulletins to the area via the Centro Regional de Sismologia para America del Sur, an intergovernmental organization.

In addition to the regional centers, the bulletins are forwarded as soon as possible to the UNESCO-PARIS Office of Disaster Response and national centers that may have an interest in data for a particular earthquake.

Twenty-three shallow earthquakes of magnitude 6.5 or better were located in or near the Pacific Basin; therefore, they initially had to be considered possibly tsunamigenic. For these shocks and others coming within reasonable limits of the response criteria, the USGS seismic observatories at Guam and Newport, Wash., function as a part of an international network of seismographs and tide stations with the purpose of furnishing tsunami warnings to all concerned in the Pacific Basin. J. N. Taggart represented the Office of Earthquake Studies at an IUGG/IOC Symposium on Tsunami Research in Ensenada, Mexico, March 23-26, 1977. In addition to participation in discussions of tsunamigenic earthquakes, Taggart contacted Soviet seismologists concerning exchanges of data, instrumentation, and scientific personnel as agreed on the Second U.S.-U.S.S.R. Meeting of Tsunami Experts held in Novosibirsk, U.S.S.R. September 1976. As a part of the bilateral understanding in 1977 A. V. Rykov, of the U.S.S.R. Akademya Nauk, installed one of his three-component ultra-long period seismograph systems at Kipapa, Oahu. The recording system for this seismograph that offers new opportunities for tsunami source generation studies was provided by the USGS. Similarly, Taggart arranged, with the help of Jon Berger (UCSD) and Mark Spaeth (NOAA/NWS), for the installation of one of the International Deployment of Accelerometers (IDA) systems

at Yuzhno-Sakhalinsk. Data will be exchanged between the sponsoring groups.

The Survey performed a 24-month study of local seismicity and associated geology in the region of Cochabamba, Bolivia, to determine seismic risk and to evaluate particular seismic microzonation problems for the Cochabamba Valley and the city of Cochabamba.

As a follow up to cooperation with Costa Rican seismologists in 1976, J. W. Dewey returned to Costa Rica to interpret seismic data from the University of Costa Rica's seismograph network. The data indicate that Costa Rica's Pacific Coast seismic zone may be significantly shallower than previously indicated. Dewey, on detail to the Organization of American States, assisted in developing a seismological program. (See Summary by Countries, p. 338.)

A seismograph network was installed for seismic investigations in Nicaragua. Results obtained help to understand location and frequency of future earthquakes and will help scientists to understand relationships between volcanos and earthquake zones, which are of worldwide interest to geologists. In Peru, the USGS is participating in cooperative projects in earthquake hazard reduction and engineering geology investigations. Techniques and expertise developed by the USGS are applied to help the pertinent Peruvian agencies strengthen, enlarge, and intensify their investigations relating to seismicity evaluation, geotechnical studies, and microzonation studies.

Under an agreement with the Government of Saudi Arabia, the Survey designed instrumentation to record a 750-km profile over the crystalline rocks in the western part of Saudi Arabia; data are being interpreted for compilation of a detailed map of the crustal and upper mantle structure beneath the profile. In Southeast Asia, as part of a UNESCO-funded project with Malaysia, the Philippine Islands, Thailand, and Hong Kong, the USGS conducted a project to strengthen and expand the seismological observatory networks in the participating countries of Southeast Asia and to create the necessary facilities for regional cooperation, in order to provide the governments of these countries with the basic knowledge of earthquake risks and thus to permit the definition of appropriate measures of protection against earthquakes.

A. H. Chidester participated in a field trip in Romania in late 1977 under the sponsorship of the Association for the Study of the Deep Zones of the Earth's Crust (AZOPRO) and the Institutul de Geologie Sr Geofizica. Members of the Institute are

coordinating studies in stratigraphy, structure, metamorphism, experimental petrology, mineralogy, and radiogenic age dating, and focusing on the complex polymetamorphic and polydeformation history of the Precambrian crystalline rocks of the Carpathian Mountains.

MULTILATERAL SCIENTIFIC PROGRAMS

The United States participates in the development and management of the International Geological Correlation Program (IGCP) by supplying one member of the IGCP Board, and several scientists working on the IGCP Scientific Committees. The Program is sponsored jointly by the International Union of Geological Sciences (IUGS) and UNESCO. Nine of the 62 IGCP projects are led by U.S. scientists, four of whom are on the Geological Survey staff. U.S. participation in IGCP is coordinated by the U.S. National Committee for the IGCP, several members of which are presently on the USGS staff. Daniel Merriam (Syracuse University) is chairman of the Committee and Linn Hoover (USGS) is secretary. J. A. Reinemund who is a member of the IGCP Board, participated in the Fifth Session of the Board, held at UNESCO headquarters in Paris in March 1977.

One objective of IGCP is to improve standards and methods used in classification, terminology, and procedures in geological research and correlation. Project 98, led by A. L. Clark, studies application of computerized data banks as a tool for analysis, resources inventory assessment, exploration and evaluation of orebodies, and integration of various kinds of information. This project held a symposium and workshop on computer modeling and data systems applications in Kenya in November 1977, in which 44 participants from 24 countries were involved.

Project 30, led by P. C. Bateman, was set up to study the relation of Mesozoic batholiths around the Pacific Basin to plate tectonics, volcanism, ore deposits, and other features. The seventh discussion meeting was held in Japan and Korea in August-September, 1977. Project 115, under the leadership of J. R. Hein, is studying siliceous deposits of the Pacific basin and neighboring geosynclines to determine basic facts about amounts and rates of deposition of silica through geologic time. The information will increase our understanding of the development of orogenic belts and provide a basis for evaluation of the economics of siliceous deposits.

Project 143, Remote sensing and mineral exploration, is headed by W. D. Carter and L. C. Rowan. It

involves testing applications of remote sensing under various climatic conditions to help in mineral exploration, and dissemination of information. The U.S. National Working Group for this project held discussion meetings and issued three newsletters to more than 70 participating scientists.

The Geological Survey is active in the Commission for the Geological Map of the World, a commission affiliated with the IUGS. The Commission is composed of representatives from more than 100 adhering geological surveys and through its subcommissions, sponsors or encourages the publication of many kinds of small-scale geological maps—tectonic, metallogenic, metamorphic belt, environmental, and hydrogeological. Other subcommissions sponsor and coordinate compilations of small-scale geological maps of continents and regions of the Earth's crust, such as Africa, the Middle East, South America, and South and East Asia. Most recently, in support of the International Geodynamics Project of the IUGS and the International Union of Geodesy and Geophysics (IUGG), new maps are being prepared that extend the geology of continental masses on to the continental shelves and slopes. In addition, the inferred geology of entire ocean basins is being compiled by using data from the National Science Foundation-sponsored Deep Sea Drilling Program. The Geological Survey is represented on the Commission by D. M. Kinney, Vice President for North America, and by P. W. Guild, President of the Subcommittee for the Metallogenic Map of the World; both Kinney and Guild are members of the Executive Committee that determines policy.

Geological Survey assistance to regional activities in East Asia was continued on behalf of the Department of State. F. H. Wang serving as Principal Marine Geologist for the Committee for Coordination of Joint Prospecting for Mineral Resources in Asian offshore areas (CCOP), has advised and assisted CCOP member countries in undertaking regional offshore investigations; establishing national petroleum data systems, and a regional center for marine research; assessing energy and mineral resources; making environmental protection studies; and in strengthening government capabilities for offshore exploration and development.

CIRCUMPACIFIC MAP PROJECT

The USGS continued its support of the international CircumPacific Map Project, sponsored by the CircumPacific Council for Energy and Mineral Re-

sources, by coordinating the efforts of five panels of about 100 earth scientists and by direct participation in map compilations. During the year, geographic and base maps of the Northwest and Northeast quadrants of the Pacific region were published by the American Association of Petroleum Geologists. Similar maps covering the Southeast and Southwest quadrants and Antarctica were prepared for printing.

Geologic maps have been compiled for most of the land areas, and work continues on the tectonic and energy and mineral resources maps. These thematic maps are to be printed on the already compiled base maps, which are on a scale of 1:10 million and equal-area projections.

Members of the five panels represent a wide spectrum of private industry, research institutions, and government agencies. USGS participation is aimed at providing a better understanding of the resource potential of the Pacific region, and, thereby, of those areas of direct U.S. interest, through a summation and analysis of what is known of its geology, tectonics, and resource occurrences.

A geologic map of China for the Northwest quadrant was compiled from tectonic and geologic maps recently published in China. Volcanos of the Northeast quadrant were compiled showing form of cone, rock type of effusive product, and status of activity. An isopach map of sedimentary basins in the Northeast quadrant was largely compiled. A plot of focal mechanisms for each quadrant was provided, and logs of Deep Sea Drilling Project (DSDP) drill holes were compiled from computer-plotted data provided by DSDP.

INTERNATIONAL REPRESENTATION

The 14th Session of CCOP was held in Manila, Philippine Islands, in September 1977. In addition to the delegates from the member countries of Indonesia, Japan, Korea, Malaysia, Papua-New Guinea, Philippines, Singapore, and Thailand, advisors and observers from Australia, France, Germany, Netherlands, Norway, U.S.S.R., United Kingdom, and the United States attended. J. A. Reinemund, W. A. Fischer, and M. J. Terman attended as special advisors from the United States. The United States reported on Project Magnet, which records close-spaced low-level magnetic intensity, and on successful application of Landsat interpretation of shallow-sea charting and oil-slick mapping. As part of the session, F. H. Wang, assisted the UNDP in

organizing a seminar on Generation and Maturation of Hydrocarbons in Sedimentary Basins. Reinemund served as alternate head of the U.S. Economic and Social Council at Geneva, Switzerland. The subject of the meeting was a review of the natural resources program of U.N. agencies and recommendations for future work.

J. O. Morgan presented two papers at the U.N. Economic and Social Commission for Asia and the Pacific (ESCAP) Intergovernmental Meeting on Remote Sensing and Satellite Surveying in Bangkok in June 1977.

U.S. coordinator J. I. Ziony, with R. A. Page and Carl Kisslinger, attended the Central Treaty Organization (CENTO) Seminar on Recent Advances in Earthquake Hazard Minimization in Iran. Their participation was funded by AID. R. L. Wesson attended a meeting of the UNESCO Preparatory Committee of Experts on Earthquake Prediction in Paris, France. The preparation committee of experts met to review the state of earthquake prediction and to discuss the possibility of a UNESCO-sponsored conference on this subject. The Committee recommended that UNESCO hold a conference on Earthquake Prediction and its Implications for Society in early 1979.

J. N. Jordan attended, as official U.S. Delegate, the XI General Assembly and Consultation III of the Pan American Institute of Geography and History (PAIGH), which is a specialized agency of the Organization of American States (OAS), held in Quito, Ecuador, August 15-31, 1977. Jordan is the U.S. Member of the Commission on Geophysics and regional editor of the PAIGH-*Revista Geofisica*, a journal for the publication, in English, Spanish, French, or Portuguese, of technical and scientific investigation in the Americas. The Quadrennial Report, USGS Circular 763 "Program Report on Selected Geophysical Activities of the United States, 1973-1976," co-editors J. N. Jordan and K. L. Svendsen (NOAA/EDS), was presented to the Assembly.

S. M. Lang attended a meeting of the International Standards Organization on representation of data elements. J. S. Cragwall, Jr., attended the Seventh Meeting of the World Meteorological Organization's Region IV Conference of North and Central American and Caribbean countries in Mexico City. W. J. Campbell participated as a coinvestigator in the third set of flights of the National

Aeronautics and Space Administration's "Polar Ice Remote Sensing Project 064" in the vicinity of Greenland. R. L. Miller presented a paper "Landsat and Seasat" at the Fifth Reunion of Central American Geologists in Managua, Nicaragua, February 1977. L. A. Heindl, chairman, met with the Soviet Hydrology Translations Committee to select U.S.S.R. hydrologic literature for publication in "Soviet Hydrology."

E. C. T. Chao visited the People's Republic of China (PRC) between December 27, 1976, and February 15, 1977. He brought with him briefing data on remote sensing, particularly on the applications of Landsat imageries to geologic problems, environmental geology, impact metamorphism, and the study of the Ries meteorite crater in Germany, recent progress on static and dynamic high-pressure and high-temperature experiments, and on micro-mineralogical techniques. The Institutes where scientific exchanges took place were the Institute of Geology, Academia Sinica, and the Chinese Academy of the Geological Sciences in Peking, and the Institute of Geochemistry, Academia Sinica in Kweiyang. The Chinese briefed him on their recent studies of (1) the February 4, 1975, predicted Haicheng earthquake and the Tangshan earthquake of July 28, 1976; (2) the Kilin meteorite shower, recent study of Mount Julmo-Lungma (Mount Everest), and (3) in geochemistry; and (4) provided tours to some of their laboratories. One copy each of a 1:4,000,000-scale geologic map of PRC, a 1:4,000,000-scale tectonic map of PRC, and two copies of a 1:5,000,000-scale geologic map of Asia were among gifts given to Chao during his visit. These maps are now in the USGS library. Chao also carried an invitation from the Chairman of the Circum-Pacific Council on Energy and Mineral Resources for Chinese participation in the Circum-Pacific Map Project, and received their comments on the manuscript geographic map of the Northeast quadrant. Chao's trip was successful in developing better communication with geoscientists of PRC, and may result in future visits between individual scientists.

D. F. Davidson served as U.S. Delegate at the XVI Meeting of the CENTO Advisory Group on Mineral Development in Tehran, Iran. The Committee reviewed activities carried out under the CENTO minerals program and planned a work program for 1978.

TECHNICAL COOPERATION AND PARTICIPANT STUDY

In contrast to the more traditional programs of transfer of technology through cooperative mineral exploration and geological mapping, the USGS has, in recent years, expanded the types of assistance provided to developing nations. Many of the projects are advisory in nature and are accomplished through short-term assignments and (or) consultative visits of USGS experts. They involve management and regulation procedures, establishing data systems and data banks for resource monitoring, as well as hydrologic and geologic projects. In addition to continuing projects, cooperative arrangements were initiated between the USGS and the following:

- Algeria, for training in optical-image interpretive methods related to resource studies and digital enhancement and manipulation, digital programming, and procurement of equipment.
- Jordan, for development of a work plan encompassing the National Resources Authority's proposed activities in mining geology over a 3-year period, for a review of the status of geo-

thermal resource data, and for implementation of activities and resolution of specific technical-operational problems.

- Nigeria, for water-resources studies, Landsat image processing and base map preparation, and geologic reconnaissance.
- Malaysia, for establishing rules and regulatory procedures for control of petroleum operations; measurement and verification of produced oil/gas volume; field development for maximum recovery and conservation and safety and environmental measures.
- Morocco, for guidance in planning and equipping analytical laboratories.

The work is done at the request of and in cooperation with, host governments and is approved by the U.S. Department of State in accordance with the U.S. Foreign Assistance Act. In the period covered by this report, USGS scientists undertook 179 assignments in 33 countries. The subjects and scope of these assignments in each country are listed in table 2, and results of many of these projects are described under the heading, "Summary by Countries," p. 338.

TABLE 2.—*Technical assistance to other countries provided by the USGS during FY 1977*

Country	USGS personnel assigned to other countries			Scientists from other countries trained in United States	
	Number	Type	Type of activity ¹	Number	Field of Training
Latin America					
Argentina -----	1	Administrator -----	A, D -----		
	2	Geologists -----	A, D -----		
	1	Hydrologist -----	A, D -----		
	1	Soils Scientist -----	A, D -----		
Bolivia -----	2	Geologist -----	D -----		
	2	Hydrologists -----	C, D -----		
Brazil -----	1	Geologists -----	D -----	1	Remote sensing
	4	Hydrologists -----	D -----	1	Theoretical and applied geophysics
Chile -----	4	Geologists -----	D -----	2	Remote sensing
	1	Hydrologist -----	C, D -----		
Colombia				1	Geology
Costa Rica -----	1	Geophysicist -----	C, D -----	1	Remote sensing
Ecuador				1	Remote sensing
Guyana				1	Remote sensing
Mexico -----	4	Chemists -----	A -----	2	Remote sensing
	1	Hydraulic Engineer -----	D -----		
	3	Hydrologists -----	A -----		
	2	Spectrographers -----	A -----		
	1	Topographic Engineer -----	A -----		
Nicaragua				1	Earthquake studies
Peru -----	5	Geologists -----	A, B -----		
	1	Physicist -----	D -----		
Venezuela -----	2	Geologists -----	D -----	1	Uranium geology
	1	Hydrologist -----	D -----	1	Geochemical exploration
				2	Remote sensing
				1	Hydrology

See footnote at end of table.

TABLE 2.—Technical assistance to other countries provided by the USGS during FY 1977—Continued

Country	USGS personnel assigned to other countries			Scientists from other countries trained in United States	
	Number	Type	Type of activity ¹	Number	Field of Training
Africa					
Algeria -----	1	Geologist -----	A -----		
	1	Remote Sensing Specialist -----	A -----		
Egypt -----	1	Cartographer -----	A -----	6	Remote sensing
	2	Geologists -----	A -----	3	Cartography
	1	Hydrologist -----	D -----	1	Minerals exploration
	1	Soils Scientist -----	D -----	1	Geological map preparation
				1	Hydrology
Ethiopia -----				1	Remote sensing
Gambia, The -----				1	Hydrology
Ghana -----				2	Hydrology
				2	Remote sensing
				1	Sediment samples
Kenya -----	2	Hydrologists -----	A, D -----		
Lesotho -----				1	Application remote sensing to land use; soil surveys
Mali -----				1	Topographic photo interpretation
Morocco -----	2	Geologists -----	D -----	1	Remote sensing
Nigeria -----	2	Administrative Officers -----	A, B -----	2	Cartography
	1	Administrator -----	A, B -----		
	2	Geologists -----	A, B -----		
	1	Engineering Geologist -----	A, B -----		
	1	Surficial Geologist -----	A, B -----		
	2	Hydrologist -----	A, B -----		
	1	Procurement Specialist -----	A, B -----		
Senegal -----	3	Hydrologists -----	C, D -----		
Sierre Leone -----				1	Remote sensing
South Africa -----				1	Remote sensing
Sudan -----	1	Cartographer -----	D -----	1	Mineral exploration
	1	Chemist -----	D -----		
	2	Geologists -----	D -----		
	1	Hydrologist -----	D -----		
Yemen -----				1	Hydrology
Near East and South Asia					
Afghanistan -----				1	Seismic systems operations maintenance
CENTO/Iran -----	1	Geologist -----	C, D -----		
	1	Earthquake Hazard Reduction Specialist -----	C, D -----		
	1	Seismic Risk Specialist -----	C, D -----		
	2	Earthquake Prediction Specialist -----	C, D -----		
CENTO/Turkey ---	1	Cartographer -----	C, D -----		
	2	Geologists -----	C, D -----		
	1	Data Processing Specialist -----	C, D -----		
	1	Remote Sensing Coordinator -----	C, D -----		
	1	Remote Sensing Specialist -----	C, D -----		
India -----	1	Hydrologist -----	D -----	8	Hydrology
				6	Remote sensing
				1	Geophysical methods for ground water
				1	Industrial minerals
				1	Geochemistry of geothermal fluids
				1	Application remote sensing to cartography
				2	Application remote sensing to hydrology
Iran -----				12	Remote sensing
Iraq -----				1	Remote sensing
Israel -----				1	Remote sensing
				1	Seismology
				1	Geothermal energy; noble gas studies
Jordan -----	1	Chemist -----	D -----		
	1	Geologist -----	A, B -----		
	1	Hydrologist -----	D -----		
Kuwait -----				1	Remote sensing
Nepal -----				1	Hydrology
				1	Topography surveys

See footnote at end of table.

TABLE 2.—*Technical assistance to other countries provided by the USGS during FY 1977—Continued*

Country	USGS personnel assigned to other countries			Scientists from other countries trained in United States	
	Number	Type	Type of activity ¹	Number	Field of Training
Near East and South Asia—Continued					
Pakistan -----				1	Uranium geology
				2	Seismic research
Qatar -----				1	Remote sensing
Saudi Arabia -----	3	Administrators -----	A, B -----	2	Business administration
	1	Administrative Officer -----	A, B -----	5	Cartography
	1	General Services Officer -----	A, B -----	1	Editing geologic publications
	1	Procurement Officer -----	A, B -----	1	Geophysics
	18	Geologists -----	A, B, D -----	1	Computer sciences
	11	Geophysicists -----	A, B, D -----	3	X-ray fluorescence
	2	Chemists -----	A, B -----	2	Hydrology
	2	Electronic Technicians -----	A, B -----	1	Geologic printing processes
	2	Topographic Engineers -----	A, B -----	1	Analytical laboratory techniques
	2	Topographic Engineers -----	A, B -----	6	Remote sensing
	1	Photogrammetrist -----	A, B -----		
	1	Remote Sensing Specialist -----	A, B -----		
	1	Photo Laboratory Chief -----	A, B -----		
	6	Computer Scientists -----	A, B, D -----		
	3	Geochronologists -----	A, B -----		
	5	Cartographers -----	A, B, D -----		
	3	Editors -----	A, B, D -----		
	2	Logistical Technicians -----	A, B, D -----		
	7	Hydrologists -----	A, B, D -----		
Syria -----				1	Hydrology
				1	Spectrophotometry
				1	Exploration geophysics
				2	Geophysics
Turkey -----	2	Hydrologists -----	D -----	1	Library sciences
				3	Remote sensing
				1	Seismology
				2	Groundwater hydrology
United Arab Emirates -----	1	Geologist -----	D -----		
Yemen -----	1	Geologist -----	A, C, D -----		
	2	Hydrologists -----	A, C, D -----		
Far East and Pacific					
Australia -----				1	Isotope geology
				2	Remote sensing
China, Republic of -----				2	Remote sensing
				1	Flood analysis; instrumentation hydrology
Indonesia -----	1	Hydrologist -----	C -----	1	Remote sensing
				1	Library sciences
Japan -----				1	Strong motion seismology
				3	Remote sensing
				1	Acidic volcanic rocks
Malaysia -----	1	Geologist -----	D -----	1	Seismology
	1	Petroleum Engineer -----	D -----		
	1	Petroleum Geologist -----	D -----		
New Zealand -----	1	Hydrologist -----	C -----		
Philippines -----	1	Hydrologist -----	D -----	1	Remote sensing
	1	Photomosaic Specialist -----	C -----	1	Seismic research
Southeast Asia -----	1	Geophysicist -----	D -----		
Sri Lanka -----	1	Hydrologist -----	C -----		
Thailand -----	1	Geologist -----	A -----	1	Oil and gas analysis
	1	Remote Sensing Specialist -----	A -----	1	Uranium geology
				2	Remote sensing
				1	Strong motion seismology
				1	Cenozoic palynology
Europe					
Belgium -----				1	Remote sensing
France -----				2	Remote sensing; hydrology
				1	Geology; geochemistry
Germany (West) -----				2	Remote sensing
				1	Seismology; earthquake research
Greece -----				1	Remote sensing

See footnote at end of table.

TABLE 2.—*Technical assistance to other countries provided by the USGS during FY 1977—Continued*

Country	USGS personnel assigned to other countries			Scientists from other countries trained in United States	
	Number	Type	Type of activity ¹	Number	Field of Training
Europe—Continued					
Italy -----	1	Geophysicist -----	D -----	1	Remote sensing
				1	Isotope geology
				1	Geochemistry; volcanology
				1	Surveillance active volcanoes
				1	Strong motion data analysis
Norway -----		-----	-----	1	Remote sensing
Poland -----		-----	-----	6	Remote sensing
				1	Geology; remote sensing
Romania -----	2	Geophysicists -----	C -----		
	1	Civil Engineer -----	C -----		
Spain -----		-----	-----	1	Remote sensing
				1	Application remote sensing to structure geology
Sweden -----		-----	-----	1	Geochemical exploration; heavy minerals
Switzerland -----		-----	-----	1	Remote sensing
United Kingdom (England) -----		-----	-----	1	Paleobotany
				1	Hydrology
				2	Remote sensing
				1	Strong motion seismology
				1	Stratigraphy
Other					
Canada -----		-----	-----	1	Digital mapping techniques
Cape Verde Islands -----	1	Hydrologist -----	C -----		
Iceland -----		-----	-----	1	Remote sensing
				1	Geodesy; photogrammetry; remote sensing
Jamaica -----		-----	-----	1	Hydrology
Trinidad and Tobago -----		-----	-----	1	Photo-lab technology
				2	Photolithography

¹ A. Broad program of assistance in developing or strengthening earth-science institutions and cadres; B. Broad program of geologic mapping and appraisal of resources; C. Special studies of geologic or hydrologic phenom-

ena or resources; D. Short-range advisory help on geologic or hydrologic problems and resources.

International activities of the USGS in 1977 were strongly influenced, as they had been in the previous 5 years, by worldwide interest in use of data obtained by the earth resources observation satellites, Landsats 1 and 2, for resources analysis and mapping (table 3). The USGS advised government officials and governmental and industrial scientists responsible for geological exploration for minerals, including oil and gas, and for water, for land-reform programs, regional development projects, and for environmental protection on subjects in which the data are applicable, on methods employed, and on institution building for efficient and effective practice.

Great demand continues for opportunities to attend the International Remote Sensing Workshop, which is presented twice yearly at the EROS Data Center. Fifty-eight scientists from 30 countries attended the eighth and ninth workshops in 1977. In addition, nine scientists from seven countries gained special experience as fellows studying or collaborat-

ing in USGS offices and in universities. Fellows from Iceland, Iran, Japan, Poland, and Saudi Arabia were sponsored by their government. USAID sponsored fellows from Lesotho and Spain.

In a demonstration of the capabilities of the Applied Technology Satellites for international television broadcasting, USAID conducted programs (AIDSAT) for 26 countries around the world. Because of the great interest in remote sensing, the USGS cooperated in those programs by providing scientists to participate in discussions, via ATS-6 and television, of Landsat applications with scientists of the host countries. The USGS also cooperated with the U.S. Information Agency in a series of presentations on Landsat applications in five African countries: Botswana, Lesotho, Swaziland, Zaire, and Zambia.

The fourth CENTO Workshop on Applications and Methods in Remote Sensing was conducted in Istanbul, Turkey, (Fary, 1977). The USGS, under USAID auspices, has been responsible for scientific

TABLE 3.—U.S. Geological Survey remote sensing activities in other countries, 1977

Cooperating country or agency	Activity*	Cooperating country or agency	Activity*
Algeria	7	Mali	4
Argentina	1, 4	Mexico	2
Australia	2	Morocco	1, 2, 4
Bahrain	5, 7	Nigeria	1, 5
Bangladesh	4	Oman	4, 5, 7
Bolivia	1, 4	Pakistan	1, 4
Botswana	1	Philippines	1
Brazil	2	Poland	2, 3
Cameroon	4	Qatar	5, 7
Canada	2	Saudi Arabia	1, 2, 7
Central African Empire	4	Sierra Leone	2, 4
Chile	2	South Africa	2
Republic of China	2	Spain	3
Costa Rica	2, 4	Sudan	4
Ecuador	2, 4	Surinam	4
Egypt	2	Swaziland	1
England	2	Switzerland	2
Ethiopia	2	Thailand	1, 2, 3, 4, 5
Ghana	2	Turkey	1, 2
Greece	2	United Arab Emirates	4, 5, 7
Guyana	2	Upper Volta	4
Haiti	4	Uruguay	4
Iceland	3	Venezuela	7
India	2	Yemen Arab Republic	4, 5
Indonesia	2	Zaire	1
Iran	1, 2, 3	Zambia	1
Israel	2	UN Economic and Social Commission for Asia and the Pacific	6
Italy	2	UN Food and Agriculture Organization	7
Ivory Coast	4	Indo-U.S. Joint Commission for Economic Cooperation	1
Jamaica	4	U.S.-Iran Joint Commission for Economic Cooperation	1
Japan	2, 3	CENTO Advisory Group on Minerals Development	1, 5
Jordan	1, 4		
Kenya	4		
Kuwait	2, 5, 7		
Lesotho	1, 3		
Liberia	4		
Libya	4		

* Activity Key

1. International cooperative program in 1977.
2. Participants in 8th and 9th Internat. Remote Sensing Workshop.
3. Participant Fellows.

4. AIDSAT.

5. USGS published report.
6. USGS papers presented at international meetings.
7. USGS briefings presented in other countries.

leadership and the manning of teams of experts for these programs. These workshops have contributed to the development of cadres of scientists in Iran, Pakistan, and Turkey who now employ Landsat data very capably in their work. Among them in the CENTO countries are university professors who are now teaching the use of the data to their students.

Under USAID sponsorship and USGS technical guidance, a remote sensing center, with staffs trained in the use of Landsat for cartography, geological exploration, geography, forestry, and land-use planning, has been established in Thailand. The program was extended through 1977 to provide additional training for key personnel and for com-

pletion of laboratory equipment (Morgan and McCord, 1977). The center now has the capability to provide photographic copies of Landsat images for conduct of national projects.

In other projects in cooperation with USAID, a USGS specialist conducted a 4-month project on preparation of photomosaics for land-use mapping for a Philippine Islands land-reform program. Three USGS staff members assisted the staff of the National Commission of Space Research of Argentina to present that country's second International Workshop on Remote Sensing for Latin America, and a fourth joined a NASA scientist in presenting workshops on the Landsat Data Collection System at the

Geological Survey of Bolivia and at the University of Santiago, Chile. A series of 12 lectures on use of remote sensing in geology was presented at the Geological Survey of Egypt. Landsat coverage was employed in conducting the geological mapping project in Jordan and confirmed the presence of faults previously suspected, as well as others that had not been previously mapped.

In addition to USAID-sponsored programs, several being performed under bilateral agreements are beginning to use Landsat data extensively. The USGS has established a Landsat applications office for the Saudi Arabian Ministry of Petroleum and Mineral Resources to support geologic analysis and preparation of base maps. Landsat data were employed in a USGS reconnaissance geologic and land-use mapping project for the Government of Nigeria that required quick action and immediate information to support the planning for the country's new Federal Capital Project. The USGS has continued the geological analysis of Landsat data and experimentation with the enhancement process that led to new areas for copper exploration in the Maski Chah region of Pakistan. This work has been done in cooperation with the National Aeronautics and Space Administration, International Business Machines Corp., the U.S. National Science Foundation, the Resource Development Corporation of Pakistan, and Dartmouth College in New Hampshire.

Under U.N. auspices a USGS hydrologist presented a month-long training program at the Turkish Water Works Agency on methods of optical enhancement of multiband photo-images for water resources research.

As a part of the USGS cooperative and assistance programs abroad, 183 earth scientists and engineers from 55 countries pursued academic, observation, or intern experience in the United States during the report period. Types of assistance to, or exchanges of, scientific experience with each country, are summarized in table 1. Under USGS guidance, a total of 1,883 participants from 101 countries have completed research, observation, academic, or intern training in the United States. In addition, the Water Resources Division alone assisted or consulted with more than 69 visitors from 32 countries.

Since the beginning of technical assistance work in 1940, more than 2,626 technical and administrative documents authored by USGS personnel have been issued. During the report period, 25 administrative and (or) technical documents were prepared, and 86 reports and maps were published or released in open file (see table 4).

TABLE 4.—*Technical and administrative documents issued during the period October 1976 through December 1977 as a result of USGS technical and scientific cooperative programs*

Country or region	Reports or maps prepared			
	Project and administrative	Approved for publication by counterpart agencies or USGS	Published	
			In technical journals	By USGS
Africa		1		
Argentina				2
Bahrain	1			1
Bolivia	1	1		1
Brazil	3	2	1	2
Cambodia				1
CENTO countries	1			
China (PRC)		2		
Colombia		1		1
Costa Rica				2
Ecuador		1		
Egypt	1			1
Great Britain				1
Guatemala				5
Guyana				1
Ireland			1	
Italy	1			
Jordan				1
Kenya				1
Kuwait	1			1
Liberia				10
Libya			1	
Mexico		1	1	2
Nepal		1		
Nicaragua			1	
Nigeria			2	2
Oman	1			1
Qatar	1			2
Romania				1
Saudi Arabia	8	10	11	4
South America				2
Sri Lanka				1
Taiwan			1	
Thailand		1		1
Turkey		1	1	1
United Arab Emirates	1			1
Yemen	3	11		11
General	2	7	2	4
Total	25	40	22	64

INTERNATIONAL HYDROLOGICAL PROGRAM AND RELATED ACTIVITIES

The International Hydrological Program (IHP), an activity of the United Nations Educational, Scientific, and Cultural Organization (UNESCO), involves about 90 countries and, in addition, several international organizations. Its activities are guided

by an Intergovernmental Council made up of representatives of 30 member countries. The United States was not a member during the 1977-78 biennium.

The five major functions of the IHP are: (1) The scientific program, including studies of the hydrologic cycle, assessment of water resources, and evaluation of the influence of man's activities on water regimens; (2) the promotion of education and training in hydrology; (3) the enhancement of exchange of information; (4) the support of technical-assistance programs; and (5) the enlargement of regional cooperation.

The United States participates in the IHP under the guidance of the U.S. National Committee on Scientific Hydrology (USNC/SH). Functions of USNC/SH are (1) to formulate the U.S. program of participation in the IHP, (2) to serve as a channel of communication among those involved, (3) to promote international hydrological activities, (4) to assist the Department of State in its preparation of the U.S. positions on water matters; and (5) to arrange for U.S. activities related to requests from other countries for information and assistance in hydrological affairs, insofar as possible.

The USNC/SH consists of the Chief Hydrologist of the USGS, who is the Chairman, the Associate Chief Hydrologist, who is the Alternate Chairman, and representatives of eight other Federal agencies and six nongovernmental organizations. J. S. Cragwall, Jr., chairman, O. M. Hackett, alternate chairman, and L. A. Heindl, executive secretary, have served on the committee since its inception in 1975.

During FY 1978, USGS hydrologists participated in a wide variety of activities related to the IHP and to other international programs related to water. These activities included symposia, meetings of working groups, workshops, intercountry exchanges of experts, and selected areas of research.

Much of the work of the IHP is done through individual rapporteurs and working groups. The rapporteurs generally work alone to prepare short reports summarizing the state of knowledge on rather narrow topics or on specific assignments such as editing or revising previously prepared report manuscripts. The working groups are composed of four to eight members representing different countries and are concerned with somewhat broader topics than the rapporteurs. There were 13 rapporteurs and 17 working groups in 1977. The United States furnished four rapporteurs and eight members to the working groups; of these, two rappor-

teurs and four working group members were from the USGS.

USGS contributions to publications

J. D. Bredehoeft reported that the United States contributed six case histories on the use of mathematical models in analyzing urban ground-water problems for the casebook being prepared by the IHP Working Group on Long-Term Prediction of Changes in Groundwater Resources Due to Human Activities.

G. H. Davis reviewed a section on ground-water-network design for the UNESCO loose-leaf publication, "Studies in Ground Water."

Thomas Maddock, Jr., submitted a case history of an irrigation development in the southwestern United States to the IHP Working Group on the Investigation of Water Regime of River Basins Affected by Irrigation, and he completed three chapters of the Working Group's final report.

R. L. Nace submitted part of his monograph on basic physical hydrology to UNESCO for review and revision. He also is editing the English translation of the USSR's "Monograph and Atlas on the World Water Balance," which will be published by UNESCO.

J. F. Poland, chairman of the IHP Working Group on Land Subsidence Due to Groundwater Exploitation, assembled several drafts of case histories of subsidence in different parts of the world as contributions to a casebook on subsidence. B. E. Lofgren also contributed to that casebook.

L. A. Heindl assisted the IHP Working Group on Investigations of the Effects of Thermal Discharges, which met in Oak Ridge, Tenn., to complete the first draft of the group's report on thermal discharges.

The National Academy of Sciences published two final reports, "Snow and Ice Hydrology in the United States—Current Status and Future Directions," by the US/IHD Work Group on the Hydrology of Snow and Ice, and "Water in Carbonate Rocks—U.S. Progress in Perspective," by the US/IHD Work Group on the Hydrology of Carbonate Terranes.

USNC/SH investigations

In Brazil, C. F. Nordin, Jr., R. H. Meade, Jr., and W. F. Curtis participated in a month-long international cooperative study directed toward providing the first full-scale measurement of the sediment load of the Amazon River in South America. R. L. Nace advised the Regional Working Group on the Water Balance of South America regarding plans and pro-

cedures. The USNC/SH also provided advisors to the UNESCO Regional Office in Montevideo in Uruguay to assist with the planning of urban-hydrology studies in Montevideo, Uruguay; Buenos Aires, Argentina; São Paulo, Brazil; and Rio de Janeiro, Brazil.

R. L. Cory (1977) continued studies of water quality and the epifauna in the South, Magothy, Rhodes, and West Rivers, in Anne Arundel County, Maryland.

Activities related to the World Meteorological Organization

J. S. Cragwall Jr., participated in the Seventh World Meteorological Organization (WMO) Region IV (North and Central America and Caribbean countries) Conference in Mexico City.

H. H. Barnes, Jr., contributed materials to the Working Group on the Guide and Technical Regulations of the WMO Commission for Hydrology regarding proposed changes in WMO Technical Regulations and in regard to the St. Johns project of the World Weather Watch.

Other international activities

The USGS cooperates with the International Standardization Organization (ISO), which is attempting to accomplish the standardization of hydrological equipment and techniques so that equipment in all countries will provide data that are mutually compatible. G. F. Smoot chaired the ISO Technical Committee on Hydrological Practices.

Domestic activities related to international programs

During 1977, the United States progressed with many studies and activities that contributed to its program of participation in the IHP. The 82 river stations in the United States, which are part of an international network, continued in operation to obtain streamflow, chemical quality, and suspended-sediment load data. This network provides a general index of the discharge of surface water and of dissolved and suspended material from the continent to the oceans. Collection of hydrologic data also was continued at 23 lake and reservoir stations and at 34 selected observation wells; these stations provide comparative reference and trend information on water-level fluctuations and on the chemical quality of lake, reservoir, and ground waters.

Hydrologic bench marks at four localities throughout the country continued to be monitored for information on hydrologic conditions generally unaffected by man's activities.

Measurements of the tritium content of water in the 20 principal rivers in the United States and of the tritium in precipitation at 16 localities are being used to evaluate the effects of precipitation on the chemical character of inland waters.

REVIEW OF HYDROLOGIC INVESTIGATIONS

During FY 1977, the USGS continued to provide technical assistance in hydrology to less developed nations, although at a reduced scale. Advice and assistance of USGS specialists were frequently sought through correspondence by inquiry from Regional Resources Attaches assigned to American embassies abroad, by inquiry from USAID missions, and by personal visits of foreign organization personnel. Long-term research projects in Kenya and the Yemen Arab Republic were completed, and final reports will be written when well-drilling programs have been completed in those countries. Except for a program in Saudi Arabia, overseas investigations consisted of short-term projects not related to continuing long-range programs.

SUMMARY BY COUNTRIES

ARGENTINA, BOLIVIA, AND PARAGUAY

Rio Pilcomayo sedimentation

J. R. Ritter (1977a) reported that results of a sedimentation reconnaissance of the Rios Pilcomayo Alto (Bolivia) and Pilcomayo Superior (Bolivia, Argentina, and Paraguay) made under the auspices of the Organization of American States (OAS) emphasized the need for a complete analysis of sediment movement in the basin before dams or irrigation projects are started. The brief study supplemented an earlier reconnaissance (Ritter, 1977b) of the Rios Pilcomayo Superior and Pilcomayo Inferior (Argentina and Paraguay) made during a period of low river discharge.

S. T. Algermissen, J. N. Jordan, and W. J. Spence (USGS), along with Bolivian coinvestigators Ramon Cabre, S. J. Flores, and Jose Flores, have started a project to assess the seismic hazard of the Cochabamba region of Bolivia. This area, which has witnessed seismic problems in the past, is scheduled for accelerated growth in the future. In Phase I, five seismograph stations are being installed as a means of establishing gross seismic patterns and as an aid in the planning of Phase II, an eight-station radio-telemetry network with central recording at the University of San Simon.

BRAZIL**Sediment studies of the Amazon River**

As part of an international research effort to determine sediment loads in the Amazon River during the 1976-77 flood season, C. F. Nordin, Jr., R. H. Meade, Jr., and W. F. Curtis measured the suspended sediment at five rated and a number of un-rated cross sections of the river and several of its major tributaries. Measurements were made from the research vessel *Alpha Helix* (operated for the National Science Foundation by Scripps Institution of Oceanography), and the research involved scientists from the United States, Brazil, Scotland, and Italy. Result of the measurements supported the prevailing view that most of the suspended sediment in the Amazon system is carried by rivers that drain the Andes. Suspended loads measured in 1976-77 at Óbidos were nearly 4×10^6 t/d, of which one-half was contributed by the Rio Solimões and at least one-fourth was contributed by the Rio Madeira. The Rio Negro contributed less than 1 percent of the total suspended sediment measured at Óbidos.

Sand ($>63 \mu\text{m}$) comprised one-fourth to one-third of the material in suspension during high water. Silt and clay particles ($>53 \mu\text{m}$) were not distributed uniformly either vertically through the water column or laterally across the river. Cross-channel differences in the concentrations of silt and clay particles could have been related to incomplete mixing of tributary inflows or to secondary circulations in the channel.

The streambed consists mostly of fine sand, but small amounts of gravel are evident near local outcrops. Such bedrock outcrops of conglomerates or clay of the Solimões or Alter do Chão Formations were encountered at several locations, especially on the outsides of meander bends.

CAMBODIA**Ground-water resources**

W. C. Rasmussen studied the subsurface geology of Cambodia in considerable detail in order to describe and evaluate the availability of ground water (Rasmussen and Bradford, 1977). He found no persistent artesian aquifer or potentially high-yielding ground-water source. Ground water is, however, a widely available supplemental source to surface water for domestic, small-scale industrial, and irrigation use.

Because of changes in governmental structure, internal boundaries, and geographic designations be-

tween 1966-74, it was necessary for G. M. Bradford to make extensive revisions in the text and maps of the final report on the ground-water resources of Cambodia.

CENTO COUNTRIES

The USGS, in support of the Department of State, USAID program, has provided leadership for a summer-long field course in the CENTO region since 1966. More than 150 graduate geologists and mining engineers from Pakistan, Iran, and Turkey have participated in the training; several comprehensive mine reports have been published, and exploration suggestions that resulted from the group's studies have led to major ore discoveries. The Ninth CENTO Training Program, under the direction of E. H. Bailey (USGS) was conducted July-September 1977 at the Angouran and Emarat zinc-lead mines in northwestern Iran. Those assisting in the instruction were J. W. Barnes, University College of Swansea (United Kingdom); M. P. Nackowski, (University of Utah); S. Ileri (Hacettepe University, Turkey); M. A. Mallakpour (Geological Survey of Iran); and Z. Ahmad (Geological Survey of Pakistan). Sixteen graduate geologists from the CENTO region participated. As part of the training, the group made a detailed geologic and topographic map of 2 km² around the Angouran mine, a regional geologic map of 150 km², two geochemical surveys, and underground maps of the Emarat mine. The structural controls that guided ore deposition were identified. The maps, along with exploration suggestions, were given to the mine owners.

CHILE

W. A. Duffield undertook a study of possible routes for tunnel construction for a hydroelectric project in the southern Andes of Chile, at the request of Empresa Nacional de Electricidad in South America.

The main objective of the project is to transfer water from one lake via a 16-km-long pressurized tunnel to a power station to be located on the shore of a second lake. Several tunnel routes are possible. Some routes are relatively far from the youngest volcanic rocks of the area, but face potentially major problems such as crossing a wide fault zone and passing beneath as much as 700 m of probably saturated rocks.

For possible alternate routes the tunnel would pass through about 1.5 km of upper Quaternary, post-glacial basaltic lava, but would avoid the fault zones and the thick overlying section. The young

lavas partly fill a glacial valley and provide the dam for the upstream lake of the project. No radiometric ages are available, but comparison of the morphology, erosion, and vegetative cover of these lavas, with other nearby lavas of known historic age suggests that the most recent eruption was at least 200-2,000 years ago. The threat of a future eruption is difficult to evaluate, but for a minimum tunnel life of 50 years needed to make the project economical, this threat seems tolerable.

The possibility of encountering hot ground water in tunneling is difficult to assess, but the fact that a major thermal spring leaks to the surface along the fault zone (just outside the project area) favors tunnel alignments through the volcanic section. Moreover, some of the most competent rock in the entire project area is found in the post-glacial lava flows. Several of these flows are more than 40 m thick and may well occur at desirable tunnel depths.

At the request of the Empresa Nacional del Petroleo (ENAP) and at Government of Chile expense, B. F. Grossling visited Santiago, Chile, to provide technical advice to ENAP on offshore seismic exploration, evaluation of petroleum prospects of various onshore and offshore areas, and overall planning and management. He reviewed all the offshore seismic sections that had been obtained between the latitude of Valpariso and Golfode Penas.

COSTA RICA

J. W. Dewey spent 3 weeks in mid-1977 at the University of Costa Rica in a cooperative USGS-OAS project to help train seismologists and upgrade seismic facilities in Costa Rica. Dewey worked principally on the interpretation of seismographic data obtained by the University network during the past year and a half. Arrival-times, first-motions, and amplitudes were read for approximately 150 earthquakes that occurred within 200 km of San Jose. Arrival times from the Instituto Costarricense de Electricidad (ICE) network in northwestern Costa Rica were available for about one-half of these earthquakes. Initially, satisfactory locations had been obtained for about 70 shocks. Extensive discussions were held over the modifications in the input data that would be necessary to obtain satisfactory solutions for the remaining earthquakes, and it is expected that most of these have now been located satisfactorily.

Local magnitudes have been assigned to earthquakes by applying the local magnitude formula of Richter directly to trace amplitudes measured on

seismograms from the SJS vertical seismograph. About 10 local earthquakes recorded by both the Wood-Anderson seismographs and the SJS vertical seismograph had nearly the same amplitudes on seismograms from both types of instruments. Therefore, it is anticipated that errors caused by use of the SJS vertical seismograph will in almost all cases be less than 0.3 magnitude unit.

Most earthquakes recorded during the past year and a half have occurred in the Pacific Coastal region of Costa Rica. This region had been identified as the major seismic region in Costa Rica on the basis of hypocenters routinely determined using data from the global network of seismographic stations. However, local hypocenters, based on both UCR and ICE data, are giving a much clearer picture of this seismic zone than is possible with hypocenters routinely determined from teleseismic data. For example, the largest Costa Rican earthquake in 1976, the shock of 1629 GMT, 25 February, was assigned a focal depth of 66 km by the NEIS, but is well located by local seismographic data (it occurred within the ICE net) at a depth of 20 km. This change of focal depth is significant; the seismic hazard associated with a 20-km deep source region in northwestern Costa Rica is far greater than that associated with a 66-km deep source region. In future years it will be necessary to reinterpret the teleseismically-located earthquakes in terms of the recently acquired data from the local network.

About 24 earthquakes, all of magnitude ≥ 3.9 , were located in the Meseta Central during the past year and a half. Seismicity has been highest at the southern margins of the Meseta Central. These earthquakes are of shallow-focus and are distinct from the Benioff Zone earthquakes. The epicenters of these earthquakes do not appear to define a single fault zone. Some of the shocks occur near major hot springs and the hypothesis that these shocks are of a type characteristic of geothermal regions elsewhere in the world is being considered. In this respect, it is noteworthy that the disastrous Cartago earthquake of 1910 occurred as part of an extended "swarm" of earthquakes; such swarms are typically associated with geothermal regions. It is also very likely that the seismicity of the Meseta Central is complicated by the proximity of the boundary between the Cocos plate and the Nazca plate. Clearly, more hypocenters are needed to better resolve the seismotectonics of the Meseta Central.

Dewey also made recommendations for a continued upgrading of seismograph stations and also outlined

areas of investigation that may be fruitful with currently available data.

DOMINICA

J. E. Case briefly visited Dominica to confer with officials of the Survey Department, Ministry of Agriculture, Lands, Fisheries, and Cooperatives on USGS assistance in appraising the natural resources of the island, at the request of the Premier. Case's recommendations include (1) analysis of the several thousand stream sediment samples that are already collected; (2) investigation of possible clay, lightweight aggregate, copper, and gold deposits; (3) appraisal of geothermal potential; and (4) study of available offshore seismic records.

EASTERN ARABIAN PENINSULA

To illustrate the applications of remote sensing in geology, hydrology, and agriculture, M. J. Grolier (1977a-e) prepared interpretations of five Landsat scenes (at 1:500,000 scale) that cover Bahrain, Kuwait, Oman, Qatar, and the United Arab Emirates (the former Trucial States). The scenes were carried to the five countries by D. F. Davidson where country officials were briefed on the possibilities of using Landsat data in those areas. The work was supported by USAID, and involved personnel from the U.S. Department of Agriculture and NASA.

EGYPT

In 1976 the USGS under the auspices of USAID initiated a cooperative program with the Egyptian Geological Survey and Mining Authority (GSE) to improve and update that organization's capability for assessing the mineral resources of Egypt. Phase I, carried out in late 1976, consisted of a preliminary evaluation of the GSE and the formulation of a phased program leading toward the principal objective. During Phase II, in 1977, the following were accomplished: (1) Installation of a cartographic office and a photographic laboratory at GSE in Cairo; (2) training of four GSE cartographers at USGS offices in the United States; (3) compilation of two geologic and two metallogenic maps in part of the Eastern Desert; (4) preliminary evaluation of GSE laboratories; and (5) a series of lectures were presented at GSE on the geologic application of remote sensing. The program will continue for another year.

Western desert development potential

G. F. Worts, Jr., (USGS) and H. L. Parkinson (USAID), made a brief evaluation of ground-water and soils potential for irrigated agriculture in the western desert of Egypt. They concluded that because of the lack of suitable soils, the high cost of drilling deep wells and the large energy requirements and costs of high pumping lifts, irrigation developments under prevailing economic conditions are not feasible except in and near existing oases (Parkinson and Worts, 1977).

GUATEMALA

After training by USGS personnel, the Instituto Nacional de Sismologia, Vulcanologia, Meteorologia, y Hidrologia (INSIVUMEH), Guatemala, has assumed responsibility for the basic analysis of seismic data record by a six-station network near Guatemala City. This includes timing of events, key-punching the data, and running a hypocenter determination program on a local computer. USGS personnel have advised INSIVUMEH on their plans to purchase instruments for the expansion of the seismic network in 1978.

Determination of earthquake hypocenters for January through June 1977 are now being completed by INSIVUMEH personnel. Seismic activity in the vicinity of the net continues at a rate approximately three times higher (30 versus 10 events per month) than the rate of seismic activity during the 11 months preceding the Guatemala earthquake of February 4, 1977.

After being relatively quiet during 1976, micro-earthquake activity at Fuego Volcano increased, beginning with a swarm of earthquakes on January 4-6, 1977. An 18 microradian tilt event occurred concurrently with this swarm. Whether or not these events are the result of tectonic faulting or magma movement is not clear. Minor eruptive activity at Fuego was observed on and during April 19, September 11-14, and October 2-9, 20, 22, 26, 29, 1977. Unexpectedly, no significant change in ground tilt was recorded before or after this activity. A small eruption on May 28, 1975, was followed by an 11 microradian tilt event showing inflation of the volcano. Even though the short-term data appear inconsistent, the long-term data indicate that the volcano has been inflating since May 1975 at a rate of roughly 3-5 microradians per month.

INDONESIA

Sediment study program assistance

J. M. Knott completed a 4-month assignment to the United Nations Development Program (UNDP) in Bandung to evaluate the existing sediment program of the Hydrochemistry Branch, Institute of Hydraulic Engineering, to observe sediment problems in Java and to train counterpart personnel in the collection, analysis, interpretation, and publication of sediment data. Final reports to UNDP included recommendations for improving current methods and equipment stocks and for future investigations.

ISRAEL AND JORDAN

J. F. Seitz has undertaken a project in Amman, Jordan. Under sponsorship of USAID, and at the request of the Jordanian National Resources Agency (NRA), the project is developing a comprehensive plan for mineral exploration activities, emphasizing advanced techniques, where appropriate. Under consideration are airborne geophysical surveying geochemical studies, and use of computerized Landsat imagery and data. Possible resources include geothermal energy, uranium, iron, and potash. On the basis of field trips in metallic mineral areas where outcrops are sparse, it was recommended that geochemical and geophysical studies be made. A new mineral associated with ettringite was discovered, and has been named hashemite in honor of the ruling family of Jordan.

A. H. Truesdell was assigned to the United Nations at Amman, Jordan, to serve as a consultant geochemist for the United Nation's geothermal exploration project. Truesdell met with officials of the United Nations Development Program (UNDP) and USGS. He made two field trips to the Zerqa Ma'in springs, two to the related Zara springs, and one to a separate hot springs system in the same aquifer. Samples were collected at each location for analysis by Jordanian NRA and USGS laboratories. A program of collection, analysis, and measurement of spring temperature and flow was suggested to the Jordanian NRA.

Dead Sea levels

S. P. Sauer (1978) reviewed historical changes in the level of the Dead Sea and factors contributing to those changes. The objective was to evaluate variations that might occur under a variety of water-management options and to consider the effects of

such variations on mineral production from the Dead Sea. He concluded that the major impact of declining water levels would be an increase in energy requirements for the production of potash or other minerals.

KENYA

Rural water-resource development

N. E. McClymonds, in cooperation with the Kenyan Ministry of Water Development and under Phase II of the USAID Kenya Livestock Development Program, continued the borehole-drilling activity in the Northeastern Province. During 1977, seven holes were completed, six of which will probably become production wells. Although USGS involvement with the program terminated late in 1977, seven more holes will be drilled during the present phase of the project and many others will be equipped, housed, and fitted with auxiliary facilities. Activities under Phase I of the program (1969-74) were described by W. V. Swarzenski and M. J. Mundorff (1977).

McClymonds also assisted the Ministry of Works by siting wells and overseeing work done by the Ministry of Water Development drilling unit, which is developing ground-water supplies for road construction between El Wak and Ramu. Advice was also provided for two ranch-water projects and several rural-water-supply schemes.

LIBERIA

Ten geologic maps that cover the country of Liberia were published as USGS maps I-771D to I-780D. The maps cover a total of 111,400 km² at a scale of 1:250,000 and make Liberia the first African country to be completely mapped geologically at so large a scale. The publication of these maps completes the folios of the 10 quadrangles, for which geographic, aeroradiometric, and aeromagnetic maps are already available.

Representing the most important product of a geologic program undertaken cooperatively by the USGS and the Liberian Geological Survey from 1963 to 1972 under sponsorship of USAID, the maps will be useful in mineral resources assessment, economic development planning, and in a wide variety of activities such as land use, urban and highway planning, agriculture, hydrology, and forestry.

The maps show the distribution, age, and structure of 70 different rock units. Key letter symbols identify the kind of data, such as magnetic, radio-

metric, and aerial photographic, used in mapping. The geology is overprinted on a shaded-relief geographic base.

A geologic feature strikingly shown on the maps is the position of scores of Jurassic dikes aligned parallel to the coastline. The dikes are believed to have formed in response to forces related to the opening of the Atlantic Ocean as the continents moved apart.

MALAYSIA

E. P. Danenberger and D. J. Bourgeois completed an assignment in Malaysia working in cooperation with Petronas, the Malaysian National Oil Company. They assisted in devising official regulations and procedures designed to control petroleum operations to assure (1) accurate measurement of produced oil/gas; (2) technologic development of petroleum fields for maximum recovery and resource conservation; (3) safety; and (4) environmental protection.

MEXICO

The cooperative USGS-Mexico program of mineral exploration in the Sonoran environment sponsored by the National Science Foundation and its counterpart in Mexico, the Consejo Nacional de Ciencia y Tecnologia, has completed maps showing distribution of the 10 most useful elements. These are based on computerized heavy-mineral concentrate and stream-sediment data.

Tropical carbonate aquifers

Scientific studies of carbonate aquifers common to Mexico and the United States were continued by a number of investigators under the auspices of the U.S. National Science Foundation and the Mexican Consejo Nacional de Ciencia y Tecnologia (CONACYT). William Back (USGS) and J. M. Lesser (Secretaria de Recursos Hidraulicos of Mexico) described hydrologic conditions on the Yucatan peninsula, reviewed water-use and water-management practices, and suggested lines of future investigation (Back and Lesser, 1977).

Another of the cooperative projects under NSF-CONACYT auspices was an extension of the mapping of the "bad-water line" from Texas to the vicinity of Monterrey, Nuevo Leon, in Northern Mexico by Back, Lesser, and B. B. Hanshaw (USGS) (1977). The "bad-water line" separates potable from nonpotable ground water in aquifers

of the Edwards Limestone and associated limestones of Cretaceous age. The nonpotable water is characterized by high concentrations of dissolved solids, particularly sulfate and sulfide, and by relatively high temperatures. Interpretation was based on chemical and isotopic analyses of water from wells and springs tapping the Cretaceous Aurora and equivalent limestones. Hypotheses were developed concerning the genesis, occurrence, areal extent, and natural controls on the waters with these particular characteristics.

Horizontal control net in a geothermal area

The U.S. Department of Energy and the Mexican Comision Federal de Electricidad have entered into an agreement for a program of cooperation for research, development, and demonstration of applications of geothermal energy, centered on the Cerro Prieto Geothermal Field in Mexicali Valley, Mexico (a continuation of the Imperial Valley of California). One element of the project is the study of land subsidence and crustal strain. B. E. Lofgren and several Mexican investigators began the study by designing, constructing, and surveying a network of 36 electronic distance measuring (EDM) stations to observe vertical displacements.

NEW ZEALAND

Ground-water flow simulator applications

P. C. Trescott (USGS) and I. G. Donaldson (Department of Scientific and Industrial Research, Government of New Zealand) investigated ground-water flow simulators and their application to the northern Canterbury Plains of New Zealand. The study, financed in part by the U.S. National Science Foundation, is an activity authorized by the Scientific and Technical Cooperation Agreement between the United States and New Zealand.

The project area is a microcosm of hydrologic features found in the United States. Better methods of treating many of these features are needed in the ground-water flow simulators that are commonly used in the United States. The experience of New Zealand scientists in simulating geothermal systems significantly aids USGS investigators by incorporating and testing proposed improvements to simulation of three-dimensional ground-water flow. Calibration of models is accomplished by measurement of river discharge from, and precipitation on, the Canterbury Plains.

NICARAGUA

D. H. Harlow reports that recent results from the 14-station seismic network in western Nicaragua included an earthquake swarm on February 13-14, 1977, near Momotombo Volcano. Twenty-four events with depths of 3 to 20 km were located, and their locus is roughly 7 km north of the volcano. An earlier, much larger, swarm occurred on September 24-27, 1975. The epicenters from this swarm were located 5-km southeast of the summit. These swarms, combined with occasional single events, make the Momotombo area the most seismically active shallow zone during the 2-year operation of the seismic net. This seismic activity is of particular interest because of the developing geothermal project at the southern foot of the volcano. These data are being used to evaluate the seismic and volcanic risk to the geothermal project, as well as the data's potential value as an exploration tool.

It now seems apparent that the previously reported increase in shallow seismic activity that began in late September 1976 in the vicinity of Concepcion Volcano on Ometepe Island was a prelude to eruptive activity. The eruption began with a late night explosion on April 4, 1977, that caused considerable anxiety and some panic among the islanders. No other eruptive activity, except for increased fumarolic emission, was observed until more than 3 weeks later on April 29. Between the early afternoon of April 29 and noon of May 1, 16 explosions were counted by an observer on the island. From light plane observations, it is known that the ash clouds from some of the explosions rose more than 1,500 m above the summit of the volcano. Minor amounts of ash reportedly fell on the city of Rivas, 25 km southwest of Concepcion.

NIGERIA

At the request of the Nigerian Federal Capital Authority (FCDA), the USGS undertook a reconnaissance geologic investigation of the newly designated Federal Capital Territory (FCT) in central Nigeria. The FCDA required base geologic, engineering, and hydrologic data for use in selection of a site for the proposed new national capital city. Reconnaissance mapping of this 7,700 km² area by a team of USGS and Nigerian Geological Survey (NGS) geologists began on March 7, 1977, and was completed on June 1, 1977 (Ege and others, 1977; Overstreet and others, 1977; U.S. Geological Survey, 1977c; Peterson and Meyer, 1977). The USGS

geologic team consisted of J. R. Ege, W. R. Griffiths, and W. C. Overstreet, the hydrologic team, of Gerald Meyer and L. R. Peterson, and logistics support was provided by L. L. Benton and F. D. Spencer.

The maps of the FCT, all at 1:100,000 scale, include a Landsat-Image geographic map (U.S. Geol. Survey, 1977) and a provisional land-use map (Overstreet and others, 1977) prepared by computer processing of Landsat tapes at the USGS Flagstaff Computer Laboratory. Three reconnaissance maps showing surficial, bedrock, and engineering geology accompany the geologic report (Ege and others, 1977). S. J. Gawarecki assisted in preparing the land-use map and defined the lineaments for the engineering geology map.

The report summarizes the engineering geology of the area, soil and rock engineering classifications, geologic hazards, and sources of construction material, and recommended suitable sites for the capital city and areas for future work. The bedrock and surficial geology are described and discussed in relation to the siting of the city.

Peterson and Meyer (1977) indicated sources for initially required water supplies and recommended a systematic investigation and collection of information for a water data base.

These maps and reports form the basis for the federal capital city site selection by FCDA and their private planning consultants.

Federal Capital Territory reconnaissance

Under an agreement between the Nigerian Federal Capital Development Authority and the USGS, L. R. Peterson and Gerald Meyer made a reconnaissance assessment of the water resources available for initial development of an area in central Nigeria to which the Capital might be relocated. They concluded that diversion from the Niger and Benue Rivers is the logical means of providing for initial requirements and probably the eventual large demands even though these rivers are outside the territorial limits. The Gurara River, which flows through the Federal Capital Territory, and sedimentary rocks that occupy the southwestern quarter of the Territory have the potential for supplying a considerable amount of water. Peterson and Meyer (1977) recommended and outlined a systematic investigation and data-collection effort to overcome present deficiencies and urged definition of institutional responsibility for such an effort.

PERU

A. L. Clark, J. M. Botbol, and N. A. Wright presented approximately 2,000 maps showing silver-copper distribution in the Toro Mocho porphyry copper deposit to officials of Centromin Peru in Lima. This was part of Phase III of the Morococha District study with emphasis on computer modeling.

S. T. Algermissen is Program Manager of a cooperative program of the USGS, the Instituto Geofísico del Peru (IGP), and the Instituto Geología y Minera that undertakes studies in earthquake hazard reduction and engineering geology. The project involves seismic hazard and zoning of the Bayovar project, a plan to build a large industrial complex and city in northern Peru. In an area sparsely settled now, at the terminus of the Peruvian oil pipeline in the Sechura Desert, a population of 250,000 is expected in the early 1980's. A suite of seismoscopes and strong-motion instruments were installed and have recorded ground motion data in the area of high concern. R. C. Bucknam and R. L. Schuster made a 2-week study of the area and possible fault activity and soil conditions for selected areas.

H. T. Evans spent 10 days in Lima, Peru, to analyze the requirements for installing an X-ray diffraction laboratory at the Instituto Peruano del Energia Nuclear. The study was made under the aegis of the Peruvian Energy and Research Development Administration and the International Energy Agency (IAEA).

Under the aegis of the Peruvian Department of Energy and the International Atomic Energy Agency, Evans also visited the laboratories of the Instituto Peruano del Energia Nuclear (IPEN) in Lima. IPEN has charge of all activities related to production of nuclear energy and needs an effective method to test raw materials. Evans gave advice on the laboratories in general, and specifically on adding an X-ray diffraction unit.

PHILIPPINE ISLANDS**Shallow ground-water potential, Subic Naval Base**

At the request of the U.S. Navy, J. T. Callahan monitored test drilling and pumping of shallow alluvial deposits in the Binictican and Boton stream valleys to determine yields and other characteristics of the aquifers. Insufficient yields for projected needs were indicated but several developmental options were proposed.

POLAND**Special Foreign Currency Program**

V. E. Swanson visited Poland relative to the project "Geochemistry of coal and computerization of coal data," to provide coordination required under the cooperative Poland-USGS project. Swanson's meeting with personnel of the Instytut Geologiczny and Gowny Instytut Gornicwa resulted in general clarification and understanding of many issues concerning three USGS projects in Poland. Swanson also met with personnel of the American Embassy in Warsaw and visited Sosnowiec and Katowice in the Upper Silesian coal basin, the Roxbark coal mine, and Zabytkowa lead-zinc district.

Two new projects, one on the characteristics of coal basins and one on the geochemistry of coal, were initiated; a third project, on base metals in carbonate rocks, completed planned geologic and mineralogic research; reports of the scientific results are being prepared. A team of USGS geologists and geophysicists met with officials of the Geological Institute in Warsaw and agreed to seek extensions and additional funds to add geophysical research to the three programs.

A comparative study of the characteristics of coal basins in Poland and the United States is being made, and research is underway to develop and test coal investigation procedures in the compact, intensively studied and mined Polish coal basins. Preliminary results indicate that the rank of coal is more erratic in the Polish basins because of local "hot spots" in underlying rocks. Also, the thermal gradient is greater, and some deep workings have encountered temperatures as high as 30°C at depths of 1,000 m.

SAUDI ARABIA**Inventory of nonmetallic mineral deposits**

L. F. Rooney reports that the only identified raw materials for structural clay products (specifically building tile) in the greater Abha-Khamis Mushayt area are wadi silts, saprolite, and colluvium. The As Sarat laterite might be amenable to beneficiation to a raw material for ceramic tile.

The Tertiary limestone deposit in the Harrat Hadan is large (50×10^6 t) and would be easily minable, but it contains too much magnesium to be a cement raw material unless it were combined with an equal amount of low-magnesium limestone. The limestone deposit contains too much silica to be a

raw material for high-purity lime, and appears to be too soft for use as aggregate.

The occurrences of asbestos southeast of Hamdah are of adequate quality but insufficient quantity to be exploited economically.

Preliminary sulfur isotopic studies

Studies of sulfur isotopes in Saudi Arabian mineral deposits by R. O. Rye in collaboration with R. J. Roberts (USGS) and Mustafa Mawad (Directorate General for Mineral Resources) throw light on the sources of sulfur and metals in the deposits, the nature of ore-forming solutions, the physical-chemical environment of ore deposition, and the genesis of the deposits. The sulfur $\delta^{34}\text{S}$ values show a wide range from strongly negative through zero to strongly positive. The strongly negative values (-46.4 to -22.9 permil) characterize syngenetic sedimentary iron sulfide deposits that formed in stagnant euxinic basins; the values that lie near zero permil characterize veins whose sulfur and metals were derived from magmatic sources, and also include some massive sulfide deposits whose metals may be of magmatic origin but whose sulfur was largely derived from sea water; and the strongly positive values (17.3 to 40.3 permil) characterize deposits whose sulfur was derived from sea water or evaporite deposits and whose metals may have come from magmatic or syngenetic sources. Many of the massive sulfide deposits show higher $\delta^{34}\text{S}$ values in deeper parts of the deposit, which suggests that the deposits may have formed in a Kuroko-type environment.

Investigation of base metal deposits

Studies were continued by C. W. Smith on base-metal deposits at Dhahar (lat $18^{\circ}13'00''$ N., long $40^{\circ}44'00''$ E.) where copper and zinc are found in metamorphic rocks of the Jiddah Group. Rock chip sampling for trace metal analyses and preliminary drill tests indicate that copper and zinc are widely, though erratically, distributed throughout metamorphosed, intermediate to silicic volcanoclastic rocks. The deposits are varied in type and range from massive pyritic and pyrrhotitic lenses bearing chalcopyrite and sphalerite within quartz crystal tuffs and pyroclastic breccias near contacts, to marbles and mafic volcanic flows, to large areas of disseminated and stockwork pyrite with associated chalcopyrite in quartz crystal tuffs, and to disseminated and stockwork zones of chalcopyrite occurring independ-

ently or with pyrite within intrusive quartz porphyry dikes that have been hydrothermally altered to quartz sericite.

The lenticular massive sulfides and the disseminated and stockwork sulfide zones fit into the volcanic model for sulfide origin and indicate that the sulfide bodies were probably formed as submarine or near-surface deposits adjacent to volcanic centers. However, the disseminated and stockwork chalcopyrite found within hydrothermally altered intrusive quartz porphyry dikes indicate a distinctly epigenetic origin associated with later plutonic rocks.

Mineralization associated with granites

J. E. Elliott continued his study of Precambrian rocks of granitic composition which are exposed over approximately 30 percent of the Arabian Shield, yet have very few known associated mineral deposits. However, available data show numerous occurrences and geochemical anomalies of tungsten, molybdenum, tin, niobium, beryllium, fluorine, and other metals associated with these rocks, principally the late syntectonic and post-tectonic granites. These younger granites (IUGS classification) may be subdivided into two series: an older, in general, calc-alkaline, and a younger alkaline to peralkaline series. Molybdenum, tungsten, and possibly tin show a stronger association with calc-alkaline series; whereas, other mineral occurrences notably of niobium, fluorine, and uranium-thorium are restricted to alkaline and peralkaline granites. Based on the distribution of these mineral occurrences and geochemical anomalies, several regions of the Shield appear to have significant potential for the discovery of commercial deposits of these minerals.

In the northwest Shield, north of latitude 26° , the discovery of the Ghurayyah deposit, an albite leucogranite stock containing major resources of niobium, zirconium, and uranium, indicates further exploration in this region is warranted. Also, palinspastic reconstruction of the Arabian-Nubian Shield by closure of the Red Sea shows this region to be adjacent to the Eastern Desert of Egypt, where numerous deposits and occurrences of tin, tungsten, tantalum and molybdenum have been found.

In the eastern Shield, between lat 21° and 24° , numerous occurrences and geochemical anomalies of tungsten and molybdenum, principally, indicate a moderate potential for discovery of commercial deposits of these metals. Low-grade resources of molybdenum and occurrences of tungsten are associated with the Uyaijah ring structure (Dodge and

Helaby, 1975; Theobald and Allcott, 1975), a plutonic complex consisting of multiple intrusions of granodiorite and calc-alkaline granite.

In the southern Shield, near lat 18° and long 44°, several granitic plutons are associated with tin anomalies. One of these, an altered leucogranite stock, is currently being investigated for tin deposits.

The Jabal Ishmas-Wadi Tathlith gold belt

R. G. Worl continued work in the Jabal Ishmas-Wadi Tathlith gold belt, which covers an area 200 km long and 20 to 30 km wide in the southeastern part of the Precambrian Shield of Saudi Arabia. The belt coincides with a major north-trending fault system and a zone of metavolcanic and metasedimentary rocks. Gold-bearing quartz veins, breccias, and stringer zones are largely confined to greenschist metamorphic facies metavolcanic and metasedimentary rocks and are spatially related to the main fault systems, which are typical associations for gold deposits of this type in other Precambrian shield areas of the world. The source, mobilization, transport, and deposition of the gold was intimately tied to the tectonic, thermal, and plutonic history of the rocks within the belt.

Gold deposits fall into five geographic groups that probably also reflect a genetic grouping. The age of emplacement and mode of development differed from group to group. Deposits in one group are related to a late stage of granodiorite to quartz monzonite intrusive activity of the Yafikh orogenic event approximately 600 m.y. ago. Another group occurs in rocks containing massive sulfide deposits. The gold-sulfide-quartz veins probably represent metals remobilized into fracture zones during regional metamorphism. Deposits in the remaining three groups are related to regional quartz veins or small gabbro or felsic intrusive bodies, and the age of deposition and source of the gold is unknown. Although all known deposits in the belt are hydrothermal, an untested potential for syngenetic gold in strata-bound deposits exists. Possible host rocks for disseminated gold include massive sulfide bodies, volcanic ironstones, quartzitic clastic rocks, shales, and porphyritic subvolcanic intrusive rocks and flows of felsic composition, all present within the gold belt.

In order to evaluate the geologic perspective of the individual deposits, a system was developed to determine the potential resources of that deposit. The system was developed from historical data on greenstone gold belts in Canada, United States, Australia, and Africa, plus data obtained from pre-

vious drilling projects in the Arabian Shield. Using any combination of physical geology parameters, channel sample results, and dump sample results, the optimum potential resource tonnage and grade for a given deposit can be estimated from the system. Although these estimates are based upon present exposures and only limited analytical data, the results indicate that hydrothermal deposits in the gold belt have modest economic potential, and only three are considered to be exploration targets. A summary of the results of the evaluation follows:

Number of deposits	Potential ore tonnage (tonnes)	Potential grade (g/t)
34	50,000	2 - 7
6	50,000-200,000	7 -17
2	200,000-300,000	10 -22
3	300,000-400,000	12 -21
1	15,000,000-20,000,000	2.5

Subsequent to this subduction-related magmatism and tectonism, called the Hijaz tectonic style, the Arabian craton was sutured to the Proterozoic African plate in a collisional event represented in Arabia and eastern Africa by the Pan-African event, which extended from prior to 650 m.y. to at least 540 m.y. and perhaps to 520 m.y. ago. Although the tectonic processes of subduction and continental collision during the period 900-500 million years ago are represented here by a single plate-tectonic model of plate convergence, the differences in age and magmatic and tectonic styles of Hijaz orogenesis from those of the Pan-African support division into at least two events. As defined by the ages of major plutonic units, the axis of magmatic and tectonic activity migrated eastward or northeastward during the Hijaz cycle. The granodiorite to granite plutonism of the Pan-African event, however, shows no geographic control because it is distributed throughout the Arabian Shield.

Age and evolution of the southern part of the Arabian Shield

Rb-Sr studies of Precambrian volcanic and plutonic rocks of the Arabian Shield by R. J. Fleck document an early development of the Arabian craton between 900 and 680 million years ago. Geologic studies by W. R. Greenwood, D. G. Hadley, R. E. Anderson, and D. L. Schmidt indicate an island-arc environment, characterized by andesitic (dioritic) magmas, volcanoclastic sedimentation, rapid deposition, and contemporaneous deformation along north- or northwest-trending axes. The ear-

liest plutonic units are diorite to trondhjemite batholiths that range from 800 to 900 million years in age and occur along the western and southwestern parts of Saudi Arabia. Younger units, from 680 to 750 million years in age, range from quartz diorite to granodiorite and become more abundant in the south-central and eastern parts of the Arabian Shield. Initial $^{87}\text{Sr}/^{86}\text{Sr}$ ratios for both groups range from 0.7023 to 0.7030, averaging 0.7027. The absence of sialic detritus in sedimentary units and the indication of an island-arc environment suggest that the early development of the Arabian craton occurred at a convergent plate margin between plates of oceanic lithosphere.

Plate tectonics and the Arabian Shield

A general consensus has been emerging over the last several years that the late Proterozoic Arabian Shield was formed in a plate-tectonic environment. The older part (1100–700 m.y. ago) of the shield is comprised mainly of calc-alkaline volcanic rocks, quartz dioritic and trondhjemitic plutons, and related graywackes that appear to be typical of rocks formed in an island arc environment. From 700 to 550 million years ago, massive amounts of granites and associated rhyolites and arkosic molasse were formed, possibly in response to a continental collisional event. Two controversial topics presently being debated are whether serpentinized ultramafic masses along suture-like zones are true ophiolites, and whether an older (Archean or older Proterozoic) basement is anywhere present in the Arabian Shield. In any case, the Arabian-Nubian Shield in general appears to be one of the prime test areas extrapolating plate tectonics back into the late Proterozoic.

Geologic mapping, geochronology, and other related work has now progressed to the point that detailed models for the evaluation of the Arabian Shield are beginning to emerge and be tested. Most of these center on a plate subduction-island arc model, although they differ radically in detail. That this mechanism operated in the middle and late Proterozoic (1100–700 m.y. ago) is indicated by massive amounts of calc-alkaline volcanic and related sedimentary rocks that are intruded by quartz-diorite to trondhjemite batholiths. These rocks do not appear to differ significantly from those of modern arcs. This period was followed by a period (700–550 m.y. ago) of intense granitic plutonism, rhyolitic volcanism and arkosic molasse sedimentation that may have been initiated by con-

tinental collision, which led to the final cratonization of the Arabian Shield.

Study of the young (650–550 m.y. ago) post-tectonic granites shows that they increase in volume and the erosional level decreases to the northeast across the shield. They include about 40 peralkaline granites that typically contain riebeckite, arfvedsonite, aegerine-augite, and more rarely barkevikite and aenigmatite. The peralkaline granites are distributed over much of the Arabian and Nubian shields, although they are completely lacking in the southwestern Arabian shield and the Precambrian of Ethiopia. These peralkaline granites probably constitute the largest field of such rocks in the world.

Paleomagnetism

Karl Kellogg reports that a modern, fully equipped paleomagnetism laboratory was established in 1977 at the USGS Mission in Saudi Arabia and an active research program begun. A Schoenstedt spinner magnetometer, capable of measuring total magnetic moments down to 2.5×10^{-8} emu is coupled with a small computer and teletype for rapid calculation of remanent directions and intensities. Unstable or low-temperature components of magnetization are removed on either a single axis A.C. demagnetizer or a thermal demagnetizer. Cores may be drilled either in the field or in the laboratory from oriented blocks.

Initial paleomagnetic studies have concentrated in three areas of the southern Arabian Shield: (1) The lower Miocene layered gabbros and dike swarm near Jabal at Tirf (Tihamat Asir), (2) the As Sarat volcanic field, and (3) the upper Proterozoic to lower Paleozoic plutons and dikes in the vicinity of Hamdah.

The mean paleomagnetic direction of 15 magnetically stable, lower Miocene rocks units in the Jabal at Tirf area, including the Jabal at Tirf gabbro and overlying granophyre as well as a suite of diabase dikes, is $D=352$, $I=11$ ($\delta_{95}=6.0$; $N=65$) defining a paleomagnetic pole at 76°N , 258°E ($dp=3.1$, $dm=6.1$), where D =declination, I =inclination, δ =sphere of confidence, and N =number of samples. The preliminary paleomagnetic results give no evidence of a seaward rotation of the coastal plain margin that can be inferred from attitudes of the dikes and layered gabbros.

Paleomagnetic studies of aplitic inclusions in a quartz monzonite pluton in the southern Arabian Shield at lat 19.0°N . and long 43.6°E . have yielded

what appears to be the first paleopole position determined from Precambrian rocks of the Shield, at paleolatitude 49.9° N, paleolongitude 101.3° E. The inclusions were cleaned in an alternating field of strength 200 oe; $\delta_{95} = 10.0$ for the stable remanent magnetization vector, based on six samples collected at the site. A late Proterozoic age of 660 m.y. has been established by Cooper and others for the pluton.

Water-resource development

Water-resources advisory services were provided to, and a number of field operations were conducted on behalf of, the Water Resources Development Department (WRDD), Ministry of Agriculture and Water (AGWAT) under the auspices of the United States-Saudi Arabian Joint Commission on Economic Cooperation (JECOR). G. C. Tibbits, Jr., succeeded D. W. Greenman as Senior Water Resources Specialist of the four-member USGS team assigned to the WRDD/AGWAT operation. The other three USGS participants were R. L. Wait, W. J. Shampine, and D. O. Moore. At year's end, the AGWAT group had 36 permanent staff members from a variety of U.S. agencies.

The USGS specialists supervised or reviewed some aspects of consulting services being provided to WRDD for test drilling and ground-water investigations, and developed specifications for extensions of this work. Considerable progress was made in planning for the computerization of storage, retrieval, and processing of hydrologic data acquired in previous investigations throughout the Kingdom and of the data continually accumulating. A compilation and evaluation of water-quality data was undertaken, with particular emphasis on radiochemical data and their application to definition of certain aquifer characteristics. A review of surface-water data and data needs in relation to stream-gaging operations has accented the necessity for development of new operational network concepts and for development of alternative means of determining some streamflow characteristics.

Future water supplies for Riyadh

S. S. Papadopoulos conducted a short-term investigation of increasing pumpage from the Wasia well field southeast of Khurais as a means of augmenting the Riyadh water supply. A previously developed digital-computer ground-water simulation model of the area was rerun to determine the effect of incrementally increasing the pumpage. Additional

observation wells were proposed to monitor pumping effects and to provide a basis for refining aquifer parameters.

SENEGAL, MAURITANIA, AND MALI

Senegal River basin data assessment

D. W. Greenman and G. L. Gallino assisted the U.S. Bureau of Reclamation in its response to USAID by reviewing the water-data collection efforts of the several member States of the Organization for the Development of the Senegal River.

They found the surface-water data-collection programs and related efforts to be well established and functioning. However, although existing ground-water data are abundant, no systematic regional compilation or evaluation has been done. Previous investigations were largely directed toward locating public, domestic, and stock-water supplies, and do not satisfy the present needs which are related to regional water management considerations.

SRI LANKA

Jaffna Peninsula irrigation development review

Under the auspices of the USAID's mission in Colombo, Harold Meisler reviewed hydrologic conditions, irrigation-development activities, and water-resource data programs on the Jaffna Peninsula of Sri Lanka. Particular concerns were areas of salt-water intrusion and upconing and unquantified ground-water discharge to the sea. Meisler (1977) concluded that recharge was considerably greater than previously thought and that discharge to the sea was not a significant element of the water balance. He suggested extensions of the data collection and analysis activities that would contribute to development of a water-management plan.

SUDAN

A. H. Chidester, T. H. Kiilsgaard, H. G. Rodis, A. P. Marranzino, and F. X. Lopez visited Sudan to develop specific project plans for a joint USGS-Sudan Geological and Mineral Resources Department (GMRD) program. The team recommended (1) a regional geology-cartography project to produce a reconnaissance geologic map of Sudan; (2) a more detailed geologic study of the Nuba Hills; and (3) a water resource study. The country geologic map will be based on available data, Landsat imagery, and supplemental field work. In addition

to ascertaining stratigraphy, structure, and mineralized areas, the Nuba Hills project will serve to provide specialized training of staff and upgrading of analytical laboratories. The water project will assess the country's water resources and establish a data-processing system that will contribute to efficient water management. The work was funded by USAID.

Water data and information management

H. C. Rodis visited Sudan to assist in the development of a joint program of earth-science studies between the USGS and Sudanese resource agencies. From a review of current methods and available documentation and by discussions with a number of key people in Sudanese water agencies, he developed a set of recommendations for updating methods of collecting, codifying, managing, and disseminating water data and information to meet the objectives and resource-management needs.

TURKEY

Morris Deutsch, through a detail to the United Nations, advised the Turkish Government on methods and techniques of multispectral image handling and trained their personnel in the techniques. In a similar assignment F. A. Kohout served as consultant in ground-water hydrology to the Turkish State Hydraulic Works.

YEMEN

Ground-water survey activities

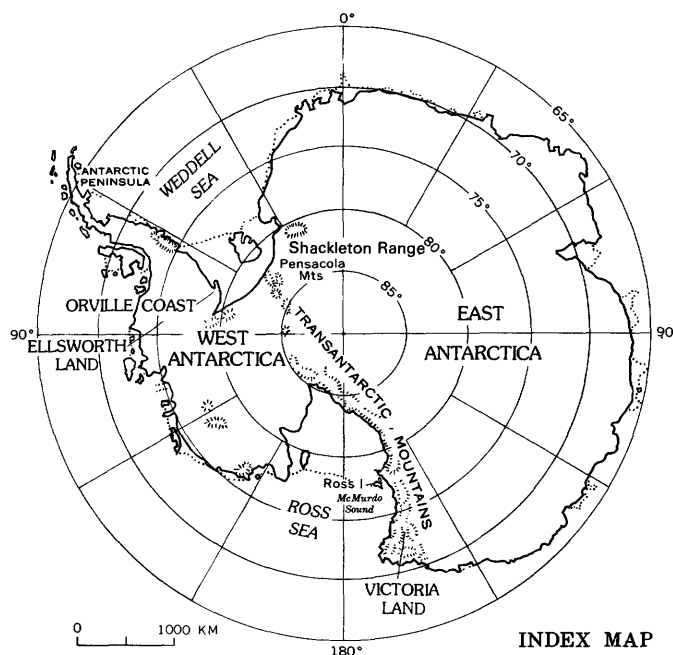
G. C. Tibbitts, Jr., under an agreement between USGS and USAID and in cooperation with the Ministry of Agriculture and the Mineral and Petroleum Authority of the Yemen Arab Republic, essentially completed the test-drilling phase of the ground-water appraisal effort in the Amran Valley. Observation-well networks in the Amran and Sana basins were maintained. Two professional counterparts were given in-country on-the-job training and seven geology students from Sana University continued, for the third summer, to receive geohydrologic field experience. Tibbitts' involvement with the project terminated late in the year. Test-drilling results indicated that there is sufficient water for both agricultural and municipal use in the Amran Valley, but ground water in the Sana Basin should be reserved for municipal use.

YUGOSLAVIA

In Yugoslavia, field work on four projects has been completed, and data analysis and preparation of reports are underway. Two USGS project officers visited Yugoslavia to review and develop plans for final scientific reports. Additional funds were allocated by the Joint Board for the preparation of the reports, and to pay for travel to the United States by the Yugoslav Principal Investigator to work with USGS counterparts on problems of data analysis and interpretation.

ANTARCTIC PROGRAMS

The Survey supports the operation of the Worldwide Standardized Seismograph Network station at the South Pole. Because of its unique location, this station, which provides essential azimuth control for many epicenter solutions in southern latitudes, receives special treatment. Because Antarctic personnel normally rotate annually, new station operators must be trained every year. Each fall the Albuquerque Seismological Laboratory (ASL) gives two part-time observers instructions in seismogram interpretation, instrument maintenance, and communication techniques. During their Antarctic tour of duty, these observers keep the South Pole seismographs in working order, determine earthquake arrival times and amplitudes, and report their readings to the USGS in Golden, Colo., via radio-telegraph.



A team of USGS geologists and topographic engineers carried out investigations along the Orville Coast at the southern end of the Antarctic Peninsula (see index map) during the austral summer 1977-1978. This area of about 30,000 km² was the last remaining large area of previously unvisited mountains on the continent. The 1977-78 fieldwork therefore essentially completes the reconnaissance geological mapping of the major exposed bedrock parts of Antarctica, an international program carried out by many Antarctic Treaty signatory nations beginning mainly in the 1959-60 austral summer. Work in the Orville Coast was carried out by ski and snowmobile traverses from tent camps, with logistical support by U.S. Navy personnel operating LC-130 (Hercules) ski-equipped aircraft based at McMurdo Station near McMurdo Sound. The work in the Orville Coast area extended earlier USGS studies of the Lassiter and Black Coasts in contiguous areas to the north.

In addition to the Orville Coast field study, work also continued on map compilation, data reduction, and laboratory studies on the petrology, geochemistry, geochronology, and paleontology of material collected during previous USGS expeditions in the Transantarctic Mountains and Antarctic Peninsula. These continuing studies and the fieldwork in Antarctica, which are part of the U.S. Antarctic Research Program (USARP), are conducted in cooperation with the Division of Polar Programs of the National Science Foundation.

Exploration of the Orville Coast of the Antarctic Peninsula

Reconnaissance geologic mapping of the Orville Coast was completed during the 1977-78 field season by P. D. Rowley (USGS), P. E. Carrara (USGS), Karl Kellogg (USGS), J. M. Boyles (University of Texas at Austin) T. S. Loudon (University of Wisconsin at Oshkosh), M. R. A. Thompson (British Exchange Scientist, British Antarctic Survey, Cambridge), and W. R. Vennum (California State College, Sonoma, at Rohnert Park). The Orville Coast is geologically similar to the previously explored Lassiter Coast (Williams and others, 1972) and northeast and eastern parts of Ellsworth Land (Laudon, 1972) that lie on strike respectively to the north and to the west.

The Orville Coast is made up of folded and thrust-faulted richly fossiliferous black shale and sandstone of the mostly Upper Jurassic Latady Formation and intertonguing volcanic rocks of silicic to intermediate composition. The sedimentary and volcanic

sequence is intruded by Upper Cretaceous Andean-type granodioritic to gabbroic stocks.

The mapped areas are here described from north to south across strike. In the northern part of the coast, the Tollefson, Olander, and Horner Nunataks area consists of Jurassic volcanic rocks that are interpreted to represent part of a former magmatic arc along the interior of the present Antarctic Peninsula. The volcanic rocks also predominate in the Sky-Hi Nunataks and the northern and central Sweeney Mountains, where they mark the southern edge of the arc. In the southern Sweeney Mountains, the volcanic rocks intertongue with the Latady Formation, which here was deposited in swamps and deltas of a marine seaway. The sedimentary and volcanic rocks of this area, and also in the Witte and Shelton Nunataks farther south, are intruded by calc-alkaline stocks of Andean type. Porphyry-type copper mineralization (noneconomic) of a granodiorite pluton in the southeastern Sky-Hi Nunataks is similar to the Lassiter Coast copper deposit (Rowley and others, 1977). In the Hauberg and Wilkins Mountains and nunataks east of the Wilkins Mountains, all rocks belong to the Latady Formation and probably were deposited in deltaic and other nearshore marine environments. Ammonite-bearing black shale of a fine-grained more seaward facies of the Latady occurs at Cape Zumberge, the southernmost exposure of the Orville Coast and located about 200 km from northernmost exposures at Horner Nunatak.

The field party also visited parts of eastern Ellsworth Land to map some areas that had not been previously explored and to conduct more detailed studies on some areas that were mapped before (Laudon, 1972). This work included remapping of a small diorite batholith in the Merrick Mountains; study and collection of Middle Jurassic marine fossils from the Latady Formation in the southern Behrendt Mountains; and the discovery and mapping of a large granodioritic stock west of the Behrendt Mountains. In the Merrick and southern Behrendt Mountains, the Latady is interbedded with silicic to intermediate volcanic rocks.

Geologic comparison of the Pensacola Mountains and Shackleton Range

The Pensacola Mountains and nearby Shackleton Range are both generally considered to belong to a late Proterozoic and Cambrian geosynclinal belt that was involved in the early Paleozoic Ross orogeny, which is recorded nearly everywhere in the Transantarctic Mountains. A. B. Ford participated

in studies of the Shackleton Range by the 22nd Soviet Antarctic Expedition (1976-77) for geologic comparisons with the Pensacola Mountains, which had been studied since the 1962-63 summer by teams of USGS geologists. Although upper Proterozoic flyschlike sequences of graywacke and slate in both mountain areas are probably correlative, they seem to record considerably different marine environments, and there is strong uncertainty that the Ross orogen, which is well documented in the Pensacola Mountains, is also recorded in the Shackleton Range (Ford, 1977a and 1977b).

Baseline soil investigations in the Pensacola Mountains

The area of Pensacola Mountains is probably one of the most pristine regions left on earth and probably less contaminated by humans than even many other parts of Antarctica. It is expected that there will be increased activity in this area in the near future by multinational parties. In order to monitor the rather certain resulting contamination in the area, soil samples were collected in December 1976 during geological studies of the Dufek Massif area. The samples were obtained, using aseptic methods, from soil areas that were believed not to have been visited previously. The samples were taken to McMurdo Station for immediate processing for microbiological content by B. C. Parker (Department of Biology; Virginia Polytechnic Institute and State University, Blacksburg, Virginia). Fungi were found to be rare components of the microbiota, which is dominated by heterotrophic aerobic bacteria (Parker and others, 1977). The results of these studies and earlier studies on soils collected in 1974 by A. B. Ford in the Cordiner Peaks and Forrestal Range (Cameron and Ford, 1974) will provide baseline data for monitoring possible future contamination in this region.

Antarctic paleobotany and coal

Coal deposits used for coking in steelmaking in Europe and North America were formed from plants with large amounts of sclerotic (thick-walled) tissue that changed into thick bands of vitrain, the most important ingredient for the coking process. Coal deposits of Gondwanaland are notably lacking in thick vitrain, as suggested by J. M. Schopf (1977) on the basis of a newly reported deposit of permineralized peat of Permian age on Mount Augusta in the Queen Alexandra Range of the Central Transantarctic Mountains. Plant structures are exceptionally well preserved in this deposit and show a

deficiency of sclerotic tissue. Glossopterid plants that are dominant in the fossil assemblage had fast-growing tissues composed of cells with thin walls. Glossopterid roots identified as species of *Vertebraria* are principal components of the deposit. An association dominated by *Glossopteris* characterizes many deposits of Gondwana coal, but preservation elsewhere is obscure. The unusual occurrence at Mount Augusta suggests that the lack of thick vitrain in Gondwana coals results from an absence of contributing thick-walled plant tissues.

Continued study of plant microfossils from coal measures of the Transantarctic Mountains strongly suggests a basis for stratigraphic zonation according to Schopf and R. A. Kyle (Ohio State University). Monosaccate pollen dominates the glacial sediments and striate and non-striate pollen characterize Upper Permian deposits. Other types of microfossils distinguish the Lower Triassic. Microfossil preservation is regrettably unpredictable and a small portion of samples provide identifiable material (Kyle and Schopf, 1977).

Other Antarctic paleobotanical studies are in progress in description of an Osmundaceous stem (Triassic) from Fremouw Peak. A new species of *Drepanophycus* (Devonian) was recently discovered in Marie Byrd Land, West Antarctica, and referred for determination to J. M. Schopf by John Wilbanks (Texas Tech University). These are the first fossils from that area.

Geologic and geophysical studies of the contact of the Dufek intrusion, Pensacola Mountains

The contact of the layered gabbroic Dufek intrusion is everywhere covered by ice, except for a single small locality in the Forrestal Range where an intrusive contact with Devonian quartzite is exposed (Ford, 1976). Detailed gravity surveys were carried out by A. W. England and W. H. Nelson in the 1976-77 field season in order to define the extent of the body near Dufek Massif more closely than was possible during earlier (1965-66) reconnaissance geophysical surveys. This work shows that the contact lies about 10 km south of Dufek Massif, under Jaburg Glacier, and swings northward to near the northern flanks of the Brown Nunataks (England and Nelson, 1977). Geologic mapping in 1976-77 by A. B. Ford, W. H. Nelson, G. K. Czamanske, C. J. Nutt, and Christine Carlson shows that, in contrast to regularity of cumulus layering elsewhere, the gabbroic rocks of Brown Nunataks are highly heterogeneous, commonly have a breccia-like appearance, and many are free of visible evidence for

cumulus origin. The heterogeneous breccia-like rocks are tentatively interpreted as being magmatic slump deposits shed off a nearby steep contact wall (Ford and others, 1977). These geologic relations there-

fore support the geophysical inference that the contact lies near the nunataks rather than 10 km to the north as suggested by the 1965-66 geophysical reconnaissance.

TOPOGRAPHIC SURVEYS AND MAPPING

FIELD SURVEYING

AERIAL PROFILING OF TERRAIN

The Aerial Profiling of Terrain surveying system is a three-coordinate scheme of reference to be used in a light aircraft; accuracy is expected to be 0.15 m vertically and 0.6 m horizontally. Design of the system was prompted by a need for obtaining terrain profiles for floodplain delineation, but other potential field applications include establishing control points for new maps or test points for evaluating the accuracy of old maps. The system under construction consists of the following modules:

- Inertial measuring unit to continuously provide the aircraft's latitude, longitude, and elevation; the unit incorporates the best available integrating gyroscopic accelerometers.
- Laser tracker to measure distances and angles to ground retroreflectors, for airborne calibration and periodic updating of the inertial measuring unit.
- Laser altimeter to measure the ground profile.
- Computer to process and adjust the measurements and provide inflight guidance.
- Tape recorder to store the profile data and imagery.

Operational procedures are to (1) establish a calibration line in the survey area with three reflectors positioned with conventional surveying methods, (2) level, orient by gyrocompassing, and stabilize the on-board instrument system at a local airport, (3) fly over and measure the calibration line to adjust the inertial measuring unit to the local datum, (4) fly the required terrain profiles, (5) re-fly the calibration line to verify and correct system performance, and (6) return to the airport for post-mission processing.

MINIMUM SAFE ALTITUDE WARNING PROJECT

USGS provided support to the Federal Aviation Administration in developing its Minimum Safe Al-

titude Warning System. In Los Angeles the project located manmade obstacles, such as buildings, towers, and tanks, within 12 m (40 ft) horizontally and 3 m (10 ft) vertically in a 33,000-km² (12,800 mi²) area centered on Los Angeles international airport. Most of the obstacles were measured in a photogrammetric system; stereomodels were set on a digitized stereoplotter, and the base and top altitudes of all visible buildings and obstructions over 30-m (100 ft) high were read. The model coordinates were fitted to the map points horizontally and vertically in a least-squares adjustment. A similar project determined the x, y, and z coordinates of the high-terrain point in each 4 nmi² (14 km²) bin within a radius of 60 nmi (111 km) of the Des Moines, Iowa, municipal airport.

SPECIAL LEVELING PROJECTS

Several special leveling projects are in progress to support ground deformation studies. Practically all of Southern California, an area of about 4,000 km², was leveled to first-order standards with eight parties supplied by USGS. The project covered a large area with a precise survey in a brief time span. The data are being used to study crustal movement and may assist in predicting earthquakes in the area.

Use of HP-97 programable printing calculators to record and check observations at each instrument station speeds up fieldwork. The calculator computes the difference between high and low scale rod readings, the backsight-foresight distance, and the elevation changes, and prints a complete record. By eliminating hand calculations, progress is faster, and the reduced data are free from blunders.

The USGS ran 150 km of second-order leveling to monitor crustal movement and land subsidence in The Geysers geothermal area of northern California and ran 185 km of first-order leveling in Yellowstone National Park in a study of ground deformation relating to volcanic and tectonic activity within the park.

PHOTOGRAMMETRY

MAPPING FROM HIGH-RESOLUTION HIGH-ALTITUDE PHOTOGRAPHS

High-altitude photographs were taken with two films to determine whether their resolution permitted compilation of standard 7½-min quadrangle maps with 20-foot contour intervals. Bar targets were placed on the Poncha Springs, Colo., quadrangle, an area containing a variety of topographic features. One camera contained Kodak 2402 film; the other, SO-022.

From microdensitometer profiles of the bar targets on diapositives of the two films, sharpness of the two films was compared and information on image motion was obtained. The profiles of targets on SO-022 film had steeper slopes, indicating that the SO-022 diapositives had higher sharpness. On both films, slopes on the density profiles were steeper for targets with bars transverse to the light of flight.

The higher resolution SO-022 film was selected for map compilation, which was evaluated against standard compilation with low-altitude photographs. Results indicate that 1:80,000-scale high-resolution high-altitude SO-022 photographs are marginal for 20-ft contour interval mapping.

RESOLUTION MEASUREMENTS WITH STAR AND BAR TARGETS

The resolution of aerial cameras is usually determined in a laboratory. Permanent resolution targets, standard bar and Siemens star, have been painted on the roof of the USGS National Center to measure resolution obtained practically. A low contrast ratio of 2.5:1 simulates the contrast normally obtained in photographs used for mapping. Earlier similar studies using target arrays with a ground contrast of 16:1 showed that the star resolution values were 3 to 6 percent higher than for bar target values, depending on differences in film type.

MICRODENSITOMETER STUDY OF SUBMERGED MARINE FEATURES

Landsat imagery of the Chagos Archipelago in the Indian Ocean revealed a major reef 8 km long that was not portrayed on the published nautical chart revised in August 1976.

From microdensitometer profiles of the newly discovered reef, later named Colvocoresses Reef, its depth was estimated. Profiles were compared with

those of a surveyed reef, Speakers Bank. Twelve scans were made with three assumptions: (1) The bank and the reef have similar reflectance characteristics, (2) both have remained relatively stable over the last 140 years since the first survey was made, and (3) soundings of the bank shown on the revised Chagos Archipelago nautical chart are correct.

The central portion of Colvocoresses Reef and the northwest portion of Speakers Bank gave correspondingly high density peaks. Since 11 m is the shallowest sounding shown in the northwest portion of the revised map and is also in the same location on the original chart, it was estimated that the central portion of Colvocoresses Reef lies at a depth of 11 m.

COMPARISON OF LANDSAT IMAGE PRODUCTS

The information content of Landsat cartographic products was studied with respect to the various types of image enhancement each had received. Forty landmarks chosen from USGS topographic maps of the northern Virginia area were compared with the corresponding points on four differently processed Landsat images of the Upper Chesapeake Bay, scene number E-1080-15192, recorded in 1972. The images in order of decreasing image detail are:

- 1:250,000-scale edge-enhanced color composite, bands 4, 5, and 7, in Cromalin color proof form, processed by IBM.
- 1:1,000,000-scale EDIES color composite transparency, bands 4, 5, and 7, by EROS Data Center.
- 1:500,000-scale precision-processed color composite, bands 4, 5, and 7, lithoprint by USGS, 1976.
- 1:500,000-scale conventional color composite, bands 4, 5, 6, and 7, lithoprint by USGS 1973, experimental edition.

The variations in detectability of selected features on the small-scale images indicate that enhancement materially increased the informational content of the images. It also indicates that edge enhancement, although it causes a few spurious signals, further increases the interpretability of cultural and natural features that have continuous edges. An unexpected finding is that one-dimensional edge enhancement approaches the results obtained by two-dimensional edge enhancement.

PHOTOIMAGE MAPPING

SIMULATING COLOR IN IMAGE MAPS

Producing color image maps by combining and assigning colors to the visible and infrared bands of black-and-white aerial film is a result of using a similar technique to produce 1:500,000-scale satellite image maps from two or more bands of imagery recorded by the Landsat multispectral scanner (MSS). Experiments indicated that MSS bands 5 and 7 are sufficient to portray the major themes of vegetation, water, and culture. Therefore, if two aerial films are filtered to have spectral responses similar to those of MSS bands 5 and 7 and simultaneously exposed, it should be practical to rectify, register, and print a 1:24,000-scale color image map in a rendition similar to that of multilayer color film. The resulting map should overcome the weaknesses of high-altitude color photographs—poor contrast and color rendition caused by atmospheric scattering. Moreover, most mapping organizations are not equipped to process color photographs. It is therefore significant that virtually no equipment changes are needed to produce color image maps from black-and-white film.

After experimenting with simulated color-infrared projects, USGS was asked by the U.S. Customs Service to try producing a simulated natural-color composite of a strip of the Canada-United States border from St. Regis, N.Y., to the Maine-New Hampshire stateline. The same halftone positives used to make a simulated color-infrared proof of the border area were used to produce the simulated natural-color proof. In simulated color-infrared rendition the panchromatic image was printed in yellow and magenta and the infrared image, in cyan; in the simulated natural-color rendition the panchromatic image was printed in yellow, cyan, and black and the infrared image, in yellow and magenta. The resulting map exhibits sharper tonal contrast and better resolution than equivalent high-altitude natural-color or color-infrared photographs. Color image maps make excellent companion maps to corresponding line maps and could eventually be incorporated into the USGS orthophotomapping program.

PHOTOBASE MAPPING

Photogrammetric map compilation and color-separation scribing become one operation with the aid of a photographic base. Clearly identifiable plani-

metric features are compiled monoscopically by final scribing on a photobase made from an orthophotoquad. Contours, single-line drainage, and other features not clearly visible on the photobase are compiled from low-altitude stereomodels scaled to the photobase. The operation has a definite sequence so that problems of workflow and register are reduced.

During the first half of fiscal 1978, 6,941 km² (2,680 mi²) of photobase mapping was compiled at 1.8 h/km² (4.7 h/mi²). A cost study, based on four projects in three States, indicates savings of \$2,000 per quadrangle compared with conventional procedures. Formal horizontal accuracy tests indicate that the line maps thus produced meet national map accuracy standards.

SATELLITE IMAGE MAPPING

In Saudi Arabia a Landsat scene of Jiddah was enlarged from 1:1,000,000 to 1:250,000 scale. Map control was obtained from published line maps. Points identifiable on both the maps and the Landsat image were used as control to enlarge the image and to fit a graticule to it.

In Nigeria an image map was requested to evaluate sites for Nigeria's new federal capital territory. The project involved not only production of the image map but also instruction of two Nigerian cartographers in the techniques used, including selection of control, control measurements, and adjustment. Materials supplied by the Nigerian government included a 1:100,000-scale map covering the entire federal capital territory, 1:50,000-scale maps covering portions of the territory, and aerial photographs covering known geodetic control points.

Three Landsat images that show the maximum extent of ice covering the Chesapeake Bay and Washington, D.C., vicinity during the winter 1976-77 were processed as a color image map at 1:500,000 scale. Two images, recorded February 7, 1977, covered a 100-mi swath from the north edge of the Dismal Swamp to the south edge of Wilmington, Del., when mosaicked together. The third image, recorded February 8, 1977, and centered on Washington, D.C., is on the side of the mosaic. This experimental image map was prepared from images digitally enhanced with the EROS Digital Image Enhancement System to emphasize ice distribution, a dominant features of the scenes, and it demonstrates Landsat capability to record temporal phenomena of general interest.

CARTOGRAPHY AND DESIGN

METRIC QUADRANGLE MAPS

The Saranac Lake, N.Y., quadrangle is the first of a series of metric topographic maps being prepared on a new format. The new design covers $7\frac{1}{2}$ -min latitude by 15 min longitude at 1:25,000 scale, uses newly designed symbology generally compatible with digital cartographic data bases, and has a re-designed map border.

In addition to traditional data such as the credit legend, bar scale, contour interval, and declination diagram, the map displays a legend explaining topographic map symbols and a metric-customary unit conversion table. All map elements—grid, contours, elevations, distances, and bathymetry—appear in metric form. The only recognition of U.S. customary units is the use of dual bar scales that retain miles and feet as well as kilometers and meters.

ONE-METER CONTOUR INTERVAL MAPPING

Maps of some areas of the country, primarily in the coastal zones, may require a 1-m contour interval to properly depict the hypsographic features. To determine the time and cost for producing 1-m contours, two projects are being compiled by different methods. The Nanticoke, Md., project, comprising six $7\frac{1}{2}$ -min quadrangles, is being compiled by field surveying methods; the Golden Hill, Md., project, comprising four $7\frac{1}{2}$ -min quadrangles, is being compiled by usual methods (153-mm focal length, flight height 1,500 m). Comparisons will be made only after assurance that vertical accuracy requirements of the National Map Accuracy Standards have been met. The areas selected are representative of the general landform types that require 1-m contours, that is, primarily tidal marshes and low-lying farmland.

SPACE OBLIQUE MERCATOR PROJECTION

Since Landsat and other Earth-viewing satellites have been launched in near-polar orbits, a conformal map projection suited to the imagery obtained has been needed. The satellites obtain a narrow strip of imagery (186-km wide) in an oblique spiral around the Earth.

The Space Oblique Mercator projection is a cylinder that moves to maintain contact with the satellite ground track on a rotating Earth and permits continuous true-to-scale mapping of satellite imagery. The ground track serves as the "prime

meridian" of the projection, which is conformal within a few degrees of the track. Two sets of equations have been formulated—one set treats the general case of any polar-orbiting satellite; the other set is specifically applied to Landsat.

The computations designed specifically for Landsat consist of three solutions; forward, inverse, and satellite groundtrack. The forward solution converts geodetic latitudes and longitudes into x and y coordinates. The inverse solution converts x and y coordinates into geodetic latitudes and longitudes. The satellite groundtrack solution yields the geodetic latitude and longitude of a point on the groundtrack given the corresponding transformed longitude. The transformed longitude is the angle that measures the progress of the satellite's orbit, 360 degrees describing one complete orbit.

DIGITAL CARTOGRAPHIC APPLICATIONS

The development of cartographic data in digital computer-compatible form is the goal of the Digital Cartographic Applications Program (DCAP). Emphasis is on providing data at an accuracy and level of detail equivalent to that of $7\frac{1}{2}$ -min 1:24,000-scale topographic maps. In addition, the program is developing a small-scale digital data base that can be used for preparing special graphic products and for generating index and status maps. Until the small-scale data base is fully developed, some current small-scale data bases, such as World Data Bank II, can meet immediate needs.

Principal types of base category data include (1) coordinate reference systems, (2), hypsography, (3) hydrography, (4) surface cover, (5) non-vegetative features, (6) boundaries, (7) transportation systems, (8) geodetic control, and (9) geographic names. During implementation of DCAP, coordination of formats and codes to enable other agencies to incorporate nonbase category data into the system must be considered.

HARDWARE

A wide variety of hardware and software contribute to an operational digital cartographic production capability. Digital map data can be collected simultaneously with the graphic data during photogrammetric stereocompilation of a map. Six analytical stereoplotter systems compile contour maps and collect both digital and graphic hypsographic and planimetric data from stereomodels. Each system comprises an optomechanical stereo-

viewer and a coordinatograph interfaced to a small general-purpose computer.

Six Altek AC189 digital data acquisition systems were purchased for use with Kern PG2 and Wild B8 analog stereoplotters. These three-axis systems feature both point and stream modes of data collection and independent scaling and translation of each of the data axes.

Increasing needs for orthophotographs and digital hypsographic data led to development of the Digital Profile Recording and Output Systems (DPROS), which collects profile data from stereomodels in stereoplotting instruments. The profiles are intended primarily for automated control of orthophoto production; however, they can later be computer processed to produce digital elevation files.

Two Gestalt Photo Mappers (GPM-2) produce orthophotographs and contour plots on photographic film and simultaneously record digital elevation data on magnetic tape. The elevation data are processed off-line to produce digital elevation files.

Map features such as public land surveys and political boundaries are not directly visible on aerial photographs. Moreover, thousands of published maps must be digitized. USGS currently has six Instronics Gradicon digitizing systems that output point and stream data on punch cards and magnetic tape. The units have microcomputer controllers for independent translation, scaling, and rotation of each axis for processing of the raw digital data before editing.

All digital map data must be edited to remove or correct errors or to revise established files as new data become available. Two digital Data Edit Systems each include three (expandable to eight) editing stations with digitizing tables and stereoplotters—all interactively interfaced with a single control processing computer. System software provides the capability to reformat data, add or delete points and lines, change the position of data, add or revise descriptive header data, or collect new data.

Six digitally controlled automated drafting systems draw computer-generated thematic line graphics, line screens, map base sheets, map collars, index graphics, and verification plots. To encode geographic name information and tag data during collection with two- and three-axis acquisition systems, USGS purchased Voice Data Entry Terminal Systems.

One current area of hardware research is an automated map digitizing system to convert feature separates from the more than 40,000 published 7½-

min maps into digital data. A map scanning and processing system is under consideration.

A second area of hardware research is high-density archival storage. Conventional magnetic storage media deteriorate unless the data are used frequently, and other techniques such as computer bubble memory, video disk, and holographic storage are being studied. Some systems under development also have the required storage densities of 10^{10} to 10^{12} bits.

SOFTWARE

Software development is highly diverse and includes the file management system to keep track of digital data in production, resampling, and reformatting data derived from different sources, topological encoding, batch editing to verify data, and graphic composition to prepare data for plotting. Major emphasis has been on developing the Unified Cartographic Line Graph Encoding System for using the manual digitizers to produce topologically encoded data. Considerable automated editing and verifying of the raw data is done according to topological characteristics.

DIGITAL CARTOGRAPHIC DATA FILES

Digital cartographic data files may be Digital Elevation Models (DEM), sampled arrays of elevations for a number of ground positions, or Digital Line Graphs (DLG), line map information in digital form. DLG data files include information on planimetric base categories, such as transportation, hydrography, and boundaries.

DEM FILES

The DEM files may be built from such data sources as contour plates, profiles, or terrain models scanned in stereophotogrammetric equipment, or digitizing orthophoto equipment. The file structure accommodates data acquired from all sources and provides a standard format for data users.

The DEM data are classified at three levels depending on editing, enhancement, and spatial structuring.

- DEM-1.—A network of raw elevation data edited only for gross blunders and not keyed to planimetry.
- DEM-2.—Elevation data smoothed for consistency, enhanced to remove noise, and filtered to reduce data volume; not keyed to planimetry.

- **DEM-3.**—Elevation data edited and modified to be consistent with planimetric features, such as streams, roads, and shorelines.

For most users of digital elevation data the DEM-2 level will be the principal product.

A DEM file is organized into a series of three logical records: (1) Information defining the general characteristics of the particular DEM, (2) elevation data and associated information, and (3) other information, such as accuracy parameters, source materials, and method of data collection.

The area covered by a DEM file is divided into patches made up of the data points. The DEM data are given in an arbitrary x, y coordinate system with an angle given to relate to a defined ground coordinate system, X, Y. The ground coordinates X, Y of the first elevation point in each regular array patch are given. For a random point distribution within the patch, the logical record contains the x, y coordinates for each elevation point. Elevations are referred to the National Geodetic Vertical Datum of 1929.

DLG FILES

The DLG files may be formed from such data sources as stable-base map separates or stereo-models in digitizing photogrammetric equipment. Both manual and automated digitizing may be used. The file structure will accommodate data acquired from all sources and provide a standard format for data users.

DLG data, like DEM data, are classified at three levels depending on editing, enhancement, and spatial structuring:

- **DLG-1.**—Line map information collected and coded to prescribed standards and edited to remove acquisition blunders.
- **DLG-2.**—Line map information edited to add attribute codes and to remove visible errors and inconsistencies.
- **DLG-3.**—DLG-2 information spatially structured to define all topological relations.

DLG-2 data are sufficient to produce a graphic output, but to support geographic information systems and automated spatial analysis, DLG-3 data are required.

All DLG data from 1:24,000-scale maps currently being collected in pilot projects are in the DLG-3 file format, using the United Cartographic Line Graph Encoding System.

FILE MANAGEMENT

For orderly growth of digital cartographic activities, an effective data management system is crucial. The first phase of a system for managing data at the file level has been completed. The management system is planned as the primary tool for public dissemination of digital cartographic data through the National Cartographic Information Center (NCIC).

The factor that most affects the form of the Digital Cartographic File Management (DCFM) system is data volume. The two GPM-2 systems are generating DEM files for 5,000 to 6,000 stereo-models annually. Considering that each model contains about 750,000 16-bit elevation points, 7×10^{10} bits of information are generated from this source alone. With increased collection of files and manual scanning of terrain elevation with the DPROS, capacity to generate digital cartographic data is approaching 10^{11} bits of information annually. The state-of-the-art in data base technology precludes effective management of this large quantity of data at the information record level (that is, individual elevations or line segments); therefore, the objective of the DCFM is to manage at the data collection, DEM or DLG, level. In the context of selective processing of information from a large data store, the DCFM performs as a staging mechanism. It brings to the user a manageable portion of the data store that contains the information records for his immediate needs.

Data volume was also instrumental in the choice of high-density magnetic tape as the archival storage medium. At 6,250 bpi recording density, a standard 2,400-ft 9-track tape can hold 10^9 bits of information. Therefore, the present annual digital cartographic output can be stored on 100 magnetic tapes. While this is a workable solution for the near future, the certain increase in digital activities and the undesirable archival characteristics of magnetic tape are leading to examination of mass storage requirements and mediums.

PILOT PRODUCTION PROJECTS

Current pilot projects for digital production are:

Coal Research Project.—33 7½-min quadrangles in Kentucky, Montana, Virginia, West Virginia, and Wyoming have been digitized for the Geologic Division in support of the National Coal Resource Data Bank. The data provided are digital elevation models, boundaries, and public land net.

Idaho Forestry Project.—180 7½-min quadrangles and 32 15-min quadrangles in central Idaho have been digitized for NASA and the State of Idaho to support a multistage inventory of the forestry resource. Data provided are public land net, boundaries, and forest ownership in five classes. The ownership was delineated by the State of Idaho.

BLM/FS/FWS.—38 7½-min quadrangles in Oregon are being digitized to support a joint Bureau of Land Management, Forest Service, and Fish and Wildlife Service management information system related to land records. The principal data categories are public land net, boundaries, hydrography, and transportation.

BLM California Desert.—The public land net and boundaries on 400 quadrangles are being digitized for an area in southeastern California to support a land management plan for the BLM California Desert Planning Staff.

DOE/NOAA.—Several categories of data are being digitized at 1:500,000 scale for the entire State of Idaho to support geothermal energy evaluations of the Department of Energy and the National Geophysical and Solar Terrestrial Data Center of the National Oceanic and Atmospheric Administration. The categories are hydrography, boundaries, transportation, significant manmade features, and the public land net. The data from this project will be at DLG-2 level. A research activity associated with

this project will investigate the use of control points from large-scale materials to improve the positional accuracy of the digital data files.

APSRs.—A series of State-oriented base maps are being prepared for NCIC using small-scale digital cartographic information in the Aerial Photography Summary Record System for automated preparation of index maps showing aerial photography coverage.

Boone County, Illinois.—The hydrography, boundaries, transportation, and public land net are being digitized. The data will be evaluated for use with census data.

USFS-DEM.—Two quadrangles of DEM data in southeastern Idaho are being formatted for the Forest Service to allow them to evaluate use of the data in their programs.

Montana 1:100,000-scale Project.—The Great Falls, Mont., 1:100,000-scale quadrangle was digitized for the State of Montana. Data categories include public land net, transportation, and hydrography.

Data from the contour plate of the Jewell Ridge, Va., 7½-min quadrangle were digitized with an automatic line follower and edited on an interactive system. The DLG-2 data set contains 2.5 million points that describe the contours and provides an excellent data base for testing various algorithms requiring digitized contours.

COMPUTER TECHNOLOGY

USGS scientists continued to rely upon advances in computer technology to meet their information and computational needs during FY 1978. The Computer Center Division expanded its capacity to meet these needs, primarily through addition of peripheral system components and enhancements to software that improved throughout.

TIME-SHARING SYSTEM ACCESS

The installation of the three Multics time-sharing computers in late 1976 (at Reston, Va., Denver, Colo., and Menlo Park, Calif.) created a need for economical access to the computers from the many USGS terminals located throughout the United States and in other countries. After an analysis of this problem, the USGS acquired through the General Services Administration (GSA), the services of TYMNET, Inc. TYMNET is a communications network service providing users an easy method of accessing any of the three Multics computers.

TYMNET provides highly reliable connections between varieties of customers' terminals and computers that are interfaced to TYMNET. Access to any of the Multics computers is available and convenient via local phone calls to the nearest TYMNET access location in most metropolitan areas, and through interconnections, from other parts of the world. This service is provided at a cost that is below the current Federal Telecommunications Service or commercial rates. In essence, users can access any of the three Multics locations from any location in the United States.

TYMNET capability was installed at Reston in October 1977, and Denver and Menlo Park received their installations in November 1977.

BATCH COMPUTING SERVICES

The Reston batch computing facility reached an overload during FY 1978. Several positive steps were taken, however, to prevent the overload from

reaching catastrophic proportions and to allow essential computing services to continue.

Acquisition of additional capacity

Since the lengthy acquisition cycle has precluded the timely replacement of the Reston batch system with a machine possessing greater capability, other means were sought to accommodate increased workload. Using the Telecommunications Services Program contract administered by GSA, the USGS acquired the services of American Management Systems (AMS). The contract specifies that AMS will provide batch computing services to the USGS in the same manner as services are provided to users by the CCD. A unique feature of this approach is that all access for batch services must come through the CCD batch processor communications controller insuring that the method of accessing batch processing procedures is identical to the user, no matter whether he is accessing the Reston batch facility or AMS. Further, AMS is required to maintain complete compatibility with the Reston system insofar as critical operating software is concerned. Thus, nearly total compatibility has been achieved, and additional batch capacity is available to the user community. The AMS contract was effective on May 10, 1978.

Index Sequential Access Method (ISAM) File Processing

A significant modification to the batch system allows simultaneous execution of jobs that access ISAM files. The improved facility reserves a file for the exclusive use of a program only during a file update operation. Previously, a file was available to only one program at a time. As a result, the system overhead required to manage ISAM jobs has been materially reduced and increased throughput of such jobs has resulted.

Overhead reduction

As the demand for batch job processing has grown, the size of the remote terminal network has increased. A study was undertaken to detect areas

in which performance of system programs is critical to the fulfilling of peak user requirements. The study revealed that much overhead was a result of rigid system management programs that were designed to accommodate normal demands but were unable to adjust themselves to peak demands. A set of programs has now been implemented that is able to expand or contract its facilities and the associated overhead requirements for managing those facilities in response to load fluctuations. It is estimated that this work has produced a savings of as much as 20 percent in system overhead. This has produced better terminal responsiveness and improved throughput.

U.S. GEOLOGICAL SURVEY PUBLICATIONS

PUBLICATIONS PROGRAM

Books and maps

Results of research and investigations conducted by the USGS are made available to the public through professional papers, bulletins, water-supply papers, circulars, miscellaneous reports, and several map and atlas series, most of which are published by the USGS. Books are printed by the Government Printing Office, and maps are printed by the USGS; both books and maps are sold by the USGS.

All books, maps other than topographic quadrangle maps, and related USGS publications are listed in the catalogs "Publications of the Geological Survey, 1879-1961" and "Publications of the Geological Survey, 1962-1970" and in yearly supplements, available on request, that keep the catalogs up to date.

New publications, including topographic quadrangle maps, are announced monthly in "New Publications of the Geological Survey." A free subscription to this list can be obtained on application to the *U.S. Geological Survey, 329 National Center, Reston, VA 22092*.

State list of publications on hydrology and geology

"Geologic and Water-Supply Reports and Maps, [State]," a series of booklets, provides a ready reference to these publications on a State basis. The booklets also list libraries in the subject State where USGS reports and maps can be consulted; these booklets are available free on request to the USGS.

Surface-water, quality-of-water, and ground-water-level records

Surface-water records through water year 1970 were published in a series of water-supply papers titled "Surface-Water Supply of the United States"; through water year 1960, each volume covered a single year, but the period 1961-70 was covered by two 5-year volumes (1961-65 and 1966-70).

Quality-of-water records through water year 1970 were published in an annual series of water-supply

papers titled "Quality of Surface Waters of the United States."

Both surface-water and quality-of-water records for water years 1971-74 were published in a series of annual reports titled "Water Resources Data for [State]." Some of these reports contained both types of data in the same volume, but others were separated into two parts, "Part 1: Surface-Water Records" and "Part 2: Water-Quality Records." Limited numbers of these reports were printed, as they were intended for local distribution only. Since the data in these reports will not be republished in the water-supply paper series, reports will be sold by the National Technical Information Service.

Records of ground-water levels in selected observation wells through calendar year 1974 were published in the series of water-supply papers titled "Ground-Water Levels in the United States." Through 1955, each volume covered a single year, but, during the period 1956-74, most volumes covered 5 years.

Starting with water year 1975, records for surface water, quality of water, and levels of ground-water-observation wells are all published under one cover in a series of annual reports issued on a State-boundary basis. Reports for water year 1975 and subsequent water years appear in a series of reports entitled "Water-Resources Data for [State]"; these reports are sold by the *National Technical Information Service, U.S. Department of Commerce, Springfield, VA 22161*.

State hydrologic unit maps

State hydrologic unit maps, which are overprints of the 1:500,000-scale State base maps, show culture in black, hydrography in blue, hydrologic subdivision boundaries and codes in red, and political (FIPS county) codes in green. The Alaska State map is at 1:2,500,000 scale, and the Puerto Rico map is at 1:240,000 scale. All river basins having drainage areas greater than 700 mi² (except for Alaska) are delineated on the maps. The hydrologic boundaries depict: (1) Water-resources regions, (2)

water-resources subregions, (3) National Water-Data Network accounting units, and (4) cataloging units of the USGS "Catalog of Information on Water Data." These maps are available for every State and Puerto Rico.

State water-resources investigations folders

A series of folders entitled "Water-Resources Investigations in [State]" is a project of the Water Resources Division to inform the public about its current programs in the 50 States and Puerto Rico, the U.S. Virgin Islands, Guam, and American Samoa. As the programs change, the folders are revised. The folders are free on request as follows: For areas east of the Mississippi River, including Minnesota, Puerto Rico, and the Virgin Islands—*Branch of Distribution, U.S. Geological Survey, 1200 South Eads Street, Arlington, VA 22202*, and for areas west of the Mississippi, including Alaska, Hawaii, Louisiana, Guam, and American Samoa—*Branch of Distribution, U.S. Geological Survey, Box 25286, Federal Center, Denver, CO 80225*.

Open-file reports

Open-file reports, which consist of manuscript reports, maps, and other preliminary material, are made available for public consultation and use. Reports and maps released only in the open files are listed monthly in "New Publications of the Geological Survey," which also lists places of availability for consultation. Most open-file reports are placed in one or more of the three USGS libraries: Room 4A100, National Center, 12201 Sunrise Valley Drive, Reston, VA 22092; 1526 Cole Boulevard at West Colfax Avenue, Golden, Colo. (mailing address: Stop 914, Box 25046, Federal Center, Denver, CO 80225); and 345 Middlefield Road, Menlo Park, CA 94025. Other depositories may include one or more of the USGS offices listed on p. 365 and interested State agencies. Many open-file reports are superseded later by formally printed publications.

Microfiche and (or) paper copies of most reports can be purchased from the *Open-File Services Section, Branch of Distribution, U.S. Geological Survey, Box 25425, Federal Center, Denver, CO 80225*.

Earthquake publications

The "Earthquake Information Bulletin" is published bimonthly by the USGS to provide information on earthquakes and seismological activities of interest to both general and specialized readers.

Each issue also lists a worldwide summary of felt earthquakes and a State seismic history.

The USGS National Earthquake Information Service locates most earthquakes above magnitude 5.0 on a worldwide basis. A chronological summary of location and magnitude data for each located earthquake is published in the monthly listing "Preliminary Determination of Epicenters." The "Earthquake Data Report," a bimonthly compilation of data used in the computation of the above listing, contains station arrival times, individual distances, azimuths, and traveltime residuals. "Earthquakes in the United States" is published quarterly as a USGS circular. The circulars supplement the information given in the monthly listing "Preliminary Determination of Epicenters" to the extent of providing detailed felt and intensity data as well as isoseismal maps for U.S. earthquakes.

"United States Earthquakes [year]" is published jointly by the National Oceanic and Atmospheric Administration and the Geological Survey. This annual sourcebook on earthquakes occurring in the United States gives location, magnitude, and intensity data. Other information such as strong-motion data fluctuations in well-water levels, tsunami data, and a list of principal earthquakes of the world is also given.

PUBLICATIONS ISSUED

During FY 1978, the USGS published 5,770 maps comprising some 22,598,417 copies:

<i>Kind of map printed</i>	<i>Number</i>
Topographic	4,889
Geologic and hydrologic	544
Maps for inclusions in book reports	30
Miscellaneous (including maps for other agencies) ..	307
Total	5,770

In addition, six issues of the "Earthquake Information Bulletin," 179 technical book reports, and 85 leaflets and maps of flood-prone areas were published.

At the beginning of FY 1978, more than 101.8 million copies of maps and 2.3 million copies of book reports were on hand in the USGS distribution centers. During the year, 9,303,781 copies of maps, including 578,828 index maps were distributed. Approximately 6.2 million maps were sold, and \$5,282,767 was deposited to Miscellaneous Receipts in the U.S. Treasury.

The USGS also distributed 161,987 copies of technical book reports, without charge and for official

use, and 1,483,793 copies of booklets, free of charge, chiefly to the general public; 269,544 copies of the monthly publications announcements and 171,500 copies of a sheet showing topographic map symbols were sent out.

The following table compares USGS map and book distribution (including map indexes and booklets, but excluding map-symbol sheets and monthly announcements) during FY 1977 and FY 1978:

Number of maps and books distributed

Publication	Fiscal Year		Change (per- cent)
	1977	1978	
Maps -----	8,664,951	9,321,340	+7.5
Books -----	453,098	215,918	-109.8
Popular publications -	1,693,355	1,483,793	-14.1
Total -----	10,811,404	11,021,051	+1.9

HOW TO OBTAIN PUBLICATIONS

OVER THE COUNTER

Book reports

Book reports (professional papers, bulletins, water-supply papers, "Topographic Instructions," "Techniques of Water-Resources Investigations," and some miscellaneous reports) can be purchased from the *Branch of Distribution, U.S. Geological Survey, 1200 South Eads Street, Arlington, VA 22202*, and from the USGS Public Inquiries Offices listed below under "Maps and Charts" (authorized agents of the Superintendent of Documents).

Some book publications that can no longer be obtained from the Superintendent of Documents are available for purchase from the above authorized agents of the Superintendent of Documents.

Maps and charts

Maps and charts can be purchased at the following USGS offices:

- 1200 South Eads Street, Arlington, Va.
- 1400 Independence Road, Rolla, Mo.
- Building 41, Federal Center, Denver Colo.
- Federal Bldg.-Box 12, 101 Twelfth Avenue, Fairbanks, Alaska
- Public Inquiries Offices:
 - Rm. 108, Skyline Bldg., 508 2d Ave., Anchorage, Alaska
 - Rm. 7638, Federal Bldg., 300 N. Los Angeles St., Los Angeles, Calif.

- Rm. 122, Bldg. 3, 345 Middlefield Road, Menlo Park, Calif.
- Rm. 504, Customhouse, 555 Battery St., San Francisco, Calif.
- Rm. 169, Federal Bldg., 1961 Stout St., Denver, Colo.
- Rm. 1028, General Services Bldg., 19th and F Sts., NW., Washington, D.C.
- Rm. 1C45, Federal Bldg., 1100 Commerce St., Dallas, Tex.
- Rm. 8105, Federal Bldg., 125 S. State St., Salt Lake City, Utah
- Rm. 1C402, National Center, 12201 Sunrise Valley Dr., Reston, Va.
- Rm. 678, U.S. Courthouse, W. 920 Riverside Ave., Spokane, Wash.

USGS maps are also sold by some 1,650 commercial dealers throughout the United States. Prices charged are generally higher than those charged by USGS offices.

Indexes showing topographic maps published for each State, Puerto Rico, the U.S. Virgin Islands, Guam, American Samoa, and Antarctica are available free on request. Publication of revised indexes to topographic mapping is announced in the monthly "New Publications of the Geological Survey." Each index also lists special and U.S. maps, as well as USGS offices and commercial dealers from which maps can be purchased.

Maps, charts, folios, and atlases that are out of print can no longer be obtained from any official source. They may be consulted at many libraries, and some can be purchased from secondhand-book dealers.

BY MAIL

Book reports

Technical book reports and some miscellaneous reports can be ordered from the *Branch of Distribution, U.S. Geological Survey, 1200 South Eads Street, Arlington, VA 22202*. Prepayment is required and should be made by check or money order in U.S. funds payable to the U.S. Geological Survey. Postage stamps are not accepted; please do not send cash. On orders of 100 copies or more of the same report sent to the same address, a 25-percent discount is allowed. Circulars, publications of general

interest (such as leaflets, pamphlets, and booklets), and some miscellaneous reports can be obtained free from the Branch of Distribution.

Maps and charts

Maps and charts, including folios and hydrologic atlases, are sold by the USGS. Address orders to *Branch of Distribution, U.S. Geological Survey, 1200 South Eads Street, Arlington, VA 22202* for maps of areas east of the Mississippi River, including Minnesota, Puerto Rico, and the U.S. Virgin Islands, and to *Branch of Distribution, U.S. Geological Survey, Box 25286, Federal Center, Denver, CO 80225* for maps of areas west of the Mississippi, including Alaska, Hawaii, Louisiana, Guam, and American Samoa. Residents of Alaska can also order maps of their State from the *Alaska Distribution Section, U.S. Geological Survey, Federal Building-Box 12, 101 Twelfth Avenue, Fairbanks, AK 99701*.

Prepayment is required. Remittances should be by check or money order in U.S. funds payable to the U.S. Geological Survey. On an order amounting to \$300 or more at the list price, a 30-percent discount is allowed. Prices are quoted in lists of publications and in indexes to topographic mapping for individual States. Prices include the cost of surface transportation.

Earthquake Information Bulletin and Preliminary Determination of Epicenters

Subscriptions to the "Earthquake Information Bulletin," and the "Preliminary Determination of Epicenters" are by application to the *Superintendent of Documents, Government Printing Office, Washington, DC 20402*. Payment is by check payable to the Superintendent of Documents or by charge to your deposit account number. Single issues can be purchased from the *Branch of Distribution, U.S. Geological Survey, 1200 South Eads Street, Arlington, VA 22202*.

National Technical Information Service

Some USGS reports, including computer programs, data and information supplemental to map or book publications, and data files, are released through the National Technical Information Service (NTIS). These reports, available either in paper copies or microfiche or sometimes on magnetic tapes, can be purchased only from the *National Technical Information Service, U.S. Department of Commerce, Springfield, VA 22161*. USGS reports that are released through NTIS, together with their NTIS order numbers and prices, are announced in the monthly "New Publications of the Geological Survey."

REFERENCES CITED

- Abrams, M. J., Ashley, R. P., and Rowan, L. C., 1977, Multispectral image mapping of hydrothermally altered rocks in the Cuprite mining district, Nevada [abs.]: W. T. Pecora Symp., 3rd, Sioux Falls, S.Dak., Oct. 30-Nov. 2, 1977. Proc.
- Abrams, M. J., Ashley, R. P., Rowan, L. C., Goetz, A. F. H., and Kahle, A. B., 1977, Use of imaging in the 0.46–2.36 μm spectral region for alteration mapping in the Cuprite mining district, Nevada: U.S. Geol. Survey open-file rept. 77–585, 10 p.
- Advisory Committee on Water Data for Public Use, 1977, Summary of 12th meeting: U.S. Geol. Survey, Ofc. of Water Data Coordination, 68 p.
- Allredge, J. R., and Bolstad, D. D., 1977, GDIST: A computer code for analysis of statistical distributions of physical data: U.S. Bur. Mines, Info. Circ. 8731, 57 p.
- Allredge, L. R., 1977, Deep mantle conductivity: Jour. of Geophys. Research, v. 82, no. 33, p. 5427–5431.
- Allegre, C. J., and Condomines, M., 1976, Fine chronology of volcanic processes using ^{238}U – ^{230}Th systematics: Earth and Planetary Sci. Letters, v. 28, p. 395–406.
- Alterman, I. B., 1972, Structure and tectonic history of the Taconic allochthon and surrounding autochthons, East-Central Pennsylvania: New York, Columbia, Univ. Ph. D. dissert.
- American Society of Planning Officials, 1977, Onshore impacts of Outer Continental Shelf oil and gas development: Sourcebook; 180 p.
- Anderson, D. G., and Stokoe, K. H. II, 1977, Shear modulus—a time-dependent material property, in Dynamic Soil and Rock Testing in the Field and Laboratory for Seismic Studies, Am. Soc. Testing and Materials. [In press].
- Anderson, J. R., Hardy, E. E., Roach, J. T., and Witmer, R. E., 1976, A land use and land classification system for use with remote sensor data: U.S. Geol. Survey Prof. Paper 964, 28 p.
- Anderson, W. H., 1977, Assessing flood damage to agriculture using infrared aerial photography: U.S. Geol. Survey open-file rept. 77–175, 29 p.
- Anderson, W. L., 1977, Interpretation of electromagnetic soundings in the Raft River geothermal area, Idaho: U.S. Geol. Survey open-file rept. 77-557, 5 p., 15 figs.
- Aronson, D. A., 1976a, Preliminary selection of storm-water basins suitable for infiltration with reclaimed water in Nassau County, Long Island, New York: U.S. Geol. Survey Open-File Rept. 76–668, 39 p.
- 1976b, Evaluation of alternative methods of supplemental recharge by storm-water basins on Long Island, New York: U.S. Geol. Survey Open-File Rept. 76–470, 56 p.
- 1978, Determination of runoff coefficients of storm-water basin drainage areas on Long Island, New York, by using maximum-stage gages: U.S. Geological Survey Journal of Research, v. 6, no. 1, p. 11–21.
- Atwater, T., and Molnar, P., 1973, Relative motion of the Pacific and North American Plates deduced from sea floor spreading in the Atlantic, Indian, and South Pacific Oceans, in Korach, R. L., and Nun, A., eds., Proceeding of the conference on tectonic problems of the San Andreas fault system: Stanford Univ., Calif. Geol. Science, v. 13, p. 136–148.
- Back, William, and Lesser, J. M., 1977, Chemical constraints on ground water management in the Yucatan Peninsula, Mexico: International Association of Hydrologists Memoir, v. XIII, pt. 1, p. G18–G29.
- Back, William, Lesser, J. M., and Hanshaw, B. B., 1977, Structural and stratigraphic occurrence of “bad water” in Coahuila, Mexico [abs.]: Geol. Soc. America, Ann. mtg., p. 885.
- Baedecker, P. A., 1971, Digital methods of photopeak integration in activation analysis: Anal. Chem. v. 43, p. 405–410.
- 1976, SPECTRA, a computer code for the resolution of gamma ray spectra for instrumental neutron activation analysis: in Taylor, R. E., ed., Advances in obsidian glass studies, Noyes Press, Park Ridge, N. J., p. 334–349.
- 1977, The precision and accuracy of iterative and non-iterative methods of photopeak integration in activation analysis with particular reference to the analysis of multiplets: Jour. Radional. Chem., v. 39, p. 239–254.
- Bailey, E. H., Black, M. C., Jr., and Jones, D. L., 1970, On-land Mesozoic oceanic crust in California coast ranges: U.S. Geol. Survey Prof. Paper 700C, p. C70–C81.
- Baird, A. K., Castro, A. J., Clark, B. C., Toulmin, Priestley III, Rose, H. J., Jr., Keil, Klaus, and Gooding, J. L., 1977, Viking X-ray experiment—sampling strategies and laboratory simulations: Jour. Geophys. Research, v. 82, p. 4595–4624.
- Banks, N. G., and Page, N. J., 1977, Some observations that bear on the origin of porphyry copper deposits: U.S. Geol. Survey open-file rept. 77–127, 14 p.
- Bargar, K. E., and Muffler, L. J. P., 1975, Geologic map of the travertine deposits, Mammoth Hot Springs, Yellowstone National Park, Wyoming: U.S. Geol. Survey Misc. field studies map, MF–659, scale 1:62,500.
- Barnes, H. H., Jr., and Jennings, M. E., 1977, Urban storm-water investigations in progress by the U.S. Geological Survey: Metropolitan sanitary district of Greater Chicago workshops on water-quality surveys, April 20–22, 1977, spec. pub., p. D1–D9.
- Bates, T. F., and Strahl, E. O., 1957, Mineralogy, petrography, and radioactivity of representative samples of Chattanooga shale: Geol. Soc. America Bull., v. 68, p. 1305–1314.
- Beckinsale, R. D., and Gale, N. H., 1969, A reappraisal of the decay constants and branching ratio of ^{40}K : Earth and Planetary Sci. Letters, v. 6, p. 289–294.

- Berg, H. C., Elliott, R. L., Koch, R. D., Carten, R. B., and Wahl, F. A., 1976, Preliminary geologic map of the Craig D-1 and parts of the Craig C-1 and D-2 quadrangles, Alaska: U.S. Geol. Survey open-file rept. 76-430, 1 sheet, scale 1:63,360.
- Berg, H. C., Elliott, R. L., Smith, J. G., and Koch, R. D., Geologic map of the Ketchikan and Prince Rupert quadrangles, Alaska: U.S. Geol. Survey open-file rept. 78-73-A, 1 sheet, scale 1:250,000. [In press].
- Berg, H. C., Jones, D. L., and Richter, D. H., 1972, Gravina-Nutzotin belt-tectonic significance of an upper Mesozoic sedimentary and volcanic sequence in southern and southeastern Alaska, in *Geological Survey Research 1972*: U.S. Geol. Survey Prof. Paper 800-D, p. D1-D24.
- Bick, K. F., 1958, Geology of the Deep Creek quadrangle, western Utah: New Haven, Conn., Yale Univ., Ph. D. dissert.
- Biemann, K., Oro, J., Toulmin, Priestley III, Orgel, L. E., Nier, A. O., Anderson, D. M., Simmonds, P. G., Flory, D., Diaz, A. V., Rushneck, D. R., Biller, J. E., and La Fleur, A. L., 1977, The search for organic substances and inorganic volatile compounds in the surface of Mars: *Jour. Geophys. Research*, v. 82, p. 4641-4658.
- Billings, M. P., 1956, The geology of New Hampshire—pt. II—Bedrock geology: Concord, N.H. State Planning and Development Comm., 203 p.
- Binder, A. B., Arvidson, R. E., Guinness, E. A., Jones, K. L., Morris, E. C., Mutch, T. A., Pieri, D. C., and Sagan, Carl, 1977, The geology of the Viking Lander 1 site: *Jour. Geophys. Research*, v. 82, p. 4439-4451.
- Birch, Francis, 1950, Flow of heat in the Front Range, Colorado: *Geol. Soc. America Bull.*, v. 61, p. 567-630.
- Black, C. C., 1967, Middle and Late Eocene mammal communities—a major discrepancy: *Science*, v. 156, p. 62-64.
- Boger, J. L., and Bergstrom, S. M., 1976, Conodont biostratigraphy of the upper Beekmantown Group and the St. Paul Group (Early and Middle Ordovician) of Maryland and West Virginia [abs.]: *Geol. Soc. America Abs. with Programs*, v. 8, no. 4, p. 465.
- Bohor, B. F., 1977, Tonsteins as correlation tools and environmental indicators of Rocky Mountain coals [abs.]: *Geol. Soc. America Abs. with Programs*, v. 9, no. 6, p. 710-11.
- Bortleson, G. C., Wilson, R. T., and Foxworthy, B. L., 1977, Water-quality effects on Baker Lake of recent volcanic activity at Mount Baker: U.S. Geological Survey Professional Paper 1022-B, 30 p.
- Boudette, E. L., 1977, Two-mica granite and uranium potential in the northern Appalachian orogen of New England, in Campbell, J. A., ed., *Short papers of the U.S. Geological Survey Uranium-Thorium Symposium, 1977*: U.S. Geol. Survey Circ. 753, p. 23-24.
- Bredenhoeft, J. D., England, A. W., Stewart, D. B., Trask, N. J., and Winograd, I. J., 1978, Geologic disposal of high-level radioactive wastes—earth-science perspectives: U.S. Geol. Survey Circ. 779, 15 p.
- Breger, I. A., and Brown, Andrew, 1962, Kerogen in the Chattanooga Shale: *Science*, v. 137, p. 221-224.
- Brew, D. A., 1971, Mississippian stratigraphy of the Diamond Peak area, Eureka County, Nevada with a section on the Biostratigraphy and age of the Carboniferous formations by Mackenzie Gorden, Jr.: U.S. Geol. Survey Prof. Paper 661, 84 p.
- Brew, D. A., Johnson B. R., Nutt, C. J., Grybeck, Donald, and Ford, A. B., 1977, Newly discovered granitic and gabbroic bodies in the Fairweather Range, Glacier Bay National Monument, Alaska, in Blean, K. M., ed., U.S. Geological Survey in Alaska; accomplishments during 1976: U.S. Geol. Survey Circ. 751-B, p. B90-B96.
- Brew, D. A., Loney, R. A., Kistler, R. W., Czamanske, G. K., Grommé, C. S., and Tatsumoto, Mitsunobu, 1977a, Probable lower Paleozoic or Precambrian rocks in the Fairweather Range, Glacier Bay National Monument, Alaska, in Blean, K. M., ed., *The U.S. Geological Survey in Alaska; accomplishments during 1976*: U.S. Geol. Survey Circ. 751-B, p. B91-B93.
- Brew, D. A., Loney, R. A., and Muffler, L. J. P., 1966, Tectonic history of southeastern Alaska: *Canadian Inst. Mining and Metallurgy Spec.* v. 8, p. 149-170.
- Brinkworth, G. L., and Kleinkopf, M. D., 1972, Bouguer gravity, in *Geologic Atlas of the Rocky Mtn. region*: Rocky Mtn. Assoc. of Geologists, p. 45-47.
- Brown, D. E., Carmony, N. B., and Turner, R. M., 1977a, compilers, Drainage map of Arizona showing perennial streams and some important wetlands: Arizona Game and Fish Department map, scale 1:1,000,000, 1 sheet.
- Brown, D. E., Carmony, N. B., and Turner, R. M., 1977b, Inventory of riparian habitats, in *Importance, preservation and management of riparian habitat*: U.S. Forest Service Gen. Tech. rept. p. 10-13.
- Brown, D. L., Blankennagel, R. K., Busby, J. F., and Lee, R. W., 1977, Preliminary data for Madison limestone test well 2, SE $\frac{1}{4}$ SE $\frac{1}{4}$ sec. 18, T. 1 N., R. 54 E., Custer County, Montana: U.S. Geological Survey open-file rept. 77-863, 143 p.
- Brown, L. D., Rflinger, R. E., Holdahl, S. R., and Balazs, E. I., 1977, Postseismic uplift near Anchorage, Alaska: *Jour. Geophys. Research*, v. 82, no. 23, p. 3369-3378.
- Brown, R. D., Jr., 1964, Geologic map of the Stonyford quadrangle, Glenn, Colusa, and Lake Counties, California: U.S. Geol. Survey Misc. Field Studies Map MF-279, scale 1:48,000.
- Bryant, N. J., George, A. V., Jr., and Hegdahl, R. W., 1977, Integration of Landsat-derived land cover information with other information for planning purposes: *Purdue Symposium on Machine Processing of Remotely Sensed Data*, 4th, June 1977, Ind., p. 313-318.
- Buchanan-Banks, J. M., Pampeyan, E. H., Wagner, H. C. and McCulloch, D. S., 1978, Preliminary map showing recency of faulting in coastal south central California: U.S. Geol. Survey Misc. Field Invest. Map I-910, scale 1:250,000.
- Byers, F. M., Jr., Carr, W. J., Christiansen, R. L., Lipman, P. W., Orkild, P. P., and Quinlivan, W. D., 1976, Geologic map of the Timber Mountain caldera area Nye County, Nevada: U.S. Geol. Survey Misc. Inv. Map 1-891, 2 sheets, scale 1:48,000.
- Cameron, R. E., and Ford, A. B., 1974, Baseline analyses of soils from the Pensacola Mountains: *Antarctic Jour. of the United States*, v. 9, no. 4, p. 116-119.
- Campbell, D. L., and Olhoeft, G. R., 1977, Laboratory measurements of complex resistivity characteristics from Saterdal no. 1 corehole, Piceance Creek Basin, Colorado: U.S. Geol. Survey open-file rept. 77-410, 7 p., 1 table, 6 figs.
- Cannon, W. F., and Klasner, J. S., 1976, Phosphorite and other apatite-bearing sedimentary rocks in the Precambrian of northern Michigan: U.S. Geol. Survey Circ. 746, 6 p.

- Carden, J. R., and Forbes, J. R., 1976, Discovery of blueschists on Kodiak Island: Alaska Div. Geol. and Geophys. Surveys Geol. rept. 51, p. 19.
- Carnegie, D. M., and Holm, C. S., 1976, Remote sensing techniques for monitoring impacts of phosphate mining in southwestern Idaho: W. T. Pecora Memorial Symp., 2nd, Am. Soc. Photogramm., Sioux Falls, S. Dak., 1976, Proc., p. 251-272.
- Carothers, W. W., and Kharaka, Y. K., 1978, Aliphatic acid anions in oil-field waters and their implications for the origin of natural gas: Am. Assoc. of Petroleum Geologists Bull. [In press].
- Carr, M. H., Crumpler, L. S., Cutts, J. A., Greeley, R., Guest, J. E., and Masursky, Harold, 1977, Martian impact craters and emplacement of ejecta by surface flow: Jour. Geophys. Research, v. 82, p. 4055-4066.
- Carr, M. H., Greeley, Ronald, Blasius, K. R., Guest, J. E., and Murray, J. B., 1977, Some martian volcanic features as viewed from the Viking Orbiters: Jour. Geophys. Research, v. 82, p. 3985-4015.
- Carter, Virginia, and Burbank, J. H., 1978, A wetland classification system for the Tennessee Valley region: Tennessee Valley Authority, TVA tech. note. [In press].
- Castle, R. O., Dixon, H. R., Grew, Edward, Grison, Andrew, and Zietz, Isidore, 1976, Structural Dislocations in Western Massachusetts: U.S. Geological Survey Bull. 1410, 39p.
- Cataldi, R., Lazzarotto, A., Muffler, L. J. P., Squarci, P., and Stefani, G. C., 1978, Assessment of geothermal potential of central and southern Tuscany: Geothermics. [In press].
- Chao, E. C. T., 1977, Preliminary interpretation of the 1973 Ries research deep drill core and a new Ries cratering model: Geol. Bavarica, v. 75, p. 421-442.
- Chao, E. C. T., and Minkin, J. A., 1977, Impact cratering phenomenon for the Ries multiring structure based on constraints of geological, geophysical, and petrological studies and the nature of the impacting body, in Impact and Explosion Cratering, Pergamon Press, p. 405-424.
- Chao, E. C. T., Minkin, J. A., and Thompson, C. L., 1977, Petrology of consortium sample 67455, from a white-matrix breccia boulder near the rim of North Ray Crater, Descartes [abs.], in Lunar Science VIII: Houston, Tex., Lunar Science Inst., p. 166-168.
- Chapman, R. M., Dettnerman, R. L., and Mangus, M. D., 1964, Geology of the Killik-Etiviluk Rivers region, Alaska: U.S. Geol. Survey Prof. Paper 303-F, p. 325-407.
- Chapman, R. M., and Sable, E. G., 1960, Geology of the Utukok-Corwin region, northwestern Alaska: U.S. Geol. Survey Prof. Paper 303-C, p. 47-176.
- Chase, R. B., and Hyndman, D. W., 1977, Mylonite detachment zone, eastern flank of Idaho batholith: Geol. Soc. America Rocky Mtn. Sec. 2, 30th Ann. Mtg. Guidebook no. 1, 31 p.
- Chatterjee, N. D., and Johannes, Wilhelm, 1974, Thermal stability and standard thermodynamic properties of synthetic $2M_1$ -muscovite, $KAl_2(AlSi_3O_{10}OH_2)$: Contr. Mineralogy and Petrology, v. 48, p. 89-114.
- Chenoweth, W. L., 1974, Uranium occurrences of the Nacimiento-Jemez region, Sandoval and Rio Arriba Counties, New Mexico, in New Mexico Geol. Soc. Guidebook, 25th Field Conf., Ghost Ranch, 1974: p. 309-313.
- Christiansen, R. L., and Blank, H. R., Jr., 1972, Volcanic stratigraphy of the Quaternary rhyolite plateau in Yellowstone National Park: U.S. Geol. Survey Prof. Paper 729B, p. B1-B18.
- Clark, B. C., Baird, A. K., Rose, H. J., Jr., Toulmin, Priestley III, Christian, R. P., Kelliher, W. C., Castro, A. J., Rowe, C. D., Keil, Klaus, and Huss, G. R., 1977, The Viking X-ray fluorescence experiment: Analytical methods and early results: Jour. Geophys. Research, v. 82, p. 4577-4594.
- Cline, D. R., 1978, Water resources of No Name Valley, Colville Indian Reservation, Washington: U.S. Geological Survey open-file rept. 78-122. [In press].
- Cline, J. D., and Holmes, M. L., 1977, Submarine seepage of natural gas in Norton Sound, Alaska: Science, v. 198, p. 1149-1153.
- Colorado Division of Mines, 1976, A summary of mineral industry activities in Colorado, 1975: Denver, Colo., 116 p.
- 1977, A summary of mineral industry activities in Colorado, 1976: Denver, Colo., 105 p.
- Conant, L. C., and Swanson, V. E., 1961, Chattanooga Shale and related rocks of Central Tennessee and nearby areas: U.S. Geol. Survey Prof. Paper 357, 91 p.
- Connor, J. J., 1977, Environmental geochemistry, Part C, in Summary report of the geology, mineral resources, engineering geology and environmental geochemistry of the Sweetwater-Kemmerer area, Wyoming: U.S. Geol. Survey open-file rept. 77-362, 22 p.
- Cory, R. L., 1977, Water quality in Rhode River at Smithsonian Pier near Annapolis, Maryland, January 1974 through December 1975: U.S. Geol. Survey Water-Resources Inv. 77-20, 48 p.
- Craig, G. S., Jr., and Rankl, J. G., 1977, Analysis of runoff from small drainage basins in Wyoming: U.S. Geological Survey open-file rept. 77-727, 88 p.
- Crittenden, M. D., Jr., 1977, Possible westward extension of Absaroka thrust into northeast Utah: Abstract of paper presented orally at joint field conference of Wyoming Geol. Assn., Montana Geol. Assn., and Utah Geol. Assn., Jackson Hole, Wyo., Sept. 1977.
- Curray, J. R., 1965, Late Quaternary history, continental shelves of the United States, in Wright, H. E. and Frey, D. G., eds., The Quaternary of the United States, Princeton, N.J., Princeton Univ. Press, p. 723-735.
- Dale, T. N., 1907, The granites of Maine: U.S. Geol. Survey Bull. 313, 202 p.
- Daniels, J. J., Scott, J. H., Blackmon, P. D., Starkey, H. S., 1977, Borehole geophysical investigations in the south Texas uranium district: U.S. Geol. Survey Jour. Research, v. 5, no. 3, p. 343-357.
- Davis, D. A., 1977, Record of ground-water exploration and development, 1975-76, Moen, Truk, Eastern Caroline Islands: U.S. Geol. Survey open-file rept. 77-739, 358 p. [Available from U.S. Geological Survey, District Office, 855 Oak Grove Avenue, Menlo Park, Calif. 94025].
- Dawdy, D. R., Lichty, R. W., and Bergmann, J. M., 1972, A rainfall-runoff simulation model for estimation of flood peaks for small drainage basins: U.S. Geol. Survey Prof. Paper 506-B, 28 p.
- Dean, W. E., and Anderson, R. Y., 1974, Application of some correlation coefficient techniques to time-series analysis: Mathematical Geology, v. 6, no. 4, p. 363-372.
- Decker, E. R., 1969, Heat flow in Colorado and New Mexico: Jour. Geophys. Research, v. 74, no. 2, p. 550-559.

- Dennison, J. M., and Boucot, A. J., 1974, The Little War Gap at Clinch Mountain provides standard reference section for Silurian Clinch Sandstone and most nearly complete Devonian section in eastern Tennessee: *Southeastern Geol.*, v. 16, no. 2, p. 79-101.
- Denson, N. M., Dover, J. H., and Osmonson, L. M., 1978a, Coal-bed distribution and coal resources of the Reno Junction-Antelope Creek area, Campbell, Converse, Niobrara, and Weston Counties, Wyoming: U.S. Geol. Survey Misc. Field Studies Map MF-960, scale 1:115,000.
- 1978b, Structure-contour and isopach maps of the Wyodak-Anderson coal bed in the Reno Junction-Antelope Creek area, Campbell and Converse Counties, Wyoming: U.S. Geol. Survey Misc. Field Studies Map MF-961, scale 1:125,000.
- Detra, D. E., 1977, Delineation of an anomalous lead-zinc area in the Philip Smith Mountains A-2 quadrangle, Alaska: U.S. Geol. Survey open-file rept. 77-223, 11 p.
- Dickinson, W. R., and Hatherton, T., 1967, Andesitic volcanism and seismicity around the Pacific: *Science*, v. 157, p. 801-803.
- Dickinson, W. R., and Snyder, W. S., 1977, Inferred plate tectonic setting of classic Laramide orogeny: *Geol. Soc. America, Abst. with Programs*, v. 9, no. 7, p. 950.
- Diller, J. S., 1903, A description of the Port Orford Quadrangle, Oregon: U.S. Geol. Survey Geol. Atlas, Folio 89, 6 p.
- Dillon, W. P., and Oldale, R. N., 1978, Late Quaternary sea-level curve: Reinterpretation based on glaciotectonic influence: *Geology*, v. 6, no. 1, p. 56-60.
- Dodge, F. C. W., and Helaby, A. M., 1975, Mineralization in the Uyaijah- Thaaban area, west-central part of the Uyaijah ring structure, Kingdom of Saudi Arabia: U.S. Geol. Survey open-file rept. 75-175 [(IR) SA-191], 43 p., 4 pls., 6 figs., and 14 tables.
- Doherty, D. J., 1976, Ground surge deposits in eastern Idaho: Wayne State, Univ. Mich., M.S. thesis, 119 p.
- Donnelly, J. M., Hearn, B. C., Jr., and Goff, F. E., 1977, The Clear Lake Volcanics, California: Geology and field trip guide, in *Field Trip Guide to The Geysers-Clear Lake Area*, 73rd Ann. Cordilleran Sec. mtg. Geol. Soc. of America, p. 25-56.
- Donnelly, M. E., and McCallum, M. E., 1977, Petrology and structure of the southern portion of the Mullen Creek mafic complex, Medicine Bow Mountains, Wyoming: *Geol. Soc. America, Abst. with Programs* v. 9, no. 6, p. 720-721.
- Draeger, W. C., Monitoring irrigated land acreage using Landsat imagery—An application example: Intern. Symposium on Remote Sensing of Environment, 11th, Ann Arbor, Mich., 1977 Proc., p. 515-524.
- Drake, A. A., Jr., and Epstein, J. B., 1967, The Martinsburg Formation (Middle and Upper Ordovician) in the Delaware Valley, Pa.-N.J.: U.S. Geol. Survey Bull. 1244-H, 16 p.
- Drost, B. W., and Seitz, H. R., 1977, Spokane Valley-Rathdrum Prairie aquifer, Washington and Idaho: U.S. Geological Survey open-file rept. 77-829, 78 p.
- Duffield, W. A., and Bacon, C. R., 1977, Preliminary geologic map of the Coso volcanic field and adjacent areas, Inyo County, Calif.: U.S. Geol. Survey open-file map 77-311.
- Dyni, J. R., 1974, Stratigraphy and nahcolite resources of the saline facies of the Green River Formation in northwest Colorado, in Murray, D. K., ed., *Guidebook to the energy resources of the Piceance Creek basin, Colorado: Rocky Mountain Assoc. of Geologists 25th Field Conf.*, p. 111-122.
- Eakin, H. M., 1916, The Yukon-Koyukuk region, Alaska: U.S. Geol. Survey Bull. 631, p. 54.
- Eargle, D. H., 1972, Revised classification and nomenclature of the Jackson Group (Eocene), south-central Texas: *Amer. Assoc. Petroleum Geologists, Bull.* v. 56, no. 3, p. 561-566.
- Eaton, G. P., Prostka, H. J., Oriol, S. S., and Pierce, K. L., 1976, Cordilleran thermotectonic anomaly—pt. 1—Geophysical and geological evidence of coherent late Cenozoic intraplate magmatism and deformation [abs.]: *Geol. Soc. America, Abs. with Programs*, v. 8, no. 6, p. 850.
- Ebens, R. J., and Connor, J. J., 1977, Cu, Pb, Zn, and Ba in carbonate residuum of southern Missouri: *Soc. Mining Engineers of A.I.M.E., Preprint no. 77-L-325*, 4 p.
- Ege, J. R., Griffiths, W. R., and Overstreet, W. C., 1977, Preliminary engineering geologic report on selection of urban sites in the Federal Capital Territory, Nigeria: U.S. Geol. Survey open-file rept. 77-488 [(IR) N-1], 78 p., 7 figs.
- Elsheimer, H. N. and Fabbi, B. P., 1977, Application of an automatic fusion technique to minor and trace element XRF analysis of silicate rocks: [abs.] *Ann. Denver X-ray Conf.*, 26th, Denver, Colo.
- Eliason, E. M. and Soderblom, L. A., 1977, An array processing system for lunar geochemical and geophysical data: *Proc. Lunar Sci. Conf.* 8th, p. 1163-1170.
- Elston, W. E., Seager, W. R., and Clemons, R. E., 1975, Emory Cauldron, Black Range, New Mexico, source of the Kneeling Nun Tuff: *New Mex. Geol. Soc. Guidebook, Field Conf.*, 26th, p. 282-292.
- England, A. W., and Nelson, W. H., 1977, Geophysical studies of the Dufek intrusion, Pensacola Mountains, Antarctica, 1976-1977: *Antarctic Jour. of the United States*, v. 12, no. 4, p. 93-94.
- Englund, K. J., King, E. R., Lesure, F. G., Perry, W. J., Jr., and others, 1977a, Mineral resource, geological, and geophysical maps of the New River Gorge area, Fayette, Raleigh, and Summers Counties, West Virginia: U.S. Geol. Survey open-file rept. OF-77-76.
- Englund, K. J., Lesure, F. G., Davies, W. E., King, E. R., and Perry, W. J., Jr., 1977b, Mineral resource appraisal of the New River Gorge, Fayette, Raleigh, and Summers Counties, West Virginia: U.S. Geol. Survey open-file rept., OF-77-207, 21 p.
- Epstein, A. G., Epstein, J. B., and Harris, L. D., 1977, Conodont Color Alteration—an Index to Organic Metamorphism: U.S. Geol. Survey Prof. Paper 995, 27 p.
- Ethington, R. L., and Clark, D. L., 1971, Lower Ordovician conodonts in North America, in Sweet, W. C., and Bergström, S. M., eds., *Eymposium on conodont biostratigraphy*: *Geol. Soc. America Memoir* 127, p. 63-82.
- Fairchild, H. S., 1912, The glacial waters of the Black and Mohawk Valleys: *New York State Mus. Bull.*, 1912, 160, 47 p.
- Fary, R. W., Compiler, 1977, Proceedings of the CENTO Workshop on Application of Remote Sensing Data and Methods, Lahore, Pakistan, Mar. 2-8, 1975: U.S. Geol. Survey open-file rept. 77-488, [(IR)CEN-10].
- Fenner, C. N., 1936, Bore-hole Investigations in Yellowstone Park: *Jour. Geology*, v. 44, p. 225-315.

- Fishman, M. J., and Spencer, R. R., 1977, Automated atomic absorption spectrometric determination of total arsenic in water and streambed materials: *Anal. Chem.*, v. 49, p. 1599.
- Fisk, H. N., 1938, Geology of Grant and La Salle Parishes: Louisiana Dept. Conserv. Geol. Bull., no. 10, 246 p.
- 1940, Geology of Avoyelles and Rapides Parishes, Louisiana Dept. Conserv. Bull., no. 18, 240 p.
- Fiske, R. S., Hopson, C. A., and Waters, A. C., 1963, Geology of Mount Rainier National Park, Washington: U.S. Geol. Survey Prof. Paper 444, 93 p.
- Fleck, R. J., Coleman, R. G., Cornwall, H. R., Greenwood, W. R., Hadley, D. G., Schmidt, L., Prinz, W. C., and Ratte, J. C., 1976, Geochronology of the Arabian Shield, Western Saudi Arabia—K-Ar results: *Geol. Soc. America Bull.*, v. 87, p. 9–21.
- Flemal, R. C., Hinkley, K. C., and Hesler, J. L., 1973, De Kalb mounds—a possible Pleistocene (Woodfordian) pingo field in north-central Illinois, in Black, R. F., Goldthwait, R. P., and Willman, H. B., eds., *The Wisconsinan stage: Geol. Soc. America Mem.* 136, p. 229–250.
- Force, E. R., Lipin, B. R., and Smith, R. E., 1976, Heavy mineral resource in Pleistocene sand of the Port Leyden Quadrangle, southwestern Adirondack Mountains, New York: U.S. Geol. Survey Misc. Field Studies Map MF-728B, scale 1:24,000.
- Ford, A. B., 1976, Stratigraphy of the layered gabbroic Dufek intrusion, Antarctica: U.S. Geol. Survey Bull. 1405–D, 36 p.
- 1977a, Tectonic framework of the southeast Weddell Sea continental margin of Antarctica [abs.]: *Geol. Soc. America Abs. with Programs*, v. 9, p. 977–978.
- 1977b, Geologic comparison of the Shackleton Range and the Pensacola Mountains during the 22nd Soviet Antarctic Expedition: *Antarctic Jour. of the United States*, v. 12, no. 4, p. 88–90.
- Ford, A. B., and Brew, D. A., 1977a, Chemical nature of Cretaceous greenstone near Juneau, Alaska, in Blean, K. M., ed., *The United States Geological Survey in Alaska: accomplishments during 1976: U.S. Geol. Survey Circ.* 751–B, p. B88–B90.
- 1977b, Truncation of regional metamorphic zonation pattern of the Juneau, Alaska, area by the Coast Range batholith, in Blean, K. M., ed., *The United States Geological Survey in Alaska; accomplishments during 1976: U.S. Geol. Survey Circ.* 751–B, p. B85–B87.
- Ford, A. B., Carlson, Christine, Czamanske, G. K., Nelson, W. H., and Nutt, C. J., 1977, Geological studies of the Dufek intrusion, Pensacola Mountains, 1976–1977: *Antarctic Jour. of the United States*, v. 12, no. 4, p. 90–92.
- Foster, H. L., Dusel-Bacon, Cynthia, and Weber, F. R., 1977, Reconnaissance geologic map of the Big Delta C-4 quadrangle, Alaska: U.S. Geol. Survey open-file rept. 77–262, 1 sheet, scale 1:63,360.
- Foster, H. L., Weber, F. R., and Dusel-Bacon, Cynthia, 1977, Gneiss dome in the Big Delta C-4 quadrangle, Yukon-Tanana Upland, Alaska, in Blean, K. M., ed., *The United States Geological Survey in Alaska; accomplishments during 1976: U.S. Geol. Survey Circ.* 751–B, p. B33.
- Fournier, R. O., White, D. E., and Truesdell, A. H., 1976, Convective heat flow in Yellowstone National Park: Second United Nations symposium on development and use of geothermal resources, San Francisco, 1975, *Proc.*, v. 1, p. 377–386.
- French, J. J., 1978, Ground-water storage in the Johnson Valley area, San Bernardino County, California: U.S. Geological Survey Water-Resources Investigation 77–130. [In press.]
- Frye, J. C. and Willman, H. B., 1973, Wisconsinan climatic history interpreted from Lake Michigan lobe deposits and soils, in Black, R. F., Goldthwaite, R. P., and Willman, H. B., eds., *The Wisconsinan Stage, Geol. Soc. America Mem.* 136, p. 135–152.
- Fuis, G. S., Friedman, M. E., and Hileman, J. A., 1977, Preliminary catalog of earthquakes in southern California, July 1974–September 1976: U.S. Geol. Survey open-file rept. 77–181, 90 p.
- Gammon, P. T., Carter, Virginia, and Shima, L. J., 1977, Classifying vegetative cover with Landsat digital data, Great Dismal Swamp, Virginia and North Carolina, in Symposium on machine processing of remotely sensed data, Indiana, 4th, 1977, *Proc. Purdue Univ. Lab. for Applications of Remote Sensing, IEEE catalog no.* 77CH1218–7 MPRSD, p. 345.
- Garbarino, J. R., and Taylor, H. E., 1977, The application of an inductively coupled plasma emission spectrometer for rapid quantitative analysis of natural waters: Federation of Analyt. Chem. and Spectro. Soc., 4th Mtg., Detroit, Mich., Nov. 7–11, 1977, *Proc.*, no. 28, p. 5.
- Gard, L. M., 1976, Geology of the north end of the Salt Valley anticline, Grand County, Utah: U.S. Geol. Survey open-file rept. 76–303.
- Garner, E. L., Murphy, T. J., Gramlich, J. W., Paulsen, P. J., and Barnes, I. L., 1976, Absolute isotope abundance ratios and the atomic weight of a reference sample of potassium: *Jour. Research of the U.S. National Bureau of Standards, sec. A*, v. 79A, p. 713–725.
- Gaydos, Leonard, and Wray, J. R., 1977, Land cover from Landsat, 1973, Washington urban area, D.C., Md., Va., with place names and census tracts, U.S. Geol. Survey Inc. Maps I-858–E and F, scale 1:100,000.
- Gaydos, Leonard, Wray, J. R., and Guptill, S. C., 1977, Digital land cover classification of the Washington urban area derived from Landsat data, 1972 and 1973 (9-track magnetic tape DOI/DF-77/003): U.S. Geol. Survey, NTIS rept. PB-246 650/3WN.
- Gere, W. C., Schell, E. M., and Moore, K. P., 1966, Stratigraphic sections and phosphate analyses of Permian rocks in the Teton Range and parts of the Snake River and Gros Ventre Ranges, Idaho and Wyoming: U.S. Geol. Survey open-file rept. 840.
- Gill, Dan, 1970, Application of a statistical zonation method to reservoir evaluation and digitized-log analysis: *Am. Assoc. Petroleum Geologists Bull.*, v. 54, no. 5, p. 719–729.
- Gilman, R. C., Goultly, N. R., Allen, C. R., Keller, R. P., and Burford, R. O., 1977, Fault creep in the Imperial Valley, California [abs.]: *EOS*, v. 58, no. 4, p. 1226.
- Goff, F. E., and Donnelly, J. M., 1977, Applications of thermal water chemistry in the Geysers-Clear Lake area, California: *Geol. Soc. America, Abs. with Programs*, v. 9, no. 7, p. 992.
- Goff, F. E., Donnelly, J. M., Thompson, J. M., and Hearn, B. C., 1977, Geothermal prospecting in The Geysers-Clear Lake area, northern California: *Geology*, v. 5, no. 8, p. 509–515.
- Green, M. W., Pierson, C. T., Bauer, D. P., and Umshler, D. B., 1977, A summary of the geology and mineral resources of the Paria Plateau-House Rock Valley area,

- Coconino County, Arizona: U.S. Geol. Survey open-file rept. 77-737, 19 p.
- Greene, H. G., Dalrymple, G. B., and Clague, D. A., 1978, Evidence for northward movement of the Emperor Seamount: *Geology*, v. 6, p. 70-74.
- Grolier, M. J., 1977, Interpretation of Landsat images; Qatar (preliminary report): U.S. Geol. Survey open-file rept. 77-295, [(IR)QA-1], 3 p., 1 fig.
- 1977b, Interpretation of Landsat images; Oman (preliminary report): U.S. Geol. Survey open-file rept. 77-296, [(IR)OM-2], 2 p., 1 fig.
- 1977c, Interpretation of Landsat images; Bahrain (preliminary report): U.S. Geol. Survey open-file rept. 77-298, [(IR)B-1], 2 p., 1 fig.
- 1977d, Interpretation of Landsat images; United Arab Emirates (preliminary report): U.S. Geol. Survey open-file rept. 77-297, [(IR)UAE-1], 3 p., 1 fig.
- 1977e, Interpretation of Landsat images; Kuwait (preliminary report): U.S. Geol. Survey open-file rept. 77-299, [(IR)KU-1], 2 p., 1 fig.
- Grossman, I. G., and Wilson, W. E. III, 1970, Hydrogeologic data for the lower Housatonic River basin, Connecticut: *Connecticut Water-Resources Bull.* 20, 50 p.
- Hack, J. T., 1942, The changing physical environment of the Hopi Indians of Arizona: *Peabody Museum Papers*, v. 35, no. 1.
- Haire, W. J., 1978, Floods in the Naguabo area, eastern Puerto Rico: U.S. Geological Survey, Hydrologic Investigation Atlas, HA-584, 1 sheet, scale 1:20,000.
- Hall, W. E., Rye, R. O., and Doe, B. R., in press, The Wood River, Idaho, District—intrusive-related lead-silver deposits derived from country rock source: *U.S. Geol. Survey Jour. Research*, v. 6, no. 5, p. 579-592.
- Hamilton, L. J., 1978, Major aquifers in Clark County, South Dakota: *South Dakota Geological Survey Information Pamphlet* no. 16, 11 p.
- Hamilton, Warren, 1965, Geology and petrogenesis of the Island Park caldera of rhyolite and basalt, eastern Idaho: *U.S. Geol. Survey Prof. Paper* 504-C, p. C1-37.
- Harbaugh, A. W., and Reilly, T. E., 1976, Analog-model analysis of effect of waste-water management on the ground-water reservoir in Nassau and Suffolk Counties, New York, Report II—Recharge with waste water: U.S. Geol. Survey open-file rept. 76-847, 34 p.
- 1977, Analog-model analysis of effect of waste-water management on the ground-water reservoir in Nassau and Suffolk Counties, New York, Report III—Reduction and redistribution of ground-water pumpage: U.S. Geol. Survey open-file rept. 77-148, 24 p.
- Harrill, J. R., 1976, Pumping and ground-water storage depletion in Las Vegas Valley, Nevada, 1955-74: *Nevada Water Resources, Bull.* 44, 70 p.
- Hass, W. H., 1956, Age and correlation of the Chattanooga Shale and the Maury Formation: *U.S. Geol. Survey Prof. Paper* 286, 47 p.
- Harwood, D. S. and Zietz, Isidore, 1976, Geologic interpretation of an aeromagnetic map of southern New England: *U.S. Geol. Survey Geophy. Inv. Map* GP-906, scale 1:250,000.
- Hathaway, J. C., Schlee, J. S., Poag, C. W., Valentine, P. C., Weed, E. G. A., Bothner, M. H., Kohout, F. A., Manheim, F. T., Schoen, Robert, Miller, R. E., and Schultz, D. M., 1976, Preliminary summary of the 1976 Atlantic Margin Coring Project of the U.S. Geological Survey, U.S. Geol. Survey open-file rept. no. 76-844, 217 p.
- Hatherton, T., and Dickinson, W. R., 1969, The relationship between andesitic volcanism and seismicity in Indonesia, the Lesser Antilles, and other island arcs: *Jour. Geophys. Research*, v. 74, p. 5301-5310.
- Hay, R. L., 1956, Pitchfork Formation, detrital facies of Early Basic Breccia, Absaroka Range, Wyoming: *Am. Assoc. Petroleum Geologists Bull.*, v. 40, p. 1863-1898.
- Hearn, B. C., Jr., Marvin, R. F., Zartman, R. E., and Naeser, C. W., 1977, Geochronology of igneous activity in the north-central Montana alkalic province: *Geol. Soc. America Abs. with Programs*, v. 9, no. 6, p. 732.
- Hedrick, W. E., Cunningham, Paul, Shay, Ralph, Lake, Brent, and McCormick, M. J., The Pacific Northwest Regional Commission's Land Resource Inventory Demonstration Project: *Practicing Planner*, January 1977, p. 18-26.
- Helgesen, J. O., 1977, Ground-water appraisal of the Pine-land Sands area, central Minnesota: U.S. Geol. Survey open-file rept. 77-102, 49 p.
- Helm, D. C., 1976a, One-dimensional simulation of aquifer-system compaction near Pixley, California—Part 2—Stress-dependent parameters: *Water Resources Research*, v. 12, no. 3, p. 375-391.
- 1976b, Estimating parameters of compacting fine-grained interbeds within a confined aquifer system by a one-dimensional simulation of field observations: *Internat. Symposium on Land Subsidence*, 2nd, Internat. Assoc. Hydrological Sciences, Anaheim, Calif., December 1976, *Proc.*, p. 145-156.
- Hertogen, J., Janssens, M. J., Takahashi, H., Palme, H., and Anders, E., 1977a, A moon-like planetesimal and other antiquities at North Ray Crater, Apollo 16 [abs.], in *Lunar Science VIII: Houston, Tex., Lunar Science Inst.*, p. 430-432.
- 1977b, Lunar basins and craters: evidence for systematic compositional changes of bombarding population: *Proc. 8th Lunar Science Conf.*, v. 1, p. 17-45.
- Hietanen, Anna, 1973, Geology of the Pulga and Bucks Lake quadrangles, Butte and Plumas Counties, California: *U.S. Geol. Survey Prof. Paper* 731, 66 p.
- Hildreth, E. W., 1977, The magma chamber of the Bishop Tuff—gradients in temperature, pressure, and composition: *Univ. Calif., Berkeley, Ph. D. thesis*, 323 p.
- Hileman, J. A., Allen, C. R., and Nordquist, J. M., 1973, Seismicity of the southern California region, January 1, 1932 to December 31, 1972: *Seismol. Lab., C.I.T., Pasadena, Ca.*, 487 p.
- Hill, D. P., Mowinkel, P., and Lahr, K. M., 1975, Catalog of earthquakes in the Imperial Valley, California, June 1973-May 1974: U.S. Geol. Survey open-file rept. 75-401, 24 p.
- Hite, R. J., 1975, An unusual northeast-trending fracture zone and its relations to basement wrench faulting in northern Paradox basin, Utah and Colorado: *Four Corners Geol. Soc. Guidebook*, 8th Field Conf., Canyonlands, p. 217-224.
- Hoare, J. M., and Coonrad, W. L., 1977, Blue amphibole occurrences in southwest Alaska, in Blean, K. M., ed., *The United States Geological Survey in Alaska; accomplishments during 1976: U.S. Geol. Survey Circ.* 751-B, p. B39.
- Hodges, C. A., Muehlberger, W. R., and Ulrich, G. E., 1973, Geologic setting of Apollo 16: *Proc. 4th Lunar Science Conf.*, v. 1, p. 1-25.
- Holley, E. R., and Yotsukura, Nobuhiro, 1978, Thermal boundary conditions for water flow with moving boundaries: *U.S. Geol. Survey, Jour. of Research*. [In press.]

- Hollick, Arthur, 1930, The Upper Cretaceous floras of Alaska: U.S. Geol. Survey Prof. Paper 159, p. 39.
- Holzer, T. L., 1977, Crustal uplift cause by ground-water withdrawal in the Lower Santa Cruz Basin, Arizona: Geol. Soc. America Abs. with programs, v. 9, no. 7, p. 1023.
- Holzer, T. L., Davis, S. N., and Lofgren, B. E., 1977, Active surface faulting caused by ground-water extraction near Picacho, Arizona: Geol. Soc. America Abs. with Programs, v. 9, no. 5, p. 437.
- Honda, S., and Muffler, L. J. P., 1970, Hydrothermal alteration in core from research drill hole Y-1, Upper Geyser Basin, Yellowstone National Park, Wyoming: Am. Mineralogist, v. 55, p. 1714-1737.
- Hooper, P. R., and Ojakangas, R. W., 1971, Multiple deformation in Archean rocks of the Vermilion district, north-eastern Minnesota: Canadian Jour. of Earth Science, v. 8, p. 423-434.
- Hudleston, P. J., 1976, Early deformational history of Archean rocks in the Vermilion district, northeastern Minnesota: Canadian Jour. of Earth Science, v. 13, p. 579-592.
- Hunt, C. B., 1969, Geologic history of the Colorado River, in The Colorado River region and John Wesley Powell: U.S. Geol. Survey Prof. Paper 669-C, p. 59-130.
- Hurlbut, C. S., Jr., Aristarain, L. F., and Erd, R. C., 1977, Hydrochlorborite from Antofagasta, Chile: Am. Mineralogist, v. 62, p. 147-150.
- Interagency Advisory Committee on Water Data, 1978, Summary of 12th meeting: U.S. Geological Survey, Ofc. of Water Data Coordination, 41 p.
- Isachsen, Yngvar W., 1975, Possible evidence for contemporary doming of the Adirondack Mountains, New York, and suggested implications for regional tectonics and seismicity: Tectonophysics, v. 29, p. 169-181.
- Jackson, H. W., and Pakiser, L. C., 1965, Seismic study of crustal structure in the southern Rocky Mountains, in Geological Survey Research 1965: U.S. Geol. Survey Prof. Paper 525D, p. D85-D92.
- Jacob, C. E., 1950, Flow of ground water, in Rouse, Hunter, ed., Engineering Hydraulics: New York, John Wiley and Sons, Inc., Chap. 5, p. 321-386.
- Jacob, C. E., and Cooper, H. H., Jr., 1940, Report on the ground-water resources of the Pensacola area in Escambia County, Florida, with a section on the geology by Sidney A. Stubbs: U.S. Geol. Survey open-file rept., 85 p.
- James, O. B., 1977, Petrology of four clasts from consortium breccia 73215, in Lunar Science VIII, The Lunar Science Institute, Houston, Tex., p. 502-504.
- James, O. B., and Hammarstrom, J. F., 1977, Petrology of four clasts from consortium breccia 73215: Proc. 8th Lunar Science Conf., p. 2459-2494.
- Janda, R. J., 1978, Summary of watershed conditions in the vicinity of Redwood National Park, California: U.S. Geol. Survey open-file rept. 78-25. [In press.]
- Jennings, J. K., and Leventhal, J. S., 1976, Interaction of oxidized uranium with humic acids, ion-exchange resins, and chelating resins to determine conditions of fixation: Geol. Soc. America, v. 8, no. 5, p. 940.
- Jennings, M. E., and Keefer, T. N., 1977, Routing of storm-water flows through storm drains: U.S. Geol. Survey Jour. of Research, v. 5, no. 3, p. 301-305.
- Jennings, M. E., and Land, L. F., 1977, Simulation studies of flow and sediment transport using a mathematical model, Atchafalaya River basin, Louisiana: U.S. Geological Survey Water-Resources Inv. 77-14, 55 p.
- Jobson, H. E., and Keefer, T. N., 1977, Thermal modeling of highly transient flows in the Chattahoochee River near Atlanta, Georgia: American Water Resources Association Special Symposium on River Quality Assessment, Tucson, Arizona, Nov. 2-3, 1977, Proc. [In press.]
- Joesting, H. R., and Case, J. E., 1962, Regional geophysical studies in Salt Valley-Cisco area, Utah and Colorado: Am. Assoc. Petroleum Geologists Bull., v. 46, no. 10, p. 1879-1889.
- Johnson, C. E., and Hadley, D. M., 1976, Tectonic implications of the Brawley earthquake swarm, Imperial Valley, California, January 1975: Seismol. Soc. Am. Bull., v. 66, p. 1133-1143.
- Johnson, S. L., and Sayre, D. M., 1973, Effects of urbanization on floods in the Houston, Texas, metropolitan area: U.S. Geol. Survey Water-Resources Inv. 3-73, 50 p.
- Johnston, R. H., and Froelich, A. J., 1977, Maps showing lithofacies and inferred subsurface distribution of channel-fill sands in the Potomac Group in Fairfax County, Virginia: U.S. Geol. Survey open-file rept. 77-287.
- Johnston, R. H., and Larson, J. D., 1977, Potentiometric surface maps (1960 and 1976) and water level change map for the lower aquifer of the Cretaceous Potomac Group in Fairfax County, Virginia: U.S. Geol. Survey open-file rept. 77-286.
- Jones, Meridee, Van der Voo, Rob, Churkin, Michael, Jr., and Eberlein, G. D., 1977, Paleozoic paleomagnetic results from the Alexander terrane of southeastern Alaska: Trans. Am. Geophys. Union, Dec. 1977, San Francisco mtg., Program.
- Kalliokoski J. A. K. 1976, Uranium and thorium occurrences in Precambrian rocks, upper peninsula of Michigan and northern Wisconsin, with thoughts on other possible settings: Energy Research and Development Agency open-file publ. GJBX-48-76.
- Kane, M. F., 1977, Correlation of major eastern earthquake centers with mafic/ultramafic basement masses: U.S. Geol. Survey open-file rep. 77-134, 16 p.
- Karlson, R. C., Curtin, G. C., Cooley, E. F., and Garnezy, Larry, 1977, Results of spectographic analyses for heavy-mineral concentrates from the western half of the Talkeetna Mountains quadrangle, Alaska: U.S. Geol. Survey Circ. 734, 23 p.
- Karlstrom, T. N. V., 1976, Quaternary and upper Tertiary time-stratigraphy of the Colorado Plateaus, continental correlations, and some paleoclimatic implications, in Mahaney, W. C., ed., Quaternary stratigraphy of North America: Stroudsburg, Pennsylvania, Dowden, Hutchinson, and Ross, p. 275-282.
- Keefer, W. R., 1971, The geologic story of Yellowstone National Park: U.S. Geol. Survey Bull. 1347, 92 p.
- Kehn, T. M., 1955, Uranium in the Chattanooga Shale, Youngs Bend Area, Eastern Highland Rem-Tennessee: U.S. Geol. Survey, Atomic Energy Comm., TEI528A, 60 p.
- Keighin, C. W. 1977, Preliminary geologic map of the Cooper Canyon quadrangle, Uintah County, Utah: U.S. Geol. Survey Misc. Field Studies Map MF-874, scale 1:24,000.
- Keith, T. E. C., White, D. E., and Beeson, M. H., in press, Hydrothermal alteration and selfsealing in Y-7 and Y-8 drill holes in northern part of the Upper Geyser Basin, Yellowstone National Park, Wyoming: U.S. Geol. Survey Prof. Paper 1054-A. [In press.]

- Kelley, V C., 1972, *Geology of The Fort Sumner Sheet, New Mexico*: New Mexico State Bureau of Mines and Mineral Resources, Bull. 98, 55 p.
- Kharaka, Y. K., Callender, Edward, and Wallace, R. H., Jr., 1977, *Geochemistry of geopressed geothermal waters from the Frio Clay in the Gulf Coast region of Texas*: *Geology*, v. 5, p. 241-244.
- Kimmel, G. E., and Harbaugh, A. W., 1976, *Analog-model analysis of effect of waste-water management on the ground-water reservoir in Nassau and Suffolk Counties, New York, Report I—Proposed and current sewerage*: U.S. Geol. Survey open-file rept. 76-441, 32 p.
- King, E. G., and Weller, W. W., 1961, *Low-temperature heat capacities and entropies at 298.15°K of diaspore, kaolinite, dickite and halloysite*: U.S. Bureau Mines rept. Inv. 5810, 6 p.
- Kirkham, V. R. D., 1931, *Snake River downwarp*: *Jour. Geol.*, v. 39, p. 456-482.
- Klitgord, K. D., and Behrendt, J. C., 1977, *Aeromagnetic anomaly map of the U.S. Atlantic continental margin*, U.S. Geol. Survey Misc. Field Studies Map, MF-913, scale 1:1,000,000, 2 sheets
- Knott, J. M., 1977, *Laboratory analysis of suspended-sediment concentration and particle-size distribution*: United Nations Development Programme rept., OTC/SF Project INS 70/527.
- , 1978, *Final report of sediment specialist*: United Nations Development Programme rept., OTC/SF Project INS 70/527.
- Kohout, F. A., Hathaway, J. C., Folger, D. W., Bothner, M. H., Walker, E. H., Delaney, D. F., Frimpter, M. H., Weed, E. G. A., and Rhodehamel, E. C., 1977, *Fresh ground water stored in aquifers under the Continental Shelf: Implications from a deep test, Nantucket Island, Massachusetts*: *American Water-Resources Assoc. Bull.*, v. 13, no. 2, p. 373-386.
- Konikow, L. F., 1978, *Hydrogeologic considerations for an interstate ground-water compact on the Madison aquifer, Northern Great Plains*: U.S. Geol. Survey open-file rept. 78-138, 8 p.
- Ku, H. F. H., Katz, B. G., Sulam, D. J., and Krulikias, R. K., 1978, *Scavenging of chromium and cadmium by aquifer material, South Farmingdale-Massapequa area, Long Island, New York*: *Ground Water*. [In press].
- Kyle, R. A., and Schopf, J. M., 1977, *Palynomorph preservation in the Beacon Superground of the Transantarctic Mountains*: *Antarctic Jour. of the United States*, v. 12, no. 4, p. 121-122.
- Lachenbruch, A. H., and Sass, J. H., 1977, *Heat flow in the United States and the thermal regime of the crust*, in Heacock, J. G., ed., *The Earth's Crust—its nature and physical properties*: *Am Geop. Union Geophys. Monogr. Sr.*, v. 20, p. 626-675.
- , 1978, *Models of an extending lithosphere and heat flow in the Basin and Range province*, in Smith, R. B., and Eaton, G. P., eds., *Cenozoic Tectonics and Regional Geophysics of the Western Cordillera*: *Geol. Soc. America Mem.* 152. [In press.]
- Lai, Chintu, 1977a, *Computer-simulation of two-dimensional unsteady flows in estuaries and embayments by the method of characteristics—basic theory and the formulation of the numerical method*: U.S. Geol. Survey, *Water-Resources Inv.* 77-85, 72 p.
- , 1977b, *Some practical techniques of two-dimensional interpolation in computational hydraulics*: *Annual Hydraulics Speciality Conference, 25th, American Society of Civil Engineers, Hydraulics Division, Texas A&M University, August 10-12, 1977, Proc.*, p. 169-178.
- Landis, K. K., 1967, *Eometamorphism, and oil and gas in time and space*: *Am. Assoc. Petroleum Geologists Bull.*, v. 51, no. 6, p. 828-841.
- Landis, K. K., and Piper, T. B., 1972, *Effect upon environment of brine cavity subsidence at Grosse Ile, Michigan*: *Solution Mining Research Inst., Inc.*, 52 p.
- Langbein, W. B., 1976, *Hydrology and environmental aspects of Erie Canal (1817-99)*: U.S. Geol. Survey *Water-Supply Paper* 2038, 92 p.
- Lanphere, M. A., and Jones, D. L., 1978, *Cretaceous time-scale for North America*, in *Contribution to geologic time scales* *Am. Assoc. Petroleum Geologists*, no. 6. [In press.]
- Lara, O. G., 1978, *Effects of urban development on the flood-flow characteristics of the Walnut Creek basin, Des Moines metropolitan area*: U.S. Geol. Survey *Water-Resources Inv.* 78-11. [In press.]
- La Roche, Hubert de, Stussi, J. M., and Grandclaude, P.H., 1976, *Global exchange and processing of information in geochemistry (GEPIC)*: Nancy, France, Roneo CRPG, Oct. 1976, 56 p.
- Laudon, T. S., 1972, *Stratigraphy of eastern Ellsworth Land, in Adie, R. J., ed., Antarctic geology and geophysics*: Oslo, Universitetsforlaget, p. 215-223.
- Lee, K. Y., 1977, *Triassic stratigraphy in the northern part of the Culpeper Basin, Virginia and Maryland*: U.S. Geol. Survey Bull. 1422-C, 1 pl., 17 p.
- Leonard, R. B., and Janzer, V. J., 1977, *Natural radioactivity in geothermal waters, Alhambra Hot Springs and nearby areas, Jefferson County, Montana*: U.S. Geol. Survey open-file rept. 77-624, 20 p.
- Leopold, L. B. and Miller, J. P., 1954, *A postglacial chronology for some alluvial valleys in Wyoming*: U.S. Geol. Survey *Water Supply Paper* 1261, 90 p.
- Leve, G. W., 1978, *Altitude and configuration of the top of the Floridan aquifer, Duval County, Florida*: U.S. Geol. Survey *Water-Resources Inv.* 77-114. [In press.]
- Leventhal, J. S., and Granger, H. C., 1977, *Conceptual-mathematical models of uranium ore formation in sandstone-type deposits*, in J. A. Campbell, ed., *Short papers of the U.S. Geol. Survey Uranium-Thorium Symposium, 1977*: U.S. Geol. Survey Circ. 753, p. 35.
- Lindstrom, M. M., Nava, D. F., Lindstrom, D. J., Winzer, S. R., Lum, R. K. L., Schuhmann, P. J., Schuhmann, S., and Philpotts, J. A., 1977a, *Geochemical studies of the white breccia boulders at North Ray Crater, Descartes region of the Lunar Highlands*: *Proc. 8th Lunar Science Conf.*, p. 2137-2151.
- , 1977b, *Geochemical studies of the white breccia boulders at North Ray Crater, Descartes Highlands [abs.]*, in *Lunar Science VIII*: Houston, Tex., Lunar Science Inst., p. 583-585.
- Lipman, P. W., 1964, *Structure and petrology of Canyon Creek pluton, Trinity Alps, northern California*, [Abs.] for 1963: *Geol. Soc. America Spec. Paper* 76, p. 280-281.
- Lipman, P. W. and Lockwood, J. P., 1977, *Structural evolution of Mauna Loa volcano, Hawaii* [Extended abs.]: *Joint General Assemblies of IASPEI/IAVCEI*, Durham, England.

- Lipman, P. W., Prostka, H. J., and Christiansen, R. L., 1972, Cenozoic volcanism and plate-tectonic evolution of the western United States—I—Early and middle Cenozoic: Royal Soc. Philos. Trans. ser. A., London, v. 271, p. 217-248.
- Loelkes, G. L., Jr., 1977, Specifications for land use and land cover and associated maps: U.S. Geol. Survey open-file rept. 77-555, 82 p.
- Loney, R. A., Brew, D. A., Muffler, L. J. P., and Pomeroy, J. S., 1975, Reconnaissance geology of Chichagof, Baranof, and Kruzof Islands, Alaska: U.S. Geol. Survey Prof. Paper 792, 105 p.
- Love, J. D., 1939, Geology along the southern margin of the Absaroka Range, Wyoming: Geol. Soc. America Spec. Paper 20, 134 p.
- Love, J. D., McGrew, P. O., and Thomas H. D., 1963, Relationship of latest Cretaceous and Tertiary deposition and deformation to oil and gas in Wyoming, in Backbone of the Americas, tectonic history from pole to pole: Am. Assoc. Petroleum Geologists Mem. 2, p. 196-208.
- Lowham, H. W., 1976, Techniques for estimating flow characteristics of Wyoming streams: U.S. Geol. Survey Water Resources Inv. 76-112, 83 p.
- Lucchitta, B. K., 1966, Structure of the Hawley Creek area, Idaho-Montana: Penn. State Univ., Ph. D. thesis. 204 p.
- , 1977, Mare ridges, topography and structure in southern Imbrium and northern Procellarum [abs.], in Lunar Science VIII, pt. 2: Houston, Tex. Lunar Science Inst. p. 595-596.
- Ludwig, K. R., 1977, Timing of uranium mineralization in Gas Hills and Crooks Gap Districts, Wyoming, as indicated by U-Pb isotope apparent ages [abs.]: Geol. Soc. America, Abs. with Programs, 1977 Ann. Mtg., v. 9, p. 1078-1079.
- Lugmair, G. W., Schenin, N. B., and Marti, K., 1975, Sm-Nd age and history of Apollo 17 basalt 75075. Evidence for early differentiation of the lunar exterior: Proc. 6th Lunar Science Conf., p. 1419-1429.
- Lupe, Robert, and Ahlbrandt, T. S., 1975, Sandstone geometry, porosity and permeability distribution, and fluid migration in eolian system reservoirs: U.S. Geol. Survey open-file rept. 75-357, 23 p.
- Lyons, J. B., and Livingston, D. E., 1977, Rb-Sr age of the New Hampshire plutonic series: Geol. Soc. America Bull., v. 88, p. 1808-1812.
- Lyons, P. C., 1977, a report on the Bedrock Geology of the Narragansett Basin of Massachusetts and Rhode Island: U.S. Geol. Survey open-file rept. 77-816, 24 pls., 42 p.
- Lystrom, D. J., and Rinella, F. A., 1978 I, A method for estimating the regional effects of land use on river-water quality, Susquehanna River basin, Pennsylvania and New York: Joint Conf. on Sensing of Environmental Pollutants, Amer. Chem. Soc., 4th, Nov. 6-11, 1977, New Orelans, La., Proc. 732-738.
- Machette, M. N., Birkeland, P. W., Markos, G., and Guccione, M. J., 1976, Soil development in Quaternary deposits in the Golden-Boulder portion of the Colorado Piedmont, in Epis, R. C., and Weimer, R. J., eds., Studies in Colorado field geology: Prof. Contr. Colorado School Mines, no. 8, p. 339-357.
- MacKevett, E. M., Jr., Brew, D. A., Hawley, C. C., Huff, L. C., and Smith, J. G., 1971, Mineral resources of Glacier Bay National Monument, Alaska: U.S. Geol. Survey Prof. Paper 632, 90 p.
- MacKevett, E. M., Jr., and Plafker, George, 1974, The Border Ranges fault in south-central Alaska: U.S. Geol. Survey Jour. of Research, v. 2, no. 3. p. 323-329.
- Maclay, R. W., and Small, T. A., 1976, Progress report on geology of the Edwards aquifer, San Antonio area, Texas, and preliminary interpretation of borehole geophysical and laboratory data on carbonate rocks: U.S. Geol. Survey open-file rept. 76-627, 65 p.
- Maldonado, Florian, 1977, Summary of the geology and physical properties of the Climax stock, Nevada Test Site: U.S. Geol. Survey open-file rept. 77-356.
- Mamet, B. L., and Skipp, B. A., 1970a, Preliminary foraminiferal correlations of early Carboniferous strata in the North American Cordillera, in Colloque sur la stratigraphie du Carbonifère: Liège Univ., Congrès et Colloques, v. 55, p. 327-348.
- , 1970b, Lower Carboniferous calcareous foraminifera; preliminary zonation and stratigraphic implications for the Mississippian of North America: Cong. Internat. Stratigraphic et Géologie Carbonifère, 6th Sheffield 1967, Comptes Rendu, 1971, v. 3, p. 1129-1146.
- Marvin, R. F., Witkind, I. J., Keefer, W. R., and Mehnert, H. H., 1973, Radiometric ages of intrusive rocks in the Little Belt Mountains, Montana: Geol. Soc. America Bull., v. 84, no. 6, p. 1977-1986.
- Masursky, Harold, Strobell, M. E., Dial, A. L., 1978, Geologic Map of the Phoenicis Lacus quadrangle of Mars: U.S. Geol. Survey Misc. Geol. Inv. Map I-896, scale 1:5,000,000.
- Masursky, Harold, Boyce, J. M., Dial, A. L., Schaber, G. G., and Strobell, M. E., 1977, Classification and time of formation of martian channels based on Viking data: Jour. Geophys. Research, v. 82, p. 4016-4038.
- McCallum, I. S., Okamura, F. P. and Ghose, S., 1975, Mineralogy and petrology of sample 67075 and the origin of lunar anorthosites: Earth and Planet. Sci. Letters, v. 26, p. 36-53.
- McCauley, J. F., 1977, Orientale and Caloris, in Comparisons of Mercury and the Moon: Phys. of Earth and Planet. Interiors, v. 15, p. 220-250.
- , 1978, Geologic map of the Coprates quadrangle of Mars: U.S. Geol. Survey Misc. Geol. Inv. Map I-897, scale 1:5,000,000.
- McCauley, J. F., Breed, C. S., and Grolier, M. J., 1978, The Great United States dust storm of February 23-25, 1977: Geol. Soc. America, Abs. with Programs, v. 10, no. 3, p. 116.
- McCormick, M. J., 1976, The Space Connection: Wash. 1976, p. 8-12.
- , 1976, Tools for emerging land use problems—An innovative approach in the Pacific Northwest: 8th Annual Land Use Symposium, Albuquerque, N. Mex., Proc., p. 72-82.
- McCulloch, D. S., Clark, S. H., Jr., Field, M. E., Scott, E. W., and Utter, P. M., 1977, A summary report on the regional geology, petroleum potential, and environmental geology of the southern proposed lease sale 53, Central and Northern California Outer Continental Shelf: U.S. Geol. Survey open-file rept. 77-593, 57 p.
- McGill, J. T., 1973, Map showing landslides in the Pacific Palisades area, city of Los Angeles, California: U.S. Geol. Survey Misc. Field Studies Map MF-471, scale 1:4,800.

- McLaughlin, R. J., 1977, Late Mesozoic-Quaternary plate tectonics and The Geysers-Clear Lake geothermal anomaly [abs.]: 73rd Ann. Cordilleran Sec. Mtg., Geol. Soc. America, Sacramento, Calif.
- Meisler, Harold, 1977, Summary of ground-water conditions in the Jaffna Peninsula, Republic of Sri Lanka, with a plan for investigating feasibility of ground-water development: U.S. Geol. Survey open-file rept. 77-558, 47 p.
- Miller, G. A., 1977, Appraisal of the water resources of Death Valley, California-Nevada: U.S. Geological Survey open-file rept. 77-728. [In press.]
- Miller, J. A., Hughes, G. H., Hull, R. W., Vecchioli, John, and Seaber, P. R., 1978, Impact of potential phosphate mining on the hydrology of Osceola National Forest, Florida: U.S. Geol. Survey Water Resources Inv. 78-6. [In press.]
- Miller, W. R., Houston, R. S., Karlstrom, K. E., Hopkins, D. M., and Ficklin, W. H., 1977, Geological and geochemical investigations of uranium occurrences in the Arrastre Lake area of the Medicine Bow Mountains, Wyoming: U.S. Geol. Survey open-file rept. 77-92, 30 p.
- Milliman, J. D., and Emery, K. O., 1968, Sea levels during the past 35,000 years: *Science*, v. 162, p. 1121-1123.
- Minkin, J. A., Thompson, C. L., and Chao, E. C. T., 1977, Apollo 16 white boulder consortium samples 67455 and 67475: Petrologic investigation: Proc. 8th Lunar Science Conf., v. 2, p. 1967-1986.
- Mitchell, W. B., Guptill, S. C., Anderson, K. E., Fegeas, R. G., and Hallam, C. A. 1977, GIRAS: A Geographic Information Retrieval and Analysis System for Handling Land Use and Land Cover Data: U.S. Geol. Survey Prof. Paper 1059, 16 p.
- Moench, A. F., 1976, Simulation of steam transport in vapor-dominated geothermal reservoirs: U.S. Geol. Survey open-file rept. 76-607, 43 p.
- Moench, A. F., and Atkinson, P. G., 1977, Transient pressure analysis in geothermal steam reservoirs with a vaporizing liquid phase—summary report: Third Workshop on Geothermal Reservoir Engineering, Stanford Univ., Stanford, Calif. Dec. 14-16, 1977, Proc.
- Molz, F. J., Warman, J. C., and Jones, T. E., 1976, Transport of water and heat in an aquifer used for hot-water storage [abs.]: EOS, Am. Geophys. Union Trans., v. 57, no. 12, p. 918.
- Morgan, J. O., and McCord, J. R., 1977, Handling and reproduction of Landsat imagery, with special reference to Thailand: U.S. Geol. Survey open-file rept. 77-595, [(IR)TH-19].
- Morse, D. R. A., and Sahlberg, J. T., Economic analysis in the Pacific Northwest Project—Theoretical considerations and preliminary results: First Conference on the Economics of Remote Sensing Information Systems, San Jose, Calif., January, 1977, Proc. p. 171-194.
- Mower, R. W., Hood, J. W., Cushman, R. L., Borton, R. L., and Galloway, S. E., 1964, An appraisal of potential ground-water salvage along the Pecos River between Acme and Artesia, New Mexico: U.S. Geol. Survey Water-Supply Paper 1659, 98 p.
- Moyle, W. R., Jr., 1977, Summary of basic hydrologic data collected at Coso Hot Springs, California: U.S. Geol. Survey open-file rept. 77-485, 53 p.
- Muffler, L. J. P., and Cataldi, Raffaele, 1978, Methods for regional assessment of geothermal resources: Geothermics. [In press.]
- Muir, K. S., 1977, Ground water in the Fresno area, California: U.S. Geol. Survey Water-Resource Inv. 77-59, 22 p.
- Mumpton, F. A., 1960, Clinoptilolite redefined: *Am. Mineralogist*, v. 45, p. 351-369.
- Murata, K. J., and Larson, R. R., 1975, Diagenesis of Miocene siliceous shales, Temblor Range, Calif.: U.S. Geol. Survey, Jour. of Research, v. 3, p. 553-566.
- Murray, C. R., and Reeves, E. B., 1977a, Water use—Estimated use of water in the United States in 1975, in Geological Survey research 1977: U.S. Geol. Survey Prof. Paper 1050, p. 127-131.
- , 1977b, Estimated use of water in the United States in 1975: U.S. Geol. Survey Circ. 765, 39 p.
- Mutch, T. A., Arvidson, R. E., Binder, A. B., Guinness, E. A., and Morris, E. C., 1977, The geology of the Viking Lander 2 site: *Jour. Geophys. Research*, v. 82, p. 4452-4467.
- Nakamura, N., Unruh, D. M., Gensho, R., Tatsumoto, M., 1977, Evolution history of lunar mare basalts: Apollo 15 samples revisited [abs.], in Lunar Science VIII, Houston, Tex., Lunar Science Inst. p. 712-713.
- Nakamura, N., Tatsumoto, M., Nunes, P. D., Unruh, D. M., Schwal, A. P., and Wildeman, T. R., 1976, 4.4 b.y.-old clast in Boulder 7. Apollo 17: A comprehensive chronological study by U-Pb, Rb-Sr and Sm-Nd methods: Proc. 7th Lunar Science Conf., p. 2309-2333.
- Nash, J. T., 1977, Geology of the Midnite uranium mine area, Washington—maps, description, and interpretation: U.S. Geol. Survey open-file rept. 77-592, 39 p.
- Nemickas, Bronius, Koszalka, E. J., and Vaupel, D. E., 1977, Hydrogeologic data from investigation of water resources of the South Fork, Suffolk County, New York: Oakdale, New York, Suffolk County Water Authority, Long Island Water Resources Bull. 7, 31 p.
- New England River Basins Commission, 1976a, Estimates for New England—Onshore facilities related to offshore oil and gas development: New England River Basins Comm., Boston, Mass., 1976, 287 p.
- , 1976b, Estimates for New England: New England River Basins Commission, Boston, Mass., Nov. 1976, 210 p., 62 fig. and 20 pl.
- Newman, K. R., 1977, Palynologic biostratigraphy of some early Tertiary nonmarine formations in central and western Washington: *Geol. Soc. America, Abs. with Programs*, v. 9, no. 7, p. 1113.
- Nichols, T. C., Jr., Savage, W. Z., and Brethauer, G. E., 1977, Stresses in some granites, with emphasis on the Barre Granite of Vermont: *Am. Nuclear Society Abs. with Programs*, April, p. 42.
- Nilsen, T. H., 1977, Paleogeography of Mississippian turbidites in south-central Idaho; in Stewart, J. H., Stevens, C. H., and Fritsche, A. E., eds., Paleozoic paleogeography of the western United States: *Soc. Econ. Paleontologists and Mineralogists, Pacific Sec., Pacific Coast Paleogeography Symp. 1*, p. 275-299.
- Nord, G. L., and James, O. B., 1977, Aphanitic matrix, an ANT-suite clast and a felsite clast in consortium breccia 73215—an electron petrographic study: Proc. 8th Lunar Science Conf., p. 2495-2506.
- Nordin, C. F., Jr., and Skinner, J. V., 1977, Sediment-sampling equipment for deep fast currents: *International*

- Association for Hydraulic Research Conference, Karlsruhe, Germany, August 15-19, 1977, Proc., v. 6, p. 606-609.
- O'Connor, Joseph T., Imhoff, E. A., Guernsey, Lee, and others, 1978, Integrated Mined-Area Reclamation and Land Use Planning—Synopsis of the Fulton County, Illinois, workshop: Chicago, Illinois, Agronne National Laboratory and Resource and Land Investigation Program, U.S. Dept. of the Interior, 32 p.
- Olhoeft, G. R., 1977, Electrical properties of water saturated basalt: preliminary results to 506°K (233°C): U.S. Geol. Survey open-file rept. 77-688, 8 p.
- Oliver, H. W., and Robbins, S. L., 1978, Gravity map of California, Fresno sheet: California Div. Mines and Geology. [In press.]
- Openshaw, R. E., Hemingway, B. S., Robie, R. A., Waldbaum, D. R., and Krupka, K. M., 1976, The heat capacities at low temperatures and entropies at 298.15°K of low albite, analbite, microcline, and high sanidine: U.S. Geol. Survey, Jour. of Research, v. 4, p. 195-204.
- Overstreet, W. C., Chavez, P., Gawarecki, S. J., and Aaron, Obiabaka, 1977, Provisional map showing land use based on interpretation of vegetation, Federal Capital Territory, Republic of Nigeria: Nigeria Federal Capital Development Authority, scale 1:100,000.
- Papanastassiou, D. A., and Wasserburg, G. J., 1973, Rb-Sr ages and initial strontium in basalts from Apollo 15: Earth and Planetary Sci. Letters, v. 17, p. 324-337.
- Parker, B. C., Ford, A. B., Allnut, T., Bishop, B., and Wendt, S., 1977, Baseline microbiological data for soils of the Dufek Massif: Antarctic Jour. of the United States, v. 12, no. 4, p. 24-26.
- Parkinson, H. L., and Worts, G. F., Jr., 1977, A brief evaluation of ground-water and soils potential for irrigated agriculture, western desert of Egypt: U.S. Geol. Survey open-file rept. 77-777, 55 p.
- Pascale, C. A., and Martin, J. B., 1977, Hydrologic monitoring of a waste-injection well near Milton, Florida, June 1975-December 1976: U.S. Geol. Survey open-file rept. 77-368, 46 p.
- , 1978, Hydrologic monitoring of a waste-injection well near Milton, Florida, June 1975-June 1977: U.S. Geol. Survey open-file rept. FL 78-101, 74 p.
- Pattison, Malka L., 1977, Socioeconomic impacts of Outer Continental Shelf oil and gas development—a bibliography: U.S. Geol. Survey Circ. 761, 63 p.
- Patton, W. W., Jr., 1973, Reconnaissance geology of the northern Yukon-Koyukuk province, Alaska: U.S. Geol. Survey Prof. Paper 774-A, p. A3-A9.
- Patton, W. W., Jr., Miller, T. P., Chapman, R. M., and Yeend, Warren, 1977, Geologic map of the Melozitna quadrangle, Alaska: U.S. Geol. Survey open-file map 77-147, scale 1:250,000.
- Peddie, N. W., 1977, Modeling the geomagnetic field with the fields of unconstrained dipoles and circular current loops, [abs.]: Trans. Am. Geophys. Union, EOS, v. 58, no. 8, p. 733.
- Penman, H. L., 1956, Evaporation—An introductory survey: Netherland Jour. of Agricultural Science, v. 4, p. 9-29.
- Pessagno, E. A., Jr., and Newport, R. L., 1972, A technique for extracting Radiolaria from radiolarian cherts: Micropaleontology, v. 18, no. 2, p. 231-234.
- Peterson, Fred, 1977, Uranium deposits related to environments in the Morrison Formation (Upper Jurassic), Henry Mountains mineral belt of southern Utah, in, Campbell, J. A., ed., Short papers of the U.S. Geological Survey Uranium-Thorium Symposium, 1977: U.S. Geol. Survey Circ. 753, p. 45-47.
- Peterson, L. R., and Meyer, Gerald, 1977, Hydrologic reconnaissance evaluation of the Federal Capital Territory and surrounding areas, Nigeria: U.S. Geological Survey open-file rept. 77-596, 30 p.
- Phair, G., and Gottfried, D., 1964, The Colorado Front Range, Colorado USA as a uranium and thorium province on the Natural Radiation Environment, Adams, A. S., and Lowder, W. M., eds.: 1966, p. 7-38.
- Pierce, K. L., Obradovich, J. D., and Friedman, Irving, 1976, Obsidian hydration dating and correlation of Bull Lake and Pinedale glaciations near West Yellowstone, Montana: Geol. Soc. America Bull., v. 87, no. 5, p. 703-710.
- Pike, R. J. Jr., 1977, Apparent depth/apparent diameter relation for lunar craters: Proc. 8th Lunar Science Conf., p. 3427-3436.
- Pitman, J. K., and Donnell, J. R., 1973, Potential shale-oil resources of a stratigraphic sequence above the Mahogany zone, Green River Formation, Piceance Creek basin, Colo.: U.S. Geol. Survey Jour. of Research, v. 1, no. 4, p. 467-473.
- Plafker, George, Jones, D. L., Hudson, Travis, and Berg, H. C., 1976, The Border Ranges fault system in the Saint Elias Mountains and Alexander Archipelago, in Cobb, E. H., ed., The U.S. Geological Survey in Alaska; accomplishments during 1975: U.S. Geol. Survey Circ. 733, p. 14-16.
- Plouff, Donald, 1977, Preliminary documentation for a FORTRAN program to compute gravity terrain corrections based on topography digitized on a geographic grid: U.S. Geol. Survey open-file rept., no. 77-535, 45 p.
- Poole, F. G., and Sandberg, C. A., 1977, Mississippian paleogeography and tectonics of the western United States, in Stewart, J. H., Stevens, C. H., and Fritsche, A. E., eds., Paleozoic paleogeography of the western United States: Soc. Econ. Paleontologists and Mineralogists, Pacific Sec., Pacific Coast Paleogeography Symp. 1, p. 67-85.
- Poole, F. G., Sandberg, C. A., and Boucot, A. J., 1977, Silurian and Devonian paleogeography of the Western United States, in Stewart, J. H., Stevens, C. H., and Fritsche, A. E., eds., Paleozoic Paleogeography of the Western United States: Soc. Econ. Paleontologists and Mineralogists, Pacific Sec., Pacific Coast Paleogeography Symposium 1, p. 39-65.
- Porcella, R. L., ed., 1976, Seismic Engineering Program Report, July-September 1976; Menlo Park, Calif., Geol. Survey Circ. 736-C.
- , 1977a, Seismic engineering program report, January-April 1977; Menlo Park, Calif., Geol. Survey Circ. 762-A.
- , 1977b, Seismic engineering program report, October-December 1976; Menlo Park, Calif., Geol. Survey Circ. 736-D.
- Poty, Bernard, 1977, Intragranitic uranium ore deposits at Limousin and Forez, France, [abs.]: Geol. Soc. America Abs. with Programs, v. 9, no. 7, p. 1133-1134.
- Powers, R. B., 1977, Assessment of oil and gas resources in the Idaho-Wyoming thrust belt, in Wyo. Geol. Assoc. Guidebook, Ann. Field Conf., 29th, 1977, p. 629-637.

- Prescott, G. C., Jr., 1968, Ground water favorability areas and surficial geology of the lower Androscoggin River basin, Maine: U.S. Geol. Survey Hydrol. Inv. Atlas HA-285, 1 sheet, scale 1:62,500.
- , 1976, Ground water favorability and surficial geology of the Portland area, Maine: U.S. Geol. Survey Hydrol. Inv. Atlas HA-561, 1 sheet, Scale 1:62,500.
- Price, Don, and Arnow, Ted, 1974, Regional appraisals of the Nation's ground-water resources—Upper Colorado region: U.S. Geol. Survey Prof. Paper 813-C, 40 p.
- Provo, L. J., Kepferle, R. C., and Potter, P. E., 1977, The Three Lick Bed—Useful stratigraphic marker in the Upper Devonian shale in eastern Kentucky and adjacent areas of Ohio, West Virginia, and Tennessee: Energy Research and Development Administration, Comprehensive Report (MERC/CR-77-2).
- Rasmussen, W. C., and Bradford, G. M., 1977, Groundwater resources of Cambodia: U.S. Geol. Survey Water-Supply Paper 1608-P, 3 pls., 122 p.
- Ray, L. L., 1974, Geomorphology and Quaternary geology of the glaciated Ohio River Valley, a reconnaissance study: U.S. Geol. Survey Prof. Paper 826, 77 p.
- Read, C. B., and Mamay, S. H., 1964, Upper Paleozoic floral zones and floral provinces of the United States (including glossary of stratigraphic terms by Grace Kerohar): U.S. Geol. Survey Prof. Paper 454-K, p. K1-K35.
- Reasenber, P. A., Cessaro, R. K., and Wilson, D. H., 1977, The Centipede seismic recording system: U.S. Geol. Survey open-file rept. 77-315, 79 p.
- Redfield, A. C., and Rubin, Meyer, 1962, The age of salt marsh peat and its relation to recent changes in sea level at Barnstable, Massachusetts: National Acad. Sciences, Proc. v. 48, no. 10, p. 1728-1735.
- Reeves, C. C., Jr., 1974, Exploration in the Marfa Basin area of west Texas [abs.]: Econ. Geology, v. 69, no. 7, p. 1186.
- Reimer, G. M., 1977, Fixed volume gas inlet system for an alpha-sensitive cell adapted for radon measurement: U.S. Geol. Survey open-file rept. 77-409, 4 p.
- Reimer, G. M., and Otton, J. K., 1976, Helium in soil gas and well water in the vicinity of a uranium deposit, Weld County, Colorado: U.S. Geol. Survey open-file rept. 76-699, 10 p.
- Reynolds, C. D., Havryluk, I., Bastaman, S., and Atmowijojo, S., 1973, The exploration of the nickel laterite deposits in Irian Barat, Indonesia: Geol. Soc. Malaysia, Bull. 6, July 1973, p. 309-323.
- Rice, D. D., 1977, Petroleum potential of the Bob Marshall Wilderness and adjacent study areas: U.S. Geol. Survey open-file rept. 77-542, 39 p.
- Riggs, H. C., 1978, Streamflow characteristics from channel size: Proceedings of the Am. Soc. of Civil Engineers, Jour. of the Hydraulics Div., v. 104, no. HY1, p. 87-96.
- Rinella, J. F., and McKenzie, S. W., 1977, Elutriation study of Willamette River bottom material and Willamette-Columbia River water: U.S. Geol. Survey open-file rept. 78-28, 8 p.
- Ritter, J. R., 1977a, Reconnaissance of sedimentation in the Rio Pilcomayo Basin, May 1975, Argentina, Bolivia, and Paraguay: U.S. Geol. Survey open-file rept. 77-327, 1 pl., 34 p.
- , 1977b, Reconnaissance of sediment transport and channel morphology in the lower Rio Bermejo basin, Argentina, *with a section on Reconnaissance of the lower Rio Pilcomayo basin, Argentina and Paraguay*: U.S. Geol. Survey open-file rept. 76-564, 41 p.
- Rittmann, Alfred, 1952, Nomenclature of volcanic rocks: Bull. Volcanology, ser. II, Tome XII, p. 75-102.
- Robinove, C. J., 1977a, A radiometric interpretative legend for Landsat digital thematic maps: Photogram. Engineering, v. 43, no. 7, p. 593-594.
- , 1977b, Experimental land systems mapping with digital Landsat images [abs.]: International Symposium on Remote Sensing of the Environment, 11th, Ann Arbor, Mich., 1977, Proc., p. 1241.
- Roddy, D. J., 1977a, Large-scale impact and explosion craters—Comparison of morphological and structural analogs, *in Impact and Explosion Cratering*, Pergamon Press, p. 185-246.
- , 1977b, Pre-impact conditions and cratering processes at the Flynn Creek crater, Tennessee, *in Impact and Explosion Cratering*, Pergamon Press, p. 277-308.
- Roddy, D. J., and Davis, Kim, 1977, Shatter cones formed in large-scale experimental explosion craters, *in Impact and Explosion Cratering*, Pergamon Press, p. 715-750.
- Roddy, D. J., Ulrich, G. W., Sauer, F. M., and Jones, G. H. S., 1977a, Cratering motions and structural deformation in the rim of the Prairie Flat multiring explosion crater: Proc. 8th Lunar Science Conf., p. 3389-3407.
- Roedder, Edwin, and Weiblen, P. W., 1977, Compositional variation in late-stage differentiates in mare lavas, as indicated by silicate melt inclusions: Proc. 8th Lunar Science Conf., p. 1767-1783.
- Rohde, W. G., Taranik, J. V., and Nelson, C. A., 1977, Inventory and mapping of flood inundation using interactive digital image analysis techniques: W. T. Pecora Memorial Symposium, 2nd, Sioux Falls, S. Dak., Oct. 1976, Proc., Am. Soc. Photogramm., p. 131-143.
- Rohrer, W. L., 1966, Geologic map of the Kisinger Lakes quadrangle, Fremont County, Wyoming: U.S. Geol. Survey Geol. Quad. Map GQ-527, scale 1:24,000.
- Resholt, J. N., Zartman, R. E., and Nkomo, I. T., 1973, Lead isotope systematic and uranium depletion in the Granite Mountains, Wyoming: Geol. Soc. America Bull., v. 84, p. 989-1002.
- Ross, C. P., 1930, Geology and ore deposits of the Seafoam, Alder Creek, Little Smoky, and Willow Creek mining districts, Custer and Camas Counties, Idaho: Idaho Bur. Mines and Geol., pamph. 33, 26 p.
- , 1934, Correlation and interpretation of Paleozoic stratigraphy in south-central Idaho, Geol. Soc. America Bull., v. 45, no. 5, p. 937-1000.
- Ross, Malcolm, 1978, The "asbestos" minerals—Definitions, description, modes for formation, physical and chemical properties, and health risk to the mining community *in Workshop on asbestos: Definitions and Measurement Methods*, National Bur. of Stds. Spec. Publ. 506. [In press.]
- Rowan, L. C., Goetz, A. F. H., and Ashley, R. P., 1977, Discrimination of hydrothermally altered and unaltered rocks in visible and near-infrared images: Geophysics, v. 42, no. 2, p. 275-287.
- Rowan, L. C., Wetlaufer, P. H., Goetz, A. F. H., Billingsley, F. C., and Stewart, J. H., 1974, Discrimination of rock types and detection of hydrothermally altered areas in south-central Nevada by the use of computer-enhanced ERTS images: U.S. Geol. Survey Prof. Paper 883, 35 p.

- Rowley, P. D., Williams, P. L., and Schmidt, D. L., 1977, Geology of an Upper Cretaceous copper deposit in the Andean Province, Lassiter Coast Antarctic Peninsula: U.S. Geol. Survey Prof. Paper 984, 36 p.
- Rubin, D.M., McCulloch, D. E., and Hill, H. R., 1977, Bedform observations with a bottom-oriented rotating side-scan sonar in San Francisco Bay, California [abs]: Trans. Am. Geophys. Union, Eds., v. 58, no. 12, p. 1162.
- Runner, G. S., 1977, Flood of April 1977 in Kentucky, Tennessee, Virginia, and West Virginia: U.S. Geological Survey, open-file rept. 77-633, 49 p.
- , 1978, Flood of April 1977 on Tug Fork, Matewan to Williamson, West Virginia-Kentucky: U.S. Geol. Survey, Hydrol. Inv. Atlas, HA-588.
- Ruppel, E. T., 1978, Medicine Lodge thrust system, east-central Idaho and southwest Montana: U.S. Geol. Survey Prof. Paper 1031, 23 p.
- Sandberg, C. A., 1975, McGowan Creek Formation, new name for Lower Mississippian flysch sequence in east-central Idaho: U.S. Geol. Survey Bull. 1405-E, p. E1-E11.
- Sandberg, C. A., and Gutschick, R. C., 1977a, Deep-water Osagean conodont faunas from a starved basin in Utah: Geol. Soc. America Abs. with Programs, v. 9, no. 5, p. 649.
- , 1977b, Paleotectonic, biostratigraphic, and economic significance of Osagean to early Meramecian starved basin in Utah: U.S. Geol. Survey open-file rept. 77-121, 16 p., 5 figs.
- Sandberg, C. A., and Poole, F. G., 1977, Conodont biostratigraphy and depositional complexes of Upper Devonian cratonic-platform and continental-shelf rocks in the Western United States, in Murphy, M.A., Berry, W. B. N., and Sandberg, C. A., eds., Western North America; Devonian, p. 144-182.
- Sando, W. J., 1957, Beekmantown Group (Lower Ordovician of Maryland): Geol. Soc. America Mem. 68, 161 p.
- Sarna-Wojcicki, A. M., William, K. M., and Yerkes, R. F., 1976, Geology of the Ventura fault, Ventura County, California: U.S. Geol. Survey Misc. Field Studies Map MF-781, scale 1:6,000.
- Sass, J. H., Ziagos, J. P., Wollenberg, H. A., Munroe, R. J., di Somma, D. E., and Lachenbruch, A. H., 1977, Application of heat-flow techniques to geothermal energy exploration, Leach Hot Springs area, Grass Valley, Nevada: U.S. Geol. Survey open-file rept. 77-762, 125 p.
- Sato, Motoaki, 1977, The driving mechanism of lunar pyroclastic eruptions inferred from the oxygen fugacity behavior of Apollo 17 orange glass: Trans. Am. Geophys. Union, EOS, v. 58, p. 425.
- Sauer, S. P., 1978, Recent and projected changes in Dead Sea level and effects on mineral production from the Sea: U.S. Geological Survey open-file rept. 78-176, 43 p.
- Savitzky, A. and Golay, M. J. E., 1964, Smoothing and differentiation of data by simplified least squares procedure: Anal. Chem. v. 36, p. 1627-1639.
- Sawatzky, D. L., 1967, Tectonic style along the Elkhorn thrust, eastern South Park and western Front Range, Park County, Colorado: Colorado School of Mines D. Sc. thesis, 206 p.
- Schoen, Robert, 1978, Role of earth science in coastal zone management: Coastal Zone 78 Proc., v. III, p. 1589-1601.
- Schopf, J. M., 1977, Coal forming elements in permineralized peat from Mount Augusta (Queen Alexandra Range): Antarctic Jour. of the United States, v. 12, no. 4, p. 110-112.
- Schopf, J. M. and Oftedahl, O. G., 1976, The Reinhardt-Thiesse coal thin section slide collection of the U.S. Geological Survey—catalog and notes: U.S. Geol. Survey Bull. 1432, 58 p.
- Schuetz, J. R., and Matthes, W. J., Jr. 1977 Fluvial sediment data for Iowa: Suspended-sediment concentrations, loads, and sizes; bed-material sizes; and reservoir siltation: Iowa Geol. Survey Tech. Info. Series, no. 6, 410 p.
- Schweitering, J. F., 1970, Devonian shales of Ohio and their eastern equivalents: unpubl. Ph. D. dissertation, Ohio State Univ.
- Scott, D. H., Diaz, J. M., and Watkins, J. A., 1977, Lunar far side tectonics and volcanism [abs.], in Lunar Science VIII, pt. 2: Houston, Tex., Lunar Science Inst., p. 863-864.
- Seeland, D. A., 1976, Uranium deposits, Powder River Basin, Wyoming, in Geological Survey Research 1976: U.S. Geol. Survey Prof. Paper 1000, p. 36-37.
- Shaler, N. S., Woodworth, J. B., and Foreste, A. F., 1899, Geology of the Narragansett Basin: U.S. Geol. Survey Mon. 33, 402 p.
- Sharp, R. V. 1976, Surface faulting in Imperial Valley during the earthquake swarm of January-February 1975: Seismol. Soc. America Bull., v. 66, p. 1145-1154.
- Shaw, H. R., Smith, R. L., and Hildreth, E. W., 1976, Thermogravitational mechanisms for chemical variations in zoned magma chambers: Geo. Soc. America Abs. with Programs, v. 8, no. 6, p. 1102.
- Shearman, J. O., 1977, Computer applications for step-backwater and floodway analyses: U.S. Geol. Survey open-file rept. 76-499, 103 p.
- Shoemaker, E. M., Roach, C. H., and Byers, F. M., Jr., 1957, Diatremes on the Navajo and Hopi Reservations, Arizona: U.S. Geol. Survey rept. TEI-700, p. 141-151.
- , 1962, Diatremes and uranium deposits in the Hopi Buttes, Arizona, in Petrologic studies—A volume in honor of A. F. Buddington: New York, Geol. Soc. America, p. 327-355.
- Sheridan, D. M., and Raymond, W. H., 1977, Preliminary data on some Precambrian deposits of zinc-copper-lead sulfides and zinc spinel (gahnite) in Colorado: U.S. Geol. Survey open-file rept. 77-607, 27 p.
- Shreve, R. L., 1966, Sherman landslide, Alaska: Science, v. 154, no. 3757, p. 1639-1643.
- Shroba, R. R., 1976, Soil development on Pinedale, Bull Lake, and pre-Bull Lake tills, Sawatch Range and Front Range, Colorado, Sangre de Cristo Range, New Mexico, and Wind River Range, Wyoming: Geol. Soc. America Abs. with Programs v. 8, no. 5, p. 629.
- Shurbet, D. H., and Reeves, C. C., Jr., 1977, The fill in Marfa basin, Texas: Am. Assoc. Petroleum Geologist Bull., v. 61, no. 4, p. 612-615.
- Siems, D. F., Curtis, C. A., Motooka, J. M., and McDanal, S. K., 1977, Analyses of stream sediment, soil, and rock samples from New River Gorge area, Fayette, Raleigh, and Summers Counties, West Virginia: U.S. Geol. Survey open-file rept. OF-77-88, 36 p.
- Silberling, N. J., and Roberts, R. L., 1962, Pre-Tertiary stratigraphy and structure of northwestern Nevada: Geol. Soc. America Spec. Paper 72, 58 p.

- Skehan, J. W., S. J., Belt, E. S., Rast, Nicholas, Murray, D. P., Hermes, O. D., and Dewey, J. F., 1976, Alleghenian deformation, sedimentation, and metamorphism in southeastern Massachusetts and Rhode Island; *in* Geol. of Southeast New England: p. 447-471.
- Skehan, J. W., S. J., Murray, D. P., Palmer, A. R., and Smith, A. T., 1977, The geological significance of Middle Cambrian trilobite-bearing phyllites from southern Narragansett Basin, Rhode Island: Geol. Soc. America, Abs. with Programs, v. 9, no. 3, p. 319.
- Sims, P. K., 1976, Early Precambrian tectonic-igneous evolution in the Vermilion district, northeastern Minnesota: Geol. Soc. America Bull., v. 87, p. 379-389.
- Skipp, B. A., 1978, Great Basin Region, Chapter P, *in* L. C. Craig, ed., Paleotectonic investigations of the Mississippian System in the United States: U.S. Geol. Survey Prof. Paper 1010. [In press.]
- Skipp, B. A., and Hait, M. H., Jr., 1977, Allochthons along the northeast margin of the Snake River Plain, Idaho, *in* Wyo. Geol. Assoc. Guidebook: Ann. Field Conf., 29th, 1977, p. 499-515.
- Skipp, B. A., and Hall, W. E., 1975, Structure and Paleozoic stratigraphy of a complex of thrust plates in the Fish Creek Reservoir area, south-central Idaho: U.S. Geol. Survey Jour. of Research, v. 3, no. 6, p. 671-689.
- Sloan, R. E., 1964, The Cretaceous System in Minnesota: Minnesota Geol. Survey rept. Inv. 5, 64 p.
- Smiley, C. J., 1969, Floral zones and correlations of Cretaceous Kukpowruk and Corwin Formations, northwestern Alaska: Am. Assoc. Petroleum Geologists Bull., v. 53, p. 2079-2093.
- Smith, B. D., Cody, J. W., Campbell, D. L., Daniels, J. J., Flanagan, V. J., 1976, A case for "other" geophysical methods in exploration for uranium deposits: Internat. Atomic Energy Agency, Vienna, 1976, Proc., p. 337-351.
- Smith, C. B., McCallum, M. E., Coopersmith, H. G., and Egger, D. H., 1977, Petrography, petrology and chemistry of kimberlite from the Colorado-Wyoming State Line and Iron Mountain, Wyoming, districts, [Extended Abs.]: Intern. Kimberlite Conf., 2nd, Santa Fe, N. Mex.
- Smith, C. B., McCallum, M. E., and Egger, D. H., 1977, Kimberlite with carbonatitic affinities at Iron Mountain, Wyoming: Geol. Soc. America Abst. with Programs, v. 9, no. 6, p. 763-764.
- Smith, G. O., 1904, Description of the Mount Stuart quadrangle, Washington: U.S. Geol. Survey, Geol. Atlas Mount Stuart, Folio no. 106, 10 p.
- Smith, G. O., and Calkins, F. C., 1906, Description of the Shoqualmie Pass quadrangle, Washington: U.S. Geol. Survey, Geol. Atlas Snoqualmie Pass, Folio 139, 14 p.
- Smith, R. L., and Bailey, R. A., 1968, Resurgent cauldrons: Geol. Soc. America Mem. 116, p. 613-662.
- Snavely, P. D., Jr., Pearl, J. E., Lander, D. L., and Scott, E. W., 1977, Interim report on petroleum resource potential and geologic hazards in the Outer Continental Shelf—Oregon and Washington Tertiary Province: U.S. Geol. Survey open-file rept. 77-282, 64 p.
- Sniegocki, R. T., 1976, Bibliography and selected abstracts of reports on water resources and related subjects for Arkansas, through 1975: Arkansas Geological Commission Water Resources Summary, Little Rock, Ark., no. 10, 237 p.
- Soderblom, L. A., Arnold, J. R., Boyce, J. M., and Lin, R. P., 1977, Regional variations in the lunar maria: Age, radioactivity, remanent magnetism: Proc. 8th Lunar Science. Conf., v. 1, p. 1191-1200.
- Soren, Julian, 1976, Basement flooding and foundation damage from water-table rise in the East New York section of Brooklyn, Long Island, New York: U.S. Geol. Survey Water-Resources Inv. 76-95, 14 p.
- , 1977, Ground-water quality near the water table in Suffolk County, Long Island, New York: Hauppauge, New York, Suffolk County Department Environmental Control, Long Island Water-Resources Bull. 8, 33 p.
- Soren, Julian, 1978a, Subsurface geology and paleogeography of Queens County, Long Island, New York: U.S. Geol. Survey Water-Resources Inv. 77-34. [In press.]
- , 1978b, Hydrogeologic conditions in the Town of Shelter Island, Suffolk County, Long Island, New York: U.S. Geol. Survey Water-Resources Inv. 77-77. [In press.]
- Spieker, E. M., 1931, The Wasatch Plateau coal field, Utah: U.S. Geol. Survey Bull. 819, 210 p.
- Spirakis, C. S., Goldhaber, M. B., and Reynolds, R. L., 1977, Thermoluminescence of sand grains around a south-Texas roll-type deposit: U.S. Geol. Survey open-file rept. 77-640, 13 p.
- Stout, M. L., 1964, Geology of a part of the south-central Cascade Mountains, Washington: Geol. Soc. America Bull., v. 75, p. 317-334.
- Stuckless, J. S., and Nkomo, I. T., 1978, Uranium-lead isotope systematics in Uraniferous alkali-rich granites from the Granite Mountains, Wyoming—Implications for uranium source rocks: Econ. Geol. [In press.]
- Swadley, W. C., 1971, The preglacial Kentucky River of northern Kentucky, *in* Geological Survey Research 1971: U. S. Geol. Survey Prof. Paper 750D, p. D127-D131.
- Swarzenski, W. V., and Mundorff, M. J., 1977, Geohydrology of North Eastern Province, Kenya: U.S. Geol. Survey Water-Supply Paper 1757-N, 5 pls., 68 p.
- Tangborn, W. V., 1978, Applications of a new hydro-meteorological streamflow prediction model: Annual Western Snow Conference, 45th, Albuquerque, New Mexico, April 19-21, 1977, Proc. [In press.]
- Taylor, F. B., 1903, The correlation and reconstruction of recessional ice borders in Berkshire County, Massachusetts: Jour. of Geology, p. 323-364.
- Taylor, H. E. and Schroder, L. J., 1978, A lithium isotope ratio technique for tracer or tagging applications in natural water samples [abs.]: 1978 Pittsburg Conference on Analytical Chemistry and Applied Spectroscopy, Cleveland, Ohio, Feb. 27-Mar. 3, 1978, Proc., p. 63.
- Terzaghi, R. D. 1969, Brinefield subsidence at Windsor, Ontario: 3d Symposium on salt, Northern Ohio Geol. Soc., Inc., v. II, p. 298-307.
- Thatcher, W., Castle, R. O., and Holdahl, S. R., 1976, Further analysis of geodetic data from southern California [abs.]: Trans. Am. Geophys. Union, EOS, v. 57, p. 898.
- Thayer, T. P., Case, J. E., and Stotelmeyer, R. E., 1977, Mineral resources of the Strawberry Mountain Wilderness and adjacent areas, Grant County, Oregon: U.S. Geol. Survey open-file rept., 77-420, 116 p.
- Theobald, P. K., and Allcott, G. H., 1975, Tungsten anomalies in the Uyaijah ring structure, Kushaymiyah igneous complex, Kingdom of Saudi Arabia, with sections on Geology and geochemistry of the Uyaijah ring struc-

- ture by Theobald, P. K., and Allcott, G. H., and Regional geophysics, by Flanigan, V. J., and Andreasen, G. E.: U.S. Geol. Survey open-file rept. 75-657 [(IR)SA-160], 86 p., 32 figs.
- Thomasson, M. R., 1959, Late Paleozoic stratigraphy and paleotectonics of central and Eastern Idaho [Nos.]: Ph.D. dissert., v. 20, no. 3, p. 999.
- Thorley, G. A., and Hood, D. R., 1977, Pacific Northwest Land Resources Inventory Demonstration Project—an overview: 23rd annual ASP/ACSM Convention, Proc., p. 29-42.
- Tilling, R. I., 1973, Boulder batholith, Montana—a product of two contemporaneous but chemically distinct magma series: Geol. Soc. America Bull., v. 84, no. 12, p. 3879-3900.
- Toulmin, Priestley III, Baird, A. K., Clark, B. C., Keil, Klaus, and Rose, H. J., Jr., 1977, Report of the Viking inorganic chemical analysis team: Jour. Geophys. Research, v. 82, p. 4575.
- Toulmin, Priestley III, Baird, A. K., Clark, B. C., Keil, Klaus, Rose, H. J., Jr., Christian, R. P., Evans, P. H., and Kelliher, W. C., 1977, Geochemical and mineralogical interpretation of the Viking inorganic chemical results: Jour. Geophys. Research, v. 82, p. 4625-4634.
- Townshend, John B., 1978, Improvements in magnetic observatory construction and operation in permafrost areas: U.S. Geol. Survey open-file rept. 78-213, 9 p., 10 figs.
- Trapp, Henry, Jr., Pascale, C. A., and Foster, J. B., 1977, Water resources of Okaloosa County and adjacent areas: U.S. Geol. Survey Water-Resources Inv. 77-9, 130 p.
- Trescott, P. C., 1975, Documentation of finite-difference model for simulation of three-dimensional ground-water flow: U.S. Geological Survey open-file rept. 75-438, 32 p.
- Trimble, S. W., 1977, the fallacy of stream equilibrium in contemporary denudation studies: Am. Jour. of Science, v. 277, p. 876-887.
- Turner-Peterson, C. E., 1977, Uranium mineralization during early burial, Newark Basin, Pennsylvania-New Jersey; in Campbell, J. A., Short papers of the U.S. Geological Survey Uranium-Thorium Symposium, 1977: U.S. Geol. Survey Circ. 753, p. 3-4.
- Tysdal, R. G., Case, J. E., Winkler, G. R., and Clark, S. H. B., 1977, Sheeted dikes, gabbro, and pillow basalt in flysch of coastal Southern Alaska, Geology, v. 5, p. 377-383.
- U.S. Army Engineer District, Corps of Engineers, Los Angeles, California, in cooperation with U.S. Department of the Interior, Geological Survey, Denver, Colorado, 1976, Report on landslide study, Pacific Palisades area, Los Angeles County, California: U.S. Army Engineer Dist., Corps of Engineers, Los Angeles, Calif., main rept., 30 p., App., 89 p., map.
- U.S. Geological Survey, 1974, Hydrologic unit map—1974: U.S. Geological Survey, Ofc. of Water Data Coordination; 47 maps by States, [1974-1977], scale 1:500,000.
- , 1976, Geological Survey Research 1976: U.S. Geol. Survey Prof. paper 1000, 414 p.
- U.S. Geological Survey, 1977a, National handbook of recommended methods for water-data acquisition: U.S. Geol. Survey, Office of Water Data Coordination, Intro., 11 p. and chap. V, 193 p.
- , 1977b, Geochemical survey of the Western energy regions, Fourth Annual Progress Report July, 1977: U.S. Geol. Survey open-file rept. 77-872, 207 p.
- , 1977c, Landsat image geographic map, Federal Capital Territory, Republic of Nigeria: Nigeria Federal Capital Development Authority, scale 1:100,000.
- U.S. Geological Survey, 1978a, Federal plus for the acquisition of water data, fiscal years 1978 and 1979: U.S. Geol. Survey, Office of Water Data Coordination, 31 p., 5 app.
- , 1978b, Regional plans for acquisition of water data, fiscal years 1978 and 1979: U.S. Geological Survey, Ofc. of Water Data Coordination (by region, 21 volumes).
- , 1978c, Catalog of information on water data: Streamflow and stage quality of surface water, and quality of ground water: U.S. Geological Survey, Ofc. of Water Data Coordination (by region, 21 volumes).
- , 1978d, Catalog of information on water data: Index to areal investigations and miscellaneous activities: U.S. Geol. Survey, Ofc. of Water Data Coordination (1 volume, 21 chapters by region).
- , 1978e, Catalog of information on water data: Index to stations in coastal areas, streamflow and stage, surface-water quality, and ground-water quality: U.S. Geological Survey, Ofc. of Water Data Coordination, 4 volumes.
- , 1978f, Catalog of information on water data: Index to stations in coal-resources areas, streamflow and stage, surface-water quality, and ground-water quality: U.S. Geological Survey, Ofc. of Water Data Coordination (East and West United States, 2 volumes).
- U.S. National Archives, 1976, Interim primary drinking regulations: Federal Register, July 9, 1976, part 141, p. 28402-28405.
- Van Andel, T. H., and Bukry, J. D., 1973, Basement ages and basement depths in the eastern Equatorial Pacific from Deep Sea Drilling Project legs 5, 8, 9, and 16: Geol. Soc. America Bull., v. 84, no. 7, p. 2361-2369.
- Van Horn, Richard and Van Driel, J. N., 1977, Computer composite map showing inferred relative stability of the land surface during earthquakes, Sugar House quadrangle, Salt Lake County, Utah: U.S. Geol. Survey Misc. Inv. Map I7660, 1 sheet, scale 1:24,000.
- Wallace, R. E., 1977, Profiles and ages of young fault scarps, north-central Nevada: Geol. Soc. America Bull., v. 88, p. 1267-1281.
- Waller, R. M., Feulner, A. J., and Tisdell, F. E., 1962, Ground-water movement in the Fort Greely area, Alaska, [abs.], in Dahlgren, George Jr., ed., Science in Alaska 1961: American Association for the Advancement of Science, Alaskan Division, Alaskan Science Conference, 12th, College, Alaska, August 28-September 1, 1961, Proceedings, p. 133-134.
- Walters, R. F. 1976, Land subsidence in central Kansas related to salt dissolution: Solution Mining Research Inst., Inc., 144 p.
- Wandle, S. W., J., 1977, Estimating the magnitude and frequency of floods on natural-flow streams in Massachusetts: U.S. Geol. Survey Water-Resources Inv. 77-39, 1 pl., 26 p.
- Ward, F. N., and Bondar, W. F., 1978, Analytical methodology in the search for metallic ores: Proc. Canadian Geoscience Council Explo 77, Ottawa, Oct. 16-21, 1977.

- Wargo, J. G., 1959, The geology of the Schoolhouse Mountain quadrangle, Grant County, New Mexico: Tucson, Ariz., Univ. Arizona Ph. D. dissert., 187 p.
- Warren, C. G., 1977, Ground water flow and the shape of uranium roll deposits, in J. A. Campbell, ed., Short papers of the U.S. Geological Survey uranium-thorium symposium, 1977: U.S. Geol. Survey Circ. 753, p. 24-25.
- Waterhouse, J. B., 1973, An ophiceratid ammonoid from the New Zealand Permian and its implications for the Permian-Triassic boundary: *Geology*, v. 110, no. 4, p. 305-329.
- , 1976, World correlations for Permian marine faunas: Univ. Queensland, Australia, Dept. Geol. Papers, v. 7, no. 2, 232 p.
- Waterhouse, J. B., and Bonham-Carter, G. E., 1976, Range, proportionate representation, and demise of brachiopod families through Permian: *Geol. Mag.*, v. 113, no. 5, p. 401-428.
- Waterways Experiment Station, 1949, Geological investigations of gravel deposits in the lower Mississippi Valley and adjacent uplands: Waterways Experiment Sta., Vicksburg, Miss., Tech. Mem. 3-273, 58 p.
- Weaver, C. E., 1912, A preliminary report on the Tertiary paleontology of western Washington: *Washington Geological Survey Bulletin* 15, 80 p.
- Webber, E. E., and Bartlett, W. P., Jr., 1977, Floods in Ohio, magnitude and frequency: Ohio Department of Natural Resources, Water Division Bull. 45, 76 p.
- Webster, D. A., 1977, Land burial of solid radioactive waste at Oak Ridge National Laboratory, Tennessee—A case history: Symposium on management of low-level radioactive waste, Atlanta, Ga., May 23-27, 1977, Proc. [In press.]
- Wershaw, R. L., and Pinckney, D. J., 1978, Methylation of humic acid fractions: *Science*, v. 199, Feb. 24th, p. 906-907.
- White, D. E., Muffler, L. J. P., Fournier, R. O., and Truesdell, A. H., 1975, Physical results of research drilling in thermal areas of Yellowstone National Park: U.S. Geol. Survey Prof. Paper 892, 70 p.
- William, P. L., 1964, Geology, structure, and uranium deposits of the Moab quadrangle, Colorado and Utah: U.S. Geol. Survey Misc. Geol. Inv. Map I-360, scale 1:250,000.
- Williams, P. L., Schmidt, D. L., Plummer, C. C., and Brown, L. E., 1972, Geology of the Lassiter Coast area, Antarctic Peninsula—preliminary report, in Adie, R. J., ed., Antarctic geology and geophysics: Oslo, Universitetsforlaget, p. 143-148.
- Wilson, L. R., 1977, Automated magnetic observatories [abs.]: *Trans. Am. Geophys. Union*, EDS. v. 58, no. 8, p. 774.
- Wilson, W. E. III, 1977, Simulated changes in ground-water levels resulting from proposed phosphate mining, west-central Florida—preliminary results: U.S. Geol. Survey open-file rept. 77-882, 46 p.
- Wilson, W. E. III, Burke, E. L., and Thomas, C. E., Jr., 1974, Water resources inventory of Connecticut, lower Housatonic River basin, Part 5: Connecticut Water-Resources Bull. 19, 79 p.
- Winner, M. D., Jr., 1978, Ground-water resources along the Blue Ridge Parkway, North Carolina: U.S. Geol. Survey Water Resources Inv. 77-65. [In press.]
- Winter, T. C., 1976, Numerical simulation analysis of the interaction of lakes and ground water: U.S. Geol. Survey Prof. Paper 1001, 45 p.
- Wintsch, R. P., 1976, Lithologic control of thrusting in eastern Connecticut [abs.]: *Geol. Soc. America Abs. with programs* v. 8, no. 2, p. 303.
- Woll, P. W., and Fischer, W. A., eds., 1977, Proceedings of the First Annual W. T. Pecora Memorial Symposium, 1975, Sioux Falls, S. Dak.: U.S. Geol. Survey Prof. Paper 1015, 370 p.
- Wood, H. B., 1976, Fluorine, in *Mineral facts and problems*, 1975 ed.: U.S. Bureau Mines Bull. 667, p. 379-399.
- Wones, D. R., 1974, Igneous petrology of some plutons in the northern part of the Penobscot Bay Area: in Osberg, P. H. ed., *Geology of east-central and north-central Maine: N.E.I.G.C. Guidebook* 1974, p. 99-125.
- Wyant, D. G., and Barker Fred, 1976, 1976, Geologic map of the Milligan Lakes quadrangle, Park County, Colorado. U.S. Geol. Survey Geol. Quad. Map GQ-1343, scale 1:24,000.
- Yotsukura, Nobuhiro, and Sayre, W. W., 1977, Reply to H. T. Shen's discussion: *Water Resources Research*, v. 13, no. 2, p. 497.
- Youd, T. L., and Perkins, D. M., 1977, Mapping of liquefaction potential using probability concepts, in *Use of probabilities in earthquake engineering: Am. Soc. Civil Engineers preprint* no. 2913, p. 61-84.
- Young, E. J., 1972, Laramide-Tertiary intrusive rocks of Colorado: U.S. Geol. Survey open-file rept. 1 pl., 206 p.
- Young, R. A., 1966, Cenozoic geology along the edge of the Colorado Plateau in northwestern Arizona: St. Louis, Mo., Washington Univ., Ph. D. dissert., 167 p.
- Zablocki, C. J., 1978, Self-potential studies in east Puna, Hawaii: Hawaii Institute of Geophys. Tech. rept., Univ. of Hawaii. [In press.]
- Zietz, Isidore, Karl, J. H., and Ostrom, M. E., 1977, Preliminary aeromagnetic map covering most of the exposed Precambrian terrane in Wisconsin: U.S. Geol. Survey Misc. Field Studies May MF-888 scale 1:250,000 [In press.]
- Zen, E-an, 1977, Some regional tectonic problems inferred from the Pioneer Mountains, Montana: *Geol. Soc. America Abs. with programs* v. 9, no. 6, p. 779.
- Zen, E-an, Marvin, R. F., and Mehnert, H. H., 1975, Preliminary petrographic, chemical, and age data on some intrusive and associated contact metamorphic rocks, Pioneer Mountains, southwestern Montana: *Geol. Soc. America Bull.*, v. 86, no. 3, p. 367-370.
- Zohdy, A. A. R., Bisdorf, R. J., and Glancy, P. A., 1977, Schlumberger soundings near Fallon, Nevada: Nevada Division of Water Resources Inf. rept. 25, 39 p.
- Zohdy, A. A. R., Jackson, D. B., and Bisdorf, R. K., 1975, Schlumberger soundings and total field measurements in the Raft River geothermal area, Idaho: U.S. Geol. Survey open-file rept. 75-130, 136 figs. 3 plates, 3 p.

INVESTIGATIONS IN PROGRESS IN THE GEOLOGICAL SURVEY

Investigations in progress during fiscal year 1978 are listed below together with the names and headquarters of the individuals in charge of each. Headquarters at main centers are indicated by NC for the National Center in Reston, Va., D for Denver, Colo., and M for Menlo Park, Calif. The lowercase letter after the name of the project leader shows the Division technical responsibility: c, Conservation Division; l, Land Information and Analysis; w, Water Resources Division; no letter, Geologic Division.

The projects are classified by principal topic. Most geologic-mapping projects involve special studies of stratigraphy, petrology, geologic structure, or mineral deposits but are listed only under "Geologic mapping" unless a special topic or commodity is the primary justification for the project. A reader interested in investigations of volcanology, for example, should look under the heading "Geologic mapping" for projects in areas of volcanic rocks, as well as under the heading "Volcanology." Likewise, most water-resource investigations involve special studies of several aspects of hydrology and geology but are listed only under "Water Resources" unless a special topic—such as floods or sedimentation—is the primary justification for the project.

Areal geologic mapping is subdivided into mapping at scales smaller than 1:62,500 (for example, 1:250,000) and mapping at scales of 1:62,500 or larger (for example, 1:24,000).

Abstracts. See Bibliographies and abstracts.

Aluminum;

Resources of the United States (S. H. Patterson, NC)

Analytical chemistry;

Activation analysis (J. J. Rowe, NC)

Analytical methods:

Textural automatic image analyzer research (M. B. Sawyer, D)

Water chemistry (M. J. Fishman, w, D)

Analytical services and research (J. I. Dinnin, NC; Claude Huffman, Jr., D; C. O. Ingamells, M)

Mineral deposits, characteristic analysis (J. M. Botbol, NC)

Organic geochemistry and infrared analysis (I. A. Berger, NC)

Organic polyelectrolytes in water (R. L. Wershaw, w, D)

Plant laboratory (T. F. Harms, D)

Radioactivation and radiochemistry (H. T. Millard, D)

Rock chemical analysis:

General (D. R. Norton, D)

Rapid (Leonard Shapiro, NC)

Services (L. B. Riley, D)

Trace analysis methods, research (F. N. Ward, D)

Ultratrace analysis (H. T. Millard, D)

X-ray spectrometer for Viking lander (Priestley Toulmin III, NC)

See also Spectroscopy.

Arctic engineering geology (Reuben Kachadoorian, M)

Artificial recharge:

Artificial recharge, Lytle Creek (M. J. Mallory, w, Laguna Niguel, Calif.)

Artificial recharge methods (W. F. Lichtler, w, Lincoln, Nebr.)

Artificial recharge methods (E. P. Weeks, w, Lubbock, Tex.)

Chemical reactions mineral surfaces (J. D. Hem, w, M)

Columbia River basalt recharge (N. P. Dion, w, Tacoma, Wash.)

Column-basin studies (Murray Garber, w, Syosset, N.Y.)

Confined aquifer San Bernadino (W. F. Hardt, w, Laguna Niguel, Calif.)

Deepwell waste injection (C. A. Pascale, w, Tallahassee, Fla.)

Fort Allen recharge (J. R. Diaz, w, Fort Buchanan, P.R.)

Fresh water in saline aquifers (I. W. Meyer, w, Miami, Fla.)

Artificial recharge—Continued

Injection wells, Santa Rosa County (C. A. Pascale, w, Tallahassee, Fla.)

Lee County freshwater injection (F. W. Meyer, w, Miami, Fla.)

Nassau County recharge (T. M. Robinson, w, Syosset, N. Y.)

Recharge, Bijou Creek (R. K. Livingston, w, D)

Recharge feasibility factors (J. Rubin, w, M)

Subsurface storage, waste heat (J. D. Bredehoeft, w, NC)

Subsurface waste disposal (R. W. Davis, w, Louisville, Ky.)

Supplemental recharge by storm basins (D. A. Aronson, w, Syosset, N. Y.)

Water management east central Florida (F. A. Watkins, w, Orlando, Fla.)

Barite:

Geology, geochemistry, and resources of barite (D. A. Brobst, NC)

Base metals. See base-metal names.

Bibliographies and abstracts:

Luna bibliography (J. H. Freeberg, M)

Outer Continental Shelf onshore impact assessment (M. L. Pattison, l, NC)

Borates:

California (N):

Furnace Creek area (J. F. McAllister)

Searles Lake area (G. I. Smith)

Chromite. See Ferro-alloy metals.

Clays:

Bentonite, resource evaluation in Rocky Mountain region (C. A. Wolfbauer, D)

State:

Georgia, kaolin investigations (S. H. Patterson, NC)

Climatic changes:

California, Quaternary (D. P. Adam, M)

Coal:

Experimental techniques to prepare geologic and resource maps (M. J. Bergin, NC; G. D. Stricker, NC)

Geochemistry of United States coal (V. E. Swanson, D)

National Coal Resources Data System (M. D. Carter, NC)

Coal—Continued*States:***Alaska:**

Bering River coal field (C, Anchorage)
Cape Beaufort-Corwin Bluff coal field (J. E. Callahan, c, Casper, Wyo.)

Nenana (Clyde Wahrhaftig, M)

Arizona, collection of coal samples for analysis (R. T. Moore, Tucson; V. E. Swanson, D)

Colorado (c, D, except as otherwise noted):

Buckhorn Lakes quadrangle (R. G. Dickinson)

Citadel Plateau (G. A. Izett)

Collection of coal samples and coal resource data in Colorado and entry of data into the USGS National Coal Resources Data System (D. K. Murray; M. D. Carter, NC)

Courthouse Mountain quadrangle (R. G. Dickinson)

Denver basin, tertiary coal zone (P. E. Soister)

Disappointment Valley, eastern (D. E. Ward, D)

Douglas Creek Arch area (B. E. Barnum)

Grand Mesa coal field (G. P. Eager)

North Park area (D. J. Madden)

Savery quadrangle (C. S. V. Barclay)

Smizer Gulch and Rough Gulch quadrangles (W. J. Hail, D)

Washboard Rock quadrangle (R. G. Dickinson)

Watkins and Watkins SE quadrangles (P. E. Soister)

Idaho, collection of coal samples in Idaho (C. R. Knowles, Moscow; V. E. Swanson, D)

Illinois, preparation of Illinois coal resource and chemical data for entry into the USGS National Coal Resources Data System (H. J. Gluskoter, Urbana; M. D. Carter, NC)

Kentucky (D):

Adams quadrangle (D. E. Ward)

Blaine quadrangle (C. L. Pillmore)

Louisa quadrangle (R. M. Flores)

Richardson quadrangle (P. T. Hayes)

Sitka quadrangle (P. T. Hayes)

Missouri, coal data collection and transfer to the National Coal Resources Data System (C. E. Robertson, Rolla; M. D. Carter, NC)

Montana:

Birney SW quadrangle (S. Volz, c, Casper, Wyo.)

Black Butte quadrangle (W. L. Rohrer, c, Casper, Wyo.)

Coal mechanics in northern Powder River basin (J. M. White, c, Billings)

Collection of coal samples in Montana (R. E. Matson, Butte; V. E. Swanson, D)

Decker quadrangle (B. E. Law, c, D)

Girard field (M. A. Soule, c, Billings)

Half Moon Hill quadrangle (V. Neirmeir, c, Casper, Wyo.)

Holmes Ranch quadrangle (N. E. Micklich, c, Casper, Wyo.)

Jordan quadrangle (G. D. Mowat, c, Billings)

Kirby quadrangle (c, Casper, Wyo.)

McCone County lignite (H. C. Taylor, c, Billings)

Monarch quadrangle (B. E. Barnum, c, D)

Pearl School quadrangle (G. L. Galyardt, c, Casper, Wyo.)

Sidney coal field (J. C. Harksen, c, Billings)

Spring Gulch quadrangle (N. E. Micklich, c, Casper, Wyo.)

Subsidence of spoil piles, Colstrip (R. A. Farrow, D; J. M. White, c, Billings)

Taintor Desert quadrangle (S. Volz), c, Casper, Wyo.)

Tongue River Dam quadrangle (N. E. Micklich, c, Casper, Wyo.)

Nevada, collection of coal samples in Nevada (J. A. Schilling, Reno; V. E. Swanson, D)

Coal—Continued*States—Continued***New Mexico:**

Alamosa Mesa West quadrangle (D. B. Umshler, c, Roswell)
Collection of coal samples in New Mexico (F. E. Kottlowski, Socorro; V. E. Swanson, D)

Gallup East quadrangle (E. D. Patterson, c, Roswell)

Gallup West quadrangle (J. E. Fassett, c, Farmington)

Manuelito quadrangle (J. E. Fassett, c, Farmington)

Ojo Encino Mesa quadrangle (D. B. Umshler, c, Roswell)

Pueblo Alto Trading Post quadrangle (R. W. Jentgen, c, Farmington)

Samson Lake quadrangle (J. E. Fassett, c, Farmington)

Star Lake quadrangle (J. E. Fassett, c, Farmington)

Tanner Lake quadrangle (D. B. Umshler, c, Roswell)

Twin Butte, quadrangle (M. L. Millgate, c, Farmington)

Western Raton field (C. L. Pillmore, D)

North Dakota (c, Billings, Mont., except as otherwise noted):

Adams, Bowman, and Slope Counties lignite resources (R. C. Lewis)

Clark Butte 15-minute quadrangle (G. D. Mowat)

North Almont quadrangle (H. L. Smith, c, D)

West-central North Dakota lignite resources (E. A. Rehbein)

Williston area lignite resources (J. M. Spencer)

Oklahoma (c, Tulsa, except as otherwise noted):

Blocker quadrangle (E. H. Hare, Jr.)

Collection of coal samples in Oklahoma (S. A. Friedman, Norman; V. E. Swanson, D)

Hackett quadrangle (E. H. Hare, Jr.)

Panama quadrangle (E. H. Hare, Jr.)

Spiro quadrangle (E. H. Hare, Jr.)

Pennsylvania (NC, except as otherwise noted):

Collection of coal samples for analysis (W. E. Edmunds, Pennsylvania State Geological Survey, Harrisburg; M. J. Bergin)

Northern anthracite field (M. J. Bergin)

Southern anthracite field (G. H. Wood, Jr.)

Utah (c, D, except as otherwise noted):

Basin Canyon quadrangle (Fred Peterson)

Big Hollow Wash quadrangle (Fred Peterson)

Blackburn Canyon quadrangle (Fred Peterson)

Butler Valley quadrangle (W. E. Bowers)

Canaan Peak quadrangle (W. E. Bowers)

Collet Top quadrangle (H. D. Zeller)

East-of-the-Navajo quadrangle (H. D. Zeller)

Fourmile Bench quadrangle (W. E. Bowers)

Geology and coal resources of Wasatch Plateau coalfield (L. F. Blanchard)

Horse Flat quadrangle (H. D. Zeller)

Horse Mountain quadrangle (W. E. Bowers)

Jessen Butte quadrangle (E. M. Schell, c, Casper, Wyo.)

Needle Eye Point quadrangle (H. D. Zeller)

Pete's Cove quadrangle (H. D. Zeller)

Ship Mountain Point quadrangle (H. D. Zeller)

Sunset Flat quadrangle (H. D. Zeller)

Virginia and West Virginia, central Appalachian Basin (K. J. Englund, NC)

Washington:

Coal resources of Washington (W. H. Lee, c, M)

Collection of coal samples for analysis (V. E. Livingston, Jr., Olympia; V. E. Swanson, D)

West Virginia:

Formatting coal data for National Coal Resources Data System (M. C. Behling, Morgantown; M. D. Carter, NC)

Coal—Continued*States—Continued***West Virginia—Continued**

Louisa quadrangle (C. W. Connor, D)

Wyoming (c, D, except as otherwise noted):

Acme quadrangle (B. E. Barnum)

Appel Butte quadrangle (G. L. Galyardt)

Bailey Lake quadrangle (M. L. Schroeder)

Beaver Creek Hills quadrangle (c, Casper)

Betty Reservoir NE quadrangle (N. McKinnie, c, Casper)

Browns Hill quadrangle (C. S. V. Barclay)

Cottonwood Rim quadrangle (C. S. V. Barclay)

Coyote Draw quadrangle (G. L. Galyardt)

Deer Creek quadrangle (M. L. Schroeder)

Eagle Rock quadrangle (S. P. Buck, c, Casper)

Fortin Draw quadrangle (B. E. Law)

Four Bar-J Ranch quadrangle (G. L. Galyardt)

Gillette East quadrangle (B. E. Law)

Gillette West quadrangle (B. E. Law)

Greenhill quadrangle (S. P. Buck, c, Casper)

Grieve Reservoir quadrangle (C. S. V. Barclay)

Hilight quadrangle (W. J. Purdon, c, Casper)

Hultz Draw quadrangle (c, Casper)

Kemmerer area (M. L. Schroeder)

Ketchum Buttes quadrangle (C. S. V. Barclay)

Little Thunder Reservoir quadrangle (G. S. Martin, c, Casper)

Monarch quadrangle (B. E. Barnum)

Moyer Springs quadrangle (B. E. Law)

Neil Butte quadrangle (S. P. Buck, c, Casper)

North Star School NE quadrangle (S. P. Buck, c, Casper)

North Star School NW quadrangle (S. P. Buck, c, Casper)

North Star School SE quadrangle (L. Jefferies, c, Casper)

North Star School SW quadrangle (L. Jefferies, c, Casper)

Open A Ranch quadrangle (G. C. Martin, c, Casper)

Oriva quadrangle (B. E. Law)

Pickle Pass quadrangle (M. L. Schroeder)

Pine Mountain-Oil Mountain area (G. J. Kerns, c, Casper)

Piney Canyon NW quadrangle (G. C. Martin, c, Casper)

Piney Canyon SW quadrangle (L. Wackwitz, c, Casper)

Rawlins coal field (C. S. V. Barclay)

Reid Canyon (G. J. Kerns, c, Casper)

Reno Junction quadrangle (L. Jefferies, c, Casper)

Reno Reservoir quadrangle (G. C. Martin, c, Casper)

Rock Springs uplift (P. J. LaPoint)

Rough Creek quadrangle (S. P. Buck, c, Casper)

Savery quadrangle (C. S. V. Barclay)

Sheridan Pass quadrangle (W. L. Rohrer, c)

Sheridan quadrangle (E. I. Winger, c, Casper)

Square Top Butte quadrangle (G. J. Kerns, c, Casper)

Teckla quadrangle (J. E. Goolsby, c, Casper)

Teckla SW quadrangle (J. E. Goolsby, c, Casper)

The Gap quadrangle (G. L. Galyardt)

Tullis quadrangle (C. S. V. Barclay)

Turnercrest NE quadrangle (G. C. Martin, c, Casper)

Weston SW quadrangle (R. W. Jones, c, Casper)

Construction and terrain problems:

Areal slope stability analysis, San Francisco Bay region (S. D. Ellen, M)

Electronics instrumentation research for engineering geology (J. B. Bennetti, D)

Engineering geology laboratory (R. A. Farrow, D)

Fissuring-subsidence research (T. L. Holzer, M)

Geotechnical measurements and services (H., W. Olsen, D)

Reactor hazards research (K. L. Pierce, D)

Construction and terrain problems—Continued

Reactor site investigations (R. H. Morris, D)

Research in rock mechanics (F. T. Lee, D)

Sino-Soviet terrain (L. D. Bonham, I, NC)

Soil engineering research (T. L. Youd, M)

Special intelligence (L. D. Bonham, I, NC)

Volcanic hazards (D. R. Crandell, D)

States:

California (M, except as otherwise noted):

Feasibility of tunneling for rapid transit, Los Angeles area (R. F. Yerkes)

Geologic environmental maps for land use planning (E. H. Pampeyan)

Geology and slope stability, western Santa Monica Mountains (R. H. Campbell)

Los Angeles County Cooperative (R. H. Campbell)

Pacific Palisades landslide area, Los Angeles (J. T. McGill, D)

California and Colorado, regional stability studies (D. H. Radruch-Hall, M)

Colorado (D):

Coal mine deformation studies, Somerset mining district (C. R. Dunrud)

Engineering geology-mapping research, Denver region (H. E. Simpson)

Massachusetts, sea-cliff erosion studies (C. A. Kaye, Boston)

Nevada:

Geologic and geomechanical investigations (J. R. Ege, D)

Seismic engineering program (K. W. King, Las Vegas)

Surface effects of nuclear explosions (R. P. Snyder, D)

Utah, coal-mine bumps (F. W. Osterwald, D)

See also Urban geology; Land use and environmental impact; Urban hydrology.

Copper:

United States and world resources (D. P. Cox, NC)

States:

Alaska, southwest Brooks Range (I. L. Tailleir, M)

Arizona (M):

Jerome and Bagdad districts (C. M. Conway)

Ray porphyry copper (H. M. Cornwall)

California, Shasta districts (C. M. Conway, M)

Maine-New Hampshire, porphyry, with molybdenum (R. G. Schmidt, NC)

Michigan (NC):

Greenland and Rockland quadrangles (J. W. Whitlow)

Michigan copper district (W. S. White)

Virginia, massive sulfides (J. E. Gair, NC)

Crustal studies. *See* Earthquake studies; Geophysics, regional.

Directories:

Department of the Interior information services (E. T. Smith, I, NC)

Drought studies:

Drought monitoring Montana (R. R. McMurtrey, w, Helena, Mont.)

Floyd River basin (W. L. Steinhilber, w, Iowa City, Iowa)

Seasonal flow characteristics (O. G. Lara, w, Iowa City, Iowa)

Earthquake studies:

Active fault analysis (R. E. Wallace, M)

Comparative elevation studies (R. O. Castle, M)

Computer fault modeling (J. H. Dieterich, M)

Computer operations and maintenance (T. C. Jackson, M)

Crustal inhomogeneity in seismically active areas (S. W. Stewart, M)

Crustal strain (J. C. Savage, M)

Crustal studies (ARPA) (Isidore Zietz, NC)

Earthquake studies—Continued

- Dynamic soil behavior (A. T. F. Chen, M)
- Earth structure studies (J. H. Healy, M)
- Earthquake field studies (W. J. Spence, C. J. Langer, J. N. Jordan, M)
- Earthquake-induced ground failures (T. L. Youd, M)
- Earthquake-induced landslides (E. L. Harp, M)
- Earthquake-induced sedimentary structures (J. D. Sims, M)
- Earthquake recurrence and history (R. D. Nason, M)
- Eastern United States (R. K. McGuire, D)
- Experimental liquefaction potential mapping (T. L. Youd, M)
- Fault-zone tectonics (J. C. Savage, M)
- Fluid injection, laboratory investigations (J. D. Byerlee, Louis Peselnick, M)
- Geologic and geotechnical factors in ground-motion analysis (R. C. Wilson, M)
- Geologic parameters of seismic source areas (F. A. McKeown, D)
- Ground failure related to the 1811-12 New Madrid earthquakes (S. F. Obermeier, NC)
- Ground failures caused by historic earthquakes (D. K. Keefer, D)
- Ground-motion modeling and prediction (W. B. Joyner, M)
- Ground-motion studies (R. D. Borchardt, R. P. Maley, M)
- Microearthquake data analysis (W. H. K. Lee, M)
- National Earthquake Information Service (A. C. Tarr, D)
- National Strong-Motion Instrumentation Network (R. B. Matthiesen, M)
- New seismic instrumentation for geothermal surveys (P. A. Reasenber, M)
- Nicaragua, Central America, technical assistance in establishing center for earthquake hazard reduction (P. L. Ward, M)
- Plate-tectonic studies (E. D. Jackson, M)
- Precursory phenomena (P. L. Ward, M)
- Prediction, animal behavior studies (P. A. Reasenber, M)
- Prediction monitoring and evaluation (R. N. Hunter, D)
- Recurrence intervals along quaternary faults (K. L. Pierce, D)
- Reduction of noise in precursor signals (J. A. Steppe, M)
- Relative activity of multiple fault strands (M. G. Bonilla, M)
- Reservoir-induced seismicity, statistical approach, (D. E. Stuart-Alexander, M)
- Seismic-risk studies (S. T. Algermissen, D)
- Seismic-source studies (W. R. Thatcher, M)
- Seismic studies for earthquake prediction (C. G. Bufe, M)
- Seismicity and Earth structure (J. N. Taggart, D)
- Seismological research observatories (J. R. Peterson, Albuquerque, N. Mex.)
- Soil engineering research (T. L. Youd, M)
- Spectral and time domain analysis of near field recordings of earthquakes (J. B. Fletcher, M)
- Stress studies (C. B. Raleigh, M)
- Synthetic strong-motion seismograms (W. B. Joyner, M)
- Tectonic studies (W. B. Hamilton, D)
- Teleseismic search for earthquake precursors (J. W. Dewey, D)
- Theoretical seismology (A. F. Espinosa, D)
- Worldwide Network of Standard Seismographs (J. R. Peterson, Albuquerque, N. Mex.)

States:**Alaska:****Earthquake hazards:**

- Anchorage (Ernest Dobrovolny, D)
- Coastal communities (R. W. Lemke, D)
- Juneau (R. D. Miller, D)
- Sitka (L. A. Yehle, D)
- Southern part (George Plafker, M)

Earthquake studies—Continued**States—Continued****Alaska—Continued**

- Microearthquake studies (R. A. Page, M)
- Turnagain Arm sediments (A. T. Ovenshine, M)
- California (M, except as otherwise noted):
 - Basement rock studies along San Andreas fault (D. C. Ross)
 - Continental Shelf fault studies (S. C. Wolf)
 - Depth of bedrock in the San Francisco Bay region (R. M. Hazlewood)
- Earthquake hazards:
 - San Francisco Bay region (E. E. Brabb)
 - Southern part (D. M. Morton, Los Angeles)
 - Foothills fault system (D. E. Stuart-Alexander, M)
 - Geodetic strain (W. H. Prescott)
 - Geophysical studies, San Andreas fault (J. H. Healy)
 - Measurement of seismic velocities for seismic zonation (J. F. Gibbs, R. D. Borchardt, T. E. Fumal)
- Microearthquake studies:
 - Central part (J. H. Pfluke)
 - New Melones (J. C. Roller)
 - Southern part (D. P. Hill)
- Recency of faulting:
 - Coastal California Desert (E. H. Pampeyan)
 - Eastern Mojave Desert (W. J. Carr)
- Tectonics:
 - Central and northern part (W. P. Irwin)
 - Central San Andreas fault (D. B. Burke, T. W. Dibblee, Jr.)
 - Salton Trough tectonics (R. V. Sharp)
 - Southern part (M. M. Clark)
 - Theory of wave propagation in anelastic media (R. D. Borchardt)
- Colorado, Rangely (C. B. Raleigh, M)
- Idaho, active faults, Snake River Plain (S. S. Oriol, M. H. Hoit, W. E. Scott, D)
- Massachusetts:
 - Fault definition, northeastern Massachusetts (A. F. Shride, D)
- Missouri, New Madrid fault-zone geophysics (M. F. Kane, D)
- Montana, Yellowstone National Park, microearthquake studies (A. M. Pitt, M)
- Nevada, tectonics, west-central (E. B. Ekren, D)
- New Mexico, seismotectonic analysis, Rio Grande rift (E. H. Baltz, Jr., D)
- South Carolina, microearthquake studies (A. C. Tarr, D)
- Washington (M):
 - Earthquake hazards, Puget Sound region (H. D. Gower, P. D. Snaveley, Jr.)
 - Hanford microearthquake studies (J. H. Pfluke)
- Engineering geologic studies.** *See* Construction and terrain problems; Urban geology.
- Environmental assessment:**
 - Amex Eagle Butte mine (J. D. Unger, I, NC)
 - Carter Oil Caballo mine (F. J. Anderson, I, NC)
 - Decker mines (N. J. King, w, D)
 - Guidelines for administration and management of EIS task forces (K. E. Vanlier, J. W. Allingham, I, NC)
 - Guidelines for preparation of EIS's (K. E. Vanlier, J. W. Allingham, I, NC)
 - Kerr-McGee East Gillette mine (F. J. Anderson, I, NC)
 - Methodology for monitoring impacts of phosphate development, Idaho (L. G. Marcus, I, NC)
 - Northern Great Plains, methodological guidebook (B. B. Hanshaw, w, NC)

Environmental assessment—Continued

- Oil-shale supplement (D. L. Schleicher, I, D)
- Peabody Rochelle mine (F. J. Anderson, I, NC)
- Powder River basin uranium (E. S. Santos, D)
- Review of environmental impact statements (L. D. Bonham, I, NC)
- South Florida environment (B. F. McPherson, w, Miami)
- Westmoreland mine (C. W. Lane, w, D)

Environmental geology:

- Quaternary dating applications—overview map (K. L. Pierce, D)
- States:

Montana:

- Environmental study of the Big Fork-Avon area (I. J. Witkind, D)
- Land resources, Helena region (R. G. Schmidt, NC; G. D. Robinson, M)

Utah:

- Cedar City 2° quadrangle (K. A. Sargent, D)
- Central Utah energy lands (I. J. Witkind, D)
- Kaiparowits Plateau coal basin (K. A. Sargent, D)

Wyoming:

- Hams Fork Coal Basin (A. B. Gibbons, D)
- See also Construction and terrain problems; Land use and environmental impact; Urban geology.

Evapotranspiration:

- Evaporation, Colorado Lakes (D. B. Adams, w, D)
- Evapotranspiration data analyses (T. E. A. van Hylckama, w, Lubbock, Tex.)
- Evapotranspiration theory (O. E. Leppanen, w, Phoenix, Ariz.)
- Mechanics of evaporation (G. E. Koberg, w, D)
- Vegetation ecohydrology (R. M. Turner, w, Tucson, Ariz.)

Extraterrestrial studies:

Lunar analog studies:

- Explosion craters (D. J. Roddy, Flagstaff, Ariz.)

Lunar data synthesis:

- Imbrium and Serenitatis Basins (J. F. McCauley, Flagstaff, Ariz.)
- Sample petrology and stratigraphy (H. G. Wilshire, M)
- Synoptic lunar geology (D. E. Wilhelms, M)

Lunar microwave (G. R. Olhoeft, Denver)

Lunar sample investigations:

- Chemical and X-ray fluorescence analysis (H. J. Rose, Jr., NC)
- Lunar igneous-textured rocks (O. B. James, NC)
- Major lunar breccia types (E. C. T. Chao, NC)
- Mineralogical analyses (R. B. Finkelman, NC)
- Oxygen fugacities and crystallization sequence (Motoaki Sato, NC)
- Petrologic studies (Edwin Roedder, NC)
- Pyroxenes (J. S. Huebner, NC)

Planetary analog studies, mass movements (E. C. Morris, Flagstaff, Ariz.)

Planetary investigations:

- Geologic mapping of Mars (D. H. Scott, J. F. McCauley, Flagstaff, Ariz.)
- Geologic synthesis of Mars (Harold Masursky, Flagstaff, Ariz.)
- Image-processing studies (L. A. Soderblom, Flagstaff, Ariz.)
- Mariner Jupiter-Saturn (L. A. Soderblom, Flagstaff, Ariz.)
- Mariner Venus-Mercury TV (N. J. Trask, NC)
- Mars mineralogy and chemistry, Viking lander (Priestley Toulmin III, H. J. Rose, Jr., NC)
- Mars topographic synthesis (S. S. C. Wu, Flagstaff, Ariz.)
- Planetary cartography (R. M. Batson, Flagstaff, Ariz.)

Extraterrestrial studies—Continued

Planetary investigations—Continued

- Radar applications (G. G. Schaber, Flagstaff, Ariz.)

Viking mission:

- Lander (E. C. Morris, Flagstaff, Ariz.)
- Orbiter TV (M. H. Carr, M)
- Physical properties of Mars (H. J. Moore, M)
- Site analysis (Harold Masursky, Flagstaff, Ariz.)

Ferro-alloy metals:

Chromium:

- Geochemistry (B. A. Morgan III, NC)
- Resource studies (T. P. Thayer, NC)
- Molybdenum-rhenium resource studies (R. U. King, D)

States:

- North Carolina, tungsten in Hamme district (J. E. Gair, NC)
- Oregon, John Day area (T. P. Thayer, NC)
- Pennsylvania, State Line district (B. A. Morgan III, NC)

Flood discharge from small drainage areas:

- Connecticut (M. D. Thomas, w, Hartford)
- Delaware (R. H. Simmons, w, Dover)
- Virginia (E. M. Miller, w, Richmond)

Flood-hazard mapping:

- Alabama (C. O. Ming, w, Montgomery)
- Arizona (B. N. Aldridge, w, Tucson)
- Arkansas (M. S. Hines, w, Little Rock)
- California (J. R. Crippen, w, M)
- Connecticut (M. A. Cervione, Jr., w, Hartford)
- Florida (S. D. Leach, w, Tallahassee)
- Georgia (McGlone Price, w, Doraville)
- Illinois (B. J. Prugh, w, Champaign)
- Indiana (J. B. Swing, w, Indianapolis)
- Iowa (O. G. Lara, w, Iowa City)
- Kansas (D. B. Richards, w, Lawrence)
- Louisiana (A. S. Lowe, w, Baton Rouge)
- Maine (R. A. Morrill, w, Augusta)
- Massachusetts (S. W. Wandle, Jr., w, Boston)
- Michigan (R. L. Knutilla, w, Okemos)
- Minnesota (G. H. Carlson, w, St. Paul)
- Mississippi (K. V. Wilson, w, Jackson)
- Missouri (L. D. Hauth, w, Rolla)
- Montana (R. J. Omang, w, Helena)
- Nebraska (G. G. Jamison, w, Lincoln)
- Nevada (D. O. Moore, w, Carson City)
- New Hampshire (S. W. Wandle, Jr., w, Boston, Mass.)
- North Carolina (R. W. Coble, w, Raleigh)
- North Dakota (O. A. Crosby, w, Bismarck)
- Ohio (D. K. Roth, w, Columbus)
- Oklahoma (W. B. Mills, w, Oklahoma City)
- Oregon (D. D. Harris, w, Portland)
- Pennsylvania (L. V. Page, w, Harrisburg)
- Puerto Rico (E. D. Cobb, w, San Juan)
- South Carolina (W. T. Utter, w, Columbia)
- Tennessee (C. R. Gamble, w, Nashville)
- Texas (J. D. Bohn, w, Austin)
- United States (G. W. Edelen, w, NC)
- Vermont (S. W. Wandle, Jr., w, Boston, Mass.)
- Virginia (E. M. Miller, w, Richmond)
- Washington (E. G. Nassar, w, Tacoma)
- West Virginia (G. S. Runner, w, Charleston)
- Wisconsin (C. L. Lawrence, w, Madison)
- Wyoming (J. F. Wilson, Jr., w, Cheyenne)

Flood-insurance studies:

- Alabama (C. O. Ming, w, Montgomery)
- Arizona (B. N. Aldridge, w, Tucson)
- Arkansas (A. H. Ludwig, w, Little Rock)

Flood-insurance studies—Continued

California (J. R. Crippen, w, M)
 Colorado (R. C. Christensen, w, D)
 Connecticut (M. A. Cervione, Jr., w, Hartford)
 Florida (S. D. Leach, w, Tallahassee)
 Georgia (McGlone Price, w, Doraville)
 Idaho (W. A. Harenberg, w, Boise)
 Illinois (G. W. Curtis, w, Champaign)
 Indiana (D. H. Rapp, w, Indianapolis)
 Iowa (A. J. Heinitz, w, Iowa City)
 Kansas (D. B. Richards, w, Lawrence)
 Kentucky (C. H. Hannum, w, Louisville)
 Louisiana (F. N. Lee, Baton Rouge)
 Maine (R. M. Morrill, w, Augusta)
 Massachusetts (L. A. Swallow, w, Boston)
 Michigan (R. M. Morrill, w, Augusta)
 Minnesota (G. H. Carlson, w, St. Paul)
 Mississippi (B. E. Colson, w, Jackson)
 Missouri (L. D. Hauth, w, Rolla)
 Montana (R. J. Omang, w, Helena)
 Nebraska (G. G. Jamison, w, Lincoln)
 Nevada (C. V. Schroer, w, Carson City)
 New Hampshire (L. A. Swallow, w, Boston, Mass.)
 New Jersey (R. D. Schopp, w, Trenton)
 New Mexico (L. P. Denis, w, Albuquerque)
 New York (R. T. Mycyk, w, Albany)
 North Carolina (N. N. Jackson, w, Raleigh)
 Ohio (D. K. Roth, w, Columbus)
 Oklahoma (T. L. Huntzinger, w, Oklahoma City)
 Oregon (D. D. Harris, w, Portland)
 Pennsylvania (Andrew Voytik, w, Harrisburg)
 Puerto Rico (J. R. Harkins, w, San Juan)
 Rhode Island (L. A. Swallow, w, Boston, Mass.)
 South Carolina (B. H. Whetstone, w, Columbia)
 Tennessee (W. J. Randolph, w, Nashville)
 Texas (J. D. Bohn, w, Austin)
 Vermont (S. S. Wandle, w, Boston, Mass.)
 Virginia (J. R. Mohler, w, Marion)
 Washington (C. H. Swift, w, Tacoma)
 Wisconsin (C. L. Lawrence, w, Madison)

Flood investigations:

Countermeasures, scour and erosion (J. C. Bruce, w, M)
 Documentation of extreme floods (H. H. Barnes, Jr., w, NC)
 Flow frequency analysis (W. O. Thomas, w, NC)
 Model bridge-site report (H. H. Barnes, w, NC)
 Nationwide flood-frequency (A. G. Scott, w, NC)
States and territories:
 Alabama, floods, bridge-site studies (C. O. Ming, w, Montgomery)
 Arkansas (M. S. Hines, w, Little Rock)
 California:
 Hydraulic techniques—HUD studies (D. E. Burkham, w, Sacramento)
 Colorado (w, D):
 Flood data for Colorado (J. F. McCain)
 Mountain rainfall floods (J. F. McCain)
 Florida (w, Tampa):
 Bridge site studies (W. C. Bridges, w, Tallahassee)
 Flood-hazard evaluation, Myakka River (W. R. Murphy, Jr.)
 Regional flood-frequency study (J. F. Turner)
 Georgia:
 Atlanta flood characteristics (E. J. Inman, w, Doraville)
 Flood and bridge site studies (McGlone Price, w, Doraville)
 Urban flood-frequency, Georgia (E. J. Inman, w, Doraville)
 Idaho (W. A. Harenberg, w, Boise)

Flood investigations—Continued*States and territories—Continued*

Illinois:
 Flood flows in small basins (G. W. Curtis, w, Champaign)
 Urban floods in northeastern Illinois (H. E. Allen, Jr., w, Dekalb)
 Indiana, flood frequency (L. G. Davis, w, Indianapolis)
 Iowa (w, Iowa City):
 Flood data for selected bridge sites (O. G. Lara)
 Flood profiles, statewide (O. G. Lara)
 Kentucky, small-area flood hydrology (J. N. Sullivan, Jr., w, Louisville)
 Louisiana, roughness coefficients (G. J. Arcement, w, Baton Rouge)
 Maryland:
 Floods—small drainage areas (D. H. Carpenter, w, Towson)
 Massachusetts:
 Small basin flood flow in Massachusetts (J. S. Wandle, w, Boston)
 Minnesota, flood-plain studies (G. H. Carlson, w, St. Paul)
 Mississippi (w, Jackson):
 Multiple-bridge hydraulics (B. E. Colson)
 Nebraska, magnitude and frequency of floods (E. W. Beckman, w, Lincoln)
 Nevada (w, Carson City):
 Environmental study, western Nevada (P. A. Glancy)
 Flood investigations (Lynn Harmsen)
 New Jersey, flood peaks and flood plains (S. J. Stankowski, w, Trenton)
 New Mexico, flood analysis (A. G. Scott, w, Santa Fe)
 New York, peak discharge of ungaged streams (Bernard Dunn, w, Albany)
 Oklahoma, small watersheds (W. O. Thomas, Jr., w, Oklahoma City)
 Puerto Rico:
 Eloise flood works, Puerto Rico (E. Colon-Diedppa, w, San Juan)
 Floods investigation program (E. D. Cobb, w, San Juan)
 South Carolina (w, Columbia):
 Hydraulic site reports (B. H. Whetstone)
 Tennessee (W. J. Randolph, w, Nashville)
 Virginia:
 Hydrology, Wytheville fish hatchery (J. R. Hendrick, w, Marion)
 Statewide (E. M. Miller, w, Richmond)
 Washington (w, Tacoma):
 Flood-inundation mapping (J. H. Bartells)
 Chehalis water resources (K. L. Walters)
 Wisconsin (w, Madison):
 Bridge flood backwater (D. A. Stedfast, w, Madison)
 Flood-control effects on Trout Creek (R. S. Grant)
 Maximum flood at Chippewa Flowage (W. R. Krug)
 St. Croix scenic river waste study (R. S. Grant)
 Wyoming, flood investigations (G. S. Craig, w, Cheyenne)
Fluorspar:
 Colorado, Bonanza and Poncha Springs quadrangles (R. E. Van Alstine, NC)
 Illinois-Kentucky district, regional structure and ore controls (D. M. Pinckney, D)
Foreign nations, geologic investigations:
 Brazil, mineral, resources and geologic training (S. A. Stanin, Rio de Janeiro)
 Poland
 Characteristics of coal basins (K. J. Englund, NC)

Foreign nations, geological investigations—Continued

Geochemistry of coal and computerization of coal data (V. E. Swanson, D)

Saudi Arabia, crystalline shield, geologic and mineral reconnaissance (F. S. Simons, Jiddah)

Spain, marine mineral resources (P. D. Snavey, Jr., M)

Thailand, remote-sensing program (J. O. Morgan, Bangkok)

Foreign nations, hydrologic investigations. *See* Water resources, foreign countries.

Fuels, organic. *See* Coal; Oil shale; Petroleum and natural gas.

Gas, natural. *See* Petroleum and natural gas.

Geochemical distribution of the elements:

Basin and Range granites (D. E. Lee, D)

Botanical exploration and research (H. L. Cannon, D)

Coding and retrieval of geologic data (T. G. Lovering, D)

Data of geochemistry (Michael Fleischer, NC)

Data systems (R. V. Mendes, D)

Element availability:

Soils (R. C. Severson, D)

Vegetation (L. P. Gough, D)

Geochemistry of belt rocks (J. J. Connor, D)

Light stable isotopes (J. R. O'Neil, M)

Phosphoria Formation, organic carbon and trace element distribution (E. K. Maughan, D)

Sedimentary rocks, chemical composition (T. P. Hill, D)

Selenium, tellurium, and thallium, geochemical exploration (H. W. Lakin, D)

Statistical geochemistry and petrology (A. T. Miesch, D)

Tippecanoe sequence, Western Craton (L. G. Schultz, D)

Trace elements in oil shale (W. E. Dean, Jr., D)

Urban geochemistry (H. A. Tourtelot, D)

Western coal regions:

Geochemical survey of rocks (R. J. Ebens, D)

Geochemical survey of soils (R. R. Tidball, D)

Geochemical survey of vegetation (J. A. Erdman, D)

Geochemical survey of waters (G. L. Feder, D)

States:

California, Sierra Nevada batholith, geochemical study (F. C. W. Dodge, M)

Colorado, Mt. Princeton igneous complex (Priestley Toulmin III, NC)

Pennsylvania, greater Pittsburgh region, environmental geochemistry (R. P. Biggs, Carnegie)

Geochemical prospecting methods:

Application and evaluation of methods of chemical analysis to diverse geochemical environments (J. G. Viets, D)

Application of silver-gold geochemistry to exploration (H. W. Laking, D)

Botanical exploration and research (H. L. Cannon, D)

Development of effective on-site methods of chemical analysis for geochemical exploration (W. L. Campbell, D)

Elements in organic-rich material (F. N. Ward, D)

Gamma-ray spectrometry (J. A. Pitkin, D)

Geochemical characterization of metallogenic provinces and mineralized areas (G. J. Neuerberg, D)

Geochemical exploration:

Glaciated areas (H. V. Alminas, D)

Research in arctic, alpine, and subalpine regions (J. H. McCarthy, D)

Techniques:

Alpine and subalpine environments (G. C. Curtin, D)

Arid environments (M. A. Chaffee, D)

Gold composition analysis in mineral exploration (J. C. Antweiler, D)

Instrumentation development (R. C. Bigelow, D)

Geochemical prospecting methods—Continued

Jasperoid, relations to ore deposits (T. G. Lovering, D)

Lateritic areas, southern Appalachian Mountains (W. R. Griffiths, D)

Mercury, geochemistry (A. P. Pierce, D)

Mineral exploration methods (G. B. Gott, D)

Mineralogical techniques in geochemical exploration (Theodore Botinelly, D)

New mineral storage and identification program (George Van Trump, Jr., D)

Ore-deposit controls (A. V. Heyl, Jr., D)

Pattern recognition and clustering methods for the graphical analysis of geochemical data (J. B. Fife, D)

Research in methods of spectrographic analysis for geochemical exploration (E. L. Mosier, D)

Sulfides, accessory in igneous rocks (G. J. Neuerberg, D)

Surface and ground water in geochemical exploration (G. A. Nowlan, D)

Volatile elements and compounds in geochemical exploration (M. E. Hinkle, D)

States:

Alaska, geochemical exploration techniques (G. C. Curtin, D)

New Mexico, Basin and Range part, geochemical reconnaissance (W. R. Griffiths, D)

Geochemistry, experimental:

Environment of ore deposition (P. B. Barton, Jr., NC)

Experimental mineralogy (R. O. Fournier, M)

Fluid inclusions in minerals (Edwin Roedder, NC)

Fluid zonation in metal deposits (J. T. Nash, M)

Geologic thermometry (J. S. Huebner, NC)

Hydrothermal alteration (J. J. Hemley, NC)

Impact metamorphism (E. C. T. Chao, NC)

Kinetics of igneous processes (H. R. Shaw, NC)

Late-stage magmatic processes (G. T. Faust, NC)

Mineral equilibria, low temperature (E-an Zen, NC)

Neutron activation (F. E. Senftle, NC)

Oil shale:

Colorado, Utah, and Wyoming (W. E. Dean, Jr., D)

Organic geochemistry (R. E. Miller, D)

Organic geochemistry (J. G. Palacas, D)

Organometallic complexes, geochemistry (Peter Zubovic, NC)

Solution-mineral equilibria (C. L. Christ, M)

Stable isotopes and ore genesis (R. O. Rye, D)

Statistical geochemistry (A. T. Miesch, D)

Geochemistry, water:

Chemical constituents in ground water, spatial distribution (William Back, w, NC)

Chemical reactions at mineral surfaces (J. D. Hem, w, M)

Chemistry of hydrosolic metals (J. D. Hem, w, M)

Computer modeling of rock-water interactions (J. L. Haas, Jr., NC)

Elements, distribution in fluvial and brackish environments (V. C. Kennedy, w, M)

Factors determining solute transfer in the unsaturated zone (Jacob Rubin, W, M)

Gases, complexes in water (D. W. Fischer, w, NC)

Geochemistry of geothermal systems (Ivan Barnes, w, M)

Geochemistry of San Francisco Bay waters and sediments (D. H. Peterson, w, M)

Geothermal trace-element reactions (E. A. Jenne, w, M)

Interaction of minerals and water in saline environments (B. F. Jones, w, NC)

Interface hydrochemistry and paleoclimatology (I. J. Winograd, w, NC)

Geochemistry, water—Continued

- Mineralogic controls of the chemistry of ground water (B. B. Hanshaw, w, NC)
- Organic geochemistry (R. L. Malcolm, w, D)
- Trace-element partitioning (E. A. Jenne, w, M)
- Western coal regions, geochemical survey of waters (G. L. Feder, D)

See also Quality of water.

Geochemistry and petrology, field studies:

- Basalt, genesis (T. L. Wright, NC)
- Basin and Range granites (D. E. Lee, D)
- Epithermal deposits (R. G. Worl, D)
- Geochemical studies in southeastern States (Henry Bell III, NC)
- Geochemistry of diagenesis (K. J. Murata, M)
- Geochemistry of marine sediments (W. E. Dean, D)
- Geochemistry of Tertiary Sequence, Western Craton (L. G. Schultz, D)
- Inclusions in basaltic rocks (E. D. Jackson, M)
- Layered Dufek intrusion, Antarctica (A. B. Ford, M)
- Layered intrusives (N. J. Page, M)
- Mercury, geochemistry and occurrence (A. P. Pierce, D)
- Niobium and tantalum, distribution in igneous rocks (David Gottfried, NC)
- Organic petrology of sedimentary rocks (N. H. Bostick, D)
- Rare-earth elements, resources and geochemistry (J. W. Adams, D)
- Regional geochemistry (W. E. Dean, Jr., D)
- Regional metamorphic studies (H. L. James, M)
- Residual minor elements in igneous rocks and veins (George Phair, NC)
- Solution transport of heavy metals (G. K. Czamanske, M)
- Submarine volcanic rocks, properties (J. G. Moore, M)
- Syngenetic ore deposition (C. M. Conway, M)
- Thermal waters, origin and characteristics (D. E. White, M)
- Trace elements in oil shale (W. E. Dean, Jr., D)
- Trondhjemites, major and minor elements, isotopes (Fred Barker, D)
- Ultramafic rocks, petrology of alpine types (R. G. Coleman, M)
- Uranium, radon and helium—gaseous emanation detection (G. M. Reimer, D)
- Western coal regions:
 - Geochemical survey of rocks (R. J. Ebens, D)
 - Geochemical survey of soils (R. R. Tidball, D)
 - Geochemical survey of vegetation (J. A. Erdman, D)
- Western energy regions:
 - Element availability—plants (L. P. Gough, D)
 - Element availability—rocks (J. M. McNeal, D)
 - Element availability—soils (R. C. Severson, D)

States:**Alaska (M):**

- La Perouse layered intrusion (R. A. Loney)
- Metasedimentary and metaigneous rocks, southwestern Brooks Range (I. L. Tailleux)

Arizona (M):

- Ray program:
 - Mineral Mountain (T. G. Theodore)
 - Silicate mineralogy, geochemistry (N. G. Banks)
- Stocks (S. C. Creasey)

California:

- Geochemistry of sediments, San Francisco Bay (D. S. McCulloch, M)
- Granitic rocks of Yosemite National Park (D. L. Peck, NC)
- Kings Canyon National Park (J. G. Moore, M)
- Long Valley Caldera-Mono Craters volcanic rocks (R. A. Bailey, NC)

Geochemistry and petrology, field studies—Continued**States—Continued****California—Continued**

- Sierra Nevada xenoliths (J. P. Lockwood, M)

Colorado:

- Petrology of Mt. Princeton igneous complex (Priestley Toulmin III, NC)

- Tertiary-Laramide intrusives (E. J. Young, D)

Hawaii, ankaramites (M. H. Beeson, M)**Idaho, Wood Rive district (W. E. Hall, M)****Idaho-Montana-Wyoming, petrology of the Yellowstone Plateau volcanic field (R. L. Christiansen, M)****Montana:**

- Diatremes, Missouri River Breaks (B. C. Hearn, Jr., NC)

- Geochronology, north-central Montana (B. C. Hearn, Jr., NC; R. F. Marvin, R. E. Zartman, D)

- Wolf Creek area, petrology (R. G. Schmidt, NC)

Nevada, igneous rocks and related ore deposits (M. L. Silberman, M)**Pennsylvania, geochemistry of Pittsburgh urban area (H. A. Tourtelot, D)****South Dakota, Keystone pegmatite area (J. J. Norton, Rapid City)****Geochronological investigations:**

- Carbon-14 method (Meyer Rubin, NC)

- Geochronology and rock magnetism (G. B. Dalrymple, M)

- Geochronology of uranium ores and their host rocks (K. R. Ludig, D)

- Igneous rocks and deformational periods (R. W. Kistler, M)

- Lead-uranium, lead-thorium, and lead-alpha methods (T. W. Stern, NC)

- Magnetic chronology, Colorado Plateau and environs (D. P. Elston, E. M. Shoemaker, Flagstaff, Ariz.)

- Quaternary dating techniques, numerical and relative-age (K. L. Pierce, D)

- Radioactive-disequilibrium studies (J. N. Rosholt, D)

- San Francisco volcanic field (P. E. Damon, University of Arizona)

States:

- Alaska, K-Ar dates, southwest Brooks Range (I. L. Tailleux, M; R. B. Forbes, D. L. Turner, Fairbanks)

- Colorado, geochronology of Denver area (C. E. Hedge, D)

See also Isotope and nuclear studies.

Geologic mapping:

- Map scale smaller than 1:62,500:

- Antarctica, Dufek Massif and Forrester Range, Pensacola Mountains (A. B. Ford, M)

- Belt basin study (J. E. Harrison, D)

- Columbia River basalt (D. A. Swanson, M)

States:**Alaska (M):**

- Ambler River and Baird Mountains quadrangles (I. L. Tailleux)

- Charley River quadrangle (E. E. Brabb)

- Craig quadrangle (G. D. Eberlein, Michael Churkin, Jr.)

- Delong Mountains quadrangle (I. L. Tailleux)

- Geologic map (H. M. Beikman)

- Glacier Bay National Monument (D. A. Brew)

- Hughes-Shungnak area (W. W. Patton, Jr.)

- Iliamna quadrangle (R. L. Detterman)

- Juneau and Taku River quadrangles (D. A. Brew)

- Metamorphic facies map (D. A. Brew)

- Natural landmarks investigation (R. L. Detterman)

- St. Lawrence Island (W. W. Patton, Jr.)

Geologic mapping—Continued:

Map scale smaller than 1:62,500—Continued

States—Continued

Arizona (Flagstaff):

- North-central part (D. P. Elston)
- Phoenix 2-degree quadrangle (T. N. V. Karlstrom)
- Shivwits Plateau (Ivo Lucchitta)

Arkansas (B. R. Haley, Little Rock)

California (M):

- Environmental maps for land use planning (E. H. Pampeyan)
- Tectonic studies, Great Valley area (J. A. Bartow, D. E. Marchand)

Colorado (D):

- Colorado Plateau geologic map (D. D. Haynes)
- Denver 2-degree quadrangle (B. H. Bryant)
- Geologic map (O. L. Tweto)
- Greeley 2-degree quadrangle, western half (W. A. Braddock)

Leadville 2-degree quadrangle (O. L. Tweto)

Pueblo 2-degree quadrangle (G. R. Scott)

Sterling 2-degree quadrangle (G. R. Scott)

Idaho (D):

- Challis Volcanics (D. H. McIntyre)
- Dubois 2-degree quadrangle (M. H. Hait and B. A. Skipp)

Idaho Falls 2-degree quadrangle (M. A. Kuntz)

Preston 2-degree quadrangle (S. S. Oriel)

Snake River Plain, central part, volcanic petrology (H. E. Malde)

Snake River Plain region, eastern part (S. S. Oriel)

Missouri, Rolla 2-degree quadrangle, mineral-resource appraisal (W. P. Pratt, D)

Montana, White Sulphur Springs 2-degree quadrangle (M. W. Reynolds, D)

Nevada:

Elko County:

- Central (K. B. Ketner, D)
- Countywide (R. A. Hope, M)
- Western (R. R. Coats, M)

Geologic map (J. H. Stewart, M)

Lincoln County, Tertiary rocks (G. L. Dixon, D)

New Mexico (D):

North Church Rock area (A. R. Kirk)

Sanostee (A. C. Huffman, Jr.)

Santa Fe 2-degree quadrangle, western half (E. H. Baltz, Jr.)

Socorro 2-degree quadrangle, (G. O. Bachman)

North Carolina, Charlotte 2-degree sheet (Richard Goldsmith, NC)

South Carolina, Charlotte 2-degree sheet (Richard Goldsmith, NC)

South Carolina-Georgia-North Carolina, Greenville 2-degree quadrangle (A. E. Nelson, NC)

Utah (M):

Delta 2-degree quadrangle (H. T. Morris)

Tooele 2-degree quadrangle (W. J. Moore)

Washington, Wenatchee 2-degree sheet (R. W. Tabor, R. B. Waitt, Jr., V. A. Frizzell, Jr., M)

Wyoming:

Geologic map (J. D. Love, Laramie)

Preston 2-degree quadrangle (S. S. Oriel, D)

Teton Wilderness (J. D. Love, Laramie)

Geologic mapping—Continued

Map scale 1:62,500, and larger:

States and territories:

Alaska:

- Anatuvuk Pass (G. B. Shearer, c, Anchorage)
- Anchorage area (Ernest Dobrovolny, D)
- Bering River coal field (R. B. Sanders, c, Anchorage)
- Cape Beaufort-Corwin Bluffs coal field (J. E. Callahan, c, Anchorage)
- Geology and mineral resources of the Ketchikan quadrangle (H. C. Berg, M)
- Juneau area (R. D. Miller, D)
- Kukpowruk River coal field (J. E. Callahan, c, Anchorage)
- Nelchina area, Mesozoic investigations (Arthur Grantz, M)
- Nenana coal investigations (Clyde Wahrhaftig, M)
- Nome area (C. L. Hummel, M)
- Utokok River and Kokolik River coal field (J. E. Callahan, c, Anchorage)

Arizona:

- Bowie zeolite area (L. H. Godwin, c, NC)
- Cummings Mesas quadrangle (Fred Peterson, c, D)
- Hackberry Mountain area (D. P. Elston, Flagstaff)
- Mt. Wrightson quadrangle (H. D. Drewes, D)
- Ray district, porphyry copper (H. R. Cornwall, M)
- Sedona area (D. P. Elston, Flagstaff)
- Western Arizona tectonic studies (Ivo Lucchitta, Flagstaff)

California (M, except as otherwise noted):

- Coast Range, ultramafic rocks (E. H. Bailey)
- Condrey Mountain and Hornbrook quadrangles (P. E. Hotz)
- Long Valley caldera (R. A. Bailey, NC)
- Malibu Beach and Topanga quadrangles (R. F. Yerkes)
- Merced Peak quadrangle (D. L. Peck, NC)
- Northern Coast Ranges (K. F. Fox, Jr.)
- Palo Alto, San Mateo, and Montara Mountain quadrangles (E. H. Pampeyan)
- Peninsular Ranges (V. R. Todd, La Jolla)
- Point Dume and Triunfo Pass quadrangles (R. H. Campbell)
- Regional fault studies (E. J. Helley, D. G. Herd, B. F. Atwater)
- Ryan quadrangle (J. F. McAllister)
- Santa Lucia Range (V. M. Seiders)
- Searles Lake area (G. I. Smith)
- Sierra Nevada batholith (P. C. Bateman)
- The Geysers-Clear Lake area (R. J. McLaughlin)
- Western Santa Monica Mountains (R. H. Campbell)

Colorado (D, except as otherwise noted):

- Aspen 15-minute quadrangle (B. H. Bryant)
- Barcus Creek quadrangle (W. J. Hail)
- Barcus Creek SE quadrangle (W. J. Hail)
- Bonanza quadrangle (R. E. Van Alstine, NC)
- Buckhorn Lakes quadrangle (R. G. Dickinson, c, D)
- Central City area (R. B. Taylor)
- Citadel Plateau (G. A. Izett, c, D)
- Coal mine deformation studies, Somerset mining district (C. R. Dunrud)
- Cochetopa area (J. C. Olson)
- Courthouse Mountain quadrangle (R. G. Dickinson, c, D)
- Denver basin, Tertiary coal zone (P. E. Soister, c, D)
- Denver metropolitan area (R. M. Lindvall)

Geologic mapping—Continued**Map scale 1:62,500, and larger—Continued***States and Territories—Continued***Colorado (except as otherwise noted)—Continued**

Desert Gulch quadrangle (R. C. Johnson, D)
 Disappointment Valley, geology and coal resources
 (D. E. Ward)

Middle Dry Fork quadrangle (R. C. Johnson, D)
 Northern Park Range (G. L. Snyder)

Poncha Springs quadrangle (R. E. Van Alstine, NC)

Rangely NE quadrangle (R. S. Garrigues, c, D)

Rocky Mountain National Park (W. A. Braddock)

Rustic quadrangle (K. L. Shaver)

Savery quadrangle (C. S. V. Barclay, c, D)

Strasburg SW quadrangle (P. E. Soister, c, D)

Thornburgh quadrangle (M. J. Reheis, c, D)

Ward and Gold Hill quadrangles (D. J. Gable)

Washboard Rock quadrangle (R. G. Dickinson, c, D)

Watkins and Watkins SE quadrangles (P. E. Soister,
 c, D)

Connecticut:

Cooperative mapping program (M. H. Pease, Jr.,
 Boston, Mass.)

Georgia:

Macon-Gordon district (S. H. Patterson, NC)

Idaho (D, except as otherwise noted):

Bayhorse area (S. W. Hobbs)

Black Pine Mountains (J. F. Smith, Jr.)

Boulder Mountains (C. M. Tschanz)

Goat Mountain quadrangle (M. H. Staatz)

Grouse quadrangle (B. A. Skipp)

Hawley Mountain quadrangle (W. J. Mapel)

Malad SE quadrangle (S. S. Oriol)

Montour quadrangle (H. E. Malde)

Palisades Dam quadrangle (D. A. Jobin, c, D)

Patterson quadrangle (E. T. Ruppel)

Strevell quadrangle (J. F. Smith)

Upper and Lower Red Rock Lake quadrangles (I. J.
 Witkind)

Wood River district (W. E. Hall, M)

Yellow Pine quadrangle (B. F. Leonard)

**Kentucky, cooperative mapping program (E. R. Cressman,
 Lexington)****Maine:**

Blue Hill quadrangle (D. B. Stewart, NC)

Castine quadrangle (D. B. Stewart, NC)

Orland quadrangle (D. R. Wones, NC)

Rumford quadrangle (R. H. Moench, D)

The Forks quadrangle (F. C. Canney, D)

Maryland (NC):

Delmarva Peninsula (J. P. Owens)

Northern Coastal Plain (J. P. Minard)

Western Maryland Piedmont (M. W. Higgins)

Massachusetts:

Boston and vicinity (C. A. Kaye, Boston)

Cooperative mapping program (J. O. Peper, NC)

**Michigan, Gogebic Range, western part (R. G. Schmidt,
 NC)****Minnesota, Vermilion greenstone belt (P. K. Sims, D)****Montana:**

Birney SW quadrangle (S. Volz, c, Casper, Wyo.)

Cooke City quadrangle (J. E. Elliott, D)

Craig quadrangle (R. G. Schmidt, NC)

Crazy Mountains Basin (B. A. Skipp, D)

Decker quadrangle (B. E. Law, c, D)

Geologic mapping—Continued**Map scale 1:62,500, and larger—Continued***States and territories—Continued***Montana—Continued**

Elk Park quadrangle (H. W. Smedes, D)

Half Moon Hill quadrangle (V. Neirmeir, c, Casper,
 Wyo.)

Holmes Ranch quadrangle (N. E. Micklich, c, Casper,
 Wyo.)

Jordan quadrangle (G. D. Mowat, c, Billings)

Kirby quadrangle (c, Casper, Wyo.)

Lemhi Pass quadrangle (M. H. Staatz, D)

Melrose phosphate field (G. D. Fraser, c, D)

Melrose quadrangle (H. W. Smedes and G. D. Fraser,
 D)

Northern Pioneer Range, geologic environment (E-an
 Zen, NC)

Pearl School quadrangle (G. L. Galyardt, c, Casper,
 Wyo.)

Spring Gulch quadrangle (N. E. Micklich, c, Casper,
 Wyo.)

Taintor Desert quadrangle (S. Volz, c, Casper, Wyo.)

Tongue River Dam quadrangle (N. E. Micklich, c,
 Casper, Wyo.)

Wolf Creek area, petrology (R. G. Schmidt, NC)

Nebraska, McCook 2-degree quadrangle (G. E. Prichard, D)**Nevada:**

Austin quadrangle (E. H. McKee, M)

Bellevue Peak quadrangle (T. B. Nolan, NC)

Carlin region (J. F. Smith, Jr., D)

Jordan Meadow and Disaster Peak quadrangles (R. C.
 Greene, M)

Kobeh Valley (T. B. Nolan, NC)

Midas-Jarbridge area (R. R. Coats, M)

Round Mountain and Manhattan quadrangles (D. R.
 Shawe, D)

Spruce Mountain 4 quadrangle (G. D. Fraser, c, D)

New Mexico:

Acoma area (C. H. Maxwell, D)

Alamosa Mesa West quadrangle (D. B. Umshler, c,
 Roswell)

Alma quadrangle (J. C. Ratté, D)

Bull Basin quadrangle (J. C. Ratté, D)

Church Rock-Smith Lake (C. T. Pierson, D)

Cretaceous stratigraphy, San Juan basin (E. R.
 Landis, D)

Dillon Mountain quadrangle (J. C. Ratté, D)

Gallup East quadrangle (E. D. Patterson, c, Roswell)

Gallup West quadrangle (J. E. Fassett, c, Farmington)

Glenwood quadrangle (J. C. Ratté, D)

Hillsboro quadrangle (D. C. Hedlund, D)

Holt Mountain quadrangle (J. C. Ratté, D)

Iron Mountain (A. V. Heyl, Jr., D)

Luna quadrangle (J. E. Fassett, c, Farmington)

Manuelito quadrangle (J. E. Fassett, c, Farmington)

Manzano Mountains (D. A. Myers, D)

Mongollon quadrangle (J. C. Ratté, D)

O-Block Canyon quadrangle (J. C. Ratté, D)

Ojo Encino Mesa quadrangle (D. B. Umshler, c,
 Roswell)

Pinos Altos Range (T. L. Finnell, D)

Pueblo Alto Trading Post quadrangle (R. W. Jentgen,
 c, Farmington)

Raton coal basin, western part (C. L. Pillmore, D)

Reserve quadrangle (J. C. Ratté, D)

Geologic mapping—Continued

Map scale 1:62,500, and larger—Continued

States and territories—Continued

New Mexico—Continued

- Saliz Pass quadrangle (J. C. Ratté, D)
- Samson Lake quadrangle (J. E. Fassett, c, Farmington)
- Star Lake quadrangle (J. E. Fassett, c, Farmington)
- Tanner Lake quadrangle (D. B. Umshler, c, Roswell)
- Twin Butte quadrangle (M. L. Millgate, c, Farmington)
- Valles Mountains, petrology (R. L. Smith, NC)

North York (NC):

- Geologic correlations and mineral resources in Precambrian rocks of St. Lawrence lowlands (C. E. Brown, NC)

North Carolina, central Piedmont (A. A. Stromquist, D)

North Dakota:

- Clark Butte 15-minute quadrangle (G. D. Mowat, c, Billings, Mont.)
- North Almont quadrangle (H. L. Smith, c, D)

Pennsylvania (NC):

- Northern anthracite field (M. J. Bergin)
- Southern anthracite field (G. H. Wood, Jr.)
- Wind Gap and adjacent quadrangles (J. B. Epstein)

Puerto Rico (R. D. Krushensky, NC)

South Dakota:

- Black Hills Precambrian (J. A. Redden, Hill City)
- Keystone pegmatite area (J. J. Norton, Rapid City)
- Medicine Mountain quadrangle (J. C. Ratté, D)

Texas:

- Agency Draw NE quadrangle (G. N. Pipiringos, D)
- Bates Knolls quadrangle (G. N. Pipiringos, D)
- Tilden-Loma Alta area (K. A. Dickinson, D)

Utah (c, D, unless otherwise noted):

- Agency Draw NW quadrangle (G. N. Pipiringos)
- Basin Canyon quadrangle (Fred Peterson)
- Big Hollow Wash quadrangle (Fred Peterson)
- Blackburn Canyon quadrangle (Fred Peterson)
- Canaan Peak quadrangle (W. E. Bowers)
- Coal mine bumps, Sunnyside mining district (F. W. Osterwald, D)
- Collet Top quadrangle (H. D. Zeller)
- Confusion Range (R. K. Hose, M)
- Crawford Mountains (W. C. Gere, c, M)
- East-of-the-Navajo quadrangle (H. D. Zeller)
- Fourmile Bench quadrangle (W. E. Bowers)
- Horse Flat quadrangle (H. D. Zeller)
- Horse Mountain quadrangle (W. E. Bowers)
- Jessen Butte quadrangle (E. M. Schell, c, Casper, Wyo.)
- Matlin Mountains (V. R. Todd, M)
- Needle Eye Point quadrangle (H. D. Zeller)
- Oak City area (D. J. Varnes, D)
- Ogden 4 NW quadrangle (R. J. Hite)
- Pete's Cove quadrangle (H. D. Zeller)
- Salt Lake City and vicinity (Richard VanHorn, D)
- Sheeprock Mountains, West Tintic district (H. T. Morris, M)
- Ship Mountain Point quadrangle (H. D. Zeller)
- Sunset Flat quadrangle (Fred Peterson)
- Wah Wah Summit quadrangle (L. F. Hintze, Salt Lake City)
- Wasatch Front surficial geology (R. D. Miller, D)
- Willard Peak area (M. D. Crittenden, Jr., M)

Virginia (NC):

- Culpeper basin (K. Y. Lee)

Geologic mapping—Continued

Map scale 1:62,500, and larger—Continued

States and territories—Continued

Virginia—Continued

- Delmarva Peninsula (J. P. Owens)
- Northern Blue Ridge (G. H. Espenshade)
- Rapidan-Rappahannock (Louis Pavlides)

Washington:

- Chewelah No. 4 quadrangle (F. K. Miller, M)
- Glacier Park area (F. W. Cater, Jr., D)
- Northern Okanogan Highlands (C. D. Rinehart, M)
- Olympic Peninsula, eastern part (W. M. Cady, D)
- Stevens County (R. G. Yates, M)
- Togo Mountain quadrangle (R. C. Pearson, D)

Wisconsin, Black River Falls and Hatfield quadrangles (Harry Klemic, NC)

Wyoming (c, D, unless otherwise noted):

- Acme quadrangle (B. E. Barnum)
- Albany and Keystone quadrangles (M. E. McCallum, D)
- Alkali Butte quadrangle (M. W. Reynolds, D)
- Appel Butte quadrangle (G. L. Galyardt)
- Badwater Creek (R. E. Thaden, D)
- Bailey Lake quadrangle (M. L. Schroeder)
- Beaver Creek Hills quadrangle (c, Casper)
- Betty Reservoir NE quadrangle (N. McKinnie, c, Casper)
- Browns Hill quadrangle (C. S. V. Barclay)
- Cottonwood Rim quadrangle (C. S. V. Barclay)
- Coyote Draw quadrangle (G. L. Galyardt)
- Crawford Mountains (W. C. Gere, c, M)
- Deer Creek quadrangle (M. L. Schroeder)
- Devils Tooth quadrangle (W. G. Pierce, M)
- Eagle Peak quadrangle (H. W. Smedes and H. J. Prostka, D)
- Eagle Rock quadrangle (S. P. Buck, c, Casper)
- Fortin Draw quadrangle (B. E. Law)
- Four Bar-J Ranch quadrangle (G. L. Galyardt)
- Gillette East quadrangle (B. E. Law)
- Gillette West quadrangle (B. E. Law)
- Grand Teton National Park (J. D. Love, Laramie)
- Greenhill quadrangle (S. P. Buck, c, Casper)
- Grieve Reservoir quadrangle (C. S. V. Barclay)
- Gros Ventre Range (F. S. Simons)
- Hilight quadrangle (W. J. Purdon, c, Casper)
- Hultz Draw quadrangle (c, Casper)
- Ketchum Buttes quadrangle (C. S. V. Barclay)
- Little Thunder Reservoir quadrangle (G. C. Martin, c, Casper)
- Monarch quadrangle (B. E. Barnum)
- Moyer Springs quadrangle (B. E. Law)
- Neil Butte quadrangle (S. P. Buck, c, Casper)
- North Star School NE quadrangle (S. P. Buck, c, Casper)
- North Star School NW quadrangle (S. P. Buck, c, Casper)
- North Star School SE quadrangle (L. Jefferies, c, Casper)
- Open A Ranch quadrangle (G. C. Martin, c, Casper)
- Oriva quadrangle (B. E. Law)
- Pickle Pass quadrangle (M. L. Schroeder)
- Pine Creek quadrangle (D. A. Jobin)
- Pine Mountain-Oil Mountain area (G. J. Kerns, c, Casper)
- Piney Canyon NW quadrangle (G. C. Martin, c, Casper)
- Piney Canyon SW quadrangle (L. Wackwitz, c, Casper)

Geologic mapping—Continued

Map scale 1:62,500, and larger—Continued

States and territories—Continued

Wyoming—Continued

- Reid Canyon quadrangle (G. J. Kerns, c, Casper)
- Reno Junction quadrangle (L. Jefferies, c, Casper)
- Reno Reservoir quadrangle (G. C. Martin, c, Casper)
- Rough Creek quadrangle (S. P. Buck, c, Casper)
- Savery quadrangle (C. S. V. Barclay)
- Sheridan Pass quadrangle (W. L. Rohrer, c, Casper)
- Sheridan quadrangle (E. I. Winger)
- Square Top Butte quadrangle (G. J. Kerns, c, Casper)
- Teckla quadrangle (J. E. Goolsby, c, Casper)
- Teckla SW quadrangle (J. E. Goolsby, c, Casper)
- The Gap quadrangle (G. L. Galyardt)
- Tullis quadrangle (C. S. V. Barclay)
- Turnercrest NE quadrangle (G. C. Martin, c, Casper)
- Two Ocean Pass quadrangle (H. W. Smedes, D)
- Wapiti quadrangle (W. G. Pierce, M)
- Weston SW quadrangle (R. W. Jones, c, Casper)

Geomagnetism:

- External geomagnetic-field variations (W. H. Campbell, D)
- Geomagnetic-data analysis (C. O. Stearns, D)
- Geomagnetic observatories (J. D. Wood, D)
- Geomagnetic secular variation (L. R. Alldredge, D)
- Magnetic-field analysis and U.S. charts (E. B. Fabiano, D)
- World magnetic charts and analysis (E. B. Fabiano, D)

Geomorphology:

- Channel adjustment, Cochiti Dam (J. D. Dewey, w, Albuquerque, N. Mex.)
- Forest geomorphology, Pacific coast (R. J. Janda, w, M)
- Morphology, provenance, and movement of desert sand (E. D. McKee, D)
- Quaternary landforms and deposits interpreted from Landsat-1 imagery, Midwest and Great Plains (R. B. Morrison, D)
- Stream channelization (J. C. Brice, w, M)
- Studies of erosion control (N. J. King, w, M)
- States:*
- Arizona, post-1890 A.D. erosion features interpreted from Landsat-1 imagery (R. B. Morrison, D)
- Idaho, surficial geology of eastern Snake River Plain (W. E. Scott, M. D. Hait, Jr., D)
- Massachusetts, sea-cliff erosion studies (C. A. Kaye, Boston)
- New Mexico, Chaco Canyon National Monument (H. E. Malde, D)
- Utah, Quaternary geology (W. E. Scott, D)
- Wyoming (D):
 - Wind River Mountains, Quaternary geology (G. M. Richmond)
 - Yellowstone National Park, glacial and postglacial geology (G. M. Richmond)

*See also Sedimentology; Geochronological investigations.***Geophysics, regional:**

- Airborne and satellite research:
 - Aeromagnetic studies (M. F. Kane, D)
 - Electromagnetic research (F. C. Frischknecht, D)
 - Gamma-ray research (J. S. Duval, D)
- Regional Studies (Isidore Zietz, NC)
- Antarctica, Pensacola Mountains, geophysical studies (J. C. Behrendt, Woods Hole, Mass.)
- Basin and Range geophysical studies (W. E. Davis, M)
- Crust and upper mantle:
 - Aeromagnetic interpretation of metamorphic rocks (Isidore Zietz, NC)

Geophysics, regional—Continued

Crust and upper mantle—Continued

- Aeromagnetic studies of the United States (Isidore Zietz, NC)
 - Analysis of travelttime data (J. C. Roller, M)
 - Seismicity and Earth structure (J. N. Taggart, D)
 - Seismologic studies (J. P. Eaton, M)
- Engineering geophysics (H. D. Ackermann, D)
- Florida Continental Shelf, gravity studies (H. L. Krivoy, NC)
- Gravity surveys:
 - Dona Ana, Otero, Lincoln, Sierra, and Socorro Counties, New Mexico (D. L. Healey, D)
 - Maryland cooperative (D. L. Daniels, NC)
- Ground-water geophysics (W. D. Stanley, D)
- Magnetic chronology, Colorado Plateau and environs (D. P. Elston, E. M. Shoemaker, Flagstaff, Ariz.)
- Mobile magnetometer profiles, Eastern United States (M. F. Kane, D)
- New England, magnetic properties of rocks (Andrew Griscom, M)
- Program and systems development (G. I. Evenden, W. L. Anderson, D)
- Rainier Mesa (J. R. Ege)
- Rocky Mountains, northern (D. L. Peterson, M. D. Kleinkopf, D)
- Southeastern States geophysical studies (Peter Popenoe, NC)
- Southwestern States geophysical studies (D. L. Peterson, NC)
- Ultramafic rocks, geophysical studies, intrusions (G. A. Thompson, M)
- United States, aeromagnetic surveys (E. R. King, NC)
- States and territories:*
- Alaska, Amblor River and Baird Mountains quadrangles, gravity studies (D. F. Barnes, M)
- California, Sierra Nevada, geophysical studies (H. W. Oliver, M)
- Idaho, Snake River Plain (D. L. Peterson, D)
- Massachusetts, geophysical studies (M. F. Kane, NC)
- Minnesota (NC):
 - Keweenaw rocks, magnetic studies (K. G. Books)
 - Southern part, aeromagnetic survey (E. R. King)
- Nevada, engineering geophysics, Nevada Test Site (R. D. Carroll, D)
- New Mexico, Rio Grande graben (L. E. Cordell, D)
- Pennsylvania, magnetic properties of rocks (Andrew Griscom, M)
- Puerto Rico, seismicity of Puerto Rico (A. C. Tarr, D)
- Geophysics, theoretical and experimental:**
- Earthquakes, local seismic studies (J. P. Eaton, M)
- Elastic and inelastic properties of Earth materials (Louis Peselnick, M)
- Electrical properties of rocks (R. D. Carroll, D)
- Electrical resistivity studies (A. A. R. Zohdy, D)
- Experimental rock mechanics (C. B. Raleigh, M)
- Gamma-ray spectrometry for uranium exploration in crystal-line terranes (J. A. Pitkin, D)
- Geomechanical studies, in-situ stress (J. R. Ege, D)
- Geophysical data, interpretation using electronic computers (R. G. Henderson, NC)
- Ground-motion studies (J. H. Healy, M)
- Infrared and ultraviolet radiation studies (R. M. Moxham, NC)
- Magnetic and luminescent properties (F. E. Senftle, NC)
- Magnetic Properties Laboratory (M. E. Beck, Jr., Bellingham, Wash.)
- Microwave studies (A. W. England, D)
- Mineral Research Petrophysics (G. R. Olhoeft, D)

Geophysics, theoretical and experimental—Continued

- Paleomagnetism, Precambrian and Tertiary chronology (D. P. Elston, Flagstaff, Ariz.)
- Remanent magnetization of rocks (C. S. Grommé, M)
- Resistivity interpretation (A. A. R. Zohdy, D)
- Rock behavior at high temperature and pressure (E. C. Robertson, NC)
- Seismicity patterns in time and space (C. G. Bufe, M)
- Stress studies (C. B. Raleigh, M)
- Theory of gamma rays for geological applications (J. S. Duval, D)
- Thermodynamic properties of rocks (R. A. Robie, NC)
- Ultramafic intrusions, geophysical studies (G. A. Thompson, M)
- Volcano geophysics (E. T. Endo, M)
- States:*
- California, mass properties of oil-field rocks (L. A. Beyer, M)
- Nevada (D):
- Nevada Test Site:
- Interpretation of geophysical logs (R. D. Carroll)
- Seismic velocity measuring techniques (R. D. Carroll)
- Vermont, in-situ stress in a granite quarry (G. E. Brethauer, D)

Geotechnical investigations:

- Electronics instrumentation research for engineering geology (J. B. Bennetti, Jr., D)
- Geotechnical measurements and services (H. W. Olsen, D)
- In-situ stress, reactor hazards research (T. C. Nichols, Jr., D)
- Miscellaneous landslide investigations (R. W. Fleming, D)
- Open-pit slope stability (F. T. Lee, D)
- Research in rock mechanics (F. T. Lee, D)
- Soil engineering research (T. L. Youd, M)
- States:*
- Colorado, coal mine deformation at Somerset (C. R. Dunrud, D)
- Utah, coal mine bumps (F. W. Osterwald, D)
- Virginia, Reston (S. F. Obermeier, NC)
- Western United States, engineering geology investigations in Powder River basin (F. W. Osterwald, D)

Geothermal Investigations:

- Broad-band electrical surveys (Mark Landisman, University of Texas)
- Colorado Plateau, potential field methods (R. R. Wahl, D)
- Convection and thermoelastic effects in narrow vertical fracture spaces:
- Analytical techniques (Gunnar Bodvarsson, Oregon State University)
- Numerical techniques (R. P. Lowell, Georgia Institute of Technology)
- Development of first-motion holography for exploration (Keiiti Aki, Massachusetts Institute of Technology)
- Electrical and electromagnetic methods in geothermal areas (D. B. Jackson, D)
- Evaluation of intermediate-period seismic waves as an exploration tool (D. M. Boore, Stanford University)
- Evaluation of noble gas studies in exploration (Emanuel Mazar, Weizmann Institute of Science, Rehovot, Israel)
- Exploration and characterization from seismic activity (E. A. Page, ENSCO, Inc.)
- Geochemical exploration (M. E. Hinkle, D)
- Geochemical indicators (A. H. Truesdell, M)
- Geochemistry of geopressured systems (Y. K. Kharaka, w. M)
- Geophysical characterization of young silicic volcanic centers, eastern Sierran Front (W. F. Isherwood, D)
- Geothermal, Coachella Valley (J. H. Robison, w, M)
- Geothermal coordination (F. H. Olmsted, w, M)
- Geothermal geophysics (D. R. Mabey, D)
- Geothermal hydrologic reconnaissance (F. H. Olmsted, w, M)

Geothermal investigations—Continued

- Geothermal petrophysics (G. R. Olhoeft, D)
- Geothermal reservoirs (Manuel Nathenson, M)
- Geothermal resource assessment (L. J. P. Muffler, M)
- Geothermal studies (A. H. Lachenbruch, M)
- Geothermal water, Verde Valley (P. P. Ross, w, Phoenix)
- Gravity variations as a monitor of water levels (J. M. Goodkind, University of California, San Diego)
- Heat flow (J. H. Sass, A. H. Lachenbruch, M)
- Isotopic and chemical studies of geothermal gases (Harmon Craig, University of California, San Diego)
- Low-frequency electromagnetic prospecting system (J. Clarke and H. F. Morrison, University of California, Berkeley)
- Mercury geochemistry as a tool for geothermal exploration (P. R. Buseck, Arizona State University)
- Oxygen isotopes (J. R. O'Neil, M)
- Physics of geothermal systems (W. H. Diment, M)
- Radioactivity series isotopic disequilibrium (J. K. Osmond and J. B. Cowart, Florida State University)
- Regional geoelectromagnetic traverse (J. F. Hermance, Brown University)
- Regional volcanology (R. L. Smith, NC)
- Remote sensing (Kenneth Watson, D)
- Rio Grande geothermal (P. H. Jones, w, Bay St. Louis, Miss.)
- Rock-water interactions (R. O. Fournier, M)
- Seismic exploration (P. L. Ward, M)
- Signal processing methods for magnetotellurics (W. C. Hernandez, ENSCO, Inc.)
- Statistical characteristics of geothermal resources, Basin and Range province (W. F. Isherwood, D)
- Thermal waters (D. E. White, M)
- States:*
- Alaska, geothermal reconnaissance (T. D. Miller, M)
- Arizona, San Francisco volcanic field (E. W. Wolfe, Flagstaff)
- California:
- Coso area, passive seismology (P. A. Reasenberg, M)
- Geology of Long Valley-Mono basin (R. A. Bailey, NC)
- Long Valley:
- Active seismology (D. P. Hill, M)
- Mercury in soils of geothermal areas (R. W. Klusman, Colorado School of Mines)
- Microearthquake monitoring:
- Imperial Valley (D. P. Hill, M)
- The Geysers-Clear Lake (C. G. Bufe, M)
- Mt. Lassen thermal areas (L. J. P. Muffler, M)
- Simulation model, Raft River basin (W. D. Nichols, w, Sacramento)
- The Geysers area:
- Seismic noise (H. M. Iyer, M)
- The Geysers-Clear Lake (B. C. Hearn, Jr., NC)
- The Geysers-Clear Lake area, pre-Tertiary geology (R. J. McLaughlin, M)
- Colorado:
- Colorado geothermal (R. E. Moran, w, D)
- Geochemical and hydrological parameters of geothermal systems (R. H. Pearl, Colorado Geological Survey)
- Geothermal resources (G. L. Galyardt, c, D)
- Relationship between geothermal resources and ground water (J. C. Romero, Colorado Geological Survey)
- Georgia, heat flow and radioactive heat generation studies in Southeastern United States (D. L. Smith, University of Florida)
- Hawaii, Kilauea Volcano, potential field methods for subsurface magma mapping (C. J. Zablocki, D)

Geothermal investigations—Continued*States—Continued***Idaho:**

- Raft River surface and subsurface geology (H. R. Covington, D)
- Snake River Plain surface and subsurface geology (M. A. Kuntz, D)
- Sugar City area (H. J. Prostka, D)
- Test drilling, Raft River valley (E. G. Crosthwaite, Boise)

Montana:

- Geothermal investigations in Montana (R. B. Leonard, w, Helena)
- Geothermal reconnaissance in southwestern Montana (R. A. Chadwick, Montana State University)

Nevada, geothermal reconnaissance (R. K. Hose, M)**New Mexico, evaluation of geothermal potential of the Basin and Range province (G. P. Landis, University of New Mexico)****Oregon:**

- Geophysical investigation of the Cascade Range (R. W. Couch, Oregon State University)
- Geophysical investigations of the Vale-Owyhee geothermal region (R. W. Couch, Oregon State University)
- Geothermal reconnaissance (N. S. MacLeod, M)
- Hydrologic reconnaissance of geothermal areas (E. A. Sammel, w, M)

Utah:

- Geothermal reconnaissance in Utah (F. E. Rush, w, Salt Lake City)
- Geothermal resources (G. L. Galyardt, c, D)
- Petrology and geochronology of late Tertiary and Quaternary volcanic rocks (W. P. Nash, University of Utah)
- Regional heat flow and geochemical studies (S. H. Ward, University of Utah)

West Virginia, eastern Warm Springs (W. A. Hobba, Jr., w, Morgantown)**Wyoming, Yellowstone thermal areas, geology (M. H. Beeson, M)****Glaciology:**

- Columbia Glacier (M. F. Meier, w, Tacoma, Wash.)
- Electromagnetic methods for measuring snow (M. F. Meier, w, Tacoma, Wash.)
- Glacier investigations (C. O. Geiger, w, Helena, Mont.)
- Ice Age modelling (D. P. Adam, M)
- Ice dynamics (W. J. Campbell, w, Tacoma, Wash.)
- Water, ice, and energy balance of mountain glaciers and ice physics (M. F. Meier, w, Tacoma, Wash.)
- World Data Center A—Glaciology (A. S. Post, w, Tacoma, Wash.)

Gold:

- Composition related to exploration (J. C. Antweiler, D)
- Great Lakes region (D. A. Seeland, D)

*States:***Alaska, Seward Peninsula, nearshore (D. M. Hopkins, M)****California, Klamath Mountains (P. E. Hotz, M)****Montana (D):**

- Cooke City quadrangle (J. E. Elliott)
- Ore deposits, southwestern part (K. L. Wier)

Nevada (M, except as otherwise noted):

- Aurora and Bodie districts, Nevada-California (F. J. Kleinhampl)
- Carlin mine (A. S. Radtke)
- Comstock district (D. H. Whitebread)
- Dun Glen quadrangle (D. H. Whitebread)

Gold—Continued*States—Continued***Nevada—Continued**

- Goldfield district (R. P. Ashley)
- Round Mountain and Manhattan districts (D. R. Shawe, D)
- New Mexico, placer deposits (Kenneth Segerstrom, D)
- North Carolina, Gold Hill area (A. A. Stromquist, D)
- Oregon-Washington, nearshore area (P. D. Snively, Jr., M)
- South Dakota, Keystone area (W. H. Raymond, D)
- Wyoming, northwestern part, conglomerates (J. C. Antweiler, D)

*See also Heavy metals.***Ground water-surface water relations:****Bank storage reconnaissance (W. D. Simons, w, M)***States:***California, confined aquifer, San Bernardino (W. H. Hardt, w, Laguna Niguel)****Florida (w, Miami, except as otherwise noted):**

- Biscayne aquifer analog model (E. H. Cordes)
- Hydrologic base, Dade County (J. E. Hull)
- Miami Canal infiltration (F. W. Meyer)

Idaho (w, Boise):**Hydrology:**

- Island Park-Henrys Lake (R. L. Whitehead)
- Weiser Basin (H. W. Young)
- Missouri, hydrology of Ozarks Basin (John Skelton, w, Rolla)
- Nebraska, Platte Basin water resources (E. G. Lappala, w, Lincoln)
- New Mexico, Pecos River, miscellaneous (G. E. Welder, w, Roswell)
- North Carolina, effect of channel improvement on hydrologic conditions in Creeping Swamp (M. D. Winner, w, Raleigh)
- Ohio, Franklin County digital model (R. E. Fidler, w, Columbus)
- Washington, water, Yakima Reservation (R. D. MacNish, w, Tacoma)

Wisconsin (w, Madison):**Hydrology:**

- Cedar Lake (R. S. McLeod)
- Nederlo Creek (P. A. Kammerer, Jr.)
- Wetlands (R. P. Novitzki)

Heavy metals:**Appalachian region:**

- Mineral resources, Connecticut-Massachusetts (J. P. D'Agostino, NC)
 - South-central (A. A. Stromquist, D)
 - Hydrogeochemistry and biogeochemistry (T. T. Chao, D)
 - Mineral paragenesis (J. T. Nash, M)
 - Regional variation in heavy-metals content of Colorado Plateau stratified rocks (R. C. Cadigan, D)
 - Rocky Mountain region, fossil beach placers (R. S. Houston, Laramie, Wyo.)
 - Solution transport (G. K. Czamanske, M)
 - Southeastern States, geochemical studies (Henry Bell III, NC)
- States:*
- Alaska (M):**
- Gulf of Alaska, nearshore placers (Erk Reimnitz)
 - Hogatza trend (T. P. Miller)
 - Southeastern part (D. A. Brew)
 - Southern Alaska Range (B. L. Reed)
 - Southwestern part (J. M. Hoare)
 - Yukon-Tanana Upland (H. L. Foster)
- Idaho, Washington Peak quadrangle (D. A. Seeland, D)**

Heavy metals—Continued

States—Continued

Nevada:

- Aurora and Bodie districts, Nevada-California (F. J. Kleinhampl, M)
- Basin and Range (D. R. Shawe, D)

Hydraulics, ground water:

- Computer analysis, ground-water problems (S. S. Papadopulos, w, NC)
- Transient phenomena in ground-water flow (C. E. Mongan, w, Boston, Mass.)
- Transport processes in fluid flows (Akio Ogata, w, Honolulu, Hawaii)

Hydraulics, surface flow:

- Dispersion by turbulent flow in open channels (Nobuhiro Yotsukura, w, NC)
- Time-of-travel studies, New York (L. A. Wagner, w, Albany, N.Y.)
- Unsteady flow and saline intrusions in rivers and estuaries (R. A. Baltzer, w, NC)

See also Hydrologic instrumentation.

Hydrologic data collection and processing:

- Data file for well records (R. S. McLeod, w, Madison, Wis.)
- Hydrologic probability models (W. H. Kirby, w, NC)
- New Mexico data bank (D. R. Posson, w, Albuquerque)
- Runoff cycle simulation (D. R. Dawdy, w, M)
- Store-retrieve hydrologic data (G. W. Hawkins, w, Mineola, N.Y.)

See also Hydrologic instrumentation.

Hydrologic instrumentation:

- Analog model unit (S. M. Longwill, w, NC)
 - Drilling techniques (Eugene Shuter, w, D)
 - GOES data collection (E. H. Cordes, w, Miami, Fla.)
 - Ground water, quality of water monitors (R. L. Whitehead, w, Boise, Idaho)
 - Instrumentation and environmental studies (G. E. Ghering, w, D)
 - Instrumentation research, water (F. C. Koopman, w, Bay St. Louis, Miss.)
 - Interagency sedimentation project (J. V. Skinner, w, Minneapolis, Minn.)
 - Laboratory research, instruments, water (G. F. Smoot, w, NC)
 - Laser spectroscopy (M. C. Goldberg, w, D)
 - Optical current meter design (Winchell Smith, w, M)
 - Remote sensing in karst terrane (J. H. Williams, w, Rolla, Mo.)
 - Satellite data relay project (R. W. Paulson, w, NC)
 - Suspended solids sensors (J. V. Skinner, w, Minneapolis, Minn.)
 - Susquehanna Landsat-DCS test (J. V. Funt, w, Harrisburg, Pa.)
 - Techniques of flood-plain mapping (R. H. Brown, w, Bay St. Louis, Miss.)
 - Telemetry evaluation program (J. F. Turner, w, Tampa, Fla.)
- See also* Hydrologic data collection and processing.

Hydrology, ground water:

- Alluvial fan deposition (W. E. Price, Jr., w, NC)
- Appalachian Basin, waste storage (P. M. Brown, w, Raleigh, N. C.)
- Aquifer systems:
 - Field research (B. E. Lofgren, w, Sacramento, Calif.)
 - Theoretical aspects (D. C. Helm, w, Sacramento, Calif.)
- Borehole geophysics (W. S. Keys, w, D)
- Consultation and research (C. V. Theis, w, Albuquerque, N. Mex.)
- Digital modeling, ground-water flow (S. P. Larson, w, NC)

Hydrology, ground water—Continued

- Fractured hydrogeologic systems (C. R. Faust, w, NC)
- Geopressed-geothermal resources (R. H. Wallace, w, Bay St. Louis, Miss.)
- Geothermal modeling (J. W. Mercer, w, NC)
- Ground-water geophysics research (A. A. R. Zohdy, w, D)
- Ground-water staff functions (S. W. Lohman, w, D)
- Ground-water tracer studies (R. J. Sun, w, NC)
- Gulf Coast hydrodynamics (P. C. Trescott, w, NC)
- Hydrologic laboratory (F. S. Riley, w, D)
- Hydrology of the Madison aquifer (E. M. Cushing, w, D)
- Hydrology of Wilcox Formation with reference to liquid waste emplacement in the Gulf Coastal Plain (R. H. Wallace, Jr., w, Bay St. Louis, Miss.)
- Impact of mining on aquifers (N. J. King, w, D)
- In-situ stress measurements (J. D. Bredehoeft, w, NC)
- Liaison, U.S. Geological Survey-Bureau of Land Management (F. W. Giessner, w, D)
- Limestone hydraulic permeability (V. T. Stringfield, w, NC)
- Microbes in ground water (G. G. Ehrlich, w, M)
- Modeling of geothermal systems (M. L. Sorey, w, M)
- Paradox basin hydrology (F. F. Rush, w, D)
- Regional ground-water-studies coordination (E. M. Cushing, w, NC)
- Role of confining clays (R. G. Wolff, w, NC)
- Transport phenomena in porous media (J. W. Mercer, w, NC)
- Tropical carbonate aquifers (William Back, w, NC)

States and territories:

Alabama:

- Cretaceous aquifer simulation (R. A. Gardner, w, Montgomery)
- Water management, Madison County (J. R. Avrett, w, University)

Alaska (w, Anchorage):

- Data summary, Cook Inlet (G. W. Freethey)
- Ground-water appraisal, Alaska region (Chester Zenone)

Arizona:

- Ground water to Colorado River (O. J. Loeltz, w, Yuma)
- Southern Apache County (T. W. Anderson, w, Flagstaff)
- Special site studies (H. M. Babcock, w, Tucson)
- Water supply, Lake Mead area (R. L. Laney, w, Phoenix)

Arkansas:

- Ground water, lower Mississippi region (J. E. Terry, Jr., w, Little Rock)
- Hydrology of Claiborne and Wilcox (M. E. Broom, w, Little Rock)

California (w, Laguna Niguel, except as otherwise noted):

- City of Merced ground water appraisal (R. W. Page, w, Sacramento)
- Data Antelope-Valley East Kern (C. E. Lamb, w, Laguna Niguel)
- Geohydrology, southwestern San Bernardino County (D. H. Schaefer)

Ground water:

- Beale Air Force Base (R. W. Page, w, Sacramento)
- Hollister area (K. S. Muir, w, M)
- Indian Wells Valley (D. J. Downing, w, Laguna Niguel)
- Napa County (J. P. Akers, w, M)
- Santa Barbara (C. E. Lamb, w, Laguna Niguel)
- Thousand Oaks (J. J. French, w, Laguna Niguel)
- Ground water model—Modesto (R. W. Page, w, Sacramento)
- Imperial Valley geothermal model (R. E. Miller)

Hydrology, ground water—Continued*States and territories—Continued***California—Continued**

- Palmdale Bulge earthquake prediction (J. R. Moyle, w, Laguna Niguel)
- Seawater intrusion, Soquel-Aptos (K. S. Muir, w, M)
- Sole-source aquifer studies (G. L. Faulkner, w, M)
- Updating ground-water information in the Eureka area (M. J. Johnson, w, M)
- Water resources, Vandenberg AFB (C. E. Lamb)

Colorado (w, D):

- Arkansas River basin (R. E. Fidler, w, Pueblo)
- Aquifer testing (F. A. Welder)
- Colorado River salinity ground water (J. W. Warner, w, D)
- Ground water, Denver basin (D. E. Hillier)
- Roan-Parachute ground-water model (R. H. Dale, d, D)
- Routt County ground water (T. R. Ford, w, Meeker)
- West Slope aquifers (T. F. Giles, w, D)

Connecticut (w, Hartford):

- Farmington ground-water potential (R. L. Melvin)
- Newton ground-water potential (F. P. Haeni)

Florida:

- Aquifer characteristics in southwest Florida (R. M. Wolansky, w, Tampa)
- Aquifer maps, Southwest Florida Water Management District (Anthony Buono, w, Tampa)
- Biscayne aquifer (Howard Klein, w, Miami)
- Broward County (C. B. Sherwood, Jr., w, Miami)
- Dade City ground water (Warren Anderson, w, Orlando)
- Fernandina saltwater intrusion investigation (C. B. Bentley, w, Jacksonville)
- Floridan aquifer—Withlacoochee (P. W. Bush, w, Orlando)
- Freshwater resources, Big Pine Key (C. E. Hanson, w, Miami)
- Geohydrology, citrus irrigation (W. E. Wilson III, w, Tampa)
- Ground water—Kissimmee River Basin (J. M. Frazee, Jr., w, Orlando)
- Hydrology, Cocoa well-field (W. D. Wood, w, Orlando)
- Hydrology of Lake Tsala Apopka (A. T. Rutledge, w, Winter Park)
- Injecting wastes in saline aquifers (F. W. Meyer, w, Miami)
- Injecting monitoring, Tampa Bay area (J. J. Hickey, w, Tampa)
- New well fields, Dade County (Howard Klein, w, Miami)
- Northwest Volusia (A. T. Rutledge, w, Orlando)
- Palm Beach County flatlands (A. L. Knight, w, Miami)
- Potentiometric maps in Southwest Florida Water Management District (P. D. Ryder, w, Tampa)
- Saltwater line, west-central Florida (E. R. Close, w, Tampa)
- Sarasota disposal well, phase 1 (Horace Sutcliffe, Jr., w, Sarasota)
- Shallow aquifer Jacksonville (L. V. Causey, w, Jacksonville)
- Shallow aquifer Palm Beach County (A. L. Knight, w, Miami)
- Springs of Florida (J. C. Rosenau, w, Ocala)
- St. Johns County Shallow aquifer study (E. C. Hayes, w, Jacksonville)
- Storage of storm waters (J. J. Hickey, w, Tampa)
- Subsurface disposal—Pinellas (J. J. Hickey, w, Tampa)
- Technical assistance Hillsborough County (J. W. Stewart, w, Tampa)

Hydrology, ground water—Continued*States and territories—Continued***Florida—Continued**

- Technical support Pinellas County (W. C. Sinclair, w, Tampa)
- Water for desalting Florida Keys (F. W. Meyer, w, Miami)
- Water resources, Canal 23, 24, 25 Basins (W. L. Miller, w, Miami)
- Water resources, Clay County (C. B. Bentley, w, Jacksonville)
- Water resources, Everglades (B. G. Waller, w, Miami)
- Water resources, Lake Worth (L. F. Land, w, Miami)
- Water resources, St. Lucie County (W. L. Miller, w, Miami)
- Water supply, Temple Terrace (J. W. Stewart, w, Tampa)
- Well fields, west central Florida (E. R. Close, w, Tampa)
- Winter Haven lakes study (R. C. Reichenbaugh, w, Tampa)

Georgia, ground water, Atlanta region (C. W. Cressler, w, Doraville)**Hawaii (w, Honolulu):**

- Ground-water appraisal, Hawaii region (K. J. Takasaki)
- Honolulu basal aquifer (R. H. Dale)

Idaho:

- Water resources of the Camas Prairie (H. W. Young, w, Boise)

Indiana (w, Indianapolis):

- Decatur County (T. K. Greenman, w, Indianapolis)
- Elkhart ground water study (D. C. Gillies, w, Indianapolis)
- Ground water near Carmel (D. C. Gilles)
- Ground water, Upper West Fork of the River basin (William Meyer)
- Indianapolis hydrology (William Meyer, w, Indianapolis)
- Jennings County fracture trace (William Meyer)
- Newton County ground water (William Meyer)
- Southeast Indiana lineaments (T. K. Greeman, w, Indianapolis)
- Vincennes ground-water study (William Meyer)

Iowa (w, Iowa City):

- Cambrian-Ordovician aquifer (W. L. Steinhilber, w, Iowa City)
- Ground water, Muscatine Island (R. E. Hansen)
- Hydrology of glaciated carbonate terranes (W. L. Steinhilber)
- Pennsylvanian aquifers, coal region (J. C. Cagle, w, Iowa City)
- Water south-central Iowa (J. W. Cagle, w, Iowa City)

Kansas:

- Arbuckle Group:
 - Liquid waste (A. J. Gogel, w, Lawrence)
 - Southeastern Kansas (K. M. Keene, w, Lawrence)
- Geohydrologic maps, southwestern Kansas (E. D. Gutentag, w, Garden City)
- Geohydrology for planning in western Kansas (E. D. Gutentag, w, Garden City)
- Great Bend Prairie (S. W. Fader, w, Lawrence)
- Greeley and Wichita Counties (S. E. Slagle, w, Garden City)
- Hydrologic data base, Ground Water Management District 3 (D. H. Lobmeyer, w, Garden City)
- Sandstone aquifer, southwest Kansas (D. H. Lobmeyer, w, Garden City)

Kentucky:

- Ground water in major aquifers (R. J. Faust, w, Louisville)
- Mississippi Plateau potentiometric map (T. W. Lambert, w, Louisville)

Louisiana (w, Baton Rouge):

- Red River waterway study (J. E. Rogers, w, Alexandria)

Hydrology, ground water—Continued

States and territories—Continued

Louisiana—Continued

- Southwestern Louisiana (D. J. Nyman, w, Baton Rouge)
- Washington Parish ground water (H. L. Case)

Maine (w, Augusta):

- Androscoggin ground water (G. C. Prescott, Jr.)
- Ground water in southwestern Maine (G. C. Prescott, Jr.)

Maryland (w, Towson):

- Environmental geohydrologic studies (E. G. Otton)
- Garrett County well inventory (L. J. Nutter, w, Towson)
- Ground water resources—urbanization Harford County (L. J. Nutter, w, Towson)

Maryland Aquifer Studies III (I. J. Kantrowitz)

- Special studies—ground water (C. A. Richardson, w, Towson)

Western Montgomery County ground water study (E. G. Otton, w, Towson)

Massachusetts (w, Boston):

- Coal hydrology, Massachusetts and Rhode Island (M. H. Frimpter)

Estimating maximum ground water levels (M. H. Frimpton, w, Boston)

Ground water:

- Cape Cod (J. H. Guswa)
- Martha's Vineyard (D. F. Delaney)
- Nantucket (E. H. Walker)

Northeastern Massachusetts river basins (R. A. Brackley, w, Boston)

Water resources Blackstone River Basin (E. H. Walker, w, Boston)

Michigan:

Ground water of coal deposits, Bay County, Michigan (J. R. Stark, w, Okemos)

Water resources Marquette iron range (N. G. Grannemann, w, Okemos)

Minnesota (w, St. Paul):

Ground water:

- Big Stone County (R. J. Wolf, w, St. Paul)
- Southwestern Minnesota (D. G. Adolphson, w, St. Paul)
- Todd, Cass, Morrison Counties (D. C. Larson, w, St. Paul)

Lake Williams—water balance (D. I. Siegel, w, St. Paul)

Pelican River sand plain (D. G. Adolphson, w, St. Paul)

Reconnaissance of sand-plain aquifers (H. W. Anderson, w, St. Paul)

Twin Cities tunnel-system hydrology (E. L. Madsen)

Water resources, Buffalo River (E. L. Madsen)

Mississippi (w, Jackson):

Hydrology-Tennessee-Tombigbee (A. G. Lamonds, w, Jackson)

Water:

- Central Delta (G. J. Dalsin)
- Developing areas (J. M. Bettendorff)
- Southwest-central Mississippi (J. M. Bettendorff)

Missouri, water in southeastern Missouri lowlands (R. R. Luckey, w, Rolla)

Montana:

Geohydrologic maps, Fort Union area (J. D. Stoner, w, Billings)

Geohydrologic maps, Madison aquifer (R. D. Feltis, w, Billings)

Ground water, Swan-Avon Valleys (K. R. Wilke, w, Helena)

Mining effects, shallow water (S. E. Slagle, w, Billings)

Powder River (W. R. Miller, w, Billings)

Pumpkin Creek (J. D. Stoner, w, Billings)

Water monitoring—coal Montana (K. R. Wilke, w, Helena)

Hydrology, ground water—Continued

States and territories—Continued

Nebraska:

Butler County, Nebraska (M. H. Ginsberg, w, Lincoln)

Hydrology Platte-Loup area NE (E. G. Lappala, w, Lincoln)

Platte-Republican watershed (J. W. Goeke, w, North Platte)

Nevada (w, Carson City):

Beatty disposal site investigation (W. D. Nichols, w, Carson City)

Fort McDermitt ground water (J. R. Harrill)

Ground-water levels, Topaz Lake (J. O. Nowlin)

Pumping effects on Devil's Hole (H. L. McQueen)

Storage depletion:

Pahrump Valley (J. R. Harrill)

Well-site evaluations, Bureau of Land Management (J. R. Harrill)

New Hampshire, ground water in Lamprey River basin (J. E. Cotton, w, Concord)

New Jersey (w, Trenton):

Digital model, Potomac-Raritan-Magothy aquifer system (J. E. Luzier)

Geohydrology, east-central New Jersey (G. M. Farlekas)

Pumpage inventory (William Kam)

New Mexico (w, Albuquerque, except as otherwise noted):

Capulin ground water (D. L. Hart, w, Albuquerque)

Effects of development in northwest New Mexico (F. P. Lyford)

Elephant Butte Irrigation District well-field evaluation (C. A. Wilson, w, Las Cruces)

Geothermal hydrology, Jemez Mountains (F. W. Trainer)

Lower Rio Grande valley (C. A. Wilson)

Navajo Indian Health Service (W. L. Hiss)

Northern High Plains (E. G. Lappala)

Rio Puerco area ground water (P. F. Frenzel, w, Albuquerque)

Roswell Basin, quantitative (G. E. Welder, w, Roswell)

Sandia-Manzano Mountains (J. B. Cooper)

Water resources:

Laguna Reservation (F. P. Lyford, w, Albuquerque)

Mimbres Basin (J. S. McLean)

Santa Fe (W. A. Mourant)

Water supply, Tijeras Canyon (J. D. Hudson)

New York:

Buried-channel aquifers, Albany (R. M. Waller, w, Albany)

Geohydrology North Brookhaven, Long Island (E. J. Koszalka, w, Syosset)

Hydrogeology of Suffolk County, New York (H. M. Jensen, w, Syosset)

Hydrologic environment, Salina Group (O. J. Cosner, w, Ithaca)

North Carolina, ground water resources Cape Lookout (M. D. Winner, w, Raleigh)

North Dakota (w, Bismarck, except as otherwise noted):

Ground water:

Adams and Bowman Counties (M. B. Croft)

Bottineau-Rolette, North Dakota (M. R. Burkart, w, Bismarck)

Emmons County (C. A. Armstrong)

Griggs and Steele Counties (J. S. Downey)

Logan County (R. L. Klausung, w, Bismarck)

McHenry County (P. G. Randich)

McIntosh County (R. L. Klausung)

Ground-water availability, Fort Union coal (M. G. Croft)

Hydrology of Madison Group (D. J. Ackerman, w, Grand Forks)

Mining and reclamation, Mercer County (M. E. Crawley)

Hydrology, ground water—Continued*States and territories—Continued*

Ohio (w, Columbus):

- Dayton digital model (R. E. Fidler)
- Piketon investigation (S. E. Norris)
- Subsurface mines as source of water (J. O. Helgesen)

Oklahoma (w, Oklahoma City):

- Arbuckle aquifer (R. W. Fairchild)
- Ogallala model, Texas County (R. B. Morton)

Oregon (w, Portland):

- Bend-Redmond ground water (J. B. Gonthier, w, Portland)
- Dalles-Monmouth ground-water study (J. B. Gonthier)
- Ground water, Clackamas County (A. R. Leonard)
- Ground water, Newberg area (F. J. Frank)
- Myrtle Creek ground-water study (F. J. Frank)
- Special studies (D. D. Harris, w, Portland)
- Water resources, lower Santiam (A. R. Leonard)

Pennsylvania (w, Harrisburg, except as otherwise noted):

- Eisenhower well test (C. R. Wood, w, Harrisburg)
- Geology and ground water, Pike County (L. D. Carswell)
- Ground water, central Columbia County (O. B. Lloyd, Jr.)
- Hydrogeology:

- Erie County (G. R. Schiner, w, Meadville)
- Great Valley (A. E. Becher)

- Hydrology of Gettysburg Formation (C. R. Wood)
- Water levels and quality monitoring (W. C. Roth)

Puerto Rico:

- Ground-water appraisal, Caribbean (J. E. Heisel, w, San Juan)
- Ground water in critical areas (J. E. Heisel, w, San Juan)
- Water-resources appraisal of St. Croix, Virgin Islands (H. J. McCoy, w, Ft. Buchanan)

Rhode Island, ground water in Pawcatuck River basin (H. E. Johnston, w, Providence)

South Carolina (w, Conway, except as otherwise noted):

- Assessment of ground-water resources (A. L. Zack)
- Capacity use study (A. L. Zack)
- Ground water resources of Sumter and Florence (B. C. Spigner, w, Columbia)
- Low country capacity use study (L. R. Hayes, w, Columbia)
- Study of geohydrologic problems (A. L. Zack)

South Dakota:

- Hydrology of the Madison Group (L. W. Howells, w, Huron)
- Water resources, Walworth County (Jack Kume, w, Vermillion)

Tennessee (w, Nashville):

- Availability of water resources (D. R. Rima)
- Ground-water appraisal, Tennessee region (P. A. Zurawski)
- Ground water in the Nashville Region, Tennessee (M. S. Moran, w, Nashville)
- Memphis aquifer studies (W. S. Parks, w, Memphis)

Texas, ground water, Palo Duro Creek Basin (P. L. Rettman, w, San Antonio):

- Salt dome hydrology (phase I) (J. E. Carr, w, Houston)

Utah (w, Salt Lake City):

- Bonneville Salt Flats (G. C. Lines)
- Coal-related hydrologic data (C. T. Sumsion, w, Salt Lake City)

Hydrology:

- Tooele Valley area (A.G. Razem)
- Navajo Sandstone:
- Southwestern Utah (R. M. Cordova)
- Reconnaissance, Fish Springs Flat (E. L. Bolke, w, Salt Lake City)

Vermont, ground water in Rutland area (R. E. Willey, w, Montpelier)

Hydrology, ground water—Continued*States and territories—Continued*

Virginia, Fairfax County urban-area study (R. H. Johnson, w, Fairfax):

- Coastal plain studies (H. T. Hopkins, w, Richmond)
- Ground water resources, Blue Ridge Parkway (H. T. Hopkins, w, Richmond)
- Hydrology of James City County (H. T. Hopkins, w, Richmond)

Washington (w, Tacoma, except as otherwise noted):

- Colville, No Name Creek study (D. R. Cline)
- Port Madison study (W.E. Lum)
- Kitsap Peninsula study (A. J. Hansen, Jr.)
- Port Gamble water resources (W. E. Lum)
- Spokane ground-water quality (I. V. Tracy, w, Spokane)
- Spokane-Rathdrum prairie aquifers (B. W. Drost, w, Tacoma)

Swinomish ground water (B. W. Drost, w, Tacoma)

Water data for coal mining (F. A. Packard)

Water Yakima Reservation (J. A. Skrivan, w, Tacoma)

West Virginia (w, Charleston):

- Elk River basin study (G. T. Tarver, w, Charleston)
- Guyandotte River study (J. S. Bader)
- Migration of saltwater (J. W. Borchers)

Wisconsin (w, Madison):

- Ground water, Dodge County (R. W. Devaul)
- Hydrogeologic maps of southeastern Wisconsin (M. G. Sherrill)
- Iron River hatchery study (S. M. Hindall, w, Madison)
- Madison area digital-computer model (R. S. Mcleod, w, Madison)
- Washington-Ozaukee Counties (H. L. Young, w, Madison)
- Water resources of Forest County, Wisconsin (H. L. Young, w, Madison)

Wyoming (w, Cheyenne):

- Bighorn Basin aquifers (M. E. Cooley)
- Digital model Uva Wyoming (D. T. Hoxie, w, Cheyenne)
- Hanna basin water resources (S. J. Rucker, w, Cheyenne)
- Paleozoic hydrology, Power River basin (J. R. Marie)
- Tertiary aquifers, Laramie County (M. A. Crist)

Hydrology, surface-water:

- Evaluation of low-flow runoff (W. D. Simons, w, M)
- Hydrology defined by rainfall simulation (G. C. Lusby, w, D)
- Modeling principles (J. P. Bennett, w, NC)
- Runoff simulation (R. W. Lichty, w, NC)
- Water-quality-model development and implementation (R. A. Baltzer, w, NC)

States:

Alabama (w, Tuscaloosa)

- Environmental study, Birmingham (R. H. Bingham)
- Small-stream studies (H. H. Jeffcoat)
- Travel-time studies (H. H. Jeffcoat)

Alaska, water resources of fish sites (G. A. McCoy, Anchorage)

Arizona, Flood hydrology of Arizona (B. N. Aldridge, w, Tucson)

Arkansas (w, Little Rock):

- Arkansas basin flows (G. G. Ducret)
- Characteristics of streams (M. S. Hines)

California (w, Sacramento, except as otherwise noted):

- California lakes and reservoirs (W. L. Bradford, w, M)
- Flood hydrology, Butte Basin (R. G. Simpson)
- Lake model test (W. L. Bradford, w, M)
- Tidal River discharge computation (R. N. Oltmann)

Colorado (w, D):

- Arkansas River Compact (F. G. Cooley, w, D)

Hydrology, surface-water—Continued*States—Continued***Colorado—Continued**

- Colorado streamflow statistics (J. F. McCain)
- Jackson County, surface water (R. K. Livingston)
- Peak discharge small watershed (R. K. Livingston, w, D)

Connecticut:

- Water quality of Lake Waramang (David Grason, w, Hartford)

Delaware, Delaware River master activity (F. T. Schaefer, w, Milford, Pa.)**Florida:**

- Freshwater inflow to estuaries (C. L. Goetz, w, Tampa)
- Hillsborough River basin water supply (C. L. Goetz, w, Tampa)
- Hydrograph simulation studies (J. F. Turner, Jr., w, Tampa)
- Hydrology Area B, Sarasota County (H. R. Sutcliffe, w, Sarasota)
- Hydrology of lakes (G. H. Hughes, w, Tallahassee)
- Jumper Creek investigation (Warren Anderson, w, Orlando)
- Low flows in northwestern Florida (R. P. Rumenik, w, Tallahassee)
- Regional flood frequency study (J. F. Turner, w, Tampa)
- Small stream flood frequencies (W. C. Bridges, w, Tallahassee)
- Volusia wetlands delineation (P. W. Bush, w, Winter Park)

Georgia (w, Doraville):

- Seasonal low flow (T. R. Dyar)
- Small-area flood hydrology (H. G. Golden)
- Storage requirements for Georgia streams (R. F. Carter)

Idaho:

- Bedload in North Fork Teton River (R. P. Williams, w, Boise)

Illinois:

- Dam ratings (R. M. Bejcek, w, DeKalb)
- Illinois River miles (R. W. Healy, w, Champaign)
- T and K studies on Illinois streams (B. J. Prugh, w, Champaign)

Indiana, coal mine lakes (M. A. Hardy, w, Indianapolis)**Kansas (w, Lawrence)**

- Big Blue River Compact (E. E. Hedman, w, Lawrence)
- Channel geometry regulated streams (E. E. Lawrence)
- Flood investigations (H. R. Hepl, Jr.)
- Sediment-active geometry (w, R. Osterkamp)
- Soldier Creek (W. J. Carswell)
- Streamflow characteristics (P. R. Jordan)
- Water yield, Kansas (W. J. Carswell, w, Lawrence)

Kentucky, Green River model study (T. W. Hale, w, Louisville)**Louisiana (w, Baton Rouge):**

- Characteristics of streams (M. J. Forbes, Jr.)
- Small-stream flood frequency (A. S. Lowe)

Maine, drainage areas (D. J. Cowing, w, Augusta):

- Hydrology of selected Maine rivers (D. J. Cowing, w, Augusta)

Maryland:

- Low-flow studies in Maryland (W. J. Herb, w, Towson)

Minnesota (w, St. Paul):

- Bridge site, project reports (C. H. Carlson)
- Movement and dispersion of solutes (G. A. Payne)

Mississippi, documentation of bridge backwater (B. E. Colson, w, Jackson)**Montana (w, Helena):**

- Bridge-site investigations (R. J. Omang)
- Peak flow, small drainage areas (R. J. Omang)

Hydrology, surface-water—Continued*States—Continued***Nevada:**

- Lake Mead recreation area flood hazards (Otto Moosburner, w, Carson City)

Nevada streamflow statistics (Otto Moosburner, w, Carson City)**Topical studies—other federal agencies (F. T. Hidaka, w, Carson City)****New Jersey, base flow studies (R. D. Schopp, w, Trenton)****New Mexico, runoff from channel geometry (A. G. Scott, w, Santa Fe)****New York:**

- Acid-rain—Adirondacks (D. E. Troutman, w, Albany)
- Hudson River basin (Level B) (R. J. Archer, w, Albany)
- Low-flow study (B. B. Eissler, w, Albany)

North Carolina (w, Raleigh):

- Channelization effects, Chicod Creek (C. P. Humphreys)
- Data site information for 208 study (C. E. Simmons)
- Effect of land use on stream quality (C. E. Simmons)
- Regionalization—minimum streamflows (R. C. Heath)

Ohio (w, Columbus):

- Hydraulics of bridge sites (R. I. Mayo)
- Low flow of Ohio streams (R. I. Mayo)
- Rural hydrology (E. E. Webber, w, Columbus)
- Time-of-travel studies of Ohio streams (A. O. Westfall)

Oklahoma, coal field hydrology (J. S. Havens, w, Oklahoma City)**Oregon, Oregon lakes and reservoirs (D. D. Harris, w, Portland)****Pennsylvania (w, Harrisburg):**

- Flow routing:
 - Susquehanna River (D. L. Bingham)
- Low-flow regionalization (H. N. Flippo)
- Mean discharge—Pennsylvania (H. N. Flippo)
- Time of travel, Lehigh River (C. D. Kaufman)

Puerto Rico:

- Islandwide 208 assistance study (Fernando Gomez-Gomez, w, San Juan)

South Carolina (w, Columbia):

- Data reports, flood forecasting (C. S. Bennett)
- Low-flow characteristics (W. M. Bloxham)

South Dakota (w, Huron):

- Flood-frequency study (L. D. Becker)
- Small-stream flood frequency (L. D. Becker)

Tennessee (w, Nashville, except as otherwise noted):

- Memphis urban flood frequency (C. W. Boning, w, Memphis)
- Metro urban development alternatives (H. C. Wibben)
- Tennessee bridge scour (W. J. Randolph)
- Tennessee flow-characteristics (R. L. Gold)

Texas (w, Austin, except as otherwise noted):

- Hydrology of small drainage areas (E. E. Schroeder)
- Small watersheds (R. D. Hawkinson)
- Trinity River time-of-travel studies (R. H. Ollman, w, Fort Worth)

Utah:

- Bear River Commission (W. N. Jibson, w, Logan)
- Mined lands rehabilitation (G. W. Sandberg, w, Cedar City)

Washington (w, Tacoma):

- Low flow (P. J. Carpenter)
- Lower Elwha Project (K. L. Walters)
- Makah Project (K. L. Walters)
- Nisqually Indian Reservation study (H. E. Pearson)
- Ozette Lake study (G. C. Bortelson)

Hydrology, surface-water—Continued*States—Continued*

West Virginia, small drainage areas (G. S. Runner, w, Charleston)

Wisconsin (w, Madison):

Flood-frequency study (D. H. Conger)

Low-flow study (W. A. Gebert)

Nonpoint source pollution (S. J. Field, w, Madison)

Pheasant Branch study (R. S. Grant, w, Madison)

Water-quality control (B. K. Holstrom)

See also Evapotranspiration; Flood investigations; Marine hydrology; Plant ecology; Urbanization, hydrologic effects.

Industrial minerals. *See* specific minerals.

Iron:

Resource studies, United States (Harry Klemic, NC)

States:

Michigan, Gogebic County, western part (G. G. Schmidt, NC)

Wisconsin, Black River Falls (Harry Klemic)

Isotope and nuclear studies:

Instrument development (F. J. Jurceka, D)

Interface of isotope hydrology and hydrogeology (I. J. Winograd, w, NC)

Isotope fractionation (T. B. Coplen II, w, NC)

Isotope ratios in rocks and minerals (Irving Friedman, D)

Isotopes in hydrology (C. T. Rightmire, w, NC)

Isotopic hydrology (F. J. Pearson, w, NC)

Lead isotopes and ore deposits (R. E. Zartman, D)

Mass spectrometry and isotopic measurements (J. S. Stacey, D)

Nuclear irradiation (G. M. Bunker, D)

Radioisotope dilution (L. P. Greenland, NC)

Reactor facility (G. P. Kraker, Jr., w, D.)

Stable isotopes and ore genesis (R. O. Rye, D)

Upper mantle studies (Mitsunobu Tatsumoto, D)

See also Geochronological investigations; Geochemistry, water; Radioactive-waste disposal.

Land resources analysis:

Idaho, eastern Snake River Plain region (S. S. Oriol, D)

Land subsidence:

Geothermal subsidence research (B. E. Lofgren, w, Sacramento, Calif.)

Land subsidence studies (B. E. Lofgren, w, Sacramento, Calif.)

States:

Arizona, land subsidence-earth fissures (R. L. Laney, w, Phoenix)

New Mexico, land subsidence in the Known Potash Leasing Area (M. L. Millgate, c, Roswell)

Texas:

Johnson Space Center artificial recharge (Sergio Garza, w, Austin)

Texas coastal subsidence studies (R. K. Gabrysch, w, Houston)

Land use and environmental impact:

Central Atlantic Regional Ecological Test Site (CARETS) Project (R. H. Alexander, I, NC)

Comparative urban land use analysis studies (J. R. Wray, I, NC)

Demonstration land use mapping (E. R. Witmer, I, NC)

Geographic Information Retrieval and Analysis System (GIRAS) (W. B. Mitchell, I, NC)

Geographic Information Systems software development (W. B. Mitchell, I, NC)

Hazard prediction and warning, socioeconomic and land use planning implications (R. H. Alexander, I, Boulder, Colo.)

Impact of the oil and gas industry on the Louisiana coast (D. W. Davis, J. L. Place, I, NC)

Land use and environmental impact—Continued

Impact of Outer Continental Shelf development on coastal land and environmental resources (H. F. Lins, I, NC)

Land use analysis for Chattahoochee River quality assessment (J. L. Place, I, NC)

Land use and land cover:

Compilation and interpretation research (G. L. Loelkes, I, NC)

Input and output processing of cover maps and data (W. B. Mitchell, I, NC)

Map accuracy determination (R. E. Witmer, I, NC)

Mapping and data compilation (G. L. Loelkes, I, NC)

Land Use Data and Analysis Program and other geographic studies (G. L. Loelkes, R. E. Witmer, I, NC)

Land use impact on solar-terrestrial energy systems (R. W. Pease, I, NC)

Land use patterns related to selected environmental problems (J. L. Place, I, NC)

Mid-Atlantic land information and analysis study (R. H. Alexander, I, NC)

Multidisciplinary studies:

Earth-science information for decisionmakers (R. D. Brown, Jr., M)

Use of Earth-science maps in land and water planning (G. D. Robinson, M; A. M. Spieker, w, M)

Review and analysis of USGS spatial data handling (Olaf Kays, I, NC)

States:

Colorado, environmental and resource demonstration study, Front Range urban corridor (W. R. Hansen, D)

Virginia, Earth-science applications study in Fairfax County (A. J. Froelich, NC)

See also Construction and terrain problems; Urban geology; Urban hydrology.

Lead, zinc, and silver:

Lead resources of United States (C. S. Bromfield, D)

Zinc resources of the United States (Helmuth Wedow, Jr., Knoxville, Tenn.)

States:

Alaska, southwest Brooks Range (I. L. Tailleux, M)

Colorado (D):

San Juan Mountains:

Eastern, reconnaissance (W. N. Sharp)

Northwestern (F. S. Fisher)

Illinois-Kentucky district, regional structure and ore controls (D. M. Pinckney, D)

Nevada (M):

Comstock district (D. H. Whitebread)

Silver Peak Range (R. P. Ashley)

Utah, Park City district (C. S. Bromfield, D)

Limnology:

Hydrology of lakes (G. C. Bortleson, w, Tacoma, Wash.)

Impoundment water quality (D. R. Williams, w, Pittsburgh, Pa.)

Interrelations of aquatic ecology and water quality (K. V. Slack, w, M)

Oxygen cycle in streams (R. E. Rathbun, w, Bay St. Louis, Miss.)

Relation of ground water to lakes (T. C. Winter, w, D)

Water quality of impoundments (J. L. Barker, w, Harrisburg, Pa.)

States and territories:

Colorado, lake reconnaissance (D. A. Wentz, w, D)

Maine, Limnological study of lakes (D. J. Cowing, w, Boston, Mass.)

Limnology—Continued

States and territories—Continued

- Massachusetts, Hager Pond nutrient study (W. D. Silvey, w, Boston)
- Montana, limnology of Valley County lakes (R. F. Ferreira, w, Helena)
- Ohio, limnology of selected lakes (R. L. Tobin, w, Columbus)
- Pennsylvania, stream health in Chester County (B. W. Lium, w, West Chester)
- Puerto Rico (w, San Juan):
 - Quality of water:
 - Lago Carraizo (Ferdinand Quinones-Marquez)
 - Laguna Tortuguero (Ferdinand Quinones-Marquez)
 - Wisconsin, hydrology of lakes (R. W. Devaul, w, Madison)

See also Quality of water.

Lunar geology. *See* Extraterrestrial studies.

Manganese. *See* Ferro-alloy metals.

Marine geology:

- Atlantic Continental Shelf:
 - Environmental impact of petroleum exploration and production (H. J. Knebel, Woods Hole, Mass.)
 - Geophysics studies (J. C. Behrendt, Woods Hole, Mass.)
 - Magnetic chronology (E. M. Shoemaker, D. P. Elston, Flagstaff, Ariz.)
 - New England coastal zone (R. N. Oldale, Woods Hole, Mass.)
 - Site surveys (W. P. Dillon, Woods Hole, Mass.)
 - Stratigraphy (J. C. Hathaway, Woods Hole, Mass.)
 - Stratigraphy and structure (J. S. Schlee, Woods Hole Mass.)
- Caribbean and Gulf of Mexico:
 - Coastal environments (H. L. Berryhill, Corpus Christi, Tex.)
 - Estuaries (C. W. Holnes, Corpus Christi, Tex.)
 - Mississippi delta studies (L. E. Garrison, Corpus Christi, Tex.)
 - Natural resources and tectonic features (R. G. Martin, Jr., Corpus Christi, Tex.)
 - Oil migration and diagenesis of sediments (C. W. Holmes, Corpus Christi, Tex.)
 - Tectonics, Caribbean (J. E. Case, Corpus Christi, Tex.)
 - Tectonics, Gulf (L. E. Garrison, Corpus Christi, Tex.)
- Geotechnical investigations (D. A. Sangrey, D)
- Marine mineral resources, worldwide (F. H. Wang, M)
- Pacific and Arctic geochemistry of sediments (W. E. Dean, D)
- Pacific coast sedimentology (H. E. Clifton, M)
- Pacific Ocean, biostratigraphy, deep ocean (J. D. Bukry, La Jolla, Calif.)
- Pacific reef studies (J. I. Tracey, Jr., NC)
- Spanish Continental Margin (Almeria Province) (P. D. Snavely, Jr., H. G. Greene, H. F. Clifton, W. P. Dillon, J. M. Robb, M)
- Volcanic geology, Mariana and Caroline Islands (Gilbert Corwin, NC)
- World offshore oil and gas (T. H. McCulloch, Seattle, Wash.)
- States and territories:*
 - Alaska (M, except as otherwise notes):
 - Arctic coastal marine processes (Erik Reimnitz)
 - Beaufort-Chukchi Sea Continental Shelf (Arthur Grantz)
 - Beaufort Sea environment studies (P. W. Barnes)
 - Bering Sea:
 - General study (D. W. Scholl)
 - Northern:
 - Environmental geologic studies (C. H. Nelson)
 - Sea floor (C. H. Nelson)
 - Coastal environments (A. T. Ovenshine)

Marine geology—Continued

States and territories—Continued

- Alaska (M, except as otherwise noted)—Continued
 - Continental Shelf resources (D. M. Hopkins)
 - Cook Inlet (L. B. Magoon III)
 - Gulf of Alaska (B. F. Molnia)
 - Seward Peninsula, nearshore (D. M. Hopkins)
 - Tectonic history (R. E. von Huene, NC)
- California (M):
 - Borderlands:
 - Geologic framework (A. E. Roberts)
 - Southern part (G. W. Moore)
 - Continental Margin, central part (E. A. Silver)
 - La Jolla marine geology laboratory (G. W. Moore)
 - Monterey Bay (H. G. Greene)
 - San Francisco Bay:
 - General study (D. S. McCulloch)
 - Geochemistry of sediments (D. H. Peterson)
 - Oregon, land-sea transect, Newport (P. D. Snavely, Jr., M)
 - Oregon-California, black sands (H. C. Clifton, M)
 - Oregon-Washington, nearshore (P. D. Snavely, Jr., M)
 - Puerto Rico, cooperative program (J. V. A. Trumbull, Santurce)
 - Texas, barrier islands (R. E. Hunter, Corpus Christi)
- Marine hydrology:**
 - Hydrologic-oceanographic studies (F. A. Kohout, w, Woods Hole, Mass.)
- States and territories:*
 - Maryland, estuarine ecology (R. L. Cory, w, Edgewater)
 - North Carolina, flow of Chowan River (C. C. Daniel, w, Raleigh)
 - Puerto Rico, San Juan lagoons (S. R. Ellis, w, San Juan)
- See also* Hydrology, surface water; Quality of water; Geochemistry, water; Marine geology.
- Mercury:**
 - Geochemistry (A. P. Pierce, D)
 - Mercury deposits and resources (E. H. Bailey, M)
- State:*
 - California, Coast Range ultramafic rocks (E. H. Bailey, M)
- Meteorites.** *See* Extraterrestrial studies.
- Mine drainage and hydrology:**
 - Chemical models—coal hydrology (D. C. Thorstenson, w, Dallas, Tex.)
- States:*
 - Indiana (w, Indianapolis):
 - Assessment of reclaimed areas (S. E. Eikenberry)
 - Metals and buffering in mine stream (S. E. Ragone)
 - Kentucky (w, Louisville):
 - Coal-mining effects:
 - Grapevine Creek (J. E. Dysart)
 - Downstream effects of coal mining (J. E. Dysart)
 - Water from coal mines (D. S. Mull)
 - Mississippi, plan for study of lignite hydrology (G. J. Dalsin, w, Jackson)
 - Montana, East Trail Creek (W. R. Hotchkiss, w, Helena)
 - New Mexico, San Juan coal monitoring (J. D. Dewey, w, Albuquerque)
 - Pennsylvania (w, Harrisburg)
 - Coal hydrology of Big Sandy Creek (D. L. Bingham)
 - Western Middle anthracite hydrology (D. J. Growitz)
 - Utah (w, Salt Lake City):
 - Huntington coal hydrology (T. W. Danielson)
 - Ferron sandstone, Castle Valley (G. C. Lines)
 - Water monitoring—coal mining Utah (K. M. Waddell)
 - West Virginia, deep-mine collapse hydrology (W. H. Hobba, w, Charleston)

Mine drainage and hydrology—Continued*States—Continued*

Wyoming, water monitoring coal mining Wyoming (S. A. Druse, w, Cheyenne)

Mineral and fuel resources—compilations and topical studies:

Application massive sulfides, Virginia deposits (J. E. Gair, NC)

Arctic mineral-resource investigations (R. M. Chapman, M)

Basin and Range, geologic studies (F. G. Poole, D)

Colorado Plateau (R. P. Fischer, D)

Information bank, computerized (J. A. Calkins, NC)

Mineral-resource surveys:

Mineral resource estimation (W. D. Menzie, M)

Mineral resources of Precambrian rocks in St. Lawrence County, New York (C. E. Brown, NC)

Minerals for energy production (L. F. Rooney, NC)

Primitive and Wilderness Areas:

Big Frog Wilderness Study Area, Tennessee (J. E. Gair, NC)

Bob Marshall Wilderness Area, Montana (R. L. Earhart, D)

Caney Creek Wilderness, Arkansas (G. E. Erickson, NC)

Citico Creek, Tennessee (E. R. Force, NC)

Cohutta Wilderness, Georgia-Tennessee (J. E. Gair, NC)

Craggy Mountain, North Carolina (F. G. Lesure, NC)

Cranberry, West Virginia (F. G. Lesure, NC)

Elkhorn Wilderness Study Area, Montana (W. R. Greenwood, D)

Ellicott Rock Wilderness, South Carolina—North Carolina—Georgia (R. W. Luce, NC)

Flint Creek Range Study Area, Montana (G. E. Ericksen, NC)

Gates of the Mountains Wilderness Area, Montana (M. W. Reynolds, D)

Gee Creek Wilderness, Tennessee (J. E. Epstein, NC)

Glacier Bay National Monument Wilderness Area, Alaska (D. A. Brew, M)

John Muir Wilderness, California (N. K. Huber, M)

Linville Gorge Wilderness, North Carolina (J. P. D'Agostino, NC)

Otter Creek Wilderness, West Virginia (K. J. Englund, NC)

Pecos Wilderness, New Mexico (R. H. Moench, D)

Rainbow Lake, Flynn Lake, and Round Lake, Wisconsin (W. F. Cannon, NC)

Rawah Wilderness Area and nearby study areas, Colorado (R. C. Pearson, D)

Selway-Bitterroot Wilderness, Idaho and Montana (W. R. Greenwood, D)

Shining Rock Wilderness, North Carolina (F. G. Lesure, NC)

Snow Mountain Wilderness Area, California (D. Grimes, D)

Snowy Range Wilderness Study Area, Wyoming (R. S. Houston, D)

Superstition Wilderness, Arizona (D. W. Peterson, D)

Wambau Swamp, South Carolina (F. G. Lesure, NC)

Washakie Wilderness, Wyoming (J. C. Antwiler, D)

Nonmetallic deposits, mineralogy (B. M. Madsen, M)

Oil and gas resources:

Central and northern California Continental Shelf (C. W. Spencer, D)

Outer Continental Shelf (R. B. Powers, E. W. Scott, D)

Mineral and fuel resources—Continued**Oil and gas resources:**

Permian Basin (G. L. Dolton, S. E. Frezon, Keith Robinson, A. B. Coury, K. L. Varnes, D)

Petroleum potential of southern California borderland appraised (C. W. Spencer, D)

Resource analysis, economics of mineral resources (J. H. DeYoung, Jr., NC)

Wilderness Program:

Geochemical services (D. J. Grimes, D)

Geophysical services (M. F. Kane, D)

*States:***Alaska (M):**

AMRAP Program (J. E. Case)

Mineral resources (E. H. Cobb)

Southwestern Brooks Range (I. L. Tailleux)

Colorado, Summitville district, alteration study (R. E. Van Loenen, D)

Missouri, Rolla 2-degree quadrangle, mineral-resource appraisal (W. P. Pratt, D)

Nevada, igneous rocks and related ore deposits (M. L. Silberman, M)

United States:

Central States, mineral-deposit controls (A. V. Heyl, Jr., D)

Iron-resources studies (Harry Klemic, NC)

Lightweight-aggregate resources (A. L. Bush, D)

Metallogenic maps (P. W. Guild, NC)

Northeastern States, peat resources (C. C. Cameron, NC)

Southeastern States, mineral-resource surveys (R. A. Laurence, Knoxville, Tenn.)

Wisconsin, northern, mineral-resource survey (C. E. Dutton, Madison)

See also specific minerals or fuels.

Mineralogy and crystallography, experimental:

Crystal chemistry (Malcolm Ross, NC)

Crystal structure, sulfides (H. T. Evans, Jr., NC)

Electrochemistry of minerals (Motoaki Sato, NC)

Mineralogic services and research (R. C. Erd, M)

Mineralogical crystal chemistry (J. R. Clark, M)

Mineralogy of heavy metals (F. A. Hildebrand, D)

Planetary mineralogical studies (Priestley Toulmin III, NC)

Research on ore minerals (B. F. Leonard, D)

See also Geochemistry, experimental.

Minor elements:

Geochemistry (George Phair, NC)

Niobium:

Colorado, Wet Mountains (R. L. Parker, D)

Niobium and tantalum, distribution in igneous rocks (David Gottfried, NC)

Phosphoria Formation, stratigraphy and resources (R. A. Gulbrandsen, M)

Nonpegmatic lithium resources (J. D. Vine, D)

Rare-earth elements, resources and geochemistry (J. W. Adams, D)

Trace-analysis methods, research (F. N. Ward, D)

Model studies, geologic and geophysical:**Computer modeling:**

Rock-water interactions (J. L. Haas, Jr., NC)

Tectonic deformation (J. H. Dieterich, M)

Ice Ages (D. P. Adam, M)

Model studies, hydrologic:

Alluvial fan deposition (W. E. Price, w, NC)

Atchafalaya River Basin model (M. E. Jennings, w, Bay St. Louis, Miss.)

Digital model, aquifer system (A. F. Robertson, w, Tampa, Fla.)

Model studies, hydrologic

- Ground-water hydrology, strip-mining areas (J. O. Helgesen, w, Columbus, Ohio)
- Hydrodynamics of a tidal estuary (R. T. Cheng, w, M)
- Miocene aquifer study (E. T. Baker, Jr., w, Austin, Tex.)
- Modeling organic solute transport (J. B. Robertson, w, M)
- Nevada Test Site hydrologic model (D. I. Leap, w, D)
- Numerical simulation (V. C. Lai, w, NC)
- Operation models, surface-water systems (M. E. Jennings, w, Bay St. Louis, Miss.)
- Physical modeling (V. R. Schneider, w, Bay St. Louis, Miss.)
- Rainfall-runoff modeling (G. H. Leavesley, w, D)
- Runoff simulation (P. H. Carrigan, w, NC)
- Simulation of hydrogeologic systems (R. L. Cooley, w, D)
- Streamflow models (P. R., Jordan, w, Lawrence, Kans.)
- Surface-water-quality modeling (S. M. Zand, w, M)
- Systems Analysis Laboratory (I. C. James, w, NC)
- Transport in fluid flow (Akio Ogata, w, M)
- Transport in ground water (L. F. Konikow, w, D)
- Water-quality modeling (D. B. Grove, w, D)
- Watershed modeling (J. F. Turner, w, Tampa, Fla.)

States and territories:**Arizona:**

- Coconino aquifer—Apache County, Arizona (P. P. Ross, w, Phoenix)

California:

- Antelope Valley ground water model (C. B. Hutchinson, w, Laguna Niguel)
- Sacramento Valley groundwater (G. L. Bertoldi, w, Sacramento)
- Salinas ground-water model (T. J. Durbin, w, M)
- Water supply forecast evaluation (K. L. Wahl, w, M)

Colorado:

- Narrows Reservoir model (A. W. Burns, w, D)
- Rocky Mountain Arsenal DIMP contamination (S. G. Robson, w, D)
- Water management—High Plains (R. G. Borman, w, D)

Delaware, Aquifer model studies—Delaware (A. L. Hodges, Jr., w, Dover)**Florida:**

- Ground water, Ft. Lauderdale (Ellis Donsky, w, Miami)
- Hydrologic effects West-Central Florida (W. E. Wilson, w, Tampa)
- Impact phosphate mining, Mid-Peace (W. E. Wilson, w, Tampa)
- Loxahatchee River basin model (D. V. Maddy, w, Miami)
- Water resources Ft. Walton Beach area (H. Trapp, w, Tallahassee)

Georgia, Ground water models (H. B. Counts, w, Doraville)**Idaho, Rathdrum Prairie aquifer (H. R. Seitz, w, Boise)****Indiana, Logansport ground-water study (D. C. Gillies, w, Indianapolis)****Kansas, ground water-surface water, north-central Kansas (L. E. Stullken, w, Lawrence)****Maryland (w, Towson):**

- Ground water from Maryland coastal plain (W. B. Fleck)
- Small basin modelling (L. J. Nutter)

Minnesota, evaluation of quality-of-water, data for management (M. S. McBride, w, St. Paul)**Mississippi:**

- Documentation of bridge backwater (B. E. Colson, w, Jackson)
- Modeling of Tupelo ground water system (M. S. McBride, w, Jackson)
- Tennessee-Tombigbee Divide digital model (M. S. McBride, w, St. Paul)

Model studies, hydrologic—Continued**States and territories—Continued****Nebraska (w, Lincoln):**

- Irrigation districts in southwestern Nebraska (E. G. Lappala)

Willow Creek dam site (E. G. Lappala)**Nevada, Eagle Valley ground-water model (F. E. Artega, w, Carson City)****New Jersey (w, Trenton):**

- Englishtown Formation (W. D. Nichols)
- Simulation of multilayer aquifer (A. W. Harbaugh)

New York:

- Hudson River estuary flow model (W. N. Embree, w, Albany)

Hydrologic modeling, phase 2 (T. E. Reilly, w, Mineola)**Tioughnioga River ground water (O. J. Cosner, w, Albany)****Ohio, Franklin County digital model (E. J. Weiss, w, Columbus)****Oklahoma, North Canadian hydrology (R. E. Davis, w, Oklahoma City)****Pennsylvania (w, Harrisburg):****Delaware River streamflow model (J. O. Shearman)****Flow routing Chemung (J. T. Armbruster)****Flow simulation, Juniata River (J. T. Armbruster)****South Dakota, water resources of Big Sioux Valley (N. C. Koch, w, Huron)****Tennessee, Memphis ground-water model (J. V. Brahana, w, Nashville)****Utah, Hydrology of Beryl-Enterprise area (R. W. Mower, w, Salt Lake City)****Washington (w, Tacoma)****Columbia River basalt model (D. B. Sapik)****Ground water-surface water model (E. A. Prych)****Spokane drainfield study (J. A. Skrivan, w, Tacoma)****Wisconsin (w, Madison):****Digital streamflow model, Rock River (W. R. Krug)****Wisconsin River model (W. R. Krug)****Wyoming, hydrology of Sweetwater Basin (W. B. Borchert, w, Cheyenne)****Molybdenum. See Ferro-alloy metals.****Moon studies. See Extraterrestrial studies.****Nickle. See Ferro-alloy metals.****Nuclear explosions, geology:****Engineering geophysics, Nevada Test Site (R. D. Carroll, D)****Environmental effects (P. P. Orkild, D)****Geologic investigations:****Computer-stored physical properties data (J. R. Ege, D)****Nevada Test Site:****Nevada Test Site (P. P. Orkild, D)****Northern Yucca Flat and Pahute Mesa (W. D. Quinlivan, D)****Pahute Mesa and central and southern Yucca Flat (G. L. Dixon, D)****Geomechanical investigations, Nevada Test Site (J. R. Ege, D)****Nuclear explosions, hydrology:****Nuclear explosive underground engineering, hydrology (J. E. Weir, w, D)****States:****Alaska, hydrology of Amchitka Island Test Site (D. D. Gonzalez, w, D)****Nevada (w, D):****Nevada Test Site:****Central, hydrology (G. A. Dinwiddie)****Hydrology (W. W. Dudley, Jr.)****Oil shale:****Oil shale and associated minerals (J. L. Renner, c, D)**

Oil shale—Continued

- Organic geochemistry (R. E. Miller, D)
- Petrology (J. R. Dyni, D)
- Regional geochemistry (W. E. Dean, Jr., D)
- Trace elements (W. E. Dean, Jr., D)
- States:
 - Alaska, Anatumuk Pass (G. B. Shearer, c, Anchorage)
- Colorado (D):
 - Central Roan Cliffs area (W. J. Hall, D)
 - Lower Yellow Creek area (W. J. Hall)
 - Northwestern Piceance Basin (G. N. Pipiringos)
 - Piceance Creek basin:
 - East-central (R. B. O'Sullivan)
 - Experimental mining (R. P. Snyder)
 - General (J. R. Donnell)
 - Stratigraphy of the Green River Formation (R. C. Johnson, D)
- Colorado-Utah-Wyoming, geochemistry (W. E. Dean, Jr., D)
- Colorado-Wyoming, Eocene rocks (H. W. Roehler, D)
- East-Central Uinta Basin (G. N. Pipiringos, D)
- Utah (W. B. Cashion, Jr., D)

Paleobotany, systematic:

- Diatom studies (G. W. Andrews, NC)
- Floras:
 - Cenozoic:
 - Pacific Northwest (J. A. Wolfe, M)
 - Western United States and Alaska (J. A. Wolfe, M)
 - Devonian (J. M. Schopf, Columbus, Ohio)
 - Paleozoic (S. H. Mamay, NC)
- Fossil wood and general paleobotany (R. A. Scott, D)
- Modern seeds, California (J. A. Wolfe, D. P. Adam, M)
- Plant microfossils:
 - Mesozoic (R. H. Tschudy, D)
 - Paleozoic (R. M. Kossanke, D)

Paleoecology:

- Faunas, Late Pleistocene, Pacific coast (W. O. Addicott, M)
- Fish, Quaternary, California (R. Casteel, D. P. Adam)
- Foraminifera, ecology (M. R. Todd, NC)
- Ostracodes, Recent, North Atlantic (J. E. Hazel, NC)
- Paleoenvironmental studies, Miocene, Atlantic Coastal Plains (T. G. Gibson, NC)
- Pollen, Quaternary, California (D. P. Adam, M)
- Tempskya*, Southwestern United States (C. B. Read, Albuquerque, N. Mex.)
- Vertebrate faunas, Ryukyu Islands, biogeography (F. C. Whitmore, Jr., NC)

Paleontology, invertebrate, systematic:

- Brachiopods:
 - Carboniferous (Mackenzie Gordon, Jr., NC)
 - Ordovician (R. B. Neuman, NC; R. J. Ross, Jr., D)
 - Upper Paleozoic (J. T. Dutro, Jr., NC)
- Bryozoans, Ordovician (O. L. Karklins, NC)
- Cephalopods:
 - Cretaceous (D. L. Jones, M)
 - Jurassic (R. W. Imlay, NC)
 - Upper Cretaceous (W. A. Cobban, D)
 - Upper Paleozoic (Mackenzie Gordon, Jr., NC)
- Chitinozoans, Lower Paleozoic (J. M. Schopf, Columbus, Ohio)
- Conodonts, Devonian and Mississippian (C. A. Sandberg, D)
- Corals, rugose:
 - Mississippian (W. J. Sando, NC)
 - Silurian-Devonian (W. A. Oliver, Jr., NC)
- Foraminifera:
 - Fusuline and orbitoline (R. C. Douglass, NC)

Paleontology, invertebrate, systematic—Continued

- Foraminifera—Continued
 - Cenozoic (M. R. Todd, NC)
 - Cenozoic, California and Alaska (P. J. Smith, M)
 - Mississippian (B. A. Skipp, D)
 - Recent, Atlantic shelf (T. G. Gibson, NC)
- Gastropods:
 - Mesozoic (N. F. Sohl, NC)
 - Miocene-Pliocene, Atlantic coast (T. G. Gibson, NC)
 - Paleozoic (E. L. Yochelson, NC)
- Graptolites, Ordovician-Silurian (R. J. Ross, Jr., D)
- Mollusks, Cenozoic, Pacific coast (W. A. Addicott, M)
- Ostracodes:
 - Lower Paleozoic (J. M. Berdan, NC)
 - Upper Cretaceous and Tertiary (J. E. Hazel, NC)
 - Upper Paleozoic (I. G. Sohn, NC)
- Pelecypods:
 - Inoceramids (D. L. Jones, M)
 - Jurassic (R. W. Imlay, NC)
 - Paleozoic (John Pojeta, Jr., NC)
 - Triassic (N. J. Silberling, M)
- Trilobites, Ordovician (R. J. Ross, Jr., D)
- Paleontology, stratigraphic:**
 - Cenozoic:
 - Diatoms, Great Plains, nonmarine (G. W. Andrews, NC)
 - Foraminifera, smaller, Pacific Ocean and islands (M. R. Todd, NC)
 - Mollusks:
 - Atlantic coast, Miocene (T. G. Gibson, NC)
 - Pacific coast, Miocene (W. O. Addicott, M)
 - Pollen and spores, Kentucky (R. H. Tschudy, D)
 - Vertebrates:
 - Atlantic coast (F. C. Whitmore, Jr., NC)
 - Pacific coast (C. A. Repenning, M)
 - Panama Canal Zone (F. C. Whitmore, Jr., NC)
 - Pleistocene (G. E. Lewis, D)
 - Mesozoic:
 - Pacific coast and Alaska (D. L. Jones, M)
 - Cretaceous:
 - Alaska (D. L. Jones, M)
 - Foraminifera:
 - Alaska (H. R. Bergquist, NC)
 - Atlantic and Gulf Coastal Plains (H. R. Bergquist, NC)
 - Pacific coast (R. L. Pierce, M)
 - Gulf Coast and Caribbean (N. F. Sohl, NC)
 - Molluscan faunas, Caribbean (N. F. Sohl, NC)
 - Western interior United States (W. A. Cobban, D)
 - Jurassic, North America (R. W. Imlay, NC)
 - Triassic, marine faunas and stratigraphy (N. J. Silberling, M)
 - Paleozoic:
 - Devonian and Mississippian conodonts, Western United States (C. A. Sandberg, D)
 - Fusuline Foraminifera, Nevada (R. C. Douglass, NC)
 - Mississippian:
 - Stratigraphy and brachiopods, northern Rocky Mountains and Alaska (J. T. Dutro, Jr., NC)
 - Stratigraphy and corals, northern Rocky Mountains (W. J. Sando, NC)
 - Mississippian biostratigraphy, Alaska (A. K. Armstrong, M)
 - Onesquethaw Stage (Devonian), stratigraphy and rugose corals (W. A. Oliver, NC)

Paleontology, stratigraphic—Continued

Paleozoic—Continued

Ordovician:

- Bryozoans, Kentucky (O. L. Karklins, NC)
- Stratigraphy and brachiopods, Eastern United States (R. B. Neuman, NC) Western United States (R. J. Roxx, Jr., D)

Paleobotany and coal studies Antartica (J. M. Schopf, Columbus, Ohio)

Palynology of cores from Naval Petroleum Reserve No. 4 (R. A. Scott, D)

Pennsylvanian:

Fusulinidae:

- Alaska (R. C. Douglass, NC)
- North-central Texas (D. A. Myers, D)

Spores and pollen, Kentucky (R. M. Kosanke, D)

Permian, floras, Southwestern United States (S. H. Mamay, NC)

Silurian-Devonian:

Corals, northeastern United States (W. A. Oliver, Jr., NC)

Upper Silurian-Lower Devonian, Eastern United States (J. M. Berdan, NC)

Subsurface rocks, Florida (J. M. Berdan, NC)

Upper Paleozoic, Western States (Mackenzie Gordon, Jr., NC)

Paleontology, vertebrate, systematic:

- Artiodactyls, primitive (F. C. Whitmore, Jr., NC)
- Pinnipedia (C. A. Repenning, M)
- Pleistocene fauna, Big Bone Lick, Kentucky (F. C. Whitmore, Jr., NC)
- Tritylodonts, American (G. E. Lewis, D)

Paleotectonic maps. See Regional studies and compilations.

Petroleum and natural gas:

- Automatic data-processing system for field and reservoir estimates (K. A. Yenne, c, Los Angeles, Calif.)
- Borehole gravimetry, application to oil exploration (J. W. Schnoker, D)
- Catagenesis of organic matter and generation of petroleum (N. H. Bostick, D)
- Devonian black shale, Appalachian Basin:
 - Borehole gravity study (J. W. Schnoker, D)
 - Clay mineralogy (J. W. Hosterman, NC)
 - Conodont maturation (A. G. Harris, NC)
 - Data storage and retrieval system
 - Geochemical study (G. E. Claypool, D)
 - Stratigraphy (J. B. Roen, NC)
 - Structural studies (L. D. Harris, NC)
 - Uranium and trace-element study (J. S. Leventhal, D)
- Gulf of Mexico, oil and gas resources of the Gulf of Mexico (B. M. Miller, D)
- Methods of recovery (F. W. Stead, D)
- Oil and gas map, North America (W. W. Mallory, D)
- Oil and gas resource appraisal methodology and procedures (B. M. Miller, D)
- Organic geochemistry (J. G. Palacas, D)
- Origin and distribution of natural gases (D. D. Rice, D)
- Origin, migration, and accumulation of petroleum (L. C. Price, D)
- Petroleum prospecting with helium detector (A. A. Roberts, D)
- Rocky Mountain States, seismic detection of stratigraphic traps (R. T. Ryder, D)
- Tight gas sands (D. D. Rice, D)
- Western Interior Cretaceous studies (C. W. Spencer, D)
- Western United States:
 - Devonian and Mississippian (C. A. Sandberg, D)

Petroleum and natural gas—Continued

Western United States—Continued

Devonian and Mississippian flysch source-rock studies (F. G. Poole, D)

- Properties of reservoir rocks (R. F. Mast, D)
- Source rocks of Permian age (E. K. Maughan, D)

States:

Alaska (M):

- Cook Inlet (L. B. Magoon III)
- North Slope, petroleum geology (R. D. Carter)
- NPRA (National Petroleum Reserve Alaska) Oil and Gas Source Rock Study (L. B. Magoon III, M)

California:

- Carpenteria and Hondo-Santa Ynez field reserves, OCS (D. G. Griggs, c, Los Angeles)
- Eastern Los Angeles basin (T. H. McCulloh, Seattle, Wash.)
- Salinas Valley (D. L. Durham, M)
- Southern San Joaquin Valley, subsurface geology (J. C. Maher, M)

Colorado (c, D, except as otherwise noted):

- Citadel Plateau (G. A. Izett)
- Denver Basin, Tertiary coal zone and associated Strata (P. A. Soister)
- Grand Junction °-degree quadrangle (W. B. Cashion, Jr., D)
- Piceance Creek basin—low permeability gas sands (R. C. Johnson, D)
- Savery quadrangle (C. S. V. Barclay)

New Mexico, San Juan Basin (E. R. Landis, D)

Utah (c, D, except as otherwise noted):

- Canaan Peak quadrangle (W. E. Bowers)
- Collet Top quadrangle (H. D. Zeller)
- Grand Junction 2-degree quadrangle (W. B. Cashion, Jr., D)

Wyoming:

- Browns Hill quadrangle (C. S. V. Barclay, c, D)
- Lander area phosphate reserve (W. L. Rohrer, c, D)
- Pine Mountain-Oil Mountain area (G. J. Kerns, c, Casper)
- Reid Canyon quadrangle (G. J. Kerns, c, Casper)
- Savery quadrangle (C. S. V. Barclay, c, D)
- Square Top Butte quadrangle (W. H. Laraway, c, Casper)
- Stratigraphy, lower Upper Cretaceous formations (E. A. Merewether, D)

Wyoming-Montana-North Dakota-South Dakota, Williston Basin (C. A. Sandberg, D)

Petrology. See Geochemistry and petrology, field studies.

Phosphate:

Phosphoria Formation, stratigraphy and resources (R. A. Gulbrandsen, M)

States:

Alaska, Anatumuk Pass (c, Anchorage)

Idaho:

- Palisades Dam quadrangle (D. A. Jobin, c, D)
- Phosphate resources (Peter Oberlindacher, c, M)

Montana, Melrose phosphate field (G. D. Fraser, c, D)

Nevada:

Spruce Mountain 4 quadrangle (G. D. Fraser, c, D)

United States, southeastern phosphate resources (J. B. Cathcart, D)

Utah:

- Crawford Mountains (W. C. Gere, c, M)
- Ogden 4 NW quadrangle (R. J. Hite, c, D)

Wyoming:

- Crawford Mountains phosphate deposits (W. C. Gere, c, M)
- Pickle Pass quadrangle (M. L. Schroeder, c, D)
- Pine Creek quadrangle (M. L. Schroeder, c, D)

Plant ecology:**Element availability:**

Soils (R. C. Severson, D)

Vegetation (L. P. Gough, D)

Periodic plant-growth phenomena and hydrology (R. L. Phipps, w, NC)

Vegetation and hydrology (R. S. Sigafos, w, NC)

Western coal regions, geochemical survey of vegetation (J. A. Erdinan, D)

See also Evapotranspiration; Geochronological investigations; Limnology.**Platinum:**

Mineralogy and occurrence (G. A. Desborough, D)

States:

Montana, Stillwater complex (N. J. Page, M)

Wyoming, Medicine Bow Mountains (M. E. McCallum, Fort Collins, Colo.)

Potash:

Arizona, Patagonia area (J. A. Crowley, c, M)

Colorado and Utah, Paradox basin (O. B. Raup, D)

Nevada, alunite (J. A. Crowley, c, M)

New Mexico, Carlsbad, potash and other saline deposits (C. L. Jones, M)

Primitive areas. *See* under Mineral and fuel resources—compilations and topical studies, mineral-resource surveys.**Public and industrial water supplies.** *See* Quality of water; Water resources.**Quality of water:**

Atlanta Central Lab atomic absorption (F. E. King, w, Doraville, Ga.)

Atlanta Central Lab automated methods (A. C. Beam, w, Doraville, Ga.)

Atlanta Central Lab—logistical support (D. K. Leifeste, w, Doraville, Ga.)

Atlanta Central Lab—manual methods (E. R. Anthony, w, Doraville, Ga.)

Atlanta Central Lab—organic analyses (L. E. Lowe, w, Doraville)

Atlanta Central Lab—special methods (D. K. Leifeste, w, Doraville, Ga.)

Adsorption process models (J. D. Hem, w, M)

Bedload samplers (D. W. Hubbell, w, D)

Benchmark network (R. R. Pickering, w, NC)

Central Laboratories (W. A. Beetem, w, NC)

Chemistry of New Zealand waters (I. K. Barnes, w, M)

Data evaluation support (R. E. Gust, w, Arvada, Colo.)

Denver Central Lab—atomic absorption (D. B. Manigold, w, D)

Denver Central Lab—automated methods (V. C. Marti, w, D)

Denver Central Lab—biological analyses (S. A. Dunca, w, D)

Denver Central Lab—logistical support (R. E. Gust, w, D)

Denver Central Lab—manual methods (S. A. Duncan, w, D)

Denver Central Lab—organic analyses (D. B. Manigold, w, D)

Denver Central Lab—physical properties (R. L. McAvoy, w, D)

Denver Central Lab—radiochemical analyses (S. A. Duncan, w, D)

Denver Central Lab—special methods (R. L. McAvoy, w, D)

Denver Central Laboratory (R. L. McAvoy, w, D)

Development of biological methods (B. W. Lium, w, Atlanta, Ga.)

Quality of water—Continued

Development of water methods (B. A. Malo, w, D)

Geochemical kinetics studies (H. C. Claassen, w, D)

Geochemistry, Western coal region (G. L. Feder, w, D)

Heat transfer (H. E. Jobson, w, Bay St. Louis, Miss.)

Hydrology of central Nevada (G. A. Dinwiddie, w, D)

Improvement of QW data system (D. A. Goolsby, w, NC)

Instrumentation, petrochemical (W. A. Beetem, w, NC)

Laboratory evaluation (V. J. Janzer, w, D)

Methods coordination (M. W. Skougstad, w, D)

Methods development (W. A. Beetem, w, NC)

Methods development support (D. K. Leifeste, w, Doraville, Ga.)

Methods for organics (W. E. Pereira, w, D)

Methods for pesticides (T. R. Steinheimer, w, D)

Methods for trace metals (H. E. Taylor, w, D)

Modeling mineral-water reactions (L. N. Plummer, w, NC)

Natural water quality (D. A. Rickert, w, Portland, Ore.)

Nevada Test Site geochemistry (A. F. White, w, D)

Nevada Test Site tracer studies (D. I. Leap, w, D)

Nevada Test Site waste management (G. A. Dinwiddie, w, D)

Nuclear hydrology services (W. W. Dudley, w, D)

Organic deep waste storage (R. L. Malcolm, w, D)

Organic substances in streams (R. E. Rathbun, w, Bay St. Louis, Miss.)

Organics in oil-shade residues (J. A. Leenheer, w, D)

Organics in water (D. F. Goerlitz, w, M)

Pesticide monitoring network (R. J. Pickering, w, NC)

Potomac Estuary studies (J. P. Bennett, w, NC)

Precipitation quality network (R. J. Pickering, w, NC)

Quality assurance (W. A. Beetem, w, NC)

Quality assurance (L. J. Schroder, w, D)

Quality assurance procedures (L. C. Friedman, w, D)

Radioanalytical methods (L. L. Thatcher, w, D)

Radiochemical network (R. J. Pickering, w, NC)

Radiochemical Techniques of Water Resources Investigations (V. J. Janzer, w, D)

Radiohydrology of explosion sites (D. D. Gonzalez, w, D)

Radionuclide migration at Nevada Test Site (W. W. Dudley, w, D)

Radionuclides on sediments (D. D. Gonzalez, w, D)

River-water quality and land use (D. J. Lystrom, w, Portland, Ore.)

Standard reference water sample program (M. J. Fishman, w, D)

Stream-temperature patterns (E. J. Pluhowski, w, NC)

Temperature modeling in natural streams (A. P. Jackman, w, M)

Thermal pollution (G. E. Harbeck, Jr., w, D)

Toxic substances in aquatic ecosystems (H. V. Leland, w, M)

Trace-element availability in sediments (S. N. Luoma, w, M)

Transport in ground water (L. F. Konikow, w, D)

Transuranium research (J. M. Cleveland, w, D)

Water-quality-data evaluation (W. H. Doyle, Jr., w, D)

States and territories:**Alabama:**

Water problems in coal-mine areas (Celso Puente, w, University)

Water resources in oil fields (W. J. Powell, w, Tuscaloosa)

Arkansas (w, Little Rock):

Soil Conservation Service watershed studies (T. E. Lamb)

Waste-assimilation capacity (C. T. Bryant)

California:

Colorado River salinity (D. T. Hartley, w, Laguna Niguel)

Hydrology, Sagehen Creek (R. G. Simpson, w, Sacramento)

Quality of water—Continued

States and territories—Continued

California—Continued

- Merced River water quality (R. J. Hoffman, w, Sacramento)
- New River water quality (J. G. Setmire, w, Laguna Niguel)
- Nitrate and nitrogen isotope study (J. M. Klein, w, Laguna Niguel)
- Quality of water, California streams (W. L. Bradford, w, M)
- San Francisco Bay urban study (R. D. Brown, M)
- Santa Barbara ground water (C. B. Hutchinson, w, Laguna Niguel)
- Thermograph network evaluation (J. T. Limerinos, w, M)
- Water resources Upper Coachella (L. A. Swain, w, Laguna Niguel)

Colorado (w, D, except as otherwise noted):

- Aquatic biology of Piceance Creek (K. J. Covay, w, Meeker)
- Effects of feedlots on ground water (S. G. Robson)
- Effects of sludge basins on ground water (S. G. Robson)
- Northwestern Colorado water quality (T. R. Ford, w, Meeker)
- Quality of water characteristics of Colorado streams (M. W. Gaydos)
- Quality of water in metal-mine drainage (D. A. Wentz)
- Quality of water in underground coal mines (R. E. Moran)
- Yampa Valley ground-water reconnaissance (W. E. Hofstra)

Connecticut, changes in ground-water quality (E. H. Handman, w, Hartford)

Florida:

- Dade storm-water quality (H. C. Mattraw, w, Miami)
- Drainage wells Orlando area (C. H. Tibbals, w, Orlando)
- Environmental studies, statewide (G. A. Irwin, w, Tallahassee)
- Ground-water quality, Dade County (Howard Klein, w, Miami)
- Lakes Faith, Hope, and Charity (A. G. Lamonds, Jr., w, Orlando)
- Radionuclides in ground water (Horace Sutcliffe, Jr., w, Sarasota)
- Subsurface waste storage (G. L. Faulkner, w, Tallahassee)
- Water quality:
 - Broward County (C. B. Sherwood, Jr., w, Miami)
 - South New River Channel (B. G. Waller, w, Miami)

Georgia (w, Doraville):

- Colonels Island test well (H. E. Gill)
- Ground water irrigation southwest Georgia (R. G. Grantham)
- Storm runoff, greater Atlanta area (J. B. McConnell)
- Stream quality southwest Georgia, agriculture area (J. B. McConnell)

Hawaii, surface-water-quality monitoring network (J. S. Yee, w, Honolulu)

Idaho (w, Boise):

- Ground-water-quality assessment (H. R. Seitz)
- Ground water—quality of water monitoring (R. L. Whitehead)

Illinois (w, Champaign):

- Sludge irrigation hydrology (R. F. Fuentes)
- Strip mine hydrology (T. P. Brabets, w, Champaign)

Indiana (w, Indianapolis):

- Ground water, Indiana dunes (W. G. Weist)
- Landfill monitoring, Marion County (J. R. Marie)
- Watershed water quality (S. E. Ragone, w, Indianapolis)

Quality of water—Continued

States and territories—Continued

Iowa:

- Water quality Iowa coal region (W. C. Steinkampf, w, Iowa City)

Kansas (w, Lawrence):

- Contamination of Equus beds (J. M. McNellis, w, Lawrence)
- Enhanced oil recovery, Kansas (D. G. Jorgensen, w, Lawrence)

- Ground-water-quality network evaluations (A. M. Diaz)
- Quality of water in mined areas in southeast (A. M. Diaz)
- Saline discharge, Smoky Hill River (J. B. Gillespie)
- South Fork, Ninnescah River basin (A. M. Diaz)

Kentucky, effects of coal mining, Kentucky River (K. L. Dyer, w, Louisville)

Louisiana (w, Baton Rouge):

- Pollution capacity of streams (R. F. Martien)

Quality of water:

- Lower Mississippi River (F. C. Wells)

Maine:

- Hydrology of Salmon Lake (D. J. Cowing, w, Augusta)
- Public inquiries (R. C. Wagner, w, Augusta)

Massachusetts:

- Impact of Otis Air Force Base waste disposal (D. R. LeBlanc, w, Boston)

- Lake Cochituate nutrients (F. B. Gay, w, Boston)

Massachusetts:

- Water quality management (M. H. Frimpter, w, Boston)

Minnesota:

- Water quality of highway runoff (M. R. Have, w, St. Paul)
- Ground-water quality network (M. F. Hult, w, St. Paul)
- Karst well hydraulics (M. F. Hult, w, St. Paul)

Mississippi:

- Tennessee-Tombigbee Divide quality-of-water monitoring (C. H. Tate, w, Jackson)

Missouri:

- Prosperity water quality (J. H. Barks, w, Rolla)

Montana:

- Environmental impact statement, Youngs Creek Mine (C. W. Lane, w, D)

- Ground water Poplar basin (R. D. Feltis, w, Billings)

- Thermal study—Madison River (A. J. Boettcher, w, Helena)

Nebraska:

- Analysis surface-water quality data (R. A. Engberg, w, Lincoln)

- Ground-water quality (R. A. Engberg, w, Lincoln)

Nevada (w, Carson City):

- Ground-water contamination by explosives wastes (A. S. Van Denburgh)

- Ground-water-quality monitoring network (J. O. Nowlin)

- Pond seepage, Weed Heights (A. S. Van Denburgh)

- Topical quality-of-water studies (J. P. Monis)

New Hampshire:

- Effects of waste disposal—Peace Air Force Base (Edward Bradley, w, Augusta)

- Eutrophication, Lake Winnisquam (W. D. Silvey, w, Concord)

- Public inquiries (J. V. Skinner, w, Concord)

New Jersey, waste-water reclamation (William Kam, w, Trenton)

New Mexico:

- Malaga Bend evaluation (J. L. Kunkler, w, Santa Fe)

- Quality-of-water monitor in Chaco River basin (Kim Ong, w, Albuquerque)

Quality of water—Continued*States and territories—Continued***New Mexico—Continued**

San Juan River valley (F. P. Lyford, w, Albuquerque)

New York (w, Albany):

Biology of landfill leaching (T. A. Ehlke)

Drilling beneath trenches, W. Valley (A. D. Randall, w, Albany)

Ground-water pollution, Olean (A. D. Randall, w, Albany)

PCB transport in the Upper Hudson (R. J. Archer, w, Albany)

Sediment nutrient dynamics (J. T. Turk)

Transport of heavy metals at Waterford (J. T. Turk)

Westchester County waste management (R. J. Archer)

North Carolina:

Chemical quality atmospheric deposition (R. C. Heath, w, Raleigh)

Effects of channelizing Black River (C. E. Simmons, w, Raleigh)

North Dakota, mining effects, Gascoyne area (M. G. Croft, w, Bismarck)

Ohio (w, Columbus):

Acid-mine drainage characterization (C. G. Angelo)

Miscellaneous water resources studies (R. V. Swisshelm, w, Columbus)

Rattlesnake Creek water quality (K. F. Evans)

Oklahoma (w, Oklahoma City):

Coal hydrology eastern Oklahoma (M. V. Marcher, w, Oklahoma City)

Saltwater infiltration (J. J. D'Lugosz)

Zinc mine water quality (J. D. Stoner)

Oregon (w, Portland):

GOES water-data system (G. L. Gallino)

Portland:

Harbor study (S. W. McKenzie)

Water-quality study (S. W. McKenzie)

Stream quality in Oregon (T. L. Miller, w, Portland)

Pennsylvania (w, Harrisburg):

Anthraxite mine discharge (D. J. Growitz)

Ground-water quality in Pennsylvania (H. E. Koester)

Nonpoint sources Pequea Creek basin (D. A. Eckhardt)

Pennsylvania Gazetteer of streams Part II (L. C. Shaw)

Stream conditions—Chester County, Pennsylvania (K. P. Kulp, w, Philadelphia)

Water quality—Blue Marsh Lake (J. L. Barker)

Water quality in Tioga River basin (J. R. Ward)

Puerto Rico (w, Fort Buchanan):

Effects of oil spillage on ground water (H. L. McCoy, w, San Juan)

Ground water reaction to refinery effluent (R. Diaz, w, San Juan)

Solid-waste study (Fernando Gomez-Gomez)

Rhode Island, public inquiries (H. E. Johnston, w, Providence)

South Carolina (w, Columbia):

Fluoride in ground water, coastal plain (J. M. Rhett)

Savannah River plant (D. I. Cahal)

Tennessee:

Burial-ground studies at Oak Ridge National Laboratory (D. A. Webster, w, Knoxville)

Pesticide migration study (Craig Sprinkle, w, Nashville)

Texas, Colorado River salinity (Jack Rawson, w, Austin)

Utah (w, Salt Lake City):

Reconnaissance of Utah coal fields (K. M. Waddell)

Surface-water quality:

Dirty Devil River basin (J. C. Mundorff)

Quality of water—Continued*States and territories—Continued***Utah (w, Salt Lake City)—Continued**

Water quality San Rafael River basin (J. C. Mundorff)

Vermont, public inquiries (R. E. Willey, w, Montpelier)

Virginia (w, Richmond):

Quality of ground water (S. M. Rogers)

Watershed water quality (S. M. Rogers)

Washington (w, Tacoma):

Columbia basin demonstration project (P. R. Boucher)

Ground-water-quality network (M. O. Fretwell)

Lake Wilderness nutrients (N. P. Dion)

Spokane ground water quality (J. B. Tracey)

Sulphur Creek program P. R. Boucher)

West Virginia, effects of deep mining (J. L. Chisolm, w, Charleston)

Wisconsin (w, Madison):

Ground-water quality, Waukesha County (M. G. Sherrill)

Irrigation and ground-water quality (S. M. Hondall)

Nederlo Creek biota (P. A. Kammerer, Jr.)

Stream reeration (R. S. Grant)

Wyoming (w, Cheyenne):

Herbicides North Platte Wyoming (H. R. Schuetz)

North Platte reservoirs (S. J. Rucker IV)

See also Geochemistry; Hydrologic instrumentation; Hydrology, surface water; Limnology; Marine hydrology; Sedimentology; Water resources.

Quicksilver. *See Mercury.*

Radioactive materials, transport in water. *See Geochemistry, water.*

Radioactive-waste disposal:

Hydrology of nuclear landfill (A. D. Randall, w, Albany, N.Y.)

Hydrology of salt domes (R. L. Hosman, w, Baton Rouge, La.)

Implications of long-term climate changes (D. P. Adam)

National Overview Atlas (J. P. Ohl, D)

Pierre Shale (G. W. Shurr, D)

Radioactive byproducts in salt (J. W. Mercer, w, Albuquerque, N. Mex.)

Radioactive-waste burial (George Debuchananne, w, NC)

Radioactive-waste-burial study (J. M. Cahill, w, Columbia, S.C.)

Radiohydrology technical coordination (George Debuchananne, w, NC)

Sheffield site investigation (J. B. Foster, w, Champaign, Ill.)

Waste-disposal sites (L. A. Wood, w, NC)

Waste emplacement crystalline rocks in conterminous United States (H. W. Smedes, D)

States:

Idaho, National Reactor Testing Station, hydrology of subsurface waste disposal (J. T. Barraclough, w, Idaho Falls)

Kentucky, Maxey Flats investigation (H. H. Zehner, w, Louisville)

New Mexico (D):

Eddy and Lea counties, exploratory drilling (C. L. Jones)

Southeastern, waste emplacement (C. L. Jones)

Utah (D):

Paradox Basin (L. M. Gard)

Salt Valley anticline (L. M. Gard)

See also Geochemistry, water.

Rare-earth metals. *See Minor elements.*

Regional studies and compilations, large areas of the United States:

Basement rock map (R. W. Bayley, M)

Characterization of crystalline rock terrane (H. W. Smedes and D. J. Gable, D)

Paleotectonic map folios:

Devonian System (E. G. Sable, D)

Regional studies and compilations, large areas of the United States
—Continued

Paleotectonic map folios—Continued

- Mississippian System (L. C. Craig, D)
- Pennsylvanian System (E. D. McKee, D)
- Physiography of Southeastern United States (J. T. Hack, NC)
- Volcanic rocks of the Appalachians (D. W. Rankin, NC)

Remote sensing:

Geologic applications:

Airborne and satellite research:

- Aeromagnetic studies (M. F. Kane, D)
- Development of an automatic analog earthquake processor (J. P. Eaton, M)
- Electromagnetic research (F. C. Frischknecht, D)
- Fraunhofer line discriminator studies (R. D. Watson, D)
- Gamma-ray research (J. S. Duyal, D)
- Geochemical plant stress (F. C. Canney, D)
- Geothermal resources (Kenneth Watson, D)
- Infrared surveillance of volcanoes (J. D. Freidman, D)
- Interpretation studies (R. H. Henderson, NC)
- National aeromagnetic survey (J. R. Henderson, D)
- Remote-sensing geophysics (Kenneth Watson, D)
- Satellite magnetometry (R. D. Regan, NC)
- Surficial and thematic mapping (T. N. V. Karlstrom, Flagstaff, Ariz.)
- Urban geologic studies (T. W. Offield, D)
- Volcanic gas monitoring (Motoaki Sato, NC)

High-resolution film recording system (George Harris, I, Sioux Falls, S. Dak.)

Landsat experiments:

- Analysis of porphyry copper prospects from Landsat digital data (R. G. Schmidt, NC)
- Evaluation of Great Plains area (R. B. Morrison, D)
- Experimental digital enhancement of Landsat images and CCT's (George Harris, I, Sioux Falls, S. Dak.)
- Geologic mapping, South America (W. D. Carter, I, NC)
- Geological and geophysical remote sensing of Iceland (R. S. Williams, Jr., I, NC)
- Geostructures of the continental crust (E. H. Lathram, M)
- Iron-absorption band for the discrimination of iron-rich zones (L. C. Rowan, NC)
- Linear features of the conterminous United States (W. D. Carter, I, NC)
- Luminescence studies (R. D. Watson, I, Flagstaff, Ariz.)
- Morphology, provenance, and movement of desert and seas in Africa, Asia, and Australia (E. D. McKee, D)
- Optimum Landsat spectral bands (G. L. Raines, D)
- Prototype volcano surveillance network (J. P. Eaton, M)
- Structural, volcanic, glaciologic, and vegetation mapping, Iceland (R. S. Williams, Jr., I, NC)
- Study of multispectral imagery, northwestern Saudi Arabia (A. J. Bodenlos, NC)
- Suspended particulate matter in nearshore surface waters, northeast Pacific Ocean and the Hawaiian Islands (P. R. Carlson, M)
- Synthetic stereo in Landsat imagery (Gordon Swann, Flagstaff, Ariz.)
- Targeting of mineral exploration effort (J. V. Taranik, I, in Sioux Falls, S. Dak.)
- Tectonic and mineral-resource investigations, Andes Mountains, South America (W. D. Carter, I, NC)

Remote sensing —Continued

Geologic applications—Continued

Landsat experiments—Continued

- Thermal surveillance of active volcanoes (J. D. Friedman, NC)

Skylab/EREP studies:

- Evaluation of Great Plains area (R. B. Morrison, D)
- Marine and coastal processes on the Puerto Rico-Virgin Islands Platform (J. V. A. Trumbull, Santurce, P. R.)

- Remote-sensing geophysics (Kenneth Watson, D)

Skylab/visual observations:

- Desert sand seas (E. D. McKee, D; C. S. Breed, Flagstaff, Ariz.)
- Volcanologic features (J. D. Friedman, D)
- Time-lapse satellite data for monitoring dynamic hydrologic phenomena (Morris Deutsch, S. Serebreny, I, NC)

States:

Alaska (M):

- Beaufort Sea, inner shelf and coastal sedimentation environment (Erk Reimnitz)
- Remote sensing of permafrost and geologic hazards (O. J. Ferrians, Jr.)

Arizona:

- Arizona Regional Ecological Test Site:
 - North-central (D. P. Elston, Flagstaff)
 - Post-1890A. D. episode erosion (R. B. Morrison, D)
- Basin and Range-Colorado Plateau boundary investigation (D. P. Elston, Ivo Lucchitta, Flagstaff)

- Colorado, effects of atmosphere on multispectral mapping of rock types by computer, Cripple Creek-Canon City (H. W. Sinedes, D)

- Colorado-Wyoming, analysis of Cortez-Uinta mineralized areas from Landsat digital data (L. C. Rowan, NC)

- New Mexico, analysis of Landsat images of Claunch and vicinity (W. A. Fischer, I, NC)

- Texas, monitoring changing geologic features, Texas Gulf Coast (R. B. Hunter, Corpus Christi)

Hydrologic applications:

- Aircraft and spacecraft observations of Arctic sea ice (W. J. Campbell, w, Tacoma, Wash.)

- Antartic sea-ice model (W. J. Campbell, w, Tacoma, Wash.)

- Application of hydrometeorological model to Sierra Nevada (L. A. Rasinussen, W. V. Tangborn, w, Tacoma, Wash.)

- Arctic Ice Dynamics Joint Experiment (W. J. Campbell, w, Tacoma, Wash.)

- Flood and flood-plain analysis (J. V. Taranik, I, Sioux Falls, S. Dak.)

High Plains Cooperative Program:

- Cloud-formation monitoring (G. A. Thorley, A. M. Kahan, I, NC)

- Meteorological-parameter monitoring with Landsat DCS (G. S. Thorley, A. M. Kahan, I, NC)

- Method of correcting distortion in SLAR imagery due to curvature of flight path (C. H. Ling, L. A. Rasinussen, W. J. Campbell, w, Tacoma, Wash.)

- Microwave remote sensing (G. K. Moore, w, Bay St. Louis, Miss.)

- Optical and computer processing and interpretation techniques for Landsat hydrologic and environmental applications (Morris Deutch, I, NC)

- Polar-ice remote sensing (W. J. Campbell, w, Tacoma, Wash.)

Remote sensing—Continued**Hydrologic applications—Continued**

Remote sensing, wetlands (V. P. Carter, w, NC)

Remote-sensing techniques (E. J. Pluhowski, w, NC)

States:

Alaska, meteor burst telemetry (R. D. Lamke, w, Anchorage)

Arizona (w, Phoenix):

Arizona Test Site (H. H. Schumann)

Snow-cover mapping (H. H. Schumann)

Connecticut, Connecticut River estuary (F. H. Ruggles, Jr., w, Hartford)

Florida, southern, Landsat (A. L. Higer, w, Miami)

Kansas, mined land hydrology, southeast Kansas (A. M. Diaz, w, Lawrence)

Pennsylvania, GOES, Juniata basin (C. D. Kauffman, w, Harrisburg)

South Dakota, hydrologic remote sensing (G. K. Moore, w, Sioux Falls)

Tennessee, Landsat digital processing of Duncan Flats quadrangle (A. L. Higer, A. E. Coker, w, Miami, Fla.)

Image processing technology:

Experimental digital enhancement of Landsat images and computer-compatible tapes (George Harris, Jr., I, Sioux Falls, S. Dak.)

High-resolution film recording system (George Harris, Jr., I, Sioux Falls, S. Dak.)

Land-resource applications:

Agricultural inventory demonstration project (W. H. Anderson, I, Sioux Falls, S. Dak.)

Applications of Landsat imagery to land systems mapping, Australia (C. J. Robinove, I, NC)

CARETS, a prototype regional environmental information system (R. H. Alexander, I, NC)

Colorado River natural resources and land use data inventory (G. A. Thorley, R. L. Hansen, I, NC)

Development of automatic techniques for land use mapping from remote-sensor data (J. R. Wray, I, NC)

Forest defoliation mapping and drainage assessment (W. G. Rohde, Technicolor Graphics, Inc.)

Forest land classification and assessment of forest succession (W. G. Rohde, Technicolor Graphics, Inc.)

Impact of strip mining on range resources and wildlife habitat (D. M. Carneggie, I, Sioux Falls, S. Dak.)

Investigation of remote-sensing techniques to assess agricultural drainage (G. A. Thorley, W. A. Lidester, I, NC)

Land systems mapping with digital Landsat data (C. J. Robinove, I, NC)

Landsat imagery for aiding objectives of the IFYGL (Morris Deutsch, A. Falconer, I, NC)

Multispectral crop canopy radiance measurement using Landsat DCS platforms (G. A. Thorley, H. D. Newkirk, I, NC)

Pacific Northwest Demonstration Project (D. R. Hood, I, Sioux Falls, S. Dak.)

Skylab/EREP investigation, census cities (J. R. Wray, I, NC)

Urban and regional land use analysis, CARETS and census cities experiment (R. H. Alexander, I, NC)

States:

Oregon-Washington, inventorying and mapping kelp and eelgrass on the coasts using Landsat digital data (G. A. Thorley, R. O. Weaver, I, NC)

South Dakota, Cooperative Land Use Demonstration Project (D. R. Hood, I, Sioux Falls)

Reservoirs. See Evapotranspiration; Sedimentology.**Resource and land investigations:**

Council of State Governments, communication of data needs (J. T. O'Connor, I, NC)

Designation of critical environmental areas (J. T. O'Connor, I, NC)

Environmental planning and Western coal development (E. T. Smith, I, NC)

Implementing critical resource area programs (E. A. Imhoff, I, NC)

Methodology for siting onshore facilities associated with OCS development in the New England region (W.W. Doyel, I, NC)

Mined-area reclamation and related land use planning (E. A. Imhoff, I, NC)

National Environmental Indicators report (E. T. Smith, I, NC)

State land inventory systems (Olaf Kays, I, NC)

State programs on wild, scenic, and recreational rivers (M. L. Pattison, I, NC)

States:

California, Redwoods National Park (J. T. O'Connor, I, NC)

Washington, Colville Indian Reservation, case study on land use planning (E. T. Smith, I, NC)

Rhenium. See Minor elements; Ferro-alloy metals.**Saline minerals:**

Mineralogy (B. M. Madsen, M)

States:

Colorado and Utah, Paradox Basin (O. B. Raup, D)

New Mexico, Carlsbad potash and other saline deposits (C. L. Jones, M)

Wyoming, Sweetwater County, Green River Formation (W. C. Culbertson, D)

Saltwater intrusion. See Marine hydrology; Quality of water.**Sedimentology:**

Arctic fluvial processes, landforms (K. M. Scott, w, Laguna Niguel, Calif.)

Bedload-transport research (W. W. Emmett, w, D)

Channel morphology (L. B. Leopold, w, Berkeley, Calif.)

Coon Creek morphology (S. W. Trimble, w, Los Angeles, Calif.)

Estuarine intertidal environments (J. L. Glenn, w, D)

Measurement of sediment-laden flows (A. G. Scott, w, NC)

Petrology Laboratory (L. G. Schultz, D)

Sediment-hillside morphology (G. P. William, w, D)

Sediment movement in rivers (R. H. Meade, Jr., w, D)

Sediment transport phenomena (D. W. Hubbell, w, D)

Transport processes (C. F. Nordin, w, D)

States:

Alabama, hydrology of Warrior coal field (Celso Puento, w, University)

Alaska, coastal environments (A. T. Ovenshine, M)

Arizona, sediment—Paria River, Lees Ferry (W. B. Garrett, w, Tucson)

California (w, M):

San Francisco Bay, circulation (T. J. Conomos)

Sediment, Feather River (George Porterfield)

Hawaii, peak flow-sediment discharge relations (B. L. Jones, w, Honolulu)

Idaho, Snake and Clearwater Rivers, sediment (W. W. Emmet w, D)

Kansas (w, Lawrence)

Estimation of sediment yield (P. R. Jordan)

Fluvial sediment in northeastern Kansas (C. D. Albert)

Sediment and geometry of channels (W. R. Osterkamp)

Kentucky, sediment yields (W. F. Curtis, w, Pikesville)

Maryland, Trap efficiency—Rock Creek (W. J. Herb, w, Towson)

Sedimentology—Continued

States—Continued

Minnesota, red clay sediment and quality-of-water evaluation (E. G. Giacomini, w, St. Paul)

North Carolina, sediment study (C. E. Simmons, w, Raleigh)

North Dakota, water monitoring—coal mining, North Dakota (W. E. Harkness, w, Bismarck)

Pennsylvania (w, Harrisburg):

Highway erosion-control measures (L. A. Reed)

Predicting sediment flow (L. A. Reed)

Study of cobble bed streams (J. R. Ritter)

Tennessee, hydrologic study, coal mining study, New River (R. S. Parker, w, Nashville)

Washington (w, Tacoma):

May Creek sediment study (W. L. Haushild)

Quileute project (M. O. Fretwell)

Sediment characteristics (L. M. Nelson)

Wisconsin (w, Madisom):

Nemadji River sediment study (S. M. Hindall)

Red clay sedimentation (S. M. Hindall)

White River reservoir study (S. M. Hindall)

See also Geochemistry, water; Geochronological investigations; Hydraulics, surface flow; Hydrologic data collection and processing; Stratigraphy and sedimentation; Urbanization, hydrologic effects.

Selenium. *See* Minor elements.

Silver. *See* Heavy metals; Lead, zinc, and silver.

Soil moisture:

Grazing exclusion, effects on soil moisture (G. C. Lusby, w, D)

Infiltration and drainage (Jacob Rubin, w, M)

Snow hydrology (W. W. Embree, w, Albany N.Y.)

Vegetation changes, effects on soil moisture (C. C. Lusby, w, D)

See also Evapotranspiration.

Spectroscopy:

Mobile spectrographic laboratory (D. J. Grimes, D)

Spectrographic analytical services and research (A. W. Helz, NC; A. T. Meyers, D; Harry Bastron, M)

X-ray spectroscopy (H. J. Rose, Jr., NC; Harry Bastron, M)

Stratigraphy and sedimentation:

Antler flysch, Western United States (F. G. Poole, D)

East Coast Continental Shelf and margin (R. H. Meade, Jr., Woods Hole, Mass.)

Middle and late Tertiary history, Northern Rocky Mountains and Great Plains (N. M. Denson, D)

Pennsylvania System stratotype section (G. H. Wood, Jr., NC)

Permian, Western United States (E. K. Maughan, D)

Phosphoria Formation, stratigraphy and resources (R. A. Gulbrandsen, M)

Rocky Mountains and Great Basin, Devonian and Mississippian conodont biostratigraphy (C. A. Sandberg, D)

Sedimentary structures, model studies (E. D. McKee, D)

Tight gas sands (D. D. Rice, D)

States:

Alabama-Florida, stratigraphy (J. A. Miller, w, Tallahassee, Fla.)

Alaska, Cretaceous (D. L. Jones, M)

Arizona:

Hermit and Supai Formations (E. D. McKee, D)

Magnetic chronology, Colorado Plateau and environs (D. P. Elston, E. M. Shoemaker, Flagstaff)

Arizona-New Mexico, paleomagnetic correlation, Colorado Plateau (D. J. Strobell, Flagstaff, Ariz.)

California, southern San Joaquin Valley, subsurface geology (J. C. Maher, M)

Stratigraphy and sedimentation—Continued

States—Continued

Colorado, Upper Triassic and marine Jurassic stratigraphy (G. N. Pippingos, D)

Louisiana, Continental Shelf (H. L. Berryhill, Jr., Corpus Christi, Tex.)

Montana, Ruby Range, Paleozoic rocks (E. T. Ruppel, D)

Montana - North Dakota - South Dakota - Wyoming, Williston basin (C. A. Sandberg, D)

Nebraska, central Nebraska basin (G. E. Prichard, D)

Nevada, Indian Trail Formation, abandonment of name (G. L. Dixon, D)

New Mexico, western and adjacent areas, Cretaceous stratigraphy (E. R. Landis, D)

Oregon-California (M):

Black sands:

Geologic investigations (H. E. Clifton)

Hydrologic investigations (P. D. Snavelly, Jr.)

Utah:

Promontory Point (R. B. Morrison, D)

Upper Triassic and marine Jurassic stratigraphy (G. N. Pippingos, D)

Wyoming (D):

Lanmont-Baroil area (M. W. Reynolds)

Upper Triassic and marine Jurassic stratigraphy (G. N. Pippingos, D)

See also Paleontology, stratigraphic; *specific areas under* Geologic mapping.

Structural geology and tectonics:

Contemporary coastal deformation (R. O. Castle, M)

Rock behavior at high temperature and pressure (E. C. Robertson, NC)

Structural studies, Basin and Range (F. G. Poole, D)

States:

Arizona, southeastern tectonics (Harold Drewes, D)

California-Nevada, transcurrent fault analysis, western Great Basin (R. E. Anderson, D)

Nevada, central, east-trending lineaments (G. L. Dixon, D)

See also specific areas under Geologic mapping.

Talc:

New York, Pope Mills and Richville quadrangles (C. E. Brown, NC)

Tantalum. *See* Minor elements.

Thorium:

Analytical support (C. M. Bunker, D)

Investigations of thorium in igneous rocks (M. H. Staatz, D)

States:

Colorado (D):

Cochetopa area (J. C. Olson)

Wet Mountains, thorium resources appraisal (T. J. Armbrustmacher)

Wyoming, Bear Lodge Mountains (M. H. Staatz, D)

Tungsten. *See* Ferro-alloy metals.

Uranium:

Exploration techniques:

Geochemical techniques (R. A. Cadigan, D)

Geochemical techniques of halo uranium (J. K. Otton, D)

Morrison Formation (L. C. Craig, D)

Uranium in streams as an exploration technique (K. J. Wenrich-Verbeek, D)

Genesis of tabular uranium deposits on the Colorado Plateau (R. A. Brooks, D)

Hydrogeochemistry of uranium deposits (C. G. Bowles, D)

Ore-forming processes (H. C. Granger, D)

Uranium—Continued

- Paleomagnetism applied to uranium exploration (R. L. Reynolds, D)
- Petrophysics (G. R. Olhoeft, D)
- Precambrian sedimentary and metasedimentary rocks (F. A. Hills, D)
- Radium and other isotopic disintegration products in springs and subsurface water (R. A. Cadigan, J. K. Felmlee, D)
- Resources of radioactive minerals (A. P. Butler, Jr., D)
- Resources of United States and world (W. I. Finch, D)
- Southern High Plains (W. I. Finch, D)
- United States:
 - Eastern:
 - Appalachian Basin Paleozoic rocks (A. F. Jacob, D)
 - Basin analysis as related to uranium potential in Triassic sedimentary rocks (C. E. Turner, D)
 - Uranium vein deposits (R. I. Grauch, D)
 - Southwestern, basin analysis related to uranium potential in Permian rocks (J. A. Campbell, D)
 - Western:
 - Relation of diagenesis and uranium deposits (M. B. Goldhaber, D)
 - Vein and disseminated deposits of uranium (J. T. Nash, D)
- Uranium daughter products in modern decaying plant remains, in soils, and in stream sediments (K. J. Wenrich-Verbeek, D)
- Volcanic source rocks (R. A. Zielinski, D)
- States:
 - Arizona-Colorado-New Mexico-Utah (D);
 - Colorado Plateau:
 - Basin analysis of uranium-bearing Jurassic rocks (Fred Peterson)
 - Tabular deposits (R. A. Brooks)
 - Arizona-Nevada-Utah, uranium potential of Basin and Range province (J. E. Peterson, D)
 - Colorado (D):
 - Cochetopa Creek uranium-thorium area (J. C. Olson)
 - Colorado Plateau (Summary) Report (R. P. Fischer)
 - Marshall Pass uranium (J. C. Olson)
 - Schwartzwalder mine (E. J. Young)
 - Uranium-bearing Triassic rocks (R. D. Lupe)
 - Colorado-New Mexico-Texas-Utah-Wyoming, organic chemistry of uranium (J. S. Leventhal, D)
 - New Mexico (D):
 - Acoma area (C. H. Maxwell)
 - Church Rock-Smith Lake (C. T. Pierson)
 - Crownpoint uranium studies (J. F. Robertson)
 - North Church Rock (A. R. Kirk)
 - San Juan Basin uranium (M. W. Green)
 - Sanostee (A. C. Huffman, Jr.)
 - Thoreau uranium studies, New Mexico (J. F. Robertson)
 - South Dakota-Wyoming, uranium-bearing pipes (C. G. Bowles, D)
 - Texas:
 - Coastal Plain, geophysical and geological studies (D. H. Eargle, Austin)
 - Tilden-Loma Alta area (K. A. Dickinson, D)
 - Uranium disequilibrium studies (F. E. Senftle, NC)
 - Texas-Wyoming, roll-type deposits (E. N. Harshman, D)
 - Utah-Colorado (D):
 - Moab quadrangle (A. P. Butler, Jr.)
 - Uinta and Piceance Creek basin (L. C. Craig)
 - Washington (D), midnite uranium mine (J. T. Nash)

Uranium—Continued*States—Continued***Wyoming (D):**

- Badwater Creek (R. E. Thaden)
- Crooks Peak quadrangle (L. J. Schmitt, Jr.)
- Granite as a source rock of uranium (J. S. Stuckless)
- Northeastern Great Divide Basin (L. J. Schmitt, Jr.)
- Powder River basin (E. S. Santos)
- Sagebrush Park quadrangle (L. J. Schmitt, Jr.)
- Stratigraphic analysis of Tertiary uranium basins of Wyoming (D. A. Seeland)
- Stratigraphic analysis of Western Interior Cretaceous uranium basins (H. W. Dodge, Jr.)

Urban geology:**Alaska (D):**

- Anchorage area (Ernest Dobrovolny)
- Juneau area (R. D. Miller)
- Sitka area (L. A. Yehle)
- Small coastal communities (R. W. Lemke)
- Arizona, Phoenix-Tucson region resources (T. G. Theodore, M)
- California (M, except as otherwise noted):
 - Coastal geologic processes (K. R. Lajoie)
 - Flatlands materials and their land use significance (E. J. Helley)
 - Geologic factors in open space (R. M. Gulliver)
 - Hillside materials and their land use significance (C. M. Wentworth, Jr.)
 - Malibu Beach and Topanga quadrangles (R. F. Yerkes)
 - Quaternary framework for earthquake studies, Los Angeles Basin (J. C. Tinsley III)
 - Regional slope stability (T. H. Nilsen)
- San Francisco Bay region, environment and resources planning study:
 - Bedrock geology (M. C. Blake)
 - Marine geology (D. S. McCulloch)
 - Open space (C. S. Danielson)
- San Andreas fault:
 - Basement studies (D. C. Ross)
 - Basin studies (J. A. Bartow)
 - Regional framework (E. E. Brabb)
 - Tectonic framework (R. D. Brown)
- San Mateo County cooperative (H. D. Gower)
- Sargent-Berrolca fault zone (R. J. McLaughlin, D. H. Sorg)
- Seismicity and ground motion (W. B. Joyner)

Southern:

- Eastern part (D. M. Morton, Riverside)
- Western part (R. F. Yerkes)

Oregon (w, Portland):

- Bear Creek water-quality study (S. W. McKenzie)
- Portland rainfall-runoff study (Antonius Laenen)

Pennsylvania (w, Harrisburg):

- Philadelphia (T. G. Ross)
- Storm-water measurements (T. G. Ross)

South Carolina, hydraulic-site reports (B. H. Whetstone, w, Columbia)**Texas (w, Fort Worth, except as otherwise noted):**

- Austin (M. L. Maderak, w, Austin)
- Dallas County urban study (B. B. Hampton)
- Dallas urban study (B. B. Hampton)
- Fort Worth urban study (R. M. Slade, Jr.)
- Houston urban study (E. L. Johnson, w, Houston)
- San Antonio urban study (R. D. Steger, w, San Antonio)

Washington, Puget Sound urban-area studies (B. L. Foxworthy, w, Tacoma)

Urban geology—Continued

Wisconsin, simulation of urban runoff (R. S. Grant, w, Madison)

Urban hydrology:

Geohydrology, urban planning (H. G. O'Connor, w, Lawrence, Kans.)

Urban-area reconnaissance (W. E. Hale, w, Albuquerque, N. Mex.)

Urban runoff networks (H. H. Barnes, Jr., w, NC)

Urban sedimentology (H. P. Guy, w, NC)

States:

Alabama, Jefferson County floodway evaluation (R. H. Bingham, w, Tuscaloosa)

Alaska:

Anchorage geohydrology (C. Zenone, w, Anchorage)

Arizona, Tucson-Phoenix urban-area pilot study (E. S. Davidson, w, Tucson)

California:

Morphology, San Francisquito (J. R. Crippen, w, M)

Perris Valley (M. W. Busby, w, Laguna Niguel)

Poway Valley (M. W. Busby, w, Laguna Niguel)

Colorado:

Climatological atlases, Colorado Front Range urban corridor (W. R. Hansen, D)

Flood frequency, urban areas (R. K. Livingston, w, D)

Front Range urban corridor (D. E. Hilher, w, D)

Storm runoff quality, Denver (S. R. Ellis, w, D)

Connecticut, Connecticut Valley urban pilot study (R. L. Melvin, w, Hartford)

Florida:

Bay Lake area (A. L. Putnam, w, Orlando)

Riviera Beach investigations (A. L. Knight, w, Miami)

Storm water quality south Florida (H. C. Matraw, w, Miami)

Tampa Bay region (G. E. Seaburn, w, Tampa)

Hawaii, hydrology, sediment in Mauna Loa (C. J. Ewart, w, Honolulu)

Illinois, quality-of-water monitoring, Bloomington-Normal (B. J. Prugh, Jr., w, Champaign)

Indiana:

Indianapolis Water Company canal study (William Meyer, w, Indianapolis)

Iowa, flow models, Walnut Creek (O. G. Lara, w, Iowa City)

Kansas, urban runoff, Wichita (D. B. Richards, w, Lawrence)

Kentucky (w, Louisville):

Hydraulics of bridge sites (C. H. Hannum)

Northern Kentucky urban hydrology (R. W. Davis, w, Louisville)

Water use and availability (D. C. Griffin)

Maryland:

Rock Creek—Anacostia River (T. H. Yorke, w, Towson)

Mississippi, bridge-site investigations (K. V. Wilson, w, Jackson)

Missouri, stream hydrology, St. Louis (T. W. Alexander, w, Rolla)

New Mexico, urban flood hydrology, Albuquerque (A. G. Scott, w, Santa Fe)

North Carolina, urban hydrology, Charlotte (W. H. Eddins, w, Raleigh)

Ohio (R. P. Hawkinson, w, Columbus)

Oregon (w, Portland):

Bear Creek water-quality study (S. W. McKenzie)

Portland rainfall-runoff study (Antonius Laenen)

Pennsylvania (w, Harrisburg):

Philadelphia (T. G. Ross)

Storm-water measurements (T. G. Ross)

Urban hydrology—Continued**States—Continued**

South Carolina, hydraulic-site reports (B. H. Whetstone, w, Columbia)

Tennessee:

Effects of urbanization on floods and quality of water (F. N. Lee, w, Nashville)

Texas (w, Fort Worth, except as otherwise noted):

Austin (M. L. Maderak, w, Austin)

Dallas County urban study (B. B. Hampton)

Dallas urban study (B. B. Hampton)

Fort Worth urban study (R. M. Slade, Jr.)

Houston urban study (S. L. Johnson, w, Houston)

San Antonio urban study (R. D. Steger, w, San Antonio)

Washington:

Bellevue urban runoff study (W. L. Haushild, w, Tacoma)

Puget Sound urban-area studies (B. L. Foxworthy, w, Tacoma)

Wisconsin, simulation of urban runoff (R. S. Grant, w, Madison)

Urbanization, hydrologic effects:

North Carolina, effect on flood flow, Charlotte area (W. H. Eddins, w, Raleigh)

Vegetation:**Element availability:**

Soils (R. C. Severson, D)

Vegetation (L. P. Gough, D)

Elements in organic-rich material (F. N. Ward, D)

Plant geochemistry, urban areas (H. A. Tourtelot, D)

Western coal regions, geochemical survey of vegetation (J. A. Erdman, D)

See also Plant ecology.

Volcanic-terrane hydrology. See Artificial recharge.**Volcanology:**

Caldron and ash-flow studies (R. L. Smith, NC)

Cascade volcanoes, geodimeter studies (D. A. Swanson, M)

Columbia River basalt (D. A. Swanson, M)

Regional volcanology (R. L. Smith, NC)

Volcanic-ash chronology (R. E. Wilcox, D)

Volcanic hazards (D. R. Crandell, D)

States:

Arizona, San Francisco volcanic field (J. F. McCauley, M)

Hawaii:

Hawaiian Volcano Observatory (Hawaii National Park)

Seismic studies (P. L. Ward, M)

Submarine volcanic rocks (J. G. Moore, M)

Idaho (D):

Central Snake River Plain, volcanic petrology (H. E. Malde)

Eastern Snake River Plain region (M. A. Kuntz, H. R. Covington)

Montana, Wolf Creek area, petrology (R. G. Schmidt, NC)

New Mexico, Valles Mountains, petrology (R. L. Smith, NC)

Wyoming, deposition of volcanic ash in the Mowry Shale and Frontier Formation (G. P. Eaton, D)

Colorado (D):

Denver-Front Range urban corridor, remote sensing (T. W. Offield)

Denver metropolitan area (R. M. Lindvall)

Denver mountain soils (P. W. Schmidt)

Denver urban area, regional geochemistry (H. A. Tourtelot)

Denver urban-area study:

Geologic maps:

Boulder-Fort Collins-Greeley area (R. B. Colton)

Volcanology—Continued*States—Continued***Colorado—Continued**

Denver urban-area study—Continued

Geologic maps—Continued

Colorado Springs-Castle Rock area (W. R. Hansen)
Greater Denver area (D. E. Trimble)

Land-use classification, Colorado Front Range urban
corridor (W. R. Hansen, L. B. Driscoll)

Engineering geology mapping research, Denver region
(H. E. Simpson)

Terrain mapping from Skylab data (H. W. Smedes)

Maryland, Baltimore-Washington urban-area study (J. T. Hack,
NC)

Massachusetts, Boston and vicinity (C. A. Kaye, Boston)

Montana, geology for planning, Helena region (R. G. Schmidt,
NC)

New Mexico, geology of urban development (H. E. Malde, D)

Pennsylvania (NC, except as otherwise noted):

Coal-mining features, Allegheny County (W. E. Davies)

Geochemistry of Pittsburgh urban area (H. A. Tourtelot, D)

Susceptibility to landsliding:

Allegheny County (J. S. Pomeroy)

Beaver, Butler, and Washington Counties (J. S.
Pomeroy)

Utah, Salt Lake City and vicinity (Richard VanHorn, D)

Virginia, geohydrologic mapping of Fairfax County (A. J.
Froelich, NC)

Water budget:

Hydrologic reconnaissance, West-Central Utah (J. S. Gates,
w, Salt Lake City, Utah)

Hydrology of Dismal Swamp (P. E. Ward, w, NC)

Water budget Eagle Lake (D. I. Siegel, w, St. Paul, Minn.)

*States:***Minnesota:**

Water budget of Shagawa Lake (D. W. Ericson, w, Grand
Rapids)

Water resources:

Central Region field coordination (J. F. Blakey, w, D)

CENTO working group on hydrogeology (J. R. Jones, w, NC)

Chattahoochee intensive river quality (R. N. Cherry, w,
Atlanta, Ga.)

Columbia-North Pacific ground water (B. L. Foxworthy, w,
Tacoma, Wash.)

Comprehensive studies, Pacific Northwest (L. E. Newcomb,
w, M)

Dams, weirs, and flumes (H. J. Tracy, w, Atlanta, Ga.)

Data coordination, acquisition, and storage:

NAWDEX Project (M. D. Edwards, w, NC)

Water Data Coordination (R. H. Langford, w, NC)

East Triassic waste-disposal study (G. L. Bain, w, Raleigh, NC)

Effects of vegetation changes (G. C. Lusby, w, D)

Environmental impact analysis support (G. H. Davis, w, NC)

Environmental impact statement, Idaho phosphate (W. J.
Schneider, w, Pocatello, Idaho)

Evaluation of land treatment (R. F. Hadley, w, D)

Foreign assistance:

PL 80-402 (J. R. Jones, w, NC)

Section 607 (J. R. Jones, w, NC)

Foreign countries:

Canada, gas pipeline (V. K. Berwick, w, Anchorage, Alaska)

India, ground-water investigations in states of Madhya
Pradesh, Gujarat, Maharashtra, and Mysore (J. R.
Jones, w, NC)

Kenya, range water resources (N. E. McClymonds, w,
Nairobi)

Water resources—Continued**Foreign countries—Continued**

Nepal, hydrogeology of Tera region (G. C. Tibbitts, Jr., w,
Katmandu)

Saudi Arabia:

Saudi Arabian advisory services (J. T. Callahan, w, NC)

Source of Riyadh water supply (J. R. Jones, w, NC)

Yemen, northern, water and mineral survey (J. R. Jones,
w, NC)

General hydrologic research (R. L. Nace, w, Raleigh, NC)

Ground water, Missouri Basin (O. J. Taylor, w, D)

Ground-water appraisal, New England region (Allen Sinnott, w,
Trenton, NJ)

Infiltration and drainage (Jacob Rubin, w, M)

Intensive river-quality assessment (D. A. Rickert, w, Portland,
Oreg.)

Intermediate-depth drilling (L. C. Dutcher, w, M)

Monitoring design, coal regions (H. H. Hudson, w, D)

Modeling principles (J. P. Bennett, w, NC)

Network design (M. E. Moss, w, NC)

Northeastern Region field coordination (J. W. Geurin, w, NC)

Northwest water-resources data center (N. A. Kallio, w, Port-
land, Oreg.)

Polaris Operations (T. T. Conomos, w, M)

Powell arid lands centennial (R. F. Hadley, w, D)

Quality-of-water accounting network (R. J. Pickering, w, NC)

Rating extensions (K. L. Wahl, w, NC)

Rehabilitation potential, energy lands (L. M. Shown, w, D)

Reservoir bank storage study (T. H. Thompson, w, M)

Southeastern Region field coordination (C. L. Holt, w, Atlanta,
Ga.)

State aid, miscellaneous (J. R. Jones, w, NC)

Water-resource activities (J. R. Carter, w, D)

Waterway treaty engineering studies (J. A. Bettendorf, w, NC)

Western Region field coordination (G. L. Bodhaine, w, M)

Yellowstone level B study (H. H. Hudson, w, D)

States and territories:

Alabama:

Drainage areas (J. C. Scott, w, Montgomery)

Low flows of Alabama streams (R. H. Bingham, w,
Tuscaloosa)

Plans, reports, and information (W. J. Powell, w, Tusca-
loosa)

Alaska (w, Anchorage, except as otherwise noted):

Arctic resources (J. M. Childers)

Coal resources study (D. R. Scully)

Collection of basic records analysis (D. R. Lanke, w,
Anchorage)

Hydrologic environment of the trans-Alaska pipeline
system (TAPS)(J. M. Childers)

Municipal water supply (G. S. Anderson)

North Slope study (G. L. Nelson, w, Fairbanks)

North Star project (G. L. Nelson, w, Fairbanks)

TAPS construction hydrology (C. E. Sloan)

Water resources of national petroleum reserves (C. E.
Sloan, w, Anchorage)

Arizona:

Black Mesa hydrologic study (R. M. Myrick, w, Tucson)

Black Mesa monitoring program (G. W. Levings, w,
Flagstaff)

Channel loss study (T. W. Anderson, w, Phoenix)

Coconino Sandstone water budget, Navajo County (L. J.
Mann, w, Flagstaff)

Copper Basin study (B. W. Thomsen, w, Phoenix)

Water resources—Continued

States and territories—Continued

Arizona—Continued

- Ground-water appraisal, Lower Colorado River (E. S. Davidson, w, Tucson)
- Sedona ground-water availability (G. W. Levings, w, Flagstaff)
- Verde Valley water resources (G. W. Levings, w, Flagstaff)
- Water resources of the Papago Reservation (L. J. Mann, w, Tucson)

Arkansas (w, Little Rock):

- Arkansas-Oklahoma Compact (R. T. Sniegocki, w, Little Rock)
- Bayo Bartholomew systems study (M. E. Broom)
- Cache River aquifer-stream system (M. E. Broom)
- Characteristics of streams (M. S. Hines)
- Investigations and hydrologic information (R. T. Sniegocki)
- Lignite hydrology (J. E. Reed, w, Little Rock)
- Time-of-travel study (T. E. Lamb)

California:

- Delta isotope study (W. L. Bradford, w, M)
- Ground water:
 - Death Valley (C. E. Lamb, w, Laguna Niguel)
 - Joshua Tree (D. J. Downing, w, Laguna Niguel)
 - Madera area, ground-water model (W. D. Nichols, w, Sacramento)
 - Santa Cruz (K. S. Muir, w, M)
 - Southern California (C. E. Lamb, w, Laguna Niguel)
- Indian reservations (C. E. Lamb, w, M)
- Power plant siting—Desert basins (J. H. Koehler, w, Laguna Niguel)
- Quality of water:
 - Ground-water quality, Suisun Bay (Chabot Kilburn, w, M)
 - Lakes and reservoirs (R. C. Averett, w, M)
 - Trace-metals control, Sacramento (R. F. Ferreira, w, Sacramento)
- San Antonio Creek ground water appraisal (C. B. Hutchinson, w, Laguna Niguel)
- Surface water:
 - Floods, small drainage areas (A. O. Waananen, w, M)
 - Sediment, Redwoods National Park (J. M. Knott, w, M)
 - Urbanization, Santa Clara County (J. M. Knott, w, M)
- Water resources California desert (J. H. Koehler, w, Laguna Niguel)

Colorado (w, D, except as otherwise noted):

- Areawide water-quality inventory (L. J. Britton)
- Coal rehabilitation (G. H. Leavesley)
- Ground water:
 - High Plains of Colorado (R. G. Borman)
 - Potentiometric surface mapping (F. A. Welder)
 - Southern Ute lands (R. E. Brogden)
 - Southwestern Colorado (R. E. Brogden)
 - U.S. Bureau of Mines prototype mine (J. B. Weeks)
- Hydrology:
 - El Paso County (R. E. Fidler, w, Pueblo)
 - Naval Oil Shale Reserve No. 1 (G. H. Leavesley)
 - Parachute-Roan Creek Basin (G. H. Leavesley)
 - San Luis Valley (R. E. Fidler, w, Pueblo)
 - South Platte River basin, Henderson to State line (R. T. Hurr)

Quality of water:

- Boulder County (D. C. Hall)
- Geochemical investigations (S. G. Robson)
- Hydrology of Jefferson County (D. C. Hall)

Water resources—Continued

States and territories—Continued

Colorado—Continued

Quality of water—Continued

- Sediment yield, Piceance Basin (V. C. Norman)
- Spring hydraulics (G. J. Saulnier)
- Water monitoring—coal mining Colorado (J. R. Little, w, D)
- Water resources, Park-Teller County (K. E. Goddard, w, Pueblo)
- Yampa River basin assessment (T. D. Steele)

Connecticut (w, Hartford):

- Hydrogeology, south-central Connecticut (R. L. Melvin)
- Integrated hydrologic network (R. L. Melvin, w, Hartford)
- Part 7, Upper Connecticut River basin (R. B. Ryder)
- Part 9, Farmington River basin (F. P. Haeni)
- Part 10, Lower Connecticut River basin (L. A. Weiss)
- Short-term studies (C. E. Thomas, Jr.)

Delaware, aquifer-model studies (R. H. Johnston, w, Dover)

Florida:

- Annual hydrologic report, southwestern Florida (K. W. Causseaux, w, Tampa)
- Broward County (C. B. Sherwood, Jr., w, Miami)
- Caloosahatchee River study (T. H. O'Donnell, w, Ft. Myers)
- East Boundary area investigation (B. G. Waller, w, Miami)
- Ground water:
 - Aquifer mapping, south Florida (Howard Klein, w, Miami)
 - Coastal springs (W. C. Sinclair, w, Miami)
 - Hallandale area (H. W. Bearden, w, Miami)
 - Hollywood area (H. W. Bearden, w, Miami)
 - Hydrogeology, middle Peace basin (W. E. Wilson III, w, Tampa)
 - Hydrology, Manatee County (D. P. Brown, w, Sarasota)
 - Ochlockonee River basin investigation (C. A. Pascale, w, Tallahassee)
 - Potentiometric surface St. Petersburg-Tampa (C. B. Hutchinson, w, Tampa)
 - Recharge, Orange County (P. W. Bush, w, Winter Park)
 - Saltwater intrusion, Fernandina (R. W. Fairchild, w, Tallahassee)
 - Sand-gravel aquifer, Pensacola (Henry Trapp, w, Tallahassee)
 - Santa Fe River basin (J. D. Hunn, w, Tallahassee)
 - Sewage effluent disposal, irrigation (L. J. Slack, w, Tallahassee)
 - Shallow aquifer, Brevard County (J. M. Frazee, Jr., w, Winter Park)
 - Shallow aquifers, Alafia and Peace Rivers (C. B. Hutchinson, w, Tampa)
 - Technical assistance, south Florida (Howard Klein, w, Miami)
 - Urban hydrology, Englewood area (Horace Sutcliffe, Jr., w, Sarasota)
 - Verna well field (Horace Sutcliffe, Jr., w, Sarasota)
- Water resources:
 - Duval and Nassau counties (G. W. Leve, w, Jacksonville)
 - Martin County (R. A. Miller, w, Miami)
 - Tequesta (A. L. Knight, w, Miami)
 - Water-supply potential, Green Swamp (H. F. Grubb, w, Orlando)

Water resources—Continued*States and territories—Continued***Florida—Continued**

Hydrogeologic maps, Seminole County (W. D. Wood, w, Winter Park)

Hydrogeology, Osceola Forest (P. R. Seaber, w, Tallahassee)

Hydrology, Volusia County (P. W. Bush, w, Orlando)

Lee County (D. H. Boggess, w, Ft. Myers)

Mapping, Green Swamp (B. F. McPherson, w, Miami)

Palm Beach County (J. N. Fischer, w, Miami)

Quality of water:

Estuarine hydrology, Tampa Bay (C. R. Goodwin, w, Tampa)

Landfill and water quality (J. E. Hull, w, Miami)

Solid waste, Hillsborough County (Mario Fernandez, Jr., w, Tampa)

Solid waste, St. Petersburg (Mario Fernandez, Jr., w, Tampa)

Technical assistance, Department of Environmental Regulation (G. A. Irwin, w, Tallahassee)

Special studies, technical assistance (C. S. Conover, w, Tallahassee)

Surface water:

Hydrology study, Fakahatchee Strand (L. J. Swayze, w, Miami)

Lakes in southwest Florida (R. C. Reichenbaugh, w, Tampa)

Manasota technical assistance (Horace Sutcliffe, Jr., w, Sarasota)

Technical assistance:

Northwest Florida Water Management District (W. B. Mann, w, Tallahassee)

Suwanee River Water Management District (J. C. Rosenau, w, Tallahassee)

Tri-county investigation (C. B. Bentley, w, Jacksonville)

Waccasassa Basin hydrology (G. F. Taylor, w, Winter Park)

Water Atlas (S. D. Leach, w, Tallahassee)

Water resources, Hendry County (T. H. O'Donnell, w, Miami)

Water resources of Manasota basin (K. W. Causseaus, w, Tampa)

Water resources, Orange County (C. H. Tibbals, w, Winter Park)

Western Collier County (W. J. Haire, w, Miami)

Georgia (w, Doraville):

Cretaceous (L. D. Pollard)

Hydrology of the Albany area (R. E. Krause)

Information system (J. R. George)

Northwest Georgia geology and water (C. W. Cressler)

Valdosta hydrology (R. E. Krause)

Hawaii (w, Honolulu):

Biology-morphology Wailuku River (J. J. S. Yee, w, Honolulu)

Data management, Guam (C. J. Huxel, Jr.)

Topical studies (F. T. Hidaka)

Idaho (w, Boise):

Flow in Silver Creek, Idaho (J. A. Moreland)

Ground-water-quality assessment (H. R. Seitz)

Kootenai Board—WWT (E. E. Harris)

Streamflow evaluation, Upper Snake River (C. A. Thomas)

Illinois, water-quality appraisal (L. G. Toler, w, Champaign)**Indiana, ground water near Fort Wayne (Michael Planert, w, Indianapolis)****Water resources—Continued***States and territories—Continued***Iowa (w, Iowa City):**

Bedrock mapping (R. E. Hansen)

East-central (K. D. Wahl)

Low flow, Iowa streams (O. G. Lara)

National eutrophication survey (I. L. Burmeister)

Sediment data (W. J. Matthes)

Kansas (w, Lawrence, except as otherwise noted):

Geohydrology Arkansas River valley southwest Kansas (R. A. Barker, w, Garden City)

Glacial deposits (J. E. Denne, w, Lawrence)

Kansas-Oklahoma Arkansas River Commission (E. R. Hedman)

Numerical modeling (J. C. Halepaska)

Special hydrologic

Saline water Wellington Formation (A. J. Gogel, w, Lawrence)

Water supply in droughts (F. C. Foley)

Kentucky (w, Louisville):

Covington-Lexington-Louisville triangle (D. S. Mull)

Ground water, Ohio River valley (J. M. Kernodle)

London-Corbin area (R. W. Davis)

Somerset hydrology (R. W. Davis)

Louisiana (w, Baton Rouge):

Baton Rouge area (C. D. Whiteman, Jr.)

Lignite hydrology (J. L. Snider, w, Alexandria)

Ground water:

Grammercy area (G. T. Cardwell)

Kisatchie Forest area (J. E. Rogers)

Terrace aquifer, central Louisiana (J. L. Snider)

New Orleans area (D. C. Dial)

Reports on special topics (M. J. Forbes)

Site studies (R. L. Hosman)

Surface water:

Flood hydraulics and hydrology (B. L. Neely, Jr.)

Velocity of Louisiana Streams (A. J. Calandro)

Maine, public inquiries (C. R. Wagner, w, Augusta)**Massachusetts (w, Boston):**

Coastal southeastern Massachusetts, Wareham to Seekonk (G. D. Tasker)

Connecticut River lowlands (E. H. Walker)

Deicing chemicals, ground water (J. R. Frost)

Nashua River basin (R. A. Brackley)

Northeast:

Coastal basins (F. B. Gay)

Public inquiries (E. S. Denison)

Michigan (w, Okemos, except as otherwise noted):

Erosion in St. Joseph Basin (T. R. Cummings)

Geohydrology, environmental planning (F. R. Twenter)

Ground water:

Models, Muskegon County (W. B. Fleck)

West Uppir Peninsula (C. J. Doonan, w, Escabana)

Minnesota (w, St. Paul):

Impact of copper-nickel mining (P. G. Olcott)

Mississippi (w, Jackson):**Ground water:**

Aquifer maps for Mississippi (E. H. Boswell)

Ground-water use (J. A. Callahan)

Salt Dome hydrology in Mississippi (C. A. Spiers, w, Jackson)

Water assimilation (G. A. Bednar)

Water use (J. A. Callahan)

Missouri (w, Rolla):

Water quality, scenic riverways (J. H. Barks)

Water resources—Continued*States and territories—Continued***Montana (w, Helena, except as otherwise noted):**

Ground water:

- Fort Belknap (R. D. Feltis, w, Billings)
- Fort Union Formation (S. E. Slagle, w, Billings)
- Hydrology, lower Flathead (A. J. Boettche)
- Powder River valley:
 - Central (W. R. Miller, w, Billings)
 - "Saline seeps" (B. D. Lewis, w, Billings)
 - Special investigations (J. A. Moreland)
 - Water availability, Madison (W. R. Miller, w, Billings)
 - Water supplies for national parks, monuments, and recreation areas (J. A. Moreland)

Nebraska (w, Lincoln):

- Hydrogeology of southwest Nebraska (E. G. Lappala)
- Movement of nitrogen into aquifers (L. R. Petri)
- Time-of-travel data (L. R. Petri)

Nevada (w, Carson City):

- Aquifers in the Fallon area (P. A. Glancy)
- Topical studies (J. P. Monis)
- Water supply:
 - Cold Spring Valley (A. S. Van Denburgh)
 - Mining districts (H. A. Shamberger)

New Hampshire (w, Concord):

- Ground-water reconnaissance, river basins (J. E. Cotton)
- Public inquiries (C. E. Hale)

New Jersey (w, Trenton):

- Automatic processing of ground-water data (William Kam)
- Miscellaneous Federal work (Harold Meisler)
- Problem river studies (J. C. Schornick, Jr.)
- Quantification nonpoint pollution (J. C. Schornick, Jr.)
- Short-term studies (Harold Meisler)
- Test drill geophysical logging (J. E. Luzier)
- Water resources, Wharton Tract (William Kam)

New Mexico (w, Albuquerque):

- Bureau of Indian Affairs water-supply investigations (F. P. Lyford)
- Cimarron Basin analysis (P. L. Soule)
- Coal-lease areas, northwest New Mexico (Kim Ong)
- Ground water:
 - Capitan Reef (W. L. Hiss)
 - Harding County (F. D. Trauger)
 - Miscellaneous activities, State Engineering (W. A. Mourant)
 - White Sands Missile Range, water levels and pumpage (H. D. Hudson)
- Rio Grande Commission (P. L. Soule)
- Surface water, Pojoaque River analyses (G. A. Hearne)
- Water resources, Acoma and Laguna Reservations (F. P. Lyford)

New York (w, Syosset, except as otherwise noted):

- Basin recharge with sewage effluent (R. C. Prill)
- Hydrogeology of southeast Nassau County (H. F. H. Ku)
- Long Island water quality (B. G. Katz)
- Management modeling (G. E. Kimmel)
- Nassau County, ground-water (Chabot Kilburn)
- Short-term studies (R. J. Dingman, w, Albany)
- Suffolk County, water-quality observation well program (Julian Soren)
- Water resources, South Fork, Long Island (Bronius Nemickas)

North Carolina (w, Raleigh):

- Hydrology of Albermarle-Pamlico area (C. C. Daniel)
- Public water supplies (T. M. Robison)

Water resources—Continued*States and territories—Continued***North Carolina—Continued**

Surface water:

- Hydrology of estuaries (G. L. Geisse)
- Requests for data (H. G. Hinson)

North Dakota (w, Bismarck, except as otherwise noted):

Ground water:

- Billings-Golden Valley Slope (L. O. Anna)
- Dickey-Lamoure (J. S. Downey)
- Dunn County (R. L. Klausning)
- Grant and Sioux Counties (P. G. Randich)
- Hydrologic changes due to mining (W. F. Horak)
- Morton County (D. J. Ackerman)
- Ramsey County (R. D. Hutchinson, w, Grand Forks)
- Ransom-Sargent (C. A. Armstrong)
- Special investigations (O. A. Crosby)
- Wibaux-Beach deposit hydrology (W. F. Horak, Jr., w, Bismarck)

Northern Mariana Islands:

- Water resources information—Northern Marianas (D. A. Davis, w, Honolulu, Haw.)

Oklahoma (w, Oklahoma City):

Ground water:

- Antlers Sand (D. L. Hart, Jr.)
- Vamoosa Formation (J. J. D'Lugosz)
- Monitor Oklahoma coal field (J. S. Havens, w, Oklahoma City)

Requests, special investigations (J. H. Irwin)

Pennsylvania (w, Harrisburg, except as otherwise noted):

- Allegheny River basin Level-B study (G. R. Schiner, w, Meadville)
- Geohydrology of Berks County (C. R. Wood)
- Geology and ground-water resources of Monroe County (L. D. Carswell, w, Philadelphia)

Ground water:

- Chester County (L. J. McGreevy, w, West Chester)
- Cumberland Valley (A. E. Beecher)
- Ground-water resources of the Williamsport area (O. B. Lloyd)

Quality of water:

- Highway construction effects on streams (J. F. Truhlar, Jr.)

Sediment from highway construction (L. A. Reed)

Western Pennsylvania (G. R. Schiner)

Puerto Rico (w, San Juan):

- Contingent requests (E. D. Cobb)
- Geohydrology of landfills, Puerto Rico (Fernando Gomez-Gomez, w, San Juan)
- Hydrologic systems modeling (M. A. Lopez)

Rhode Island, public inquiries (H. E. Johnston, w, Providence)**South Carolina (w, Columbia):**

- Cooper River redirection (P. W. Johnson)
- Reconnaissance of estuaries (F. A. Johnson)

South Dakota (w, Huron, except as otherwise noted):

- Cheyenne and Standing Rock Indian Reservations (L. W. Howells)
- Clark County (L. J. Hamilton)
- Deuel and Hamlin Counties (Jack Kume, w, Vermillion)
- Ground water, Hand and Hyde Counties (N. C. Koch)
- McPherson, Edmunds, and Faulk Counties (L. J. Hamilton)
- Water resources:
 - Aurora and Jerauld Counties (L. J. Hamilton)
 - Davison-Hanson Counties (J. E. Powell, w, Huron)
 - Miner County (Jack Kume, w, Vermillion)

Water resources—Continued*States and territories—Continued***South Dakota—Continued****Water resources—Continued**

Yankton County (J. E. Powell, w, Huron)

Tennessee (w, Nashville, except as otherwise noted):

Terrace-deposits study (W. S. Parks, w, Memphis)

Water for Murfreesboro (D. R. Rima)

Wetlands delineation (E. F. Hollyday)

Texas:**Ground water:**

El Paso (W. R. Meyer, w, El Paso)

Galveston County continuing quantitative studies (R. K. Gabrysch, w, Houston)

Houston (R. K. Gabrysch, w, Houston)

Model study, Chicot and Evangeline aquifers (D. G. Jorgensen, w, Houston)

Orange County (G. D. McAdoo, w, Houston)

Rio Grande environmental study (J. S. Gates, w, El Paso)

Salt encroachment at Houston (D. G. Jorgensen, w, Houston)

San Antonio (R. D. Reeves, w, San Antonio)

Hydrologic investigations:

Limestone hydrology study (R. W. Maclay, w, San Antonio)

Quality of water, bays and estuaries (D. C. Hahl, w, Austin)**Trust territory, water-resource information (D. A. Davis, w, Honolulu, Hawaii)****Utah (w, Salt Lake City, except as otherwise noted):****Environmental impacts (Donald Price)****Ground water:**

Oil-shale hydrology (F. K. Fields)

Statewide ground-water conditions (J. C. Stephens)

Navajo Sandstone, southeastern Utah (J. W. Hood)

Program enhancement (Theodore Arnow)

Quality of water, Flamingo Gorge Reservoir (E. L. Bolke)

Surface water:

Canal-loss studies (R. W. Cruff)

Inflow to Great Salt Lake (J. C. Mundorff)

Vermont:

Ground water, Upper Winooski Basin (A. L. Hodges, Jr., w, Montpelier)

Public inquiries (R. E. Willey, w, Montpelier)

Water quality, Black River (W. D. Silvey, w, Boston, Mass.)

Virginia (w, Richmond):**Ground water:**

Geohydrologic data (R. L. Wait)

Hydrology of Prince William Forest Park (H. T. Hopkins)

South of James River (O. J. Cosner)

Service work (H. T. Hopkins)

Surface water, project planning and public inquiries (P. M. Frye)

Washington (w, Tacoma):**Ground water:**

Special hydrologic problems (R. A. MacNish)

Spokane Basin water resources (J. A. Skrivan)

Test drillings (K. L. Walters)

Model simulation for water management (R. D. MacNish)

Real-time data collection (R. R. Adsit)

Surface-water network reevaluation (W. L. Haushild)

Tulalip water resources (B. W. Drost)

West Virginia (w, Charleston):

Quantitative mine-water studies (G. G. Wyrick)

Water resources—Continued*States and territories—Continued***West Virginia (w, Charleston):**

Salt water (J. B. Foster)

Studies for unforeseen needs (G. G. Wyrick)

Wisconsin (w, Madison):**Ground water:**

Columbia County (C. A. Harr)

Low flow of small streams (S. J. Field)

Nederlo Creek hydrology (P. A. Kammerer, w, Madison)

Quality of water:

Ground-water-quality monitoring (C. A. Harr)

Menomonee River sediment study (E. R. Zuehls)

Pine River basin (P. A. Kammerer, Jr.)

Washington county sediment study (S. M. Hindall)

Surface water:

Drainage areas (E. W. Henrich)

Recreation reservoirs (B. K. Holstrom)

Wyoming (w, Cheyenne):

Arikaree Formation, Lusk (M. A. Crist)

Effluent monitor, national parks (E. R. Cox)

Green River basin water supply (H. W. Lowham)

Water resources, Powder River basin (M. E. Lowry)

Water use:

National water use data program (J. R. Ruggles, w, NC)

*States:***Connecticut:**

Water use (F. P. Haeni, w, Hartford)

Florida:

Ground-water use, Peace basin (A. D. Duerr, w, Tampa)

Water use, statewide (S. D. Leach, w, Tallahassee)

Water use southwest Florida (A. D. Duerr, w, Tampa)

Hawaii, water-use data (R. H. Nakahara, w, Honolulu)

Kansas:

Estimating ground-water withdrawals (C. H. Baker, Jr., w, Lawrence)

Water use (C. H. Baker, Jr., w, Lawrence)

Louisiana, water use, 1975 (G. C. Cardwell, w, Baton Rouge)

Maryland:

Water use (F. K. Mack, w, Towson)

Massachusetts:

Water use (J. A. Baker, w, Boston)

Michigan:

Water use (F. R. Twenter, w, Lansing)

North Carolina:

Water-use data collection North Carolina (R. C. Heath, w, Raleigh)

Nebraska:

Availability and use of water, Nebraska (E. K. Steele, w, Lincoln)

North Dakota:

Water use (Dale Frink, w, Bismarck)

Ohio:

Water use (R. M. Hathaway, w, Columbus)

Pennsylvania:

Water use (A. E. Becher, w, Harrisburg)

Utah:

Water use (R. W. Cruff, w, Salt Lake City)

West Virginia:

Water use (G. G. Wyrick, w, Charleston)

Washington, water use (G. G. Parker, w, Tacoma)

Waterpower classification:*California (c, Sacramento):*

Mokelumne River Basin, examination of pumped storage sites (D. E. Wilson)

Waterpower classification:**California (c, Sacramento)—Continued**

Review of withdrawals:

Owens River Basin, George Creek to Olancha Creek
(R. D. Morgan)

Westside tributaries (R. D. Morgan)

Idaho (c, Portland, Oreg.):

Pahsimeroi River, reservoir and dam site (K. J. St. Mary)

Oregon (c, Portland):

Review of withdrawals:

Clackamas River basin (L. O. Moe)

Coquille River basin (S. R. Osborne)

Nestucca River basin (K. J. St. Mary)

North Umpqua River (K. J. St. Mary)

South Umpqua River (L. O. Moe)

Washington (c, Portland, Oreg.):Blanca Lake and Troublesome Creek pumped storage site,
Skykomish River (J. B. Dugwyler, Jr.)**Waterpower classification—Continued****Washington (c, Portland, Oreg.)—Continued**Columbia River, vicinity of developed Wells Project, review
of withdrawals (J. B. Dugwyler, Jr.)Wood Plateau—Coyote Creek and John Day pool pumped
storage site, Columbia River (J. B. Dugwyler, Jr.)**Wyoming (c, D):**

Shoshone River Basin, review of withdrawals (G. A. Lutz)

Wilderness Program. *See Primitive and Wilderness Areas under
Mineral and fuel resources—compilations and topical studies,
mineral-resources surveys.***Zeolites:**California (southeastern), Oregon, and Arizona (R. A. Shep-
pard, D)**Zinc.** *See Lead, zinc, and silver.*

SUBJECT INDEX

A

- absolute age** *see also* geochronology; isotopes
- absolute age—dates**
- alluvium*: Uranium-trend dating of alluvium deposits 192
 - basalt*: Triassic and Jurassic rocks in the South Carolina coastal plain 51-52
 - biotite*: Age of quartz diorite at Bishop Spring in northwestern Oregon 74
 - Geology and oil-shale resources of the South Elko Basin in Nevada 26
 - K-Ar dating of the Albian 191
 - Middle Proterozoic tectonics in the Wyoming Age Province 64
 - gneiss*: Strontium-isotope data from Pioneer batholith in southwestern Montana 61
 - granite*: Tectonic implications of granite ages, southwestern Montana 60-61
 - igneous rocks*: Age and evolution of the southern part of the Arabian Shield 348-349
 - Ages of alkalic igneous activity in north-central Montana 59-60
 - Glaciation near Togwotee Pass in the Wind River Mountains of Wyoming 27
 - Youngest movement on Melones fault zone in California 267
 - metasedimentary rocks*: Archean age of major sedimentary sequences in southwestern Montana 62
 - obsidian*: Soil development and age of Bull Lake Glaciation in the Rocky Mountains 57
 - ore deposits*: Geochronology of uranium ores 34-35
 - peat*: Postglacial sea levels on the inner continental shelf of southern New England 146-147
 - Time of Pinedale deglaciation in the Park Range of Colorado 57
 - tuff*: Paleocene deposition and Eocene deformation in South Park, Colorado 63
 - volcanic rocks*: Age of volcanism at Togwotee Pass area in Wyoming 183
 - zircon*: Discordancy of zircons in the Saudi Arabian Shield 191
- absolute age—interpretation**
- ophiolite*: Mesozoic thrust-bound terranes in the San Juan Islands, Washington 79-80
 - plutonic rocks*: New data on modification of K-Ar ages by Tertiary thrust faulting in eastern Nevada 185
- absolute age—methods**
- Sm/Nd*: Samarium-neodymium systematics in gabbro from Fairweather Range in Alaska 192
- aerial photography** *see under* remote sensing
- aeromagnetic surveys** *see* magnetic surveys
- under* geophysical surveys *under* Wisconsin
- Africa** *see also* Egypt; Kenya; Liberia; Nigeria; Sudan
- Africa—hydrogeology**
- hydrology*: Senegal, Mauritania, and Mali 350
 - Senegal River basin data assessment 350
- Alabama—economic geology**
- lithium*: Lithium in flint clays 43-44
- Alabama—hydrogeology**
- hydrology*: Alabama 103-104
 - Effects of surface coal mining on the hydrology of Warrior coal field 103
 - Relation of geology to low flow in Alabama streams 103-104
 - Statistical analyses of water quality 103
- Alaska—areal geology**
- east-central*: East-central Alaska 83
 - Gulf of Alaska*: Environmental geologic studies, northeastern Gulf of Alaska 153-155
 - Ketchikan Quadrangle*: New data on Ketchikan and Prince Rupert quadrangles 84-85
 - north*: Northern Alaska 80-82
 - Prince Rupert Quadrangle*: New data on Ketchikan and Prince Rupert quadrangles 84-85
 - regional*: Alaska 80-87
 - General 80
 - south*: Southern Alaska 84
 - southeast*: Southeastern Alaska 84-87
 - southwest*: Southern Alaska 83-84
 - west-central*: West-central Alaska 82-83
- Alaska—economic geology**
- heavy minerals*: Reconnaissance geochemical studies in Alaska 10
 - lead-zinc deposits*: Strata-bound lead-zinc mineralization, Philip Smith Mountains quadrangle 82
 - mineral resources*: Mineral appraisals of Alaska on schedule; levels of studies 80
 - petroleum*: Alaska 17-18
 - Petroleum potential of Lisburne Group in the North Slope 17-18
 - Petroleum potential of Tertiary formations on Alaska peninsula 18
 - uranium*: An occurrence of parsonite, a secondary uranium mineral, in west-central Alaska 33
 - Uranium studies in western Alaska 32-33
- Alaska—engineering geology**
- permafrost*: Offshore permafrost in the Prudhoe Bay region 81
 - shorelines*: Effects of a major storm on the northern Bering Sea coastline 156
 - Gravel resources and erosional problems on the coast of Beaufort Sea 81-82
- Alaska—environmental geology**
- ecology*: Benthic invertebrates in a north-flowing stream and a south-flowing stream in Brooks Range, Alaska 243
 - geologic hazards*: Delicate environment of Alaska's coal lands 273
 - impact statements*: Environmental analysis of NPRA 323
- Alaska—geochemistry**
- heavy minerals*: Reconnaissance geochemical studies in Alaska 10
 - trace elements*: Content of nonplatinum-group minor metals in the Douglas Island Volcanics, Juneau quadrangle 86

- Platinum-group metals in the Douglas Island Volcanics, Juneau quadrangle 86
- Alaska—geochronology**
absolute age: Samarium-neodymium systematics in gabbro from Fairweather Range in Alaska 192
- Alaska—geomorphology**
glacial geology: Snowfall on Alaskan glaciers in 1976-77 212
mass movements: Landslides near Melozitna River Canyon 83
 — Planetary geologic processes and histories 294-295
- Alaska—geophysical surveys**
remote sensing: Geohydrologic analysis 303
 — Geology 303
 — Vegetation classification 302-303
- Alaska—hydrogeology**
hydrology: Alaska 125-126
 — Reconnaissance of lakes in the National Petroleum Reserve in Alaska 242-243
springs: Large springs north of Delta Junction 125-126
- Alaska—mineralogy**
orthosilicates: Lawsonite in Hagemeister Island quadrangle 83-84
- Alaska—oceanography**
continental shelf: Continental shelf structure, northwestern Gulf of Alaska 155
marine geology: Alaskan continental margin 153-157
ocean basins: Heat flow data for the Bering Sea basin 155
sedimentation: Bedform movement in lower Cook inlet 155
- Alaska—paleontology**
Mollusca: North Atlantic Cenozoic mollusks in northern Alaska 229
- Alaska—petrology**
igneous rocks: Distribution of intrusive rocks in the Fairweather Range, Glacier Bay National Monument, Alaska 86-87
intrusions: Contacts of the gabbro at Mount La Perous, Mount Fairweather quadrangle 86
metamorphic rocks: Aluminosilicate minerals in the Big Delta Quadrangle 83
- Alaska—sedimentary petrology**
sedimentation: Paleotransport directions in Nanushuk Group 81
- Alaska—seismology**
earthquakes: Seismogenic zones of Alaska and adjacent continental shelf 257
 — Southern Alaska 261-262
 — The 1899 Yakutat Bay earthquakes 257-258
- Alaska—stratigraphy**
Carboniferous: Paleomagnetic results from the Alexander terrane and from eastern North America agree on Paleozoic paleolatitudes 85-86
Cretaceous: Basal Cretaceous rocks discovered at south margin of Yukon-Koyukuk province 82
 — Paleomagnetic poles from the Valdez(?) and Orca Groups, Alaska 167
- Devonian*: Paleomagnetic results from the Alexander terrane and from eastern North America agree on Paleozoic paleolatitudes 85-86
Paleogene: Sedimentary facies in Tertiary rocks in the Tyonek quadrangle 84
Paleozoic: Probable pre-Ordovician age of metamorphic complex in northern Kuskokwim Mountains 82-83
 — Radiolaria date chert in Big Delta quadrangle as late Paleozoic 83
 — Tectonic significance of newly discovered lower Paleozoic strata in the Healy A-6 quadrangle 84
Pleistocene: Early or Middle Pleistocene glaciation in the National Petroleum Reserve in Alaska 80-81
- Alaska—tectonophysics**
plate tectonics: Microplate tectonics of the southern part of Alaska 80
 — Tarr Inlet suture zone, Glacier Bay National Monument, Alaska 87
- Alaska—volcanology**
Aniakchak: Post-caldera airfall pumice at Aniakchak caldera 84
- algae—biochemistry**
nitrogen: NO₃-N uptake by algae in a streamlike environment 187
- algae—diatoms**
Miocene: Miocene diatoms from the Montesano Formation of Weaver (1912), Washington 229
- algae—nannofossils**
Quaternary: Nannofossil ages for East Pacific Rise fast spreading sites 158-159
- aluminum** *see also under economic geology under United States*
- Antarctica—areal geology**
maps: Exploration of the Orville Coast of the Antarctic Peninsula 352
Pensacola Mountains: Geologic comparison of the Pensacola Mountains and Shackleton Range 352-353
regional: Antarctic programs 351-354
Shackleton Range: Geologic comparison of the Pensacola Mountains and Shackleton Range 352-353
- Antarctica—geochronology**
Neogene: Paleomagnetic dating of glacial sediments underlying Taylor Dry Valley in Antarctica 168
- Antarctica—geophysical surveys**
gravity surveys: Geologic and geophysical studies of the contact of the Dufek intrusion, Pensacola Mountains 353-354
- Antarctica—paleobotany**
Plantae: Antarctic paleobotany and coal 353
- Antarctica—soils**
surveys: Baseline soil investigations in the Pensacola Mountains 353
- Anthozoa** *see under Coelenterata*
- Appalachians—areal geology**
research: Appalachian Highlands and the Coastal Plains 48-52
- Appalachians—economic geology**
natural gas: Appalachian Basin and Florida 22-23
 — Possible stratigraphic controls for Devonian gasfields in the Appalachian Basin 22
petroleum: Appalachian Basin and Florida 22-23
- Appalachians—environmental geology**
geologic hazards: Appalachian flood of April 1977 in Kentucky, Tennessee, Virginia, and West Virginia 281
- Appalachians—petrology**
metamorphic rocks: The Baltimore Complex, a disrupted ophiolite 184
- Appalachians—stratigraphy**
Devonian: Possible stratigraphic controls for Devonian gasfields in the Appalachian Basin 22
Ordovician: Lower-Middle Ordovician boundary in south-central Appalachian Basin-conformity and unconformity; the Beekmantown Group "updated" 231
- aquifers** *see under ground water*
- Arabian Peninsula** *see also Saudi Arabia; Yemen*
- Arabian Peninsula—geophysical surveys**
remote sensing: Eastern Arabian Peninsula 342
- Arabian Peninsula—tectonophysics**
plate tectonics: Age and evolution of the southern part of the Arabian Shield 348-349
 — Plate tectonics and the Arabian Shield 349
- Archean** *see also under geochronology under Montana*
- archeology** *see archaeology under occurrence under fossil man*
- Arctic Ocean—geophysical surveys**
remote sensing: Radar imagery study of Beaufort Sea ice 245
- Arctic Ocean—oceanography**
continental shelf: Sediment transport on the inner shelf of the Beaufort Sea 157
sedimentation: Rates of Arctic marine geologic processes 157
- Arctic region** *see also Greenland*
- Arctic region—paleontology**
Mammalia: Pliocene and Pleistocene holarctic correlation of microtid rodents 228
- Arizona—economic geology**
copper: Another model of porphyry copper generation 7-8
 — Characteristics of a porphyry copper stock in Globe-Miami district of Arizona 7
geothermal energy: Crustal melting in the San Francisco volcanic field in Arizona 41
 — Geothermal water studies in the Verde Valley of Arizona 40
lithium: New occurrences of the lithium-rich smectite, hectorite 42-43
maps: Mineral exploration potential 13-14

- uranium*: Character of the conglomerate of the Shinarump Member of the Chinle Formation at Window Rock in Arizona 29
- Geology and mineral resources in north-central Arizona 30
 - Intermontane basin uranium occurrences in Arizona 30
 - Uranium in the Date Creek Basin area of west-central Arizona 27
- Arizona—engineering geology**
- earthquakes*: Fort Yuma Earthquake of 1852 267
 - land subsidence*: Elastic expansion of the lithosphere caused by ground-water depletion 291
 - Subsidence investigation in central Arizona 289
 - Surface faulting in Arizona induced by ground-water withdrawal coincident with a geologic fault 291
- Arizona—geochemistry**
- magmas*: Petrochemistry trends, distribution coefficients, and quality of minor element data 186
- Arizona—geochronology**
- Phanerozoic*: Geochronology of the San Francisco volcanic field in Arizona 207
- Arizona—geomorphology**
- processes*: Reinterpretation of Grand Canyon geomorphology 71-72
- Arizona—geophysical surveys**
- magnetotelluric surveys*: Audio-magnetotelluric measurements on the Papago Indian Reservation in Arizona 172
 - surveys*: Geophysical surveys near Picacho, Arizona 265
- Arizona—hydrogeology**
- ground water*: Water use may double in Apache County 126
 - hydrology*: Arizona 126
 - Evapotranspiration from saltcedar in the Gila River flood plain in Arizona 239-240
 - Soil moisture along a bajada in southern Arizona 240
 - maps*: Perennial streams and wetlands of Arizona 233-234
- Arizona—petrology**
- igneous rocks*: Calc-alkalic intrusive rocks at Mineral Mountain, south-central Arizona 73-74
 - Jurassic plutonism and volcanism in south-central Arizona 73
 - Tertiary volcanic sequence at Mineral Mountain in Arizona 182-183
 - intrusions*: Calc-alkaline intrusive relations at Mineral Mountains in Arizona 186
- Arizona—stratigraphy**
- Holocene*: Tree rings and alluvial history on Black Mesa, Arizona 214-215
 - Mississippian*: Mississippian rocks of Pedregosa basin in southwesternmost New Mexico and adjacent Arizona 72-73
 - Quaternary*: Geology contributes to archaeology and climate studies in northeast Arizona 268
- Triassic*: Origin of natural remanent magnetization in red sedimentary rocks of the Moenkopi Formation in Arizona 168
- Arkansas—structural geology**
- structural analysis*: Multiple deformation of gneiss dome near Rincon Mountains in southeastern Arizona 73
 - tectonics*: Cenozoic volcanism and tectonism in west-central Arizona 72
- Arkansas—areal geology**
- maps*: Quadrangle compilation manuscript available for 1976 geologic map of Arkansas 88
- Arkansas—hydrogeology**
- bibliography*: Water-resource literature for Arkansas annotated 111
 - hydrology*: Arkansas 111
- Arkansas—stratigraphy**
- Cretaceous*: Cretaceous biostratigraphy in Arkansas 230
 - Dinoflagellates and acritarchs prove useful in the biostratigraphic and paleoecologic analysis of Santonian-Age formation in southwestern Arkansas 228
- arsenic—analysis**
- chemical analysis*: Arsenic and selenium 248
- Asia** *see also* Arabian Peninsula; Cambodia; Indonesia; Malay Archipelago; Malaysia; Philippine Islands; Sri Lanka
- associations—general**
- International Standardization Organization*: Other international activities 339
- associations—hydrogeology**
- U. S. National Committee on Scientific Hydrology*: USNC/SH investigations 338-339
- Atlantic Coastal Plain—environmental geology**
- land use*: Land use and land cover research and analysis 320-322
- Atlantic Coastal Plain—hydrogeology**
- ground water*: Freshwater in offshore aquifers 224
 - hydrology*: Atlantic and Gulf Coast 159-161
 - Distribution of biologically reactive substances in the Potomac Estuary 159-160
 - Estuarine sediment sources of the Potomac Estuary 159
 - Interstate studies 103
 - Southeastern region 102-108
- Atlantic Coastal Plain—stratigraphy**
- Pleistocene*: Inland limit of the Croatan Sea; Pliocene and Pleistocene beds at Fountain, North Carolina 228
- Atlantic Ocean—economic geology**
- petroleum*: Petroleum potential of the Mid-Atlantic continental margin 145
- Atlantic Ocean—engineering geology**
- geologic hazards*: Geologic environment of the Atlantic continental shelf 145-146
 - Glacial deposits of the continental shelf 146
 - marine installations*: Environmental studies of the Mid-Atlantic outer continental shelf 147-148
- Atlantic Ocean—geochemistry**
- isotopes*: Pb-210 profiles in continental shelf sediments; an index to rates of sediment reworking 146
 - organic materials*: Environmental organic geochemistry of Mid-Atlantic shelf sediments 148
 - Organic geochemistry of heavy hydrocarbons in Florida-Hatteras outer continental shelf sediments 148
 - trace elements*: Vertical distribution of trace metals in sediments of Georges Bank 146
- Atlantic Ocean—geophysical surveys**
- seismic surveys*: Analyses of sidescan sonar and high resolution seismic records for the Carolina to Florida continental shelf 148
 - Evidence from Massachusetts onshore and offshore areas for thrusting coastal end moraines and a fluctuating ice margin of Woodfordian age 147
 - surveys*: Stratigraphy and structure of the Atlantic continental margin and adjacent deep-sea floor 144-145
- Atlantic Ocean—oceanography**
- continental slope*: Atlantic continental margin 144-148
 - ocean circulation*: Currents and bottom sediment movement on Georges Bank 146
 - sediments*: Environmental assessment of the South Atlantic continental shelf 148
- atmosphere—composition**
- mercury*: Mercury outgassing in Hawaii 289
- Australasia** *see also* New Zealand
- automatic data processing—engineering geology**
- waste disposal*: Simulation of the effects of containment of nuclear wastes in layered salt deposits 279
- automatic data processing—environmental geology**
- land use*: Geographic information systems software development 319-320
- automatic data processing—general**
- cartography*: DEM files 359-360
 - Digital cartographic applications 358
 - Digital cartographic data files 359
 - DLG files 360
 - File management 360
 - Hardware 358-359
 - Pilot production projects 360-361
 - Software 359
 - maps*: Useful applications of map data file 87
- automatic data processing—geochemistry**
- computer programs*: Frequency distributions of elements 188-189
 - maps*: Geochemical anomalies 189
 - neutron activation analysis*: Instrumental neutron activation of geological materials 246-247

- automatic data processing—geophysical surveys**
 - data processing:* Geomagnetic array data processing 174
 - digital techniques:* Digital terrain corrections for gravity data 175
 - microcomputers:* New magnetotelluric field processing system 174
 - remote sensing:* Data Analysis Laboratory 301
- automatic data processing—hydrogeology**
 - data bases:* Data management and instrumentation 137
 - National Water Data Exchange 135-136
 - Water-Data Storage System 136
 - information systems:* Water data and information management 351
 - models:* Model studies 139
 - programs:* Office of Water Data Coordination 133-135
 - Special water-resource programs, data coordination, acquisition, and storage 133-143
- automatic data processing—methods**
 - batch processing:* Acquisition of additional capacity 362
 - Batch computing services 362
 - Index Sequential Access Method (ISAM) File Processing 362
 - Overhead reduction 362-363
 - technology:* Computer technology 362
 - time sharing:* Time-sharing system access 362
- automatic data processing—seismology**
 - data processing:* Equipment development 255

B

- Basin and Range Province—areal geology**
 - regional:* Basin and Range region 69-74
 - Stratigraphic and structural studies 69-73
- Basin and Range Province—economic geology**
 - geothermal energy:* Geothermal potential of the eastern margin of the Basin and Range province in Utah 205-206
 - metals:* Mineral-resource studies 69
- Basin and Range Province—geochemistry**
 - igneous rocks:* Semiquantitative spectrographic data from granitoid rocks of the Basin-Range Province 186
- Basin and Range Province—geochronology**
 - absolute age:* Geochronologic studies 74
- Basin and Range Province—petrology**
 - igneous rocks:* Igneous rocks 73-74
- Basin and Range Province—tectonophysics**
 - heat flow:* Models of an extending lithosphere and heat flow in the Basin and Range province 200
- beptonite** *see also under* economic geology *under* Montana; Wyoming
- Bering Sea—geochemistry**
 - organic materials:* Thermogenic gas seep on the sea floor of Norton Sound 155-156

- Bering Sea—geophysical surveys**
 - heat flow:* Heat flow data for the Bering Sea basin 155
 - seismic surveys:* Navarin Basin complex, Bering Sea outer continental shelf 155
- Bering Sea—oceanography**
 - ocean circulation:* Bottom boundary layers and sediment transport on the floor of Norton Sound in Alaska 156-157
- beryllium—analysis**
 - spectroscopy:* Determination of beryllium in geologic materials 246
- beryllium—geochemistry**
 - power plants:* Mass balances of trace elements at powerplants 16
- bibliography** *see also under* hydrogeology *under* Arkansas
- biogeography—Mammalia**
 - Pliocene:* Pliocene and Pleistocene holarctic correlation of microtid rodents 228
- biogeography—Mollusca**
 - Cenozoic:* North Atlantic Cenozoic mollusks in northern Alaska 229
- Black Sea—stratigraphy**
 - Pleistocene:* Hypersaline epoch in the Black Sea 159
- borates** *see under* minerals
- boron—abundance**
 - water:* Boron in natural water 247
- Brazil—hydrogeology**
 - hydrology:* Brazil 340
 - Sediment studies of the Amazon River 340
- Brazil—sedimentary petrology**
 - sedimentation:* Sampler for large streams 212
- brines** *see also under* economic geology *under* Nevada

C

- cadmium—geochemistry**
 - waste disposal:* Extraction of chromium and cadmium from aquifer material 97
- California—areal geology**
 - regional:* California 74-77
- California—economic geology**
 - geothermal energy:* Evaluation of geothermal systems using teleseisms 205
 - Geothermal potential northeast of Clear Lake in California 40
 - Geothermal water studies in the Coso Hot Springs of California 40
 - Mercury anomalies in the Long Valley, California geothermal area 208
 - Noble gases and dissolved ions in geothermal exploration 205
 - P-wave delay studies in geothermal areas 199
 - Relation of mercury mineralization to The Geysers hydrothermal system 198-199
 - Seismicity of The Geysers-Clear Lake geothermal area in California 195
 - Strike-slip faulting and crustal spreading in the Coso Range, California 195
 - Water-rock reaction in the Salton Sea Geothermal Field in California 207-208

- gold:** Gold and silver in ash of incinerated sewage sludge 43
- maps:** Mineral exploration potential maps 13-14
- natural gas:** Great Basin and California 20-22
- Oil and gas resources of the Outer Continental Shelf 23
- petroleum:** Detection of marine oil slicks as a petroleum exploration tool 23-24
- Great Basin and California 20-22
- Oil and gas resources of the Outer Continental Shelf 23
- Sedimentation, tectonics, and petroleum potential of California Coast Ranges 21-22
- phosphate:** California phosphorite 43
- silver:** Gold and silver in ash of incinerated sewage sludge 43
- California—engineering geology**
 - earthquakes:* Fort Yuma Earthquake of 1852 267
 - Ground response in the Los Angeles region 262
 - Ground response in the San Francisco Bay region 262-263
 - Seismic intensities of the 1906 California earthquake 262
 - geologic hazards:* Ancient landslide dated in The Geysers steam field, California 266
 - Deformational structures in soft sediments 264
 - Landslide data available for Pacific Palisades area in Los Angeles, California 265
 - Potential fault hazard in Ventura, California 291
 - Research in geologic hazards 265
 - Streamside landsliding near Redwood National Park 266
 - land subsidence:* Application of subsidence model 290
 - Drought verified changed storage parameters in California 289-290
 - tunnels:* Analyses of subsurface data to assist planners in evaluating feasibility of tunneling for rapid-transit systems 318
- California—environmental geology**
 - ecology:* Benthic-community structure in San Francisco Bay 163
 - Distribution of biologically reactive substances in northern San Francisco Bay 162
 - Estimates of phytoplankton productivity in San Francisco Bay 162
 - In vivo fluorescence studies in the San Francisco Bay 162
 - Seasonal phytoplankton distribution in San Francisco Bay 162-163
 - geologic hazards:* Geologic response of southern California to contemporary climate 217
 - Potential volcanic activity near Clear Lake in California 182
 - land use:* Geologic aspects of off-road vehicle use 273

- Integrated terrain mapping 306
- pollution*: Studies show pollution of streams 126
- California—geochemistry**
- isotopes*: Strontium isotopic variation in a compositionally zoned granitic pluton 189
- rare earths*: Jurassic zoned tonalite-trondhjemite pluton in Trinity Alps of Klamath Mountains in California 185
- trace elements*: Emplacement sequence and chemical evolution of Pleistocene rhyolites in Coso Range, California 181-182
- California—geochronology**
- Pleistocene*: Geomagnetic polarity event from Cobb Mountain in California 167
- California—geomorphology**
- fluvial features*: Effects of clearcutting redwoods in the Redwood National Park of California 211
- California—geophysical surveys**
- electrical surveys*: Geoelectrical investigations in the Coso Hot Springs area in California 201-202
- gravity surveys*: Gravity data reveal buried ophiolite belt in California 172
- remote sensing*: Luminescence studies 308
- Lunar radar studies 297
- California—hydrogeology**
- ground water*: Ground-water studies in desert basins 127-128
- Water supply at Beale Air Force Base unchanged 128
- hydrology*: California 126-128
- Copper cycles and copper sulfate algal capacity in two California lakes 241-242
- Nitrogen studied in the Santa Ana River basin 127
- Studies show pollution of streams 126
- springs*: Geothermal gradient is 800°C at Coso Hot Springs 126-127
- thermal waters*: Helium-3 in Yellowstone, Lassen, and The Geysers' fluids indicates mantle connection 201
- Water chemistry predicts occurrences of Great Valley sequence 75
- California—mineralogy**
- sulfides*: New alkali metal sulfides from California 178
- California—oceanography**
- ocean circulation*: Current-measurement studies in San Francisco Bay 161
- Distribution of biologically reactive substances in northern San Francisco Bay 162
- Hydrographic framework of San Francisco Bay 161-162
- sedimentation*: Beach-sand retention landward of a nearshore submarine canyon 151
- Migration of sand waves in central San Francisco Bay 161
- Sedimentological features and growth of the Monterey deep-sea fan off central California 151
- Separate and superimposed equilibrium bedforms; a synthesis of flume and San Francisco Bay observations 152-153
- California—petrology**
- igneous rocks*: Upper Cenozoic basaltic and phonolitic lavas in central Sierra Nevada 75
- magmas*: Petrology of post-caldera rhyolites in Long Valley, California 182
- metamorphic rocks*: Garnet clues for lost Sierra Nevada tail 74-75
- metamorphism*: Maximum temperature of formation of Franciscan melange 76-77
- metasomatic rocks*: Serpentine emplacement, Northern California Coast Ranges 76
- metasomatism*: Laumontite alteration 187
- California—sedimentary petrology**
- diagenesis*: Thermal history in siliceous shales 186-187
- California—seismology**
- earthquakes*: Analyses of seismic data 255
- Cucamonga fault scarps 77
- Deformational regime assessed 77
- Earthquake swarms in Imperial Valley, California 194-195
- seismicity*: Seismicity of The Geysers-Clear Lake geothermal area in California 195
- California—stratigraphy**
- Cenozoic*: Three-million-year isotopic record of paleoclimate at Death Valley in California 216
- Three million years of climate history at Searles Lake 216-217
- Miocene*: Deep-water sedimentation influenced by an actively-shifting source terrane 77
- California—structural geology**
- neotectonics*: California coastal tectonics 259
- Deformational regime assessed 77
- Geology of the Monterey Bay region 151
- Recent faulting of seafloor off Humboldt Bay in California 151-152
- Santa Maria River Fault, California 267
- Southern California tectonics 258-259
- Tectonic framework of the San Francisco Bay Region 258
- Trench investigation of faults 261
- Youngest movement on Melones fault zone in California 267
- tectonics*: Faulting in coastal South-central California 150-151
- Melones fault zone in the northern Sierra Nevada 75
- Sedimentation, tectonics, and petroleum potential of California Coast Ranges 21-22
- Southern Elsinore fault zone in California 267
- Tectonics and sedimentology of upper Tertiary fluvial deposits along Maacama fault studies 76
- California—tectonophysics**
- plate tectonics*: Plate tectonics and The Geysers geothermal anomaly 75-76
- Cambodia—hydrogeology**
- ground water*: Ground-water resources 340
- surveys*: Cambodia 340
- Cambrian** *see also under stratigraphy under Massachusetts; Rhode Island*
- Canada** *see also Appalachians; Atlantic Coastal Plain; Great Lakes region; Great Plains; Rocky Mountains*
- carbon—geochemistry**
- black shale*: Uranium, thorium, carbon, and sulfur in Devonian black shale from West Virginia, Kentucky, and New York 39
- carbon— isotopes**
- C-13/C-12*: Application of stable carbon isotopic ratios to exploration for deep-water source sediments 24
- Hydrocarbon maturation in Kentucky and Virginia 22
- Three-million-year isotopic record of paleoclimate at Death Valley in California 216
- Water temperature of corals shown by isotopic analysis 216
- carbonate rocks** *see under sedimentary rocks*
- Carboniferous** *see also under stratigraphy under Alaska; Massachusetts*
- Caribbean region—areal geology**
- maps*: Geologic-tectonic map of the Caribbean 88
- Caribbean region—geophysical surveys**
- surveys*: Circum-Caribbean mafic-ultramafic belts 170-171
- Cenozoic** *see also under geochronology under Wyoming; see also under stratigraphy under California; Georgia; Mississippi Valley; Texas; Utah; Wyoming*
- Cenozoic—paleontology**
- research*: Mesozoic and Cenozoic studies 227-230
- Central America** *see also Costa Rica; Guatemala; Nicaragua*
- Ceylon** *see Sri Lanka*
- changes of level** *see also under stratigraphy under New England*
- chemical analysis—methods**
- applications*: Pesticides 249
- chromatography*: Biological methods 249
- Determination of acetone 248
- Hydrophobic organic acids 248-249
- neutron activation analysis*: Instrumental neutron activation of geological materials 246-247
- Neutron activation 246-247
- research*: Analytical chemistry 245-247
- Analytical methods 245-249
- trace-element analyses*: Anodic stripping voltammetry 248
- chemical analysis—techniques**
- applications*: Analysis of water 247-249
- sample preparation*: Organic solutes 248
- Chile—engineering geology**
- tunnels*: Chile 340-341

- Chile—mineralogy**
borates: Crystal structure of hydrochloroborite 177-178
- chromatography** *see under methods under chemical analysis*
- chromite—production**
global: Geological analysis of world chromite production 1
- chromium—geochemistry**
power plants: Mass balances of trace elements at powerplants 16
waste disposal: Extraction of chromium and cadmium from aquifer material 97
- clastic rocks** *see under sedimentary rocks*
- clastic sediments** *see under sediments*
- clay mineralogy—areal studies**
New Mexico: Montmorillonite in coal partings 15
- clay mineralogy—mineral data**
kaolinite: Heat capacities of feldspars and kaolinite 176
- coal** *see also under economic geology under Colorado; Illinois; New Mexico; North Dakota; Ohio; Poland; United States; Utah; West Virginia; Wyoming*
- coal—geochemistry**
trace elements: Scanning electron microscopy study of the accessory minerals in coal 247
- coal—resources**
collections: Reinhardt Thiessen collection now at Reston, Virginia 14
data: Growth of the National Coal Resources Data System 14
exploration: Coal 13
reserves: Coal resources 14-16
- Coastal Plains—areal geology**
research: Appalachian Highlands and the Coastal Plains 48-52
- Coelenterata—Anthozoa**
Mississippian: Coral zones and problems of Mississippian stratigraphy in the Williston Basin 232
- Coelenterata—biochemistry**
isotopes: Water temperature of corals shown by isotopic analysis 216
- Colorado—economic geology**
coal: Coal rank related to depth of burial and buried intrusive rocks 15-16
geothermal energy: Potential geothermal reservoirs in southern Colorado 208
industrial minerals: Production of quartz-muscovite schist from Poncha Pass area in Colorado 6
lead: Source of lead in ores of the San Juan Mountains in Colorado 189-190
metals: Trace elements in galena and sphalerite in the Montezuma district of Colorado 11
mineral resources: Trace elements in minerals 11
natural gas: Hydrocarbon accumulation in Cretaceous shallow-marine sandstones of the northern Denver Basin 20
oil shale: Contact between the Parachute Creek Member of the Green River Formation and the Uinta Formation of south-central Piceance Creek Basin in Colorado 26
- Intertonguing of the Green River and Uinta Formations in Rio Blanco County, Colorado 25-26
- Isolation of zones in oil shale with distinctive chemical characteristics using statistical techniques 25
- petroleum*: Hydrocarbon accumulation in Cretaceous shallow-marine sandstones of the northern Denver Basin 20
- thorium*: Stable isotope studies of thorium-bearing veins in the Wet Mountains of Colorado 33
- uranium*: Structural and lithologic controls for uranium at the Pitch mine in Colorado 31
- Uranium and Tertiary volcanic rocks in the Marshall Pass district of Colorado 32
- Uranium potential of the Lower Cretaceous, Piceance Basin of Colorado 28-29
- zinc*: Potential economic significance of gahnite (zinc spinel) in Colorado 6
- Colorado—engineering geology**
reservoirs: Effects of proposed "Narrows" reservoir on South Platte River 113
rock mechanics: Radar-transport oil shales 173-174
- Colorado—environmental geology**
ecology: Benthic invertebrates in Piceance Creek, northwestern Colorado 111
geologic hazards: Landslides in northwestern Colorado 56
land use: Environmental geology of oil shale and coal lands, in northwest Colorado 272
- Geologic and hydrologic mapping in the Colorado Front Range Urban Corridor to aid local regional planners 317-318
- pollution*: Organic contamination of the Arkansas River in Pueblo County, Colorado 284-285
- waste disposal*: Water-level fluctuations and residential waste-treatment systems 114
- Colorado—geochemistry**
Paleocene: Paleocene deposition and Eocene deformation in South Park, Colorado 63
surveys: Soil geochemistry in the Uinta and Piceance Basins 288
trace elements: Minor element geochemistry and strontium isotopes of Tertiary stocks in Colorado mineral belt 192-193
- Trace elements in galena and sphalerite in the Montezuma district of Colorado 11
- Trace elements in minerals 11
- Colorado—geomorphology**
glacial geology: Time of Pinedale deglaciation in the Park Range of Colorado 57
processes: Storm-event aggradation of ephemeral streams 211
- Colorado—geophysical surveys**
heat flow: Distribution of radioactivity with depth in the Front Range Uranium and Thorium Provinces 202
remote sensing: Landsat investigations of the northern Paradox Basin, Utah and Colorado 311-312
surveys: Geophysical studies of the Silver Cliff area in Colorado 173
- Colorado—hydrogeology**
ground water: Availability and quality of ground water in the Gunnison-Crested Butte area 111
- Piceance Basin model 113
- Reconditioning of geohydrologic test holes in an oil-shale formation 113
- Two-dimensional finite-difference model developed for the closed-basin area of San Luis Valley 114
- Water-table aquifers in the Boulder-Fort Collins-Greeley area of the Front Range Urban Corridor 112
- hydrology*: Colorado 111-114
- Estimating regional water use and residuals output from energy development 140
- Flow and salinity modeling of proposed reservoirs in the Yampa River basin 242
- Water-management plans for the South Platte River valley 112-113
- Water quality in Boulder County 112
- springs*: Water quality of springs and productivity of wells in the Piceance Basin 113-114
- Colorado—petrology**
igneous rocks: Magmatic diversification and crust-mantle structure in Colorado 185-186
- intrusions*: Multiple-intruded carbonatite dike in the Wet Mountains of Colorado 33
- Colorado—stratigraphy**
Cretaceous: Uranium potential of the Lower Cretaceous, Piceance Basin of Colorado 28-29
Eocene: Contact between the Parachute Creek Member of the Green River Formation and the Uinta Formation of south-central Piceance Creek Basin in Colorado 26
Tertiary: Intertonguing of the Green River and Uinta Formations in Rio Blanco County, Colorado 25-26
- Uranium and Tertiary volcanic rocks in the Marshall Pass district of Colorado 32
- Colorado—structural geology**
maps: Rio Grande rift system in Colorado 88
tectonics: Paleocene deposition and Eocene deformation in South Park, Colorado 63
- Tectonics 63-68
- Colorado Plateau—stratigraphy**
Cretaceous: New age data, Early Cretaceous, Colorado Plateau 229

- Columbia Plateau—geochemistry**
lava: Petrogenesis of Columbia River Basalt Group 181
- Columbia Plateau—petrology**
lava: Columbia River plateau studies 180-181
- congresses** *see* symposia
- Connecticut—hydrogeology**
ground water: Appraisal of ground-water availability and quality in Farmington 91
 — Evaluation of the stratified-drift aquifer in the Pootatuck River valley 91
hydrology: Connecticut 91-92
 — FCB concentrations in bottom sediments of the Housatonic River 91-92
- Connecticut—stratigraphy**
Paleozoic: Correlation of Scotland Schist and Hebron Formation in eastern Connecticut with Oakdale Formation in Massachusetts 47
- Connecticut—structural geology**
faults: Syntectonic faults in eastern Connecticut 47-48
- conodonts—biostratigraphy**
Ordovician: Conodont-based Lower Ordovician correlations in eastern Pennsylvania 231-232
 — Lower-Middle Ordovician boundary in south-central Appalachian Basin—conformity and unconformity; the Beekmantown Group "updated" 231
- conodonts—paleoecology**
nektonic environment: Paleoecology and biofacies of Osagean conodonts 232
- conservation** *see also under* environmental geology *under* United States
- construction materials** *see also* limestone
- continental shelf** *see also under* oceanography *under* Alaska; Arctic Ocean; Eastern U.S.; Gulf of Mexico; Pacific Ocean
- continental slope** *see also under* oceanography *under* Atlantic Ocean; Eastern U.S.
- copper** *see also under* economic geology *under* Arizona; Michigan; Minnesota; Montana; New Mexico; Oregon; Puerto Rico
- copper—geochemistry**
power plants: Mass balances of trace elements at powerplants 16
- Costa Rica—seismology**
earthquakes: Costa Rica 341-342
- Cretaceous** *see also under* geochronology *under* North America; Wyoming; *see also under* stratigraphy *under* Alaska; Arkansas; Colorado; Colorado Plateau; Georgia; Maryland; Minnesota; North Carolina; South Dakota
- crust** *see also under* seismology *under* Nevada; South Carolina
- crust—observations**
international cooperation: Crustal studies 327-329
- crust—structure**
global: Worldwide three-dimensional seismic crustal studies 209
- crystal chemistry** *see also* minerals
- crystal chemistry—mineral data**
experimental studies: Mineralogic studies and crystal chemistry 177-179
- crystal growth** *see also* crystal chemistry; minerals
- crystal structure** *see also* crystal chemistry; minerals
- crystal structure—borates**
hydrochlorborite: Crystal structure of hydrochlorborite 177-178
- crystal structure—chain silicates, pyroxene group**
orthopyroxene: Fine structure of orthopyroxene 178
- ## D
- deformation** *see also* geophysics; structural analysis
- Devonian** *see also under* stratigraphy *under* Alaska; Appalachians; Nevada; Tennessee
- diagenesis** *see also* sedimentation
- diagenesis—geochemistry**
experimental studies: Diagenetic studies 186-187
- diagenesis—materials**
reefs: Reef destruction by boring organisms 159
shale: Thermal history in siliceous shales 186-187
- diatoms** *see under* algae
- dikes** *see under* intrusions
- District of Columbia—environmental geology**
land use: Land-use climatology 214
- dunes** *see under* eolian features *under* geomorphology
- ## E
- Earth—magnetic field**
diurnal variations: Geomagnetic diurnal variation 169
models: U. S. and World Magnetic Charts 169
observations: Geomagnetic observatories 168-169
 — Magnetic stations for the International Magnetospheric Study 169
secular variations: Geomagnetic secular change 169
variations: Deep mantle conductivity estimated from geomagnetic variations 169
- earthquakes** *see also* engineering geology; seismology; *see also under* engineering geology *under* Arizona; California; South Carolina; Utah; *see also under* seismology *under* Alaska; California; Costa Rica; Guatemala; Nicaragua; Pacific Coast; South Carolina; Texas; United States; Western U.S.; Wyoming
- earthquakes—mechanism**
models: Source of earthquake energy 262
stress: Analysis of stress-concentration mechanism for intraplate earthquakes 172-173
- earthquakes—prediction**
experimental studies: Laboratory studies 256-257
research: Earthquake mechanics and prediction studies 253-257
- Eastern Hemisphere** *see also* Africa; Antarctica; Arctic Ocean; Atlantic Ocean; Indian Ocean
- Eastern U.S.—economic geology**
phosphate: Phosphate resources in the southeastern United States 43
uranium: Genesis of tabular uranium bodies in Triassic and Jurassic basins in Eastern United States 27
- Eastern U.S.—environmental geology**
pollution: Environmental studies of the Mid-Atlantic outer continental shelf 147-148
- Eastern U.S.—geophysical surveys**
heat flow: Low heat flow values in the Southeastern United States 210
- Eastern U.S.—hydrogeology**
hydrology: Northeastern region 90-102
- Eastern U.S.—oceanography**
continental shelf: Analyses of sidescan sonar and high resolution seismic records for the Carolina to Florida continental shelf 148
 — Atlantic continental margin 144-148
 — Petroleum potential of the Mid-Atlantic continental margin 145
 — Stratigraphy and structure of the Atlantic continental margin and adjacent deep-sea floor 144-145
continental slope: Geologic environment of the Atlantic continental shelf 145-146
- ecology** *see also under* environmental geology *under* Alaska; California; Colorado; Georgia; Louisiana; North Carolina; Vermont; Virginia; Wisconsin; Wyoming; *see also under* paleontology *under* Florida
- ecology—Plantae**
terrestrial environment: Plant ecology 233-234
- Egypt—economic geology**
mineral resources: Egypt 342
- Egypt—hydrogeology**
ground water: Western Desert development potential 342
- elastic waves** *see under* seismology
- electrical logging** *see* well-logging
- electrical surveys** *see under* geophysical surveys *under* California; Florida; Hawaii; Minnesota
- electromagnetic surveys** *see under* geophysical surveys *under* Idaho
- electron microscopy—techniques**
trace-element analyses: Scanning electron microscopy study of the accessory minerals in coal 247
- energy sources** *see also under* economic geology *under* United States
- energy sources—resources**
international cooperation: Energy resources studies on behalf of other agencies 326
- engineering geology** *see also* environmental geology; geodesy; geophysical methods; ground water; land subsidence; mining geology; rock mechanics; soil mechanics

- engineering geology—general**
research: Engineering geology 264-265
- engineering geology—methods**
photogrammetry: Photogrammetry 356
- environmental geology** *see also* engineering geology
- environmental geology—general**
research: Geology and climate 213-218
 — Land use and environmental impact 317-323
- environmental geology—objectives**
mediation: Conflict resolution 325
- environmental geology—surveys**
United States: Environmental geochemistry 288-289
- Eocene** *see also* under stratigraphy under Colorado; Idaho; Texas; Wyoming
- eolian features** *see* under geomorphology
- erosion** *see* under processes under geomorphology
- Eurasia** *see also* Black Sea
- Europe** *see also* the individual nations
- explosions** *see also* under engineering geology under United States

F

- faults—displacements**
normal faults: Intertonguing, paleochannels, and faults in the Wasatch Plateau in Utah 14-15
 — Southern Elsinore fault zone in California 267
strike-slip faults: A major left-lateral strike-slip fault in the Wood River area of Idaho 66
 — Strike-slip faulting and crustal spreading in the Coso Range, California 195
 — Strike-slip faults in Lake Mead area of southern Nevada 71
thrust faults: Three structural styles in the Sapphire thrust belt in western Montana 67
 — Thrust faults near the Lewis and Clark line in Montana 68
 — Thrusts in City Creek Canyon near Salt Lake City, Utah 71
transform faults: Possible continental transform fault in northwest Washington 79
uplifts: Possible Lake George faulting 45
- faults—distribution**
active faults: Active faults in central Utah 56
basins: New information on tectonic framework on the Culpeper Triassic and Jurassic basin 51
conglomerate: Revised thickness of Hailey Conglomerate Member, Wood River Formation of central Idaho 58-59
continental margin: Faulting in coastal South-central California 150-151
deep-seated structures: Major deep-seated faults near Helena, Montana 67-68
fault scarps: Potential fault hazard in Ventura, California 291
fault zones: Geology of the northern Portneuf Range in southeastern Idaho 64-65

- metasedimentary rocks*: Age of rocks in Lake Char fault zone in south-central Massachusetts 46
- ore deposits*: Faulting in the Duluth Complex in Minnesota 6
- thrust belts*: The fold and thrust belt in southwestern Montana 66-67
- faults—systems**
fault zones: Syntectonic faults in eastern Connecticut 47-48
grabens: Reserve graben of west-central New Mexico 72
horsts: Faults south of Wenatchee, Washington 78
- fission-track dating** *see* under geochronology
- floods** *see* under rivers and streams under hydrology
- Florida—economic geology**
natural gas: Appalachian Basin and Florida 22-23
petroleum: Appalachian Basin and Florida 22-23
 — Source-rock potential of South Florida Basin 23
phosphate: Phosphate resources in the southeastern United States 43
- Florida—engineering geology**
waste disposal: Subsurface waste disposal 221-222
- Florida—environmental geology**
pollution: Environmental pollution of the Everglades in Florida 16-17
 — Ground-water contamination from percolation ponds 286
 — Impact of phosphate mining on the hydrology of Osceola National Forest, Florida 287
- Florida—geophysical surveys**
electrical surveys: Surface resistivity used in locating major aquifer 223
- Florida—hydrogeology**
ground water: Availability of water from a shallow limestone aquifer in the Jacksonville area 104
 — Contamination of a shallow aquifer by irrigation 106
 — Effects of phosphate mining on the Floridan aquifer 105
 — Identification of a limestone aquifer in southern Hendry County 105
 — Induced infiltration to new well fields 106
 — Leaky confined-aquifer conditions indicated in a sand-and-gravel aquifer at Pensacola 105
 — Paving does not necessarily reduce ground-water recharge 219
 — Potential sources of pollution to the Biscayne aquifer 105-106
 — Pumpage shutdown in industrial area yields significant information on recovery of water levels 104
 — Pumpage shutdown yields water-level recovery information 224-225
 — Saltwater intrusion causes abandonment of municipal-supply wells 105
 — Saltwater intrusion in Florida 222-223

- Saltwater intrusion in well fields 106
 — Top of Floridan Aquifer mapped 104
 — Water-bearing zone in the Hawthorn Formation identified in Lee County 105
 — Water from shallow aquifers in St. Johns County 104
hydrology: Availability of water in the Santa Fe River subbasin 104
 — Data management and instrumentation 137
 — Florida 104-106
 — Source of urban runoff in southern Florida 137
 — Water quality and well yield of the Ochlockonee River basin 104-105
- Florida—oceanography**
ocean circulation: Circulation modeling and turbidity monitoring in Tampa Bay, Florida 160
- Florida—paleontology**
ecology: Water temperature of corals shown by isotopic analysis 216
- fluid inclusions—analysis**
chemical analysis: A new ultramicrochemical analytical technique for fluid inclusions 177
- folds—distribution**
fold belts: The fold and thrust belt in southwestern Montana 66-67
volcanic rocks: Folds in Huckleberry Ridge Tuff (Pleistocene) in eastern Idaho 183
- foliation** *see also* structural analysis
- fossil man—occurrence**
archaeology: Geology contributes to archaeology and climate studies in northeast Arizona 268
- fossils** *see* appropriate fossil group
- foundations** *see also* rock mechanics; soil mechanics

G

- garnet** *see* under orthosilicates, garnet group under minerals
- genesis of ore deposits** *see* mineral deposits, genesis
- geochemistry—cycles**
nitrogen: NO₃-N uptake by algae in a streamlike environment 187
- geochemistry—experimental studies**
hydrochemistry: Experimental studies on chemistry of water 187-188
lead hydroxide: Lead hydroxide formation constants 187
water: Geochemistry of water and sediments 186-188
- geochemistry—general**
research: Experimental and theoretical geochemistry 176-177
 — Isotope and nuclear geochemistry 189-193
- geochemistry—methods**
statistical methods: Frequency distributions of elements 188-189
 — Geochemical anomalies 189
 — Statistical geochemistry and petrology 188-189

- geochemistry—processes**
diffusion: Aqueous geochemical kinetics studies 188
hydrogenation: Hydrogenation of coal and sulfide minerals 16
precipitation: Coprecipitation of metals with manganese oxide 187
- geochemistry—properties**
electrochemical properties: Adsorption of lead at variable-charge mineral surface 187
solubility: Salt and anhydrite 276
specific conductivity: Specific conductance and pH 247
thermodynamic properties: Thermodynamic behavior of titanomagnetite 177
- geochemistry—surveys**
Great Plains: Availability of soil elements to native plants 88-289
Missouri: Anomalous geochemical variability in Washington County, Missouri 188
United States: Environmental geochemistry 288-289
Western U.S.: Geochemical survey of the western energy regions 288
- geochronology** *see also* absolute age
- geochronology—fission-track dating**
zircon: Fission-track dating of the type Ordovician and Silurian 191
- geochronology—methods**
research: Advances in geochronometry 191-193
- geochronology—paleomagnetism**
correlation: Origin of natural remanent magnetization in red sedimentary rocks of the Moenkopi Formation in Arizona 168
lava: Picture Gorge Basalt coeval with middle part of Grande Ronde Basalt 180-181
reversals: Geomagnetic polarity event from Cobb Mountain in California 167
 — Paleomagnetic dating of glacial sediments underlying Taylor Dry Valley in Antarctica 168
- geochronology—tephrochronology**
eruptions: Post-caldera airfall pumice at Aniakchak caldera 84
floods: Age of the last major scabland flood of eastern Washington 78
- geochronology—time scales**
Cenozoic: Revised late Cenozoic geomagnetic polarity time-scale 167
Cretaceous: Cretaceous timescale for North America 229
Phanerozoic: Geochronology of the San Francisco volcanic field in Arizona 207
- geodesy—methods**
field studies: Field surveying 355
leveling: Special leveling projects 355
terrain classification: Aerial profiling of terrain 355
topography: Topographic surveys and mapping 355-361
- geologic hazards** *see also* land subsidence; *see also* under engineering geology under Atlantic Ocean; California; Guatemala; Mississippi; Nigeria; North Dakota; Pacific Coast; Utah; Virginia; *see also* under environmental geology under Alaska; Appalachians; California; Colorado; Georgia; Great Plains; Kansas; Massachusetts; Missouri; Montana; Nevada; Ohio; Pennsylvania; Rocky Mountains; Utah; Washington
- geologic hazards—earthquakes**
ground motion: Dynamic response of soils to shear 263
 — Estimation of design ground motions 263
 — Ground motion investigations 262-263
 — Research in soils engineering 264-265
landslides: The effect of scale on seismic-induced landslides 266
prediction: Earthquake mechanics and prediction studies 253-257
research: Earthquake hazard studies 257-264
 — Earthquake studies 250-264
 — Tectonic framework and fault investigations 257-261
strong motion: Processing of strong motion records 263
 — Strong-motion recording program 264
- geologic hazards—effects**
research: Topical and areal research 266-267
- geologic hazards—floods**
frequency: Flood frequency studies 281-283
maps: Flood mapping 283-284
research: Floods 280-284
statistical analysis: Flood-frequency estimates based on censored samples 283
- geologic hazards—land subsidence**
solution mining: Solution mine subsidence hazards 290-291
 — Solution mine subsidence hazards 292
- geologic hazards—landslides**
earthquakes: Landslides 263
field studies: Ground failure investigations 263-264
research: Landslide hazards 265-266
- geologic hazards—prediction**
research: Geology and hydrology applied to hazard assessment and environment 250-292
 — Hazards information and warnings 291-292
- geologic hazards—site exploration**
nuclear facilities: Reactor hazards 266-268
- geology—practice**
international cooperation: International cooperation in the earth sciences 326-354
 — Technical cooperation and participant study 332-337
publications: Book reports 366
 — Book reports 366-367
 — Books and maps 364
 — By mail 366-367
- How to obtain publications 366-367
 — Maps and charts 366
 — Maps and charts 367
 — National Technical Information Service 367
 — Open-file reports 365
 — Over the counter 366
 — Publications issued 365-366
 — Publications program 364-365
 — State list of publications on hydrology and geology 364
 — U. S. Geological Survey publications 364-367
- geology—research**
current research: Geochemistry, mineralogy, and petrology 176-189
general: Geologic and hydrologic principles, processes, and techniques 167-249
international cooperation: Cooperative scientific investigation and exchange 327-330
programs: Multilateral scientific programs 329-330
- geomorphology** *see also* glacial geology
- geomorphology—eolian features**
changes: Modification of eolian deposits 212
dunes: Daily cycles in coastal dune deposits 159
- geomorphology—fluvial features**
buried channels: Schlumberger soundings near Moorhead, Minnesota 172
channel geometry: Effects of clearcutting redwoods in the Redwood National Park of California 211
 — Shrinking channels of the North Platte and Platte Rivers 118
drainage patterns: Changes in ground-water quality caused by realignment of the Red River in northern Avoyelles Parish 116
 — Circular feature in Pennsylvania 308
 — Effects of the Teton Dam failure 211
 — New evidence supports Nebraskan age for origin of Ohio River drainage system 52-53
streams: Stream morphology 211-212
- geomorphology—landform description**
fault scarps: Cucamonga fault scarps 77
 — Geomorphology of fault scarps 260-261
terraces: Tentative dating of pre-Pleistocene deposits along the Kentucky River of central Kentucky 53
weathering: Geomorphology of the Augusta, Georgia area 52
- geomorphology—mass movements**
landslides: Ancient landslide dated in The Geysers steam field, California 266
 — Landslides near Melozitna River Canyon 83
 — Planetary geologic processes and histories 294-295
- geomorphology—processes**
aggradation: Storm-event aggradation of ephemeral streams 211
erosion: Reinterpretation of Grand Canyon geomorphology 71-72

- sedimentation*: Relationship between channel gradient and mean discharge 212
— Sediment accumulation rates in stream valleys of Wisconsin 211-212
- geomorphology—volcanic features**
calderas: Caldera on Snake River Plain 171
- geophysical methods—electrical methods**
applications: Nonlinear complex resistivity applied to ground-water and mineral chemistry 170
- geophysical methods—gravity methods**
accuracy: Accuracy of borehole gravity data 25
instruments: Variations in superconducting gravimeters 208
techniques: Digital terrain corrections for gravity data 175
- geophysical methods—magnetic methods**
interpretation: Magnetic depth estimates 173
techniques: Geomagnetic array data processing 174
- geophysical methods—magnetotelluric methods**
instruments: A d.c. SQUID magnetometer for geothermal exploration 207
interpretation: Noise problem in audiomagnetotelluric survey 174
techniques: New magnetotelluric field processing system 174
- geophysical methods—methods**
applications: Applied geophysical techniques 170-176
— Detection of shallow faults 175
— Underground fires in coal mines located by geophysical surveys 168
interpretation: Electrokinetic potential and magnetic anomalies 174
- geophysical methods—seismic methods**
applications: New seismic procedure for locating stratigraphic traps 24-25
instruments: New seismic instrumentation for geothermal surveys 195
- geophysical surveys** *see* electrical surveys *under* geophysical surveys *under* California; Florida; Hawaii; Minnesota; *see* electromagnetic surveys *under* geophysical surveys *under* Idaho; *see* gravity surveys *under* geophysical surveys *under* Antarctica; California; New Mexico; Wyoming; *see* magnetic surveys *under* geophysical surveys *under* Wisconsin; *see* magnetotelluric surveys *under* geophysical surveys *under* Arizona; Southwestern U.S.; *see* radioactivity surveys *under* geophysical surveys *under* South Carolina; *see* seismic surveys *under* geophysical surveys *under* Atlantic Ocean; Bering Sea; Gulf of Mexico; Hawaii; Idaho; Pacific Coast; Pacific Ocean; *see* surveys *under* geophysical surveys *under* Arizona; Atlantic Ocean; Caribbean region; Colorado; Idaho; Montana; Nevada; Pacific Ocean; Wyoming; *see also* geophysical methods
- geophysics** *see also* engineering geology
- geophysics—experimental studies**
general: Experimental geophysics 167-170
particulate materials: Infrared spectral behavior of fine particulate solids 170
petrophysics: Petrophysics 169-170
- Georgia—economic geology**
kaolin: Geologic mapping of Cretaceous and Tertiary kaolin in the Macon-Gordon district of Georgia 4
- Georgia—environmental geology**
ecology: Biology of the upper Chattahoochee River in Georgia 243
geologic hazards: Flood-depth frequency relations on natural streams in Georgia 282
— Magnitude and frequency of floods in metropolitan Atlanta, Georgia 281-282
- Georgia—geomorphology**
landform description: Geomorphology of the Augusta, Georgia area 52
- Georgia—hydrogeology**
ground water: Determination of depth to saltwater in the Albany area 106
— Dewatering operation indicates yield potential of crystalline rocks 107
— Results of long-term monitoring for saltwater in the Savannah area of Georgia and South Carolina 103
hydrology: Georgia 106-107
— Irrigation increasing in southwestern Georgia 139
— Variations in low-flow characteristics 106
- Georgia—sedimentary petrology**
sedimentation: Nearshore sedimentation in Upper Cretaceous deposits in Western Georgia 52
- Georgia—stratigraphy**
Cenozoic: Georgia subsurface studies 50-51
Cretaceous: Georgia subsurface studies 50-51
- geotechnics** *see* engineering geology
- geothermal energy** *see also* economic geology *under* Arizona; Basin and Range Province; California; Colorado; Hawaii; Idaho; Mexico; Montana; Nevada; New Zealand; Oregon; United States; Western U.S.
- geothermal energy—production**
reservoir rocks: Transient pressure analysis in vapor-dominated geothermal reservoirs 193
- geothermal energy—properties**
geothermal systems: Geothermal systems 193-210
reservoir properties: Numerical analysis of convection and thermoelastic effects in fault effecting geothermal systems 208-209
reservoir rocks: Electrical properties in a geothermal environment 169-170
- geothermal energy—resources**
data: Geotherm file 14
nomenclature: Terminology for geothermal resources assessment 41
- geothermal energy—theoretical studies**
geothermal systems: Two and three dimensional modeling of geothermal systems 193
- glacial geology** *see also* geomorphology
- glacial geology—glacial features**
glacial lakes: Middle Wisconsinan glacial lake near Scobbey, Montana 58
pingos: Pingo scars in southwestern South Dakota 57-58
- glacial geology—glaciation**
age: Glaciation near Togwotee Pass in the Wind River Mountains of Wyoming 27
— Soil development and age of Bull Lake Glaciation in the Rocky Mountains 57
deglaciation: Deglaciation in the Leominster-Fitchburg area, Massachusetts 45-46
— Time of Pinedale deglaciation in the Park Range of Colorado 57
extent: Early or Middle Pleistocene glaciation in the National Petroleum Reserve in Alaska 80-81
ice movement: Evidence from Massachusetts onshore and offshore areas for thrust coastal end moraines and a fluctuating ice margin of Woodfordian age 147
lakes: Glacial Lake Housatonic was complex 46
- glacial geology—glaciers**
ablation: Increased ablation in the Western United States in 1977 213
atlas: Atlas of glaciers 306
avalanches: Volcanic effects on snow and ice on Mount Baker, Washington 213
ice movement: Climate and glaciers 215
ice sheets: Mapping of the Greenland ice sheet 245
instruments: Hot-water drill for use in temperate glaciers 213
research: Glaciology 212-213
snow: Snowfall on Alaskan glaciers in 1976-77 212
- glaciation** *see under* glacial geology
- glaciers** *see under* glacial geology
- gold** *see also* economic geology *under* California; Idaho; Nevada; Oregon; Saudi Arabia; South Carolina; South Dakota; Wyoming
- gold—geochemistry**
tracer experiments: Anion complex of gold as ground-water tracer 223
- grabens** *see under* systems *under* faults
- granite** *see also* *under* granite-granodiorite family *under* igneous rocks
- gravity surveys** *see under* geophysical surveys *under* Antarctica; California; New Mexico; Wyoming
- Great Basin—economic geology**
natural gas: Great Basin and California 20-22
petroleum: Great Basin and California 20-22
— Permian source rocks, northeastern Great Basin 20
— Rates of sedimentation of petroleum source rocks in Utah, Nevada, and Idaho 21

- Great Britain—geochronology**
Silurian: Fission-track dating of the type Ordovician and Silurian 191
- Great Lakes region—areal geology**
research: Lake Superior region 53-54
- Great Lakes region—environmental geology**
waste disposal: Reevaluation of water resources of the Marquette Iron Range 95
- Great Plains—areal geology**
research: Rocky Mountains and the Great Plains 55-68
- Great Plains—economic geology**
natural gas: Natural gas resources of shallow, low-permeability (tight) reservoirs of the northern Great Plains 19-20
 — Rocky Mountains and Great Plains 18-20
petroleum: Rocky Mountains and Great Plains 18-20
- Great Plains—environmental geology**
geologic hazards: Duststorm of 1977 in the High Plains 217
 — Environmental geology 56-58
land use: Environmental geology 56-58
reclamation: Rehabilitation potential of coal lands in the central region evaluated 110-111
- Great Plains—geochemistry**
surveys: Availability of soil elements to native plants 88-289
- Great Plains—geophysical surveys**
heat flow: Geothermal gradients in the Northern Great Plains 201
- Great Plains—hydrogeology**
ground water: Hydrogeologic considerations for an interstate ground-water compact on Madison Aquifer, northern Great Plains 110
- Great Plains—stratigraphy**
Mississippian: Coral zones and problems of Mississippian stratigraphy in the Williston Basin 232
- Greenland—geophysical surveys**
maps: Mapping of the Greenland ice sheet 245
- ground water** *see also* hydrogeology; hydrology
- ground water—aquifers**
models: Aquifer-model studies 218-220
water storage: Long-term storage of fresh-water in saline aquifer 225
- ground water—contamination**
pollutants: Fate of wood preservatives in ground water 284
radioactive waste: Hydrologic investigations relative to the disposal of low level radioactive waste 280
research: Effects of pollutants on water quality 284-288
- ground water—geochemistry**
hydrochemistry: Nonlinear complex resistivity applied to ground-water and mineral chemistry 170
water: Water sampling for uranium exploration 37-38
- ground water—levels**
changes: Barometric effects on water levels in unconfined aquifers 223
- ground water—models**
heat storage: Simulation of heat-energy storage in a ground-water reservoir 218
systems analogs: Hydrogeologic system simulation 219
transport: Solute-transport model for ground water 109
- ground water—movement**
cycles: Relation between surface water and ground water 238-239
tracer experiments: Anion complex of gold as ground-water tracer 223
- ground water—recharge**
artificial recharge: Artificial recharge 220-221
- ground water—surveys**
Alaska: Geohydrologic analysis 303
 — Large springs north of Delta Junction 125-126
Arbuckle Aquifer: Geohydrology of the Arbuckle aquifer, south-central Oklahoma 119
Arikaree Aquifer: Digital model predicts water-level declines and streamflow depletions near Wheatland 124
 — Preliminary digital model of the Sweet-water River basin 123
Arkansas: Water-resource literature for Arkansas annotated 111
Atlantic Coastal Plain: Freshwater in offshore aquifers 224
 — Results of long-term monitoring for saltwater in the Savannah area of Georgia and South Carolina 103
 — Southeastern region 102-108
Big Sioux Aquifer: Big Sioux aquifer in parts of eastern South Dakota extends beyond stream valleys 120-121
Biscayne Aquifer: Potential sources of pollution to the Biscayne aquifer 105-106
Buffalo Aquifer: Appraisal of the Buffalo aquifer 96
California: Geothermal gradient is 800°C at Coso Hot Springs 126-127
 — Ground-water studies in desert basins 127-128
 — Nitrogen studied in the Santa Ana River basin 127
 — Water supply at Beale Air Force Base unchanged 128
Cambodia: Ground-water resources 340
Chicot Aquifer: Model of the Chicot and Evangeline aquifers in Houston, Texas 218
 — Potential saltwater encroachment in southwestern Louisiana 160
Coconino Aquifer: Water use may double in Apache County 126
Colorado: Availability and quality of ground water in the Gunnison-Crested Butte area 111
 — Geologic and hydrologic mapping in the Colorado Front Range Urban Corridor to aid local regional planners 317-318
- Piceance Basin model 113
 — Reconditioning of geohydrologic test holes in an oil-shale formation 113
 — Two-dimensional finite-difference model developed for the closed-basin area of San Luis Valley 114
 — Water-level fluctuations and residential waste-treatment systems 114
 — Water-management plans for the South Platte River valley 112-113
 — Water quality in Boulder County 112
 — Water quality of springs and productivity of wells in the Piceance Basin 113-114
 — Water-table aquifers in the Boulder-Fort Collins-Greeley area of the Front Range Urban Corridor 112
Connecticut: Appraisal of ground-water availability and quality in Farmington 91
 — Evaluation of the stratified-drift aquifer in the Pootatuck River valley 91
Eastern U.S.: Northeastern region 90-102
Edwards Aquifer: Effects of carbonate facies and faulting on hydrogeology of the Edwards Aquifer 223-224
Egypt: Western Desert development potential 342
Evangeline Aquifer: Model of the Chicot and Evangeline aquifers in Houston, Texas 218
Florida: Availability of water from a shallow limestone aquifer in the Jacksonville area 104
 — Contamination of a shallow aquifer by irrigation 106
 — Ground-water contamination from percolation ponds 286
 — Identification of a limestone aquifer in southern Hendry County 105
 — Induced infiltration to new well fields 106
 — Leaky confined-aquifer conditions indicated in a sand-and-gravel aquifer at Pensacola 105
 — Pumpage shutdown yields water-level recovery information 224-225
 — Saltwater intrusion causes abandonment of municipal-supply wells 105
 — Saltwater intrusion in Florida 222-223
 — Saltwater intrusion in well fields 106
 — Surface resistivity used in locating major aquifer 223
 — Water from shallow aquifers in St. Johns County 104
Floridan Aquifer: Availability of water in the Santa Fe River subbasin 104
 — Effects of phosphate mining on the Floridan aquifer 105
 — Impact of phosphate mining on the hydrology of Osceola National Forest, Florida 287
 — Paving does not necessarily reduce ground-water recharge 219
 — Pumpage shutdown in industrial area yields significant information on recovery of water levels 104

- Subsurface waste disposal 221-222
- Top of Floridan Aquifer mapped 104
- Water-bearing zone in the Hawthorn Formation identified in Lee County 105
- Water quality and well yield of the Ochlockonee River basin 104-105
- Georgia*: Determination of depth to saltwater in the Albany area 106
- Dewatering operation indicates yield potential of crystalline rocks 107
- Great Plains*: Quality of water in abandoned zinc mines in northeastern Oklahoma and southeastern Kansas 111
- Rehabilitation potential of coal lands in the central region evaluated 110-111
- Idaho*: Ground-water stress in southeastern Idaho 128-129
- Hydrology of subsurface waste disposal, Idaho National Engineering Laboratory in Idaho 279
- Pollution of the Snake Plain aquifer 286
- "Sole-source" study 125
- Water resources in Camas Prairie 129
- Illinois*: Hydrologic evaluation of a radioactive-waste burial site near Sheffield, Illinois 280
- Sludge-irrigation hydrology 92
- Indiana*: Availability of ground water in the Upper White River basin 92
- Geology and hydrology of the Indiana Dunes National Lakeshore area 92
- Leachate movement in opposite directions in outwash aquifer separated into two units by clay 93
- Unconsolidated aquifers near Logansport 92-93
- Iowa*: Drought effect and recovery noted in Iowa carbonate aquifers 114
- Jasper Aquifer*: Jasper aquifer mapped in the Coastal Plain of Texas 121
- Kansas*: Chemical quality of ground water in Kansas 236
- Chloride concentration of ground-water discharge to Smoky Hill River in Kansas 115
- Geohydrology of saline water occurrence in the Wellington Formation in central Kansas 115
- Ground-water mining in west-central Kansas 114-115
- Modeling of river valleys in north-central Kansas 115
- Streamflow losses in the Arkansas River, western Kansas 115
- Kenya*: Rural water-resource development 343
- Louisiana*: Changes in ground-water quality caused by realinement of the Red River in northern Avoyelles Parish 116
- Fresh ground water mapped in St. James Parish in Louisiana 116
- Freshwater anomalies over three Louisiana salt domes 116
- Ground-water in lignite areas of De Soto Parish 116
- Ground-water resources of Washington Parish 116
- Madison Aquifer*: Hydrogeologic considerations for an interstate ground-water compact on Madison Aquifer, northern Great Plains 110
- Second test well completed in the Madison aquifer 118
- Maine*: Geohydrology of the Androscoggin Valley Regional Planning Area 93
- Ground-water resources in the Portland area 93
- Massachusetts*: A water budget for Nantucket Island 95
- Freshwater-saltwater relations on Cape Cod 94
- Ground-water assessment in the lower Merrimack River basin 94-95
- Ground-water development on Cape Cod 95
- Results of water-level survey at Martha's Vineyard 93-94
- Trace metals in ground water on Cape Cod 94
- Mexico*: Tropical carbonate aquifers 344
- Michigan*: Effects of waste-water irrigation on ground-water conditions 218-219
- Reevaluation of water resources of the Marquette Iron Range 95
- Micronesia*: Ground-water yields small in Truk Islands 128
- Minnesota*: Appraisal of a sand-plain aquifer in central Minnesota 96
- Availability of ground water in southwestern Minnesota 96
- Ground-water appraisal in sand plains of Benton, Sherburne, Stearns, and Wright Counties 96-97
- Hydrology and ground-water quality in a potential mining area in northeastern Minnesota 95-96
- Interflow in uncased multiaquifer wells 96
- Planning study in the Pelican River sand plain 96
- Mississippi*: Base of freshwater above salt domes 225
- Montana*: Ground-water resources of the Poplar River basin, northeastern Montana 116-117
- Localized saline seep development in Hailstone Basin in Montana 117-118
- Site-specific coal-land reclamation study near East Trail Creek, southern Montana 117
- Thermal ground water 117
- Nebraska*: High nitrate concentrations found under a Nebraska prairie 236
- Natural filtration used in artificial recharge investigation 220-221
- Nevada*: Aquifers underlie Carson Desert 130
- Chemical character of ground water associated with the Soda Lakes geothermal area near Fallon, Nevada 193-194
- Hydrologic evaluation of radioactive waste buried near Beatty, Nevada 280
- Hydrologic investigation of the Eleana Formation, Nevada Test Site 279
- Hydrology and geology of the Carson City area 129
- Iodide- and bromide-tracer studies in carbonate rocks 223
- Kinetic controls on ground-water chemistry in a volcanic aquifer 187-188
- Monitoring ground-water quality in Nevada 286
- Overdraft in Pahrump Valley 129-130
- Waste brines are rich in metals 129
- Water supply stable in Fort McDermitt Indian Reservation 129
- New Jersey*: Saltwater intrusion into the Old Bridge Sand Member of the Magoghy Formation of New Jersey 160-161
- Water-resources potential of the Wharton Tract 97
- New Mexico*: Digital-computer model simulates ground-water flow in the lower Mesilla Valley of Texas and New Mexico 111
- Geohydrology of the Proposed Waste Isolation Pilot Plant in southeastern New Mexico 278-279
- Ground water near Capulin 118-119
- New York*: Areas of contamination delineated in ground water in Suffolk County 98
- Artificial recharge 138
- Beds of clay impose limits on available fresh ground water on Shelter Island 98
- Diversion of the Hudson River in Pleistocene time 97
- Effects of wastewater-management schemes on ground-water reservoir evaluated 97
- Extraction of chromium and cadmium from aquifer material 97
- Glacial deposits may be thin at artificial-recharge site 98
- Investigation of nitrogen in ground water on Long Island, New York 285
- Movement of bacteria in the Cretaceous Magoghy Formation 286
- Nitrate in ground water 285-286
- Position of freshwater-saltwater interface on South Fork, Long Island 97
- Storm-water basins for aquifer recharge with reclaimed water 220
- Water-table recovery causes flooding problems 98
- New Zealand*: Ground-water flow simulator applications 344
- North Carolina*: Water sources and geology along the Blue Ridge Parkway 107
- North Dakota*: Buried glaciofluvial aquifer system in southeastern McIntosh County in North Dakota 119
- Ground-water flow model of Harmon lignite at Gascoyne Mine, North Dakota 119

- Hydrologic evaluation of mining and reclamation in the Beulah Trench area of North Dakota 119
- Ogallala Formation*: Effects of mixing injected and native waters 220
- Ohio*: Steady state flow conditions simulated for potential strip mining areas in Ohio 219-220
- Oklahoma*: Quality of ground-water varies in prospective coal-lease areas of east-central Oklahoma 119-120
- Oregon*: Ground water in southern Douglas County 130
- Philippine Islands*: Shallow ground-water potential, Subic Naval Base 346
- Piney Point Aquifer*: Two-dimensional model of the Piney Point Aquifer 93
- Puerto Rico*: Artificial recharge with wastewater 221
- Rhode Island*: Measurement of aquifer characteristics in the Pawcatuck River basin 99
- Saudi Arabia*: Future water supplies for Riyadh 350
- Water-resource development 350
- South Carolina*: Hydrologic evaluation of radioactive waste buried in Barnwell County, South Carolina 280
- Saltwater encroachment in the principal artesian aquifer for Beaufort, Colleton, Hampton, and Jasper Counties 107-108
- South Dakota*: A thick glacial-drift deposit contains several outwash aquifers in Miner County 121
- Extensive aquifers occur in alluvium and outwash deposits in Walworth County 121
- Large ground-water yields in northeastern South Dakota 121
- Madison Group only a part of a major aquifer system in South Dakota 120
- Major outwash aquifers located in southeastern South Dakota 120
- Sri Lanka*: Jaffna Peninsula irrigation development review 350
- Tennessee*: Ground-water exploration in carbonate rocks 108
- Using infrared aerial photographs for ground-water exploration 313
- Texas*: Digital-computer model simulates ground-water flow in the lower Mesilla Valley of Texas and New Mexico 111
- Geohydrology of the Northeastern Texas salt-dome basin 121-122
- Turkey*: Turkey 351
- Tuscaloosa Aquifer*: "Tuscaloosa aquifer system" in Mississippi 107
- United States*: Central region 108-124
- Interstate studies 110-111
- Multistate studies 109
- Utah*: Declining ground-water levels in the Beryl-Enterprise area of southwestern Utah 123
- Evaluation of aquifers in southern Utah 122
- Navajo Sandstone evaluated as an alternative source of water for energy development in the Kaiparowits Plateau area in south-central Utah 123
- Navajo Sandstone source of ground water for future energy-related development in southeastern Utah 122
- Reasons for deterioration of the Bonneville Salt Flats 122-123
- Spring discharge and water-quality data on coal areas of east-central Utah 123
- Vermont*: Ground-water resources in the Rutland area 99
- Virginia*: Geohydrologic studies to guide exploratory drilling for ground water in Fairfax County, Virginia 317
- Wabash River*: Saline ground water near Vincennes 92
- Washington*: Coal-hydrology studies 132
- Colville (No Name Creek basin) 130-131
- Lower Elwha 131
- Port Gamble 131
- Port Madison 131
- "Sole-source" study 125
- Swinomish 131
- Test well drilling in Washington State 132
- Tulalip 131
- Yakima 131-132
- West Virginia*: Hydrology of the Guyandotte River basin 100
- Western U.S.*: Interstate studies 125
- Western region 124-133
- Wisconsin*: Concentrations of toxic heavy metals in water from wells in Wisconsin 101
- Simulation of pumping in Dane County, Wisconsin 220
- Wyoming*: Shallow ground-water flow systems in the northern Powder River basin 110
- Yemen*: Ground-water survey activities 351
- Guatemala—economic geology**
- petroleum*: Application of helium surveys to petroleum exploration 24
- Guatemala—engineering geology**
- geologic hazards*: Seismic engineering studies 264
- Guatemala—seismology**
- earthquakes*: Guatemala 262
- Guatemala 342
- Gulf Coastal Plain—environmental geology**
- land use*: Land use and land cover research and analysis 320-322
- Gulf Coastal Plain—hydrogeology**
- hydrology*: Atlantic and Gulf Coast 159-161
- thermal waters*: Geochemistry of geopressed geothermal waters 203
- Gulf of Mexico—economic geology**
- natural gas*: Oil and gas resources of the Gulf of Mexico 23
- petroleum*: Oil and gas resources of the Gulf of Mexico 23
- Gulf of Mexico—geophysical surveys**
- seismic surveys*: Multichannel seismic data raise questions concerning the Mesozoic age of the crust beneath the Gulf of Mexico 148-149
- Gulf of Mexico—oceanography**
- continental shelf*: Sediment deposition and movement, Gulf of Mexico continental shelf 149
- marine geology*: Gulf of Mexico and Caribbean Sea 148-150
- sedimentation*: Sediments of Corpus Christi Bay 149-150
- Submarine landslides on the Mississippi Delta 149
- gymnosperms—Coniferales**
- Holocene*: Tree-growth rates reflect changes resulting from drainage construction 233
- ## H
- Hawaii—economic geology**
- geothermal energy*: Characteristics of a Hawaiian geothermal system 204
- mineral resources*: Soil-gas investigations, Hawaii Volcanoes National Park in Hawaii 10-11
- Hawaii—environmental geology**
- pollution*: Mercury outgassing in Hawaii 289
- Hawaii—geochemistry**
- isotopes*: ^{18}O and δD values of Hawaiian basalts and xenoliths 190-191
- soil gases*: Soil-gas investigations, Hawaii Volcanoes National Park in Hawaii 10-11
- Hawaii—geophysical surveys**
- electrical surveys*: Self-potential anomalies on volcanos 172
- seismic surveys*: Refraction study of the southeast coast of Kilauea 195
- Hawaii—hydrogeology**
- hydrology*: Hawaii 128
- Wailuku River basin characterized 128
- Water use in Hawaii in 1975 139
- Hawaii—petrology**
- volcanology*: Hawaiian volcano studies 179-180
- Hawaii—volcanology**
- Kilauea*: Activity at Kilauea Volcano in 1977 179
- Paths of magma ascent in the Earth 180
- Mauna Loa*: Rate of inflation shows at Mauna Loa Volcano 179
- Structural evolution of Mauna Loa Volcano 179-180
- heat flow** *see also under* geophysical surveys *under* Bering Sea; Colorado; Eastern U.S.; Great Plains; Idaho; Wyoming; *see also under* tectonophysics *under* Basin and Range Province; Nevada; Western U.S.
- heavy minerals** *see also under* economic geology *under* Alaska; New York; South Carolina
- helium—geochemistry**
- soil gases*: Mobile helium-detection equipment used in uranium exploration 37
- surveys*: Application of helium surveys to petroleum exploration 24

- water*: Helium and radon in uranium exploration 12
- Holocene** *see also* under stratigraphy under Arizona; Washington
- hydrocarbons** *see* under organic materials
- hydrogeology** *see also* ground water; hydrology
- hydrogeology—general**
research: Ground-water hydrology 218-225
 — Miscellaneous studies 221-225
- hydrogeology—methods**
research: New hydrologic instruments and techniques 244
- hydrogeology—practice**
international cooperation: International Hydrological Program and related activities 337-351
 — Other international activities 339
publications: State hydrologic unit maps 364-365
 — State list of publications on hydrology and geology 364
 — State water-resources investigations folders 365
 — Surface-water, quality-of-water, and ground-water-level records 364
 — USGS contributions to publications 338
research: Domestic activities related to international programs 339
review: Review of hydrologic investigations 339
 — Summary by countries 339-351
U. S. National Committee on Scientific Hydrology: USNC/SH investigations 338-339
- hydrogeology—textbooks**
lakes: Primer on limnology 132
- hydrology** *see also* ground water; hydrogeology
- hydrology—cycles**
evapotranspiration: Evaporation and transpiration 239-240
models: Model studies 139
 — Water-table configuration related to lake seepage 239
research: Relation between surface water and ground water 238-239
- hydrology—general**
programs: International Hydrological Program and related activities 337-351
research: Chemical, physical, and biological characteristics of water 234-238
- hydrology—instruments**
drills: Hot-water drill for use in temperate glaciers 213
samplers: Design requirements for pumping samplers 212
- hydrology—limnology**
research: Limnology and potamology 240-244
- hydrology—methods**
remote sensing: Applications to hydrologic studies 312-314
 — Landsat surveillance of water turbidity and color 313
- Surface-water applications of Landsat data 313-314
research: New hydrologic instruments and techniques 244
- hydrology—rivers and streams**
estuaries: Estuarine and coastal hydrology 159-163
floods: Flood-frequency estimates based on censored samples 283
 — Flood frequency studies 281-283
 — Flood mapping 283-284
 — Floods 280-284
hydrochemistry: Investigations of volatile organic compounds and gases in streams 238
models: Applications of modeling 225-227
research: Surface-water hydrology 225
sedimentation: Variability of sediment discharge 210
streamflow: Estimating flow characteristics at ungaged sites 225
- hydrology—surveys**
Africa: Senegal, Mauritania, and Mali 350
Alabama: Alabama 103-104
 — Effects of surface coal mining on the hydrology of Warrior coal field 103
 — Relation of geology to low flow in Alabama streams 103-104
 — Statistical analyses of water quality 103
Alaska: Alaska 125-126
 — Benthic invertebrates in a north-flowing stream and a south-flowing stream in Brooks Range, Alaska 243
 — Large springs north of Delta Junction 125-126
 — Reconnaissance of lakes in the National Petroleum Reserve in Alaska 242-243
Amazon River: Sediment studies of the Amazon River 340
Androscoggin River: Geohydrology of the Androscoggin Valley Regional Planning Area 93
Appalachians: Appalachian flood of April 1977 in Kentucky, Tennessee, Virginia, and West Virginia 281
Argentina: Argentina, Bolivia, and Paraguay 339
Arizona: Arizona 126
 — Perennial streams and wetlands of Arizona 233-234
Arkansas: Arkansas 111
 — Water-resource literature for Arkansas annotated 111
Arkansas River: Organic contamination of the Arkansas River in Pueblo County, Colorado 284-285
 — Streamflow losses in the Arkansas River, western Kansas 115
Atlantic Coastal Plain: Atlantic and Gulf Coast 159-161
 — Interstate studies 103
 — Southeastern region 102-108
Black River: Low-flow characteristics of streams in the Trempealeau-Black River basin 101-102
- Bolivia*: Argentina, Bolivia, and Paraguay 339
Brazil: Brazil 340
California: California 126-128
 — Copper cycles and copper sulfate algal capacity in two California lakes 241-242
Cambodia: Cambodia 340
Chattahoochee River: Biology of the upper Chattahoochee River in Georgia 243
Colorado: Benthic invertebrates in Piceance Creek, northwestern Colorado 111
 — Colorado 111-114
 — Water quality in Boulder County 112
Connecticut: Connecticut 91-92
Eastern U.S.: Northeastern region 90-102
- Florida*: Data management and instrumentation 137
 — Florida 104-106
 — Impact of phosphate mining on the hydrology of Osceola National Forest, Florida 287
 — Source of urban runoff in southern Florida 137
Fox River: Low-flow characteristics of streams in the Rock-Fox River basin 101
Georgia: Flood-depth frequency relations on natural streams in Georgia 282
 — Georgia 106-107
 — Irrigation increasing in southwestern Georgia 139
 — Magnitude and frequency of floods in metropolitan Atlanta, Georgia 281-282
 — Variations in low-flow characteristics 106
Gila River: Evapotranspiration from saltcedar in the Gila River flood plain in Arizona 239-240
Green River basin: Green River basin water-quality investigations 234
 — Stream-temperature model for the Green River basin in Wyoming 124
Guyandotte River basin: Hydrology of the Guyandotte River basin 100
Hawaii: Hawaii 128
 — Water use in Hawaii in 1975 139
Housatonic River: FCB concentrations in bottom sediments of the Housatonic River 91-92
Hudson River: Dye used to study mixing of waters of the Hudson River estuary 98
 — PCB and suspended-sediment transport in the Hudson River 284
Idaho: Channel width as an indicator of discharge characteristics in Idaho 227
 — Idaho 128-129
Illinois: Illinois 92
Indiana: Indiana 92-93
Indonesia: Indonesia 343
 — Sediment study program assistance 343
Iowa: Drought effect and recovery noted in Iowa carbonate aquifers 114
 — Iowa 114

- Iowa sediment-data compiled 114
- Kansas*: Flood-hazard mapping in Kansas 283
- Kansas 114-115
- Modeling of river valleys in north-central Kansas 115
- Lake Champlain*: Marsh plants depend on nitrogen and phosphorus from sediments 241
- Lake Koochanusa*: Lake Koochanusa water quality program 242
- Laramie River*: Digital model predicts water-level declines and streamflow depletions near Wheatland 124
- Louisiana*: Louisiana 115-116
- Time of travel of solutes in Louisiana streams 115-116
- Maine*: Limnology of Maine lakes 240-241
- Maine 93
- Maryland*: Maryland 93
- Massachusetts*: Deglaciation in the Leominster-Fitchburg area, Massachusetts 45-46
- Flood-frequency model for small streams in Massachusetts 282
- Massachusetts 93-95
- Michigan*: Michigan 95
- Minnesota*: Hydrology and ground-water quality in a potential mining area in northeastern Minnesota 95-96
- Minnesota 95-97
- Mississippi*: Mississippi 107
- Scour at a bridge in Mississippi 281
- Mississippi River*: Benthic invertebrates of the lower Mississippi River 243-244
- Organic compounds in the Lower Mississippi River 237
- Missouri*: Effects of mining on water quality 286
- Floods in Missouri and Kansas in 1977 281
- Magnitude and frequency of floods in St. Louis County, Missouri 282
- Soil temperatures indicate gaining and losing streams 239
- Montana*: Flood-insurance study for Belt, Montana 283
- Floods of June 1976 in Culbertson, Montana 280
- Localized saline seep development in Hailstone Basin in Montana 117-118
- Montana 116-118
- Site-specific coal-land reclamation study near East Trail Creek, southern Montana 117
- Water quality of selected streams in the Fort Union coal area, southeastern Montana 117
- Nebraska*: Nebraska 118
- Nevada*: Flood hazards in Carson City, Nevada 283
- Nevada 129-130
- New Jersey*: New Jersey 97
- New Jersey water-quality investigations 235
- New Mexico*: New Mexico 118-119
- New River*: Studies show pollution of streams 126
- New York*: Effects of wastewater-management schemes on ground-water reservoir evaluated 97
- Modeling lake drawdown caused by well pumpage 238-239
- New York 97-98
- New Zealand*: New Zealand 344
- Nigeria*: Federal Capital Territory reconstruction 345
- Nisqually Lake*: Nisqually, an undeveloped lake 133
- North Carolina*: Chemical quality of streams in North Carolina 234-235
- North Carolina 107
- North Dakota*: North Dakota 119
- North Platte River*: Algal growth potential of North Platte reservoirs 242
- Shrinking channels of the North Platte and Platte Rivers 118
- Ochlockonee River*: Water quality and well yield of the Ochlockonee River basin 104-105
- Ohio*: Assessment of water quality in an Ohio watershed 235
- Magnitude and frequency of Ohio floods 282-283
- Oklahoma*: Oklahoma 119-120
- Quality of water in Oklahoma's abandoned coal pits 120
- Stream-water quality in eastern Oklahoma coalfield 120
- Oneida Lake*: Large concentrations of ferromanganese nodules found in Oneida Lake, New York 241
- Oregon*: Oregon 130
- Red colonies on fecal-coliform-bacteria plates identified 238
- Streets contribute much lead to urban runoff 130
- Water quality of active and inactive log ponds 241
- Ozette Lake*: Salmon propagation in Ozette Lake 133
- Pacific Coast*: Pacific Coast 161-163
- Pamlico Sound*: Water budget of Pamlico Sound, North Carolina 161
- Paraguay*: Argentina, Bolivia, and Paraguay 339
- Pecos River*: Hydrologic effects of saltcedar control on the Pecos River flood plain in New Mexico 240
- Pennsylvania*: Floods of July 1977 in the Johnstown area of western Pennsylvania 281
- Nutrient and sediment discharges for agricultural land 98-99
- Pennsylvania 98-99
- Philippine Islands*: Philippine Islands 346
- Platte River*: Shrinking channels of the North Platte and Platte Rivers 118
- Potomac River*: Distribution of biologically reactive substances in the Potomac Estuary 159-160
- Estuarine sediment sources of the Potomac Estuary 159
- Puerto Rico*: Inundation maps of urban areas 283-284
- Rhode Island*: Rhode Island 99
- Rio Pilcomayo*: Rio Pilcomayo sedimentation 339
- Rock River*: Low-flow characteristics of streams in the Rock-Fox River basin 101
- Saint Joseph River*: Agricultural land use related to chemical and physical erosion 95
- Santa Ana River basin*: Nitrogen studied in the Santa Ana River basin 127
- Santa Fe River*: Availability of water in the Santa Fe River subbasin 104
- Senegal River*: Senegal River basin data assessment 350
- South Carolina*: South Carolina 107-108
- South Cascade Glacier*: Subglacier dye-injection test 213
- South Dakota*: South Dakota 120-121
- South Platte River*: Effects of proposed "Narrows" reservoir on South Platte River 113
- Water-management plans for the South Platte River valley 112-113
- Sri Lanka*: Sri Lanka 350
- Sulphur Creek Basin*: Cyclic variations in drain-water quality 133
- Susquehanna River basin*: Effects of land use on water quality of rivers 234
- Sweetwater River*: Preliminary digital model of the Sweetwater River basin 123
- Tennessee*: Tennessee 108
- Texas*: Texas 121-122
- Water quality of selected reservoirs in Texas 242
- Tillamook River*: Estuarine sediment sources in the Tillamook Estuary in Oregon 163
- Trempealeau River*: Low-flow characteristics of streams in the Trempealeau-Black River basin 101-102
- United States*: Central region 108-124
- Comparison of USGS urban-basin model and rational-method estimate of peak discharge 137
- Estimated use of water in the United States in 1975 139
- Flood-frequency studies 137
- Maps of flood-prone areas 283
- Marine geology and coastal hydrology 144-163
- National Stream-Quality Accounting Network 140-143
- National Water Data Exchange 135-136
- National water quality programs 140
- Office of Water Data Coordination 133-135
- Special water-resource programs, data coordination, acquisition, and storage 133-143
- Urban water program 136-139
- Water-Data Storage System 136
- Water-quality changes 142-143
- Water-quality conditions 140-142

- Water-quality studies 138-139
 - Water resources investigations 89-143
 - Water use 139-140
 - Utah*: Utah 122-123
 - Vermont*: Vermont 99
 - Wailuku River*: Wailuku River basin characterized 128
 - Washington*: Coal-hydrology studies 132
 - Colville (No Name Creek basin) 130-131
 - Irrigation increased in Horse Heaven Hills 132
 - Lake studies 132-133
 - Makah 131
 - Model predicts snowmelt runoff 133
 - Port Madison 131
 - Primer on limnology 132
 - Southern Cascade Range borehole drilling program 212-213
 - Studies on Indian reservations 130-132
 - Swinomish 131
 - Tulalip 131
 - Washington 130-133
 - Water-quality effects of underground coal mining 243
 - Water use in Washington for 1975 139-140
 - Yakima 131-132
 - West Virginia*: Effects of deep mining on base flow 99
 - West Virginia 99-100
 - Western U.S.*: Interstate studies 125
 - Western region 124-133
 - White River*: Traveltime and dispersion characteristics of the White River in the Uinta Basin oil-shale area 122
 - White River basin*: Availability of ground water in the Upper White River basin 92
 - Wilderness Lake*: Nutrient loading and budget of Wilderness Lake 132-133
 - Willamette River*: Analyses of Willamette River bottom material and elutriates 236
 - Wisconsin*: Effects of a powerplant on streamflow and lake levels 100
 - Low-flow characteristics of small streams in 32 basins 100
 - Preimpoundment conditions in a small drainage basin 101
 - Wetland vegetation reflects hydrology 233
 - Wisconsin 100-102
 - Wisconsin River*: Low-flow characteristics at gaging stations on the Wisconsin, Fox, and Wolf rivers 100
 - Low-flow characteristics of streams in the lower Wisconsin River basin 100-101
 - Wood River*: Measurement of aquifer characteristics in the Pawcatuck River basin 99
 - Wyoming*: Analysis of runoff from small drainage basins in Wyoming 123-124
 - Wyoming 123
 - Yakima River basin*: Irrigation return flows in the lower Yakima River basin of Washington 210
 - Yalobusha River*: Flood elevations of canalized stream in Mississippi 282
 - Yampa River*: Estimating regional water use and residuals output from energy development 140
 - Yampa River basin*: Flow and salinity modeling of proposed reservoirs in the Yampa River basin 242
 - Yellowstone National Park*: Size of glacial streams in Yellowstone National Park 215-216
 - Yemen*: Yemen 351
 - hydrology—techniques**
 - laser probe*: Suspended-sediment analysis by laser-light methods 212
 - spectroscopy*: Chemical reactivity of sediment in aqueous systems 235-236
 - hydrothermal alteration** *see under* processes *under* metasomatism
- I
- Idaho—economic geology**
 - base metals*: Mineralized volcanic arc in westernmost Idaho and adjacent Oregon 69
 - geothermal energy*: Seismic refraction of Raft River in Idaho 40
 - Snake River plain, Idaho, geothermal well studies 39-40
 - gold*: Trace elements in silver-lead-gold veins in Idaho 9-10
 - lead*: Trace elements in silver-lead-gold veins in Idaho 9-10
 - petroleum*: Economic geology 55-56
 - Hydrocarbon potential north of Snake River Plain of Idaho and Montana 55
 - Permian source rocks, northeastern Great Basin 20
 - Rates of sedimentation of petroleum source rocks in Utah, Nevada, and Idaho 21
 - phosphate*: Methodology for post-EIS monitoring 322
 - Phosphate resources of the Hawley Creek area in Idaho 44
 - silver*: Trace elements in silver-lead-gold veins in Idaho 9-10
 - Idaho—engineering geology**
 - waste disposal*: Hydrology of subsurface waste disposal, Idaho National Engineering Laboratory in Idaho 279
 - Idaho—environmental geology**
 - pollution*: Pollution of the Snake Plain aquifer 286
 - Idaho—geochemistry**
 - trace elements*: Trace elements in silver-lead-gold veins in Idaho 9-10
 - Idaho—geomorphology**
 - fluvial features*: Effects of the Teton Dam failure 211
 - Idaho—geophysical surveys**
 - electromagnetic surveys*: EM modeling and inversion programs 174
 - heat flow*: Temperatures and heat flow in wells near the Raft River geothermal area of Cassia County in Idaho 197
 - remote sensing*: Evaluation of algorithms for geological thermal-inertia mapping 310-311
 - seismic surveys*: Seismic refraction of Raft River in Idaho 40
 - surveys*: Caldera on Snake River Plain 171
 - Magnetic and gravity expressions of the Lewis and Clark Line 170
 - Idaho—hydrogeology**
 - ground water*: Ground-water stress in southeastern Idaho 128-129
 - “Sole-source” study 125
 - Water resources in Camas Prairie 129
 - hydrology*: Channel width as an indicator of discharge characteristics in Idaho 227
 - Idaho 128-129
 - Idaho—petrology**
 - igneous rocks*: Igneous rocks 59-62
 - volcanism*: The Heise caldera in southeastern Idaho 61
 - Idaho—stratigraphy**
 - Eocene*: Paleozoic strata and Eocene(?) granites along eastern margin of Idaho batholith 59
 - Paleozoic*: Paleozoic strata and Eocene(?) granites along eastern margin of Idaho batholith 59
 - Stratigraphy 58-59
 - Pennsylvanian*: Revised thickness of Hailey Conglomerate Member, Wood River Formation of central Idaho 58-59
 - Stratigraphy 58-59
 - Permian*: Permian-Triassic boundary in western Wyoming and parts of Idaho and Montana 232-233
 - Triassic*: Permian-Triassic boundary in western Wyoming and parts of Idaho and Montana 232-233
 - Idaho—structural geology**
 - faults*: A major left-lateral strike-slip fault in the Wood River area of Idaho 66
 - folds*: Folds in Huckleberry Ridge Tuff (Pleistocene) in eastern Idaho 183
 - neotectonics*: Surficial geology and tectonics in the Snake River Plain 260
 - tectonics*: Geology of the northern Portneuf Range in southeastern Idaho 64-65
 - Late Paleozoic depositional patterns suggest separate crustal responses north and south of eastern Snake River Plain 65
 - New light on the Beaverhead Mountains in Idaho 67
 - Structure and volcanism in eastern Snake River Plain, of Idaho 65-66
 - Tectonics 63-68
 - igneous rocks** *see also* magmas; metamorphic rocks; metasomatism; phase equilibria
 - igneous rocks—basalt family**
 - composition*: Triassic and Jurassic rocks in the South Carolina coastal plain 51-52
 - geochemistry*: Carbon dioxide-filled vesicles in deep-sea basalt 184

- igneous rocks—composition**
alkalic composition: Ages of alkalic igneous activity in north-central Montana 59-60
- igneous rocks—granite-granodiorite family**
granite: Paleozoic strata and Eocene(?) granites along eastern margin of Idaho batholith 59
 — Tectonic implications of granite ages, southwestern Montana 60-61
two-mica granite: Uranium in two-mica granite in northern New England 38-39
- igneous rocks—lamprophyre and carbonatite family**
dikes: Multiple-intruded carbonatite dike in the Wet Mountains of Colorado 33
- igneous rocks—petrology**
complexes: Jurassic plutonism and volcanism in south-central Arizona 73
distribution: Igneous rocks 59-62
general: Igneous rocks 73-74
- igneous rocks—plutonic rocks**
calc-alkalic composition: Calc-alkalic intrusive rocks at Mineral Mountain, south-central Arizona 73-74
distribution: Distribution of intrusive rocks in the Fairweather Range, Glacier Bay National Monument, Alaska 86-87
genesis: Magmatic diversification and crust-mantle structure in Colorado 185-186
geochemistry: Semiquantitative spectrographic data from granitoid rocks of the Basin-Range Province 186
petrology: Plutonic rocks and magmatic processes 184-186
- igneous rocks—pyroclastics and glasses**
tuff: The Heise caldera in southeastern Idaho 61
- igneous rocks—ultramafic family**
kimberlite: Carbonate-rich kimberlite in southeastern Wyoming 61-62
ophiolite: Circum-Caribbean mafic-ultramafic belts 170-171
 — Gravity data reveal buried ophiolite belt in California 172
 — Red Sea opening 184
 — Serpentine emplacement, Northern California Coast Ranges 76
- igneous rocks—volcanic rocks**
chemical composition: Chemical trends of Tertiary volcanic rocks in the Pioneer Mountains of Montana 60
distribution: Tertiary volcanic rocks in southwestern New Mexico 74
lava: Upper Cenozoic basaltic and phonolitic lavas in central Sierra Nevada 75
lithostratigraphy: Stratigraphy of volcanic rocks as a guide to uranium in the Thomas Range, Utah 32
 — Uranium and Tertiary volcanic rocks in the Marshall Pass district of Colorado 32
petrology: Cenozoic volcanism and tectonism in west-central Arizona 72
 — Tertiary volcanic sequence at Mineral Mountain in Arizona 182-183
- Volcanic rocks in western United States 182-183
Precambrian: Distinct volcanic assemblages indentified in Missouri Precambrian 54
- Illinois—economic geology**
coal: Sphalerite-bearing coal in Illinois 16
lithium: Lithium in flint clays 43-44
- Illinois—engineering geology**
waste disposal: Hydrologic evaluation of a radioactive-waste burial site near Sheffield, Illinois 280
- Illinois—environmental geology**
reclamation: Sludge-irrigation hydrology 92
- Illinois—geochemistry**
trace elements: Sphalerite-bearing coal in Illinois 16
- Illinois—hydrogeology**
hydrology: Illinois 92
- impact statements** *see also* under environmental geology under Alaska; Wyoming
- impact statements—land use**
monitoring: Methodology for post-EIS monitoring 322
research: Environmental impact studies 322-323
- inclusions** *see also* fluid inclusions
- Indian Ocean—oceanography**
ocean floors: Microdensitometer study of submerged marine features 356
- Indiana—environmental geology**
pollution: Leachate movement in opposite directions in outwash aquifer separated into two units by clay 93
- Indiana—hydrogeology**
ground water: Geology and hydrology of the Indiana Dunes National Lakeshore area 92
 — Saline ground water near Vincennes 92
 — Unconsolidated aquifers near Logan-sport 92-93
hydrology: Availability of ground water in the Upper White River basin 92
 — Indiana 92-93
- Indonesia—hydrogeology**
hydrology: Indonesia 343
 — Sediment study program assistance 343
- industrial minerals** *see also* under economic geology under Colorado
- inert gases** *see* noble gases
- intrusions—contact**
gravity surveys: Geologic and geophysical studies of the contact of the Dufek intrusion, Pensacola Mountains 353-354
- intrusions—dikes**
carbonatite: Multiple-intruded carbonatite dike in the Wet Mountains of Colorado 33
orientation: Gently dipping feeder dikes for Columbia River Basalt Group 180
- intrusions—layered intrusions**
contact: Contacts of the gabbro at Mount La Perous, Mount Fairweather quadrangle 86
- intrusions—plutons**
age: Calc-alkaline intrusive relations at Mineral Mountains in Arizona 186
geochemistry: Jurassic zoned tonalite-trondhjemite pluton in Trinity Alps of Klamath Mountains in California 185
 — Strontium isotopic variation in a compositionally zoned granitic pluton 189
granulite: Fitchburg pluton in Massachusetts 46
- intrusions—stocks**
geochemistry: Minor element geochemistry and strontium isotopes of Tertiary stocks in Colorado mineral belt 192-193
- Invertebrata** *see also* Coelenterata; Mollusca; Ostracoda; Radiolaria
- Invertebrata—ecology**
benthonic taxa: Benthic invertebrates in Piceance Creek, northwestern Colorado 111
- Iowa—hydrogeology**
hydrology: Drought effect and recovery noted in Iowa carbonate aquifers 114
 — Iowa 114
 — Iowa sediment-data compiled 114
- iron** *see also* under economic geology under New York; Virginia; West Virginia; Wyoming
- isotope dating** *see* absolute age
- isotopes** *see also* absolute age; geochronology
- isotopes—abundance**
basalt: ^{18}O and δD values of Hawaiian basalts and xenoliths 190-191
- isotopes—carbon**
C-13/C-12: Application of stable carbon isotopic ratios to exploration for deep-water source sediments 24
 — Hydrocarbon maturation in Kentucky and Virginia 22
- isotopes—corals**
temperature: Water temperature of corals shown by isotopic analysis 216
- isotopes—helium**
He-4/He-3: Helium-3 in Yellowstone, Lassen, and The Geysers' fluids indicates mantle connection 201
- isotopes—igneous rocks**
two-mica granite: Uranium in two-mica granite in northern New England 38-39
- isotopes—lead**
Pb-210: Pb-210 profiles in continental shelf sediments; an index to rates of sediment reworking 146
ratios: Source of lead in ores of the San Juan Mountains in Colorado 189-190
- isotopes—lithium**
analysis: Lithium isotopes 249
- isotopes—noble gases**
abundance: Noble and active gases in the Larderello Geothermal Field in Italy 202-203
- isotopes—oxygen**
O-18/O-16: Snake River plain, Idaho, geothermal well studies 39-40
 — Stable isotope studies of thorium-bearing veins in the Wet Mountains of Colorado 33

- isotopes—ratios**
paleoclimatology: Three-million-year isotopic record of paleoclimate at Death Valley in California 216
stable isotopes: Stable isotope ratios 249
 — Stable isotopes 190-191
- isotopes—strontium**
Sr-87/Sr-86: Strontium-isotope data from Pioneer batholith in southwestern Montana 61
 — Strontium isotopic variation in a compositionally zoned granitic pluton 189
- isotopes—sulfur**
S-34/S-32: Iron sulfide minerals and sulfur isotopes associated with roll-type uranium deposits 33-34
- isotopes—tracer experiments**
research: Isotope tracer studies 189-190
- isotopes—uranium**
ratios: Uranium-isotope ratio characterization of geothermal waters 204-205
- Israel—economic geology**
water resources: Dead Sea levels 343
- Israel—hydrogeology**
ground water: Hydrogeologic system simulation 219
- Italy—hydrogeology**
thermal waters: Noble and active gases in the Larderello Geothermal Field in Italy 202-203
- J**
- Jordan—economic geology**
mineral resources: Israel and Jordan 343
water resources: Dead Sea levels 343
- Jurassic** *see also under stratigraphy under South Carolina*
- K**
- Kansas—environmental geology**
geologic hazards: Floods in Missouri and Kansas in 1977 281
maps: Flood-hazard mapping in Kansas 283
pollution: Chloride concentration of ground-water discharge to Smoky Hill River in Kansas 115
- Kansas—hydrogeology**
ground water: Chemical quality of ground water in Kansas 236
 — Geohydrology of saline water occurrence in the Wellington Formation in central Kansas 115
 — Ground-water mining in west-central Kansas 114-115
 — Quality of water in abandoned zinc mines in northeastern Oklahoma and southeastern Kansas 111
hydrology: Kansas 114-115
 — Modeling of river valleys in north-central Kansas 115
 — Streamflow losses in the Arkansas River, western Kansas 115
- kaolin** *see also under economic geology under Georgia*
- Kentucky—areal geology**
research: Kentucky 52-53
- Kentucky—economic geology**
lithium: Lithium in flint clays 43-44
natural gas: Hydrocarbon maturation in Kentucky and Virginia 22
 — Possible stratigraphic controls for Devonian gasfields in the Appalachian Basin 22
thorium: Uranium, thorium, carbon, and sulfur in Devonian black shale from West Virginia, Kentucky, and New York 39
uranium: Uranium, thorium, carbon, and sulfur in Devonian black shale from West Virginia, Kentucky, and New York 39
- Kentucky—geomorphology**
landform description: Tentative dating of pre-Pleistocene deposits along the Kentucky River of central Kentucky 53
- Kentucky—stratigraphy**
Pleistocene: New evidence supports Nebraskan age for origin of Ohio River drainage system 52-53
- Kenya—economic geology**
water resources: Kenya 343
- Kenya—hydrogeology**
ground water: Rural water-resource development 343
- L**
- land subsidence—mines**
solution mining: Solution mine subsidence hazards 290-291
 — Solution mine subsidence hazards 292
- land use** *see also under environmental geology under Atlantic Coastal Plain; automatic data processing; California; Colorado; District of Columbia; Great Plains; Gulf Coastal Plain; Maryland; New Mexico; Nigeria; North Carolina; Pacific Coast; Rocky Mountains; South Dakota; United States; Virginia; Western U.S.; Wyoming*
- land use—classification**
wetlands: National wetland-classification system 233
- land use—general**
research: Land use and environmental impact 317-323
- land use—management**
coastal zone: Coastal zone management coordination 325
- land use—maps**
cartography: Cooperative land use mapping and data projects 319
 — Geographic information systems software development 319-320
 — Land use and land cover mapping 319
 — Land use and land cover maps and data and other geographic studies 318-322
- land use—natural resources**
energy sources: Energy resources studies on behalf of other agencies 326
 — Environmental aspects of energy 268-273
international cooperation: International resources assessment 326-327
- programs*: Resource and land investigation programs 325-326
 — Resources attache and reporting program 326-327
- land use—planning**
education: Integrated surface mine reclamation and land use planning 325
 — Technology transfer workshops for state and local officials 325
- land use—regional planning**
natural resources: Multidisciplinary studies in support of land-use planning and decisionmaking 317-318
- land use—remote sensing**
applications: Assessing the impact of surface mining 304-305
- landform description** *see under geomorphology*
- landslides** *see under earthquakes under geologic hazards; see under slope stability; see under mass movements under geomorphology*
- lava** *see also igneous rocks; magmas*
- lava—age**
lava domes: Emplacement sequence and chemical evolution of Pleistocene rhyolites in Coso Range, California 181-182
- lava—geochemistry**
basalt: Petrogenesis of Columbia River Basalt Group 181
- lead** *see also under economic geology under Colorado; Idaho*
- lead—abundance**
water: Streets contribute much lead to urban runoff 130
- lead—geochemistry**
aqueous solutions: Lead hydroxide formation constants 187
peat: Environmental pollution of the Everglades in Florida 16-17
pollutants: Bioavailability of sediment-bound lead and zinc to estuarine clams 285
- Liberia—environmental geology**
maps: Liberia 343-344
- limestone—composition**
applications: Carbonate rocks for sulfur dioxide gas recovery 44
- limnology** *see under hydrology*
- lineation** *see also structural analysis*
- lithium** *see also under economic geology under Alabama; Arizona; Illinois; Kentucky; Maryland; Missouri; Nevada; New Mexico; Ohio; Pennsylvania*
- lithium— isotopes**
analysis: Lithium isotopes 249
- lithium—resources**
sedimentary rocks: Origin of lithium in sedimentary rocks and brines 42
- Louisiana—engineering geology**
marine installations: Submarine landslides on the Mississippi Delta 149
- Louisiana—environmental geology**
ecology: Benthic invertebrates of the lower Mississippi River 243-244
pollution: Time of travel of solutes in Louisiana streams 115-116

- Louisiana—hydrogeology**
ground water: Changes in ground-water quality caused by realignment of the Red River in northern Avoyelles Parish 116
 — Fresh ground water mapped in St. James Parish in Louisiana 116
 — Freshwater anomalies over three Louisiana salt domes 116
 — Ground-water in lignite areas of De Soto Parish 116
 — Ground-water resources of Washington Parish 116
 — Potential saltwater encroachment in southwestern Louisiana 160
hydrology: Louisiana 115-116
 — Organic compounds in the Lower Mississippi River 237
thermal waters: Radium-228 found in water from a geopressured-geothermal well 237
- lunar studies** *see* Moon
- M**
- magmas** *see also* igneous rocks; intrusions; lava
- magmas—differentiation**
geochemistry: Petrology of post-caldera rhyolites in Long Valley, California 182
- magmas—geochemistry**
evolution: Chemical evolution of silicic magma chambers 181-182
minor elements: Petrochemistry trends, distribution coefficients, and quality of minor element data 186
- magnetic field** *see under* Earth
- magnetic surveys** *see under* geophysical surveys *under* Wisconsin
- magnetotelluric surveys** *see under* geophysical surveys *under* Arizona; Southwestern U.S.
- Maine—geophysical surveys**
remote sensing: Maine 304
 — Orland lineament and structural control in eastern Maine 312
- Maine—hydrogeology**
ground water: Geohydrology of the Androscoggin Valley Regional Planning Area 93
 — Ground-water resources in the Portland area 93
hydrology: Limnology of Maine lakes 240-241
 — Maine 93
- Maine—stratigraphy**
Paleozoic: Vassalboro-pre-Vassalboro stratigraphic relations 45
- Malay Archipelago—economic geology**
nickel: Nickel laterites 307
- Malaysia—economic geology**
petroleum: Malaysia 344
- Mammalia—biostratigraphy**
Eocene: Correlation and structure of Eocene rocks in southwestern Bighorn Basin of Wyoming 58
- Mammalia—Rodentia**
Pliocene: Pliocene and Pleistocene holarctic correlation of microtoid rodents 228
- man, fossil** *see* fossil man
- mantle—properties**
conductivity: Deep mantle conductivity estimated from geomagnetic variations 169
- maps** *see also under* areal geology *under* Antarctica; Arkansas; Caribbean region; Maryland; New York; *see also under* economic geology *under* Arizona; California; Nevada; Oregon; *see also under* environmental geology *under* Kansas; Liberia; Montana; Puerto Rico; United States; *see also under* general *under* automatic data processing; Pacific region; *see also under* geochemistry *under* automatic data processing; *see also under* geomorphology *under* United States; *see also under* geophysical surveys *under* Greenland; Montana; Nevada; United States; Washington; Wisconsin; Wyoming; *see also under* hydrogeology *under* Arizona; *see also under* structural geology *under* Colorado
- maps—cartography**
aerial photography: Mapping from high-resolution high-altitude photographs 356
automatic data processing: DEM files 359-360
 — Digital cartographic applications 358
 — Digital cartographic data files 359
 — DLG files 360
 — File management 360
 — Hardware 358-359
 — Software 359
 — Useful applications of map data file 87
design: Cartography and design 358-361
environmental geology maps: Flood mapping 283-284
geologic maps: Geologic maps 87-88
land use: Cooperative land use mapping and data projects 319
 — Land use and land cover mapping 319
 — Land use and land cover maps and data and other geographic studies 318-322
photogeology: Photobase mapping 357
 — Photoimage mapping 357
 — Satellite image mapping 357
 — Simulating color in image maps 357
projections: Space oblique Mercator projection 315
 — Space oblique Mercator projection 358
projects: Pilot production projects 360-361
 — Topographic surveys and mapping 355-361
remote sensing: Applications to cartographic studies 314-316
 — Landsat-3 investigations 314
 — Parameters for an automated mapping satellite (Mapsat) 315-316
 — Satellite image maps 314-315
- marble** *see also under* economic geology *under* New York
- marine geology** *see also* oceanography; *see also under* oceanography *under* Alaska; Gulf of Mexico; Pacific Ocean; United States
- marine geology—observations**
processes: Studies of marine and coastal processes 159
- marine installations** *see also under* engineering geology *under* Atlantic Ocean; Louisiana; Texas
- Mars—exploration**
Viking: The Viking Mars Mission 293-294
- Mars—geomorphology**
environment: Climatic changes on Mars 217-218
landform description: Planetary geologic processes and histories 294-295
- Maryland—areal geology**
maps: One-meter contour interval mapping 358
- Maryland—economic geology**
lithium: Lithium in flint clays 43-44
- Maryland—environmental geology**
land use: Land-use climatology 214
- Maryland—hydrogeology**
ground water: Two-dimensional model of the Piney Point Aquifer 93
hydrology: Maryland 93
- Maryland—sedimentary petrology**
sedimentary rocks: Synorogenic mudflow deposit 52
- Maryland—stratigraphy**
Cretaceous: A new Upper Cretaceous ostracode zone 230
Triassic: Upper Triassic stratigraphy in the Culpeper Basin of Virginia and Maryland 48-49
- Maryland—structural geology**
tectonics: New information on tectonic framework on the Culpeper Triassic and Jurassic basin 51
- mass movements** *see under* geomorphology
- Massachusetts—engineering geology**
nuclear facilities: Expected ground motion at proposed nuclear power plant sites 268
- Massachusetts—environmental geology**
geologic hazards: Flood-frequency model for small streams in Massachusetts 282
- Massachusetts—geomorphology**
glacial geology: Deglaciation in the Leominster-Fitchburg area, Massachusetts 45-46
 — Glacial Lake Housatonic was complex 46
- Massachusetts—hydrogeology**
ground water: A water budget for Nantucket Island 95
 — Freshwater-saltwater relations on Cape Cod 94
 — Ground-water assessment in the lower Merrimack River basin 94-95
 — Ground-water development on Cape Cod 95
 — Results of water-level survey at Martha's Vineyard 93-94

- Trace metals in ground water on Cape Cod 94
hydrology: Massachusetts 93-95
- Massachusetts—petrology**
intrusions: Fitchburg pluton in Massachusetts 46
metamorphic rocks: Granite gneiss terrane in southeastern Massachusetts 47
- Massachusetts—stratigraphy**
Cambrian: Hoppin Hill unconformity, new fossils 46-47
Carboniferous: Coal and stratigraphy in the Narragansett Basin of Massachusetts 48
Paleozoic: Correlation of Scotland Schist and Hebron Formation in eastern Connecticut with Oakdale Formation in Massachusetts 47
- Massachusetts—structural geology**
faults: Age of rocks in Lake Char fault zone in south-central Massachusetts 46
- mathematical geology** *see also* automatic data processing
- meetings** *see* symposia
- melange** *see under* interpretation *under* structural analysis; *see under* P-T conditions *under* metamorphism
- mercury** *see also under* economic geology *under* Nevada; Oregon; Pacific Coast
- mercury—abundance**
thermal waters: Relation of mercury to geothermal areas in Yellowstone National Park in Wyoming 207
- mercury—geochemistry**
pollution: Mercury outgassing in Hawaii 289
- Mesozoic** *see also under* stratigraphy *under* Oregon
- Mesozoic—paleontology**
research: Mesozoic and Cenozoic studies 227-230
- metals** *see also* arsenic; beryllium; chromite; *see also under* economic geology *under* Basin and Range Province; Colorado; Mexico; Nevada; Saudi Arabia; Utah; Western U.S.; Wyoming
- metals—abundance**
metavolcanic rocks: Content of non-platinum-group minor metals in the Douglas Island Volcanics, Juneau quadrangle 86
 — Platinum-group metals in the Douglas Island Volcanics, Juneau quadrangle 86
water: Concentrations of toxic heavy metals in water from wells in Wisconsin 101
- metamorphic rocks** *see also* igneous rocks; metamorphism; metasomatism
- metamorphic rocks—age**
absolute age: Strontium-isotope data from Pioneer batholith in southwestern Montana 61
complexes: Probable pre-Ordovician age of metamorphic complex in northern Kuskokwim Mountains 82-83
- metamorphic rocks—composition**
mineral composition: Nature of Cambrian trilobite-bearing rocks from Beavertail Point 48
- metamorphic rocks—gneisses**
granite gneiss: Granite gneiss terrane in southeastern Massachusetts 47
mineral assemblages: Aluminosilicate minerals in the Big Delta Quadrangle 83
occurrence: Garnet clues for lost Sierra Nevada tail 74-75
- metamorphic rocks—lithostratigraphy**
correlation: Correlation of Scotland Schist and Hebron Formation in eastern Connecticut with Oakdale Formation in Massachusetts 47
mylonite: Age of rocks in Lake Char fault zone in south-central Massachusetts 46
Paleozoic: Vassalboro-pre-Vassalboro stratigraphic relations 45
- metamorphic rocks—metasedimentary rocks**
petrology: Farmington Canyon Complex, Wasatch Mountains, Utah 62-63
- metamorphic rocks—petrology**
complexes: Mafic complex of Mullen Creek in the Medicine Bow Mountains of Wyoming 63
ophiolite: The Baltimore Complex, a disrupted ophiolite 184
- metamorphism—P-T conditions**
melange: Maximum temperature of formation of Franciscan melange 76-77
- metasomatic rocks—serpentinite**
genesis: Serpentine emplacement, Northern California Coast Ranges 76
- metasomatic rocks—skarn**
mineral assemblages: Experimental studies in the MgO-CaO-SiO₂-H₂O-HCl system 176
- metasomatism—environment**
volcanism: Mineral alteration in volcanic environments 183
- metasomatism—processes**
hydrothermal alteration: Hydrothermal alteration in Carnegie I Drill Hole, Upper Geyser Basin, Yellowstone Park 196
 — Water-rock reaction in the Salton Sea Geothermal Field in California 207-208
zeolitization: Laumontite alteration 187
- meteorology—practice**
World Meteorological Organization: Activities related to the World Meteorological Organization 339
 — Activities related to the World Meteorological Organization 339
- Mexico** *see also* Gulf Coastal Plain
- Mexico—economic geology**
geothermal energy: Aquifer pressure lowering at Cerro Prieto, Mexico, causing boiling and temperature decrease 198
 — Horizontal control net in a geothermal area 344
metals: Stream-sediment and panned-concentrate investigations, northern Sonora, Mexico 10
- mineral resources*: Mexico 344
- Mexico—geochemistry**
rare earths: Stream-sediment and panned-concentrate investigations, northern Sonora, Mexico 10
- Mexico—geochronology**
Precambrian: Chronometric-geologic charts for Precambrian, United States and Mexico 87
- Mexico—hydrogeology**
ground water: Tropical carbonate aquifers 344
- Mexico—stratigraphy**
Quaternary: Pleistocene and Holocene climate in central Mexico 215
- Michigan—economic geology**
copper: Keweenaw igneous complex identified in Michigan 5
nickel: Keweenaw igneous complex identified in Michigan 5
thorium: High radioactivity in basement rocks of Michigan 31-32
uranium: High radioactivity in basement rocks of Michigan 31-32
- Michigan—environmental geology**
pollution: Reevaluation of water resources of the Marquette Iron Range 95
waste disposal: Effects of waste-water irrigation on ground-water conditions 218-219
- Michigan—hydrogeology**
hydrology: Agricultural land use related to chemical and physical erosion 95
 — Michigan 95
- Micronesia—hydrogeology**
ground water: Ground-water yields small in Truk Islands 128
- Middle East** *see also* Israel; Jordan; Turkey
- Midwest—areal geology**
research: Central region 52-53
- Midwest—paleontology**
Mollusca: New information about the evolution of mollusks during the Cambrian and Ordovician 230-231
- mineral deposits, genesis—controls**
structural controls: Strata-bound lead-zinc mineralization, Philip Smith Mountains quadrangle 82
 — West-northwesterly structural zone controlled gold mineralization at Manhattan in Nevada 8-9
- mineral deposits, genesis—copper**
models: Another model of porphyry copper generation 7-8
- mineral deposits, genesis—metals**
age: Age of volcanism and mineralization in Tonopah mining district, southwestern Nevada 69
environment: Preliminary sulfur isotopic studies 347
- mineral deposits, genesis—processes**
hydrothermal processes: Hydrothermal system of the East Tintic District in Utah 190
plate tectonics: Mesozoic and Cenozoic metallogenesis in the western United States 2

- mineral deposits, genesis—uranium**
controls: Structural and lithologic controls for uranium at the Pitch mine in Colorado 31
hydrothermal processes: Emplacement of uranium into Midnite mine deposits 31
leaching: Uranium mobility during interaction of rhyolitic glass with alkaline solutions 35-36
models: Computer modeling of roll-type uranium deposits 37
oxidation: Pyrite oxidation and the origin of roll-front uranium deposits 34
sedimentation: Conceptual-mathematical models of uranium ore formation in sandstone-type deposits 36
- mineral exploration—geochemical methods**
helium: Mobile helium-detection equipment used in uranium exploration 37
radon: Radon analyses of water in Carbon County, Wyoming 11
rare earths: Stream-sediment and panned-concentrate investigations, northern Sonora, Mexico 10
soil gases: Soil-gas investigations, Hawaii Volcanoes National Park in Hawaii 10-11
statistical methods: Anomalous geochemical variability in Washington County, Missouri 188
stream sediments: Water sampling for uranium exploration 37-38
surveys: Geochemical anomalies associated with mercury deposits in Nevada and Oregon 10
— Litho-geochemical studies in Missouri 9
— Reconnaissance geochemical studies in Alaska 10
techniques: Analytical methodology and its usefulness in geochemical exploration 245-246
— Evaluation of analytical methods for the geochemical exploration of uranium 246
trace elements: Trace elements in galena and sphalerite in the Montezuma district of Colorado 11
— Trace elements in minerals 11
— Trace elements in silver-lead-gold veins in Idaho 9-10
water: Geochemical studies of water 11-12
— Helium and radon in uranium exploration 12
— Radioactive spring site guides to uranium in southwestern United States 12
— Stream water sampling in Puerto Rico 11-12
- mineral exploration—geophysical methods**
anomalies: Ground checks of aeroradioactivity anomalies in the Atlantic Coastal Plain of South Carolina 4
gravity surveys: Geophysical studies in southwestern New Mexico 11
uranium: Electromagnetic methods aid in detection of mineralization associated with uranium 39
- well-logging*: In-hole gamma ray studies in Texas 11
— Physical properties changes associated with uranium deposits can be detected by borehole geophysical measurements 175-176
- mineral exploration—methods**
applications: Geochemical and geophysical techniques in resource assessments 9-14
— Regional geochemical and geophysical studies 9-11
maps: Mineral exploration potential maps 13-14
thermoluminescence: Thermoluminescence of sand grains near a uranium deposit 37
- mineral exploration—programs**
current research: Mineral appraisals of Alaska on schedule; levels of studies 80
- mineral exploration—remote sensing**
infrared methods: Spectral signatures of minerals in the visible and near-infrared regions of the spectrum 310
interpretation: Effects of atmosphere on Landsat data 306-307
nickel: Nickel laterites 307
satellite methods: Targeting mineral exploration 306-309
— William T. Pecora Memorial Symposium 306
uranium: Remote sensing for uranium exploration 309-310
- mineral prospecting** *see* mineral exploration
- mineral resources** *see also* under economic geology under Alaska; Colorado; Egypt; Hawaii; Jordan; Mexico; Missouri; Nevada; South Carolina; Tennessee; United States; West Indies; West Virginia; Wyoming
- mineral resources—economics**
land use: Mineral-resources assessment of land areas 2
ore deposits: Geologic studies of mineral districts and mineral-bearing areas 4
- mineral resources—exploration**
geochemical methods: Geochemical and geophysical techniques in resource assessments 9-14
methods: New analytical methods and techniques 12
- mineral resources—resources**
global: Mineral-resource and mineral-fuel investigations 1-44
models: Mineral resource information systems and analysis 12-13
- minerals** *see also* crystal chemistry; crystal structure
- minerals—borates**
hydrochlorborite: Crystal structure of hydrochlorborite 177-178
- minerals—chain silicates, pyroxene group**
orthopyroxene: Fine structure of orthopyroxene 178
- minerals—experimental studies**
infrared spectra: Infrared spectral behavior of fine particulate solids 170
- minerals—mineral data**
crystal chemistry: Mineralogic studies and crystal chemistry 177-179
- minerals—orthosilicates**
lawsonite: Lawsonite in Hagemeister Island quadrangle 83-84
- minerals—orthosilicates, garnet group**
garnet: Garnet clues for lost Sierra Nevada tail 74-75
- minerals—oxides**
titanomagnetite: Thermodynamic behavior of titanomagnetite 177
- minerals—phosphates**
parsonite: An occurrence of parsonite, a secondary uranium mineral, in west-central Alaska 33
- minerals—sheet silicates, clay minerals**
hectorite: New occurrences of the lithium-rich smectite, hectorite 42-43
- minerals—silicates**
chemical composition: Electron microprobe analyses of uraninite and coffinite 35
thermal properties: Heat capacities of feldspars and kaolinite 176
- minerals—sulfides**
alkali-metal sulfides: New alkali metal sulfides from California 178
sphalerite: Sphalerite-bearing coal in Illinois 16
- mining geology—practice**
international cooperation: CENTO countries 340
- Minnesota—economic geology**
copper: Faulting in the Duluth Complex in Minnesota 6
nickel: Faulting in the Duluth Complex in Minnesota 6
peat: Peat resources in part of Lake of the Woods County in Minnesota 5
- Minnesota—engineering geology**
tunnels: Analyses of subsurface data to assist planners in evaluating feasibility of tunneling for rapid-transit systems 318
- Minnesota—geophysical surveys**
electrical surveys: Schlumberger soundings near Moorhead, Minnesota 172
- Minnesota—hydrogeology**
ground water: Appraisal of a sand-plain aquifer in central Minnesota 96
— Appraisal of the Buffalo aquifer 96
— Availability of ground water in southwestern Minnesota 96
— Ground-water appraisal in sand plains of Benton, Sherburne, Stearns, and Wright Counties 96-97
— Interflow in uncased multiaquifer wells 96
— Planning study in the Pelican River sand plain 96
hydrology: Hydrology and ground-water quality in a potential mining area in northeastern Minnesota 95-96
— Minnesota 95-97

- Minnesota—stratigraphy**
Cretaceous: New biostratigraphic, paleogeographic, and tectonic data on Cretaceous rocks in Minnesota and eastern South Dakota 18-19
- Minnesota—structural geology**
folds: Lake Superior region 53-54
tectonics: New biostratigraphic, paleogeographic, and tectonic data on Cretaceous rocks in Minnesota and eastern South Dakota 18-19
 — Structural evolution of the Vermilion district of Minnesota 53-54
- Miocene** *see also under stratigraphy under California; Washington*
- Mississippi—areal geology**
research: Upper Mississippi Embayment 52
- Mississippi—engineering geology**
geologic hazards: Flood elevations of canalized stream in Mississippi 282
waste disposal: Base of freshwater above salt domes 225
waterways: Scour at a bridge in Mississippi 281
- Mississippi—hydrogeology**
ground water: "Tuscaloosa aquifer system" in Mississippi 107
hydrology: Mississippi 107
- Mississippi Valley—stratigraphy**
Cenozoic: Late Cenozoic history of the upper Mississippi embayment 53
- Mississippian** *see also under stratigraphy under Arizona; Great Plains; Nevada; New Mexico; Virginia; West Virginia*
- Mississippian—paleontology**
conodonts: Paleocology and biofacies of Osagean conodonts 232
- Missouri—areal geology**
research: Missouri 54
- Missouri—economic geology**
lithium: Lithium in flint clays 43-44
mineral resources: Lithochemical studies in Missouri 9
- Missouri—environmental geology**
geologic hazards: Floods in Missouri and Kansas in 1977 281
 — Magnitude and frequency of floods in St. Louis County, Missouri 282
pollution: Effects of mining on water quality 286
- Missouri—geochemistry**
surveys: Anomalous geochemical variability in Washington County, Missouri 188
trace elements: Lithochemical studies in Missouri 9
- Missouri—hydrogeology**
hydrology: Soil temperatures indicate gaining and losing streams 239
- Missouri—petrology**
igneous rocks: Distinct volcanic assemblages identified in Missouri Precambrian 54
- Mohorovicic discontinuity** *see also mantle*
- Mollusca—biogeography**
affinities: North Atlantic Cenozoic mollusks in northern Alaska 229
- Mollusca—Bivalvia**
Ordovician: New information about the evolution of mollusks during the Cambrian and Ordovician 230-231
Pliocene: Inland limit of the Croatan Sea; Pliocene and Pleistocene beds at Fountain, North Carolina 228
- molybdenum** *see also undereconomic geology under Nevada*
- Montana—economic geology**
 bentonite: Physical and chemical properties of bentonite 43
copper: Copper in Belt rocks of Montana 62
geothermal energy: Geothermal reconnaissance of southwestern Montana 209
natural gas: Hydrocarbon potential of Disturbed Belt in northwestern Montana 18
 — Hydrocarbon potential of proposed Great Bear Wilderness in western Montana 18
petroleum: Economic geology 55-56
 — Hydrocarbon potential north of Snake River Plain of Idaho and Montana 55
 — Hydrocarbon potential of Disturbed Belt in northwestern Montana 18
 — Hydrocarbon potential of proposed Great Bear Wilderness in western Montana 18
uranium: Uranium mineralization at the Upper Cretaceous Fox Hills Sandstone-Lance Formation interface 27-28
- Montana—engineering geology**
slope stability: Potential rockfall at Billings, Montana 292
- Montana—environmental geology**
geologic hazards: Floods of June 1976 in Culbertson, Montana 280
maps: Flood-insurance study for Belt, Montana 283
pollution: Radium-228 found in Montana hot springs 287-288
reclamation: Site-specific coal-land reclamation study near East Trail Creek, southern Montana 117
- Montana—geochemistry**
isotopes: Strontium-isotope data from Pioneer batholith in southwestern Montana 61
- Montana—geochronology**
Archean: Archean age of major sedimentary sequences in southwestern Montana 62
Proterozoic: Middle Proterozoic tectonics in the Wyoming Age Province 64
- Montana—geomorphology**
glacial geology: Middle Wisconsinan glacial lake near Scobbey, Montana 58
 — Soil development and age of Bull Lake Glaciation in the Rocky Mountains 57
- Montana—geophysical surveys**
maps: Montana/Wyoming image maps 315
- surveys*: Magnetic and gravity expressions of the Lewis and Clark Line 170
- Montana—hydrogeology**
ground water: Ground-water resources of the Poplar River basin, northeastern Montana 116-117
 — Shallow ground-water flow systems in the northern Powder River basin 110
hydrology: Lake Koocanusa water quality program 242
 — Localized saline seep development in Hailstone Basin in Montana 117-118
 — Montana 116-118
 — Water quality of selected streams in the Fort Union coal area, southeastern Montana 117
springs: Radium-228 found in Montana hot springs 287-288
thermal waters: Thermal ground water 117
- Montana—petrology**
igneous rocks: Ages of alkalic igneous activity in north-central Montana 59-60
 — Chemical trends of Tertiary volcanic rocks in the Pioneer Mountains of Montana 60
 — Igneous rocks 59-62
 — Tectonic implications of granite ages, southwestern Montana 60-61
intrusions: Ages of alkalic igneous activity in north-central Montana 59-60
- Montana—stratigraphy**
Permian: Permian-Triassic boundary in western Wyoming and parts of Idaho and Montana 232-233
Precambrian: Copper in Belt rocks of Montana 62
 — Precambrian rocks 62-63
Triassic: Permian-Triassic boundary in western Wyoming and parts of Idaho and Montana 232-233
- Montana—structural geology**
folds: The fold and thrust belt in southwestern Montana 66-67
tectonics: Major deep-seated faults near Helena, Montana 67-68
 — Middle Proterozoic tectonics in the Wyoming Age Province 64
 — Tectonic implications of granite ages, southwestern Montana 60-61
 — Tectonics 63-68
 — Three structural styles in the Sapphire thrust belt in western Montana 67
 — Thrust faults near the Lewis and Clark line in Montana 68
- Moon—exploration**
research: Lunar investigations 295-297
- Moon—geochronology**
absolute age: Samarium-neodymium chronology of lunar samples 299
- Moon—geomorphology**
craters: Basin and crater studies 295-296
volcanic features: Volcanism and tectonism studies 296-297
- Moon—geophysical surveys**
remote sensing: Lunar radar studies 297

- Moon—paleomagnetism**
research: Geochemical, geophysical, and geological consortium studies 297
- Moon—petrology**
breccia: Consortium studies of Apollo 17 breccias 298
 — Petrology of Apollo 16 samples 298-299
lava: Late-stage differentiates in mare lavas 299-300
research: Lunar sample investigations 298-300
volcanology: Studies of lunar pyroclastic eruption mechanisms 299
- mud volcanoes** *see also* volcanology

N

- natural gas** *see also under* economic geology *under* Appalachians; California; Colorado; Florida; Great Basin; Great Plains; Gulf of Mexico; Kentucky; Montana; Ohio; Oregon; Rocky Mountains; Utah; Virginia; Washington; West Virginia
- natural gas—exploration**
isotopes: Application of stable carbon isotopic ratios to exploration for deep-water source sediments 24
techniques: New exploration and production techniques 23-25
- natural gas—production**
techniques: New exploration and production techniques 23-25
- natural gas—resources**
distribution: Oil and gas resources 17-25
nonconventional resources: Nonconventional natural gas resources 25
offshore: Offshore areas 23
- Nebraska—hydrogeology**
ground water: High nitrate concentrations found under a Nebraska prairie 236
 — Natural filtration used in artificial recharge investigation 220-221
hydrology: Nebraska 118
 — Shrinking channels of the North Platte and Platte Rivers 118
- Neogene** *see also under* geochronology *under* Antarctica; Oregon
- neotectonics** *see also under* structural geology *under* California; Idaho; Nevada; United States; Utah; Washington
- Nevada—economic geology**
brines: Geophysical characterization of brine deposits 42
geothermal energy: Thermal regime of Leach Hot Springs area of Grass Valley in Nevada 199-200
gold: West-northwesterly structural zone controlled gold mineralization at Manhattan in Nevada 8-9
lithium: Lithium-rich rocks in Nevada 42
 — New occurrences of the lithium-rich smectite, hectorite 42-43
maps: Mineral exploration potential maps 13-14
mercury: Geochemical anomalies associated with mercury deposits in Nevada and Oregon 10
- metals*: Age of volcanism and mineralization in Tonopah mining district, southwestern Nevada 69
mineral resources: Geology of the Cuprite mining district of Esmeralda County in Nevada 8
molybdenum: Molybdenum mineralization in the Battle Mountain mining district of Lander County, Nevada 8
oil shale: Geology and oil-shale resources of the South Elko Basin in Nevada 26
petroleum: Permian source rocks, northeastern Great Basin 20
 — Rates of sedimentation of petroleum source rocks in Utah, Nevada, and Idaho 21
- Nevada—engineering geology**
land subsidence: Effects of continuing land subsidence in Las Vegas Valley, Nevada 290
 — Potential surface faulting related to ground-water withdrawal in Las Vegas Valley, Nevada 292
waste disposal: Hydrologic evaluation of radioactive waste buried near Beatty, Nevada 280
 — Hydrologic investigation of the Eleana Formation, Nevada Test Site 279
 — Nevada Test Site 277-278
- Nevada—environmental geology**
geologic hazards: Flood hazards in Carson City, Nevada 283
 — Hydrology and geology of the Carson City area 129
pollution: Monitoring ground-water quality in Nevada 286
waste disposal: Waste brines are rich in metals 129
- Nevada—geochemistry**
surveys: Geochemical anomalies associated with mercury deposits in Nevada and Oregon 10
- Nevada—geochronology**
absolute age: New data on modification of K-Ar ages by Tertiary thrust faulting in eastern Nevada 185
Tertiary: Age of volcanism and mineralization in Tonopah mining district, southwestern Nevada 69
- Nevada—geophysical surveys**
maps: Digital aeromagnetic data set for Nevada 70
remote sensing: Mapping altered rocks using multispectral aircraft images 309
 — Playa surface mapping 308
 — Quantitative study of Landsat data 308-309
surveys: Geophysical characterization of brine deposits 42
- Nevada—hydrogeology**
ground water: Aquifers underlie Carson Desert 130
 — Hydrogeologic system simulation 219
 — Iodide- and bromide-tracer studies in carbonate rocks 223
 — Kinetic controls on ground-water chemistry in a volcanic aquifer 187-188
- Overdraft in Pahrump Valley 129-130
 — Water supply stable in Fort McDermitt Indian Reservation 129
hydrology: Nevada 129-130
thermal waters: Chemical character of ground water associated with the Soda Lakes geothermal area near Fallon, Nevada 193-194
 — Chemistry of geothermal waters 236-237
- Nevada—seismology**
crust: Crustal thinning over area of high heat flow 206
- Nevada—stratigraphy**
Devonian: Allochthonous Devonian chert in northern Shoshone Range in North-central Nevada 70
 — Devonian Woodruff Formation in central Nevada 70-71
Mississippian: Mississippian flysch in Toiyabe Range in central Nevada 70
Tertiary: Geology and oil-shale resources of the South Elko Basin in Nevada 26
Triassic: Triassic rocks in southern Toiyabe Range in central Nevada 70
- Nevada—structural geology**
neotectonics: Quaternary faulting in Clayton Valley in southwestern Nevada 69-70
 — Seismotectonics of Utah and Nevada 259-260
tectonics: Strike-slip faults in Lake Mead area of southern Nevada 71
- Nevada—tectonophysics**
heat flow: Crustal thinning over area of high heat flow 206
- New England—areal geology**
research: New England 45-48
- New England—economic geology**
thorium: Uranium in two-mica granite in northern New England 38-39
uranium: Uranium in two-mica granite in northern New England 38-39
- New England—stratigraphy**
changes of level: Postglacial sea levels on the inner continental shelf of southern New England 146-147
- New England—structural geology**
faults: Possible Lake George faulting 45
tectonics: Zone of detachment in the Hoo-sac Mountain area 46
- New Jersey—hydrogeology**
ground water: Saltwater intrusion into the Old Bridge Sand Member of the Magoghy Formation of New Jersey 160-161
 — Water-resources potential of the Whar-ton Tract 97
hydrology: New Jersey 97
 — New Jersey water-quality investigations 235
- New Mexico—economic geology**
coal: Montmorillonite in coal partings 15
copper: Geophysical studies in southwestern New Mexico 11

- lithium*: Lithium-rich rocks in Nevada 42
- uranium*: Electron microprobe analyses of uraninite and coffinite 35
- Uranium anomaly in Canada de la Cueva, New Mexico 37
- Uranium mineralization in the Morrison Formation at the Dennison-Bunn Prospect in New Mexico 30
- New Mexico—engineering geology**
- waste disposal*: Geohydrology of the Proposed Waste Isolation Pilot Plant in southeastern New Mexico 278-279
- Southeast New Mexico 278
- New Mexico—environmental geology**
- land use*: Geologic aspects of off-road vehicle use 273
- reclamation*: Surficial deposits in San Juan Basin of New Mexico 56
- New Mexico—geophysical surveys**
- gravity surveys*: Geophysical studies in southwestern New Mexico 11
- remote sensing*: Luminescence studies 308
- Multidisciplinary study in New Mexico 308
- New Mexico—hydrogeology**
- ground water*: Digital-computer model simulates ground-water flow in the lower Mesilla Valley of Texas and New Mexico 111
- Ground water near Capulin 118-119
- hydrology*: Hydrologic effects of saltcedar control on the Pecos River flood plain in New Mexico 240
- New Mexico 118-119
- New Mexico—petrology**
- igneous rocks*: Tertiary volcanic rocks in southwestern New Mexico 74
- New Mexico—stratigraphy**
- Mississippian*: Mississippian rocks of Pecos basin in southwesternmost New Mexico and adjacent Arizona 72-73
- New Mexico—structural geology**
- tectonics*: Reserve graben of west-central New Mexico 72
- New York—areal geology**
- maps*: Metric quadrangle maps 358
- New York—economic geology**
- heavy minerals*: Geology of Port Leyden, New York, heavy mineral deposit 5
- iron*: High temperature magnetic separation tests of titaniferous magnetites 176
- marble*: High-calcium marble in the Beaver Creek area of St. Lawrence County in New York 5
- thorium*: Uranium, thorium, carbon, and sulfur in Devonian black shale from West Virginia, Kentucky, and New York 39
- uranium*: Uranium, thorium, carbon, and sulfur in Devonian black shale from West Virginia, Kentucky, and New York 39
- New York—engineering geology**
- waste disposal*: Gamma spectral borehole logging, West Valley, New York 279
- waterways*: Impact of climate on the Erie Canal 214
- New York—environmental geology**
- pollution*: Investigation of nitrogen in ground water on Long Island, New York 285
- Movement of bacteria in the Cretaceous Magothy Formation 286
- Nitrate in ground water 285-286
- PCB and suspended-sediment transport in the Hudson River 284
- waste disposal*: Effects of wastewater-management schemes on ground-water reservoir evaluated 97
- New York—hydrogeology**
- ground water*: Areas of contamination delineated in ground water in Suffolk County 98
- Artificial recharge 138
- Beds of clay impose limits on available fresh ground water on Shelter Island 98
- Diversion of the Hudson River in Pleistocene time 97
- Extraction of chromium and cadmium from aquifer material 97
- Glacial deposits may be thin at artificial-recharge site 98
- Position of freshwater-saltwater interface on South Fork, Long Island 97
- Storm-water basins for aquifer recharge with reclaimed water 220
- Water-table recovery causes flooding problems 98
- hydrology*: Dye used to study mixing of waters of the Hudson River estuary 98
- Large concentrations of ferromanganese nodules found in Oneida Lake, New York 241
- Modeling lake drawdown caused by well pumpage 238-239
- New York 97-98
- New Zealand—economic geology**
- geothermal energy*: Ages and continuities of most New Zealand geothermal systems not well-defined 196-197
- New Zealand—hydrogeology**
- ground water*: Ground-water flow simulator applications 344
- hydrology*: New Zealand 344
- Nicaragua—seismology**
- earthquakes*: Nicaragua 345
- nickel** *see also under* economic geology *under* Malay Archipelago; Michigan; Minnesota
- nickel—geochemistry**
- power plants*: Mass balances of trace elements at powerplants 16
- Nigeria—engineering geology**
- geologic hazards*: Nigeria 345
- Nigeria—environmental geology**
- land use*: Federal Capital Territory reconnaissance 345
- Nigeria 345
- nitrogen—geochemistry**
- cycles*: NO₃-N uptake by algae in a stream-like environment 187
- noble gases** *see also* helium; radon
- noble gases—geochemistry**
- geothermal systems*: Noble gases and dissolved ions in geothermal exploration 205
- nodules—manganese**
- composition*: Sediment-nodule geochemistry of deep sea manganese nodules 157-158
- nonmetals** *see also* boron; sulfur; *see also under* economic geology *under* Saudi Arabia
- North America** *see also* Appalachians; Atlantic Coastal Plain; Great Lakes region; Great Plains; Gulf Coastal Plain; Mexico; Rocky Mountains; United States
- North America—geochronology**
- Cretaceous*: Cretaceous timescale for North America 229
- North America—stratigraphy**
- Paleozoic*: Radiolarian age-dating of Paleozoic cherts 230
- Tertiary*: Paleomagnetic poles from the Valdez(?) and Orca Groups, Alaska 167
- North Carolina—economic geology**
- phosphate*: Phosphate resources in the southeastern United States 43
- North Carolina—environmental geology**
- ecology*: Tree-growth rates reflect changes resulting from drainage construction 233
- land use*: Wetland vegetation studies 313
- North Carolina—hydrogeology**
- ground water*: Water sources and geology along the Blue Ridge Parkway 107
- hydrology*: Chemical quality of streams in North Carolina 234-235
- North Carolina 107
- Water budget of Pamlico Sound, North Carolina 161
- North Carolina—stratigraphy**
- Cretaceous*: Age of basal Cretaceous in North Carolina 51
- Pliocene*: Inland limit of the Croatan Sea; Pliocene and Pleistocene beds at Fountain, North Carolina 228
- North Dakota—economic geology**
- coal*: Hydrogenation of coal and sulfide minerals 16
- North Dakota—engineering geology**
- geologic hazards*: Surficial geology and geologic hazards in the Williston Basin in North Dakota 272-273
- North Dakota—environmental geology**
- reclamation*: Hydrologic evaluation of mining and reclamation in the Beulah Trench area of North Dakota 119
- North Dakota—geochemistry**
- processes*: Hydrogenation of coal and sulfide minerals 16
- North Dakota—hydrogeology**
- ground water*: Buried glaciofluvial aquifer system in southeastern McIntosh County in North Dakota 119
- Ground-water flow model of Harmon lignite at Gascoyne Mine, North Dakota 119
- hydrology*: North Dakota 119

Northern Hemisphere *see also* Africa; Arctic Ocean; Atlantic Ocean; North America; Pacific Ocean

nuclear facilities *see also under* engineering geology *under* Massachusetts; Oregon

nuclear facilities—geologic hazards
research: Reactor hazards 266-268

O

ocean basins *see also under* oceanography *under* Alaska

ocean circulation *see also under* oceanography *under* Atlantic Ocean; Bering Sea; California; Florida

ocean floors *see also under* oceanography *under* Indian Ocean

oceanography—research
general: Oceanic studies 157-159

oceanography—sea ice
experimental studies: Results of AIDJEX main experiment 244-245
models: Sea-ice model 245
remote sensing: Radar imagery study of Beaufort Sea ice 245
research: Sea-ice studies 244-245

Ohio—economic geology
coal: Neutron activation and magnetism of coal 17
lithium: Lithium in flint clays 43-44
natural gas: Possible stratigraphic controls for Devonian gasfields in the Appalachian Basin 22

Ohio—environmental geology
geologic hazards: Magnitude and frequency of Ohio floods 282-283

Ohio—hydrogeology
ground water: Steady state flow conditions simulated for potential strip mining areas in Ohio 219-220
hydrology: Assessment of water quality in an Ohio watershed 235

oil shale *see also under* economic geology *under* Colorado; Nevada; Utah

oil shale—resources
distribution: Oil-shale resources 25-26

Oklahoma—economic geology
petroleum: Application of helium surveys to petroleum exploration 24

Oklahoma—hydrogeology
ground water: Geohydrology of the Arbuckle aquifer, south-central Oklahoma 119
— Quality of ground-water varies in prospective coal-lease areas of east-central Oklahoma 119-120
— Quality of water in abandoned zinc mines in northeastern Oklahoma and southeastern Kansas 111
hydrology: Oklahoma 119-120
— Quality of water in Oklahoma's abandoned coal pits 120
— Stream-water quality in eastern Oklahoma coalfield 120

ophiolite *see under* petrology *under* metamorphic rocks; *see under* ultramafic family *under* igneous rocks

Ordovician *see also under* geochronology *under* United Kingdom; *see also under* stratigraphy *under* Appalachians; Pennsylvania

Oregon—areal geology
regional: Oregon 77-78

Oregon—economic geology
base metals: Mineralized volcanic arc in westernmost Idaho and adjacent Oregon 69
copper: Relationships of copper and gold deposits in the ophiolitic Canyon Mountain Complex in Grant County, Oregon 6-7

geothermal energy: Geothermal hydrology and geochemistry of the Klamath Falls area in Oregon 206-207

— Newberry Volcano in Oregon 194

gold: Relationships of copper and gold deposits in the ophiolitic Canyon Mountain Complex in Grant County, Oregon 6-7

maps: Mineral exploration potential maps 13-14

mercury: Geochemical anomalies associated with mercury deposits in Nevada and Oregon 10

natural gas: Oil and gas resources of the Outer Continental Shelf 23

petroleum: Oil and gas resources of the Outer Continental Shelf 23

Oregon—engineering geology
nuclear facilities: Expected ground motion at proposed nuclear power plant sites 268

Oregon—environmental geology
pollution: Analyses of Yamette River bottom material and elutriates 236
— Streets contribute much lead to urban runoff 130

Oregon—geochemistry
surveys: Geochemical anomalies associated with mercury deposits in Nevada and Oregon 10

Oregon—geochronology
Neogene: Picture Gorge Basalt coeval with middle part of Grande Ronde Basalt 180-181

Triassic: Age of quartz diorite at Bishop Spring in northwestern Oregon 74

Oregon—geomorphology
olian features: Daily cycles in coastal dune deposits 159

Oregon—geophysical surveys
remote sensing: Aeromagnetic mapping in the Vale-Owyhee area of Oregon 206
— Geophysical mapping of the central Cascades 206

Oregon—hydrogeology
ground water: Ground water in southern Douglas County 130
hydrology: Estuarine sediment sources in the Tillamook Estuary in Oregon 163
— Oregon 130
— Red colonies on fecal-coliform-bacteria plates identified 238
— Streets contribute much lead to urban runoff 130

— Water quality of active and inactive log ponds 241

Oregon—petrology
intrusions: Gently dipping feeder dikes for Columbia River Basalt Group 180

Oregon—stratigraphy
Mesozoic: Radiolarians from Mesozoic rocks in western Oregon 77-78

organic materials—analysis
chemical analysis: Organic solutes 248
chromatography: Biological methods 249
— Determination of acetone 248
— Hydrophobic organic acids 248-249
— Pesticides 249

organic materials—humic acids
geochemistry: Organic materials and conditions of uranium fixation 36-37
structure: Humic acids 249

organic materials—hydrocarbons
abundance: Environmental organic geochemistry of Mid-Atlantic shelf sediments 148
— Organic gases in geothermal fluids 201

— Organic geochemistry of heavy hydrocarbons in Florida-Hatteras outer continental shelf sediments 148
sediments: Thermogenic gas seep on the sea floor of Norton Sound 155-156

orthosilicates *see under* minerals

Ostracoda—biostratigraphy
Cretaceous: A new Upper Cretaceous ostracode zone 230
— Cretaceous biostratigraphy in Arkansas 230

oxides *see under* minerals

oxygen— isotopes
O-18/O-16: Snake River plain, Idaho, geothermal well studies 39-40
— Stable isotope studies of thorium-bearing veins in the Wet Mountains of Colorado 33
— Three-million-year isotopic record of paleoclimate at Death Valley in California 216
— Water temperature of corals shown by isotopic analysis 216

P

Pacific Coast—areal geology
regional: Pacific Coast region 74-87

Pacific Coast—economic geology
mercury: Relation of mercury mineralization to The Geysers hydrothermal system 198-199
petroleum: California to Washington 150

Pacific Coast—engineering geology
geologic hazards: Petroleum resources potential and geologic hazards of the Oregon-Washington outer continental shelf 152

Pacific Coast—environmental geology
land use: Land use and land cover research and analysis 320-322
— Pacific Northwest Demonstration Project 303

- Pacific Coast—geophysical surveys**
seismic surveys: Recent faulting of seafloor off Humboldt Bay in California 151-152
springs: Geothermal gradient is 800°C at Coso Hot Springs 126-127
- Pacific Coast—hydrogeology**
hydrology: Pacific Coast 161-163
- Pacific Coast—seismology**
earthquakes: Geology of the Monterey Bay region 151
- Pacific Ocean** *see also* Bering Sea; Micronesia
- Pacific Ocean—economic geology**
petroleum: Petroleum resources potential and geologic hazards of the Oregon-Washington outer continental shelf 152
- Pacific Ocean—geochemistry**
nodules: Sediment-nodule geochemistry of deep sea manganese nodules 157-158
- Pacific Ocean—geophysical surveys**
remote sensing: Trust territories 306
seismic surveys: Geology of the Monterey Bay region 151
surveys: California to Washington 150
 — Deep-tow studies of the East Pacific Rise, Pacific Ocean basin 158
- Pacific Ocean—oceanography**
continental shelf: Potential petroleum reservoirs within Tertiary melange, coastal Olympic Peninsula and adjacent OCS 78
marine geology: Pacific continental margin 150-153
reefs: Coral caps on seamounts of the Emperor Seamount Chain 158
- Pacific Ocean—stratigraphy**
Quaternary: Nannofossil ages for East Pacific Rise fast spreading sites 158-159
- Pacific Ocean—tectonophysics**
plate tectonics: Magnetic depth estimates 173
sea-floor spreading: Nannofossil ages for East Pacific Rise fast spreading sites 158-159
- Pacific region—general**
maps: Circumpacific map project 330
- paleoclimatology—Cenozoic**
California: Three-million-year isotopic record of paleoclimate at Death Valley in California 216
 — Three million years of climate history at Searles Lake 216-217
- paleoclimatology—Holocene**
Arizona: Tree rings and alluvial history on Black Mesa, Arizona 214-215
- paleoclimatology—indicators**
isotopes: Water temperature of corals shown by isotopic analysis 216
- paleoclimatology—Quaternary**
Mexico: Pleistocene and Holocene climate in central Mexico 215
- Paleogene** *see also under* stratigraphy *under* Alaska; Washington
- paleogeography—Cretaceous**
Minnesota: New biostratigraphic, paleogeographic, and tectonic data on Cretaceous rocks in Minnesota and eastern South Dakota 18-19
- paleogeography—Eocene**
Wyoming: Course of Eocene Wind River locates auriferous sedimentary rocks in the western Wind River Basin in Wyoming 6
- paleomagnetism—Alaska**
Paleozoic: Paleomagnetic results from the Alexander terrane and from eastern North America agree on Paleozoic paleolatitudes 85-86
- paleomagnetism—experimental studies**
general: Rock magnetism 167-168
- paleomagnetism—pole positions**
anomalies: Paleomagnetic poles from the Valdez(?) and Orca Groups, Alaska 167
- paleomagnetism—Proterozoic**
Saudi Arabia: Paleomagnetism 349-350
- paleomagnetism—Triassic**
Arizona: Origin of natural remanent magnetization in red sedimentary rocks of the Moenkopi Formation in Arizona 168
- paleontology—general**
research: Paleontology 227-233
- Paleozoic** *see also under* stratigraphy *under* Alaska; Connecticut; Idaho; Maine; Massachusetts; North America; United States
- palynomorphs—biostratigraphy**
Cretaceous: Dinoflagellates and acritarchs prove useful in the biostratigraphic and paleoecologic analysis of Santonian-Age formation in southwestern Arkansas 228
- palynomorphs—miospores**
Cretaceous: New age data, Early Cretaceous, Colorado Plateau 229
- peat** *see also under* economic geology *under* Minnesota
- peat—geochemistry**
trace elements: Environmental pollution of the Everglades in Florida 16-17
- Pelecypoda** *see* Bivalvia *under* Mollusca
- Pennsylvania—economic geology**
lithium: Lithium in flint clays 43-44
- Pennsylvania—environmental geology**
geologic hazards: Floods of July 1977 in the Johnstown area of western Pennsylvania 281
- Pennsylvania—geophysical surveys**
remote sensing: Circular feature in Pennsylvania 308
- Pennsylvania—hydrogeology**
hydrology: Effects of land use on water quality of rivers 234
 — Nutrient and sediment discharges for agricultural land 98-99
 — Pennsylvania 98-99
- Pennsylvania—stratigraphy**
Ordovician: Conodont-based Lower Ordovician correlations in eastern Pennsylvania 231-232
 — Ordovician clastic rocks of eastern Pennsylvania 50
- Pennsylvanian** *see also under* stratigraphy *under* Idaho
- permafrost** *see also under* engineering geology *under* Alaska
- Permian** *see also under* stratigraphy *under* Idaho; Montana; Wyoming
- Peru—areal geology**
regional: Peru 345-346
- petroleum** *see also under* economic geology *under* Alaska; Appalachians; Atlantic Ocean; California; Colorado; Florida; Great Basin; Great Plains; Guatemala; Gulf of Mexico; Idaho; Malaysia; Montana; Nevada; Oklahoma; Oregon; Pacific Coast; Pacific Ocean; Rocky Mountains; Utah; Washington; Wyoming
- petroleum—exploration**
gravity methods: Accuracy of borehole gravity data 25
isotopes: Application of stable carbon isotopic ratios to exploration for deep-water source sediments 24
techniques: New exploration and production techniques 23-25
- petroleum—production**
eolian deposits: Studies of eolian deposits aid production problems 24
techniques: New exploration and production techniques 23-25
- petroleum—resources**
distribution: Oil and gas resources 17-25
offshore: Offshore areas 23
- Phanerozoic** *see also under* geochronology *under* Arizona
- phase equilibria—chemically precipitated rocks**
experimental studies: Salt and anhydrite 276
- phase equilibria—experimental studies**
 $Al_2O_3-SiO_2-H_2O$: Solubilities in the system $Al_2O_3-SiO_2-H_2O$ 183
 $MgO-CaO-SiO_2-H_2O-HCl$: Experimental studies in the $MgO-CaO-SiO_2-H_2O-HCl$ system 176
- Philippine Islands—hydrogeology**
ground water: Shallow ground-water potential, Subic Naval Base 346
hydrology: Philippine Islands 346
- phosphate** *see also under* economic geology *under* California; Eastern U.S.; Florida; Idaho; North Carolina
- phosphates** *see under* minerals
- phosphorus—geochemistry**
peat: Environmental pollution of the Everglades in Florida 16-17
- planetology** *see also* Mars; Moon
- planetology—general**
research: Astrogeology 292-300
 — Planetary investigations 293-295
- Plantae** *see also* algae; gymnosperms; palynomorphs; pteridophytes
- Plantae—ecology**
terrestrial environment: Plant ecology 233-234
- Plantae—occurrence**
peat: Antarctic paleobotany and coal 353
- plate tectonics** *see also under* tectonophysics *under* Alaska; Arabian Peninsula; California; Pacific Ocean; Red Sea region

- plate tectonics—indicators**
carbon dioxide: Relationship of carbon dioxide to seismogenic zones 261
- plate tectonics—mechanism**
seismotectonics: Analysis of stress-concentration mechanism for intraplate earthquakes 172-173
- Pleistocene** *see also under* geochronology *under* California; Washington; *see also under* stratigraphy *under* Alaska; Atlantic Coastal Plain; Black Sea; Kentucky
- Pleistocene—geochronology**
time scales: Revised late Cenozoic geomagnetic polarity time-scale 167
- Pliocene** *see also under* stratigraphy *under* North Carolina
- Pliocene—geochronology**
time scales: Revised late Cenozoic geomagnetic polarity time-scale 167
- plutons** *see under* intrusions
- Poland—economic geology**
coal: Poland 346
 — Special Foreign Currency Program 346
- pollution** *see also under* environmental geology *under* California; Colorado; Eastern U.S.; Florida; Hawaii; Idaho; Indiana; Kansas; Louisiana; Michigan; Missouri; Montana; Nevada; New York; Oregon; Washington
- pollution—pollutants**
asbestos: Health aspects of the asbestos minerals as they relate to the mining industry 178-179
lead: Bioavailability of sediment-bound lead and zinc to estuarine clams 285
toxicity: Characterizing levels of chronic toxicity 285
trace elements: Mass balances of trace elements at powerplants 16
- pollution—waste disposal**
radioactive waste: Hydrologic investigations relative to the disposal of low level radioactive waste 280
 — Relation of radioactive waste to the hydrologic environment 278-280
- pollution—water**
experimental studies: Transport of organic solutes by in situ oil shale retorting 284
ground water: Fate of wood preservatives in ground water 284
research: Effects of pollutants on water quality 284-288
- Precambrian** *see also under* geochronology *under* Mexico; United States; *see also under* stratigraphy *under* Montana; South Dakota; Utah; Wyoming
- Proterozoic** *see also under* geochronology *under* Montana; Saudi Arabia; Wyoming; *see also under* stratigraphy *under* Saudi Arabia; Utah
- pteridophytes—biostratigraphy**
Mississippian: New floral zone in Mississippian of Virginia and West Virginia 230
- Puerto Rico—economic geology**
copper: Stream water sampling in Puerto Rico 11-12
- Puerto Rico—environmental geology**
maps: Inundation maps of urban areas 283-284
 — Maps of flood-prone areas 283
- Puerto Rico—hydrogeology**
ground water: Artificial recharge with wastewater 221
- Puerto Rico—oceanography**
sedimentation: Dispersal paths of river sediments on the north shelf of Puerto Rico 150
- pyrite** *see also under* economic geology *under* South Carolina
- Q**
- Quaternary** *see also under* geochronology *under* Wyoming; *see also under* stratigraphy *under* Arizona; Mexico; Pacific Ocean
- Quaternary—geochronology**
absolute age: Uranium-trend dating of alluvium deposits 192
- R**
- radioactive dating** *see* absolute age
- radioactivity surveys** *see under* geophysical surveys *under* South Carolina
- Radiolaria—biostratigraphy**
Mesozoic: Radiolarians from Mesozoic rocks in western Oregon 77-78
Paleozoic: Radiolarian age-dating of Paleozoic cherts 230
- radon—geochemistry**
water: Helium and radon in uranium exploration 12
- rare earths—abundance**
plutonic rocks: Jurassic zoned tonalite-trondhjemite pluton in Trinity Alps of Klamath Mountains in California 185
- reclamation** *see also under* environmental geology *under* Great Plains; Illinois; Montana; New Mexico; North Dakota; Western Interior; Western U.S.
- Red Sea region—tectonophysics**
plate tectonics: Red Sea opening 184
- reefs** *see also under* oceanography *under* Pacific Ocean
- reefs—evolution**
diagenesis: Reef destruction by boring organisms 159
- regional geology** *see* areal geology *under* the appropriate area term
- remote sensing** *see also* geophysical methods; *see also under* geophysical surveys *under* Alaska; Arabian Peninsula; Arctic Ocean; automatic data processing; California; Colorado; Idaho; Maine; Moon; Nevada; New Mexico; Oregon; Pacific Ocean; Pennsylvania; South America; Tennessee; Turkey; United States; Utah; Virginia; Wyoming
- remote sensing—airial photography**
maps: Mapping from high-resolution high-altitude photographs 356
techniques: Resolution measurements with star and bar targets 356
- remote sensing—applications**
aviation: Minimum safe altitude warning project 355
cartography: Applications to cartographic studies 314-316
 — Landsat-3 investigations 314
 — Parameters for an automated mapping satellite (Mapsat) 315-316
 — Satellite image maps 314-315
 — Space oblique Mercator projection 315
- defoliation*: Forest defoliation 305
environment: Studying the global environment 305
general: Remote sensing application to geologic studies 309-312
geodesy: Aerial profiling of terrain 355
glaciers: Atlas of glaciers 306
hydrology: Applications to hydrologic studies 312-314
 — Landsat surveillance of water turbidity and color 313
 — Surface-water applications of Landsat data 313-314
land use: Assessing the impact of surface mining 304-305
meteorology: Cloud top temperature monitoring 305
military geology: Nighttime images of the Earth from space 314
mineral exploration: Targeting mineral exploration 306-309
 — William T. Pecora Memorial Symposium 306
monitoring: Monitoring the environment 301-305
petrology: Landsat filters for rock type discrimination 311
- remote sensing—automatic data processing**
EROS: Data Analysis Laboratory 301
- remote sensing—general**
research: Cooperative projects with states 303-304
 — Cooperative projects with the Bureau of Land Management 301-303
 — Cooperative projects with the Bureau of Reclamation 304
- remote sensing—instruments**
detectors: A plastic detector for aerial gamma-ray surveys 174-175
electronic units: Compact, low-power telemetry controller and transmitter unit for volcanic gas monitoring 176-177
- remote sensing—interpretation**
corrections: Effects of atmosphere on Landsat data 306-307
multispectral analysis: Correlation of Landsat data with geophysical data 307
spectral analysis: Origin of bands in mineral and rock spectra in the three-micrometer range 310
 — Spectral signatures of minerals in the visible and near-infrared regions of the spectrum 310

- stereoscopic projection*: Stereoscopic projection system to interpret Landsat data 307-308
- remote sensing—methods**
research: Remote sensing and advanced techniques 301-316
satellite methods: Earth Resources Observation Systems program 301-309
- reservoirs** *see also* engineering geology under Colorado
- Rhode Island—hydrogeology**
hydrology: Measurement of aquifer characteristics in the Pawcatuck River basin 99
 — Rhode Island 99
- Rhode Island—stratigraphy**
Cambrian: Nature of Cambrian trilobite-bearing rocks from Beavertail Point 48
- rock mechanics** *see also* soil mechanics
- rock mechanics—deformation**
fractures: Pressurized fractures in hot rock 199
stress: In-situ stress on Barre Granite in Vermont 267-268
- rock mechanics—materials, properties**
oil shale: Radar-transport oil shales 173-174
research: Research in rock mechanics 264
reservoir rocks: Electrical properties in a geothermal environment 169-170
thermal conductivity: Thermal conductivities of rocks 194
 — Thermal properties 277
- Rocky Mountains—areal geology**
research: Rocky Mountains and the Great Plains 55-68
- Rocky Mountains—economic geology**
natural gas: Rocky Mountains and Great Plains 18-20
petroleum: Rocky Mountains and Great Plains 18-20
- Rocky Mountains—environmental geology**
geologic hazards: Environmental geology 56-58
land use: Environmental geology 56-58
- Rocky Mountains—geochronology**
absolute age: Soil development and age of Bull Lake Glaciation in the Rocky Mountains 57
- Rocky Mountains—stratigraphy**
Triassic: Permian-Triassic boundary in western Wyoming and parts of Idaho and Montana 232-233
- S**
- Saudi Arabia—areal geology**
regional: Saudi Arabia 346-350
- Saudi Arabia—economic geology**
base metals: Investigation of base metal deposits 347
gold: The Jabal Ishmas-Wadi Tathlith gold belt 348
metals: Mineralization associated with granites 347-348
 — Preliminary sulfur isotopic studies 347
- nonmetals*: Inventory of nonmetallic mineral deposits 346-347
water resources: Water-resource development 350
- Saudi Arabia—geochronology**
Proterozoic: Age and evolution of the southern part of the Arabian Shield 348-349
 — Discordancy of zircons in the Saudi Arabian Shield 191
- Saudi Arabia—hydrogeology**
ground water: Future water supplies for Riyadh 350
- Saudi Arabia—paleontology**
Vertebrata: Paleocene vertebrates from southern Hijaz Province, Kingdom of Saudi Arabia 227
- Saudi Arabia—petrology**
igneous rocks: Red Sea opening 184
- Saudi Arabia—stratigraphy**
Proterozoic: Paleomagnetism 349-350
- sea-floor spreading** *see also* under tectonophysics under Pacific Ocean
- sea water—geochemistry**
hydrocarbons: Detection of marine oil slicks as a petroleum exploration tool 23-24
- sedimentary petrology—general**
research: Sedimentology 210-212
- sedimentary petrology—instruments**
samplers: Design requirements for pumping samplers 212
 — Helley-Smith bedload sampler 212
 — Instrumentation 212
- sedimentary petrology—techniques**
laser probe: Suspended-sediment analysis by laser-light methods 212
samplers: Sampler for large streams 212
- sedimentary rocks** *see also* sedimentary structures; sedimentation; sediments
- sedimentary rocks—carbonate rocks**
chemical composition: Source-rock potential of South Florida Basin 23
- sedimentary rocks—clastic rocks**
black shale: Hydrocarbon maturation in Kentucky and Virginia 22
clasts: Synorogenic mudflow deposit 52
conglomerate: Character of the conglomerate of the Shinarump Member of the Chinle Formation at Window Rock in Arizona 29
flysch: Mississippian flysch in Toiyabe Range in central Nevada 70
lithofacies: Facies change related to ore deposition 28
 — Genesis of tabular uranium bodies in Triassic and Jurassic basins in Eastern United States 27
mineral composition: Mineralogic character of some hydrocarbon reservoirs in Uinta Basin, Utah 21
Ordovician: Ordovician clastic rocks of eastern Pennsylvania 50
- sedimentary rocks—environmental analysis**
braided streams: Sedimentary facies in Tertiary rocks in the Tyonek quadrangle 84
- sedimentary rocks—geochemistry—geochemistry**
trace elements: uranium: black shale: Uranium, thorium, carbon, and sulfur in Devonian black shale from West Virginia, Kentucky, and New York 39
trace elements: Isolation of zones in oil shale with distinctive chemical characteristics using statistical techniques 25
- sedimentary rocks—lithofacies**
phosphorite: California phosphorite 43
- sedimentary rocks—lithostratigraphy**
Paleozoic: Late Paleozoic depositional patterns suggest separate crustal responses north and south of eastern Snake River Plain 65
- sedimentary structures** *see also* sedimentary rocks; sediments
- sedimentary structures—planar bedding structures**
channels: Diversion of the Hudson River in Pleistocene time 97
- sedimentation—controls**
structural controls: Tectonics and sedimentology of upper Tertiary fluvial deposits along Maacama fault studies 76
- sedimentation—cyclic processes**
dunes: Daily cycles in coastal dune deposits 159
- sedimentation—deposition**
Paleozoic: Late Paleozoic depositional patterns suggest separate crustal responses north and south of eastern Snake River Plain 65
submarine fans: Sedimentological features and growth of the Monterey deep-sea fan off central California 151
tracer experiments: Sediment deposition and movement, Gulf of Mexico continental shelf 149
- sedimentation—environment**
arctic environment: Rates of Arctic marine geologic processes 157
barrier islands: Nearshore sedimentation in Upper Cretaceous deposits in Western Georgia 52
high-energy environment: California phosphorite 43
marine environment: Gulf of Mexico and Caribbean Sea 148-150
paleochannels: Intertonguing, paleochannels, and faults in the Wasatch Plateau in Utah 14-15
terrestrial environment: Uranium in Triassic rocks in southeast Utah 28
 — Uranium mineralization at the Upper Cretaceous Fox Hills Sandstone-Lance Formation interface 27-28
- sedimentation—processes**
bioturbation: Bioturbation traces 212
 — Interactions of oil and burrowing fauna experiment at Willapa Bay 153
deposition: Sedimentation, tectonics, and petroleum potential of California Coast Ranges 21-22

- sedimentation—provenance**
clastic rocks: Deep-water sedimentation influenced by an actively-shifting source terrane 77
 — Paleotransport directions in Nanushuk Group 81
estuaries: Estuarine sediment sources in the Tillamook Estuary in Oregon 163
heavy minerals: Heavy-mineral assemblages of Willapa Bay in Washington 153
- sedimentation—rates**
reworking: Pb-210 profiles in continental shelf sediments; an index to rates of sediment reworking 146
source rocks: Rates of sedimentation of petroleum source rocks in Utah, Nevada, and Idaho 21
- sedimentation—transport**
channels: Character of the conglomerate of the Shinarump Member of the Chinle Formation at Window Rock in Arizona 29
marine transport: Beach-sand retention landward of a nearshore submarine canyon 151
 — Bedform movement in lower Cook inlet 155
 — Bottom boundary layers and sediment transport on the floor of Norton Sound in Alaska 156-157
 — Currents and bottom sediment movement on Georges Bank 146
 — Dispersal paths of river sediments on the north shelf of Puerto Rico 150
 — Migration of sand waves in central San Francisco Bay 161
 — Sediment transport on the inner shelf of the Beaufort Sea 157
 — Separate and superimposed equilibrium bedforms; a synthesis of flume and San Francisco Bay observations 152-153
mass movements: Submarine landslides on the Mississippi Delta 149
stream transport: Analyses of long-term sediment records 210
 — Bedload-transport rates 210
 — Iowa sediment-data compiled 114
 — Reinterpretation of Grand Canyon geomorphology 71-72
 — Sediment studies of the Amazon River 340
 — Variability of sediment discharge 210
wind transport: Modification of eolian deposits 212
- sediments** *see also* sedimentary rocks; sedimentary structures; sedimentation
- sediments—clastic sediments**
genesis: Surficial deposits in San Juan Basin of New Mexico 56
- sediments—distribution**
bays: Sediments of Corpus Christi Bay 149-150
- sediments—geochemistry**
organic materials: Environmental organic geochemistry of Mid-Atlantic shelf sediments 148
 — Organic geochemistry of heavy hydrocarbons in Florida-Hatteras outer continental shelf sediments 148
trace metals: Vertical distribution of trace metals in sediments of Georges Bank 146
- sediments—pore water**
environmental analysis: Hypersaline epoch in the Black Sea 159
- sediments—textures**
grain size: Environmental assessment of the South Atlantic continental shelf 148
- seismic surveys** *see under* geophysical surveys *under* Atlantic Ocean; Bering Sea; Gulf of Mexico; Hawaii; Idaho; Pacific Coast; Pacific Ocean
- seismology** *see also* engineering geology
- seismology—crust**
models: Worldwide three-dimensional seismic crustal studies 209
- seismology—earthquakes**
aftershocks: Guatemala 262
ground motion: Estimation of design ground motions 263
 — Ground motion investigations 262-263
 — Ground response in the Los Angeles region 262
 — Ground response in the Salt Lake City region 263
 — Ground response in the San Francisco Bay region 262-263
 — Seismic intensities of the 1906 California earthquake 262
mechanism: Source of earthquake energy 262
occurrence: Kermit, Texas 261
prediction: Analyses of seismic data 255
 — Earthquake mechanics and prediction studies 253-257
 — Hydrofracturing 255-256
 — Laboratory studies 256-257
 — Land deformation 253-254
publications: Earthquake Information Bulletin, and Preliminary Determination of Epicenters 367
 — Earthquake publications 365
research: Earthquake studies 250-264
seismotectonics: Tectonic framework and fault investigations 257-261
strong motion: Strong-motion recording program 264
- seismology—elastic waves**
P-waves: P-wave delay studies in geothermal areas 199
- seismology—methods**
instruments: Equipment development 255
- seismology—observatories**
international cooperation: Crustal studies 327-329
National Earthquake Information Service: National Earthquake Information Service 250-251
networks: Observatory and seismic data systems 251
- seismology—seismicity**
faults: Seismicity of The Geysers-Clear Lake geothermal area in California 195
research: Seismicity 250-253
 — Seismicity and seismic parameters research 251-253
 — Seismicity investigations 261-262
seismotectonics: California coastal tectonics 259
 — Relationship of carbon dioxide to seismogenic zones 261
 — Seismogenic zones of Alaska and adjacent continental shelf 257
 — Seismotectonics of the Mississippi embayment 260
 — Seismotectonics of Utah and Nevada 259-260
 — Southern California tectonics 258-259
 — Tectonic framework of the San Francisco Bay Region 258
 — The 1899 Yakutat Bay earthquakes 257-258
 — Trench investigation of faults 261
zoning: Charleston, South Carolina 261
- seismology—volcanology**
eruptions: Southern Alaska 261-262
- selenium—analysis**
chemical analysis: Arsenic and selenium 248
- shorelines** *see also under* engineering geology *under* Alaska
- silicates** *see under* minerals
- Silurian** *see also under* geochronology *under* Great Britain
- silver** *see also under* economic geology *under* California; Idaho
- slope stability** *see also* engineering geology; geomorphology; *see also under* engineering geology *under* Montana; Washington; Wyoming
- slope stability—landslides**
earthquakes: Landslides 263
field studies: Ground failure investigations 263-264
research: Landslide hazards 265-266
seismicity: The effect of scale on seismic-induced landslides 266
- soil mechanics** *see also* rock mechanics
- soil mechanics—deformation**
shear modulus: Dynamic response of soils to shear 263
- soils—analysis**
sample preparation: Sample preparation effects elements extractions of soils 245
- soils—surveys**
Antarctica: Baseline soil investigations in the Pensacola Mountains 353
Arizona: Soil moisture along a bajada in southern Arizona 240
Colorado: Soil geochemistry in the Uinta and Piceance Basins 288
Rocky Mountains: Soil development and age of Bull Lake Glaciation in the Rocky Mountains 57
Washington: Irrigation increased in Horse Heaven Hills 132
- solubility** *see under* properties *under* geochemistry

- South America** *see also* Brazil; Chile; Peru
- South America—geophysical surveys**
remote sensing: South America 306
- South America—hydrogeology**
hydrology: Argentina, Bolivia, and Paraguay 339
 — Rio Pilcomayo sedimentation 339
- South Carolina—economic geology**
gold: Mineralization controls at the Haile gold mine in South Carolina 4
heavy minerals: Ground checks of aeroradioactivity anomalies in the Atlantic Coastal Plain of South Carolina 4
mineral resources: Mineral-resource potential of Wambaw Swamp Wilderness Study Area in South Carolina 3
pyrite: Mineralization controls at the Haile gold mine in South Carolina 4
- South Carolina—engineering geology**
earthquakes: Hydrofracturing 255-256
waste disposal: Hydrologic evaluation of radioactive waste buried in Barnwell County, South Carolina 280
- South Carolina—geophysical surveys**
radioactivity surveys: Ground checks of aeroradioactivity anomalies in the Atlantic Coastal Plain of South Carolina 4
- South Carolina—hydrogeology**
ground water: Results of long-term monitoring for saltwater in the Savannah area of Georgia and South Carolina 103
 — Saltwater encroachment in the principal artesian aquifer for Beaufort, Colleton, Hampton, and Jasper Counties 107-108
hydrology: South Carolina 107-108
- South Carolina—seismology**
crust: Upper-crustal structures near Charleston, South Carolina 171
earthquakes: Charleston, South Carolina 261
- South Carolina—stratigraphy**
Jurassic: Triassic and Jurassic rocks in the South Carolina coastal plain 51-52
Triassic: Triassic and Jurassic rocks in the South Carolina coastal plain 51-52
- South Carolina—structural geology**
folds: Inner Piedmont Deformation 50
- South Dakota—economic geology**
gold: Uranium, thorium, and gold in Precambrian conglomerate in Black Hills, South Dakota 30-31
thorium: Uranium, thorium, and gold in Precambrian conglomerate in Black Hills, South Dakota 30-31
uranium: Uranium, thorium, and gold in Precambrian conglomerate in Black Hills, South Dakota 30-31
- South Dakota—environmental geology**
land use: South Dakota 303-304
- South Dakota—geomorphology**
glacial geology: Pingo scars in southwestern South Dakota 57-58
- South Dakota—hydrogeology**
ground water: A thick glacial-drift deposit contains several outwash aquifers in Miner County 121
 — Big Sioux aquifer in parts of eastern South Dakota extends beyond stream valleys 120-121
 — Extensive aquifers occur in alluvium and outwash deposits in Walworth County 121
 — Large ground-water yields in northeastern South Dakota 121
 — Madison Group only a part of a major aquifer system in South Dakota 120
 — Major outwash aquifers located in southeastern South Dakota 120
hydrology: South Dakota 120-121
- South Dakota—stratigraphy**
Cretaceous: New biostratigraphic, paleogeographic, and tectonic data on Cretaceous rocks in Minnesota and eastern South Dakota 18-19
Precambrian: Uranium, thorium, and gold in Precambrian conglomerate in Black Hills, South Dakota 30-31
- South Dakota—structural geology**
tectonics: New biostratigraphic, paleogeographic, and tectonic data on Cretaceous rocks in Minnesota and eastern South Dakota 18-19
- Southern Hemisphere** *see also* Africa; Antarctica; Atlantic Ocean; Indian Ocean; Pacific Ocean; South America
- Southwestern U.S.—economic geology**
uranium: Radioactive spring site guides to uranium in southwestern United States 12
- Southwestern U.S.—geophysical surveys**
magnetotelluric surveys: Magnetotelluric survey of the Southwest 207
- spectrometry** *see* spectroscopy
- spectroscopy—methods**
atomic absorption: Lithium isotopes 249
 — New analytical methods and techniques 12
 — New atomic-absorption method for tellurium 12
mass spectroscopy: Stable isotope ratios 249
- spectroscopy—techniques**
emission spectroscopy: Plasma emission spectrometry 247-248
plasma emission spectroscopy: Argon inductively coupled plasma in the analysis of geological materials by atomic emission spectrometry 246
research: Emission spectroscopy 246
- springs** *see also* ground water; *see also under* hydrogeology *under* Alaska; California; Colorado; Montana; Utah; Wyoming
- springs—geochemistry**
theoretical studies: Chemical modeling of geothermal waters 193
- Sri Lanka—hydrogeology**
ground water: Jaffna Peninsula irrigation development review 350
hydrology: Sri Lanka 350
- standard materials—analysis**
beryllium: Determination of beryllium in geologic materials 246
thallium: Thallium contents of 16 USGS standard rocks 246
- strontium— isotopes**
Sr-87/Sr-86: Crustal melting in the San Francisco volcanic field in Arizona 41
 — Strontium-isotope data from Pioneer batholith in southwestern Montana 61
 — Uranium in two-mica granite in northern New England 38-39
- structural analysis** *see also* folds
- structural analysis—folds**
foliation: Fitchburg pluton in Massachusetts 46
mapping: Structural evolution of the Vermilion district of Minnesota 53-54
phases: Inner Piedmont Deformation 50
- structural analysis—interpretation**
interference patterns: Multiple deformation of gneiss dome near Rincon Mountains in southeastern Arizona 73
melange: Potential petroleum reservoirs within Tertiary melange, coastal Olympic Peninsula and adjacent OCS 78
- structural petrology** *see* structural analysis
- Sudan—areal geology**
regional: Sudan 350-351
- Sudan—economic geology**
water resources: Water data and information management 351
- sulfides** *see under* minerals
- sulfur—geochemistry**
black shale: Uranium, thorium, carbon, and sulfur in Devonian black shale from West Virginia, Kentucky, and New York 39
- sulfur— isotopes**
S-34/S-32: Iron sulfide minerals and sulfur isotopes associated with roll-type uranium deposits 33-34
- sulphur** *see* Sulfur
- surveys—hydrogeology**
ground water: Second test well completed in the Madison aquifer 118
- surveys—research**
U. S. Geological Survey: Cooperation with other Federal agencies 166
 — How to obtain publications 366-367
 — Publications issued 365-366
 — U. S. Geological Survey publications 364-367
- symposia—economic geology**
mineral exploration: William T. Pecora Memorial Symposium 306
- symposia—general**
research: International representation 330-331

T

- tectonics** *see also* faults; folds; structural analysis; *see also under* structural geology *under* Arizona; California; Colorado; Idaho; Maryland; Minnesota; Montana; Nevada; New England; New Mexico; South Dakota; United States; Utah; Virginia; Washington; Wyoming
- tellurium—analysis**
spectroscopy: New atomic-absorption method for tellurium 12

- Tennessee—economic geology**
mineral resources: Mineral-resource assessment of the Citico Creek Wilderness Study Area in Tennessee 3
thorium: Uranium, thorium, carbon, and sulfur in Devonian black shale from West Virginia, Kentucky, and New York 39
uranium: Uranium, thorium, carbon, and sulfur in Devonian black shale from West Virginia, Kentucky, and New York 39
- Tennessee—engineering geology**
waste disposal: Detection of gamma-emitting radioisotopes in boreholes 279-280
- Tennessee—geophysical surveys**
remote sensing: Using infrared aerial photographs for ground-water exploration 313
- Tennessee—hydrogeology**
ground water: Ground-water exploration in carbonate rocks 108
hydrology: Tennessee 108
- Tennessee—stratigraphy**
Devonian: Devonian black shale stratigraphy 49-50
- tephrochronology** *see under* geochronology
- Tertiary** *see also under* geochronology *under* Nevada; *see also under* stratigraphy *under* Colorado; Nevada; North America; Utah
- Texas—economic geology**
uranium: In-hole gamma ray studies in Texas 11
 — Iron sulfide minerals and sulfur isotopes associated with roll-type uranium deposits 33-34
 — Modern day formation of a uranium orebody in Bee County, Texas 176
 — Stratigraphic relations in the Whitsett Formation in South Texas 29
 — Uranium possibilities of Marfa Basin in Texas 29
- Texas—engineering geology**
land subsidence: Subsidence rate decreasing in the Houston-Galveston area of Texas 289
marine installations: Sediments of Corpus Christi Bay 149-150
- Texas—geophysical surveys**
radioactivity methods: In-hole gamma ray studies in Texas 11
- Texas—hydrogeology**
ground water: Digital-computer model simulates ground-water flow in the lower Mesilla Valley of Texas and New Mexico 111
 — Effects of carbonate facies and faulting on hydrogeology of the Edwards Aquifer 223-224
 — Effects of mixing injected and native waters 220
 — Geohydrology of the Northeastern Texas salt-dome basin 121-122
 — Jasper aquifer mapped in the Coastal Plain of Texas 121
 — Model of the Chicot and Evangeline aquifers in Houston, Texas 218
hydrology: Texas 121-122
 — Water quality of selected reservoirs in Texas 242
- Texas—seismology**
earthquakes: Kermit, Texas 261
- Texas—stratigraphy**
Cenozoic: Uranium possibilities of Marfa Basin in Texas 29
Eocene: Stratigraphic relations in the Whitsett Formation in South Texas 29
- thallium—analysis**
spectroscopy: Thallium contents of 16 USGS standard rocks 246
- thermal waters** *see also under* hydrogeology *under* California; Gulf Coastal Plain; Italy; Louisiana; Montana; Nevada; Utah; Wyoming
- thermal waters—geochemistry**
gases: Isotopic and chemical studies of geothermal gases 204
isotopes: Uranium-isotope ratio characterization of geothermal waters 204-205
precipitation: Precipitation of quartz in convecting hydrothermal systems 204
properties: Viscosity of water and ionic substances 207
trace elements: Chemical modeling of geothermal waters 193
- thorium** *see also under* economic geology *under* Colorado; Kentucky; Michigan; New England; New York; South Dakota; Tennessee; West Virginia
- thorium—geochemistry**
black shale: Uranium, thorium, carbon, and sulfur in Devonian black shale from West Virginia, Kentucky, and New York 39
- thrust faults** *see under* displacements *under* faults
- trace elements** *see under* geochemical methods *under* mineral exploration; *see under* geochemistry *under* Alaska; Atlantic Ocean; California; coal; Colorado; sedimentary rocks; Idaho; Illinois; Missouri; peat; sedimentary rocks; thermal waters; United States; *see under* pollutants *under* pollution
- Triassic** *see also under* geochronology *under* Oregon; *see also under* stratigraphy *under* Arizona; Idaho; Maryland; Montana; Nevada; Rocky Mountains; South Carolina; Virginia; Wyoming
- tunnels** *see also under* engineering geology *under* California; Chile; Minnesota
- Turkey—geophysical surveys**
remote sensing: Turkey 351

U

underground water *see* ground water

United Kingdom—geochronology

Ordovician: Fission-track dating of the type Ordovician and Silurian 191

United States *see also* the individual states and regions

United States—areal geology

research: Regional geologic investigations 45-88

United States—economic geology

aluminum: Alunite resources of the United States 2

coal: Coal resource occurrence/development potential maps 165

— Geochemistry of U. S. coal resources 16-17

— Known recoverable coal resource areas 165

— Vanadium content in coal 16

energy sources: Nuclear-fuel resources 26-39

fluorspar: Fluorine provinces, reserves, and resources of the United States 1-2

geothermal energy: Geothermal resources 39-44

lead-zinc deposits: Potential for massive sulfides in eastern and central United States 2

mineral resources: Nuclear-fuel resources 26-39

— Regional geochemical and geophysical studies 9-11

— United States and world mineral-resource assessments 1-8

United States—engineering geology

explosions: Geology and hydrology related to national security 273-275

land subsidence: Land subsidence 289-291

United States—environmental geology

conservation: Classification and evaluation of mineral lands 164-165

— Classified land 164

— Coal resource occurrence/development potential maps 165

— Known geologic structures of producing oil and gas fields 165

— Known geothermal resources areas 165

— Known leasing areas for potassium, phosphate, and sodium 165

— Known recoverable coal resource areas 165

— Management of natural resources on Federal and Indian lands 164-166

— OCS lease sales for oil and gas 166

— Supervision of mineral leasing 165-166

— Waterpower classification; preservation of reservoir sites 165

land use: Urban water program 136-139

maps: Maps of flood-prone areas 283

United States—geochemistry

trace elements: Geochemistry of U. S. coal resources 16-17

vanadium: Vanadium content in coal 16

United States—geochronology

Precambrian: Chronometric-geologic charts for Precambrian, United States and Mexico 87

United States—geomorphology

maps: Quaternary map of the conterminous United States 88

United States—geophysical surveys

maps: Heat flow in the United States and the thermal regime of the crust 200-201

— Temporal mapping with Landsat data 314

- Upper Chesapeake Bay 314-315
- remote sensing*: Crustal magnetic anomalies from satellite data 173
- Lineament patterns interpreted from radar images of the Mississippi embayment 312
- United States—hydrogeology**
- ground water*: Interstate studies 110-111
- Multistate studies 109
- hydrology*: Central region 108-124
- Comparison of USGS urban-basin model and rational-method estimate of peak discharge 137
- Estimated use of water in the United States in 1975 139
- Flood-frequency studies 137
- National Stream-Quality Accounting Network 140-143
- National Water Data Exchange 135-136
- National water quality programs 140
- Office of Water Data Coordination 133-135
- Special water-resource programs, data coordination, acquisition, and storage 133-143
- Water-Data Storage System 136
- Water-quality changes 142-143
- Water-quality conditions 140-142
- Water-quality studies 138-139
- Water resources investigations 89-143
- Water use 139-140
- United States—oceanography**
- marine geology*: Coastal and marine geology 144-159
- Marine geology and coastal hydrology 144-163
- United States—seismology**
- earthquakes*: National Earthquake Information Service 250-251
- United States—stratigraphy**
- Paleozoic*: Paleozoic studies 230-233
- United States—structural geology**
- neotectonics*: Seismotectonics of the Mississippi embayment 260
- tectonics*: Geophysical anomalies in the Mississippi Embayment 171
- uranium** *see also under* economic geology under Alaska; Arizona; Colorado; Eastern U.S.; Kentucky; Michigan; Montana; New England; New Mexico; New York; South Dakota; Southwestern U.S.; Tennessee; Texas; Utah; Washington; West Virginia; Wyoming
- uranium—exploration**
- electromagnetic methods*: Electromagnetic methods aid in detection of mineralization associated with uranium 39
- geochemical methods*: Helium and radon in uranium exploration 12
- methods*: Evaluation of analytical methods for the geochemical exploration of uranium 246
- Mobile helium-detection equipment used in uranium exploration 37
- thermoluminescence*: Thermoluminescence of sand grains near a uranium deposit 37
- water*: Water sampling for uranium exploration 37-38
- well-logging*: Physical properties changes associated with uranium deposits can be detected by borehole geophysical measurements 175-176
- uranium—genesis**
- mobility*: Uranium mobility during interaction of rhyolitic glass with alkaline solutions 35-36
- models*: Computer modeling of roll-type uranium deposits 37
- ore deposits*: Organic materials and conditions of uranium fixation 36-37
- oxidation*: Pyrite oxidation and the origin of roll-front uranium deposits 34
- uranium—geochemistry**
- silica*: Uranium in secondary silica as a guide for describing uranium mobility 36
- uranium—properties**
- sandstone*: Conceptual-mathematical models of uranium ore formation in sandstone-type deposits 36
- Utah—economic geology**
- coal*: Intertonguing, paleochannels, and faults in the Wasatch Plateau in Utah 14-15
- metals*: Hydrothermal system of the East Tintic District in Utah 190
- natural gas*: Early gas discovery in Cordilleran hingeline area in Utah 20-21
- oil shale*: Geology of the Bates Knolls quadrangle of east-central Uinta Basin in Utah 26
- Lower Tertiary rocks in the southeastern Uinta Basin of Utah 25
- petroleum*: Mineralogic character of some hydrocarbon reservoirs in Uinta Basin, Utah 21
- Permian source rocks, northeastern Great Basin 20
- Rates of sedimentation of petroleum source rocks in Utah, Nevada, and Idaho 21
- uranium*: Sedimentological guide to uranium deposits in southern Utah 26-27
- Spring-deposited radioactive barite in the Great Salt Lake area of Utah 38
- Stratigraphy of volcanic rocks as a guide to uranium in the Thomas Range, Utah 32
- Uranium in Triassic rocks in southeast Utah 28
- Utah—engineering geology**
- earthquakes*: Ground response in the Salt Lake City region 263
- geologic hazards*: Land stability in Salt Lake City in Utah 263-264
- waste disposal*: Regional studies in Paradox Basin in Utah 277
- Utah—environmental geology**
- geologic hazards*: Active faults in central Utah 56
- Utah—geochemistry**
- surveys*: Soil geochemistry in the Uinta and Piceance Basins 288
- weathering*: Reasons for deterioration of the Bonneville Salt Flats 122-123
- Utah—geomorphology**
- landform description*: Geomorphology of fault scarps 260-261
- Utah—geophysical surveys**
- remote sensing*: Landsat investigations of the northern Paradox Basin, Utah and Colorado 311-312
- Mapping altered rocks using multispectral aircraft images 309
- Utah—hydrogeology**
- ground water*: Declining ground-water levels in the Beryl-Enterprise area of southwestern Utah 123
- Evaluation of aquifers in southern Utah 122
- Navajo Sandstone evaluated as an alternative source of water for energy development in the Kaiparowits Plateau area in south-central Utah 123
- Navajo Sandstone source of ground water for future energy-related development in southeastern Utah 122
- hydrology*: Traveltime and dispersion characteristics of the White River in the Uinta Basin oil-shale area 122
- Utah 122-123
- springs*: Spring discharge and water-quality data on coal areas of east-central Utah 123
- thermal waters*: Geothermal potential of the eastern margin of the Basin and Range province in Utah 205-206
- Utah—petrology**
- intrusions*: Pressurized fractures in hot rock 199
- Utah—stratigraphy**
- Cenozoic*: Stratigraphy of volcanic rocks as a guide to uranium in the Thomas Range, Utah 32
- Precambrian*: Farmington Canyon Complex, Wasatch Mountains, Utah 62-63
- Precambrian rocks 62-63
- Proterozoic*: Proterozoic (Precambrian Z) stratigraphy clarified in Deep Creek Mountains of westernmost Utah 71
- Tertiary*: Geology of the Bates Knolls quadrangle of east-central Uinta Basin in Utah 26
- Lower Tertiary rocks in the southeastern Uinta Basin of Utah 25
- Utah—structural geology**
- neotectonics*: Seismotectonics of Utah and Nevada 259-260
- tectonics*: Thrusts in City Creek Canyon near Salt Lake City, Utah 71

V

- vanadium—geochemistry**
- coal*: Vanadium content in coal 16
- power plants*: Mass balances of trace elements at powerplants 16
- Vermont—engineering geology**
- rock mechanics*: In-situ stress on Barre Granite in Vermont 267-268

- Vermont—environmental geology**
ecology: Marsh plants depend on nitrogen and phosphorus from sediments 241
- Vermont—hydrogeology**
ground water: Ground-water resources in the Rutland area 99
hydrology: Vermont 99
- Vertebrata** *see also* fossil man; Mammalia
- Vertebrata—faunal studies**
Paleocene: Paleocene vertebrates from southern Hijaz Province, Kingdom of Saudi Arabia 227
- Virginia—economic geology**
iron: Large submarginal iron resources in Mill Creek, Peters Mountain, and Mountain Lake Wilderness study areas in Virginia and West Virginia 3
natural gas: Hydrocarbon maturation in Kentucky and Virginia 22
- Virginia—engineering geology**
geologic hazards: Landslides related to fracture systems in Fairfax County, Virginia 266
- Virginia—environmental geology**
ecology: Distribution of forest plants reflects differences in environment 233
land use: Wetland vegetation studies 313
- Virginia—geophysical surveys**
remote sensing: Comparison of Landsat image products 356
- Virginia—hydrogeology**
ground water: Geohydrologic studies to guide exploratory drilling for ground water in Fairfax County, Virginia 317
- Virginia—stratigraphy**
Mississippian: New floral zone in Mississippian of Virginia and West Virginia 230
Triassic: Upper Triassic stratigraphy in the Culpeper Basin of Virginia and Maryland 48-49
- Virginia—structural geology**
tectonics: New information on tectonic framework on the Culpeper Triassic and Jurassic basin 51
 — Tectonic model for northeast Virginia Piedmont 51
- volcanic features** *see under* geomorphology
- volcanism** *see under* volcanology
- volcanoes** *see under* volcanology
- volcanology—volcanism**
calderas: The Heise caldera in southeastern Idaho 61
controls: Olympic-Wallowa Lineament influenced Cascade-Columbia River volcanism 180
eruptions: Potential volcanic activity near Clear Lake in California 182
gases: Compact, low-power telemetry controller and transmitter unit for volcanic gas monitoring 176-177
processes: Volcanic rocks and processes 179-184
rift zones: Structure and volcanism in eastern Snake River Plain, of Idaho 65-66
submarine environment: Submarine volcanism 184
- volcanology—volcanoes**
Alaska: Southern Alaska 261-262
Guatemala: Guatemala 342
Hawaii: Activity at Kilauea Volcano in 1977 179
 — Hawaiian volcano studies 179-180
 — Paths of magma ascent in the Earth 180
 — Rate of inflation shows at Mauna Loa Volcano 179
 — Refraction study of the southeast coast of Kilauea 195
 — Structural evolution of Mauna Loa Volcano 179-180
Nicaragua: Nicaragua 345
- W**
- Washington—areal geology**
regional: Washington 78-80
- Washington—economic geology**
natural gas: Oil and gas resources of the Outer Continental Shelf 23
petroleum: Oil and gas resources of the Outer Continental Shelf 23
 — Potential petroleum reservoirs within Tertiary melange, coastal Olympic Peninsula and adjacent OCS 78
uranium: Emplacement of uranium into Midnite mine deposits 31
- Washington—engineering geology**
slope stability: Potential submarine landslides in Puget Sound 79
- Washington—environmental geology**
geologic hazards: Puget Sound project; hazard evaluation on Mount Baker 318
pollution: Interactions of oil and burrowing fauna experiment at Willapa Bay 153
 — Mercury release from contaminated estuarine sediments 159
 — Water-quality effects of underground coal mining 243
waste disposal: Coal-hydrology studies 132
- Washington—geochronology**
Pleistocene: Age of the last major scabland flood of eastern Washington 78
- Washington—geophysical surveys**
maps: Wenatchee, Washington 315
- Washington—hydrogeology**
ground water: Lower Elwha 131
 — Port Gamble 131
 — "Sole-source" study 125
 — Test well drilling in Washington State 132
hydrology: Colville (No Name Creek basin) 130-131
 — Cyclic variations in drain-water quality 133
 — Irrigation increased in Horse Heaven Hills 132
 — Irrigation return flows in the lower Yakima River basin of Washington 210
 — Lake studies 132-133
 — Makah 131
 — Model predicts snowmelt runoff 133
 — Nisqually, an undeveloped lake 133
- Nutrient loading and budget of Wilderness Lake 132-133
 — Port Madison 131
 — Primer on limnology 132
 — Salmon propagation in Ozette Lake 133
 — Southern Cascade Range borehole drilling program 212-213
 — Studies on Indian reservations 130-132
 — Subglacier dye-injection test 213
 — Swinomish 131
 — Tulalip 131
 — Washington 130-133
 — Water use in Washington for 1975 139-140
 — Yakima 131-132
- Washington—oceanography**
sedimentation: Heavy-mineral assemblages of Willapa Bay in Washington 153
- Washington—petrology**
volcanology: Olympic-Wallowa Lineament influenced Cascade-Columbia River volcanism 180
- Washington—stratigraphy**
Holocene: Climate and glaciers 215
Miocene: Miocene diatoms from the Montesano Formation of Weaver (1912), Washington 229
Paleogene: Revision of Naches Formation 78-79
- Washington—structural geology**
neotectonics: Possible Quaternary faulting in the Puget Sound region 79
tectonics: Faults south of Wenatchee, Washington 78
 — Mesozoic thrust-bound terranes in the San Juan Islands, Washington 79-80
 — Possible continental transform fault in northwest Washington 79
- Washington—volcanology**
Mount Baker: Volcanic effects on snow and ice on Mount Baker, Washington 213
waste disposal *see also under* engineering geology *under* automatic data processing; Florida; Idaho; Illinois; Mississippi; Nevada; New Mexico; New York; South Carolina; Tennessee; Utah; *see also under* environmental geology *under* Colorado; Great Lakes region; Michigan; Nevada; New York; Washington
- waste disposal—radioactive waste**
effects: Hydrologic investigations relative to the disposal of low level radioactive waste 280
 — Relation of radioactive waste to the hydrologic environment 278-280
feasibility studies: Studies of potential repository sites 277-278
management: Geologic aspects of radioactive waste management 275-278
media: Crystalline rocks 276-277
 — Salt and anhydrite 276
 — Thermal properties 277
models: Simulation of the effects of containment of nuclear wastes in layered salt deposits 279

- research: Studies of media* 276-277
- water resources** *see also under* economic geology *under* Israel; Jordan; Kenya; Saudi Arabia; Sudan
- waterways** *see also under* engineering geology *under* Mississippi; New York
- weathering** *see also under* geochemistry *under* Utah
- well-logging—electrical logging**
interpretation: Physical properties changes associated with uranium deposits can be detected by borehole geophysical measurements 175-176
- well-logging—methods**
accuracy: Accuracy of borehole gravity data 25
neutron methods: Neutron activation and magnetics of coal 17
- well-logging—radioactivity**
gamma-ray methods: Quick evaluation by gamma-ray intensity and density crossplot of Devonian shale in West Virginia 22-23
techniques: Optimum size source for borehole gamma-ray analysis 175
- West Indies** *see also* Puerto Rico
- West Indies—economic geology**
mineral resources: Dominica 342
- West Virginia—economic geology**
coal: Coal in the New River Gorge area in West Virginia 14
— Coal rank related to depth of burial and buried intrusive rocks 15-16
iron: Large submarginal iron resources in Mill Creek, Peters Mountain, and Mountain Lake Wilderness study areas in Virginia and West Virginia 3
mineral resources: New River Gorge in West Virginia 3
natural gas: Possible stratigraphic controls for Devonian gasfields in the Appalachian Basin 22
— Quick evaluation by gamma-ray intensity and density crossplot of Devonian shale in West Virginia 22-23
thorium: Uranium, thorium, carbon, and sulfur in Devonian black shale from West Virginia, Kentucky, and New York 39
uranium: Uranium, thorium, carbon, and sulfur in Devonian black shale from West Virginia, Kentucky, and New York 39
- West Virginia—hydrogeology**
ground water: Hydrology of the Guyandotte River basin 100
hydrology: Effects of deep mining on base flow 99
— West Virginia 99-100
- West Virginia—stratigraphy**
Mississippian: New floral zone in Mississippian of Virginia and West Virginia 230
- Western Hemisphere** *see also* Atlantic Ocean; North America; Pacific Ocean; South America
- Western Interior—environmental geology**
reclamation: Rehabilitation potential of coal lands in the central region evaluated 110-111
- Western U.S.—economic geology**
geothermal energy: Geothermal potential of Western United States related to silica geothermometry of nonthermal ground waters and regional heat flow 209
metals: Mesozoic and Cenozoic metallogenesis in the western United States 2
- Western U.S.—environmental geology**
land use: Impact of western energy development 325-326
reclamation: Climatic assessment of rehabilitation potential 214
— Geochemical survey of the western energy regions 288
- Western U.S.—geomorphology**
glacial geology: Increased ablation in the Western United States in 1977 213
- Western U.S.—hydrogeology**
hydrology: Interstate studies 125
— Western region 124-133
- Western U.S.—petrology**
igneous rocks: Volcanic rocks in western United States 182-183
- Western U.S.—seismology**
earthquakes: Land deformation 253-254
- Western U.S.—tectonophysics**
heat flow: Heat flow in the United States and the thermal regime of the crust 200-201
- Wisconsin—economic geology**
lead-zinc deposits: Previously unreported mineralization found in the Darlington quadrangle of southwestern Wisconsin 5
- Wisconsin—environmental geology**
ecology: Wetland vegetation reflects hydrology 233
- Wisconsin—geomorphology**
processes: Sediment accumulation rates in stream valleys of Wisconsin 211-212
- Wisconsin—geophysical surveys**
magnetic surveys: Geologic interpretation of aeromagnetic map of part of northern Wisconsin 54
maps: Geologic interpretation of aeromagnetic map of part of northern Wisconsin 54
- Wisconsin—hydrogeology**
ground water: Concentrations of toxic heavy metals in water from wells in Wisconsin 101
— Simulation of pumping in Dane County, Wisconsin 220
hydrology: Effects of a powerplant on streamflow and lake levels 100
— Low-flow characteristics at gaging stations on the Wisconsin, Fox, and Wolf rivers 100
— Low-flow characteristics of small streams in 32 basins 100
— Low-flow characteristics of streams in the lower Wisconsin River basin 100-101
— Low-flow characteristics of streams in the Rock-Fox River basin 101
— Low-flow characteristics of streams in the Trempealeau-Black River basin 101-102
- Preimpoundment conditions in a small drainage basin 101
— Wisconsin 100-102
- Wisconsin—structural geology**
folds: Geologic interpretation of aeromagnetic map of part of northern Wisconsin 54
— Lake Superior region 53-54
- Wyoming—economic geology**
bentonite: Physical and chemical properties of bentonite 43
coal: Coal in Powder River basin in Wyoming 55
— Economic geology 55-56
gold: Course of Eocene Wind River locates auriferous sedimentary rocks in the western Wind River Basin in Wyoming 6
iron: Economic geology 55-56
— Proterozoic rocks and iron deposits, Hartville Uplift, Wyoming 55-56
metals: Mineral resource appraisal of the Washakie Wilderness in Wyoming 3-4
mineral resources: Carbonatite dikes in Bear Lodge Mountains, Wyoming 6
petroleum: New seismic procedure for locating stratigraphic traps 24-25
uranium: Characterization of granitic uranium source rocks 35
— Electron microprobe analyses of uraninite and coffinite 35
— Facies change related to ore deposition 28
— Geochronology of uranium ores 34-35
— Iron sulfide minerals and sulfur isotopes associated with roll-type uranium deposits 33-34
— Radon analyses of water in Carbon County, Wyoming 11
— Remote sensing for uranium exploration 309-310
— Uranium-bearing, quartz-pebble conglomerate found in Sierra Madre, Wyoming 31
— Uranium deposits at Copper Mountain in Wyoming 28
— Uranium in secondary silica as a guide for describing uranium mobility 36
— Uranium mineralization at the Upper Cretaceous Fox Hills Sandstone-Lance Formation interface 27-28
- Wyoming—engineering geology**
slope stability: Stability of highwalls in surface coal mines, western Powder River basin 266
- Wyoming—environmental geology**
ecology: Algal growth potential of North Platte reservoirs 242
impact statements: Modified format for site-specific EIS 323
land use: Environmental geology of coal development, Powder River basin in Wyoming 269-271
- Wyoming—geochronology**
Cenozoic: Geochronology of uranium ores 34-35
Cretaceous: K-Ar dating of the Albian 191

- Proterozoic*: Middle Proterozoic tectonics in the Wyoming Age Province 64
- Quaternary*: Age of volcanism at Togwotee Pass area in Wyoming 183
- Wyoming—geomorphology**
- glacial geology*: Glaciation near Togwotee Pass in the Wind River Mountains of Wyoming 27
- Wyoming—geophysical surveys**
- gravity surveys*: Delineation of buried thermal bodies by precision releveing and gravity reobservations 205
- heat flow*: Conductive component of total heat flow in research drill holes of Yellowstone Park and relation of heat flow to vegetation patterns 203-204
- maps*: Montana/Wyoming image maps 315
- remote sensing*: Presentation and interpretation of aerial radiometric data 311
- surveys*: Underground fires in coal mines located by geophysical surveys 168
- Wyoming—hydrogeology**
- ground water*: Shallow ground-water flow systems in the northern Powder River basin 110
- hydrology*: Analysis of runoff from small drainage basins in Wyoming 123-124
- Digital model predicts water-level declines and streamflow depletions near Wheatland 124
- Green River basin water-quality investigations 234
- Preliminary digital model of the Sweet-water River basin 123
- Size of glacial streams in Yellowstone National Park 215-216
- Stream-temperature model for the Green River basin in Wyoming 124
- Wyoming 123
- springs*: Hot springs in Jackson Hole in northwestern Wyoming 56-57
- thermal waters*: Geology and thermal history of Mammoth Hot Springs 197-198
- Helium-3 in Yellowstone, Lassen, and The Geysers' fluids indicates mantle connection 201
- Hot springs in Jackson Hole in northwestern Wyoming 56-57
- Improved estimates of carbonate alkalinity in geothermal waters 202
- Relation of mercury to geothermal areas in Yellowstone National Park in Wyoming 207
- Wyoming—petrology**
- igneous rocks*: Carbonate-rich kimberlite in southeastern Wyoming 61-62
- Igneous rocks 59-62
- metasomatism*: Hydrothermal alteration in Carnegie I Drill Hole, Upper Geyser Basin, Yellowstone Park 196
- Wyoming—seismology**
- earthquakes*: Seismicity and tectonics at Yellowstone National Park 195-196
- Wyoming—stratigraphy**
- Cenozoic*: Tectonic significance and post-Laramide giant boulders in southeastern Wyoming 63-64
- Eocene*: Correlation and structure of Eocene rocks in southwestern Bighorn Basin of Wyoming 58
- Stratigraphy 58-59
- Permian*: Permian-Triassic boundary in western Wyoming and parts of Idaho and Montana 232-233
- Precambrian*: Mafic complex of Mullen Creek in the Medicine Bow Mountains of Wyoming 63
- Precambrian rocks 62-63
- Uranium-bearing, quartz-pebble conglomerate found in Sierra Madre, Wyoming 31
- Triassic*: Permian-Triassic boundary in western Wyoming and parts of Idaho and Montana 232-233
- Wyoming—structural geology**
- tectonics*: Mafic complex of Mullen Creek in the Medicine Bow Mountains of Wyoming 63
- Middle Proterozoic tectonics in the Wyoming Age Province 64
- Tectonic significance and post-Laramide giant boulders in southeastern Wyoming 63-64
- Tectonics 63-68

X

- X-ray analysis—X-ray fluorescence**
- applications*: XRF glass disc fusion method for silicate rock analysis 247
- research*: X-ray fluorescence 247
- X-ray fluorescence** *see under* X-ray analysis

Y

- Yemen—hydrogeology**
- ground water*: Ground-water survey activities 351
- hydrology*: Yemen 351
- Yugoslavia—general**
- research*: Yugoslavia 351

Z

- zinc** *see also under* economic geology *under* Colorado
- zinc—geochemistry**
- peat*: Environmental pollution of the Everglades in Florida 16-17
- pollutants*: Bioavailability of sediment-bound lead and zinc to estuarine clams 285
- sphalerite*: Sphalerite-bearing coal in Illinois 16

INVESTIGATOR INDEX

A

Ackermann, H. D.	40, 171
Adams, D. B.	242
Adolphson, D. G.	96
Ahlbrandt, T. S.	24, 81, 212
Ahmad, Z.	340
Aiken, G. R.	248
Aki, K.	209
Albert, C. D.	236, 286
Alexander, T. W.	282
Algermissen, S. T.	257, 339, 345
Allcott, G. H.	10
Alldredge, L. R.	169
Allen, H. E., Jr.	137
Allen, R. V.	255
Alley, W. M.	139
Altschuler, Z. S.	16
Anderson, B. M.	288
Anderson, D. G.	263
Anderson, F. J.	323
Anderson, H. W., Jr.	96
Anderson, R. E.	259, 260, 348
Anderson, W. L.	174
Andrews, D. J.	262
Andrews, S.	212
Antweiler, J. C.	3
Arihood, L. D.	92
Armbruster, J. T.	225
Armbrustmacher, T. J.	33
Armstrong, A. K.	72
Arnou, T.	123
Aronson, D. A.	98, 220
Arteaga, F. E.	129
Arth One, J. G.	61
Arthur, D. W. G.	296
Aruscavage, P. J.	246
Ashley, J. W.	99
Ashley, R. P.	8, 69, 309
Attig, J. W., Jr.	93

B

Back, W.	344
Bacon, C. R.	181
Bader, J. S.	100
Baedecker, P. A.	246
Bailey, E. H.	340
Bailey, R. A.	182
Baird, A. K.	293
Baker, E. T., Jr.	121
Bakun, W. H.	255
Balch, A. H.	24
Ball, J. W.	193, 202, 236
Baltzer, R. A.	313
Banks, N. G.	186
Barber, D. W.	256
Barczak, V. J.	216
Bargar, K. E.	197
Barker, F.	185

Barker, R. A.	115
Barks, J. H.	286
Barnes, D. F.	253
Barnes, H. H., Jr.	339
Barnes, I.	261
Barnes, J. W.	340
Barnes, P. W.	157
Barr, D. E.	222
Barraclough, J. T.	279
Barron, J. A.	229
Bartlett, W. P., Jr.	282
Barton, H. N.	10
Batchelder, J. N.	8, 58, 66, 184, 190
Bateman, P. C.	189, 329
Bath, G. D.	273
Bauer, D. P.	242
Beeson, M. H.	196
Behrendt, J. C.	144
Belkin, H. E.	278
Bell, H.	4
Bentley, C. B.	104, 224
Bentley, R. D.	180
Benton, L. L.	345
Berg, H. C.	80, 84
Berger, J.	327
Beverage, J. P.	212
Bhattacharyya, B. K.	173
Billingsley, F. C.	304
Bingham, J. W.	138
Bingham, R. H.	103
Bird, K. J.	17
Bischoff, J. L.	157
Bisdorf, R. J.	172
Bishop, L. J.	279
Blackwelder, B. W.	51, 228
Blair, W. N.	77
Blake, D. W.	8
Blakely, R. J.	173
Blanchard, L. F.	14
Bohannon, R. G.	71
Bohor, B. F.	15
Bolm, J. G.	18
Bond, S. V.	283
Bonelli, J. E.	248
Bonham, H. F., Jr.	69
Bonilla, M. G.	261
Borcherdt, R. D.	262
Borchers, J. W.	100
Borchert, W. B.	123
Bortleson, G. C.	133
Boswell, E. H.	107
Botbol, J. M.	345
Bothner, M. H.	146, 159
Botinelly, T.	11
Boucher, P. R.	133
Boudette, E. L.	38
Bouma, A. H.	155
Bourgeois, D. J.	344
Bowin, C. O.	144
Bowles, C. G.	71
Bown, T. M.	58
Boyce, J. M.	296
Boyd, E. L.	112

Boyles, J. M.	352
Brabb, E. E.	258
Bradbury, J. P.	215
Bradford, G. M.	340
Bradford, W. L.	127
Branson, F. A.	110
Bredehoeft, J. D.	338
Breed, C. S.	217, 294
Breger, I. A.	16
Brenner-Tourtelot, E. F.	42
Brethauer, G. E.	273
Brew, D. A.	86, 87
Briskey, J. A., Jr.	73
Brock, M. R.	31
Bromfield, C. S.	30
Brook, C. A.	26
Brouwers, E.	230
Brown, C. E.	5
Brown, D. E.	233
Brown, D. W.	187
Brown, F. H.	205
Brown, G. A.	98
Brown, G. E.	177
Brown, R. D.	76
Browne, P. R. L.	196
Brownfield, I. K.	33
Brua, S. A.	281
Bruns, T. R.	153
Bryant, B. H.	62, 63
Buchanan-Banks, J. M.	258
Bucknam, R. C.	259, 260, 345
Bufe, C. G.	195, 255
Buie, B. F.	4
Bukry, J. D.	158
Burbank, J. H.	313
Burchard, J. M.	193, 236
Burford, R. O.	253
Burke, R. C.	57
Burns, A. W.	112
Buseck, P. R.	207
Butler, H. M.	251
Butman, B.	146
Butterfield, D.	99
Byerlee, J. D.	256
Byerly, G. R.	78, 180
Byers, F. M., Jr.	273

C

Cabre, R.	339
Cacchione, D. A.	156
Cadigan, R. A.	12, 38
Cady, W. M.	62
Cahill, J. M.	280
Cain, D. L.	112
Cain, J. C.	169
Calandro, A. J.	115
Callahan, J. T.	346
Cameron, C. C.	3, 5
Campbell, D. L.	39, 171, 172, 173
Campbell, E. Y.	246
Campbell, J. A.	84

Campbell, W. J. 244, 245, 330
 Cannon, W. F. 5, 54
 Carlson, C. 353
 Carlson, K. H. 23
 Carlson, M. A. 250
 Carlson, P. R. 153
 Carmony, N. B. 233
 Carnegie, D. M. 304
 Carpenter, D. H. 225
 Carr, J. E. 121, 218
 Carr, M. H. 217, 293
 Carrara, P. E. 272, 352
 Carswell, W. J., Jr. 281
 Carter, R. F. 106
 Carter, V. 233, 313
 Carter, W. D. 304, 306, 307, 308, 329
 Case, H. L., III 116
 Case, J. E. 88, 170, 342
 Cashion, W. B. 25
 Cassidy, R. J. 23
 Castle, R. O. 253
 Caswell, W. B. 304
 Cataldi, R. 41
 Cathcart, J. B. 43
 Causey, L. V. 104
 Chadwick, R. A. 209
 Chao, E. C. T. 295, 298, 330
 Chao, T. T. 11, 12
 Chapman, R. M. 82, 83
 Chappell, B. 189
 Cheng, R. T. 161
 Cherry, R. N. 243
 Chidester, A. H. 327, 350
 Childs, J. R. 155
 Chleborad, A. F. 269
 Choy, G. L. 251
 Christian, R. P. 293
 Christopher, R. A. 51
 Chrzastowski, M. J. 79
 Claassen, H. C. 188
 Clague, D. A. 158
 Clark, A. L. 329, 345
 Clark, B. C. 293
 Clark, H. E., Jr. 251
 Clark, J. R. 177
 Clark, M. M. 258, 265
 Clarke, J. 207
 Claypool, G. E. 18, 22
 Clifton, H. E. 153
 Cloern, J. E. 162
 Clynne, M. A. 176, 276
 Coates, D. A. 269
 Cobban, W. A. 18, 191
 Cody, J. W. 39
 Coleman, R. G. 184
 Coleman, S. L. 15
 Collinson, J. W. 70
 Colton, R. B. 58
 Colvocoresses, A. P. 315
 Connor, C. W. 289
 Connor, J. J. 188, 269, 288, 289
 Conomos, T. J. 159, 161
 Conrad, G. 256
 Cooley, R. L. 219
 Coonrad, W. L. 83
 Cooper, A. K. 155
 Cooper, J. A. 191
 Cooper, R. W. 6
 Coplen, T. 216

Coplen, T. B., II 249
 Coppersmith, H. G. 61
 Corbett, M. K. 64
 Corchary, G. S. 273
 Cordova, R. M. 122
 Cormier, V. 251
 Cory, R. L. 338
 Couch, R. W. 206
 Counts, H. B. 103
 Covay, K. J. 111
 Cowan, D. S. 79
 Cowart, J. 204, 216
 Cowing, D. J. 240
 Cragwall, J. S., Jr. 330, 339
 Craig, G. S., Jr. 123
 Craig, H. 204
 Craig, L. C. 28, 229
 Cramer, H. R. 50
 Crawley, M. E. 119
 Creasey, S. C. 7, 73, 182
 Cressler, C. W. 107
 Crittenden, M. D., Jr. 71
 Croft, M. G. 119
 Csejtey, B., Jr. 84
 Cummings, L. R. 95
 Cunningham, C. G. 184
 Curtis, W. F. 338, 340
 Cushing, E. M. 118
 Czamanske, G. K. 86, 178, 192, 353

D

Dale, R. H. 242
 Dalrymple, G. B. 158, 167
 Dalziel, M. 24
 Damon, P. E. 207
 Danenberger, E. P. 344
 Daniels, J. J. 39, 175
 Davidson, D. F. 330, 342
 Davis, D. A. 128
 Davis, D. W. 320
 Davis, G. H. 338
 Davis, J. R. 69
 Davis, R. E. 111, 119, 120
 Dawdy, D. R. 282
 de Witt, W., Jr. 49
 Dean, W. E. 25, 241, 288
 Delaney, D. F. 93, 94
 Delevaux, M. H. 189
 DeLong, L. L. 234
 Demas, C. R. 243
 Denson, N. M. 55
 Derr, J. S. 253
 Desborough, G. A. 70, 74
 Detra, D. E. 82
 Deutsch, M. 351
 Dewey, J. W. 251, 268, 327, 341
 di Somma, D. E. 199
 Dial, D. C. 116
 Diaz, A. M. 286
 Diaz, J. M. 296
 Diaz, J. R. 221
 Dickerman, D. C. 99
 Dickinson, K. A. 29, 84
 Dieterich, J. H. 256
 Diment, W. H. 197, 257
 Dingler, J. R. 151
 Dinwiddie, G. A. 273, 279
 Dion, N. P. 132, 133, 139

Dixon, H. R. 46
 Dodge, F. C. 75
 Dodge, H. W., Jr. 27
 Doe, B. R. 189
 Doherty, D. J. 61
 Donaldson, I. G. 344
 Donato, M. M. 184
 Donnell, J. R. 25
 Donnelly, J. M. 40, 75, 167, 182, 198
 Donovan, T. J. 23, 24
 Doty, G. C. 273, 290
 Dover, J. H. 55
 Doyle, W. H., Jr. 137, 139
 Draeger, W. C. 302
 Drake, A. A., Jr. 50, 231
 Drake, D. E. 156, 157
 Drewes, H. D. 73
 Drost, B. R. 125
 Drost, B. W. 131
 Duffield, W. A. 181, 340
 Dunn, B. 98
 Dunn, M. L. 3
 Dunrud, C. R. 269, 290
 Dutro, J. T., Jr. 82
 Duval, J. S. 174, 311

E

Earhart, R. L. 18
 Ebaugh, W. F. 269
 Ebens, R. J. 188, 269
 Eckhardt, D. A. 98
 Edelen, G. W., Jr. 283
 Edwards, K. L. 293
 Ege, J. R. 273, 345
 Eggers, D. E. 244, 279
 Ehrlich, G. G. 286
 Elder, J. F. 241
 Elders, W. A. 207
 Eliason, E. M. 293
 Elliot, R. L. 84
 Elliott, J. E. 347
 Ellis, W. L. 273
 Elsheimer, H. N. 247
 Elston, D. P. 168
 Embree, G. F. 183
 Emiliani, C. 216
 Emmett, W. W. 210
 Engelke, M. J., Jr. 234
 England, A. W. 353
 Englund, K. J. 14
 Erd, R. C. 176
 Erdman, J. A. 269, 288
 Erdmann, D. E. 247
 Erickson, R. L. 9
 Ericson, D. W. 95
 Evans, H. T. 345
 Evans, K. F. 235
 Ewart, C. J., II 128

F

Fabbi, B. P. 247
 Fabiano, E. B. 169
 Fabro, R. J. 146
 Fairchild, R. 119
 Farrar, C. D. 40
 Fejfar, O. 228

Felmlee, J. K. 12, 38
 Feltis, R. D. 58, 116
 Fenner, C. N. 196
 Fernald, A. T. 273
 Ferrigno, J. 306
 Field, S. J. 100
 Finkelman, R. B. 247
 Finn, D. W. 122
 Fischer, J. N. 223
 Fischer, W. A. 308, 326, 330
 Fishel, D. K. 235
 Fisher, F. S. 3, 189
 Fisher, M. E. 155
 Fishman, M. J. 248
 Fitterman, D. V. 174
 Flanigan, V. J. 39, 175
 Fleck, R. J. 348
 Fleck, W. B. 218
 Flores, J. 339
 Flores, R. M. 14
 Flores, S. J. 339
 Foehner, O. H. 305
 Folger, D. W. 146, 147
 Foose, M. P. 6
 Force, E. R. 4, 5
 Ford, A. B. 86, 352, 353
 Ford, T. R. 111
 Forgey, R. L. 24
 Foster, H. L. 83
 Foster, J. B. 222, 280
 Fouch, T. D. 21
 Fournier, R. O. 203, 204
 Fox, J. E. 81
 Frahme, C. W. 43
 Frank, D. G. 213
 Frank, F. J. 130
 French, J. J. 127
 Fretwell, M. O. 132, 133, 243
 Frey, D. G. 216
 Frickel, D. G. 211
 Friedman, J. D. 311
 Frimpter, M. H. 94
 Frizzell, V. A., Jr. 78
 Fuentes, R. F. 92
 Fuis, G. S. 194
 Fullerton, D. S. 269
 Fumal, T. E. 262
 Fuste, L. A. 132, 243

G

Gabrysch, R. K. 289
 Gallino, G. L. 350
 Gammon, P. T. 313
 Garbarino, J. R. 247
 Garber, M. S. 138
 Garrison, L. E. 149
 Garside, L. J. 69
 Gates, J. S. 111
 Gaum, W. C. 78
 Gawarecki, S. J. 345
 Gay, F. B. 94
 Gebert, W. A. 100
 Gibbons, A. B. 52
 Gibbs, J. F. 262
 Giese, G. L. 161
 Giles, T. F. 111
 Gillespie, J. B. 115
 Gillespie, W. H. 230

Gillies, D. C. 92
 Giovannelli, R. F. 137
 Girard, O. W. 145
 Glancy, P. A. 130
 Glanzman, R. K. 42
 Glenn, J. L. 159, 163
 Gluskoter, H. J. 16
 Goddard, K. E. 284
 Godsy, E. M. 286
 Goerlitz, D. F. 284
 Goetz, A. F. H. 309
 Goff, F. E. 40, 75, 182
 Gogel, A. J. 115, 221
 Gohn, G. S. 51
 Goldberg, M. C. 212, 235
 Golden, H. G. 281
 Goldhaber, M. B. 33, 34, 37, 39
 Goldsmith, R. 46, 47
 Golightly, D. W. 246
 Gonzalez, D. D. 273
 Gonzalez Quintero, L. 215
 Goodkind, J. M. 208
 Goodwin, C. R. 160
 Gordon, D. W. 251
 Gordon, M., Jr. 72
 Gough, L. P. 88, 288
 Gower, H. D. 79
 Graff, P. J. 31
 Granger, H. C. 36
 Grannemann, N. 95
 Grantham, R. G. 139
 Grauch, R. I. 35
 Gralee, G. C., Jr. 98
 Green, M. W. 30
 Greene, H. G. 151, 158
 Greenlee, D. D. 301
 Greenman, D. W. 350
 Greenwood, W. R. 348
 Griffiths, W. R. 345
 Grolier, M. J. 217, 342
 Gromme, C. S. 167
 Gromme, S. 85
 Grossling, B. F. 340
 Grossman, I. G. 138
 Grosz, A. 4
 Grow, J. A. 144, 145
 Guild, P. W. 2, 329
 Gulbrandsen, R. A. 43
 Guswa, J. H. 94, 95
 Gutentag, E. D. 114
 Gutschick, R. C. 20, 232
 Guy, H. P. 210

H

Hadley, D. G. 348
 Hadley, R. F. 110
 Haeni, F. P. 91
 Haffty, J. 86
 Hail, W. J. 26
 Hait, M. H., Jr. 55
 Hall, C. A., Jr. 267
 Hall, D. C. 112, 114
 Hall, R. B. 2
 Hall, W. B. 307
 Hall, W. E. 58, 66
 Hallet, B. 217
 Hamilton, L. J. 120, 121
 Hammarstrom, J. M. 60

Hampson, J. C., Jr. 153
 Hampton, M. A. 155
 Handman, E. H. 138
 Hansen, A. J., Jr. 139
 Hansen, R. L. 304
 Hanshaw, B. B. 344
 Happ, S. C. 211
 Harbough, A. W. 97
 Harden, D. R. 266
 Harlow, D. H. 344, 345
 Harms, T. F. 289
 Harned, D. A. 234
 Harp, E. L. 263
 Harr, C. A. 101
 Harrill, J. R. 129
 Harris, A. G. 76, 230, 231
 Harris, L. D. 22, 231
 Harrison, J. E. 62, 87
 Hart, D. L., Jr. 118
 Hartz, R. W. 81
 Harvey, E. J. 239
 Harwood, D. S. 46
 Haubert, A. W. 86
 Haushild, W. L. 132
 Hauth, L. D. 281
 Havens, J. S. 119
 Haxel, G. B. 73
 Hay, R. L. 216
 Hayes, E. C. 104
 Hayes, L. R. 107, 222
 Hayes, P. T. 14
 Hays, W. W. 263
 Hazel, J. E. 230
 Healey, D. L. 273, 277
 Hearn, B. C., Jr. 40, 59, 75, 182
 Hedge, C. E. 62, 192
 Hedges, L. S. 120
 Hedlund, D. C. 74
 Hein, J. R. 155
 Heindl, L. A. 330, 338
 Helgesen, J. O. 96, 219
 Helley, E. J. 198
 Helm, D. C. 290
 Hem, J. D. 187
 Hemingway, B. S. 176
 Hemley, J. J. 176, 183
 Hemphill, W. R. 23
 Hendricks, J. D. 171
 Henry, M. E. 23
 Herd, D. G. 258
 Hereford, R. 268
 Hermance, J. F. 207
 Hess, A. E. 279
 Hess, G. R. 151, 158
 Hetrick, J. H. 4
 Hietanen, A. M. 75
 Higgins, B. B. 51
 Hildenbrand, T. G. 171
 Hildenbrand, T. G. 260
 Hill, D. P. 195
 Hill, G. W. 105
 Hillhouse, J. W. 167
 Hillier, D. E. 112
 Hills, F. A. 30
 Himmelberg, G. R. 86
 Hindall, S. M. 101
 Hinkle, M. E. 10
 Hinkley, T. K. 288
 Hinrichs, E. N. 269

Hitchcock, T. 199
 Hoare, J. M. 83
 Hobba, W. A., Jr. 99
 Hodge, S. M. 212, 213
 Hodges, C. A. 295
 Hodges, R. E. 279
 Hodgson, J. 327
 Hodson, J. N. 277
 Holcombe, T. L. 88
 Holdsworth, B. 70, 230
 Holley, E. R. 225
 Hollyday, E. F. 108, 313
 Holm, R. F. 41
 Holmes, C. W. 149
 Holmes, M. L. 187
 Holmstrom, B. K. 100, 101
 Holt, H. E. 268
 Holzer, T. L. 258, 265, 291, 292
 Hood, D. R. 303
 Hoover, D. B. 168, 174
 Hoover, D. L. 277
 Hoover, L. 329
 Hopkins, D. M. 81
 Horne, A. J. 241
 Hose, R. K. 70
 Hotchkiss, W. R. 110, 117
 Houston, R. S. 31
 Hovland, R. D. 44
 Howell, D. G. 21
 Howells, L. W. 120
 Hoxie, D. T. 124
 Hubbel, D. W. 212
 Hubert, A. E. 12
 Hudson, J. H. 159
 Huettner, R. 295
 Huffman, A. C. 81
 Hull, J. E. 105, 106
 Hult, M. F. 96
 Hunn, J. D. 104
 Hunt, G. R. 170, 310, 311
 Hunter, R. E. 156, 159
 Hunter, R. N. 253
 Hurr, R. T. 112
 Husid, R. 264
 Hutchinson, C. F. 306

I

Ierley, D. L. 233
 Ileri, S. 340
 Imhoff, E. A. 325
 Inman, E. J. 281
 Irwin, W. P. 261
 Iyer, M. 199
 Izett, G. A. 191

J

Jachens, R. C. 253
 Jackson, D. B. 201
 Jacob, C. E. 221
 Jaksha, L. H. 251
 James, I. C., II 283
 James, O. B. 298
 Janda, R. J. 211, 266
 Janzer, V. J. 237, 287
 Jenkins, E. C. 273
 Jenkins, W. 201

Jenne, E. A. 193, 202, 236
 Jenner, C. B. 320
 Jennings, J. K. 36
 Jennings, M. E. 137, 139, 225
 Jenson, S. K. 301
 Jobson, H. E. 225
 Johnson, B. R. 32, 86, 87
 Johnson, D. A. 296
 Johnson, G. R. 305
 Johnson, M. V. 280, 283
 Johnston, H. E. 99
 Johnston, M. J. 253
 Jones, A. C. 253
 Jones, D. L. 70, 79, 80, 83, 229, 230
 Jones, M. 85
 Jordan, J. N. 330, 339
 Jordan, P. R. 210, 225
 Jorgensen, D. G. 115
 Joyner, W. B. 263
 Julian, B. R. 251
 Junkins, J. 315

K

Kammerer, P. A. 101
 Kane, M. F. 260
 Kanizay, S. P. 269
 Kaplan-Henry, T. A. 261
 Karlstrom, E. 268
 Karlstrom, T. N. V. 214, 268
 Katz, B. G. 97, 285
 Katzer, T. L. 129
 Kauahikaua, J. P. 174
 Kauffman, C. D., Jr. 244
 Keefer, T. N. 139, 225
 Keil, K. 293
 Keith, J. R. 288
 Keith, T. E. C. 196
 Keith, W. J. 73, 182, 186
 Kellogg, K. 349, 352
 Kennedy, V. C. 187
 Kepferle, R. C. 49
 Kestin, J. 207
 Keys, W. S. 279
 Kharaka, Y. K. 203
 Kibler, J. D. 273
 Kiilsgaard, T. H. 350
 Kilty, K. T. 201
 Kimmel, G. E. 97, 285
 Kinney, D. M. 329
 Kirby, S. H. 256
 Kisslinger, C. 330
 Kistler, R. W. 189
 Kiteley, L. W. 20
 Klasner, J. S. 5
 Klausung, R. L. 119
 Klein, F. W. 255
 Klein, H. 105, 106
 Klein, J. M. 127
 Kleinkopf, M. D. 170, 173
 Klemic, H. 176
 Klepper, M. R. 67
 Kline, R. J. 310
 Klitgord, K. D. 144
 Klusman, R. W. 208, 288
 Knapton, J. R. 117, 242
 Knebel, H. J. 147
 Knott, J. M. 343
 Koch, N. C. 120

Koch, R. O. 84
 Kohout, F. A. 224, 351
 Konikow, L. F. 109, 110
 Koopman, F. C. 244
 Kork, J. O. 188
 Koszalka, E. J. 97
 Kouma, E. 220, 236
 Kowalik, W. S. 308
 Krause, R. E. 106
 Kreidler, C. W. 285
 Kretschmer, E. L. 8
 Krimmel, R. M. 213
 Krug, W. R. 100
 Krulik, R. K. 97, 98
 Ku, H. F. H. 97, 285
 Kuberry, R. W. 169
 Kume, J. 121
 Kuntz, M. A. 65
 Kurklin, J. 120
 Kvenvolden, K. A. 153, 155
 Kyle, R. A. 353

L

Lachenbruch, A. H. 199, 200
 Lahr, J. C. 261
 Lai, C. 225
 Lajoie, K. R. 259
 Lambert, G. D. 23
 Lamothe, P. J. 246
 Lamphere, M. A. 41
 Land, L. F. 225
 Lander, D. L. 152
 Landis, K. K. 198
 Laney, R. L. 289
 Lang, S. M. 330
 Langbein, W. B. 214
 Langer, C. J. 251, 261, 262
 Lanphere, M. A. 229
 Lantz, R. J. 187
 Lapham, W. W. 92
 Lara, O. G. 137
 Larson, S. P. 218
 Lash, G. G. 50
 Leap, D. I. 223, 244
 Learned, R. E. 11
 LeBlanc, D. R. 94, 95
 Lee, D. E. 185, 186
 Lee, F. T. 264
 Lee, K. Y. 48
 Lee, M. W. 24
 Lee, R. W. 110
 Lee, W. H. K. 255
 Leenheer, J. A. 284
 Leggat, E. R. 111
 Leland, H. V. 285
 Leonard, R. B. 117
 Leopold, E. B. 216
 Leopold, L. B. 210
 Lesser, J. M. 344
 Lesure, F. G. 3
 Leve, G. W. 104
 Leventhal, J. S. 36, 39
 Lewis, B. D. 110, 117
 Lewis, J. E. 320
 Lewis, R. E. 39, 286
 Lewis, R. E., Jr. 56
 Lichtler, w. F. 220, 236
 Lichty, R. W. 225

Liddicoat, J. C. 216
 Lidz, B. H. 159
 Lind, C. J. 187
 Lindholm, G. F. 96
 Lindner, J. B. 285
 Lindsey, D. A. 32
 Lindskov, K. L. 122
 Lines, G. C. 122
 Ling, C. H. 245
 Lins, H. F., Jr. 320
 Lipin, B. R. 1
 Lipman, P. W. 189
 Liscum, F. 137, 225
 Lium, B. W. 243
 Locker, S. D. 146
 Loferski, P. J. 176
 Lofgren, B. E. 344
 Lofgren, B. F. 289
 Londquist, C. J. 114
 Loney, R. A. 86
 Long, A. T. 150, 151
 Long, C. L. 172
 Lopez, D. 67
 Lopez, F. X. 350
 Lopez, M. A. 137
 Loskot, C. J. 218
 Loudon, T. S. 352
 Love, J. D. 56, 63
 Lowell, R. P. 208
 Lowham, H. W. 124
 Lucas, J. R. 304
 Lucchitta, B. K. 294, 296
 Lucchitta, I. 72
 Luce, R. W. 4, 176
 Ludwig, K. R. 34
 Luepke, G. 153
 Lum, W. E., II 131, 132, 139
 Lund, J. W. 206
 Luoma, S. N. 285
 Lupe, R. D. 28
 Lyle, W. M. 18
 Lynch, R. S. 106
 Lyons, P. C. 46, 48
 Lystrom, D. J. 234
 Lyttle, P. T. 50

M

Mabey, D. R. 171
 MacLeod, N. S. 194
 Madden, C. T. 227
 Maddock, T., Jr. 338
 Madole, R. F. 56, 57
 Magner, J. E. 273
 Malcolm, R. L. 248
 Maldonado, F. 277
 Mallakpour, M. A. 340
 Mamet, B. L. 72
 Manheim, F. T. 159
 Mankinen, E. A. 167
 Mann, L. J. 126
 Manon, A. 198
 Marcus, K. L. 78
 Marcus, L. C. 322
 Marincovich, L. N. 229
 Markewich, W. 23
 Marks, S. M. 195
 Marley, W. E. 14
 Marlow, M. S. 155

Marranzino, A. P. 350
 Marrs, R. J. 269
 Marsh, S. 308
 Marshall, B. V. 155
 Martin, A., Jr. 92
 Martin, E. A. 149
 Martin, J. B. 221
 Martin, R. G. 148
 Marvin, R. F. 59, 60, 63, 74, 185
 Massey, B. C. 137, 139
 Masursky, H. 293
 Matthes, W. J., Jr. 114
 Matthiesen, R. B. 264
 Mattick, R. E. 145
 Mattraw, H. C., Jr. 137, 138
 Maughan, E. K. 20, 232
 Mawad, M. 347
 May, F. E. 81, 228
 Mayo, L. R. 212
 Mays, R. E. 86
 Mazor, E. 202, 205
 Mazzaferro, D. L. 91
 McCallum, M. E. 61, 63
 McCarthy, R. P. 251
 McCauley, J. F. 217, 294, 295
 McClymonds, N. E. 343
 McCulloch, D. S. 23, 150, 151, 161
 McCulloh, T. H. 187
 McDonald, M. G. 218
 McGee, K. A. 176
 McGill, J. T. 265
 McGuire, R. K. 263
 McKay, J. R. 160
 McKenzie, S. W. 130, 138, 236
 McKinley, P. W. 117
 McLaughlin, R. J. 75, 76, 198, 266
 McLean, H. 21, 155
 McLeod, R. S. 101, 220
 McMurray, G. 162
 McNeal, J. M. 88, 245
 McQueen, I. S. 110
 Meade, R. H., Jr. 338, 340
 Medina, K. D. 283
 Medlin, J. H. 15, 16
 Mehnert, H. H. 63, 74, 185
 Meisler, H. 350
 Mendieta, H. B. 242
 Mercer, J. W. 193, 278
 Merewether, E. A. 18
 Merriam, D. 329
 Merritt, V. M. 63
 Meyer, F. W. 225
 Meyer, G. 345
 Meyer, W. 92
 Meyer, W. R. 218
 Miesch, A. T. 188, 189
 Milazzo, V. A. 320
 Millard, H. T., Jr. 185
 Miller, B. M. 23
 Miller, C. H. 269
 Miller, F. K. 77
 Miller, G. A. 127
 Miller, R. A. 137, 138
 Miller, R. E. 148
 Miller, R. F. 110
 Miller, S. H. 310
 Miller, T. L. 130, 138
 Miller, T. P. 32, 33, 84
 Miller, W. A. 302

Miller, W. L. 106
 Miller, W. R. 11
 Minges, D. R. 113
 Minkin, J. A. 295, 298
 Moench, A. F. 193
 Molenaar, D. 132
 Molnia, B. F. 153
 Monroe, R. J. 199
 Moore, D. O. 350
 Moore, G. K. 313
 Moore, H. J. 293, 294, 296
 Moore, J. G. 75, 184
 Moore, R. B. 41
 Morgan, B. A. 184
 Morgan, J. O. 330
 Morrell, R. P. 86, 87
 Morris, E. C. 293
 Morris, H. T. 71
 Morrison, H. F. 207
 Mortensen, C. E. 253
 Morton, D. M. 77
 Mosier, E. L. 9, 10
 Moulton, G. F. 216
 Mower, R. W. 123
 Moxham, R. M. 11
 Moyle, W. R., Jr. 40, 126
 Mudge, M. R. 18
 Mudrey, M. G., Jr. 54
 Mueller, H. W. 298
 Muffler, L. J. P. 41, 203
 Mull, C. G. 81
 Muller, D. C. 273
 Mullineaux, D. R. 78
 Mummie, S. T. 160
 Mundorff, M. J. 343
 Murata, K. J. 186
 Murray, C. R. 139

N

Nace, R. L. 338
 Nackowski, M. P. 340
 Naeser, C. W. 59, 63, 191, 269
 Nakahara, R. H. 139
 Nakamura, N. 299
 Nakata, J. K. 217
 Naqvi, I. M. 227
 Nash, J. T. 31
 Nash, W. P. 205
 Nason, R. D. 262
 Nathenson, M. 197
 Nauman, J. W. 243
 Neeley, C. L. 4
 Neely, B. L., Jr. 225
 Nehring, N. L. 201
 Nelson, A. E. 50
 Nelson, C. A. 301, 302, 304
 Nelson, C. H. 155
 Nelson, G. L. 125
 Nelson, L. M. 210
 Nelson, R. E. 81
 Nelson, W. H. 84, 353
 Nemickas, B. 97
 Newell, W. L. 51, 52
 Newhall, C. G. 41
 Newkirk, H. D. 304
 Newton, J. G. 103
 Nicholas, F. W. 320
 Nichols, F. H. 163

Nichols, T. C., Jr. 264
 Nichols, W. D. 280
 Nilsen, T. H. 76
 Noble, M. A. 146
 Nolan, K. M. 211, 266
 Nord, G. L., Jr. 178
 Nordin, C. F., Jr. 212, 338, 340
 Normark, W. R. 151, 158
 Novitzki, R. P. 233
 Nowlin, J. O. 286
 Nutt, C. J. 353
 Nyman, D. W. 160

O

Oaksford, E. J. 138
 Oberlindacher, P. 44
 Obermeier, S. F. 266
 Obradovich, J. D. 183, 191
 O'Connor, J. T. 325
 O'Connor, L. J. 39
 O'Donnell, T. H. 105
 Offield, T. W. 309
 O'Hara, C. J. 146, 147
 Ohl, J. P. 273
 Ohlen, D. O. 302, 304
 Oldale, R. N. 146, 147
 O'Leary, D. W. 312
 Olhoeft, G. R. 169, 170, 173
 Olive, W. W. 53
 Oliver, H. W. 172
 Olmsted, F. H. 236
 Olson, J. C. 32
 Oman, C. L. 16
 Omang, R. J. 283
 O'Neil, J. R. 190
 Oppenheimer, D. H. 199
 Orkild, P. P. 273
 Orr, B. R. 278
 Osberg, P. H. 45
 Osmond, J. K. 204
 Osmonson, L. M. 33, 55
 Osterkamp, W. R. 212
 Osterwald, F. W. 269
 Otton, J. K. 27
 Overstreet, W. C. 345
 Owens, J. P. 51

P

Pabst, M. E. 114
 Packard, F. A. 132, 243
 Page, R. A. 330
 Page, R. W. 128
 Pakiser, L. C. 253
 Palacas, J. G. 23
 Palmer, I. F. 18
 Papadopoulos, S. S. 350
 Papp, C. S. E. 289
 Parker, B. C. 353
 Parker, R. S. 286
 Parkinson, H. L. 342
 Pascale, C. A. 104, 221, 222
 Pasternack, I. 81
 Patterson, G. L. 92
 Patterson, S. H. 4
 Patton, W. W., Jr. 82, 83
 Paulson, R. W. 306

Pavich, M. J. 52
 Pavlides, L. 51
 Pearl, J. E. 78, 152
 Pearson, H. E. 132, 133
 Pease, M. H., Jr. 47
 Pease, R. W. 320
 Peck, D. L. 189
 Peddie, N. W. 169
 Peek, C. O. 225, 283
 Penman, H. L. 240
 Perkins, D. M. 257, 264
 Perry, W. J., Jr. 52
 Person, W. J. 250
 Peselnick, L. 256
 Pessagno, E., Jr. 79
 Pessl, F., Jr. 79
 Peterman, Z. E. 64, 276
 Peters, H. B. 121
 Peterson, D. H. 159, 162
 Peterson, F. 26
 Peterson, L. R. 345
 Pettijohn, R. A. 93
 Pfefferkorn, H. W. 230
 Phair, G. 185, 202
 Phelps, G. G. 104
 Phillips, J. D. 171
 Philpott, B. C. 268
 Phipps, R. L. 233
 Pierce, K. L. 215
 Pierson, C. T. 30
 Pike, R. S. 23
 Pilkey, O. 148, 150
 Pinckney, D. J. 249
 Piper, D. Z. 157
 Pippingos, G. N. 26
 Pitman, J. K. 21
 Pitt, A. M. 195
 Pitt, W. A. J., Jr. 106, 286
 Place, J. L. 320
 Playton, S. J. 111, 120
 Plouff, D. 175
 Poggioli, R. S. 97
 Pojeta, J., Jr. 230
 Poland, J. F. 338
 Pollard, D. D. 199
 Poole, F. G. 21, 69, 70, 74
 Popenoe, P. 50, 148
 Potter, D. B. 46
 Potter, R. W. 176, 276
 Powers, R. B. 23
 Pratt, W. P. 54
 Prescott, G. C., Jr. 93
 Prescott, W. H. 253
 Price, D. 123
 Price, M. 282
 Priestly, K. F. 206
 Prill, R. C. 138
 Prostka, H. J. 61, 183
 Prugh, B. J., Jr. 138
 Puente, C. 103
 Purucker, M. E. 168
 Putnam, S. A. 106

R

Ragone, S. E. 285
 Raines, G. L. 309
 Rankin, D. W. 3
 Rankl, J. G. 123, 225

Rasmussen, L. A. 245
 Rasmussen, W. C. 340
 Ratcliffe, N. M. 46
 Rathbun, R. E. 238
 Ratte, J. C. 72
 Raup, R. B., Jr. 272
 Raymond, W. H. 6
 Reasenber, P. A. 195
 Redden, G. D. 153
 Reeder, J. W. 261
 Reeves, C. C., Jr. 29
 Reeves, E. B. 139
 Reilly, T. E. 97
 Reimer, G. M. 12, 37
 Reimnitz, E. 157
 Reinemund, J. A. 326, 329, 330
 Remmenga, E. E. 23
 Repenning, C. A. 228
 Repetski, J. E. 230, 231
 Reussow, J. P. 92
 Reynolds, M. W. 68, 170
 Reynolds, R. L. 33, 34, 37
 Rhea, B. S. 312
 Rice, D. D. 18, 19
 Richard, J. K. 303
 Richards, D. B. 283
 Richmond, G. M. 88
 Ridgley, J. L. 30
 Riggs, H. C. 227
 Rinella, F. A. 234
 Rinella, J. F. 236, 241
 Ringrose, C. D. 288
 Ritter, J. R. 339
 Roberts, A. A. 24
 Roberts, A. E. 43
 Roberts, R. J. 347
 Robertson, E. C. 194, 277
 Robertson, J. B. 284
 Robie, R. A. 176
 Robinson, P. 46
 Robinson, S. W. 266
 Robison, T. M. 98
 Robson, S. G. 113
 Roddy, D. J. 295
 Rodis, H. G. 350, 351
 Roedder, E. 177, 278, 299
 Roen, J. B. 49
 Rogers, A. M. 261, 262
 Rohde, W. G. 302, 304
 Rohrer, W. L. 27, 183
 Rolston, J. L. 138
 Romero, J. C. 208
 Rooney, L. F. 346
 Rose, H. J. 293
 Rosholt, J. N. 192
 Ross, D. C. 74
 Ross, M. 178
 Ross, P. P. 40
 Ross, R. J. 191
 Rowan, L. C. 329
 Rowe, J. J. 246
 Rowley, P. D. 352
 Rubin, D. M. 152, 161
 Rubin, M. 57
 Rucker, S. J., IV 242
 Runnegar, B. 230
 Runner, G. S. 281
 Ruppel, B. D. 187
 Ruppel, E. T. 66

Russ, D. P. 260
 Russo, T. N. 103
 Rutledge, A. T. 222
 Ryals, G. N. 116
 Ryder, R. T. 24, 77
 Rye, R. O. 33, 347
 Rykov, A. V. 327
 Rythuba, J. J. 10

S

Sahai, S. K. 307
 Sallenger, A. H. 156
 Sanchez, J. D. 14
 Sandberg, C. A. 20, 21, 232
 Sandberg, G. W. 123
 Sandeen, W. M. 218
 Sando, W. J. 232
 Santos, E. S. 28
 Sanzolone, R. F. 12
 Sarna-Wojcicki, A. M. 216
 Sass, J. H. 199, 200
 Sato, M. 177, 299
 Sauer, S. P. 343
 Saulnier, G. J., Jr. 113
 Savage, J. C. 253
 Savage, W. Z. 266, 269
 Sayre, W. W. 225
 Schaber, G. G. 296, 297
 Schaefer, F. L. 160
 Schaeffer, O. A. 298
 Schafer, J. P. 268
 Schefter, J. E. 140
 Schifflett, C. M. 44
 Schlee, J. S. 144, 145
 Schlocker, L. B. 74
 Schmidt, D. L. 227, 348
 Schmidt-Kaeler, H. 295
 Schmidt, R. G. 67
 Schmoker, J. W. 22, 25
 Schmoll, H. R. 273
 Schneider, W. J. 323
 Schock, W. 232
 Scholl, D. W. 155
 Scholle, P. A. 24, 145
 Schopf, J. M. 353
 Schornick, J. C., Jr. 235
 Schroder, L. J., II. 249
 Schroer, C. V. 129, 283
 Schuetz, J. R. 114
 Schultz, D. M. 148
 Schuster, R. L. 345
 Schwab, W. C. 153
 Scott, D. H. 294, 296
 Scott, E. W. 23
 Scott, G. R. 56
 Scott, J. H. 175
 Scott, M. 240
 Scott, R. A. 81
 Scott, W. B. 105
 Scott, W. E. 260
 Seaber, P. R. 287
 Sebetich, M. J. 187
 Seeland, D. A. 6
 Seeley, J. L. 246
 Seiders, V. M. 76
 Seitz, H. R. 125, 128
 Seitz, J. F. 343
 Senftle, F. E. 11, 175, 279

Setmire, J. G. 126
 Severson, R. C. 88, 245, 288
 Shampine, W. J. 350
 Sharp, R. V. 258, 261
 Shaw, H. R. 180, 279
 Shawe, D. R. 8
 Shearman, J. O. 225
 Shedlock, R. J. 92
 Sheehan, C. A. 303
 Shell, J. D. 282
 Sheridan, D. M. 6
 Sherrill, M. G. 101
 Shima, L. J. 313
 Shinn, E. A. 159
 Shoaf, W. T., III. 249
 Shown, L. M. 110
 Shultz, D. J. 238
 Shurr, G. W. 18, 19
 Siegel, D. I. 95
 Sigafos, R. A. 233
 Signor, D. C. 220
 Silberling, N. J. 70
 Silberman, M. L. 69
 Simmons, C. E. 234
 Simmons, E. C. 192
 Simmons, R. H. 225
 Simon, F. O. 246
 Simpson, S. L. 311, 312
 Sims, J. D. 264
 Sims, P. K. 53, 54
 Skelton, J. 239
 Skinner, J. V. 212
 Skipp, B. A. 55, 65
 Skrivan, J. A. 131
 Slack, J. F. 3
 Slack, K. V. 243
 Slagle, S. E. 110
 Sloan, C. E. 242
 Smith, B. D. 39, 42
 Smith, B. E. 253
 Smith, C. B. 61
 Smith, C. S. 118
 Smith, C. W. 347
 Smith, D. L. 210
 Smith, G. I. 216
 Smith, J. A. 283
 Smith, J. G. 84
 Smith, P. A. 81
 Smith, R. B. 205
 Smith, R. L. 181
 Smith, W. K. 266, 269
 Smoot, G. F. 339
 Snavely, P. D., Jr. 23, 78, 152
 Snider, J. L. 116
 Sniegocki, R. T. 111
 Snyder, G. L. 55
 Snyder, J. 315
 Soderblom, L. A. 293, 297
 Solomon, B. J. 26
 Soren, J. 97, 98
 Sorg, D. H. 198
 Southwick, D. W. 53
 Spaeth, M. 327
 Spalding, R. 236
 Spall, H. R. 168
 Spence, W. J. 251, 253, 268, 339
 Spencer, D. W. 282
 Spencer, F. D. 345
 Spencer, R. R. 247, 248

Spiers, C. A. 225
 Spirakis, C. S. 37
 Staatz, M. H. 6
 Stacey, J. S. 189, 191
 Stanley, R. S. 46
 Stanley, W. D. 174
 Stannard, D. I. 220, 236
 Steele, T. D. 242
 Steinheimer, T. R. 249
 Stephens, C. D. 261
 Stephens, D. W. 238
 Steven, T. A. 189
 Stevens, H. H., Jr. 212
 Stewart, R. M. 255, 256
 Stokoe, K. H. 263
 Stone, B. D. 5, 45
 Stoner, J. D. 117
 Stover, C. W. 250
 Stuber, H. A. 284
 Stullken, L. E. 115
 Sturdevant, J. A. 304
 Sulam, D. J. 97, 285
 Sumsion, C. T. 123
 Sun, R. J. 223
 Suneson, N. H. 72
 Svendsen, K. L. 330
 Swadley, W. C. 52, 53
 Swanberg, C. A. 209
 Swanson, D. A. 78, 180
 Swanson, V. E. 346
 Swarzenski, W. V. 343
 Szabo, B. J. 216

T

Tabor, R. W. 78
 Taggart, J. N. 327
 Tai, D. Y. 248
 Tangborn, W. V. 133, 213
 Tanner, A. B. 11
 Taranik, J. V. 304, 306, 307
 Tatsumoto, M. 192, 299
 Taylor, H. E. 247, 248, 249, 288
 Taylor, P. L. 213
 Terman, M. J. 326, 330
 Teter, G. A. 304
 Thaden, R. E. 28, 29
 Thatcher, L. L. 223
 Thatcher, W. R. 257
 Thayer, T. P. 1
 Theisen, A. F. 23
 Theobald, P. K., Jr. 10
 Theodore, T. G. 8, 73, 182, 186
 Thomas, C. A. 227
 Thomas, M. P. 225
 Thompson, C. L. 295, 298
 Thompson, J. M. 75
 Thompson, M. R. A. 352
 Thomson, A. F. 77
 Thorman, C. H. 73
 Threlkeld, C. N. 22
 Thurman, E. M. 248
 Tibbals, C. H. 219, 221
 Tibbitts, G. C., Jr. 350
 Tibbitts, G. C., Jr. 351
 Tidball, R. R. 288
 Tilley, L. J. 243
 Toimil, L. J. 157
 Toler, L. G. 286

Torgensen, T. 201
 Toulmin, P., III..... 293
 Tourtelot, H. A. 43
 Townshend, J. B. 168
 Toy, T. J..... 214
 Trabant, D. C..... 212
 Trapp, H., Jr. 105, 222
 Trautwein, C. M. 306
 Trent, V. A..... 15
 Trescott, P. C..... 238, 344
 Trexler, D..... 129
 Trimble, D. E..... 57, 272
 Trimble, S. W..... 211
 Truesdell, A. H. 198, 201, 203, 343
 Trumbull, J. V. A. 150
 Tschanz, C. M. 9, 59
 Tschudy, B. D. 229
 Tschudy, R. H. 229
 Tucci, P. 92
 Tucker, R. D. 46
 Turk, J. T. 241, 284
 Turner-Peterson, C. E..... 27
 Turner, R. M. 233
 Tweto, O. L. 88

U

Ulrich, G. E. 41
 Urban, T. C. 197
 Utter, P. A. 150, 151

V

Valenza, M..... 177
 Van Alstine, R. E. 1, 6
 Van Denburgh, A. S. 129, 193, 236
 Van der Voo, R. 85
 Van Driel, J. N. 263
 Van Horn, R. 71, 263
 van Hylckama, T. E. A..... 239, 240
 Vanschaack, J. R. 255
 Vecchioli, J. 221
 Vedder, J. G..... 21
 Vennum, W. R..... 352
 Viets, J. G. 9
 Vietti, B. T. 23
 Villalobos, H. A..... 261
 Vine, J. D. 42
 Vivit, D. V. 202, 236
 Volckmann, R. P. 51
 von Huene, R. E. 155

W

Waddall, K. M..... 139
 Wait, R. L. 350
 Waitt, R. B..... 215

Walker, E. H. 95
 Walker, R. L., Jr. 160
 Wallace, C. A. 67
 Wallace, L. G..... 49
 Wallace, R. E..... 259, 260
 Walling, D. E..... 210
 Walter, A. W. 195
 Walters, A. 201
 Walters, K. L. 131
 Wandle, S. W., Jr. 282
 Wang, F. H. 326, 329, 330
 Ward, F. N. 245, 246
 Ward, J. R. 98
 Ward, L. W. 228
 Ward, R. W. 205
 Ward, S. M. 99
 Ward, W. A. 294
 Wardlaw, B. R. 70, 230, 232
 Warren, C. G. 37
 Warren, C. R. 46
 Watkins, J. A. 296
 Watson, D. E..... 168
 Watson, K. 310
 Watson, R. D. 23, 308
 Watts, K. R. 115
 Weaver, C..... 195, 201
 Webber, E. E. 282
 Wedow, H., Jr. 2
 Weeks, E. P. 220, 223
 Weiblen, P. W. 299
 Weiner, E. R. 212, 235
 Weiner, M. S. 234
 Weiss, E. J. 219
 Welder, F. A. 113
 Welder, G. E. 240
 Wells, F. C. 237, 243
 Wenrich-Verbeek, K. J. 37
 Wershaw, R. L. 249
 Wesson, R. L. 330
 West, M. N. 49
 West, W. S. 5
 Whetten, J. T..... 79
 Whipple, J. W. 67
 White, A. F. 187, 188
 White, D. E. 111, 196, 203
 Whitfield, M. S., Jr. 116
 Whitkind, I. J..... 56
 Whitney, J. W. 272
 Wiczorek, G. F. 263
 Wilbanks, J..... 353
 Wilcox, D. E. 125
 Wilhelms, D. E..... 295
 Willey, R. E. 99
 Williams, B. B. 3
 Williams, G. P. 118
 Williams, J. F..... 93
 Williams, R. P. 211
 Williams, R. S., Jr. 306

Williams, V. S. 269
 Wilshire, H. G. 217, 273
 Wilson, K. V. 281
 Wilson, L. D. 137, 139
 Wilson, L. R..... 168
 Wilson, R. C. 266
 Wilson, W. E., III..... 105
 Winkler, S. 81
 Winner, M. D., Jr. 107
 Winograd, I. J. 216
 Winter, T. C..... 239
 Wisconsin Geological and Natural History
 Survey 101
 Wittenberg, L. A. 238
 Wold, R. J. 45
 Wolf, R. J..... 96
 Wolfe, E. W. 41
 Wollenberg, H. A. 199
 Wood, M. D..... 255
 Wood, W. W. 220
 Worl, R. G..... 348
 Worts, G. F., Jr. 342
 Wright, N. A. 345
 Wright, T. L. 180, 181
 Wrucke, C. T., Jr..... 70
 Wyant, T. S. 283
 Wynn, J. C. 11
 Wyrick, G. G..... 100

Y

Yee, J. J. S. 128
 Yeend, W. E. 80
 Yehle, L. A. 273
 Yerkes, R. F..... 77, 265
 Yotsukura, N. 225
 Youd, T. L. 264, 265
 Young, H. L. 238
 Young, H. W. 39, 129
 Yount, J. C..... 215
 Yukutake, T. 169
 Yurewicz, M. C..... 235

Z

Zablocki, C. J..... 172
 Zapecza, O. S..... 97
 Zartman, R. E. 59, 79
 Zen, E-an..... 46, 48, 60, 61
 Ziagos, J. P..... 199
 Zielinski, R. A. 35, 36
 Ziony, J. I. 257, 330
 Zoback, M. D. 255
 Zohdy, A. A. R. 172
 Zubovic, P. 16
 Zucca, J. J. 195
 Zurawski, P. 108